IMPLICATIONS OF HUMAN INTERACTION FOR HEALTH OF PAST POPULATIONS IN ASIA

Melandri Vlok

A thesis submitted for the degree of Doctor of Philosophy at the University of Otago
Dunedin, New Zealand

July 2020

ABSTRACT

Drivers of human mobility such as migration, trade and conflict is today recognised to considerably influence the spread and prevalence of infectious diseases globally. Additionally, these factors are known to impact nutritional levels of migrating populations. However, the impacts of interactions between two or more populations, which occurs following human mobility, has received little attention in the palaeopathological literature. This thesis investigates whether *human population interaction* significantly influenced the health of prehistoric populations in Asia. Six skeletal assemblages across three case studies (n=450) in Asia's prehistory were explored to assess the level of nutritional and infectious diseases. These were the Middle to Late and Final Jomon (5000-2300BP), Pre-Neolithic to Neolithic Vietnam (6900-3500BP) and Bronze Age to Xiongnu Period Mongolia (4500 to 1800BP).

The questions proposed for this thesis were:

1) *Did increasing levels of population interaction over time significantly affect the health of populations in prehistoric Asia?* And;

2) *How did population interaction interplay with a range of other sociocultural, biological and ecological factors to influence the health of populations in prehistoric Asia?*

It was hypothesised that human interaction would have a considerable impact on the health of prehistoric populations from Asia, but that other sociocultural, environmental and biological factors would mediate the degree of impact. To assess the implications of human population interaction on prehistoric health, protocols of weighted diagnostic criteria for differential diagnosis of infectious diseases, nutritional diseases and anaemias in dry bone were developed to standardise identification where they do not yet exist in the palaeopathological literature. Additionally, inclusion criteria for an overall infectious disease prevalence, that encompasses specific and non-specific infectious diseases, was developed. A three-stage statistical approach was applied to address the research questions. This involved analysis within assemblages (*site level*), diachronically across two assemblages in the same region (*regional level*) and across all assemblages to assess general trends in the influence of human population interaction on disease dynamics (*continent level*). The results of this study demonstrated that varying levels of human population

interaction influenced the prevalences and diversity of infectious diseases in Asia, but only indirectly influenced the prevalences of nutritional diseases. However, residential mobility and population density served to mediate the impact that human population interaction had on infectious disease prevalences and diversity in past populations. Therefore, the hypothesis was supported for infectious diseases but not nutritional diseases. Additionally, the impact of disease on mortality was variable and dependent on the pathogens introduced through human population interaction processes.

ACKNOWLEDGMENTS

Given that this thesis has involved research in three different countries, you can imagine that the support and collaborative efforts were immense. They say it takes a village to raise a child, but apparently it also takes a village of academics from around the world to raise a PhD student. So to anyone reading this acknowledgement, strap yourself in, because there is a lot of people to thank.

First and foremost, I need to thank the great supervisor Professor Hallie Buckley. To say the achievement of this project was a challenge, is a bit of an understatement. To find a supervisor willing to dive in with you and have good stab at that challenge is unique. There were many highs and many lows that we sailed together, and there were a few times where I doubted myself and felt perhaps we should just shoot for plan B, a simpler version of the project. Each time Hallie would just turn me around to face towards forward, and gently nudge me in the right direction. What I have learnt is not to bail out on plan A when plan A is still working, even if it feels like an impossible task. And to trust my instincts. Hallie's dedication to the science, which often meant challenging me to go deeper, and to question literally everything, is an exceptionally rare thing. I'm a better researcher because of this. I will also note here, Hallie's particular 'dedication' to radiographs. Every time I was overseas and had found something really interesting, the email response would always be "Did you get x-rays?". These words have inadvertently led to probably the most extensive radiographic collection of prehistoric Asian material to date, and a shared giggle over the thought of me just tattooing those words on my arm for future reference. Honestly, I could not have thought of a better supervisor for my PhD.

Secondly, I need to thank my honours supervisor Professor Marc Oxenham who stayed on as a committee member for my PhD and has been one of my biggest supporters. Marc has literally been there from the start. When we met, I was a nineteen year old 1st year undergraduate, fresh out of high school, with a bad buzz cut (from a hairdresser trip that went horribly wrong), excessive amounts of energy and a complete inability to sit still. Marc, I truly apologise for all my troublemaking antics in the field way back, and I'm glad you saw past all that to mentor me through these years.

I am also indebted to Associate Professor Dorothy Oorschot, Associate Professor Siân Halcrow, and Dr. Michael Knapp for their guidance as members of my supervisory panel for the last three years. Your encouragement through the years helped instil confidence in me to keep going.

One of the greatest unsung heroes of this PhD has been Tran Thi Minh. Minh was by my side every day at the Institute of Archaeology in Hanoi when I was collecting data for the Vietnamese assemblage. Minh assisted with laying out skeletons, facilitating paperwork and every aspect of administration that comes with international collaboration, and also arranging radiographs to be completed at a nearby clinic where the doctors only spoke Vietnamese. Minh also translated the abstract of our first publication based off of this thesis work. She did all this while also caring for the most adorable 7-month-old baby in existence. Her passion and dedication to the bioarchaeology of Vietnam is inspiring, and I, and other Otago PhD students who worked on the assemblage, wouldn't have been able to complete our research without her. I would also like to thank Minh's husband Dr. Bui Van Khan as he also helped a great deal in finding a clinic who would be happy to scan skeletal remains. Dr. Nguyen Thi Mai Huong, Professor Nguyen Lan Cuong, Dr. Hiep Hoang Trinh and Mr. Nghia Truong Huu from the Institute of Archaeology at Hanoi were equally invaluable to my research in Vietnam and continue to be exceptional collaborators.

I want to thank Professor Nakatsukasa, Dr. Kazuhiro Sakaue and Ms. Hikari Ishijima for all the effort they went to make sure I had radiographs for my Jomon assemblage. Nowhere in Kyoto was willing to radiograph the bones, so the bones were shipped to National Museum of Science and Nature in Tokyo. There Dr. Sakaue and Ms. Ishijima radiographed all the Jomon individuals in their own time and at no cost. I'm indebted to Professor Nakatsukasa for allowing me access to the Jomon collections. Dr. Sakaue also provided invaluable information in regards to Jomon palaeopathology.

I want to thank Professor Hirofumi Matsumura, who was elemental to my research in Vietnam as well as assisting with access to skeletal collections in Japan. Professor Matsumura's encouraging words and support were also most helpful throughout the years.

I am also grateful to Professor Erdene Myagmar for allowing access to Mongolian assemblages, and for also helping me with radiographs. I also learnt so much from Professor

Erdene about bioarchaeology in Mongolia, and her passion on the subject was truly inspiring. I want to thank Dr. Dagvasumberel Munkhbaatar for allowing us to use his radiology clinic and assisting us with x-rays after hours for the Mongolian assemblage.

The original palaeopathological work up for Man Bac was completed by Associate Professor Kate Domett. Kate provided excellent discussion on disease at the site over the years, and was particularly excellent at picking up all my typos in our manuscripts. Dr. Annie Sohler-Snoddy was similarly excellent at pointing out my grammar mistakes while proof reading my thesis chapters.

The statistical methods used in this thesis would not have been possible without the assistance of Drs. Clare and Michael McFadden. I never knew stats could be this fun, and I was glad I wasn't the only one excited about the numbers.

I also want to thank Dr. Rebecca Crozier. Although Rebecca didn't play a role in my PhD, she mentored me throughout my honours, and certainly played a role in my decision to shoot my shot and apply for PhD. Rebecca helped foster my confidence in human skeletal analysis, and is probably one of the most patient people I have ever met. She also was the first person I trusted to read my thesis proposal.

I want to thank all the people who had my back when things were tough: Mum, dad, Liz, Tim, Liam, Matt, Fletcher, Marie, Viv, Lucy, Tom, Meg, Clare, Monica, Annie, Charlotte, Alisha, Nellissa, and Melanie. Thanks for picking me up when I was down. You all know how important you are to me. I will of course give you all a great big hug to say thank you.

Lastly, a special mention to Celine Dion, whose bangers got me through the months of Covid-19 lockdown.

This thesis is dedicated to the memory of Professor Colin Groves.
Colin's wonder of the world around him ignited the curiosity of his students. His light is greatly missed.

And

To my parents, Heidi and Carlo Vlok.
As immigrants, you gave up everything so that your two children could have the best chance. I'm only here today because of the sacrifices you made.

TABLE OF CONTENTS

LIST OF FIGURES

CHAPTER 6:

CHAPTER 7:

CHAPTER 8:

CHAPTER 9:

CHAPTER 10:

LIST OF TABLES

CHAPTER 6:

CHAPTER 7:

CHAPTER 8:

CHAPTER 9:

CHAPTER 10:

CHAPTER 1:
INTRODUCTION

"The link between infectious diseases and population mobility must thus be understood in relation to the different forms, conditions and patterns of migration, which have very different influences on the distribution and spread of infectious diseases." (Saker et al. 2004: 37).

Today, large-scale migrations following conflict and environmental crises are demonstrable risk factors for epidemic outbreaks (WHO 2000). This is not a recent phenomenon. Human population interactions succeeding migration, trade and conflict have facilitated the spread of infectious diseases throughout the past (Roberts and Manchester 2012; Steckel 2005; Tatem et al. 2006; Wilson 1995). A long term co-evolutionary understanding of the spread of infectious diseases and human population interaction patterns can, therefore, contribute essential information on pathogen behaviour. Past epidemiological information is needed to inform modern models of potential outbreaks (Coburn et al. 2009; Comas and Gagneux 2009; Duintjer Tebbens et al. 2005). *Palaeopathology* has traditionally been considered the 'study of ancient disease' in skeletal or mummified human remains, although historical contexts are also studied in the field (Grauer 2011). The basis of identification of disease in the field is that of *differential diagnosis*. In this process, potential diseases that share similar appearances in bone are compared and the least likely causes are excluded through a process of elimination (Ortner 2012). This process is of great importance as each pathogen is suited to different biological, social and environmental contexts, and the identification of a particular disease may provide a vast amount of knowledge on these contexts, which would not otherwise be accessible through other archaeological investigations.

Palaeopathological information on previous epidemiological transitions such as with emerging agriculture, may also help predict consequences of changing biosocial conditions today and how they relate to the dynamics of infectious disease (Harper and Armelagos 2010). However, despite their potential importance, migration, trade and conflict receive little attention in palaeopathological models, that instead focus on impacts of population density and subsistence change (see Armelagos and Cohen 1984; Eshed et al. 2010; Johansson and Horowitz 1986; Martin and Goodman 2002; Pinhasi and Stock 2011; Temple 2010). In fact, to date no research in the field has attempted to directly consider how infectious diseases introduced via migration, trade or conflict influenced morbidity and

mortality of previously unexposed populations. As Saker et al.'s (2004) report for the World Health Organization notes above, to completely understand how infectious diseases spread in present day, and similarly with the past, requires understanding of how different population interaction events influenced the epidemiology and behaviour of pathogens.

Moreover, the influence of nutritional status on the transmission of infectious pathogens via migrant groups, has received much attention by epidemiologists, particularly in the light of uncontrollable outbreaks of infectious disease associated with forcibly displaced persons such as refugees (Rowland and Nosten 2001). Specifically, the morbidity and mortality rate of infectious diseases at refugee camps are well documented to be far more severe in times of nutritional crises such as famines. Movements of malnourished people, who are more likely to contract infectious diseases, is linked to increased potential for the disease to spread further within the population (Chowdhury and Chen 1977). In palaeopathology, recognition of the synergism between infectious and nutritional diseases is paramount to the study of population level impacts of disease (Roberts and Brickley 2018). However, the discussion of the impact of migration, as a possible disruptive factor impacting both sides of the infectious disease and nutritional disease synergy is a topic of research yet to be addressed. This project addresses this gap in the field by investigating the impact of increasing population interaction on disease following population mobility in prehistoric Asia.

1.1 Modelling Disease in the Past

Our understanding of human populations and respective disease response has been largely reliant on data from the contexts of Europe and North America (Armelagos and Cohen 1984; Donoghue et al. 2015; Manchester and Roberts 1989; Martin and Goodman 2002; Mays 2014; Powell and Cook 2005; Roberts 2015; Steckel et al. 2002). Investigation of prehistoric health in other regions such as Southeast Asia and the Pacific have received systematic attention only within the last two decades (Buckley 2000; Oxenham and Buckley 2016; Oxenham et al. 2005; Tayles and Buckley 2004; Willis and Oxenham 2013). The field of palaeopathology is advancing towards an evolutionary perspective on population studies that actively considers the changing dynamics of humans and pathogens over time (DeWitte 2016; Zuckerman et al. 2012). With this perspective, large-scale statistical models that incorporate multiple variables to analyse the health conditions of human groups in the past

are becoming more common (Roberts 2012; Steckel 2005; Steckel and Rose 2002; Zuckerman et al. 2012). For example, using the Western Hemisphere Database compiled as part of the Global History of Health Project, with a sample size of 4078 individuals from Pre-Columbian North America, Steckel and Rose (2002) developed a health index that integrates a number of skeletal indicators of morbidity, identifying physiological insults due to disease. Steckel (2005) then created regression models to associate this health index with factors such as settlement patterns, elevation, subsistence and coastal vs. inland groups. While this model, as acknowledged by the authors, is limited by the treatment of all skeletal indicators as having equal impacts on morbidity and mortality, the basis of the *continent level* model can also be appropriately applied to specific diseases in isolation, such as assessing infectious and nutritional diseases. A more focal assessment of "health" may be more appropriate when smaller samples sizes are available. It is important note here that evidence of disease does not equate to poor health and assessing "health" is challenging in the archaeological record. These issues will be addressed in sections below in light of the osteological paradox.

Reconstruction of the co-evolutionary history of humans and pathogens addresses crucial anthropological questions surrounding the spread of infectious diseases with migration in the past. With increasing reliance on ancient DNA that can provide detailed evolutionary data on pathogens and migration, macroscopic analysis is more necessary than ever to highlight individuals with the potential for pathogen DNA sampling at a later stage (Spigelman et al. 2012). Furthermore, in regions such as Southeast Asia where extraction of DNA has yielded poor results due to DNA preservation issues, the primary form of identification of infectious diseases remains by macroscopic assessment. Finally, models such as those proposed in this thesis clearly demonstrate the merit of macroscopic data in its own right.

1.2 The Spread of Infectious Diseases in Prehistoric Asia

Reliance on agriculture particularly rice and millet occurred in China alongside the Holocene Thermal Maximum, a period of global warming and increased precipitation, which peaked at 7,200 to 6000 years ago (Zhao 2011). Human mobility, particularly with migration for new agricultural land subsequently intensified in Asia (Renssen et al. 2012;

Tao et al. 2010; Zhao 2011). Alongside agricultural expansion, population size increased and interaction between populations north, west and south of China occurred (Bellwood and Oxenham 2008; Liu et al. 2009). This social transition may have enabled the emergence of epidemics on a large scale. The earliest convincing evidence for specific infectious disease in Asia comes from an individual with probable tuberculosis from Meishan, a Neolithic Longshan site in China dating from 4500 to 4000BP (Pechenkina et al. 2007). Subsequent evidence of specific infectious disease is sparse both geographically and temporally until the Metal Ages (from approximately the 5th Century BC to 5th Century AD) onwards where skeletal evidence of leprosy and tuberculosis has been found in Central, Eastern and Southeast Asia (Blau and Yagodin 2005; Murphy et al. 2009; Suzuki et al. 2008; Suzuki and Inoue 2007; Tayles and Buckley 2004). Following the agricultural expansion, the emergence of large states, systems of high mobility, social and cultural exchange may have provided opportunistic environments for pathogen repositories. Exchange routes such as in the Middle Asian Interaction Sphere, the Bay of Bengal Interaction Sphere, the Eurasian steppes and the Silk Roads, may have facilitated the spread of infectious diseases into new regions such as East and Southeast Asia (Buckley and Oxenham 2016; Gupta 2007; Pechenkina and Oxenham 2013). Consequently this may have resulted in an increase in the number of different types of specific infectious diseases in the archaeological record. For this reason, more research investigating population interactions within Asia is required to understand the spread of infectious diseases throughout Asia's prehistory.

Palaeopathological research in Asia is also relevant to research conducted in the Pacific, as colonisation events of the Pacific originated from the greater Asian region and evidence for exchange and migration between Asia and the Pacific are well documented (Larson et al. 2007; Sheppard et al. 2011; Storey et al. 2010; Tykot and Chia 1996). Intensive palaeopathological research in the Pacific has revealed the presence of leprosy and treponematosis in this region by approximately 1200BP (Buckley and Oxenham 2016). However, questions remain as to the route of introduction of treponematosis into the region, particularly as prehistoric evidence of this disease in Mainland and Island Southeast Asia has to date not been identified. Further palaeopathological research within Southeast Asia also has potential impact for understanding the spread of these pathogens into the Pacific (Buckley and Oxenham 2016; Trembly 1995). A palaeopathological exploration of samples from Mainland Southeast Asia then provides an opportunity to investigate factors of

migration, social change, impact of settlement, and disease burden which influences understanding of many populations in and beyond Asia.

Research on continental Asia also provides an opportunity to test large multi-variable palaeoepidemiological models in a region with highly geographically variable social, biological and environmental factors. Such variation enables study of major ecological and social influencers of disease patterns and pathogen evolution. Furthermore, systematic palaeopathological studies in Asia remain sparse. This thesis applies statistical models to sites across Asia, thereby addressing a number of gaps in the current palaeopathological literature.

1.3 Human Population Interaction as a Factor in Palaeopathological Study

The term *mobility* has in the past been employed in bioarchaeological studies that associate migration with the spread of infectious diseases (e.g Roberts et al. 2013). However, this definition is broad and has been employed in many different ways in bioarchaeological research. Moreover, the term does little to describe the complex processes involved with an event of human population mobility in terms of the effect on health.

Today humans occupy over 50% of the earth's habitable terrain surface (WWF 2016), and interaction between populations following mobility in the face of globalisation is inevitable. In contrast, mobility in the past did not necessarily involve contact between two or more populations. Therefore, the experience and consequence on health of human groups who colonise new lands (such as the prehistoric colonisation of Remote Oceania), are separate from populations of migrants who interacted with pre-existing local populations within a territory. In the former scenario, all infectious diseases experienced are either incidental infections from interactions with the surrounding environment or pre-existing within the colonising population (Waguespack 2002).

In the latter scenario, where human population interaction is occurring, transmission of infectious diseases can also occur between the interacting human populations or via their domesticated animals (Wilson 2007). Depending on the disease's influence on morbidity and mortality, this newly introduced pathogen can have significant consequences on the

"health" of populations who have not been previously exposed to the pathogen, and have therefore not developed an ancestral immunity. For example, ancestral resistance due to strong selection pressure from the high mortality of smallpox in Europe is suggested to have led to a significant rise of the CCR5-Δ32 deletion, a dominant allele which provided resistance to death from the disease as early as 1000 to 1200 years ago (Galvani and Slatkin 2003). Significant mortality (sometimes as high as 90%) occurred, however, when smallpox was introduced to Native Americans by Europeans following the Columbus voyage in 1492 (Black 2004). While the latter case is a result of a syndemic where structural and physical violence led to malnutrition and susceptibility to pathogens (Cameron et al. 2015), the divergent experiences between *colonising* and *interacting* populations can produce distinctly different disease patterns, and needs to be considered as two separate entities influencing the prevalence and spread of pathogens in the past. Of course this distinction is not always clear within the narrative of human mobility. For example, it has been suggested that the Lapita people, Austronesian colonisers of Near and Remote Oceania through Island Southeast Asia (~3000 years ago) brought with them *Plasmodium falciparum* malaria, introducing the disease to local indigenous Australo-Papuan people who have inhabited Near Oceania for at least 50,000 years, before colonising uninhabited islands in Remote Oceania (Groube 1993; Kirch 1997).

Secondly, the term mobility in of itself has had different interpretations within bioarchaeology. For example, Killgrove (2010) combined strontium isotope and palaeopathological research to study the differences of health in migrants and locals in Imperial Rome. Killgrove (2010) used the term mobility synonymously with migration into urban cities. The author's research aligns with similar aims in this thesis. However, the term mobility has also been used to describe biomechanical adaptions in association with activity. For example, Huffer and Oxenham (2015) assessed mobility patterns through changes in rugosity in muscle and tendon insertions between Pre-Neolithic and Neolithic Northern Vietnam. The latter definition is derived from the model by Binford (1980) that describes dynamics of residential or logistic mobility for resource procurement.

Lastly, the term mobility outside of the bioarchaeological sphere, has a considerably different meaning in archaeology. Archaeologists who study mobility, attempt to understand the experience of movement across the landscape of past human groups. Such approaches

include rhythm analysis of landscapes travelled, and the incorporation of GIS to map visibility and topography between sites in the discussion of experience and embodiment of human mobility (Aldred 2014; Seitsonen et al. 2014). These researchers distinctly argue that an archaeological site cannot capture a decision to migrate or the mobile process of migration, rather a completed event of human movement (Aldred 2014). Therefore, what bioarchaeologists may capture within their skeletal data are not only of the actual process of human movement, but also the experiences succeeding the process, whether this results in interaction with new populations, and/or results in adaptive experiences of colonisers in new environments. For this reason, this thesis does not investigate the health effects of mobility, rather the consequences of interaction between populations following mobility. Therefore in this thesis, the terms *human population interaction* or *population interaction* are used to describe the process that may enable the transmission of infectious diseases from one group to another.

Human population interaction is introduced in this thesis as new terminology to describe the process of contact and 'interaction' between two or more populations or human groups following human mobility which can result from conflict, trade, migration or any combination therein. This definition is significant in the study of the spread of infectious diseases as it describes the means where infectious diseases have the potential to spread from one population to another.

There are two major forms of population interaction which have different outcomes on disease dynamics; intrapopulation and interpopulation interaction. *Interpopulation interaction* is defined here as the contact between two demonstrable culturally and/or biologically distinct populations. That is, the potential for introduction of new diseases can be a consequence of this interaction, as different biocultural histories can be observed for the interacting populations. The populations are at least partially exogenous to each other and carry the potential for differential ancestral exposure to infectious diseases. An example of interpopulation interaction includes the long distance trade along the Silk Roads that connected civilisations of Europe and Asia for centuries, and functioned as a route of cultural and genetic exchange alongside the transmission of infectious diseases as early as 2000 years ago (Yeh et al. 2016).

In contrast, *intrapopulation interaction* occurs within one culturally or biologically distinct population, and results from community level population movements where drivers of migration, trade or other mobility processes established regions of interaction within this cultural or biological group. Intrapopulation interaction can include regional trade networks and intermarriage between groups initiating the movement of people. Movement due to intermarriage occurs in many societies. For example, inter-island female migration for marriage was common prior to European colonisation of Tonga and Samoa (Gunson 1997). Further discussion on the association between human population interaction, infectious diseases and nutritional diseases is found in Chapter 2.

1.4 Theoretical Framework: Palaeoepidemiology and the Biocultural Approach

The theoretical frameworks within which this thesis has been conducted are presented here. This thesis functions within the subfield of palaeoepidemiology, as population level disease dynamics of the past are statistically modelled. Investigation of disease dynamics include the assessment of morbidity and mortality of diseases. Challenges surrounding describing disease dynamics include the reconstruction of the archaeological and biological context of disease within the *biocultural approach* and the issues related to estimating health from populations that are already deceased, termed the *osteological paradox*. Both of these concepts are essential to interpretation of disease dynamics and are described below.

Viral, fungal and bacterial pathogens have co-adapted with human populations since before the emergence of anatomically modern humans (Aufderheide et al. 1998). The evolution of pathogens that infect humans influence and in turn are influenced by the social decisions of human populations (Roberts and Manchester 2012). The impacts of pathogens on human populations over time is not static, and therefore it must be recognised that both pathogens and humans adapt over time when comparing disease presence in the archaeological record. This evolutionary process has been described as an ‘arms race’ between host and pathogen as the opposing organisms in this dynamic are in constant adaptive response to the malicious mechanisms of the other (Ewald 2000; Gagneux 2012; Woolhouse et al. 2002). Pathogens and human hosts then constantly evolve alongside each other in a process known as *co-evolution* (Gagneux 2012; Woolhouse et al. 2002).

Zuckerman et al. (2012) argue that the field of palaeopathology should aim to reconstruct this evolutionary dynamic between pathogen and human hosts in order to inform on the ability of pathogens to adapt to biological and social changes in human populations over time. *Palaeoepidemiology*, the study of past population level disease dynamics, is a subfield of palaeopathology and provides temporal depth to the study of co-evolution between humans and the pathogens in ways that modern epidemiological studies cannot (DeWitte 2016; DeWitte and Stojanowski 2015: 398; Roberts 2012). This subfield applies population level statistical models to assess changes in disease dynamics over time. *Disease dynamics* include changes in morbidity (the state of being diseased) and mortality (the state of dying from disease). It is important when considering disease impact in the archaeological record that the biological, social and environmental contexts of the assemblage are considered. Pathogens that have the ability to exploit human cells in their own reproductive cycles have had, and do have a considerable impact on the demographics, evolutionary pathways, social decisions, and overall wellbeing of humans (Buckley and Oxenham 2016; DeWitte 2014a; DeWitte 2014b; Fincher et al. 2008). The multitude of factors involved in the relationship between pathogens and their human hosts requires multidisciplinary understanding at both biological and social levels. Termed the *biocultural approach*, this framework assesses biology and culture as influential on the other, and consequently driving mechanisms for evolutionary change (Goodman and Leatherman 2010; Zuckerman et al. 2012).

The approach taken within this thesis continues this movement in palaeopathological research, striving for a framework of thinking that acknowledges social, cultural, environmental and biological processes as dynamic and driving adaptive change in human groups. The palaeoepidemiological approach applied in this thesis enables quantitative assessment of this adaptation, particularly in relation to the co-evolutionary change of human groups alongside pathogens.

1.4.1 The Osteological Paradox

In 1992, Wood et al. published a seminal paper summarising concerns bioarchaeologists had in regards to the impact of mortality on the presence of disease in archaeological skeletal populations. In general, the paper determined that it was unknown whether the presence of skeletal markers for stress or disease in an archaeological

assemblage indicated survivorship or susceptibility. That is, morbidity did not directly equate to evidence of "poor health" in comparison to others individuals in the assemblage. Termed the *osteological paradox*, Wood et al. (1992) outlined three major problems: selective mortality, demographic non-stationarity and hidden heterogeneity in risks.

Selective mortality refers to the bias within palaeopathological assessment, where all skeletal material assessed is at the worst state of health, death. Therefore, assumption of poor or good health is skewed and does not reflect a representative sample of the living population (Wood et al. 1992). *Demographic non-stationarity* tests the assumption that a population does not undergo flux in regards to demographics. Factors which change over time include migration, fertility and mortality rates. Archaeological populations are likely to have undergone flux, but are statistically considered as a single population wherein the demographic state is treated as having remained the same (Boldsen and Milner 2012; Wood et al. 1992). The consequence of this is that changes in fertility have more influence on the age distribution of skeletal assemblages than mortality. Therefore, changes in population level life expectancy predominantly reflects changes in fertility and should not be discussed in regards to reflection of health and susceptibility to death. Finally, the problem of *hidden heterogeneity in risks* highlights that each individual within a population has a different level of *frailty,* which is defined as 'susceptibility to death and disease' (Wood et al. 1992: 345). This variation includes endogenous factors such as genetics and biology, and exogenous factors such as socioeconomic and environmental conditions that vary within the population (DeWitte and Stojanowski 2015; Wood et al. 1992). Therefore, a population based approach masks the variability within the population and assessing factors such as age, sex, ancestry and status do not sufficiently control for the variables highlighted by the osteological paradox (Reitsema and McIlvaine 2014).

Frailty influences whether skeletal markers of disease are present in the individual. For example, a very frail individual can succumb to the disease prior to progression of the disease to a stage of bone response, yet in an archaeological population, this individual is inseparable from the state of an individual who did not have disease. Those with skeletal markers of disease survived long enough for abnormal bone change to occur and therefore inherently demonstrate some form of survivorship to the disease (Wood et al. 1992). For this reason, reliance on morbidity to assess good or poor health is erroneous, and the

presence or absence of skeletal markers of stress or disease therefore does not directly reflect the state of health of an individual.

As there have been over two decades, since Wood et al.'s (1992) paper, the field has advanced in terms of addressing these three issues. However, as DeWitte and Stojanowski (2015) note, the osteological paradox is often mentioned but overall still very poorly directly addressed in research design. DeWitte and Stojanowski (2015) identified few papers that aligned with Wood et al's (1992) recommendation to counter the problems of demographic non-stationarity. These papers assessed simple egalitarian societies or cemeteries with a short time frame (see Assis et al. 2011; Capasso 2007; Crist and Sorg 2014; Geber and Murphy 2012; Mitchell 2006; Palubeckaitė et al. 2006). DeWitte and Hughes-Morey (2012) for example, studied the impacts of stature on susceptibility to the Black Death in a cemetery which was used over the course of two years during the pandemic as a mass grave. While the argument of demographic non-stationarity as an osteological problem is legitimate, restricting palaeopathological research to only certain skeletal assemblages will result in significant reduction of assessment of regions where these cemeteries do not exist. In general, this would include any palaeoepidemiological research associated with the agricultural transition, one of the major focuses of the field, where increase in fertility is a large factor of this transition (Bocquet-Appel et al. 2012). Secondly entire continents (including Asia and Africa) where historical information for cemeteries of short duration do not exist except in recent history, are therefore not acceptable regions of study according to this recommendation.

There are methods that researchers have begun to employ to address the osteological paradox in regards to heterogeneity in risk. For example, Ward (2019) incorporated intrasite spatial statistics to assess the relationship between stress and socioeconomic status within a Thai Iron Age assemblage. In regards to selective mortality, DeWitte (2014a; 2014b) and Redfern and DeWitte (2011) have intensively researched the impact of risk of death through the application of hazard models, which enable assessment of factors such as sex, childhood stress, or pathology on susceptibility to mortality. DeWitte applied these models to demonstrate that there was an increased survivorship (reduced frailty) following the end of the Black Plague epidemic in England, therefore likely the plague had selective mortality on more frail individuals. This thesis includes direct engagement with the issue of selective mortality by applying mortality statistics to the assessment of disease impact.

While the osteological paradox does consider the impact of mortality in population statistics, investigation of the impact of morbidity is still valuable. As Goodman (1993) notes, there remains a physiological cost of living with morbidity which cannot be ignored in the literature, and mortality alone does not describe the impact of disease on past human populations. For this reason, morbidity and mortality are both assessed in this research.

1.5 Research Aims, Questions and Objectives

This thesis aims to assess the relationship between human population interaction and prevalence and diversity of infectious and nutritional diseases by assessing skeletal markers for disease from three different regions of Asia (Mongolia, Vietnam and Japan; see Table 1.1 and Figure 1.1). Integral to this aim, this thesis also explores how nutritional disease levels could be associated with interactions between populations as well.

The research aims can be focused into two questions:

1. Did increasing levels of population interaction over time significantly affect the health of populations in prehistoric Asia?

2. How did population interaction interplay with a range of other sociocultural, biological and ecological factors to influence the health of populations in prehistoric Asia?

Table 1.1: *Regions and interaction events addressed in this thesis.*

REGION	SITES	TIMES PERIOD	DATE	CLIMATE	POPULATION INTERACTION EVENT	N=
Japan	*Ota* *Tsukumo*	Middle to Late/ Final Jomon	5000-4000BP[1] 4000-2300BP[1]	Temperate[1] (slightly warmer than today- following Holocene Thermal Maximum (HTM))	Migration to refuge zones following climate cooling after HTM (no external interaction outside of Japan)[1]	34 30
Vietnam	*Con Co Ngua* *Man Bac*	Pre-Neolithic (Da But) to Neolithic (Phung Nguyen)	6900-6200BP[2] 4000-3500BP[3]	Subtropical (slightly warmer than today- following Holocene Thermal Maximum[2,3] (HTM))	Large migration event[3,4]	155 70
Mongolia	*Numerous sites*	Bronze Age to Xiongnu Period (Late Iron Age)	4500-2300BP[5] 2300-1800BP[6]	Subarctic/ Arid[7]	Increasing migration and trade alongside centralised state formation[8]	92 69
Total						450

[1](Temple 2007); [2](Oxenham et al. 2018); [3](Oxenham et al. 2011); [4](Matsumura and Oxenham 2014); [5](Lee 2013); [6] (Keyser-Tracqui et al. 2006); [7] (Frachetti et al. 2012); [8](Makarewicz 2011); [9](Ventresca Miller and Makarewicz 2019)

To address the research question, the objectives of this thesis are:

1. To assess the demographic profile of each of the skeletal samples and their appropriateness to study of disease within this thesis.

2. Record all evidence of non-articular macroscopic pathological changes (lesions) in the cranium and postcranium.

3. Perform differential diagnoses to identify specific diseases related to infectious and nutritional aetiologies. Create standards for identification of these diseases where they do not yet exist in the literature, whereby clinical and palaeopathological literature are employed to assess the likely aetiology of the pathological change (Table 1.2).

4. Conduct a three stage approach to the statistical analysis, assessing epidemiological trends at a site, a regional, and a continent level. For the first stage, assess the trends of morbidity and mortality of infectious and nutritional diseases within each site, including across age and sex.

5. For the second stage, assess the trends of morbidity and mortality of the diseases across time within each of the three cases (Vietnam, Mongolia, and Japan), and investigate whether the prevalence or diversity of nutritional and infectious diseases increased over time with increasing human interaction, and how other contextual factors including culture, environment and biology concomitantly influenced the pattern observed in the skeletal record.

6. For the final stage, develop a model using statistical techniques to assess whether human interpopulation interaction as a factor is impacting the prevalence of nutritional and infectious diseases in all of the skeletal samples employed in this thesis.

It is hypothesised that increased human population interaction played a key role in increasing the diversity (number of diseases) and the prevalence of both infectious and nutritional diseases in Asia. However, it also hypothesised that the degree of impact of human interaction on disease prevalence and diversity is dependent on other sociocultural, biological and environmental factors.

Three case studies were selected to encompass variations in interaction levels, climate, and social structure. The selection of these case studies enables statistical analyses of co-variates to meet objectives 5 and 6. The three case studies assessed in this thesis are as follows:

Case Study 1: Japan

The Middle Period Jomon (5000-4000BP) site of Ota is compared to the Late/Final Jomon (4000-23000BP) site of Tsukumo to investigate the impact on health of increased intrapopulation interaction following climate cooling and population displacement in Japan.

Case Study 2: Vietnam

The Pre-Neolithic site of Con Co Ngua (6900-6200BP) is compared to the Neolithic site of Man Bac (4000-3500BP) to assess the health impact of increased interpopulation interaction, in the form of a large migration which introduced agriculture to the region.

Case Study 3: Mongolia

Sites from the Early to Late Bronze Age Period (4500-2300BP) are compared to sites from the Xiongnu Period (2300-1800BP) in Mongolia to assess whether increasing migration, trade and conflict alongside centralisation and expansion of political power was associated with disease increase.

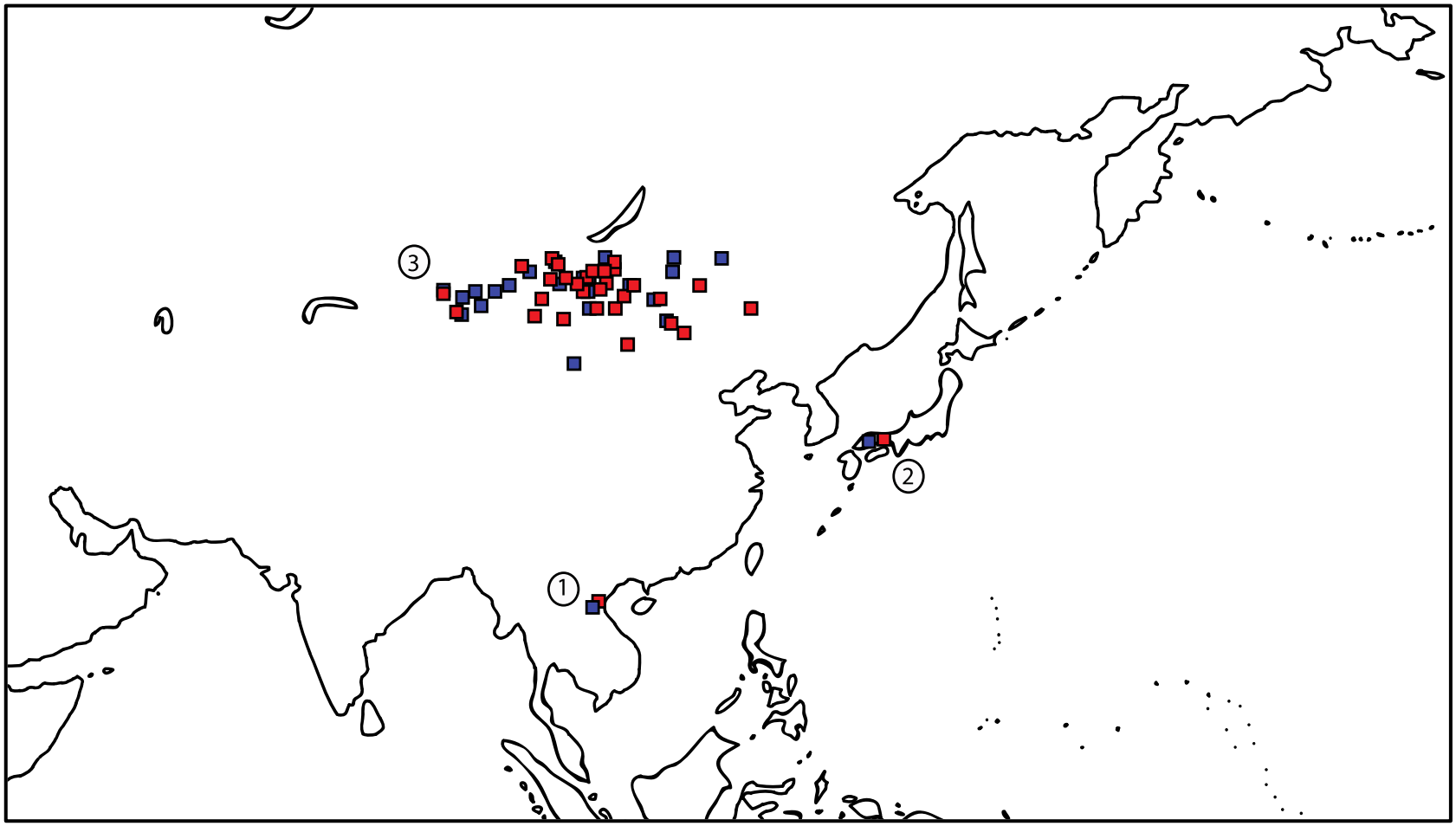

Figure 1.1: *Map of the sites of study in this thesis. Three regions of Asia were selected for investigation. 1) Pre-Neolithic to Neolithic Vietnam, 2) Pre-Neolithic Middle Jomon to Pre-Neolithic Late/Final Jomon Japan, and 3) Bronze Age to Xiongnu Period (Late Iron Age) Mongolia. Sites in blue are representative of the time period prior to the interaction event, whereas the sites in red are representative of the time period after the interaction event. Modern political divisions of countries have been purposely removed from this map (Image: author's own)*

Table 1.2: *Infectious and nutritional diseases assessed in this thesis*

DISEASE	INFECTIOUS OR NUTRITIONAL DISEASE	STANDARDS CREATED IN THIS THESIS?
Tuberculosis	Infectious	Yes
Leprosy	Infectious	Yes
Treponematosis	Infectious	Yes
Brucellosis	Infectious	Yes
Hydatic Echinococcosis	Infectious	Yes
Mycosis	Infectious	Yes
Rickets/ Osteomalacia	Nutritional	No (Brickley and Ives, 2010)
Scurvy	Nutritional	No (Snoddy et al. 2018)
Iron Deficiency Anaemia	Non-specific	Yes
Thalassaemia	Genetic (may be associated with infectious disease [malaria])	Yes
Osteomyelitis	Infectious (non-specific)	Yes
Mastoiditis/ Otitis Media	Infectious (non-specific)	Yes

1.6 Limitations of this Thesis

This thesis combines investigation of morbidity and mortality to describe the disease patterns in each assemblage assessed. Assessment of mortality through survivorship analysis techniques directly addresses the osteological paradox in relation to selective mortality by assessing the differences in frailty between individuals with and without skeletal evidence for disease. However, it is acknowledged that the samples within this thesis are likely represented by non-stationary demographics. Intrasite analysis of differences across age and sex are employed to assess heterogeneity in risk. However, the statistics employed likely do not directly address all aspects of heterogeneity in risk which require further investigation in the future.

Wood et al. (1992) argue that selective mortality reflects an over-representation of the disease in skeletal populations. However, this is not straight forward as not all cases of chronic diseases with the potential to affect the skeleton directly cause death, and the mortality rate of the disease influences the overall prevalence rate. Furthermore, skeletal involvement of specific disease is generally between 10-20% of cases, so this is a poor representation of the true prevalence of disease (Ortner 2009). Either way a deeply complex interaction of mortality, which is defined by both an individual's own susceptibility to disease and also the mortality rate of the disease itself occurs. This complexity cannot be properly described in its entirety with the analytical tools currently available to palaeoepidemiologists.

In regards to the differential diagnosis of specific disease, not all diseases can be diagnosed from dry bone, and multiple disease possibilities are often the outcome due to the physiological restriction of bone response (Zuckerman et al. 2012). While parameters for including non-specific subperiosteal new bone patterns within infectious disease frameworks are presented in this thesis, it is acknowledged that these do not provide the same level of context as a diagnosis of specific disease does in terms of impact on morbidity, mortality and the mechanism of infection.

Finally, in regards to the continent level statistical models that employ all sites analysed in this thesis, these do not encompass variation in mortality rates of the different disease prevalences across the sites employed in the analysis. They assess variations in morbidity only. For this reason, this analysis is accompanied by a contextualised assessment of disease morbidity and mortality at a site and regional level.

1.7 Publications

This thesis follows a hybrid thesis structure wherein parts of two publications have been integrated into the text of this thesis. Each chapter explicitly states where information from these publications has been included. These papers are included in the appendices according to University of Otago guidelines. The contributions to these papers are included in Table 1.3.

The two papers are:

1. Vlok M, Oxenham M, Domett K, Tran MT, Mai Huong NT, Matsumura H, Trinh HH, Higham T, Higham CF, Huu NT et al. . 2020. Two Probable Cases of Infection with *Treponema pallidum* during the Neolithic Period in Northern Vietnam (ca. 2000-1500B.C.). *Bioarchaeology International* 4(1):15-39. (see Appendix 4)

2. Vlok M, Oxenham MF, Domett K, Hiep TH, Minh TT, Mai Huong NT, Matsumura H, McFadden C, Huu NT, and Buckley H. in review. Subadult Nutritional Stress during the Agricultural Transition in Southeast Asia: Perspectives from a Neolithic site in Northern Vietnam. *International Journal of Paleopathology*. (see Appendix 5).

Table 1.3: *Relative contributions to papers published during this thesis.*

DISEASE	BI (2020)	IJPP (IN REVIEW)
Data Collection and Analysis	Melandri Vlok (primary data collection and analysis of pathology), Hallie Buckley (data analysis), Tran Thi Minh (laboratory assistant), Kate Domett (pilot data), Tom Higham (radiocarbon data collection and analysis). Marc Oxenham (human skeletal data collection	Melandri Vlok (primary data collection), Tran Thi Minh (laboratory assistant), Kate Domett (pilot data), Marc Oxenham (human skeletal data collection)
Editor Support	Melandri Vlok, Marc Oxenham, Kate Domett, Hirofumi Matsumura. Hiep Hoang Trinh, Ngyuen Thi Mai Huong, Nghia Truong Huu, Hallie Buckley, Charles Higham, Tom Higham	Melandri Vlok, Marc Oxenham, Kate Domett, Hirofumi Matsumura. Hiep Hoang Trinh, Ngyuen Thi Mai Huong, Nghia Truong Huu, Hallie Buckley, Clare McFadden
Major contributions to the text	Melandri Vlok	Melandri Vlok
Minor contributions to the text	Hallie Buckley, Marc Oxenham	Hallie Buckley, Marc Oxenham, Clare McFadden
Study Design	Melandri Vlok, Hallie Buckley	Melandri Vlok

1.8 Thesis Summary

Chapter two provides a literature review of the mechanisms that spread infectious diseases between human populations in both the present and the past. Epidemiological literature on human population interaction and the spread of pathogens is explored to address the significant gap in palaeoepidemiological literature and to provide a foundation for a new area of research in palaeoepidemiology, the investigation of the impact of human population interaction on disease.

Chapter three provides an overview of the pathogenesis, pathophysiology and epidemiology of major infectious diseases, nutritional diseases and anaemias that affect bone and are assessed within this thesis. This chapter draws from predominantly clinical and epidemiological literature to outline the progression of disease in the body beyond what is observed in dry bone.

Chapter four presents methodology for human skeletal analysis and census data for the samples assessed for pathology in this thesis. The methods employed for age and sex estimation, and recording of completeness and preservation are first presented. Following on, the age and sex distribution, skeletal completeness and preservation of each assemblage is assessed, and evaluations are made as to their appropriateness for investigation in this study.

Chapter five presents the methodology for lesion recording and differential diagnosis of diseases explored in this thesis. This chapter continues from chapter 3 and explores the pathologies observed macroscopically and radiographically in dry bone. Threshold criteria for diagnosis of disease are presented. New standards for differential diagnosis are presented in this chapter wherever standardised criteria for diagnosis do not yet exist in literature for a disease.

Chapters six, seven and eight present the case studies which explore disease patterns at site and regional levels. These include the outcomes of differential diagnosis and also assessment of the morbidity and mortality of the diseases. *Chapter six* presents the outcome of analysis for the Middle to Late/Final Periods of the Jomon of Japan, *chapter seven* presents the outcomes for the Pre-Neolithic to Neolithic Periods of Northern Vietnam, and *chapter eight* presents the analysis of Bronze Age to Xiongnu Periods of Mongolia.

The overall statistical analysis incorporating all of the data collected for this thesis, to assess continent level trends of disease related to population interaction levels, is presented in *chapter nine*. Finally, *chapter ten* summarises and discusses the findings of this thesis. Major conclusions, and future directions are presented.

CHAPTER 2:
HUMAN MOBILITY, POPULATION INTERACTION AND CONSEQUENCES TO HEALTH

2.1 Introduction

This chapter provides an overview of the literature pertaining to human mobility and population interaction. The background presented here is essential to establishing the epidemiological parameters for human population interaction and addressing the research questions of this thesis. Modern epidemiological studies on infectious disease spread are relevant to prehistoric contexts, and the theoretical basis for pathogen spread in epidemiological literature is instrumental to understanding how diseases spread in the past. As such, it is necessary to draw from modern epidemiological studies to define a model for disease spread in prehistoric populations, the final objective of this thesis (see Chapter 10). Firstly, the definitions of infectious disease dynamics, human mobility and interaction, as applied in modern epidemiological studies of human populations are discussed. The various factors which influence infectious disease dynamics and the relationship to human mobility and population interaction are explored. Subsequently, aspects of migrant health beyond disease transmission are examined. The final section of this chapter pertains to applications of the epidemiological theories addressed here within prehistoric contexts.

2.2 Epidemiological Definitions

It is important to correctly define disease processes in order to best describe how infectious diseases impacted populations in the past. The following terms are frequently used in epidemiological and palaeoepidemiological literature to define infectious disease dynamics in the present and the past. The terms introduced here are employed in this thesis.

An *epidemic* of infectious disease occurs when the prevalence of the disease exceeds what would normally be expected in that region (Kalra et al. 2015). The term is often used to describe significant outbreaks of infectious diseases. In contrast, a disease is considered *endemic* when it spreads at a constant rate throughout the population, and is considered stable but persistent in a region (Codeço 2001). Epidemics and endemics then are expected to have considerably different patterns in disease transmission and proliferation.

Epidemics and endemics are measured through their *incidence* and *prevalence* rates. The incidence rate measures the number of new cases observed in a given time period, whereas the prevalence rate measures the total number of cases (Lombardi and García Cáceres 2000; Waldron 1991). While both measures are valuable in epidemiology, only the prevalence is observed in palaeoepidemiology as new cases cannot be observed in the archaeological record (Waldron 1991). Therefore, from here on, only the prevalences of diseases are discussed.

Pathogens and parasites have variable modes of transmission. A pathogen can spread directly from host to host, or through a vector, another organism that is responsible for disease transmission (Ewald 1994). Vector borne diseases include for example malaria, a parasite (*Falciparum* sp.) that is reliant on the *Anopheles* mosquito feeding on humans to spread (Miller et al. 1994). Vectorborne diseases have greater potential to be lethal, as they do not require the host to be ambulatory and directly interacting with other hosts in order to spread (Ewald 1994). In contrast non-vector transmission involves direct transmission from host to host. Some parasitic diseases (such as echinococcosis), have multiple hosts during their lifecycle. A host infected during the larval stage is termed an *intermediate host*, whereas a host infected by sexually mature adults is termed a *definitive* host (Poulin and Randhawa 2015; Webster and McConkey 2010). Non-vector transmissions include:

1. waterborne diseases spread through drinking (such as cholera),
2. airborne or respiratory diseases spread through air droplets (such as tuberculosis),
3. non-sexual skin transmission (such as endemic syphilis),
4. sexual transmission (such as HIV),
5. vertical transmission from mother to foetus (such as venereal syphilis), and;
6. foodborne diseases spread through eating (such as helminthiasis).

2.3 The Impact of Human Mobility on Health Today

Recent epidemics of SARS (2002), H1N1 (2009), and COVID-19 (2019) viruses have demonstrated the significant health issue that international travel poses to the risks of global transmission, particularly of highly virile pathogens (MacPherson et al. 2009; Wells et al. 2020; Zhou et al. 2004). The volume, rapidity and complexity of overseas travel when faced with pathogens such as these overwhelm the capacity of quarantine and border control

measures (MacPherson et al. 2009). However, local and regional networks of mobility are of considerable epidemiological importance, as they both fuel epidemics and sustain endemic disease. Today regional human mobility factors provide the single largest challenge to eradication programs. Certainly in cases such as malaria, reintroduction of the disease due to human population movement into areas where eradication program efforts have been focused, has prevented eradication of the disease (Prothero 1977). The emergence of the AIDS epidemic and eventual pandemic has been retrospectively linked to major roadways serving as corridors of disease transmission in Africa. Additionally, the spread of HIV from urban to rural areas was likely driven by the return of migrant workers to their home communities (Quinn 1994).

Human mobility has both short range and long range influences on the spread of cholera, a diarrheal disease caused by the bacterium *Vibrio cholerae*. Human mobility was particularly impactful in regards to people visiting infected areas and returning to unaffected regions and introducing the disease to waterways (Mari et al. 2012). This problem is exacerbated by the predominance of mild symptoms in many individuals who then unknowingly introduce the disease to an unaffected region (Mari et al. 2012). Indeed, epidemiological models produced by Mari et al. (2012) for the 2000-2002 cholera outbreak in Kwazulu-Natal, South Africa demonstrated that human mobility was paramount in the epidemic of cholera spreading outside of hydrological catchments. Human mobility is then crucial in crossing natural geographic barriers to the spread of pathogens, even in the context of high population densities of the modern day.

Human mobility not only influences infectious disease transmission but can contribute to malnutrition of interacting populations. The process of migration can induce nutritional stress as migrant groups acclimatise to new environments and are required to adapt their resource acquirement practices (Zezza et al. 2011). This impact on health has consequences for all migrants whether colonising new lands or interacting with other populations. However beyond the health effects of migration, population interaction also specifically influences nutritional stress. Conflict and warfare directly influence the nutritional profiles of engaging groups and of populations caught within regions of conflict. In conflict, economic instability drives starvation amongst civilians, and coupled with chronic stress also increases susceptibility to infectious diseases (Gayer et al. 2007). Moreover, interaction with new populations is often associated with a dietary shift as

migrants frequently adopt the diet of their place of destination out of necessity, which can have both a negative or a positive influence on their overall health (Zezza et al. 2011). Considerable health disparities due to shifts in socio-economic conditions can also contribute to increased nutritional stress in migrant populations. These conditions are particularly detrimental when they extend from lack of skilled labour practice or education in their place of origin, such as in urban migration to escape rural poverty. Núñez-Rocha et al. (1998) observed that almost 52% of migrant pre-schoolers surveyed in Mexico suffered chronic malnutrition in comparison to non-migrant children where malnutrition was only prevalent in 29%. Indeed, where socio-economic disparities are not a key factor, there may not necessarily be a variable influence on nutritional stress (Karamba et al. 2011; Sharghi et al. 2011). The relationship between migration and nutritional stress is then highly context specific.

2.4 Human Mobility and Interaction as Factors in Infectious Disease Dynamics

In epidemiology, *interaction* is defined as the connection between two nodes, where a *node* represents a single host, which may allow disease transmission (Bansal et al. 2010). Approximately 2-3% of the world's population today live in a nation other than one's place of birth, and approximately 2 billion people move across large geographic spaces around the world (Gushulak and MacPherson 2004; MacPherson et al. 2009). For these reasons, the term human mobility is often used in epidemiological literature to describe the process of interaction, as these two factors inevitably end in the same result. Human mobility is described as "a network of interacting communities where the connections and the corresponding intensity represent the flow of people among them" (Balcan et al. 2009: 21484). Prehistoric populations are marked by slower population mobility, lower global population size, and the rate of population mobility was restricted by technology (Tatem et al. 2006; Wilson 1995). Global population mobility can now be achieved in a matter of hours, which, put simply, was not a factor of consideration in the past (Prothero 1977). However, epidemiological considerations of human mobility, interaction and infectious disease transmission are useful for reconstructing the emergence of infectious diseases in the prehistoric past.

The impacts of interaction are multi-scale and epidemics spread both within local interaction networks *and* regionally via long distance movement (Belik et al. 2011; Dalziel

et al. 2013). Interaction and mobility of human populations across the landscape is dynamic, transient and episodic, as social relationships between individuals change over time (Bansal et al. 2010). Subsequently, epidemics occur in waves, and transmission is best described through diffusion, rather than through direct routes from place of origin to place of destination (Belik et al. 2011). Realistically, no human is isolated and at a local level, interactions amongst individuals occur on a daily basis (Belik et al. 2011).

Human mobility is therefore, difficult to model as it occurs as a repeated process rather than a single event, although it may be treated as such in epidemiology (Quinn 1994). However, the risk of disease transmission is recognised to be mediated by the dynamics of interaction and human mobility (Vazquez-Prokopec et al. 2013). Human groups with varying levels of human mobility may differ in their rate of transmission of infectious diseases (Dalziel et al. 2013). While population density is a factor of disease transmission, Dalziel et al. (2013) observed that the dynamics of epidemics did not necessarily have to rely on the number of potential hosts (population density) but in the amount of different types of human mobility within a population.

Additionally, human mobility and interaction patterns disrupt the spaciotemporal dynamics of an epidemic (Merler and Ajelli 2010). For example, the increase of symptomatic malaria in Colombia, where the disease is endemic, is strongly correlated with immigration of nonimmune individuals into endemic regions (Sevilla-Casas 1993). Long term endemicity of a disease will eventually lead to immunisation of affected populations, stabilising the transmission rate. Therefore, introduction of the pathogen to naïve populations who do not have prior exposure, will significantly alter the morbidity and mortality rate of the disease (Bansal et al. 2010). Introduction of infectious diseases into naïve populations through processes of human mobility and interaction, can initiate an epidemic of more severe proportions than in the original population (Bansal et al. 2010). As more individuals in the naïve population are susceptible to disease, these epidemics can drive demographic change which in turn can increase the mutation rate of the pathogen and alter the host-pathogen relationship and subsequent disease dynamics (Cui et al. 2013). The introduction of the pathogen into a new population can also significantly disrupt the evolutionary trajectories of human hosts and pathogens (Kodaman et al. 2014).

In summary, human mobility and interaction have significant consequences on the dynamics of infectious diseases. In modern day epidemiological studies, the terms are commonly used in tandem. However, it is clear that while these processes relate, they are both different but essential components to the spread of infectious diseases. Interaction enables the spread of infectious disease from one host to another. However, interaction cannot transpire without a process of human mobility occurring.

2.4.1 Population Level Interaction Disease Dynamics

In their most basal form, infectious pathogens spread within a close network of interactions between individuals (Bansal et al. 2010). Within a community, transmission of human to human infectious diseases tends to occur in predictive patterns. Individuals travel between home and work and a few limited locations (Belik et al. 2011; Vazquez-Prokopec et al. 2013). The chance of transmission is dependent on the *return rate*, the number of times an individual leaves home to another location, and the *dwelling time*, the amount of time spent at a particular location (Belik et al. 2011). These places of aggregation then may serve to enable the spread of infectious diseases between households, and the return of an infected individual to their home enables the spread within the household (Belik et al. 2011). Different patterns of mobility between individuals within a household are then modelled as a lattice of disease transmission across space (Figure 2.1).

On a larger scale, migrants can spread infectious diseases between communities. Interactions between communities are often essential for the procurement of critical resources through regional exchange networks (Wiessner 2002). The nature of these regional exchange networks are crucial in the development of outbreaks beyond their point of origin, and variation in inter-community mobility influences the potential for disease transmission (Tatem and Smith 2010). Even further, long-distance migration enables the spread of disease across significant geographical and political boundaries. Today, international travel is responsible for the spread of pathogens on a global scale, particularly from regions where infectious diseases are endemic (Ratnam et al. 2013; van der Bij and Pitout 2012). When diseases are introduced into a community they spread further through community interactions. Therefore, significant contact between migrants and locals is not necessary for the proliferation of newly introduced pathogens in a community. However,

increased contact of locals with long distance migrants does increase the rate of transmission of a disease. Indeed, historically, infectious disease outbreaks have focused around maritime trade ports, where interactions between locals, international traders and seamen were high (Gushulak and MacPherson 2004; MacPherson and Gushulak 2001; Prothero 1977). Overall, it is clear that interaction networks occur across various scales, within communities, between communities and across larger regional networks, all influencing the dynamics of infectious disease transmission.

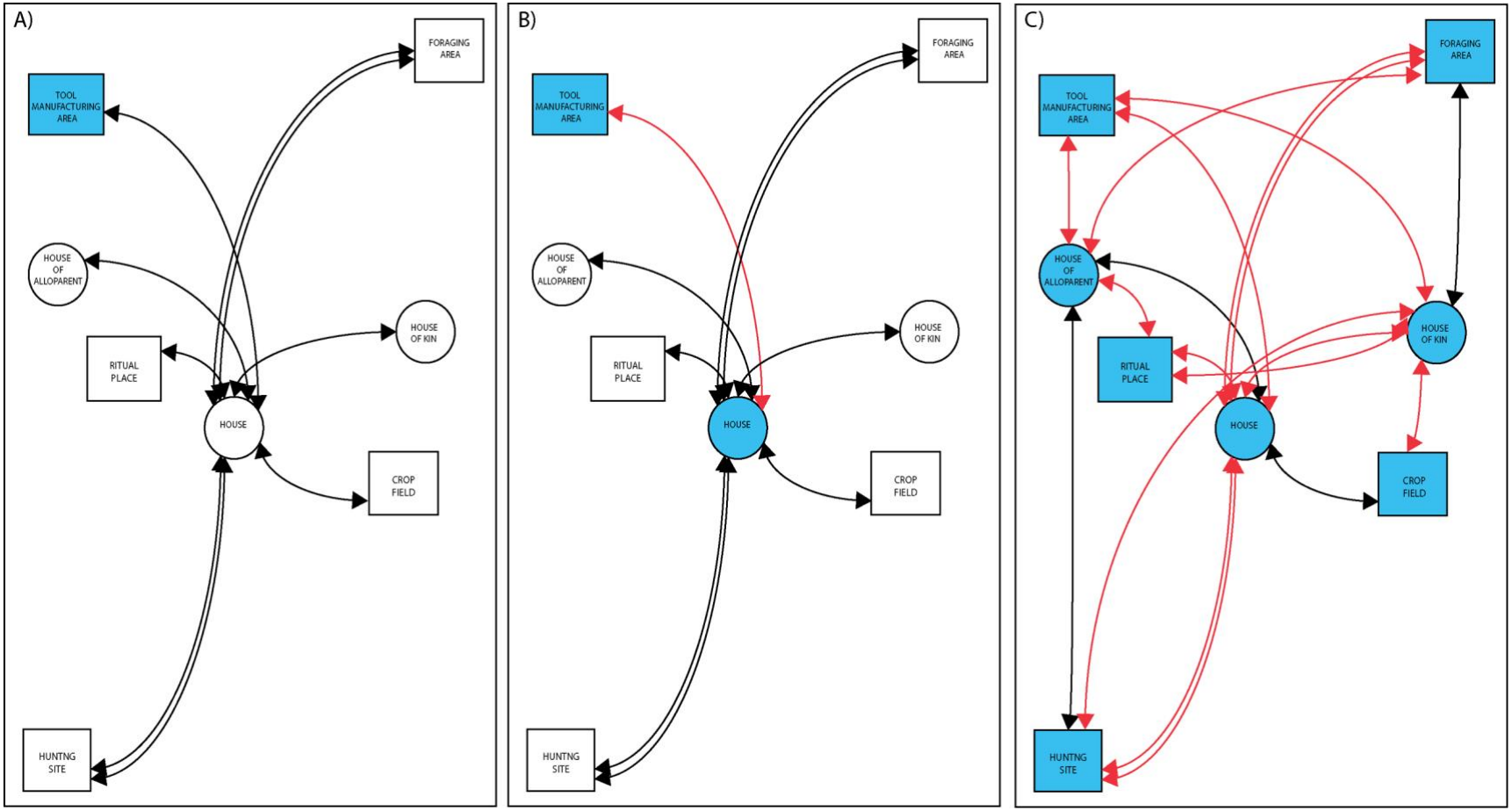

Figure 2.1: *Model of community spread of human to human infection (community interaction) (adapted from Belik et al. 2011). Circles indicate households, whereas squares indicate areas of aggregation. This model demonstrates how contact with an infected individual at site of aggregation (in blue) can spread the disease throughout a community via one household. A) An infected individual interacts with others at a place of aggregation, infecting others. B) A newly infected individual then returns home and introduces the disease to household members. C) Infected household members then travel to various places of aggregation and close contact households thereby continuing the spread of disease. Even if not all individuals of the household are infected (travel of non-infectious people: black arrows), the disease still spreads rapidly amongst the community as more households become infected. Image: author's own.*

2.4.2 Variations in the Impact of Human Mobility and Interaction on Infectious Disease Transmission

The impact of mobility on disease spread varies considerably and is also reliant on pathogen-mediated conditions (Tizzoni et al. 2014; Vazquez-Prokopec et al. 2013). For example, respiratory diseases that spread through air droplets do not require direct contact between individuals, and proximate distance within enclosed spaces is sufficient for transmission. Therefore, respiratory diseases can be spread effectively by a number of human mobility processes (Leder and Newman 2005). However, diseases of the skin require more close contact between individuals and are therefore reliant on the relationship of physically interacting individuals (Grin 1956). Transmission of these diseases through mobility then tends to occur along community or familial lines. This has been observed in yaws, a tropical disease spread through skin contact (Mitjà et al. 2013).

Additionally, the mode of transmission will also influence which demographic groups serve as reservoirs for the disease, and dissemination of the disease due to human mobility will depend on whether the reservoirs are mobile. For example, the spread of HIV in West Africa was associated with increased urban migration of sexually mature young males who were migrating for better job prospects (Quinn 1994). Where transmission is reliant on a vector, human mobility may be necessary for the transmission of the disease across large regions. Long distance spread of dengue fever and malaria, reliant on mosquito vectors for transmission, is facilitated by human mobility as mosquitos themselves tend to travel over very short distances (Wesolowski et al. 2015). Human transmission is then essential to the spread of malaria across different mosquito habitats.

The suitability of the pathogen to particular environmental conditions means mobile individuals may have a positive, neutral or negative impact on the epidemiology of the place of destination (MacPherson and Gushulak 2001). For example, an individual carrying a tropical disease to a temperate region is not likely to induce an epidemic (MacPherson and Gushulak 2001). Certainly this has been documented historically in the case of yaws epidemics in China. Epidemics of yaws were frequently observed in Southern China. However, cases of yaws in Northern China were sporadic, only documented in 1st degree migrants from Southern China, and never proliferated beyond the case identified (Hill 1953). Furthermore, the disease appeared to resolve itself in the migrant individuals, likely due to unviability of the pathogen

in the temperate climate (Hill 1953). In sum, the characteristics of both the pathogen and the host underlie disease dynamics (Merler and Ajelli 2010).

2.4.3 Epidemiological Considerations of Migrant Health and Susceptibility to Infectious Disease

Migrant health is defined by three points of migration: the health characteristics of place of origin (*pre-departure phase*), transition through new environments during the migration (*movement phase),* and the characteristics of the new destination (*arrival phase*) (Gushulak and MacPherson 2004; MacPherson and Gushulak 2001). For example, the disease profile or social and economic instability of the region of origin may be both a driver for migration and an impact on health. A desire to flee a region undergoing an epidemic may increase migration and contribute to the transmission of the disease (Prothero 1977). Moreover, increased physiological stress due to the migration may also increase the susceptibility of infection, affecting the health of a migrant before and during the migration (Prothero 1977). The migration can be particularly taxing on the health of displaced persons who travel through refugee camps, or are forced to move through environments that are not well known to them (Gushulak and MacPherson 2004). Lastly, the epidemiological implications of integrating with new populations, and experiencing new environmental conditions at place of destination can also be a contributor to poor health.

Where the disease characteristics differ from the place of origin and the point of destination, transmission of infectious diseases can occur (Gushulak and MacPherson 2004). This transmission is defined as *epidemiological bridging* between the two populations (Gushulak and MacPherson 2004). Two major factors influence the impact of this epidemiological bridging on the prevalence of infectious epidemics at the destination region: these are the size of the migrant population and the degree of health disparity between the region of origin and the region of destination (Gushulak and MacPherson 2004). That is, the larger the bridge, and the greater the cline of pathogen prevalence between region of origin and of destination the greater the overall epidemiological impact.

Secondary to these two major factors, other influences include individual health status, socio-economic factors, healthcare access, education, cultural health responses, genetics, dietary influences, psychosocial behaviour, and risk of co-morbid non-communicable diseases

(Gushulak and MacPherson 2004; MacPherson and Gushulak 2001). The conditions of these factors also differ between the pre-departure phase, the movement phase and the arrival phase. Therefore, the ultimate context of transmission at place of destination has been shaped and changed dynamically even prior to this point (MacPherson and Gushulak 2001).

Epidemiologists define a migrant who carries an infectious disease as an *active transmitter*, with the receiver of the infectious disease at the region of destination identified as a *passive acquirer*. However, it is recognised that an individual may be both an active transmitter and a passive acquirer of various infectious pathogens (Prothero 1977). Furthermore, it needs to also be considered that migrant populations may be vulnerable to disease at the region of destination and therefore migrants can also be *passive acquirers* of infectious disease and susceptible to the epidemiological conditions of the region of destination (MacPherson and Gushulak 2001).

Interestingly chronic diseases such as those identified in the skeletal record (e.g. tuberculosis) have considerable impact as the latency phase of certain infections mean the disease may only present clinically long after arrival at the region of destination (Gushulak and MacPherson 2004; MacPherson and Gushulak 2001). In modern contexts, these diseases are not identified through current quarantine protocols, and the epidemiological impact occurs at a later stage. Furthermore, these diseases increase susceptibility to non-communicable diseases such as cardiovascular disease and stroke, that are also of concern to population health (MacPherson and Gushulak 2001). Both chronic infection and non-communicable consequences are over-represented in migrant populations (MacPherson and Gushulak 2001).

2.5 Defining Human Interaction Processes in the Past

As previously mentioned, the concept of population mobility is complex, and therefore difficult to apply to the archaeological record when assessing the impact on health. Instead, human population interaction is proposed in this thesis as an alternative and applicable concept to questions surrounding disease transmission in the prehistoric past. Levels of human population interaction can be summarised as the potential increase in the epidemiological bridge between two interacting populations. An increase in the *frequency* (number of episodes of interaction) and *intensity* of interaction (size of the interaction in terms of number of individuals involved) may then increase the size of the epidemiological bridge and therefore

probability of the transmission of infectious diseases (Figure 2.2). This section introduces some of the classifications of human mobility and human population interaction in the past in order to demonstrate the viability of exploring the research question posed in this thesis from a palaeoepidemiological perspective. Classification of different levels of human interaction for statistical purposes is explored in Chapter 9.

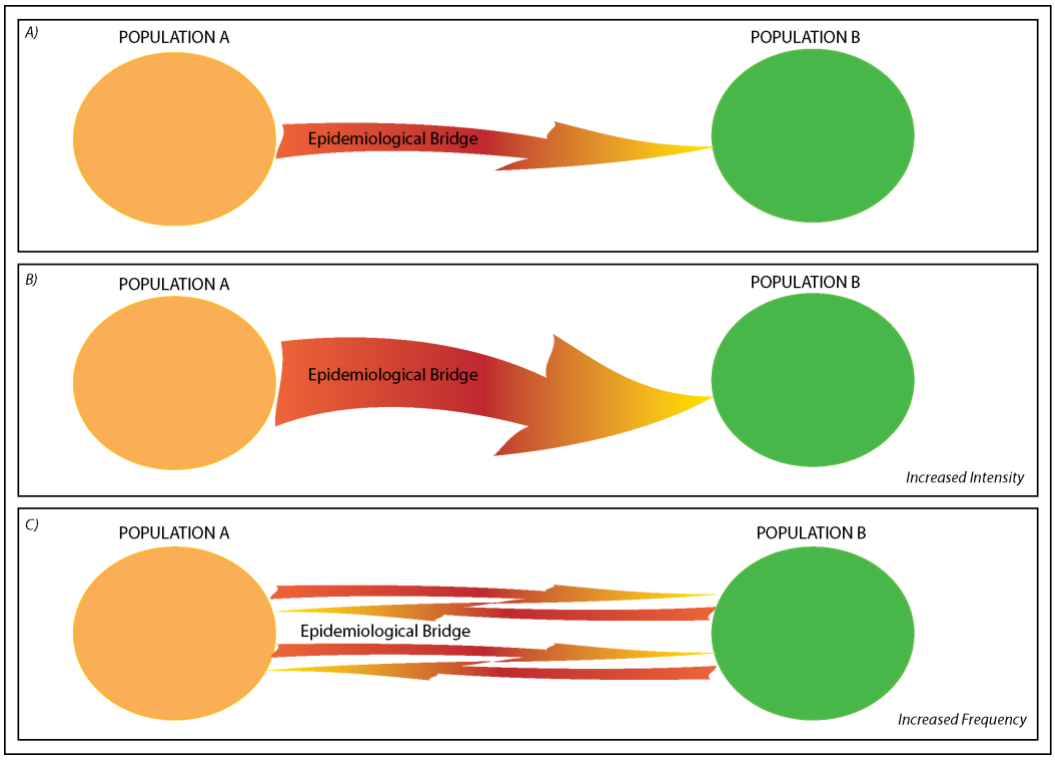

Figure 2.2: *Model of transmission of infectious diseases with varying levels of human population interaction. A) Human interaction enables an open system of pathogen transmission between populations. B) An increase in the number of individuals contributing to the interaction (increase in intensity) widens the epidemiological bridge and increases the potential for disease transmission. C) While the number of individuals contributing to interaction may be low, episodic interaction (increase in frequency) also increases the epidemiological bridge. Episodic interaction is more often due to cyclical forms of human mobility that enable multi-direction disease transmission effecting both interacting populations. Image: author's own.*

2.5.1 Identifying Types of Population Mobility and Geographic Spaces of Interaction in the Past

Human mobility processes can be separated into three broad categories: *permanent movement*, *temporary movement* and *secondary movement* (also known as *circulation*) (Gushulak and MacPherson 2004; Quinn 1994). Permanent movement involves a single interaction with permanently sustained habitation at the region of destination by the migrant group; temporary movement involves a return to region of origin, and secondary movement

involves two or more rotations between region of origin and region of destination, and therefore involves cyclical migration (Prothero 1977; Quinn 1994). Some forms of migration therefore have longer duration of interaction than others. Moreover, temporary and cyclical migrations enable epidemiological bridges that do not occur in a single direction but have implications for the health of both interacting populations (Prothero 1977). The range of human mobility processes that may lead to population interaction in the past are summarised in Table 2.1.

The purpose of migration is usually invisible in the archaeological record. Therefore, it is argued here that it is more suitable to archaeological research, especially palaeopathological research, to define archaeological sites, or clusters of sites as *interaction zones*. These interaction zones are geographic spaces where human population interaction occurs as a consequence of the human mobility processes described above. An archaeological site can be defined by more than one form of interaction zone, and therefore these classifications are not mutually exclusive. They are however, useful classifications to describe the human mobility processes that occur within these zones, as they enable consideration of multiple levels and different types of mobility processes which occur simultaneously. The classification of interaction zones applied within this thesis are summarised in Table 2.2. These processes define the types of population movements and the potential for permanent compared to episodic interactions that influence the epidemiological bridging described above.

***Table 2.1**: Types of Past Human Mobility Processes. These are the underlying reasons why humans choose to migrate.*

Human Mobility Process	Permanent, Temporary or Secondary Movement and Interaction	Description	References
Relocation	Permanent	Permanent movement- may be voluntary or forced	(Gushulak and MacPherson 2004)
Trade	Temporary or Secondary	Contact between groups to initiate commercial exchange	(Belyi et al. 2017)
Intermarriage	Permanent	Gender-mediated relocations resulting in migration of a particular gender away from their place of birth	(Fan and Huang 1998)
Warfare	Temporary or Secondary	Movement of a large group of individuals to engage in combat along political boundaries	(Apostolopoulos and Sönmez 2007)
Religious Pilgrimage or Diplomatic Mission	Permanent, Temporary or Secondary	Relocation in order to spread religious ideology to contact group, or to establish political relations.	(Apostolopoulos and Sönmez 2007)
Exploration	Permanent, Temporary or Secondary	Purposeful movement to explore new territories	(Apostolopoulos and Sönmez 2007)
Resource Procurement	Temporary or Secondary	Mobile movements in order to procure food or other resources, or movements to increase economic prosperity (migration of seasonal workers).	(Gushulak and MacPherson 2004)

***Table 2.2**: Geographic spaces of human interaction (interaction zones). Processes of human mobility that lead to interaction at these zones.*

Interaction Zone	Description	Possible Consequences for Health	References
Refuge Zones	Environmental or social factors such as climatic cooling or conflict which leave only particular geographic spaces habitable or provide sanctuary for human groups. (e.g. Last Glacial Maximum, and post-Holocene Thermal Maximum events)	Conflict or environmental disasters can be a driver for migration wherein *place of origin* is no longer suitable to reside. Refuge zones may be places where health outcomes improve as there is an increase of resource availability and lower pathogen load. However, as is the case in modern day refugee camps, the conditions of refuge zones where migrants of already poor health are surviving on minimal resources and interacting with individuals from high pathogen load areas, the health outcomes can be negative.	(Hughes et al. 2017; MacPherson and Gushulak 2001; Prothero 1977; Straus 1991)
Friction Zones	Frontier of forager and farmer interaction. Gradual expansion of farmers with increasing desire of agricultural land, resulting in interactions with foragers in new environments.	Possible adoption of subsistence practices between foragers and farmers influencing underlying nutrition levels. May increase or decrease health outcomes.	(Ammerman 1973; Bellwood 2001; Bellwood and Oxenham 2008; Bocquet-Appel et al. 2012; Higham et al. 2011)

Interaction Zone	Description	Possible Consequences for Health	References
Commerce Zones	Cities or regions where trade or commerce was particularly important, often as part of trade routes (e.g. oasis cities along the Silk Road)	Potential pathogen "high-ways" as traders passed through these points of population aggregation.	(Achtman 2016; Green 2017; Green and Jones 2020)
Exchange Zones	Zones of non-commercial exchange such as intermarriage or kinship relocations.	Transmission of infectious diseases including those transmitted through physical contact.	(Anglewicz 2012; Fan and Huang 1998; Gunson 1997; Saggurti et al. 2012)
Fission-Fusion Interaction Zones (Nodes of Interaction)	Spaces of interaction at shared pastoral or foraging land, can be seasonally restricted and therefore these spaces can move dynamically across the landscape with changing climatic conditions. Defined by the processes of intermittent population aggregation and dispersal.	Fission and fusion mobility dynamics are known to sustain infectious disease epidemics and transitions through different ecological environments and can increase susceptibility to ecologically based disease (through exposure to vectors) which are then transmitted to other groups at nodes of interaction. Malarial epidemics of Somali-speaking pastoralists in Africa are documented to be sustained by the fission-fusion dynamics.	(Frachetti 2009; Prothero 1977)
Conflict Zones	Geographic regions of warfare	Spread of pathogens between two warring populations. Conflict causing widespread malnutrition and increasing risk of infectious disease transmission. Breakdown of systems of healthcare also increases morbidity and mortality to diseases.	(Gayer et al. 2007; Green 2017)
Zones of Colonialism	Interactions between populations where one seeks to retain authority over the other	Most commonly an unequal influence on health, with significant deleterious health consequences of the colonised populations. Colonialism is well known to be the cause of significant epidemics and population decline of numerous indigenous populations.	(Campbell 1983; Lovell 1992; Tsuda et al. 2015)
Zones of Exploitation	Forced migration and contact due to empowerment of one group over the other (e.g. slavery)	Large global movements of malnourished slaves, placed in conditions of poor hygiene, and high population aggregation for considerable amounts of time. Slavery has been linked to the global spread of a number of tropical diseases including dengue and yellow fevers.	(Apostolopoulos and Sönmez 2007; Green 2017; Green and Jones 2020; Tatem et al. 2006)
Urban Zones	Urban centres which attract migration due to commerce and lifestyle, or escaping rural poverty.	In urban zones, rapid migration can result in increasing population sizes in urban zones incapable of accommodating such change and migrants may need to cope with inadequate housing, inadequate water and food resources, poor sanitation and waste disposal.	(Burkle 2007; Prothero 1977)

2.6 Identification of Human Interaction in the Archaeological Record

Tsuda et al. (2015) argues that short term or cyclical migrations cannot be captured in the archaeological record. However, in regards to understanding the impact on health, consideration of the micro-level effects of interaction is crucial. As will be evident in the following chapters of this thesis, there are multiple instances where seasonal or cyclical human movements have been documented by archaeological data such as through isotopic research. Moreover, the presence of trade items themselves indicate temporary population movements resulting in the interactions between people on a smaller scale. Clark (2001) is correct in stating that forms of human population movement are invisible to archaeologists and that understanding the social implications of migration requires large scale data. However, the combination of archaeological and epidemiological data on human population movement and interaction in relation to the spread of infectious diseases is of considerable value for the reconstruction of disease dynamics in the past. When considering the implications of health, these population movements are more than just 'background noise' as stated by Clark (2001). Again, this discussion outlines the difference between studies on 'migration' or 'mobility' in comparison to 'population interaction' influences on health and disease.

Furthermore, human mobility patterns are recognised to involve interactions at any given distance, and realistically infectious diseases spread amongst individuals who interact at a short distance. Therefore, disease spread should be visualised more as a network of transmission than as a direct transmission route from region of origin to region of destination (Balcan et al. 2009; Tizzoni et al. 2014). Archaeologically, solely relying on markers of migration such as the use of strontium isotopes to identify migrants, over simplifies this network at play. For example, Roberts et al. (2013) assessed the oxygen and strontium isotopes of 14th to 16th Century burials from England, of which some individuals exhibited treponematosis. Of six individuals with possible or probable treponematosis, only two were considered non-local from their isotopic values. The authors concluded that migration had a negligible effect on disease transmission of treponematosis. However, the approach taken in this research limited the interpretation of disease transmission, as it aimed to identify a direct relationship between long distance migration and disease spread, and did not consider infectious disease spread as a result of a network of interactions between hosts.

While not to the degree of mobility in the present day, in the past maritime transport and travel by horse meant long distances could be covered (Wilson 1995). However, archaeological signatures of long-distance migrants may not exist. Instead, network interactions form over a long distance (i.e. the Silk Roads) and enable transmission of infectious disease over vast expanses via many hosts. For this reason, constructing evidence of population interaction from as many contexts as available (including archaeological and historical evidence, aDNA analysis, morphometric analysis, isotope studies) are required to best inform the complexity of the interaction at each site of consideration.

2.6.1 Isotopic Evidence of Migration

Isotopic variation of strontium, oxygen, and lead in bones and tooth enamel can be used to explore mobility in the archaeological record. As tooth enamel forms in childhood, and the skeleton remodels, differences in the ratios of these isotopes in tooth enamel and bone may indicate migration. Different isotopic signatures from neighbouring ecologies can also be used to identify a migrant (termed a non-local in isotopic studies). A number of factors including rainfall, temperature, seasonality, altitude, latitude, and aridity influence the evaporation of the stable oxygen isotope ^{16}O in water sources (Turner et al. 2012). Therefore, the ratio of stable oxygen isotopes ($^{16}O/^{18}O$) varies across differing bodies of water, beneficial for establishing provenance. Strontium isotope ratios enable geographic provenance in relation to foundational bedrock. The radiogenic isotope ^{87}Sr is formed through decay of ^{87}Rb (radiogenic rubidium) in bedrock, whereas the stable strontium isotope ^{86}Sr values remain the same over time. The age of the bedrock then determines the $^{87}Sr/^{86}Sr$ value (Bentley 2006). The strontium ratios of underlying bedrock are taken up through regional food and water sources. This relationship is not a closed system and can be influenced by factors such as erosion and weathering (Bentley 2006). Lead isotope analysis is applied similarly to strontium isotope analysis and reliant on lead in the surrounding geology. However, multiple radiogenic lead isotopes exist therefore a number of ratios are employed including most commonly $^{206}Pb/^{204}Pb$ and $^{207}Pb/^{204}Pb$ (Carlson 1996). Geographic provenance is most accurate when multiple isotopic approaches are applied. As isotopes may capture migrants who have died at their place of destination, isotopic signatures are likely to underestimate the amount of interaction, as the temporary or secondary forms of human mobility, such as trade, may not necessarily be identified.

2.6.2 Ancient DNA and Morphometric Evidence of Genetic Admixture

Construction of genome wide DNA analysis has been commonly employed in biological anthropology for over the last decade (Stoneking and Krause 2011). These techniques have enabled the documentation of substantial genetic phylogenies in the past, and are particularly useful for identifying interaction between populations in the form of genetic admixture (Feldman et al. 2019; He et al. 2019; Llorente et al. 2015). More traditional methods of DNA analysis, mitochondrial and Y-chromosome analysis are still employed and are useful for assessing admixture along matrilineal and patrilineal lines respectively (Duggan et al. 2017; Harney et al. 2019; Kivisild 2017). Commensal models including analysis of genetic phylogenies of animals and plants intricately linked to human migration are also useful for reconstructing systems of mobility and interaction. For example, the spread of the Pacific rat (*Rattus exulans)*, domestic dogs, chickens and pigs across the Pacific were reliant on colonization by human populations (Matisoo-Smith 2009). These commensal models provide sound proxies particularly when access to destructive analysis of human skeletal remains is restricted (Storey et al. 2013). They may also be useful in identifying interaction processes that have not resulted in the genetic admixture of human populations (e.g. trade). Variations in the phylogenetic dynamics between human and commensal models is then expected.

While seemingly usurped by genome wide DNA analysis, osteological morphometric analysis of prehistoric assemblages can also provide important detail on the population history of prehistoric human groups. The usefulness of morphometric analysis is particularly important in regions of the world such as tropical Southeast Asia and the Pacific islands where DNA degradation is high, or destructive analysis of human skeletal remains is not a viable option (Kumar et al. 2000). Morphometric methods aim to quantify morphological similarities or differences between populations thereby identifying variations in population history or consequences of admixture (Matsumura 2006; Salzano 2011). This technique is limited in the level of complexity that is revealed in the data and usually results in simplified explanations of population histories.

2.6.3 Archaeological Evidence of Population Interaction

Archaeological evidence of emulation and exchange indicate considerable interaction between populations. Emulation describes the process of changes in material culture, where one culture adopts the practices of another (Clark 2001). This process assumes cultural

exchange of knowledge that is only possible through interaction between populations. Moreover, the presence of artefacts or raw materials external to the environment is also evidence of exchange through trade (Clark 2001). Trade items may be traced to their origin through their design, chemical composition or distinct *chaînes opératoires* (Favereau and Bellina 2016). The archaeological evidence of emulation and exchange are useful in identifying complex and sustained networks within and between populations (Hung et al. 2013), and can suggest multiple episodes of potential disease transmission.

2.6.4 Historical Documentation of Interaction Events

For some populations, textual history of migration, trade and conflict exist and therefore historical documents may be particularly useful in informing on past population interactions. It should be noted that historical documentations may reflect a level of bias in the reporting of details, particularly in the case of conflicts. Therefore caution should be taken in the application of historical documentation to palaeopathological studies (Mitchell 2012).

2.7 Population Interaction within the Realms of the 'Bioarchaeology of Migration'

The choice to migrate is economically defined as "an investment in an individual's future productivity" (Kontuly and Smith 1995: 179). That is, it is recognised by a migrant that a region of destination may have increased returns than that of the current region of origin (Greenwood 1985). Migration may also be driven by environmental, economic or political disruptions in the place of residence rather than due to prospects of the place of arrival (Tsuda and Baker 2015). Migrants then make decisions to weigh the costs and benefits of migration. In an archaeological context, increased migrations are known to occur alongside social stratification changes and the disparity of goods and land for cultivation which drive exchange and expansion. Certainly perceived potential for increased returns and better probability of survival may have been particularly strong drivers of migration in the past (Tung 2012; Tung 2008).

Migrant experiences are an important social issue in the past as is the case today. Factors surrounding "othering" of migrants are of bioarchaeological consideration in terms of social inclusion, but also may have influenced health in the past in regards to access to healthcare and resources (Grove and Zwi 2006; Tung 2012). Additionally, the social regard of particular immigrant groups as "disease carriers" carry real social consequences today, and

may have been a factor in the past, particularly if the immigrant group introduced a new infectious disease (Grove and Zwi 2006). For this reason, understanding the context of disease transmission through population interaction could be said to overlap with the *bioarchaeology of migration.* This subfield is concerned with identity and health of migrant diasporas in the past (Tung 2012; Tung 2008). Social considerations of migrant health are beyond the scope of this thesis, but it is recognised here that the social experience of migration and interaction of the case studies presented in subsequent chapters is an area for further study.

What is of important concern in this thesis regarding migrant health in the past is that unlike in epidemiology of living populations, the pre-departure phase and the movement phase (see section above) remain invisible in the archaeological record. Archaeologically, skeletal evidence of migrant poor health can be assumed to be a composite of all three of these states of migration. This limitation must be recognised when considering the impactions of human interaction on health, as is the focus of this thesis.

2.8 Chapter Summary

This chapter provided a brief consideration of current epidemiological thought surrounding interaction, mobility and the impact on health of populations. Population interaction through the process of human mobility is multi-layered and consists of networks of contact at community, cross-community, and inter-regional levels. The intensity and frequency of human interaction increases the risk of disease transmission, and therefore is a substantial element of study from a palaeoepidemiological perspective. Assessment of population interaction as a factor of disease transmission is also more suited to archaeological assemblages than human mobility as it enables consideration of multiple forms and layers of human movement. The epidemiological considerations addressed in this chapter are elemental to the research design of this thesis.

CHAPTER 3:
SPECIFIC AND NON-SPECIFIC DISEASES IN THE CONTEXT OF PALAEOPATHOLOGY

3.1 Introduction

This chapter reviews the pathogenesis, pathophysiology and epidemiology of the specific diseases employed in the differential diagnoses for this thesis. Identification of specific diseases provides the foundation for the statistical assessments employed in this thesis (outlined in Chapter 5) and differential diagnosis (objective 3, outlined in Chapter 1). The purpose of this chapter is to present the key elements of disease in living populations prior to manifestations of pathology that may eventually be observed in dry bone. It is important to understand the disease progression (pathogenesis) and subsequent disordered processes in the body due to disease progression (pathophysiology). While palaeopathologists usually study evidence of disease in bone, these lesions are representative of chronic disease progression that has also affected the soft tissue, and inferring the stages of disease progression prior to skeletal involvement is essential to interpretation (Ortner 2011). Moreover, due to the unique characteristics of each disease, individuals of variable age, sex, socioeconomic status, geographic region, and genetics are differently impacted in terms of susceptibility to both morbidity and mortality.

The definitions of specific disease, non-specific disease and non-specific infection as they are defined in palaeopathology and within this thesis are first addressed. Subsequently details of the specific diseases are presented. The skeletal manifestations of each disease are briefly mentioned here. However, they are described in detail in Chapter 5 alongside the differential diagnostic protocol for each disease. As non-specific bone infections such as osteomyelitis and otitis media (ear infection) are caused by a considerable number of pathogens with variable pathogeneses and epidemiology, they are dealt with at length in the methodology (Chapter 5). The skeletal changes recognised in these infections are not discussed within this chapter.

The introduction sections of the diseases treponematosis, tuberculosis, leprosy, brucellosis and mycosis have been published in Vlok et al. (2020). The section on calcium

deficiency rickets has been included in Vlok et al. (in review). These publications can be accessed in Appendices 4 and 5 respectively.

3.2 Specific Disease, Non-Specific Disease and Non-Specific Infection

Disease is clinically defined as "an interruption, cessation, or disorder of body functions, systems, or organs... A morbid entity characterised usually by at least two of these criteria: recognised aetiological agent(s), identifiable group of signs and symptoms, or consistent anatomical alterations..." (Stedman's Medical Dictionary (26th Edition), 1995: 492 in Grauer 2011). In palaeopathology, this definition, specifically refers to observed interruptions to the skeletal system, where 'anatomical alterations' of other organs and tissues are inferred. Bone can only respond to disease either in the form of deposition (bone formation), lysis (bone resorption), or both (Waldron 2008). Some infectious and nutritional diseases influence the homeostasis of bone deposition and resorption, and therefore result in abnormal bone development causing *lesions* on bone (Ortner 2003; see Chapter 5 for more discussion). The expression of some diseases can take the form of osteoblastic inflammation on the surface of the bone called *subperiosteal new bone* (SPNB). SPNB can have various aetiologies, including trauma, infection, and metabolic bone disease. For this reason SPNB should be considered as a *non-specific* indicator of disease (Buikstra 2019; Ortner 2011). That is, the aetiology of the disease causing SPNB cannot be determined (Weston 2008). For this reason the assumption that SPNB is the result of infection, as is the case in a number of palaeopathological studies (e.g. Ikehara-Quebral et al. 2017; Pietrusewsky and Douglas 2001; Pietrusewsky et al. 2019) can lead to erroneous interpretations of the health of past populations (Weston 2012).

Non-specific infection is also a term used by palaeopathologists. This term describes patterns of skeletal markers that are specifically indicative of infection (such as the presence of pus draining holes in bone termed cloacae which develop in bone due to pyogenic infection), but can be caused by a myriad of bacteria, fungi or viruses, and the specific pathogen cannot be identified (Ortner 2003). While there is not always clear demarcation in the palaeopathological literature, non-specific disease and non-specific infection are terms that are differentiated from each other in this thesis. Non-specific disease is here used when discussing SPNB, whereas non-specific infection refers to osteomyelitis, mastoiditis and otitis media.

In contrast, a particular skeletal pattern of bone formation or lysis can aid in the diagnosis of *specific diseases*, where the aetiology of the skeletal pattern can be directly identified, or at least inferred, such as in the case of tuberculosis or treponematosis (Ortner 2003; Roberts and Manchester 2012; Waldron 2008). The following section introduces the specific diseases assessed in this thesis, their pathogenesis, pathophysiology and epidemiology, in order to provide essential background to the differential diagnosis methodology presented in Chapter 5. The potential relationship between some infectious and nutritional diseases observable in dry bone is also discussed.

3.3 Tuberculosis

The Mycobacterium tuberculosis complex (MTBC) is a group of infectious, slow growing, gram positive bacteria that can cause granulomatous necrotising abscesses throughout the entire body (Flynn and Chan 2001; Haque 1990; Knechel 2009). The MTBC consists of *Mycobacterium* strains which infect a number of mammalian primary hosts but all can infect humans. These include: *M. tuberculosis* (humans), *M. bovis* (domestic livestock), *M. canetti* (humans), *M. microti* (voles, hyrax, llama, rarely humans), *M. caprae* (goats), *M. pinnipedii* (seals and sea lions, rarely humans), and *M. africanum* (humans) (Roberts 2012). The most common form is *M. tuberculosis* which is a human specific respiratory disease that affects the lungs and other organs and will be described in detail here.

Approximately 1 in 3 of the global population are infected with a non-infectious asymptomatic form of tuberculosis (De la Rua-Domenech 2006; World Health Organization 2013). *M. tuberculosis* is most often spread through air droplets from coughing, sneezing and talking (Knechel 2009; World Health Organization 2013), whereas zoonotic forms such as *M. bovis* tend to spread to humans through ingestion (De la Rua-Domenech 2006). The symptoms of the disease are highly variable depending on which body systems are affected. However, more commonly coughing, fever, weight loss in the form of wasting, fatigue, malaise, shortness of breath and chest pain due to respiratory disease occurs (Fanning 1999; Knechel 2009). The disease can be fatal, if untreated, particularly in immunocompromised people (Raviglione et al. 1995).

3.3.1 Pathogenesis and Pathophysiology of Tuberculosis

In pulmonary tuberculosis, the bacilli travel through and rest in the upper parts of the air way. If not trapped in the mucus lining the airway and lungs, they will travel to the alveoli of the lungs (Knechel 2009). Macrophages in the alveoli will surround the bacilli but the pathogen will continue to replicate within the macrophages (Knechel 2009). The body cannot eliminate the bacteria and therefore T cells subsequently migrate to the infected area and initiate a granulomatous response to contain it (Flynn and Chan 2001; Knechel 2009; Ortner 2003). The granuloma contains macrophages, giant cells, T cells, fibroblasts and B cells which migrate to the infection site (Flynn and Chan 2001). This process occurs between 2 to 12 weeks of initial infection (Knechel 2009).

In most individuals, the containment of the bacteria leads to an asymptomatic non-infectious form. However, two forms of *active tuberculosis* can occur. In individuals with immature immune systems such as young children or severely immunocompromised adults, failure of containment of the disease results in *primary tuberculosis* (Haque 1990). In this form, the bacteria are free to multiply and disseminate through lymph nodes and into the blood stream. Cavities due to necrosis of granulomatous tissue form in various organs especially the lungs. Most commonly, this form affects children between the ages of 1 to 3 years and young adults (Haque 1990; Lewis 2017). The bacteria disseminate through haematogenous routes to the upper lobes of the lungs, brain, renal cortices and epiphyses of long bones (Haque 1990).

Secondary tuberculosis also known as reactivation pulmonary tuberculosis ensues when necrosis and breakdown of the granuloma occurs due to fluctuations in immune function and a release of the bacteria into the body following a period of latency (Flynn and Chan 2001; Haque 1990). Most commonly this starts as a form of necrotising pneumonia in the upper lung causing cavitation (Haque 1990).

Extrapulmonary tuberculosis most commonly occurs in immunocompromised individuals and spreads through circulatory and lymphatic systems to various organs in the body (Roberts 2012). Progression to an extrapulmonary form can affect varying organ systems. For example, infection of the central nervous system can cause meningitis which is fatal if not treated. Infection of the bloodstream and lymph nodes leads to infection of a

number of organ systems including the skeletal system and reinfection of the lungs (Figure 3.1; Knechel 2009). Extrapulmonary skeletal involvement of tuberculosis will occur in approximately only 3-5% of cases (Jaffe 1972).

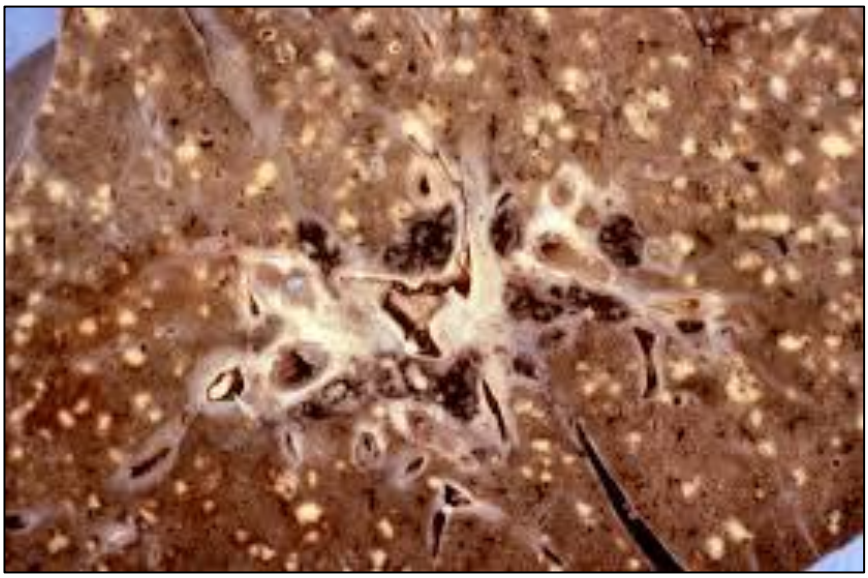

Figure 3.1: *Miliary tuberculosis (haematogenous spread) of the lung. Multiple necrotic abscesses are present. Image: The Wellcome Collection (Creative Commons).*

3.3.2 Epidemiology of Tuberculosis

Transmission through air droplets enables *M. tuberculosis* to be efficiently spread throughout large populations, whereas the spread of *M. bovis* is restricted to regions where infected livestock are consumed. However, given the body's ability to contain the disease, certain conditions cause symptomatic morbidity and mortality from active tuberculosis. For, example demographically, infants, children, older adults and pregnant women appear to be the most susceptible (Marais et al. 2013). In regards to sex, males more often than females are susceptible to the disease (World Health Organization 2013). This difference may be related to sex specific hormones and their role in mediating immune response to the bacteria (Nhamoyebonde and Leslie 2014).

Population density and crowding has been strongly associated with the emergence of endemic human tuberculosis (Roberts 2012). Due to high population numbers throughout the world *M. tuberculosis* has a global geographic distribution. However, a high prevalence corresponds to regions of the world where ineffective healthcare is present, as tuberculosis is predominantly a treatable disease. Furthermore, a strong co-morbidity with HIV is well

recognised, but is not relevant to this thesis (World Health Organization 2013). Regions where medical care is not sufficient to manage outbreaks of tuberculosis, poverty, overcrowding, and poor sanitation are also factors related to the high prevalence of the disease (DeWitte 2016; Roberts 2012; Roberts and Buikstra 2003; World Health Organization 2013). Colder climates are likewise known to increase the risk of respiratory diseases, including tuberculosis (Roberts 2012). Finally, increased travel and migration are well known risk factors for the spread of tuberculosis (Albert and Davies 2008).

The rarity of skeletal forms of tuberculosis can be partially attributed to the high mortality rates in absence of modern medical treatment. Up to 70% of untreated cases reported resulted in death within 10 years of initial infection (Tiemersma et al. 2011; World Health Organization 2013).

3.4 Treponemal Disease (Treponematosis)

Treponemal disease is a group of systemic diseases caused by a bacterial spirochete which primarily affects the skin, but can also affect bones and other organs (Hook and Marra 1992). Four diseases including yaws (*Treponema pallidum pertenue),* pinta (*T. carateum),* venereal syphilis (*T. pallidum pallidum)* and endemic syphilis *(T. pallidum endemicum)* have similar bacterial morphology and share a similar pathogenesis (Hook and Marra 1992; Marks et al. 2014; Willcox 1974). However, they occupy different ecological niches (Marks et al. 2014).

3.4.1 Pathogenesis and Pathophysiology of Treponematosis

While the four treponemal diseases cause a variation of symptoms, there is overlap in the progression of these diseases (Marks et al. 2014). However, pinta only affects the skin, not bone, and therefore is not discussed here further. The treponemes travel to the lymph nodes after initial infection (Marks et al. 2014). Initial infection induces a cell-mediated immune response (Peeling and Hook 2006). A primary skin lesion forms at the site of inoculation within a few weeks of initial infection and subsequently appears to resolve itself (Peeling and Hook 2006).

In the secondary phase, the skin rash reappears and becomes more diffuse and is associated with swelling of lymph nodes (lymphadenopathy) (Peeling and Hook 2006).

Other soft tissue secondary changes are specific to the type of treponemal disease. The secondary phase is then followed by an asymptomatic latent phase (Hackett 1953). As is the case in tuberculosis, described above, chronic infection (except in pinta) leads to a granulomatous response, and the pathogen is contained (Peeling and Hook 2006). Latency can last somewhere from 3 to 10 years since initial infection. Sometimes no latency occurs (Hackett 1953). It is thought that the low metabolic rate of the pathogen allows it to avoid immune recognition in the latent stage (Marks et al. 2014). Spontaneous recovery from primary and secondary stages can be attributed to ongoing cell mediated immune response (Peeling and Hook 2006).

Following a period of latency, a destructive tertiary stage begins, where necrosis of the granulomas occurs causing *gummatous* lesions of skin, internal organs and bones. During the tertiary stage, secondary lesions stop forming (Hackett 1953). While early treponemal lesions can heal within a few months, the late (tertiary) stage lesions can last for more than a year and leave permanent changes in bone and skin (Hackett 1978). The following sections focus on the treponemal diseases that can be observed in the skeletal record.

3.4.2 Yaws

Yaws *(Treponema pallidum pertenue)* is a treponemal disease that today is restricted to the tropical belt and can only survive in hot and humid climates (Willcox 1974). The pathogen has recently been identified in archaeological assemblages from 15th Century Northern Europe, suggesting that in the past some strains were not tropically restricted, but may have originated from tropical Africa (Giffin et al. 2020). It is predominantly a disease of childhood due to skin contact being the primary route of transmission, and transmission is exacerbated if there is trauma to the skin surface (Willcox 1974). Yaws remains endemic to Pacific countries including Papua New Guinea and the Solomon Islands, and also in Ghana, Africa (Marks et al. 2014).

In primary yaws, an ulcerous skin rash occurs at the site of inoculation within 1 to 2 weeks of initial infection (Hackett 1951; Marks et al. 2014). At this point, spontaneous healing can occur, otherwise the disease progresses to secondary yaws with widespread skin involvement and sometimes an osseous response (Marks et al. 2014). The secondary effects

to the skin can include ulcerous rashes, and hyperkeratotic lesions of the hands and feet commonly known as *crab yaws* (Gip 1989*)*. *Goundou* is an inflammation of the nasolabial lymph nodes that can occur in the secondary stage and may cause SPNB deposition on the anterior maxillae (Hackett 1946; Harper et al. 2011; Lewis 2017). Osseous involvement is strictly osteoblastic and can cause dactylitis, and widespread SPNB response of the long bones (Marks et al. 2014). A condition known as *sabre shin* has been reported where prolific SPNB deposit results in anterior pathological pseudobowing of the tibiae (Hackett 1946; Hackett 1951). Skeletal involvement can also continue beyond the period where the secondary skin lesions have healed, termed the late secondary stage (Hackett 1951). In approximately 10% of untreated individuals a destructive tertiary stage can form wherein granulomatous nodules cause tissue necrosis and superficial bone destruction (Figure 3.2) (Hackett 1951; Marks et al. 2014). Furthermore, at this stage joint destruction, destruction of the nasal region (gangosa) (Figure 3.3), and fluid accumulation (hydroarthrosis) within the knee joint can occur (Hackett 1953).

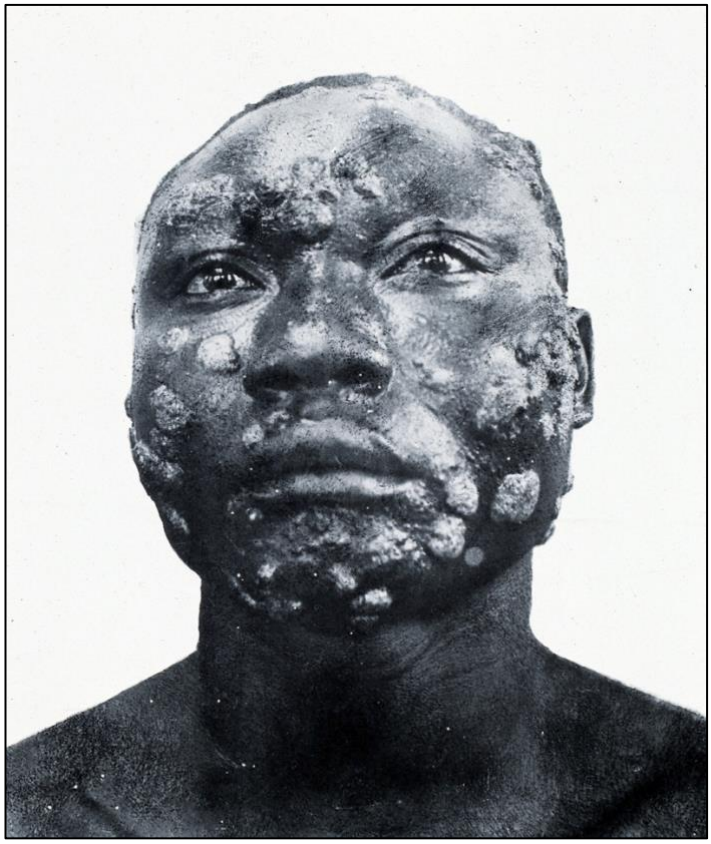

Figure 3.2: *Destructive gummatous lesions of the face and neck in tertiary yaws. Image: The Wellcome Collection (Creative Commons).*

Figure 3.3: *Destructive gangosa of the nasofacial region in tertiary yaws. Image: The Wellcome Collection (Creative Commons).*

3.4.3 Endemic Syphilis

Endemic syphilis *(Treponema pallidum endemicum)* exists in warm but dry areas, particularly areas bordering the tropical belt including the Middle East and Saharan and Kalahari Africa (Marks et al. 2014; Willcox 1974). Skin contact, and therefore mode of transmission, is restricted as the organism survives in mucous areas of the body. Transmission commonly occurs through kissing, sharing of eating or drinking vessels, contact of fingers and can also occur through sexual contact (Pace and Csonka 1984; Willcox 1974). Skin lesions are generally also restricted to moist areas of the body such as the lips, groin and armpits (Hackett 1936; Hackett 1978; Willcox 1974). Most commonly the primary lesion develops in the oropharynx or nasopharynx and is generally undetectable until secondary stage (Marks et al. 2014). Secondary lesions develop between 3 to 6 months after infection with a diffuse skin rash, infection of the lymph nodes (lymphadenopathy) and osteoblastic bone response similar to yaws. However, the rash differs to that of yaws in that it appears as papules rather than ulcerous (Marks et al. 2014). As is the case with yaws, a

tertiary stage marked by destruction from gummatous lesions can occur and gross destruction of the nasopharynx has been frequently reported (Marks et al. 2014).

3.4.4 Venereal Syphilis

Venereal syphilis *(Treponema pallidum pallidum)* is a ubiquitous (globally prevalent) disease (Willcox 1974). Unlike with the other treponemes, venereal syphilis predominantly spreads through sexual contact (Hook and Marra 1992). For this reason most cases of acquired venereal syphilis occur in adults (Marks et al. 2014). Primary skin lesions called chancres form at the site of infection, most commonly in the groin region, generally within 21 days after initial infection (Hook and Marra 1992). The secondary stage is defined by a diffuse papular rash and ulcerations (Figure 3.4), with concentration in moist areas (Hook and Marra 1992). A secondary stage can be accompanied by fever and alopecia, as well as multi organ involvement (Hook and Marra 1992; Peeling and Hook 2006).

Figure 3.4: *Secondary skin lesion in venereal syphilis. Image: The Wellcome Collection (Creative Commons).*

Tertiary stages of venereal syphilis result in similar gummatous lesions such as yaws and endemic syphilis (Figure 3.5). However, more severe complications can occur. Aortic aneurysms and neurological deficits (termed neurosyphilis) are fatal consequences of this disease (Peeling and Hook 2006). Neurological deficits can involve tremors, dementia, loss of pain sensation, and loss of facial-muscle tone (Peeling and Hook 2006). Prior to penicillin

treatment, syphilis was a leading cause in neurologic and cardiovascular diseases (Hook and Marra 1992).

Figure 3.5: *A case of tertiary venereal syphilis to the back and arms. Image: The Wellcome Collection (Creative Commons).*

While there are some reports of congenital transmissions of yaws and endemic syphilis, congenital transmission has been most commonly documented in venereal syphilis (Arslanagić et al. 1989; Engelhardt 1959; Hook and Marra 1992; Lewis 2017; Ortner 2003). Transmission occurs through the placental barrier after approximately the 16th week, with most after the 6th month of pregnancy (Fiumara and Lessell 1970). For this reason, congenital syphilis does not proceed in the stages identified in acquired syphilis. In approximately 30 to 50% of cases, pregnancies of syphilitic women end in miscarriage or still birth (Peeling and Hook 2006). Infant deaths are due to issues of prematurity, an

enlarged liver (hepatomegaly), spleen (splenomegaly) and changes to the lung (Saxoni et al. 1967). If the infant survives, lifelong lesions occur. This form results in distinctive changes to the skeleton. Changes can include frontal bone bossing due to SPNB deposition, short maxilla, saddle nose due to reoccurring rhinitis (syphilitic snuffles, Figure 3.6), osteochondritis, a high palatal arch, and dental hypoplasias (Hutchinson's incisors, Moon's molars and Mulberry molars) (Fiumara and Lessell 1970; Lewis 2017). Other features include corneal scarring, and eighth nerve deafness due to chronic inner ear infection (Fiumara and Lessell 1970).

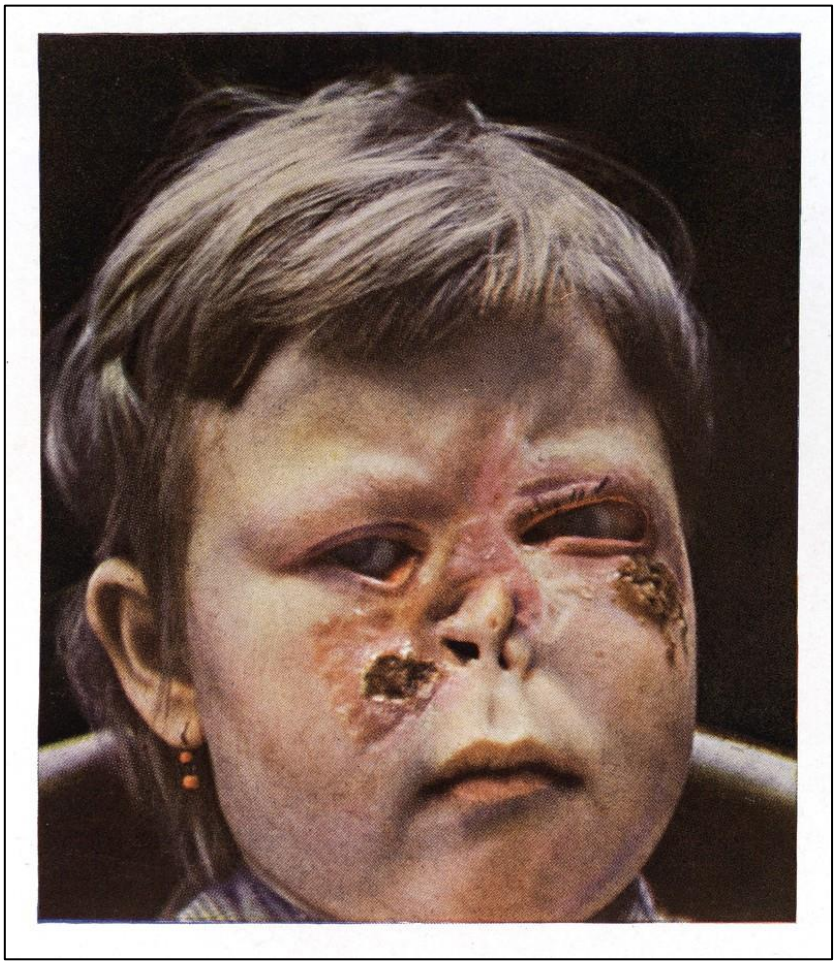

Figure 3.6: *Destruction of the nasofacial region resulting in saddle nose of congenital syphilis. Image: The Wellcome Collection (Creative Commons).*

3.4.5 Epidemiology of Treponematosis

Peak in vivo proliferation of treponemes occurs between an internal body temperature of 35 and 37°C, and the bacteria are easily killed when dried (Hollander and

Turner 1954; Perine et al. 1984). As described above, the treponeme has adapted to arid climates through survival within moist areas of the body. As is the case in endemic syphilis, where yaws has been observed in slightly drier climates, the treponeme is more often restricted to areas of the armpit, groin, anus and lips (Hackett 1936; Hackett 1978). The endemic treponemes spread particularly in areas of poor sanitation and where there is constant skin contact amongst individuals (Marks et al. 2014; Willcox 1974). Historically, mass migrations have been considered to play a role in the spread of the treponemes globally such as with the forced migrations of the African slave trade (Willcox 1974). Travel by sea has been implicated in the rapid spread of venereal syphilis globally (Willcox 1974). In regards to mortality, due to the neurological and cardiovascular effects of venereal syphilis, this treponeme is considered to have a higher mortality rate than the endemic treponemes (Hook and Marra 1992; Peeling and Hook 2006). The reduced mortality in endemic treponemes does increase chances of these diseases being present in the skeletal archaeological record.

3.5 Leprosy

Leprosy is a chronic bacterial infection caused by *Mycobacterium leprae or M. lepromatosis* which primarily affects the skin, nasal mucosa and peripheral nerves (Abulafia and Vignale 1999; Bokhary and Phung 2016; Eichelmann et al. 2013; Saonere 2011). Transmission of the disease is still not well understood. However, the spread of bacteria from the nasal mucosa through secretions to the upper respiratory tract has been proposed (Bhat and Prakash 2012; Menger et al. 2007). It is possible the disease may also spread through skin contact (Bhat and Prakash 2012). The disease used to have a global distribution, but today is restricted to developing countries in tropical regions (Foss and Motta 2012).

3.5.1 Pathogenesis and Pathophysiology of Leprosy

At a cellular level, the mycobacterium targets Schwann cells of the peripheral nervous system, endothelial cells, pericytes, monocytes and macrophages (Abulafia and Vignale 1999). The mycobacteria replicate slowly at approximately 20 to 30 days leading to slow progression of the disease (Abulafia and Vignale 1999). Furthermore, the incubation period is extremely variable lasting from a few weeks to up to 10 years (Bokhary and Phung 2016; Lockwood 2004). The bacteria spreads through the body by both lymph and blood vessels (Abulafia and Vignale 1999). Schwann cells are the primary site of replication as

these cells are not capable of destroying the bacteria, and the bacteria can reprogram Schwann cells to encourage dissemination of the bacteria to other tissues (Abulafia and Vignale 1999; Masaki et al. 2013). Invasion of perineural cells adjacent to infected Schwann cells appears to be the primary driver of a granulomatous response in the body (Abulafia and Vignale 1999).

The symptoms of the disease vary along a spectrum and are highly dependent on individual immune response (Abulafia and Vignale 1999; Bokhary and Phung 2016; Eichelmann et al. 2013). Tuberculoid leprosy is a milder form which is often non-contagious, whereas lepromatous leprosy is more systemic, infectious, and causes more severe symptoms (Bokhary and Phung 2016; Eichelmann et al. 2013; Saonere 2011). In the tuberculoid form, cell mediated immunity predominates and granulomas rarely form except in epithelioid tissue (Abulafia and Vignale 1999; Bokhary and Phung 2016). In contrast, in the lepromatous form macrophages are incapable of destroying the bacteria in their entirety and a strong immune response occurs in the body wherein the bacilli are contained within granulomas (Abulafia and Vignale 1999). Clinically, a continuum between the tuberculoid and lepromatous form is recognised and expression intermediate between the two extremes (borderline forms) is frequently documented (Abulafia and Vignale 1999).

As symptoms progress, peripheral neuropathy occurs which could be permanent (Bhat and Prakash 2012; World Health Organization 1998). Schwann cells become injured and demyelinated resulting in loss of motor and sensory function (Bhat and Prakash 2012). Skin changes in response to tuberculoid leprosy tend to be large, localised and few in number (Figure 3.7) whereas skin changes in the lepromatous form are diffuse and lead to systemic subcutaneous granulomatous nodules (Figure 3.8; Bhat and Prakash 2012). The affected epidermis can also become thicker (Bhat and Prakash 2012). A concentration of bacilli is found within each papule (Bhat and Prakash 2012). Other organs such as the eyes can be affected by the lepromatous nodules causing blindness (Bhat and Prakash 2012; Menger et al. 2007). In all forms, skin changes are associated with neuritis (inflammation of the peripheral nerves) (Bhat and Prakash 2012; World Health Organization 1998). Neuritis leading to an increased likelihood of secondary infections from open wound trauma, or pressure ulcers due to sensory loss, results in lack of associated pain, and therefore unawareness of the progression of infection (Saha et al. 2019). Advanced necrosis following secondary infection is believed to be the primary cause of skeletal manifestations of leprosy,

and can cause significant erosive destruction particularly to the nasofacial region (Figure 3.9). Saddle nose deformities similar to those seen in treponemal disease can occur once this skeletal erosion progresses (Menger et al. 2007; Shah et al. 2009).

Figure 3.7: *Skin rash in tuberculoid leprosy. Image: The Wellcome Collection (Creative Commons).*

Figure 3.8: *Skin changes due to lepromatous leprosy. Image: The Wellcome Collection (Creative Commons).*

Figure 3.9: *Nasopalatine and maxillary destruction in advanced stage of lepromatous leprosy. Image: The Wellcome Collection (Creative Commons).*

3.5.2 Epidemiology of Leprosy

In regions where *M. leprae* is endemic, individuals are at more risk of contracting the disease (Bokhary and Phung 2016). Conditions of poor hygiene, contaminated water and malnutrition increase the risk of immune susceptibility to the pathogen (Bhat and Prakash 2012). Furthermore, a myriad of mutations at loci pertaining to innate immune pathogen detection and response influence susceptibility to the disease (Bokhary and Phung 2016). Leprosy from *M. lepramatosis* is more recently described and very little epidemiological research exists (Bhat and Prakash 2012).

The age distribution of those affected by the disease tends to be bimodal with children between 10 to 14 years of age, and older adults presenting with higher prevalences

of the disease (Noordeen 1998). Potential explanations for this bimodal age distribution include predominant infection in childhood followed by reinfection later on in adulthood when immunity declines (Noordeen 1998).

Males tend to be more frequently infected than females at a frequency of 2:1 (Noordeen 1998). The disease can be geographically wide spread but appears to have a predilection for tropical regions (Menger et al. 2007). However, the disease also favours temperatures below 37°C (Rendall and McDougall 1976). Mortality directly from the disease is low and when fatal is associated with co-morbidities such as secondary infections (Noordeen 1998).

3.6 Brucellosis

Brucellosis (also known as Bang's disease, undulant fever, Mediterranean fever and Malta fever) is a zoonotic bacterial disease commonly associated with animal husbandry (Al-Shahed et al. 1994; Corbel 2006; Franco et al. 2007; Galinska and Zagórski 2013). The disease is mainly caused by six species of bacteria: *Brucella abortus, B. suis, B. canis, B. melitensis, B. neotomae,* and *B. ovis* (Al-Shahed et al. 1994; Corbel 2006; Franco et al. 2007; Galinska and Zagórski 2013). However, there are rare sylvatic *Brucella* strains in wild terrestrial (voles, foxes and rabbits, *B. suis* biovar 5 and *B. microti*) or marine mammals (whales, dolphins and seals, *B. marina*) that are of relevance for brucellosis infection in archaeological assemblages, due to the range of animals exploited by prehistoric groups (Al Dahouk et al. 2013; Corbel 2006; Galinska and Zagórski 2013). The bacteria are transmitted to humans mostly through ingestion of animal products such as dairy, but can be transmitted through skin lesions or air droplets in circumstances of close contact with animals (Corbel 2006; d'Anastasio et al. 2011; Franco et al. 2007; Mehmet et al. 2002). In extremely rare cases, the bacteria can also be spread between humans through breastfeeding from mother to infant, or through sexual contact (Corbel 2006; Meltzer et al. 2010). Each strain is predominantly associated with a different animal. *B. abortus* is associated with cattle, camels, bison, yak, elk and buffalo, *B. melitensis* with sheep and goats, *B. ovis* with sheep, *B. canis* with dogs, *B. neotomae* in rats, and *B. suis* with pigs, reindeer and rodents (Al Dahouk et al. 2013; Corbel 2006; Galinska and Zagórski 2013).

3.6.1 Pathogenesis and Pathophysiology of Brucellosis

Following initial infection, the *Brucella* bacteria bind to cells of the mononuclear phagocyte system, a group of cells that include marrow progenitors, blood monocytes and macrophages found in hematopoietic regions of the body including the liver, spleen and bone (Campbell et al. 1994; Corbel 2006; Hume 2006). The disease spreads through the body via the lymphatic system (Galinska and Zagórski 2013).

Symptoms of brucellosis are non-specific and therefore present a diagnostic problem for clinicians except in light of molecular or serological confirmation, therefore the disease is often overlooked as a possible aetiology for clinical symptoms in a patient (Al Dahouk et al. 2013; Franco et al. 2007; Galinska and Zagórski 2013). The disease usually begins as an acute or insidious (gradual) form and progresses to a chronic disease in advanced stages (Corbel 2006). In the acute stage, fever is associated with sweating, appetite loss, headaches, joint pain, back pain, diarrhoea, and malaise, whereas in the insidious form symptoms occur gradually over time increasing in severity (Corbel 2006; Franco et al. 2007). Hepatomegaly, splenomegaly and lymphadenopathy may occur (Corbel 2006; Franco et al. 2007). This infection persists for weeks or months and becomes chronic where cell mediated immunity leads to granulomatous containment of the bacterium (Corbel 2006; Franco et al. 2007). Symptomatic chronic forms develop from relapse, or persistence of the disease with continued progression in the absence of acute symptoms (Corbel 2006). A diffuse or localised form of the disease can subsequently develop in any organ of the body including the skin, heart and brain (Al-Shahed et al. 1994). Skin response can vary from papular, ulcerous, or nodular rashes (Corbel 2006). Musculoskeletal complications are common in brucellosis occurring in up to 40% of cases, and spondylitis is frequent (Al Dahouk et al. 2013; Al-Shahed et al. 1994; Corbel 2006; Mehmet et al. 2002). In diffuse forms the disease infects multiple organs (Al-Shahed et al. 1994). The presentation of localised or diffuse forms are reliant on individual level immune effectiveness (Galinska and Zagórski 2013).

3.6.2 Epidemiology of Brucellosis

Pasteurisation and cooking is effective in eliminating the bacteria from meat and dairy products and preventing human disease (Al Dahouk et al. 2013; Corbel 1989). Therefore, poor hygiene and food handling greatly increases the risk of brucellosis infection (Corbel 2006). The disease is endemic today in regions of pastoralism and is not

geographically restricted (Galinska and Zagórski 2013). There is a direct correlation of a high prevalence in animals to increased transmission to humans (Al Dahouk et al. 2013). Shepherd dogs and livestock can both be reservoirs for brucellosis therefore pastoralists employing dogs for herding are at a particular risk for infection (Galinska and Zagórski 2013). Pastoralists who rely on the livestock for dairy also have increased risk of infection as *Brucella* are frequently shed in milk (Aparicio 2013). The disease can occur in individuals of any age or sex (Corbel 2006; Franco et al. 2007). Introduction of infected animals into uninfected livestock groups is the main mode for widespread transmission of the disease in animals, therefore migration and interaction of livestock is a risk factor for infection (Aparicio 2013). Contact of livestock with infected wild animals (i.e. transmission of infected buffalos to cattle) is another mode of transmission, albeit less frequently (Aparicio 2013).

Death from brucellosis is rare but infections of the heart and/or central nervous system are known to be fatal (Corbel 2006; Franco et al. 2007). The placenta is an enriched region of haematopoiesis wherein the *Brucella* bacteria thrives (placentitis) and spontaneous abortion occurs in both animals and humans through placental transmission of *Brucella* (Aparicio 2013; Corbel 2006).

3.7 Cystic Hydatids Disease

Species of *Echinococcus* tapeworm including *E. granulosis, E. vogeli, E. multilocularis, E. ortleppi, E. canadensis* and *E. intermedius* can cause parasitic infection in humans (Deplazes et al. 2017; Rausch and D'Alessandro 1999). This group of diseases rely on a cycle between a definitive host and an intermediate host (Beggs 1985). Only the larvae of *E. granulosis* and *E. multilocularis* can proliferate in bone and are the focus of this section (Rausch and D'Alessandro 1999).

E. granulosis is the most common form of hydatids disease and is characteristic for the development of parasitic cysts in the body (Beggs 1985). An alveolar form of hydatids disease occurs with *E. multilocularis* (Brunetti et al. 2010). This form is far more rare, more lethal and does not cause the cyst-like changes in soft tissue that occur in *E. granulosis* (Brunetti et al. 2010; Rausch and D'Alessandro 1999). However, alveolar and cystic echinococcosis are indistinguishable in bone (Merkle et al. 1997).

3.7.1 Pathogenesis and Pathophysiology of Hydatids Disease

In *E. granulosis* dogs serve as the *definitive* (end of life cycle) host whereas a number of ruminants including sheep, goat, cattle, and buffalo serve as the intermediate host (Beggs 1985). In sylvatic (wild) strains of *E. granulosis*, wild animals such as deer are the intermediate hosts whereas wolves, and other wild canids, can serve as the definitive host (Rausch and D'Alessandro 1999). In *E. multilocularis* foxes are more commonly the definitive hosts, with rodents serving as the intended intermediate host (Czermak et al. 2001). Dogs are infected through eating viscera of livestock either through feeding domestic dogs offal of infected livestock or scavenging of livestock carcasses (Eslami and Hosseini 1998). The adult (a tapeworm) lives in the intestines of the definitive host. Hundreds of eggs are discharged by each hydatid worm into the intestines where the eggs are subsequently excreted in the faeces. Faecal matter is ingested by the ruminating intermediate hosts (Beggs 1985). Humans are accidental intermediate hosts (Rausch and D'Alessandro 1999; Vatankhah et al. 2015). In the case of humans, consumption of contaminated water or vegetables is the most common form of transmission (Figure 3.10; Beggs 1985).

In intermediate hosts, parasitic embryos form and pass through the intestine wall and spread throughout the body through the venous or lymphatic system (Beggs 1985). In *E. granulosis* larvae begin to grow in a vesicle of germinal tissue encased in laminated fluid filled cysts (Rausch and D'Alessandro 1999; Vatankhah et al. 2015). The cyst has three layers: an outer layer (the pericyst) which develops from the intermediate host's inflammatory response and is comprised mostly of modified host cells, the middle laminated layer which enables passage of nutrients but prevents invasion of bacteria, and the inner germinal layer which produces the laminations of the middle layer (Figure 3.11; Beggs 1985). Concentric enlargement of the vesicle occurs until an approximate maximum size of 6 to 7cm (Rausch and D'Alessandro 1999). The cyst can reach the size of 5mm within 3 months (Beggs 1985). In rare circumstances, these cysts can calcify and can remain in the archaeological record (Beggs 1985). Cysts can be simple, multifocal or multichambered and can proliferate in any organ, but are most commonly found in the liver (Rausch and D'Alessandro 1999; Vatankhah et al. 2015). Up to 75% of cases involve the liver, followed in frequency by the lung (approximately 15%) (Beggs 1985; Song et al. 2007; Vatankhah et al. 2015).

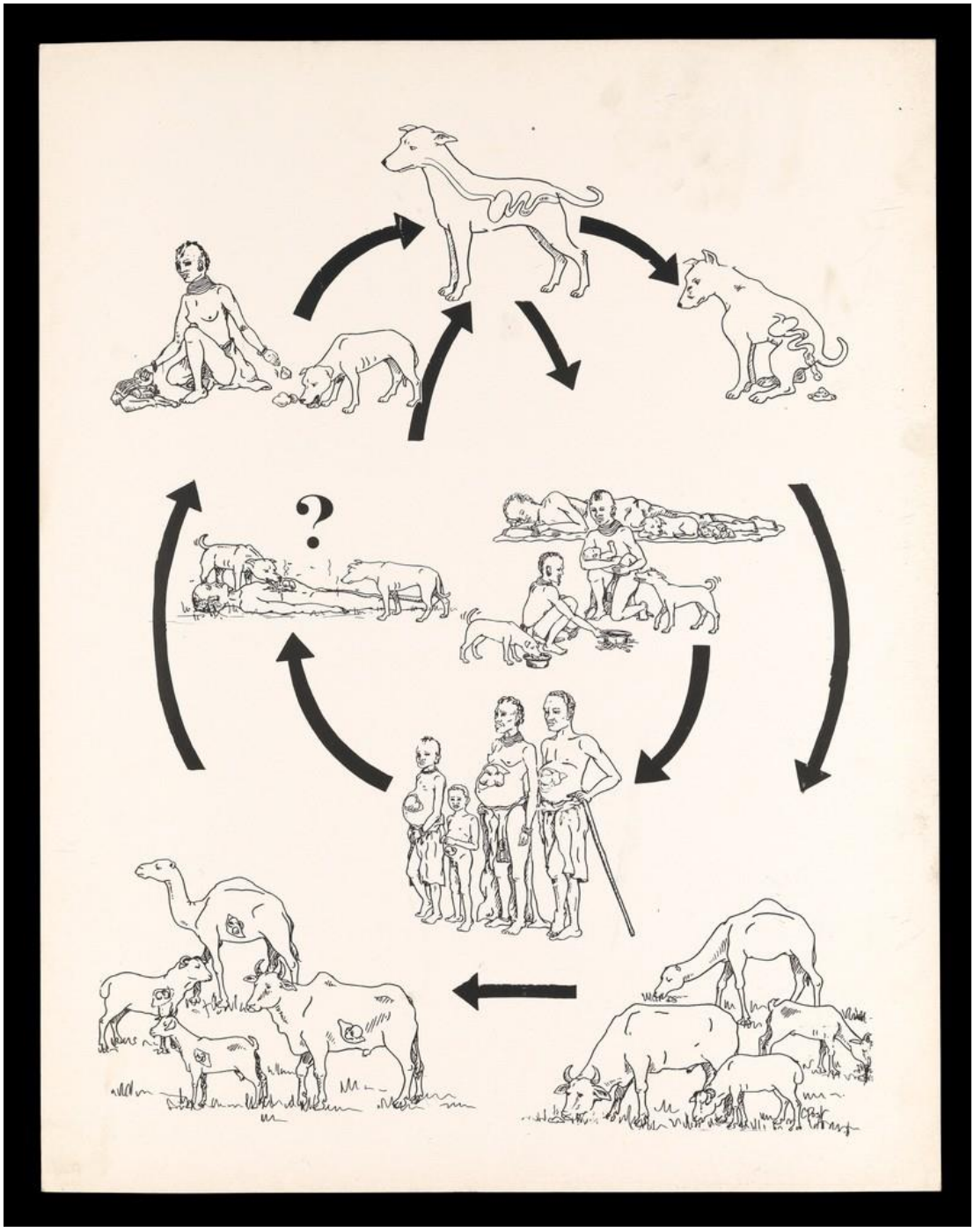

Figure 3.10: *Life cycle of Echinococcus granulosis with humans as hosts. Humans are most often infected by the eggs from the definitive host (dogs) which have close contact with the intermediate host (livestock). Image: The Wellcome Collection (Creative Commons).*

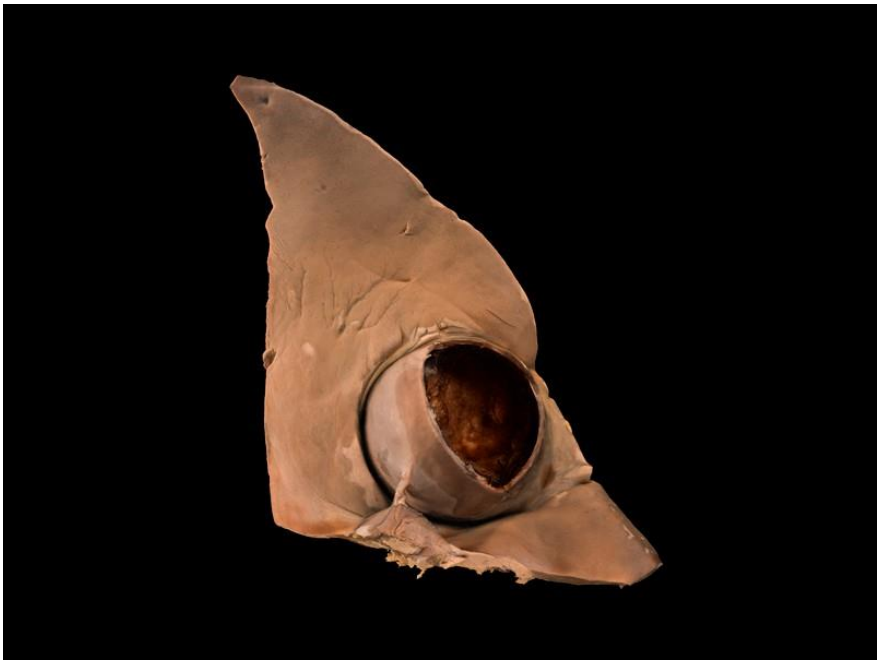

Figure 3.11: *Echinococcus granulosis cyst in a horse liver. Image: The Wellcome Collection (Creative Commons).*

In contrast, the growth and proliferation of *E. multilocularis* larvae have been equated to metastatic growth in cancer (Czermak et al. 2001; Toussaint et al. 2001). The lesions are multilocular, and resemble the alveoli of the lungs (Czermak et al. 2001). Lesions (daughter cysts) proliferate as peripheral extensions of a parent lesion, similar to the growth of a tumour (Czermak et al. 2001). The lesions initiate necrosis at the site of development and cause significant destruction to organs (Czermak et al. 2001; Toussaint et al. 2001).

Bone is an exception where a pericyst does not form in *E. granulosis*, and due to preference of vascularised areas such as trabecular bone and in the medullary canal, proliferation can be extensive and rapid as in the case of *E. multilocularis* (Beggs 1985). Bone infection occurs through infiltration of larvae from adjacent infected tissue or from the bloodstream (Beggs 1985; Song et al. 2007).

3.7.2 Epidemiology of Hydatids Disease

A close relationship with dogs and ruminants are directly associated with human hydatids disease, and pastoralists are particularly at risk for this disease (Beggs 1985; Deplazes et al. 2017). Sylvatic strains are more rare and in present day are associated with regions of high altitude (Beggs 1985). There does not appear to be a direct relationship

between the prevalence in dogs or livestock and the prevalence in humans infected by *E. granulosis* in endemic regions (Eslami and Hosseini 1998).

Most cases in humans are acquired in childhood, but due to the slow progression of disease, clinical symptoms tend to not present until approximately 30 or 40 years of age (Agarwal et al. 1992; Beggs 1985). The disease can be fatal, and mortality is particularly associated with the rupture of cysts that can induce an anaphylactic response. Death can also occur due to a secondary infection (Beggs 1985). A heightened inflammatory response in skeletal hydatids disease, due to lack of pericyst formation, is also associated with increased risk of death (Song et al. 2007).

3.8 Mycosis

Various fungal infections are known to result in skeletal involvement. These fungal spores thrive in soils (Goodwin et al. 1981; Oberoi et al. 2012). Diseases including coccidioidomycosis *(Coccidiodes immitis* and *C. posadasii)*, blastomycosis (*Blastomyces dermatitidis)*, histoplasmosis *(Histoplasma capsulatum* and *H. duboisii)*, aspergillosis (various *Aspergillus* sp.), and cryptococcosis *(Cryptococcus neoformans neoformans* and *C. neoformans gattii)* rarely affect the musculoskeletal system, but are more frequent in immunocompromised individuals (Corr 2011; Denning 1998; Goodwin et al. 1981; Oberoi et al. 2012; Perfect and Casadevall 2002).

3.8.1 Pathogenesis and Pathophysiology of Mycosis

Transmission of fungal spores into the human body often occurs through open wounds or through the respiratory tract whereby haematogenous spread occurs (Corr 2011; Oberoi et al. 2012; Pappas et al. 1993). Mycosis is predominantly subclinical, with a cellular immune response containing the infection (Bradsher et al. 2003; Denning 1998). In acute forms mycotic infection can imitate pneumonia and are self-limited, lasting only 1 to 3 weeks (Bradsher et al. 2003; Oberoi et al. 2012; Pappas et al. 1993). Symptoms include fever, coughing, body aches, weakness and loss of appetite (Oberoi et al. 2012). However, when infected through the respiratory tract, the spores can be phagocytosed by innate immune cells in the lung alveoli as an immune response wherein granulomas form (Anstead and Graybill 2020). In chronic forms of the disease, the granulomas burst and release high numbers of spores in the lungs that are then subsequently formed into further granulomas

(Anstead and Graybill 2020; Goodwin et al. 1981). Similar to other granulomatous infections, these granulomas can become necrotic in severe cases and cause cystic cavities (Figure 3.12; Anstead and Graybill 2020). In this sense, mycotic infections mimic the symptoms and clinical signs of chronic tuberculosis (Goodwin et al. 1981).

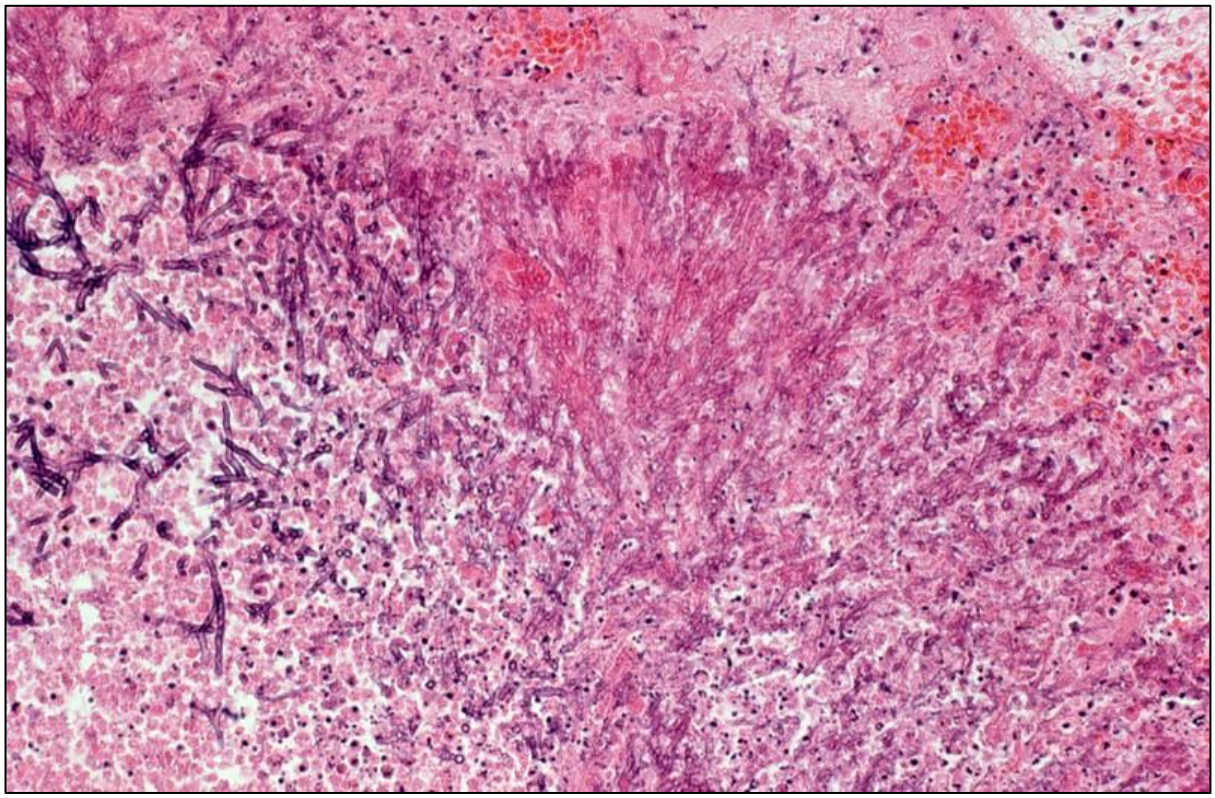

Figure 3.12: *Invasive aspergillosis of the lungs with associated necrosis (dark purple stain). The Aspergillus fungi are closely packed. This individual was immunocompromised through HIV co-infection. Image: The Wellcome Collection (Creative Commons).*

A disseminated form of disease can develop particularly in immunocompromised individuals where spores infect other regions of the body (Corr 2011; Goodwin et al. 1981; Oberoi et al. 2012). The frequency of disseminated disease varies between the different mycotic infections. For example, in coccidioidomycosis, only 0.5-1% of infected individuals develop disseminated disease where bone infection can develop, whereas bone infection is more common in blastomycosis (Anstead and Graybill 2020; Oberoi et al. 2012; Pappas et al. 1993). Disseminated disease can affect every organ but primarily causes papules, nodes or abscesses of the skin and infiltrates the central nervous system (Anstead and Graybill 2020; Bradsher et al. 2003). Rare complications of mycotic disease include pericarditis and mediastinal fibrosis or mediastinal granulomas (Goodwin et al. 1981).

Systemic hypersensitivity can occur from acute infection in coccidioidomycosis, and a disease known as Valley Fever develops (Anstead and Graybill 2020). Fever, severe system wide inflammatory response particularly in skin and fatty tissue, and joint pain occurs in this condition (Anstead and Graybill 2020). However, death only occurs if the disease progresses to a chronic form (Dickson and Gifford 1938).

3.8.2 Epidemiology of Mycosis

The mycotic infections generally have geographic restrictions. Coccidioidomycosis is found in the Americas in arid environments, blastomycosis in North America and Africa, histoplasmosis in temperate regions, and *C. neoformans gattii* cryptococcosis is found in subtropical regions of the world (Goodwin et al. 1981; Oberoi et al. 2012; Pappas et al. 1993; Perfect and Casadevall 2002). Aspergillosis and *C. neoformans neoformans* cryptococcosis are found globally (Denning 1998; Perfect and Casadevall 2002). Therefore, some consideration of geographic spread of fungi needs to be taken into consideration in the differential diagnosis of skeletal mycosis. Cryptococcosis, histoplasmosis and aspergillosis are then of primary focus in skeletal collections of Asia. However, geographical boundaries of present day fungi may not reflect those of the prehistoric past and all fungi should be considered in differential diagnoses.

Immunocompromised individuals and women in their third trimester of pregnancy are at higher risk of symptomatic mycosis (Anstead and Graybill 2020; Denning 1998; Pappas et al. 1993). Inadequate neutrophil (innate immune cell) response may be an underlying cause for system failure to contain the spores leading to disseminated disease (Pappas et al. 1993). Approximately one-third of cases of disseminated coccidioidomycosis result in death, particularly when the central nervous system is involved (Anstead and Graybill 2020). Similarly, deaths from blastomycosis are associated with disseminated disease leading to fatal meningitis (Pappas et al. 1993). A high risk of mortality can be assumed in skeletal cases of mycosis.

3.9 Summary of the Specific Infectious Diseases That Affect Bone

A range of bacterial, fungal and parasitic infections were addressed in the section above. While these pathogens vary in their pathogenesis, pathophysiology and epidemiology, the human host response is shared amongst these diseases. For all of them, if

the host fails to eliminate the pathogen, the immune response aims to contain the pathogen within granulomas. Disseminated disease leading to skeletal expression occurs with necrosis of these granulomas. The degree of overlap in the expression of specific infectious diseases in bone, then necessitates differential diagnosis. Chapter 5 will explore in detail differences in skeletal expression of these diseases that may enable identification of these diseases in archaeological dry bone. The following section discusses the pathogenesis, pathophysiology and epidemiology of nutritional diseases that affect the skeleton.

3.10 Bone Modelling and Remodelling

Nutritional diseases affect bone metabolism during growth and maintenance, therefore the normal processes of these aspects need to be understood. Bone *modelling* is the initial process of skeletal growth prior to maturation in nonadults (Scheuer and Black 2000). Bone *remodelling* is the process of bone turnover that occurs in growing nonadults and mature adults. Skeletal tissue continually undergoes *remodelling* processes in homeostasis. Bone *modelling* and *remodelling* involves the activity of osteoclasts which resorb old bone, and are then followed by osteoblasts depositing an unmineralised matrix called *osteoid* (Junqueira and Carneiro 1980; Stout and Crowder 2012). The bone is then subsequently mineralised by osteoblasts which release inorganic hydroxyapatite crystals, constructed of mostly phosphate and calcium (Anderson 1989; Raggatt and Partridge 2010; Stout and Crowder 2012).

In the process of *modelling,* bones form from ossification centres within soft tissue following a cartilage template (appendicular skeleton) or from apposition on soft tissue (intramembranous in most of cranium) (Scheuer and Black 2000; White et al. 2012). Primary ossification centres form within the endochondral template approximately 9 weeks after conception (Bagnall et al. 1982). For long bones, the centre of the shaft (diaphysis) is the first to ossify (Bagnall et al. 1982; White et al. 2012). From this ossification centre bones grow longitudinally (linear) as well as appositionally (White et al. 2012). Ossification occurs through the production of osteoblasts from a thin membrane which surrounds the cartilage known as a *perichondrium,* the precursor for the *periosteum* (White et al. 2012). These bones do not possess epiphyses which ossify and develop independently to longitudinal growth (Bagnall et al. 1982; White et al. 2012). When initially mineralised during modelling (in bone growth), the bone takes on a woven appearance before reorganising into dense, smooth

and compact lamellar bone. In normal remodelling of compact bone, microscopic concentric units termed osteons form, where vascular channels for nutrients and nerve communication are surrounded by circular deposits of lamellar bone (Su et al. 2003).

The *remodelling* process is essential for continued maintenance and upkeep of the skeletal system, that as a living organ, provides important metabolic functions in the body (Hadjidakis and Androulakis 2006). In nonadults the remodelling process is much faster than in adults due to growth and development (Parfitt et al. 2000). In adults the remodelling process, leading to a complete replacement of the bone matrix, can take up to 15 years for some skeletal elements (Bell et al. 2001).

3.11 Scurvy

Ascorbic acid (Vitamin C) is an antioxidant free radical compound with the ability to bind to aggressive oxidative compounds and make them less reactive, thereby playing a crucial role in the maintenance of the cellular membrane of intracellular organelles (Linster and Van Schaftingen 2007). It also plays an antioxidant role in the plasma surrounding the lung, lens and retina of the eye (Bendich et al. 1986). Oxidation occurs due to inflammatory immune response to pathogens, therefore Vitamin C plays an essential role in immune function (Wintergerst et al. 2006). Most mammals synthesise ascorbic acid. However, humans and other haplorrhine primates cannot, and require dietary Vitamin C (Hirschmann and Raugi 1999; Keenan et al. 2002). Vitamin C is also essential in the production of collagen and cement formation in the body. Lysyl and prolyl (procollagen molecules) are hydroxylised by enzymes which require ascorbic acid for proper function. Collagen fibres are rendered unstable, weakening collagen-based structures in the body such as blood vessels (Hirschmann and Raugi 1999; Maat 2004). Chronic haemorrhaging subsequently occurs in Vitamin C deficiency due to repeated rupturing of weak blood vessels causing the nutritional disease known as scurvy (Hirschmann and Raugi 1999).

3.11.1 Pathogenesis and Pathophysiology of Scurvy

At minimum 10mg a day is required to prevent clinical scurvy (Hirschmann and Raugi 1999). Within a few weeks of restricted dietary Vitamin C, fatigue develops as the first symptom (Hirschmann and Raugi 1999). Within 90 days of deficiency, bodily stores of Vitamin C are depleted (Hirschmann and Raugi 1999). Extended periods of scurvy over a

few months can then result in hyperkeratotic papules around hair follicles, corkscrew hairs and eventually perifollicular and subperiosteal haemorrhaging due to weakened blood vessels (Figure 3.13; Hirschmann and Raugi 1999; Lewis et al. 1998). Haemorrhages have been reported to occur in the conjunctiva, eye lids, retrobulbar space, the sheaths of the optic nerve and in the limbs (which can cause neuropathy) (Hirschmann and Raugi 1999; Lewis et al. 1998). Healed wounds prior to deficiency have also been known to reopen due to disruption in maintenance of collagen scar tissue (Hirschmann and Raugi 1999). In advanced cases, swelling and bleeding of gums occurs, that can become necrotic especially in association with gingivitis, and eventually lead to tooth loss (Hirschmann and Raugi 1999).

A multitude of other symptoms can occur including joint pain, joint effusions, ankle oedema, mucosal ulceration, weakness, shortness of breath, and insufficiency fractures of the spine (Hirschmann and Raugi 1999; Keenan et al. 2002; Lewis et al. 1998). Pain associated with swelling of joints, movement of limbs, and bone pain predominantly due to haemorrhaging can sometimes lead to inability to walk (Hirschmann and Raugi 1999; Keenan et al. 2002; Ortner and Ericksen 1997). Increased activity levels initially encourage the development of haemorrhaging and oedema, particularly in the limbs (Keenan et al. 2002).

The production of abnormal type X collagen in children can cause metaphyseal deformities (Keenan et al. 2002). Calcified cartilage at the provisional zone of calcification of the metaphyseal plates, during growth, lacks osteoid, as Vitamin C plays a role in osteoid production (Keenan et al. 2002). This results in thinning trabeculae in metaphyses and an increased occurrence of microfractures (Keenan et al. 2002). Lastly, death can occur due to pulmonary hypertension, myocardial haemorrhaging, pericardial haemorrhaging, and most commonly fatal shock due to internal blood loss and impaired vasoconstriction (Hirschmann and Raugi 1999).

3.11.2 Epidemiology of Scurvy

Diets poor in Vitamin C generally result in Vitamin C deficiency. In developed countries scurvy is exceedingly rare due to the variety of foods available. Scurvy remains a risk for individuals who consume high quantities of alcohol and in individuals highly selective of the foods they eat, restricting dietary availability (Keenan et al. 2002; Léger 2008). Scurvy remains a risk in diets that over rely on crop foods, which contain sufficient

quantities of macronutrients, but at the expense of sufficient micronutrients. Scurvy is common in situations of famine and poor access to food sources, or in refugee camps where relief foods provide macronutrient requirements but are poor in vitamin C (Desenclos et al. 1989; Tontisirin et al. 2002). Finally, processing of foods through cooking also can reduce the content of Vitamin C by 20 to 40% of the original raw food product thereby reducing bioavailability (Hirschmann and Raugi 1999).

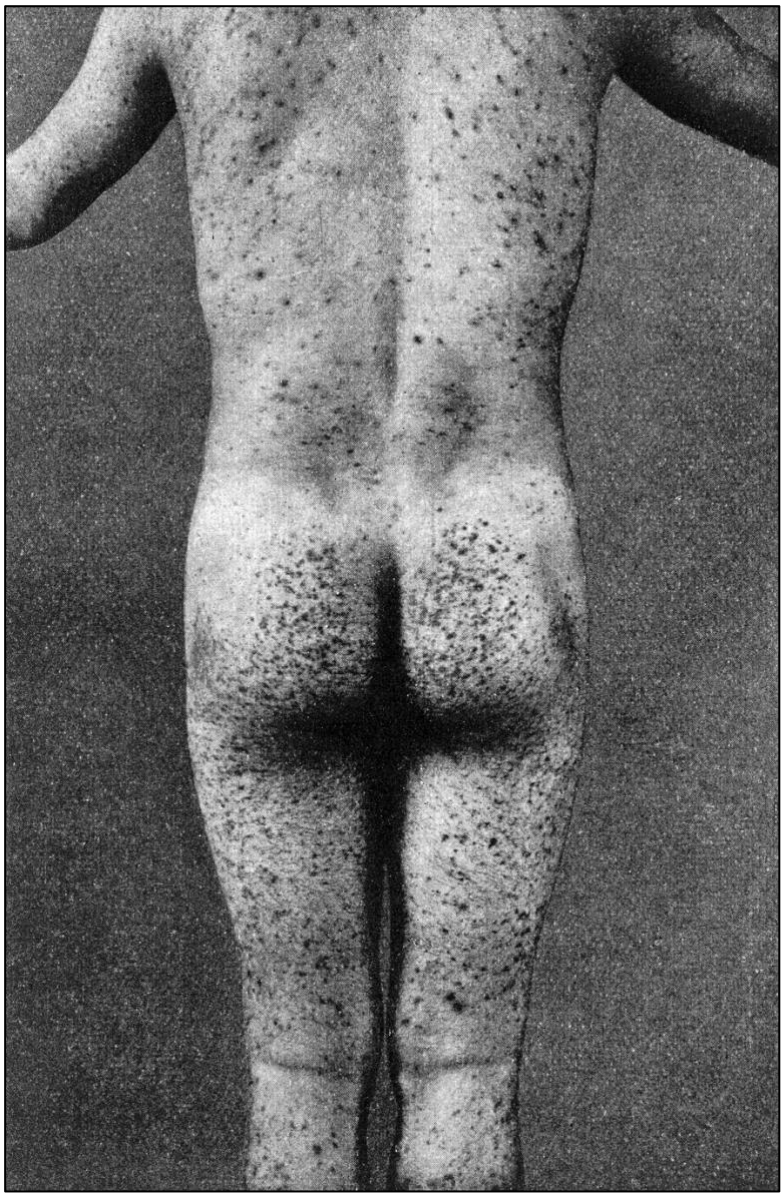

Figure 3.13: *Subcutaneous haemorrhaging in scurvy. Image: The Wellcome Collection (Creative Commons).*

A genetic susceptibility for scurvy has also been determined particularly amongst Asian populations with the Haptoglobin 2-2 genotype. This allele is responsible for an

increase in in-vivo oxidation of ascorbic acid resulting in lower blood concentrations of the vitamin (Delanghe et al. 2007). The development of clinical scurvy therefore results from an interaction between genetics, activity levels and the bioavailability of Vitamin C.

Direct mortality rates for scurvy are difficult to discern from clinical data due to the rarity of the disease today, the intentions of clinical research to prevent death in reported cases, as well as scurvy being common in conditions where multiple nutrient deficiencies have occurred (Nieburg et al. 1992). However, scurvy has been associated with increased mortality in individuals with various disease co-morbidities (Raynaud-Simon et al. 2010). Given the reparative function of Vitamin C in the body, deficiency can play a significant role in mortality from infectious and cardiovascular diseases (Khaw and Woodhouse 1995).

3.12 Rickets and Osteomalacia

Rickets and osteomalacia are bone deforming metabolic diseases caused by poor mineralisation of the skeleton (Wharton and Bishop 2003). These diseases occur due to disruption of bone intake of calcium or phosphate in the process of mineralisation which can be affected by dietary, hormonal, genetic and environmental factors (Brickley and Ives 2010). The pathogenesis of the diseases are complex and often arise from a suite of interacting factors which lead to disorder (Wharton and Bishop 2003). Deficiency of Vitamin D, a regulator of calcium and phosphate in the body, is the most common cause of bone mineralisation disorders causing rickets (childhood mineralisation disorder) and osteomalacia (adult mineralisation disorder).

3.12.1 Vitamin D, Calcium and Phosphate

Vitamin D, particularly in its most active metabolic form 1,25-dihydroxyvitamin D_3, plays a number of roles in the body. It can act as a modulator in the expression of a number of genes including but not restricted to the *TP53* tumour suppressor gene, DNA repair, metabolism, oxidative stress and membrane transport (Morris and Anderson 2010). 1,25-dihydroxyvitamin D_3 functions as a regulator in the intestinal absorption of calcium and phosphate, and regulates the homeostasis of calcium and phosphate in extracellular fluid (Morris and Anderson 2010). As such, Vitamin D deficiency leads to abnormal bone changes as it influences the absorption of calcium and phosphate, both required for bone mineralisation (Morris and Anderson 2010). It has also been proposed that Vitamin D

directly mediates bone remodelling through osteoblast differentiation, osteoclastogenesis and bone mineralisation (Anderson et al. 2011). Primary synthesis of Vitamin D occurs through UV-B irradiation of skin tissue, but cholecalciferol, a dietary available source, can be found in a number foods including fatty fishes (Lamberg-Allardt 2006; Morris and Anderson 2010). Pre-Vitamin D_3 is synthesised using UV-B rays from 7-dehydrocholesterol in the skin (Morris and Anderson 2010). The entire chemical synthesis chain from pre-Vitamin D_3 to 1,25-dihydroxyvitamin D_3 can occur at skin level (Morris and Anderson 2010). Blood concentrations of 25-dihydroxyvitamin D_3 (the inactive pre-metabolite form) less than 10-12 ng/ml and 25-30 ng/mol trigger clinical symptoms of rickets and osteomalacia respectively (Pettifor et al. 2018). 25-dihydroxyvitamin D_3 has a half-life of 2 to 3 weeks in soft tissue, therefore stores are rapidly depleted if not replenished (Pettifor et al. 2018).

Calcium and phosphate comprise the major non-organic elements of bone in the form of hydroxyapatite (Viswanath et al. 2010). Deficiency or disruption of absorption of calcium or phosphate then causes issues in mineralisation during growth and maintenance of bone tissue resulting in mineralisation disorders (Pettifor 2004; Viswanath et al. 2010). When plasma levels of 1,25-dihydroxyvitamin D_3 and calcium decrease, parathyroid hormones increase (Morris and Anderson 2010). High levels of parathyroid hormones increase the synthesis of 1,25-dihydroxyvitamin D_3 in the renal system and also regulates calcium absorption levels in order to maintain homeostasis (Morris and Anderson 2010; Munson 1955). Disruptions to calcium, Vitamin D, phosphate and parathyroid hormone levels can then all cause demineralisation disorders (Brickley and Ives 2010).

3.12.2 Pathogenesis and Pathophysiology of Rickets and Osteomalacia

Mineralisation disorders are clinically referred to as rickets when bone modelling is disrupted (Wharton and Bishop 2003). Osteomalacia is the term used to describe physiological disruption to bone remodelling. In adults, the process of bone modelling is no longer occurring and disruptions in mineralisation are restricted to remodelling. Therefore in nonadults both rickets and osteomalacia occurs, whereas in adults the skeletal changes are restricted to osteomalacia only. However, for ease of description all skeletal changes in nonadults tend to be referred to as rickets (Brickley and Ives 2010). This thesis follows this terminology. Here the term *rickets* will apply to mineralisation disorders in nonadults, and *osteomalacia* will apply to mineralisation disorders in adults. However, as discussed in

Chapter 8, a level of overlap in the clinical manifestations of these conditions is observed in older adolescents. *Residual rickets* is a term that defines clinical symptoms of rickets observed in adults, representing severe bone mineralisation disorders in childhood, leaving 'residual' changes to bone (Brickley and Ives 2010).

Poorly mineralised osteoid leads to plastic yet fragile bones in osteomalacia (Bhan et al. 2010; Jaffe 1972). Fractures (particularly infractions/ psuedofractures) and bending are characteristic of this disease (Bhan et al. 2010; Jaffe 1972). Bones which take high biomechanical loading or have higher rates of remodelling, for example the vertebral column, pelvis, ribs and sternum, are more commonly affected (Jaffe 1972).

In nonadults, disruption of mineralisation leads to extensive deposits of unmineralised bone at the site of endochondral ossification as well as demineralisation and "softening" of bones (Wharton and Bishop 2003). Bowing of the long bones is accompanied by expansion of the growth plates characterised by cupping, swelling and/or flaring of the metaphyses (Figure 3.14; Klein and Simmons 1993; Wharton and Bishop 2003). Areas of biomechanical load become softened and deformities such as *coxa vara* (decrease in the angle of the femoral neck) can also occur (see Figure 3.15). While bowing deformities and *coxa vara* of long bones can occur in osteomalacia this is not common and is more characteristic of rickets (Jaffe 1972). Demineralisation of the skull vault means the vault bones can become soft and thin (craniotabes), and bossing (anterior protrusion) of the skull can occur (Klein and Simmons 1993).

Clinically, rickets and osteomalacia are associated with convulsions due to hypocalcaemia, tetany (muscular contractions), and in severe cases heart failure (Jaffe 1972; Wharton and Bishop 2003). In advanced cases pseudoparalysis develops due extensive bone deformities, and delays in motor development have also been documented (Bhan et al. 2010; Klein and Simmons 1993; Wharton and Bishop 2003). Fractures in children are rare, but do occur due to the fragility of poorly mineralised bone (Wharton and Bishop 2003). In adults, fractures are frequent in osteomalacia (Jaffe 1972). Change of body position such as rising from squatting or sitting down can cause debilitating bone and muscular pain, due to severe bone deformity (Bhan et al. 2010; Jaffe 1972). Links to increase in disorders later on in life including type 1 diabetes, multiple sclerosis, cancers, schizophrenia and heart disease

following childhood Vitamin D deficiency have been reported (Grant 2002; McGrath 2001; van der Mei et al. 2001; Wharton and Bishop 2003).

A number of genetic causes interrupt conversion of various Vitamin D products in forms useable by the body (e.g. calcidiol to calcitriol) and cause severe forms of rickets (Wharton and Bishop 2003). Hypophosphatemic rickets (previously termed Vitamin D resistant rickets) are also predominantly caused by genetic mutations which disrupt regulation and absorption of phosphate (Verge et al. 1991). Only in extreme circumstances of starvation does hypophosphatemia result from dietary factors and generally this is an acute form (Fitzgerald 1978; Waldholtz and Andersen 1988).

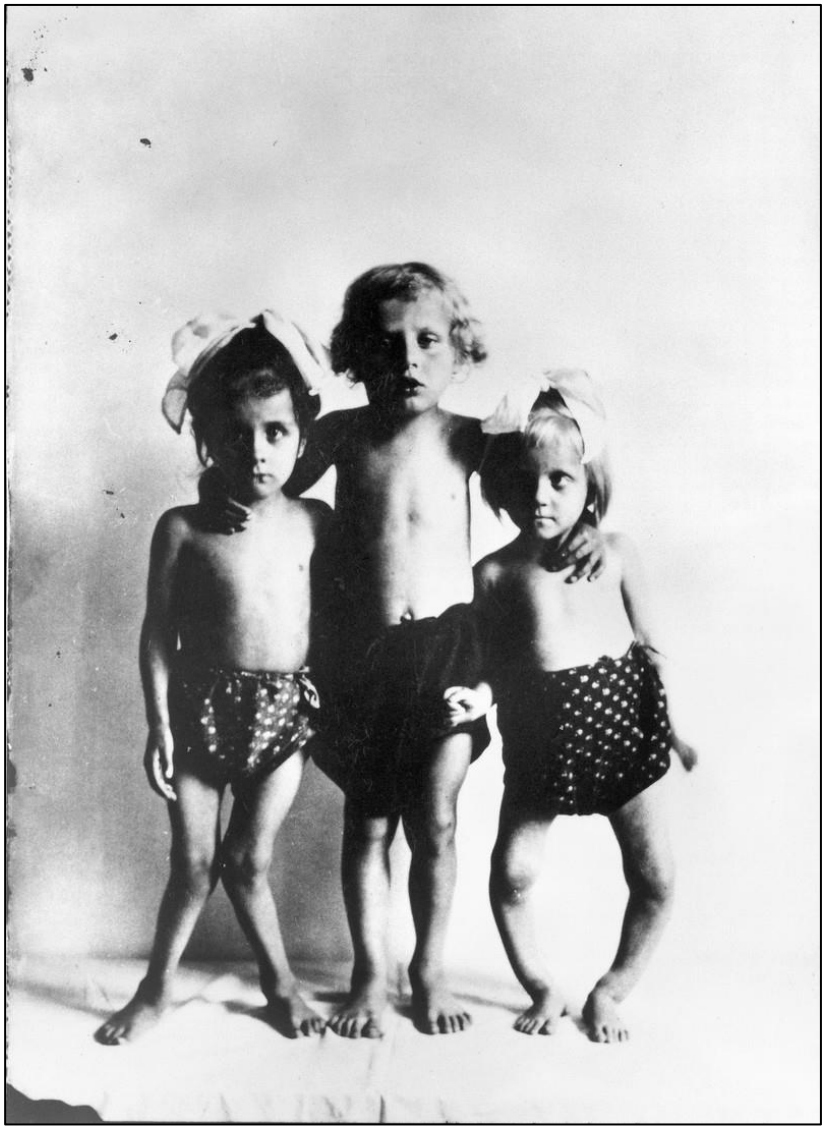

Figure 3.14: *Three children with long bone bending deformities due to rickets. Image: The Wellcome Collection (Creative Commons).*

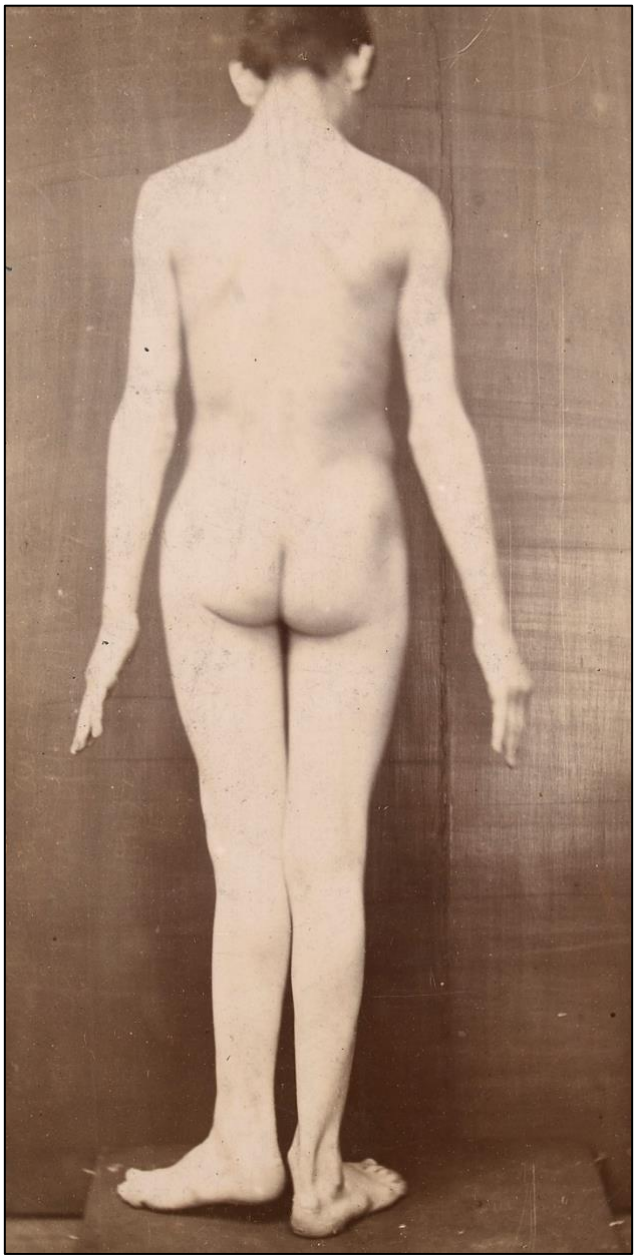

Figure 3.15: *Individual with coxa vara of the left femur. Image: The Wellcome Collection (Creative Commons).*

3.12.3 Epidemiology of Rickets and Osteomalacia

Genetic factors for risk of rickets are complex. Rickets has been associated with an increased frequency of Vitamin D receptor polymorphism genotype *FF* (Mao and Huang 2014). Enigmatically, this genotype codes for a better functioning receptor for Vitamin D, and the association between rickets and the *FF* genotype is unclear (Fischer et al. 2000; Pettifor et al. 2018). The *FF* genotype is lower in European and Asian populations (Fischer et al. 2000).

As Vitamin D is primarily synthesised by the sun, lack of exposure to ultraviolet light increases susceptibility of disease, particularly where dietary substitutes of Vitamin D are not present (Pettifor et al. 2018). Factors which affect sun exposure include latitude, atmospheric pollution, confinement indoors and the wearing of clothing that covers most areas of the skin (Klein and Simmons 1993; Pettifor et al. 2018). Inadequate UV penetrates the atmosphere in latitudes above 40°C N or S (such as in Mongolia studied in this thesis) to be synthesised in the skin presenting significant risk of Vitamin D deficiency in these regions of the world (Pettifor et al. 2018).

An agricultural crop base increases the risk for calcium deficiency where supplements from dairy are lacking (Pettifor 2004). The crop base provides inadequate amounts of calcium, and the phytates in grains such as wheat and rice inhibit absorption of calcium in the gut (Pettifor 2004). Calcium deficiency in isolation is not known to cause osteomalacia and instead causes osteoporosis of the skeleton (Pettifor 2004). Calcium deficiency is then only expected to be observed in nonadults.

Females, particularly during pregnancy, are at an increased risk for osteomalacia from Vitamin D deficiency due to the increased demands of the foetus (Jaffe 1972). A high mortality of both infant and mother is associated with osteomalacia due to the narrowing of the pelvis (Jaffe 1972). Additionally, while calcium deficiency does not lead to osteomalacia, a mother's bones tend to be leached for calcium in periods of nutritional stress to compensate for the growing foetus in pregnancy. Research suggests dietary intake is independent of calcium secretion in breast milk, except in states of severe deficiency (Olausson et al. 2012). Foetal evidence for calcium deficiency then implies severe calcium deficiency in their mother. Additionally, dietary requirements for calcium increase in the first 6 months after birth, compared to foetal requirements, rendering post-natal infants susceptible to calcium deficiency (Almaghamsi et al. 2018).

3.13 Summary of Summary of Specific Nutritional Diseases That Affect Bone

Scurvy and rickets/osteomalacia impact the deposit and mineralisation of osteoid respectively. Therefore, these conditions are readily observable in the archaeological record. Unlike in infectious diseases, that leave skeletal markers due to granulomatous response, nutritional disorders directly affect the growth and maintenance of bone and therefore

produce considerably different skeletal markers. However, there is a degree of overlap between the two nutritional diseases as to their impact on bone, and differential diagnosis is required. The identification of these skeletal markers is discussed in further detail in Chapter 5.

3.14 Anaemia

Anaemia is a condition where there is a reduction of red blood cells carrying oxygen throughout the body (Stedman's Medical Dictionary 1995). The condition arises from a number of aetiologies including trauma, dietary deficiencies (iron, B12, folate), genetic disorders (thalassaemias and sickle cell anaemia), infection, neoplasms and autoimmune disorders (Mehta and Hoffbrand 2009). While the specific aetiology commonly cannot be determined, skeletal lesions do form in chronic anaemia during childhood and therefore are present in the archaeological record (discussed further in Chapter 5). The following section discusses two major causes of anaemia that are of interest in the three case studies presented in this thesis.

3.15 Iron Deficiency Anaemia

Iron deficiency anaemia is the most common form of anaemia and nutritional disease globally, therefore it can be expected to contribute a significant proportion of evidence of anaemia in the skeletal record (Camaschella 2015; Clark 2008; Killip et al. 2007). Iron functions in respiration, energy production, DNA synthesis and cell proliferation (Camaschella 2015). Particularly it is important in reactions essential for oxygen transport and storage in the bloodstream, and the production of adenosine triphosphate (Clark 2008). Iron is found in every cell of the body, therefore deficiency has considerable impact on all body functions (Clark 2008). Severe iron deficiency causes anaemia, which is clinically associated with microcytic hypochromic red cell development (discolouration of red blood cells due to decrease in oxygen in the blood) (Camaschella 2015).

3.15.1 Pathogenesis and Pathophysiology of Iron Deficiency Anaemia

Iron is initially absorbed from dietary sources in the jejunum (Killip et al. 2007). Dietary sources include haem iron from meat and non-haem iron from plant and dairy sources (Killip et al. 2007). Non-haem iron is not directly bioavailable, requires acid

digestion, and absorption is readily inhibited by other dietary compounds such as calcium and fibre (Killip et al. 2007).

Iron is stored and recycled in the body (Camaschella 2015). However, iron is only absorbed at the rate of approximately 1 to 2mg a day to prevent iron overload (Camaschella 2015). In non-menstruating people 1mg of iron is lost a day (Killip et al. 2007). Recycling of iron in the body occurs through phagocytosis of dead erythrocytes (Camaschella 2015). Hepcidin, a peptide hormone, is primarily responsible for the homeostasis of iron acquisition in the body (Camaschella 2015). Increased levels of hepcidin is produced following heightened erythropoiesis, and counteracts cellular iron absorption processes in a negative feedback loop, which stabilises the levels of active iron in the body (Camaschella 2015). In states of low iron availability the production of hepcidin is inhibited, and absorption can increase three to fivefold as a buffer to iron deficiency (Camaschella 2015). Severe and long-term restriction of availability then leads to anaemia following depletion of the body's iron stores (Clark 2008).

Iron deficiency causes microcytic anaemia (small hypochromic red blood cell production) (Killip et al. 2007). Iron is essential for the synthesis of the haem group in the haemoglobin of red blood cells which plays a primary role in the transport of oxygen throughout the bloodstream to cells of organs and tissues in the body (Hsia 1998; Lopez et al. 2016). The small size of red blood cells occur due to decreased production of haemoglobin (DeLoughery 2014). Iron deficiency anaemia then restricts oxygen transport in the body resulting in system wide oxygen starvation termed *hypoxia* (Camaschella 2015).

Iron deficiency anaemia causes fatigue, weakness and increased susceptibility to infectious diseases due to hypoxia and disruption of immune cell proliferation (Camaschella 2015; Ekiz et al. 2005). In children, anaemia can delay mental and motor development (Camaschella 2015; Killip et al. 2007). Increased newborn and maternal mortality is associated with iron deficiency anaemia during pregnancy (Camaschella 2015).

3.15.2 Epidemiology of Iron Deficiency Anaemia

Iron deficiency affects approximately one third of the global population, with anaemia occurring in one-third of iron deficient individuals (Camaschella 2015). Therefore,

it is a common disease and a significant nutritional factor of consideration in archaeological skeletal assemblages. The primary causes for global iron deficiency are due to direct dietary factors and/or parasitic infestations of the gut particularly of intestinal worms (Camaschella 2015).

Increased demand for iron due to growth in infancy and adolescence, menstruation, and pregnancy increases the risk of developing anaemia if insufficient dietary sources are available (Camaschella 2015; Clark 2008). Therefore children and premenopausal women are at an increased risk of developing iron deficiency anaemia (Camaschella 2015). Factors restricting iron absorption including inflammatory conditions, infectious diseases which thrive on iron stores in the body, or diseases of chronic blood loss also increase the risk of developing anaemia (Camaschella 2015; Clark 2008; DeLoughery 2014). Iron deficiency is also associated with increasing age (Camaschella 2015). Paradoxically, the skeletal indicators for anaemia only occur in childhood (Brickley 2018; Stuart-Macadam 1985). A rare autosomal recessive disease identified as iron-refractory iron-deficiency anaemia, which results in dietary iron resistance, mimics the clinical symptoms of dietary or parasitic iron deficiency (Camaschella 2015). This disease may also be a cause for skeletal lesions of anaemia in the archaeological record.

3.16 Thalassaemia

Thalassaemia is the most common genetic anaemia worldwide (Aydinok 2012). In normal haemoglobin production, the two components: the alpha-globin and beta-globin chains partner. The two forms of disease, alpha and beta thalassaemia, causes disruption of the synthesis of the alpha or beta chains respectively, resulting in malformation of haemoglobin which is a tetramer compound (Aydinok 2012; Galanello and Cao 2011). This tetramer structure is essential in the role haemoglobin plays in transporting oxygen throughout the body (Hsia 1998). Three forms are recognised: a severe homozygous form (thalassaemia major), a moderate homozygous form (thalassaemia intermedia) and mild homozygous or heterozygous form (thalassaemia minor) (Aydinok 2012). While the three forms of thalassaemia are clinically established, a great number of mutations and deletions in both beta and alpha thalassaemia result in a spectrum of clinical expression, and skeletal changes can vary greatly (Aydinok 2012; Galanello and Cao 2011).

3.16.1 Pathogenesis and Pathophysiology of Thalassaemia

Alpha and beta- globin chains are essential in the formation of haemoglobin tetramers (Aydinok 2012). As the primary function of haemoglobin is to transport oxygen throughout the blood stream for use by body tissues (Hsia 1998). The function of haemoglobin is highly reliant on its tetramer structure and in the case of thalassaemia where synthesis of alpha- or beta- globin is disrupted, malformed haemoglobin molecules are formed and oxygen transport is affected (Aydinok 2012; Galanello and Cao 2011; Hsia 1998).

In homozygous thalassaemia, both chromosomes carrying the alpha- or beta-globin genes are affected (Aydinok 2012; Weatherall 2008). Alpha- and beta- globin genes are coded on the 16^{th} and 11^{th} chromosomes respectively (Aydinok 2012; Galanello and Cao 2011). A heterozygous form is usually asymptomatic (Aydinok 2012). The severity of the alpha and beta thalassaemia is reliant on minor mutations which result in diminished or absent alpha- or beta-globin chains (Aydinok 2012; Weatherall 2008). Due to poor synthesis of beta-chains in beta thalassaemia, an overproduction of non-bound alpha chains increases oxidative damage of the cell membrane and haemolysis of the red cells occur (Aydinok 2012). The *vice versa* process occurs in alpha thalassaemia (Galanello and Cao 2011). As the mutations occur on different chromosomes, alpha and beta thalassaemia can also be co-inherited (Aydinok 2012). Severe anaemia causes ineffective erythropoiesis and expansion of marrow leading to bone deformities (Aydinok 2012).

Symptomatic expression of beta thalassaemia generally begins at around 3 months of age as foetal haemoglobin are gradually replaced with mature haemoglobin from the time of birth (Aydinok 2012; Thein and Menzel 2009). However foetal forms do occur in alpha thalassaemia major (Bart hydrops fetalis syndrome) that mostly leads to death in utero (Galanello and Cao 2011). Foetal haemoglobin contains pairings of alpha- and gamma-globin chains, whereas adult haemoglobin involves the alpha- and beta-globin pairing affecting the difference in the timing of alpha and beta thalassaemia onset (Thein and Menzel 2009). Distinct skeletal deformities occur in Bart hydrops fetalis syndrome that can be present in the archaeological skeletal record (Galanello and Cao 2011).

Thalassaemia is associated with increased iron absorption, and anaemia and iron overload distinctively co-occurs (Aydinok 2012). A number of subsequent complications such as liver disease, endocrine disruptions and cardiac issues occur due to iron overload (Aydinok 2012). Increased erythropoiesis also results in abnormal enlargement of the spleen (splenomegaly) (Aydinok 2012). Severe skeletal changes in beta thalassaemia major and intermedia are caused by increased marrow proliferation, thinning of cortical bone and widening of the diploic spaces (Bouguila et al. 2015). *Rodent face* (or rodent facies) a distinct characteristic skeletal deformity of beta thalassaemia is the outcome from expansion and protrusion of the facial region due to prolonged anaemia (Bouguila et al. 2015).

3.16.2 Epidemiology of Thalassaemia

Thalassaemia is found worldwide but particularly prevalent in Africa, the Middle East, Southeast Asia and the Western Pacific (Aydinok 2012). Clinically significant and non-expressive carrier forms of thalassaemia are demonstrated to provide protection against malaria (Aydinok 2012; Weatherall 2008). Malaria is a disease transmitted by the female anopheles mosquito (White et al. 2014). Four species of the parasite cause disease in humans: *Plasmodium falciparum, P. vivax, P. malariae* and *P. ovale* (Weatherall 2008; White et al. 2014). The disease invades and destroys red blood cells (Weatherall 2008; White et al. 2014). Regions of high prevalence of thalassaemia have been associated with global endemic areas of malaria (Figure 3.16; Aydinok 2012; Weatherall 2008). It is proposed in these regions that malaria, an infectious disease with high mortality, led to stabilising selection for the heterozygous form of thalassaemia (Weatherall 2008). *Falciparum* malaria is particularly associated with high mortality and is the one of the strongest selection pressures currently known (Weatherall 2008). However, *vivax* malaria which causes chronic disease is endemic in the Asia-Pacific region and may have also been a past selection pressure for the emergence of the high prevalence of thalassaemia in Southeast Asia and the Pacific (Flint et al. 1986; Weatherall 2008).

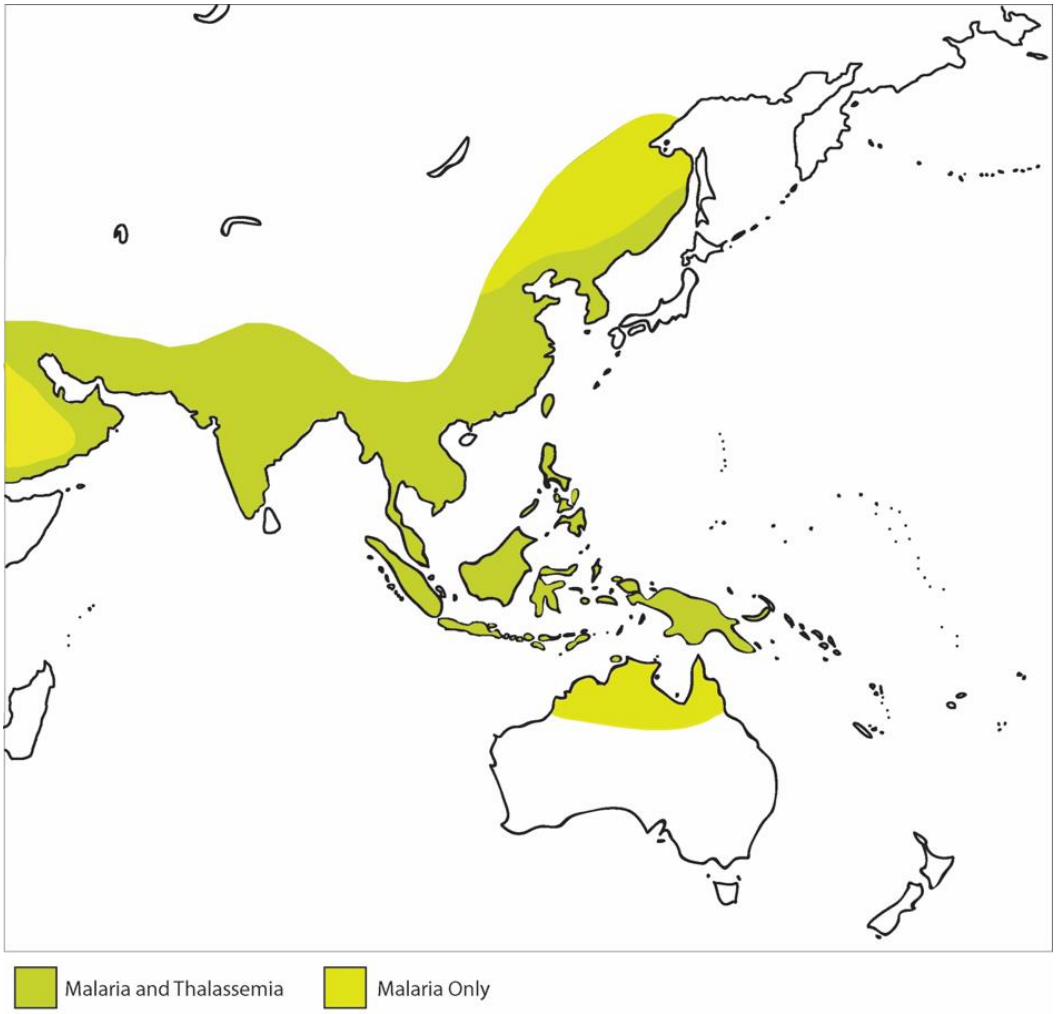

Figure 3.16: *Distribution of Malaria and Thalassaemia in Asia prior to eradication programs. In all regions where thalassaemia is present, malaria is also endemic. Image: adapted from Weatherall (2008: 277).*

3.17 Co-morbidity of Specific Infectious and Nutritional Diseases

Complex co-morbidity between nutritional and infectious diseases exist and this co-morbidity is important in the consideration of overall morbidity and mortality in archaeological skeletal remains. The presence of nutritional deficiency or infectious disease makes one susceptible to the other (Stephensen 2001). Many vitamins and minerals function as regulators in the immune system, whereas pathogens can decrease the availability or increase the demands of certain micronutrients in the body. For this reason, infectious diseases in the archaeological record should not be considered without establishing the level of nutritional stress also (Roberts and Brickley 2018). Skeletal evidence of nutritional stress may also be an indicator of increased pathogen loads, wherein the effects of the pathogen itself is not observable in skeletal material (Buckley 2000).

3.17.1 Vitamin D and Infection

Vitamin D deficiency is a well-known risk factor for both morbidity and mortality to active tuberculosis (Talat et al. 2010). Vitamin D supplementation has been used in the treatment of tuberculosis, and co-morbidity of these diseases has been known for over a century (Zasloff 2006). However, Vitamin D deficiency is now recognised as a risk factor in a wide range of other infectious diseases (de Haan et al. 2014). Vitamin D plays a significant role in cell mediated immunity, responsible for the granulomatous response to bacilli (Nnoaham and Clarke 2008). In the case of tuberculosis, reactivation from latency, or chronic disease can occur due to Vitamin D deficiency (Nnoaham and Clarke 2008). Vitamin D binds to antimicrobial peptides in cells, particularly in neutrophils which are responsible for eliminating a number of viral, bacterial and fungal pathogens (Ginde et al. 2009; Zasloff 2006). Vitamin D deficiency has also been associated with increased mortality when co-occurring with infection as considerable complications such as hypocalcaemia increase in severity alongside sepsis (de Haan et al. 2014).

3.17.2 Vitamin C and Infection

Vitamin C deficiency is associated with increased transmission, mortality and severity of infectious diseases (Sadun et al. 1951). Given the role of ascorbic acid in immunoresponse, deficiency increases the susceptibility of infectious disease. Phagocytosis of pathogens by neutrophils in cell mediated immunity is dependent on the consumption of ascorbate, and ascorbic acid regulates B cell activity. Therefore, systemic levels of vitamin C is a considerably significant factor in the formation of the granulomatous response in the chronic infectious diseases discussed in sections above (Amakye-Anim et al. 2000). In contrast, certain pathogens deplete levels of ascorbate in leukocytes which increases the systemic demand for ascorbic acid (Amakye-Anim et al. 2000). Infections that cause diarrhoea, particularly in infants, are associated with increased excretion of Vitamin C levels and reducing absorption in the gut, thereby decreasing body stores available for phagocytosis to fight infection (Abt et al. 1940).

3.17.3 Iron, Infection and the Iron Withholding Hypothesis

An oxygen rich environment is required for a number of pathogens such as mycobacteria to thrive in the body and require iron in the host to grow. Iron is scavenged from the host body, which can induce the body to *withhold* iron, therefore iron deficiency is

often associated with infection (Boelaert et al. 2007; Knechel 2009; Ratledge 2004; Roberts 2012). This process has been termed the *iron withholding hypothesis*, an evolutionary adaptive suppression of available iron in the body to starve pathogens of oxygen necessary for continued proliferation in the host (Ong et al. 2006). Inflammation increases the production of hepcidin subsequently reducing available iron within the body and may be an underlying adaptive response to infection (Camaschella 2015). However, the relationship between dietary iron and infection is complex. For example, no direct relationship between iron deficiency and tuberculosis has been established, instead iron overload has been demonstrated to increase susceptibility to tuberculosis (Boelaert et al. 2007; Isanaka et al. 2011). Non-haem iron availability is significantly disrupted by inflammation of the gut in infectious diseases such as *Helicobacter pylori* and diarrhoea from these conditions have been demonstrated to impede absorption in the gut (Annibale et al. 2000; de Vizia et al. 1992). Finally, a relationship between malaria and anaemia has been well documented in the clinical literature. However, the relationship with iron deficiency is but one factor in malarial anaemia. The *Plasmodium* parasite destroys red blood cells, slows down production of new red blood cells, decreases iron absorption, and increases folate requirements, all contributing to anaemia morbidity (Menendez et al. 2000).

3.18 Chapter Summary

This chapter has reviewed the literature on the pathogenesis, pathophysiology and epidemiology of infectious diseases, nutritional diseases and anaemias known to leave skeletal markers in the archaeological record. The pathogenesis and pathophysiology of each disease was described to provide background context to pathologies observed in dry bone. Lesions due to infectious diseases observed in the skeletal record are a product of pathogen mediated disease progression *and* human host immune response. The lesions observed in nutritional diseases are a product of the impact of vitamin deficiencies on bone metabolism during growth and maintenance. Additionally, the epidemiology of each of these diseases was discussed to examine which demographic groups are at an increased risk of morbidity and mortality to these diseases.

CHAPTER 4:
SKELETAL CENSUS

4.1 Introduction

This chapter introduces the human skeletal census for each of the six assemblages investigated in this thesis from Vietnam, Mongolia and Japan. The methodological theory for age and sex estimation in human skeletal analysis is first explored, prior to presentation of the methods used in this thesis. Subsequently, the methods of recording of completeness and taphonomy are presented. Finally, a brief introduction, age and sex estimates and discussion on taphonomy and completeness are provided for each assemblage. Estimation of age and sex are essential to meet objectives 4 and 5 of this thesis. These objectives pertain to the assessment of morbidity and mortality of diseases across site and region levels. Additionally, taphonomy factors into disease analysis as poor preservation impedes observation of pathology in dry bone.

4.2 Age and Sex

The minimal standard for demographic analysis in any palaeoepidemiological assessment is that of age and sex (Ortner 2003). The assessment of intra-site variation using these parameters allows for investigation of the impacts of a disease on a population affected by biologically determined susceptibility, an objective of this thesis. Pre-existing age and sex data were used for the Northern Vietnam sites of Man Bac and Con Co Ngua provided by Professor Marc Oxenham (Australian National University) and Associate Professor Kate Domett (James Cook University). The estimation techniques employed for Man Bac and Con Co Ngua align with those employed for the other samples in this thesis. Sex and age estimates for the Mongolian and Japanese samples were assessed by myself.

4.3 Sex Estimation

4.3.1 Sex as a Factor in Palaeoepidemiological Study

Considerable differences in the immuno-response of males and females, as well as underlying gendered differences in risk of exposure and access to resources, means assessing sex as a factor in intrapopulation disease dynamics is necessary in palaeoepidemiological

analysis. Differences in the biology of males and females lead to different levels of susceptibility, during various stages in life. For example, during adolescence males are more susceptible to infectious diseases than females, due to the immunosuppressant properties of testosterone to accommodate rapid growth and maturation during puberty (Bupp 2015). An enhanced female adaptive immune response may counter the trade-off of the detrimental physiological effects of pregnancy (Klein and Flanagan 2016; Ortner 2003). While not directly captured in analysis of sex, differences in exposure to diseases may also stem from gendered divisions in the activities of males and females within a group (Temple et al. 2011). The following section explores the techniques employed by bioarchaeologists to estimate sex prior to justifying the most appropriate methods used in this thesis.

4.3.2 Nonadult Sex Estimation

The estimation of sex in nonadult skeletons, remains one of the largest road blocks in bioarchaeology, particularly to palaeodemography and palaeopathology. Standard sex estimation techniques of adults rely on the development of secondary sex characteristics which only develop with puberty. As such, they are not useful for the determination of sex in nonadults. The analysis of DNA to identify the presence of X and Y chromosomes avoids many of the issues surrounding skeletal analysis of sex in nonadults (Faerman et al. 1998; Kaestle and Horsburgh 2002). DNA assessment is not feasible in palaeoepidemiological studies due to the cost and destructive nature, and low chance of success, of the analysis (Milner and Boldsen 2012).

A recent sex estimation technique developed by Parker et al. (2019) employing the presence of amelogenin protein fragments coded on the X and Y chromosomes and persistent in tooth enamel, has been attempted on deciduous teeth. Good preservation of amelogenin protein fragments in dental material avoids most of the preservation issues in relation to DNA sex estimation. This method currently requires specialised training and equipment in order to estimate sex. As such, it is not universally applied in the field, but provides future opportunities. Due to the issues outlined above, sex estimation of nonadults under the age of approximately 15 was not attempted in this investigation.

4.3.3 Adult Sex Estimation

Morphological and metric adult sex estimation techniques rely on skeletal maturation of secondary sex characteristics following puberty (Krishan et al. 2016). DNA and protein estimation of sex may be possible in adults. However, morphological or metric techniques are more feasible in larger studies. Non-metric sex estimation of adults differentiate features in the cranium and pelvis, whereas sex estimation with metric methods are theoretically possible on all skeletal elements (White et al. 2012). Metric discriminative methods are not discussed here as to date methods applicable to Asian archaeological populations do not exist.

4.3.4 Cranial Non- metric Sex Estimation

The premise of cranial sex estimation is that following puberty, males tend to develop more robust cranial features than females, due to testosterone changes to the musculoskeletal system (Rowbotham 2016; White et al. 2012). A number of cranial sex estimation techniques exist, and rely on the scoring of the degree of robusticity of a cranial feature (Acsádi et al. 1970; Buikstra and Ubelaker 1994; Walrath et al. 2004). Therefore, a trait that is more *gracile* is considered a female trait, and a trait that is *robust* is considered a male trait. An inherent limitation of morphological scoring systems is that these features occur along a continuum (Milner and Boldsen 2012). For example Buikstra and Ubelaker (1994) after Acsádi et al. (1970) present five features of the cranium and mandible with a score range from ‘minimal expression’ (1) to ‘maximum expression’ (5). Features such as the nuchal crest of the occipital bone, mastoid crest of the temporal bone, mental eminence of the mandible and supraorbital margin of the frontal bone are classically reported as sexually dimorphic features (Acsádi et al. 1970; Buikstra and Ubelaker 1994; Ferembach 1980). The recommendation is that techniques that employ multiple cranial features with clear descriptions are more reliable, this is particularly true due to the compounding factor of ancestry, which plays a significant role in the morphology of the skull (Buikstra and Ubelaker 1994; Walrath et al. 2004). The factor of ancestry is pertinent to samples used in this thesis, as there are different population histories for each of the three regions investigated. Walrath et al. (2004) presented ten traits modified from Buikstra and Ubelaker (1994) and Ferembach (1980) based on 42 Inuit crania. Each trait has an independent weighting in accordance with the significance of that feature in sex estimation, resulting in a weighted score. What is recognised in this method is that not all cranial features are of

equal value in the estimation of sex, and that differential preservation of the cranium affects the confidence of sex estimation. Due to the multiple factors that influence cranial morphology, including physiology, behaviour, and genetics, these techniques are considered less reliable than estimation from the pelvis (White et al. 2012).

4.3.5 Pelvic Non-metric Sex Estimation

Due to functional differences in relation to pregnancy in females, the pelvis provides the best indicator for sex estimation and is more reliable than cranial estimates (Tague 1992; White et al. 2012). It is argued that population specific factors have less of an effect on the pelvis than other skeletal elements (González et al. 2007; Steyn and Patriquin 2009). During puberty, females form wider and more rounded pelves, and as a result form wider greater sciatic notches, wider subpubic angles, and morphological difference to the pubic and preauricular areas in comparison to males. An assessment of a number of pelvic features in sex estimation is recommended (Bruzek 2002; Buikstra and Ubelaker 1994; Phenice 1969). The Phenice (1969) method is considered to be the most accurate method (McFadden and Oxenham 2016; White et al. 2012). This method relies on the presence of three feminine traits on the pubis: a ventral arc, subpubic concavity and an ischio-pubic ramus ridge (Figure 4.1). Assessment based on the greater sciatic notch and the preauricular sulcus is also presented in Buikstra and Ubelaker (1994) and scored along a scale similar to that of cranial morphological characteristics. In this instance, maximum expression of the feature is considered a more feminine trait.

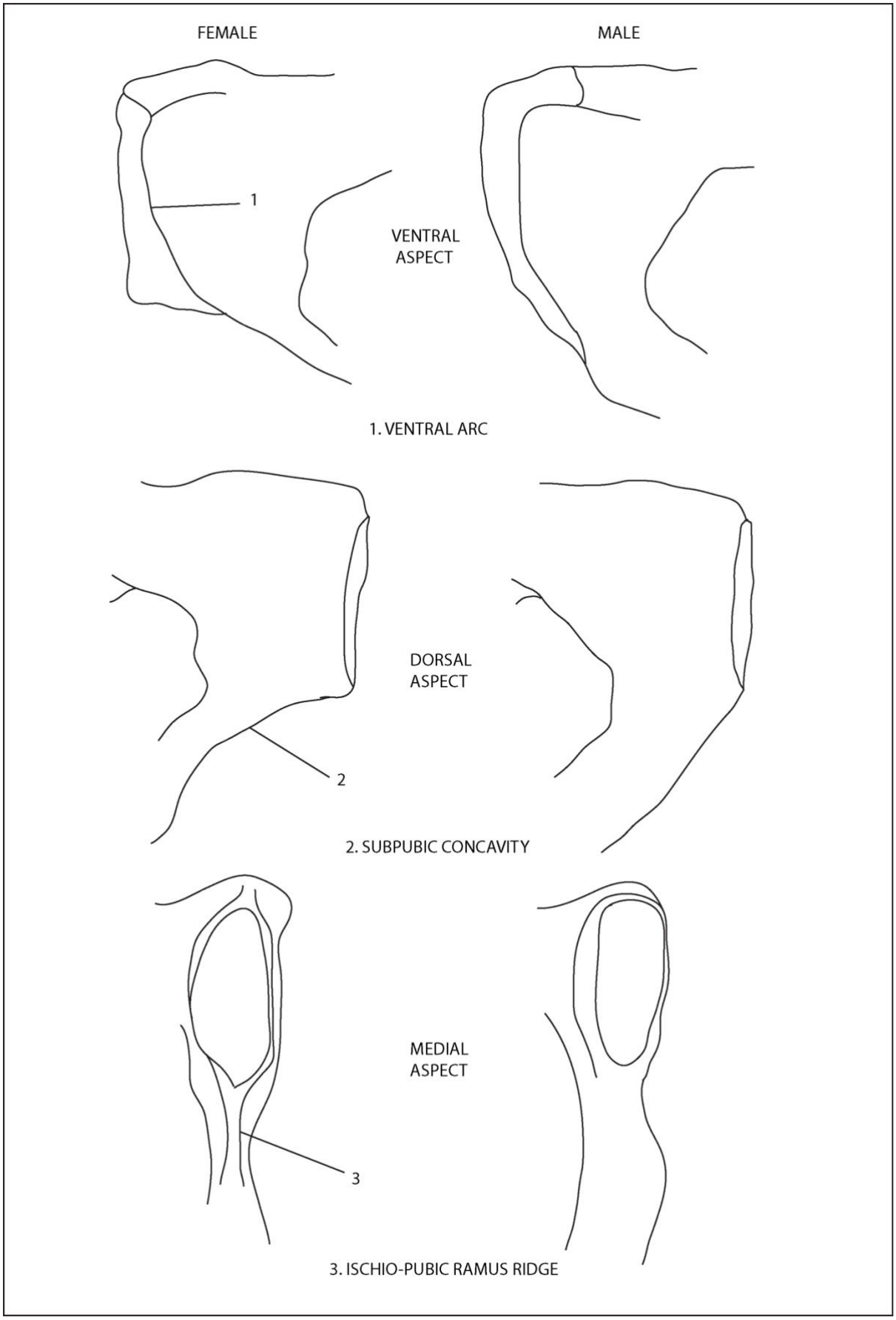

Figure 4.1**:** *The comparison of male and female morphology assessed in the Phenice (1969) sex estimation technique. Image: author's own.*

4.3.6 Sex Estimation Methods Used in this Thesis

Both cranial and pelvic morphological assessments were performed, with pelvic estimates considered more reliable. The Phenice method (1969) was considered the most reliable estimate and took precedence, supplemented with scoring of the greater sciatic and pre-auricular sulcus following standards by Buikstra and Ubelaker (1994). For cranial estimation, the Walrath method (2004) was employed due to the weighting of features more related to sexual differentiation, and least likely to be influenced by ancestry. Where the pelvis was available, pelvic sex estimation took precedence in the final sex estimation. Reliance on cranial sex estimation only occurred where the pelvis was not available, or pelvic sex estimation was ambiguous. Individuals were classified as *probable male*, *possible male*, *indeterminate*, *possible female* and *probable female* in accordance with the degree of expression of the sex characteristics. Due to ancestral confounding factors in cranial sex estimation, where only cranial traits were available, an individual was determined as *possible male*, *possible female* or *indeterminate* only. For statistical purposes, probable/possible females and probable/possible males, were considered together as male and female in this thesis. Indeterminates were not assessed in the statistical analyses for sex. However, they were included in other statistical analyses.

Chi square goodness of fit was used to assess whether there were statistically significant differences between the presence of males and females in an assemblage. A p-value of less than 0.1 meant the assemblage was not suitable for statistical assessment of disease differences across sex. Appendix 1 provides information on the number of individuals assessed with each method across the six assemblages.

3.4 Age Estimation

4.4.1 Age as a Factor in Palaeoepidemiological Study

Age is one of the most important factors influencing the morbidity and mortality of diseases. When reconstructing age, bioarchaeologists are faced with recording the physiological age of the skeleton which does not directly reflect chronological age (Halcrow et al. 2007). Population approaches such as those taken in this thesis, however, are not as concerned with estimating the chronological age of the individual rather the functional age of the individual in relation to the rest of the population (Tayles and Halcrow 2016). The

objectives of this thesis are to assess the impact of human population interaction on disease morbidity and mortality. As mortality is a function of age, techniques that accurately seriate the ages of individuals in each sample are necessary to statistically assess population trends in disease mortality.

Immunocompetence of an individual fluctuates over their life time (Bupp 2015; Szulc et al. 2000). Additionally, the remodelling rate of bone and therefore skeletal response to disease also changes with age. In general, the increasing age of nonadults is associated with an increased immunocompetency with the development of an acquired immune system over time, while simultaneously being associated with decrease of bone turnover rate as growth rate decreases with age (Lewis 2017).

Babies are born with passive immunity that is passed trans-placentally from the mother, providing a buffer to infection in infancy (Morein et al. 2007). This passive immunity is also passed through breast milk and colostrum and provides some level of protection until weaning (Field 2005). The attainment of active immunity occurs from around 2 years of age, but its maturation is reliant on the exposure of the body to antigens (Kelly and Coutts 2000; Lewis 2017). Susceptibility to infection in young children prior to the maturation of antigen recognition and clearance cells responsible for acquired immunity is then dependent on weaning age until a sufficient acquired immunity begins to form. The result is an increase in susceptibility to infection following birth in infancy, followed by a decrease in susceptibility to infection with age with maturation of acquired immunity. *Exogenous* factors such as infectious disease and malnutrition are most often associated with post-neonatal death (after the first month) (Lewis and Gowland 2007). Within the first month of life *endogenous* factors such as congenital defects, other genetic factors, birth trauma and the intrauterine environment are the primary drivers of mortality, and consideration of the transition from endogenous to exogenous mortality is essential when assessing the influence of age on infectious and nutritional disease morbidity and mortality in human skeletal assemblages (Lewis and Gowland 2007).

In adults, bone turnover and immunocompetence both generally decrease with age (Steinmann 1986). However, the life history of immunocompetency in adults is far more complex and is dependent on a multitude of exogenous and endogenous factors. This is the result of individual differences in susceptibility to disease as previously discussed in relation

to the *osteological paradox* (Chapter 1). When considering overall mortality within a cemetery assemblage, high frequencies of individuals in infancy to early childhood, and of old adults would reflect a natural population mortality distribution. Age-at-death distributions of cemetery assemblages need to be carefully considered, particularly when applying palaeoepidemiological analysis as is the case in this thesis.

4.4.2 Nonadult Age Estimation

Age estimation of nonadults is reliant on using reference population parameters for growth and development of the skeleton. Due to the nature of growth (a fast rate of growth at infancy to the eventual slowing and termination of growth in adulthood), nonadult age techniques are more accurate for infants than post-infant nonadults. Nonadult age estimates are reliant on dental calcification and eruption, long bone growth, and the timing of primary and secondary fusion of the skeleton. These methods are affected by population specific parameters of the original reference population, and when applied to archaeological populations must be done with a level of caution. Population specific variation in growth and development is well acknowledged in bioarchaeology as a limitation to age estimation of nonadults (Halcrow et al. 2007). Not one particular technique is suitable for the entire phase of skeletal growth and maturation. Skeletal methods for nonadult age estimation are presented here prior to dental age estimation techniques.

In this thesis, both the mean age in years and age stages (infant, child or adolescent) are used to describe nonadults (see Table 4.1). Age stages are presented in this thesis to allow discussion of the relative stage of development in nonadults. Age brackets which follow the approximate development of the immune system (Buckley 2016; Lewis 2017) are also employed to describe disease prevalence with age stage (see Table 4.1).

Table 4.1**:** *Nonadult age stages and age brackets used in this thesis for analysis. The average age produced from age assessment determines the classification of the age stage.*

NONADULT AGE BRACKETS ASSESSED IN THIS THESIS	**AGE STAGE**
Preterm to under 6 months old	*Infant*
6 months to under 1 year old	
1 to 5 years	*Child*
6 to 10 years	
11 to 14 years	*Adolescent*
15 to under 20 years	

A nonadult under the age of 1 year is termed an *infant* (Lewis 2011b). *Neonate* is also used in this thesis to describe infants from birth to approximately 27 postnatal days and the term *perinate* is used to refer to infants around birth (from 24 weeks gestation to 7 postnatal days) (Lewis 2011a). Adolescence has been previously defined for bioarchaeology by Lewis (2011b) as nonadults over the age of 14 years of age. However, due to population variation in skeletal growth, and variation in fertility of the six samples (see Chapter 9) puberty onset may have been earlier or later. Therefore, *adolescence* is here conservatively defined as over 10 years to under 20 years of age. *Childhood* is then defined as the period between infancy and adolescence (1 to 10 years of age). These terms are employed in the results chapters (Chapters 6 to 8).

4.4.3 Long Bone Length Age Estimation (Diaphyseal Length)

Bone modelling has been discussed in Chapter 3. The process of bone modelling as it pertains to diaphyseal long bone growth is valuable in the estimate of nonadult age. In infants, measurement of diaphyseal length of long bones is the primary form of age estimation prior to the eruption of teeth (Lewis and Gowland 2007). Methods correlating chronological age to diaphyseal length have been produced from measurements taken from dry bones and radiographs in modern populations (Fazekas and Kosa 1978; Jeanty 1983; Maresh 1970; Scheuer et al. 1980). Multiple factors affect relative growth, therefore with increasing age, the use of the method becomes increasingly unreliable. Genetics determine the peak attainable height of an individual, and population specific differences in height can be particularly dramatic (McEvoy and Visscher 2009). Under nutrition and infection also impede the development of genetically determined attainable height as a physiological trade-off for survival (Bailey et al. 1984; Bogin and MacVean 1978; Temple et al. 2014). As palaeoepidemiological studies often assess health and disease in compromised individuals, estimations from diaphyseal lengths are likely to underage malnourished individuals post-infancy (Hoppa and Gruspier 1996).

4.4.4 Age Estimation from Fusion of Primary Elements and Secondary Centres of Ossification

The mechanism of maturation of the skeleton can also be used for age estimation (McKern and Stewart 1957; Schaefer et al. 2009). In some bones of the axial skeleton and the pelvis, primary ossification, as described above, also includes the fusion of separate bone

elements to form as a single bone (e.g. the fusion of the neural archs to the vertebral bodies to form a single vertebra), and the timing of this fusion is a useful indicator of childhood age.

Following primary ossification, most bones undergo a secondary ossification where the fusion of growth plates (epiphyses) enable maturation of the skeleton in adolescence (Mackie et al. 2008; Scheuer and Black 2000). The delay of epiphyseal fusion until adolescence in humans enables increased longitudinal growth, and growth of pelvis and thorax breadth. In adolescence, the skeleton is nearing the completion of diaphyseal growth, fusion of primary elements, and dental development (Scheuer and Black 2000). Therefore, epiphyseal fusion techniques play a predominant role in estimation of age in adolescence. Additionally, later fusing epiphyses are also beneficial in the estimation of age in young adults (Scheuer and Black 2000). An important consideration in the assessment of secondary ossification is that of puberty, which determines the timing of the fusion of epiphyses (Shapland and Lewis 2013). The onset of puberty is influenced by population specific factors (Shapland and Lewis 2013). Additionally, differences exist in the timing of fusion in males and females, with females maturing at an earlier age (Ubelaker 1987). A more conservative age estimate is needed where sex cannot be determined, as the epiphyseal fusion variation for both males and females need to be included in the age estimate.

4.4.5 Dental Calcification and Eruption Estimation

Age estimation based on dental development is possible due to differential timing of the formation and eruption of teeth. As humans develop two sets of teeth, a deciduous and a permanent set, with each tooth type erupting at different times, age estimation through dental techniques are possible for almost the entirety of childhood and adolescence. Furthermore, as teeth are more resilient to taphonomic factors than bone, teeth are more likely to be preserved in the skeletal record. Dental development is less susceptible to biological and environmental factors than skeletal methods of age estimation in nonadults. However, the timing of dental development is not completely impervious to the effects of genetics, nutrition levels, and hormones (Garn et al. 1965). Differences in the timing of tooth development between the sexes cannot be corrected for in bioarchaeology due to the challenges of determining sex in nonadults, and could be as much as a year depending on the tooth, population and standard used (Demirjian and Levesque 1980; Höuffding et al.

1984). Furthermore, as is the case for all nonadult age estimation methods, population specific differences in the timing of development is a confounding factor. For example, Ubelaker (1987) identified accelerated development in Native Americans compared to European American reference samples. Similarly, Halcrow et al. (2007) note that dental development could be delayed up to a year in Thai children, suggesting that the application of dental age estimation standards for prehistoric Asian populations, such as assessed in this thesis, are likely less reliable in regards to estimating true chronological age. However, these age estimation techniques still provide a method with which to seriate nonadults in a population based palaeoepidemiological approach, and therefore have value in addressing the research questions presented in this thesis. The reliability of dental formation and eruption methods is attributed to the strong physiological regulation of incremental deposit of dental tissue (Dean 2000). Initial enamel mineralisation occurs at the head of the crown and continues growing, with the root forming as the last component of tooth development (Dean 2000).

Assessment of the timing of dental formation and dental eruption are the two main methods employed in nonadult dental age estimation. Dental eruption methods rely on the timing of initial eruption of the crown in the alveolar bed up until the final position of the teeth in occlusion. In the dental formation method, radiographs are taken so that the calcification of the entire tooth can be considered from initial formation of the crown inside the mandible and maxillae to the completion of the root apex (Moorrees et al. 1963). As the eruption method only accounts for the final stages of tooth formation, it is widely considered to be the least accurate of the two methods (Buikstra and Ubelaker 1994; Halcrow et al. 2007; Ubelaker 1987). Differences between the sexes are minimal in the earlier stages of calcification, further suggesting the formation method is more accurate (Demirjian and Levesque 1980; Moorrees et al. 1963). However, as the dental formation method requires the employment of radiographs in order to identify the development of roots and unerupted teeth, where radiographs are not available, the eruption technique is still valuable for age estimation. Additionally, the dental formation method can be employed when teeth are exposed or isolated due to taphonomic damage in an archaeological context (Halcrow et al. 2007). What needs to be considered in this case, is that fewer teeth may be available for analysis using dental formation methods, increasing the level of error. Dental calcification and eruption estimates also become increasingly unreliable with older age particularly by the time of adolescence, where the eruption and occlusion of permanent teeth are near

completion. The eruption of the third molar is the most variable tooth. Additionally, up to a third of individuals within Asian populations have agenesis of the third molar (Alam et al. 2014; White et al. 2012). The lack of a third molar then does not indicate an individual is a nonadult.

4.4.6 Nonadult Age Estimation Methods in this Thesis

While the dental formation method arguably provides the most accurate method of age assessment for nonadults, a complete assessment requires radiographs, unless teeth are loose from the mandible and maxilla. Radiographs were only available for the Man Bac nonadults (Domett and Oxenham 2011). For these individuals the dental formation standards of Moorrees et al. (1963) were employed. Additionally, this technique was employed when loose teeth were available during macroscopic assessment of the other assemblages. Where radiographs or loose teeth were not available, the dental eruption standard of Ubelaker (1987) was primarily used. For young children, standards for timing of fusion of primary elements of the axial skeleton following Schaefer et al. (2009) provided a secondary form of age assessment for individuals with teeth. This was also the primary standard applied in the assessment of nonadult age in children without available teeth. Timing of epiphyseal fusion served as a primary form of age estimation in adolescents following Schaefer et al. (2009).

Measurements from diaphyseal lengths of long bones were primarily used in infant age assessment (Fazekas and Kosa 1978; Maresh 1970). Newborn and perinatal long bones were assessed using Fazekas and Kosa (1978). Maresh (1970) was applied to individuals over the age of 1.5 months. If only long bone measurements were available for an individual over the age of 1 year, the long bones were compared to that of nonadults with dental age estimates. Where intrasample comparisons could not be made, the Maresh (1970) standard was applied. Acknowledgement of the underlying population differences between the reference and sample populations was the reason for this decision. Long bone measurements were taken twice to evaluate intraobserver error. Any discrepancies in measurements were minimal (a maximum of 2mm error) and none demonstrated a change in the assessment of the individual's age between the two measurements.

4.4.7 Adult Age Estimation

Adult age estimation methods are generally reliant on degeneration of certain joints which can result in considerable deviation of the estimated skeletal age from the actual chronological age of the individual (Tayles and Halcrow 2016). The estimation parameters used are dependent on the ancestry and sample size of the reference population, the ease of applying the technique, and the experience of the assessor with the technique (Baccino et al. 1999; Saunders et al. 1992; Wärmländer and Sholts 2011). As the techniques are reliant on degeneration, individual activity levels and physiology also play a role in the relationship between the individual's true age and skeletal age. The methods applied in bioarchaeology involve the assessment of degeneration of fibrocartilaginous, cartilaginous and synovial joints of the pelvis and ribs where effects of activity and biomechanics are minimal (Becker et al. 2010; Cartmill et al. 1987). Other forms of estimation of age rely on population specific seriation of tooth wear, and the fusion of cranial sutures (Meindl and Lovejoy 1985; Molnar 1971). Though some forms of age estimation are considered more accurate than others (i.e. pubic symphysis and auricular surfaces), applying multiple methods provides the best estimate overall (Acsádi et al. 1970; Baccino et al. 1999; Lovejoy et al. 1985). A common central bias is recognised for all techniques, where younger individuals tend to be over-estimated and older individuals under-estimated in age (Buckberry and Chamberlain 2002; Gocha et al. 2015). *Age mimicry* wherein the distribution of the estimated population will reflect that of the reference population is also a recognised problem of traditional techniques (Hens and Godde 2016). Lastly, these techniques become unreliable past the age of 50 years of age as the rate of degeneration becomes too variable, considerably restricting the extent of age estimation in older ages (White et al. 2012).

As presented below, no age estimation technique is strictly suitable to the assessment of Asian populations, particularly in consideration of prehistoric skeletal material (Gocha et al. 2015). However, the application of these methods enable seriation of individuals within the assemblage, and are still useful in population level palaeoepidemiological statistics (Oxenham 2000). When discussing individual cases, the use of broad age categories is more appropriate (Tayles and Halcrow 2016). Age stages for adult case studies presented in this thesis follow Buikstra and Ubelaker (1994) (Table 4.2). The mean age of death is employed in mortality statistical analysis (see Chapter 5), and 10 year brackets (20-29, 30-39 etc.) are used for graphical representation of the association of disease prevalence with age.

Table 4.2**:** *Adult age stages used in this thesis and their relative age bracket. The mean age in years produced from age assessment determines the classification of the age stage (Buikstra and Ubelaker 1994).*

AGE STAGE	ASSOCIATED AGE BRACKET
Young Adult	20 to 34 years
Middle Aged Adult	35 to 49 years
Old Adult	50+ years

4.4.8 Age Estimation of the Pubic Symphysis

The pubic symphysis is the articulation between the left and right anterior *os coxae.* The pubic symphysis is predominantly comprised of fibrocartilage, bound by two bony surfaces from the left and right pubic bones known as the pubic symphyseal surfaces (or faces). The joint's primary functions are to absorb shock during movement of the lower limbs, provide mechanical stability of the pelvic girdle and allow movement during parturition (Becker et al. 2010). Given that there is a reduced association with activity related skeletal changes, the degeneration of the pubic symphysis is considered one of the best areas for estimating age in adults (Baccino et al. 1999; Wärmländer and Sholts 2011; White et al. 2012).

Age estimation methods of the pubic symphysis (Acsádi et al. 1970; Brooks and Suchey 1990; Gilbert and McKern 1973; Todd 1920) attempt to classify the continuum of degeneration into stages with associated age brackets. In general, the pubic symphyseal face transforms from a youthful *billowing* appearance, to an eventual depression of the surface with degeneration of the margins associated with irregular osteophytic activity. Todd (1920) initially introduced ten stages of degeneration. This standard was revised by Brooks and Suchey (1990) to six stages. The revised standard included a larger sample (n= 1225), inclusion of both males and females in the reference population, and simplification of the technique to reduce interobserver error. Limitations of this method are that often the left and right pubic symphysis present with different stages, and at times the descriptions of the stages do not encompass the variation observed in the progression of degeneration (Overbury et al. 2009). Given the role of the pelvis in parity, the morphology and rate of degeneration of the pubic symphyseal surfaces differ between the sexes. Further, trauma associated with late stages of parity and parturition accelerates degeneration of the pubic symphysis which introduces a level of uncertainty in archaeological samples that needs to be considered if fertility rates are high and multiparity can be assumed for women of childbearing age (Gilbert and McKern 1973). Osteologists vary in their application of the

method. For example, some may choose to only record a single side, whereas others will record both sides and include a larger margin of error in their estimate (Garvin and Passalacqua 2012). A challenge with age estimation from the pubic symphyseal face in archaeology is that the pubic bone is often poorly preserved (White et al. 2012). Therefore, often other methods are necessary.

4.4.9 Age Estimation of the Auricular Surface

The auricular surface forms the inferior portion of the sacroiliac joint. While this is a synovial joint, the range of mobility is limited (Cartmill et al. 1987), as such this region, is also useful for assessment of skeletal age. In contrast to the pubic symphysis, the auricular surface area is more robust to taphonomic factors and is more likely to be sufficiently preserved for assessment (White et al. 2012). The auricular surface transforms from a fine billowing appearance, to granular and uniform appearance, and finally breakdown of the margins with erratic densification of the surface. Similar to the Suchey-Brooks method for the pubic symphysis, auricular surface methods attempt to identify stages of senescence that occur along a continuum (Lovejoy et al. 1985).

The auricular surface presents with similar challenges to that of the pubic symphysis: interobserver error, and genetic, biological and environmental variation. The Lovejoy auricular surface method is derived from a reference population of only approximately 100 individuals (Lovejoy et al. 1985). However, the method is considered by some to be more accurate than the pubic symphysis for estimating individuals of older age cohorts (Schmitt 2004; White et al. 2012). In order to combat the challenges of variation in degeneration Buckberry and Chamberlain (2002) have since produced a technique which enables the scoring of independent morphological features of the auricular surface (macroporosity, granulation, microporosity etc), as opposed to the original Lovejoy et al. (1985) method which considers these traits in combination. The outcomes of the two techniques appeared similar enough that Hens and Godde (2016) remarked that the best method would be the one the researcher is most comfortable with.

4.4.10 Tooth Wear

In contrast to the skeleton, tooth enamel is made from non-remodelling tissue. Therefore, following the completion of dental development, irreversible degeneration occurs. As such, tooth wear degeneration can be used for age estimation purposes. The rate of tooth wear is highly population specific, due to dietary, disease and societal factors impacting the tooth wear rate (Molnar 2011). To calibrate the association of age with degree of wear in adults from the same population, a functional age is derived from the rate of wear identified between the first, second and third molars in adolescents. The method assumes the rate of wear remains unchanged with increasing age (Miles 2001). The reality is that the rate of wear is highly variable over an individual's life time (Kaidonis 2008). Different methods for recording tooth wear exist. Scott (1979) introduced a method of recording four quadrants of the molars separately to account for the variation of wear across the surface of a tooth, and Molnar (1971) provided descriptions of dental wear of anterior teeth. While tooth wear charts exist based on reference populations, such as Brothwell (1981), individuals can only be placed in large age categories and in case study situations, the tooth wear technique is predominantly a last resort method (Garvin and Passalacqua 2012). The employment of tooth wear in archaeological samples is more common as prehistoric populations tend to have more wear in teeth than modern populations. It has been demonstrated that tooth wear rates considerably underestimate the age of old adults, and in populations with advanced tooth wear rates, the technique is restricted to use in younger ages of adulthood (Miles 2001).

Seriation of tooth wear can also be incorporated into regional age estimation standards such as by Oxenham (2000), where regression models, developed from a relationship between tooth wear and pubic symphysis or auricular surface age, allows for age estimates of individuals where the pelvis was too fragmented or not available for assessment. The assumption in these models are that both pelvic age estimates and dental wear have a similar relationship to skeletal age, but they evade the issues of the rate of wear being derived from only adolescents in the collection. Given the degree of variation accepted in the dental wear methods, other methods are often prioritised, but tooth wear methods remain valuable in population based studies, particularly where fragmentation of the skeleton restricts the application of pelvic age estimation techniques.

4.4.11 Cranial Sutures

Over time the fibrous joints between the cranial sutures ossify and fuse. There is differentiation in the timing of the fusion of different sutures, with the tendency of the sagittal suture to fuse early and the pterion much later on in adulthood, if at all. The fusion timing of the different cranial sutures span adulthood; therefore, they can be employed to estimate age. Estimates for ectocranial, endocranial and palatal sutures are employed (Acsádi et al. 1970; Buikstra and Ubelaker 1994; Meindl and Lovejoy 1985). The methods themselves include large margins of error due to the degree of variation in the timing of suture closure, and rely on the premise that suture closure will occur which is not the case in many individuals. There is considerable difference in the suture timing between populations and these methods are particularly unreliable for Southeast Asian populations (Gocha et al. 2015). As such, this method is generally applied when other age estimation methods are not possible, and frequently only used as an indicator of relative age stage of life (Garvin and Passalacqua 2012).

4.4.12 Adult Age Estimation Methods in this Thesis

Where possible, a combination of Lovejoy's (1985) auricular surface and the Suchey-Brooks method (1990) for pubic symphysis age estimation was employed to assess adult age. If both methods could not be employed due to preservation issues, estimation of age depended on the assessment of only one of these morphological approaches. Both the left and right sides were assessed, if available, with the estimate inclusive of both scores (e.g. an estimation of age could be stage 5 and 6, accompanied with a larger age estimate margin). Scott's (1979) dental attrition scores were assessed for all adult individuals with molars present. Individuals within each assemblage were seriated based on their degree of tooth wear. Relative tooth wear scores were compared to those with predetermined age categories from the auricular surface and pubic symphysis regions. Tooth wear seriation age estimation was only used where the other age estimation methods were not available.

For the Con Co Ngua sample from Northern Vietnam, regression estimations produced by Oxenham (2000) based on the 1980 Con Co Ngua skeletal assemblage were used to translate the raw Scott tooth wear scores (provided by M. Oxenham) into ages in years for population statistics purposes. This was the only deviation to the methodology

outlined above and was a necessary due to poor preservation of the pelves in this assemblage, possibly in relation to the squatted burial position.

4.5 Completeness and Recording of Taphonomic Processes

The recording of both skeletal completeness, the percentage of presence of the skeleton, taphonomic damage, and assessment of the degree of postmortem degradation processes (whether they be environmental, biological or cultural), is essential in palaeopathological assessment (Nawrocki 1995). The degree of skeletal completeness and postmortem damage influences the visibility and presence of disease.

Overall skeletal completeness and skeletal element completeness were assessed. Overall skeletal completeness was modified from Buikstra and Ubelaker (1994) and completeness ranged from *complete* (over 75% presence) to *crushed* (mostly fine fragments and bone powder) (Table 4.3). A *skeletal element* was defined as a single bone, except in the case of vertebrae (where cervical, thoracic, lumbar and sacral vertebral groups were each considered as different single elements), sternum (the sternal body, manubrium and xiphoid process are considered together as a single element), ribs (left and right sides were considered as two different elements), hands (carpals, metacarpals, and phalanges were considered as different elements), and feet (tarsals, metatarsals, and phalanges were considered as different elements). All skeletal elements were also identified as present or absent. If more than 2/3 of the skeletal element was missing, the bone was marked as absent.

Table 4.3: *Classification of overall skeletal completeness employed in this thesis*.

COMPLETENESS	DESCRIPTION
Complete	More than 75% of the skeleton is present
Near Complete	Approximately 66 to 75% of the skeleton is present
Partially Complete	Approximately 50 to 66% of the skeleton is present
Incomplete	Approximately 33 to 66% of the skeleton is present
Fragmented	Less than 33% of the skeleton is present or the skeletal elements are heavily fragmented
Crushed	The skeleton is mostly fine fragments or resembles bone powder.

As different diseases vary in their skeletal expression, skeletal element completeness is useful in assessing whether the assemblages are valid in terms of their potential to represent the diseases assessed in this thesis (Chapter 5). Skeletal element completeness of

long bones, hands and feet, vertebrae, and neurocranium was systematically recorded following White's (1992) Index:

$$\frac{\text{Number of segments observed}}{\text{Number of segments expected}} \text{ X } 100$$

For hands and feet, vertebrae and neurocranium, each individual bone was counted. For adult long bones, upper third shaft, middle third shaft, lower third shaft, proximal epiphysis and distal epiphysis were counted as separate segments (each long bone then has a maximum score of 5). For nonadult long bones only the upper, middle and lower third shafts were included in assessment of completeness (each long bone has a maximum score of 3).

Taphonomic processes of the bone were described following Buikstra and Ubelaker (1994). Animal gnaw marks, surface preservation, colour changes, root etching and water damage were noted. All descriptions of completeness and postmortem taphonomic damage of bone for each individual in this study is presented in Appendix 2. The following section outlines the results for each assemblage in relation to sex, age and taphonomy.

4.6 Ota: Middle Jomon Japan

4.6.1 Background

Ota is a Middle Jomon Period site dating between 5000-4000 BP, in the Chugoku District of Western Japan along Mikawa Bay (Figure 4.2; Kusaka et al. 2010; Temple 2007). The site was initially excavated in 1926 by Kenji Kiyono. Of the 55 skeletal remains reported to have been excavated at the site (Kiyono 1969), 33 were included in the palaeopathological assessment. Ota is the pre-interaction site assessed in Chapter 6.

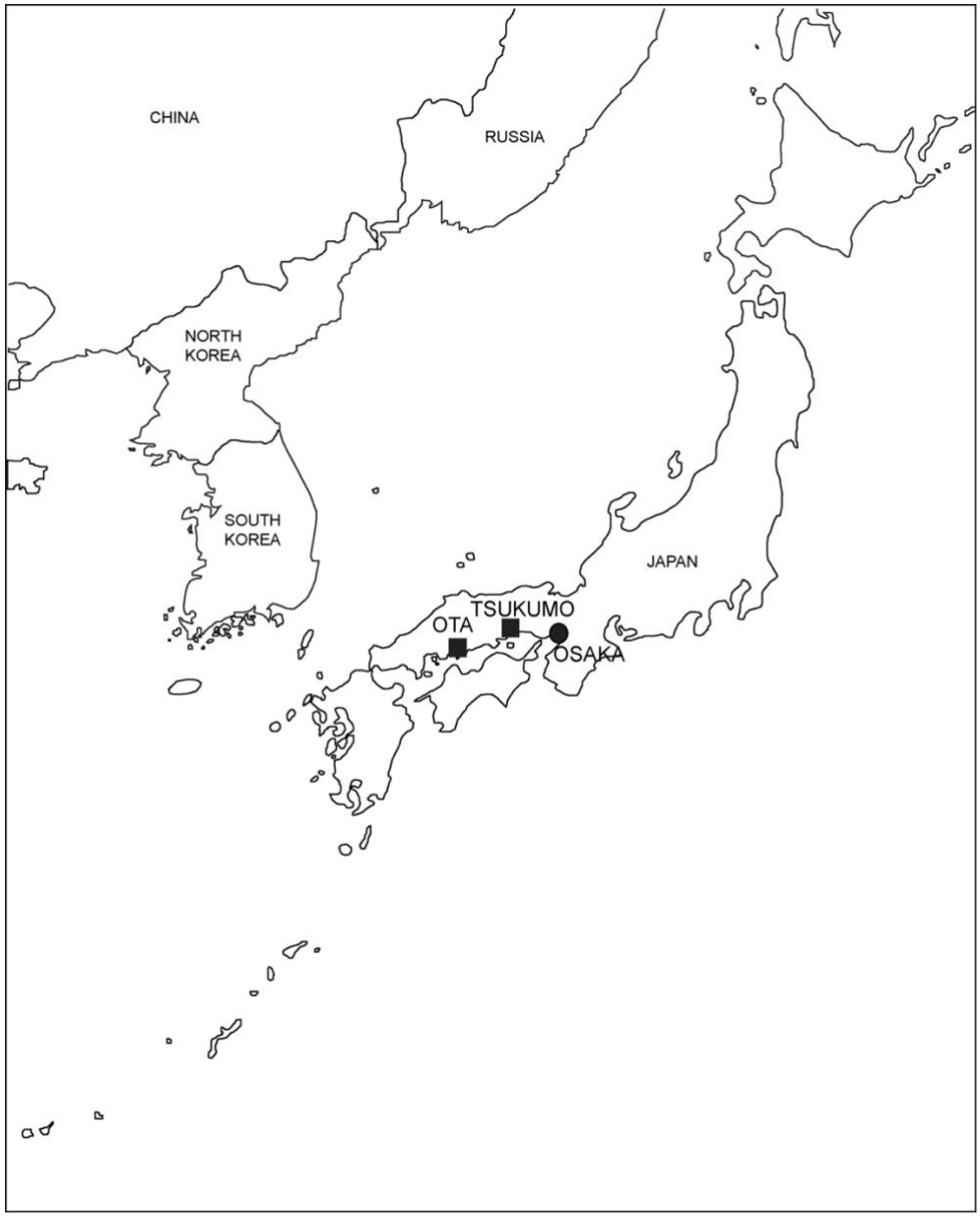

Figure 4.2: *Location of the two sites from Japan investigated in this thesis. Ota represents a site prior to and Tsukumo represents a site following intrapopulation interaction. The modern city of Osaka is here presented for geographical reference. Image: author's own.*

4.6.2 Sample Completeness and Taphonomy

All three nonadults from the Ota assemblage were fragmented, whereas over 50% of the adults were at least partially complete (more than 50% completeness) (Table 4.4 and Table 4.6). However, 16% of the Ota adult assemblage were fragmented. Long bones were the best represented skeletal elements for both adults and nonadults, whereas as the hands and feet of both adults and nonadults were poorly preserved (Table 4.5 and Table 4.7).

Most bone surfaces were of good preservation, that is that larger subperiosteal new bone deposits, particularly remodelled ones were easily observable, but postmortem loss of smaller discrete or active deposits is possible. However, some elements had distinct colour changes which made observation of bone surfaces difficult. Three individuals (Ota 664, 678B, 687, and 697) had some skeletal elements which were charcoal black in colour. Commingling of this assemblage was common and due to the individual approach (as opposed to assessment of pathology with skeletal element as the denominator) many individuals were excluded from analysis due to the comingling. Individuals who were commingled but could be separated with confidence were included. Usually this involved the inclusion of two individuals with distinct morphological differences assigned to a single number. Postmortem breakage was common, and ribs were predominantly heavily fragmented, if present. Individuals Ota 715A and 678B also had rodent gnaw marks which restricted observation of the bone surfaces.

Table 4.4: *Overall completeness of the adult skeletal assemblage at Ota (adapted from Buikstra and Ubelaker 1994).*

COMPLETENESS	*Fragmented (<33%)*	*Incomplete (~33 to 50%)*	*Partially Complete (~50%- 66.7%)*	*Near Complete (~66.7% to 75%)*	*Complete (> 75%)*
Count	5/31	10/31	4/31	5/31	7/31
%	16.1	32.3	12.9	16.1	22.5

Table 4.5: *Completeness of different skeletal elements of the Ota adults. Following White (1992).*

	Range (%)	**Mean (%)**
Long Bone Survival Index	0 to 96.67	54.33
Hands and Feet Survival Index	0 to 59.43	17.48
Vertebrae Survival Index	0 to 95.8	39.38
Neurocranium Survival Index	0 to 87.5	46.77

Table 4.6**:** *Overall completeness of the nonadult skeletal assemblage at Ota (adapted from Buikstra and Ubelaker 1994).*

COMPLETENESS	*Fragmented (<33%*	*Incomplete (~33 to 50%)*	*Partially Complete (~50%- 66.7%)*	*Near Complete (~66.7% to 75%)*	*Complete (> 75%)*
Count	3/3	0/3	0/3	0/3	0/3
%	100	0	0	0	0

Table 4.7: *Completeness of different skeletal elements of the Ota nonadults. Following White (1992).*

	Range (%)	Mean (%)
Long Bone Survival Index	0 to 41.67	26.84
Hands and Feet Survival Index	0 to 1.89	0.63
Vertebrae Survival Index	0 to 8.33	2.78
Neurocranium Survival Index	0 to 0	0

4.6.3 Sex Distribution

Of the 32 individuals over the age of 15, only 10 individuals were confidently identified as *probable male* and *probable female*, with 25% of the assemblage being of *indeterminate* sex (Table 4.8; Figure 4.3). The high number of indeterminates in this assemblage is a combination of cranial trait ambiguity (the skull is neither gracile nor robust) and individuals missing both crania and pelvis for estimation. For the individuals identified as female from the pelvis, the crania tended to be ambiguous, and were generally more robust than gracile. Therefore it is likely that at least some of the crania identified as indeterminate may be female, contributing to the skew in sex in the assemblage with a high number of males present. Individuals identified as *possible males* by crania, due to missing pelves, were highly robust. This suggests the employment of the Walraith cranial estimation technique on the Jomon is likely not useful for estimation of female sex. The high numbers of *possible males* compared to *probable males* is due to poor preservation of pelvic elements for estimation of sex. As stated above, the robusticity of the crania does suggest these individuals are males. However, for consistency, a conservative approach has been taken here, and these individuals are considered as *possible males* only. The chi square test for goodness of fit does not demonstrate any significant differences in the number of individuals in each of the sex cohorts (X^2 6.00, p= 0.112).

Table 4.8: *Estimation of sex in Ota individuals over the age of 15 years.*

SEX ESTIMATION	# INDIVIDUALS FINAL SEX ESTIMATION
Probable Male	7
Possible Male	11
Indeterminate	8
Possible Female	3
Probable Female	3
Total	32

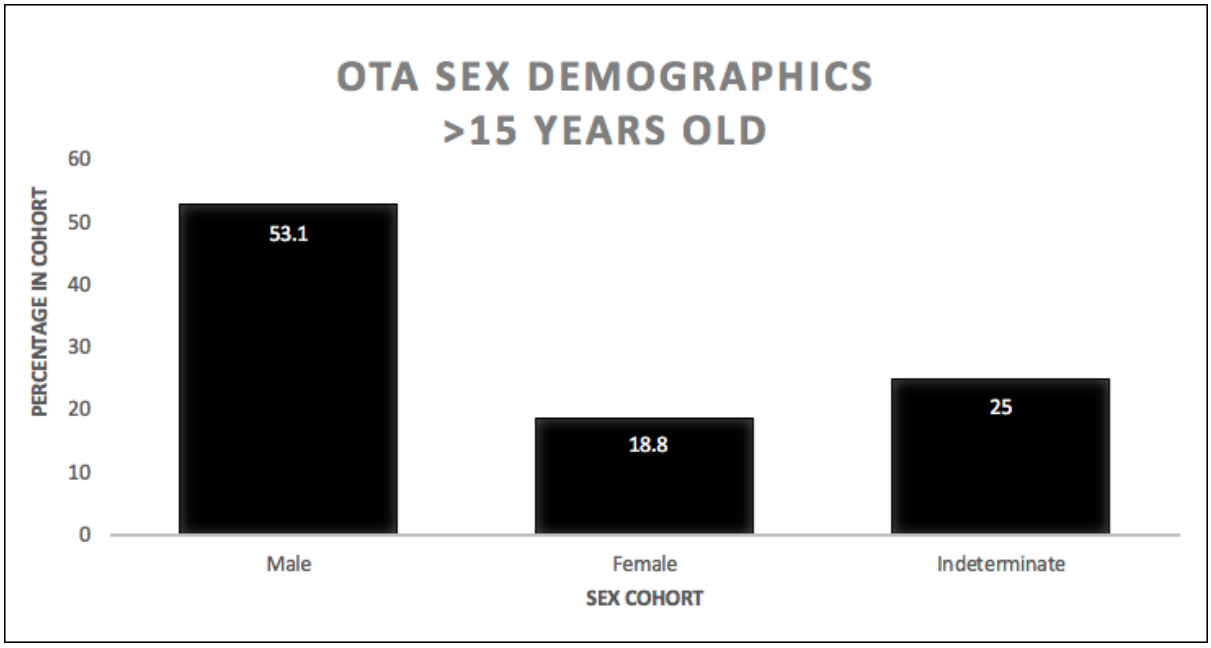

Figure 4.3**:** *Percentage of individuals over the age of 15 in each cohort of estimated sex at Ota. Image: author's own.*

4.6.4 Age-at-Death Distribution

Nonadults were considerably underrepresented in this assemblage, and it may be possible the nonadults with the exception of adolescents were not excavated (Table 4.9). The two infants identified in this assemblage were found amongst a bag of faunal remains, so they may have not been recognised as human by the excavators. A higher percentage of middle aged adults compared to young adults indicate an increased risk of death of middle aged adults, which is consistent with a typical mortality distribution (Figure 4.4). However, the under-representation of older adults in the assemblage is not consistent with a typical mortality distribution.

Table 4.9: *Age-at-death distribution of individuals included for palaeopathological assessment at Ota. Some adult individuals in the assemblage were excluded due to commingling.*

AGE COHORT	# INDIVIDUALS	(%)
0 to <6 months	2	7.4
6 months to <1 year	0	0
1 to 5 years	0	0
6 to 10 years	0	0
11 to 14 years	0	0
15 to 19 years	1	3.7
20 to 29 years	5	18.5
30 to 39 years	10	37
40 to 49 years	7	25.9
50+ years	2	7.4
Total	27	

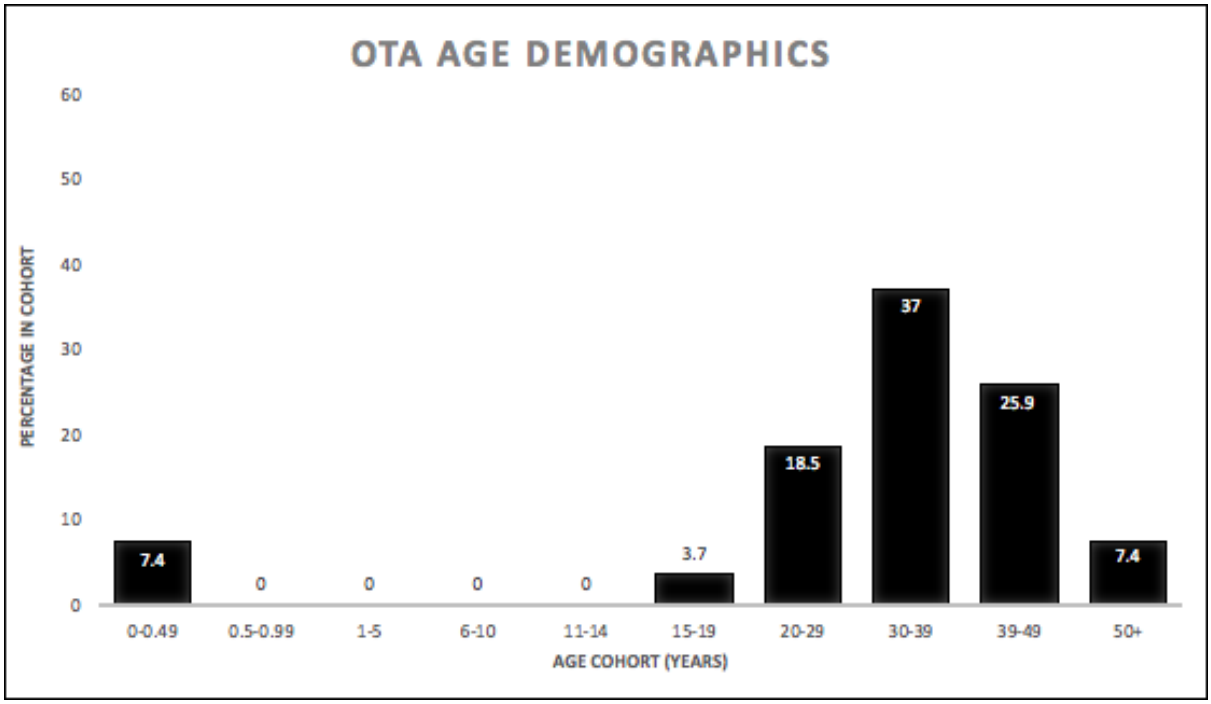

Figure 4.4: *Overall percentage age-at-death distribution of the Ota sample. Image: author's own.*

4.7 Tsukumo: Late to Final Jomon Japan

4.7.1 Background

Tsukumo, a Late to Final Jomon site dated to 3200-2800 BP by pottery (Kiyono 1969; Kusaka et al. 2010), was excavated in the 1910's to 1920's by three different excavators: Ogushi, Kiyono and Hasebe, and therefore the overall assemblage is housed at different institutions in Japan. Thirty individuals from the Kiyono assemblage excavated in 1920-22 (out of a reported 72 individuals) were assessed for palaeopathology in this thesis. Tsukumo is the post-interaction site assessed in Chapter 6.

4.7.2 Sample Completeness and Taphonomy

Over 68% of the adults in the assemblage were complete (more than 75%) whereas only 27% of nonadults were complete (Table 4.10 and 4.12). Forty-five percent of the nonadult assemblage were incomplete or fragmented. The nonadults who were complete had preserved metaphyses of the long bones which were available for radiographic assessment of nutritional deficiency (see Chapter 5). The long bones and neurocranium were the best preserved elements for both the adults and nonadults (Table 4.11 and Table 4.13).

The hands and feet of nonadults were poorly preserved (Table 4.13), whereas all elements were well represented in the adult assemblage (Table 4.11).

Surfaces of the bones were in good condition. The vertebrae of two individuals were commingled (Tsukumo 42 and Tsukumo 58), and therefore their vertebrae were excluded from analysis. No pathology was noted on these vertebrae. Postmortem breakage of the axial skeleton was common. The ribs of the adults were predominantly fragmented. Postmortem grey deposits of an unknown matrix (possibly mould) were present on the surfaces of long bones and crania in some individuals which appeared similar to active subperiosteal deposits. Subperiosteal new bone deposits were only recorded if they could be confidently differentiated from this unknown matrix.

Table 4.10: *Overall completeness of the adult skeletal assemblage at Tsukumo (adapted from Buikstra and Ubelaker 1994).*

COMPLETENESS	*Fragmented (<33%)*	*Incomplete (~33 to 50%)*	*Partially Complete (~50%- 66.7%)*	*Near Complete (~66.7% to 75%)*	*Complete (> 75%)*
Count	0/19	0/19	2/19	4/19	13/19
%	0	0	10.5	21.1	68.4

Table 4.11: *Completeness of different skeletal elements of the Tsukumo adults. Following White (1992).*

	Range (%)	**Mean (%)**
Long Bone Survival Index	48.33 to 100	86.67
Hands and Feet Survival Index	16.98 to 67.92	62.48
Vertebrae Survival Index	0 to 100	72.36
Neurocranium Survival Index	0 to 100	82.24

Table 4.12: *Overall completeness of the nonadult skeletal assemblage at Tsukumo (adapted from Buikstra and Ubelaker 1994).*

COMPLETENESS	*Fragmented (<33%*	*Incomplete (~33 to 50%)*	*Partially Complete (~50%- 66.7%)*	*Near Complete (~66.7% to 75%)*	*Complete (> 75%)*
Count	1/11	4/11	1/11	2/11	3/1
%	9.1	36.4	9.1	18.2	27.3

Table 4.13: *Completeness of different skeletal elements of the Tsukumo nonadults. Following White (1992).*

	Range (%)	**Mean (%)**
Long Bone Survival Index	0 to 100	65.66
Hands and Feet Survival Index	0 to 62.26	9.95
Vertebrae Survival Index	0 to 100	35.23
Neurocranium Survival Index	0 to 87.5	50

4.7.3 Sex Distribution

Of the 22 individuals over the age of 15, only one individual was estimated as indeterminate. Most individuals could be confidently estimated as *probable male* or *probable female* (Table 4.14). Approximately 55% of the assemblage were estimated as male, and 40.9% as female (Figure 4.5). The variation between the presence of males and females were not statistically different (X^2 0.429, p= 0.934), and therefore the assessment of differences of disease between males and females at Tsukumo is valid.

Table 4.14: *Estimation of sex in Tsukumo individuals over the age of 15 years.*

SEX ESTIMATION	# INDIVIDUALS FINAL SEX ESTIMATION
Probable Male	10
Possible Male	2
Indeterminate	1
Possible Female	2
Probable Female	7
Total	22

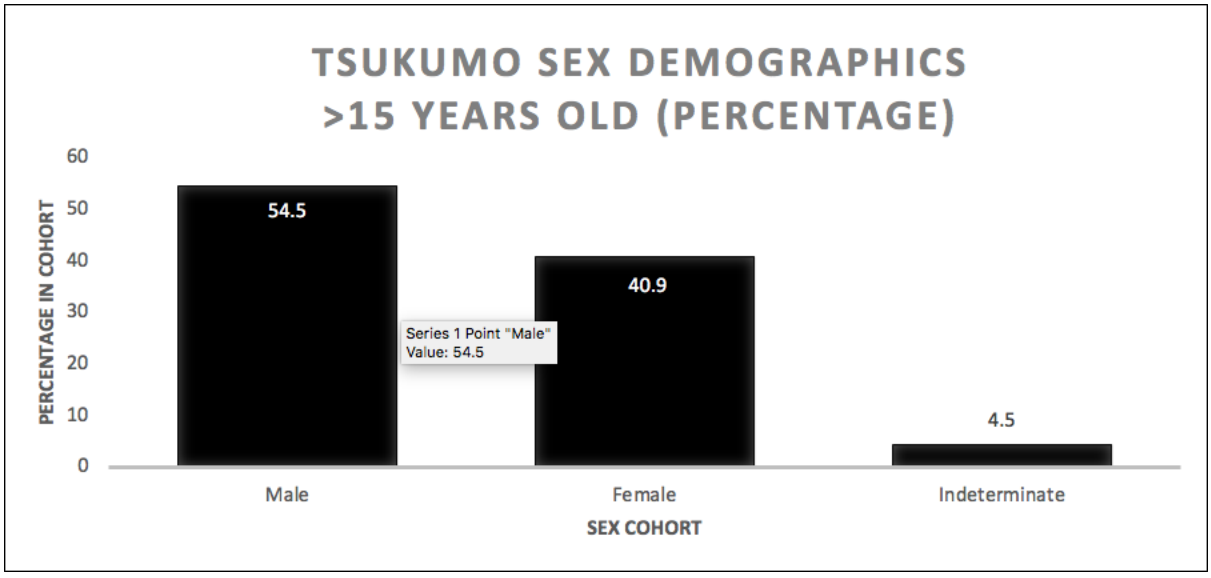

Figure 4.5: *Percentage of individuals over the age of 15 in each cohort of estimated sex at Tsukumo. Image: author's own.*

4.7.4 Age-at-Death Distribution

No infants and older children are present in the assemblage. Due to time constraints, priority was placed on recording nonadults prior to adults, and the percentage of nonadults (27.6%) compared to adults (63.2%) is conflated. However, this is not considered to be an

issue in this research as nonadults and adults were assessed separately. It is apparent that young adults were at an increased risk of death in relation to adults of older age, which does not reflect what is expected for a typical mortality distribution, wherein higher percentages of older adults would be expected (Table 4.15; Figure 4.6).

Table 4.15: *Age-at-death distribution of individuals included for palaeopathological assessment at Tsukumo.*

AGE COHORT	# INDIVIDUALS	(%)
0 to <6 months	0	0
6 months to <1 year	0	0
1 to 5 years	7	23.3
6 to 10 years	0	0
11 to 14 years	2	3.3
15 to 19 years	2	1
20 to 29 years	10	33.3
30 to 39 years	4	13.3
40 to 49 years	4	13.3
50+ years	1	3.3
Total	30	

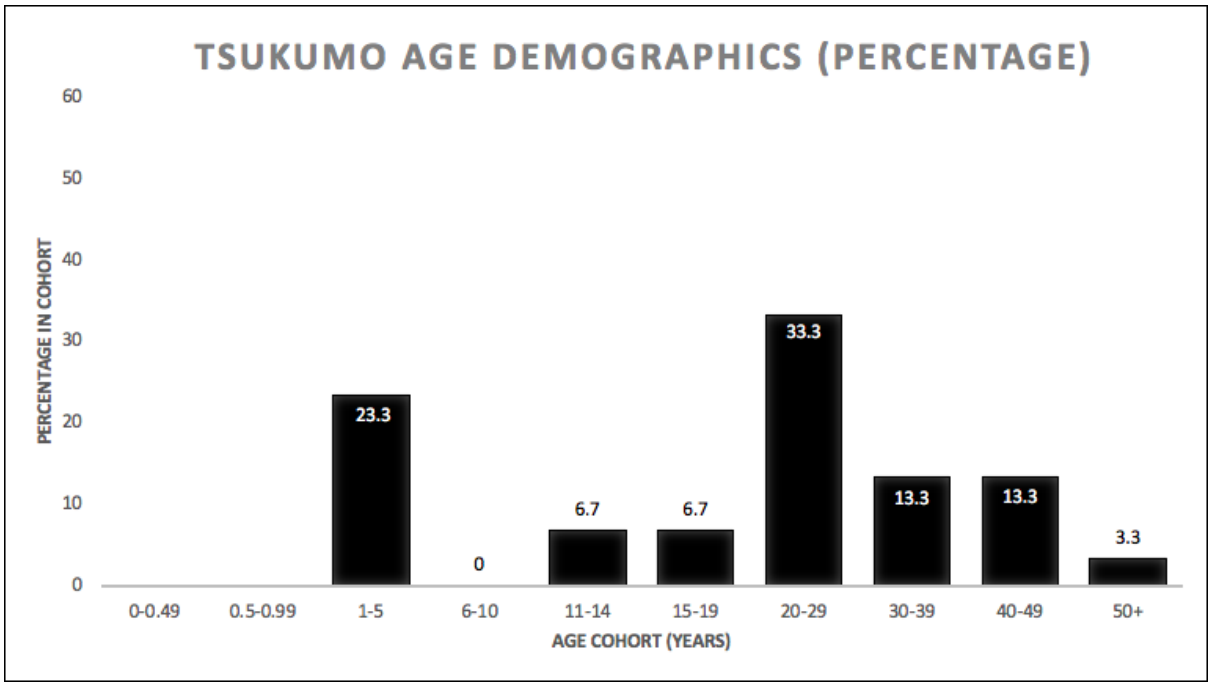

Figure 4.6: *Overall percentage age-at-death distribution of the Tsukumo sample. Image: author's own.*

4.8 Con Co Ngua: Pre-Neolithic Vietnam

4.8.1 Background

Con Co Ngua is a Pre-Neolithic sedentary forager cemetery located approximately 30km from the coast in Northern Vietnam (Figure 4.7). The site dates from 6200-6700 cal BP *terminus ante quem* by radiocarbon dating of tooth enamel (Oxenham et al. 2018).

Palaeopathological and taphonomic recording of adults and post-infant nonadults was completed by H. Buckley, and the recording of cribra orbitalia data was completed by M. Oxenham. The raw palaeopathological data for Con Co Ngua was provided for analysis and interpretation in this thesis. Recording of lesions in the Con Co Ngua infants was undertaken by myself. Of the total 274 individuals excavated in 1979, 1980 and 2013, 155 individuals from the 2013 excavation were included in the palaeopathological assessment. Con Co Ngua is the pre-interaction site assessed in Chapter 7.

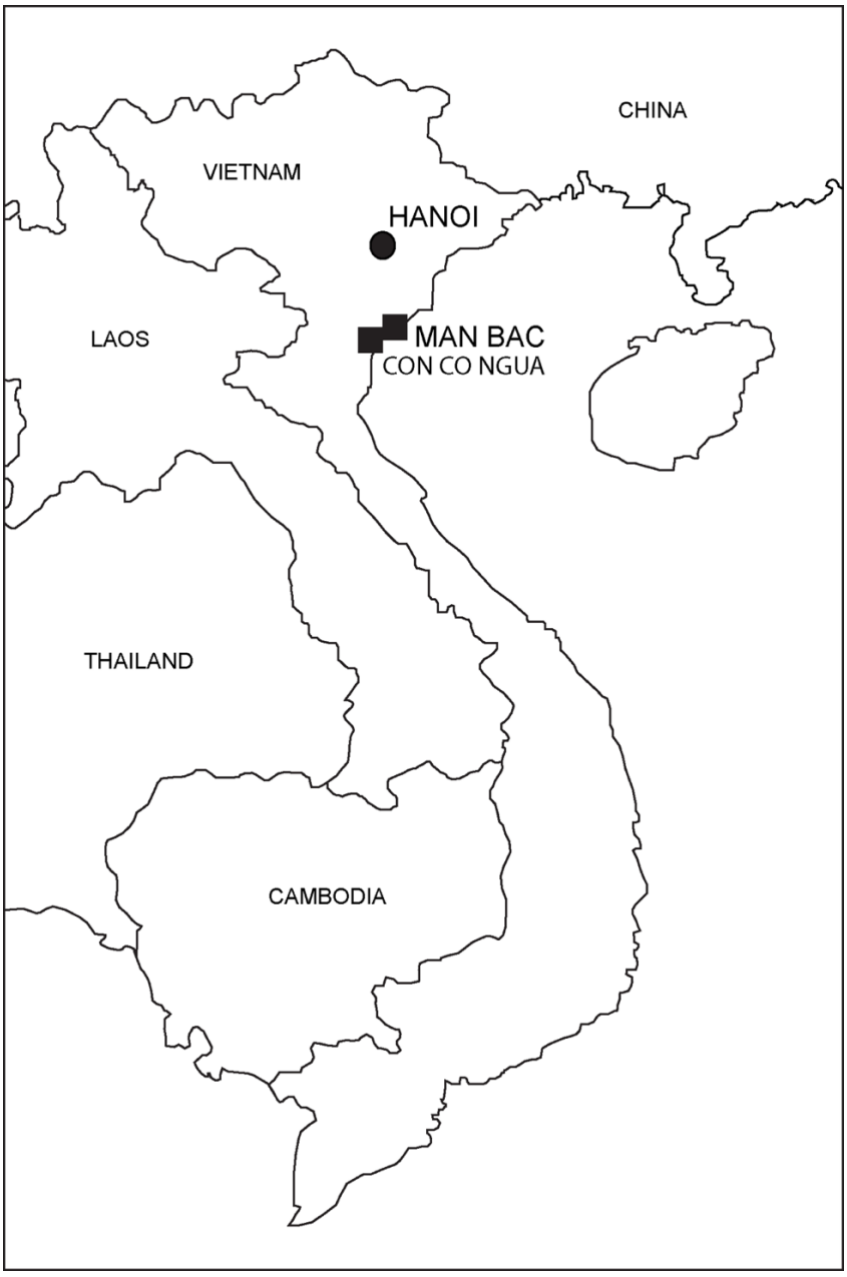

Figure 4.7: *Location of the two sites from Vietnam investigated in this thesis. Con Co Ngua represents a site prior to and Man Bac represents a site following interpopulation interaction. Image: author's own.*

4.8.2 Sample Completeness and Taphonomy

Palaeopathological raw data for the Con Co Ngua cemetery were provided by H. Buckley, therefore indices for skeletal elements are not present. However, generally speaking, individuals were predominantly partially (50-66%) to near complete (66 to 75%). Nonadult preservation most often ranged from fragmented (<33%) to partially complete (50-66%). As previously noted by Oxenham (2000), the axial skeleton and the pelvis was poorly preserved in this collection. Long bones shafts were better preserved with mixed excellent to poor preservation of the epiphyses of long bones. Bones suffered significant postmortem breakage, but most bones could be reconstructed with relative ease. Vertebrae and ribs were often fragmented. Surfaces exhibited some erosion but evidence of subperiosteal new bone deposits were still observable.

4.8.3 Sex Distribution

Twenty-four individuals could not be classified as male or female, which results predominantly from preservation issues rather than lack of sexual dimorphism in the assemblage (Table 4.16). This is represented by the large percentage of individuals confidently estimated as *probable male* or *probable female*. Forty-eight percent of the entire cohort over the age of 15 analysed in this thesis were estimated to be male (Figure 4.8). However, the variation between the presence of males and females were not statistically different (X^2 4.545, p= 0.208), and therefore assessment of differences of disease between males and females at Con Co Ngua is valid.

Table 4.16: *Estimation of sex in Con Co Ngua individuals over the age of 15.*

SEX ESTIMATION	# INDIVIDUALS
Probable Male	49
Possible Male	5
Indeterminate	24
Possible Female	11
Probable Female	23
Total	112

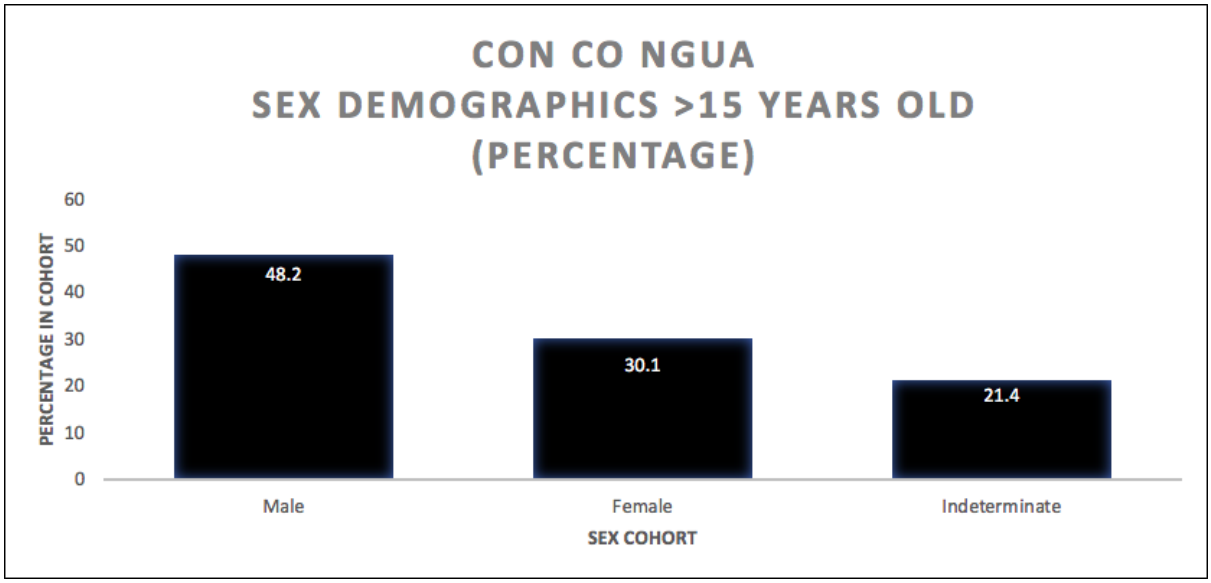

Figure 4.8: *Percentage of individuals over the age of 15 in each cohort of estimated sex at Con Co Ngua. Image: author's own.*

4.8.4 Age-at-Death Distribution

Due to poor preservation the age of six nonadults and 11 adults could not be properly estimated. Approximately 39% of the Con Co Ngua assemblage assessed in this thesis are under the age of 20, with a total of 54 nonadults represented in the sample (Table 4.17; Figure 4.9). A good representation of nonadults in the overall assemblage reflects representation of a natural cemetery population.

Table 4.17: *Age-at-death distribution of individuals included for palaeopathological assessment at Con Co Ngua. Some individuals were excluded from the analysis including a small number of foetal and neonate remains represented by single isolated bone fragments.*

AGE COHORT	# INDIVIDUALS	(%)
0 to <6 months	9	6.5
6 months to <1 year	4	2.9
1 to 5 years	11	8
6 to 10 years	8	5.8
11 to 14 years	5	3.6
15 to 19 years	17	12.3
20 to 29 years	30	21.7
30 to 39 years	22	15.9
40 to 49 years	16	11.6
50+ years	16	11.6
Total	138	

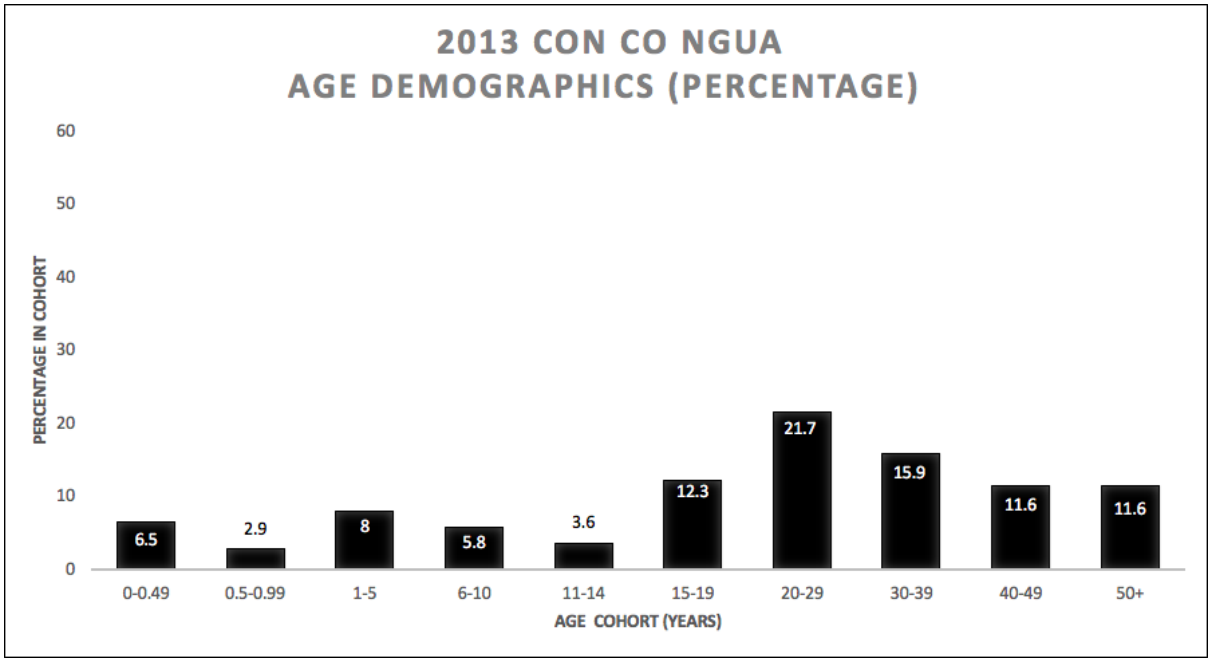

Figure 4.9: *Overall percentage age-at-death distribution of the Con Co Ngua sample. Image: author's own.*

4.9 Man Bac: Neolithic Vietnam

4.9.1 Background

Man Bac is an early Neolithic site in the Ninh Binh province of Northern Vietnam situated on a karst limestone plain. Today the site is approximately 25km from the ocean (Oxenham et al. 2011). The site was excavated in a number of seasons during 1999, 2004/5 and 2007. However, the site was likely approximately 1km from the ocean in an estuarine zone during occupation between 3906-2523 cal BP (Hiep 2004; Tanabe et al. 2006; Vlok et al. 2020). Over 100 individuals have been identified at Man Bac from the 1999 to 2007 excavations. However, only 70 individuals were preserved enough to be included in palaeopathological analysis. Man Bac is assessed as the post-interaction site in Chapter 7.

4.9.2 Sample Completeness and Taphonomy

Both the nonadult and adult assemblage of Man Bac were well represented with adults being better preserved than the nonadults (Table 4.18- 4.21). Almost 75% of the adults and 55% of the nonadults were complete (>75% preservation of the skeleton). For nonadults, the metaphyseal ends of the long bones were predominantly intact, therefore radiographs of nonadult long bones were valuable for diagnosis of nutritional disease (see Chapter 5 for radiographic diagnosis of nutritional disease from metaphyses of nonadults). For both adults

and nonadults, long bones were the best preserved skeletal elements (Table 4.19 and Table 4.21). The hands and feet of the nonadults were predominantly incomplete, this was particularly true for infants and children.

The bone surfaces of the Man Bac collection were in excellent condition, that is subperiosteal new bone deposits, even small discrete deposits, were easily identifiable on the surfaces of the bones. For some nonadults, concretions of dried clay adhered to the endocranium and vertebral bodies. These surfaces could not be cleaned and therefore were not observed and were recorded as missing. One individual (MB07H2M29) presents with a combination of beetle gnawing and carnivore punctures of the tibiae, fibulae and femora. The animal scavenging marks did not prevent observation of disease in this individual (see Chapter 7 for discussion of disease in Man Bac). Some soil in the medullary canal were present in the radiographs of Man Bac individuals. However, soil was not extensive and did not obstruct radiographic assessment.

Table 4.18: *Overall completeness of the adult skeletal assemblage at Man Bac (adapted from Buikstra and Ubelaker 1994).*

COMPLETENESS	*Fragmented (<33%)*	*Incomplete (~33 to 50%)*	*Partially Complete (~50%- 66.7%)*	*Near Complete (~66.7% to 75%)*	*Complete (> 75%)*
Count	2/26	1/26	1/26	3/26	19/26
%	7.7	3.8	3.8	11.5	73.1

Table 4.19: *Completeness of different skeletal elements of the Man Bac adults. Following White (1992).*

	Range (%)	**Mean (%)**
Long Bone Survival Index	0 to 100	82.69
Hands and Feet Survival Index	0 to 100	62.48
Vertebrae Survival Index	0 to 100	74.52
Neurocranium Survival Index	0 to 100	81.25

Table 4.20**:** *Overall completeness of the nonadult skeletal assemblage at Man Bac (adapted from Buikstra and Ubelaker 1994).*

COMPLETENESS	*Fragmented (<33%*	*Incomplete (~33 to 50%)*	*Partially Complete (~50%- 66.7%)*	*Near Complete (~66.7% to 75%)*	*Complete (> 75%)*
Count	5/44	6/44	3/44	6/44	24/44
%	11.4	13.6	6.8	13.6	54.5

Table 4.21: *Completeness of different skeletal elements of the Man Bac nonadults. Following White (1992).*

	Range (%)	Mean (%)
Long Bone Survival Index	5.6 to 100	75.84
Hands and Feet Survival Index	0 to 88.68	20.05
Vertebrae Survival Index	8.3 to 100	63.35
Neurocranium Survival Index	0 to 100	63.07

4.9.3 Sex Distribution

Of the 29 adults included in palaeopathological assessment, 25 were assigned a sex estimation (Table 4.22). Four individuals could not be classified as male or female. Fifty percent of the entire cohort over the age of 15 analysed in this thesis were estimated to be male, compared to approximately 37% females (Figure 4.10). However, the variation between the presence of males and females were not statistically different (X^2 0.615, p= 0.893), and therefore assessment of differences of disease between males and females at Man Bac is valid.

Table 4.22: *Estimation of sex in Man Bac individuals over the age of 15. Data was provided by M. Oxenham and K. Domett.*

SEX ESTIMATION	# INDIVIDUALS
Probable Male	11
Possible Male	4
Indeterminate	4
Possible Female	3
Probable Female	7
Total	29

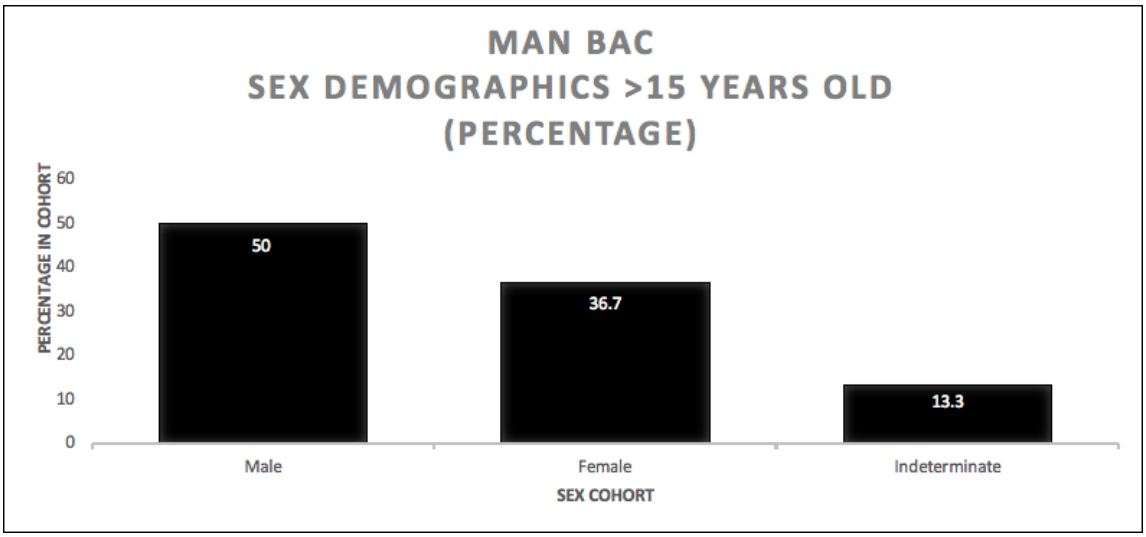

Figure 4.10: *Percentage of individuals over the age of 15 in each cohort of estimated sex at Man Bac. Image: author's own.*

4.9.4 Age-at-Death Distribution

Approximately 63% of the Man Bac assemblage were under the age of 20, with almost 49% aged 5 years or younger (Table 4.23; Figure 4.11). The high number of nonadults at Man Bac is likely due to excellent preservation, an exceptionally high fertility ratio (McFadden et al. 2018), and inclusion of nonadults in the overall burial practices at Man Bac (Oxenham et al. 2011). Therefore, it is likely the assemblage properly characterises the underlying mortality and fertility distribution of the population. This is particularly visible in Figure 4.12, where it is clear the highest percentage of deaths are occurring within the first year of life. The nonadult age-at-death distribution trend follows common epidemiological patterns of death, with highest mortality of nonadults under the age of 5 followed by a period of low mortality until adulthood. The adult age-at-death distribution does not follow a typical mortality distribution where increase in percentage of deaths with increasing age is expected. Instead, higher numbers of deaths in early adulthood occurred (Figure 4.12).

Table 4.23: *Age-at-death distribution of individuals included for palaeopathological assessment at Man Bac.*

AGE COHORT	# INDIVIDUALS	(%)
0 to <6 months	8	11.4
6 months to <1 year	6	8.6
1 to 5 years	20	28.6
6 to 10 years	3	4.3
11 to 14 years	3	4.3
15 to 19 years	4	5.7
20 to 29 years	9	12.9
30 to 39 years	6	8.6
40 to 49 years	8	11.4
50+ years	3	4.3
Total	70	

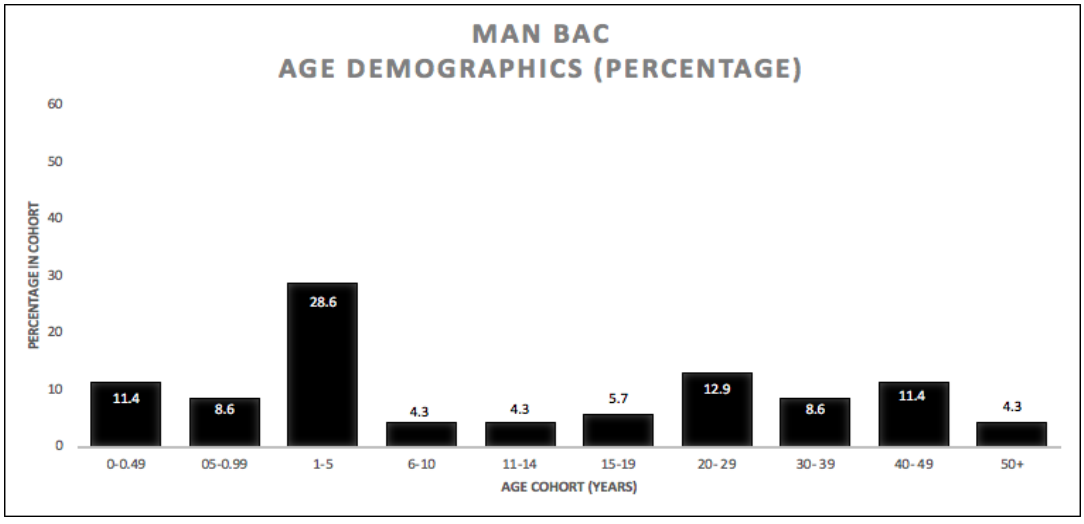

Figure 4.11: *Overall percentage age-at-death distribution of the Man Bac sample. Image: author's own.*

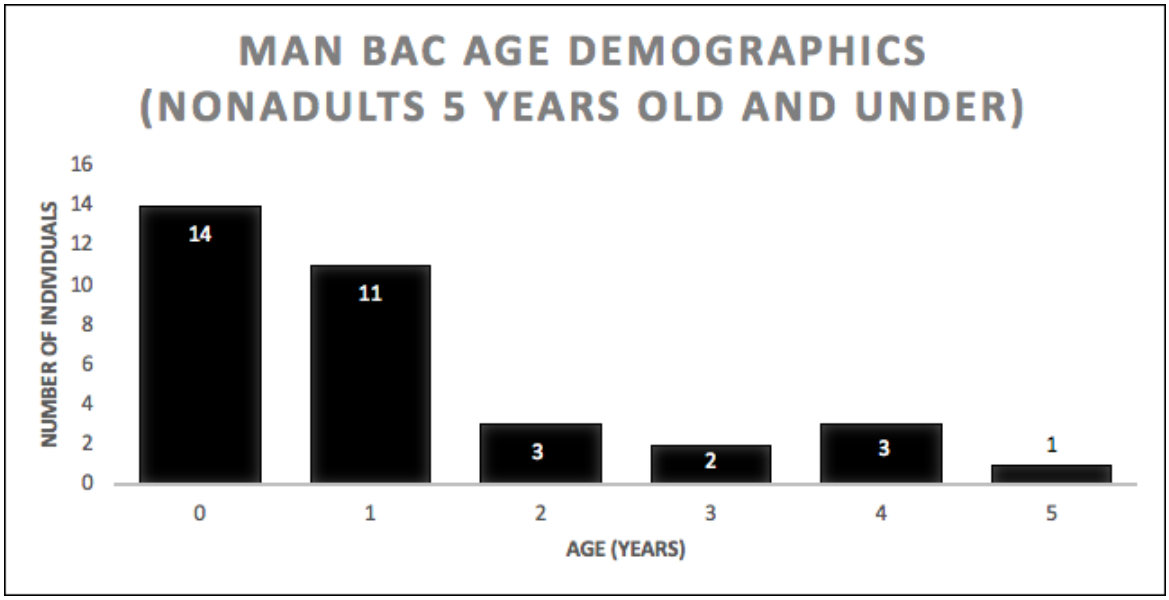

Figure 4.12: *Age-at-death distribution of individuals 5 years and under in the Man Bac sample. Image: author's own.*

4.10 Bronze Age Mongolia

4.10.1 Background

The Bronze Age Mongolian assemblage is an accumulation of a number of sites across Mongolia, as low numbers of burials are generally found at each site (Figure 4.13). The sites date from the Early to Final Bronze Ages, approximately 5000-2300 BP (Dashtseveg et al. 2013; Taylor et al. 2019). Ninety-two individuals were included in the palaeopathological assessment of Bronze Age Mongolia. The overall assemblage is comprised of seven cultures, described in greater detail in Chapter 8 (Figure 4.14). The assemblage represents the pre-interaction time period investigated in Chapter 8.

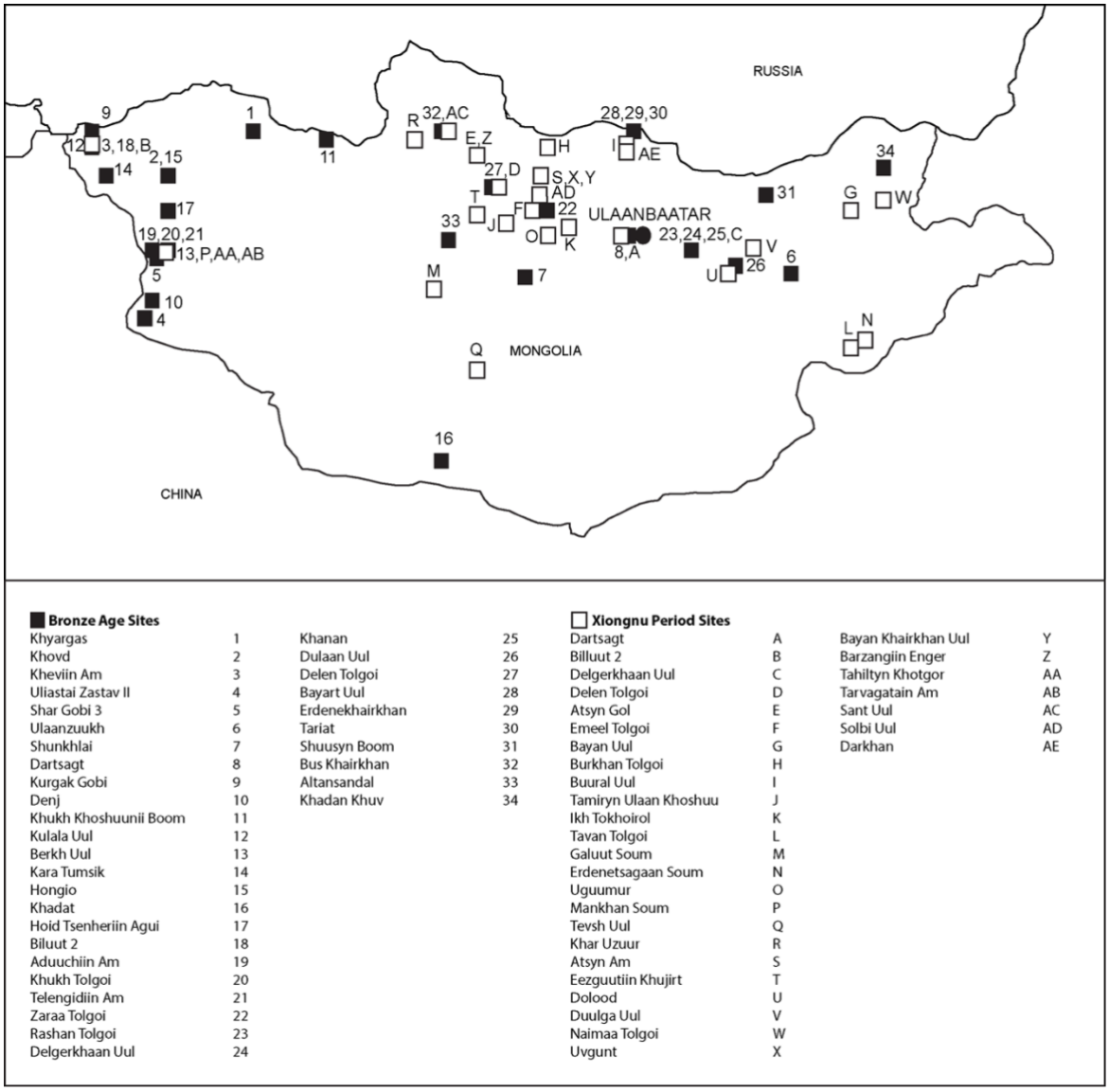

Figure 4.13: *Location of the sites from Mongolia investigated in this thesis. Black squares represent Bronze Age sites and white squares represent Xiongnu Period sites. The modern city of Ulaanbaatar is here presented for geographical reference. Image: author's own.*

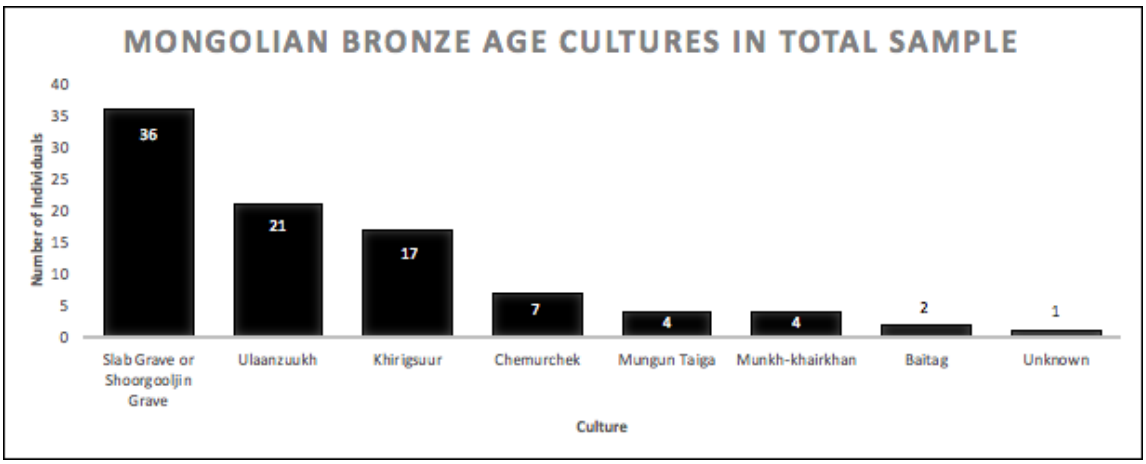

Figure 4.14: *Number of individuals from each cultural group within the Bronze Age Mongolia assemblage. Image: author's own.*

4.10.2 Sample Completeness and Taphonomy

While only 20% of the adult assemblage were complete (more than 75% of skeletal elements present), over 70% were at least partially complete (Table 4.24). The cranium of most individuals were absent, accounting for the low mean preservation of the neurocranium for the overall population (Table 4.25). However, for individuals where the cranium was present, it was intact and excellently preserved. Long bones and vertebrae were the better preserved skeletal elements of the assemblage (Table 4.25). Nonadults were less well preserved than adults (Table 4.26). However more nonadults had cranial elements present than adults (Table 4.27). Once again long bones were the best preserved skeletal elements for nonadults.

Due to the arid climate, most surfaces were in excellent condition. That is, subperiosteal new bone deposits, even small discrete deposits, were easily identifiable on the surfaces of the bones. For some individuals root etching of the limb bones, weathering or covering of dry soil impacted the visibility of the surfaces but they could still be recorded. Fourteen individuals had weathering and animal scavenging which obscured the bone surfaces (see Appendix 2). There was also a moderate amount of postmortem breakage of preserved skeletal elements.

Table 4.24*: *Overall completeness of the adult Bronze Age Mongolia skeletal assemblage (adapted from Buikstra and Ubelaker 1994).

COMPLETENESS	*Fragmented (<33%)*	*Incomplete (~33 to 50%)*	*Partially Complete (~50%- 66.7%)*	*Near Complete (~66.7% to 75%)*	*Complete (> 75%)*
Count	1/74	19/74	26/74	13/74	15/74
%	1.4	25.7	35.1	17.6	20.3

Table 4.25*: *Completeness of different skeletal elements of the Bronze Age Mongolia adults. Following White (1992).

	Range (%)	**Mean (%)**
Long Bone Survival Index	0 to 100	65.38
Hands and Feet Survival Index	0 to 65.09	16.55
Vertebrae Survival Index	0 to 100	41.55
Neurocranium Survival Index	0 to 100	28.25

Table 4.26: *Overall completeness of the nonadult Bronze Age Mongolia skeletal assemblage (adapted from Buikstra and Ubelaker 1994).*

COMPLETENESS	*Fragmented (<33%*	*Incomplete (~33 to 50%)*	*Partially Complete (~50%- 66.7%)*	*Near Complete (~66.7% to 75%)*	*Complete (> 75%)*
Count	0/18	8/18	3/18	4/18	3/18
%	0	44.4	16.7	22.2	16.7

Table 4.27: *Completeness of different skeletal elements of the Bronze Age Mongolia nonadults. Following White (1992).*

	Range (%)	**Mean (%)**
Long Bone Survival Index	0 to 100	52.19
Hands and Feet Survival Index	0 to 64.15	8.75
Vertebrae Survival Index	0 to 95.83	31.48
Neurocranium Survival Index	0 to 100	38.19

4.10.3 Sex Distribution

Of the 81 individuals over 15 years old included in palaeopathological assessment, 67 individuals were assigned an estimation (Table 4.28). Fourteen individuals could not be classified as male nor female. Almost 50% of the entire cohort over the age of 15 were estimated to be male (Figure 4.15). However, the variation between the presence of males and females were not statistically different (X^2 1.806, p= 0.614), and therefore assessment of differences of disease between males and females in Bronze Age Mongolia is valid.

Table 4.28: *Estimation of sex in Bronze Age Mongolia individuals over the age of 15.*

SEX ESTIMATION	**# INDIVIDUALS FINAL SEX ESTIMATION**
Probable Male	20
Possible Male	19
Indeterminate	14
Possible Female	11
Probable Female	17
Total	81

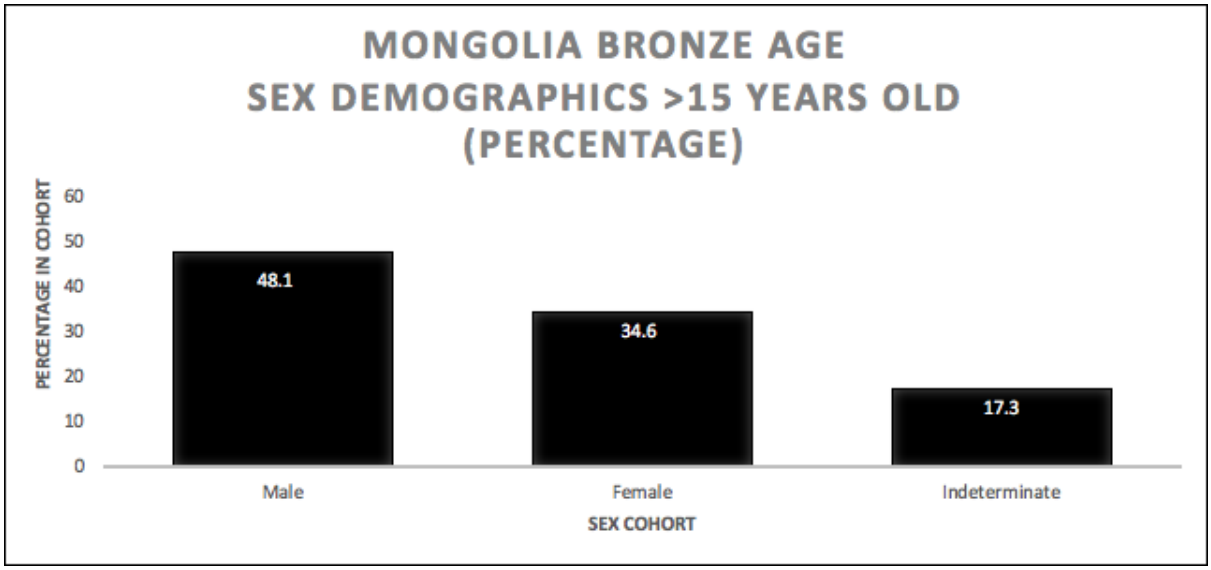

Figure 4.15: *Percentage of individuals over the age of 15 in each cohort of estimated sex in Bronze Age Mongolia. Image: author's own.*

4.10.4 Age-at-Death Distribution

While only 25% of individuals the assemblage were under the age of 20, all nonadult age stages were represented. In a typical mortality distribution it would be expected that a higher number of infant deaths would be present. However, the percentage of infants under 1 year of age was higher than other nonadults until the age of 15 to 19 years, which does follow a typical mortality distribution (Table 4.29; Figure 4.16). A low fertility rate may be the cause for the low numbers of infants in the assemblage. Almost 15% of the overall assemblage were old adults (over the age of 50 years). While the adult age-at-death distribution is inconsistent with a typical mortality distribution, there may be a high survivorship reflected in the assemblage.

Table 4.29: *Age-at-death distribution of individuals included for palaeopathological assessment of Bronze Age Mongolia*

AGE COHORT	# INDIVIDUALS	(%)
0 to <6 months	2	2.8
6 months to <1 year	2	2.8
1 to 5 years	2	2.8
6 to 10 years	3	4.2
11 to 14 years	3	4.2
15 to 19 years	6	8.5
20 to 29 years	10	14.1
30 to 39 years	20	28.2
40 to 49 years	13	18.3
50+ years	10	14.1
Total	71	

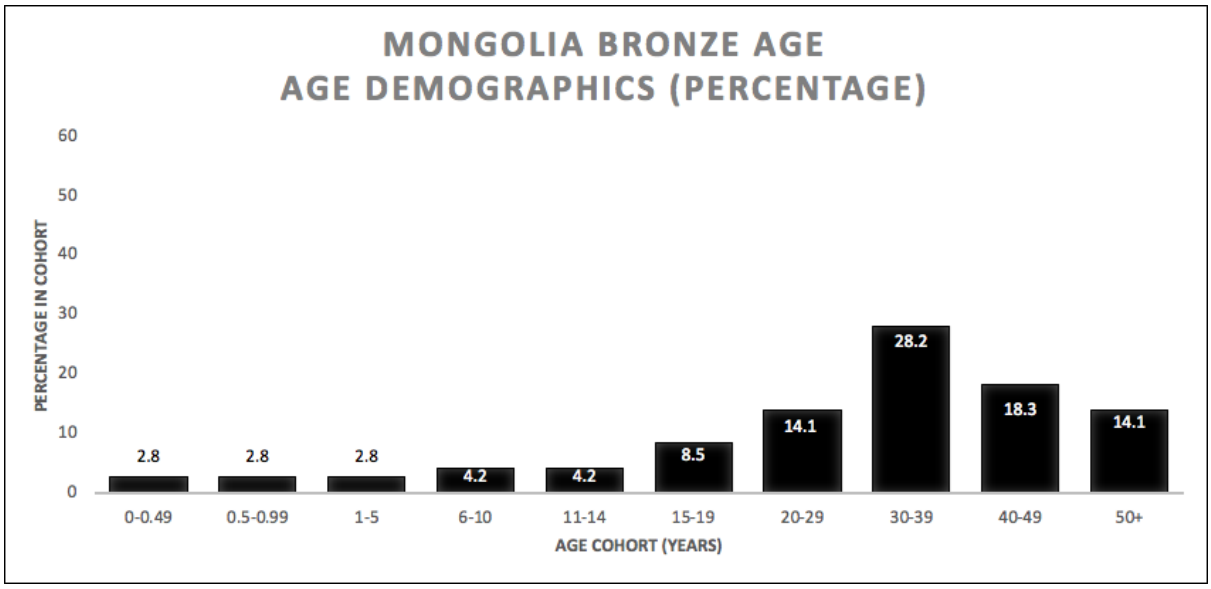

Figure 4.16: *Overall percentage age-at-death distribution of the Bronze Age Mongolia sample. Image: author's own.*

4.11 Xiongnu Period (Iron Age) Mongolia

4.11.1 Background

The Xiongnu Mongolian assemblage is an accumulation of a number of sites across Mongolia, as a low number of burials are generally found at each site. The sites date to the Xiongnu Empire (2300-1800 BP), the first confederate state of the Mongolian region focused on mobile pastoralism (Keyser-Tracqui et al. 2006; Wright et al. 2009). Sixty-nine individuals from the Xiongnu Period were assessed for this thesis. The assemblage represents the post-interaction time period in Chapter 8.

4.11.2 Sample Completeness and Taphonomy

Only approximately 30% of the adults in the assemblage were complete (more than 75% of skeletal elements present). However, over 96% were at least partially complete (Table 4.30). Only the postcranium of most individuals were present, accounting for the low mean preservation of the neurocranium for the overall population, and the predominance of near complete individuals (Table 4.31). However, for individuals where the cranium was present, it was intact and excellently preserved. Long bones and vertebrae were the better preserved skeletal elements of the skeletal assemblage (Table 4.31). Nonadults were

predominantly complete or incomplete (Table 4.32). Adolescents were the better preserved individuals (complete individuals), with infants and children being less well preserved. (Table 4.33).

Preservation of surfaces in most individuals were excellent. That is, that subperiosteal new bone deposits, even small discrete deposits, were easily identifiable on the surfaces of the bones. In two individuals the aridity preserved portions of mummified periosteum, and there appeared to be no apparent postmortem damage to the skeletons. Weathering, gnaw marks and dry dust of bone surfaces were present in the assemblage but infrequent (see Appendix 2). Postmortem breakage was also minimal in the assemblage.

Table 4.30: *Overall completeness of the adult Xiongnu Period Mongolia skeletal assemblage (adapted from Buikstra and Ubelaker 1994).*

COMPLETENESS	*Fragmented (<33%)*	*Incomplete (~33 to 50%)*	*Partially Complete (~50%- 66.7%)*	*Near Complete (~66.7% to 75%)*	*Complete (> 75%)*
Count	0/51	2/51	8/51	25/51	16/51
%	0.0	3.9	15.7	49.0	31.4

Table 4.31: *Completeness of different skeletal elements of the Xiongnu Period Mongolia adults. Following White (1992).*

	Range (%)	**Mean (%)**
Long Bone Survival Index	0 to 100	78.43
Hands and Feet Survival Index	0 to 56.60	14.48
Vertebrae Survival Index	0 to 100	62.99
Neurocranium Survival Index	0 to 100	36.02

Table 4.32**:** *Overall completeness of the nonadult Bronze Age Mongolia skeletal assemblage (adapted from Buikstra and Ubelaker 1994).*

COMPLETENESS	*Fragmented (<33%*	*Incomplete (~33 to 50%)*	*Partially Complete (~50%- 66.7%)*	*Near Complete (~66.7% to 75%)*	*Complete (> 75%)*
Count	0/18	7/18	1/18	4/18	6/18
%	0	38.9	5.6	22.2	33.3

Table 4.33: *Completeness of different skeletal elements of the Bronze Age Mongolia nonadults. Following White (1992).*

	Range (%)	**Mean (%)**
Long Bone Survival Index	0 to 100	65.89
Hands and Feet Survival Index	0 to 37.74	8.07
Vertebrae Survival Index	0 to 100	41.67
Neurocranium Survival Index	0 to 100	38.89

4.11.3 Sex Distribution

Of the total of 60 individuals over the age of 15 only 6.6% (4 individuals) could not be estimated by sex (Figure 4.17). A near 1:1 ratio of males and females is present in the assemblage (Table 4.34). The variation between the presence of males and females were then not statistically different (X^2 0.018, p= 0.999), and therefore assessment of differences of disease between males and females in Xiongnu Period Mongolia is valid.

***Table 4.34*:** *Estimation of sex in Xiongnu Period Mongolia individuals over the age of 15.*

SEX ESTIMATION	# INDIVIDUALS FINAL SEX ESTIMATION
Probable Male	23
Possible Male	6
Indeterminate	4
Possible Female	9
Probable Female	18
Total	60

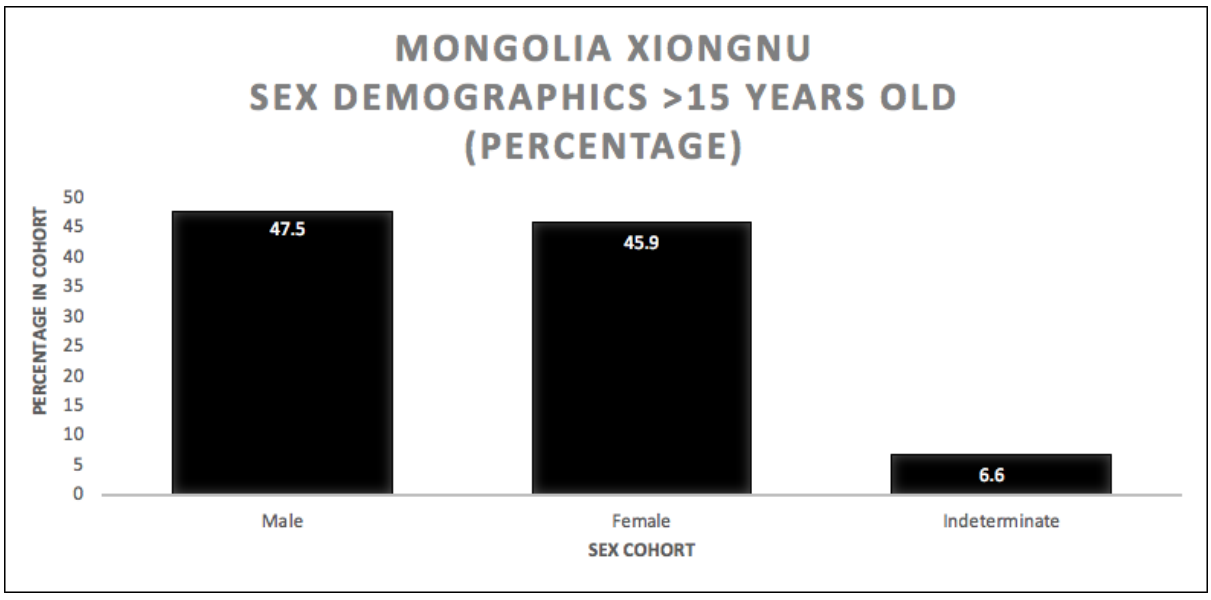

Figure 4.17: *Percentage of individuals over the age of 15 in each cohort of estimated sex in Xiongnu Period Mongolia. Image: author's own.*

4.11.4 Age-at-Death Distribution

Twenty-seven percent of the assemblage were under the age of 20, predominantly represented by adolescents, and no infants between 6 months and 1 year of age were represented (Table 4.35; Figure 4.18). Given the low percentage of infants under 1 years of

age, the assemblage is not representative of a normal mortality distribution. A low fertility rate may be the cause for the low numbers of infants in the assemblage. Almost 14% of the overall assemblage were old adults (over the age of 50 years), which denotes an excellent representation of adult age categories, likely due to excellent preservation of the assemblage. However, with 50% of the sample between the age of 20 and 39, the adult assemblage is also not entirely representative of a typical mortality distribution.

Table 4.35: *Age-at-death distribution of individuals included for palaeopathological assessment of Xiongnu Period Mongolia*

AGE COHORT	# INDIVIDUALS	(%)
0 to <6 months	1	1.5
6 months to <1 year	0	0
1 to 5 years	3	4.5
6 to 10 years	4	6.1
11 to 14 years	1	4.5
15 to 19 years	9	13.6
20 to 29 years	18	27.3
30 to 39 years	16	24.2
40 to 49 years	5	7.6
50+ years	9	13.6
Total	66	

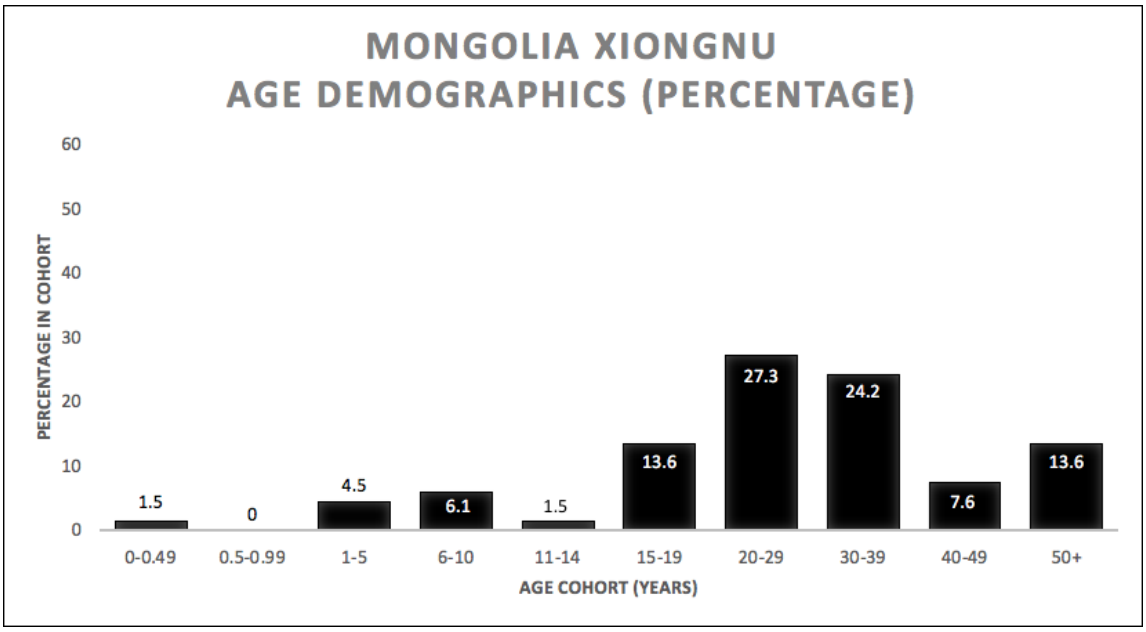

Figure 4.18: *Overall percentage age-at-death distribution of the Xiongnu Period Mongolia sample. Image: author's own.*

4.12 Chapter Summary

This chapter provided an overview of the methods and results for age, sex and recording of taphonomic damage for the six assemblages employed in this thesis. The first half of the chapter introduced the theory fundamental to the methodology for estimating the parameters of age and sex. The rationale for particular methods and standards employed were then described. Methods for describing post depositional taphonomic processes on the skeletal assemblages were also presented. The second half of this chapter focused on descriptors of age, sex and taphonomy for each of the assemblages which are essential to appropriately interpret the population disease level assessments in the subsequent chapters.

CHAPTER 5:
METHODOLOGY FOR RECORDING PATHOLOGY AND DIAGNOSIS OF DISEASE

5.1 Introduction

The differential diagnosis of disease provides the foundations for all analysis in this thesis, and a robust diagnostic protocol is essential to correctly identify disease in the past. The first section of this chapter outlines the processes for differential diagnosis employed in this thesis. Systematic and detailed lesion recording protocols are fundamental for the classification of diseases through differential diagnosis, as differentiation of diseases in the skeleton can at times be dependent upon arguably diminutive differences in lesion patterning. For this reason, the methodology employed in this thesis for the macroscopic and radiographic recording of lesions in dry bone is outlined here. Subsequent to the methodology of lesion recording, the methodology for a standardised approach to differential diagnoses for specific and non-specific infectious disease, specific nutritional disease, and anaemias is presented. The pathophysiology, lesion type and distribution across the skeleton for each disease is presented prior to the diagnostic protocol applied to identify this disease in the skeletal archaeological record. Following this, the second section of this chapter introduces the statistical analyses applied to assess the mortality and morbidity of the diseases diagnosed in accordance with the objectives of this thesis.

Some of the background of the skeletal manifestations of tuberculosis, leprosy, treponematosis, brucellosis and osteomyelitis, the diagnostic criteria of treponematosis, and the parameters for diagnostic lesion scoring is published in *Bioarchaeology International* (Vlok et al. 2020). The description of the employment of relative risk ratios for the assessment of morbidity in palaeoepidemiology was submitted in a manuscript to the *International Journal of Paleopathology* (Vlok et al. in review).

PART ONE: DIAGNOSIS OF DISEASE

5.2 Assessment of Disease in Palaeopathology

Palaeopathological assessment of dry bone provides the foundation for identification of disease in this thesis. The following section presents the biological basis of disease expression in the skeleton, and the identification of *specific* disease, prior to presenting the methods of identification and diagnosis of *non-specific* and *specific* disease used in this thesis. Finally, the diagnostic criteria for each disease under investigation is presented.

5.2.1 Pathological Bone Response

An abnormal response to bone can be caused by trauma or disease (infection, nutritional deficiency, hormonal or cancerous insults) (Klaus and Lynnerup 2019). As is the case with normal bone remodelling (see Chapter 3), only osteolytic (bone loss) and/ or osteoblastic (bone production) cellular processes can occur. When one cellular process overtakes the other the bone response is considered pathological (Klaus and Lynnerup 2019). This abnormal response, as previously described is termed a *lesion*. The most common form of response is subperiosteal new bone (SPNB) formation (Weston 2012). The initial appearance of SPNB develops from woven (active) to lamellar (remodelled) bone (Weston 2012). The unorganised formation of the woven SPNB can leave traces on the surface of the bone even when remodelling has begun. The identification of osteolytic and osteoblastic lesions in bone form the foundations for palaeopathological research of skeletal remains as they are often the only macroscopically visible remnants of a disease, which likely interacted with soft tissue no longer available for study (Ortner 2003). In growing children, the initial modelling of the bones (see Chapter 3) can also be disrupted and leading to shape deformities and mechanical failure of the bone (Brickley and Ives 2010; Lewis 2017; Ortner et al. 2001).

5.3 Methods of Lesion Recording

The limited response of bone to disease presents a challenge to palaeopathology. In regards to SPNB deposits, which can result from many aetiologies, as it is the primary skeletal inflammatory response to physiological insult, clear description is vital for interpretation of the underlying cause (Table 5.1; Weston 2008; Weston 2012). Description of the skeletal element affected, severity, level of remodelling (active, mixed or remodelled),

and alterations to bone shape should be recorded. Similarly, description of the size, shape, margin definition, localisation and level of sclerotic response in an osteolytic lesion is important for specific diagnosis where possible (Table 5.1; Buikstra and Ubelaker 1994). For each lesion, the skeletal element, aspect and position on the element, the type of bone affected (cortical, trabecular or medullary canal intrusion), laterality, and symmetricity were noted. Distortion of the bone shape was also noted and described when identified. Osteoblastic lesions, osteolytic lesions and porosity were coded separately. Where a lesion had an osteoblastic and an osteolytic component, or involved an inflammatory and porotic response, the lesion was coded as having both. Where a lesion was considered to have diagnostic potential for identification of a specific disease, the skeletal element was radiographed, enabling observation of internal changes to the cortex, trabeculae and medullary canals. Specifications for radiograph machine and images were not recorded due to issues with the language barrier between myself and radiograph technicians.

Table 5.1: *Parameters for description of osteoblastic and osteolytic lesions recorded in this thesis. X designates that the lesion parameter was recorded.*

Lesion Description Parameters	Osteoblastic Lesions	Osteolytic Lesions
Lesion location on the bone - proximal epiphysis/ proximal metaphysis/ proximal third shaft/ middle third shaft/ distal metaphysis or distal epiphysis - body or arches - endocranium or ectocranium	X	X
Aspect of bone affected - anterior/ posterior/ medial/ lateral/ superior and/or inferior	X	X
Percentage of bone affected	X	X
Completeness of bone - complete/ near complete/ partially complete/ incomplete or fragmented	X	X
Bone type affected - cortical/ trabecular and/or medullary canal	X	X
Is there shape change associated? - description of shape change	X	X
Associated fracture? - description of fracture	X	X
Lesion healing - active/ mixed/ or remodelled	X	X
Margins - defined, defined with sclerotic reaction or undefined		X
Associated sequestra?	X	X
Focality? - Focal/ multifocal/ multifocal and coalesced/ diffuse	X	X
Bilateral?	X	X
Symmetrical?	X	X
Lesion Diameter - Measured with sliding calipers (mm)		X

5.3.1 Osteoblastic Lesion Recording

Coding of proliferative lesions were adapted from Buckley and Tayles (2003) and Steckel et al. (2011). Buckley and Tayles (2003) is a useful method for recording osteoblastic lesions, as it is straightforward to apply, and provided the basis for the recording of lesions within this thesis. However, the lesion recording method does not distinguish SPNB deposits from lesions leading to cortical enlargement, and, eventually, medullary closure. The authors primarily developed this code to describe osteoblastic lesions possibly related to treponematosis. The code adapted in this thesis enables consideration of extensive new bone deposits with or without enlargement of the underlying cortex (Table 5.2, Figure 5.1- 5.6). Cortical enlargement, sometimes described in the literature as cortical expansion, is a term defined by SPNB and endosteal apposition of new bone that results in abnormal enlargement of the cortex width (Ortner 2003). For the purposes of differential diagnosis, consideration of small localised discrete deposits of new bone is also necessary, as this may be indicative of underlying Vitamin C deficiency (see the scurvy section below), therefore this score was adopted from Steckel et al. (2011). However, the remainder of the lesion recording code by Steckel et al. (2011) is not directly used here as the authors do not describe the justification for their severity scores. For example, 'moderate involvement of the periosteum' does not explain the degree of SPNB deposit required to classify a deposit as such. However, the terms *slight*, *moderate* and *extensive* as used by Steckel et al. (2011) are employed in this thesis. These terms are defined in the recording code (Table 5.2).

Table 5.2: *Codes used for recording of Osteoblastic (OB) Lesions compared to Buckley and Tayles (2003) and Steckel et al. (2011).*

OB Code ***Steckel et al. (2011)***	**Description**	**OB Code** ***Buckley and Tayles (2003)***	**Description**	**OB Code** ***used in this thesis***	**Description**
1	No osteoperiostitis present	***1***	Formation of subperiosteal new bone as part of a response to infection or an aetiology of non-infectious origin: uneven distribution of disorganised new bone and/or cortical porosity on the cortical surface of the bone	***1***	Slight discrete patches of SPNB (in long bones this involves less than one quarter of the diaphysis)
2	Markedly accentuated longitudinal striations			***2***	Slight SPNB but more diffuse along the length of the bone element (> ¼ of the bone element)
3	Slight, discrete patches of reactive bone involving less than one quarter of the long bone surface	***2***	More diffuse apposition of subperiosteal new bone, with incipient new bone production on the endosteal aspect	***3***	Moderate SPNB: projection of SPNB from the surface of the underlying cortical bone, there is distinct change to the surface morphology
4	Moderate involvement of the periosteum			***4***	Similar to OB3 but with cortical enlargement (radiographs or postmortem breaks are required to identify this grade)
5	Extensive periosteal reaction involving over half of the diaphysis, with cortical expansion, pronounced deformation	***3***	Gross and diffuse apposition of new bone on the subperiosteal and endosteal margins of the bone. The thickness of the cortex will be increased (radiography required to identify this grade)	***5***	Extensive SPNB: significant gross apposition of SPNB and pronounced deformation of the external cortex margin
6	Osteomyelitis (infection involving most of the diaphysis with cloacae)			***6***	Similar to OB5 but with cortical enlargement (radiographs or postmortem breaks are required to identify this grade)
7	Osteoperiostitis associated with a fracture	***4***	Complete closure of medullary canal due to endosteal expansion of disorganised new bone.		

***Figure 5.1**: OB Grade 1 (Edo Period [15th to 19th Century AD] Japan, Scapula). Image: author's own*

***Figure 5.2**: OB Grade 2 (Edo Period Japan, Tibia). Image: authors own.*

Figure 5.3: *OB Grade 3 (Edo Period Japan, Clavicles). The subperiosteal new bone deposit is similar to that of the OB2 grade lesion in Figure 5.2. However, the deposit projects from the underlying cortex, changes the contour of the outer surface and there is no evidence of cortical enlargement (white arrow). Image: authors own.*

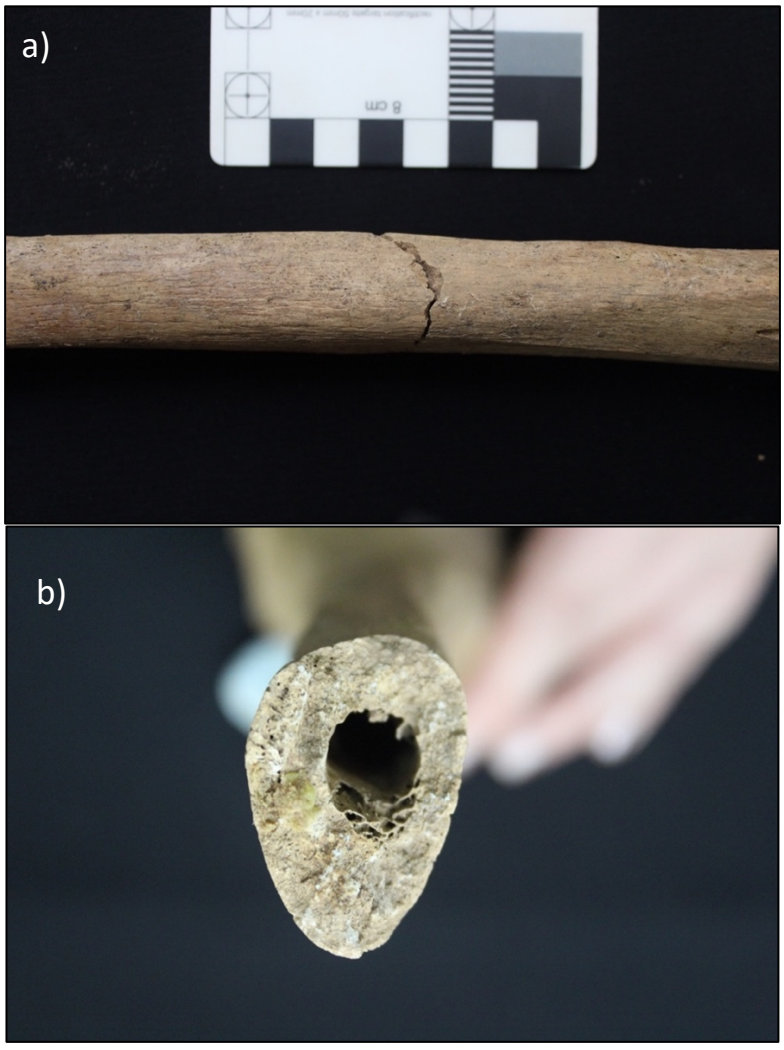

Figure 5.4*: OB Grade 4 (Neolithic Vietnam, Tibia). a) note the cortical thickness b) transverse view shows clear cortical enlargement. Image: author's own.*

Figure 5.5: *OB Grade 5 (Ancient Egypt, Femur). Image: Wellcome Library. creative commons.*

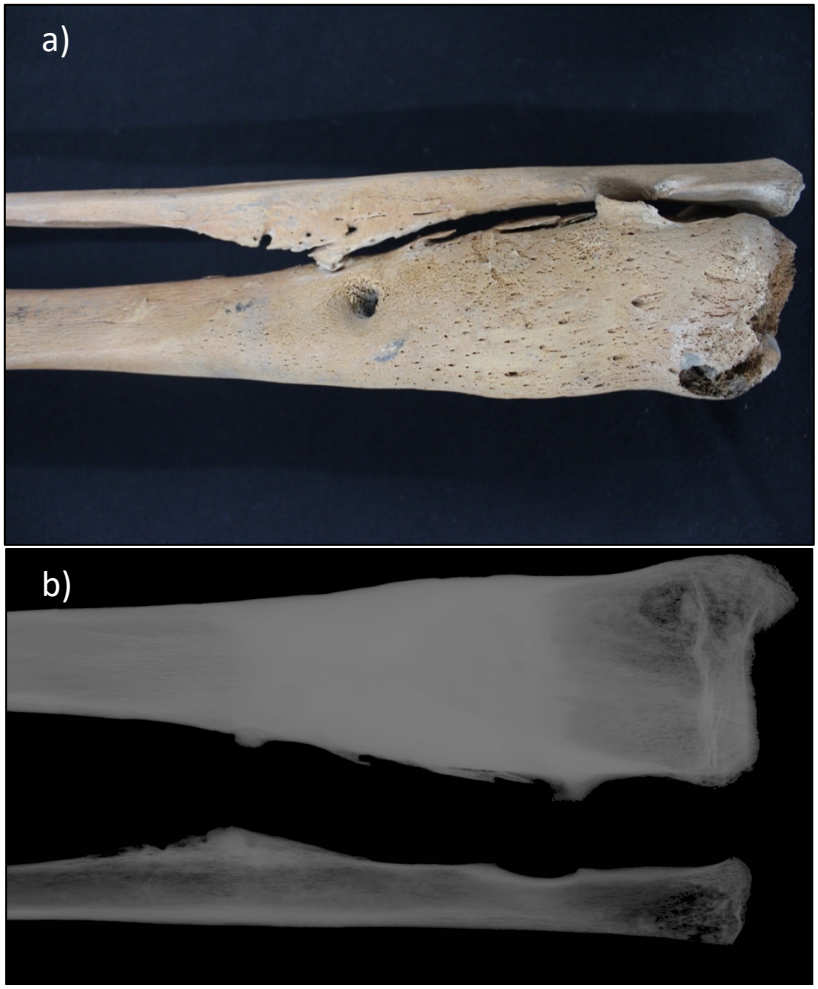

Figure 5.6: *OB Grade 6 (Edo Period Japan, Tibia). Extensive new bone response with cortical enlargement. This tibia also presents with pathology consistent with osteomyelitis (see below for description of osteomyelitis diagnosis) Image: authors own.*

5.3.2 Osteolytic Lesion Recording

Recording of osteolytic lesions followed protocol presented by Buikstra and Ubelaker (1994). The osteolytic lesion recording from Buckley and Tayles (2003) was not followed, as it was based on the progression of osteolytic lesions which form in treponemal disease specifically and is therefore not appropriate for description of other osteolytic lesions. Severity was based on the size of the lesions (Table 5.3, Figure 5.7- 5.9). However, when lytic erosion occurred on margins (e.g. the nasal margin), the approximate area of bone loss was difficult to determine. In these circumstances the entire area was measured (e.g. the entire nasal cavity; see Figure 5.9 for an example). Descriptors of focality, depth, margin description, level of sclerotic response (osteoblastic response alongside the osteolytic destruction) on the margins and in the base, and location on the skeletal element were more important for describing the osteolytic lesion for differential diagnosis (after recommendations by Ortner 2003).

Table 5.3: *Codes used for recording of Osteolytic (OL) Lesions*

Osteolytic (OL) code	Description
1	Bone loss covering < 1cm area
2	Bone loss 1-5cm area
3	Bone loss >5cm

5.3.3 Osteoblastic and Osteolytic Lesions Scores and their Relationship to Diagnosis

It is important to note that the codes used for recording of osteoblastic and osteoclastic lesions do not directly relate to diagnosis of disease. While these codes are useful in defining the relative severity of a lesion, and necessary for comprehensive and standardised macroscopic assessment of bone pathology, diagnosis is considerably dependent on lesion type and distribution within the skeleton (see below). Further discussion on the severity of lesions and their potential value to future diagnostic protocols is presented in Chapter 10.

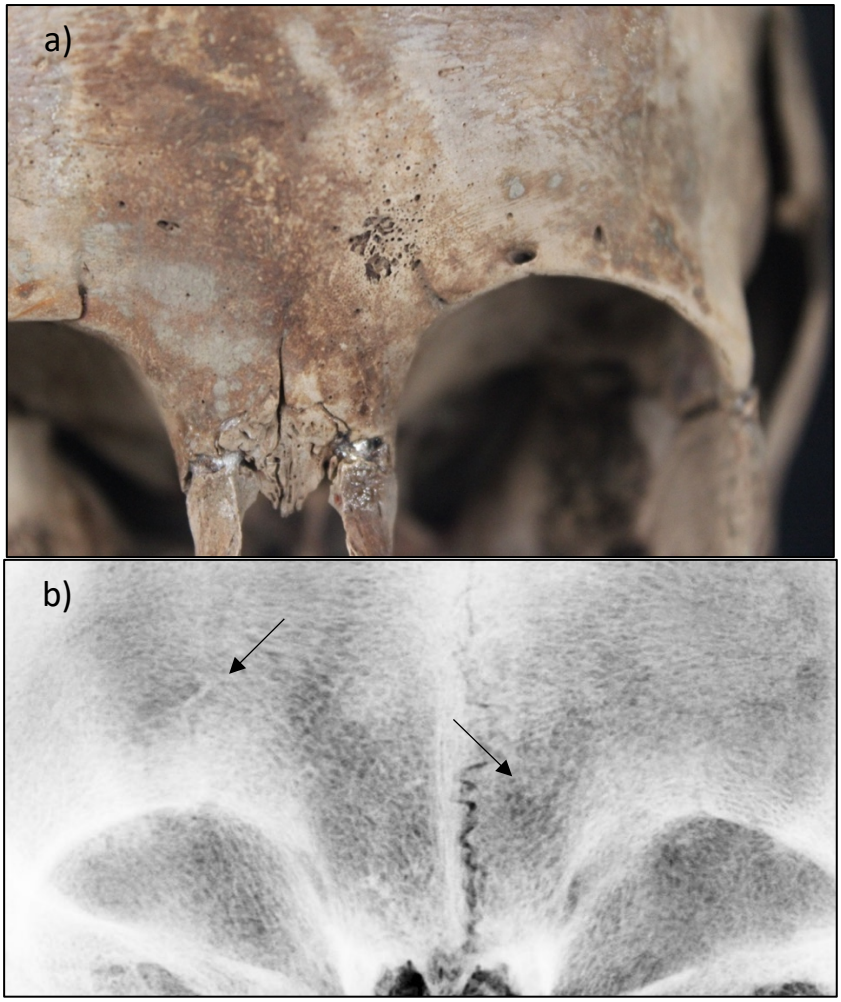

Figure 5.7: *OL Grade 1 (Edo Period Japan, Cranium). a) The lesion is multifocal and coalesced with defined margins, no evidence of sclerotic reaction, and loss of both cortical and trabecular bone. b) Radiographs demostrated two osteolytic regions with minimal bone response. The lesion on the left while macroscopically observeable is faint radiographically, but multifocal lytic destruction is observable. However, the lesion on the right is more clear on the radiograph. As the lesion on the right does not penetrate the external cortex, these lesions are not due to taphonomic damage. Image: author's own.*

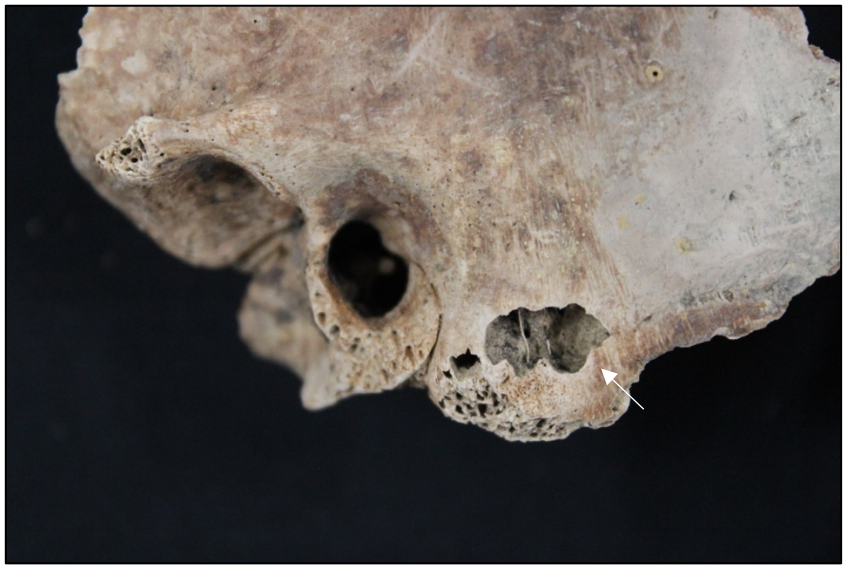

Figure 5.8: *OL Grade 2 (Edo Period Japan, Temporal Bone). The lesion is described as multifocal coalesced, and deep. There is postmortem damage to the margins except to a small portion of the inferior margin where it is clear the lesion penetrated the cortex (white arrow). Osteolytic destruction of the internal air cells of the mastoid is between 10-50mm in maximum diameter. Image: author's own.*

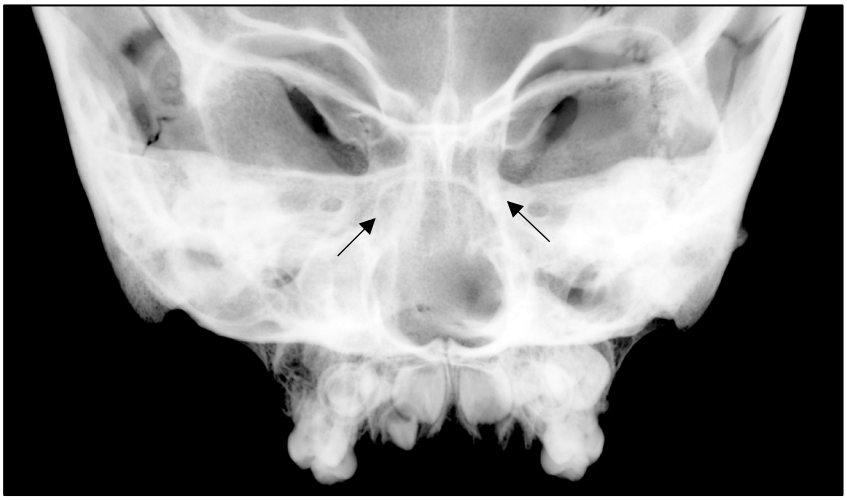

Figure 5.9: *OL Grade 3 (Edo Period Japan, Cranium). This lesion was not observed macroscopically. Radiographs demonstrate a circular focal lesion with sclerotic margins of the nasal cavity. The original size of the nasal cavity could not be estimated, and bone loss occurred spherically therefore the maximum diameter of the nasal margin was used as a basis for lesion coding (over 5cm in diameter). Image: author's own.*

5.3.4 Porosity Lesion Recording

Porosity both normal and abnormal in the skeleton is widely described in the palaeopathological literature. Ortner and Ericksen (1997) argued that differentiation of porosity of the cranium and postcranium is necessary for differential diagnosis. However, porosity remains poorly defined, and as of the publication of the 3rd edition of Ortner's

Identification of Pathological Conditions in Human Skeletal Remains (Buikstra 2019), a definition for porosity in of itself is not presented, although the term is widely used within the text. *Porotic lesions* in this thesis are defined as abnormal multifocal osteolytic formations, small and numerous in number, which have a wide range of aetiologies. Traditional lesion coding methods such as Buikstra and Ubelaker (1994) include porosity within osteolytic codes (as they are due to an osteolytic process). However, due to the advancement of palaeopathological methods requiring more specific descriptions of porosity for diagnosis, they have been coded separately from osteolytic lesions here in this thesis.

Abnormal porous lesions can form in existing cortical bone or in SPNB deposits (Ortner 2012). This porosity is formed by a separate process from the porous structure of woven bone, although they are commonly confused in the literature. The porosity is a remnant of a system of capillaries across the surface of the bone, almost as a negative impression of the vascular tissue that has since decomposed (Klaus 2017). Such lesions have been associated with subperiosteal haematoma formations which elicit osteoblastic response from blood pooling and subsequently increased vascularisation at the site of the haematoma to drain the fluid from the region (Ortner et al. 1999). This porosity is termed *abnormal cortical porosity* (after Snoddy et al. 2018), and can be found in any region of the skeleton where vascularisation occurs close to the surface of bone (Figure 5.10).

Cribra orbitalia is a term used here to describe trabecular expansion leading to porosity, specifically of the orbital roof, which occurs in childhood anaemia (see section on anaemia diagnosis below) (Stuart-Macadam 1985). Unlike abnormal cortical porosity, the porosity from anaemia is deep as it extends from within the trabecular bone underlying the supraorbital surface. The porosity is restricted to the region close to the supraorbital margin where the trabecular bone is denser, commonly presenting as a distinct crescent shaped lesion, although severe forms can extend beyond this region (Klaus 2017). The porosity also forms in childhood and therefore remodelling or remodelled regions are observed in adults (Stuart-Macadam 1985). As mentioned above, abnormal cortical porosity can be present on any skeletal element, including the orbits. Therefore, the distinction between the two different porosities is most difficult when on the supraorbital surfaces. However, abnormal cortical porosity is most often accompanied with a SPNB deposit. In abnormal cortical

porosity the regions of porosity may be symmetrical between the left and right orbit, yet the actual formation of the porosity in of itself is unevenly distributed (Figure 5.10). Additionally, abnormal cortical porosity does not appear to extend from the underlying diploe, and instead appears to penetrate inwards from the surface (Klaus 2017). Abnormal cortical porosity may also be associated with vascular impressions, presenting as horizontal formations of blood vessels embedded in bone due to SPNB forming around vessels which have since decomposed (Brown and Ortner 2011).

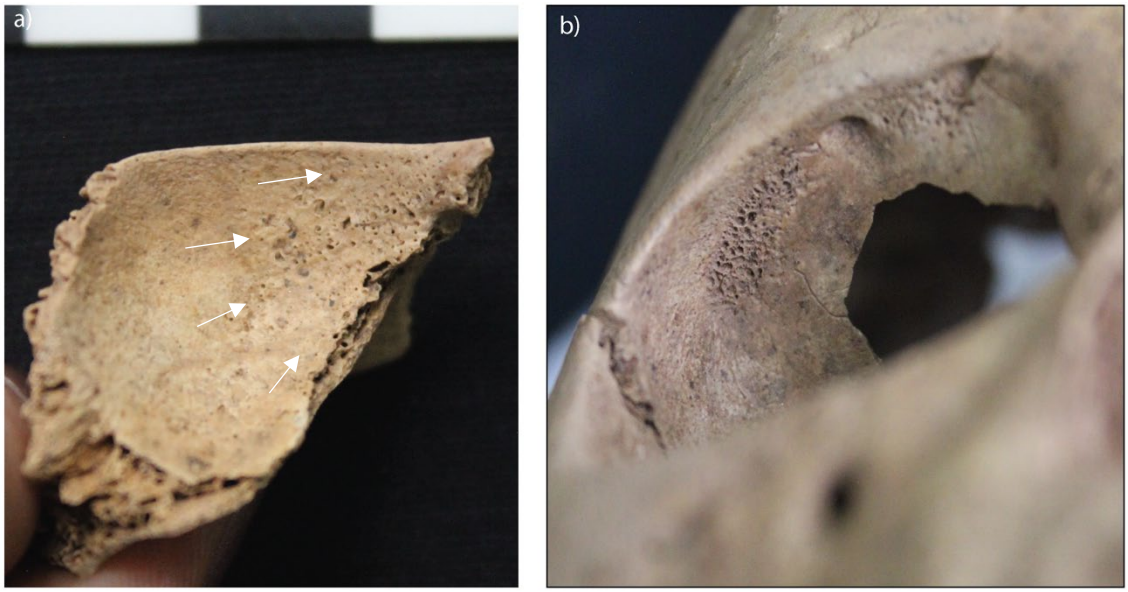

Figure 5.10: *Differences between abnormal cortical porosity and cribra orbitalia on the orbital roofs. Abnormal cortical porosity (a) (Northern Vietnam ~3 years old) can be identified through its association with subperiosteal new bone deposit (outlined by the white arrows) and uneven distribution and size of pores across the bone surface. In contrast cribra orbitalia due to anaemia (b) (Northern Vietnam, ~5 years old) appears evenly distributed and remains localised in a crescent shaped region on the orbital roof. Image: author's own.*

Trabecular porosity known as *porotic hyperostosis* which occurs on the ectocranial vault, due to anaemia, may also appear similar to cortical porosity of the ectocranium (Ortner 2012). The definition and diagnosis of porotic hyperostosis in this thesis is dealt with further below in regards to the differential diagnosis of anaemia. However, I briefly mention here that once again this porosity is restricted to regions of dense trabeculae and is associated with diploic expansion, and therefore associated with increased thickness of the ectocranium.

Finally, defective deposit or mineralisation of the osteoid in childhood bone modelling can cause abnormal porosity in regions of growth, such as the metaphyseal plates. Porosity of the metaphysis is present in the normal process of growth as bone is removed from the end to alter the shape and size of the growing bone (Buikstra and Ubelaker 1994; Ortner 2012). However, the extent of porosity termed *endochondral porosity* determines whether the porosity could be considered abnormal. Currently abnormal porosity is arbitrarily determined by Ortner and Ericksen (1997) as being more than 10mm from the metaphyseal plate regardless of skeletal element type. To date this measure remains the standard in palaeopathology as employed by Brickley and Ives (2010) and Snoddy et al. (2017). It is important to recognise some porosity in the skeleton is normal (for example superficial porosity of the ectocranial vault in adults due to normal nutrient foramina formation), and it is the extent, severity, and region in the skeleton and association with other abnormal osteolytic and osteoblastic changes which render them abnormal (Klaus and Lynnerup 2019).

The grades of porosity recorded in this thesis are adapted from the protocol by Stuart-Macadam (1985) for cribra orbitalia (Table 5.4, Figure 5.11- 5.15). This protocol was adapted to include the further two types of porosity since identified to occur in relation to nutritional deficiency and beneficial for diagnosis of specific nutritional diseases (abnormal cortical porosity and abnormal endochondral porosity of the metaphyses of long bones) (Ortner et al. 2001; Snoddy et al. 2018; Snoddy et al. 2017). Therefore, the codes for porosity do not strictly identify an increased degree of severity with increasing grade such as with the osteoblastic and osteolytic codes in this thesis. Instead the different grades for porosity are useful for classifying porosity caused by different pathological aetiologies.

The degree of porotic hyperostosis also followed the Stuart-Macadam (1985) codes. However, as described below, in the final diagnosis of porotic hyperostosis further stipulations were required. Where the mechanism of the porosity was unknown (i.e. the lesion was too slight to determine strictly cortical or trabecular origin), the code of 'P2' was given. The aetiologies of abnormal cortical porosity and cribra orbitalia vary greatly, therefore, ambiguous cases assigned P2 were excluded from analysis as they did not contribute to differential diagnosis. Other forms of postcranial porosity were not given a recording code, rather they were described. Terms of description following Buikstra and

Ubelaker (1994), often applied in palaeopathological literature were used. Descriptions included microporosity (less than 1mm in size), macroporosity (more than 1mm in size), or combination of the two, cortically restricted versus deep porosity, and descriptions of sharp versus rounded margins.

Table 5.4: *Codes used for recording of Porosity. Codes 2 to 4 are adapted from Stuart-Macadam (1985:392).*

Porosity (P) code	Description
1	Fine abnormal porosity less than 1mm in size, focused in a discrete area (in cortical bone only)
2	Light: Scattered fine foramina.
3	Medium: large and small isolated foramina that have coalesced to form a trabecular structure. Thickening of diploic bone in area of porosity
4	Severe: outgrowth in trabecular structure from the normal contour of the outer table.
5	Abnormal endochondral porosity beyond 10mm from metaphyseal plate (nonadults only)

Figure 5.11*: P Grade 1 (Edo Period Japan, Maxilla). Note that the abnormal cortical porosity (white arrow) on the posterior maxilla is in association with subperiosteal new bone deposit (here a lighter colour than the surrounding bone) and vascular impressions (yellow arrows). Note that the porosity appears to have an uneven distribution and size of the pores across the surface of the bone surface. This nonadult was diagnosed with probable scurvy. Image: author's own.*

Figure 5.12: *P Grade 2. "Scattered fine foramina" of the orbital roof after Stuart-Macadam (1985:392). (Edo Period Japan, Cranium). Given the restricted location of the lesion to the region where the underlying trabecular bone is dense, it is possible this lesion is due to anaemia. However, such a lesion is too mild for inclusion in the final analysis of anaemia within this thesis as it may be a normal anatomical variant, or abnormal cortical porosity. Image: author's own.*

Figure 5.13: *P Grade 3. Medium Cribra Orbitalia. Note the porosity appears restricted towards the superior margin where the underlying trabecular bone is dense. The porosity has coalesced in some areas resulting in larger cavities. (Edo Period Japan, Cranium). Image: author's own.*

Figure 5.14**:** *P Grade 4. Severe Cribra Orbitalia. The trabecular expansions are raised from the orbital roof. Such lesions, particularly in nonadults, can be easily mistaken as active subperiosteal new bone deposits with abnormal cortical porosity. However, there is expansion of the contour of the bone surface associated with this lesion (within white circle) and porosity projects outward from the bone rather than toward the bone surface (white arrows). (Neolithic Vietnam, Cranium). Image: author's own.*

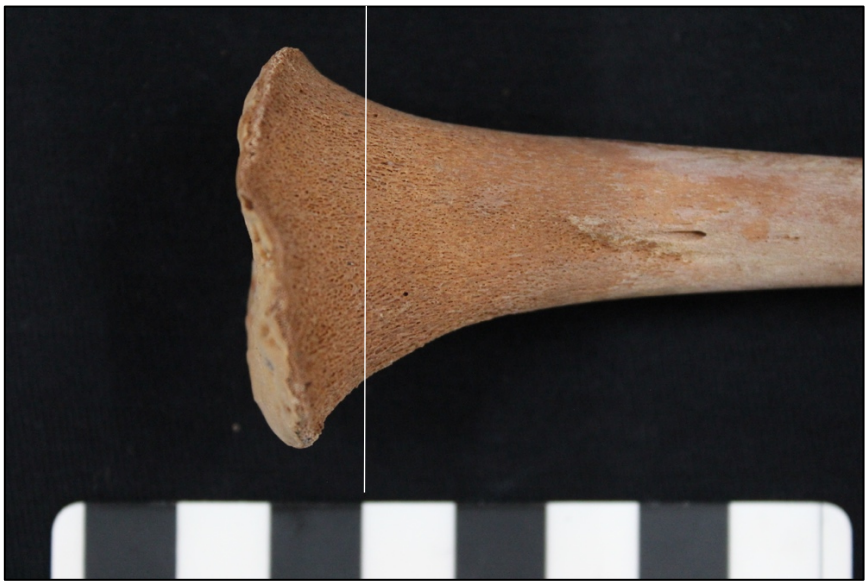

Figure 5.15: *P Grade 5. Deep endochondral porosity exceeding well beyond 10mm from the metaphyseal plate. 10mm is demarcated by the white line. The porosity resembles 'stripping' of the outer cortex. (Edo Period Japan, Humerus). Image: author's own*

5.4 Specific Disease and Differential Diagnosis Protocol

All recorded skeletal lesions, with the exception of porotic lesions coded as P2, in both cranial and postcranial remains, were considered in differential diagnosis. A differential diagnosis is the standard protocol for the identification of specific disease in palaeopathology. All possible causes of the lesion expression at an individual level was considered in order to infer which disease or diseases has caused the observed pathology.

5.4.1 Methods for Differential Diagnosis of Disease

Ortner (1991) argued that standardisation of disease diagnosis was essential for applying evolutionary thought in palaeopathology. However, it is only recently that applicable methodologies have been developed which enable realistic comparisons of archaeological cases of disease. That is, that diagnostic protocol has gone beyond comparative qualitative description as has defined the last century of the literature body, even if these have been somewhat standardised in the past. The new form of diagnostic criteria standardises diagnostic strength of pathologies according to their specificity to a disease. Thresholds can be developed to determine whether the observed pathologies are appropriate for diagnosis of a specific disease. This approach is termed *weighted diagnostic criteria*. Examples include diagnostic criteria developed by Harper et al. (2011) for treponemal disease, Brickley and Ives (2010) for varying nutritional diseases such as scurvy and rickets, and Snoddy et al. (2018) for scurvy.

The argued benefits for standardisation include 1) a decreased interobserver error, 2) increased transparency and objectivity in the reporting of lesions attributed to a specific disease, 3) decreased instances of the introduction of claimed cases of disease of poor diagnostic strength into the body of palaeopathological literature, and 4) an increased interaction with clinical literature as the basis for diagnostic criteria (Zuckerman et al. 2012). Potential limitations to this approach are discussed in Chapter 10.

Presented here are the skeletal diagnostic criteria for identification of selected nutritional and infectious diseases known to affect bone and well documented in palaeopathology: tuberculosis, leprosy, treponematosis, brucellosis, mycotic infections, hydatids disease, rickets, osteomalacia, and scurvy. Protocols for the identification of non-

genetic and genetic anaemias (thalassaemia) were also developed due to their indirect relationship to nutritional deficiencies and non-skeletal infectious diseases such as malaria. Diagnostic protocols for non-specific infectious diseases, osteomyelitis, otitis media and mastoiditis, which can be caused by a number of bacterial, fungal and viral agents are also presented (Ortner 2003).

Nutritional diseases such as hypervitaminosis A, hypovitaminosis A, and pellagra (niacin deficiency) were excluded from the analysis but are recognised to possibly contribute to the overall lesion presence as they can often mimic the skeletal changes in scurvy and rickets (Jaffe 1972; Paine and Brenton 2006). Only in extreme cases may these diseases be differentiated in the skeletal record. No such cases were identified in the assemblages assessed in this thesis.

While pre-existing diagnostic criteria exist for scurvy (following Snoddy et al. 2018 and Brickley and Ives 2010) rickets (following Brickley and Ives 2010), and treponemal disease (Harper et al. 2011), diagnostic criteria for the remaining diseases were produced by myself to achieve the aims of this thesis. Diagnostic criteria for treponemal diseases were also adapted as the Harper et al. (2011) criteria does not provide thresholds for *possible* or *probable* cases of treponemal diseases and therefore is not a useful diagnostic protocol to employ in this thesis in accordance with the objectives. Instead the methodology by Vlok et al. (2020) developed through the course of this thesis was used here.

A differential diagnosis was performed with the basis drawn from seminal literature in palaeopathology, as well as clinical literature concerning specific diseases. Lesions were characterized as *diagnostic* and *suggestive* of specific disease based on recommendations by Snoddy et al. (2018). In Snoddy et.al (2018)'s criteria, lesions are only considered to be diagnostic if there is strong clinical basis or considerable body of palaeopathological work supporting the diagnostic weight of the lesion. Pathologies that have no consensus in the clinical or palaeopathological literature, but remain anatomically intuitive, are designated a suggestive value. In addition, lesions that have been considered elsewhere as pathognomonic for disease are here scored as *strongly diagnostic* (after Brickley and Ives 2010). For a *probable* diagnosis of disease at least one strongly diagnostic or two diagnostic lesions are required (Brickley and Ives 2010; Snoddy et al. 2018). A *possible* diagnosis of

disease requires a minimum of one diagnostic lesion or two suggestive lesions (Snoddy et al. 2018). Diseases where there currently remains no strong clinical or palaeopathological literature were diagnosed as possible cases at best. The diagnostic criteria for each of the diseases assessed in this thesis are presented here. Discussion on the pathogenesis and pathophysiology of these diseases was presented in Chapter 3, and only the skeletal manifestations of the diseases are discussed here.

5.4.2 Tuberculosis (TB)

Tuberculosis is a pathogen which spreads throughout the blood stream, and therefore skeletal manifestations of the disease are associated with dissemination of the TB bacilli from the bloodstream to surrounding bone (particularly regions of haematopoiesis), and can invade cartilage and joint spaces (Davidson and Horowitz 1970). Therefore, in its chronic form, tuberculosis can cause widespread granulomatous skeletal destruction with minimal new bone response, predominantly in regions of high trabecular bone content such as the vertebral bodies, and the articular surfaces (Jaffe 1972: 956; Key 1940; LaFond 1958; Ortner 2003).

The most commonly affected skeletal elements in skeletal TB are the vertebrae, particularly the lower thoracic and upper lumbar regions (Ortner 2003: 231; Roberts and Buikstra 2003). In the most advanced form, destruction of the vertebral bodies, particularly of the anterior aspects, causes collapse referred to as gibbus formation or Pott's disease of the spine. This bone destruction is considered *pathognomonic* for tuberculosis and therefore here is considered as a strongly diagnostic lesion (Figure 5.16; Table 5.5; Davidson and Horowitz 1970; Jaffe 1972: 958-961; Turgut 2001).

Cranial destruction can occur albeit rarely, and when present is consistently more advanced on the endocranium (Lewis 2017: 156-157; Ortner 2003: 248; Snoddy et al. 2020). As the TB bacterium is particularly selective to destruction of areas of haematopoiesis, in children the lesions can be more widespread across the skeleton due to distribution of red bone marrow in developing skeletons, causing destruction of the metaphyses of the long bones (Lewis 2017: 161; Ortner 2003: 245; Teo and Peh 2004). In both adults and children, septic arthritis can occur, particularly in the hip (Moon et al. 2012; Saraf and Tuli 2015). SPNB or erosion on the internal ribs, rib heads or within the interior ilia can contribute

supportive evidence of respiratory or gastric infection depending on whether the transmission has been from air droplets (*Mycobacterium tuberculosis*) or ingested (zoonotic TB such as *Mycobacterium bovis*) (Figure 5.17; Davidson and Horowitz 1970; Murphy et al. 2009; Roberts et al. 1998). As primary infection occurs in the gut of those infected with *M. bovis,* differences in skeletal manifestations of bovine compared to human tuberculosis may occur (Manchester 1984; Murphy et al. 2009). Similar lesions of the spine and hip, such as observed in TB also occur in brucellosis, mycotic infections, osteomyelitis and hydatid's disease, therefore these infectious diseases need to be considered in the differential diagnosis (Ortner 2003).

Figure 5.16: *Pott's disease of the spine in a young adult male (Liao Dynasty, Mongolia). Lytic destruction has progressed to complete destruction of the T8 vertebral body leading to anterior collapse (kyphosis). Note how the vertebral archs remain unaffected which is characteristic for tuberculosis infection of the spine. Image: author's own.*

Figure 5.17: *New bone deposition and osteolytic changes to the ribs of a young adult male (Liao Dynasty [10th to 12th Century AD], Mongolia). The new bone is mostly remodelled (yellow arrow), but some activity remains (white arrow). Osteolytic changes are present on the 8th to 10th ribs and extruded into the subchondral bone (blue arrow). Image: author's own.*

Table 5.5: *Diagnostic Criteria for Identification of Tuberculosis (SD= strongly diagnostic, D= diagnostic, and S= suggestive).*

Pathology	Diagnostic Strength	Differential Diagnosis	Reference
Pott's Spine: vertebral collapse with gibbus formation following osteolytic destruction of vertebral body/ bodies	**SD**	Brucellosis, mycosis, neoplasms, osteomyelitis, trauma	(Davidson and Horowitz 1970; Jaffe 1972: 958-961; Ortner 2003: 235)
Single isolated (may be multiple), 'punched out' osteolytic lesions of both tables of frontal or parietal bones o*r* "moth eaten", round foci and larger on endocranial vault (juvenile). Focal osteolytic lesion with larger defect on the endocranium and minimal sequestration (adult)	**D**	Treponematosis, mycosis, neoplasms	(Lewis 2017: 156-157; Ortner 2003: 248-253)

Pathology	Diagnostic Strength	Differential Diagnosis	Reference
Focal osteolytic formation without sclerotic response on scapula and pelvis. Osteolytic foci with surrounding bone (juvenile)	**D**	Brucellosis, mycosis, neoplasms, osteomyelitis	(Lewis 2017: 158)
Focal osteolytic formation without sclerotic response of the vertebral bodies starting anterior-superior (initiation from intervertebral disk) and following the vessels (juvenile).	**D**	Brucellosis, mycosis, neoplasms, osteomyelitis	(Lewis 2017: 158-160)
Focal osteolytic lesions and/ or erosive lesions on the inferior margins and/or pleural aspect of the ribs, with or without new bone on the ribs	**D**	Brucellosis, mycosis, neoplasms, osteomyelitis	(Davidson and Horowitz 1970; Kelley and Micozzi 1984; Ortner 2003: 246-247)
Focal osteolytic lesions at growth plates and metaphyses of the hip, knee and ankle (juvenile)	**D**	Brucellosis, mycosis, neoplasms, osteomyelitis, treponematosis	(Lewis 2017: 160-161)
Radiographic: Honey-comb osteolytic foci in the metaphyses (juvenile)	**D**	Thalassaemia	(Jaffe 1972: 975; Lewis 2017: 161-162)
Focal osteolytic lesions of the vertebral body focused anteriorly with minimal bone response concentrated around the first lumbar vertebra region. Often with two adjacent vertebrae affected	**D**	Brucellosis, mycosis, neoplasms, osteomyelitis	(Jaffe 1972: 983; Ortner 2003: 231)
Flared bony extensions (extensive reactive SPNB) on spine due to psoas abscess	**D**	Brucellosis, mycosis, neoplasms, osteomyelitis	(Jaffe 1972: 985; Ortner 2003: 232)
Tuberculosis arthritis of the hip: affecting acetabulum and femoral head and neck. May involve destruction of femoral head/ neck and acetabulum, necrosis of the hip, and/ or bony ankylosis	**D**	Brucellosis, mycosis, neoplasms, osteomyelitis, trauma, Gaucher's disease, sickle cell anaemia, diseases diminishing blood flow	(Davidson and Horowitz 1970; Ortner 2003: 235-239; Snoddy et al. 2020)
Focal osteolytic bone destruction on the ilium along the psoas muscle and may be accompanied with ossification of the abscess wall	**D**	Brucellosis, mycosis, neoplasms, osteomyelitis	(Ortner 2003: 239)
Focal destruction of subarticular bones and/ or tuberculosis arthritis of the knee, ankle, shoulder, or forearm joints with minimal bone response. May be associated with sequestra	**D**	Non-specific infectious arthritis, brucellosis, mycosis, trauma	(Ortner 2003: 240-243)
Tuberculosis dactylitis (spina ventosa) with involvement of metacarpals, metatarsals and phalanges (predominantly juveniles). Marked concentric expansion of the tubular hand and feet bones.	**D**	Leprosy, treponematosis, thalassaemia, sickle cell disease, osteomyelitis	(Lewis 2017: 162; Ortner 2003: 242)
Orbit or paranasal sinus infection (juvenile >1 year)	**S**	Leprosy, non-specific infection, treponematosis	(Lewis 2017: 156-157)

Pathology	Diagnostic Strength	Differential Diagnosis	Reference
Otitis Media (juvenile) *(see otitis media diagnostic criteria)*	**S**	Various infectious diseases	(Lewis 2017: 156-157)
Focal circumvallate osteolytic destruction of the lateral orbits, zygomatic bones, nasal bones and/ or maxillae with minimal sclerotic response (juvenile)	**S**	Mycosis, treponematosis, leprosy	(Lewis 2017: 156-157)
Active endocranial new bone which may be associated with arachnoid granuloma like osteolytic lesions and/or endocranial new bone lesions with deep vascular impressions (Lewis type 3 and 4) (*serpens endocranial symmetrica*) (juvenile)	**S**	Non-specific infection, various anaemias, scurvy, rickets	(Lewis 2017: 156-157)
SPNB on the visceral surface of the ribs	**S**	Various respiratory illnesses, trauma, scurvy, rickets,	(Lewis 2017: 160; Ortner 2003; Roberts et al. 1998)
Focal osteolytic lesions further from the lower thoracic to upper lumbar region. May also involve the arch in the cervical spine	**S**	Brucellosis, mycosis, osteomyelitis, neoplasms	(Ortner 2003: 230)
Focal osteolytic lesions on the vertebral bodies with sequestrae or SPNB bone response	**S**	Brucellosis, mycosis, osteomyelitis, neoplasms	(Ortner 2003: 230-235)
Isolated focal osteolytic lesions with minimal bone response on the ilium, sternum, and scapula	**S**	Brucellosis, mycosis, osteomyelitis, neoplasms	(Ortner 2003: 239-247)
Focal destruction of the greater trochanter	**S**	Brucellosis, mycosis, osteomyelitis, neoplasms, trauma	(Ortner 2003: 239)
Focal osteolytic lesions in long bone ends (metaphysis) with marked bone response (in juveniles), minimal bone response (in adults)	**S**	Brucellosis, mycosis, osteomyelitis, neoplasms, treponematosis	(Lewis 2017: 161; Ortner 2003: 239)

5.4.3 Treponematosis

Three *Treponema pallidum* subspecies, yaws *(T. pallidum pertenue)*, endemic syphilis *(T. pallidum endemicum)*, and venereal syphilis *(T. pallidum pallidum)* can cause bony lesions in both the secondary and tertiary stages of the disease's pathophysiology. The three treponemes that affect the bone cannot be distinguished by their skeletal expression alone (Harper et al. 2011). During the secondary stages skeletal manifestations of treponemal disease are osteoblastic only and are due to inflammatory response to dissemination of the treponemal bacteria through the bloodstream and the lymph nodes (Buckley and Dias 2002). SPNB with cortical enlargement which can present as *nodes* of new bone appear at sites of lymph nodes and drainage (Hackett 1975; Hackett 1976: 362-

396). As the tertiary stage commences, marked osteoblastic bone response ceases, and destructive osteolytic lesions occur. In this stage SPNB deposit may only occur around the margins of the destructive bone lesions (Hackett 1953; Hackett 1976).

Treponematosis is distinctive for its gross destruction of the face, skull, limbs, and in the case of venereal syphilis, the axial skeleton from infected arterial vessels and organs in later stages of the disease (Goh 2005). However, the disease can affect any part of the skeleton (Ortner 2003: 280). Bone deformities such as sabre shin can be present from the secondary stage onwards where anterior new bone formation presents as *pseudo-bowing* of the tibiae. That is, the bone appears to have anterior bowing due to gross apposition of SPNB deposit and cortical enlargement towards the anterior aspect, without actual bowing of the medullary canal as see in true bowing deformities (Lewis 2017: 179). This lesion is suggestive for treponemal diseases as it can manifest in other diseases such as leprosy and osteomyelitis (Hackett 1951: 28). True anterior tibial bowing can also occur if infected in childhood or adolescence (Harper et al. 2011; Lewis 2017: 175).

The granulomatous 'gummatous' lesions of the tertiary stage are distinctive and specific to all treponemal diseases, and are universally accepted as highly diagnostic for treponemal syndromes (Table 5.6; Harper et al. 2011; Ortner 2003). Tertiary lesions on the skull, *caries sicca,* which present on the ectocranium, are the most well recognised lesion of the disease (Figure 5.18-5.19). Early stage gumma are focal lesions termed 'superficial cavitations' which advance on the ectocranium and the outer cortex of long bones. The development of lesions in treponematosis were described by Hackett (1976). Gummatous lesions are distinct in that they rarely penetrate the cortex. Furthermore, the superficial cavitations of postcranial bones are only strongly diagnostic when in direct association with nodes of new bone or cortical enlargement (Hackett 1975; Hackett 1976: 429-433; Harper et al. 2011).

Tertiary lesions of treponemal disease are associated with sclerotic response on the margins and base of the lesion, seen as smooth edges to the lesion (Hackett 1976). Gross destruction of the palate and the nose can also occur, particularly in yaws (Hackett 1946). In the case of venereal syphilis, trans-placental transmission can cause congenital syphilis which leaves distinctive bone and dental deformities in infants and young children up until puberty (Lewis 2017). These involve hypoplastic changes to the permanent incisors called

Hutchinson's incisor and changes to the occlusal surfaces of permanent molars (*Moon's molars*) (see Figure 5.20). Another dental change to the molars called *Mulberry molars* is strongly associated with syphilis, but is also recognised as being symptomatic of a number of preterm systemic conditions (Harper et al. 2011; Hillson et al. 1998).

No diagnostic lesions form during the secondary stage, and skeletal manifestations of secondary stage treponemal disease cannot be confidently differentially diagnosed from other infectious diseases, such as leprosy, as the proliferative lesions are only suggestive of treponemal disease (Harper et al. 2011). Tertiary gummatous lesions, however, are distinct and only found in the treponemal diseases (Harper et al. 2011).

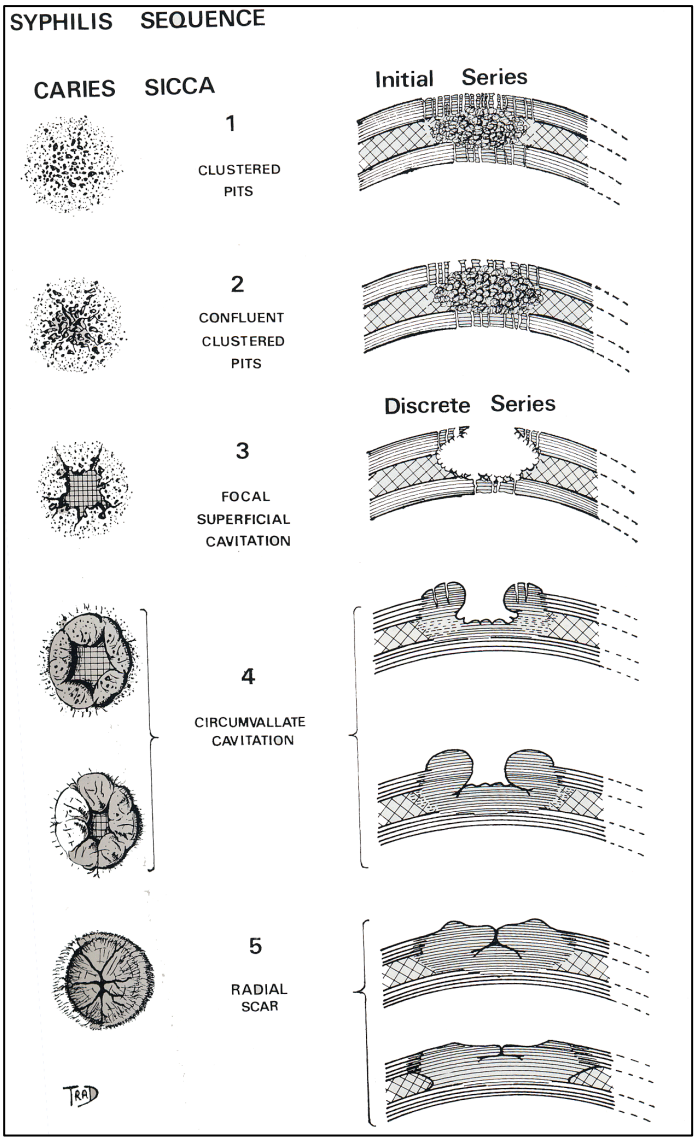

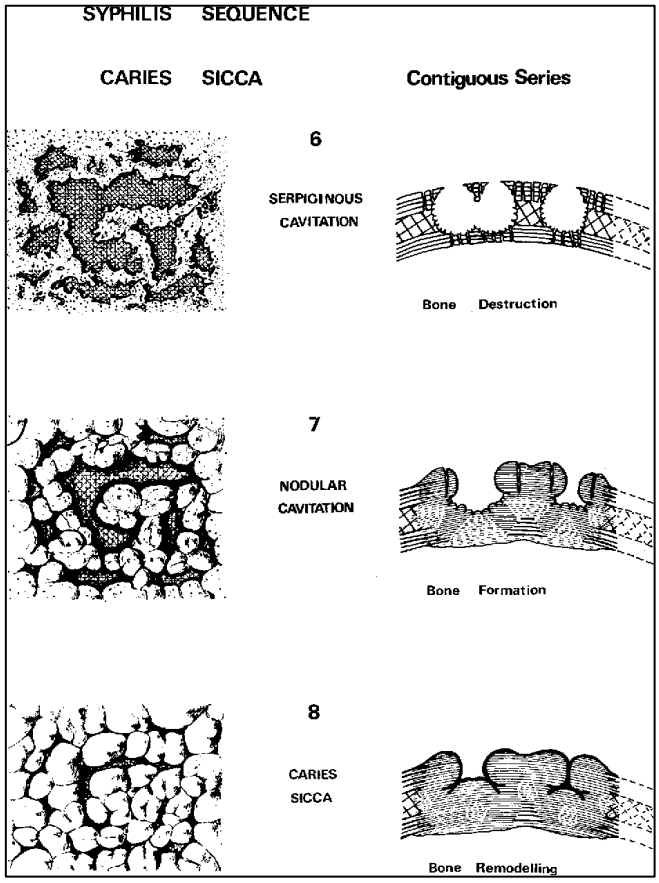

Figure 5.18: *Hackett's (1976) Scheme for the advancement of the caries sicca sequence of treponematosis. Image: Springer. Permission pending.*

Figure 5.19: *Caries sicca of the cranium (Taumako, Solomon Islands) Image: H. Buckley. Used with permission.*

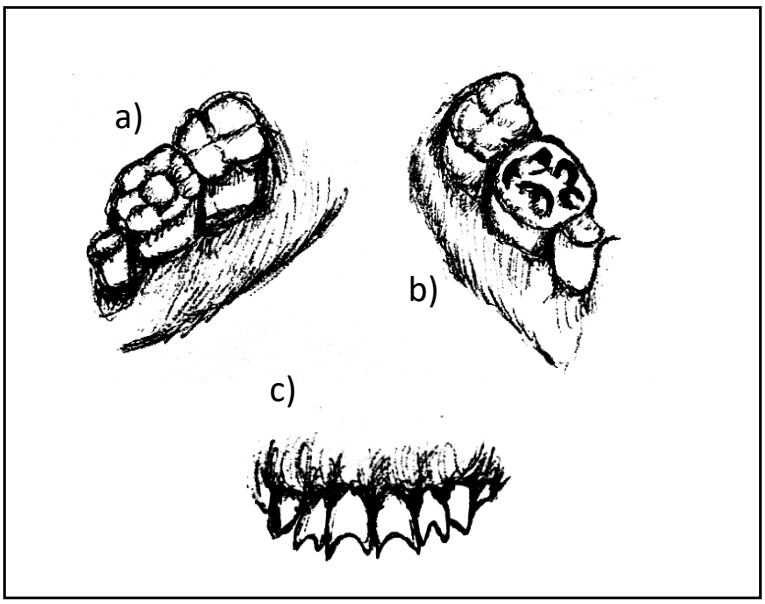

Figure 5.20: *Dental abnormalities in permanent teeth caused by congenital syphilis. a) Moon's molars b) Mulberry molars and c) Hutchinson's incisors. Image: author's own.*

Table 5.6: *Diagnostic Criteria for Identification of Treponematosis (SD= strongly diagnostic, D= diagnostic, and S= suggestive). Published in Vlok et al. (2020).*

Pathology	Diagnostic Strength	Differential Diagnosis	Reference
Caries Sicca Stages 4-8: circumvallate cavitation, radial scars, serpiginous cavitation, nodular cavitation and *caries sicca* of the ectocranium	**SD**		(Hackett 1975; Hackett 1976: 362-396; Harper et al. 2011)
Gummatous lesions on any skeletal element: focal superficial cavitations in direct relation with nodes or expansions (enlargements) of new bone	**SD**		(Hackett 1975; Hackett 1976: 429-433; Harper et al. 2011)
Hutchinson's incisors (congenital)	**SD**	Normal morphology	(Hackett 1976: 441; Harper et al. 2011; Hillson et al. 1998; Lewis 2017: 179; Pessoa and Galvão 2011; Stokes and Gardner 1923)
Moon's Molars (congenital)	**SD**	Growth disruption	(Hackett 1976: 441; Harper et al. 2011; Hillson et al. 1998; Lewis 2017: 179)
Congenital syphilis (Caffey's) triad: osteochondritis, bilateral thick SPNB of the long bones *and* osteomyelitis of metaphyseal ends (early congenital)	**D**	Non-specific osteomyelitis, infantile cortical hyperostosis, Paget's disease.	(Caffey 1939; Jaffe 1972: 910; Lewis 2017: 178)
Caries sicca sequence stages 1-3: clustered pits, confluent clustered pits, focal superficial cavitation of the ectocranium *or* focal superficial cavitation of the cortex of long bones not within a distinct node or expansion (enlargement).	**D**	Mycosis, tuberculosis, Langerhans's cell histiocytosis, multiple myeloma and other metastatic neoplasms	(Hackett 1975; Hackett 1976: 362-396)

Pathology	Diagnostic Strength	Differential Diagnosis	Reference
Gross rhinomaxillary and palatal destruction (gangosa)	**D**	Leprosy, tuberculosis, mycosis, destructive neoplasms, trauma, leishmaniasis.	(Fiumara and Lessell 1970; Hackett 1951: 164-168; Hackett 1975; Hackett 1976: 399-401; Lewis 2017: 175)
Wimberger's corner sign (congenital): bilateral widening band of decreased calcification of the metaphyses leading to destruction	**D**	Non-specific osteomyelitis, trauma, scurvy	(Brackett and Standley 2019; Harper et al. 2011; Lewis 2017: 178; Rasool and Govender 1989)
Mulberry (Fournier's) molars	**D**	Mercury use, growth disruption	(Harper et al. 2011; Hillson et al. 1998; Lewis 2017: 179)
Thick SPNB deposition and exostoses on the maxillae (goundou)	**S**	Scurvy, osteomyelitis, leprosy, infantile cortical hyperostosis, Paget's disease, genetic anaemias	(Buckley 2016: 30; Harper et al. 2011; Lewis 2017: 175)
Higoumenakis' Sign: unilateral enlargement of the sternal end of the clavicle (congenital)	**S**	Trauma, non-specific osteomyelitis, normal variant	(Dax and Stewart 1939; Frangos et al. 2011; Harper et al. 2011; Lewis 2017: 179; Yang 1940)
Sabre shin (pseudobowing of the tibia without bowing of the medullary canal)	**S**	Leprosy, osteomyelitis, various benign and malignant bone tumours, Paget's disease, hyperfluorosis	(Hackett 1951: 28; Harper et al. 2011)
Boomerang leg: True anterior tibial bowing with bowing of medullary canal (until adolescence)	**S**	Rickets, skeletal dysplasias, osteogenesis imperfecta, fracture	(Harper et al. 2011; Lewis 2017: 175)
Dactylitis (subperiosteal new bone enlargement of the hand and feet bones)	**S**	Tuberculosis, non-specific osteomyelitis, genetic anaemias	(Hackett 1951: 30; Harper et al. 2011; Lewis 2017: 178-179; Rasool and Govender 1989)
Charcot's joint (resorption of weight bearing joints)	**S**	Septic arthritis, diabetes, osteoarthritis, syringomyelia, tuberculosis	(Hackett 1976; Harper et al. 2011; Johns 1970; Lewis 2017: 179; Sequeira 1994)
Opera glass fingers: diaphyseal tapering of the bone	**S**	Leprosy, rheumatoid arthritis, syringomyelia, diabetes, osteomyelitis, erosive osteoarthritis	(Hackett 1951: 153-154; Jones 1972; Ortner 2003: 278; Swezey et al. 1972)
Radiographic: Saw tooth appearance of metaphyseal ends *or* macroscopic symmetrical destruction of metaphyses attributed to osteochondritis (early congenital)	**S**	Rickets, scurvy, trauma, tuberculosis	(Harper et al. 2011; Jaffe 1972: 910-912; Lewis 2017; Rasool and Govender 1989)

Pathology	Diagnostic Strength	Differential Diagnosis	Reference
Thick deposit of mixed active and remodelled SPNB on the long bones, thickest at the midshaft (congenital) or long bone endosteal nodes or expansions (enlargements) with medullary canal intrusion	**S**	Paget's disease, non-specific osteomyelitis, neoplasms, tuberculosis	(Hackett 1951; Hackett 1975; Hackett 1976: 411-433; Harper et al. 2011; Lewis 2017: 178-179)
Saddle nose (congenital): loss of nose height and collapse of the bridge.	**S**	Leprosy, trauma, non-specific osteomyelitis	(Fiumara and Lessell 1970; Harper et al. 2011; Lewis 2017; Pavithran 1987)
High palatal arch (congenital)	**S**	Various congenital deformities including: Turner's syndrome and Klippel-Feil syndrome.	(Lewis 2017: 177; Pavithran 1987)

5.4.4 Leprosy

Due to peripheral neuropathy and loss of sensation from leprosy, the high chance of skin trauma leading to secondary infections in open wounds can progress to affect the skeleton (Saha et al. 2019). Secondary infections then cause slow progression of erosive lesions that are accompanied by inflammatory bone response in the form of SPNB and abnormal cortical porosity around the margins of erosion (Table 5.7; Møller-Christensen 1961; Møller-Christensen 1978; Ortner 2003: 264-265). In advanced forms of leprosy, destruction of the nasal mucosa subsequently causes erosion of surrounding tissue and bone (Menger et al. 2007). The causes of nasal mucosal destruction are not well known and destruction of the skeleton may be due to secondary infection from exposed cartilage following mucosal destruction or through secondary vascular ischemia resulting in necrosis (Menger et al. 2007; Shah et al. 2009). Destruction of the alveolar region around the central incisors can occur and has been associated with direct infiltration of *M. leprae* into surrounding soft tissue causing periapical granulomas, suggesting skeleton erosion from the primary infection may also occur (Rendall and McDougall 1976). The degree of skeletal involvement depends on whether leprosy has advanced in its tuberculoid or lepromatous form, with more distinct features of the condition expressed in the latter (Manchester 1984; Tayles and Buckley 2004).

Slow erosive progression of naso-palatal margins including resorption of the anterior nasal spine, and resorption of the alveolar margins of the maxillary central incisors with associated proliferative SPNB and abnormal cortical porosity (also termed cortical pitting

in the literature) are considered as here as diagnostic features of this disease (Møller-Christensen 1961; Møller-Christensen 1978; Møller-Christensen et al. 1952). The resorption of the alveolar margins of the central incisors can eventually lead to antemortem loss of these teeth (Manchester 1984; Møller-Christensen 1978; Ortner 2003: 264-265). These two pathologies together are described by Møller-Christensen (1961) as *facies leprosa*, which is pathognomonic for leprosy. Juvenile forms of leprosy are similar to adult forms with the exception of distinct dental changes termed *leprogenic odontodysplasia* which can occur in children. In this condition inflammatory changes to the maxilla leads to concentric constriction of the roots of the developing maxillary incisors (Lewis 2017: 167).

Erosive destruction of the nose and face needs to be differentially diagnosed from similar changes that occur in treponematosis (Hackett 1976). In treponematosis, the changes cause gross destruction, whereas in leprosy subtler changes such as erosion of the nasal aperture and anterior nasal spine occur (Hackett 1976; Møller-Christensen 1978). Moreover, perforation of the hard palate can occur in both conditions. However, in leprosy destruction of the palate often follows erosion of the inferior palatal surface (Møller-Christensen 1961: Plate II). In treponemal disease, the palatal destruction is an extension of nasal destruction (gangosa) and most often accompanies other more distinct changes of the disease, which can enable differential diagnosis between the two diseases (Satter and Tokarz 2010).

Table 5.7: *Diagnostic Criteria for Identification of Leprosy (SD= strongly diagnostic, D= diagnostic, and S= suggestive).*

Pathology	Diagnostic Strength	Differential Diagnosis	Reference
Concentric atrophy of phalanges	**D**	Quadriparesis, developmental disorder, treponematosis	(Møller-Christensen 1961; Ortner 2003: 264-265)
"Tear Drop" remodelling of small bones of the extremities especially distal phalanges	**D**	Treponematosis	(Ortner 2003: 264-265)
Atrophy and absorption of the anterior nasal spine (*facies leprosa)*	**D**	Treponematosis	(Andersen and Manchester 1992; Møller-Christensen 1961; Møller-Christensen 1978)
Recession and atrophy of the alveolar maxillary process beginning centrally at prosthion and causing loosening and eventual loss of relevant teeth (*facies leprosa)*	**D**	Treponematosis, periodontal disease, cleft palate	(Andersen and Manchester 1992; Møller-Christensen 1961; Møller-Christensen 1978)
Inflammatory pitting (abnormal cortical porosity) of the oral palatine and/or nasal palatine surface	**D**	Treponematosis, osteomyelitis	(Andersen and Manchester 1992; Lewis 2017: 165;

Pathology	Diagnostic Strength	Differential Diagnosis	Reference
			Møller-Christensen 1978)
Destruction of the hard palate	**D**	Treponematosis, tuberculosis, leishmaniasis	(Møller-Christensen 1961; Ortner 2003: 264-265)
Dens leprosus/ leprogenic odontodysplasia: concentric constriction of the roots of the maxillary incisors (juvenile)	**D**		(Lewis 2017: 167; Møller-Christensen 1978; Ortner 2003: 264-265)
Absorption of the nasal aperture, without gross destruction of the entire nasal region as in syphilis (*facies leprosa)*	**D**	Treponematosis	(Andersen and Manchester 1992; Lewis 2017: 167; Møller-Christensen 1961; Møller-Christensen 1978)
Endonasal inflammatory changes (pitting or new bone)	**S**	Various infectious diseases	(Lewis 2017: 165; Møller-Christensen 1978)
Maxillary sinusitis	**S**	Various infectious diseases	(Lewis 2017: 165)
Septic arthritis	**S**	Various infectious diseases	(Lewis 2017: 165)
Claw hand and foot and/ or drop hand or foot	**S**	Various neuromuscular disorders, trauma	(Lewis 2017: 165; Manchester 1984; Ortner 2003: 264-265)
Osteomyelitis *(see osteomyelitis diagnostic criteria)*	**S**	Various infectious diseases	(Lewis 2017: 165)
Ossification of interosseous membrane	**S**	Osteomyelitis	(Lewis 2017: 165)
Bone ulcers (localised osteitis with SPNB)	**S**	Treponematosis, osteomyelitis, neoplasms	(Lewis 2017: 165; Ortner 2003: 264-265)
Tarsal disintegration	**S**	Treponematosis, trauma	(Manchester 1984)
Inflammatory pitting and generalised osteolytic destruction of the tubular hand and feet bones	**S**	Treponematosis, tuberculosis, osteomyelitis	(Lewis 2017: 165)
Enlarged nutrient foramen of the hands/feet	**S**	Thalassaemia, sickle cell anaemia, osteomyelitis	(Lewis 2017: 165)

5.4.5 Brucellosis

Skeletal involvement is common in brucellosis and therefore likely to be present in the archaeological skeletal record (Al-Shahed et al. 1994; Mehmet et al. 2002). Once chronic it can affect the skeleton in both focal or diffuse forms and therefore skeletal lesions can be localised or widespread throughout the skeleton (Al-Shahed et al. 1994). Granulomatous focal destructive lesions, which are often but not always accompanied by sclerotic reaction due to their slow development, are the predominant skeletal lesions which form in brucellosis (Roberts and Buikstra 2019).

Similar to tuberculosis, brucellosis has a predilection for articular regions of the skeleton (Madkour et al. 1988). Septic arthritis is the most common form of skeletal change associated with this disease. However, this is not a diagnostic lesion (Madkour et al. 1988). Focal destruction of the spine is a primary characteristic of this disease, followed by involvement of the sacroiliac joint (Al-Shahed et al. 1994; Madkour et al. 1988). The pathogen infects the spine from within the intervertebral disks and the superior vertebral bodies are the most commonly affected (Al-Shahed et al. 1994). Macroscopic and radiographic evidence of bone destruction on the superior margin of the anterior vertebral bodies, with sclerotic margins is diagnostic for this disease (Table 5.8; Al-Shahed et al. 1994; Madkour et al. 1988). Remodelling can cause the presence of parrot's beak osteophytes on the superior margin of the anterior vertebral bodies, which although not unique to brucellosis, is suggestive of this disease (Al-Shahed et al. 1994). Osteolytic lesions can also frequently develop in regions of haematopoiesis including the hip, knee and ankle joints (Al-Shahed et al. 1994; Mehmet et al. 2002).

Less has been described about the skeletal pathology of brucellosis than tuberculosis, and questions remain about how to distinctly differentiate between the two, and whether this is even possible in many cases (Al-Shahed et al. 1994). Brucellosis appears to affect similar regions of the spine to tuberculosis, but does tend to affect the lumbar more often than thoracic spine (Klaus and Lynnerup 2019; Ortner 2003: 215-221). Potential markers for differentiation lies in the likelihood that brucellosis can cause more widespread destruction of the skeleton, skeletal involvement is more common than in tuberculosis, and a sclerotic response is common in brucellosis whereas this is not usually the case for tuberculosis (Al-Shahed et al. 1994; Mehmet et al. 2002). In extraspinal regions, such as the hip joint, differential diagnosis between tuberculosis and brucellosis may be impossible (Al-Shahed et al. 1994). While collapse of the spine can occur in brucellosis, it is rare for the lytic destruction to advance to the severity seen in tuberculosis (Roberts and Buikstra 2019). Given the dearth of discussion on this disease in palaeopathology and the similarity of skeletal lesions of brucellosis to that of tuberculosis, any cases of brucellosis diagnosed with the criteria used in this thesis lead to a *possible* not a *probable* case.

Table 5.8: *Diagnostic Criteria for Identification of Brucellosis (SD= strongly diagnostic, D= diagnostic, and S= suggestive).*

Pathology	Diagnostic Strength	Differential Diagnosis	Reference
Osteolysis of the superior vertebral body (more likely anterior margin) with a sclerotic response or osteophytes around the region (intervertebral origin)	**D**	Tuberculosis, trauma, osteomyelitis, mycosis	(Al-Shahed et al. 1994; Madkour et al. 1988; Ortner 2003: 215-221)
Multiple foci osteolytic destructive process of joint cavities of the limbs with minimal to slight sclerotic response	**S**	Tuberculosis, osteomyelitis, mycosis	(Ortner 2003: 215-221)
Multiple circumscribed lytic foci on the ilium or sacrum with minimal to slight sclerotic response	**S**	Tuberculosis, osteomyelitis, mycosis, echinococcosis	(Ortner 2003: 215-221)
Osteolysis on the inferior margin of the vertebral body	**S**	Tuberculosis, osteomyelitis, mycosis, echinococcosis	(Ortner 2003: 215-221)
Parrot's beak of the superior margin of the anterior vertebral body	**S**	Osteoporosis, trauma, non-specific infection	(Al-Shahed et al. 1994)
Septic arthritis	**S**	Osteoarthritis, non-specific infection	(Madkour et al. 1988)

5.4.6 Echinococcosis (Hydatids Disease)

Larvae of *Echinococcus granulosis* and *E. multilocularis* are small enough to pass through the pores of skeletal tissue (microvesicular dissemination) (Zlitni et al. 2001). As the larvae grow, the bone surrounding the cyst is destroyed in a spherical manner, with minimal sclerotic response occurring (Zlitni et al. 2001). As a pericyst does not form within the skeleton, large cysts do not tend to be found in bone although this can occur. Instead cysts are most commonly small and multifocal, and resemble a "bunch of grapes" on radiographs, strongly diagnostic for hydatids disease (Table 5.9; Kalinova et al. 2005; Ortner 2003: 337-338; Zlitni et al. 2001: 76). Over time the cortex may resorb, and eventually penetration of the cortex may occur, where the parasite continues to reinfect the surrounding soft tissue and organs (Song et al. 2007; Zlitni et al. 2001). Macroscopic evidence of cortex penetration is, however, not clinically diagnostic for hydatids disease. Bone necrosis and pathological fractures due to failure of the structural integrity can occur in advanced cases (Zlitni et al. 2001). In regions such as the pelvis, osteoblastic bone response can develop to accommodate an expanding cyst or form due to secondary osteomyelitis (Agarwal et al. 1992; Ortner 2003: 337-338).

Hydatic cysts grow in regions of the skeleton where there is least resistance (Beggs 1985). That is regions with high trabecular volume and the medullary cavities are the most common sites of parasitic growth (Ortner 2003: 337-338; Zlitni et al. 2001). Infection of adjacent bones can occur, but this is rare due to the thickness of the cortex in joint regions (Jaffe 1972: 1073; Ortner 2003: 337-338). Most commonly, the disease is located to a single bone (Jaffe 1972: 1073; Ortner 2003: 337-338). While all bones of the skeleton can be affected, the vertebrae and the pelvis are the most frequently affected bones, followed by the metaphyseal regions of the humerus, tibia, fibula and femur (Jaffe 1972: 1073; Ortner 2003: 337-338; Zlitni et al. 2001). As the cystic bone lesions are located within the metaphyses of long bones, the spine and the pelvis, tuberculosis, mycosis, and osteomyelitis need to be included within the differential diagnosis (Jaffe 1972; Song et al. 2007). Furthermore, aneurysmal cysts, metastatic cancers, osteochondritis dissecans and benign tumours can present very similar macroscopic circular destructive lesions on the long bone ends (Agarwal et al. 1992; Oxenham et al. 2005; Song et al. 2007).

Soft tissue hydatids cysts are known to calcify following the death of the parasite, and rarely these cysts survive in the archaeological record (Dervenis et al. 2005; Waters-Rist et al. 2014). If a calcified cyst is found, it must first be differentiated from calcified tumours and various cysts or soft tissue nodes within the body (Komar and Buikstra 2003). The presence of multiple layers of the calcified cyst wall, and the presence of septa which demonstrates evidence of daughter cysts are crucial for the differential diagnosis of the calcified hydatids cyst (Komar and Buikstra 2003; Oxenham et al. 2018).

Table 5.9: *Diagnostic Criteria for Identification of Hydatids (SD= strongly diagnostic, D= diagnostic, and S= suggestive).*

Pathology	Diagnostic Strength	Differential Diagnosis	Reference
Calcified Hydatid cyst: clear evidence of a double-sub layered calcified pericyst, hollow, ellipsoid in shape with septa demonstrating evidence of daughter cyst formation.	**SD**	Calcified ovary, ovarian cyst or fibroma, lymph node, omental nodule, renal cyst or abscess; lithopaedion; urinary calculus; leiomyoma, mesenteric carcinoid tumour or cyst; lipoleiomyoma; faecalith; appendicolith; psammoma body; calcified neoplasm, alveolar *Echinococcus* cyst	(Komar and Buikstra 2003; Waters-Rist et al. 2014)
Small and numerous circular osteolytic cysts (multifocal or coalesced) in regions of trabecular bone or marrow cavity with 1) minimal or no reactive SPNB response, resembling a bunch of grapes, 2) lack of clear boundaries, 3) and lack of morphological changes to the bone. These lesions are not widespread throughout the body and typically do not cross articular regions as the cyst does not invade the epiphysis. Vertebrae, innominate, humerus, tibia, fibula and femur most commonly involved. Cysts can become large in the marrow space.	**SD**	Hyperparathyroidism	(Beggs 1985; Jaffe 1972: 1073; Ortner 2003: 337-338; Zlitni et al. 2001).
Combination of multilocular cysts and reactive sclerosis involving a large expansion of the pelvis	**D**	Tuberculosis, neoplasms	(Agarwal et al. 1992; Song et al. 2007)
Radiographic: Thin cortex around the region of cystic lytic response	**S**	Various nutritional deficiencies	(Song et al. 2007; Zlitni et al. 2001)
Radiographic: Ischemic necrosis of the marrow area	**S**	Osteomyelitis	(Zlitni et al. 2001)
Collapse of vertebrae	**S**	Tuberculosis, osteomyelitis, mycosis	(Ortner 2003: 337-338)
Secondary osteomyelitis or SPNB at site of cystic lytic response	**S**	Various infectious disease	(Agarwal et al. 1992; Ortner 2003: 337-338)
Pathological fracture associated with bone cyst	**S**	Trauma	(Zlitni et al. 2001).
Large circular destruction of the cortex due to cortex breeching and continued infection of surrounding soft tissue.	**S**	Tuberculosis, mycosis, osteomyelitis, neoplasms, osteochondritis dissecans or erosive arthropathies of the long bones	(Song et al. 2007)

5.4.7 Mycosis

Mycoses can become systemic through haematogenous routes but can directly affect bone through adjacent infected soft tissue as well (Corr 2011; Oberoi et al. 2012; Ortner 2003; Pappas et al. 1993). The bone lesion is primarily a deep circular area of focal lytic destruction which may or may not be associated with localised SPNB deposit around the

osteolytic foci (Jaffe 1972: 1060). Mycotic infections do not appear to be selective of particular regions of the skeleton as is the case with most infections, and a seemingly random distribution of focal destructive lesions may indicate a case of mycosis over other aetiologies (Table 5.10; Ortner 2003). These pathogens can affect any bone in the body (Jaffe 1972: 1060). However mycotic infections such as coccidioidomycosis and blastomycosis do appear to have some predilection for articular ends of long bones, likely related to the haematogenous spread of the spores (Jaffe 1972: 1064).

Due to the ambiguity of the skeletal lesions, mycotic infections have been traditionally diagnosed in palaeopathology where other options including tuberculosis, osteomyelitis, brucellosis, hydatids disease and metastatic cancers have been excluded as improbable causes (Micarelli et al. 2019; Ortner 2003). Clinically, mycotic lesions can appear indistinct from skeletal tuberculosis (Jaffe 1972). Given the lack of distinct criteria for mycotic infection, any cases of mycosis with the diagnostic criteria used in this thesis is diagnosed a *possible* not a *probable* case.

Table 5.10: *Diagnostic Criteria for Identification of Mycosis (SD= strongly diagnostic, D= diagnostic, and S= suggestive).*

Pathology	Diagnostic Strength	Differential Diagnosis	Reference
Multiple osteolytic focal lesions with defined margins and associated sclerotic reaction with apparent random distribution (bilateral unlikely) of the cranium, ribs, clavicles, sternum and/or vertebrae. Can be with or without localised SPNB around the osteolytic lesion.	**D**	Tuberculosis, osteomyelitis, neoplasms, multiple myeloma, brucellosis, echinococcosis	(Jaffe 1972: 1060-1066; Ortner 2003: 325-332)
Severe vertebral collapse causing in kyphosis	**S**	Tuberculosis, osteomyelitis, trauma, osteoporosis, brucellosis	(Ortner 2003: 325-332)
SPNB along the vertebrae in relation to paravertebral abscesses	**S**	Tuberculosis, brucellosis, neoplasms of the spine, osteomyelitis	(Jaffe 1972: 1066; Ortner 2003: 325-332)
Multiple osteolytic foci with well-defined margins towards the long bone ends (epiphyseal and metaphyseal regions)	**S**	Tuberculosis, osteomyelitis, neoplasms, multiple myeloma, brucellosis, echinococcosis	(Jaffe 1972: 1060-1066; Ortner 2003: 325-332)
Osteolytic foci of the extremities (hands and feet)	**S**	Tuberculosis, osteomyelitis, neoplasms, echinococcosis	(Jaffe 1972: 1060-1066; Ortner 2003: 325-332)
Osteolytic focal destruction of the paranasal sinuses/ unilateral hard palate/maxillary sinus	**S**	Tuberculosis, treponematosis, leprosy, osteomyelitis	(Ortner 2003: 325-332)

5.4.8 Osteomyelitis

Pyogenic (pus forming) osteomyelitis is a non-specific infection of bone producing a characteristic suite of lesions of bone death from loss of blood supply (sequestrum), combining an osteolytic lesion (circular pus-draining cloaca) and a osteoblastic healing response (involucrum) (Ikpeme et al. 2010). The major causative agents are *Staphylococcus* or *Streptococcus* bacterial species although other pathogens can infect bone (Acosta et al. 2004; Ikpeme et al. 2010). Initial transmission generally occurs through soft tissue infection of open wounds and, less frequently, secondary to respiratory, food-borne or water-borne diseases (Giaccai and Idriss 1952; Honda and McDonald 2009; Jaffe 1972: 1015-1046; Miller et al. 1963; Vohra et al. 1997).

The pathogenic agent enters the bone through the bloodstream and infiltrates through nutrient arteries (Jaffe 1972: 1015-1020). Proliferation within bone generally begins in the metaphyseal region, and eventually spreads to the cortex through the Haversian canals (Ikpeme et al. 2010; Jaffe 1972: 1020). Substantial deposits of SPNB occurs particularly in the long bones causing a shell of new bone termed the involucrum (Ikpeme et al. 2010; Kharbanda and Dhir 1991). Disruption to blood supply by the involucrum subsequently causes bone death (sequestrum) (Ikpeme et al. 2010; Kharbanda and Dhir 1991). Finally, cloacae develop within the involucrum in order to drain pus which has accumulated in the medullary canal (Ikpeme et al. 2010; Kharbanda and Dhir 1991). Osteomyelitis can cause nodes of SPNB only, like treponemal disease and bone cancers, therefore osteomyelitis is only diagnostic when there is clear evidence of pyogenic infection (Hackett 1976: 424). The presence of sequestra, cloacae and involucrum are all strongly diagnostic signs of pyogenic osteomyelitis, but may not necessarily all be present (Figure 5.21; Table 5.11).

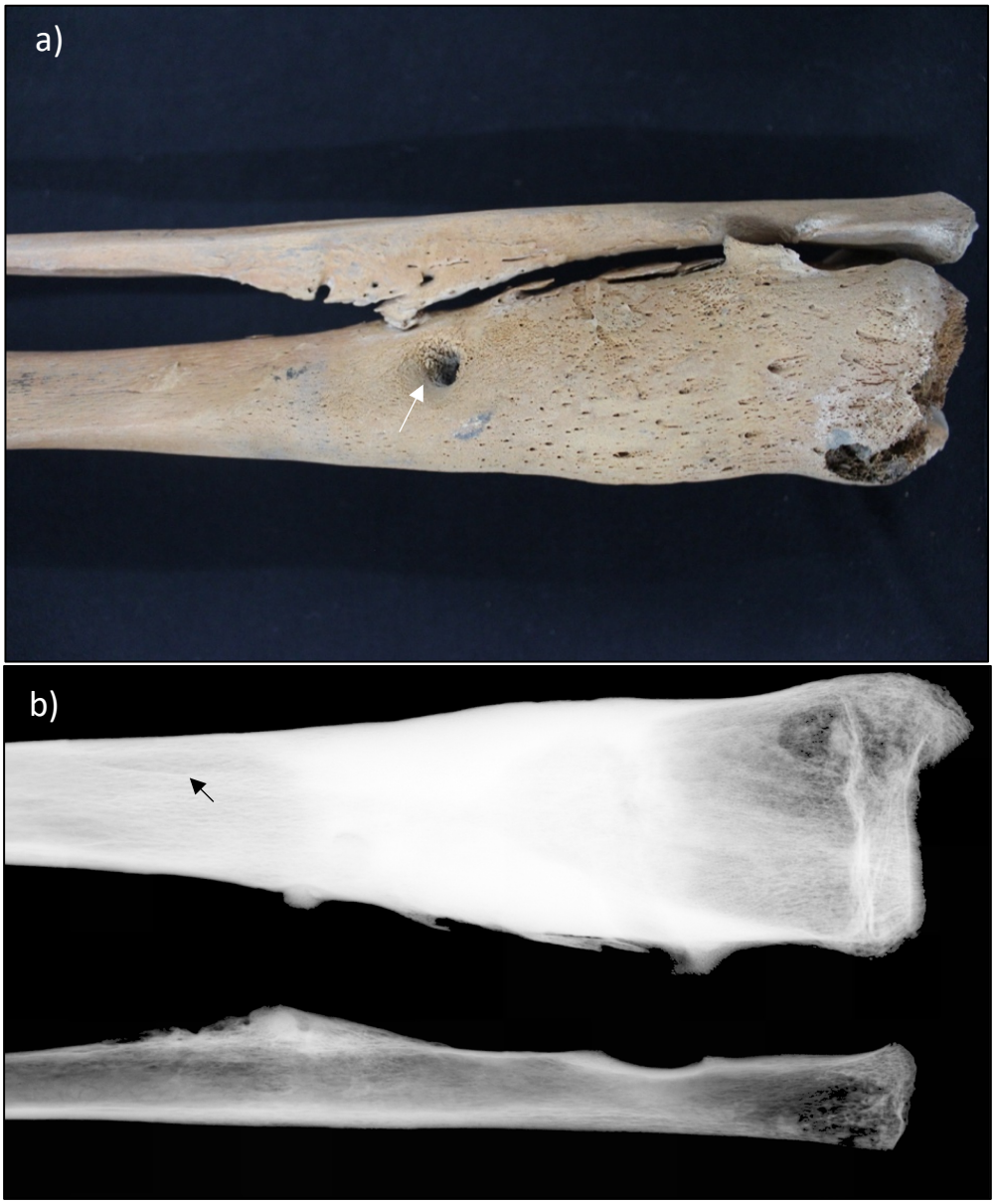

Figure 5.21: *Osteomyelitis of the tibia. a) Note the presence of cloacae (indicated by white arrow) and development of the involucrum. b) A small sheath of radiolucent bone (indicated by blue arrow) is consistent with sequestration (Edo Period Japan). Images author's own.*

Table 5.11: *Diagnostic Criteria for Identification of Osteomyelitis (SD= strongly diagnostic, D= diagnostic, and S= suggestive).*

Pathology	Diagnostic Strength	Reference
Osteoblastic new bone deposition (involucrum) with cloacae	**SD**	(Ortner 2003: 181-190)
Presence of involucrum and sequestrum	**SD**	(Ortner 2003: 181-190)

5.4.9 Mastoiditis and Otitis Media

Chronic bacterial and viral infections of the ear, which when untreated, can lead to proliferative bone response and lytic destruction of the ear canal (*otitis media*) and mastoid (*mastoiditis*) (Sadé and Berco 1974). Destruction of the air cells of the mastoid, and expansion of the auditory canal with lytic destruction of the auditory ossicles occurs due to pyogenesis (Lewis 2017: 140). SPNB deposits around and within the ear canal region can occur due to the inflammatory response to infection (Lewis 2017: 140). Radiographic evidence of the destruction of air cells of the mastoid or macroscopic evidence of mastoid destruction, either due to penetration of the outer cortex or exposed through postmortem damage, are strongly diagnostic for mastoiditis (Table 5.12; Figure 5.22; Flohr and Schultz 2009). Often skeletal evidence of ear infections are evident on radiographs only as most destruction occurs internally within the mastoid and ear canal (Flohr and Schultz 2009). Temporal bones in this thesis were not consistently radiographed, therefore identification relied on advanced cases or incidental finds on radiographs of the skull for other diagnostic reasons. Thus, the prevalences of otitis media in this thesis are likely under reported. Cholesteatoma, a rare but destructive tumour which can result in osteolytic destruction of the inner ear and mastoid needs to be considered in the differential diagnosis (Sadé and Berco 1974). However, this tumour can inadvertently cause infectious in of itself leading to pyogenic ear infection (Derlacki and Clemis 1965).

***Table 5.12*:** *Diagnostic Criteria for Identification of Otitis Media and Mastoiditis (SD= strongly diagnostic, D= diagnostic, and S= suggestive).*

Pathology	Diagnostic Strength	Differential Diagnosis	Reference
Osteolytic destruction of the mastoid region with destruction of the internal air cells	**SD**	Cholesteatoma	(Lewis 2017: 140-141)
Radiographic: Radiolucent region of osteolytic destruction in the internal mastoid or radiodensity of the internal mastoid	**SD**	Cholesteatoma	(Flohr and Schultz 2009; Lewis 2017: 140-141)
Osteolytic erosion of the auditory ossicles (often only seen under microscope)	**SD**	Cholesteatoma	(Lewis 2017: 140-141; Sadé and Berco 1974)
SPNB formation localised around the external ear canal region	**S**	Infection of the external crania, scurvy, rickets, cholesteatoma	(Lewis 2017: 140-141)
Internal draining fistula from mastoid region	**S**	Normal variant of the mastoid foramen	(Lewis 2017: 140-141)
Asymmetric mastoid process	**S**	Normal variant, congenital deformities	(Lewis 2017: 140-141)

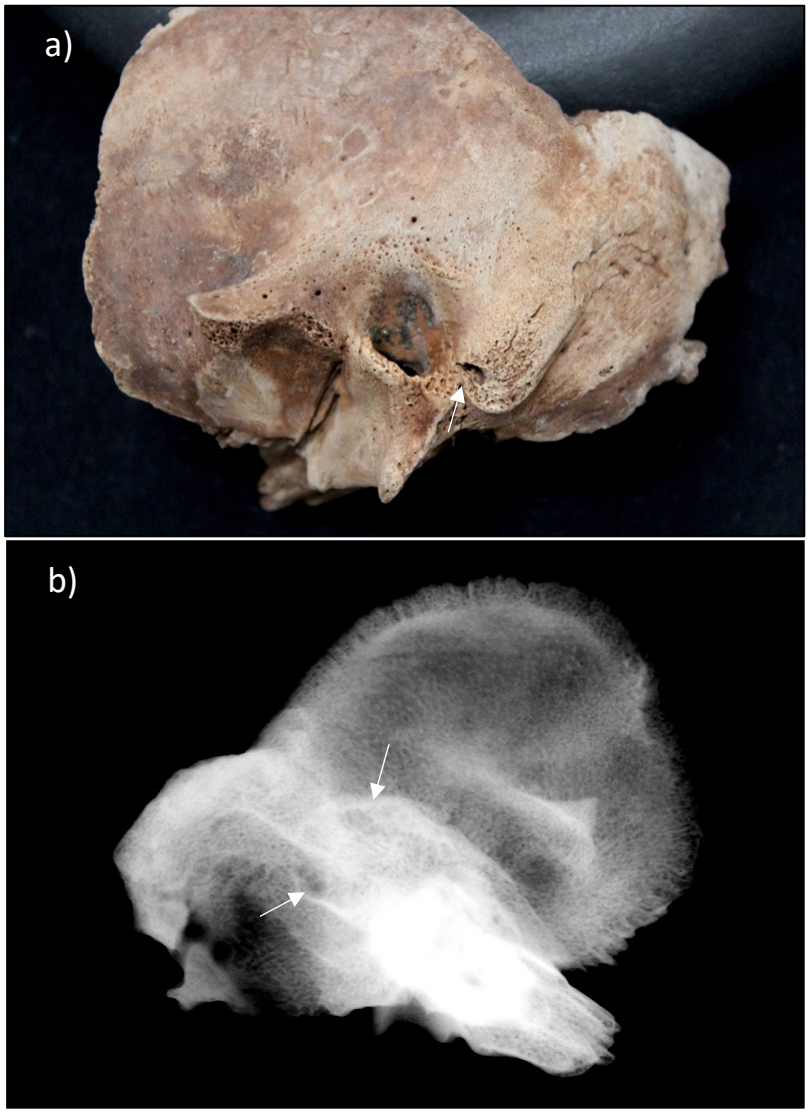

Figure 5.22: *Mastoiditis in a child (Edo period Japan, Temporal Bone). a) Small focal osteolytic lesion on the external aspect of the mastoid (white arrow). b) The radiographs demonstrate considerable internal lytic destruction (white arrows). Image: author's own*

5.4.10 Scurvy

Skeletal evidence of scurvy is caused by both direct and indirect impacts of malproduction of collagen in skeletal tissue (Fain 2005). Reoccurring haematomas form in scurvy due to insufficient collagen in blood vessels which then rupture (Hirschmann and Raugi 1999; Lewis et al. 1998). Haematoma formation around the cranial and postcranial bones has been demonstrated in adults and nonadults with scurvy, and the pooling of blood adjacent to the bone surface causes localised and discrete deposits of SPNB (Maat 2004; Resnick 1995b; Snoddy et al. 2017). Abnormal cortical porosity subsequently occurs due to increased capillary formation at the site of haematoma formation as a consequence of the

repeated microtrauma (Ortner and Ericksen 1997). In growing children, Vitamin C deficiency disrupts initial osteoid production which has deleterious effects on bone growth. This disruption causes bone loss around the regions of the metaphyseal plate, which leads to the formation of abnormal endochondral deep porosity (Brickley and Ives 2010: 65; Ortner et al. 2001).

Regions of the body where there is an association between blood vessels and habitually used muscles in contact with bone encourage repeated episodes of vessel rupture that lead to SPNB formation as an inflammatory response (Brickley and Ives 2010). The external greater wing of the sphenoid bone, and temporal bone are regions known to express pathology related to scurvy due to the use of the *temporalis* muscles in the chewing of food (Table 5.13; Ortner and Ericksen 1997). Similarly, use of the *supraspinatus* and *infraspinatus* muscles leads to pooling of blood, subsequent SPNB and abnormal cortical porosity in the supraspinous and infraspinous fossae of the scapula (Snoddy et al. 2018). Symmetrical discrete deposits of SPNB and abnormal cortical porosity in these regions are diagnostic for scurvy (Table 5.13; Figure 5.23). While many features in relation to the inflammatory response to microtrauma in scurvy have been described in infants, these also occur in adults, albeit likely to a lesser degree. Infants have a looser periosteum, and therefore it is expected they would present with more distinct osteoblastic lesions than in adults (Subbarao 1987). Lesions in scurvy are most commonly symmetrical as microtrauma tends to occur simultaneously in bilateral regions of the body (Ortner and Ericksen 1997; Snoddy et al. 2018).

The skeletal indicators of scurvy can be observed macroscopically and radiographically. Abnormal endochondral porosity radiographically presents as a translucent zone in the metaphyseal region called a ‘Trummerfeld’ or ‘Scurvy’ line (Jaffe 1972; Resnick 1995b). This area of radiolucency is often accompanied by an adjacent radiodense metaphyseal plate, termed a ‘White line of Fraenkel’ (Figure 5.24). A similar radiodense line around the epiphyseal plate occurs due to poor resorption of calcified cartilage, termed a ‘Wimberger ring sign’ (Snoddy et al. 2018). Fractures of the corners of the metaphyseal plates termed Pelkan spurs can occur given the disruption to osteoid formation where the structural integrity of the bone is compromised (Snoddy et al. 2018).

As scurvy lesions form from repeated microtrauma, trauma as a cause of the lesions unrelated to scurvy needs to be considered in the differential diagnosis. These lesions are less likely to be bilateral and symmetrical (Snoddy et al. 2018). Abnormal cortical porosity of the supraorbital roofs and the ectocranium can be misdiagnosed as trabecular porosity in these regions can be related to anaemia (see anaemia section below for differentiation between anaemia and scurvy of the ectocranium). Clear evidence that the porosity is restricted to the cortex is required to the differentiate between the two diseases (Klaus 2017). Finally, some rachitic lesions overlap with those of scurvy, and therefore rickets must always be considered in the differential diagnosis if scurvy is suspected (Lewis 2017). However, rickets and scurvy commonly co-occur, further complicating diagnosis of these two conditions (Schattmann et al. 2016).

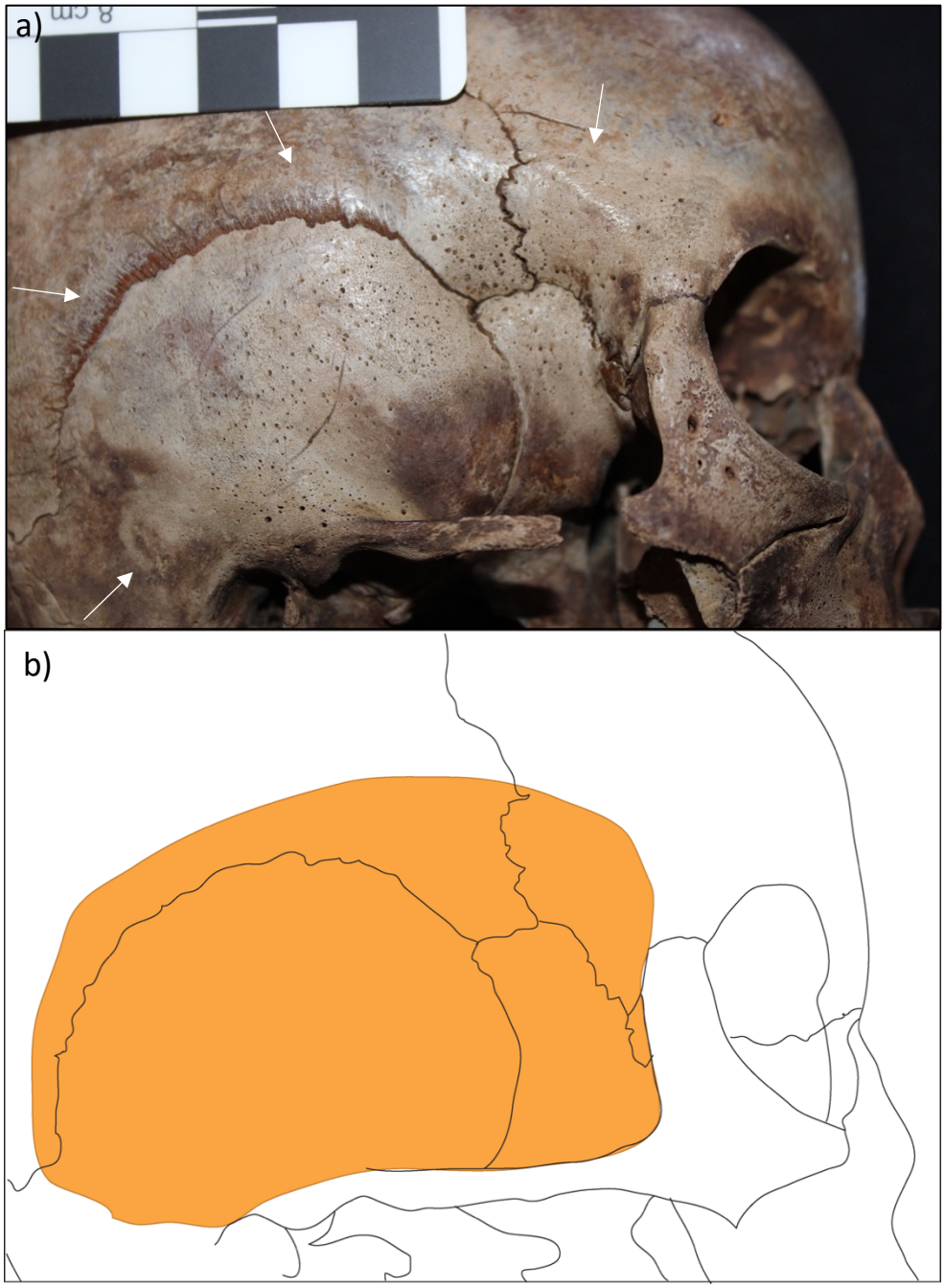

Figure 5.23: *Diagnostic lesion for scurvy. a) Discrete deposit of SPNB with abnormal cortical porosity on the lateral ectocranium including the sphenoid bone, the frontal bone, the temporal bone and parietal bone (white arrows). The lesion of this individual is consistent with a haematoma of the temporalis muscle and a symmetrical lesion was present on the right side of the cranium. b) An overlay of the region of the temporalis muscle in this individual, estimated from the muscle attachment sites. (Edo Period Japan) Image: author's own*

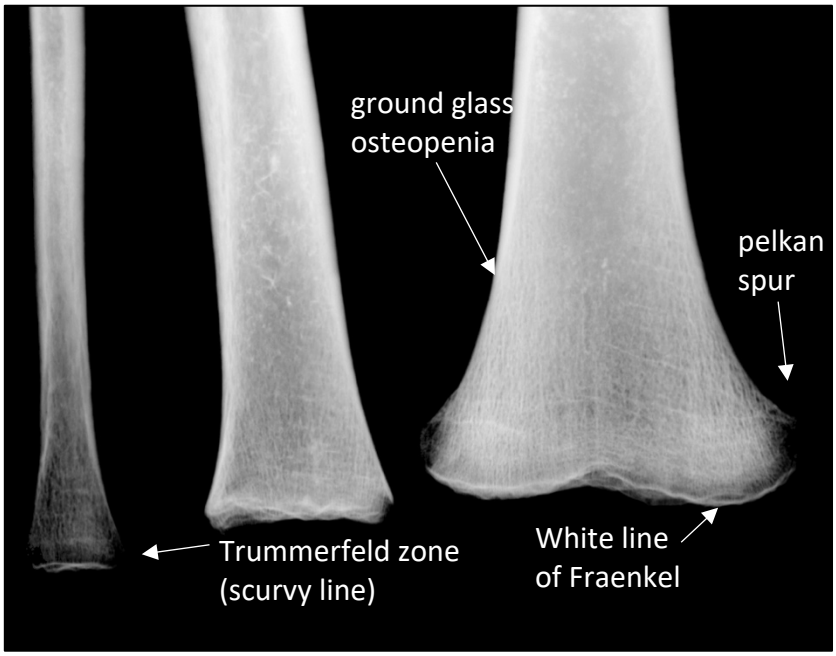

Figure 5.24: *Radiographic features of scurvy. (Edo Period Japan). Image: author's own*

Table 5.13: *Diagnostic Criteria for Identification of Scurvy (SD= strongly diagnostic, D= diagnostic, and S= suggestive) SPNB= subperiosteal new bone deposit.*

Pathology	Diagnostic Strength	Differential Diagnosis	Reference
Abnormal cortical porosity/ SPNB on ectocranial parietal bone/squamous temporal bone	**D**	Trauma, infection, anaemia	(Snoddy et al. 2018)
Abnormal cortical porosity/ SPNB on external greater wing of sphenoid bone	**D**	Trauma, infection	(Snoddy et al. 2018)
SPNB around foramen rotundum	**D**	Appositional growth (juveniles)	(Snoddy et al. 2018)
Abnormal cortical porosity/ SPNB on pterygoid fossae and/or plates	**D**	Appositional growth (juveniles)	(Snoddy et al. 2018)
Abnormal cortical porosity/ SPNB on anterior surface of maxillae/ infraorbital foramina	**D**	Trauma, infection	(Snoddy et al. 2018)
Abnormal cortical porosity/ SPNB on posterior surface of maxilla	**D**	Alveolar resorption	(Snoddy et al. 2018)
Abnormal cortical porosity/ SPNB on palatal surface of maxillae	**D**	Infection, trauma	(Snoddy et al. 2018)
Abnormal cortical porosity/ SPNB on medial surfaces of coronoid processes of mandible	**D**	Infection, trauma	(Snoddy et al. 2018)
Abnormal cortical porosity/ SPNB on the supraspinous fossae of the scapula	**D**	Trauma, appositional growth	(Snoddy et al. 2018)
Abnormal cortical porosity/ SPNB on the infraspinous fossae of the scapula	**D**	Trauma, appositional growth	(Snoddy et al. 2018)
Abnormal cortical porosity/ SPNB on orbital roof	**D**	Trauma, anaemia	(Snoddy et al. 2018)
Abnormal endochondral porosity extending >10mm from the distal metaphyseal plate of long bones	**D**	Rickets, longitudinal growth	(Ortner et al. 2001; Snoddy et al. 2017)
Radiographic: White line of Fraenkel	**D**	Normal variation, lead toxicity, rickets	(Brickley and Ives 2010: 65)
Radiographic: Trummerfeld line	**D**	Osteopenia, trauma, amaemia	(Brickley and Ives 2010; Resnick 1995b)

Pathology	Diagnostic Strength	Differential Diagnosis	Reference
Radiographic: Wimberger ring sign	**D**	Normal variation	(Brickley and Ives 2010: 65)
Corner fracture at position of dense zone of calcification (Pelkan's spur)	**D**	Trauma	(Brickley and Ives 2010: 65)
Abnormal cortical porosity and islands of SPNB on the endocranium	**S**	Inflammation of the meninges including trauma and infection	(Snoddy et al. 2018)
Abnormal cortical porosity on the lesser wing of the sphenoid bone	**S**	Normal variation, appositional growth (juveniles)	(Snoddy et al. 2018)
Abnormal cortical porosity/ SPNB on the posterior aspect of the zygomatic bones	**S**	Infection	(Snoddy et al. 2018)
Abnormal cortical porosity/ SPNB on the lateral portion of the anterior aspect of the zygomatic bones	**S**	Infection	(Snoddy et al. 2018)
SPNB around the mylohyoid line of the mandible	**S**	Trauma, infection	(Snoddy et al. 2018)
Inferior surface of the pars basilaris	**S**	Normal appositional growth	(Moore and Koon 2017; Snoddy et al. 2018)
Abnormal cortical porosity/ SPNB and/or vascular impressions on the visceral surface of the ilium	**S**	Infection, trauma	(Snoddy et al. 2018)
Flaring and swelling of the costochondral junction of the ribs	**S**	Rickets	(Schattmann et al. 2016)
SPNB deposit on the external shafts of the ribs	**S**	Normal appositional growth, trauma, infection	(Snoddy et al. 2017)
SPNB around region of the linea aspera of the femur	**S**	Entheseal changes	(Buckley et al. 2014; Snoddy et al. 2018)
Biconcavity of the vertebrae	**S**	Osteomalacia, osteoporosis, trauma	(Snoddy et al. 2018)
Bilateral ossified haematomas of the long bones	**S**	Trauma, osteogenesis imperfecta, haemophilia, pellagra	(Snoddy et al. 2018)
Metaphyseal cupping/flaring	**S**	Rickets	(Snoddy et al. 2018)
Ground glass osteopenia	**S**	Hyperfluorosis	(Brickley and Ives 2010: 65)

Note: Snoddy et al. (2018) also treat bilateral SPNB of the limbs in infants as diagnostic for scurvy (in cases where cranial diagnostic lesions are also present). Given this is a common response in many of the nutritional and infectious diseases assessed in this study, it was not included as a diagnostic feature for scurvy in this thesis.

5.4.11 Rickets and Osteomalacia

Disruption to the balance of minerals and hormones which regulate mineralisation of osteoid (calcium, phosphate, parathyroid hormone and Vitamin D) interrupts the normal modelling and remodelling processes of bone. Poor mineralisation of bone then causes rickets (nonadults) and osteomalacia (adults), as the bone strength is insufficient and therefore bone shape, contingent on the influence of gravity and the biomechanics of the bone, is deformed (Klein and Simmons 1993; Wharton and Bishop 2003). Internal bone loss is also associated with the disorder, and osteopenia of the cortical margins and trabeculae can occur (Brickley and Ives 2010: 106).

In osteomalacia, structural failure leads to pseudofractures (infractions), and bone deformity in the form of buckling can occur (Figure 5.25; Table 5.14). While pseudofractures can form from microtrauma, they are strongly diagnostic when found symmetrically at regions of weight bearing. These pseudofractures occur in multiple regions of the body, and when in the process of remodelling are associated with a callus with clear evidence of poor mineralised new bone (Brickley and Ives 2010: 118-119). In advanced forms, bone bending deformities particularly in regions of weight bearing such as the pelvis and proximal femur occur, and are also diagnostic for osteomalacia (Brickley and Ives 2010: 127-131). In children, defective mineralisation causes distinctive flaring, cupping and fraying of the growing long bone ends (Figure 5.26; Brickley and Ives 2010: 103-105). These features present both macroscopically and radiographically and are diagnostic for rickets. Bending deformities of the long bone shafts and alterations to the cranial shape also occur in rickets (Figure 5.27). If rachitic changes are observed in adults, *residual rickets* is diagnosed (Brickley and Ives 2010). Bending deformities, particularly of long bones, need to be differentiated from congenital developmental disorders such as skeletal dysplasias, and a level of overlap of lesion expression in rickets occurs with scurvy (Lewis 2017; Schattmann et al. 2016).

Figure 5.25: *Pseudofracture with poorly mineralised callous on the margins (Chandman Early Iron Age Mongolia [700-400 BC], Sacrum). The fracture has only just begun to remodel and is indicated by the white arrow, and the poorly mineralised callous indicated by the yellow arrows. The S3 body is also impacted into the S2 causing anterior angulation of the sacrum. Image: author's own*

Figure 5.26: *Fraying and rachitic porosity of the proximal metaphyses (Edo Period Japan, Humeri). Image: author's own*

Figure 5.27: *Anterior bending deformity of the shaft (Edo Period Japan, Femur). Image: author's own*

Table 5.14: *Diagnostic Criteria for Identification of Mineralisation Disorders (Rickets and Osteomalacia) (SD= strongly diagnostic, D= diagnostic, and S= suggestive).*

Pathology	Diagnostic Strength	Differential Diagnosis	Reference
Rickets (Nonadult mineralisation disorder)			
Layers of spiculated, irregular, porous SPNB on ectocranium, when healing there are irregular trabecular spurs	**D**	Normal growth, scurvy, anaemia	(Brickley and Ives 2010: 103-107)

Pathology	Diagnostic Strength	Differential Diagnosis	Reference
Medial angulation of mandibular ramus**	**D**		(Brickley and Ives 2010: 103-107)
Kyphosis or scoliosis of the T9 to L3 vertebrae**	**D**	Congenital or developmental anomalies	(Brickley and Ives 2010: 103-107)
Alteration in rib neck angle (>3 months of age) **	**D**		(Brickley and Ives 2010: 103-107)
Lateral straightening of rib shaft (>3 months of age) **	**D**		(Brickley and Ives 2010: 103-107)
Enlargement of costochondral rib junction	**D**	scurvy	(Brickley and Ives 2010: 103-107)
Acetabulae are pushed dorsally and angled anteriorly** (*protrusio acetabulae*)	**D**	Developmental abnormalities	(Brickley and Ives 2010: 103-107)
Flaring and swelling of distal metaphyses	**D**	Scurvy	(Brickley and Ives 2010: 103-107)
Fraying and or porosity of metaphyseal plate (macroscopic or radiological)	**D**	Postmortem damage	(Brickley and Ives 2010: 103-107; Schattmann et al. 2016)
Bending deformities of the limbs**	**D**	Developmental deformities	(Brickley and Ives 2010: 103-107)
Angulation (depression) of the femoral neck (*coxa vara*)**	**D**	Osteopenia,	(Brickley and Ives 2010: 103-107)
Cupping of metaphyseal plates	**D**	Postmortem damage, trauma, scurvy	(Brickley and Ives 2010: 103-107)
Long bone "thickening" (cortical enlargement) or Radiographic: Thick cortex with SPNB apposition**	**S**	Scurvy, congenital syphilis, non-specific infection, trauma	(Brickley and Ives 2010: 103-107) *
Delayed Fontanelle closure	**S**	Hydrocephalus, congenital or developmental conditions	(Brickley and Ives 2010: 103-107)
Thinning cranial bones	**S**	Osteopenia	(Brickley and Ives 2010: 103-107)
Craniotabes	**S**	Normal variation, prematurity, congenital syphilis, osteogenesis imperfecta	(Brickley and Ives 2010: 103-107)
Formation of large square shaped head**	**S**	Normal variant, swaddling or binding	(Brickley and Ives 2010: 103-107)
Disproportionate growth of pelvis**	**S**		(Brickley and Ives 2010: 103-107)
Shortening of limbs and growth stunting	**S**	Various childhood diseases and trauma	(Brickley and Ives 2010: 103-107)
Fractures at regions of weight bearing	**S**	Osteogenesis imperfecta, congenital syphilis, scurvy	(Brickley and Ives 2010: 103-107)
Radiographic: Trabecular coarsening in the distal metaphyses of long bones	**S**	Anaemia, scurvy	(Schattmann et al. 2016)
Radiographic: Loss of integrity at the sternal end of the ribs	**S**	Scurvy	(Schattmann et al. 2016)
Osteomalacia (Adult mineralisation disorder)			
Pseudofractures superior/inferior pubic rami. True fractures or buckling deformities	**SD**	Trauma	(Brickley and Ives 2010: 127-131)
Pubic rami lie adjacent rather than opposing, dislocation of the pubic symphysis. Obstruction of the pelvic inlet	**SD**		(Brickley and Ives 2010: 127-131)
Pseudofractures in medial aspect of the ilium adjacent to greater sciatic notch	**SD**		(Brickley and Ives 2010: 127-131)
Multiple pseudofractures as linear ridges of irregular, spiculated bone formation	**SD**	Infection, trauma	(Brickley and Ives 2010: 127-131)

Pathology	Diagnostic Strength	Differential Diagnosis	Reference
Looser's zones: pseudofractures affecting lateral border and inferior lateral margin of spinous process of the scapula	**SD**	Residual rickets	(Brickley and Ives 2010: 127-131)
Pseudofractures affecting the medial femoral neck or and medial trochanteric level	**SD**	Paget's disease	(Brickley and Ives 2010: 127-131)
Buckling and folding of the vertebrae	**D**	Osteoporosis	(Brickley and Ives 2010: 127-131)
Multiple complete fractures, numerous may appear adjacent	**D**		(Brickley and Ives 2010: 127-131)
Irregularly formed trabecular spicules at fracture margins	**D**		(Brickley and Ives 2010: 127-131)
Lateral straightening of rib shafts where the extreme may show medial indentations	**D**	Residual rickets	(Brickley and Ives 2010: 127-131)
Bending of the sternum	**D**		(Brickley and Ives 2010: 127-131)
Protrusion of ilia into pelvic inlet	**D**		(Brickley and Ives 2010: 127-131)
Narrowing of pelvis and curvature of ilia	**D**	Residual rickets	(Brickley and Ives 2010: 127-131)
Anterior facing of acetabulae and protrusion into pelvic inlet	**D**	Residual rickets	(Brickley and Ives 2010: 127-131)
Thinning of the ilia, collapse and buckling/ folding (anterior) and the fracture of the iliac crest	**D**	Osteopenia, paget's diseases	(Brickley and Ives 2010: 127-131)
Antero-lateral bending of femoral shaft	**D**	Residual rickets, congenital deformities	(Brickley and Ives 2010: 127-131)
Coxa vara of femoral necks	**D**	Residual rickets, congenital deformities	(Brickley and Ives 2010: 127-131)
Genu valgum ("knocked-knees") angulations	**D**	Blount's disease	(Brickley and Ives 2010: 127-131)
Pseudofractures affecting proximal ulna shaft beneath proximal joint surface as well as distal third of shaft	**D**	Trauma, activity related	(Brickley and Ives 2010: 127-131)
Irregularity of poorly mineralised bone accumulation at site of muscle attachments	**D**		(Brickley and Ives 2010: 127-131)
Pseudofractures of the clavicles, humeri, tibiae and fibulae	**D**	Stress fractures	(Brickley and Ives 2010: 127-131)
Increased posterior curvature of scapula blade	**D**	Residual rickets	(Brickley and Ives 2010: 127-131)
Buckling/ collapse of the superior border of the scapula	**D**		(Brickley and Ives 2010: 127-131)
Pseudofractures of the metacarpals and metatarsals	**D**	Stress fractures, trauma	(Brickley and Ives 2010: 127-131)
Radiographic: Osteopenia of the cortical margin and trabeculae of the vertebrae	**D**	Various metabolic disorders	(Brickley and Ives 2010: 127-131)
Loss of body height and irregularity of endplates of vertebrae	**D**		(Brickley and Ives 2010: 127-131)
Multiple sites of biconcave compression superior and inferior surfaces of the vertebral bodies. Radiographic: *codfish* sign	**D**	Sickle cell disease; osteoporosis	(Brickley and Ives 2010: 127-131; Ntagiopoulos et al. 2007)
Fine pitting/ diffuse porosity of cortical surface of cranial bones with low weight (can include basilar invagination)	**S**	Paget's disease, rickets	(Brickley and Ives 2010: 127-131)
Antemortem tooth loss	**S**	Dental disease, age, metabolic or infectious aetiologies	(Brickley and Ives 2010: 127-131)
Kyphosis and/ or scoliosis	**S**	Congenital and developmental disorders, metabolic or infectious disorders, trauma	(Brickley and Ives 2010: 127-131)

Pathology	Diagnostic Strength	Differential Diagnosis	Reference
Extreme ventral angulation of the of the sacrum, typically at S3	**S**	Residual rickets, trauma, sexual dimorphism	(Brickley and Ives 2010: 127-131)
Pseudofractures of the radial shaft	**S**	Osteopenia	(Brickley and Ives 2010: 127-131)
Radiographic: Thinning and coarsening of trabeculae	**S**	Various metabolic disorders	(Brickley and Ives 2010: 127-131)

* Brickley and Ives (2010) treats cortical bone thickening (cortical enlargement) as diagnostic. Due to the large variety of other pathologies where bone "thickening" can also occur, it is treated here as a suggestive feature. Particularly when radiographs are not possible. **These traits can be found in adults in the form of residual rickets.

5.4.12 Anaemia

To accommodate anaemic conditions during childhood, porosity of the external cranium and orbital roofs can develop as expansion of red bone marrow occurs (Brickley 2018). Porosity extending from the trabecular bone, associated with expansion of the diploë particularly on the ectocranium (porotic hyperostosis) and the orbital roofs (cribra orbitalia), is characteristic of this disorder (Table 5.15; Figure 5.28). In severe cases the expansions can take a "hair-on-end" appearance, where the porosity appears to project outwards perpendicular to the surface of the bone, usually visualised in radiographs (Ortner 2003: 103).

The term *porotic hyperostosis* has been defined in different ways in literature (e.g. Ortner (2012) following Angel (1966), uses the term to describe any form of abnormal porosity on the ectocranium), and there remains no consensus on the use of the term in the literature. In this thesis, the term is used to specifically describe trabecular expansions (marrow hyperplasia) causing porosity on the ectocranium and associated with expansion of the vault. This terminology separates conditions likely as a consequence of anaemia from other forms of pathological porosity such as the presence of islands of SPNB and abnormal cortical porosity on the parietal and temporal bones in individuals with scurvy (Snoddy et al. 2018). Defining porotic hyperostosis as a skeletal pathology specifically relating to anaemia is now possible due to the advances in the identification of porosity since Angel (1966) first discussed porotic hyperostosis and the relationship of this lesion to anaemia (Klaus 2017).

Trabecular expansions can also occur in the long bones of nonadults where red bone marrow persists prior to conversion to yellow bone marrow (Brickley 2018; Lewis 2017). However, given the dearth of discussion of postcranial changes in response to anaemia, these

were excluded from analysis. The term *cribra orbitalia* is used to describe trabecular porosity on the orbital roofs. Only medium or severe cases of cribra orbitalia (porosity grade 3 or 4) were considered in the diagnosis, as mild cases were ambiguous and could be caused by other conditions, or even be a normal anatomical variant (Cole and Waldron 2019). To identify porotic hyperostosis from other conditions which cause porosity on the ectocranium, this condition was only identified if there were at least two cranial bones that present with trabecular porosity, and there was a widespread and uniform distribution across the cranial element (Klaus 2017). As discussed in Chapter 3, anaemia is caused by a number of aetiologies, and therefore the specific cause for porotic hyperostosis and cribra orbitalia cannot be determined. When diagnosing anaemia, scurvy, rickets, and infection need to be included in the differential diagnosis as these can cause abnormal cortical porosity of the ectocranium which can appear similar to the trabecular porosity caused by anaemia, particularly in mild or remodelled forms (Klaus 2017). Porosity from anaemia tends to be in equidistant and symmetrical areas of affected bone in regards to the spread of the porosity across the cranial vault, whereas non-hyperplastic cortical porosity is more often asymmetrical in size and distribution (Klaus 2017: 99). It is recognised here that issues remain with the identification of anaemia from the cranium, particularly when radiographs are not standardly applied in the diagnosis. The following results chapters (6 to 8) present a variation of lesions that meet the criteria for porotic hyperostosis according to this thesis, it is clear that further research into the diagnosis of anaemia is necessary.

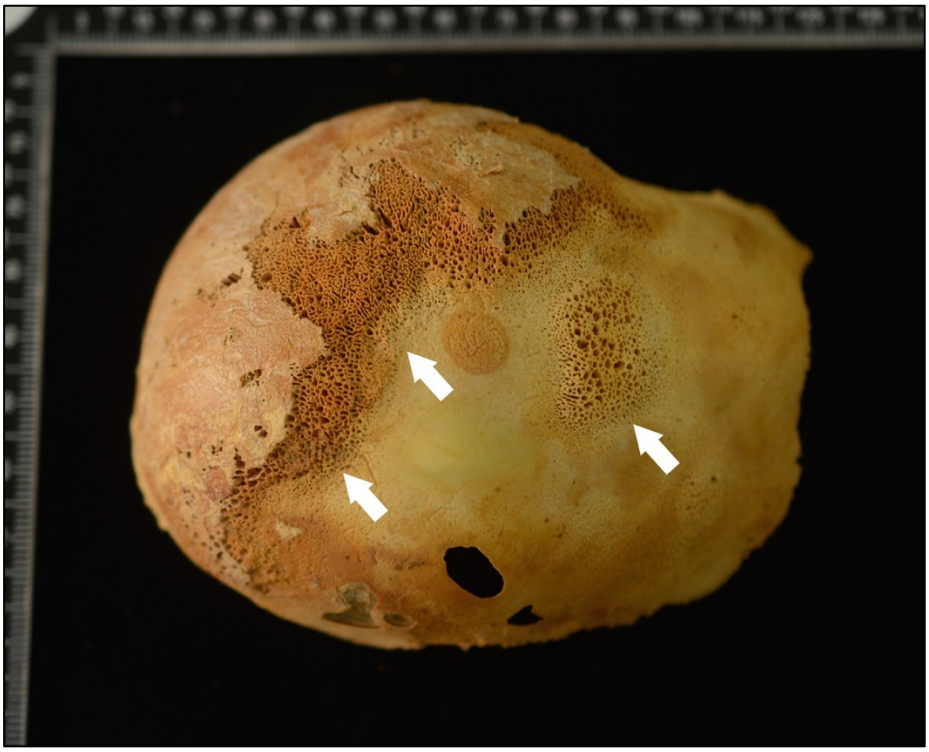

Figure 5.28: *Severe Porotic Hyperostosis in an infant between 9 months to 1 year of age (Formative Period, Atacama Desert, Chile). The porosity on the ectocranium of this individual is clearly associated with diploic expansion and has taken on a "hair-on-end" lesion expression. Image: Sohler (2017) used with permission courtesy of Dr. Annie Sohler- Snoddy,*

Table 5.15: *Diagnostic Criteria for Identification of Anaemia (SD= strongly diagnostic, D= diagnostic, and S= suggestive).*

Pathology	Diagnostic Strength	Differential Diagnosis	Reference
Porotic hyperostosis in at least two cranial elements with diploic expansion of cranial vault *or* moderate to severe cribra orbitalia	**SD**	Cortical porosity and thick cranial vault from scurvy, rickets and infection, other anaemias can cause the same lesions.	(Buckley 2016; Klaus 2017; Ortner 2003: 102-103; Stuart-Macadam 1985)

5.4.13 Thalassaemia

Thalassaemia is a genetic haemolytic anaemia, therefore skeletal changes in regards to increased marrow proliferation resemble those of non-specific anaemia as presented above. However, an extreme expression characterises the pathological changes which occur to the skeleton in thalassaemia (Papavasiliou 2012). Clinical research on the skeletal manifestations of thalassaemia are restricted to beta-thalassaemia only. Severe porotic hyperostosis leading to a "hair-on-end" appearance is a common skeletal manifestation of

thalassaemia and has been reported in cases of thalassaemia major and minor (Cambouris 1989; Sfikakis 1989).

Extensive marrow hyperplasia of the medullary canal and within trabecular bone cause considerable thinning of the bone cortex and expansion of the area of the medullary canal (Cambouris 1989). The severe marrow hyperplasia causes thinning trabeculae. However, osteoblastic response to the trabecular destruction instigates coarsening of trabeculae instead which is observed radiographically (Cambouris 1989). In extreme cases cortical thinning can progress to destruction of the cortex and subsequent honeycomb appearance of the bone surface, although these changes are recorded in anatomical cases who received treatment (Figure 5.29; Ortner 2003: 366).

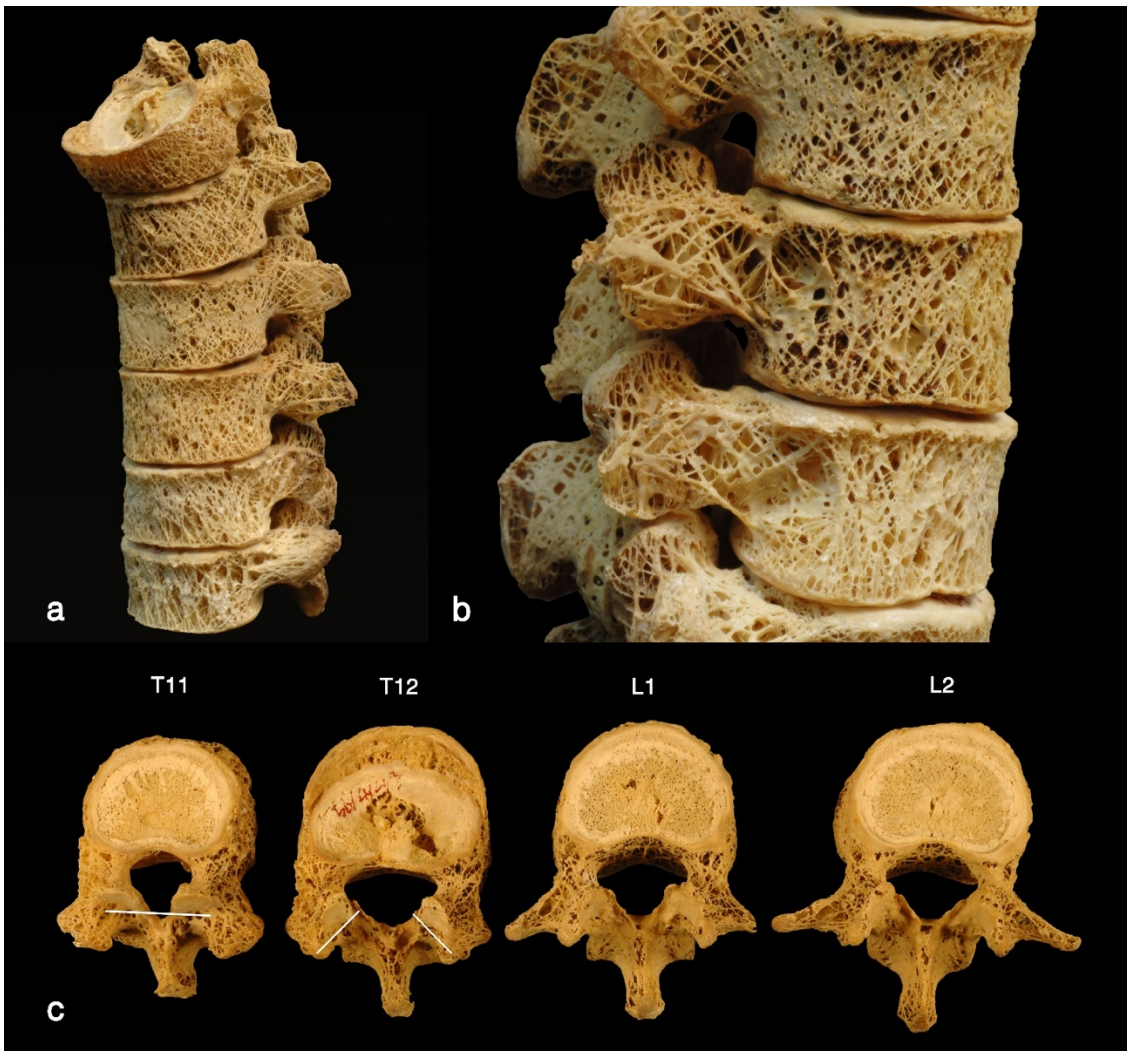

Figure 5.29: *Honeycomb appearance of the spine in a clinically diagnosed case of beta thalassaemia major in a Thai female (aged 49 years at death). Note the honeycombing on the vertebral bodies (a-b) and the archs (c). This individual received blood transfusion treatment and iron chelation therapy. Image: used with permission courtesy of Dr. Nawaporn Techataweewan.*

As mentioned in Chapter 3, a distinct facial deformity called *rodent facies* occurs in severe cases, particularly in beta thalassaemia major, whereby extensive marrow proliferation of the maxillae and zygomatic bones creates anterior bulging of the face, and lack of pneumatisation (formation of air cavities) of the maxillary, sphenoidal and frontal sinuses (Cambouris 1989; Lewis 2012; Scutellari et al. 1989; Tunacı et al. 1999). This pathology is strongly diagnostic for thalassaemia, particularly of beta thalassaemia major (Table 5.16; Cambouris 1989; Tunacı et al. 1999). The marrow proliferation also causes anterior teeth protrusion and malocclusion of the remaining teeth (Lewis 2012). A radiographic diagnostic feature of this disorder is the "rib with in a rib" sign. This feature is produced by extensive marrow hypertrophy perforating the thin cortex of the rib associated with a radiodense line in the middle of the medullary canal (Adamopoulos and Petrocheilou in press; Lewis 2012; Lewis 2017; Tunacı et al. 1999). Hypertrophic changes to the hands and feet of infants (with expanded foramina in the phalanges) is also characteristic of the disease as this lesion indicates an extreme form of anaemia unlikely to be associated with non-genetic aetiologies (Cambouris 1989; Tayles 1996).

Marrow perforation of the cortex known as extramedullary haematopoiesis occurs in extensive marrow proliferation. In certain circumstances SPNB response, similar to the "hair-on-end" appearance of the skull, surrounding thin cortices of postcranial bones, can occur as a consequence of marrow perforation (Adamopoulos and Petrocheilou in press; Colavita et al. 1987). This skeletal response has been documented to lead to premature fusion of the epiphyses of long bones particularly of the proximal humerus and distal femur (Cambouris 1989; Colavita et al. 1987). This lesion has not been well documented in the clinical literature but is more common in cases of thalassaemia intermedia (Colavita et al. 1987). Colavita et al. (1987) argue that a clinical emphasis in the literature on thalassaemia major patients who require blood transfusions to survive is likely the predominant reason for the dearth of reporting of this feature. Bone infarction (necrosis), while less common in thalassaemia than sickle cell anaemia, also has been reported. In this pathological condition, bone death occurs followed by inflammatory new bone response around the region of necrosis, and has a distinct appearance on radiographs (Kanthawang et al. 2016).

As thalassaemia is a heterogenous disorder, it is likely that the degree of skeletal expression in this disease also varies (Aydinok 2012; Galanello and Cao 2011). This heterogeneity provides a challenge in differential diagnosis as milder forms such as

thalassaemia intermedia and minor may be virtually indistinct from other forms of non-genetic anaemia, particularly if the overall epidemiology of an archaeological skeletal assemblage indicates that a number of causes for anaemia may have been responsible. For example, the thinning of cortices and expansion of the medullary canal observed in thalassaemia is also seen in other haemolytic anaemias (Resnick 1995a). Cases of severe skeletal forms of anaemia may also attributed to nongenetic haemolytic anaemias as is the case recorded by Sohler (2017) in Figure 5.28, and the archaeological context of the case is crucial to the differential diagnosis. Consideration of the regional distribution today, and the relationship of present day high prevalence of thalassaemia in regional zones of malarial endemicity is of significance in the diagnosis of thalassaemia in the past (Weatherall 2008).

Table 5.16: *Diagnostic Criteria for Identification of Thalassaemia (SD= strongly diagnostic, D= diagnostic, and S= suggestive).*

Pathology	Diagnostic Strength	Differential Diagnosis	Reference
Marrow hyperplasia of the facial bones: maxillae- leading to ventral displacement of central incisors, zygomatic bones- leading to orbital displacement, and/ or mandible (*rodent facies* deformity)	**SD**		(Adamopoulos and Petrocheilou in press; Cambouris 1989; Lewis 2012; Ortner 2003: 365; Scutellari et al. 1989; Tunacı et al. 1999)
Poor or lack of pneumatisation of the paranasal and cranial sinuses sparing the ethmoid sinuses.	**D**	Neoplasms, Paget's disease, trauma, hypopituitarism, hypothyroidism, osteopetrosis, sickle cell anaemia	(Cambouris 1989; Tunacı et al. 1999)
Widening of entire rib, or widening of the rib head and neck with pronounced bulbous appearance posteriorly (costal osteomas). Associated with radiograph appearance of erosion of the inner cortex.	**D**	Neuroblastoma, Nieman-Pick disease, Leukemia	(Cambouris 1989; Lawson et al. 1981; Lewis 2012; Tunacı et al. 1999)
Radiographic: "rib within a rib" appearance, related to the above sign.	**D**	Sickle cell anaemia, osteomyelitis, leukemia	(Cambouris 1989; Lawson et al. 1981; Lewis 2012; Tunacı et al. 1999)
Enlarged tubular bones of the hands and feet due to marrow hyperplasia (infants) sometimes associated with enlarged nutrient foramina *or* Radiographic: coarse trabecular patterns of the hands or feet, sometimes associated with cyst-like lucencies due to focal collection of hyperplastic marrow	**D**	Treponemal disease, leprosy, tuberculosis	(Cambouris 1989; Lewis 2012; Tayles 1996; Tunacı et al. 1999)
Premature fusion of epiphyseal plates particularly of the proximal humerus and distal femur, often causing short long bone maximum length	**D**	Scurvy, hypervitaminosis A, trauma, achondroplasia, Morquio's disease, Ellis-van Creveld disease, peripheral dysostosis, poliomyelitis	(Cambouris 1989; Currarino and Erlandson 1964; Lewis 2012; Tayles 1996; Tunacı et al. 1999)

Pathology	Diagnostic Strength	Differential Diagnosis	Reference
Extensive marrow proliferation of the long bones leading to expansion of the medullary canal, associated with thin cortices (and in extreme circumstances honeycomb-like porosity) resulting in swollen appearance or metaphyseal flasked shaped deformities	**S**	Other haemolytic anaemias, scurvy, rickets, metaphyseal dysplasia, Gaucher's disease, osteomyelitis	(Cambouris 1989; Lawson et al. 1983; Lewis 2012)
Severe porotic hyperostosis of vault and maxilla and/ or Cribra Orbitalia (*see iron deficiency anaemia diagnostic criteria*)	**S**	Other haemolytic anaemias	(Cambouris 1989; Lewis 2012; Tunacı et al. 1999)
Wide dental spacing	**S**	Skeletal dysplasias, normal variation	(Lewis 2012)
Spiculated or scalloped proliferation of subperiosteal reactive new bone on the shafts of the limb bones and the clavicles	**S**	Infectious diseases, rickets, scurvy, hypertrophic osteoarthropathy	(Adamopoulos and Petrocheilou in press; Colavita et al. 1987; Tayles 1996)
Marked osteoporosis and cortical thinning of the vertebrae, with compression fractures in severe cases	**S**	Age related osteoporosis, osteomalacia, scurvy, trauma	(Tunacı et al. 1999)
Bone infarction	**S**	Osteomyelitis, sickle cell anaemia, osteosarcoma	(Kanthawang et al. 2016)
Enlargement and alteration of the trabecular pattern in flat bones (pelvis and scapula)	**S**	Other haemolytic anaemias, leukemia	(Ortner 2003: 365)

5.4.14 Summary of Differential Diagnosis Protocols in this Thesis

Standardised protocols for differential diagnosis were produced for six infectious diseases, and two anaemias. Furthermore, published protocols for two nutritional diseases were adapted (Brickley and Ives 2010; Snoddy et al. 2018). The following section defines the methodology applied for statistical analyses based on prevalences derived from differential diagnosis of the diseases described above.

PART TWO: Palaeoepidemiological Assessment

5.5 Structure of Statistical Analysis

It is important to consider the impact of human population interaction on the health of past populations at multiple levels of investigation. For this reason, the impact of human population interaction is considered in this thesis within three phases of focus: 1. site, 2. region, and 3. continent level. Where analysis at a site level enables introspection of differential health effects within a population (e.g. age and sex), the regional level will enable discussion of contextually embedded changes to disease patterns with an increase of human population interaction levels. Different statistical models are employed suited to each stage. For site and regional levels, statistical analysis is used to assess both the *morbidity* and *mortality* of diseases. The analytical tools used for site and region level (as employed in

Chapters 6, 7 and 8) are presented here. A detailed description of the statistical methods employed at the continent level is provided in Chapter 9.

5.6 Selection of Disease Prevalence Estimates

Lesion prevalence estimates within this thesis are based on the individual as a denominator rather than skeletal element analysis, enabling demographic assessment of epidemiological impact. In estimates of specific disease, an individual is defined as having the presence of at least two skeletal elements which have the potential to express 'diagnostic' lesions (see tables outlining 'diagnostic' lesions for each of these above) (adapted from Buckley 2016). A specific requirement for identifying anaemia required the presence of at minimum one orbital roof, or at least the frontal bone and one parietal bone in order to identify cribra orbitalia or porotic hyperostosis. Similarly, identification of mastoiditis or otitis media required the presence of at least one temporal bone with the mastoid and ear canal intact.

5.6.1 Infectious and Nutritional Disease Prevalence Parameters

As skeletal evidence for infectious disease can be both specific and non-specific, parameters for the construction of infectious disease prevalences presented in this thesis are inclusive of both categories. Statistically, this is necessary due to the low prevalences of specific infectious diseases identified in an archaeological context. As previously stated, SPNB deposits can be caused by number of pathologies including trauma, cancer, nutritional, metabolic disease and infection (Weston 2012). Previous researchers have separated systemic from non-systemic disease through the identification of systemic disease as involving two or more skeletal elements (Buckley and Tayles 2003; Ortner et al. 2001). This is not beneficial in differentiating infection from metabolic, endocrinal and cancerous aetiologies, as they all fall into this category (Brickley and Ives 2010; Loyer et al. 2019). Researchers such as DeWitte (2014a) and Temple (2007) have previously used bilateral SPNB deposits on the tibiae as a proxy for infectious disease. However, the tibiae are particularly susceptible to traumatic insult, and can be equally affected bilaterally in nutritional diseases such as in scurvy (Brickley and Ives 2010; Maat 2004; Steinbock 1976).

In the case of scurvy, lesions in adults tend to be more discrete as they result from haematoma formation (Maat 2004), and in the case of residual rickets, by adulthood the

surfaces are often already well remodelled and there is no longer signs of abnormal bone tissue on the outer cortex surface (Brickley and Ives 2010). Therefore, diffuse SPNB deposits across multiple elements in adults may be a better proxy for an infectious process. As such, it is proposed that wherein two skeletal elements have been identified to have SPNB deposits that extends beyond ¼ of the bone surface, this is sufficient to consider as likely due to infection. As osteoblastic bone response to infection can be unilateral, bilateral spread is not a necessary component of the criteria such as in DeWitte (2014a) and Temple (2007)'s work. Only individuals over the age of 15 are considered within this parameter as the periosteum is more loose in children, and nutritional diseases such as scurvy are well known to cause widespread SPNB particularly in the long bones (Snoddy et al. 2018; Subbarao 1987).

It is recognised here that the parameters for identification of infection from SPNB deposits only, can lead to the inclusion of other individuals where infection was not the underlying cause for the skeletal expression of new bone. For example, hypertrophic osteoarthropathy is a rare systemic condition caused by a number of disorders including neoplasms, which produce diffuse SPNB deposits across multiple skeletal elements, particularly in the appendicular skeleton (Loyer et al. 2019). However, the parameters presented here attempt to minimise the *probability* of inclusion of other non-infectious aetiologies, and in most cases these parameters would indicate an infectious cause. In cases where a cancerous aetiology was identified, the SPNB deposits were not considered to be from infectious causes, and therefore excluded. This is very rare and cases of diffuse SPNB in association with other pathological evidence for cancer was found in only two individuals in this thesis, one from Xiongnu Mongolia and another from Jomon Japan (see Chapters 6 and 8).

The parameters for infection in this thesis are:

1. Specific infectious disease has been identified using the diagnostic criteria
2. Minimum of 2 skeletal elements with more than ¼ of the bone surface covered with SPNB deposits where cancerous pathologies have not been identified (diffuse lesions not discrete [OB grades 2-6]). Individual is >15 years of age.
3. Evidence of non-specific infection: otitis media, mastoiditis and osteomyelitis

Only specific metabolic diseases were used to identify the prevalence of nutritional deficiency for both adults and nonadults, as parameters for inclusion of non-specific cases of malnutrition cannot be constructed, due to the variable nature of skeletal expression of nutritional deficiency. The prevalence of each nutritional disease was dealt with separately, in contrast to the case of the combined infectious disease prevalence, particularly as specific nutritional disease prevalences are considerably higher than the prevalences of specific infectious diseases (see Chapters 6, 7 and 8).

5.7 Statistical Analysis: Assessment of Morbidity

The statistical assessment of morbidity was an essential component to meeting objectives 4 and 5 which relate to investigating disease dynamics at site and regional level. Assessment of morbidity, specifically relates to the prevalence of individuals within each sample who present with evidence of disease. The assessment of morbidity involved the employment of relative risk ratios and Fisher's exact analyses to determine whether there were statistically significant differences in the proportions of disease amongst different demographic groups. Tests for both site and regional levels were undertaken for the prevalence of each specific nutritional disease identified in this thesis (the prevalence of combined possible and probable cases, and the prevalence of probable only cases were both statistically assessed), the prevalence of anaemia, and the overall proportion of infectious disease as outlined in the above section.

5.7.1 Determining the Significance for Statistical Assessment

Palaeoepidemiological analyses typically apply a p-value of <0.05 as the measure of statistical significance (Lukacs 1992; Mays 2005; Scaffidi 2020). However, this is often not accompanied by consideration of the size of the effect (when measurable), the statistical test applied, and the sample size that influences the appropriate consideration of what is a *significant* outcome. As Dahiru (2008) notes the $p<0.05$ convention has been directly adopted from R.A Fisher's initial analysis when he pioneered the idea of significance testing, and applying this p-value as a *standard* is a fallacy in statistical analysis. This convention has no objective status in statistical analysis and the decision of what is considered statistically significant is an arbitrary distinction that should consider the nature of the data (its size, statistical power, variable type), and the statistical analysis applied. Palaeoepidemiological studies are often affected by low statistical power which reduces the

probability of achieving $p<0.05$. As Smith (2020) argues, the size of the effect (the level of difference between the two samples) is likely a better valuation of significance as the nature of the data in biological anthropology is prone to false negatives (Type II error). The p-value itself does not provide any information on the size of the effect. While p-values were employed in this thesis, the effect sizes and confidence intervals were considered within the analysis, and are provided in the results chapters (Chapters 6 to 8). Additionally, p-values were adjusted to suit the appropriateness of the statistical tests to the data presented (see sections below on specific p-values according to each statistical test). This determination in threshold value follows standard applications of p-values in statistics where decisions are made to determine what threshold is appropriate to provide evidence against the null hypothesis (Dahiru 2008). This approach has been applied in some palaeoepidemiological analyses (see Godde et al. 2020).

5.7.2 Relative Risk Ratios for Morbidity Analysis

Relative risk (RR) ratios are a common statistical technique employed in the field of medicine and epidemiology to assess whether a disease has differential influence across two independent categories (dichotomous variable) (Altman 1990). While the test is not yet commonly used in palaeoepidemiology (a recent example of its use is Collier and Primeau 2019), a similar assessment interpreted in the palaeopathological literature as assessing relative risk is that of the odds ratio. While commonly applied in palaeoepidemiological studies (Molto et al. 2019; Smith-Guzmán 2015; Waldron 1991), the odds ratio (OR) purely describes the probability of one event over the other. As such, claims such as 6 times the greater risk due to an odds ratio of 6 is erroneous (Schmidt and Kohlmann 2008). In contrast the relative risk ratio is a direct measure of the relative risk, the susceptibility of one cohort acquiring a disease compared to another cohort. It is recognised in epidemiology that the odds ratio can greatly overstate the 'relative risk' of one event, especially if the outcomes are not rare (Schmidt and Kohlmann 2008). That is relative risk ratios are more appropriate in instances where the prevalence rate of a disease is high. Where the prevalence rate of a disease is low in both cohorts being statistically assessed the odds ratio and the relative risk ratios will appear similar (Cummings 2009). It is recognised that both relative risk ratios and odds ratios tests are modern epidemiological analytical tests, therefore they are limited in their application to archaeological samples. Many confounding factors that can be controlled

for in modern day cohort studies are not possible in palaeoepidemiological analyses (Klaus 2014).

Relative risk ratios were employed to test the probability that the dichotomous variables being assessed (e.g. presence or absence of disease) were associated with a positive vs. a negative outcome, and that an *exposed* group was associated with a higher probability of a bad outcome, than the *treatment* group (McKillup 2006). In this thesis the exposed group was selected as the variable most likely at risk (e.g. females as the exposed group compared to males as the treatment group). That is, relative risk ratios were used in instances where it was likely that the disease had a higher impact on health of one category compared to the other in terms of morbidity. Relative risk ratios were calculated using MedCalc Software Ltd 2020. Due to the sample sizes employed in this thesis, statistical significance was set at P <0.10. The p-value was also evaluated in the context of the size of the effect (relative risk and confidence interval).

The formula for relative risk ratios are:

$$RR = \frac{a/(a+b)}{c/(c+d)}$$

Simply put the relative risk ratio is the ratio of two probabilities, and for morbidity is calculated as:

The number of individuals in the *exposed* group with *disease present* / the total number of individuals in the *exposed* group

---

The number of individuals in the *control* group with *disease absent* /the total number of individuals in the assemblage in the *control* group (Table 5.17).

Table 5.17: *Assessment of morbidity using relative risk ratios*

	Exposed *Category likely at risk*	**Control** *Category not likely at risk*
Positive (bad outcome) *Disease Present*	a	c
Negative (good outcome) *Disease Absent*	b	d

5.7.3 Fisher's Exacts for Morbidity Analysis

The Fisher's exact test is a statistical tool which calculates the probability that two samples exhibit differences in observed and expected frequencies of two categorical variables, thereby testing the association between categories and samples (McKillup 2006: 309). This statistical test is commonly used as an alternative to the Chi-square test for datasets with a small sample size. Fisher's exact tests were employed in instances where it was not known which variable can be treated as an *exposed* group. Fisher's exact tests were performed in Microsoft Excel 16.16.18. Statistical significance was set at $P< 0.05$.

5.7.4 Morbidity Analysis at Site Level

Relative risk ratios were employed to assess the influence of disease prevalence within in each assemblage across sex (male vs. female), nonadult age (<1 year of age vs. >1 <20 year of age, <5 years of age vs. >5 <20 years of age, and <10 years of age vs. >10 <20 years of age) and adult age (>14 <20 years of age vs. >20 years of age, >14 <30 years of age vs. >30 years of age, and >14 <40 years of age vs. >40 years of age). The category of >14 <20 year olds were included in both nonadult and adult age statistical analyses, as the period marks a transition from childhood to adulthood. Nonadults and adults were assessed separately, as the differential rate of bone remodelling in nonadults compared to adults, and therefore differential disease response is a confounding factor.

Fisher's exact tests were employed for Bronze Age Mongolia to assess possible differences in disease between Bronze Age cultures of Eastern and Western Mongolia, as the archaeological material and mortuary patterns differ significantly between these two regions. The Fisher's exact test assessed whether it was appropriate to combine the assemblage as a single sample for the regional and continent statistical assessments.

5.7.5 Morbidity Analysis at Region Level

Relative risk ratios were employed to assess changes in disease prevalences with increasing interaction levels. The post-interaction site for each of the three regions (Tsukumo, Man Bac, and Xiongnu Mongolian assemblages) were treated as the *exposed* group. Only diseases that were present in both the pre-interaction and the post-interaction assemblages for each region were statistically assessed for differences.

5.8 Statistical Analysis: Assessment of Mortality

Statistical assessment of mortality also meets objectives 4 and 5 of this thesis. Additionally, the mortality analysis enables direct engagement of the outcomes of this thesis with the osteological paradox (see Chapter 1). The assessment of mortality relates to the risk of death associated with the presence of a particularly disease within the sample (DeWitte and Stojanowski 2015). Statistical assessments of mortality are necessary, as underlying mortality rates within an assemblage influences the morbidity prevalence, a factor identified by Wood et al. (1992). As can be observed by the age-at-death distributions of the assemblages presented in Chapter 4, raw age-at-death distributions from cemetery samples do not necessarily reflect a natural mortality distribution. Therefore, assessment of mortality purely from cross-cohort comparative age-at-death distributions (e.g. Halcrow et al. 2016), is not an appropriate technique, as the age-at-death distributions are not necessarily representative of mortality rates only, and are influenced by other factors such as fertility rates, selective burial practices and discriminatory post-mortem depositional processes (Hoppa 1999; Wright and Yoder 2003).

The age dependent mortality distribution (Gompertz model) is associated with decreasing risk of death with increasing age in childhood, and increasing risk of death with senescence in adulthood. This model has previously been employed in bioarchaeological assemblages to assess the impacts of variables such as sex (Redfern and DeWitte 2011), stature (DeWitte and Hughes-Morey 2012), and the impact of the bubonic plague (DeWitte 2014b) as co-variates on the risk of death. The Gompertz and Gompertz-Makeham models are traditionally demographic models, which require the estimation of multiple parameters beyond the age-at-death distribution, readily estimated in a living population. To employ these statistics in palaeodemography, age-distributions were produced through transition analysis, a technique whereby age estimates were modelled based on conditional

probabilities produced from 17th Century Danish parish records.(DeWitte and Hughes-Morey 2012). Therefore, the models are potentially influenced by age mimicry and restricted to the mortality conditions of the Danish records, and may not be entirely appropriate for application in prehistoric assemblages. Additionally, assessing the *difference* in mortality of two samples by 'refitting' the mortality distributions to the *same* model of generalised mortality may be counterproductive to the intended outcomes of the model, particularly as it remains unknown whether the prehistoric samples exhibited a generalised mortality distribution. Instead, relative risk ratios, Kaplan-Meier survival curves and Cox proportional hazard regression models are applied in this thesis as they do not assume an underlying mortality distribution. That is, they do not require estimation of parameters, and enable better comparisons of changing mortality rates between two prehistoric skeletal samples.

Tests for the mortality of diseases at both site and regional levels were undertaken on the prevalence of each specific nutritional disease identified in this thesis (the prevalence of combined possible and probable cases, and the prevalence of probable only cases were both statistically assessed), the prevalence of anaemia, and the overall proportion of infectious diseases. It is recognised here that the activity of the disease (active vs. mixed vs. healed) factors into mortality analysis. However, due to the sample sizes of the assemblages, mortality was restricted to assessment of presence and absence of disease. Further discussion on limitations and future mortality research involving activity of disease is addressed in Chapter 10. A relationship of disease presence with increased mortality is defined as increased *frailty*, where as a relationship of disease presence with decreased mortality is defined as *survivorship*.

5.8.1 Relative Risk Ratios for Mortality Analysis

In order to assess mortality using relative risk ratios, the positive (bad) outcome was defined as death before a certain age (*x* age in years). Therefore, relative risk at death could be calculated over a number of different age brackets. In nonadults, the tested categories were <1 year of age vs. >1 <20 year of age, <5 years of age vs. >5 <20 years of age, and <10 years of age vs. >10 <20 years of age. In adult age the categories tested were >14 <20 years of age vs. >20 years of age, >14 <30 years of age vs. >30 years of age, and >14 <40 years of age vs. >40 years of age. The category of >14 <20 year olds were included in both nonadult and adult age statistical analyses, like in the morbidity analysis. Nonadults and

adults were assessed separately, as the different rates of bone remodelling in nonadults compared to adults, and therefore differential disease response is a confounding factor.

The relative risk ratio for mortality is calculated as:

$$\frac{\text{The number of individuals in the } \textit{exposed} \text{ group who } \textit{died before age x} \text{ / the total number of individuals in the assemblage in the } \textit{exposed} \text{ group}}{\text{The number of individuals in the } \textit{control} \text{ group who } \textit{survived after age x} \text{ / the total number of individuals in the assemblage in the } \textit{control} \text{ group (Table 5.18).}}$$

Table 5.18: *Assessment of mortality using relative risk ratios*

	Exposed *Category likely at risk*	**Control** *Category not likely at risk*
Positive (bad outcome) *Age of Non-survivors (died before age x)*	a	c
Negative (good outcome) *Age of Survivors (survived after age x)*	b	d

5.8.2 Kaplan-Meier Curves for Mortality Analysis

The Kaplan-Meier survival function is a univariate non-parametric statistical test commonly used in epidemiological and clinical studies to assess the impact of disease or a particular medical treatment on the survivorship across a sample (Liu 2018). The test is also now frequently used in palaeoepidemiology (DeWitte 2014a; McFadden and Oxenham 2020; Milner and Boldsen 2017). The Kaplan-Meier estimates the probability of surviving an event past a certain age, therefore producing a survivorship function (Tolley et al. 2016). Like the relative risk ratios, the test is used to compare the relationship of age to a binary variable. However, unlike relative risk ratios, the age variable is not dichotomous, and is instead a continuous variable (Liu 2018). In palaeoepidemiology, the Kaplan-Meier survival curves can be employed to assess selective mortality, and whether the presence of a disease

within an assemblage is associated with survivorship or frailty to that disease (DeWitte 2014a).

The Kaplan-Meier survival function is defined by the probability of surviving to the next interval (age in years). For each interval, P= 1- (number of deaths / number of survivors at the start of the interval). The formula for the Kaplan Meier survival function is:

$$\widehat{S}(t) = \prod_{i:\, t_i \leq t} \left(1 - \frac{d_i}{n_i}\right),$$

$\widehat{S}(t)$ = survival function

d_i = number of deaths

t_i= time

n_i= number of individuals survived up to time t_i

In order to employ the Kaplan-Meier survival function, point age estimates (age of individuals in years) need to be produced. As standard age estimation methods were employed in this thesis, mean age estimates were used. This provides a limitation to the use of the statistical method as traditional age methods have relatively large standard deviations from the mean and are not useful past the age of 60 (see Chapter 4). However, as the Kaplan-Meier function does not assume an underlying age-at-death distribution, the function can accommodate point age estimates that are concentrated around means produced from morphological stages (e.g. the Suchey-Brooks and Lovejoy methods). Statistical significance was set at $P < 0.15$ due to the small sample sizes, the use of mean age estimates, and due to the use of standard age estimators which restricted the oldest age demographic to 50+ years of age.

The assumptions of the Kaplan-Meier survival function is related to the independence of censoring and recruiting time. Censoring time is a condition specific to clinical studies where individuals exit the study, leading to missing data, and recruiting time is associated with the inclusion of individuals at a later stage in the study (Koletsi and Pandis 2017). This is not relevant to bioarchaeological contexts. As the Kaplan-Meier is a univariate model, confounding factors (such as co-morbidity) and their impact on mortality is not considered in this model (Liu 2018). For example, when assessing the association of

infectious disease levels to survivorship, the model does not consider the impact of nutritional deficiency on infectious disease susceptibility to mortality (see Chapter 3). However, in this thesis the Kaplan-Meier survival functions have been independently applied on both infectious disease and nutritional disease levels to assess their relative impact on the overall mortality of the assemblage.

5.8.3 Cox Proportional Hazards Regression for Mortality Analysis

The Cox proportional hazards model (also known as Cox regression) is a statistical technique commonly employed in clinical medicine and epidemiology, and tests the association between the survival time (*x* age in years) and one or more predictor variables (such as the presence of disease) (Lane et al. 1986). Much like the Kaplan-Meier survival analysis, the Cox regression model is now applied frequently in palaeoepidemiological studies (Godde et al. 2020; McFadden and Oxenham 2020; Walter and DeWitte 2017). Unlike the Kaplan-Meier test which determines a relationship of an event to the survival time, the Cox proportional hazard model is a regression model which estimates a *hazard rate* contingent on the independent variables (Liu 2018). Furthermore, the Cox regression model can be applied when the data is non-categorical (such as continuous variables), and can also be employed as a multivariate model (Wang et al. 2011). In this model the hazard function tests the probability of the event occurring at a particular interval given the individual survived to that interval (in this case *x* age in years; Liu 2018).

The Cox proportion hazards function is:

$$\log\ [\mathrm{h}\,(\mathrm{ti})\,/\mathrm{h}_0\,(\mathrm{ti})] = \beta_1 \mathrm{X}_1 + \beta_2 \mathrm{X}_2 + \beta_3 \mathrm{X}_3 + \cdots \beta_\mathrm{k} \mathrm{X}_\mathrm{k}$$

t= time

h(ti)= the hazard function (the risk of dying at time t)

h_0(ti)= the hazard of a particular individual when the independent variables are zero

X= covariates (treatment)

β= regression coefficients (slope of the regression)

The Cox proportional hazard regression model assumes that the survival curves for the variables must have hazard functions that are proportional over time (Liu 2018). That is the effect of the hazard remains the same over time, across age intervals (Hess 1995). As is

the case for the Kaplan-Meier Survival functions, point age estimates are required. For the same reasons given for the Kaplan-Meier survival functions, statistical significance was set at $P < 0.15$.

While Cox regressions can enable the inclusion of co-variates (such as the association to mortality of the presence or absence of nutritional disease as a co-variate to assessing the mortality of the presence or absence of infectious disease), this function is usually applied in a living sample. In a cemetery sample, the issue of differential mortality in relation to the skeletal expression of different diseases makes it difficult to identify a clear relationship to mortality when a multivariate model is used. That is, if a particular infectious disease (variable 1) has a low mortality rate and presents with a high level of skeletal expression, and a particular nutritional disease as a co-variate (variable 2) is associated with high mortality and few individuals who suffered the disease developed skeletal lesions, the final association of mortality as determined by the Cox regression may not necessarily reflect the true association of the living population. Univariate models that enable consideration of a direct relationship of a single disease to mortality were then applied in this thesis only.

5.8.4 Mortality Analysis at Site Level

At a site level, the mortality of diseases were assessed with relative risk ratios. *Disease presence* was treated as the *exposed* group, to test whether the presence of disease was significantly associated with increased risk of death before *x* age in years. Kaplan-Meier survival curves were produced to assess whether either the presence or the absence of a disease was associated with increased risk of death. Where Kaplan-Meier survival curves identified a clear relationship between mortality and lesion presence (there was a clear increased risk of death with the presence of disease, there was a clear increased probability of survivorship to older age with the presence of disease, or there was seemingly no differences in mortality between the presence or absence of disease), Cox regressions were also applied as a different function of survivorship to further investigate the validity of the relationship between disease and mortality.

5.8.5 Mortality Analysis at Region Level

Relative risk ratios, Kaplan-Meier survival curves and Cox regressions were also employed at region level in the same manner as that of site level. However, the post-interaction assemblage for each region was treated as the *exposed* group, to assess whether there were changes in the overall mortality between the pre- and post-interaction assemblages for each region. The mortality analysis at region level involves the assessment of diachronic changes to mortality overall. Differences in fertility rates are likely a considerable confounding factor in assessing overall mortality in nonadults as higher infant representation occurs in assemblages with high fertility ratios. Assemblages with higher fertility ratios will appear to have higher mortality rates with survival analyses. Therefore, only adults were assessed.

5.8.6 Summary of Morbidity and Mortality Analysis Employed in this Thesis

Morbidity and mortality analysis was assessed both within sites, and across sites within each region. These techniques were employed in accordance with the objectives of this thesis, which are 1) to assess the epidemiological trends in terms of mortality and morbidity within each site (objective 4), and 2) to assess changing trends in the mortality and morbidity of infectious and nutritional diseases across time, within the three regions (Vietnam, Japan and Mongolia) alongside increasing levels of human population interaction (objective 5). Fisher's exact and relative risk ratio analysis were applied to assess morbidity, and relative risk ratios, Kaplan- Meier survival functions, and Cox proportional hazard regression models were applied to assess mortality of the diseases diagnosed in this thesis. Additionally, the mortality and morbidity analyses were cross referenced in order to assess the relationship between morbidity and mortality of the diseases.

Table 5.19 *Summary of statistical analyses for site and regional level*

LEVEL OF ANALYSIS	COMPARISONS	MORBIDITY ANALYSIS	MORTALITY ANALYSIS
Site Level	Age, sex, cultural group (Mongolia only)	Relative risk ratios, Fisher's exact	Relative risk ratios, Kaplan-Meier Survival analysis, Cox regression
Region Level	Across time periods	Relative risk ratios	

5.9 Chapter Summary

This chapter outlined the methodology for the entire process of disease diagnosis through to statistical analyses of disease prevalences employed in this thesis. Methodologies for macroscopic and radiographic lesion recording, the standards for differential diagnosis of disease, and finally statistical analysis of the morbidity and mortality of disease are defined. This chapter then contributes to the third objective of this thesis, to create standards for differential diagnosis for diseases where they do not yet exist in the literature. The methodology presented for statistical analysis of morbidity and mortality provides a basis for the fourth objective of this thesis, to conduct a three stage analysis of disease patterns and their relationship with human population interaction levels at a site and region level. The results of the methodologies outlined in this chapter are presented in Chapters 6, 7 and 8.

CHAPTER 6:
CLIMATE CHANGE AND REFUGE: DISEASE AND ENVIRONMENT TRANSFORMATIONS OF THE WESTERN JAPANESE JOMON

6.1 Introduction

The first out of three cases studies in this thesis is presented in this chapter: disease and population movement from the Middle to Late and Final Jomon Periods in Western Japan. This case study explores the potential impacts of intrapopulation interaction in a population isolated from mainland inhabitants. First, a broad background of the Jomon is presented to provide context to the results presented in this chapter. Then, the archaeological context and previous palaeopathological research of the Middle Period Jomon site of Ota is presented. Following on, differential diagnosis, and analysis of morbidity and mortality of disease at Ota is given, succeeded by discussion of disease context at the site. A similar format is then followed for disease outcomes at the Late to Final Period Jomon site of Tsukumo. Lastly, diachronic changes to the morbidity and mortality of disease are explored in light of the role played by increasing population interaction from the Middle to the Final Jomon Periods. This chapter meets objectives 3 to 5 of this thesis, which includes differential diagnosis of disease, and site and regional analysis of disease (stages 1 and 2 of statistical analysis).

6.2 The Emergence and Decline of the Jomon Hunter-Gatherers of Japan

The Jomon were prehistoric hunter-gatherer-fisher-foragers from Japan (Koyama 1979). These foragers arose in Japan as early as approximately 15,000 years ago (Matsui and Kanehara 2006). Six distinct periods of the Jomon have been recognised dating from approximately 16,500-1700BP (Table 6.1). The Jomon are named after their unique cordmarked pottery styles (Nakashima et al. 2010). The Jomon pottery, particularly of the Middle Jomon Period, are characteristic for their elaborate forms commonly termed as *flame pottery* due to their stylistic flame like design (Pearson 2007). Jomon archaeological sites vary from shell mounds filled with fishing tools such as harpoons, hooks, net weights and

burials to large sedentary villages with extensive evidence for food storage in pits (Koyama 1979). The Jomon exploited a considerable amount of marine and terrestrial resources with at least 354 species of shellfish, 71 fishes, 35 birds, 70 mammals and 39 plants excavated from archaeological sites (Koyama 1979: 24; Kusaka et al. 2015). Macro evidence from flotation of rice and millet have been found in North-eastern Honshu (central main island of Japan) and in Kyushu (southern main island of Japan), from the Middle Jomon onwards (D'Andrea 1995; Matsui and Kanehara 2006). However, no evidence of domestication (agriculture) has been documented at Jomon sites, and these crops were probably the result of cultivation (D'Andrea 1995). Considerable evidence of cultivation of chestnuts and herbaceous plants have also been identified in wetland sites where botanical remains have been well preserved (Matsui and Kanehara 2006). However, it is likely cultivation provided a smaller portion of the overall Jomon diet compared to hunting, foraging and fishing exploits (Matsui and Kanehara 2006).

Table 6.1: *Chronological Time Periods of the Jomon Pottery (after Habu 2004: 39). Most dates for Jomon sites remain uncalibrated and are therefore approximate dates. Regional variation also occurs in regards to these dates. Calibrated dates indicate the start of the Incipient Jomon as early as 16,500 years ago (Nakamura et al. 2001).*

TIME PERIODS	YEARS BP (uncalibrated)
Incipient	16,500- 9500
Initial	9500- 6000
Early	6000- 5000
Middle	5000- 4000
Late	4000-3000
Final	3000-2300
Epi	2300-1700

Habitation sites of the Jomon from the Initial Jomon Period mark an increase in sedentism (Pearson 2006; Watanabe 1966; Watanabe 1986). These sites comprised of permanent houses, large pottery vessels, stone tools, ritual objects and ornaments (Pearson 2006). Large polished adzes were probably used for building houses and dugout canoes, while ventilated hearths were possibly used for smoking food. Storage pits permitted the long term storage of food, such as nuts, that enabled sedentary habitation without agriculture (Pearson 2006). The Jomon also appear to have been predominantly egalitarian, with possible age based or kinship affiliated identity playing a role in social organisation (Temple et al. 2011). Some stratification has been proposed in both the East and the West of Japan (Pearson 2007; Takahashi 2001). Overall, high cultural and social diversity across

geographic and temporal borders indicates considerable complexity in the social structure of the Jomon (Pearson 2006).

There remain competing theories in regards to the origins of the Jomon population in Japan. The Jomon are not the first inhabitants of the Japanese islands with evidence from human occupation as early as 23,000 years ago (Bronk Ramsey, 2009). Kaifu et al (2011) do not see continuation between these populations and Jomon, arguing that the first settlers of Japan are the direct descendants of the first modern humans to arrive in Asia approximately 60,000 years ago (Oxenham and Buckley 2016). Ancient DNA of the Hokkaido (northern main island of Japan) Jomon and Epi-Jomon suggest links to Siberian populations in the lower Amur region in the Russian Far East (Adachi et al, 2011). Palaeolithic stone implement types of this period are also similar between Japan and Siberia (Adachi et al. 2011; Inada 2001). It is possible that the Siberian migration was associated with climatic factors during the Last Glacial Maximum (LGM). Hokkaido may have been a refuge from inhabitable regions further north during the LGM (Izuho et al. 2014). The Siberian migration probably occurred through the Levant with population movement into eastern Eurasia by 45,000 years ago. This migration was separate from the first migration of anatomically modern humans 60,000 years ago which occurred along a southern route in Asia (Oxenham and Buckley 2016).

Y chromosome DNA analysis suggests the Jomon were at least partially descended from Central Asian populations (Hammer et al. 2006; Seguchi et al. 2017). Morphometric evidence appears to support a relationship between Northeast Asian populations and the Jomon (Dashtseveg 2013; Temple and Matsumura 2011). Clinal variation in cranial morphometrics supports the idea of a northern entry into Japan through Hokkaido (Hanihara and Ishida 2009). However, the Jomon also appear to share affinities with early Southeast Asians related to the first migration into Asia (Oxenham and Matsumura 2008). Furthermore, increased body mass in the Hokkaido Jomon are consistent with adaptation to colder climate, but the Jomon also appear to have elongated limbs such as reported in the body proportions of assemblages from tropical areas (Temple and Matsumura 2011). The Jomon may then genetically represent a meeting of the first anatomical modern humans in Asia with later descendants of the northern route people post-LGM (Oxenham and Buckley 2016).

6.2.1 The Incipient, Initial and Early Jomon (16,500-5000BP)

The earliest radiocarbon dates for the Jomon date to 16,500-15,170 cal BP (Nakamura et al. 2001). This stage termed the Incipient Jomon was marked by a slow trend toward sedentism. Non-seasonal sedentary villages are apparent by 12,000 cal. BP in Kyushu (Pearson 2006). The vast amounts of pottery excavated during the subsequent Initial and Early Jomon may suggest not just the storing but the sharing of food amongst the community (Pearson 2006). A trend to sedentary habitation continued during these periods, with the expansion of more complex craft production and ritual (Pearson 2006). A relatively rapid population increase from the Initial to Middle Jomon Period marked this time frame (Habu 2008; Koyama 1979).

6.2.2 Middle Period Jomon (5000-4000BP)

The Middle Jomon Period (5000-4000BP) was marked by the peak of population density and cultural complexity of the Jomon (Pechenkina and Oxenham 2013). Large scale Middle Jomon settlements in Japan indicate considerable settlement planning and are discovered in high densities from this period (Koyama 1979). The population expansion, social stability, cultural continuity and sustained sedentism was further encouraged by climate stability during and following the Holocene Thermal Maximum, a period of global warming associated with sea level rise, with a peak at between 8-6000 years ago in Asia (Hoover and Matsumura 2008; Schmidt et al. 2019). The annual mean temperature during the Middle Jomon Period was approximately 2 degrees higher, and vegetation zones included a dominance of evergreen oaks, and an abundance of terrestrial resource returns such as woodland flora and fauna (Hoover and Matsumura 2008; Koyama 1979).

Estimates of population size indicate an increase from 150,000 to 260,000 people from the Early to Middle Jomon Periods (Hoover and Matsumura 2008; Koyama 1979). The Middle Jomon Period also saw a diversification of ceramic styles, with variation occurring along a North to South cline (Hoover and Matsumura 2008).

6.2.3 Late and Final Jomon (4000-2300BP)

Following the end of the Holocene Thermal Maximum, about 5000 years ago (Schmidt et al. 2019), climatic cooling and increase in precipitation initiated significant ecological change in Japan, which appears to be associated with significant population

decline after the Middle Jomon Period (Koyama 1979; Temple 2007a). A shift from evergreen oaks to coniferous forests occurred in Western and Central Japan alongside the climate cooling (Koyama 1979). A population decline of approximately 100,000 individuals, considerable loss of cultural diversity, site density and increased regional heterogeneity of subsistence base marked the Late and Final Jomon Periods (Hoover and Matsumura 2008; Pechenkina and Oxenham 2013; Temple 2007a). While considerable subsistence variation between Eastern, Western and Northern Jomon already existed prior to the Late Jomon Period (Kusaka et al. 2015), the Jomon of Western Japan increasingly exploited forest and freshwater sources with seasonal marine input in the diet. In contrast, Eastern and Northern diets saw a higher intake of marine resources (Kusaka et al. 2015). It is likely this period marked an increase in the use of terrestrial resources particularly in the Western Honshu Jomon (Kusaka et al. 2015; Temple 2007a). During this time, populations were displaced from inland and Eastern areas (Kusaka et al. 2015; Temple 2007b), with a continued gradual increase in population density in warmer areas to the West (Habu 2004).

A connection between climate cooling and population decrease has been suggested, but questions still remain as to how the climate cooling resulted in population decline (Habu 2008). Habu (2008) proposed this decline was a result of overspecialisation of resource reliance during the Middle Jomon Period, which were no longer available during climate change. However, when considered from a perspective of resilience it is possible social change occurred instead as an adaptive response to climate cooling given the variable methods of resource exploitation performed by Jomon communities (Kawashima 2013; Temple 2018). An increase in plant processing artefacts found in Late to Final Jomon in Western Japan supports an argument for adaptation to a changing environment (Temple 2008). Further still, the potential reduction in resource returns, driving nutritional stress, and subsequent population displacement and decline has been proposed, but to date no direct evidence of diminished food returns exists. However, the climatic shift probably disrupted the cultivation efforts of chestnuts in North-eastern Japan (Kawahata 2019; Kawahata et al. 2009; Temple 2018). If reduced food returns played a role in population decline, displacement to *refuge zones* such as Central and Western Japan may have increased already underlying nutritional stress (Hoover and Matsumura 2008; Temple 2007a).

6.2.4 The Yayoi Expansion and Epi-Jomon Period (from 2300BP)

As early as 2800BP, farmers from the Korean Peninsula migrated to Japan initiating the agricultural transition (Pearson 2007). The Yayoi were a population of wet rice farmers of Southeast Asian descent (Hoover and Matsumura 2008). Rapid adoption of agriculture occurred in Western Honshu (by 2300BP) following this expansion, with slower spread of agriculture occurring in the East possibly related to the marine reliance in Eastern Japan (Temple 2007a). In contrast, the Jomon of Northern Japan (Hokkaido) persisted until 1700BP (Oxenham and Matsumura 2008), with a short period of persistence of Jomon in Kyushu during the Yayoi Period as well (Hoover and Hudson 2016; Temple 2018). Termed the Epi Jomon Period, these populations lived contemporaneously with the Yayoi who occupied Honshu (Oxenham and Matsumura 2008). Specialisation in fish subsistence and reduction in social complexity marked the Epi Jomon Period (Hoover and Matsumura 2008).

6.2.5 Spatial and Temporal Differences in the Health of the Jomon

Linear enamel hypoplasia (LEH), non-specific indicators of stress in teeth, and cribra orbitalia prevalences are high across sites in the Jomon (Hoover and Matsumura 2008; Temple 2007a; Temple 2007b). However, the Western Jomon had higher prevalences of LEH than the Eastern Jomon, supporting regional variation in society and subsistence (Temple 2007b). It is possible that an increased reliance on terrestrial resources in Western Honshu contributed to increased nutritional stress (Temple 2007b). Higher rates of caries in Honshu compared to Hokkaido were also observed which may be related to a greater carbohydrate content in Honshu Jomon diets (Oxenham and Matsumura 2008).

Temple (2007a) found little difference in overall non-specific stress markers such as LEH and cribra orbitalia between Middle to Late and Late to Final Jomon sites, and therefore did not find evidence to support an increase in dietary stress with climatic cooling. However, Temple (2007b) recorded higher levels of bilateral tibial subperiosteal new bone deposits (SPNB) in the Late to Final Jomon compared to Middle to Late Jomon sites, which were attributed to infection. Similarly the author found a decrease in stature in Late to Final Jomon sites in Japan which may reflect exposure to chronic infection (Temple 2008; Temple et al. 2012). Temple (2008) argues that increased contact with infectious pathogens during this period may have been related to population aggregation. Suzuki (1998) also found a high prevalence of SPNB deposits across Jomon sites, which the author attributed to infection,

without any evidence of pyogenic osteomyelitis. Suzuki (1998) concluded that nutritional instability in the Jomon may have prevented progression to advanced bone infection, suggesting a high mortality rate from infection in the Jomon. To date there remains no research on specific nutritional and infectious diseases in the Jomon, which may further enable investigation into the impacts of climate cooling and population displacement on health. This chapter addresses this gap in the literature.

6.2.6 Climatic Cooling, Population Dispersal and Disease

The Jomon are thought to have been in isolation for 10,000 years due to post-LGM sea level rise (Nakashima et al. 2010). However, by the Late Jomon some evidence of artefact exchange is evident with the Korean Peninsula (Hoover and Matsumura 2008). Therefore, the Jomon are likely to have had some but limited interpopulation interaction with the mainland. However, population displacement and movement to *refuge zones* with climate cooling may have increased the intrapopulation interaction following the Middle Jomon Period. Alongside gradual increase in population density, similar artefacts as those previously found in Eastern Japan emerge at Western Japanese Jomon sites, suggesting migration from the East to the West (Matsumoto et al. 2017). The case study presented in this chapter then aims to assess if there was an increase in infectious diseases with movement of populations to refuge zones in Western Honshu following climate cooling in Japan. Additionally, the chapter aims to assess whether an increase in nutritional stress may have accompanied infectious disease increase and contributed to population decline. The aim of this case study fits within the broader research questions of this thesis which is to assess how infectious and nutritional disease levels were influenced by increase in human population interaction.

6.3 Ota

The Ota site, relatively dated by pottery chronologies to 5000-4000BP, is a Jomon shell midden site in Southwestern Honshu bordering the Inland Sea (Kiyono 1969; Shiomi et al. 1971). As a Middle Jomon site, the site dates to a time period of climatic stability. The shell midden site was classified as similar to sites where pit dwellings are found, and exhibited tools for both foraging and ritual purposes (Kiyono 1969; Temple 2018). As was the case with other Middle Jomon sites, Ota was likely a place of longstanding occupation, and a sedentary settlement (Kiyono 1969).

The Ota assemblage consists of mostly adults, with three individuals under the age of 20 identified. It is possible given that excavation occurred in the 1920s, that some sample bias (including a possible predilection for excavating adults) is present. For this reason, estimations of the fertility rate and therefore rate of natural population increase was not possible (further assessed in Chapter 9). There were no differences in ornamentation of burials at Ota which suggests no differentiation in the identity of Ota individuals in death (Temple 2018). However, some ritual tooth ablation was present at Ota which indicates a level of social complexity and group or kin identity that remains poorly understood (Temple 2018). There appears to be no association of tooth ablation to migration at Ota, and it is possible tooth ablation was related to age achieved kin related identity (Fujita 1997; Kusaka et al. 2012; Temple et al. 2011).

Palaeodietary reconstruction of the Ota diet using stable carbon and nitrogen isotopes indicates that food resources were predominantly terrestrial with between 6-13% reliance on marine resources (Kusaka et al. 2010; Kusaka et al. 2015). Marine resources were then likely an important protein source (Kusaka et al. 2010; Kusaka et al. 2015). Carbon and nitrogen isotopes also suggest possible sex-based differences in the diet (Kusaka et al. 2010; Kusaka et al. 2015). Males had significantly higher carbon and nitrogen values indicating males consumed greater proportions of marine foods than females highlighting possible differential access to food. The authors attributed this difference to gender related food procurement roles. A high prevalence of auditory exostoses in Ota males and none in females supports frequent cold water fishing and diving of males (Miyake and Imamichi (1931) in Kusaka et al. 2015).

Temple (2007b) reported a linear enamel hyperplasia prevalence per individual of 63.2% and carious lesion rate of 3.8% at Ota. This outcome suggests high levels of systemic stress in Ota individuals. However, their diet does not appear to consist of highly cariogenic foods such as roots, tubers and processed nuts (Temple 2018). Temple (2007b) also reported a low prevalence of cribra orbitalia (15.7%) for Ota and no evidence of bilateral tibial SPNB deposits. Dietary differences between males and females appears to also be supported by sex-based differences in dental caries prevalence. Females exhibited higher caries prevalences than males, argued by Temple (2007b) to indicate an increase in carbohydrates in female diets. However, higher levels of caries are often prevalent in females due to the

relationship between immunosuppression in pregnancy and decreased oral health (Willis and Oxenham 2013).

Strontium isotopes indicate minimal migration to Ota during the Middle Jomon Period. Kusaka et al. (2012) identified one non-local in the Ota assemblage through strontium signatures from tooth enamel and ribs which differed to others at the site and the surrounding bedrock (Kusaka et al. 2012). The presence of a single non-local indicates some regional interaction with other Middle Period Jomon sites. The following section presents the differential diagnosis for infectious and nutritional disease at Ota, followed by statistical analysis of morbidity and mortality of these diseases.

6.4 Results: Ota Skeletal Pathology

6.4.1 Summary of Pathological Lesions at Ota

Of the 34 individuals assessed for pathology, 50% (17/34) of the Ota assemblage exhibited osteoblastic lesions (Table 6.2). Osteoblastic lesions were present on both crania and postcrania (Figure 6.1- 6.2). However, these lesions were predominantly unilateral and present on long bones particularly the tibiae. Most lesions both cranial and postcranial were discrete and remodelled with 8.8% (3/34) of individuals exhibiting diffuse lesions across more than two skeletal elements. These individuals also exhibited diffuse SPNB deposits across multiple internal and external ribs. Cranial lesions were also commonly symmetrical and accompanied with abnormal cortical porosity. Additionally abnormal cortical porosity was also observed in absence of SPNB on the crania. Of the three preserved nonadults in the Ota assemblage, one neonate presented with diffuse active SPNB on the preserved left femur, and discrete deposits of SPNB were presented on the preserved crania of an adolescent.

Osteolytic lesions were present in 20.6% (7/34) of Ota individuals. Only adults were affected by osteolytic lesions (22.6%, 7/31). However, nonadults in the Ota assemblage were poorly preserved, therefore it is not possible to infer whether or not nonadults were similarly affected as adults. The osteolytic lesions in adults were predominantly restricted to the mastoid region (38.9%, 3/7), with the remainder of the lesions present on other parts of the crania, long bones, sternum, and ilia (Figure 6.3). The osteolytic lesions outside of the mastoid were predominantly OL1 focal lesions with or without sclerotic response. Finally,

only one individual (Ota 697, a young adult female) presented with skeletal deformity exhibiting moderate lateral bending deformities of the ulnae.

Table 6.2: *Summary of OB and OL lesion prevalences at Ota*

	NONADULT (aff/obs)	**NONADULT (%)**	**ADULT (aff/obs)**	**ADULT (%)**	**TOTAL (aff/obs)**	**TOTAL (%)**
OB Lesion	2/3	66.7	16/31	51.6	16/34	50
OL Lesion	0/3	0	7/31	22.6	7/34	20.6

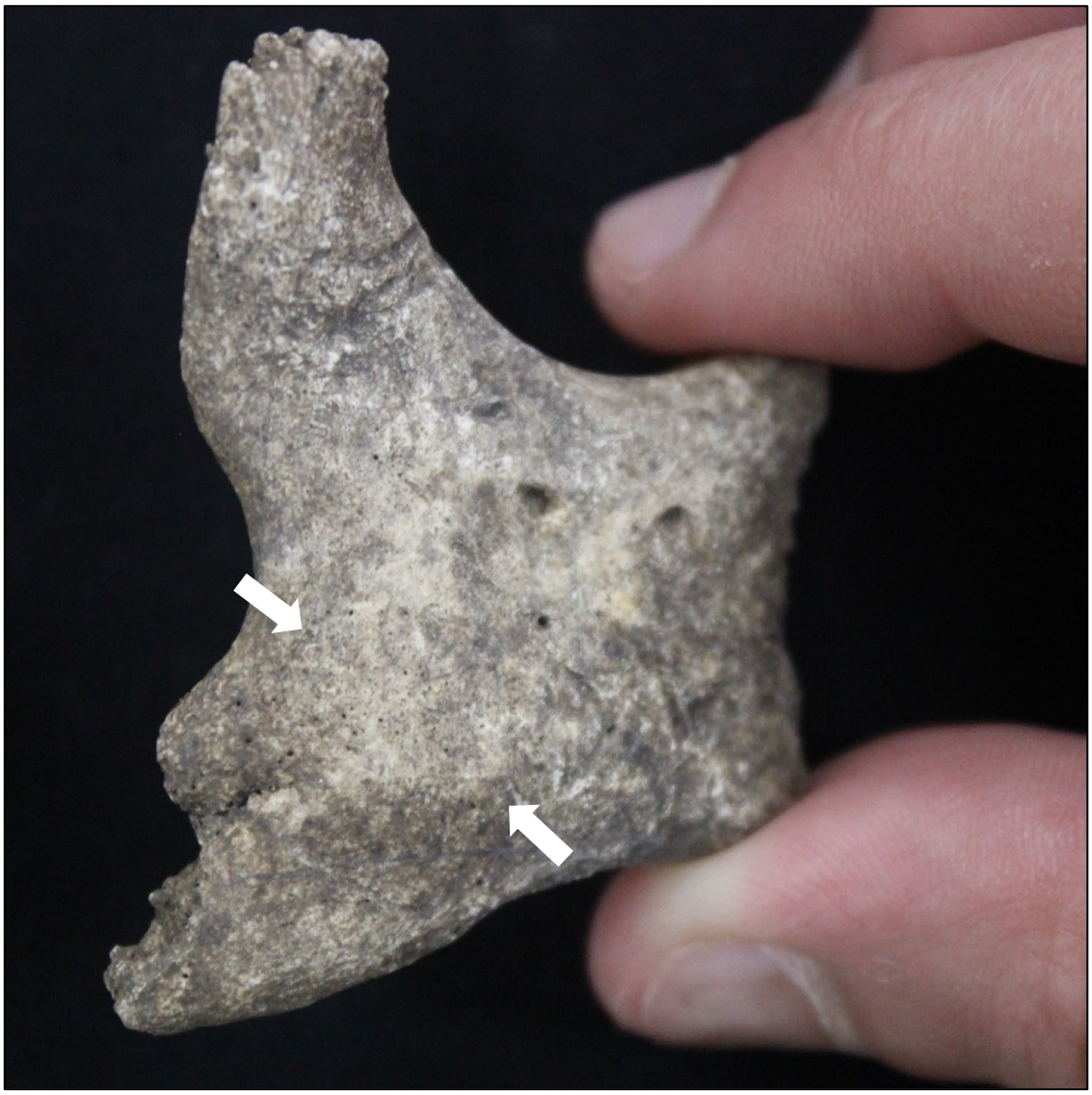

Figure 6.1: *Remodelled discrete deposit of SPNB with abnormal cortical porosity on the anterior right zygoma (white arrow, Ota 666a, middle aged adult male). Image: author's own*

Figure 6.2: *Mixed active and remodelled diffuse deposit of SPNB with abnormal cortical porosity on the middle shaft of the left femur (white arrow, Ota 666a, middle aged adult male). Image: author's own*

Figure 6.3: *Postcranial osteolytic lesions at Ota. a-c) Focal oval lesion of the distal posterior right radius. Note the lesion has a margin which projects from the underlying surface of the bone. Sclerosis of the margin is evident on the radiograph (Ota 666a, a middle aged adult male). d) Focal lesion with sclerotic response on the posterior sternum. The lesion is not consistent with a sternal foramen (Ota 674, a young aged adult male). e) Focal circular osteolytic lesion with minimal sclerotic response on the right lateral iliac body (Ota 710, young aged adult female). Image: author's own.*

6.4.2 Diagnosis of Infectious Disease at Ota

Overall, 20.6% (7/34) of Ota individuals exhibited lesions consistent with an infectious origin. Three individuals (8.8%, 3/34) had diffuse SPNB (more than ¼ of the bone surface) across two skeletal elements. However, one individual exhibited sunburst SPNB across the thoracic and lumbar spine consistent with possible neoplastic origin (Jaffe 1972; Resnick 1995). The diagnosis of neoplasms is beyond the scope of this thesis, and the individual was not included in the overall infectious disease prevalence (Figure 6.4). The other two individuals met the criteria for inclusion in the overall infectious disease prevalence (Table 6.3). These two individuals exhibited SPNB of multiple ribs on the pleural aspect, which may indicate respiratory disease.

Figure 6.4: *Active sunburst SPNB of an upper lumbar vertebral arch. While this individual has widespread SPNB throughout the postcranium involving the ribs, vertebrae, scapulae, ilia, and limb bones consistent with infectious disease, the sunburst pattern is more reminiscent of neoplastic osteoblastic response as seen in bone cancers such as osteosarcomas (Jaffe 1972; Resnick 1995). Given the uncertainty of the lesion aetiology, the individual was excluded from the infectious disease criteria (719, middle aged adult male). Image: author's own.*

Of the seven individuals with osteolytic lesions, three individuals met the criteria for probable, and one individual met the criteria for possible otitis media or mastoiditis (11.7%, 4/18). Mastoiditis presented in the form of destruction of internal air cells, internally draining fistulas from the mastoid foramen and focal lesions around the external auditory

canal (Figure 6.5). Individuals with osteolytic lesions around the mastoid also exhibited SPNB and cortical porosity around the external auditory canal. Of the osteolytic lesions not pertaining to otitis media and mastoiditis, only one individual presented with lesions consistent for diagnosis with specific infectious disease. Ota 670A, a middle aged adult of indeterminate sex, exhibited three focal oval shaped OL1 lesions of the cranium (Figure 6.6). Lesions were present on the medial frontal process and lateral to the anterior nasal spine of the left maxilla, as well as on the inferior aspect of the pars basilaris. Furthermore, osteolysis with sclerotic response within the left hypoglossal canal, was also present (Figure 6.6). With exception of the lesion in the right hypoglossal canal, the focal lesions appear to have penetrated beyond the original cortex margin into the trabeculae underneath. There was sclerotic response on the margins and the base of the maxillary lesions, with minimal sclerosis of the pars basilaris lesion. The random distribution of the focal lesions in the cranium is diagnostic for mycotic infection. Therefore, the pathology of Ota 670A is consistent with possible mycosis. These lesions are not consistent with tuberculosis, which can affect the cranium, but most often extend endocranially from the diploe (Ortner 2003). Similarly, the lesions are not consistent with leprosy. While osteolytic destruction is present near the anterior nasal spine of Ota 670A, in leprosy destruction appears as marginal erosion of the anterior nasal spine with associated inflammatory pitting (Møller-Christensen 1961). It is possible that the osteolytic lesions from other individuals are also of mycotic aetiology (Figure 6.3). All lesions were found around nasal and respiratory regions, other axial regions or metaphyses of long bones and appear similar to the lesions exhibited in Ota 670A. Furthermore, all lesions were unilateral. This trend is consistent with mycotic infection. However, these lesions can also form from non-infectious pathologies such as benign cysts (Hakim et al. 2015), therefore they did not meet the criteria for infectious disease in this thesis. Furthermore, skeletal mycosis is exceptionally rare (Behrman et al. 1990), therefore mycotic infection in 11.7% (4/34) of individuals in an assemblage would be unusual.

Table 6.3: *Summary of infectious disease at Ota*

	POSSIBLE			**PROBABLE**			**POSSIBLE AND PROBABLE**		
	Affected	*Observed*	*(%)*	*Affected*	*Observed*	*(%)*	*Affected*	*Observed*	*(%)*
Mycosis									
15 to 19 years	0	1	0	0	1	0	0	1	0
20 to 29 years	0	5	0	0	5	0	0	5	0
30 to 39 years	1	10	10	0	10	0	1	10	10
40 to 49 years	0	7	0	0	7	0	0	7	0
50+ years	0	2	0	0	2	0	0	2	0
Male	0	18	0	0	18	0	0	18	0
Female	0	6	0	0	6	0	0	6	0
Total adults	1	31	3.2	0	31	0	1	31	3.2
Total	1	34	2.9	0	34	0	1	34	2.9
Otitis Media									
15 to 19 years	0	0	0	0	0	0	0	0	0
20 to 29 years	0	1	0	0	1	0	0	1	0
30 to 39 years	0	8	0	1	8	12.5	1	8	12.5
40 to 49 years	0	6	0	2	6	33.3	2	6	33.3
50+ years	1	1	100	0	1	0	1	1	100
Male	1	12	8.3	2	12	16.7	3	12	25
Female	0	4	0	1	4	25	1	4	25
Total adults	1	18	5.6	3	18	16.7	4	18	22.2
Total	1	18	5.6	3	18	16.7	4	18	22.2
							CRITERIA PREVALENCE		
							Affected	*Observed*	*(%)*
Overall infectious disease criteria									
0 to 5 months							0	2	0
15 to 19 years							0	1	0
20 to 29 years							2	5	40
30 to 39 years							1	10	10
40 to 49 years							3	7	42.9
50+ years							1	2	50
Male							5	18	27.8
Female							1	6	16.7
Total adults							7	31	22.6
Total							7	34	20.6

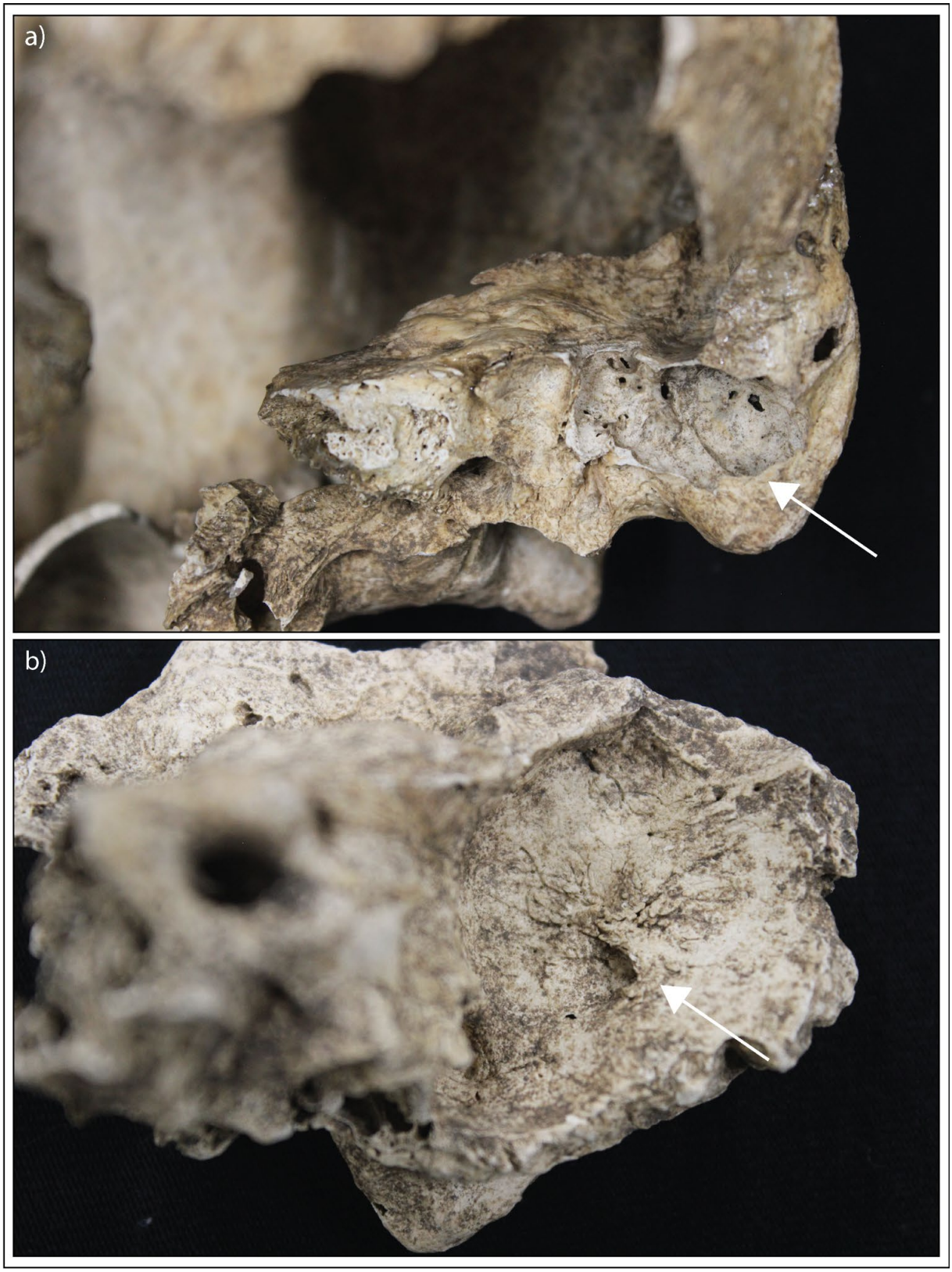

Figure 6.5: *Lesions consistent with otitis media. a) Destruction of mastoid air cells (Ota 670A, middle aged adult). b) Internally draining fistula (Ota 703, old adult male). Image: author's own.*

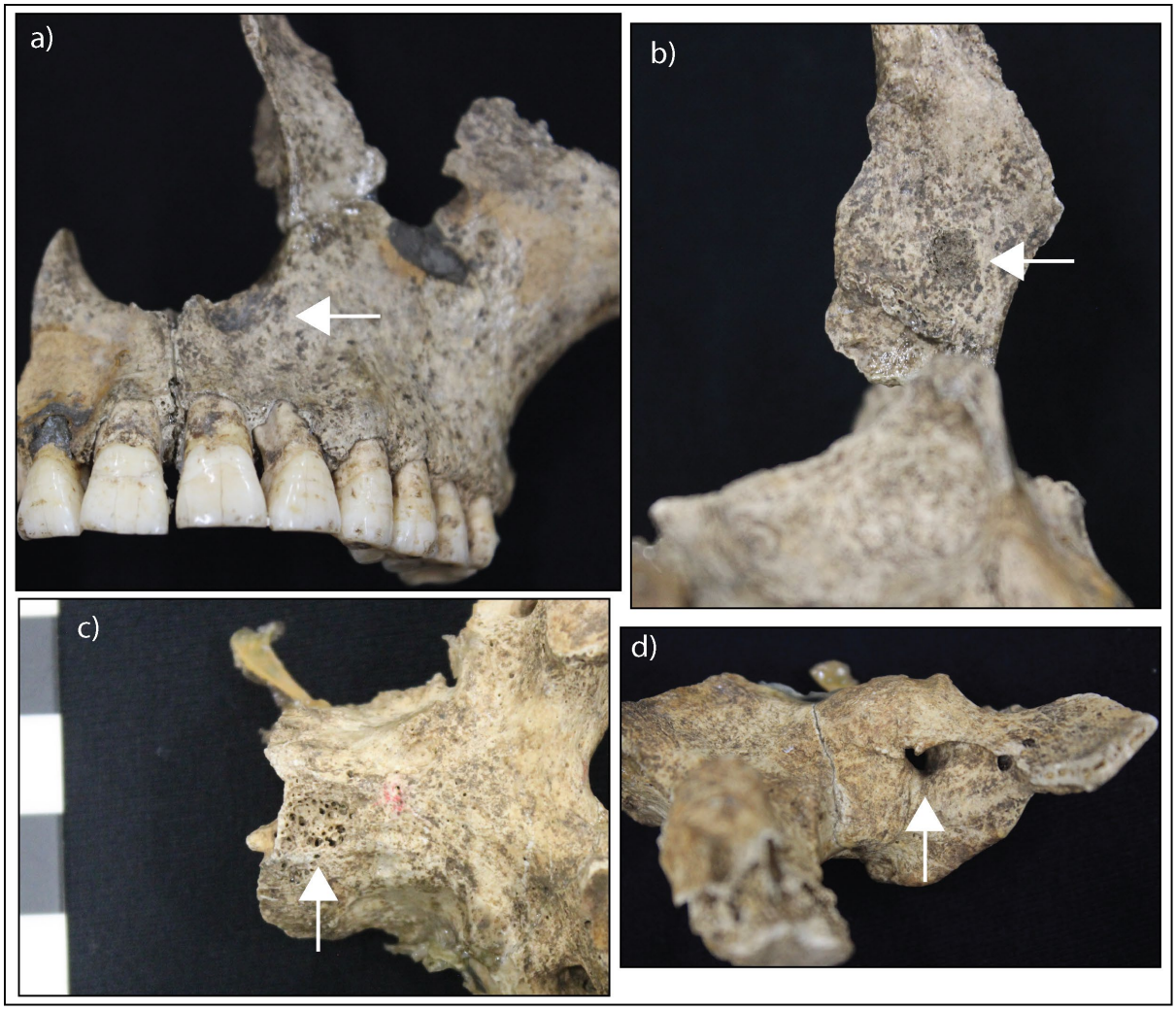

Figure 6.6: *Lesions consistent with possible mycosis in Ota 670A, a middle aged adult of indeterminate sex. a) Focal lesion with sclerosis lateral to the anterior nasal spine. b) Focal lesion with sclerosis on the interior nasal region (medial aspect of the frontal process) of the left maxilla. c) Possible focal lesion with minimal sclerosis on the inferior pars basilaris of the occipital. d) Fistula like lesion extending from the right hypoglossal canal. Image: author's own.*

6.4.3 Morbidity of Infectious Disease at Ota

While males (27.8%, 5/18) presented with a higher prevalence of infectious diseases than females (16.7%, 1/6), this was not statistically significant (n=24, RR=0.6000, p=0.6054; Table 6.4). Similarly, no statistically significant differences were apparent in adult age related morbidity. This outcome indicates morbidity of infectious disease was shared across sex and adult age groups.

Table 6.4: *Relative risk of infectious disease morbidity at Ota across sex and age cohorts.*

EXPOSED GROUP/ CONTROL GROUP	**OUTCOME**		**RR**	**P-VALUE**	**95%CI**
	Positive: *Infection Present*	***Negative:*** *Infection Absent*			
Sex					
Female/ Male	1/5	5/13	0.6000	0.6054	0.0864- 4.1673
Adults					
<20 yrs/ >20 yrs	0/7	1/17	0.8333	0.8852	0.0702- 9.8921
<30 yrs/ >30 yrs	2/5	4/14	1.2667	0.7331	0.3255- 4.9299
<40 yrs/>40 yrs	3/4	13/5	0.4219	0.1776	0.1203- 1.4793

A relative risk (RR) >1 denotes a relationship of the exposed group with an increase in disease prevalence, whereas RR <1 denotes a relationship of the control group with an increase in disease prevalence.
*= statistically significant (p<0.10). **= statistically significant when considering size of the effect of RR.

6.4.4 Mortality of Infectious Disease at Ota

Relative risk ratio analysis indicates no significant relationship of skeletal evidence of infectious disease with increased mortality (Table 6.5). Similarly Kaplan-Meier analysis indicates no significant relationship to mortality (n=25, X^2=0.692, df=1, p=0.406). The Kaplan-Meier cumulative survivorship function indicates similar survivorship trends between Ota individuals with evidence of infectious disease and individuals without (Table 6.6; Figure 6.7). Overall, survivorship analysis indicates no relationship of infectious disease with increased mortality.

Table 6.5: *Relative risk of infectious disease mortality at Ota across age cohorts.*

POSITIVE OUTCOME/ NEGATIVE OUTCOME	**TREATMENT**		**RR**	**P-VALUE**	**95%CI**
	Exposed Group: *Infection Present*	***Control Group:*** *Infection Absent*			
Adults					
<20 yrs/ >20 yrs	0/7	1/17	0.7917	0.8823	0.0359- 17.4373
<30 yrs/ >30 yrs	2/5	4/14	1.2857	0.7351	0.2999- 5.5123
<40 yrs/>40 yrs	3/4	13/5	0.5934	0.2569	0.2408- 1.4626

A relative risk (RR) >1 denotes a relationship of the disease presence with the positive outcome (susceptibility to mortality), whereas RR <1 denotes a relationship of the disease absence with a negative outcome (survivorship).
*= statistically significant (p<0.10). **= statistically significant when considering size of the effect of RR.

Table 6.6: *Statistical summary for Kaplan-Meier function of infectious disease mortality of adults at Ota.*

INFECTIOUS DISEASE	ESTIMATE	STD. ERROR	95% CI	LOG RANK (MANTEL-COX)		
				CHI SQUARE	DF	P-VALUE
Mean				0.692	1	0.406
Absent	35.556	2.168	31.306- 39.805			
Present	38.857	4.533	29.973- 47.741			
Overall	36.480	1.982	32.596- 40.364			
Median						
Absent	35.000	3.162	28.802- 41.198			
Present	42.000	9.165	24.036- 59.964			
Overall	35.000	2.082	30.920- 39.080			

*= statistical significance (p<0.15).

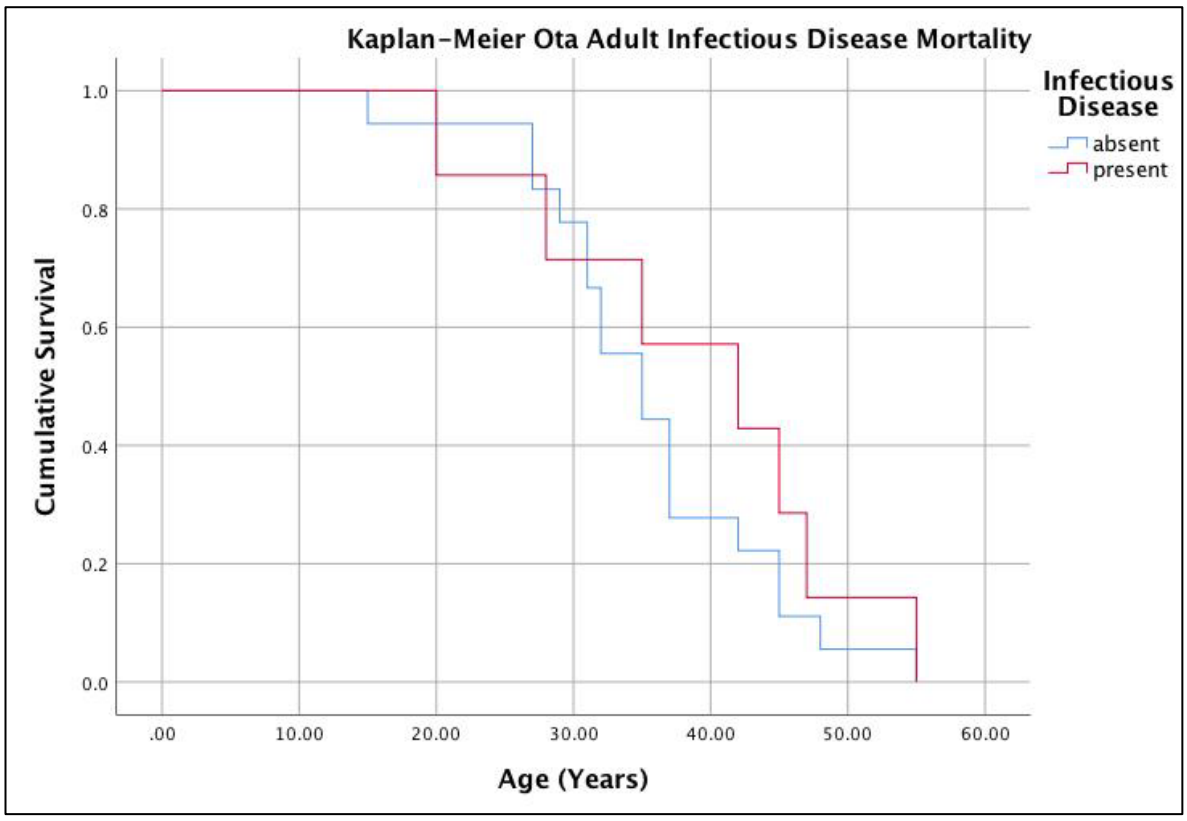

Figure 6.7: *Kaplan-Meier cumulative survival function of adult infectious disease mortality at Ota. Image: author's own*

6.4.5 Diagnosis of Nutritional Disease at Ota

Over thirty-four percent (34.4%, 11/32) of the Ota assemblage had lesions consistent with a diagnosis of a possible or probable case of scurvy (Table 6.7). As the Ota assemblage is comprised of predominantly adults, discrete symmetrical SPNB and abnormal porosity on the cranium were the most diagnostic lesions exhibited. These lesions presented symmetrically on the orbital roofs, anterior and posterior zygomatic bones, anterior and

posterior maxillae, lateral greater wings and pterygoid processes of the sphenoid bones, and the medial coronoid processes and mylohyoid lines of the mandibles (Figure 6.8). The two neonates were only represented by long bone shafts and therefore diagnostic lesions for scurvy could not be observed. Therefore, the neonates were excluded from analysis of scurvy. The adolescent (Ota 715B, 15-19 years of age) exhibited discrete SPNB deposits with abnormal cortical porosity on the mylohyoid line, right coronoid process of the preserved right hemimandible and anterior right zygoma consistent with possible scurvy (Figure 6.8c). Possible and probable cases of scurvy was identified predominantly in adults between 30 and 50 years of age (Table 6.7; Figure 6.9). However, no adult over the age of 40 exhibited lesions consistent with a probable case.

The bilateral bending deformities of the ulnae of Ota 697, a young adult female, are not characteristic of residual rickets which tends to affect the lower limb bones of adults more often than upper limbs (Brickley and Ives 2010). It is possible these deformities were associated with congenital deformity or were activity related. Consideration of the non-nutritional aetiology of these deformities is beyond the scope of this thesis. As such there remains no evidence of mineralisation disorders in the Ota assemblage.

Table 6.7: *Summary of nutritional disease at Ota*

SCURVY	**POSSIBLE**			**PROBABLE**			**POSSIBLE AND PROBABLE**		
	Affected	*Observed*	*(%)*	*Affected*	*Observed*	*(%)*	*Affected*	*Observed*	*(%)*
15 to 19 years	1	1	100	0	1	0	1	1	100
20 to 29 years	0	5	0	1	5	20	1	5	20
30 to 39 years	2	10	20	4	10	40	6	10	60
40 to 49 years	3	7	42.9	0	7	0	3	7	42.9
50+ years	0	2	0	0	2	0	0	2	0
Total nonadults	1	1	100	0	1	0	1	1	100
Males	3	18	16.7	4	18	22.2	7	18	38.9
Females	2	6	33.3	0	6	0	2	6	33.3
Total adults	6	31	19.4	5	31	16.1	11	31	35.5
Total	6	32	18.8	5	32	15.6	11	32	34.4

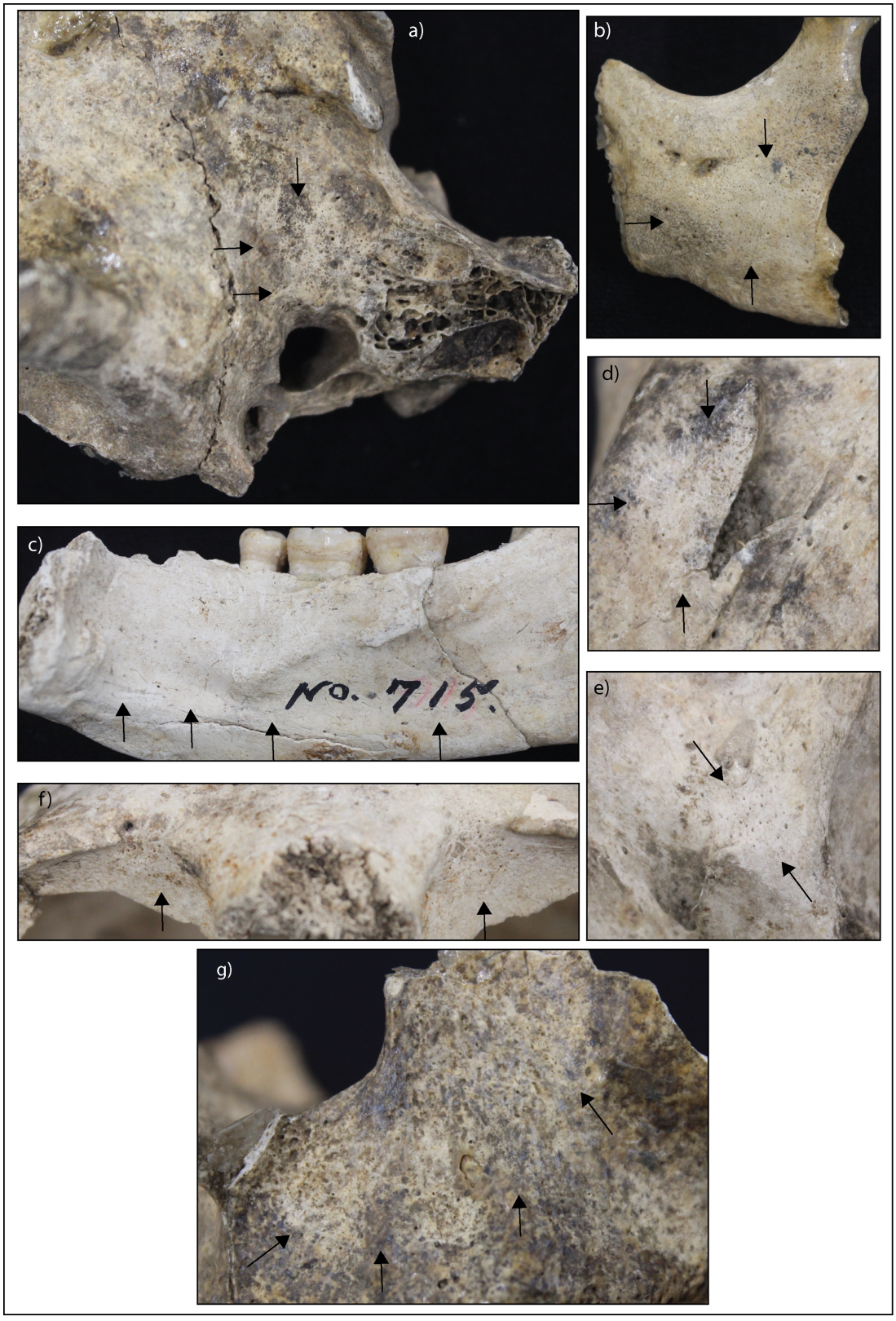

Figure 6.8: *Discrete deposits of SPNB with abnormal cortical porosity consistent with scurvy at Ota. a) Pterygoid process and lateral greater wing of sphenoid bone. The lesion extends onto the temporal bone (Ota 719, middle aged adult male). b) Anterior left zygoma (Ota 718, middle aged adult male). c) Inferior to the right mylohyoid line on the mandible. Note the vascular impressions (Ota 715, 15-19 years old). d) Around the right mandibular foramen (Ota 719, middle aged adult male). e) medial aspect of the left coronoid process of the mandible (Ota 718, middle aged adult male). f) Superior orbital roofs (Ota 710, young adult female). g) Anterior left maxilla (Ota 674, young adult male). Image: authors own.*

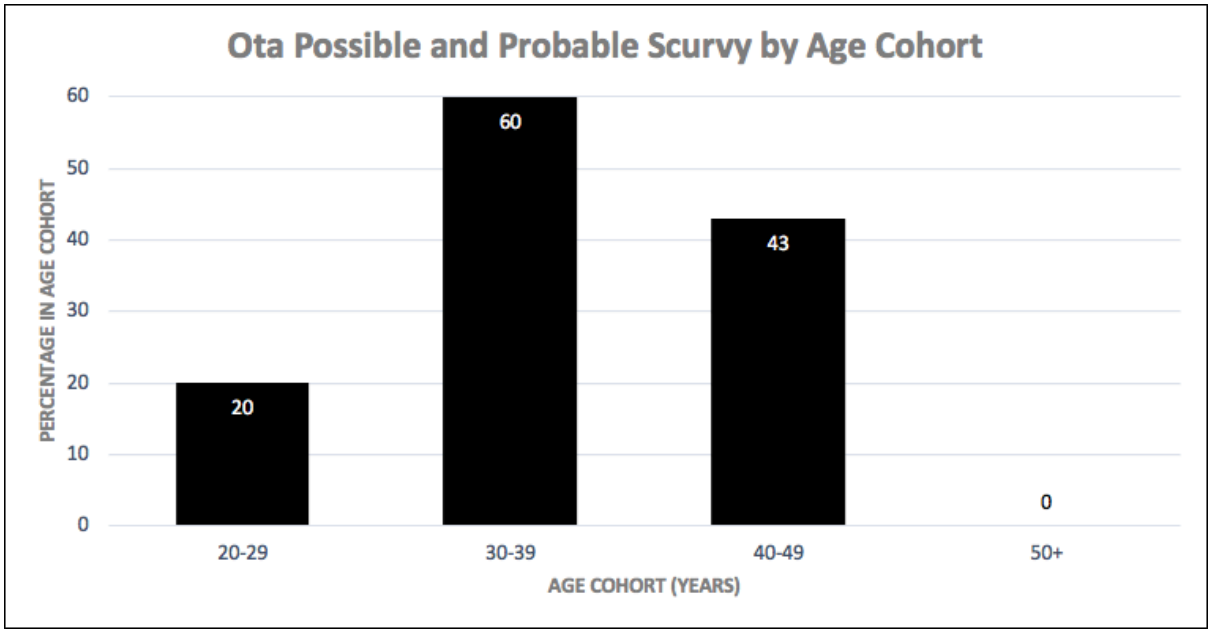

Figure 6.9: *Age-at-death distribution of possible and probable cases of scurvy at Ota. Image: author's own.*

6.4.6 Morbidity of Nutritional Disease at Ota

Morbidity of individuals under the age of 20 was not assessed as only one nonadult was observable for scurvy in the Ota assemblage. No significant differences in the prevalence of combined possible and probable and probable only diagnosed cases of scurvy are observed between males and females (Table 6.8). However, there appears to be age related differences in morbidity. Individuals under the age of 40 were 6.5 times more likely to have probable scurvy than over the age of 40, which was statistically significant given the size of the effect (n=25, RR=6.4706, p=0.1892).

Table 6.8: *Relative risk of scurvy morbidity at Ota across sex and age cohorts.*

EXPOSED GROUP/ CONTROL GROUP	OUTCOME		RR	P-VALUE	95%CI
	Positive: *Scurvy Present*	***Negative:*** *Scurvy Absent*			
Possible and Probable (combined)					
Sex					
Female/ Male	2/7	4/11	0.8571	0.8121	0.2404- 3.0558
Adults					
<20 yrs/ >20 yrs	-	-	-	-	-
<30 yrs/ >30 yrs	2/9	4/10	0.7037	0.5745	0.2063- 2.4000
<40 yrs/>40 yrs	8/3	8/6	1.5000	0.4473	0.5271- 4.2687
Probable Only					
Sex					
Female/ Male	0/4	6/14	0.3016	0.3998	0.0185- 4.9117
Adults					
<20 yrs/ >20 yrs	-	-	-	-	-
<30 yrs/ >30 yrs	1/4	5/15	0.7917	0.8180	0.1082- 5.7907
<40 yrs/>40 yrs	5/0	11/9	**6.4706**	**0.1892****	0.3983- 105.1107

A relative risk (RR) >1 denotes a relationship of the exposed group with an increase in disease prevalence, whereas RR <1 denotes a relationship of the control group with an increase in disease prevalence.
*= statistically significant (p<0.10). **= statistically significant when considering size of the effect of RR.

6.4.7 Mortality of Nutritional Disease at Ota

No statistically significant differences in mortality between those with possible or probable cases of scurvy compared to those without was apparent in the relative risk ratio analysis (Table 6.9). This outcome was reflected in the Kaplan-Meier survival analysis (n=25, X^2=0.921, df=1, p=0.337; Table 6.10; Figure 6.10). However, relative risk ratio analysis indicated a significant increase in the mortality of individuals under the age of 40 years of age with evidence of probable scurvy (n=25, RR=1.812, p=0.0031). Individuals were 1.8 times more likely to die before the age of 40 years of age with evidence of probable scurvy than without. The Kaplan-Meier (n=25, X^2=2.764, df=1, p=0.096) and Cox regression analysis (n=25, Wald= 2.441, df=1, p=0.118) supports a statistically significant relationship between the presence of probable scurvy and increased risked of death at Ota (Tables 6.11 -6.12, Figures 6.11 -6.12). The overall survivorship statistical analyses then indicate that the presence of skeletal signs of probable scurvy at Ota were associated with increased frailty.

Table 6.9: *Relative risk of scurvy mortality at Ota across age cohorts.*

POSITIVE OUTCOME/ NEGATIVE OUTCOME	**TREATMENT**		**RR**	**P-VALUE**	**95%CI**
	Exposed Group: *Scurvy Present*	***Control Group:*** *Scurvy Absent*			
Possible and Probable (combined)					
Adults					
<20 yrs/ >20 yrs	1/10	0/14	3.7500	0.4047	0.1674- 84.0239
<30 yrs/ >30 yrs	2/9	4/10	0.6364	0.5555	0.1416- 2.8592
<40 yrs/>40 yrs	8/3	8/6	1.2727	0.4153	0.7124- 2.2739
Probable Only					
Adults					
<20 yrs/ >20 yrs	0/5	1/19	1.1667	0.9216	0.0542- 25.1165
<30 yrs/ >30 yrs	1/4	5/15	0.8000	0.8189	0.1184- 5.4045
<40 yrs/>40 yrs	5/0	11/9	**1.8182**	**0.0031***	1.2231- 2.7027

A relative risk (RR) >1 denotes a relationship of the disease presence with the positive outcome (susceptibility to mortality), whereas RR <1 denotes a relationship of the disease absence with a negative outcome (survivorship).
*= statistically significant (p<0.10). **= statistically significant when considering size of the effect of RR.

Table 6.10: *Statistical summary for Kaplan-Meier function of possible and probable scurvy mortality of adults at Ota.*

POSSIBLE AND PROBABLE SCURVY	**ESTIMATE**	**STD. ERROR**	**95% CI**	**LOG RANK (MANTEL-COX)**		
				CHI SQUARE	**DF**	**P-VALUE**
Mean				0.921	1	0.337
Absent	38.000	2.799	32.514- 43.486			
Present	34.545	2.791	29.076- 40.015			
Overall	36.480	1.982	32.596- 40.364			
Median						
Absent	37.000	3.086	30.951- 43.049			
Present	35.000	1.477	32.105- 37.895			
Overall	35.000	2.082	30.920- 39.080			

*= statistical significance (p<0.15).

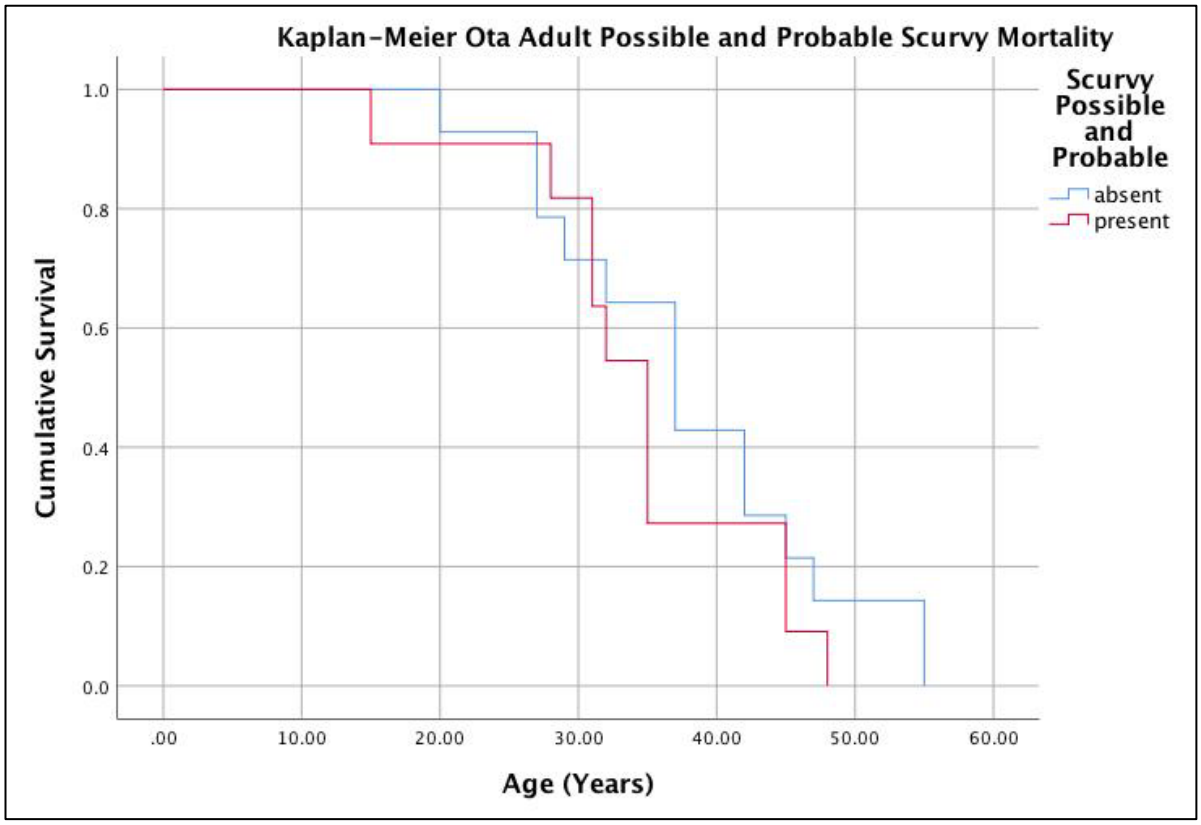

Figure 6.10: *Kaplan-Meier cumulative survival function of adult possible and probable scurvy mortality at Ota. Image: author's own*

Table 6.11: *Statistical summary for Kaplan-Meier function of probable scurvy mortality of adults at Ota.*

PROBABLE SCURVY	ESTIMATE	STD. ERROR	95% CI	LOG RANK (MANTEL-COX)		
				CHI SQUARE	DF	P-VALUE
Mean				2.764	1	**0.096***
Absent	37.400	2.423	32.651- 42.149			
Present	32.800	1.428	30.001- 35.599			
Overall	36.480	1.982	32.596- 40.364			
Median						
Absent	37.000	3.708	29.732- 44.268			
Present	35.000	0.000	-			
Overall	35.000	2.082	30.920- 39.080			

*= statistical significance (p<0.15).

Table 6.12: *Statistical summary for Cox regression function of probable scurvy mortality of adults at Ota.*

PROBABLE SCURVY	COEFFICIENT (β)	STD. ERROR	WALD	DF	P-VALUE	ODDS RATIO (Exp(β))
	-0.892	0.571	2.441	1	**0.118***	0.410

*= statistical significance (p<0.15).

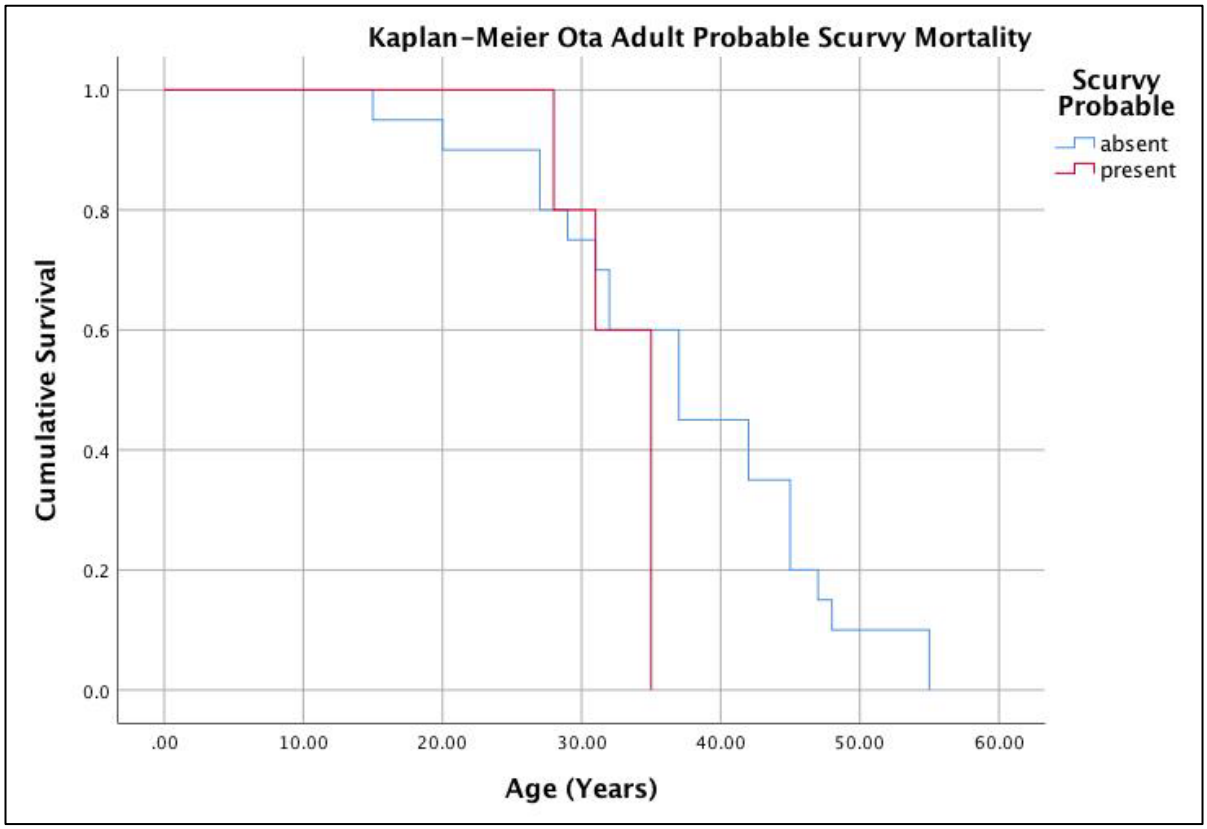

Figure 6.11: *Kaplan-Meier cumulative survival function of adult probable scurvy mortality at Ota. Image: author's own*

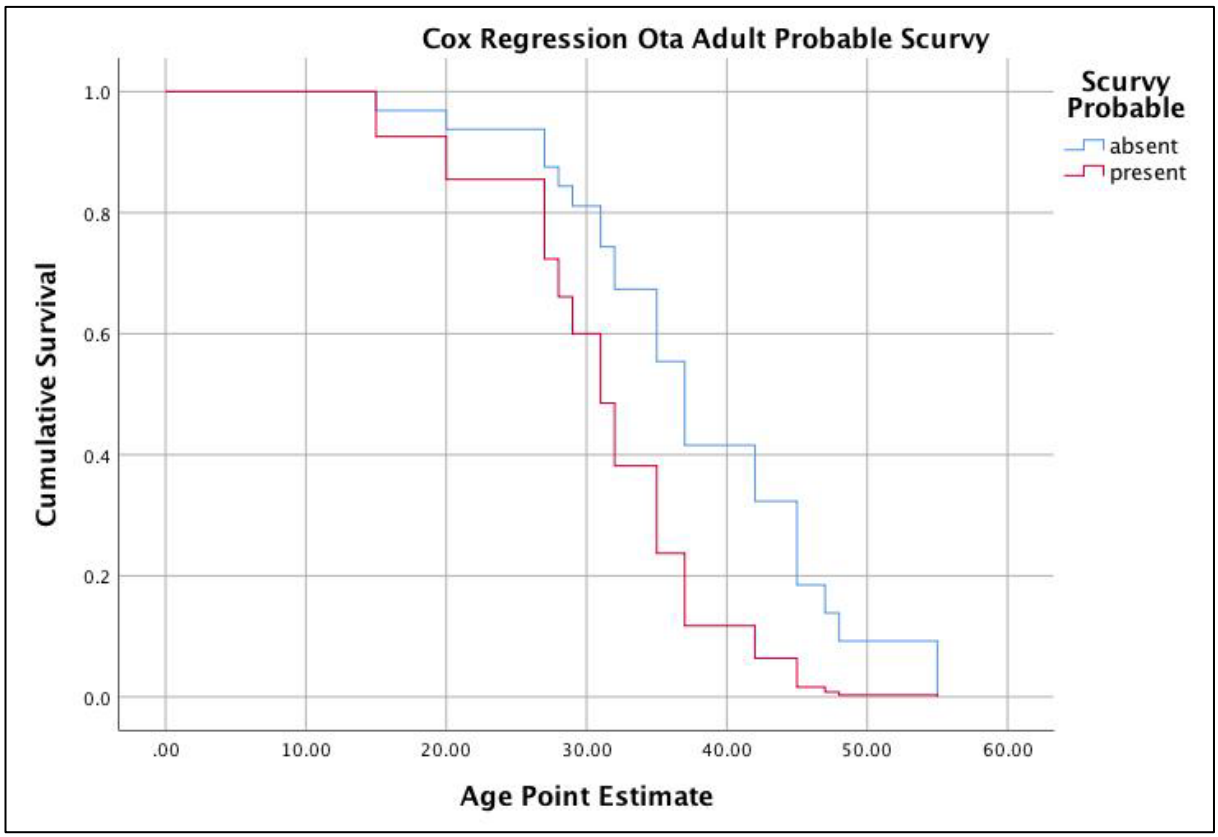

Figure 6.12: *Cox regression cumulative survival function of adult probable scurvy mortality at Ota. Image: author's own.*

6.4.8 Diagnosis of Anaemia at Ota

A high percentage (63.2%, 12/19) of the Ota adults exhibited medium or severe grade cribra orbitalia and/or porotic hyperostosis consistent with a diagnosis of anaemia (Table 6.13; Figure 6.13). Lack of preservation of the cranial vault and orbits in the nonadults means anaemia could not be observed. Porotic hyperostosis (47.1%, 8/17) was slightly more common in the Ota adults than medium or severe grade cribra orbitalia (35.3%, 6/17). However, a considerable number of individuals with porotic hyperostosis also had mild grade cribra orbitalia. Individuals aged between 30-39 had the highest prevalence of childhood anaemia (87.5%, 7/8) with no individuals over the age 50 years exhibiting skeletal evidence for anaemia (Figure 6.14).

Table 6.13: *Summary of anaemia at Ota.*

ANAEMIA	**CO**			**Cranial PH**			**PH and/or CO**		
	Affected	*Observed*	*(%)*	*Affected*	*Observed*	*(%)*	*Affected*	*Observed*	*(%)*
20 to 29 years	1	2	50	0	2	0	1	2	50
30 to 39 years	3	7	42.9	5	7	71.4	7	8	87.5
40 to 49 years	1	4	25	2	5	40	2	5	40
50+ years	0	1	0	0	1	0	0	1	0
Males	5	11	45.5	6	11	54.5	9	12	75
Females	0	5	0	1	4	25	1	5	20
Total adults	6	17	35.3	8	17	47.1	12	19	63.2
Total	6	17	35.3	8	17	47.1	12	19	63.2

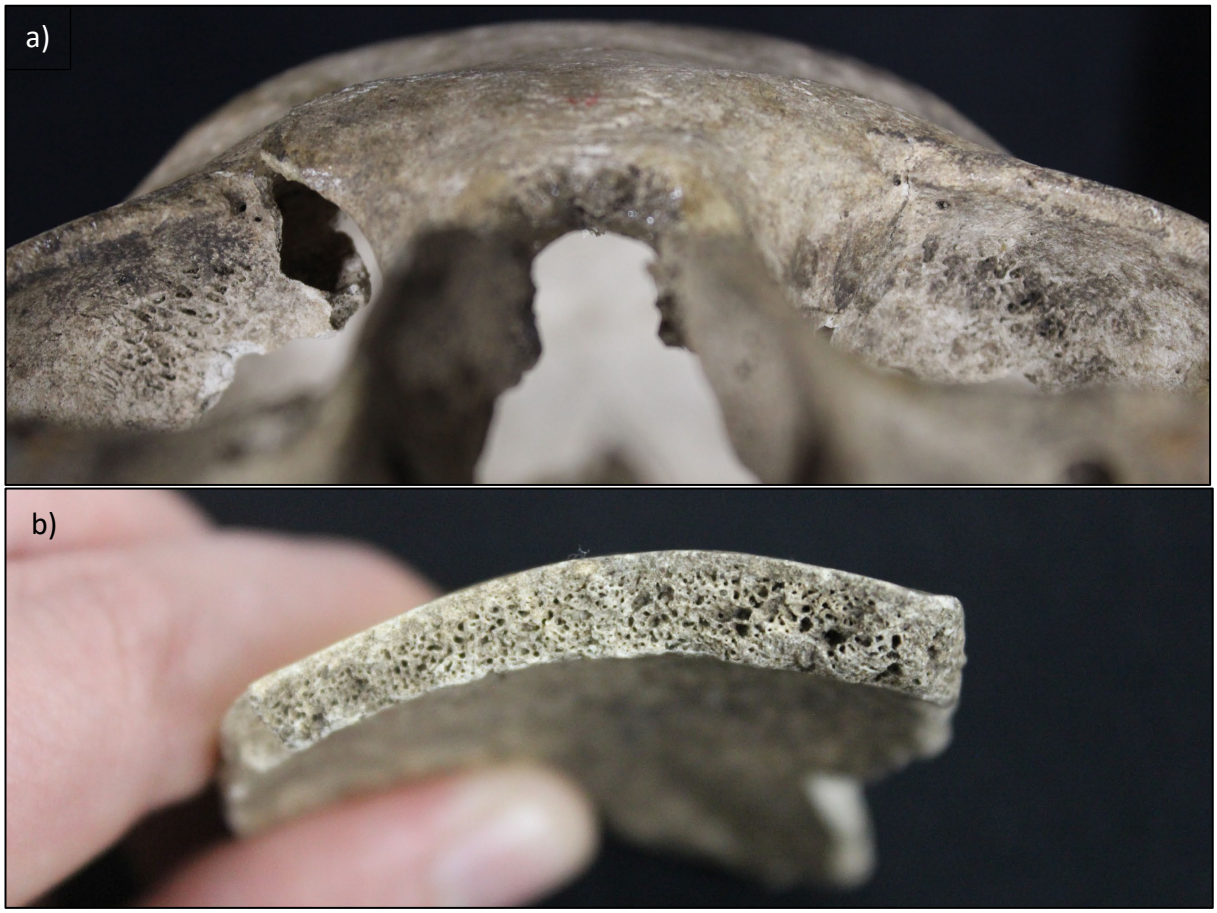

Figure 6.13: *Lesions consistent with anaemia at Ota. a) Medium grade cribra orbitalia (Ota 668B, middle aged adult male). b) Diploic expansion. This pathology was associated with porosity on the ectocranium (Ota 683, young adult male). Image: author's own.*

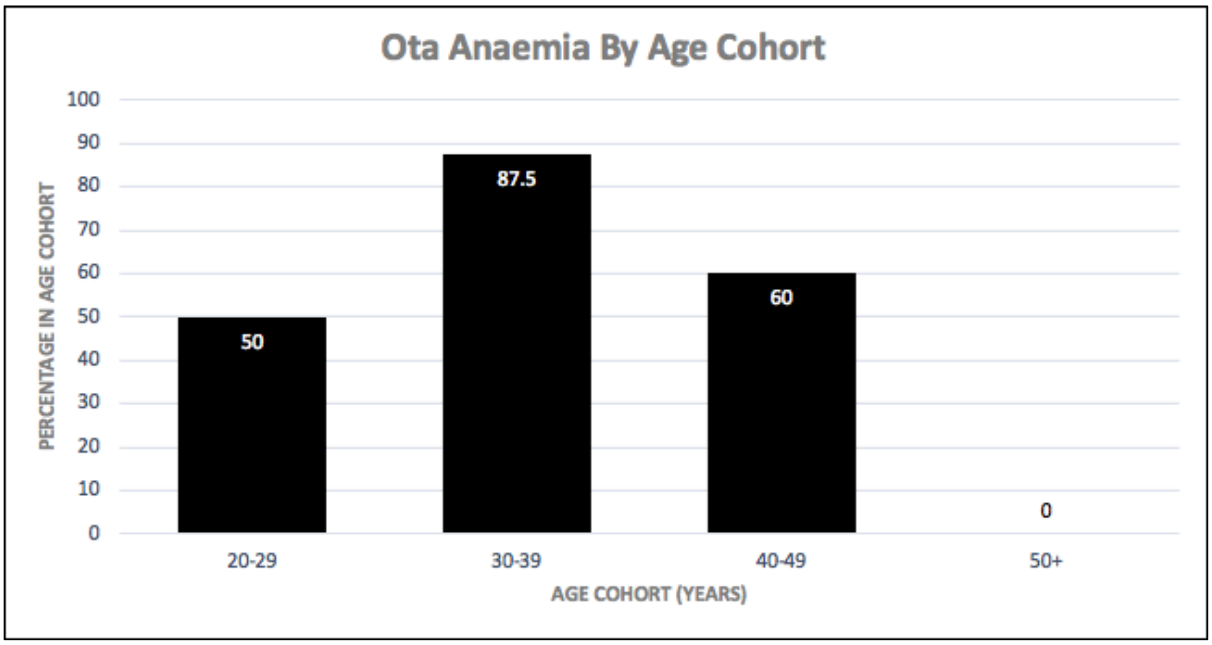

Figure 6.14: *Age-at-death distribution of anaemia at Ota. Image: author's own.*

6.4.9 Morbidity of Anaemia at Ota

The morbidity of anaemia could not be assessed for nonadults, as no individual under 20 years of age had preserved cranial nor orbital elements. Ota adults were 2.4 times more likely to have signs of childhood anaemia under the age of 40 compared to over (Table 6.14). This was statistically significant given the size of the effect (n=16, RR= 2.4000, p= 0.1436). However, males were 3.7 times more likely to have anaemia than females, which was statistically significant given the size of the effect (n=17, RR=0.2667, p=0.1463). This outcome suggests males were at an increased risk of developing anaemia in childhood compared to females.

Table 6.14: *Relative risk of anaemia morbidity at Ota across sex and age cohorts.*

EXPOSED GROUP/ CONTROL GROUP	**OUTCOME**		**RR**	**P-VALUE**	**95%CI**
	Positive: *Anaemia Present*	***Negative:*** *Anaemia Absent*			
Sex					
Female/ Male	1/9	4/3	**0.2667**	**0.1463****	0.0448- 1.5864
Adults					
<20 yrs/ >20 yrs	-	-	-	-	-
<30 yrs/ >30 yrs	1/9	1/5	0.7778	0.7323	0.1843- 3.2824
<40 yrs/>40 yrs	8/2	2/4	**2.4000**	**0.1463****	0.7424- 7.7581

A relative risk (RR) >1 denotes a relationship of the exposed group with an increase in disease prevalence, whereas RR <1 denotes a relationship of the control group with an increase in disease prevalence.
*= statistically significant (p<0.10). **= statistically significant when considering size of the effect of RR.

6.4.10 Mortality of Anaemia at Ota

Relative risk ratio analysis demonstrated a significantly increased risk of death in individuals with skeletal signs of anaemia (Table 6.15). Ota individuals were 2.4 times more likely to die before the age of 40 years with skeletal signs of childhood anaemia. This was statistically significant given the size of the effect (n=16, RR= 2.4000, p= 0.1436). Similarly, significantly increased mortality of individuals exhibiting skeletal signs of anaemia was observed with both the Kaplan-Meier (n=16, X^2=4.019, df=1, p=0.045; Table 6.16; Figure 6.15) and Cox Regression (n=16, Wald=3.189, df=1, p=0.074; Table 6.17; Figure 6.16) analyses. The Kaplan-Meier cumulative survival function (Figure 6.15) clearly indicates differential survival between those with and those without skeletal signs of childhood anaemia. Individuals were less likely to survive to old age if they had experienced stressors which contributed to development of skeletal signs of anaemia in their childhood.

Table 6.15: *Relative risk of anaemia mortality at Ota across age cohorts.*

POSITIVE OUTCOME/ NEGATIVE OUTCOME	**TREATMENT**		**RR**	**P-VALUE**	**95%CI**
	Exposed Group: *Anaemia Present*	***Control Group:*** *Anaemia Absent*			
Adults					
<20 yrs/ >20 yrs	-	-	-	-	-
<30 yrs/ >30 yrs	1/9	1/5	0.6000	0.6980	0.0454- 7.9219
<40 yrs/>40 yrs	8/2	2/4	**2.4000**	**0.1463****	0.7424- 7.7581

A relative risk (RR) >1 denotes a relationship of the disease presence with the positive outcome (susceptibility to mortality), whereas RR <1 denotes a relationship of the disease absence with a negative outcome (survivorship).
*= statistically significant (p<0.10). **= statistically significant when considering size of the effect of RR.

Table 6.16: *Statistical summary for Kaplan-Meier function of anaemia mortality of adults at Ota.*

ANAEMIA	**ESTIMATE**	**STD. ERROR**	**95% CI**	**LOG RANK (MANTEL-COX)**		
				CHI SQUARE	**DF**	**P-VALUE**
Mean				4.019	1	**0.045***
Absent	42.333	3.930	34.631- 50.036			
Present	34.600	1.655	31.357- 37.843			
Overall	37.500	1.973	33.633- 41.367			
Median						
Absent	42.000	4.899	32.398- 51.602			
Present	32.000	1.265	29.521- 34.479			
Overall	35.000	1.984	31.111- 38.889			

*= statistical significance (p<0.15).

Table 6.17: *Statistical summary for Cox regression function of anaemia mortality of adults at Ota.*

ANAEMIA	**COEFFICIENT (β)**	**STD. ERROR**	**WALD**	**DF**	**P-VALUE**	**ODDS RATIO (Exp(β))**
	-1.103	0.618	3.189	1	**0.074***	0.332

*= statistical significance (p<0.15).

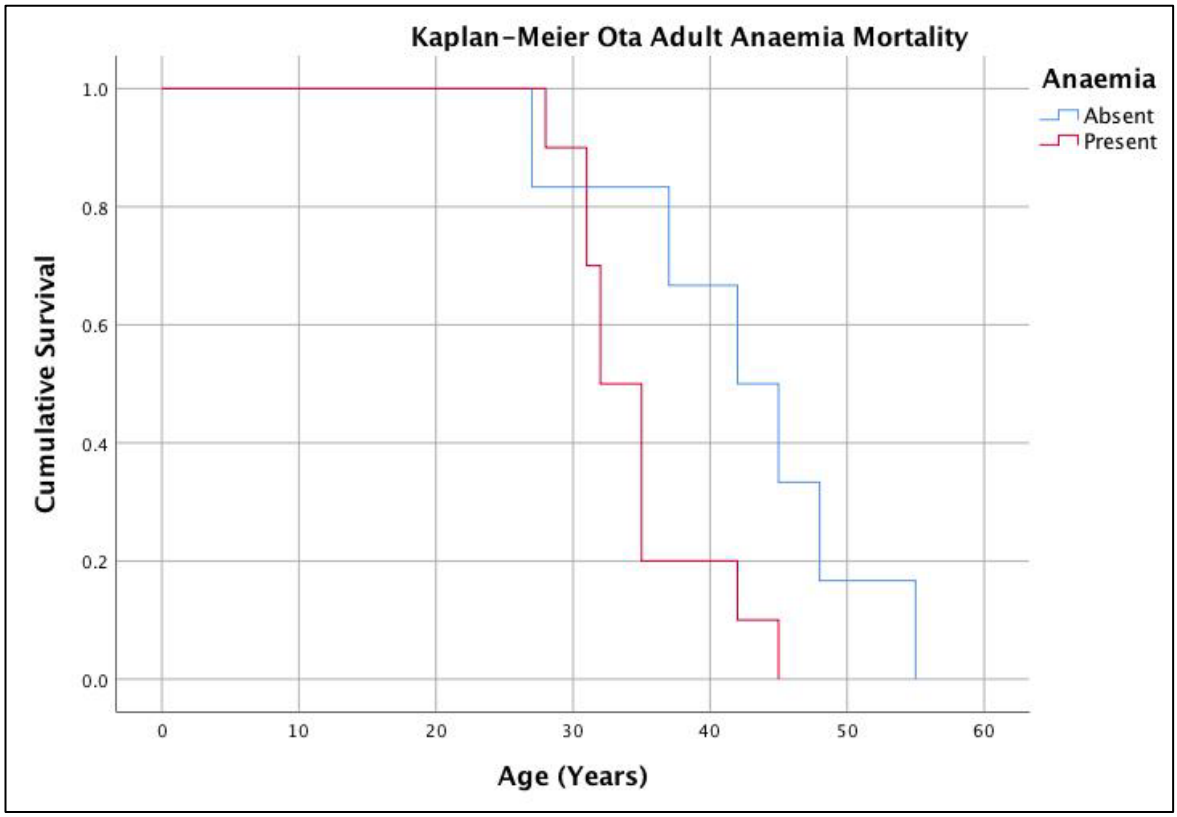

Figure 6.15: *Kaplan-Meier cumulative survival function of adult anaemia mortality at Ota. Image: author's own*

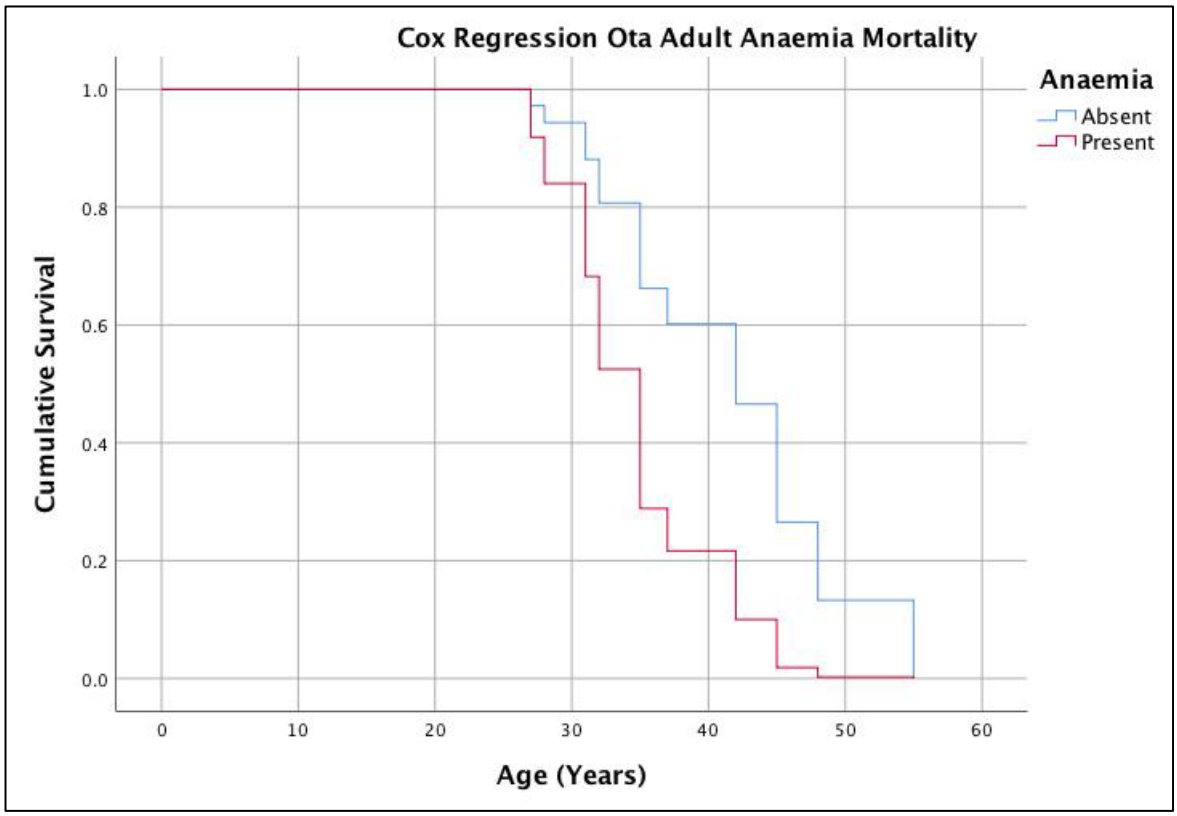

Figure 6.16: *Cox regression cumulative survival function of adult anaemia mortality at Ota. Image: author's own.*

6.4.11 Summary of Diagnosis and Context of Disease at Ota

Individuals in the Ota assemblage had considerable evidence for infectious and nutritional disease burden. Over twenty percent (20.6%, 7/34) exhibited signs of infectious diseases. Furthermore, 34.4% (11/32) of the assemblage were diagnosed with a possible or probable case of scurvy and 63.2% (12/19) exhibited skeletal evidence for anaemia.

6.4.11.1 Mycosis at Ota

Fungal infection is commonly caused by exposure to fungal spores in the environment, as these spores thrive in soils (Behrman et al. 1990; Goodwin et al. 1981; Mathews et al. 2016; Oberoi et al. 2012). As such, a possible case of mycotic infection at Ota is plausible given the hunter-fisher-foraging efforts which were employed by the Ota community, particularly the exploitation of terrestrial environments. Given the geographical spread of fungal diseases today, cryptococcosis (*Cryptococcus neoformans neoformans)*, aspergillosis (various *Aspergillus* sp.) and histoplasmosis *(Histoplasma capsulatum* and *H. duboisii)* are primary candidates for mycotic infection in prehistoric Japan. It is recognised that geographic distributions of fungi may have differed in the past. However, given that Japan has an island geography, significant differences to distributions are unlikely. Cryptococcosis most commonly affects single skeletal sites, and if lesions are multifocal, these are often found in contiguous regions as is the case of the two lesions of the nasal cavity of Ota 670A (Behrman et al. 1990). Cranial involvement in skeletal histoplasmosis is common, and sinusitis can occur in aspergillosis which may spread the spores directly through the respiratory and nasal tracts into surrounding bone (Bodey and Vartivarian 1989; Mathews et al. 2016). Aspergillosis is also known to invade the mastoid and temporal bone and cause otitis media (Bodey and Vartivarian 1989). In sum, the skeletal expression of Ota 670A is consistent with a number of possible candidates for mycosis.

6.4.11.2 Scurvy at Ota

Scurvy is commonly associated with agricultural transitions and the restriction of micronutrients with reliance on staple crops (Snoddy et al. 2017). The question then remains, how did the Jomon, a forager group, exploiting a variety of resources suffer from severe Vitamin C deficiency? In order for skeletal lesions of scurvy to develop, an individual must be in the process of recovery, as Vitamin C deficiency leads to obstruction of osteoblastic

deposit of SPNB (Brickley and Ives 2010). Some re-introduction into the diet is then necessary for skeletal evidence of haematomas to form. Therefore, skeletal evidence of scurvy at Ota likely indicates that cyclical Vitamin C restriction and recovery was present indicating fluctuations in the Ota diet. Most lesions related to scurvy diagnosis in the Ota adults were remodelled, and therefore do not indicate instances of scurvy that directly contributed to the cause of death in these individuals. Research into Vitamin C deficiency in prehistoric South American and Pacific skeletal assemblages have reached similar conclusions (Buckley 2000; Buckley et al. 2014; Snoddy et al. 2017). Given the seasonal climate of temperate Japan, available resources fluctuated significantly across seasons. During the winter months reliance on boar and deer increased at the expense of Vitamin C rich roots, tubers, fruits and nuts that were readily available during the summer and springtime (Habu 2004). However, chestnuts, some shellfish and animal liver, available during the winter time, may have provided sufficient quantities to prevent clinical Vitamin C deficiency (Table 6.18).

Table 6.18: *Dietary sources of the Jomon during summer/ spring and winter/autumn periods (Habu 2004). (<6.5 to 10mg a day results in Vitamin C deficiency). Vitamin C estimates: (US Department of Agriculture 2019).*

WINTER/ AUTUMN		**SPRING/ SUMMER**	
Food Type	***Vitamin C (mg) per 100g***	***Food Type***	***Vitamin C (mg) per 100g***
Acorns	0	Mulberry Fruit	36.4
Chestnuts	40.2	Gourd	8.5
Walnuts	1.3	Yam	17.1
Boar	0.6	Mussel/ shellfish	13.6
Venison	0	Fish	3.6
Fish	3.6	Tuber (Sweet Potato)	2.4
		Taro	5

There are a number of plausible explanations for a high prevalence of scurvy even if sufficient dietary sources for Vitamin C were available. Vitamin C is easily leached from food during processing. Certain acorns and horse chestnuts required a considerable leaching process, where toxins were removed in order for them to be edible. This process likely involved boiling or leaching stages that occurred over a number of days to two weeks (Kawashima 2016; Sakaguchi 2009). In Western Japan, it appears that evergreen acorns, which required little processing, predominate the archaeological assemblage over that of Vitamin C rich chestnuts (Takahashi and Hosoya 2016). Furthermore, it is more common for ‘wet-type’ storage pits to be found in Western Japan, where food was stored in water that may have naturally leached out Vitamin C from the nuts (Sakaguchi 2009). In long term

storage in water, this may have had considerable influence on the levels of Vitamin C and other water soluble vitamins in the stored foods. Finally, if animal liver provided a primary source for Vitamin C, this may have consequently caused hypervitaminosis A, particularly in children, as the liver of animals is exceptionally enriched with Vitamin A. The effects of hypervitaminosis A occur more rapidly than that of scurvy, and are more immediately drastic. This condition can cause blindness, changes in consciousness, liver damage, and severe anaemia (Perrotta et al. 2002). In sum, where dietary sources were high in Vitamin C, the actual bioavailability of the Vitamin C may have been considerably reduced due to food storage or processing methods, and/or the Jomon may have made strategic choices to forage for foods easier to process, but lower in Vitamin C.

Less than half (42.8%, 3/7) of individuals with infectious disease were also diagnosed with a possible or probable case of scurvy. This outcome does not indicate a strong association in skeletal evidence of co-morbidities between infectious and nutritional diseases at Ota. Nevertheless, dissemination of spores as is the case in skeletal mycosis is often the result of immunocompromisation which occurs in instances of malnutrition or micronutrient deficiency (Corr 2011; Goodwin et al. 1981; Oberoi et al. 2012). Indeed, Ota 670A, the middle aged adult diagnosed with possible mycosis was also diagnosed with probable scurvy, as well as otitis media which presumably developed in childhood. Furthermore, this individual exhibited multiple linear enamel hypoplasia defects of the permanent teeth indicating repeated exposure to stressors in childhood (Temple 2007b). Comparisons of cases of nutritional and infectious disease co-morbidities with other skeletal signs of non-specific stress is beyond the focus of this thesis, but an intriguing avenue for further research.

6.4.11.3 Anaemia at Ota

Given that Ota and Tsukumo are coastal sites, likely an exploitation of marine resources increased parasitic load which would have contributed to the prevalence of porotic hyperostosis and cribra orbitalia (Temple 2007a). The consumption of raw marine foods such as fish is well associated with parasitism (Søe et al. 2018). Significant numbers of whipworm eggs (*Trichuris trichuria*) in coprolites have been identified by Kanehara (1995) at the Early to Middle Jomon Period Sannai Maruyama site in Northern Honshu, also indicating a high parasitic burden may have been caused by exposure to contaminated soil

or water often associated with sedentary habitation (Søe et al. 2018). However, scurvy is also strongly correlated with iron deficiency anaemia due to repeated internal haemorrhaging resulting in chronic blood loss, which may have also contributed to childhood anaemia (Brickley and Ives, 2010). Furthermore, a number of vitamin deficiencies including A, folate and B12 could have been indirect contributors to anaemia (Bloem et al. 1989; Gowland and Western 2012). These vitamins are commonly found in sources such as fish, shellfish and meat, and anaemia due to micronutrient deficiency likely only occurred in times of severe food scarcity (Navarra 2014; Watanabe 2007). Additionally, inflammatory iron deficiency anaemia as a result of infectious disease may have been a contributor to the overall prevalence of anaemia at Ota (Camaschella 2015).

It is evident that the presence of skeletal signs of childhood anaemia significantly affected survivorship to old age of Ota adults. This outcome implies that childhood exposure to stressors causing anaemia may have contributed to increased risk of death to disease later on in life.

6.4.11.4 Intrapopulation Variation of Disease at Ota

Males had consistently higher prevalences of disease at Ota. However, this was only statistically significant for anaemia. Carbon and nitrogen isotopic levels of bone collagen varied significantly between males and females, indicating males exploited more marine resources than females (Kusaka et al. 2010; Kusaka et al. 2015). As previously mentioned, the authors argued that the difference may have been related to gendered labour division in food resource procurement. However, gendered differences in exposure to marine foods are also documented in communities due to gender specific food taboos. For example, in Fiji women are prohibited from consuming fish and shellfish around pregnancy (Henrich and Henrich 2010). The research in this thesis does support the argument by Kusaka et al. (2010) if these gendered differences in diet extended from childhood with boys eating a richer marine diet than girls, increasing their access to marine parasites and therefore chronic anaemia. However, Kusaka et al. (2010) did not find significant differences in the carbon isotopes of tooth enamel, which forms in childhoods. Given the complex aetiologies of anaemia, exploring gendered patterns in the diet of Ota males and females is similarly complex and beyond the scope of this thesis.

6.5 Tsukumo

Tsukumo, like Ota, is classified as a shell midden site (Kiyono 1969). Relative dating places this site in the Late to Final Jomon Period (4000-2300BP) during the period of climatic cooling (Kiyono 1969). The Tsukumo assemblage is comprised of predominantly adults. However, there is a greater number of preserved nonadults than was the case for Ota. A distinct lack of infants under 1 year of age and older children does indicate some bias in the sample. As the nonadults who are present in the assemblage were well preserved, and given the assemblage was excavated in the 1920's, it was suspected during analysis that some level of curation bias exists. For this reason fertility rates and rates of natural population increase for the site was not estimated.

While similar to Ota in regards to sedentary dwellings along the Inland Sea, and similar foraging and fishing tools were excavated from the shell midden (Kiyono et al. 1920), Tsukumo does have some distinct differences which indicate considerable social change from the Middle to the Late and Final Jomon Periods in this region. Kiyono (1969) identified fashioned deer antlers placed along the right hip of three individuals at Tsukumo, which were described as *hip ornaments* and animal bone implements were found in 33% of graves. These were not found at Ota. Temple (2018) has argued that these artefacts indicate social differentiation in identity at Tsukumo. As was the case at Ota, tooth ablation was practiced at Tsukumo (Kusaka et al. 2012; Temple 2018). However, different forms of tooth ablation and an increase in the number of individuals with ablated teeth was apparent at Tsukumo in contrast to Ota (Temple 2018). While there remains no evidence for socioeconomic inequality, this may indicate the beginnings of social stratification in the Late to Final Jomon in Western Japan (Temple 2018).

In regards to the Tsukumo diet, Kusaka et al. (2010) found no differences in the carbon and nitrogen isotope values between males and females, contrasting the outcome at Ota. Tsukumo individuals also exhibited significantly lower nitrogen values than Ota individuals indicating an increased proportion of terrestrial sources in the Tsukumo diet. The Tsukumo assemblage exhibited a carious lesion prevalence rate of 9.6%, considerably higher than that of Ota (Temple 2007b). The increased rate of carious lesions of Late and Final Jomon compared to Middle Period Jomon indicates an increased carbohydrate intake supported by the isotopic findings of Kusaka et al. (2010) for an increased reliance on

terrestrial food resources. The prevalence of linear enamel hypoplasia per individual was similar to that of Ota at 66.7% in the Tsukumo assemblage (Temple 2007b).

Kusaka et al. (2012) identified no non-locals in the Tsukumo assemblage. However, it is important to note that the ambiguity of the dating of Tsukumo plays a significant role in the interpretation of the role of Tsukumo in the migration of Jomon to refuge zones following climate cooling. It is expected such a migration would have been gradual, and therefore interpretation of Tsukumo as a proxy for assessing intrapopulation interaction in Western Honshu does not necessarily rely on the identification of first degree migrants (see Chapter 2 for discussion on limitations of assessing human mobility solely through isotopes). Kusaka et al. (2009) and Kusaka et al. (2011) did identify an increase of migrants in Central Japan during the Late to Final Jomon, which share cultural affinity and social interactions with Western Honshu sites during this time. Additionally, as Tsukumo burials extend into the Final Jomon Period, presumably migration may have stabilised but the epidemiological implications of the population interaction would have been long lasting. The following section presents the results for disease diagnosis and analysis of morbidity and mortality of these diseases at the Tsukumo site.

6.6 Results: Tsukumo Skeletal Pathology

6.6.1 Summary of Pathological Lesions at Tsukumo

Of the 30 individuals from the Tsukumo assemblage assessed for skeletal pathology, all individuals, both adults and nonadults exhibited at least one osteoblastic lesion (Table 6.19; Figure 6.17). While some individuals exhibited diffuse deposits of SPNB across the long bones, the lesions were overwhelmingly symmetrical and discrete deposits of SPNB across the crania and postcrania that were often directly associated with abnormal cortical porosity.

Three adults (15.8%, 3/19) exhibited OL1 focal destruction of the mastoid. Two of these individuals and one other exhibited an osteolytic fistula draining from the mastoid foramen. One individual (Tsukumo 6, a young adult female) exhibited multifocal and coalesced OL2 osteolytic destruction with irregular margins and sclerotic response of the inferior posterior vertebral body of the T12, superior posterior vertebral body of the L1, and superior anterior vertebral body of the L2. The lesions of the superior vertebral body of the

L2 was the most severe and was accompanied with osteophytic response on the anterior margin (Figure 6.18). The T12 and L2 lesion appear to form from a single point of lysis, therefore two regions of destruction are apparent in Tsukumo 6's spine. Additionally, a cloaca was observed extending from the inferior T12 body. This individual also exhibited expansions of the foramina of the left proximal and intermediate digit phalanges. Nonadults did not exhibit any osteolytic lesions, and no individual in the Tsukumo assemblage exhibited any skeletal deformities.

Table 6.19: *Summary of OB and OL lesion prevalences at Tsukumo*

	NONADULT (aff/obs)	**NONADULT (%)**	**ADULT (aff/obs)**	**ADULT (%)**	**TOTAL (aff/obs)**	**TOTAL (%)**
OB Lesion	11/11	100	19/19	100	30/30	100
OL Lesion	0/11	0	5/19	26.3%	5/30	16.7

Figure 6.17: *Discrete deposit of SPNB on the proximal right medial femur (Tsukumo 37, middle aged adult female). This lesion is also associated with abnormal cortical porosity and vascular impressions. Image: author's own.*

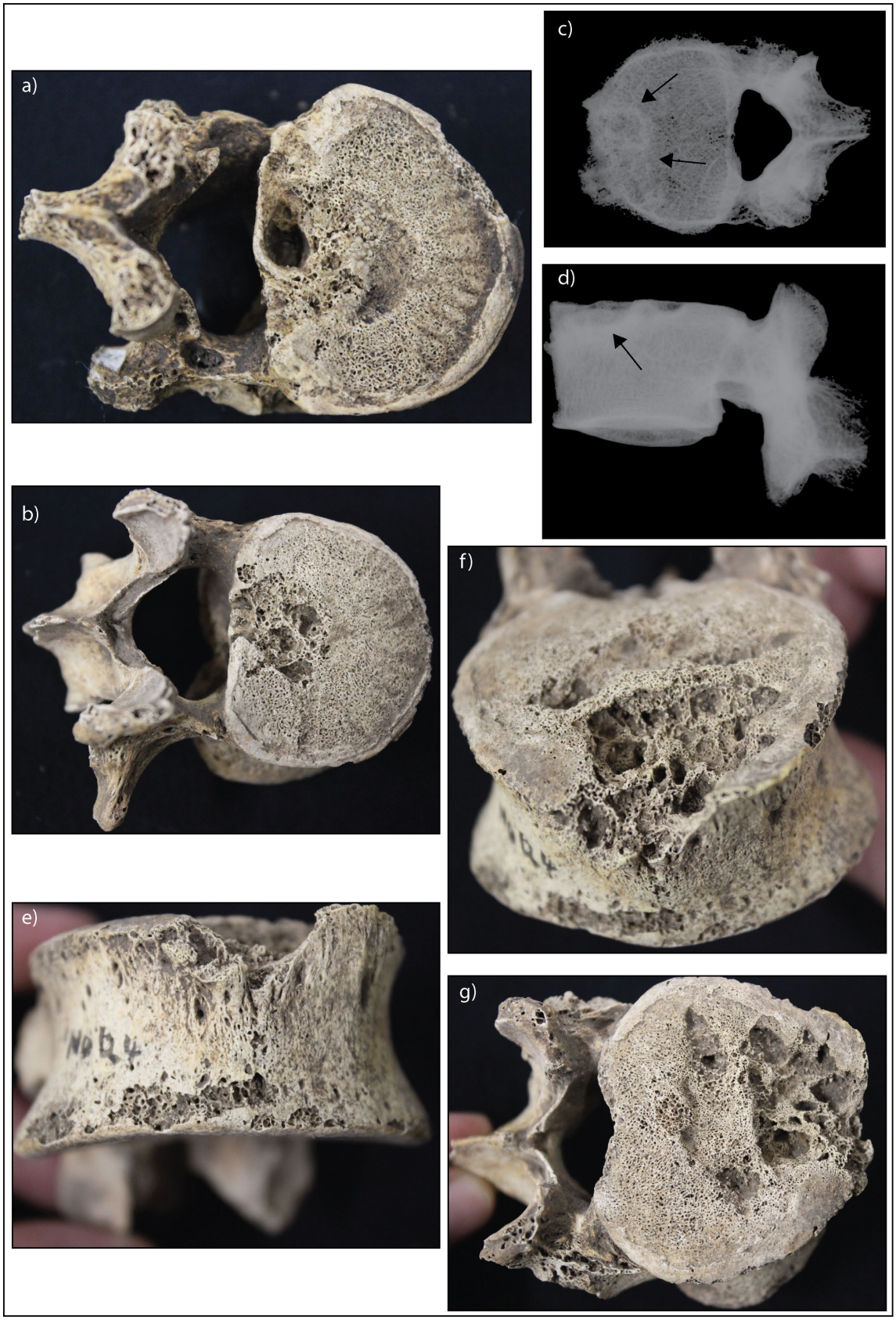

Figure 6.18: *Osteolytic lesions of the vertebral bodies of Tsukumo 6, young adult female. a) Inferior vertebral body of the T12. Note the cloaca on the posterior margin indicating pyogenic infection. b) Superior vertebral body of the L1. c-d) radiographs of L2. Note the sclerosis of the lesion margins (black arrows). e-g) Superior vertebral body of L2. While there are burst fractures evident on the vertebral bodies, these do not appear to be related to the progression of the osteolytic lesion. Image: author's own*

6.6.2 Diagnosis of Infectious Disease at Tsukumo

A high percentage (46.7%, 14/30) of the overall Tsukumo assemblage had pathologies consistent with an infectious aetiology (Table 6.20). Eleven individuals (36.7% 11/30) exhibited diffuse SPNB across more than 2 skeletal elements and were therefore included in the overall infectious disease criteria. One of these individuals was an adolescent (Tsukumo 29, female, ~16 years of age). The focal destruction of the mastoid region in three individuals (10%, 3/30) was consistent with a diagnosis of probable mastoiditis. Additionally one individual with a fistula draining from the mastoid foramen also presented with asymmetric development of the mastoid processes consistent with a possible case of mastoiditis (Figure 6.19).

The vertebral osteolytic destruction of Tsukumo 6 was consistent with a number of infectious diseases that spread through a haematogenous route, including tuberculosis, brucellosis, mycosis and osteomyelitis. The adjacent lysis of T12 and L1 indicate an intervertebral origin likely from the intervertebral disc. The focus of the lysis on the posterior vertebral body of the T12 and L1 are rare occurrences in both tuberculosis and brucellosis. Additionally, osteophytic response is not typical of the osteolytic destruction of tuberculosis (Jaffe 1972; Ortner 2003), and brucellosis is exceedingly rare in non-pastoralists communities but are found in marine animals in Japan that may have been consumed by the Jomon (Hernández-Mora et al. 2013). While mycosis remains a possibility, the presence of cloacae on the posterior vertebral body of the T12 indicates a pyogenic infection consistent with probable vertebral osteomyelitis. Pyogenic osteomyelitis often involves the development of a distinct involucrum particularly on the long bones (Ortner 2003), this does not appear to be the case in vertebral osteomyelitis where irregular osteolytic destruction is more common (Carragee 1997). As is the case in Tsukumo 6, reactive sclerosis at the site of the osteolytic destruction occurs in vertebral osteomyelitis instead of development of an involucrum (Skaf et al. 2010).

Table 6.20: *Summary of infectious disease at Tsukumo*

	POSSIBLE			**PROBABLE**			**POSSIBLE AND PROBABLE**		
	Affected	*Observed*	*(%)*	*Affected*	*Observed*	*(%)*	*Affected*	*Observed*	*(%)*
Osteomyelitis									
1 to 5 years	0	7	0	0	7	0	0	7	0
6 to 10 years	0	0	0	0	0	0	0	0	0
11 to 14 years	0	1	0	0	1	0	0	1	0
15 to 19 years	0	3	0	0	3	0	0	3	0
20 to 29 years	0	10	0	1	10	10	1	10	10
30 to 39 years	0	4	0	0	4	0	0	4	0
40 to 49 years	0	4	0	0	4	0	0	4	0
50+ years	0	1	0	0	1	0	0	1	0
Male	0	12	0	0	12	0	0	12	0
Female	0	9	0	1	9	11.1	1	9	11.1
Total adults	0	19	0	1	19	0	1	19	0
Total	0	30	0	1	30	3.3	1	30	3.3
Otitis Media									
1 to 5 years	0	3	0	0	3	0	0	3	0
6 to 10 years	0	0	0	0	0	0	0	0	0
11 to 14 years	0	1	0	0	1	0	0	1	0
15 to 19 years	0	2	0	0	2	0	0	2	0
20 to 29 years	0	9	0	1	9	11.1	1	10	11.1
30 to 39 years	0	3	0	0	3	0	0	3	0
40 to 49 years	1	3	33.3	1	3	33.3	2	3	66.7
50+ years	0	1	0	1	1	100	1	1	100
Male	1	10	10	2	10	20	3	10	30
Female	0	8	0	1	8	12.5	1	8	12.5
Total adults	1	16	6.25	3	16	18.75	4	16	25
Total	1	22	4.5	3	22	13.6	4	22	18.1

	CRITERIA PREVALENCE		
	Affected	*Observed*	*(%)*
Overall infectious disease criteria			
1 to 5 years	0	7	0
6 to 10 years	0	0	0
11 to 14 years	0	1	0
15 to 19 years	1	3	33.3
20 to 29 years	9	10	90
30 to 39 years	1	4	25
40 to 49 years	2	4	50
50+ years	1	1	100
Male	7	12	58.3
Female	7	9	77.8
Total nonadults	1	11	9.1
Total adults	13	19	68.4
Total	14	30	46.7

Figure 6.19: *Remodelled osteolytic destruction of the mastoid strongly diagnostic for mastoiditis (Tsukumo 23, old aged adult male).*

6.6.3 Morbidity of Infectious Disease at Tsukumo

Given the distribution of nonadult age groups, relative risk ratios were restricted to assessment of individuals under and over the age of 5 years of age. No statistically significant differences were identified in the morbidity of infectious disease at Tsukumo across nonadult age cohorts, adult age cohort or between males and females (Table 6. 21).

Table 6.21: *Relative risk of infectious disease morbidity at Tsukumo across sex and age cohorts.*

EXPOSED GROUP/ CONTROL GROUP	**OUTCOME**		**RR**	**P-VALUE**	**95%CI**
	Positive: *Infection Present*	***Negative:*** *Infection Absent*			
Sex					
Female/ Male	7/7	2/5	1.3333	0.3410	0.7375- 2.4105
Nonadults					
<1 yr/ >1 yr	-	-	-	-	-
<5 yrs/ >5yrs	0/1	7/3	0.2083	0.3053	0.0104- 4.1815
<10 yrs/ >10yrs	-	-	-	-	-
Adults					
<20 yrs/ >20 yrs	1/13	2/6	0.4872	0.3870	0.0955- 2.4846
<30 yrs/ >30 yrs	10/4	3/5	1.7308	0.1729	0.7864- 3.8090
<40 yrs/>40 yrs	11/3	6/2	1.0784	0.8527	0.4859- 2.3933

A relative risk (RR) >1 denotes a relationship of the exposed group with an increase in disease prevalence, whereas RR <1 denotes a relationship of the control group with an increase in disease prevalence.
*= statistically significant (p<0.10). **= statistically significant when considering size of the effect of RR.

6.6.4 Mortality of Infectious Disease at Tsukumo

Relative risk ratio analysis identified no clear relationship with the presence of skeletal signs of infectious disease and increased mortality for both nonadult and adult age cohorts (Table 6.22). Kaplan-Meier survival analysis was not attempted on the nonadult cohort as only one individual, an adolescent, had skeletal lesions consistent with infectious disease. Kaplan-Meier survival analysis identified no statistically significant differences in mortality of individuals with or without skeletal evidence for infectious disease (n=22, X^2=0.073, df=1, p=0.787; Table 6.23; Figure 6.20), which supports the outcome of the relative risk ratio analysis. Additionally, the Kaplan-Meier cumulative survival graph (Figure 6.20) indicates similar trends in survivorship between those with and without skeletal signs of infectious disease.

Table 6.22: *Relative risk of infectious disease mortality at Tsukumo across age cohorts.*

POSITIVE OUTCOME/ NEGATIVE OUTCOME	**TREATMENT**		**RR**	**P-VALUE**	**95%CI**
	Exposed Group: *Infection Present*	***Control Group:*** *Infection Absent*			
Nonadults					
<1 yr/ >1 yr	-	-	-	-	-
<5 yrs/ >5yrs	0/1	7/3	0.3667	0.4192	0.0321- 4.1825
<10 yrs/ >10yrs	-	-	-	-	-
Adults					
<20 yrs/ >20 yrs	1/13	2/6	0.2587	0.2725	0.0305- 2.6779
<30 yrs/ >30 yrs	10/4	3/5	0.9048	0.1856	0.7337- 4.9448
<40 yrs/>40 yrs	11/3	6/2	1.0476	0.8508	0.6452- 1.7010

A relative risk (RR) >1 denotes a relationship of the disease presence with the positive outcome (susceptibility to mortality), whereas RR <1 denotes a relationship of the disease absence with a negative outcome (survivorship).
*= statistically significant (p<0.10). **= statistically significant when considering size of the effect of RR.

Table 6.23: *Statistical summary for Kaplan-Meier function of infectious disease mortality of adults at Tsukumo.*

INFECTIOUS DISEASE	**ESTIMATE**	**STD. ERROR**	**95% CI**	**LOG RANK (MANTEL-COX)**		
				CHI SQUARE	**DF**	**P-VALUE**
Mean				0.073	1	0.787
Absent	29.125	3.993	21.299- 36.951			
Present	28.643	2.580	23.587- 33.699			
Overall	28.818	2.135	24.634- 33.002			
Median						
Absent	30.000	2.041	-			
Present	25.000	1.389	2.173			
Overall	25.000	2.010	2.350			

*= statistical significance (p<0.15).

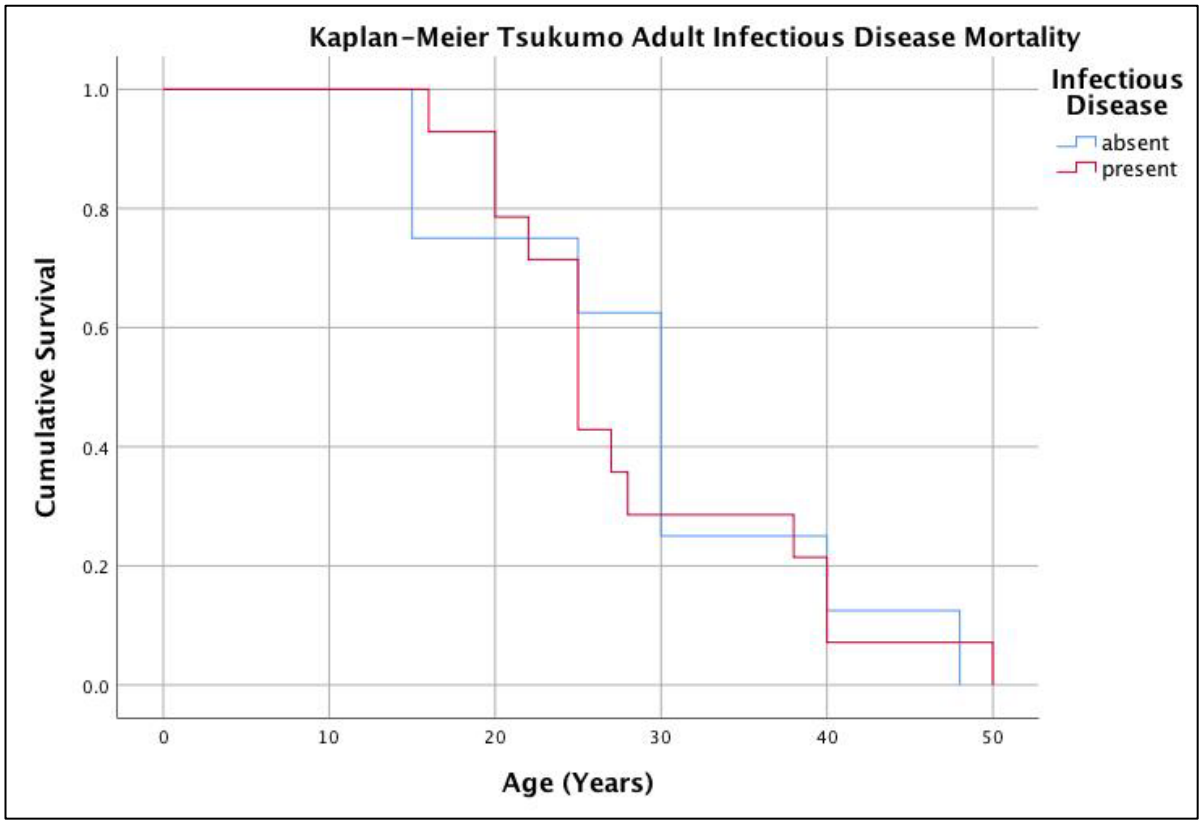

Figure 6.20: *Kaplan-Meier cumulative survival function of adult infectious disease mortality at Tsukumo. Image: author's own*

6.6.5 Diagnosis of Nutritional Disease at Tsukumo

6.6.5.1 Diagnosis of Nutritional Disease in Nonadults

Sixty-four percent (63.6%, 7/11) of nonadults exhibited lesions consistent with a diagnosis of probable, and 18.2% (2/11) exhibited lesions consistent with a possible diagnosis of scurvy (Table 6.24). Macroscopic lesions diagnostic for scurvy consisted of bilateral and symmetrical SPNB deposits associated with abnormal cortical porosity and sometimes vascular impressions on the sphenoid bones, temporal bones, maxillae, zygomatic bones, mandibles, superior orbits, as well as abnormal endochondral porosity exceeding 10mm from the metaphyseal plates of long bones (Figure 6.21). Radiographic signs of scurvy were observed in three nonadults aged between approximately 2 to 3 years. Radiographic signs included ground glass osteopenia, and white line of Fraenkel in combination with Trummerfeld zones (Figure 6.21a). Overall, 81.8% of the nonadult assemblage at Tsukumo presented with skeletal signs of scurvy consistent with a possible or probable diagnosis.

6.6.5.2 Diagnosis of Nutritional Disease in Adults

All Tsukumo adults (100%, 19/19) exhibited lesions that met the threshold criteria for at least a possible diagnosis with scurvy, and almost 80% (78.9%, 15/19) of Tsukumo adults exhibited lesions consistent with a diagnosis of probable scurvy. Discrete bilateral and symmetrical SPNB were present on both the crania (100%, 19/19) and postcrania (26.3%, 5/19). As was the case in nonadults, SPNB deposits were present symmetrically on the sphenoid bones, temporal bones, maxillae, and mandibles of adults (Figure 6.22). In many adults the SPNB was well remodelled. The prevalence of probable scurvy was high in all age cohorts (Figure 6.23). No individual in the Tsukumo assemblage had any signs of mineralisation disorders such as rickets or osteomalacia.

Table 6.24: *Summary of nutritional disease at Tsukumo*

SCURVY	**POSSIBLE**			**PROBABLE**			**POSSIBLE AND PROBABLE**		
	Affected	*Observed*	*(%)*	*Affected*	*Observed*	*(%)*	*Affected*	*Observed*	*(%)*
1 to 5 years	0	7	0	5	7	71.4	5	7	71.4
6 to 10 years	0	0	0	0	0	0	0	0	0
11 to 14 years	1	2	50	1	2	50	2	2	100
15 to 19 years	1	2	50	1	2	50	2	2	100
20 to 29 years	2	10	20	8	10	80	10	10	100
30 to 39 years	2	4	50	2	4	50	4	4	100
40 to 49 years	0	4	0	4	4	100	4	4	100
50+ years	0	1	0	1	1	100	1	1	100
Total nonadults	2	11	18.2	7	11	63.6	9	11	81.8
Males	2	12	16.7	10	12	83.3	12	12	100
Females	3	9	33.3	6	9	66.7	9	9	100
Total adults	4	19	21.1	15	19	78.9	19	19	100
Total	6	30	20	22	30	73.3	28	30	93.3

Figure 6.21: *Lesions in Tsukumo nonadults consistent with scurvy. a) White lines of Fraenkel (white arrows) and Trummerfeld zones (yellow arrow) of the metaphyseal plates of the tibia (Tsukumo 71, approx. 2 years). b) SPNB and abnormal cortical porosity on the lateral right sphenoid. Note the vascular impression (black arrow; Tsukumo 31, approx. 2 years). c) SPNB and abnormal cortical porosity on the posterior left maxilla and zygoma. Note the vascular impressions (black arrow, Tsukumo 56, approx. 3 years). d) Abnormal endochondral porosity exceeding 10mm from the metaphyseal plates of the tibia (Tsukumo 21, approx. 3 years). e) SPNB and abnormal cortical porosity of the superior left orbit. Note the vascular impressions (black arrows, Tsukumo 21, approx. 3 years). f) SPNB of the medial left coronoid process of the mandible (Tsukumo 21, approx. 3 years). g) SPNB and abnormal cortical porosity of the inferior pars basilaris (Tsukumo 26, approx. 1.5 years). h) SPNB and abnormal cortical porosity of the palatal surface of the maxilla (Tsukumo 21, approx. 3 years). i) SPNB and abnormal cortical porosity on the anterior maxilla (Tsukumo 31, approx. 2 years). j) SPNB and abnormal cortical porosity on the medial left coronoid process of the mandible (Tsukumo 56, approx. 3 years). Image: author's own.*

Figure 6.22: *Lesions in Tsukumo adults consistent with scurvy. a-b) SPNB and abnormal cortical porosity on the anterior and posterior maxilla (black arrows). SPNB is extending from around the infraorbital foramen (Tsukumo 3, young adult male). c) SPNB and abnormal cortical porosity on the posterior left zygoma (Tsukumo 60, young adult female). d) SPNB and abnormal cortical porosity on the left lateral sphenoid bone and temporal bone (Tsukumo 3, young adult male). e) SPNB and cortical porosity on the anterior right zygoma. Note the vascular impression (black arrow, Tsukumo 30, young adult male). f) SPNB and abnormal cortical porosity on the medial right coronoid process of the mandible (Tsukumo 23, old adult male). g) SPNB on the supraspinous fossa of the right scapula (Tsukumo 23, old adult male). Image: author's own.*

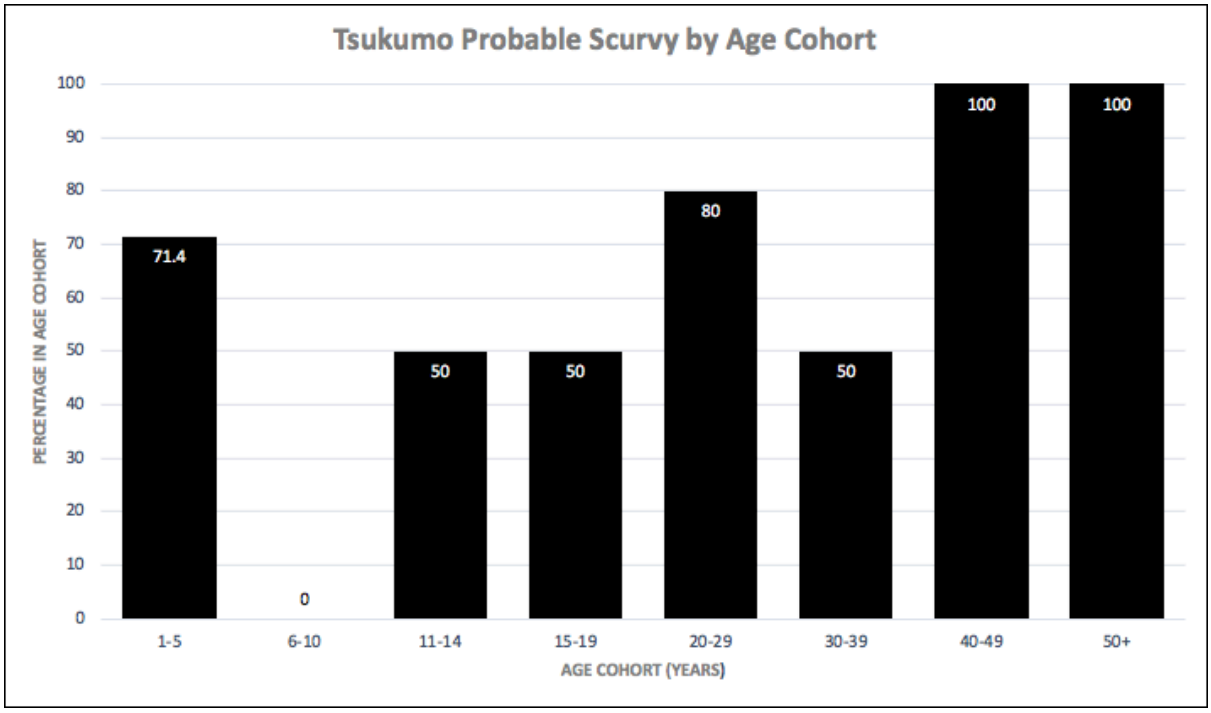

Figure 6.23: *Age-at-death distribution of probable scurvy at Tsukumo. Image: author's own.*

6.6.6 Morbidity of Nutritional Disease at Tsukumo

Nonadult morbidity could only be assessed between age groups under and over 5 years of age, due to a lack of individuals representing infants and older childhood age groups. No statistically significant differences in morbidity with combined possible and probable cases of scurvy were apparent between males and females, and across adult and nonadult cohorts (Table 6.25). This outcome was expected given that 100% of the Tsukumo adults exhibited lesions at least consistent with a diagnosis of possible scurvy. However, there was a significantly higher level of morbidity of probable scurvy in Tsukumo adults over the age of 40 years of age (n=22, RR=0.6471, p=0.0151). Tsukumo adults over 40 years of age were 1.5 times more likely to exhibit lesions consistent with a probable diagnosis of scurvy, than those under 40 years of age. There remained no significant differences between males and females, even when considering probable only cases (n=21, RR=0.8000, p=0.4064).

Table 6.25: *Relative risk of scurvy morbidity at Tsukumo across sex and age cohorts.*

EXPOSED GROUP/ CONTROL GROUP	OUTCOME		RR	P-VALUE	95%CI
	Positive: *Scurvy Present*	***Negative:*** *Scurvy Absent*			
Possible and Probable (combined)					
Sex					
Female/ Male	9/12	0/0	1.0000	1.0000	1.0000
Nonadults					
<1 yr/ >1 yr	-	-	-	-	-
<5 yrs/ >5yrs	5/4	2/0	0.7143	0.1593	0.4471- 1.1412
<10 yrs/ >10yrs	-	-	-	-	-
Adults					
<20 yrs/ >20 yrs	3/19	0/0	1.0000	1.0000	1.0000
<30 yrs/ >30 yrs	13/9	0/0	1.0000	1.0000	1.0000
<40 yrs/>40 yrs	17/5	0/0	1.0000	1.0000	1.0000
Probable Only					
Sex					
Female/ Male	6/10	3/2	0.8000	0.4064	0.4724- 1.3547
Nonadults					
<1 yr/ >1 yr	-	-	-	-	-
<5 yrs/ >5yrs	5/4	2/0	0.7143	0.1593	0.4471- 1.1412
<10 yrs/ >10yrs	-	-	-	-	-
Adults					
<20 yrs/ >20 yrs	1/15	2/4	0.4222	0.2960	0.0838- 2.1273
<30 yrs/ >30 yrs	9/7	4/2	0.8901	0.6503	0.5381- 1.4724
<40 yrs/>40 yrs	11/5	6/0	**0.6471**	**0.0151***	0.4555- 0.9192

A relative risk (RR) >1 denotes a relationship of the exposed group with an increase in disease prevalence, whereas RR <1 denotes a relationship of the control group with an increase in disease prevalence.
*= statistically significant (p<0.10). **= statistically significant when considering size of the effect of RR.

6.6.7 Mortality of Nutritional Disease at Tsukumo

Nonadults with a diagnosis of probable scurvy exhibited significantly better survivorship past the age of 5 years than those without a probable diagnosis in relative risk ratio analysis (n=11, RR=0.5556, p= 0.0487). Nonadults without skeletal signs for probable scurvy were then almost 2 times more likely to die before the age of 5 years of age (Table 6.26). As no possible cases of scurvy were diagnosed in the Tsukumo nonadults, the outcome remained the same for combined possible and probable cases. Similarly Tsukumo adults diagnosed with probable cases of scurvy were 5.3 times more likely to survive past the age of 20 than their adolescent counter parts (15-19 years) which was statistically

significant (n=22, RR=0.1875, p=0.0487). These adults diagnosed with probable scurvy were also almost 1.5 times more likely to survive past 40 years of age (n=22, RR=0.687, p=0.0262).

Kaplan-Meier survival analysis (n=11, X^2=1.798, df=1, p=0.180; Table 6.27) and Cox regression (n=11, Wald=1.378, df=1, p=0.240; Table 6.28) indicate no statistically significant differences between probable cases of scurvy in nonadults compared to those not diagnosed. The cumulative survival graph for the Kaplan-Meier (Figure 6.24) and Cox regression (Figure 6.25) demonstrate the opposite than identified with relative risk ratio analysis, with a lower survival trend in individuals with skeletal evidence from scurvy. Disparities between the statistical techniques is likely due to the low sample size (n=11) and poor representation of individuals across nonadult age cohorts. For this reason, the relationship of probable scurvy in nonadults to mortality remains undetermined.

Kaplan-Meier survival analysis was not conducted on combined possible and probable cases of scurvy in adults, as all adults in the Tsukumo assemblage met these criteria. A statistically significant relationship of probable scurvy with survivorship in Tsukumo adults is identified by the Kaplan-Meier survival analysis (n=22,X^2=2.490, df=1, p=0.115; Table 6.29). Whereas a statistically significant relationship was not identified in Cox regression (n=22, Wald=2.067, df=1, p=0.151; Table 6.30). Given the small sample size of the assemblage, and the conservative estimate of Cox regression, this outcome does not negate evidence of survivorship of adults in Tsukumo with skeletal lesions consistent with probable scurvy. This is additionally supported by the size of the effect of the odds ratio from the Cox regression output (OR=2.080; Table 6.30). Figures 6.26 and 6.27 indicate clear differences in the trend of survivorship between those diagnosed with probable scurvy and the remainder of the Tsukumo assemblage diagnosed with possible scurvy. Overall skeletal signs of probable adult scurvy in the Tsukumo assemblage are consistent with increased survivorship to older age.

Table 6.26: *Relative risk of scurvy mortality at Tsukumo across age cohorts.*

POSITIVE OUTCOME/ NEGATIVE OUTCOME	TREATMENT		RR	P-VALUE	95%CI
	Exposed Group: *Scurvy Present*	***Control Group:*** *Scurvy Absent*			
Possible and Probable (combined)					
Nonadults					
<1 yr/ >1 yr	-	-	-	-	-
<5 yrs/ >5yrs	5/4	2/0	**0.5556**	**0.0487***	0.3097- 0.9966
<10 yrs/ >10yrs	-	-	-	-	-
Adults					
<20 yrs/ >20 yrs	3/19	0/0	0.3043	0.2858	0.0342- 2.7046
<30 yrs/ >30 yrs	13/9	0/0	1.1739	0.8745	0.1605- 8.5857
<40 yrs/>40 yrs	17/5	0/0	1.5217	0.6767	0.2115- 10.9485
Probable Only					
Nonadults					
<1 yr/ >1 yr	-	-	-	-	-
<5 yrs/ >5yrs	5/4	2/0	**0.5556**	**0.0487***	0.3097- 0.9966
<10 yrs/ >10yrs	-	-	-	-	-
Adults					
<20 yrs/ >20 yrs	1/15	2/4	**0.1875**	**0.1376****	0.0206- 1.7084
<30 yrs/ >30 yrs	9/7	4/2	0.8438	0.6400	0.4140- 1.7195
<40 yrs/>40 yrs	11/5	6/0	**0.6875**	**0.0262***	0.4941- 0.9566

A relative risk (RR) >1 denotes a relationship of the disease presence with the positive outcome (susceptibility to mortality), whereas RR <1 denotes a relationship of the disease absence with a negative outcome (survivorship).
*= statistically significant (p<0.10). **= statistically significant when considering size of the effect of RR.

Table 6.27: *Statistical summary for Kaplan-Meier function of probable scurvy mortality of nonadults at Tsukumo.*

PROBABLE SCURVY	ESTIMATE	STD. ERROR	95% CI	LOG RANK (MANTEL-COX)		
				CHI SQUARE	DF	P-VALUE
Mean				1.798	1	0.180
Absent	9.250	2.121	2.121- 16.379			
Present	5.500	1.681	1.381- 9.619			
Overall	6.864	3.220	3.220- 10.507			
Median						
Absent	4.000	6.500	0.000- 16.740			
Present	3.000	0.598	1.829- 4.171			
Overall	3.000	1.101	0.842- 5.158			

*= statistical significance (p<0.15).

Table 6.28: *Statistical summary for Cox regression function of probable scurvy mortality of nonadults at Tsukumo.*

PROBABLE SCURVY	COEFFICIENT (β)	STD. ERROR	WALD	DF	P-VALUE	ODDS RATIO (Exp(β))
	-0.829	0.707	1.378	1	0.240	0.436

*= statistical significance (p<0.15).

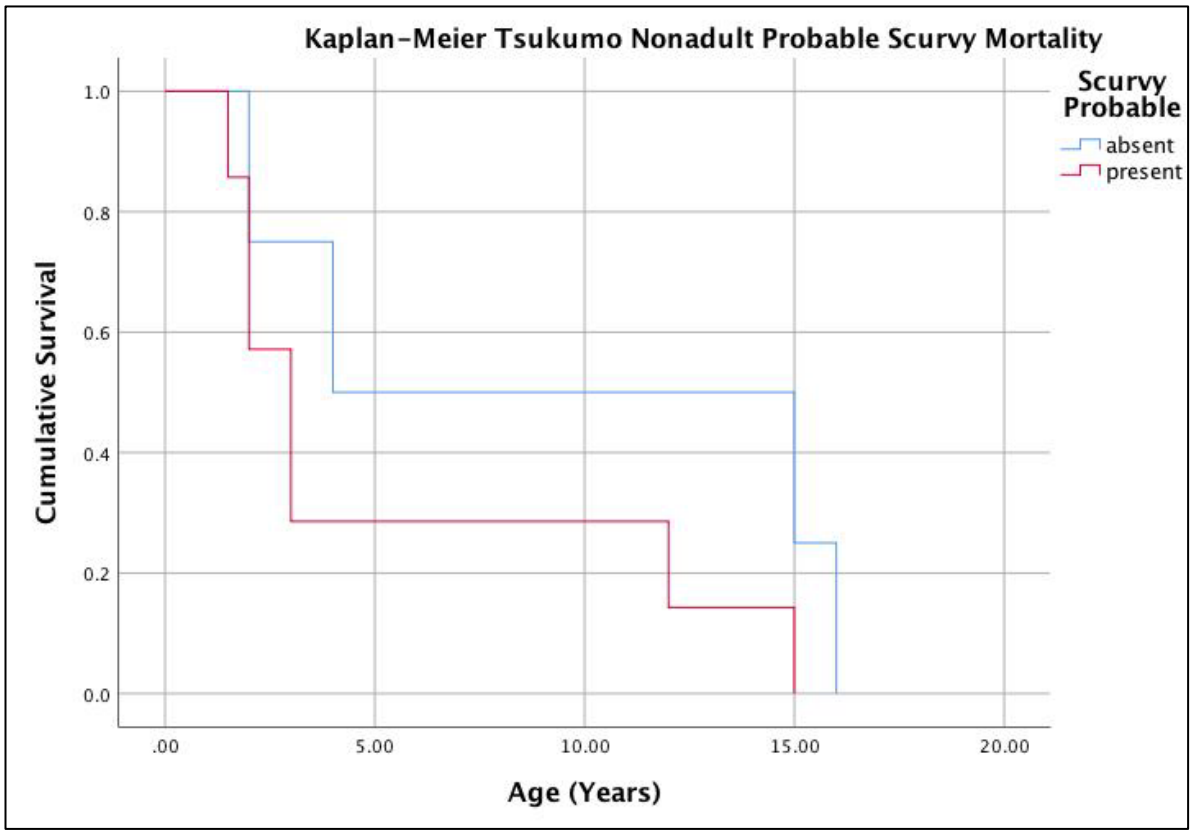

Figure 6.24: *Kaplan-Meier cumulative survival function of nonadult probable scurvy mortality at Tsukumo. Image: author's own*

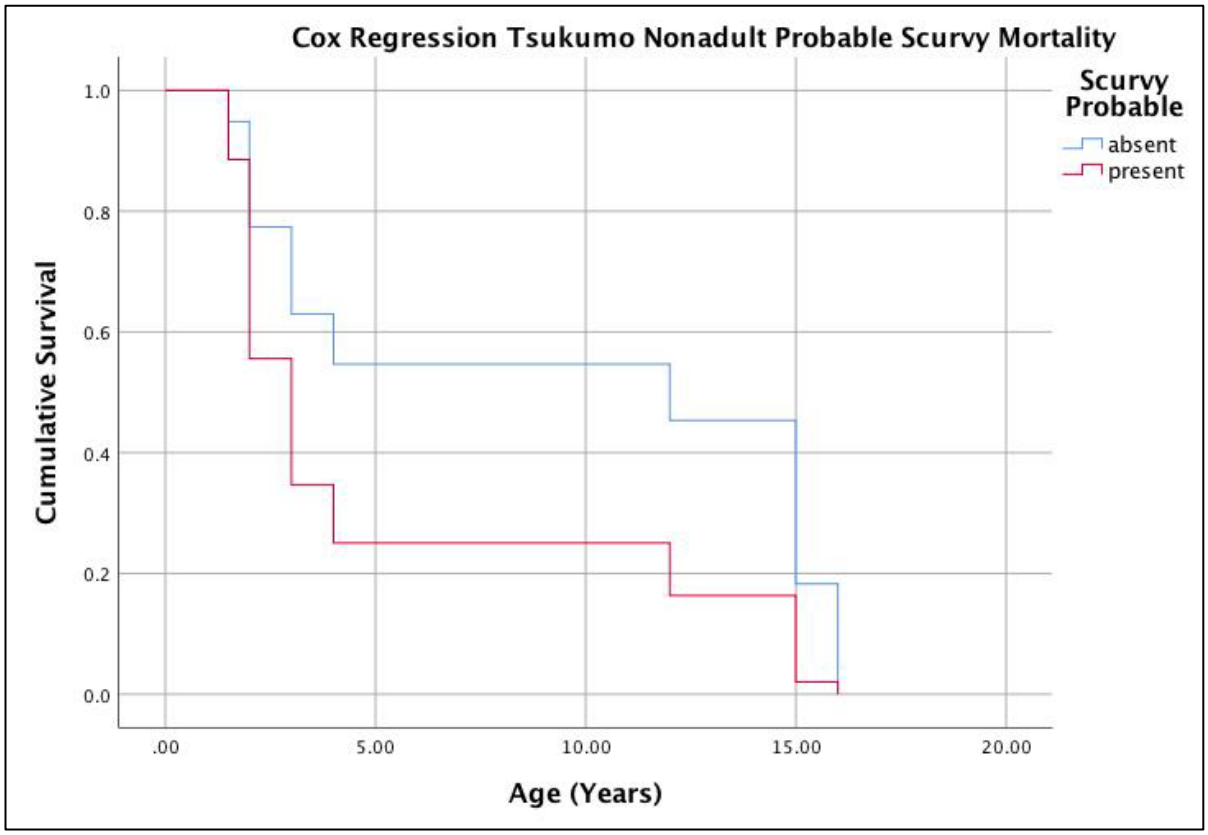

Figure 6.25: *Cox regression cumulative survival function of nonadult probable scurvy mortality at Tsukumo. Image: author's own*

Table 6.29: *Statistical summary for Kaplan-Meier function of probable scurvy mortality of adults at Tsukumo.*

PROBABLE SCURVY	ESTIMATE	STD. ERROR	95% CI	LOG RANK (MANTEL-COX)		
				CHI SQUARE	DF	P-VALUE
Mean				2.490	1	**0.115***
Absent	24.000	3.624	16.897- 25.693			
Present	30.625	2.516	25.693- 35.557			
Overall	28.818	2.135	24.634- 33.002			
Median						
Absent	20.000	5.511	9.198- 30.802			
Present	27.000	3.000	21.120- 32.880			
Overall	25.000	2.010	21.060- 28.940			

*= statistical significance (p<0.15).

Table 6.30: *Statistical summary for Cox regression function of probable scurvy mortality of adults at Tsukumo.*

PROBABLE SCURVY	COEFFICIENT (β)	STD. ERROR	WALD	DF	P-VALUE	ODDS RATIO (Exp(β))
	0.732	0.509	2.067	1	0.151	2.080

*= statistical significance (p<0.15).

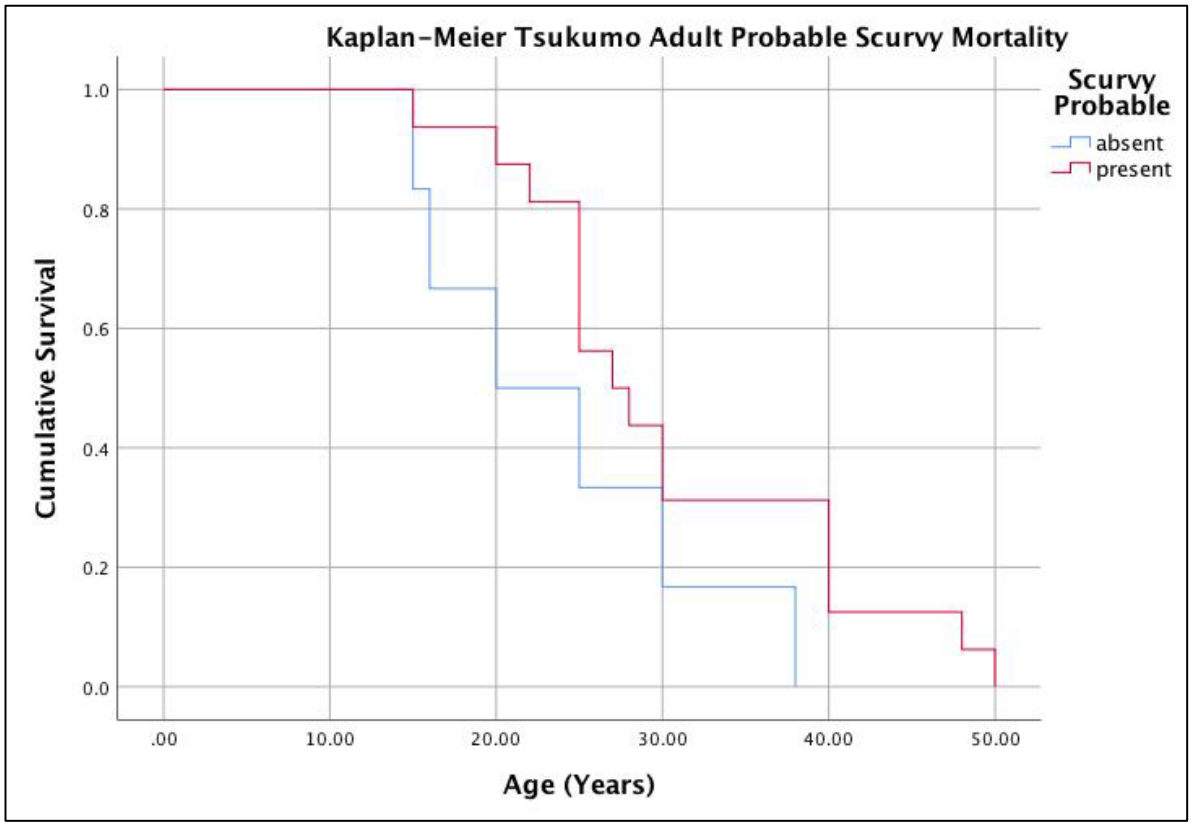

Figure 6.26: *Kaplan-Meier cumulative survival function of adult probable scurvy mortality at Tsukumo. Image: author's own*

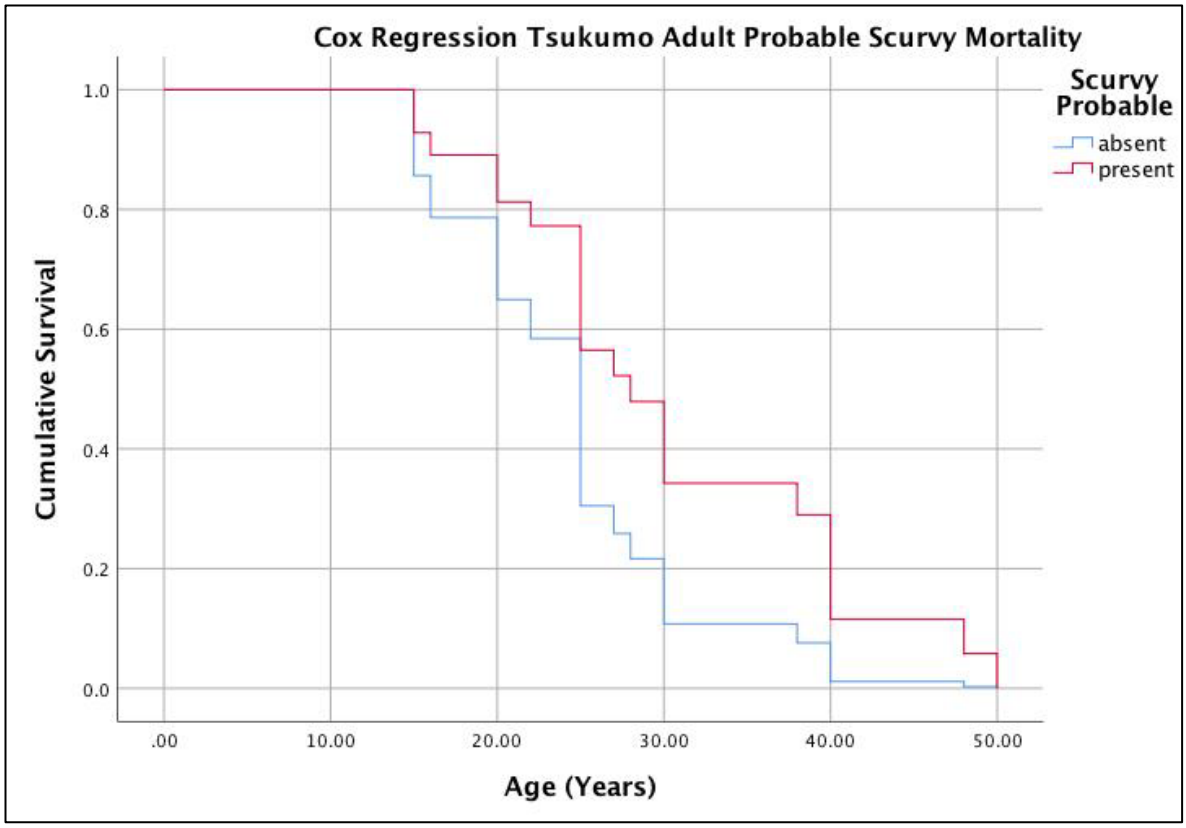

Figure 6.27: *Cox regression cumulative survival function of adult probable scurvy mortality at Tsukumo. Image: author's own*

6.6.8 Diagnosis of Anaemia at Tsukumo

Almost 70% (69.2%, 18/26) of the overall Tsukumo assemblage exhibited moderate or severe grade cribra orbitalia, and/or porotic hyperostosis consistent with a diagnosis of childhood anaemia (Table 6.31; Figure 6.28). As was the case in Ota, individuals diagnosed with anaemia from porotic hyperostosis only also exhibited mild grade cribra orbitalia. Skeletal signs of anaemia were only found in individuals over the age of 15 years. All age cohorts from 15 years onwards exhibited high prevalences of anaemia (Figure 6.29). All males (100%, 11/11) experienced childhood anaemia, whereas only 66.7% of females (6/9) showed skeletal signs of childhood anaemia.

Table 6.31: *Summary of anaemia at Tsukumo.*

ANAEMIA	**CO**			**Cranial PH**			**PH and/or CO**		
	Affected	*Observed*	*(%)*	*Affected*	*Observed*	*(%)*	*Affected*	*Observed*	*(%)*
1 to 5 years	0	4	0	0	4	0	0	5	0
6 to 10 years	0	0	0	0	0	0	0	0	0
11 to 14 years	0	1	0	0	1	0	0	1	0
15 to 19 years	1	2	50	2	2	100	2	2	100
20 to 29 years	6	8	75	6	9	66.7	7	9	77.8
30 to 39 years	2	4	50	3	4	75	3	4	75
40 to 49 years	2	4	50	4	4	100	4	4	100
50+ years	1	1	100	1	1	100	1	1	100
Males	7	10	70	10	11	90.9	11	11	100
Females	4	8	50	6	9	66.7	6	9	66.7
Total nonadults	1	7	14.3	2	8	25	2	8	25
Total adults	11	17	64.7	14	18	77.8	15	18	83.3
Total	12	24	50	16	26	61.5	18	26	69.2

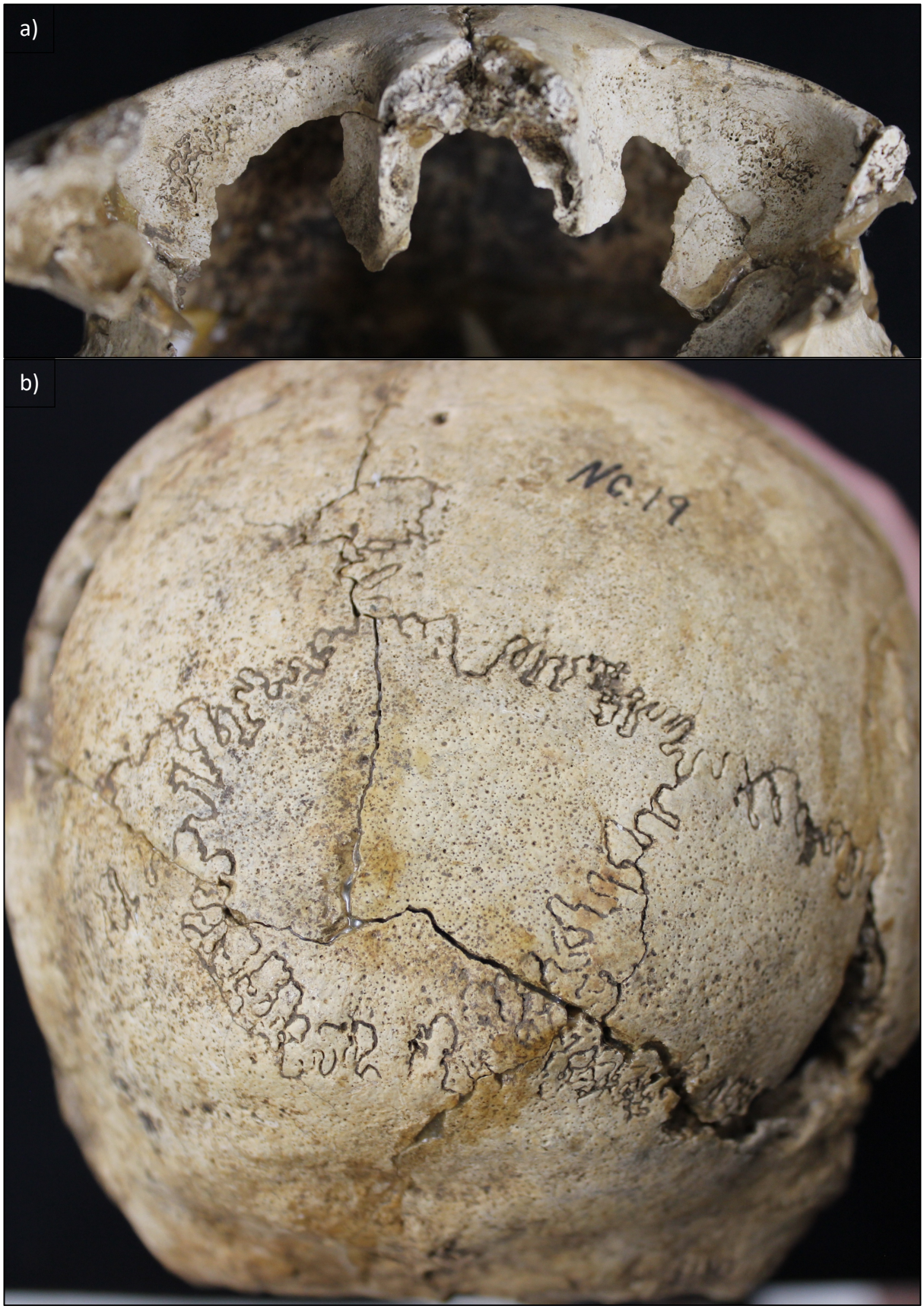

Figure 6.28: *Lesions consistent with anaemia in Tsukumo. a) Moderate grade cribra orbitalia (Tsukumo 60, young adult female). b) Porotic hyperostosis of the cranial vault. Diploic expansion could be observed through postmortem breaks in the vault (Tsukumo 19, middle aged adult male). Image: author's own.*

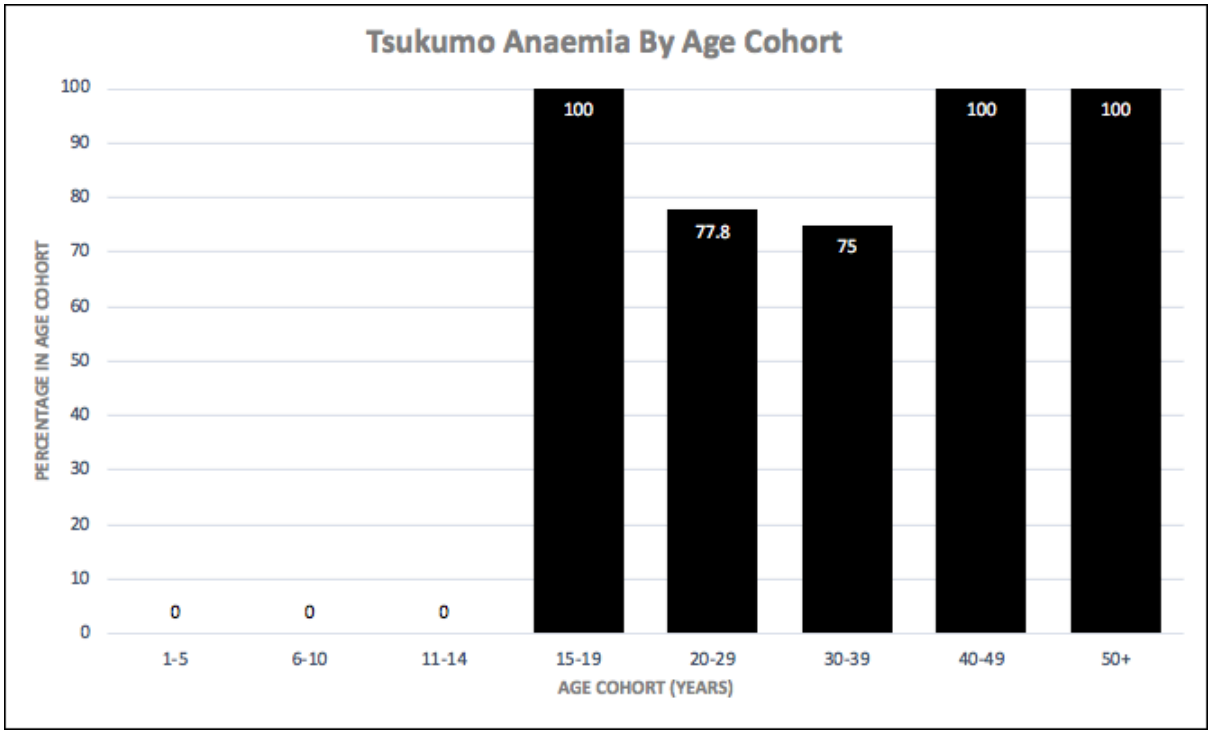

Figure 6.29: *Age-at-death distribution of anaemia at Tsukumo. Image: author's own.*

6.6.9 Morbidity of Anaemia at Tsukumo

A statistically significant difference in the prevalence of anaemia in males compared to females was identified (n=20, RR=0.6667, p=0.0854). Males were 1.5 times more likely to have anaemia than females (Table 6.32). There was a statistical relationship between the presence of anaemia and older nonadults. Nonadults over the age of 5 years of age were 8.4 times more likely to have anaemia, than those under 5 years of age (n=9, RR=0.1190, p=0.1245). Adolescents (15-19 year olds) were 1.2 times more likely to exhibit anaemia than adults over 20 years of age, which was statistically significant (n=20, RR=1.200, p=0.0854). However, adults were 1.2 times more likely to have evidence of childhood anaemia when under 40 years of age (n=20, RR=0.8000, p=0.0839).

Table 6.32: *Relative risk of anaemia morbidity at Tsukumo across sex and age cohorts.*

EXPOSED GROUP/ CONTROL GROUP	OUTCOME		RR	P-VALUE	95%CI
	Positive: *Anaemia Present*	***Negative:*** *Anaemia Absent*			
Sex					
Female/ Male	6/11	3/0	**0.6667**	**0.0854***	0.4200- 1.0581
Nonadults					
<1 yr/ >1 yr	-	-	-	-	-
<5 yrs/ >5yrs	0/3	5/1	**0.1190**	**0.1245****	0.0079- 1.7985
<10 yrs/ >10yrs	-	-	-	-	-
Adults					
<20 yrs/ >20 yrs	2/15	0/3	**1.2000**	**0.0837***	0.9760- 1.4754
<30 yrs/ >30 yrs	9/8	2/1	0.9205	0.6535	0.6410- 1.3218
<40 yrs/>40 yrs	12/5	3/0	**0.8000**	**0.0839***	0.6212- 1.0303

A relative risk (RR) >1 denotes a relationship of the exposed group with an increase in disease prevalence, whereas RR <1 denotes a relationship of the control group with an increase in disease prevalence.
*= statistically significant (p<0.10). **= statistically significant when considering size of the effect of RR.

6.6.10 Mortality of Anaemia at Tsukumo

A statistically significant relationship with increased survivorship was identified for individuals exhibiting skeletal signs of anaemia in the nonadult cohort (n=9, RR=0.1591, p=0.1693; Table 6.32). Nonadults with skeletal signs for anaemia were 6.3 times more likely to survive past 5 years than those without skeletal evidence for anaemia. Additionally, Tsukumo adults were 1.4 times more likely to survive past the age of 40 years if they exhibited skeletal signs of childhood anaemia (n=20, RR=0.7059, p=0.0261).

Kaplan-Meier survivorship analysis was not conducted for the nonadult cohort due to the poor representation of individuals across age groups, and a sample size of only 9 individuals. No statistically significant relationship with increased mortality of individuals with skeletal signs of anaemia was identified with Kaplan-Meier survival analysis of adults (n=20, X^2=0.196, df=1, p=0.658; Table 6.34). However, as evidenced on the Kaplan-Meier cumulative survival graph (Figure 6.30), cumulative survival of individuals without skeletal signs of anaemia reaches 0% prior to the age of 40 years. It is then possible that there may be a slight effect of survivorship to old age in individuals with skeletal signs for anaemia.

Table 6.33: *Relative risk of anaemia mortality at Tsukumo across age cohorts.*

POSITIVE OUTCOME/ NEGATIVE OUTCOME	**TREATMENT**		**RR**	**P-VALUE**	**95%CI**
	Exposed Group: *Anaemia Present*	***Control Group:*** *Anaemia Absent*			
Nonadults					
<1 yr/ >1 yr	-	-	-	-	-
<5 yrs/ >5yrs	0/3	5/1	**0.1591**	**0.1693****	0.0351- 4.7712
<10 yrs/ >10yrs	-	-	-	-	-
Adults					
<20 yrs/ >20 yrs	2/15	0/3	1.1111	0.9420	0.0651- 18.9520
<30 yrs/ >30 yrs	9/8	2/1	0.7941	0.6223	0.3174- 1.9870
<40 yrs/>40 yrs	12/5	3/0	**0.7059**	**0.0261***	0.5194- 0.9594

A relative risk (RR) >1 denotes a relationship of the disease presence with the positive outcome (susceptibility to mortality), whereas RR <1 denotes a relationship of the disease absence with a negative outcome (survivorship).
*= statistically significant (p<0.10). **= statistically significant when considering size of the effect of RR.

Table 6.34: *Statistical summary for Kaplan-Meier function of anaemia mortality of adults at Tsukumo.*

ANAEMIA	**ESTIMATE**	**STD. ERROR**	**95% CI**	**LOG RANK (MANTEL-COX)**		
				CHI SQUARE	**DF**	**P-VALUE**
Mean				0.196	1	0.658
Absent	29.333	4.333	20.840- 37.827			
Present	29.222	2.499	24.324- 34.120			
Overall	29.238	2.195	24.936- 33.541			
Median						
Absent	25.000	-	-			
Present	27.000	3.182	20.763- 33.237			
Overall	27.000	1.962	23.155- 30.845			

*= statistical significance (p<0.15).

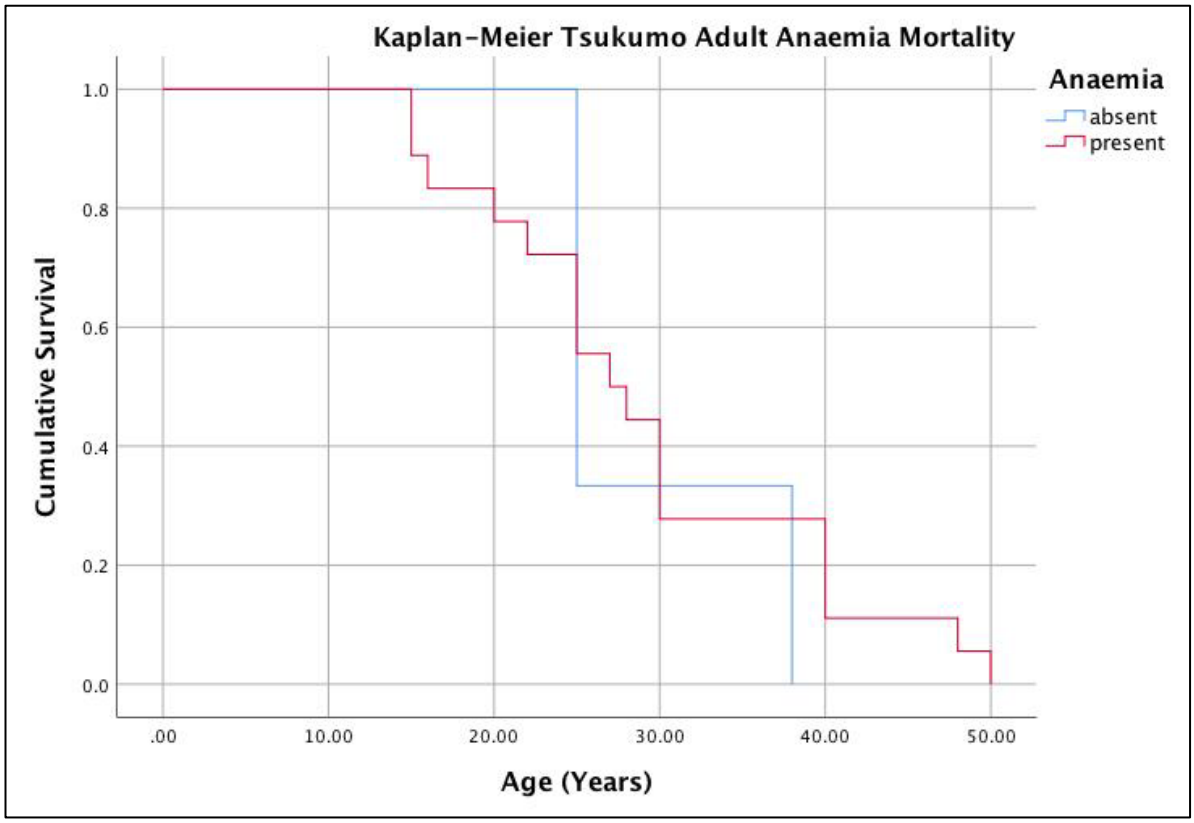

Figure 6.30: *Kaplan-Meier cumulative survival function of adult anaemia mortality at Tsukumo. Image: author's own*

6.6.11 Summary of Diagnosis and Context of Disease at Tsukumo

Overall a high infectious and nutritional disease burden was apparent in the Tsukumo community. Almost fifty percent (46.7%, 14/30) of the overall Tsukumo assemblage exhibited infectious disease, whereas nearly all Tsukumo individuals (93.3%, 28/30) were diagnosed with a possible or probable case of scurvy. Additionally, 69.2% (18/26) exhibited skeletal evidence for anaemia during their childhood.

6.6.11.1 Vertebral Body Osteomyelitis at Tsukumo

While direct traumatic introduction of pathogens is common in osteomyelitis, this is only clinically documented in vertebral body osteomyelitis where pathogens have been introduced through spinal surgery (Carragee 1997; Skaf et al. 2010). Therefore, it is more likely the vertebral body osteomyelitis in Tsukumo 6 was related to a systemic origin. Non-surgically related vertebral body osteomyelitis is most commonly associated with genito-urinary infections spread through the bloodstream to the intervertebral discs of the lower thoracic and lumbar spine (spondylodiscitis) eventually infecting bone (Carragee 1997; Skaf et al. 2010). Given the systemic origin, vertebral body osteomyelitis is most commonly

associated with immunocompromised individuals (Carragee 1997; Skaf et al. 2010). Tsukumo 6 was also diagnosed with probable scurvy, and some scorbutic lesions remained active indicating that the individual had experienced a recent case of scurvy prior to death.

6.6.11.2 Scurvy at Tsukumo

Similar circumstances for the prevalence of scurvy at Ota can be argued for Tsukumo. That is, that a combination of seasonal restriction of Vitamin C available foods, food processing techniques, food storage methods and selective eating may have contributed to the burden of scurvy in the Tsukumo community. An increased reliance on terrestrial foods by the Tsukumo inhabitants decreased supplementation of marine sources with Vitamin C, possibly contributing to the high prevalence of scurvy. Reduced food returns from the forest following climate cooling may have also increased periods of food scarcity and poor resource returns that may have had a significant impact on Tsukumo given their reliance on terrestrial resources.

Almost all Tsukumo individuals both adults and nonadults were diagnosed with at least possible scurvy, which indicates a shared burden of micronutrient deficiency throughout the community. The Hadza hunter-gatherers of Northern Tanzania demonstrate an increased sharing of food provisions during times of resource scarcity, or to prevent periods of food shortage (Hawkes et al. 2014). It is possible a similar foraging strategy was employed by the Tsukumo inhabitants during times of nutritional stress. Given that scurvy lesions form only during recovery of Vitamin C, a high prevalence of scurvy in the Tsukumo does also indicate that almost all individuals in Tsukumo survived the active progression of scurvy, and exhibited some recovery of Vitamin C. This finding supports the possibility of the Tsukumo inhabitants employing a strategy that increased community morbidity with nutritional stress but reduced the community's mortality burden overall.

Adults with lesions consistent with a probable diagnosis presented with increased survivorship compared to the remainder of Tsukumo adults diagnosed with possible scurvy. It is possible individuals with probable scurvy suffered scurvy for prolonged periods, or a number of seasonal cycles enabling development of more skeletal lesions. Lesions in middle-aged and old adults were predominantly remodelled and may have accumulated in

the skeleton over time over multiple instances of scurvy. Such individuals then were less frail than other individuals who succumbed with scurvy at an earlier stage in time.

Seventy-five percent (9/12) of adults with infectious disease and 50% (4/8) without infectious disease were diagnosed with probable scurvy. Therefore, there is not clear evidence for skeletal co-morbidity of infectious and nutritional disease. However, it is likely the overall infectious disease burden, including diseases that do not alter bone, increased the bodily needs for Vitamin C and therefore may have contributed to the overall prevalence of scurvy in the Tsukumo community.

6.6.11.3 Anaemia at Tsukumo

As was the case with scurvy, the conditions which resulted in childhood anaemia at Ota are also likely to have resulted in anaemia in Tsukumo inhabitants. That is, childhood anaemia was likely related to a combination of nutritional stress, parasitic load, and infection. If children were involved in foraging tasks, given the variety of ecologies exploited by the Jomon, exposure to parasites or infection from pathogens in the environment was likely. With periods of reduced terrestrial food returns in the Tsukumo community, this may have also increased nutritional stress, increased iron, vitamins A and B12, and folate deficiency contributing to the overall anaemia prevalence in the Tsukumo assemblage. Exposure to stressors causing anaemia in childhood may have contributed to death prior to achieving old age in Tsukumo adults, as no individual over the age of 40 years exhibited cribra orbitalia or porotic hyperostosis. As such, childhood stress may have had long lasting effects on the health of Tsukumo adults.

6.6.11.4 Intrapopulation Variation of Disease at Tsukumo

As was the case in the Ota assemblage, Tsukumo males exhibited significantly higher prevalences of childhood anaemia than Tsukumo females. All males in the Tsukumo assemblage had developed skeletal signs of anaemia in childhood. Interestingly, Kusaka et al. (2010) did not find dietary differences between males and females in the Tsukumo assemblage, suggesting that differences between Tsukumo boys and girls may not be related to gender-specific diets. However, if children contributed to foraging, Tsukumo boys may have been involved in different foraging practices than Tsukumo girls, which increased the exposure of Tsukumo boys to pathogens in their surrounding environment. However,

females (77.8%, 7/9) exhibited higher levels of infectious disease than males (58.3%, 7/12), but this was not statistically significant. Tsukumo boys may then have been at higher risk of nutritional stress. Males (83.3%, 10/12) exhibited higher prevalences of scurvy than females (66.7%, 6/9), which supports the latter argument. Again this was not statistically significant and the differential outcome is likely to be a complex interaction between both biological factors of disease between sex and social variations in resource access and use across genders. Further consideration of differences in the childhood stress of Tsukumo males and females is beyond the scope of this thesis but remains an interesting area for further research. The following section will assess the role of human population interaction on the changing disease dynamics from the Middle to Late and Final Periods of the Western Honshu Jomon.

6.7 Regional Level Results: Middle to Late/Final Western Honshu Jomon

6.7.1 Diachronic Assessment of Morbidity of Infectious Disease from Middle to Late/Final Jomon

Due to the dearth of nonadults in the Ota assemblage, diachronic changes in infectious disease morbidity was only assessed for adults. Tsukumo adults were almost 3 times more likely to have had infectious disease than Ota adults which was statistically significant (n=54, RR=2.9091, p=0.0040; Table 6.35).

Table 6.35: *Relative risk of infectious disease morbidity from the Middle to Late/Final Jomon.*

EXPOSED GROUP/ CONTROL GROUP	**OUTCOME**		**RR**	**P-VALUE**	**95%CI**
	Positive: *Infectious Disease Present*	***Negative:*** *Infectious Disease Absent*			
Adults					
Tsukumo/ Ota	14/7	8/25	**2.9091**	**0.0040***	1.4061- 6.0185

A relative risk (RR) >1 denotes a relationship of the exposed group with an increase in disease prevalence, whereas RR <1 denotes a relationship of the control group with an increase in disease prevalence.
*= statistically significant (p<0.10). **= statistically significant when considering size of the effect of RR.

6.7.2 Diachronic Assessment of Morbidity of Nutritional Disease from Middle to Late/Final Jomon

Overall morbidity of scurvy was significantly higher in the Tsukumo adults when considering combined possible and probable, and probable only cases of scurvy (Table 6.36). Tsukumo adults were over 4.5 times more likely to exhibit lesions consistent with a probable diagnosis of scurvy than Ota adults (n=54, RR=4.6545, p=0.0004).

Table 6.36: *Relative risk of scurvy morbidity from the Middle to Late/Final Jomon.*

EXPOSED GROUP/ CONTROL GROUP	**OUTCOME**		**RR**	**P-VALUE**	**95%CI**
	Positive: *Scurvy Present*	***Negative:*** *Scurvy Absent*			
Possible and Probable (combined) Scurvy					
Adults					
Tsukumo/ Ota	22/11	0/21	**2.9091**	**<0.0001***	1.8024- 4.6954
Probable Only Scurvy					
Adults					
Tsukumo/ Ota	16/5	6/27	**4.6545**	**0.0004***	1.9997- 10.8339

A relative risk (RR) >1 denotes a relationship of the exposed group with an increase in disease prevalence, whereas RR <1 denotes a relationship of the control group with an increase in disease prevalence.
*= statistically significant (p<0.10). **= statistically significant when considering size of the effect of RR.

6.7.3 Diachronic Assessment of Morbidity of Anaemia from Middle to Late/Final Jomon

There was a significant difference in the prevalence of anaemia when comparing the Ota adults to the Tsukumo adults (n=39, RR=1.3571, p=0.1203; Table 6.37). However, Tsukumo adults were only at a 1.4 times increased risk of developing anaemia in childhood.

Table 6.37: *Relative risk of anaemia morbidity from the Middle to Late/Final Jomon.*

EXPOSED GROUP/ CONTROL GROUP	**OUTCOME**		**RR**	**P-VALUE**	**95%CI**
	Positive: *Anaemia Present*	***Negative:*** *Anaemia Absent*			
Adults					
Tsukumo/ Ota	18/12	2/7	**1.4250**	**0.0629***	0.9811- 2.0697

A relative risk (RR) >1 denotes a relationship of the exposed group with an increase in disease prevalence, whereas RR <1 denotes a relationship of the control group with an increase in disease prevalence.
*= statistically significant (p<0.10). **= statistically significant when considering size of the effect of RR.

6.7.4 Diachronic Assessment of Overall Mortality from Middle to Late/Final Jomon

Relative risk ratio analysis indicates a significant increase in risk of mortality of Tsukumo adults under the age of 30 years, compared to Ota adults (Table 6.38). Tsukumo adults were 2.5 times more likely to die before the age of 30 years compared to Ota adults (n=47, RR=2.4621, p=0.0235).

Kaplan-Meier survival analysis indicates a significant increase in the risk of mortality of Tsukumo adults compared to Ota adults (n=47, X^2=4.875, df=1, p=0.027; Table 6.39). A statistically significant increase in risk of mortality was also met with Cox regression analysis (n=47, Wald=4.319, df=1, p=0.038; Table 6.40). The Kaplan-Meier (Figure 6.31) and Cox regression (Figure 6.32) cumulative survival functions indicate clear differences in trends of survivorship between Tsukumo and Ota adults.

Table 6.38: *Relative risk of overall mortality from the Middle to Late/Final Jomon across age cohorts.*

POSITIVE OUTCOME/ NEGATIVE OUTCOME	**TREATMENT**		**RR**	**P-VALUE**	**95%CI**
	Exposed Group: *Tsukumo*	***Control Group:*** *Ota*			
<20 yrs/ >20 yrs	3/1	19/24	3.4091	0.2722	0.3817- 30.4453
<30 yrs/ >30 yrs	13/6	9/19	**2.4621**	**0.0235***	1.1293- 5.3679
<40 yrs/>40 yrs	17/16	5/9	1.2074	0.3197	0.8330- 1.7501

A relative risk (RR) >1 denotes a relationship of the disease presence with the positive outcome (susceptibility to mortality), whereas RR <1 denotes a relationship of the disease absence with a negative outcome (survivorship).
*= statistically significant (p<0.10). **= statistically significant when considering size of the effect of RR.

Table 6.39: *Statistical summary for Kaplan-Meier function of overall mortality of adults from the Middle Period to Late/Final Periods Jomon Japan.*

OVERALL MORTALITY	**ESTIMATE**	**STD. ERROR**	**95% CI**	**LOG RANK (MANTEL-COX)**		
				CHI SQUARE	**DF**	**P-VALUE**
Mean				4.875	1	**0.027***
Absent	36.480	1.982	32.596- 40.364			
Present	28.818	2.135	24.634- 33.002			
Overall	32.894	1.543	29.869- 35.918			
Median						
Absent	35.000	2.082	30.920- 39.080			
Present	25.000	2.010	21.060- 28.940			
Overall	31.000	1.469	28.121- 33.879			

*= statistical significance (p<0.15).

Table 6.40: *Statistical summary for Cox regression function of overall mortality of adults from the Middle Period to Late/Final Periods Jomon Japan.*

OVERALL MORTALITY	COEFFICIENT (β)	STD. ERROR	WALD	DF	P-VALUE	ODDS RATIO (Exp(β))
	-0.630	0.303	4.319	1	**0.038***	0.533

*= statistical significance (p<0.15).

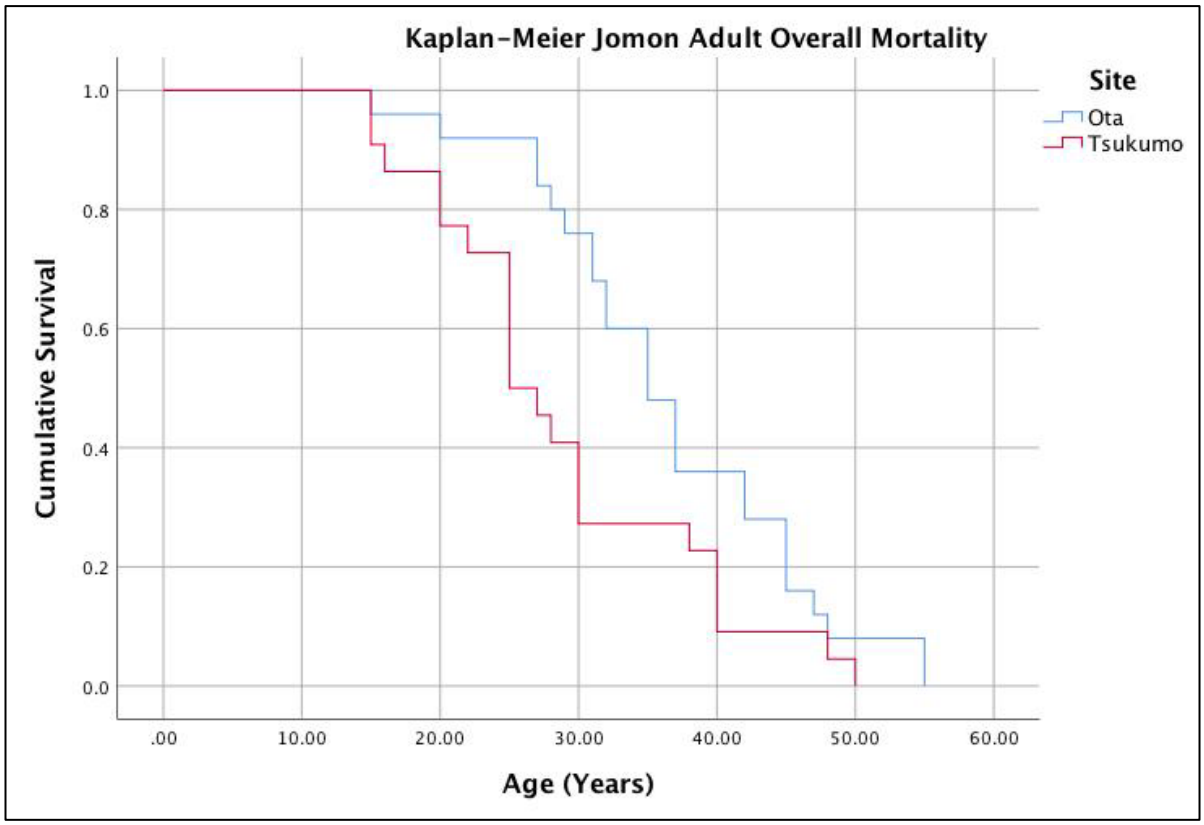

Figure 6.31: *Kaplan-Meier cumulative survival function of adult overall mortality from Middle Period to Late/Final Periods of Jomon Japan. Image: author's own*

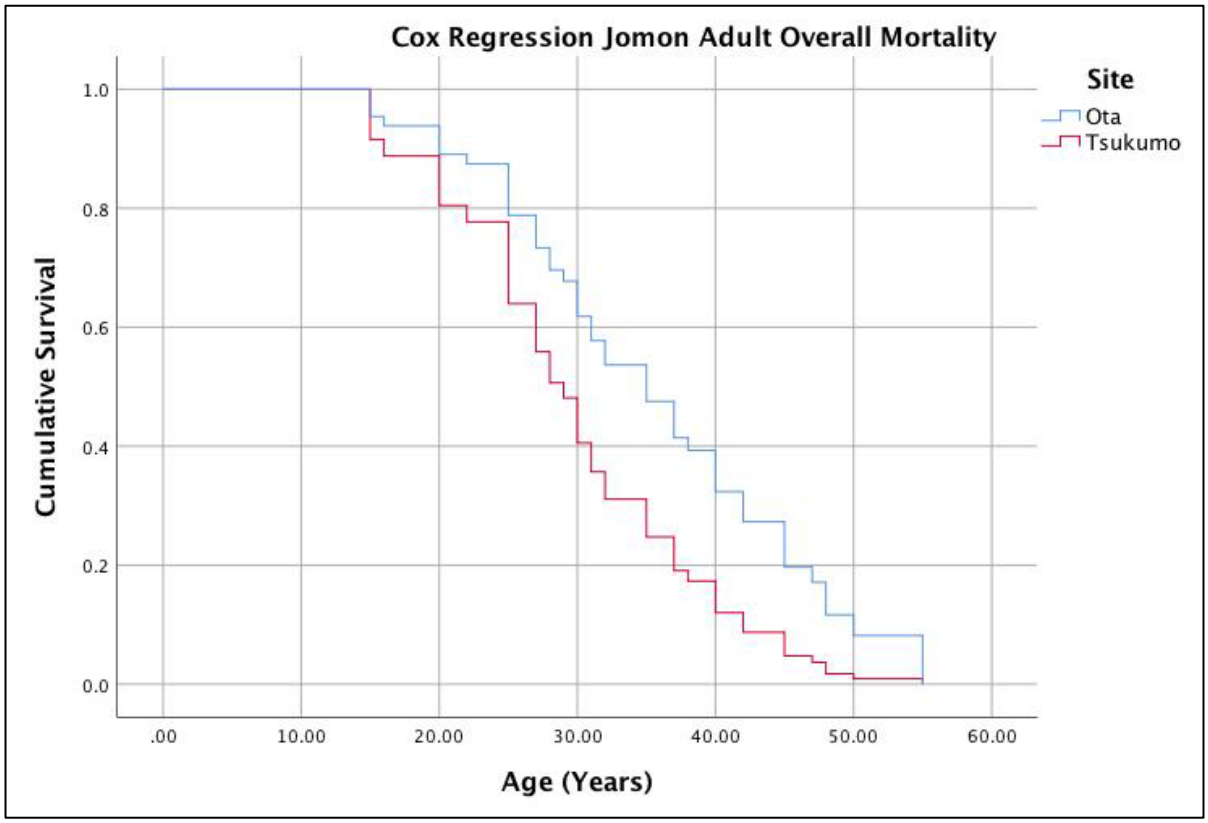

Figure 6.32: *Cox regression cumulative survival function of adult overall mortality from Middle Period to Late/Final Periods of Jomon Japan. Image: author's own*

6.8 Discussion: Diachronic Changes in Disease from Middle to Final Jomon

The results presented in this chapter demonstrated significant increases in the morbidity of infectious disease, scurvy and anaemia from the Middle Period to Late/Final Periods of the Western Honshu Jomon. This outcome indicates an increase in micronutrient deficiencies and levels of infectious disease following climate cooling.

An increase in the mortality rate of Late to Final Jomon individuals was also apparent. This outcome indicates that the population increase from the Middle through to Final Jomon Periods in Western Honshu (identified through an increase in archaeological sites) may be associated with a considerable increase in fertility or migration as the overall mortality rate increased. An increase in the fertility rate during this time would be unusual as there was considerable evidence for an increase of nutritional stress in the later periods, during the climate cooling; evidence for possible resource scarcity. Such factors more often result in a decline in fertility rates (Bentley et al. 1999; Huss-Ashmore 1980; Luck et al. 1995; Lummaa and Clutton-Brock 2002). The Late and Final Jomon do not see a rise in

large villages in Western Honshu, instead an increase in the number of smaller house pits and storage pit sites are documented throughout the region (Habu 2004; Sakaguchi 2009), which is not consistent with a high fertility rate where villages would need to accommodate a large number of children per household. Furthermore, as previously mentioned the settlement patterns, artefacts and subsistence which marks the Late to Final Jomon of Western Japan, are similar to those of Eastern Japan prior to climate cooling, leading authors such as Matsumoto et al. (2017) to argue that there remains a strong link between migration and population increase in Western Japan. As such, migration may have played a considerable role in the increase of population size and site densities of the Late and Final Jomon Periods of Western Japan. It is important to note that a case study of two sites is presented here, and further research across the Middle to Final Jomon Periods of Western and Central Japan is necessary to corroborate these findings.

6.8.1 Changes in Infectious Disease with Increasing Population Interaction in Western Japan

As population density increased during the Late to Final Jomon in Western Honshu, it is difficult to discern to what degree human population interaction factored into the increase of infectious diseases during this period. However, as stated above, it is likely that increased population interaction in Western Honshu may have been a driver for increased population density. The lack of development of large villages during the Late to Final Jomon in Western Honshu also means that an association between an overall regional increase in population density and an increase in infectious disease prevalence may then only have occurred in the light of complex intrapopulation interaction within and between villages. Furthermore, the scarcity of these villages in Western Honshu has also thrown into question the permanence of settlements, and it is argued that the Jomon of the Late to Final Periods in Western Honshu may have been more mobile than previously thought, highlighting a much more dynamic landscape of human population movement and interaction than previously considered (Yamaguchi 2010).

There was no increase in the number of different infectious diseases from the Middle to the Late and Final Jomon Periods. As intrapopulation interaction likely increased, it would not be expected that new infectious diseases be introduced not already existing in Japan during this time. While specific infectious disease (mycosis) was only identified in Ota,

given the rarity of skeletal mycosis it is unlikely that a similar case would have been diagnosed at Tsukumo. However, it does need to be considered that other osteolytic lesions identified at Ota, that did not meet the threshold for diagnosis, may have also had a mycotic aetiology, which then indicates the possibility of varying risks of exposure to different pathogens between the two sites. Even when these osteolytic lesions are considered within the infectious disease criteria, statistically significant differences between Tsukumo and Ota remain (n=54, RR=2.1000, p=0.0165). While a traumatic origin for pathogens is common in non-specific infection (Dubey et al. 1988; Lew and Waldvogel 2004; Ortner 2003), given the high prevalence of individuals in the Tsukumo assemblage with skeletal lesions across multiple skeletal elements, it can be assumed that at least a large proportion of these involved systemic infection from a non-traumatic aetiology. As previously mentioned, the case of vertebral osteomyelitis is likely not related to trauma, indicating the presence of infectious disease in the Tsukumo community not strictly tied to risk of infection from foraging activities. As such, an argument could be made that an increase in regional population interaction in Western Honshu during the Late to Final Jomon likely contributed, at least in part, to an increase in the prevalence of infectious disease.

It should be noted here that otitis media and mastoiditis presented a significant component of the prevalences of infectious disease at both Ota and Tsukumo. This disease primarily occurs in childhood due to the small size and shape of the Eustachian tubes, although the infection can reoccur in adulthood (Klein 1994; Lewis 2017). Critical assessment of the inclusion of otitis media and mastoiditis in infectious disease survival analysis, particularly due the likelihood that it is a marker of infection in childhood, is dealt with in Chapter 10. Ear infections are more common in swimmers, and the high prevalences identified in both Jomon skeletal assemblages is possibly an artefact of having lived in a marine environment (Wang et al. 2005). Auditory exostoses are also known to increase the prevalence of ear infections as they increase the risk of accumulating debris in the ear canal (Wang et al. 2005).

6.8.2 Changes in Specific Nutritional Disease with Increasing Population Interaction in Western Japan

A statistically significant increase in scurvy between the Ota and Tsukumo does indicate an increase in nutritional stress which contrasts the findings by Temple (2007a;

2007b) who found no difference in non-specific stress markers (linear enamel hypoplasia and cribra orbitalia) between the Middle to Late and the Late to Final Jomon in Western Honshu. Temple (2007a; 2007b) attributed these non-specific stress markers to evidence of nutritional stress in Western Honshu Jomon. Temple's argument was in light of very low levels of "bilateral tibial periostitis" and therefore little evidence of infectious disease burden in Western Honshu Jomon skeletal assemblages, which included Ota and Tsukumo (Temple 2007b). However, the research in this thesis indicates a relatively high burden of infectious disease in Ota and Tsukumo assemblages, indicating that infection in childhood may have also contributed to the development of linear enamel hypoplasia and cribra orbitalia. The diagnosis of scurvy provides a direct indicator of nutritional stress, supporting the argument for increased nutritional stress in the Late and Final Jomon Periods due to decreased terrestrial food returns.

It is possible that an increase in population interaction associated with population increase amplified the stress on natural terrestrial resources in the region, thereby indirectly influencing the increase in the prevalence of scurvy in the Late to Final Jomon Periods. Furthermore, an increase in infection would have contributed to increased bodily demands of Vitamin C, which in turn may have made Jomon people more susceptible to morbidity and mortality of infectious diseases. As such, environmental change following climate cooling appears to be the main driver in the increase of nutritional and infectious diseases. However, population interaction was likely a large contributor (Figure 6.33).

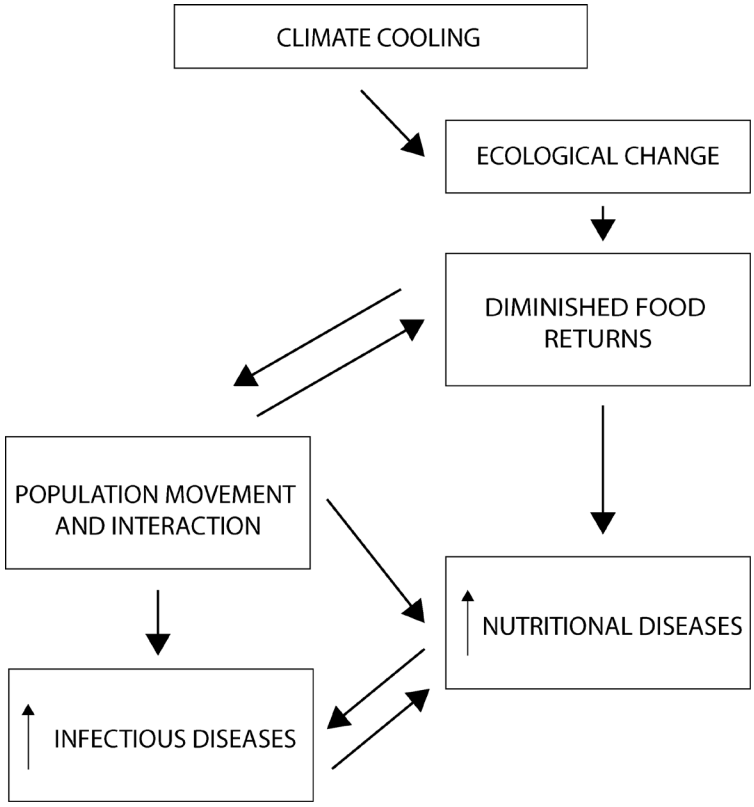

Figure 6.33: *Relationships between factors driving increase in infectious and nutritional disease in the Late to Final Western Honshu Jomon. Climate cooling provided the main driver for ecological change and subsequent diminished food returns. Diminished food returns likely resulted in migrations to warmer regions such as in Central and Western Honshu. However, the increasing population pressure due to migration may have then added strain to already decreasing food returns from terrestrial resources in Western Honshu increasing the levels of nutritional disease, and also increasing the levels of infectious disease. Finally, the increase in nutritional and infectious disease likely led to increased susceptibility of the other. Image: author's own.*

6.8.3 Changes in Anaemia with Increasing Population Interaction in Western Japan

While statistically significant, in contrast to the levels of infection and scurvy, the size of the effect between the prevalences of anaemia at Ota and Tsukumo was not particularly high (RR=1.4250). This outcome reflects the equifinality of skeletal manifestations of anaemia, and it is not possible to discern with great detail whether the aetiologies of anaemia were the same or differed between the two sites. Given the coastal location of both sites and similar subsistence strategies it is likely that a large proportion of anaemia at both Ota and Tsukumo can be attributed to exposure to marine parasites. Interestingly, there was a reduction in marine resource exploitation, but a slight increase in the risk of morbidity of anaemia in the Tsukumo, which was statistically significant. It is possible then that at Tsukumo, increased nutritional stress may have further contributed to the levels of childhood anaemia, albeit this effect may have been minimal given the already

underlying exposure to other stressors of a coastal lifestyle. As such, population interaction may have a had a minor impact on the prevalence of anaemia at Ota and Tsukumo.

6.9 Chapter Summary

This chapter explored site and regional level differences in infectious and nutritional diseases across the Middle to Late and Final Periods of the Jomon of Western Japan. There was a significant increase in infectious and nutritional disease morbidity with increased intrapopulation interaction in Western Japan. Population density and interaction in Western Japan after the Middle Period is said to have increased following migration from the North and East alongside climate cooling and ecological change. The site of Ota, a Middle Period site was compared to the Late and Final Period site of Tsukumo. Mycosis was identified at the Ota site, whereas only non-specific infection was identified at Tsukumo. However, the levels of infectious disease are significantly higher at Tsukumo than Ota. Infectious disease did not appear to increase the risk of death at either site. Scurvy was prevalent at both sites. However, the prevalence of scurvy was exceptionally high at Tsukumo where all adults exhibited signs of Vitamin C deficiency. Interestingly, individuals diagnosed with probable scurvy exhibited an increased risk of death at Ota, whereas in contrast, the presence of probable scurvy indicated increased survivorship (decreased risk of death) at Tsukumo. Finally, there was an increase in the mortality rate of Late and Final Jomon individuals. An increase in intrapopulation interaction in Western Japan following climate cooling appears to then have been associated with increased morbidity and mortality of disease.

CHAPTER 7:
AGRICULTURE AND MIGRATION: A CHANGING EPIDEMIOLOGICAL DYNAMIC OF PREHISTORIC NORTHERN VIETNAM

7.1 Introduction

This chapter presents the second case study: the Pre-Neolithic to Neolithic transition in Northern Vietnam. The Neolithic transition of Southeast Asia is explored first to provide context to the human population interaction increase during this period. Following this, previous archaeological and palaeopathological research of the Pre-Neolithic site of Con Co Ngua is presented, prior to site level differential diagnosis of disease and analysis of disease morbidity and mortality. Subsequently, the similar information will be presented for the early Neolithic site of Man Bac. The presentation of these site level results meet objectives 3 and 4 of this thesis (differential diagnosis, and stage 1 statistical analysis: site level analysis of epidemiological trends). Diachronic changes in the morbidity of infectious and nutritional diseases, and changes to the overall mortality are assessed in accordance with objective 5 (stage 2 of statistical analysis: temporal level analysis of epidemiological trends). Finally, the observed changes to disease prevalences are discussed in regards to the increasing population interaction levels from the Pre-Neolithic to the Neolithic in Northern Vietnam.

Parts of a paper published in *Bioarchaeology International* (Vlok et al. 2020) have been presented in the following sections including the differential diagnosis of treponemal disease and discussion of the origins of treponemal disease in Mainland Southeast Asia. Parts of a paper under review in the *International Journal of Paleopathology* (Vlok et al. in review) is presented in the section on the Neolithic transition in Southeast Asia, the background on the Man Bac site, diagnosis of nonadult nutritional disease, morbidity of nonadult nutritional disease and discussion on the factors influencing nutritional disease levels at Man Bac.

7.2 The Neolithic Transition of Southeast Asia and the Role of Migration

Anatomically modern humans have inhabited Mainland Southeast Asia (MSEA) for at least 60,000 years (Matsumura and Oxenham 2014). For most of this time period, the region has been predominantly occupied by groups of foragers, with agriculture emerging as recently as 4500 years ago (Bellwood and Oxenham 2008; Higham et al. 2011). These foragers (which include a great number of cultures including the Son Vi, the Hoabinhian, and the Da But) have been recognised to share morphological affinity to modern day Australo-Papuan groups (previously termed Australo-Melanesians) of near Oceania, which include Australian Aboriginals and modern day Papua New Guineans (Cuong 1986; Cuong 2007; Matsumura et al. 2017; Matsumura et al. 2001). By 10,000 years ago, a group of complex sedentary hunter-gatherers known as the Dingsishan culture had emerged in Southern China and Northern Vietnam (Fu 2002; Oxenham et al. 2018). Dingsishan sites are characteristic for their large open air cemeteries associated with material culture including polished stone tools, fish hooks, knives, arrows, and spears, demonstrating exploitation of a wide range of ecologies (Fu 2002; Zhang and Hung 2012). The diverse taxa of the faunal assemblages and floral phytoliths associated with these sites further establish that the Dingsishan were foragers who consumed a diverse range of animals and plants (Zhang and Hung 2012). Evidence of this culture in Northern Vietnam (known in Vietnam as the Da But culture) appears possibly as early as 7500 years ago, although this is based on relative dating (Zhang and Hung 2012). Evidence of rice has not been identified at any Dingsishan-Da But sites (Zhang and Hung 2012). These pottery-producing hunter-gatherers likely emerged due to the suitable conditions of the Holocene Thermal Maximum (11-5000 years ago), a period of increased temperature and humidity which stimulated ecological diversity of the region. An abundance of food resources were available to sustain such large sedentary foraging groups (Fu 2002; Oxenham et al. 2018).

The earliest evidence for rice domestication in Asia developed in the Yangtze River Valley in China approximately 9000 years ago with dependence on agriculture in this region occurring later from 6-5000 years ago (Oxenham et al. 2018; Zhao 2011). Approximately 4500-4000 years ago, farmers from Southern China migrated to MSEA and interacted with local indigenous foragers, initiating the Neolithic Period in the region (Bellwood and Oxenham 2008). These Neolithic sites are characterised by the presence of polished axes, adzes, grinding stones, chisels, arrows, pottery distinct from those identified in the Pre-

Neolithic sites, and the presence of domesticated crops (rice and millet), pigs and dogs (Khoach 1980; Oxenham et al. 2015). Intensification of regional interaction and exchange networks appear as characteristic aspects of Neolithic sites throughout MSEA (Frieman et al. 2017; Higham et al. 2011; Khoach 1980; Oxenham et al. 2015).

The migration of farmers from Southern China induced a significant change to the population history of MSEA. Mainland Southeast Asians (modern day Austro-Asiatic speaking peoples) more resemble these migrants in terms of their genetics as well as skeletal morphology (Lipson et al. 2018; Matsumura and Oxenham 2014; Matsumura et al. 2008; McColl et al. 2018). This migration prompted a subsistence transition with the introduction of domesticated pigs and dogs, and rice and/or millet farming (Castillo 2011; Jones et al. 2019; Piper et al. 2014; Weber et al. 2010). However, agricultural intensification was regionally mosaic, with variation within MSEA as to the degree of adoption of agriculture and therefore likely leading to differential impact on health (King et al. 2017; Oxenham et al. 2015). The adoption of agriculture in MSEA aligns with a period of climate cooling following the Holocene Thermal Maximum, and it is possible the changing ecology of the region, as it became colder and drier, potentially caused diminished food returns that may have contributed to the adoption of agriculture from Southern Chinese farmers (Oxenham et al. 2018).

Foraging occurred alongside agricultural food production at many sites in the region, and may have provided a buffer to nutritional deficiencies caused by a reliance of a single staple (Higham and Thosarat 2005; Jones et al. 2019; Oxenham et al. 2011). Furthermore, there was variation in the domesticated plants initially adopted throughout MSEA. While Northern Vietnam is associated with rice agriculture, Neolithic sites in Central Thailand instead have been demonstrated to have initially taken up millet instead, prior to adopting rice as a subsistence base (Castillo 2011; Jones et al. 2019; Mai Huong 2016; Weber et al. 2010). Complete dependence of an agricultural subsistence base did not occur until the Iron Age (500BC to 500AD) with the intensification of wet rice agriculture and the construction of moats (Halcrow et al. 2016; Higham 2007; Higham et al. 2014; King et al. 2014; McGrath and Boyd 2001). Therefore, it has been argued that a gradual intensification and eventual agricultural dependency in MSEA may have ameliorated the impact of agriculture on health in comparison to other regions of the world (Oxenham and Tayles 2006).

Neolithic sites in Mainland Southeast Asia (including Khok Phanom Di in Southern Thailand and Man Bac in Northern Vietnam) are marked by high fertility rates and rates of natural population increase in contrast to earlier Pre-Neolithic forager and later Bronze and Iron Age sites (McFadden et al. 2018). This high fertility demonstrates significant demographic changes during the initial agricultural transition in the region.

It is clear that human population interaction following migration has had a significant impact on the population history and social structure of human groups in MSEA during the Neolithic. The initial interaction between foragers and farmers, identified as *friction zones* by Bellwood and Oxenham (2008), is then of particular interest in regards to health, as these interactions have the potential to influence the demography and subsistence bases of both groups. Specifically, the interacting forager and farmer groups would have needed to navigate the differences in society and subsistence, instigating a host of changes to both groups, which could have influenced their health. The aim of this case is to explore if the agricultural transition of Northern Vietnam induced by human population interaction through migration, resulted in a change in the morbidity and mortality of nutritional disease due to subsistence transition, and potentially infectious diseases, via the introduction of new pathogens.

7.3 Con Co Ngua

Con Co Ngua is a large open air Pre-Neolithic cemetery site in Thanh Hoa province in Northern Vietnam identified as belonging to the Dingsishan-Da But forager complex (Oxenham 2000; Oxenham et al. 2018). As is the case with all Da But sites, Con Co Ngua appears to have been occupied by sedentary foragers (Huffer and Oxenham 2015; Nguyen 2005). The individuals from the site share a biological affinity with earlier Hoabinhian hunter-gatherers in Vietnam, and modern day Australo-Papuan groups (Matsumura and Oxenham 2014; Oxenham et al. 2018). Dating at minimum from 6200-6700 cal BP, the site was occupied at the height of the Holocene Thermal Maximum which occurred between 7200-6000 years ago in East Asia (Oxenham et al. 2018; Tao et al. 2010). While approximately 30km from the ocean today, sea levels were higher during the Holocene Thermal Maximum and the site was adjacent to the ocean during occupation (Hiep 2004; Tanabe et al. 2006). Today, the climate in the region is subtropical, with two distinct seasons, a hot and cold season, where high levels of humidity are sustained year round (Oxenham

2006; Oxenham et al. 2011). At the peak of the Holocene Thermal Maximum, the surface temperature in East Asia was 1-4°C higher than present day, with significantly increased rainfall (between 40 to 100% higher) (Tao et al. 2010).

Individuals in the Con Co Ngua cemetery were predominantly buried in a flexed position, which was a common Pre-Neolithic burial type in MSEA (Figure 7.1; Higham et al. 2011; Oxenham 2000; Oxenham et al. 2018). Some individuals in later phases of the site were buried in a side flexed position which may indicate temporal change in burial practice at the site (Muir 2019). Seventy-two percent of the burials also exhibited post-mortem ritual mutilation in the form of chopping of the long bone shafts (Muir 2019; Oxenham et al. 2018). Most nonadults were found within the grave fill of an adult burial, and when complete were also more likely to be buried in side flexed positions than adults. Different burial practices between adults and nonadults might indicate some age based social differentiation at Con Co Ngua (Muir 2019).

Figure 7.1: *Burial position of an individual from Con Co Ngua. Notice the squatting tight flexed position. Image: courtesy of Prof M. Oxenham (used with permission).*

The inhabitants of Con Co Ngua exploited a vast variety of resources in the surrounding landscape. *Canarium* sp. fragments (a genus which includes Chinese white and black olives) which are cultivated for their fruits and nuts today, were found at Con Co Ngua

(Oxenham et al. 2018). While other plants in the region, which may serve as food resources, were not identified at the site, the rich ecology of Northern Vietnam during the Holocene Thermal Maximum included Indian gooseberries *(Phyllanthus embelica),* melons *(Cucumis* sp.*)*, gourd *(Lagenaria sp.)*, Areca nuts *(Areca* sp.*)*, Livistona fruits *(Livistona* sp.*)* and cherry like fruits *(Prunus* sp.). It is possible some of these plants were also exploited by the Con Co Ngua inhabitants (Mai Huong 2013). As is the case with all Dingsishan-Da But sites, no rice phytoliths were found at Con Co Ngua from flotation.

The vertebrate taxa identified at Con Co Ngua include mammals, reptiles, fish, sharks, rays and birds from a wide range of ecological habitats (including woodland, wetland, estuarine and offshore environments) and represent the diversity of food available to the foragers of Con Co Ngua (Jones et al. 2019; Oxenham et al. 2018). Water buffalo dominated the assemblage, and the types of skeletal injuries sustained by the inhabitants, possibly from buffalo, suggests that this animal may have been managed or herded by the Con Co Ngua community (Scott et al. 2019). Macaques (*Macaca* spp), deer, monitor lizards (*Varanus* spp.), hard-shell (Geoemydidae spp.) and soft-shell tortoises (Trionychidae spp.), pangolins and a tiger (*Panthera tigris)* were also present in the assemblage (Jones et al. 2019; Oxenham et al. 2018). Butchering marks on these animals, particularly on buffalo and deer, indicate that processing occurred on site (Oxenham et al. 2018).

The fertility rate (D0-14/D) and rate of natural population increase (RNPI) of Con Co Ngua (D0-14/D= 0.30, RNPI= 1.37) is not particularly high for MSEA and is comparative to Bronze Age and Iron Age sites of Thailand. However, they are considerably lower than the Neolithic sites of Man Bac (D0-14/D= 0.59, RNPI= 4.32) and Khok Phanom Di (D0-14/D= 0.56, RNPI= 4.01) (McFadden et al. 2018). Twenty-two percent of the 2013 assemblage died before 5 years of age (Oxenham et al. 2018).

Non-specific stress markers including linear enamel hypoplasia (LEH) and cribra orbitalia have been recorded for the 1979/1980 assemblage by Oxenham (2006; 2000). Eighty-one percent of individuals exhibited cribra orbitalia (mild to severe) with 72% displaying canine LEH, indicating a high burden of non-specific stress in the Pre-Neolithic. Furthermore, Oxenham et al. (2018) identified a calcified hydatid cyst in association with metaphyseal osteolytic lesions, which is strongly diagnostic for the presence of the *Echinococcus* parasite (see Chapter 5). A similar metaphyseal osteolytic lesion was

identified in an individual from the 1979/1980 assemblage by Oxenham et al. (2005) and a further 19 individuals were observed to have such lesions by Buckley et al. (2018) in the 2013 assemblage. Buckley et al. (2018) posited the possibility of hydatids disease amongst these individuals. Further discussion on the diagnosis of hydatids disease at Con Co Ngua is found below. The following section presents the results for differential diagnosis of infectious disease, nutritional disease, and anaemia at Con Co Ngua followed by the statistical assessment of morbidity and mortality of these diseases within the site.

7.4 Results: Con Co Ngua Skeletal Pathology

7.4.1 Summary of Pathological Lesions at Con Co Ngua

Of the 155 individuals included in this palaeopathological analysis 30.3% (47/155) exhibited osteoblastic lesions (Table 7.1). Osteoblastic lesions in the adults (27.7%, 28/101) were predominantly restricted to unilateral flakes of subperiosteal new bone (SPNB) of the long bones (particularly the femur, tibia and fibula). However, four individuals had unilateral or bilateral remodelled cortical enlargement of the shafts of the long bones including the femur, humerus, radius, and ulna. Shafts of these individuals radiographically present as *bone within a bone* or *double cortex* appearance likely indicating remodelled thick SPNB and endosteal enlargement. In one individual, this was possibly observed macroscopically in a cross section of the shaft (Figure 7.2). There was a slightly higher prevalence of SPNB deposits in nonadults (35.2%, 19/54) than adults (Table 7.1). Lesions were predominantly bilateral and symmetrical discrete SPNB in infants with a mixture of bilateral and unilateral lesions in older nonadults, particularly adolescents. In infants postcranial and cranial elements were equally affected, whereas postcranial SPNB was predominant in adolescents.

Nineteen individuals (1 adolescent and 18 adults) presented with predominantly unilateral (sometimes bilateral) circular OL2 osteolytic cyst-like lesions with or without sclerosis of the margins and base in the metaphyses of the long bones (Figure 7.3). These osteolytic lesions were predominantly observed on the distal humerus (52.4% of lesions), acetabulae (23.8% of lesions), and distal femora (9.5% of lesions). One individual (CCN13M133a) demonstrated a combination of osteoblastic and severe erosive changes to the articular surfaces of the left distal tibia and talus. The subchondral bone of the distal left tibia has completely eroded with the presence of a cloaca on the medial malleolus.

Table 7.1: *Summary of OB and OL lesion prevalences at Con Co Ngua*

	NONADULT (aff/obs)	**NONADULT (%)**	**ADULT (aff/obs)**	**ADULT (%)**	**TOTAL (aff/obs)**	**TOTAL (%)**
OB Lesion	19/54	35.2	28/101	27.7	47/155	30.3
OL Lesion	1/54	1.9	18/101	17.8	19/155	12.3

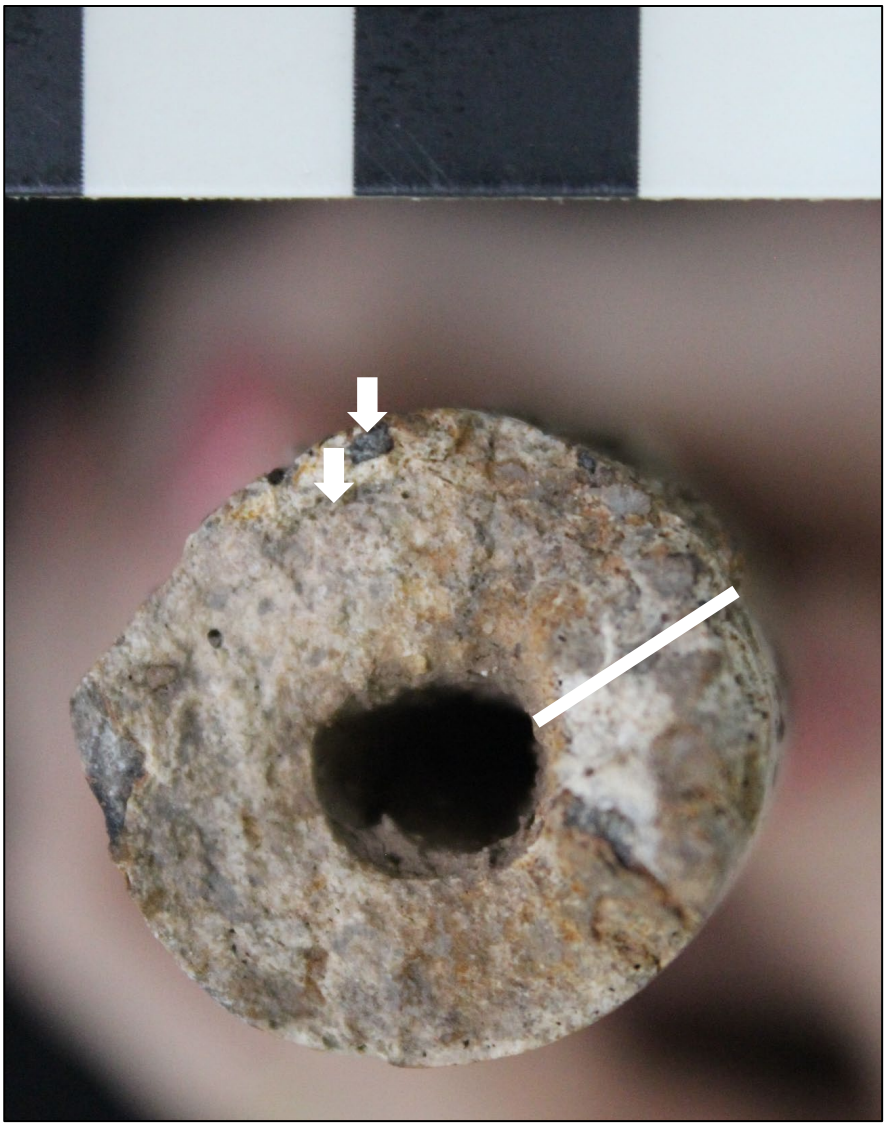

Figure 7.2: "*Double cortex" appearance of the femoral shaft of an individual from Con Co Ngua (CCN13M67a, adolescent >16 years). Note the overall cortical expansion (white line), medullary stenosis and possibly two distinct margins of the cortex (white arrows). Image: courtesy of Ms M. Walker (used with permission).*

Figure 7.3: *Large cystic lesion of the right distal humerus (CCN13M12a, young adult male). While there is postmortem damage to the margins note the sclerotic base. The internal structure of the lesion is multilocular. Image: author's own.*

7.4.2 Diagnosis of Infectious Disease at Con Co Ngua

Five individuals (3.2%, 5/155) present with diffuse SPNB involving more than ¼ of the bone surface across two or more skeletal elements and were therefore included in the overall infectious disease prevalence at Con Co Ngua (Table 7.2). The presence of SPNB and cloacae of the distal tibia of CCN13M133a (a middle aged adult female) is strongly diagnostic for osteomyelitis. Additionally, the erosive destruction of the subchondral surfaces of the talus and distal tibia is consistent with septic arthritis (Figure 7.4). This case was described by Scott et al. (2019) and it is likely the osteomyelitis is related to trauma as amputation of the distal fourth and fifth metatarsals was also observed.

As previously mentioned, a calcified hydatid cyst was identified by Oxenham et al. (2018) which is strongly diagnostic for hydatids disease (specifically *Echinococcus granulosis*). The cyst was found within the soil matrix in the pelvis of individual CCN13M59a (an old adult male). This individual also exhibited circular OL2 osteolytic cyst-like lesions with minimal sclerosis of the margins and base in the metaphysis of the right distal humerus (Figure 7.5a). This lesion was identified in 12.3% (19/155) of the overall assemblage. These lesions are *suggestive* for hydatids disease. The osteolytic lesion of one individual (CCN13M113a, middle aged adult male) appears to originate within the subchondral bone of the distal right femur which is not consistent with hydatids disease where infection occurs from within the marrow space or internal trabeculae, and may be more characteristic of osteochondritis dissecans. CCN13M113a also does not present with radiographic signs of hydatids disease.

Radiographs of seven individuals with macroscopic cyst-like lesions identified small and numerous multifocal cystic lesions resembling a "bunch of grapes" within the marrow and trabecular regions of the bone. This radiographic sign is strongly diagnostic for hydatids disease (Figure 7.6). Therefore, 4.5% (7/155) of the Con Co Ngua assemblage demonstrated lesions consistent with probable hydatids disease (Table 7.2). Of these individuals, five also presented with ischemic necrosis of the marrow area surrounding the multifocal osteolytic lesions (Figure 7.6). One individual (CCN13M21a, adult female) displayed a pathological fracture at the lesion site (left distal humerus) which is known to occur in hydatids disease (Zlitni et al. 2001). Radiographs were not available for the remaining 11 individuals with cyst-like macroscopic lesions. Given the similarity of the lesions between those radiographed and those not radiographed, hydatids could be considered a likely cause for all individuals. However, the disease is diagnostic with the presence of radiographs only (see Chapter 5), and therefore these individuals were not considered in the statistics in this thesis. The disease affected both sexes, all adult age groups, and adolescents over the age of 15 years of age (Figure 7.7).

Table 7.2: *Summary of infectious disease at Con Co Ngua*

	POSSIBLE			**PROBABLE**			**POSSIBLE AND PROBABLE**		
	Affected	*Observed*	*(%)*	*Affected*	*Observed*	*(%)*	*Affected*	*Observed*	*(%)*
Hydatids Disease									
15 to 20 years	0	17	0	1	17	5.9	1	17	5.9
20 to 30 years	0	30	0	1	30	3.3	1	30	3.3
30 to 40 years	0	22	0	1	22	4.5	1	22	4.5
40 to 50 years	0	16	0	1	16	6.3	1	16	6.3
50+ years	0	16	0	2	16	12.5	2	16	12.5
Total nonadults	0	54	0	1	54			54	
Males	0	54	0	3	54	5.6	3	54	5.6
Females	0	34	0	2	34	5.9	2	34	5.9
Total adults	0	84	0	6	84	7.1	6	84	7.1
Total	0	155	0	7	155	4.5	7	155	4.5
Osteomyelitis									
20 to 30 years	0	30	0	0	30	0	0	30	0
30 to 40 years	0	22	0	1	22	4.5	1	22	4.5
40 to 50 years	0	16	0	0	16	0	0	16	0
50+ years	0	16	0	0	16	0	0	16	0
Male	0	54	0	0	54	0	0	54	0
Female	0	34	0	1	34	2.9	1	34	2.9
Total	0	155	0	1	155	0.7	1	155	0.6
Overall infectious disease criteria									
15 to 20 years							3	17	17.6
20 to 30 years							2	30	6.7
30 to 40 years							2	22	9.1
40 to 50 years							3	16	18.8
50+ years							3	16	18.8
Total nonadults									
Male							5	54	9.3
Female							5	34	14.7
Total adults							10	84	11.9
Total							13	155	8.4

Figure 7.4: *Osteomyelitis of the left distal tibia and talus of CCN13M133a, a middle aged adult female. Note the cloaca on the medial malleolus (white arrow). Image: courtesy of Prof H. Buckley. Used with permission.*

Figure 7.5: *Macroscopic cyst-like lesions suggestive of hydatids disease at Con Co Ngua. a) Anterior right distal humerus. This individual was found with a calcified hydatid cyst (CCN13M59a, old adult male). b) Posterior right distal humerus (CCN13M67a, adolescent >16 years). c) Right acetabulum (CCN13M45a, old adult). d) Lateral right distal humerus (CCN13M32a, young adult). e) Posterior distal right humerus (CCN13M12a, young adult male). f) Anterior distal left humerus (CCN13M12a, young adult male). Image: authors own.*

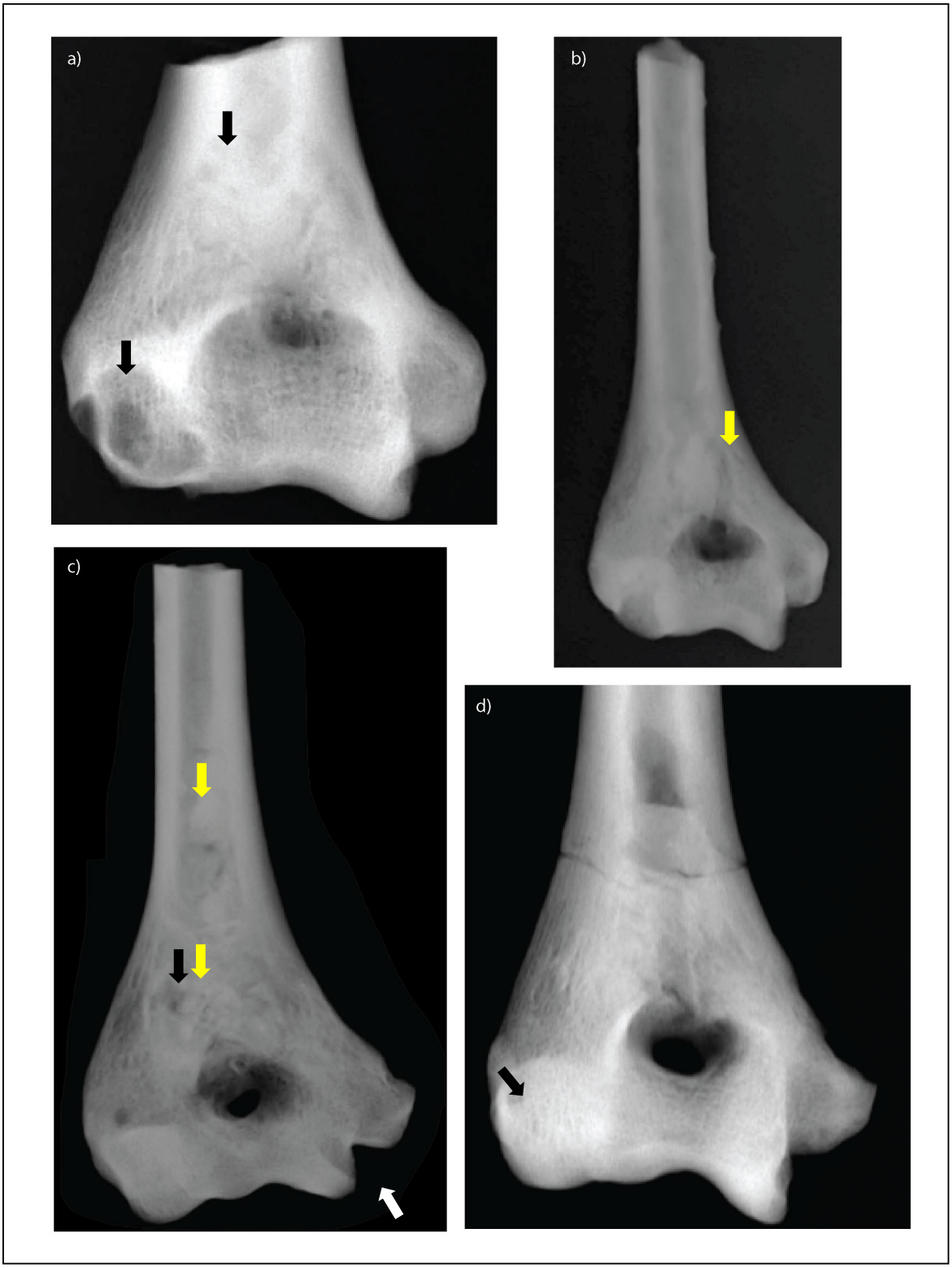

Figure 7.6: *Radiographic signs of hydatids disease at Con Co Ngua. a) Radiographic evidence of small and multilocular lesions throughout the trabeculae terminating in a cortex breech with clear sclerotic margins (black arrows; CCN13M12a, young adult male)). b) Ischemic necrosis of the trabecular bone extending from the medullary canal (yellow arrow; CCN13M59a, old adult male)). c) Ischemic necrosis of the trabeculae extending from the medullary canal (yellow arrows). There is a large oval radiolucent region which is comprised of small and numerous multilocular lucencies resembling a "bunch of grapes" (black arrow). There is also a pathological fracture which has deformed (depressed) the medial epicondyle (white arrow; CCN13M21a, adult female). d) Two small circular lesions extending into the subchondral bone (CCN13M72a, adolescent to young adult). Image: authors own*

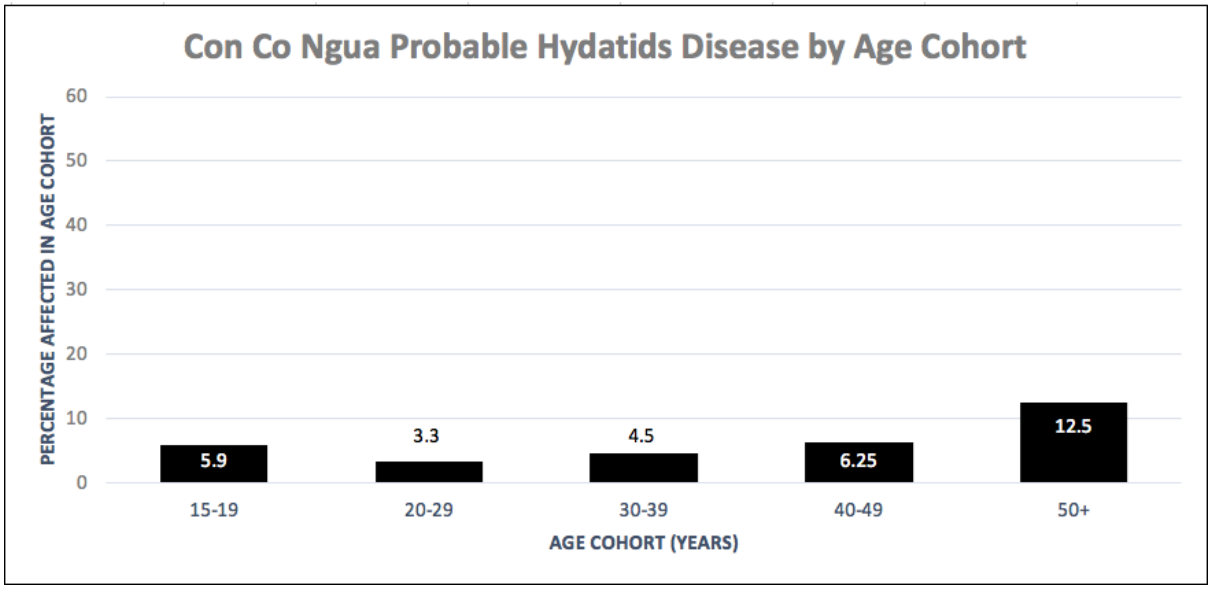

Figure 7.7: *Age-at-death distribution of probable cases of hydatids disease at Con Co Ngua. Image: authors own*

7.4.3 Morbidity of Infectious Disease at Con Co Ngua

No significant differences in the prevalences of infectious diseases were apparent between males (9.3%, 5/54) and females (14.7%, 5/34), across nonadult age cohorts nor across adult age cohorts at Con Co Ngua (Table 7.3).

Table 7.3: *Relative risk of infectious disease morbidity at Con Co Ngua across sex and age cohorts.*

EXPOSED GROUP/ CONTROL GROUP	**OUTCOME**		**RR**	**P-VALUE**	**95%CI**
	Positive: *Infection Present*	***Negative:*** *Infection Absent*			
Sex					
Female/ Male	5/5	29/49	1.5882	0.4356	0.4964-5.0815
Nonadults					
<1 yr/ >1 yr	0/2	13/39	0.6000	0.7365	0.0306- 11.7604
<5 yrs/ >5yrs	0/2	23/29	0.2667	0.3862	0.0134- 5.3025
<10 yrs/ >10yrs	0/2	31/21	0.1500	0.2136	0.0075- 2.9827
Adults					
<20 yrs/ >20 yrs	3/10	14/74	1.4824	0.5133	0.4554- 4.8253
<30 yrs/ >30 yrs	5/8	42/46	0.7181	0.5352	0.2521- 2.0453
<40 yrs/>40 yrs	7/6	62/26	0.5411	0.2317	0.1977- 1.4806

A relative risk (RR) >1 denotes a relationship of the exposed group with an increase in disease prevalence, whereas RR <1 denotes a relationship of the control group with an increase in disease prevalence.
*= statistically significant (p<0.10). **= statistically significant when considering size of the effect of RR.

7.4.4 Mortality of Infectious Disease at Con Co Ngua

Relative risk ratio analysis presented no statistically significant differences in risk of death between individuals with or without skeletal signs of infectious disease across all adult and nonadult age cohorts at Con Co Ngua (Table 7.4). The Kaplan-Meier survivorship function also indicated no significant differences in the mortality of adults with infectious disease present (n=101, X^2=1.255, df=1, p=0.263; Figure 7.8). Significant overlap between the confidence intervals of infectious disease presence and infectious disease absence further supports this outcome (Table 7.5). As only two nonadults presented with infectious disease, a Kaplan-Meier survival function was not produced for nonadults.

Table 7.4: *Relative risk of infectious disease mortality at Con Co Ngua across age cohorts.*

POSITIVE OUTCOME/ NEGATIVE OUTCOME	**TREATMENT**		**RR**	**P-VALUE**	**95%CI**
	Exposed Group: *Infection Present*	***Control Group:*** *Infection Absent*			
Nonadults					
<1 yr/ >1 yr	0/2	13/39	0.6543	0.7465	0.0500- 8.5656
<5 yrs/ >5yrs	0/2	23/29	0.3759	0.4517	0.0294- 4.8057
<10 yrs/ >10yrs	0/2	31/21	0.2804	0.3266	0.0221- 3.5561
Adults					
<20 yrs/ >20 yrs	3/10	14/74	1.4505	0.5085	0.4816- 4.3691
<30 yrs/ >30 yrs	5/8	42/46	0.8059	0.5577	0.3916- 1.6581
<40 yrs/>40 yrs	7/6	62/26	0.7643	0.3120	0.4539- 1.2870

A relative risk (RR) >1 denotes a relationship of the disease presence with the positive outcome (susceptibility to mortality), whereas RR <1 denotes a relationship of the disease absence with a negative outcome (survivorship).
*= statistically significant (p<0.10). **= statistically significant when considering size of the effect of RR.

Table 7.5: *Statistical summary for Kaplan-Meier function of infectious disease mortality of adults at Con Co Ngua.*

INFECTIOUS DISEASE	**ESTIMATE**	**STD. ERROR**	**95% CI**	**LOG RANK (MANTEL-COX)**		
				CHI SQUARE	**DF**	**P-VALUE**
Mean				1.255	1	0.263
Absent	32.135	1.253	29.679- 34.591			
Present	36.250	3.850	28.705- 43.795			
Overall	32.624	1.195	30.281-34.967			
Median						
Absent	35.000	1.788	31.496- 38.504			
Present	35.000	6.928	21.421-48.579			
Overall	35.000	1.798	31.475-38.525			

*= statistical significance (p<0.15).

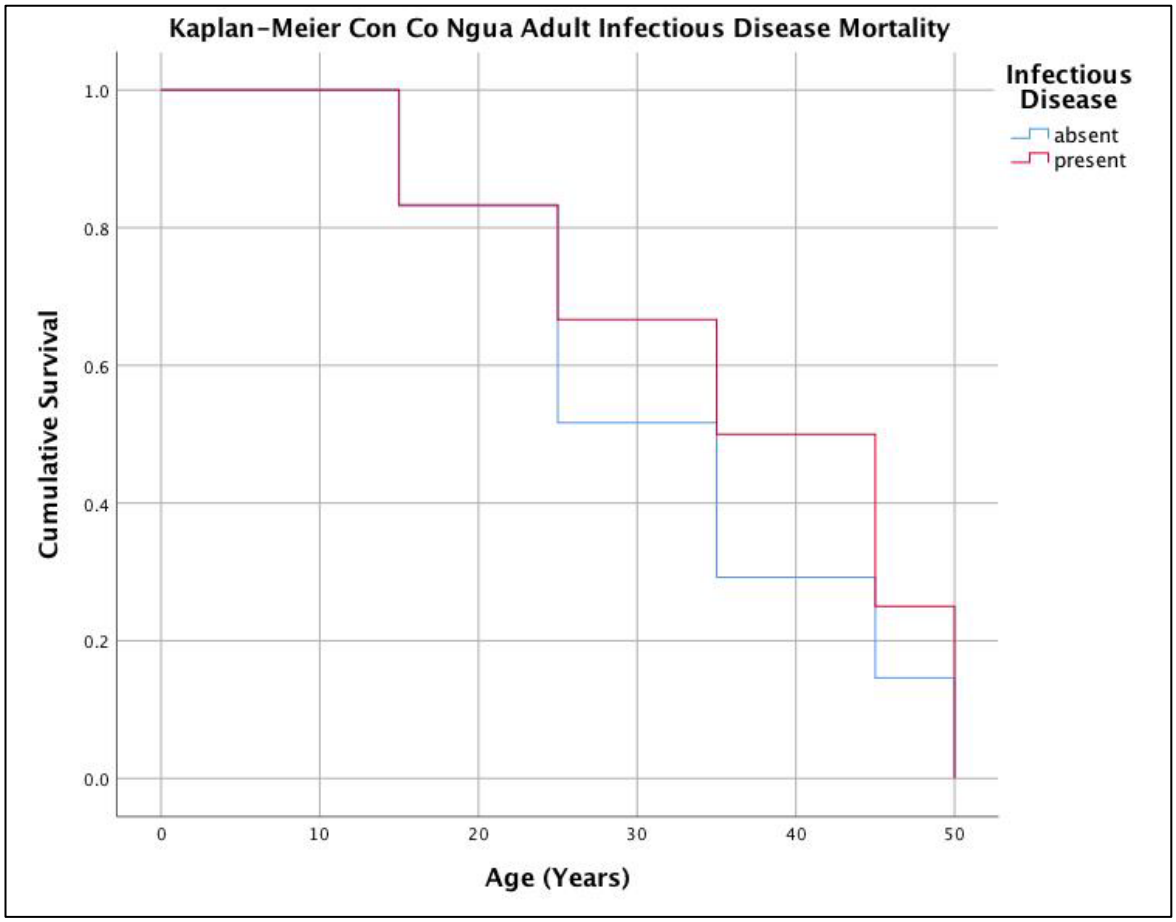

Figure 7.8: *Kaplan-Meier cumulative survival function of adult infectious disease mortality at Con Co Ngua. Image: author's own*

7.4.5 Diagnosis of Nutritional Disease at Con Co Ngua

Over 6% (6.5%, 10/155) of the overall Con Co Ngua assemblage presented with pathologies consistent with a possible or probable diagnosis of scurvy. Only two individuals, both perinates, had lesions consistent with a diagnosis of probable scurvy (Figure 7.9). CCN13M36a, an infant at around 37 foetal weeks of age exhibited bilateral active SPNB on the temporal squama, the left superior orbital roof, left zygomatic process of the frontal bone, and bilaterally across the shafts of the limb bones. CCN13M167a, another infant around 37 foetal weeks in age exhibited active SPNB on the left superior orbital roof, left zygomatic process of the frontal bone, right temporal squama, endocranium, and symmetrically on the shafts of the tibiae. These SPNB lesions were not associated with abnormal cortical porosity. As such, it is possible these lesions were caused by normal growth variation in infants, particularly when considering the poor preservation of these individuals. However, the lesions on the frontal bones do appear to be discrete and consistent with haematoma formation around the region of the *temporalis* which can occur in scurvy. Additionally,

CCN13M36a (37 foetal weeks) also presented with abnormal endochondral porosity exceeding 10mm from the metaphyseal plate of the proximal right tibia, which indicates disruptions to the osteoid production during growth due to scurvy (Figure 7.9). Furthermore, there was evidence of scurvy in children past the age of infancy, where normal SPNB in growth is not a significant confounding factor (Table 7.6).

No adults exhibited any evidence of specific nutritional disease, and in total 18.5% (10/54) of nonadults had lesions consistent with possible or probable scurvy. Evidence of scurvy was highest within the first year of life (61.5%, 8/13), with sporadic cases of scurvy occurring in later childhood and adolescence (Table 7.6; Figure 7.10). No evidence of other specific nutritional diseases such as rickets and osteomalacia was identified at Con Co Ngua. Overall, evidence of nutritional disease at Con Co Ngua was predominantly restricted to possible cases of scurvy at a low prevalence rate.

Table 7.6: *Summary of nutritional disease at Con Co Ngua*

SCURVY	**POSSIBLE**			**PROBABLE**			**POSSIBLE AND PROBABLE**		
	Affected	*Observed*	*(%)*	*Affected*	*Observed*	*(%)*	*Affected*	*Observed*	*(%)*
0 to 6 months	4	9	44.4	2	9	22.2	6	9	66.7
6 months to 1 year	2	4	50	0	4	0	2	4	50
1 to 5 years	0	11	0	0	11	0	0	11	0
5 to 10 years	1	8	12.5	0	8	0	1	8	12.5
10 to 15 years	0	5	0	0	5	0	0	5	0
15 to 20 years	1	17	5.9	0	17	5.9	1	17	5.9
20 to 30 years	0	30	0	0	30	0	0	30	0
30 to 40 years	0	22	0	0	22	0	0	22	0
40 to 50 years	0	16	0	0	16	0	0	16	0
50+ years	0	16	0	0	16	0	0	16	0
Total nonadults	8	54	14.8	2	54	3.7	10	54	18.5
Males	0	54	0	0	54	0	0	54	0
Females	0	34	0	0	34	0	0	34	0
Total adults	0	84	0	0	84	0	0	84	0
Total	8	155	5.2	2	155	1.3	10	155	6.5

Figure 7.9: *Macroscopic lesions consistent with foetal scurvy in Con Co Ngua. a) Active SPNB on the left zygomatic process of the frontal (white arrows; CCN13M36a). b) Active SPNB on the left temporal squama (white arrow; CCN13M36a). c) Abnormal endochondral porosity exceeding 10mm from the metaphyseal plate on the proximal tibia (white arrow; CCN13M36a). d) Active SPNB on the right orbital roof (white arrow). The SPNB is layered which may be a sign of appositional growth rather than abnormal SPNB. Note the possible vascular impression (CN13M167a; black arrow). e) Active SPNB on the right zygomatic process of the frontal (CN13M167a; white arrows).*

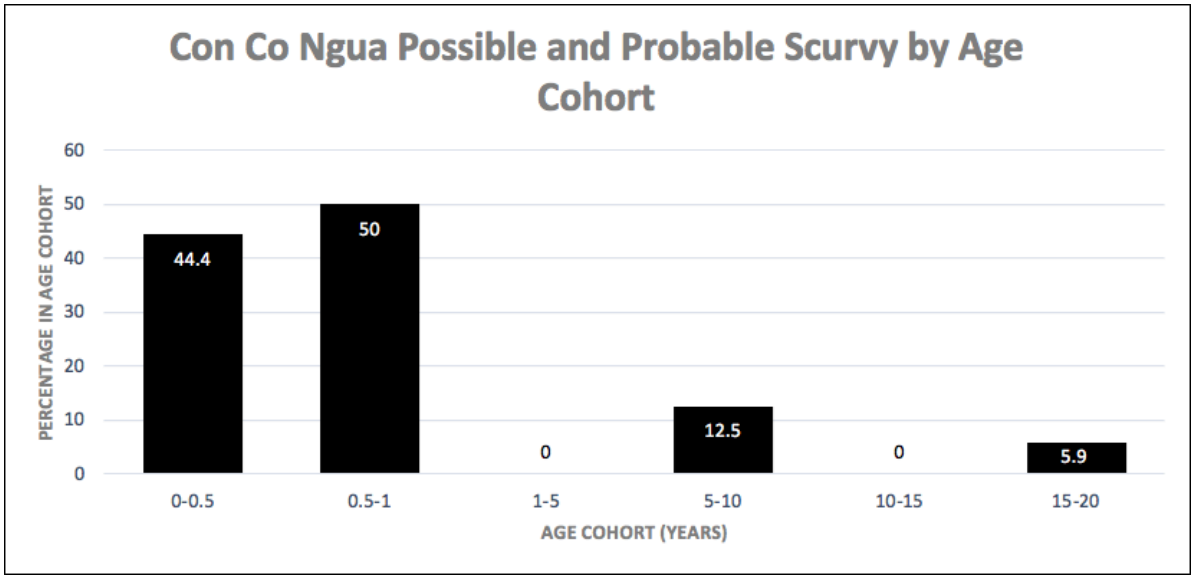

Figure 7.10: *Age-at-death distribution of possible and probable cases of scurvy at Con Co Ngua. Image: author's own.*

7.4.6 Morbidity of Nutritional Disease at Con Co Ngua

As no adults presented with evidence of scurvy, statistical analysis was restricted to assessment of scurvy morbidity across nonadult age cohorts. The presence of possible or probable scurvy was significantly higher in younger nonadults than older nonadults, in all relative risk tests across age (Table 7.7). Notably, the morbidity of scurvy at Con Co Ngua was exceptionally higher in infants under 1 year of age, than in post-infancy nonadults. This pattern was consistent when considering both combined possible and probable, and probable only cases. Individuals were 12 times more likely to present with skeletal evidence of possible or probable scurvy before 1 year of age (n=54, RR=12.6154, p=0.0005). In probable only cases, individuals before 1 year of age were 15 times more likely to present with skeletal evidence of scurvy (n=54, RR= 5.000, p=0.0745). The trend of higher morbidity of probable scurvy in younger nonadults was not consistent across all tested nonadults age cohorts as there was no statistical significance at 5 and 10 years of age (Table 7.7). This pattern is likely due to the low frequency of probable cases of scurvy at Con Co Ngua.

Table 7.7: *Relative risk of scurvy morbidity at Con Co Ngua across sex and age cohorts.*

EXPOSED GROUP/ CONTROL GROUP	OUTCOME		RR	P-VALUE	95%CI
	Positive: *Scurvy Present*	***Negative:*** *Scurvy Absent*			
Possible and Probable (combined)					
Nonadults					
<1 yr/ >1 yr	8/2	5/39	**12.6154**	**0.0005***	3.0543- 52.1068
<5 yrs/ >5yrs	8/2	15/29	**5.3913**	**0.0230***	1.2614- 23.0436
<10 yrs/ >10yrs	9/1	22/22	**6.6774**	**0.0620***	0.9088- 49.0626
Probable Only					
Nonadults					
<1 yr/ >1 yr	2/0	11/41	**15.000**	**0.0745***	0.7653- 294.0097
<5 yrs/ >5yrs	2/0	21/31	6.6667	0.2136	0.3353- 132.5629
<10 yrs/ >10yrs	2/0	29/23	3.7500	0.3862	0.1886- 74.5666

A relative risk (RR) >1 denotes a relationship of the exposed group with an increase in disease prevalence, whereas RR <1 denotes a relationship of the control group with an increase in disease prevalence.
*= statistically significant (p<0.10). **= statistically significant when considering size of the effect of RR.

7.4.7 Mortality of Nutritional Disease at Con Co Ngua

As no adults exhibited evidence of scurvy, statistical analysis was restricted to assessment of scurvy mortality and nonadult age. Relative risk analysis of mortality to scurvy indicates a statistically significant relationship of the presence of scurvy to frailty at a younger age. While the prevalence of scurvy was consistently higher in the younger age cohorts (Table 7.8), this was particularly high at 1 year of age. Infants under 1 year of age were 7 times more likely to die with skeletal evidence of possible or probable scurvy than those without (n=54, RR=7.0400, p<0.0001). This pattern was also observed in probable only cases.

Kaplan-Meier and Cox regression analyses were applied for combined possible and probable cases of scurvy in nonadults. Consistently higher frailty of nonadults with skeletal evidence of scurvy was observed in the Kaplan-Meier and Cox regression functions (Table 7.9-7.10, Figure 7.11-7.12). Statistical significance was achieved for both analyses (KM: n=54, X^2=11.634, df=1, p=0.001; Cox: n=54, Wald= 7.482, df=1, p= 0.006). Overall, the presence of scurvy in the assemblage was associated with very high frailty, particularly when the lack of evidence for adult scurvy at Con Co Ngua is also considered.

Table 7.8: *Relative risk of scurvy mortality at Con Co Ngua across age cohorts.*

POSITIVE OUTCOME/ NEGATIVE OUTCOME	TREATMENT		RR	P-VALUE	95%CI
	Exposed Group: *Scurvy Present*	***Control Group:*** *Scurvy Absent*			
Possible and Probable (combined)					
Nonadults					
<1 yr/ >1 yr	8/2	5/39	**7.0400**	**<0.0001***	2.9157- 16.9983
<5 yrs/ >5yrs	8/2	15/29	**2.3467**	**0.0012***	1.4027- 3.9260
<10 yrs/ >10yrs	9/1	22/22	**1.800**	**0.0014***	1.2551- 2.5814
Probable Only					
Nonadults					
<1 yr/ >1 yr	2/0	11/41	**4.7273**	**<0.0001***	2.7972- 7.9892
<5 yrs/ >5yrs	2/0	21/31	**2.4762**	**<0.0001***	1.7798- 3.4451
<10 yrs/ >10yrs	2/0	29/23	**1.7931**	**<0.0001***	1.4076- 2.2842

A relative risk (RR) >1 denotes a relationship of the disease presence with the positive outcome (susceptibility to mortality), whereas RR <1 denotes a relationship of the disease absence with a negative outcome (survivorship).
*= statistically significant (p<0.10). **= statistically significant when considering size of the effect of RR.

Table 7.9: *Statistical summary for Kaplan-Meier function of possible and probable scurvy mortality of nonadults at Con Co Ngua.*

POSSIBLE AND PROBABLE SCURVY	ESTIMATE	STD. ERROR	95% CI	LOG RANK (MANTEL-COX)		
				CHI SQUARE	DF	P-VALUE
Mean				11.634	1	**0.001***
Absent	8.776	0.883	7.046- 10.505			
Present	2.463	1.624	0.000- 5.645			
Overall	7.606	0.843	5.954- 9.259			
Median						
Absent	8.000	1.960	11.841			
Present	0.000	-	-			
Overall	7.000	4.001	9.999			

*= statistical significance (p<0.15).

Table 7.10: *Statistical summary for Cox regression function of possible and probable scurvy mortality of nonadults at Con Co Ngua.*

POSSIBLE AND PROBABLE SCURVY	COEFFICIENT (β)	STD. ERROR	WALD	DF	P-VALUE	ODDS RATIO (Exp(β))
	-0.984	0.360	7.482	1	**0.006***	0.374

*= statistical significance (p<0.15).

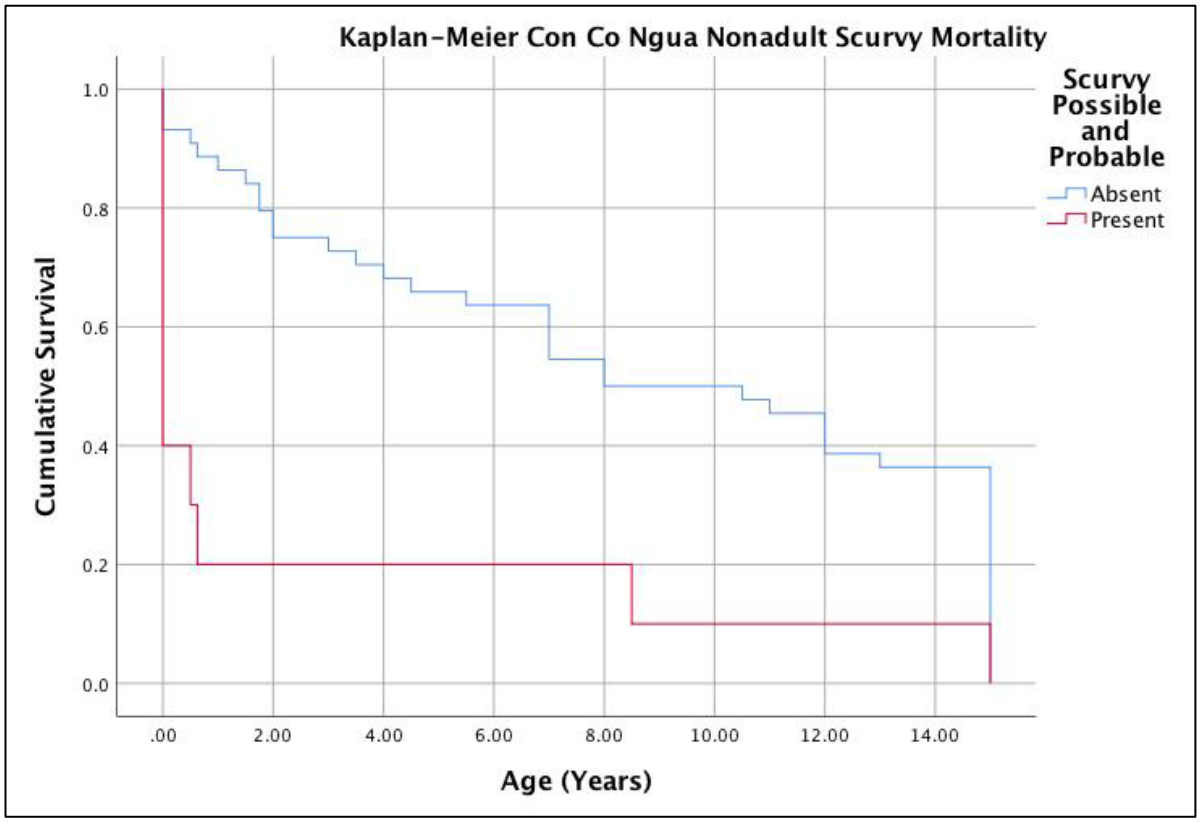

Figure 7.11: *Kaplan-Meier cumulative survival function of nonadult possible and probable scurvy mortality at Con Co Ngua. Image: author's own.*

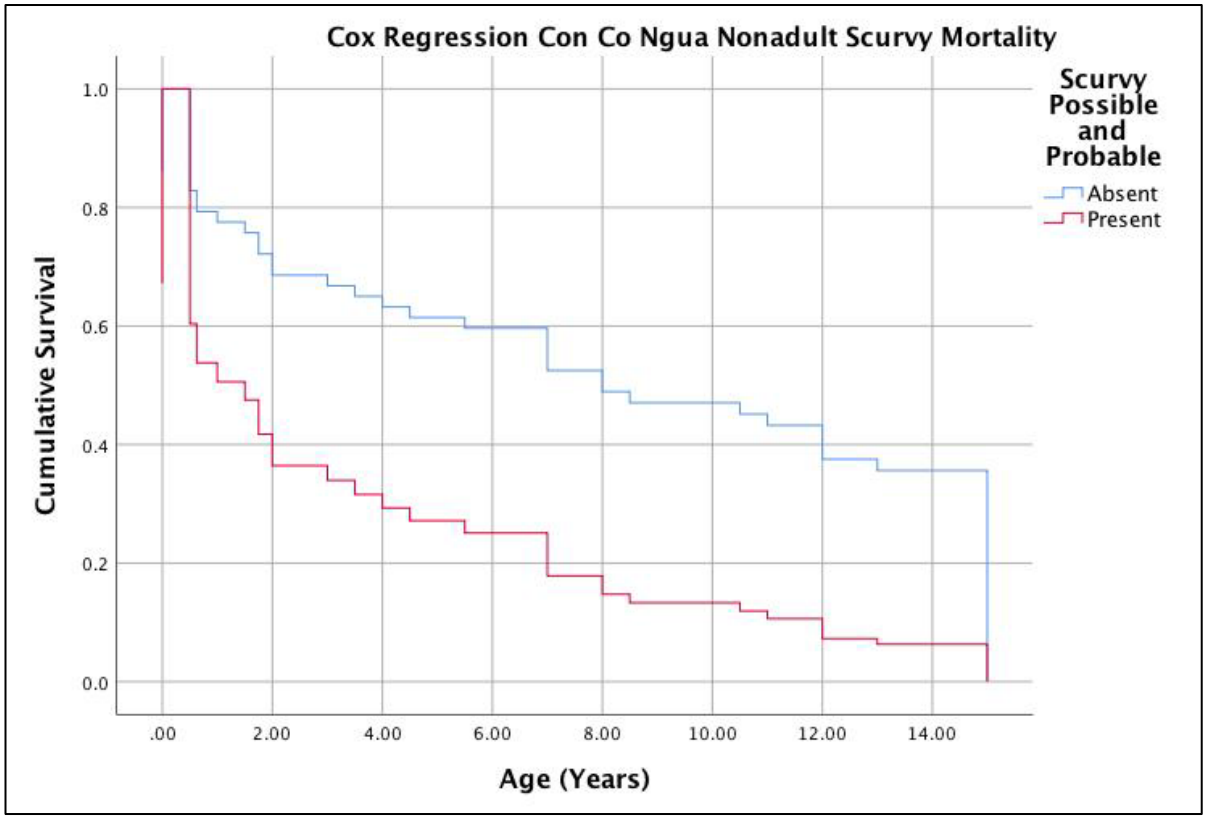

Figure 7.12: *Cox regression cumulative survival function of nonadult possible and probable scurvy mortality at Con Co Ngua. Image: author's own.*

7.4.8 Diagnosis of Anaemia at Con Co Ngua

Thirty-three percent of the overall Con Co Ngua assemblage exhibited medium or severe grade cribra orbitalia and/or porotic hyperostosis, consistent with a diagnosis of anaemia (Table 7.2). Cribra orbitalia was more common (31.7%, 40/126) than porotic hyperostosis (3.2%, 4/126), and no nonadults had porotic hyperostosis. Out of the four individuals with porotic hyperostosis, three of these also had medium or severe grade cribra orbitalia. The youngest individual in the collection with evidence of anaemia was an 8-9 year old child with medium grade cribra orbitalia. A steady increase in the percentage of anaemia is apparent with increasing adult age (Table 7.11; Figure 7.13).

As previously mentioned, seven individuals exhibited macroscopic and/or radiographic "double cortex" or "bone within a bone" signs (Figure 7.2). These pathologies are synonymous with macroscopic SPNB on the shafts of limb bones due to extramedullary haematopoiesis in thalassaemia, but can also be caused by infection or residual rickets. This lesion is therefore a suggestive trait, and alone is not diagnostic for thalassaemia (see Chapter 5). However, CCN13M113a, a middle aged adult male, also exhibited radiographic evidence for bone infarction (ischemic necrosis), another suggestive trait indicating the presence of possible thalassaemia at Con Co Ngua in at least one individual (Figure 7.14). This trait can also occur in hydatids disease (as seen in Figure 7.6). However, in CCN13M113a the infarctions are far more widespread than in the cases where necrosis has been identified as a result of hydatids disease which remains restricted to the region of lysis.

Table 7.11: *Summary of anaemia at Con Co Ngua*

ANAEMIA	CO			Cranial PH			PH and/or CO		
	Affected	*Observed*	*(%)*	*Affected*	*Observed*	*(%)*	*Affected*	*Observed*	*(%)*
0 to 6 months	0	6	0	0	6	0	0	6	0
6 months to 1 year	0	2	0	0	2	0	0	2	0
1 to 5 years	0	9	0	0	9	0	0	9	0
5 to 10 years	1	5	20	0	5	0	1	5	20
10 to 15 years	1	5	20	0	5	0	1	5	20
15 to 20 years	2	16	12.5	0	16	0	2	16	12.5
20 to 30 years	11	29	37.9	2	29	37.9	11	29	37.9
30 to 40 years	9	22	40.9	1	22	4.5	9	22	40.9
40 to 50 years	7	16	43.8	1	16	6.25	8	16	50
50+ years	9	15	60	0	15	0	9	15	60
Total nonadults	4	43	9.3	0	43	0	4	43	9.3
Males	21	53	39.6	4	53	7.5	21	53	39.6
Females	15	33	45.5	1	33	3.0	16	33	48.5
Total adults	36	82	43.9	4	82	4.9	37	82	45.1
Total	40	126	31.7	4	126	3.2	41	126	32.5

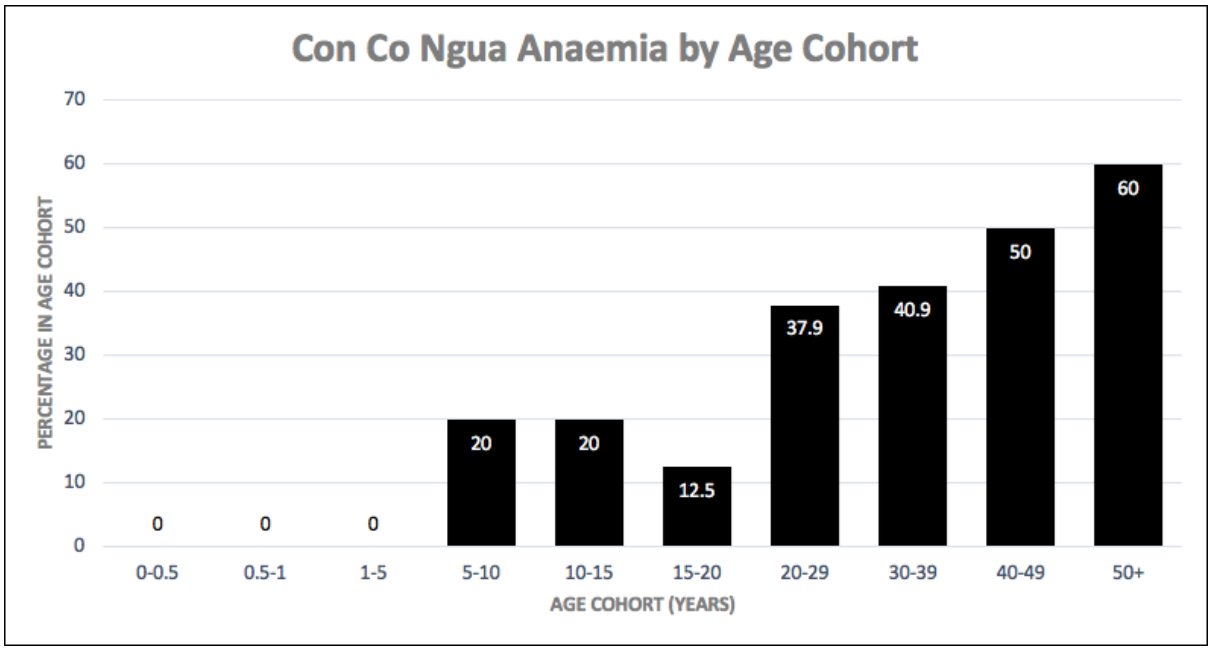

Figure 7.13: *Age-at-death distribution of anaemia at Con Co Ngua. Image: author's own.*

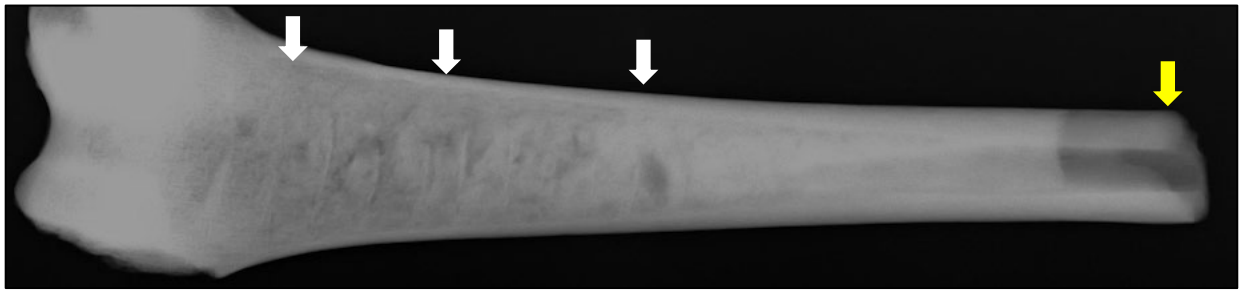

Figure 7.14: *Radiographic lesions suggestive of possible thalassemia in CCN13M113a, middle aged adult male. Note the widespread ischemic necrosis (white arrows), and the "double cortex" sign (yellow arrow).*

7.4.9 Morbidity of Anaemia at Con Co Ngua

The presence of thalassaemia was not statistically assessed as the disease patterns of this genetic anaemia is not directly associated with nutritional and infectious disease levels. The presence of this disease as possible indirect evidence of malaria is dealt with in the discussion section below. Assessment of anaemia morbidity at Con Co Ngua is restricted to those who presented with porotic hyperostosis and/or medium or severe grade cribra orbitalia, and therefore anaemia.

No statistically significant differences between the presence and absence of anaemia were apparent between males (39.6%, 21/53) and females (48.5%, 16/31) at Con Co Ngua (n=86, RR=1.2237, p=0.4136). Similarly, there were no significant differences in the prevalence of anaemia across nonadult age cohorts (Table 7.12). However, prevalence of skeletal evidence of anaemia was significantly higher in older age cohorts. This trend was consistent for individuals over the age of 20, 30 and 40 years. Adults were 3.6 times more likely to have evidence of anaemia after the age of 20 years than adolescents aged 15-19 years (n=98, RR=0.2770, p=0.0563). Because cribra orbitalia and porotic hyperostosis form in childhood, the trend observed is more likely reflective of childhood survivorship with anaemia which is assessed in the section below.

Table 7.12: *Relative risk of anaemia morbidity at Con Co Ngua across sex and age cohorts.*

EXPOSED GROUP/ CONTROL GROUP	OUTCOME		RR	P-VALUE	95%CI
	Positive: *Anaemia Present*	***Negative:*** *Anaemia Absent*			
Sex					
Female/ Male	16/21	17/32	1.2237	0.4136	0.7543- 1.9852
Nonadults					
<1 yr/ >1 yr	0/4	8/32	0.4568	0.5873	0.0270- 7.7369
<5 yrs/ >5yrs	0/4	16/24	0.1895	0.2543	0.0109- 3.3090
<10 yrs/ >10yrs	1/3	22/18	0.3043	0.2858	0.0342- 2.7046
Adults					
<20 yrs/ >20 yrs	2/37	14/45	**0.2770**	**0.0563***	0.0741- 1.0352
<30 yrs/ >30 yrs	13/26	32/27	**0.5589**	**0.0521***	0.3452- 1.0047
<40 yrs/>40 yrs	22/17	45/14	**0.5988**	**0.0318***	0.3749- 0.9564

A relative risk (RR) >1 denotes a relationship of the exposed group with an increase in disease prevalence, whereas RR <1 denotes a relationship of the control group with an increase in disease prevalence.
*= statistically significant (p<0.10). **= statistically significant when considering size of the effect of RR.

7.4.10 Mortality of Anaemia at Con Co Ngua

Relative risk ratios for both nonadults and adults indicated that the presence of skeletal anaemia at Con Co Ngua is related to increased likelihood of survival to older age. However, this relationship was only statistically significant in the adult age cohorts and not in the nonadult cohorts (Table 7.13). Con Co Ngua adults were 4.6 times more likely to have survived past the age of 20 years of age with skeletal evidence of possible childhood anaemia than die before this age (n=98, RR=0.2161, p=0.0352). The relative risk gradually increased at 30 years (n=98, RR=0.6111, p=0.0701) and 40 years of age (n=98, RR=0.7211, p=0.0415), which suggests the relationship with survivorship decreased with increasing adult age.

Kaplan-Meier distribution analysis indicates no significant differences between survivorship of nonadults with and without evidence of anaemia (n=44, X^2=0.352, df=1, p=0.352; Table 7.14; Figure 7.15). However, statistically significant survivorship of adults with skeletal signs of anaemia was identified with the Kaplan-Meier distribution (n=98, X^2=6.164, df=1, p=0.013; Table 7.15; Figure 7.16) and the Cox regression function (n=98, Wald=3.341, df=1, p=0.068; Table 7.16; Figure 7.17). These outcomes support the relative risk ratio analysis outcome for anaemia mortality.

Table 7.13: *Relative risk of anaemia mortality at Con Co Ngua across age cohorts.*

POSITIVE OUTCOME/ NEGATIVE OUTCOME	**TREATMENT**		**RR**	**P-VALUE**	**95%CI**
	Exposed Group: *Anaemia Present*	***Control Group:*** *Anaemia Absent*			
Nonadults					
<1 yr/ >1 yr	0/4	8/32	0.4824	0.5962	0.0325- 7.1549
<5 yrs/ >5yrs	0/4	16/24	0.2485	0.3042	0.0175- 3.5380
<10 yrs/ >10yrs	1/3	22/18	0.4545	0.3690	0.0814- 2.5394
Adults					
<20 yrs/ >20 yrs	2/37	14/45	**0.2161**	**0.0352***	0.0520- 0.8989
<30 yrs/ >30 yrs	13/26	32/27	**0.6111**	**0.0701***	0.3573- 1.0452
<40 yrs/>40 yrs	22/17	45/14	**0.7211**	**0.0415***	0.5266- 0.9875

A relative risk (RR) >1 denotes a relationship of the disease presence with the positive outcome (susceptibility to mortality), whereas RR <1 denotes a relationship of the disease absence with a negative outcome (survivorship).
*= statistically significant (p<0.10). **= statistically significant when considering size of the effect of RR.

Table 7.14: *Statistical summary for Kaplan-Meier function of anaemia mortality of nonadults at Con Co Ngua.*

ANAEMIA	**ESTIMATE**	**STD. ERROR**	**95% CI**	**LOG RANK (MANTEL-COX)**		
				CHI SQUARE	**DF**	**P-VALUE**
Mean				0.868	1	0.352
Absent	7.984	0.982	6.060- 9.909			
Present	12.750	1.652	9.512- 15.988			
Overall	8.418	0.925	6.605- 10.231			
Median						
Absent	7.000	1.579	3.905- 10.095			
Present	13.000	2.333	8.427- 17.573			
Overall	8.000	2.154	3.779- 12.221			

*= statistical significance (p<0.15).

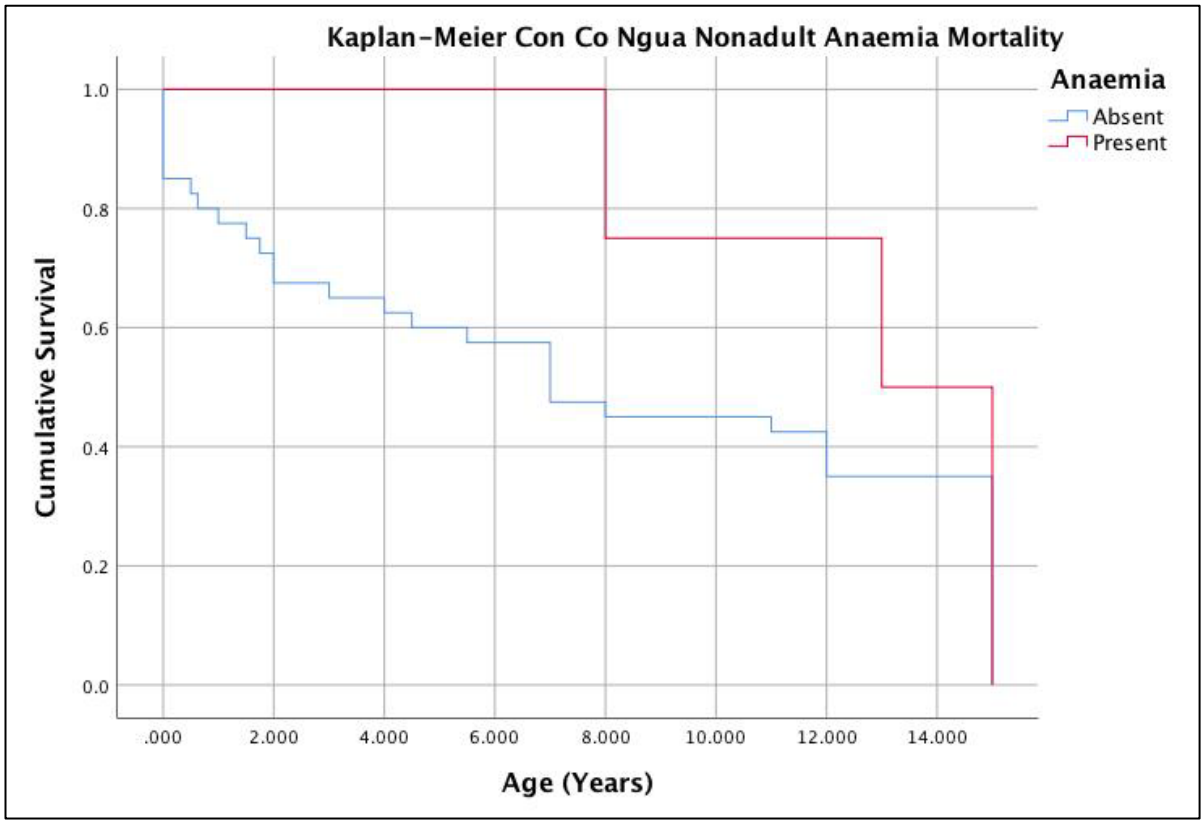

Figure 7.15: *Kaplan-Meier cumulative survival function of nonadult anaemia mortality at Con Co Ngua. Image: author's own.*

Table 7.15: *Statistical summary for Kaplan-Meier function of anaemia mortality of adults at Con Co Ngua.*

ANAEMIA	ESTIMATE	STD. ERROR	95% CI	LOG RANK (MANTEL-COX)		
				CHI SQUARE	DF	P-VALUE
Mean				6.164	1	**0.013***
Absent	30.085	1.541	27.065- 33.105			
Present	36.665	1.765	33.207- 40.126			
Overall	32.704	1.203	30.346- 35.062			
Median						
Absent	25.000	2.469	20.161- 29.839			
Present	35.000	3.441	28.256- 41.744			
Overall	35.000	1.805	31.461- 38.539			

*= statistical significance (p<0.15).

Table 7.16: *Statistical summary and equation for Cox regression function of anaemia mortality of adults at Con Co Ngua.*

ANAEMIA	COEFFICIENT (β)	STD. ERROR	WALD	DF	P-VALUE	ODDS RATIO (Exp(β))
	0.380	0.208	3.341	1	**0.068***	1.463

**= statistical significance (p<0.15).*

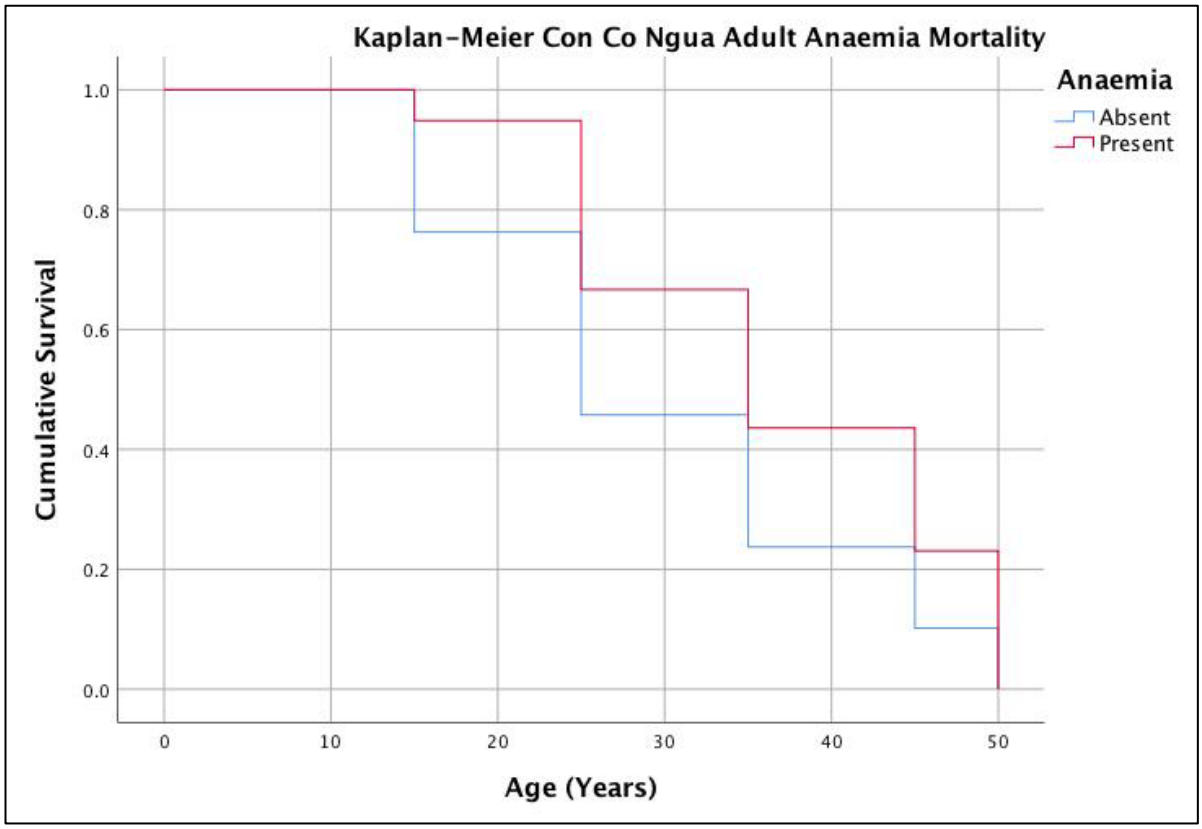

Figure 7.16: *Kaplan-Meier cumulative survival function of anaemia mortality at Con Co Ngua. Image: author's own.*

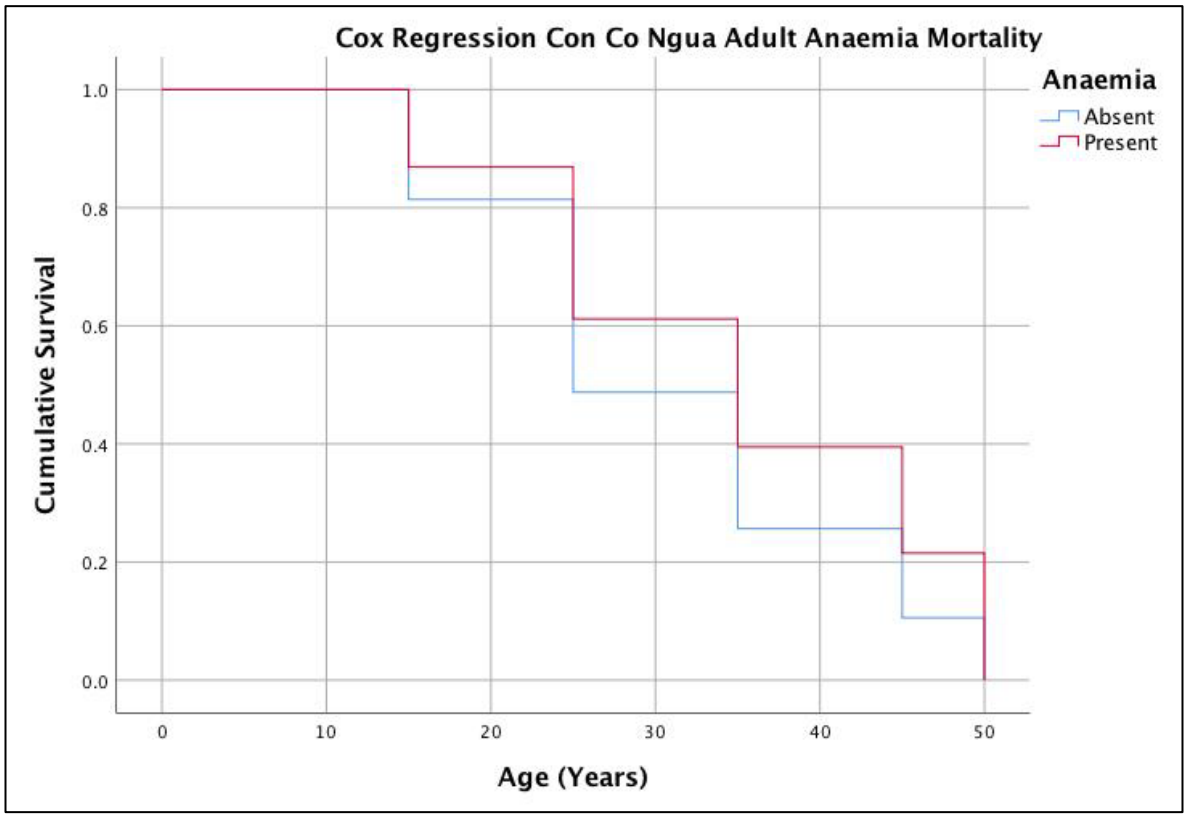

Figure 7.17: *Cox regression cumulative survival function of adult anaemia mortality at Con Co Ngua. Image: author's own.*

7.4.11 Summary of Diagnosis and Context of Disease at Con Co Ngua

Overall infectious diseases, which included hydatids disease and non-specific infection (8.4%,13/255), scurvy (6.5%, 10/155), and anaemia (32.5%,41/126) were identified at Con Co Ngua.

7.4.11.1 Infectious Disease at Con Co Ngua

The identification of osteomyelitis in an individual from a foraging community is not unusual due to the varying hunting, gathering and foraging activities which could result in exposure to a variety of pathogens which infect the skeleton, particularly when related to trauma. However, the diagnosis of seven cases of probable hydatids disease requires further discussion. The calcified cyst suggests that *Echinococcus granulosis* is the likely cause for the hydatids disease at Con Co Ngua. Hydatids disease is predominantly associated with pastoralism and requires a contiguous relationship between human groups, dogs and ungulates for humans to become an accidental intermediate host (Beggs 1985). While sylvatic (wild) strains do occur, they rarely infect humans. Such strains are known to affect deer as intermediate hosts and wolves as definitive hosts, and are found in the northern hemisphere (Rausch and D'Alessandro 1999). Buffalo and deer dominate the faunal assemblage and evidence of butchery marks on the animal bone indicate processing of the full carcass at the site which could suggest hunting of animals nearby to residence (Oxenham et al. 2018). Buffalo are also known to be intermediate hosts for *E. granulosis* non-sylvatic strains (Beggs 1985). Evidence of accidental trauma at Con Co Ngua indicates a close relationship with buffalo through the management of wild herds (Scott et al. 2019). The prevalence and patterns of trauma at the site were most closely related to those observed at agropastoralist sites. As was proposed in Oxenham et al. (2018), these two species (deer and buffalo) are posited as plausible intermediate hosts at Con Co Ngua, and a number of carnivorous animals such as civets, jackals, wolves, leopards, and foxes may have served as the definitive host (Jones 2017; Oxenham et al. 2018). In both sylvatic and non-sylvatic strains of *E. granulosis*, contamination of water source is a primary route of accidental infection in humans (Beggs 1985). It is plausible that water sources shared with buffalo and/or deer, and carnivores led to the infection of Con Co Ngua habitants with hydatids disease.

There was no significant relationship with mortality or age of morbidity in the Con Co Ngua individuals with infectious disease. This outcome is expected, considering that the overall infectious disease prevalence was predominantly representative of individuals diagnosed with hydatids disease. While the disease is recognised to have a high mortality rate once it has affected the skeleton, the disease often lies dormant for decades in organs prior to skeletal infection. The relationship of skeletal hydatids disease to mortality is determined by the age of onset (Song et al. 2007). Adolescents and adults of all age cohorts were infected, so were both males and females, suggesting that at the very least all adults were at risk of exposure to the disease. Children may have also been infected without progression of the disease to a skeletal stage.

7.4.11.2 Scurvy at Con Co Ngua

A low prevalence of scurvy is expected given the vast tropical resources available to inhabitants at Con Co Ngua. Oxenham et al. (2018) have previously suggested the Holocene Thermal Maximum may have provided favourable conditions for wild faunal and floral resources available to sedentary foragers in Northern Vietnam and Southern China from the Dingsishan-Da But period. This is supported by palaeobotanical and zooarchaeological studies of resources of Pre-Neolithic foragers (Jones 2017; Mai Huong 2013; Oxenham et al. 2018). The Vitamin C content of *Canarium* sp., found at Con Co Ngua, provides up to 12.33mg/100g, levels sufficient to prevent scurvy in an adult male if consumed in adequate quantities (Chang et al. 2017; Hirschmann and Raugi 1999). The high association between scurvy presence and infant mortality at Con Co Ngua suggests scurvy may represent an extreme in the assemblage. Food shortage, possibly due to seasonal fluctuations, typhoons or other climatic events may have diminished food returns, and the most vulnerable individuals succumbed to malnourishment at an early age (Oxenham 2006). As the causes of scurvy are often multifactorial, infection may have also increased the bodily demand for Vitamin C in these individuals (Buckley 2000). Notably, as the two probable cases of scurvy are perinatal, it does suggest a lack of Vitamin C passed placentally, implicating Vitamin C deficiency in the mother as well (Snoddy et al. 2017). It does need to be noted that as nonadults were often found disturbed by other adult burials impacting preservation, this may have influenced the age-at-death distribution of nonadults and subsequently findings in regards to scurvy prevalences across nonadult age cohorts.

7.4.11.3 Anaemia and Thalassaemia at Con Co Ngua

The higher prevalence of anaemia in comparison to scurvy and infection at Con Co Ngua is likely due to the variable factors which cause anaemia. Iron deficiency can occur due to insufficient dietary intake, inflammation to the gut disrupting absorption into the bloodstream and possibly due to iron withholding during infection (Annibale et al. 2000; Tontisirin et al. 2002). Parasites such as helminths (parasitic worms) are primary factors causing iron deficiency anaemia, due to parasitic diarrhoea, in tropical regions and in populations who exploit marine fish, such as at Con Co Ngua (Bathurst 2005; de Vizia et al. 1992; Foy and Nelson 1963; Temple 2007). Hydatids disease is caused by a helminth and has been linked to iron deficiency (Somily et al. 2005). However, because humans get infected with *Echinococcus* sp. as intermediate hosts, adult worms directly influencing infection in the gut (such as is the case in hookworm and ascaris) does not occur, and iron deficiency is usually mild in cystic hydatids disease (Gilles 1968; Somily et al. 2005). Therefore, anaemia as directly caused by hydatids disease is unlikely to have significantly contributed to the development of skeletal signs of anaemia at Con Co Ngua.

The overall prevalence of anaemia is also probably not restricted to the representation of only iron deficiency anaemia, and can be caused by genetic disorders or vitamin deficiencies (such as Vitamin A and B12) (Gowland and Western 2012; Mejia 1993; Oh and Brown 2003). The diagnosis of one possible case of thalassaemia suggests that multiple aetiologies including possibly genetic factors are influencing the prevalence of anaemia at Con Co Ngua. The significant relationship of anaemia presence to adult survivorship indicates those who were exposed to factors inducing skeletal evidence of anaemia, survived better to the overall conditions at Con Co Ngua than those who did not form porotic hyperostosis or cribra orbitalia.

7.4.11.4 Intrapopulation Variation of Disease at Con Co Ngua

No differences between males and females were identified for any of the diagnosed diseases at Con Co Ngua. In conclusion, the disease pattern observed at Con Co Ngua emphasises a community with low levels of specific nutritional disease (due to sufficient dietary diversity), a considerable burden of specific infectious disease, but overall pervasive stressors were particularly evident in the form of skeletal evidence for anaemia.

7.5 Man Bac

Man Bac is an early Neolithic habitation and burial site in Ninh Binh province of Northern Vietnam dating to 3906-3523 cal BP (Vlok et al. in press; Oxenham et al. 2011; Vlok et al. 2020). Today the site is on a lowland plain, coastal and surrounded by limestone karsts. While today the site is currently 25km from the ocean, Man Bac would have been adjacent to the sea during its time of occupation due to higher sea levels in the past (Tanabe et al. 2006). As is the case with Con Co Ngua, the site is within the subtropical zone (Oxenham et al. 2011). During the Neolithic, the temperature was likely slightly warmer and more humid than present day, although not to the degree as during the occupation of Con Co Ngua (Oxenham et al. 2018). The surrounding ecology likely included riverine, coastal and estuarine flora and fauna (Tanabe et al. 2006).

Man Bac forms part of the Phung Nguyen complex, a series of sites found along the Red River Delta. The presence of contemporaneous Phung Nguyen pottery styles suggests extensive interaction between the sites further inland along the river, as well as shared archaeological material with agricultural sites in Southern China (Bellwood 2008; Nguyen 2008). The type site of Phung Nguyen is approximately 160km from today's coastline, which represents the possible extent of interaction of farming settlements within Northern Vietnam, although this site is dated to slightly later at around 3500BP (Khoach 1980). Evidence of housing type was not found at Man Bac. However, housing may have been similar to other Phung Nguyen habitation sites where evidence of large houses on stilts appear to have been built possibly for similar reasons as constructed in mountainous regions of Vietnam today, in order to keep out snakes and small animals (Khoach 1980).

Storms including large typhoons are common for the region today and were likely a common occurrence in prehistory, possibly disrupting both agricultural efforts and wild plant resources (Oxenham 2006). To date it is the only site in Southeast Asia where co-habitation of indigenous foragers with affinity to Australo-Papuan populations and migrant farmers morphologically similar to cold adapted East Asian populations, have been documented through morphometric and DNA research (Lipson et al. 2018; Matsumura and Oxenham 2013; Matsumura and Oxenham 2014; McColl et al. 2018). As such, Man Bac is a site of significance for understanding the agricultural transition of Southeast Asia. Long grain rice phytoliths were found within the cultural layers of Man Bac, as has been identified

at other Phung Nguyen sites (Bellwood and Oxenham 2008; Jones et al. 2019; Mai Huong 2013; Mai Huong 2016; Willis and Oxenham 2013). Evidence of domesticated pigs has been found, and the faunal assemblage exhibits restricted diversity of faunal taxa when compared to Con Co Ngua (Jones et al. 2019; Oxenham et al. 2018; Sawada et al. 2011). However, preliminary carbon isotope results suggest a lower reliance on C3 plants than subsequent Metal Period assemblages in Vietnam (Oxenham et al. 2011; Yoneda 2008). Along, with faunal evidence demonstrating a continued exploitation of marine fauna from brackish and estuarine waters, and terrestrial sources from forests, grasslands and watered lowlands, a mixed subsistence base of foraging and farming is proposed for Man Bac (Jones 2017; Jones et al. 2019; Sawada et al. 2011; Toizumi et al. 2011).

It is not possible to estimate the population density of the Man Bac community because the number of burials is not likely representative of the numbers in the living population. Additionally, the full extent of the site was not excavated. However, the Man Bac cemetery sample is characterized by a high fertility rate and rate of natural population growth (D0-14/D= 0.59, RNPI= 4.32), the highest of any MSEA prehistoric site (McFadden et al. 2018). All burials, with the exception of three flexed inhumations, were in a supine extended position, which is the normative pattern of burial at this time throughout Southeast Asia (Figure 7.18; Higham et al. 2011). Grave goods suggest an age-based social hierarchy, and ritual tooth removal (ablation) indicates affinal kinship relationships, which may have impacted the distribution of resources within the community (Huffer et al. in press; Tilley and Oxenham 2016).

Figure 7.18: *The excavation of Man Bac. Note that the burials are extended and supine as is common for Neolithic and post-Neolithic burials in Mainland Southeast Asia. Individuals were buried with earthenware characteristic of the Phung Nguyen Culture. Image: courtesy of Prof M. Oxenham (used with permission).*

Previous palaeopathological research has demonstrated high levels of non-specific stress; 92.3% of males and 53.8% of females presented with cribra orbitalia (mild to severe) and 64.9% of the total assemblage exhibited linear enamel hypoplasia of the incisors or canines (Oxenham et al. 2011). Forty-two per cent of individuals had localised primary canine hypoplasia which may be related to calcium, Vitamin A, or Vitamin D deficiencies during gestation (McDonell and Oxenham 2014). Therefore, stresses either from parasitic, dietary or infectious origin were commonplace experiences during childhood for many of the individuals from Man Bac. The following section presents the results for differential diagnosis of infectious disease, nutritional disease, and anaemia at Man Bac followed by the statistical assessment of morbidity and mortality of these diseases at the site.

7.6 Results: Man Bac Skeletal Pathology

7.6.1 Summary of Pathological Lesions at Man Bac

A high percentage (88.6%, 62/70) of individuals from Man Bac presented with at least one osteoblastic lesion (Table 7.17). All except one nonadult had osteoblastic lesions

(97.7%, 43/44), with a lower prevalence observed in the adults (73.1%, 19/26). The osteoblastic lesions in the assemblage were overwhelmingly discrete and symmetrical SPNB affecting the crania (Figure 7.19). Furthermore, the cranial SPNB was commonly associated with abnormal cortical porosity and vascular impressions were also frequent, particularly in nonadults. Diffuse symmetrical SPNB was also common in the postcrania of both adults and nonadults. Twenty-nine percent (29.4%, 10/34) of individuals over 15 years of age also exhibited diffuse SPNB across multiple limb bones predominantly with cortical enlargement (Figure 7.20), and cortical enlargement was present in 20.5% (9/44) of nonadults. In one adult (MB05M20, young adult male) and one nonadult (MB07H2M29, approx. 7 years old), bilateral cortical enlargement of the anterior surfaces of the tibiae caused mild anterior pseudobowing. Additionally, 12.9% (8/62) of the assemblage that presented with preserved hands/or feet, exhibited dactylitis.

Four individuals (5.7%, 4/70) in the collection presented with superficial oval osteolytic lesions of the external cortex of long bones shafts with sclerotic smooth margins and base (Figure 7.21). These lesions were predominantly grade OL2, with the exception of an osteolytic lesion in an approximate 18-month old (MB05M5) that was less than 10mm in size (OL1). No lesions were macroscopically observed in the axial skeleton. All lesions demonstrated sclerotic margins on the radiographs and were either found within discrete nodes of SPNB and/or on a long bone with cortical enlargement of the shaft. Furthermore, diffuse SPNB across multiple long bones was identified in every individual with these osteolytic lesions.

With the exception of pseudobowing of the tibiae from extensive SPNB in one adult, no adults exhibited any true skeletal deformities indicative of infectious or nutritional disease. Bending of the shafts (8/44, 18.2%), and flaring (10/44, 22.7%), fraying (5/44, 11.4%) and cupping of the metaphyseal plates (18/44, 40.9%) of long bones were present in some nonadults. Additionally, over half (52.3%, 23/44) of nonadults presented with abnormal deep endochondral porosity extending more than 10mm from the metaphyseal plates. Four nonadults (9.1%, 4/44) also presented with an enlarged and bulbous appearance of the zygomatic bones, maxillae and in one individual the mandible with associated crowding of the teeth. Two of these nonadults with anterior protrusions of the facial bones and one other (6.8%, 3/44), also exhibited thick and short ilia and/or scapulae in comparison to other infants of similar age in the assemblage.

Table 7.17: *Summary of OB and OL lesion prevalences, and skeletal deformities at Man Bac*

	NONADULT (aff/obs)	NONADULT (%)	ADULT (aff/obs)	ADULT (%)	TOTAL (aff/obs)	TOTAL (%)
OB Lesion	43/44	97.7	19/26	73.1	62/70	88.6
OL Lesion	2/44	4.5	2/26	7.7	4/70	5.7
Cupping	18/44	40.9	0/26	0	18/70	25.7
Flaring	10/44	22.7	0/26	0	10/70	14.3
Fraying	5/44	11.4	0/26	0	5/70	7.1
Bending of Long Bone Shafts	8/44	18.2	0/26	0	8/70	11.4
Facial Deformity	4/44	9.1	0/26	0	4/70	5.7
Other Skeletal Deformities	3/44	6.8	0/26	0	3/70	4.3

Figure 7.19: *Discrete deposit of remodelled SPNB and abnormal cortical porosity inferior to the right oblique line of the mandible (white arrows) of MB07H2M19, young adult male. There is also a symmetrical lesion on the left side. Image: author's own.*

Figure 7.20: *Diffuse SPNB with cortical enlargement especially distally (OB4, white arrows) across the shafts and metaphyses of the tibiae and fibulae of MB07H2M18, female ~16 years of age. Image: author's own.*

Figure 7.21: *Superficial oval osteolytic lesion on the anterior lateral epicondyle of the right humerus (MB05M20, young adult male). Image: author's own.*

7.6.2 Diagnosis of Infectious Disease at Man Bac

Seven individuals over the age of 15 (7/70, 10%) displayed diffuse SPNB involving more than ¼ of the bone surface across two or more skeletal elements, and were therefore included in the overall infectious disease prevalence at Man Bac (Table 7.18). One individual, MB05M10, a nonadult approximately 9 years of age, exhibited a small deep focal OL1 osteolytic lesion with minimal sclerosis of the margin of the right mastoid, and associated remodelled SPNB and cortical porosity around the margins of the external auditory canals. Radiographs demonstrate extensive multifocal and coalesced osteolytic destruction extending from the mastoid into the petrous portion superior to the auditory canal (Figure 7.22). Osteolytic destruction of the mastoid is strongly diagnostic for mastoiditis consistent with the diagnosis of a probable case.

Two individuals, MB05M20 (young adult male) and MB07H2M29 (child approximately 7 years of age), presented with superficial focal cavitations within striated nodes of SPNB which is strongly diagnostic for treponemal disease, and consistent with a diagnosis of a probable case (Figure 7.23, Table 7.18). Both individuals exhibited sabre shin, and MB07H2M29 displayed dactylitis, which supports this diagnosis (Figures 7.24 and 7.25). Unilateral enlargement of the sternal end of the clavicle was also observed in MB07H2M29, and this lesion has been noted in cases of late onset congenital syphilis (Dax and Stewart 1939; Frangos et al. 2011; Harper et al. 2011; Lewis 2017; Yang 1940). This so-called *Higoumenakis sign* presents as layers of SPNB on the sternal end of the clavicle unilaterally (Frangos et al. 2011). The lack of macroscopic or radiographic trace of SPNB or cortical enlargement on the sternal end of MB07H2M29's left clavicle makes the identification of this pathology as a clear Higoumenakis sign difficult. However, MB07H2M29 also presented with evidence of nutritional disease (probable scurvy and rickets) which may have resulted in cortical thinning (see section on nutritional disease below). These two cases are published in Vlok et al. (2020).

Four other individuals exhibited lesions consistent with possible treponemal disease. MB05M5 is an infant approximately 18 months of age with endosteal enlargement of the long bones associated with superficial osteolytic lesions, and a distinct node of SPNB of the tibia. While the radiographs demonstrate a superficial focal sclerotic response in the distal metaphysis of the left humerus and superior acromial end of the clavicle, these lesions are

small (lesion on humerus is 3.9x1.7mm, and on clavicle is 3x3mm), impeding confidence that these lesions are *superficial focal cavitations* as described by Hackett (1976). MB05M29 is a middle-aged adult male with dactylitis and diffuse SPNB in the forearms and legs associated with endosteal enlargements. Two focal superficial lesions with sclerotic response are present on the medial distal right fibula. However, these lesions are not within a distinct node of SPNB, do not strictly fit the definition of *superficial cavitation* by Hackett (1976), and are therefore not strongly diagnostic. These lesions have been considered diagnostic instead (Vlok et al. 2020). A further three individuals presented with endosteal nodes/enlargements of long bones, and/or dactylitis which are also consistent with treponemal disease. All lesions follow a postcranial pattern of lymphatic dissemination consistent with treponemal disease (Buckley and Dias 2002). One individual (MB07H2M17, 11-15 years of age) exhibited diffuse SPNB without endosteal enlargement as well as dactylitis. This individual did not meet the criteria for possible treponemal disease due the lack of evidence of cortical enlargement or nodes of SPNB. However, as the overall skeletal lesion expression was consistent with others identified with possible and probable treponemal disease (diffuse SPNB across the appendicular skeleton), the individual was included in the overall infectious disease prevalence for Man Bac. Possible and probable cases of treponemal disease were present in all post-infant age cohorts up until the age of 40 years of age, and both males and females were affected (Table 7.18; Figure 7.26).

Figure 7.22: *Mastoiditis in a nonadult at Man Bac. a) Deep oval osteolytic lesion the mastoid of MB05M10 (approx. 9 years of age, white arrow). The margin is preserved on the inferior portion, with some postmortem damage on the superior portion of the lesion. b) Radiographs demonstrate extensive internal multifocal and coalesced osteolytic destruction beyond what is macroscopically visible (region indicated by the white arrow). Image: author's own.*

Table 7.18: *Summary of infectious disease at Man Bac*

	POSSIBLE			**PROBABLE**			**POSSIBLE AND PROBABLE**		
	Affected	*Observed*	*(%)*	*Affected*	*Observed*	*(%)*	*Affected*	*Observed*	*(%)*
Otitis Media									
0 to 6 months	0	6	0	0	6	0	0	6	0
6 months to 1 year	0	7	0	0	7	0	0	7	0
1 to 5 years	0	15	0	0	15	0	0	15	0
5 to 10 years	0	2	0	1	2	50	1	2	50
10 to 15 years	0	3	0	0	3	0	0	3	0
15 to 20 years	0	4	0	0	4	0	0	4	0
Total nonadults	0	37	0	1	37	2.7	1	37	2.7
Total	0	61	0	1	61	1.6	1	61	1.6
Treponemal Disease									
0 to 6 months	0	8	0	0	8	0	0	8	0
6 months to 1 year	0	6	0	0	6	0	0	6	0
1 to 5 years	1	20	5	0	20	0	1	20	5
5 to 10 years	1	3	33.3	1	3	33.3	2	3	66.7
10 to 15 years	0	3	0	0	3	0	0	3	0
15 to 20 years	1	4	25	0	4	0	1	4	25
20 to 30 years	0	9	0	1	9	11.1	1	9	11.1
30 to 40 years	1	6	16.7	0	6	0	1	6	16.7
40 to 50 years	0	8	0	0	8	0	0	8	0
50+ years	0	3	0	0	3	0	0	3	0
Total nonadults	3	44	6.8	1	44	2.3	4	44	9.1
Males	1	15	6.7	1	15	6.7	2	15	13.3
Females	1	11	9.1	0	11	0	1	11	9.1
Total adults	1	26	3.8	1	26	3.8	2	26	7.7
Total	4	70	5.7	2	70	2.9	6	70	8.5
							CRITERIA PREVALENCE		
							Affected	*Observed*	*(%)*
Overall infectious disease criteria									
0 to 6 months							0	8	0
6 months to 1 year							0	6	0
1 to 5 years							1	20	5
5 to 10 years							2	3	66.7
10 to 15 years							1	3	33.7
15 to 20 years							3	4	75
20 to 30 years							1	9	11.1
30 to 40 years							4	6	66.7
40 to 50 years							2	8	25
50+ years							0	3	0
Total nonadults							7	44	15.9
Males							6	15	40
Females							2	11	18.2
Total adults							7	26	26.9
Total							14	70	20

Figure 7.23: *Strongly Diagnostic and Diagnostic Macroscopic Lesions for Treponemal Disease in MB05M20 (M20) and MB07H2M29 (M29). a) Superficial focal cavitation of the medial left calcaneus (M20). b) Superficial focal cavitation of the anterior lateral epicondyle of the right humerus (M20). c) Superficial focal cavitation of the posterior lateral epicondyle of the right humerus (M20). d) Superficial focal cavitations within a distinct node of new bone of the right distal fibular shaft M20). e) Superficial focal cavitations within a distinct node of new bone of the right distal fibular shaft (M20). f) Focal cavitation of the right distal fibular shaft with sclerotic margins within a distinct node of new bone (M29). g) Superficial focal cavitation of the proximal right fibula (M20). h) Focal cavitation of the right distal fibular shaft with sclerotic margins within a distinct node of new bone, same lesion as 5f. (M29). i) Focal cavitations of the right mid ulnar and radial shafts with sclerotic margins within a distinct node of new bone (M29). Image: author's own from Vlok et al. (2020).*

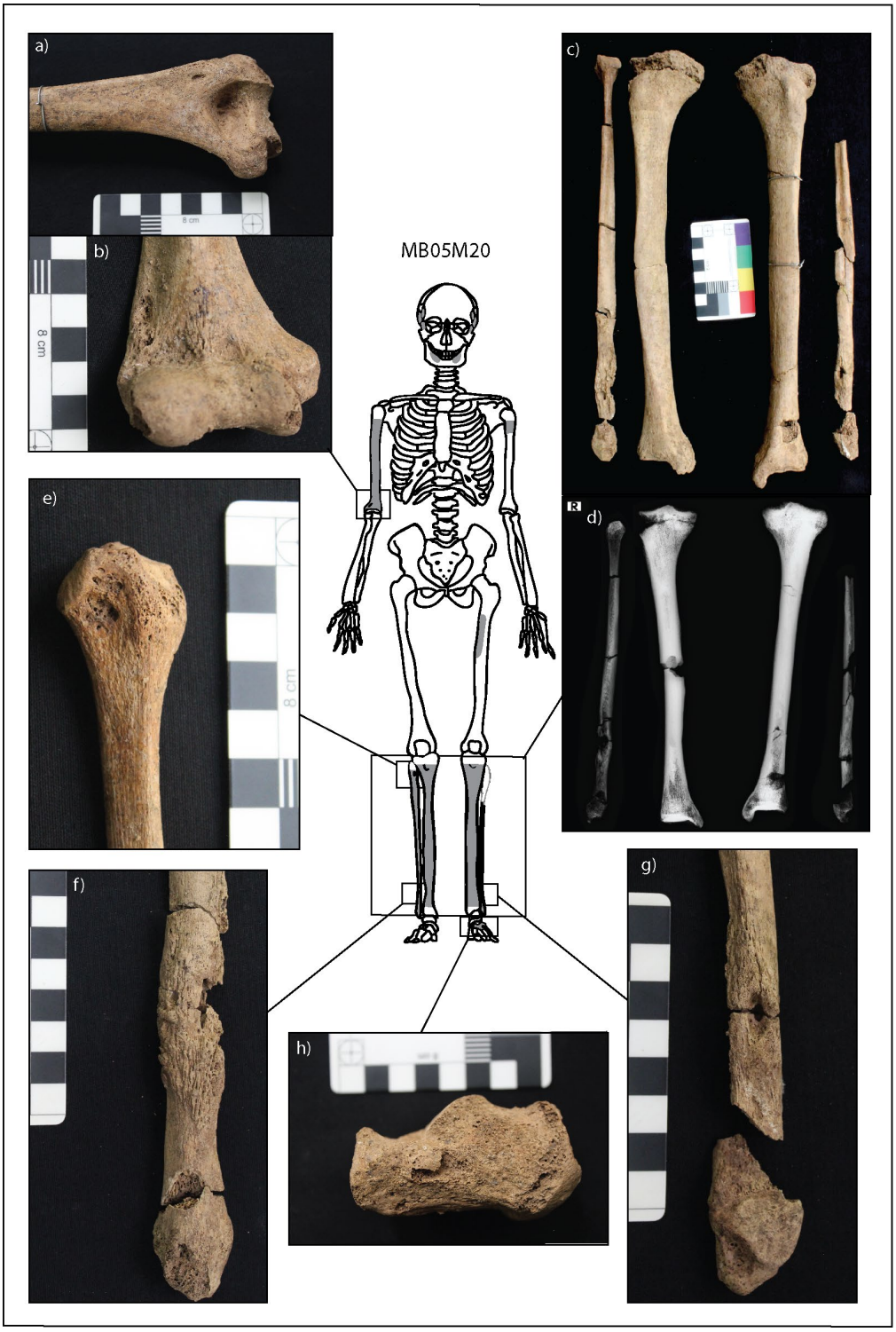

Figure 7.24: *Expression of lesions related to infectious disease in MB05M20. Preserved bones are outlined in black, with absent bones outlined in light grey. The skeletal extent of osteoblastic lesions is indicated by dark grey fill. a) and b) Superficial focal cavitations with smooth sclerotic margins not within distinct nodes of SPNB on the anterior and posterior lateral epicondyle of the right humerus. c) Cortical enlargements throughout the shafts of the tibiae with striated nodes of SPNB on the distal fibulae. d) Radiographs of the tibiae and fibulae: a distinct node of new bone with medullary intrusion is present on the medial middle shaft of the right tibia. e) Superficial focal cavitation not within a distinct node of SPNB on the proximal right fibula. f) Two focal superficial cavitations on the lateral aspect of the right distal fibula within a distinct node of striated new bone. g) Focal superficial cavitation on the medial aspect of the right distal fibula within a distinct node of striated SPNB. h) Focal superficial cavitation on the medial left calcaneal body, not within a distinct node of SPNB. Image: author's own from Vlok et al. (2020).*

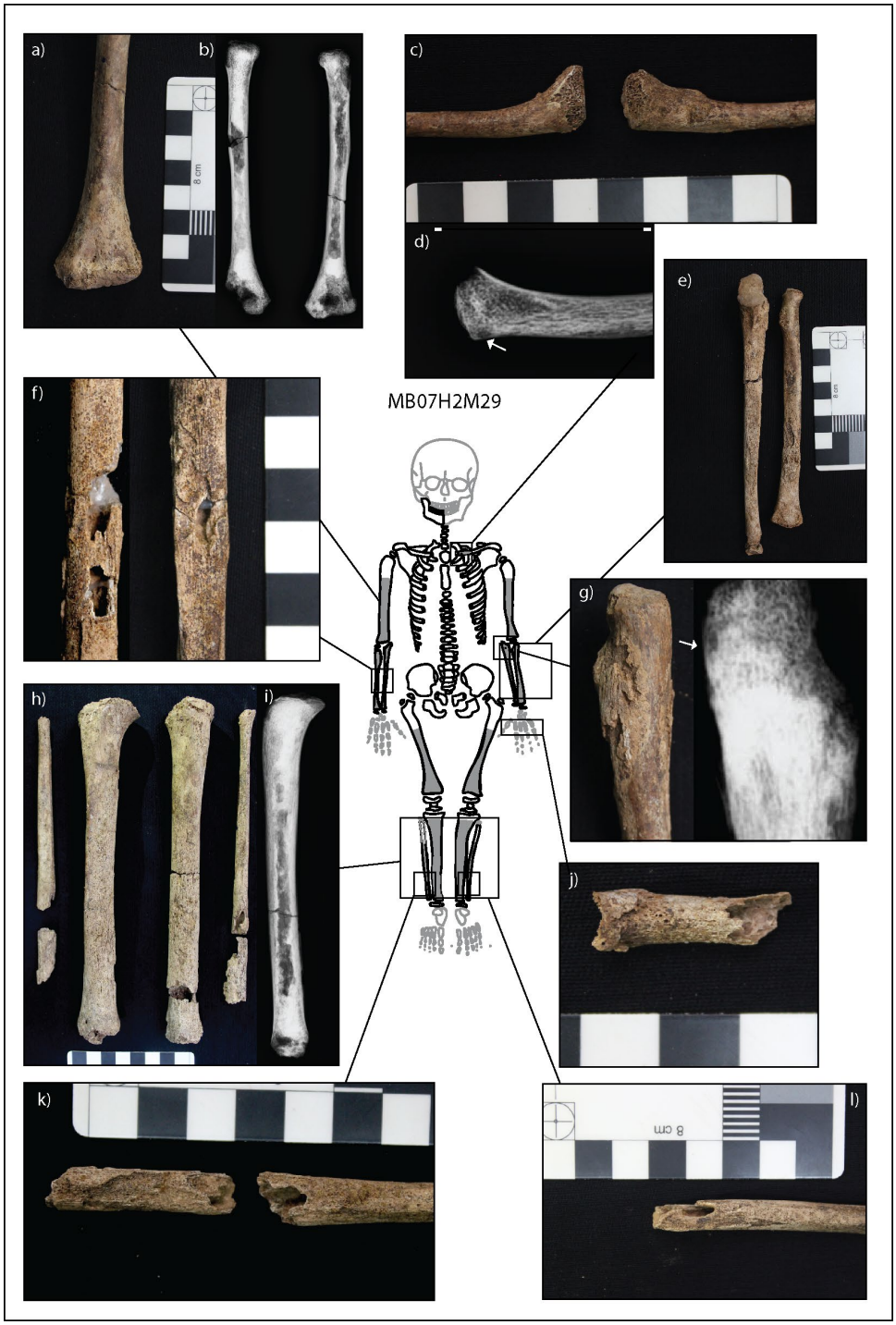

Figure 7.25: *Expression of lesions related to infectious disease in MB07H2M29. Preserved bones are outlined in black, with absent bones outlined in light grey. An undetermined metacarpal is also present but not demonstrated in the figure as its skeletal position is unknown. The skeletal extent of OB lesions is indicated by dark grey fill. a) and b) SPNB on the distal ends of the humeri with cortical enlargement. c) Possible Higoumenakis sign of the left clavicle. d) Oval osteolytic lesion with a radiodense sclerotic margin on the inferior medial metaphysis of the left clavicle. e) Diffuse SPNB across the radii and ulnae. f) Two cavitations within nodes of SPNB on the midshafts of the right radius and ulna. g) Large node of SPNB on the proximal left ulna. Radiographs demonstrate a small oval osteolytic lesion with sclerotic margins within the node. h) Prolific SPNB across the tibiae and fibulae. i) Radiograph of the right tibia demonstrating sabre shin j) Dactylitis of a metacarpal. k) and l) Focal cavitations of the distal fibulae. The lesions are within nodes of new bone. Image: author's own from Vlok et al. (2020).*

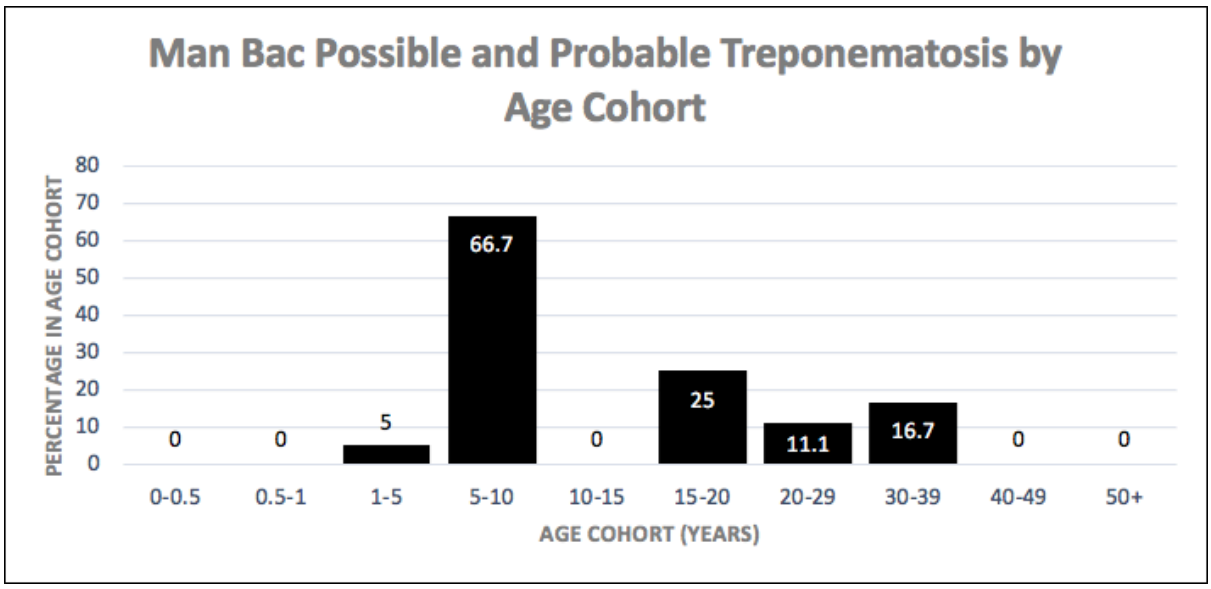

Figure 7.26: *Age-at-death distribution of possible and probable cases of treponematosis at Man Bac. Image: author's own.*

7.6.3 Morbidity of Infectious Disease at Man Bac

No significant differences between the prevalence of infectious disease amongst males and females were identified (n=25, RR=0.5000, p=0.3270; Table 7.19). There was a significant increase in morbidity of older nonadults compared to younger nonadults. Nonadults over the age of 5 years were almost 18 times more likely to have infectious disease than those under the age of 5 (n=44, RR=0.0556, p=0.0047). Nonadults 10 years of age and over were 7 times more likely to have infectious disease than those under the age of 10 (n=44, RR=0.1419, p=0.0024), which is a reduction in relative risk compared to statistical analysis at 5 years of age. This outcome suggests a particularly increased morbidity of infectious disease in pre-adolescent children over 5 years of age. In adults, there was no statistically significant differences except when assessing the differences between adults over and under 20 years of age. Adolescents between 15-19 years old, had significantly higher morbidity than adults (n=29, RR=3.7143, p<0.0001). Again, this outcome suggests a high nonadult morbidity.

Table 7.19: *Relative risk of infectious disease morbidity at Man Bac across sex and age cohorts.*

EXPOSED GROUP/ CONTROL GROUP	OUTCOME		RR	P-VALUE	95%CI
	Positive: *Infectious Disease Present*	***Negative:*** *Infectious Disease Absent*			
Sex					
Female/ Male	2/6	8/9	0.500	0.3270	0.1250- 1.9993
Nonadults					
<1 yr/ >1 yr	0/7	14/23	0.1378	0.1646	0.0084- 2.2558
<5 yrs/ >5yrs	1/6	32/5	**0.0556**	**0.0047***	0.0075- 0.4122
<10 yrs/ >10yrs	3/4	34/3	**0.1419**	**0.0024***	0.0402- 0.5004
Adults					
<20 yrs/ >20 yrs	3/7	0/19	**3.7143**	**<0.0001***	1.9717- 6.9969
<30 yrs/ >30 yrs	4/6	8/11	0.9444	0.9131	0.3382- 2.6373
<40 yrs/>40 yrs	8/2	10/9	2.4444	0.1963	0.6300- 9.4846

A relative risk (RR) >1 denotes a relationship of the exposed group with an increase in disease prevalence, whereas RR <1 denotes a relationship of the control group with an increase in disease prevalence.
*= statistically significant (p<0.10). **= statistically significant when considering size of the effect of RR.

7.6.4 Mortality of Infectious Disease at Man Bac

A statistically significant survivorship is observed in the relative risk ratio analysis of nonadults, with significant survivorship of those with infectious diseases observed after 5 years (n=44, RR=0.1652, p=0.0524) and 10 years of age (n=44, RR=0.4664, 0.0824). No cases of infectious disease was identified in the infants (Table 7.20). As was the case with the relative risk of morbidity across adult age cohorts, there was no statistical difference in adult mortality of infectious disease at Man Bac, with the exception of individuals between 15-19 years having over 12 times the risk of death with skeletal signs of infectious disease than adults over the age of 20 (n=29, RR=12.7273, p=0.0824).

Kaplan-Meier survival analysis indicates a statistically significant relationship between infectious disease presence and survivorship to older age in nonadults (n=44, X^2=7.846, df=1, p=0.005; Table 7.21; Figure 7.27). In contrast, a statistically significant relationship with frailty was identified in adults with skeletal evidence for infectious disease in the Kaplan-Meier survival analysis (n=29, X^2=2.378, df=1, p=0.123; Table 7.22). That is, individuals with infectious disease had a significantly lower survivorship that those without evidence for infectious disease. However, Cox regression analysis identified no statistically significant differences in mortality (n=29, Wald=1.637, df=1, p=0.201; Table 7.23). Figure 7.28, and Figure 7.29 present similar Kaplan-Meier and Cox regression

survival curves for adults with or without infectious disease presence indicating low association with infectious disease to frailty. The overall outcome of mortality analysis indicates survivorship of nonadults with infectious disease prevalence at Man Bac, whereas there appears to be low level frailty of adults with skeletal signs of infectious disease. The presence of infectious disease at Man Bac then appears to have a low effect on mortality in the adults.

Table 7.20: *Relative risk of infectious disease mortality at Man Bac across age cohorts.*

POSITIVE OUTCOME/ NEGATIVE OUTCOME	**TREATMENT**		**RR**	**P-VALUE**	**95%CI**
	Exposed Group: *Infectious Disease Present*	***Control Group:*** *Infectious Disease Absent*			
Nonadults					
<1 yr/ >1 yr	0/7	14/23	0.1638	0.1914	0.0109- 2.4720
<5 yrs/ >5yrs	1/6	32/5	**0.1652**	**0.0524***	0.0268- 1.0185
<10 yrs/ >10yrs	¾	34/3	**0.4664**	**0.0824***	0.1972- 1.1030
Adults					
<20 yrs/ >20 yrs	3/7	0/19	**12.7273**	**0.0824***	0.7213- 224.5722
<30 yrs/ >30 yrs	4/6	8/11	0.950	0.9134	0.3770- 2.3940
<40 yrs/>40 yrs	8/2	10/9	1.5200	0.1196	0.8971- 2.5753

A relative risk (RR) >1 denotes a relationship of the disease presence with the positive outcome (susceptibility to mortality), whereas RR <1 denotes a relationship of the disease absence with a negative outcome (survivorship).
*= statistically significant (p<0.10). **= statistically significant when considering size of the effect of RR.

Table 7.21: *Statistical summary for Kaplan-Meier function of infectious disease mortality of nonadults at Man Bac.*

INFECTIOUS DISEASE	**ESTIMATE**	**STD. ERROR**	**95% CI**	**LOG RANK (MANTEL-COX)**		
				CHI SQUARE	**DF**	**P-VALUE**
Mean				7.846	1	**0.005***
Absent	2.678	0.664	1.376- 3.980			
Present	11.071	2.071	7.011- 15.131			
Overall	4.014	0.791	2.464- 5.563			
Median						
Absent	1.500	0.091	1.322- 1.678			
Present	13.000	5.237	2.735- 23.265			
Overall	1.5000	0.091	1.321- 1.679			

*= statistical significance (p<0.15).

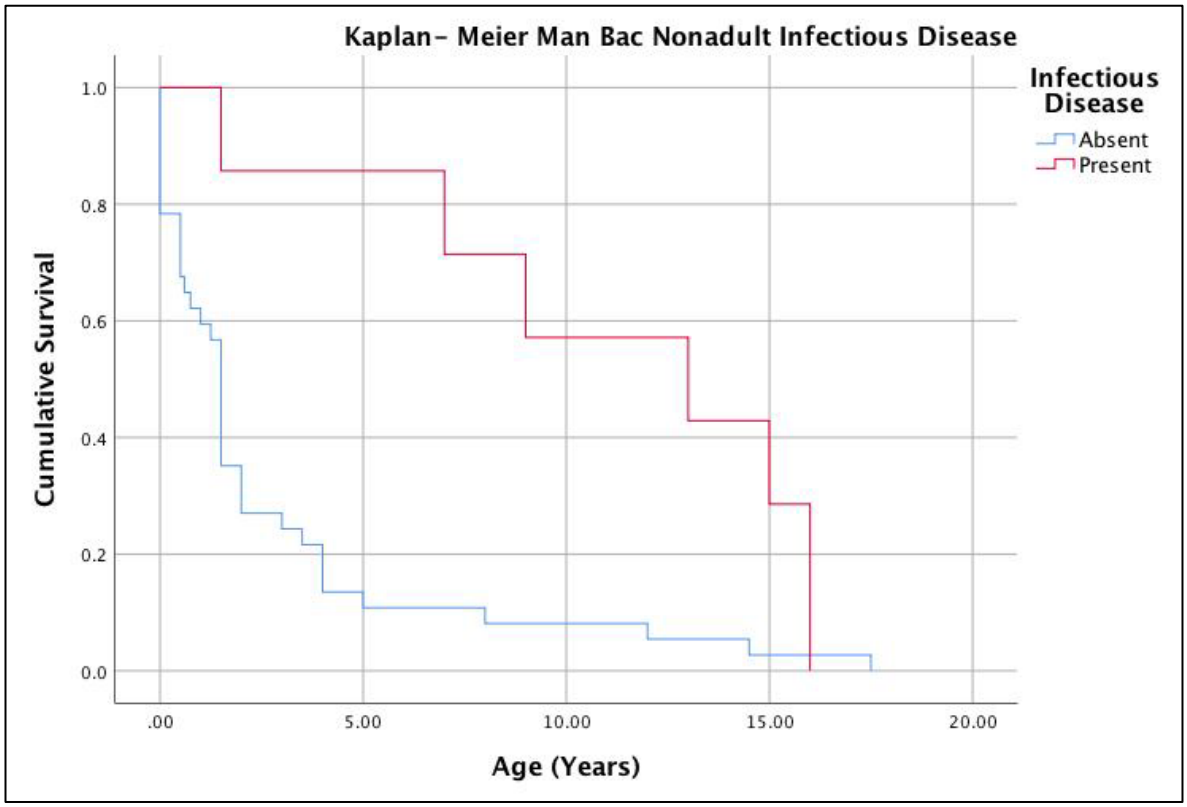

Figure 7.27: *Kaplan-Meier cumulative survival function of nonadult infectious disease mortality at Man Bac. Image: author's own.*

Table 7.22: *Statistical summary for Kaplan-Meier function of infectious disease mortality of adults at Man Bac.*

INFECTIOUS DISEASE	ESTIMATE	STD. ERROR	95% CI	LOG RANK (MANTEL-COX)		
				CHI SQUARE	DF	P-VALUE
Mean				2.378	1	**0.123***
Absent	35.684	2.565	30.657- 40.712			
Present	29.900	3.698	22.652- 37.148			
Overall	33.690	2.135	29.506- 37.874			
Median						
Absent	35.000	4.897	25.402- 44.598			
Present	35.000	4.111	26.943- 43.057			
Overall	35.000	3.484	28.171- 41.829			

*= statistical significance (p<0.15).

Table 7.23: *Statistical summary and equation for Cox regression function of infectious disease) mortality of adults at Man Bac.*

INFECTIOUS DISEASE	COEFFICIENT (β)	STD. ERROR	WALD	DF	P-VALUE	ODDS RATIO (Exp(β))
	-0.523	0.409	1.637	1	0.201	0.593

*= statistical significance (p<0.15).

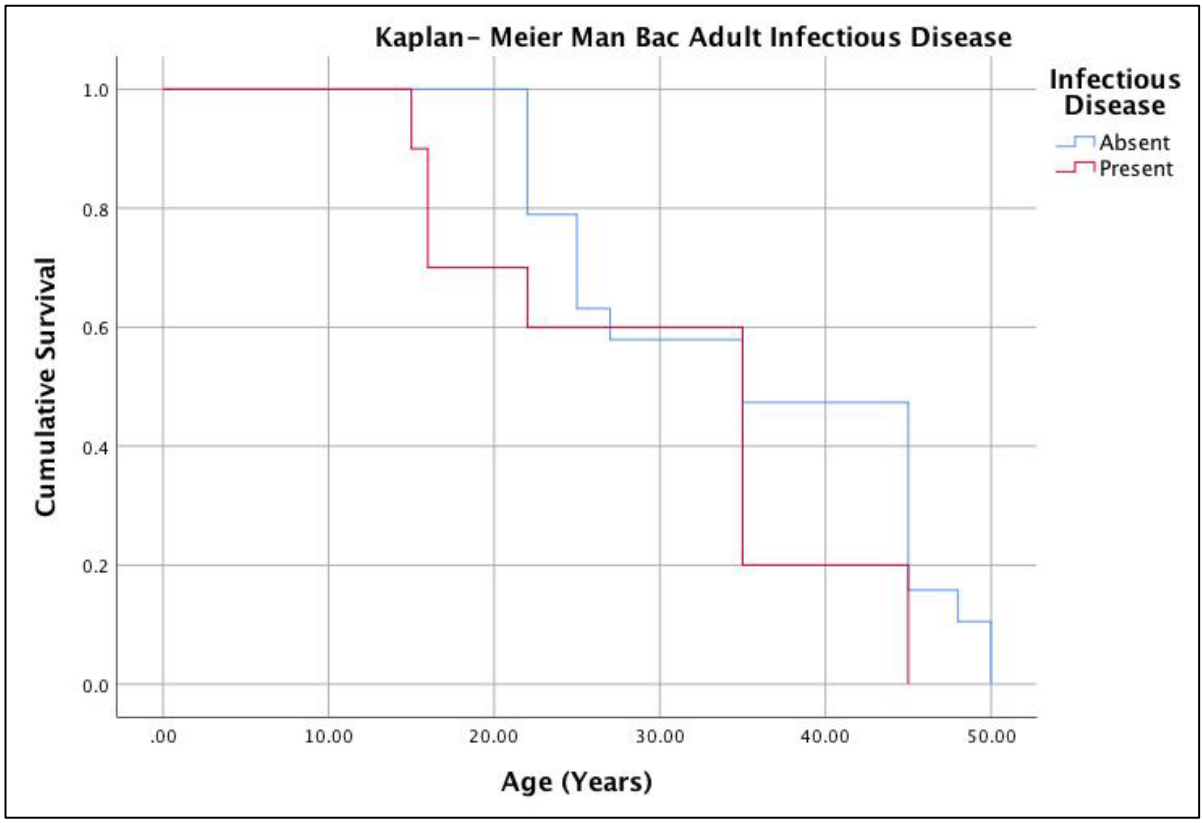

Figure 7.28: *Kaplan-Meier cumulative survival function of adult infectious disease mortality at Man Bac. Image: author's own.*

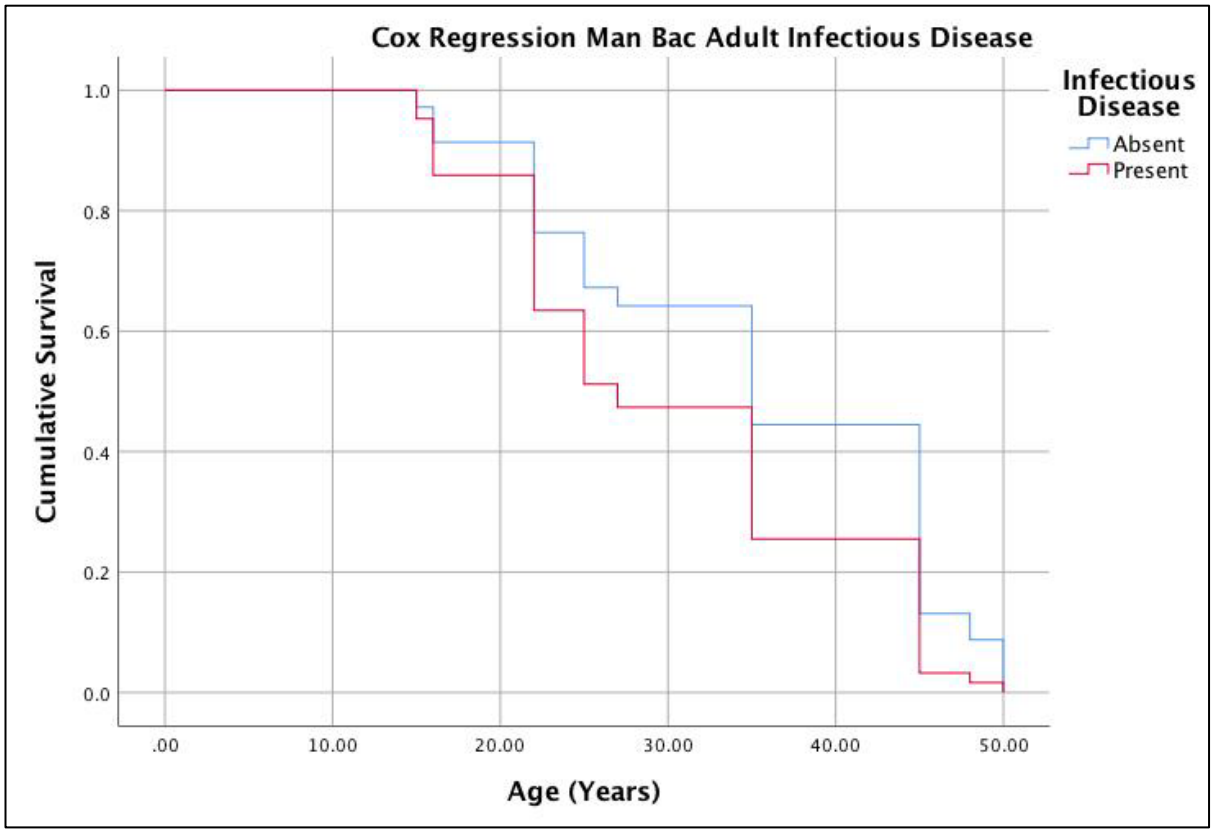

Figure 7.29: *Cox regression cumulative survival function of adult infectious disease mortality at Man Bac. Image: author's own.*

7.6.5 Diagnosis of Nutritional Disease at Man Bac

7.6.5.1 Diagnosis of Nutritional Disease in Nonadults

Over 79% (79.5%, 35/44) of nonadults at Man Bac met the threshold for probable scurvy and 95.5% (42/44) met the threshold criteria for at minimum possible scurvy (Table 7.24; Figure 7.30-7.31). Macroscopic lesions consistent with scurvy were predominantly bilateral and symmetrical discrete deposits of SPNB associated with abnormal cortical porosity of the crania and mandibles indicating repeated haemorrhaging events (Figure 7.31). Fifty percent (22/44) of the nonadults presented with radiographic signs of scurvy (white line of Fraenkel, Trummerfeld zone and/ or Pelkan spurs) alongside macroscopic evidence (figure 7.31f).

Fifty-percent (22/44) of nonadults met the criteria for at minimum a possible diagnosis of rickets, and 31.8% (14/44) met the criteria for probable diagnosis (Table 7.24; Figure 7.32). These features included bending of the diaphyses, fraying, flaring and cupping of metaphyseal plates, thinning cranial bones and deposits of SPNB on the cranium and long bones which appear poorly mineralized (Figure 7.32). Fraying, an indicator of active rickets, was only found in nonadults under 2 years of age (11.4%, 5/44) and no evidence of rickets was found in individuals over 10 years of age. Probable cases of rickets were particularly high in the 6 months to under 1 year age cohort, with 83.3% (5/6) of individuals diagnosed with probable rickets (Figure 7.33). Clear co-morbidities between rickets and scurvy are apparent in the nonadult cohort from Man Bac with almost 32% (31.8%, 14/44) of individuals in the nonadult cohort presenting with probable rickets and probable scurvy. All cases diagnosed as possible or probable rickets were also diagnosed with probable scurvy.

Table 7.24: *Summary of nutritional disease at Man Bac*

	POSSIBLE			PROBABLE			POSSIBLE AND PROBABLE		
	Affected	*Observed*	*(%)*	*Affected*	*Observed*	*(%)*	*Affected*	*Observed*	*(%)*
Scurvy									
0 to 6 months	3	8	37.5	5	8	62.5	8	8	100
6 months to 1 year	0	6	0	6	6	100	6	6	100
1 to 5 years	3	20	15	16	20	80	19	20	95
5 to 10 years	0	3	0	3	3	100	3	3	100
10 to 15 years	1	3	33.3	2	3	66.7	3	3	100
15 to 20 years	0	4	0	3	4	75	3	4	75
20 to 30 years	0	9	0	5	9	55.6	5	9	55.6
30 to 40 years	2	6	33.3	1	6	16.7	3	6	50
40 to 50 years	1	8	12.5	2	8	25	3	8	37.5
50+ years	0	3	0	1	3	33.3	1	3	33.3
Total nonadults	7	44	16	35	44	79.5	42	44	95.5
Males	2	15	13.3	7	15	46.7	9	15	60
Females	2	11	18.2	2	11	18.2	4	11	36.4
Total adults	3	26	11.5	9	26	34.6	12	26	46.2
Total	10	70	14.3	44	70	62.9	54	70	77.1
Rickets									
0 to 6 months	0	8	0	2	8	25	2	8	25
6 months to 1 year	0	6	0	5	6	83.3	5	6	83.3
1 to 5 years	7	20	35	6	20	30	13	20	65
5 to 10 years	1	3	33.3	1	3	33.3	2	3	66.7
10 to 15 years	0	3	0	0	3	0	0	3	0
15 to 20 years	0	4	0	0	4	0	0	4	0
Total nonadults	8	44	18.2	14	44	31.8	22	44	50
Total	8	70	11.4	14	70	20	22	70	31.4

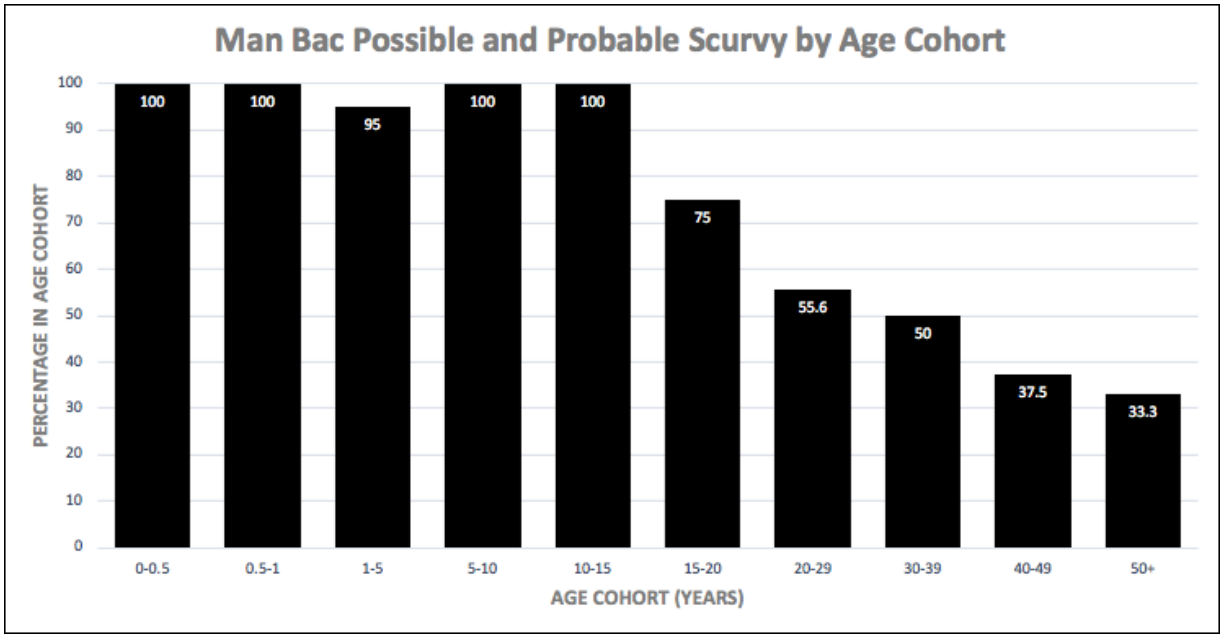

Figure 7.30: *Age-at-death distribution of possible and probable cases of scurvy at Man Bac. Image: author's own.*

Figure 7.31: *Lesions in Man Bac nonadults diagnostic for scurvy. Active SPNB and abnormal cortical porosity: a) On the palate (MB05M36, ~3 years) b) The anterior maxilla extending from the infraorbital foramen (MB05M36, ~3 years), c) Anterior maxilla, note the vascular impressions (MB05M25, ~5 years), d) Medial coronoid process of the mandible (MB05M25, ~5 years), e) Supraspinous fossa of the scapula (MB05M5, ~1.5 years), f) White lines of Fraenkel and Trummerfeld zones of the distal long bones (MB07H2M6, ~2 years). g) SPNB and abnormal cortical porosity: on the anterior maxilla (MB05M2, neonate), h) External sphenoid (MB05M12, ~2 years i) Abnormal endochondral porosity extending more than 10mm from the distal metaphyseal plate of the femur (MB07H2M16, ~1.5 years), j) SPNB and abnormal cortical porosity on the posterior zygoma (MB05M2, neonate) k) Pterygoid fossae of the sphenoid (MB05M25, ~5 years). Image: author's own adapted from Vlok et al. (in review).*

Figure 7.32: *Lesions in Man Bac nonadults consistent with a diagnosis for rickets. a) Thin layers of poorly mineralised new bone of the ectocranium and overall thinning of the cranial bone (MB07H2M21, ~9 months), b) Thick SPNB deposits on the femora and slight cupping of the distal metaphysis (MB05M30, ~6 months), c) Slight cupping of proximal tibia (MB05M25, ~5 years), d) Fraying, cupping and flaring of the proximal tibia (MB05M18, ~1.5 years), e) Fraying, flaring and cupping of the distal femur (MB05M18, ~1.5 years), f) Bending of the humeral shafts with fraying of the proximal metaphyses (MB05M3, ~6 months), g) Thickened cortex with mixed coarsened and ground glass trabeculae. Metaphyseal ends are also thickened. (MB05M30, ~6 months). Image: author's own from Vlok et al. (in review).*

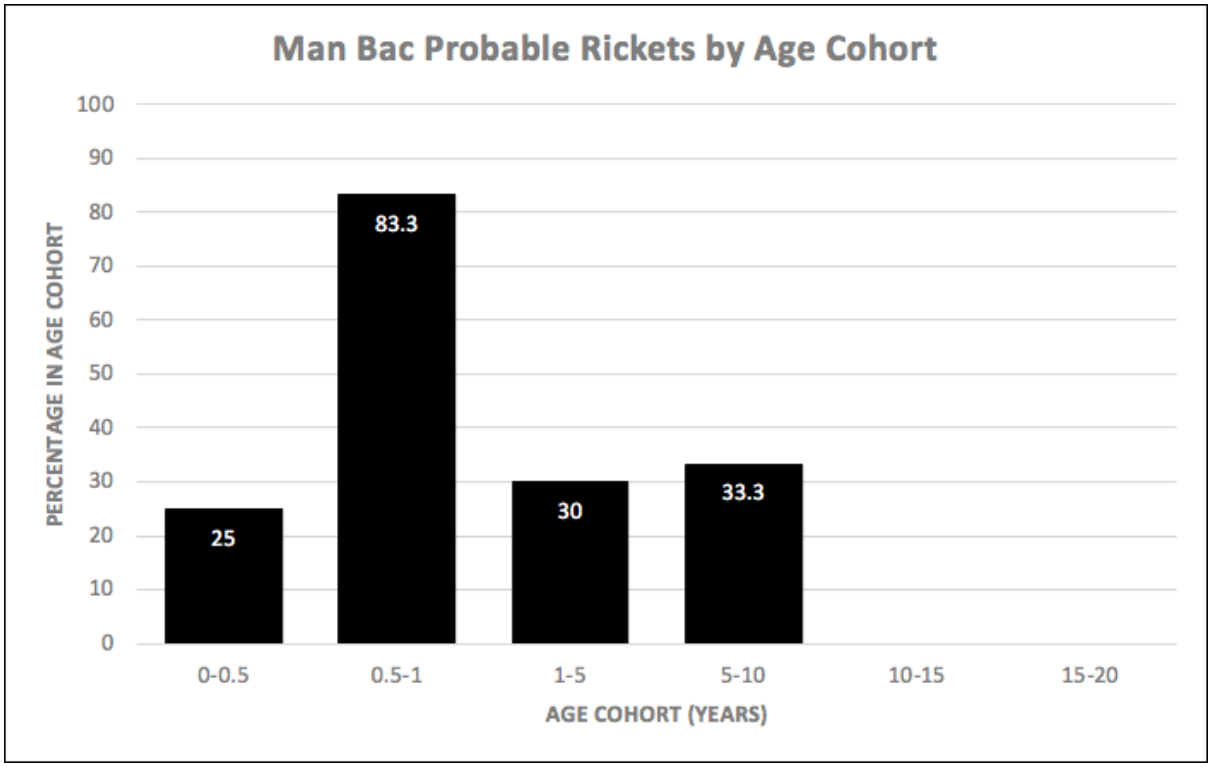

Figure 7.33: *Age-at-death distribution of probable cases of rickets at Man Bac. Image: author's own.*

7.6.5.2 Diagnosis of Nutritional Disease in Adults

In adults, 46.2% (12/26) met the criteria for at minimum possible case of scurvy with 34.6% (9/26) having lesions consistent with a probable diagnosis (Table 7.24; Figure 7.34). Lesions in adults were restricted to evidence of symmetrical discrete SPNB and abnormal cortical porosity, particularly of the crania and mandibles. There is a decreasing trend in the prevalence of adult scurvy with increasing age at death (Figure 7.30). One adult exhibited slight lateral bending of the right humerus (MB07H2M12, old aged adult female). In adults, unilateral bending deformities of the upper limb are more often activity or trauma related (Brickley and Ives 2010). No adults displayed signs of osteomalacia.

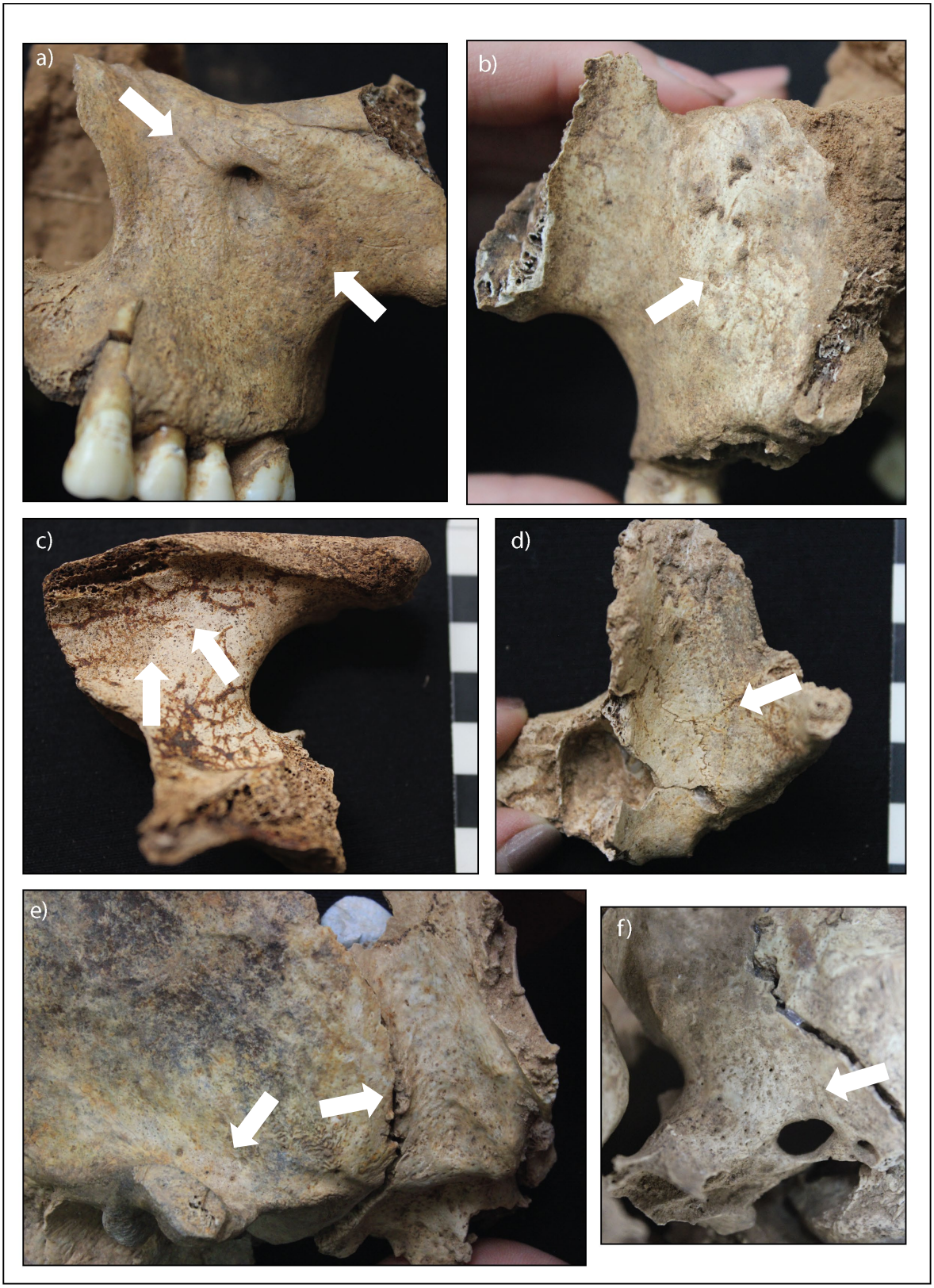

Figure 7.34: *Macroscopic lesions in Man Bac adults and adolescents diagnostic for scurvy. a) Remodelled deposit of SPNB with vascular impressions, and b) Remodelled deposit of SPNB with abnormal cortical porosity and vascular impressions (MB05M11, young adult male). c) Active SPNB inferior to scapular spine on infraspinous fossa of right scapula (MB05M29, middle aged adult male), d) Remodelled SPNB and abnormal cortical porosity on the posterior right zygoma, e) Right external greater wing of sphenoid and temporal squama (MB07H2M19, young adult male). f) Remodelled SPNB and abnormal cortical porosity on external left sphenoid around pterygoid region (MB07H2M18, male, 14-18 years). Image: author's own.*

7.6.6 Morbidity of Nutritional Disease at Man Bac

Scurvy was prevalent in adults and nonadults, therefore the morbidity of scurvy could be assessed for both groups (Table 7.25). No statistically significant differences were identified in the morbidity of scurvy between males and females for combined possible and probable (n=25, RR=0.6667, p=0.3578) and probable only cases (n=25, RR=0.4286, p=0.2195). There was also no statistically significant differences between the prevalence of scurvy across nonadult age cohorts for both combined possible and probable and probable only scurvy (Table 7.25). This statistical outcome is expected given that the prevalence of scurvy was high across all nonadult age cohorts. The morbidity of combined cases of possible and probable scurvy was significantly higher for adolescents (15-19 years old) compared to adults over 20 years of age. Adolescents between 15-19 years of age were 2.2 times more likely to have scurvy than their adult counterparts (n=29, RR=2.1667, p=0.0003). When considering probable only cases of scurvy, significantly higher morbidity in individuals under 20 years of age was achieved (n=29, RR=3.2500, p=0.0001) and significantly higher prevalences was also attained for those under 30 years of age (n=29, RR=3.7778, p=0.0181). However, a significantly higher prevalence of probable scurvy was not found for those under 40 years of age. The relative risk of morbidity of probable scurvy under 20 years of age (RR=3.2500) was similar to the relative risk of probable scurvy morbidity under 30 years of age (RR=3.7778). This outcome identifies similar morbidity in adults between 20-29 and 30-39 years of age, with reduced morbidity from 40 years of age.

Bone mineralisation disorders (rickets and osteomalacia) were only identified in nonadults at Man Bac, therefore statistical assessment of rickets was restricted to nonadults. As no nonadults over the age of 10 years were diagnosed with rickets, nonadults were 9.5 times more likely to exhibit possible or probable rickets before 10 years of age, which was statistically significant when considering the size of the effect (n=44, RR=9.4737, p=0.1022). Nonadults were also 2.1 times more likely to be diagnosed with a probable case of rickets before 1 year of age, which was statistically significant (n=44, RR=2.1429, p=0.0732).

Table 7.25: *Relative risk of nutritional disease morbidity at Man Bac across sex and age cohorts.*

EXPOSED GROUP/ CONTROL GROUP	**OUTCOME**		**RR**	**P-VALUE**	**95%CI**
	Positive: *Disease Present*	***Negative:*** *Disease Absent*			
Possible and Probable Scurvy (combined)					
Sex					
Female/ Male	4/9	6/6	0.6667	0.3578	0.2809- 1.5822
Nonadults					
<1 yr/ >1 yr	14/28	0/2	1.0714	0.1574	0.9737- 1.1790
<5 yrs/ >5yrs	32/10	1/1	1.0667	0.5195	0.8765- 1.2981
<10 yrs/ >10yrs	36/6	1/1	1.1351	0.4186	0.8349- 1.5433
Adults					
<20 yrs/ >20 yrs	3/12	0/14	**2.1667**	**0.0003***	1.4305- 3.2817
<30 yrs/ >30 yrs	8/7	4/10	1.6190	0.1741	0.8081- 3.2438
<40 yrs/>40 yrs	11/4	7/7	1.6806	0.2391	0.7081- 3.9885
Probable Only Scurvy					
Sex					
Female/ Male	2/7	8/8	0.4286	0.2195	0.1108- 1.6574
Nonadults					
<1 yr/ >1 yr	11/24	3/6	0.9821	0.9140	0.7083- 1.3619
<5 yrs/ >5yrs	26/9	7/2	1.1030	0.7012	0.6684- 1.8202
<10 yrs/ >10yrs	30/5	7/2	1.1351	0.6148	0.6928- 1.8598
Adults					
<20 yrs/ >20 yrs	3/8	0/18	**3.2500**	**0.0001***	1.8259- 5.7848
<30 yrs/ >30 yrs	8/3	4/14	**3.7778**	**0.0181***	1.2549- 11.3729
<40 yrs/>40 yrs	9/2	9/9	2.7500	0.1378	0.7229- 10.4608
Possible and Probable Rickets (combined)					
Nonadults					
<1 yr/ >1 yr	7/15	7/15	1.0000	1.0000	0.5303- 1.8859
<5 yrs/ >5yrs	19/3	14/8	2.1111	0.1464	0.7701- 5.7876
<10 yrs/ >10yrs	22/0	15/7	**9.4737**	**0.1022****	0.6387- 140.5132
Probable Only Rickets					
Nonadults					
<1 yr/ >1 yr	7/7	7/23	**2.1429**	**0.0732***	0.9309- 4.9327
<5 yrs/ >5yrs	13/1	20/10	4.3333	0.1336	0.6378- 29.4426
<10 yrs/ >10yrs	14/0	23/7	6.1053	0.1914	0.4045- 92.1432

A relative risk (RR) >1 denotes a relationship of the exposed group with an increase in disease prevalence, whereas RR <1 denotes a relationship of the control group with an increase in disease prevalence.
*= statistically significant ($p<0.10$). **= statistically significant when considering size of the effect of RR.

7.6.7 Mortality of Nutritional Disease at Man Bac

7.6.7.1 Man Bac Scurvy Mortality

No statistical significance between mortality and the presence of possible and probable cases of scurvy was identified in relative risk ratio analysis for both adults and nonadults at Man Bac. This outcome is expected given the overall high morbidity of scurvy across all age cohorts. However, when considering probable only cases there is a statistically significant risk of death with the presence of scurvy in adults. The significant relationship between probable adult scurvy and frailty is prevalent at 20, 30 and 40 years of age (Table 7.26). Individuals were over 11 times more likely to die before 20 years of age with probable scurvy (n=29, RR=11.08033, p=0.1009), indicating a higher mortality rate in nonadults compared to adults. The relative risk of death decreased with increasing age, with 3.3 times the risk of death before 30 years of age (n=29, RR=3.2727, p=0.0131), and only 1.6 times the risk of death under 40 years of age (n=29, RR=1.6364, p=0.0736). This outcome indicates young adults were at a higher risk of death than older adults if they developed skeletal signs of probable scurvy.

Kaplan-Meier statistical analysis identified a statistically significant relationship with frailty in nonadults with possible or probable diagnoses for scurvy (n=44, X^2=2.911, df=1, p=0.088; Table 7.27; Figure 7.35). Cox regression analysis was not statistically significant (n=44, Wald=2.072, df=1, p=0.150; Table 7.28), as was the case with relative risk ratio analysis. The ambiguity of the relationship of nonadult scurvy to mortality is likely due to the lower number of absent cases of scurvy in the nonadult cohort. However, the Cox regression accumulative survival function (Figure 7.36) does demonstrate increased frailty in individuals with present cases of possible or probable scurvy. There was no relationship to mortality determined by Kaplan-Meier (n=44, X^2=0.003, df=1, p=0.958; Table 7.29; Figure 7.37) nor Cox regression analyses (n=44, Wald= 0.002, p=0.961; Table 7.30) for probable cases of nonadult scurvy. The Cox regression cumulative survival function (Figure 7.38) demonstrates a near identical relationship to mortality between probable and non-probable cases of nonadult scurvy. Therefore, overall no association of nonadult scurvy to mortality was determined.

As was the case with the relative risk ratio analysis, the Kaplan-Meier survival analysis indicated no relationship with mortality in possible or probable cases of adult scurvy

(n=29, X^2=1.673, df=1, p=0.196; Table 7.31; Figure 7.39). However, a statistically significant relationship with frailty in probable cases of adult scurvy was apparent in the Kaplan-Meier (n=29, X^2=3.764, df=1, p=0.052; Table 7.32; Figure 7.40) and the Cox regression analysis (n=29, Wald=2.379, df=1, p=0.123; Table 7.33; Figure 7.41). Overall, given that there was a significantly higher association with mortality in adolescents than nonadults, with a statistically significant relationship with frailty in probable cases of adult scurvy, it is likely that the presence of scurvy is related to frailty at Man Bac. While, at a nonadult level this statistical relationship was not significant, this was likely due to the high prevalence of the disease in individuals who did not survive until adulthood.

Table 7.26: *Relative risk of scurvy mortality at Man Bac across age cohorts.*

POSITIVE OUTCOME/ NEGATIVE OUTCOME	**TREATMENT**		**RR**	**P-VALUE**	**95%CI**
	Exposed Group: *Disease Present*	***Control Group:*** *Disease Absent*			
Possible and Probable Scurvy (combined)					
Nonadults					
<1 yr/ >1 yr	14/28	0/2	2.0233	0.5902	0.1557- 26.2987
<5 yrs/ >5yrs	32/10	1/1	1.5238	0.5543	0.3722- 6.1559
<10 yrs/ >10yrs	36/6	1/1	1.7143	0.4477	0.4264- 6.8924
Adults					
<20 yrs/ >20 yrs	3/12	0/14	6.5625	0.2001	0.3690- 116.7072
<30 yrs/ >30 yrs	8/7	4/10	1.8667	0.1997	0.7190- 4.8459
<40 yrs/>40 yrs	11/4	7/7	1.4667	0.2156	0.7999- 2.6892
Probable Only Scurvy					
Nonadults					
<1 yr/ >1 yr	11/24	3/6	0.9429	0.9122	0.3314- 2.6824
<5 yrs/ >5yrs	26/9	7/2	0.9551	0.8219	0.6403- 1.4248
<10 yrs/ >10yrs	30/5	7/2	1.1020	0.6111	0.7578- 1.6027
Adults					
<20 yrs/ >20 yrs	3/8	0/18	**11.0833**	**0.1009****	0.6261- 196.2127
<30 yrs/ >30 yrs	8/3	4/14	**3.2727**	**0.0131***	1.2823- 8.3529
<40 yrs/>40 yrs	9/2	9/9	**1.6364**	**0.0736***	0.9541- 2.8065

A relative risk (RR) >1 denotes a relationship of the disease presence with the positive outcome (susceptibility to mortality), whereas RR <1 denotes a relationship of the disease absence with a negative outcome (survivorship).
*= statistically significant (p<0.10). **= statistically significant when considering size of the effect of RR.

Table 7.27: *Statistical summary for Kaplan-Meier function of possible and probable scurvy mortality of nonadults at Man Bac.*

POSSIBLE AND PROBABLE SCURVY	ESTIMATE	STD. ERROR	95% CI	LOG RANK (MANTEL-COX)		
				CHI SQUARE	DF	P-VALUE
Mean				2.911	1	**0.088***
Absent	9.500	8.000	0.000- 25.180			
Present	3.752	0.759	2.265- 5.240			
Overall	4.014	0.791	2.464- 5.563			
Median						
Absent	1.500	-	-			
Present	1.500	0.100	1.304- 1.696			
Overall	1.500	0.091	1.321- 1.679			

*= statistical significance (p<0.15).

Table 7.28: *Statistical summary for Cox regression function of possible and probable scurvy mortality of nonadults at Man Bac.*

POSSIBLE AND PROBABLE SCURVY	COEFFICIENT (β)	STD. ERROR	WALD	DF	P-VALUE	ODDS RATIO (Exp(β))
	-1.471	1.022	2.072	1	0.150	0.230

*= statistical significance (p<0.15).

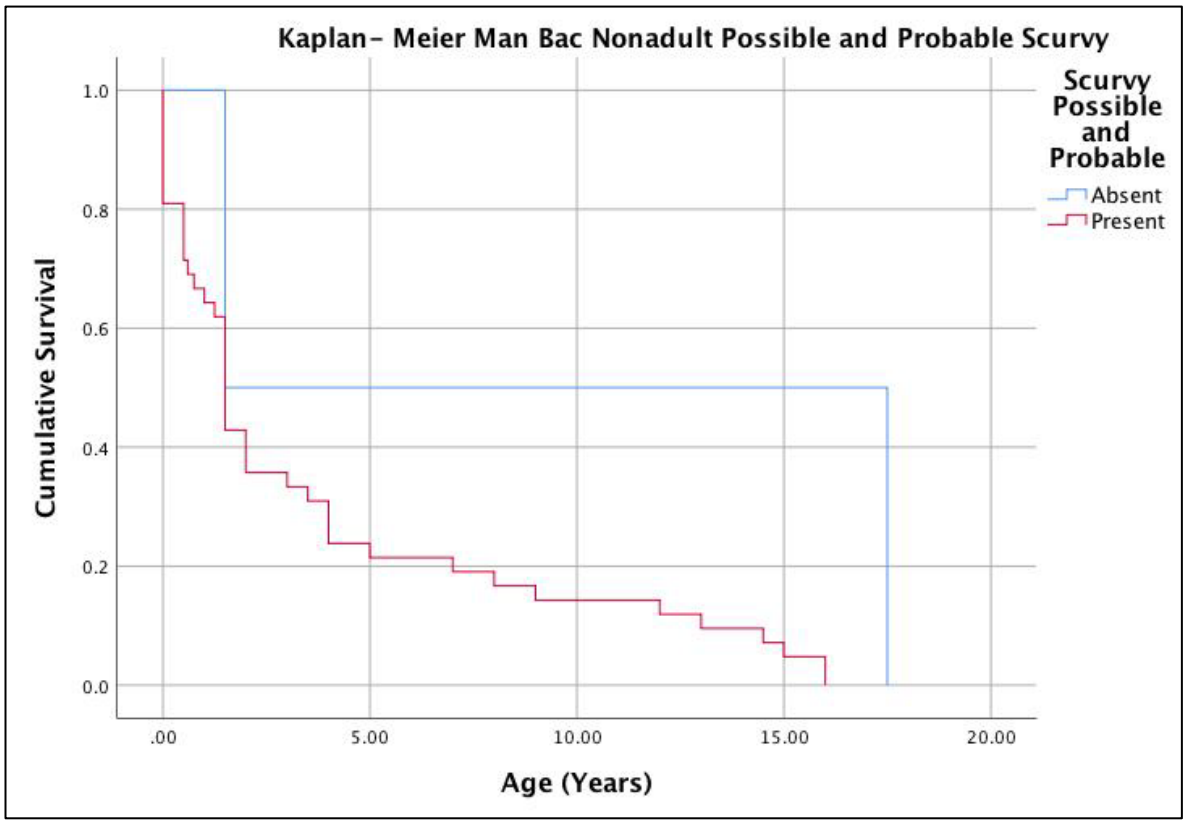

Figure 7.35: *Kaplan-Meier cumulative survival function of nonadult possible and probable scurvy mortality at Man Bac. Image: author's own.*

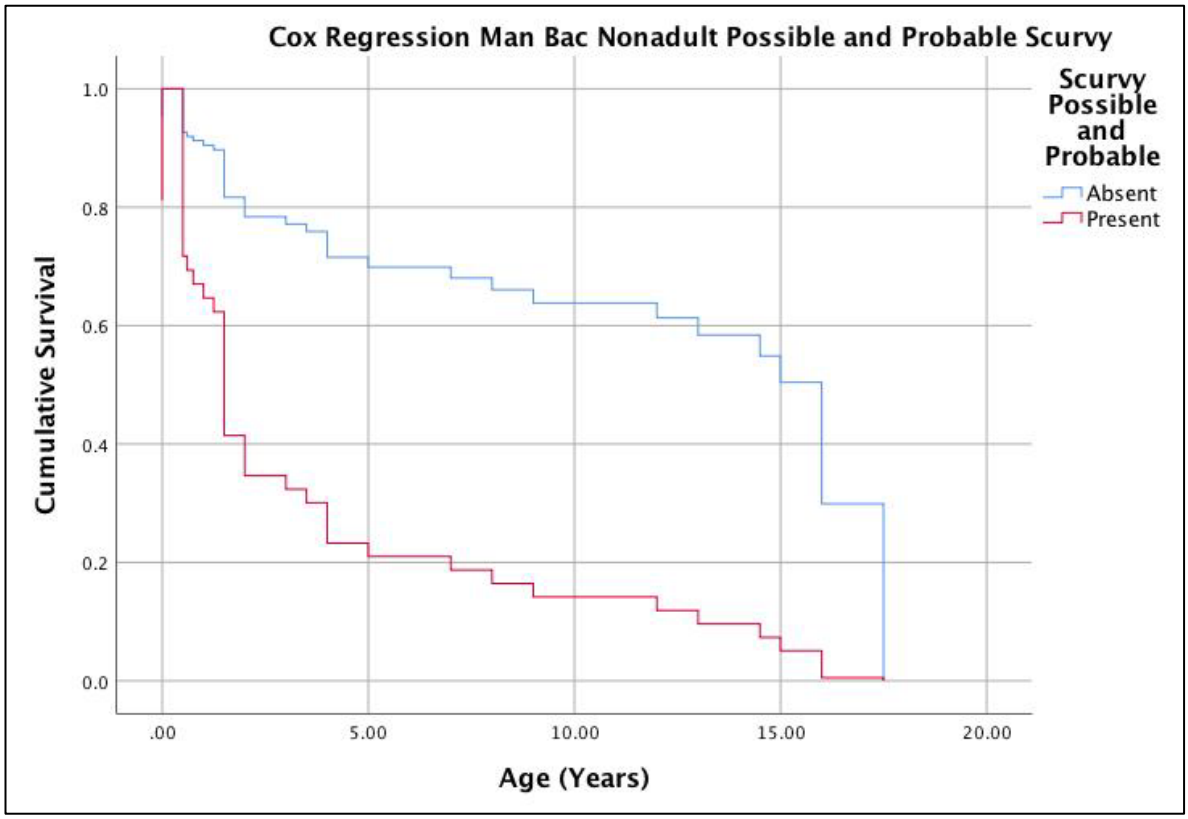

Figure 7.36: *Cox Regression cumulative survival function of nonadult possible and probable scurvy mortality at Man Bac. Image: author's own.*

Table 7.29: *Statistical summary for Kaplan-Meier function of probable scurvy mortality of nonadults at Man Bac.*

PROBABLE SCURVY	ESTIMATE	STD. ERROR	95% CI	LOG RANK (MANTEL-COX)		
				CHI SQUARE	DF	P-VALUE
Mean				0.003	1	0.958
Absent	3.917	2.110	0.000- 8.052			
Present	4.039	0.851	2.370- 5.707			
Overall	4.014	0.791	2.464-5.563			
Median						
Absent	1.500	0.104	1.296- 1.704			
Present	1.500	0.329	0.856- 2.144			
Overall	1.500	0.091	1.321- 1.679			

*= statistical significance (p<0.15).

Table 7.30: *Statistical summary for Cox regression function of probable scurvy mortality of nonadults at Man Bac.*

PROBABLE SCURVY	COEFFICIENT (β)	STD. ERROR	WALD	DF	P-VALUE	ODDS RATIO (Exp(β))
	-0.019	0.395	0.002	1	0.961	0.981

*= statistical significance (p<0.15).

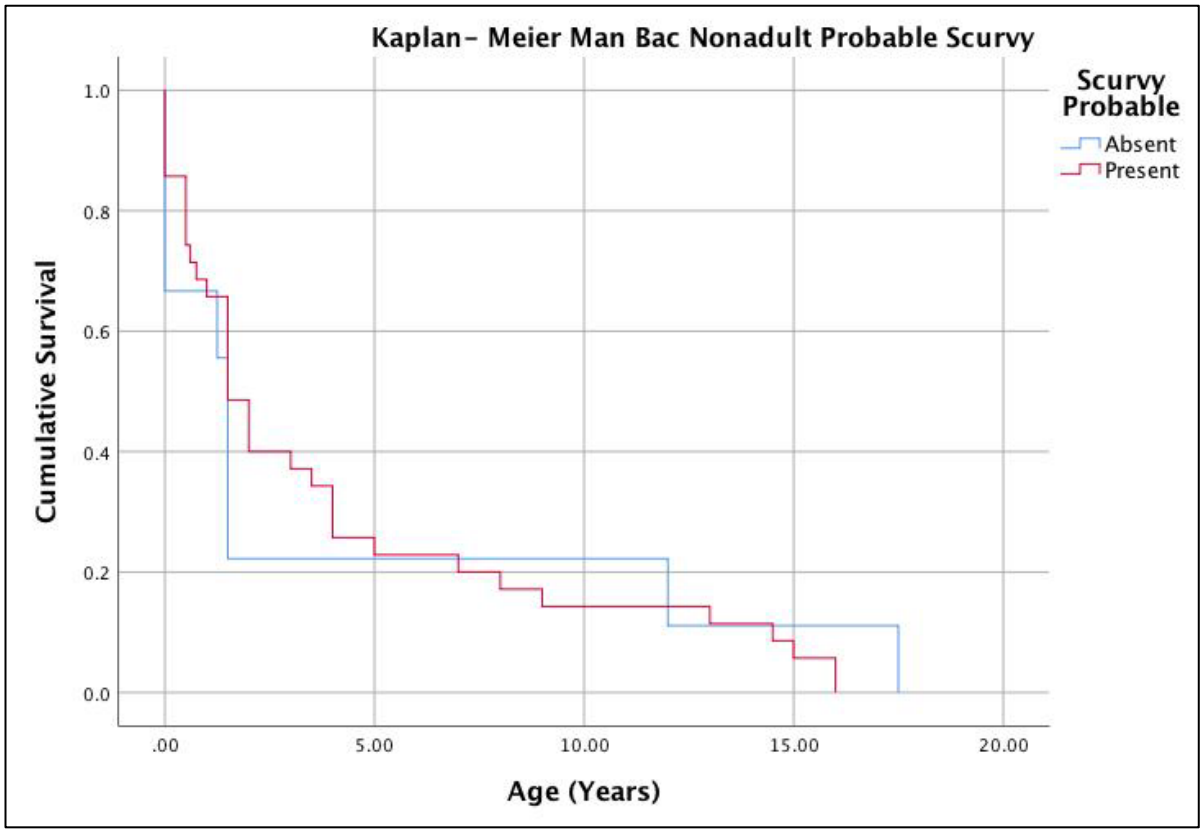

Figure 7.37: *Kaplan-Meier cumulative survival function of nonadult probable scurvy mortality at Man Bac. Image: author's own.*

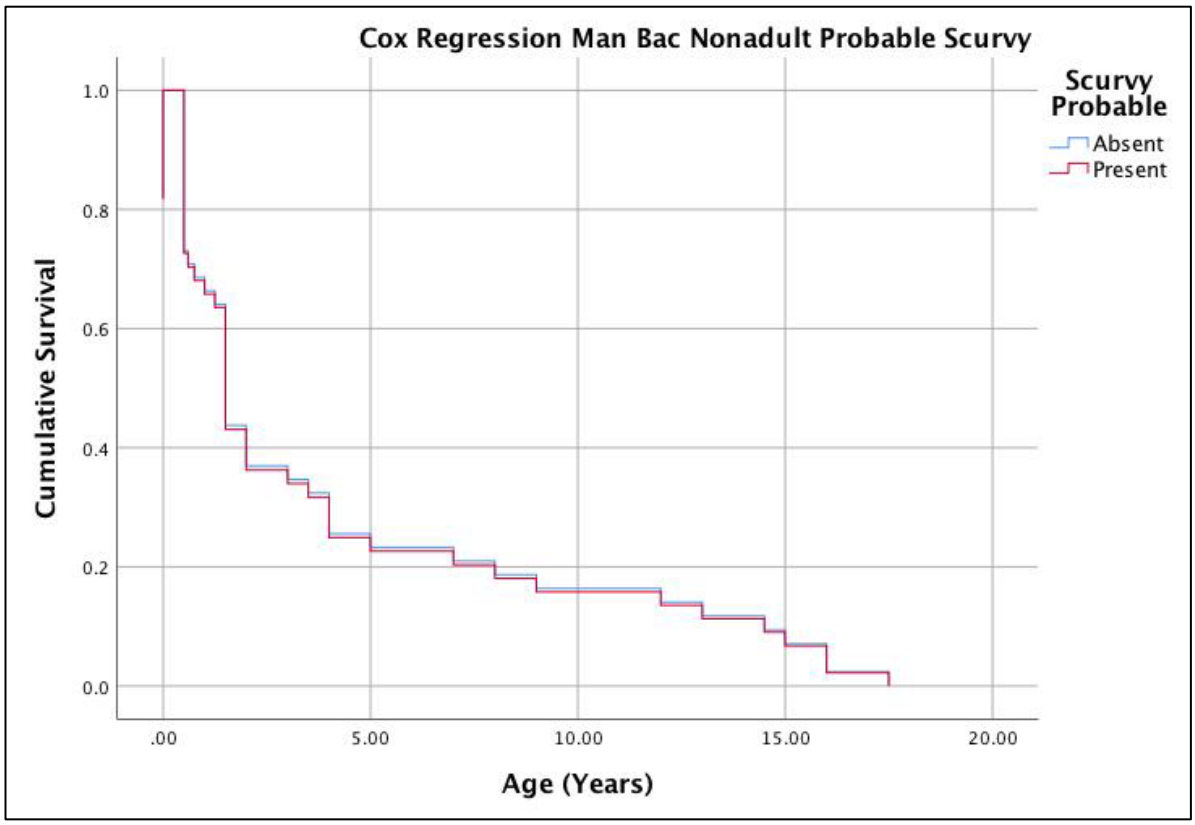

Figure 7.38: *Cox regression cumulative survival function of nonadult probable scurvy mortality at Man Bac. Image: author's own.*

Table 7.31: *Statistical summary for Kaplan-Meier function of possible and probable scurvy mortality of adults at Man Bac.*

POSSIBLE AND PROBABLE SCURVY	ESTIMATE	STD. ERROR	95% CI	LOG RANK (MANTEL-COX)		
				CHI SQUARE	DF	P-VALUE
Mean				1.673	1	0.196
Absent	37.286	2.732	31.930- 42.641			
Present	30.333	3.079	24.298- 36.369			
Overall	33.690	2.135	29.506- 37.874			
Median						
Absent	35.000	4.677	25.833- 44.167			
Present	27.000	5.024	17.154- 36.846			
Overall	35.000	3.484	28.171- 41.829			

*= statistical significance (p<0.15).

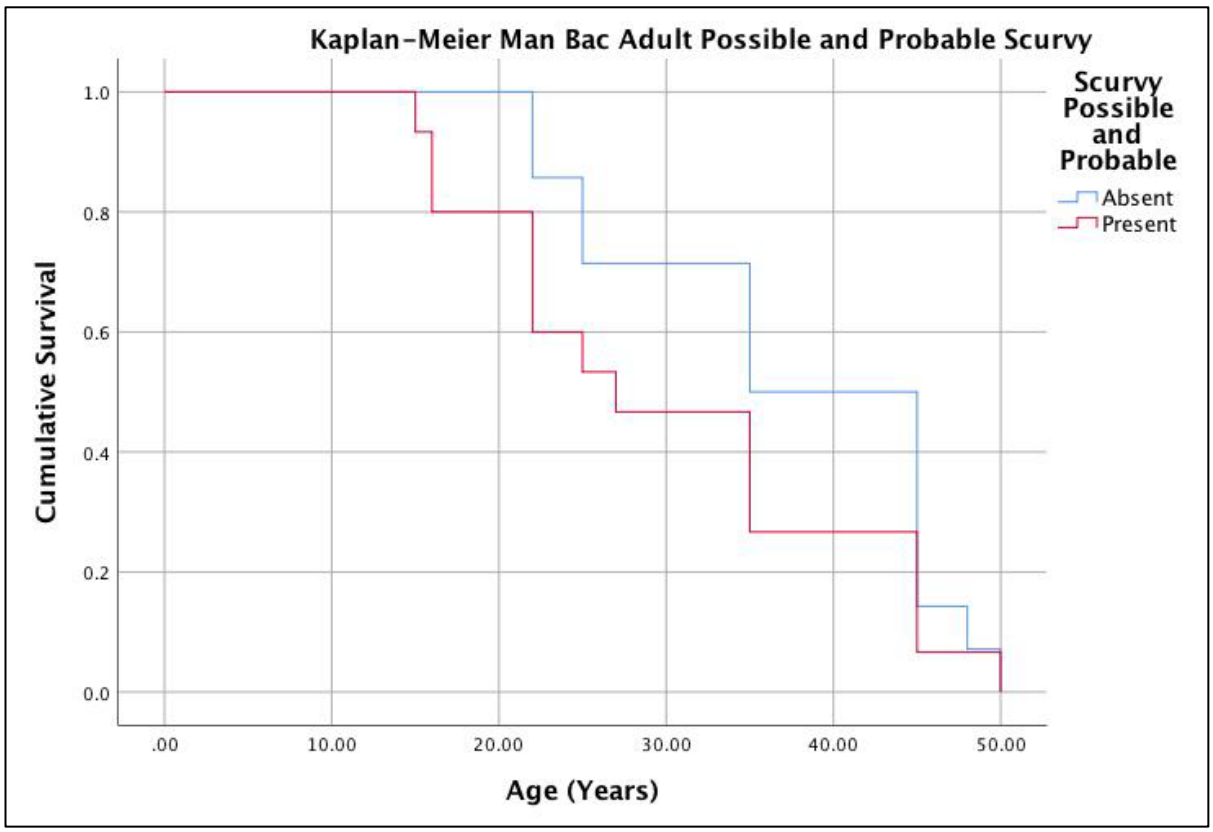

Figure 7.39: *Kaplan-Meier cumulative survival function of adult possible and probable scurvy mortality at Man Bac. Image: author's own.*

Table 7.32: *Statistical summary for Kaplan-Meier function of probable scurvy mortality of adults at Man Bac.*

PROBABLE SCURVY	ESTIMATE	STD. ERROR	95% CI	LOG RANK (MANTEL-COX)		
				CHI SQUARE	DF	P-VALUE
Mean				3.764	1	**0.052***
Absent	37.889	2.201	33.576- 42.202			
Present	26.818	3.544	19.872- 33.765			
Overall	33.690	2.135	29.506- 37.874			
Median						
Absent	35.000	3.536	28.070- 41.930			
Present	22.000	3.716	14.717- 29.283			
Overall	35.000	3.484	28.171- 41.829			

*= statistical significance (p<0.15).

Table 7.33: *Statistical summary for Cox regression function of probable scurvy mortality of adults at Man Bac.*

PROBABLE SCURVY	COEFFICIENT (β)	STD. ERROR	WALD	DF	P-VALUE	ODDS RATIO (Exp(β))
	-0.606	0.393	2.379	1	**0.123***	0.545

*= statistical significance (p<0.15).

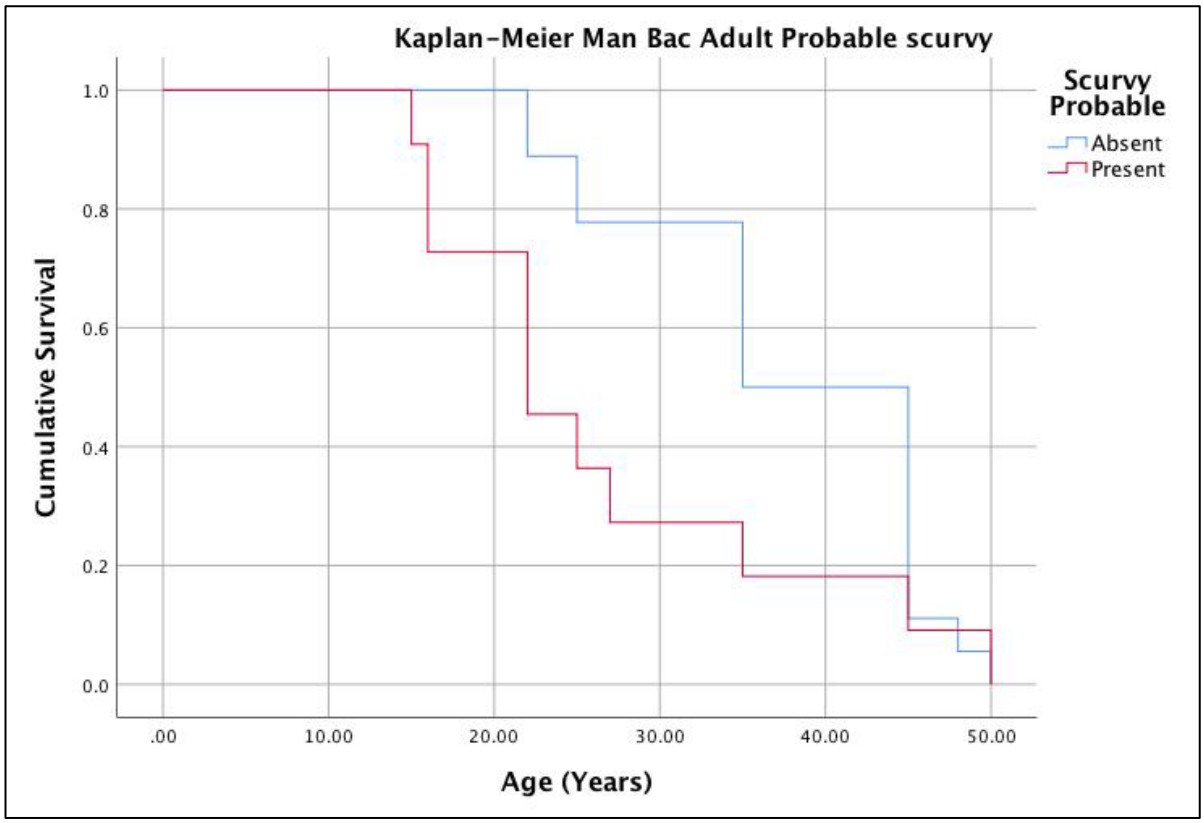

Figure 7.40: *Kaplan-Meier cumulative survival function of adult probable scurvy mortality at Man Bac. Image: author's own.*

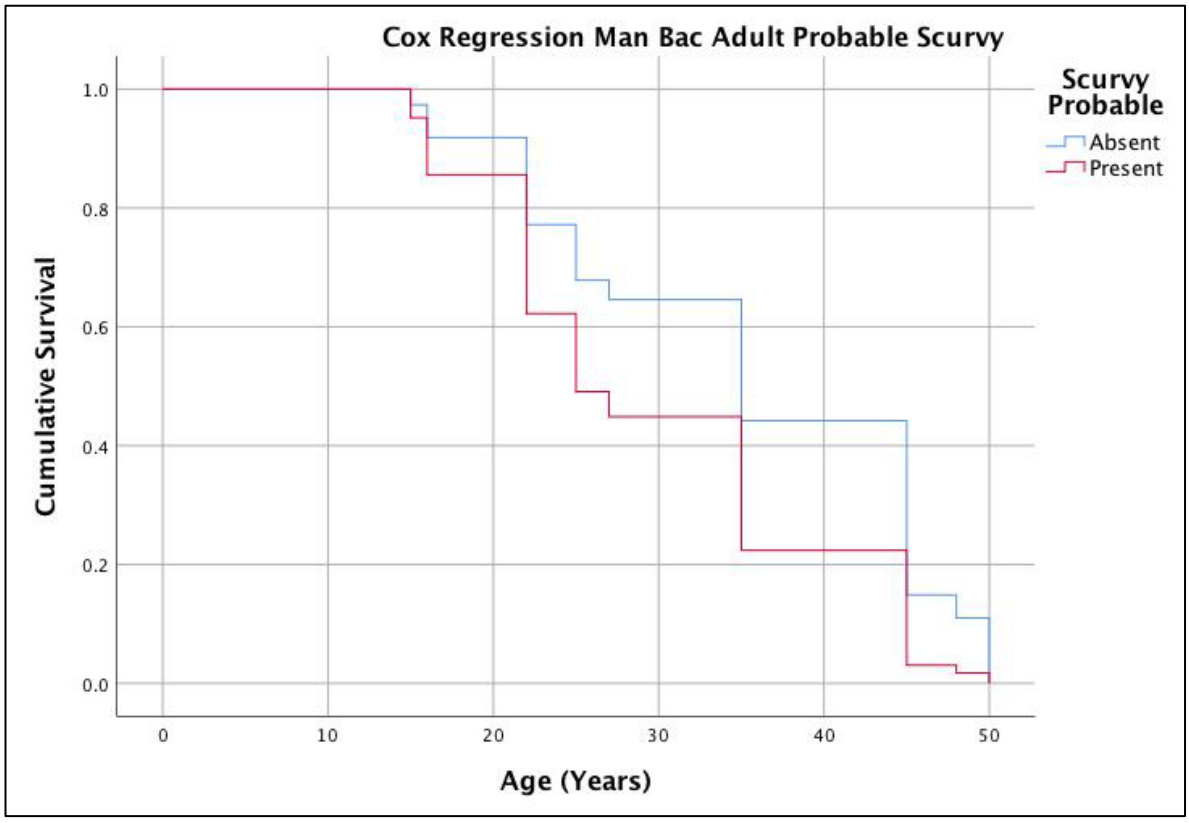

Figure 7.41: *Cox regression cumulative survival function of adult probable scurvy mortality at Man Bac. Image: author's own.*

7.6.7.2 Man Bac Rickets Mortality

A statistically significant relationship with frailty was identified in cases of combined possible and probable, and probable only cases of rickets (Table 7.34). For probable only cases, the relationship with frailty was statistically significant at all tested age groups (1, 5 and 10 years of age), whereas for combined possible and probable cases significance was found at under 5 and under 10 year age groups only. However, relative risk overall is not particularly high with the risk of death before the age of 1 year being only 2 times higher in the cases of probable only rickets (n=44, RR=2.1429, p=0.0732). The lack of significance in the prevalence of infant compared to post-infant cases of combined possible and probable rickets, is likely due to the large variation in the prevalences between 0 to under 6 month olds, compared to 6 months to 1 year olds in the nonadult assemblage (Figure 7.34). Infants over the age of 6 months had considerably higher prevalence of rickets than those under 6 months of age. Underlying reasons for this disparity are discussed below.

Kaplan-Meier survival analysis identified statistically significant frailty in individuals with possible or probable (n=44, X^2=4.212, df=1, p=0.040; Table 7.35; Figure 7.42), as well as probable only (n=44, X^2=5.335, df=1, p=0.021; Table 7.37; Figure 7.44) cases of rickets. Similarly, significant frailty for combined possible or probable (n=44, Wald= 3.480, df=1, p=0.062; Table 7.36; Figure 7.43), as well as probable only (n=44, Wald=4.334, d=1, p=0.037; Table 7.38; Figure 7.45) cases of rickets were also identified in the Cox regression analysis. Overall, mortality statistics identifies a clear relationship of frailty with the presence of rickets in nonadults.

Table 7.34: *Relative risk of rickets mortality at Man Bac across age cohorts.*

POSITIVE OUTCOME/ NEGATIVE OUTCOME	**TREATMENT**		**RR**	**P-VALUE**	**95%CI**
	Exposed Group: *Disease Present*	***Control Group:*** *Disease Absent*			
Possible and Probable Rickets (combined)					
Nonadults					
<1 yr/ >1 yr	7/15	7/15	1.000	1.000	0.4210- 2.3752
<5 yrs/ >5yrs	19/3	14/8	**1.3571**	**0.0935***	0.9498- 1.9391
<10 yrs/ >10yrs	22/0	15/7	**1.4667**	**0.0085***	1.1024- 1.9512
Probable Only Rickets					
Nonadults					
<1 yr/ >1 yr	7/7	7/23	**2.1429**	**0.0732***	0.9309- 4.9327
<5 yrs/ >5yrs	13/1	20/10	**1.3929**	**0.0260***	1.0404- 1.8648
<10 yrs/ >10yrs	14/0	23/7	**1.3043**	**0.0083***	1.0707- 1.5890

A relative risk (RR) >1 denotes a relationship of the disease presence with the positive outcome (susceptibility to mortality), whereas RR <1 denotes a relationship of the disease absence with a negative outcome (survivorship).
*= statistically significant (p<0.10). **= statistically significant when considering size of the effect of RR.

Table 7.35: *Statistical summary for Kaplan-Meier function of possible and probable rickets mortality of nonadults at Man Bac.*

POSSIBLE AND PROBABLE RICKETS	**ESTIMATE**	**STD. ERROR**	**95% CI**	**LOG RANK (MANTEL-COX)**		
				CHI SQUARE	**DF**	**P-VALUE**
Mean				4.212	1	**0.040***
Absent	5.830	1.424	3.038- 8.621			
Present	2.198	0.466	1.285- 3.110			
Overall	4.014	0.791	2.464- 5.563			
Median						
Absent	1.500	0.821	0.000- 3.109			
Present	1.500	0.188	1.131- 1.869			
Overall	1.500	0.091	1.321- 1.679			

*= statistical significance (p<0.15).

Table 7.36: *Statistical summary for Cox regression function of possible and probable rickets mortality of nonadults at Man Bac.*

POSSIBLE AND PROBABLE RICKETS	COEFFICIENT (β)	STD. ERROR	WALD	DF	P-VALUE	ODDS RATIO (Exp(β))
	-0.654	0.351	3.480	1	**0.062***	0.520

*= statistical significance (p<0.15).

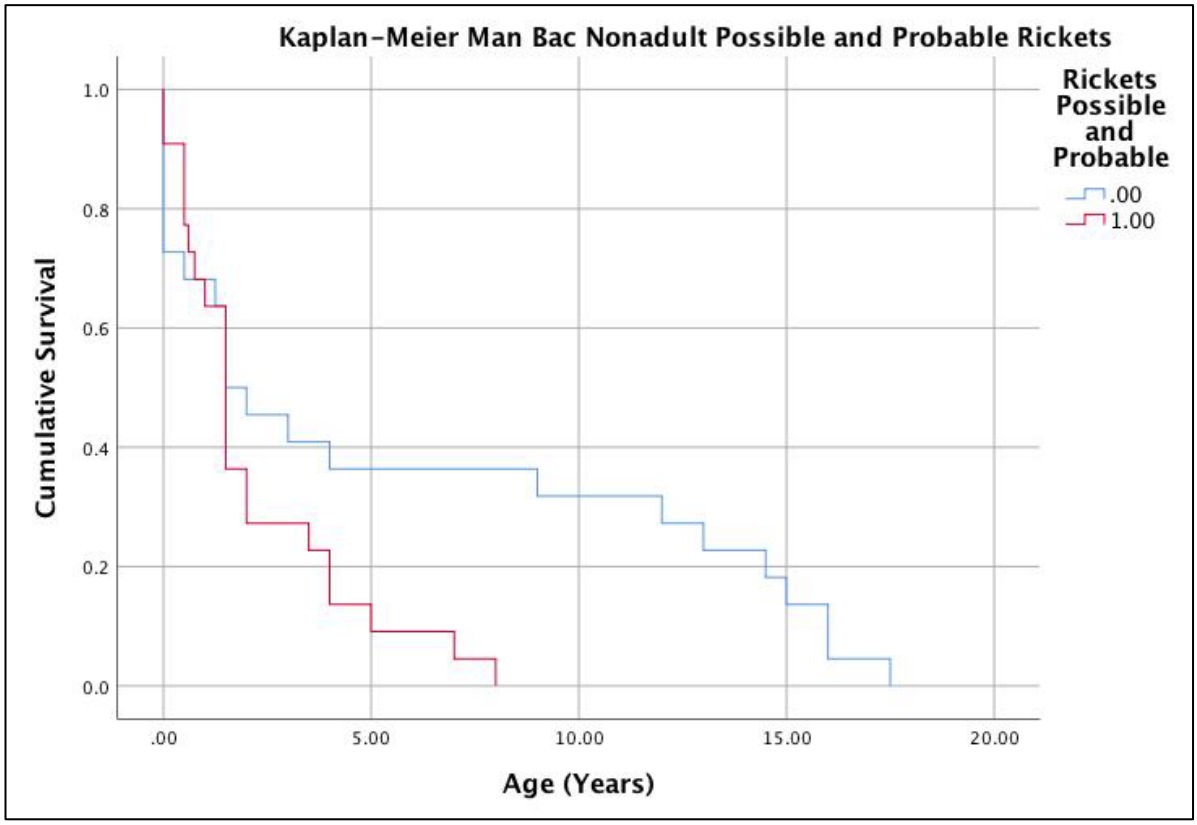

Figure 7.42: *Kaplan-Meier cumulative survival function of nonadult possible and probable rickets mortality at Man Bac. Image: author's own.*

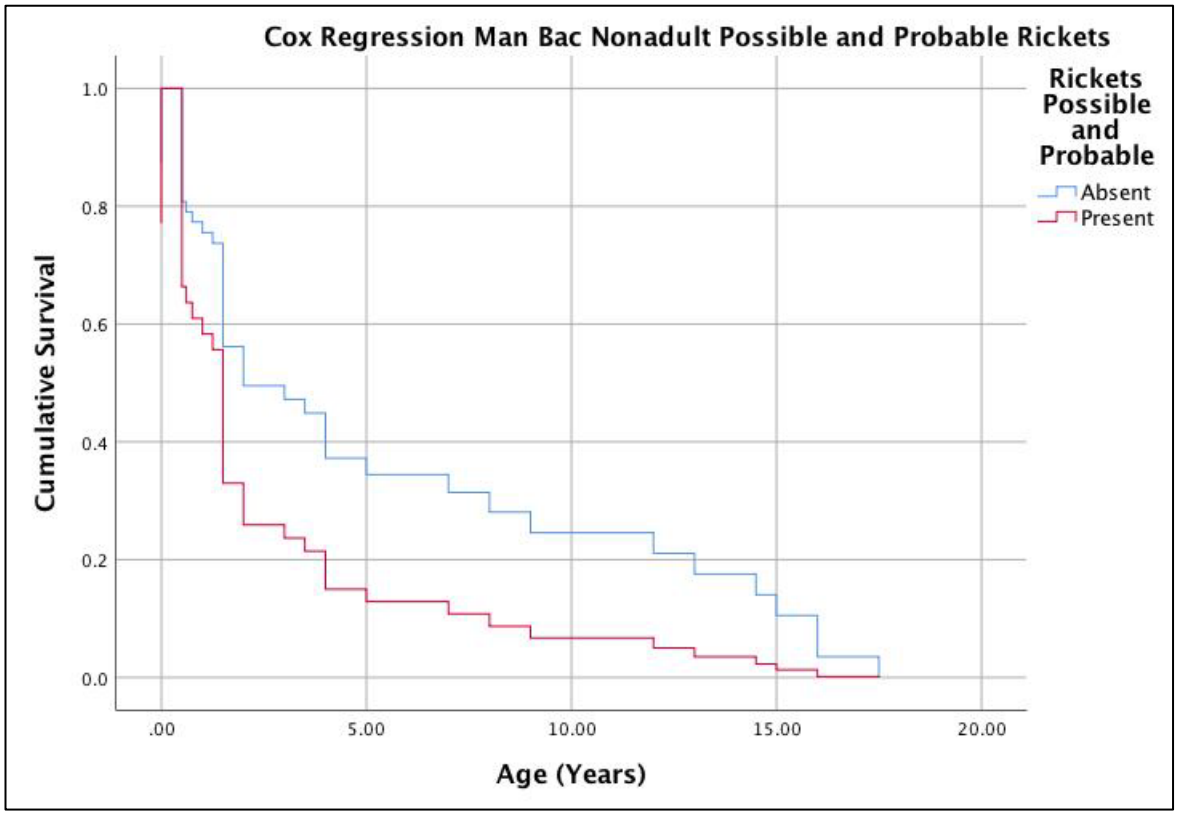

Figure 7.43: *Cox Regression cumulative survival function of nonadult possible and probable rickets mortality at Man Bac. Image: author's own.*

Table 7.37: *Statistical summary for Kaplan-Meier function of probable rickets mortality of nonadults at Man Bac.*

PROBABLE RICKETS	ESTIMATE	STD. ERROR	95% CI	LOG RANK (MANTEL-COX)		
				CHI SQUARE	DF	P-VALUE
Mean				5.335	1	**0.021***
Absent	5.142	1.081	3.023- 7.261			
Present	1.596	0.501	0.614- 2.579			
Overall	4.014	0.791	2.464- 5.563			
Median						
Absent	1.500	0.599	0.326- 2.674			
Present	0.750	0.421	0.000- 1.575			
Overall	0.091	0.091	1.321- 1.679			

*= statistical significance (p<0.15).

Table 7.38: *Statistical summary for Cox regression function of probable rickets mortality of nonadults at Man Bac.*

PROBABLE RICKETS	COEFFICIENT (β)	STD. ERROR	WALD	DF	P-VALUE	ODDS RATIO (Exp(β))
	-0.733	0.352	4.334	1	**0.037***	0.480

*= statistical significance (p<0.15).

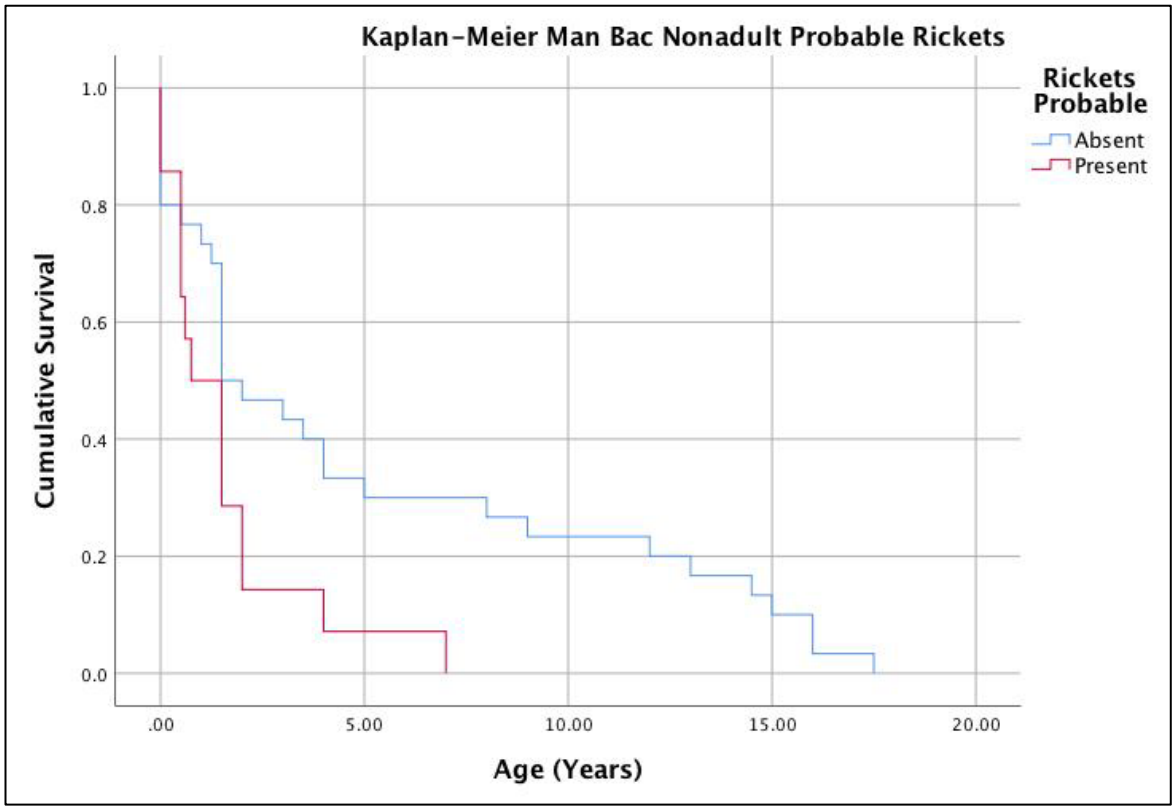

Figure 7.44: *Kaplan-Meier cumulative survival function of nonadult probable rickets mortality at Man Bac. Image: author's own.*

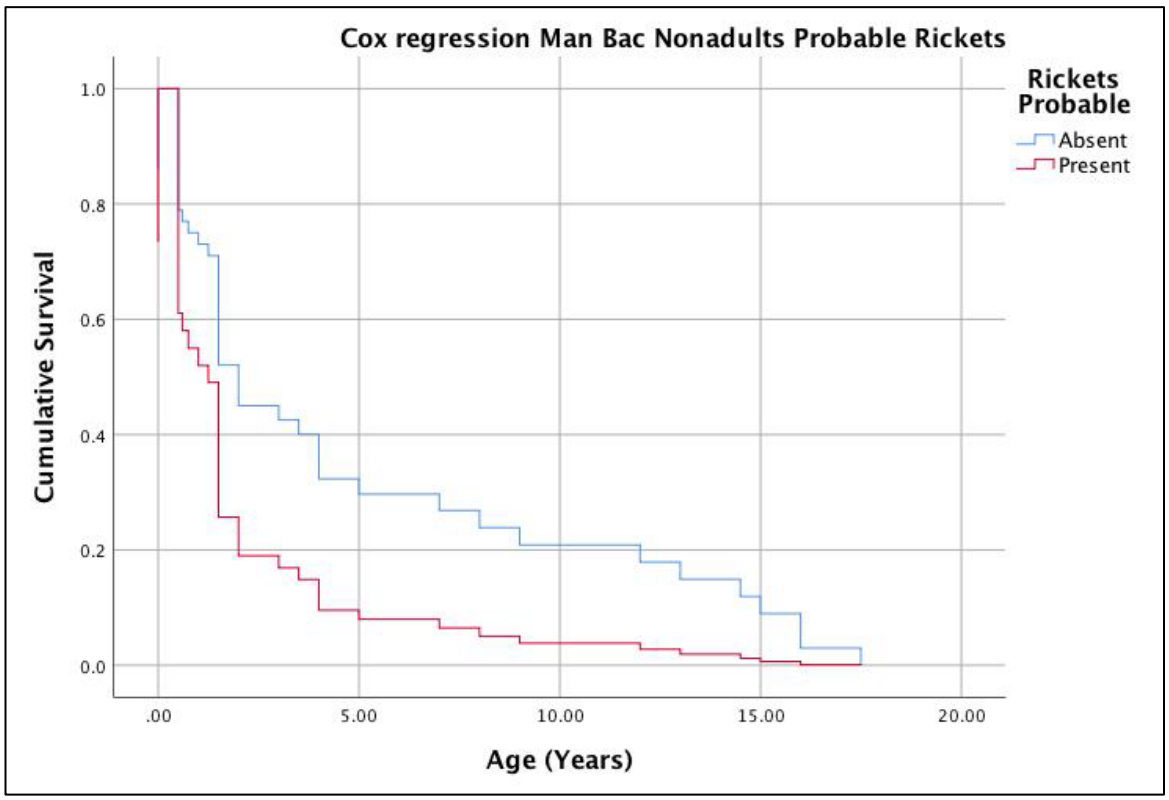

Figure 7.45: *Cox Regression cumulative survival function of nonadult probable rickets mortality at Man Bac. Image: author's own.*

7.6.8 Diagnosis of Anaemia at Man Bac

Out of 57 individuals with preserved cranial and/or orbital skeletal elements, 47.3% (27/57) exhibited medium or severe grade cribra orbitalia and/or porotic hyperostosis consistent with anaemia (Table 7.39). The presence of porotic hyperostosis (54.5%, 12/22) in adults was more common than medium or severe grade cribra orbitalia (38.1%, 8/21). However, all individuals with porotic hyperostosis (Figure 7.46) exhibited at minimum mild grade cribra orbitalia. The youngest individual with evidence of anaemia was 1.5 years of age (MB07H2M16). However, one neonate (MB07H1M12) exhibited diploic expansion of one preserved left temporal without ectocranial porosity, which was not included in the overall prevalence of anaemia. The possible aetiology of the diploic expansion is dealt with below. The prevalence of anaemia in adults was highest under 40 years of age, with lower prevalences in adults over the age of 40 years of age (Figure 7.47).

Table 7.39: *Summary of anaemia at Man Bac*

ANAEMIA	**CO**			**Cranial PH**			**PH and/or CO**		
	Affected	*Observed*	*(%)*	*Affected*	*Observed*	*(%)*	*Affected*	*Observed*	*(%)*
0 to 6 months	0	6	0	0	1	0	0	6	0
6 months to 1 year	0	5	0	0	5	0	0	5	0
1 to 5 years	5	14	35.7	2	14	14.3	5	15	33.3
5 to 10 years	1	2	50	0	2	0	1	2	50
10 to 15 years	3	3	100	1	3	33.3	3	3	100
15 to 20 years	2	4	50	3	4	75	3	4	75
20 to 30 years	2	7	28.6	5	7	71.4	7	7	100
30 to 40 years	4	6	66.7	5	6	83.3	6	6	100
40 to 50 years	2	6	33.3	2	7	28.6	3	7	42.9
50+ years	0	2	0	0	2	0	0	2	0
Total nonadults	11	34	32.4	6	29	20.7	12	35	34.3
Males	6	13	46.2	11	13	84.6	11	13	84.6
Females	4	11	36.4	5	10	50	7	11	63.6
Total adults	8	21	38.1	12	22	54.5	15	22	68.2
Total	19	55	34.5	18	51	35.3	27	57	47.4

Figure 7.46: *Remodelled porotic hyperostosis (MB05M11, young adult male). Marrow hyperplasia has resulted in diploic expansion of the parietal bones. Note the clear margin where porosity ceases above the temporal line (porosity: white arrow, temporal line: black arrow). This is not consistent with scorbutic porosity which often is found within the bone surface in contact with the temporalis muscle due to haemorrhaging from muscle use.*

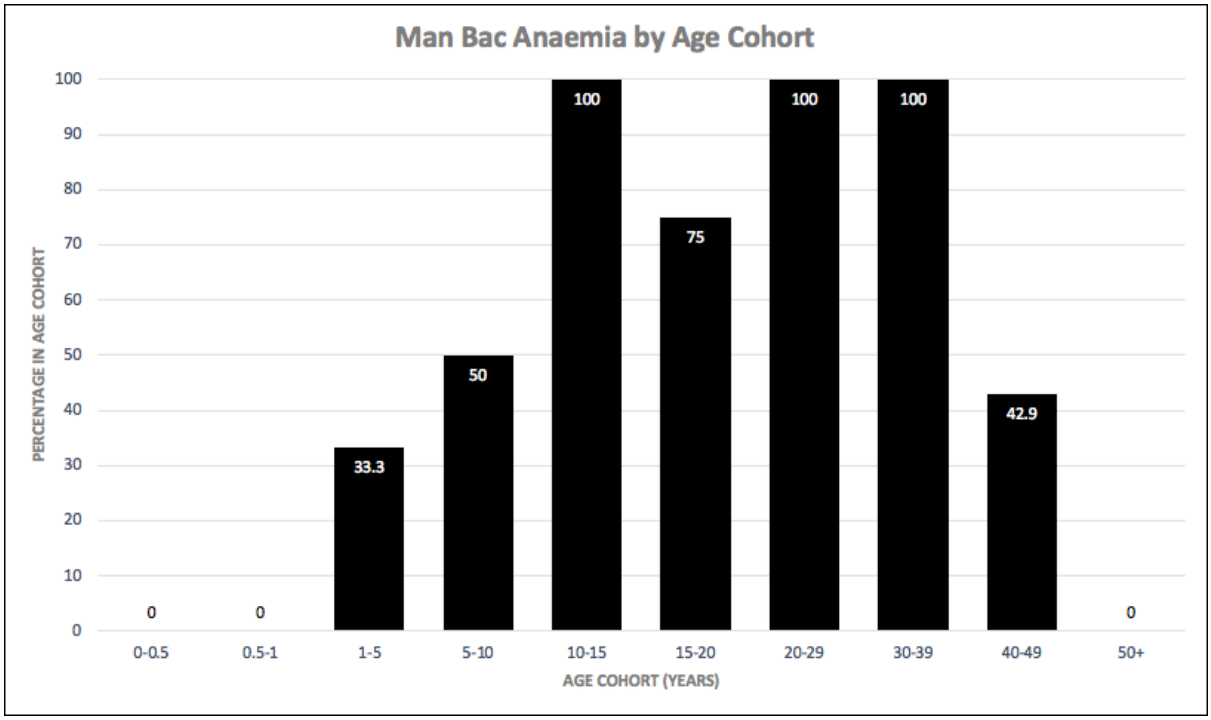

Figure 7.47: *Age-at-death distribution of anaemia at Man Bac. Image: author's own.*

One individual exhibited skeletal pathology consistent with possible, and six individuals consistent with a probable case of thalassaemia (10%, 7/70; Table 7.40). Four individuals exhibited marrow hyperplasia of the zygomatic bones, maxilla and/or mandible consistent with rodent facies (Figure 7.48). Rodent facies was associated with crowding and anterior protrusion of the anterior maxillary teeth. Radiographs confirmed marrow hyperplasia of the facial bones, strongly diagnostic for thalassaemia. Additionally, lack of pneumatisation of the paranasal and frontal sinuses were present in two individuals (Figure 7.48e). Three individuals also presented with radiographic "rib-within-a-rib" sign (Figure 7.49) and three individuals exhibited severe cribra orbitalia (Figure 7.48j). Diploic expansion was not associated with ectocranial porosity. However, in two individuals, hair-on-end endocranial lesions were also present (Figure 7.48d). Limb bones exhibited marrow hyperplasia associated with cortical thinning (rarefaction) or spiculated diffuse SPNB (extramedullary haematopoiesis). Only one adult was identified with pathology consistent with thalassemia (MB07H1M8, middle aged adult male). This individual exhibited radiographic "rib-within-a-rib" sign as well as enlarged foramina of the phalanges. Marrow hyperplasia of the phalanges was observed on the radiographs (Figure 7.49b). A neonate with diploic expansion of the temporal bone also exhibited enlarged scapulae and ilia. These elements exhibited alteration in the structure of the trabeculae consistent with thalassaemia.

This neonate constitutes the only possible case identified in the assemblage. Cases of thalassaemia were identified in nearly all age cohorts of nonadults. The adult (MB07H1M8, middle aged adult male) did not exhibit any gross macroscopically observable morphological changes to the skeleton, whereas gross morphological changes were present in all nonadults diagnosed with possible or probable thalassaemia.

Table 7.40: *Summary of possible and probable thalassaemia at Man Bac*

THALASSAEMIA	**POSSIBLE**			**PROBABLE**			**POSSIBLE AND PROBABLE**		
	Affected	*Observed*	*(%)*	*Affected*	*Observed*	*(%)*	*Affected*	*Observed*	*(%)*
0 to 6 months	1	8	12.5	0	8	0	1	8	12.5
6 months to 1 year	0	6	0	1	6	16.7	1	6	16.7
1 to 5 years	0	20	0	2	20	10	2	20	10
5 to 10 years	0	3	0	0	3	0	0	3	0
10 to 15 years	0	3	0	1	3	33.3	1	3	33.3
15 to 20 years	0	4	0	0	4	0	0	4	0
20 to 30 years	0	9	0	0	9	0	0	9	0
30 to 40 years	0	6	0	1	6	16.7	1	6	16.7
40 to 50 years	0	8	0	0	8	0	0	8	0
50+ years	0	3	0	0	3	0	0	3	0
Total nonadults	1	44	2.3	4	44	9.1	5	44	11.4
Total adults	0	26	0	1	26	3.8	1	26	3.8
Total	1	70	1.4	5	70	7.1	6	70	8.6

Figure 7.48: *Cranial lesions consistent with thalassaemia at Man Bac. a) Anterior protrusion of the zygomatic bones consistent with rodent facies (MB05M3, approx. 6 months old). b) and d) Diploic expansion of the cranial vault. There is no porosity on the ectocranium but hair-on-end formations are present on the endocranium (MB05M12, approx. 2 years). c) Marrow hyperplasia of the zygomatic bones (MB05M12). e) Lack of pneumatisation of the frontal sinus (MB07H1M1, approx. 12 years). f) and g) Marrow hyperplasia of the maxilla (MB07H1M1). h) Rodent facies of the maxilla, mandible and zygoma (MB07H2M26, approx. 1.5 years). i) Hyperplasia of the left zygoma (MB07H1M1). j) Severe cribra orbitalia (white arrow) and diploic expansion of the crania (black arrow) (MB07H1M1). Image: author's own.*

Figure 7.49: *Postcranial lesions consistent with thalassaemia at Man Bac. a) Enlarged rib (MB05M3, approx. 6 months old). b) and d) Expanded foramina of the phalanges (black arrow) with marrow hyperplasia (white arrow (MB07H1M8, middle aged adult). c) "Rib-within-a-rib" sign (MB07H1M8). e) Alteration of the trabecular structure of the ilia. Note the radiating pattern (MB07H1M12, neonate). f) "Rib-within-a-rib" sign (MB07H2M26, approx. 1.5 years). g) Enlargement of the scapular spines (MB07H1M12, neonate). h) Marrow hyperplasia of the humerus (MB05M12, approx. 2 years). Image: author's own.*

7.6.9 Morbidity of Anaemia at Man Bac

No statistically significant differences in anaemia were identified between males and females at Man Bac (n=23, RR=0.7091, p=0.2261). A relationship with morbidity of anaemia and older nonadult age groups was statistically significant at all tested cohorts (1, 5 and 10 years; Table 7.41). In contrast, adults were associated with increased risk of morbidity in individuals under 30 years of age (n=26, RR=1.600, p=0.0544), as well as under 40 years of age (n=26, RR=3.1250, p=0.0194). As previously mentioned, skeletal lesions for anaemia develop in childhood therefore, it is likely this outcome is directly related to mortality which is assessed below. However, as hyperplasia from childhood may be completely remodelled in older age groups (Stuart-Macadam 1985), age of onset in childhood may in part be influencing the adult age trend at Man Bac.

Table 7.41: *Relative risk of anaemia morbidity at Man Bac across sex and age cohorts.*

EXPOSED GROUP/ CONTROL GROUP	**OUTCOME**		**RR**	**P-VALUE**	**95%CI**
	Positive: *Anaemia Present*	***Negative:*** *Anaemia Absent*			
Sex					
Female/ Male	6/11	4/2	0.7091	0.2261	0.4064- 1.2372
Nonadults					
<1 yr/ >1 yr	0/12	11/12	**0.0833**	**0.0757***	0.0054- 1.2927
<5 yrs/ >5yrs	4/8	21/2	**0.2000**	**0.0009***	0.0773- 0.5172
<10 yrs/ >10yrs	6/6	22/1	**0.2500**	**0.0004***	0.1156- 0.5405
Adults					
<20 yrs/ >20 yrs	2/16	1/7	0.9583	0.9213	0.4118- 2.2301
<30 yrs/ >30 yrs	9/9	1/7	**1.600**	**0.0544***	0.9911- 2.5831
<40 yrs/>40 yrs	15/3	3/7	**3.1250**	**0.0194***	1.2023- 8.1224

A relative risk (RR) >1 denotes a relationship of the exposed group with an increase in disease prevalence, whereas RR <1 denotes a relationship of the control group with an increase in disease prevalence.
*= statistically significant (p<0.10). **= statistically significant when considering size of the effect of RR.

7.6.10 Mortality of Anaemia at Man Bac

Relative risk ratio analysis demonstrated a high association of survivorship in nonadults with skeletal evidence of anaemia (cribra orbitalia or porotic hyperostosis), which was statistically significant across all tested nonadult age cohorts (after 1, 5 and 10 years of age; Table 7.42). In contrast, an association with frailty was evident for skeletal signs of anaemia in adults. However, this association was only statistically significant for adults under 40 years of age (n=28, RR=6.6667, p=0.0439). This outcome suggests survivorship

to old age of those without skeletal evidence for anaemia. The relative risk of mortality was higher than was the case for adult morbidity at 40 years of age, indicating a stronger influence of mortality than factors of morbidity such as remodelling lesions.

Statistically significant higher survivorship in nonadults with the presence anaemia was identified in both Kaplan-Meier (n=35, X^2=11.863, df=1, p=0.001; Table 7.43: Figure 7.50) and Cox regression (n=35, Wald= 9.397, df=1, p=0.002; Table 7.44; Figure 7.51) analyses. In contrast, as was the case in relative risk ratio analysis, a relationship with frailty was identified in both Kaplan-Meier (n=26, X^2= 9.673, df=1, p=0.002; Table 7.45; Figure 7.52) and Cox regression (n=26, Wald=5.999, df=1, p=0.014; Table 7.46; Figure 7.53) analyses. Overall, an association with survivorship of nonadults, and frailty of adults with skeletal evidence of anaemia is apparent.

Table 7.42: *Relative risk of anaemia mortality at Man Bac across age cohorts.*

POSITIVE OUTCOME/ NEGATIVE OUTCOME	**TREATMENT**		**RR**	**P-VALUE**	**95%CI**
	Exposed Group: *Anaemia Present*	***Control Group:*** *Anaemia Absent*			
Nonadults					
<1 yr/ >1 yr	0/12	11/12	**0.0803**	**0.0722***	0.0051- 1.2554
<5 yrs/ >5yrs	4/8	21/2	**0.3651**	**0.0148***	0.1624- 0.8207
<10 yrs/ >10yrs	6/6	22/1	**0.5227**	**0.0264***	0.2949- 0.9266
Adults					
<20 yrs/ >20 yrs	2/16	1/7	0.8889	0.9183	0.0936- 8.4453
<30 yrs/ >30 yrs	9/9	1/7	4.0000	0.1507	0.6039- 26.4965
<40 yrs/>40 yrs	15/3	3/7	**6.6667**	**0.0439***	1.0535- 42.1880

A relative risk (RR) >1 denotes a relationship of the disease presence with the positive outcome (susceptibility to mortality), whereas RR <1 denotes a relationship of the disease absence with a negative outcome (survivorship).
*= statistically significant (p<0.10). **= statistically significant when considering size of the effect of RR.

Table 7.43: *Statistical summary for Kaplan-Meier function of anaemia mortality of nonadults at Man Bac.*

ANAEMIA	**ESTIMATE**	**STD. ERROR**	**95% CI**	**LOG RANK (MANTEL-COX)**		
				CHI SQUARE	**DF**	**P-VALUE**
Mean				11.863	1	**0.001***
Absent	2.146	0.754	0.668- 3.623			
Present	9.375	1.704	6.036- 12.714			
Overall	4.624	0.954	2.755- 6.494			
Median						
Absent	1.500	0.271	0.969- 2.031			
Present	8.000	6.062	0.000- 19.882			
Overall	1.500	0.411	0.695- 2.305			

*= statistical significance (p<0.15).

Table 7.44: *Statistical summary for Cox regression function of anaemia mortality of nonadults at Man Bac.*

ANAEMIA	COEFFICIENT (β)	STD. ERROR	WALD	DF	P-VALUE	ODDS RATIO (Exp(β))
	1.193	0.389	9.397	1	**0.002***	3.298

*= statistical significance (p<0.15).

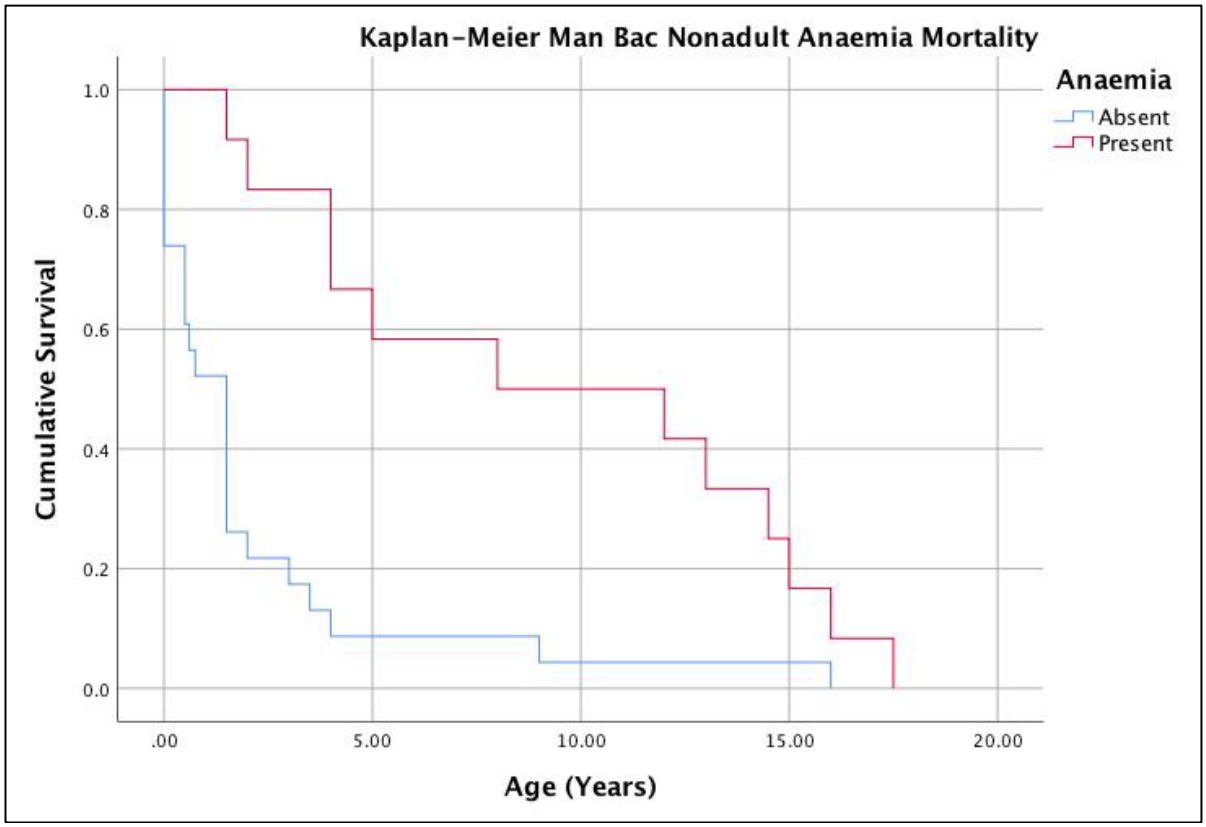

Figure 7.50: *Kaplan-Meier cumulative survival function of nonadult anaemia mortality at Man Bac. Image: author's own.*

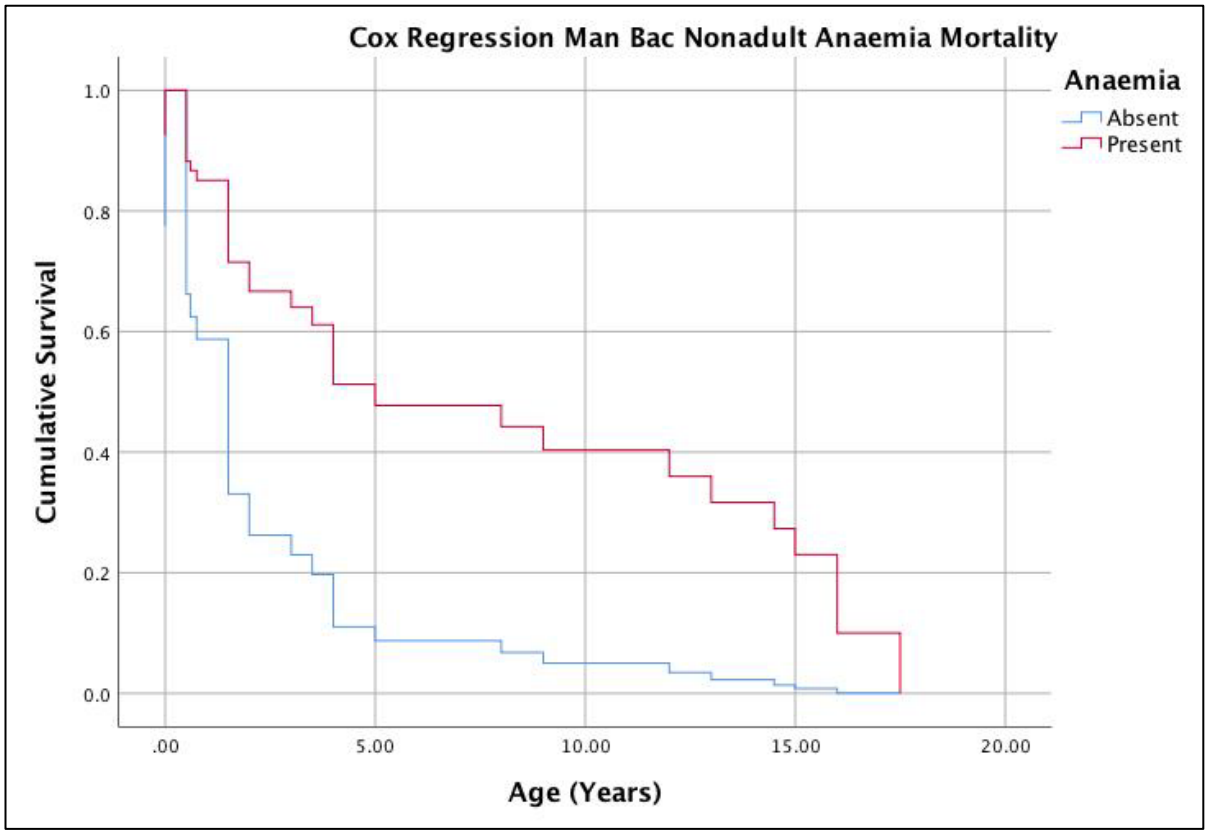

Figure 7.51: *Cox regression cumulative survival function of nonadult anaemia mortality at Man Bac. Image: author's own*

Table 7.45: *Statistical summary for Kaplan-Meier function of anaemia mortality of adults at Man Bac.*

ANAEMIA	ESTIMATE	STD. ERROR	95% CI	LOG RANK (MANTEL-COX)		
				CHI SQUARE	DF	P-VALUE
Mean				9.673	1	**0.002***
Absent	43.000	3.937	35.283- 50.717			
Present	30.222	2.230	25.852- 34.592			
Overall	34.154	2.251	29.742- 38.566			
Median						
Absent	45.000	9.927	25.542- 64.458			
Present	27.000	3.030	21.060- 32.940			
Overall	35.000	3.308	28.517- 41.483			

*= statistical significance (p<0.15).

Table 7.46: *Statistical summary for Cox regression function anaemia mortality of adults at Man Bac.*

ANAEMIA	COEFFICIENT (β)	STD. ERROR	WALD	DF	P-VALUE	ODDS RATIO (Exp(β))
	-1.292	0.527	5.999	1	**0.014***	0.275

*= statistical significance (p<0.15).

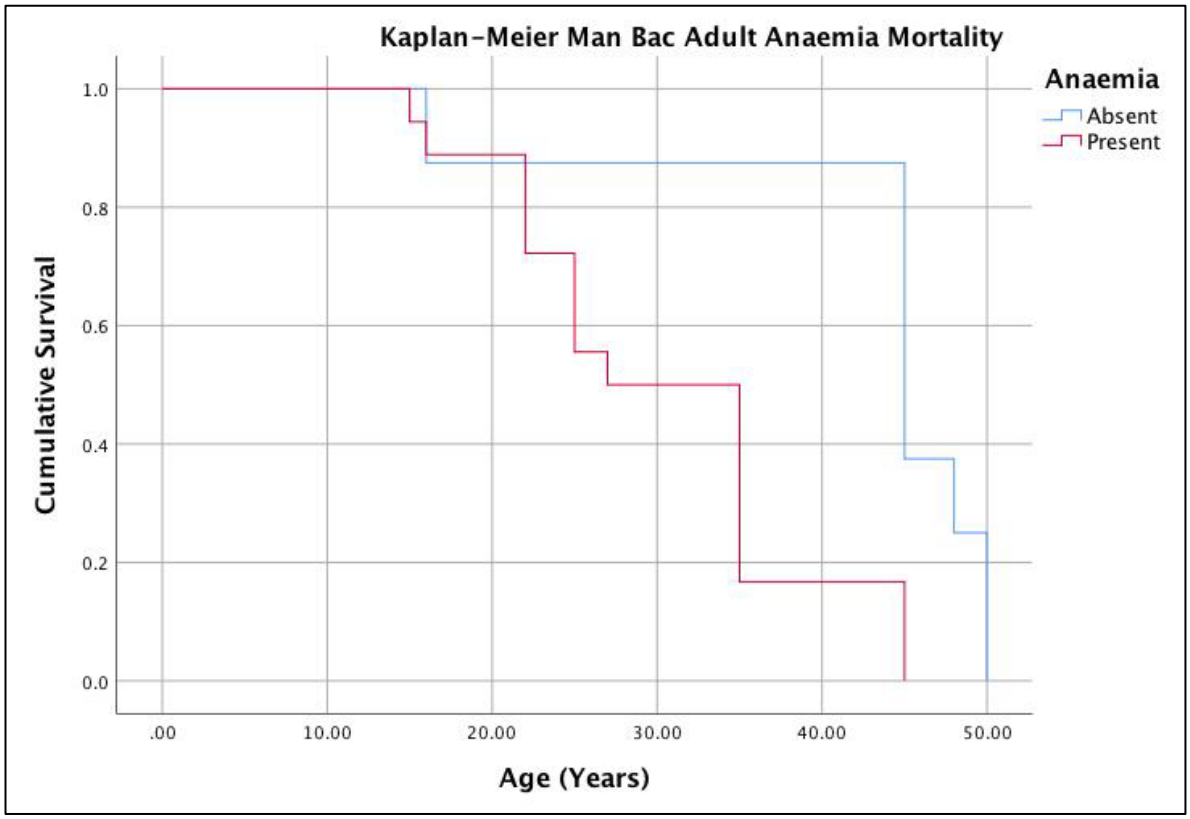

Figure 7.52: *Kaplan-Meier cumulative survival function of adult anaemia mortality at Man Bac. Image: author's own*

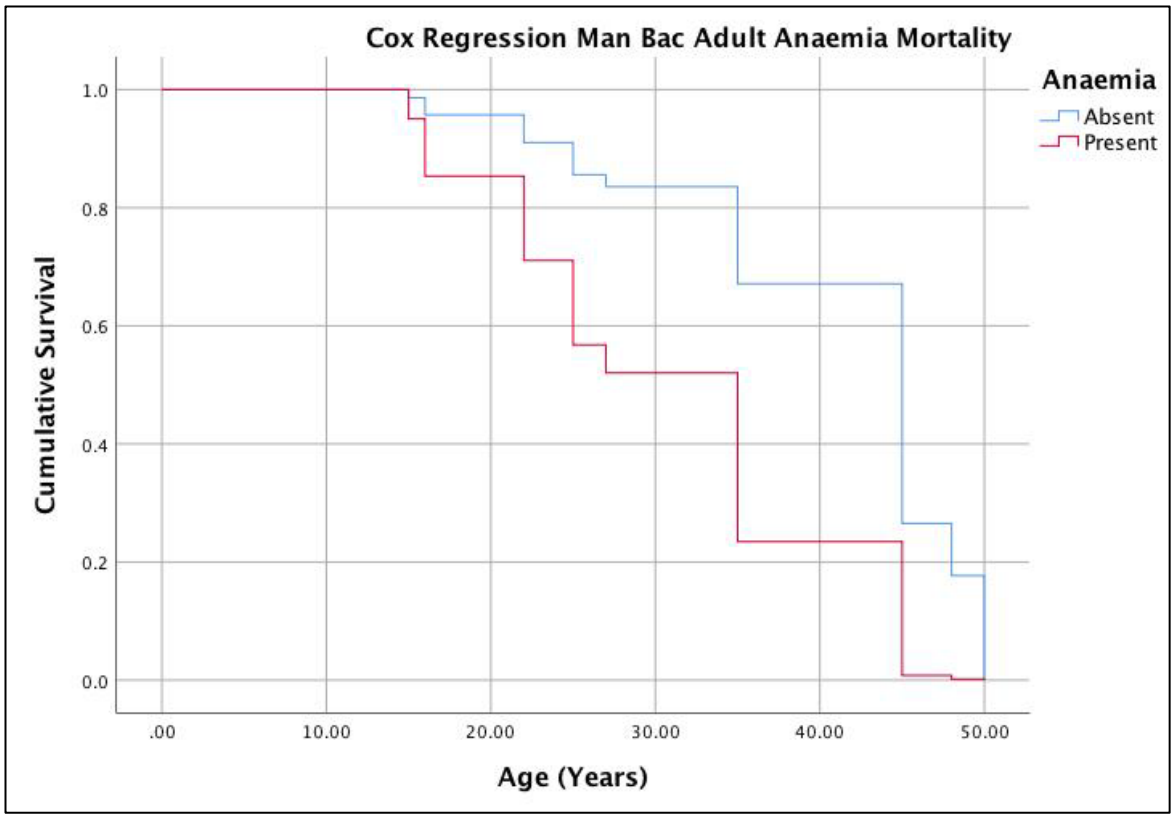

Figure 7.53: *Cox regression cumulative survival function of adult anaemia mortality at Man Bac. Image: author's own*

7.6.11 Summary of Diagnosis and Context of Disease at Man Bac

Overall a considerable disease burden was apparent at Man Bac. Twenty percent (14/70) of the assemblage exhibited lesions consistent with infectious disease. Evidence of nutritional disease was very high with 77.1% (54/70) of the assemblage displaying skeletal evidence for scurvy and/or rickets. Additionally, 46.6% (27/58) of the assemblage had skeletal evidence of anaemia, with 10% (7/70) exhibiting skeletal signs specific for thalassaemia.

7.6.11.1 Treponemal Disease at Man Bac

As mentioned in Chapter 5, treponemal diseases that affect the skeleton cannot be distinguished from their skeletal pathology alone. However, the epidemiological, social, and environmental contexts of the disease do allow some discussion on the treponeme responsible. Climatically, Vietnam is within latitudinal boundaries where yaws has been historically documented (Mitjà et al. 2013). With consideration of all possible and probable cases at Man Bac, it is clear the lesions are predominantly in nonadults, with only two adults presenting lesions consistent with treponemal disease. The epidemiological distribution in terms of age does suggest a non-venereal form such as yaws, where initial infection most often occurs between the ages of 2 and 15 years (Mitjà et al. 2013). The climatic suitability of yaws to Northern Vietnam is discussed in detail in Vlok et al. (2020) (see Appendix 4). Relative risk ratio analysis identified a high morbidity of the disease in childhood. Furthermore, mortality analysis identified a low association of the disease to mortality. Low mortality and high childhood morbidity rates are both characteristic of yaws (Mitjà et al. 2013).

The social contexts of Man Bac fostered an environment that was advantageous to the spread of non-venereal treponemal disease in the community. Agricultural transitions such as that which occurred at Man Bac have been universally documented to have resulted in epidemiological transitions, as farming practices encouraged sedentism, population growth and increased susceptibility to infection due to nutritional stress (Armelagos and Cohen 1984; Cohen and Crane-Kramer 2007; Larsen 2006). Coastal habitations, such as prehistoric Man Bac, have been associated with higher yaws prevalence in historical contexts due to the abundance of water and vegetation increasing population density (Hackett 1953: 135; Kazadi et al. 2014). Furthermore, pre-industrialised agricultural

communities have also been associated with increased prevalence of yaws (Guimarães 1953; Hackett 1953: 135). The increase in fertility and population growth at Man Bac was likely associated with an increase in infants and children within the community, who are known to be the primary transmitters of yaws (McFadden et al. 2018; Mitjà et al. 2013).

7.6.11.2 Scurvy at Man Bac

Consideration of the reasons for the presence of scurvy at Man Bac is required given the high levels observed. Firstly, the excellent preservation of bone surfaces at Man Bac is of particular note as active SPNB can be lost through taphonomic factors (Roberts and Connell 2004). Given the number of diagnostic lesions for scurvy that occur on the neurocranium, mandible, maxillae and zygomatic bones, the excellent preservation of crania at Man Bac may have contributed to this high observable prevalence (Brickley and Ives 2010; Snoddy et al. 2018). It is also conceivable that the frequencies of possible cases of scurvy in nonadults present an overrepresentation of individuals with clinical scurvy, due to the confounding factor of growth. However, this does not explain the high prevalences of scurvy observed in adults. As previously mentioned, treponemal disease has been identified in the Man Bac assemblage and is a possible contributor to the SPNB recorded in the nonadult assemblage. In infants and children, infection with *Treponema pallidum* can result in SPNB deposits on the face and neurocranium (Lewis 2017). For example, bilateral SPNB formations on the anterior maxillae due to inflammation of the nasolabial lymph nodes in yaws (*Treponema pallidum pertenue)* could mimic haematoma formations on the anterior maxillae due to scurvy (Hackett 1946; Harper et al. 2011; Lewis 2017). However, in regards to probable cases, 84.1% (37/44) of Man Bac nonadults had more than 3 diagnostic lesions for scurvy, and 56.8% (25/44) also presented with radiographic signs of scurvy further strengthening the argument for high levels of scurvy in the nonadults at Man Bac.

Man Bac inhabitants had a broad based diet. As mentioned, it is currently not known to what degree rice or other indigenous plants supplemented the diet of the people at Man Bac, but the evidence for fruits and nuts of a wide variety found in Pre-Neolithic sites in Northern Vietnam may have been available during the Neolithic Period. However, following climate cooling after the terminus of the Holocene Thermal Maximum, approximately 6000 years ago, which would have significantly altered the ecology of the region, it is difficult to determine what indigenous plants were available 4-3500 years ago at Man Bac. The diverse

ecologies exploited by the Man Bac community for meat may have also provided a range of available fruits and nuts. Globally, dietary diversity decreased with the transition to agriculture, and a similar pattern is present at Man Bac in regards to faunal exploitation, where the diversity of taxa decreased during the early Neolithic transition in Northern Vietnam (Jones et al. 2019). It is possible, a similar reduction in dietary diversity of flora occurred with the introduction of rice and the cooling climate, and would explain the high levels of scurvy identified at Man Bac. Furthermore, tropical storms are frequent in Northern Vietnam so it is also possible that both wild and cultivated food sources were occasionally disrupted, potentially increasing the nutritional stress already experienced after the decrease in dietary diversity (Oxenham 2006).

Although at Man Bac there is a high reliance on marine species from freshwater and brackish environments with the exploitation of sea bream, sharks, rays, mullet, barramundi, groupers and flathead, all fish types provide inadequate levels of Vitamin C, with raw Mullet providing the highest amounts at only 1.2mg/100g of ascorbic acid. At minimum 6.5mg/day is required to prevent clinical scurvy in an adult male (Hodges et al. 1971; US Department of Agriculture 2019). Sea bream represented more than 50% of the fish assemblage at Man Bac, and no detectable levels of Vitamin C are identified in this fish (Toizumi et al. 2011). Similarly, the faunal assemblage which included pigs, deer, dogs, rats, otter, civets, buffalo, and rhino would not have yielded sufficient levels of Vitamin C (Sawada et al. 2011). Additionally, the cooking and processing of these foods would have further reduced the dietary available Vitamin C (Rumm-Kreuter and Demmel 1990). The interaction between local foragers and migrant farmers was also likely to have had an impact on nutritional stress as migrants adapted to establishing domesticated crops in new environments.

Lastly, adequate intake of Vitamin C is essential for immune function, and a high pathogen load where phagocytes are activated in the immune response, increases oxidative stress and results in an overall increased demand for Vitamin C in the body (Hemilä 2017; Khaw and Woodhouse 1995; Rokkas et al. 1995). Scurvy consequently causes an increased susceptibility to infectious diseases. Of the 14 individuals with skeletal signs of infectious disease, 79% (11/14) of individuals concurrently exhibited at minimum a possible case of scurvy, indicating a high association between scurvy and infectious disease at Man Bac. Indeed, in a subtropical climate a high pathogen load from many infectious diseases is expected. Hookworm, roundworm, *Shigella* sp., *Salmonella* sp., schistosomiasis, and

Escherichia coli are all possible causes for infectious diarrhoea which decreases absorption of vitamin C, particularly in a sedentary agricultural community such as Man Bac (King et al. 2017). Weanling diarrhoea, associated with the introduction of foods to supplement breast feeding may have also increased the dietary requirement for Vitamin C in infants. This synergy is likely driving the frequencies of scurvy identified in the Man Bac infants and has been argued to be a contributing factor in other tropical environments (Buckley 2000). To date, no isotopic research has identified terminal age of weaning at Man Bac, but passive immunity from the maternal intrauterine environment is known to be reduced by 3 months of age (Lewis 2017). Furthermore, the high levels of fertility at Man Bac indicates shorter birth intervals which may have been facilitated by the early introduction of weaning foods (Buikstra et al. 1986; McFadden and Oxenham 2018). It is possible the increased frequency of probable scurvy after 6 months of age is related to the decreased efficacy of passive immunity from the intrauterine environment combined with introduction of weaning foods, increasing susceptibility of pathogens and the requirements for Vitamin C deficiency in these infants. In sum, a combination of restricted dietary diversity due to environmental factors and adoption of agricultural subsistence, and high pathogen loads are likely underlying the outcome of high levels of nonadult scurvy at Man Bac.

The inhabitants of Man Bac appear to have had an aged based hierarchy which may have impacted the distribution of resources towards older individuals in the community (Oxenham et al. 2008). A decrease in the prevalence of scurvy with increasing age is apparent in the adults which may support evidence for distribution of available resources in the community detrimental to children and adolescents. Evidence of association with probable adult scurvy cases and frailty suggests that in severe cases of scurvy, this redistribution of resources may have influenced mortality of individuals in young adulthood.

7.6.11.3 Rickets at Man Bac

The causes for the skeletal manifestations of rickets are complex and result from an imbalance of calcium and phosphate regulation by Vitamin D and parathyroid hormones (Brickley and Ives 2010; Pettifor et al. 1981). Therefore, disturbances to any part of the mineralisation process can cause rickets. Given that the faunal assemblage at Man Bac includes a significant percentage of domestic pig and marine resources, which provide sufficient phosphorous, it is unlikely that phosphate deficiency is the underlying cause here

(Moe et al. 2011). Preliminary isotope research at Man Bac does not show any sex related differences in nitrogen and carbon values, suggesting mothers (and therefore their foetuses) likely had sufficient access to meat (Oxenham et al. 2011). Hypophosphatemic rickets is also most commonly caused by a genetic disorder, and hypophosphatemia from malnourishment is extremely rare (Lentz et al. 1978; Yamazaki et al. 2002). Finally, Vitamin D deficiency is strongly associated with high latitudes and reduced sun exposure which is unusual in subtropical regions unless social factors (such as clothing) inhibit sun exposure.

Rice is high in phytates and restricts calcium absorption in the gut while also having overall low calcium levels (Pettifor 2004). Rice *(Oryza sativa japonica)* is presumed to have approximately 32 mg/100g with levels less than 125mg/day resulting in skeletal deformities (Pettifor et al. 1981; US Department of Agriculture 2019). Therefore, calcium deficiency is probably the most likely cause for rickets in the infants and children of Man Bac due to the evidence of rice introduction. This is further supported by the presence of high levels of localised primary canine hypoplasia (LHPC) defects in Man Bac nonadults which have been partially attributed to calcium deficiency (McDonell and Oxenham 2014).

Calcium deficiency rickets has been documented in agriculturally dependent temperate and tropical regions globally today (Pettifor 2004). Dietary calcium deficiency does not cause osteomalacia in adults (which is absent in the adults of Man Bac), unlike in Vitamin D and phosphorous deficiency (Pettifor 2004). The presence of high levels of rickets at 6 months old and not younger, where likely breastfeeding provided a buffer against deficiency, also supports an argument for calcium deficiency as a primary cause of rickets at Man Bac (Butte et al. 2002). Lower calcium levels are required in the tropics due to increased absorption of Vitamin D from UV rays (Pettifor 2004), for this reason skeletal representation of calcium deficiency suggests severe restriction of dietary calcium at Man Bac. Additionally, dietary requirements for calcium increase in the first 6 months after birth, compared to foetal requirements (Almaghamsi et al. 2018). A pregnant woman's bones tend to be leached for calcium in periods of nutritional stress to compensate for the growing foetus, and research suggests dietary intake is independent of calcium secretion in breast milk, except in states of severe deficiency (Olausson et al. 2012). Given that 25% of neonates presented with probable active rickets suggests that in some Man Bac mothers, calcium deficiency was extreme. A continued decline of calcium deficiency with increasing age at Man Bac is not surprising due to the decline in calcium requirements of a growing child

(Prentice 1995). As also is the case with ascorbic acid, a relationship with infectious diarrhoea and calcium deficiency has been observed (Foldenauer et al. 1998). The combination of high levels of scurvy and rickets at Man Bac suggests a restricted diet likely related to subsistence transition contributing to scarce micronutrients in the diet. Therefore, life stage is a significant factor in rickets, with dietary requirements increasing in infancy at a time when breastfeeding was insufficient for providing the required quantity of calcium for normal skeletal development.

7.6.11.4 Anaemia at Man Bac

Given the high percentage of meat (protein content) in the diet, a direct dietary aetiology to the presence of anaemia at Man Bac is unlikely. Haem iron which is resistant to phytates is found in abundant quantities in meat and fish, suggesting anaemia at Man Bac is not likely a result of insufficient dietary iron levels except in cases of chronic malnutrition following food shortage (Marangoni et al. 2016). The aetiology of anaemia at Man Bac is likely to be multivariable. Calcium is an inhibitor to non-haeme iron absorption in the gut, whereas ascorbic acid plays an essential role in iron absorption, demonstrating a complex relationship of micronutrient deficiencies with anaemia (Bloem et al. 1989; Bouis and Welch 2010; Marangoni et al. 2016). Low grade inflammation in the gut can result in imbalances of microflora or from pathogen invasion, influencing absorption of iron through the basolateral membrane into the bloodstream (Tontisirin et al. 2002). As mentioned in Chapter 6, parasitism in the gut following raw fish consumption in coastal communities can also restrict iron absorption (Temple 2007). Scurvy is also inextricably linked to iron deficiency due to repeated internal haemorrhaging inducing an anaemic state (Cox et al. 1967). As mentioned above, B12 and Vitamin A deficiency are also strongly correlated with anaemia, and while B12 was likely sufficient due to the availability in meat, the fish exploited by Man Bac inhabitants were not rich in Vitamin A (McDonell and Oxenham 2014; Semba and Bloem 2002).

7.6.11.5 Thalassaemia at Man Bac

The identification of thalassaemia at Man Bac indicates in part a strong genetic influence in the presence of cribra orbitalia and porotic hyperostosis not related to dietary or infectious anaemia. Thalassaemia has previously been identified at the contemporaneous Neolithic site of Khok Phanom Di in Southern Thailand which supports the possibility of a

genetic basis for some anaemia in the region (Tayles 1996). Malaria has been strongly linked to a high prevalence of thalassaemia in Southeast Asia (Aydinok 2012; Weatherall 2008), and as posited by Tayles (1996) may suggest the presence of malaria in Mainland Southeast Asia during the Neolithic. With 8.6% (6/70) of the Man Bac assemblage exhibiting skeletal evidence for thalassaemia, an adaptive response to malaria increasing the prevalence of diagnosed cases, is a plausible cause. The presence of rodent facies in most of the diagnosed nonadults has been associated with beta thalassaemia major or intermedia, the homozygous forms with particularly high mortality rates (Adamopoulos and Petrocheilou in press; Bouguila et al. 2015). However, the presence of possible thalassaemia in one neonate suggests instead Bart hydrops fetalis syndrome, the homozygous alpha thalassaemia form, as beta chains do not form until well after birth (Galanello and Cao 2011; Thein and Menzel 2009). Alpha and beta thalassaemia, both exist in high abundance in Southeast Asia today and coinheritance has been frequently reported (Winichagoon et al. 1985). Therefore, alpha and beta thalassaemia co-occurrence cannot be ruled out. Co-occurrence is demonstrated to reduce rather than increase the severity of beta thalassemia major in the modern Thai populations, and may enhance the survivorship and therefore presence of individuals with homozygous beta thalassaemia in archaeological assemblages (Winichagoon et al. 1985).

A detailed review of the origins of thalassaemia at Man Bac is beyond the scope of this thesis. However, the relationship between the prevalence of thalassaemia in Southeast Asia and malarial endemicity is of interest in the consideration of the overall infectious disease epidemiology of Man Bac. Wet rice agriculture (irrigation) was only introduced during the Iron Age (2500-1500BP) in Southeast Asia (Castillo et al. 2018). This form of agriculture has been archaeologically linked to increased malarial vectors compared to dry rice agriculture in Mainland Southeast Asia (King et al. 2017). However, present day reports of differences in malarial vector prevalence in irrigated versus non-irrigated farming localities varies and depends on other ecological dynamics such as seasonality (Koudou et al. 2005). Additionally, in tropical forested areas of Mainland Southeast Asia, malarial vectors are common. Low land flood plains in Vietnam, such as where Man Bac is located have low reported malarial cases and vectors, as is the case with coastal and estuarine environments (Poolsuwan 1995). However, the diverse ecology of the region surrounding Man Bac included exposure to fringe forests, brackish water, and riverine areas that may have placed the inhabitants of Man Bac at risk of a number of different *Anopheles* mosquito species (Poolsuwan 1995). Possible interaction between other Phung Nguyen sites further

inland, where higher vector densities have been reported (Poolsuwan 1995), may have also contributed to the possible prevalence of malaria. Alternatively, gene flow of thalassaemia alleles from other inland Phung Nguyen sites may be responsible for the prevalence at Man Bac, and therefore the presence of thalassaemia at Man Bac does not necessarily indicate malaria was present.

7.6.11.7 Intrapopulation Variation of Disease at Man Bac

No differences between males and females were identified for any of the diagnosed diseases at Man Bac, indicating that differences in the exposure to infectious disease or nutritional stress may have been similar at Man Bac. The following section will explore the role of human population interaction in the changing epidemiology between the Pre-Neolithic to Neolithic Northern Vietnam.

7.7 Regional Level Results: Pre-Neolithic to Neolithic Period Northern Vietnam

7.7.1 Diachronic Assessment of Morbidity of Infectious Disease from Pre-Neolithic to Neolithic Vietnam

Changes in overall morbidity of infectious disease with increasing human population interaction levels were assessed separately for adults and nonadults. There were no statistically significant differences between infectious disease prevalences of nonadults from Con Co Ngua compared to Man Bac (n=98, RR=2.1477, p=0.1974; Table 7.47). However, Man Bac adults were almost 3 times more likely to have infectious disease than Con Co Ngua adults which was statistically significant (n=141, RR=2.7586, p=0.0046).

Table 7.47: *Relative risk of infectious disease morbidity from the pre-Neolithic to Neolithic Vietnam.*

EXPOSED GROUP/ CONTROL GROUP	**OUTCOME**		**RR**	**P-VALUE**	**95%CI**
	Positive: *Infectious Disease Present*	***Negative:*** *Infectious Disease Absent*			
Nonadults					
Man Bac/Con Co Ngua	7/4	37/50	2.1477	0.1974	0.6718- 6.8663
Adults					
Man Bac/Con Co Ngua	10/14	19/98	**2.7586**	**0.0046***	1.3681- 5.5623

A relative risk (RR) >1 denotes a relationship of the exposed group with an increase in disease prevalence, whereas RR <1 denotes a relationship of the control group with an increase in disease prevalence.
*= statistically significant (p<0.10). **= statistically significant when considering size of the effect of RR.

7.7.2 Diachronic Assessment of Morbidity of Nutritional Disease from Pre-Neolithic to Neolithic Vietnam

Overall morbidity of scurvy was significantly higher at Man Bac compared to Con Co Ngua for both adults and nonadults (Table 7.48). This statistical significance occurred when considering combined possible and probable cases as well as probable cases only. As no cases of adult probable scurvy were identified at Con Co Ngua, Man Bac adults were over 86 times more likely to have scurvy than adults at Con Co Ngua (n=141, RR=86.6333, p=0.0018). Furthermore, rickets was only identified at Man Bac. Overall, a considerable increase in specific micronutrient deficiency with the transition to the Neolithic Period in Northern Vietnam is apparent.

Table 7.48: *Relative risk of scurvy morbidity from the pre-Neolithic to Neolithic Vietnam.*

EXPOSED GROUP/ CONTROL GROUP	**OUTCOME**		**RR**	**P-VALUE**	**95%CI**
	Positive: *Disease Present*	***Negative:*** *Disease Absent*			
Possible and Probable Scurvy (combined)					
Nonadults					
Man Bac/Con Co Ngua	42/10	2/44	**5.1545**	**<0.0001***	2.9350- 9.052
Adults					
Man Bac/Con Co Ngua	15/1	14/111	**57.9310**	**0.0001***	7.9773- 42.6968

Probable Only Scurvy					
Nonadults					
Man Bac/Con Co Ngua	35/2	9/52	**21.4773**	**<0.0001**	5.4671- 84.3729
Adults					
Man Bac/Con Co Ngua	11/0	18/112	**86.6333**	**0.0018***	5.2539- 1428.5255

A relative risk (RR) >1 denotes a relationship of the exposed group with an increase in disease prevalence, whereas RR <1 denotes a relationship of the control group with an increase in disease prevalence.
*= statistically significant (p<0.10). **= statistically significant when considering size of the effect of RR.

7.7.3 Diachronic Assessment of Morbidity of Anaemia from Pre-Neolithic to Neolithic Vietnam

As was the case for scurvy, a statistically significant increase in the prevalence of anaemia was evident for Man Bac when compared to Con Co Ngua (Table 7.49). However, the size of the effects are considerably lower than was the case for scurvy. Man Bac adults were only 2 times more likely to have anaemia than Con Co Ngua adults (n=138, RR=1.9349, p=0.0003), and Man Bac nonadults were 3 times more likely to have skeletal evidence for anaemia (n=79, RR=3.0171, p=0.0219).

Table 7.49: *Relative risk of anaemia morbidity from the pre-Neolithic to Neolithic Vietnam.*

EXPOSED GROUP/ CONTROL GROUP	**OUTCOME**		**RR**	**P-VALUE**	**95%CI**
	Positive: *Anaemia Present*	***Negative:*** *Anaemia Absent*			
Nonadults					
Man Bac/Con Co Ngua	12/5	23/39	**3.0171**	**0.0219***	1.1737- 7.7558
Adults					
Man Bac/Con Co Ngua	18/39	8/70	**1.9349**	**0.0003***	1.3512- 7.7558

A relative risk (RR) >1 denotes a relationship of the exposed group with an increase in disease prevalence, whereas RR <1 denotes a relationship of the control group with an increase in disease prevalence.
*= statistically significant (p<0.10). **= statistically significant when considering size of the effect of RR.

7.7.4 Diachronic Assessment of Overall Mortality from Pre-Neolithic to Neolithic Vietnam

Changes in mortality rates between the Pre-Neolithic and Neolithic Vietnam were assessed for adults only, as comparisons between age-at-death distributions of nonadults are likely to reflect fertility rather than mortality. While there were significant increases to the morbidity of infectious and nutritional diseases at Man Bac compared to Con Co Ngua, there was no statistically significant differences between the overall mortality rates of Man Bac

adults when compared to Con Co Ngua adults (Table 7.50-5.52; Figure 7.54-7.55). The Cox regression cumulative survival function (Figure 7. 55) indicates a near identical trend in mortality in the Man Bac adults compared to the Con Co Ngua adults

Table 7.50: *Relative risk of overall mortality from the pre-Neolithic to Neolithic Vietnam across age cohorts.*

POSITIVE OUTCOME/ NEGATIVE OUTCOME	**TREATMENT**		**RR**	**P-VALUE**	**95%CI**
	Exposed Group: *Man Bac*	***Control Group:*** *Con Co Ngua*			
<20 yrs/ >20 yrs	3/26	17/84	0.6146	0.4091	0.1935- 1.9524
<30 yrs/ >30 yrs	12/17	47/54	0.8892	0.6323	0.5497- 1.4385
<40 yrs/>40 yrs	18/11	69/32	0.9085	0.5494	0.6637- 1.2437

A relative risk (RR) >1 denotes a relationship of the disease presence with the positive outcome (susceptibility to mortality), whereas RR <1 denotes a relationship of the disease absence with a negative outcome (survivorship).
*= statistically significant (p<0.10). **= statistically significant when considering size of the effect of RR.

Table 7.51: *Statistical summary for Kaplan-Meier function of overall mortality of adults from the pre-Neolithic to Neolithic Vietnam.*

OVERALL MORTALITY	**ESTIMATE**	**STD. ERROR**	**95% CI**	**LOG RANK (MANTEL-COX)**		
				CHI SQUARE	**DF**	**P-VALUE**
Mean				0.160	1	0.689
Con Co Ngua	32.624	1.195	30.281- 34.967			
Man Bac	33.690	2.135	29.506- 37.874			
Overall	32.862	1.040	30.822- 34.901			
Median						
Con Co Ngua	35.000	1.798	31.475- 38.525			
Man Bac	35.000	3.484	28.171- 41.829			
Overall	35.000	1.850	31.374- 38.626			

*= statistical significance (p<0.15).

Table 7.52: *Statistical summary for Cox regression function of overall mortality of adults from the pre-Neolithic to Neolithic Vietnam.*

OVERALL MORTALITY	**COEFFICIENT (β)**	**STD. ERROR**	**WALD**	**DF**	**P-VALUE**	**ODDS RATIO (Exp(β))**
	-0.066	0.212	0.098	1	0.754	0.936

*= statistical significance (p<0.15).

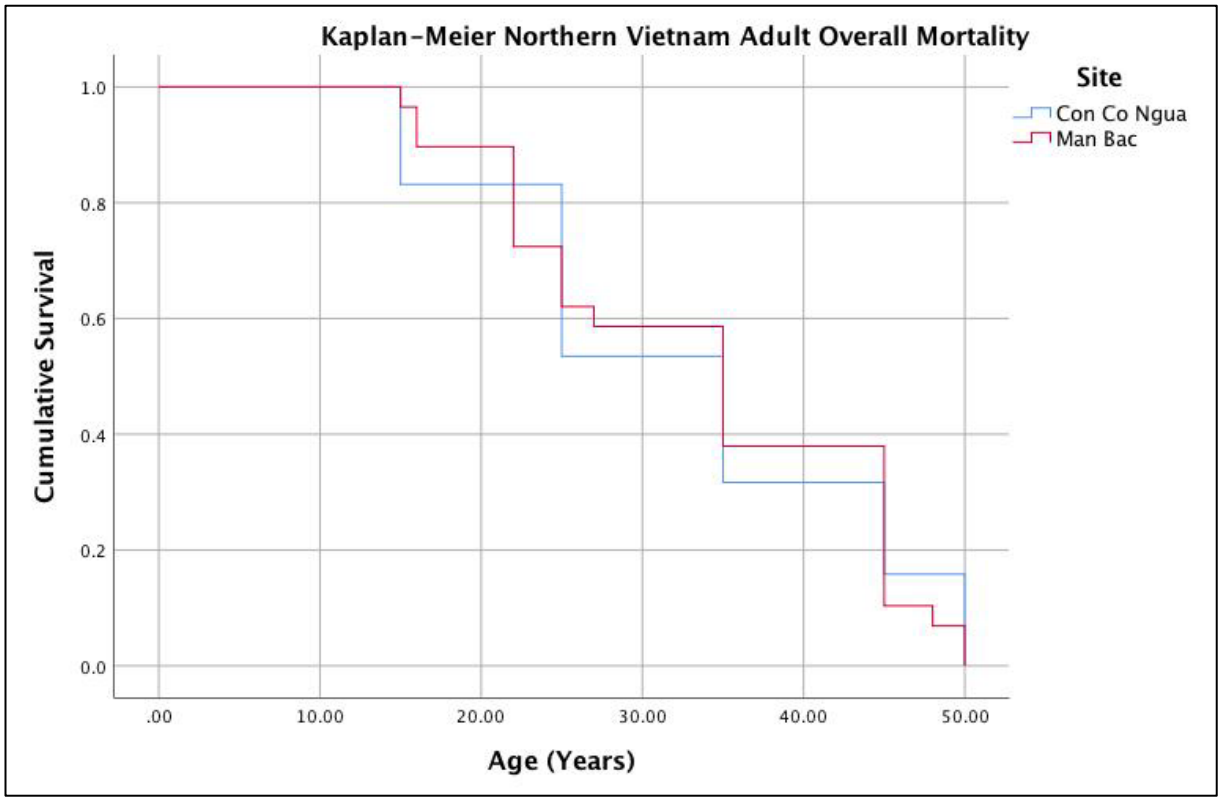

Figure 7.54: *Kaplan-Meier cumulative survival function of adult overall mortality from the pre-Neolithic to Neolithic Vietnam. Image: author's own*

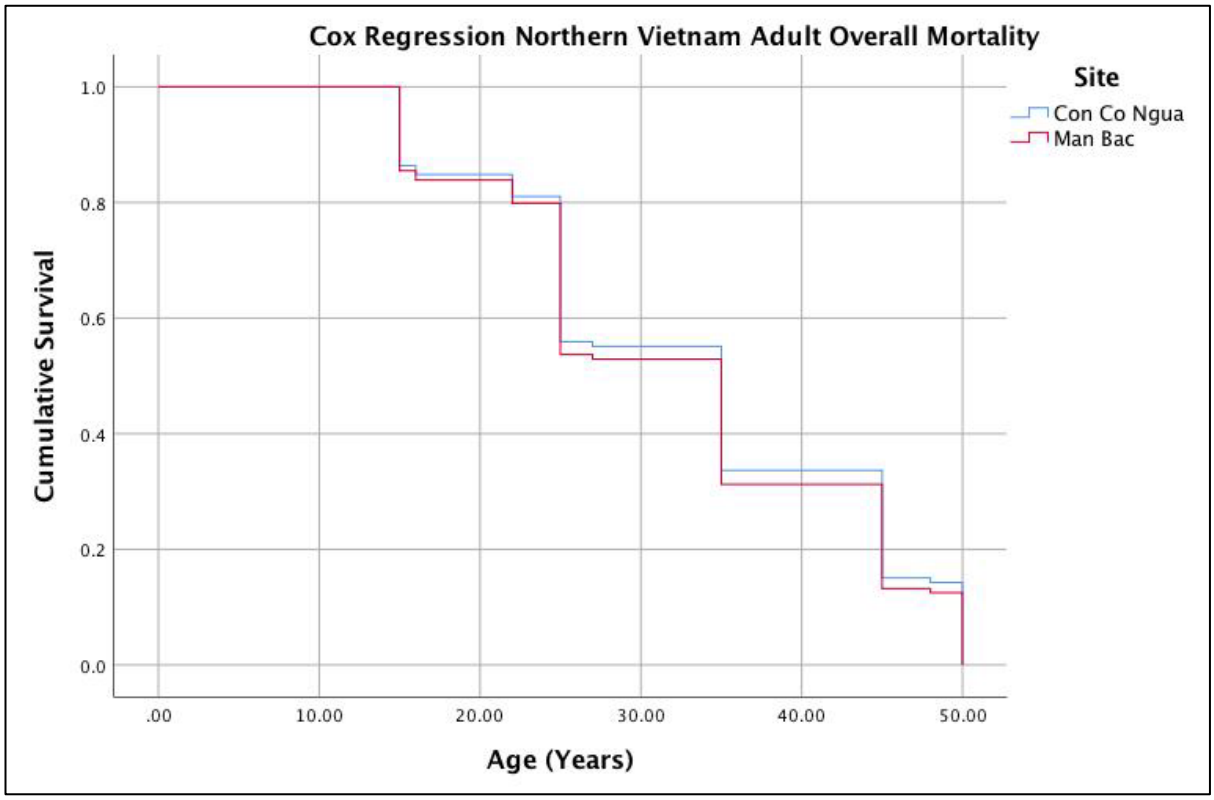

Figure 7.55: *Cox regression cumulative survival function of adult overall mortality from the pre-Neolithic to Neolithic Vietnam. Image: author's own*

7.8 Discussion: Diachronic Changes in Disease from Pre-Neolithic to Neolithic Vietnam

Significant increases in the morbidity of infectious diseases, nutritional diseases and anaemia were apparent with the transition from the Pre-Neolithic to the Neolithic in Northern Vietnam. However, the increase in morbidity of disease across the two sites was not accompanied with an increase in overall mortality. That is, evidence of epidemiological change across time periods is apparent, but this may not have affected the overall mortality burden. This outcome suggests that while changes in the morbidity of nutritional and infectious diseases are apparent, other factors influencing overall disease burden negated the differentiating factors in infectious and nutritional disease mortality between the two time periods.

7.8.1 Changes in Infectious Disease with Increasing Population Interaction in Northern Vietnam

There was no increase between the number of infectious disease types identified at Con Co Ngua and Man Bac, and therefore there was no recognised increase in the diversity of infectious diseases, with increasing human population interaction levels in prehistoric Northern Vietnam. Con Co Ngua exhibited cases of osteomyelitis (non-specific infection) and hydatids disease, whereas Man Bac exhibited cases of mastoiditis (non-specific infection) and treponemal disease. However, hydatids disease is an infectious disease associated with animal interactions, and in the case of Con Co Ngua, where no evidence of domesticated species exist, was more likely a product of environmental interfaces between humans, ungulates and carnivores. In contrast, treponemal disease is an infectious disease transmitted predominantly between humans, and therefore may be related to the increase in population interaction in the Neolithic.

It is not possible at this point to determine confidently whether treponemal disease was introduced by the migrant farmers from Southern China. However, spread of treponemal disease into Mainland Southeast Asia (MSEA) with migrant farmers during the Neolithic is plausible when considering the extent of the migration and the sedentary agricultural contexts they brought with them (Bellwood and Oxenham 2008). There is no archaeological evidence for contact with other groups apart from Southern Chinese farmers outside of MSEA at this time. Admixture with indigenous foragers in Northern Vietnam

(further expansion across the friction frontier) may have enabled further transmission of treponemal disease throughout MSEA, although currently no further evidence for prehistoric treponemal disease exists in Southeast Asian skeletal collections. While it is recognised that absence of evidence is not evidence of absence, and a deep antiquity of treponemal disease in MSEA is possible prior to the agricultural transition, there is no identification of human to human transmissive diseases (such as tuberculosis, treponematosis, or leprosy) prior to this time in MSEA despite intensive bioarchaeological research in the region (Buckley and Oxenham 2016). Although Man Bac is positioned at the present day upper geographical limit of the survival of yaws, documented cases of yaws existed in southern China and Taiwan prior to worldwide eradication attempts (Hill 1953). In light of pre-eradication clinical evidence of yaws in this region, a possible origin for the spread of treponemal disease into Mainland Southeast Asia from farmers originating in Southern China from approximately 4000 years ago is plausible. Given the presence of treponemal disease at Man Bac, regional interactions throughout the Red River delta also presents possible routes of transmission to and from other Phung Nguyen sites where archaeological material indicates contact with agricultural groups of Southern China (Khoach 1980; Nguyen 2008). Further investigation of existing and newly excavated skeletal assemblages in Southern China and MSEA may provide further insight into the origins and antiquity of this disease within the region.

7.8.2 Changes in Specific Nutritional Disease with Increasing Population Interaction in Northern Vietnam

A clear increase in the prevalence of specific nutritional disease (Vitamin C and calcium deficiency) is apparent with the Neolithic transition in Northern Vietnam. As mentioned, the high prevalence of nutritional disease at Man Bac was likely a combination of the introduction of rice agriculture, possible decrease in the diversity of indigenous food sources due to climate cooling, and a high pathogen load. In contrast, the Pre-Neolithic inhabitants of Con Co Ngua exploited a diverse range of resources available due to advantageous climatic conditions during the Holocene Thermal Maximum. It is possible the initial adoption of agriculture in Mainland Southeast Asia was stimulated by the changing climate and diminishing indigenous resources (Oxenham et al. 2018). Domesticated animals and rice crops likely provided supplementation for foraging during the early Neolithic, which supports this argument (Yoneda 2008). The increase in nutritional deficiencies from

the Pre-Neolithic to the Neolithic are then distinctly tied to the shift to agriculture. However, as the adoption of agriculture in MSEA was enabled through the interactions between indigenous foragers and migrant farms from Southern China, the process of human population interaction was integral to this shift and therefore influenced the prevalence of nutritional disease over time, albeit indirectly.

7.8.3 Changes in Anaemia with Increasing Population Interaction in Northern Vietnam

An increase in anaemia morbidity is apparent from the Pre-Neolithic to the Neolithic in Northern Vietnam. As anaemia is relatively non-specific and multifactorial, the relationship with human population interaction is difficult to determine between these two sites. Con Co Ngua and Man Bac likely shared similar exposure to marine parasites due to the exploitation of aquatic environments, and possible iron deficiency anaemia through parasitism is likely. Similarly, at both sites a dietary iron deficiency is not likely a major cause except in cases of malnutrition. Interestingly, skeletal signs of anaemia at Con Co Ngua is associated with adult survivorship, whereas at Man Bac these pathologies are associated with frailty. This outcome potentially suggests an increased negative impact, of the aetiologies that lead to anaemia, on health over time.

7.8.4 Changes in Thalassaemia Inheritance with Increasing Population Interaction in Northern Vietnam

While there remains tentative evidence for thalassaemia at Con Co Ngua, considerable evidence for thalassaemia at Man Bac has been identified. Questions in regards to the antiquity of thalassaemia in Mainland Southeast Asia and the likely relationship to malarial endemicity remain. These questions are of concern in regards to human population interaction, the potential transmission of malaria between populations in the region as well as gene flow of the genetic anaemia. It is interesting to note here that the one adult with probable thalassaemia from Man Bac has dental and skeletal affinity to Australo-Papuan populations such as those from Con Co Ngua (and all Pre-Neolithic foraging groups from Vietnam), and inhabitants from the Neolithic Southern Thailand site of Khok Phanom Di represent mixed dental affinities (Matsumura and Oxenham 2014). Deep antiquity of thalassaemia in the region prior to the Neolithic remains a possibility. However, the complexity of gene flow and stabilising selection in the region exceeds the limitations of

morphometric data. Nevertheless, the population interactions between indigenous and migrant groups during the Neolithic are crucial to understanding the dynamics of thalassaemia inheritance and malaria in Mainland Southeast Asia and present an area for further research.

7.9 Chapter Summary

This chapter explored site and regional level differences in infectious and nutritional diseases across the Pre-Neolithic to the Neolithic of Northern Vietnam. Overall a significant change in disease morbidity was identified with increasing levels of human population interaction. The sites of Con Co Ngua, a Pre-Neolithic foraging site with low levels of human interaction was compared to Man Bac, a Neolithic site with direct evidence of population interaction between indigenous foragers and migrant farmers from Southern China. Hydatids disease, a zoonotic disease was identified at Con Co Ngua whereas treponemal disease, a human transmissive disease, was identified at Man Bac. These diseases appeared to have low association with mortality. Furthermore, a very low prevalence of scurvy was identified at Con Co Ngua whereas at Man Bac a high prevalence of scurvy and calcium deficiency rickets was identified. These diseases were demonstrated to have a high relationship with frailty. A significant increase in the prevalences of infectious and nutritional diseases is apparent with the introduction of agriculture alongside large scale migration of migrant farmers from Southern China approximately 4000 years ago. The population interaction between indigenous foragers and migrant farmers initiated a host of changes including subsistence change, resulting in a decrease in dietary diversity, and the possible introduction of human to human transmissive disease into Mainland Southeast Asia. However, the increase in human population interaction did not increase the mortality rate of populations in Northern Vietnam over time.

CHAPTER 8:
BORDERS, FRONTIERS AND SILK ROADS: DISEASE AND THE INTENSIFICATION OF POPULATION INTERACTION FROM THE BRONZE AGE TO XIONGNU PERIOD IN MONGOLIA

8.1 Introduction

The final of the three case studies in this thesis is presented in this chapter: increasing interpopulation interaction from the Bronze Age to the Xiongnu Period in Mongolia. This chapter assesses how an increase in external migration, conflict and trade impacted the health of prehistoric pastoral nomads. A format similar to the previous case study chapters will be followed here, and the results outlined in this chapter meet objectives 3-5 of the thesis. Firstly, a background on the emergence of pastoralism in the Bronze Age and the eventual rise of the nomadic Xiongnu Empire is presented. Secondly, the background to the Bronze Age is presented followed by differential diagnosis, morbidity and mortality analysis of Bronze Age disease. A similar format is then presented for the Xiongnu Period. Lastly, it is explored whether an increase in interpopulation interaction from the Bronze Age to Xiongnu Period was accompanied with increasing levels of mortality and morbidity of infectious and nutritional diseases.

8.2 The Emergence of a Pastoralist Economy and Empire in Prehistoric Mongolia

8.2.1 Pastoralism during the Bronze Age of Mongolia

Following a period of climate cooling and increased aridity, populations on the Eurasian steppe abandoned sedentary agriculture and eventually developed a specialised mobile pastoralist subsistence (Allard and Erdenebaatar 2005; Kuzmina 1998). By 5000 years ago, during the Bronze Age, mobile pastoralism emerged as the primary life way of Mongolian populations (Honeychurch 2015; Wilkin et al. 2020b). A range of livestock including camel, yak, goat, sheep and eventually horse, became important in subsistence and travel (Taylor et al. 2020). The emergence of horse dairying on the Eastern Eurasian Steppe coincided with the first evidence for horseback riding approximately 3200 years ago, that inevitably changed pastoral lifeways (Wilkin et al. 2020b). The practice of pastoralism

itself likely arrived in Mongolia from Western Steppe cultures such as the Afanasievo, through the Altai Mountains (Janz et al. 2017; Wilkin et al. 2020b).

While dairying and pastoralism may have originated from steppe cultures, the genetics of the Bronze Age pastoralists from Mongolia more resemble hunter-gatherers who inhabited Mongolia prior to the adoption of agriculture (Jeong et al. 2020). This genetic profile persisted throughout the Bronze and Iron Ages of Mongolia. However, there is also genetic evidence to indicate some admixture of Western Mongolian people with European Cordwear associated populations of the Western Steppe, while there remained an absence of genetic admixture in Eastern Mongolian populations. It then appears, that Western Steppe peoples who introduced pastoralism to Mongolia, left very little genetic foot print but exacted significant influence on subsistence and modes of life of Bronze Age people in Mongolia (Jeong et al. 2018).

Mobile pastoralism of the Bronze Age relied on dynamic and fluctuating networks of interaction, dubbed *nodes of interaction* by Frachetti (2009). The combination of low population density, and diverse ecology lead to disproportionally more animals to humans, likely assisting the establishments of these regional networks of connection (Spengler et al. 2013). The development of these nodes fluctuated seasonally as groups migrated throughout the landscape to viable pastures (Frachetti et al. 2012). Within these nodes of interaction, the population density would have temporarily increased (Spengler et al. 2013), possibly enabling the spread of infectious diseases throughout pastoral groups.

8.2.2 The Rise of the Xiongnu Empire

By 2200BP, these pastoralists developed a multilingual and multiethnic empire that eventually controlled an area over approximately 4 million square kilometres (Rogers 2017). This region covered areas of Central Asia to Siberia (Kim et al. 2010). Dubbed the *Xiongnu* by their Han counterparts in China, this empire was defined by the emergence of hierarchical polities, a complex internal social organisation, and established economic systems and trade within and outside of the empire (Rogers 2017). Urban settlements also emerged in contrast to the mobile villages of the Bronze Age, but these remained peripheral, as the empire continued to be focused on mobile pastoralism (Rogers 2017).

Gene flow increased considerably with the Xiongnu Period (Late Iron Age) compared to the Bronze Age, which stands testament to significant increase in migration to Mongolia during the Xiongnu Period (Jeong et al. 2020). Xiongnu populations also included genetic admixture with prehistoric Iranian, Samartian and East Asian populations outside of Mongolia. The Xiongnu also appear to represent admixture between the Western and Eastern Bronze Age populations (Jeong et al. 2020). Additionally, historical records indicate significant trade of resources between Han China and the Xiongnu Empire (Eng and Quanchao 2013). The expansion of the Xiongnu Empire also increased contact with groups not previously encountered during the Bronze Age (Eng 2016). Increase in migration and trade also ushered in the introduction of millet into Xiongnu subsistence. Ventresca Miller and Makarewicz (2019) demonstrated an increase in C4 plants in the subsistence of Xiongnu Period individuals through carbon and nitrogen isotope analysis. The authors argue that the introduction of millet accompanied intensified involvement in political exchange networks.

Conflict between Xiongnu and other polities, particularly Han China was essential to the rapid expansion of the Xiongnu Empire. The Xiongnu-Han Wars culminated following persistent raids of the Xiongnu warriors across the Chinese frontier resulting in declaration of war by the Han multiple times over the Xiongnu Period (Kradin 2011; Psarras 2003). This conflict only further led to the establishment of trade and exchange, albeit unequally between the Han and the Xiongnu, in order to establish political stability and reduce the raiding of Han territory. The warring was so significant that the Han Chinese established the construction of a defensive wall which eventually emerged as the Great Wall of China (Kradin 2011). Overall, the Xiongnu Empire relied on political interactions which involved migrations to the centre of the empire within Mongolia, and political control of trade maintained through raiding and warring with outer territories.

8.2.3 Pastoral Interactions and the Spread of Infectious Diseases

High mobility of mobile pastoralists in the Western Steppe has been argued to have spread the plague during the Bronze Age. DNA of *Yersinia pestis*, the pathogen responsible for the bubonic plague, was identified in individuals who belonged to the Afanasievo culture (4909-4677BP) and the Andronovo culture (3746-3626BP) of Altai Siberia (Rasmussen et al. 2015). The presence of *Mycobacterium bovis* has also been identified through pathogen DNA analysis in Iron Age Siberian Altai (2300-1700BP) (Murphy et al. 2009). The

identification of these infectious diseases in mobile pastoralists demonstrate population movements due to pastoralism may have played a significant role in the spread of infectious diseases across Eurasia. These populations had direct contact with Mongolian populations which then prompts investigation for the presence of infectious diseases in Mongolian nomads. This case study then investigates whether intensification of migration and trade increased the prevalence and diversity of infectious diseases from the Bronze Age to the Xiongnu Period. Increase in conflict and the introduction of millet may also have increased micronutrient deficiency in the Mongolian population following the development of the Xiongnu Empire. Therefore, this chapter also explores the role of increased human population interaction on nutritional stability from the Bronze Age to Xiongnu Period in Mongolia.

8.3 Mongolian Bronze Age Assemblage

The Bronze Age assemblage is comprised of burials from throughout Mongolia. These date from the Early to Final Bronze Age (5000-2300BP). During this period, Mongolia was occupied by specialist nomadic pastoralists who maintained regional interactions likely through the development of shared ritual and fluctuating social stratification in a trans-egalitarian society (Wright 2012). As such, these pastoralists, particularly populations of Western Mongolia, emerged as monument builders who constructed large stone mound structures (Khirigsuurs) often associated with burials of animal remains, especially horse heads and sometimes containing human burials as its centre piece (Allard and Erdenebaatar 2005; Houle 2016; Wright 2012). Erect stone structures known as *deer stones*, were often associated with these Khirigsuurs, named as such for their elaborate stone iconographies that often depicted stylised deer, but contained a range of symbols including other animals or weaponry of significant importance to these nomads (Houle 2016). These monuments stand testament to temporary aggregations of an overall low density population. The presence of these monuments, wanes further east, and deer stones and Khirigsuurs are not found past Central Mongolia. Instead, pastoralists in Eastern Mongolia appeared to have buried their dead in stone slabs, a ritual that continued through to the Early Iron Age (Allard and Erdenebaatar 2005; Houle 2016). The pastoralists of Bronze Age Mongolia inhabited variable ecologies in Mongolia, extending from the forest steppes and mountainous regions to the North and West, and the arid climate of the Gobi Desert to the south. Regionalised adaptive strategies were employed that involved

husbandry practices of the specific animal species suited to each biosphere (Machicek and Beach 2013; Taylor et al. 2020).

Seven different cultures were included within the overall assemblage used in this thesis, representing the heterogeneity of cultures that emerged across space and time in Bronze Age Mongolia. Due to the low population density and low number of burials at any given Bronze Age site, an aggregated assemblage was necessary for analysis of this region. Similar ecological and subsistence factors allow for aggregation of these different cultures. Nevertheless, potential differences between these cultures are assessed in the results below to determine the suitability of an aggregated sample. Potential variations between the Eastern and Western Mongolian cultures are also statistically assessed.

The cultures included in the assemblage are:

Chemurchek culture: An Early Bronze Age culture dated to approximately 5000-3700 cal BP by radiocarbon dating of bone, wood and charcoal (Kovalev and Erdenebaatar 2009; Taylor et al. 2019). This cultural group presents the earliest evidence for nomadic pastoralism in the Eastern Eurasian steppe region. Burials are found in barrows and in rectangular stone graves, inside larger stone crypts orientated east to west and sometimes associated with anthropomorphic standing stone figures (Kovalev and Erdenebaatar 2009; Taylor et al. 2019). Artefacts associated with the burial complexes include bronze awls, bone daggers and arrowheads, stone tools and stone and ceramic vessels (Kovalev and Erdenebaatar 2009). Burial complexes of this culture are found in Mongolia, Russia and China, and indicate cultural interactions on both sides of the Altai mountains (Kovalev and Erdenebaatar 2009). Morphology of crania from the Mongolian Chemurchek sites indicate European origin, and it is suggested the Chemurchek people co-existed with the Afanasievo culture of Siberian Altai, although this has remained controversial (Kovalev and Erdenebaatar 2009). Complete genomic analysis of the Chemurchek has indicated genetic affinity to Afanasievo as well as Central Asian populations (Kazakhstan) (Jeong et al. 2020). The Chemurchek consumed milk from sheep and goat (Wilkin et al. 2020b).

Ulaanzuukh culture: A Middle Bronze Age culture dated to approximately 3500-3300 cal BP by radiocarbon dating of the burials (Taylor et al. 2019). Individuals were placed in rectangular stone graves in rows or groups, and buried in prone extended position

with artefacts including bone beads and pottery (Dashtseveg et al. 2013). The Ulaanzuukh were involved in dairying of ruminants including goat and sheep (Wilkin et al. 2020b).

*Munkhkhairkhan (*Mönkhkhairkhan) culture: A Middle Bronze Age culture dating to approximately 3800-2600 cal BP by radiocarbon dating (Dashtseveg et al. 2013; Kovalev and Erdenebaatar 2009). Individuals were buried in barrows. A report on a single burial indicates a flexed position. Artefacts include bronze ornaments and blades, and stone and shell beads (Kovalev and Erdenebaatar 2009). Genomic analysis indicates these individuals have some genetic affinity to Western Steppe populations (Jeong et al. 2020). There is currently no information on dairying for this culture.

Deer Stone- Khirigsuur Complex (DSKC): A Late Bronze Age culture of Western Mongolia dated between approximately 3400-2700 cal BP by radiocarbon dating of human and faunal bone samples (Honeychurch 2015). The sites are comprised of large stone mound monuments known as Khirigsuurs or Kurgans, with stone enclosures. These can be isolated, or a complex of Khirigsuurs may be found across the landscape. These mounds may have hearth or burial features that involve the burial of animal remains such as horse heads or human skeletal remains (Honeychurch 2015). Deer stones associated with the DSKC culture, have been found in Western and Central Mongolia, Siberia, and Central China indicating a vast geographic network of cultural interactions (Honeychurch 2015). There is some genetic affinity with Western Steppe populations indicating admixture with populations who likely introduced pastoralism to Mongolia (Jeong et al. 2020). Sheep and goat dairying was identified in DSKC (Wilkin et al. 2020b).

Mungun Taiga culture: A Late Bronze Age culture, where individuals are buried in Kurgan mounds similar to the Khirigsuurs of Western Mongolia (Honeychurch 2015). It is possible that these mounds are of the same cultural group as the DSKC culture, but represent different social status (Tsybiktarov 2002).

Slab Grave and *Shorgooljin Grave* (figured grave) culture: A Late to Final Bronze Age culture of Eastern and Southern Mongolia dating to 3600-2300BP (Dashtseveg et al. 2013). The figured graves, stone graves of an hourglass figure possibly represent an earlier part of the culture, and may be related to the earlier Ulaanzuukh culture, but these grave types remain poorly understood, as few have been excavated (Honeychurch 2015). Similar

genetic profiles between the Ulaanzuukh and Slab Grave peoples support the argument for ties between the two cultures (Jeong et al. 2020). Later slab grave burials, possibly originating from around 2100BP, and extending into the Early Iron Age, were rectangular shaped burials constructed through the use of large stone slabs (Honeychurch 2015). Unlike the Khirigsuurs, there were a higher number of burials within the complexes. Ceramics, bone beads, domesticated animal remains, horse harnesses, stone tools and bronze ornaments are associated with the graves (Honeychurch 2015). Individuals from the Slab Grave culture present the earliest evidence of horse dairying on the Eastern Eurasian steppe dating to 3200cal BP (Wilkin et al. 2020b). Sheep, goat and cow dairying was also identified in the Slab Grave culture (Wilkin et al. 2020b).

Baitag culture: A Late Bronze Age culture of Western Mongolia radiocarbon dated to around 3100-2940 cal BP (Taylor et al. 2019). Little is understood about this culture, but individuals are buried supine with knees up within a circular hollow (Taylor et al. 2019). Genomic analysis indicates these individuals have some genetic admixture with Western Steppe populations (Jeong et al. 2020). Sheep, goat, cow and horse dairying was identified in the Baitag (Wilkin et al. 2020b).

While there was a representation of all nonadult age cohorts in the Bronze Age sample and they were in excellent condition of preservation, the overall proportion of nonadults in the assemblage was low, a phenomenon also observed by Littleton et al. (2012) for DSKC burials. Therefore, a low fertility rate may have been apparent (D0-14/D=0.30) (after McFadden and Oxenham 2018a). A natural population decrease was also observed (RNPI=-0.30) (after McFadden and Oxenham 2018b). It is possible that nonadults were buried elsewhere affecting the measurement of fertility. However, no such nonadult burial ground has been found in Mongolia, and this result is consistent with the low population density observed for these populations.

A previous bioarchaeological study of 25 individuals from Khovsgol Aimag in Western Mongolia identified no evidence of scurvy nor rickets, and only 12% of individuals had osteoblastic lesions (Karstens et al. 2018). One individual was diagnosed with non-specific infection. It is noted here that the pathology recorded by Karstens et al. (2018) is consistent with bone destruction from other diseases including brucellosis or tuberculosis, but a complete differential diagnosis was not the objective of the paper. Karstens et al.

(2018) also recorded carious lesions in one individual, with 50% of the sample exhibiting dental calculus. One study has reported "Vitamin C deficiency" in two Bronze Age individuals from Central Mongolia, but provided no further details (Grupe et al. 2019). Antemortem tooth loss (AMTL) was common in the Bronze Age, with over 39% of the sample exhibiting loss of teeth prior to death (Erdene 2014). Similarly Erdene (2014) found no dental caries in the aggregated Bronze Age assemblage used in this thesis. Periapical lesions were present in over 50% of individuals, that was more common in males compared to females. Similarly, AMTL also presented in more than half of the overall assemblage, again a predominance in males was noted, likely related to the development of periapical lesions. Furthermore, there was considerable increase in the AMTL of Western Mongolian populations compared to Eastern populations. The following section will present the results for differential diagnosis and analysis of morbidity and mortality of disease in the Bronze Age assemblage.

8.4 Results: Bronze Age Skeletal Pathology

8.4.1 Summary of Pathological Lesions in the Bronze Age Assemblage

Of the 92 individuals included in the palaeopathological assessment, 26.1% (24/92) presented with osteoblastic lesions. Over half (55.6%, 10/18) of the nonadult assemblage displayed osteoblastic lesions, whereas the prevalence in adults was lower (18.9%, 14/74; Table 8.1). Lesions were predominantly bilateral discrete SPNB deposits of the cranium, and unilateral or bilateral discrete deposits of SPNB on the lower limbs, particularly the tibia (Figure 8.1). Only one adult (AT-233, a young adult male) exhibited diffuse SPNB across multiple elements including the left tibia, left femur and left os coxa (Figure 8.2).

Table 8.1: *Summary of OB and OL lesion prevalences, and skeletal deformities in the Bronze Age*

	NONADULT (aff/obs)	**NONADULT (%)**	**ADULT (aff/obs)**	**ADULT (%)**	**TOTAL (aff/obs)**	**TOTAL (%)**
OB Lesion	10/18	55.6	14/74	18.9	24/92	26.1
OL Lesion	0/18	0	3/74	4.1	3/92	3.3
Cupping	0/18	0	0/74	0	0/92	0
Flaring	0/18	0	0/74	0	0/92	0
Fraying	2/18	11.1	0/74	0	2/92	2.2
Bending of Long Bone Shafts	5/18	27.8	13/74	17.6	18/92	19.6
Cranial Deformity	0/11	0	1/27	3.7	1/38	2.6
Other Skeletal Deformities	2/18	11.1	5/74	6.8	8/92	8.7
Pathological Fracture	0/18	0	0/74	0	0/92	0

Three individuals, all adults, exhibited osteolytic lesions of the pelvis. However, all three individuals exhibited lesions of different types. AT-630, an old adult female, presented with unilateral OL1 and OL2 multifocal deep circumscribed osteolytic lesions with defined margins and sclerosis of the base in the inferior-lateral portion of the right acetabulum, and extending into the acetabular fossa (Figure 8.3). These lesions were associated with articular changes to the inferior margin of the right acetabulum. AT-630 also exhibited a remodelled focal deep circumscribed lesion extending into the superior left mastoid process (Figure 8.3).

AT-865, a middle aged adult female, presented with bilateral multifocal deep and coalesced (OL2) irregular osteolytic destruction of the acetabulae and femoral heads with minimal sclerotic response (Figure 8.4). Gross osteophytic changes to the superior and posterior acetabulae and femoral heads were associated with the destruction, and necrosis of the left femoral head. Small multifocal macroporotic changes consistent with joint destruction were present on the superior S1 body, and bilaterally on the articulating auricular surfaces of the sacrum and os coxae. Finally, bilateral osteophytic changes associated with multifocal destruction were apparent on the anatomical necks of the humeri marginal to the joint.

Figure 8.1: *Remodelled discrete deposit of SPNB on the left proximal tibia (white arrows, Khovd-Tomb 10-5, male, ~19 years old). Image: author's own.*

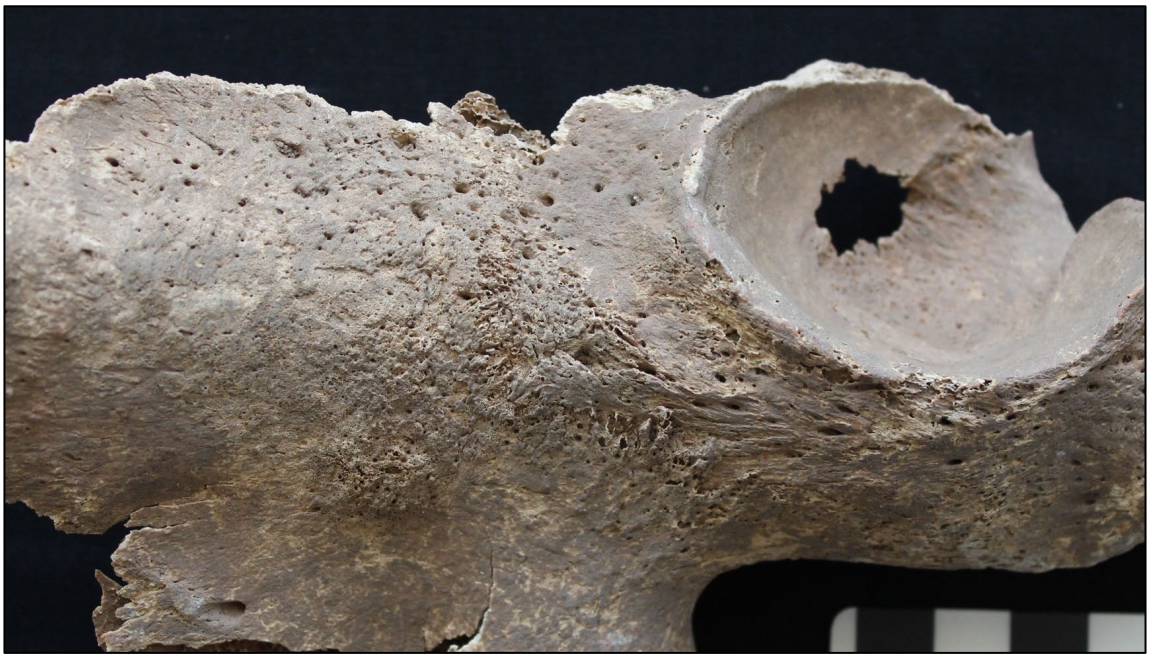

Figure 8.2: *Mixed active and remodelled diffuse SPNB across the right os coxa (AT-233, young adult male). Image: author's own.*

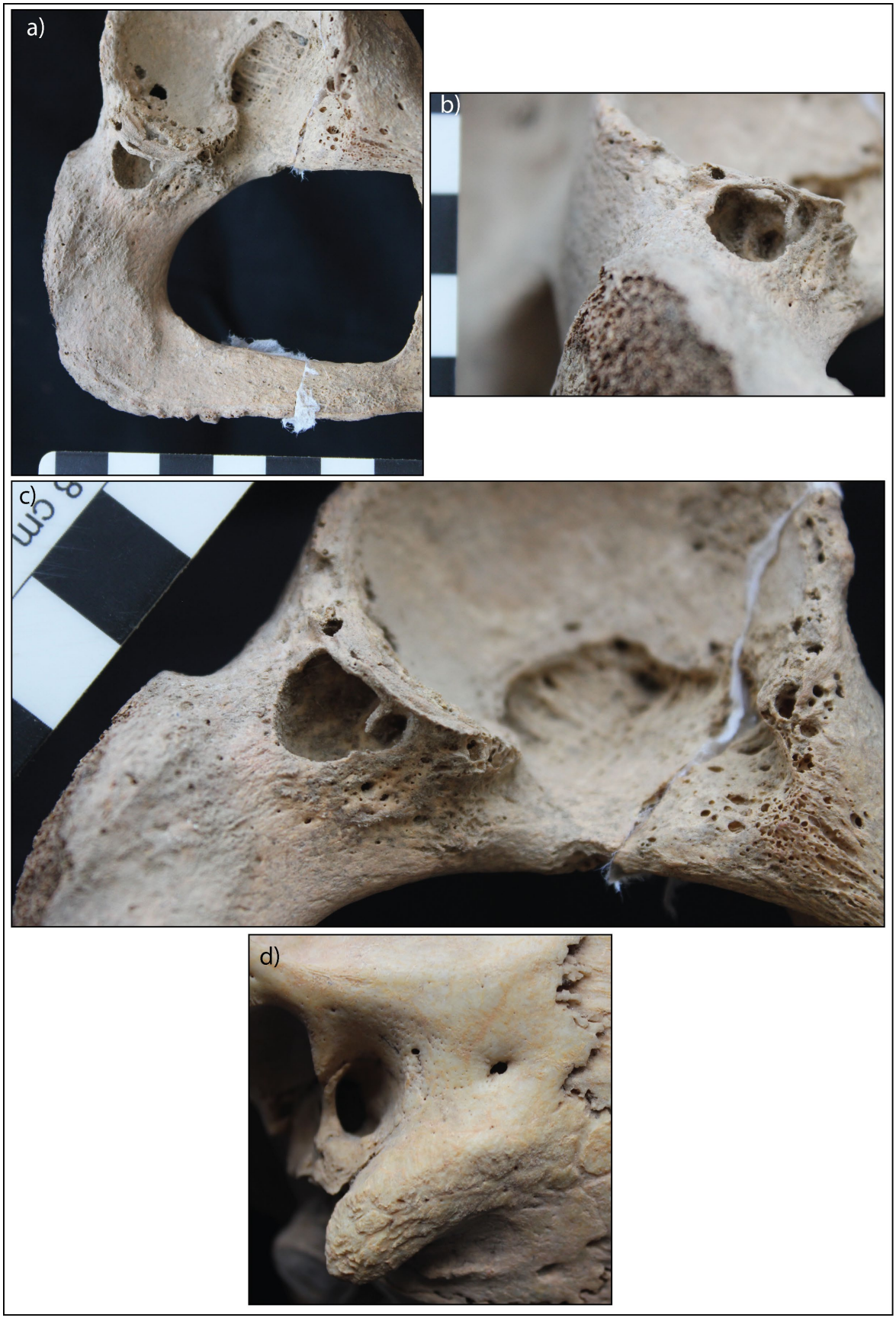

Figure 8.3: *Osteolytic lesions of AT-630, an old adult female, Chemurchek culture. a-c) Large and deep circumscribed focal lesions of the right acetabulum. d) Osteolytic perforation of the superior left mastoid process. Image: author's own.*

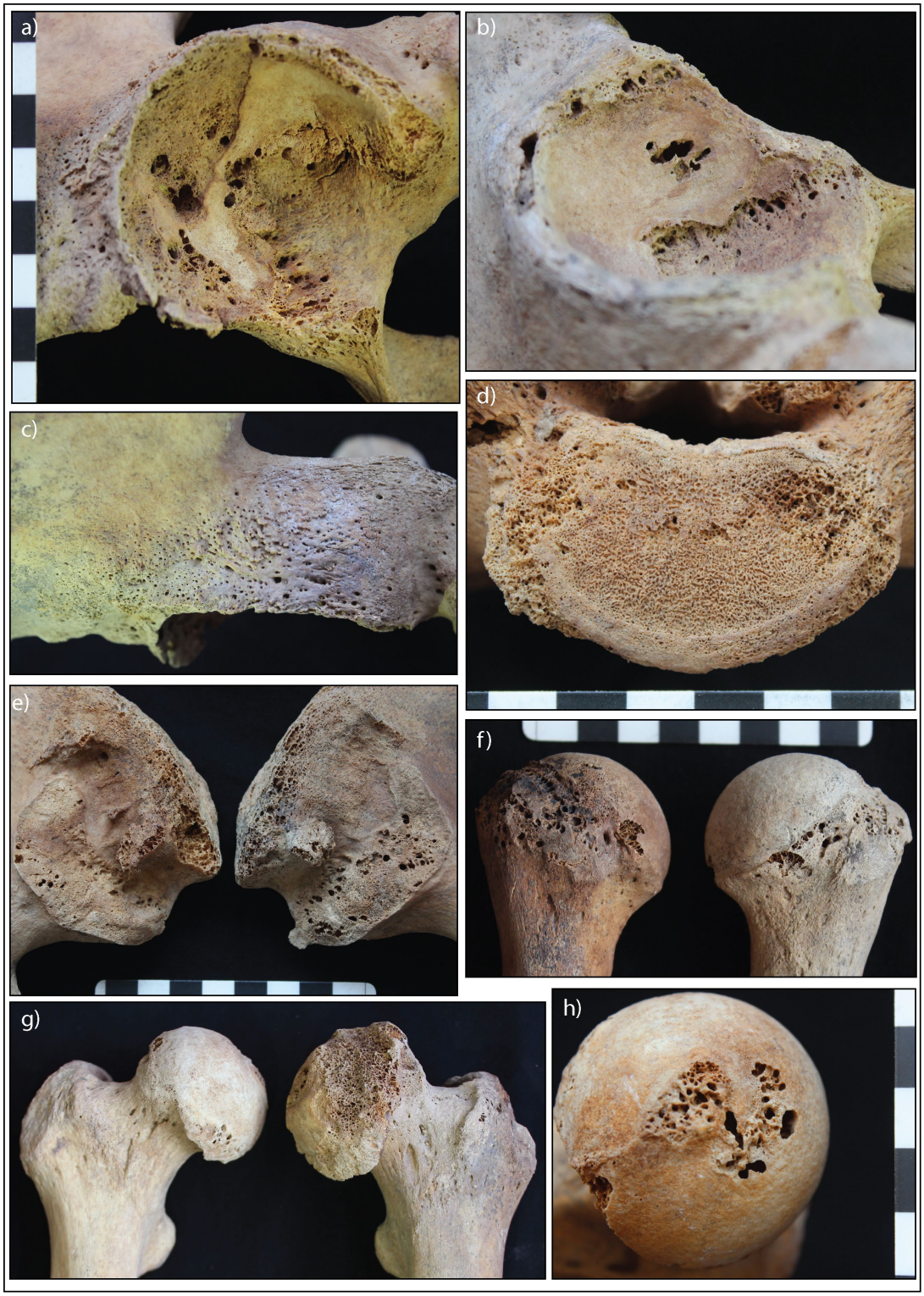

Figure 8.4: *Osteolytic lesions of AT-865, a middle aged adult female, Mungun Taiga culture. a) Multifocal and deep coalesced osteolysis of the left acetabulum. Note the marginal lipping. b) Multifocal and deep coalesced osteolysis of the right acetabulum. Again, note marginal lipping. c) Reactive SPNB associated with osteolytic pathology of the right acetabulum. d) Erosive destruction of the superior vertebral body of the S1. The osteolytic response is associated with lipping. e) Multifocal osteolysis of the auricular surface of the os coxae. f) Multifocal osteolysis and associated new bone response of the anatomical necks of the humeri, marginal to the joint. The lesions look similar to those on the auricular surfaces. g) Erosive changes to the femoral heads. Note the destruction and necrosis of the left femoral head and osteophytes. h) Osteolytic lesions of the right femoral head. Image: author's own.*

AT-272, a middle aged adult male, exhibited OL1 and OL2 deep and remodelled multifocal channel-like osteolytic lesions with sclerotic margins, medial to the antero-medial border of the right acetabulum extending behind the acetabulum into the pubis (Figure 8.5). These osteolytic lesions were present within thick remodelled SPNB. Gross osteophytic changes of the acetabulum and articulating femoral head was associated with the pathology. Additionally, there was ankylosis of the right sacroiliac joint.

Almost 20% (19.6%, 18/92) of the overall assemblage exhibited abnormal bending of the long bones. More nonadults (27.8%, 5/18) than adults (17.6%, 13/74) displayed these bending deformities. Additionally two nonadults (one adolescent, one infant) had fraying of the metaphyseal plates. Postcranial skeletal deformities were also present in adults (6.8%, 5/74). These included kyphosis of the spine, alterations of rib angles, and buckling of the sterna, scapulae, vertebrae, and sacra. One individual (AT-984, old adult female) also exhibited a distinctly brachycephalic, large square shaped skull.

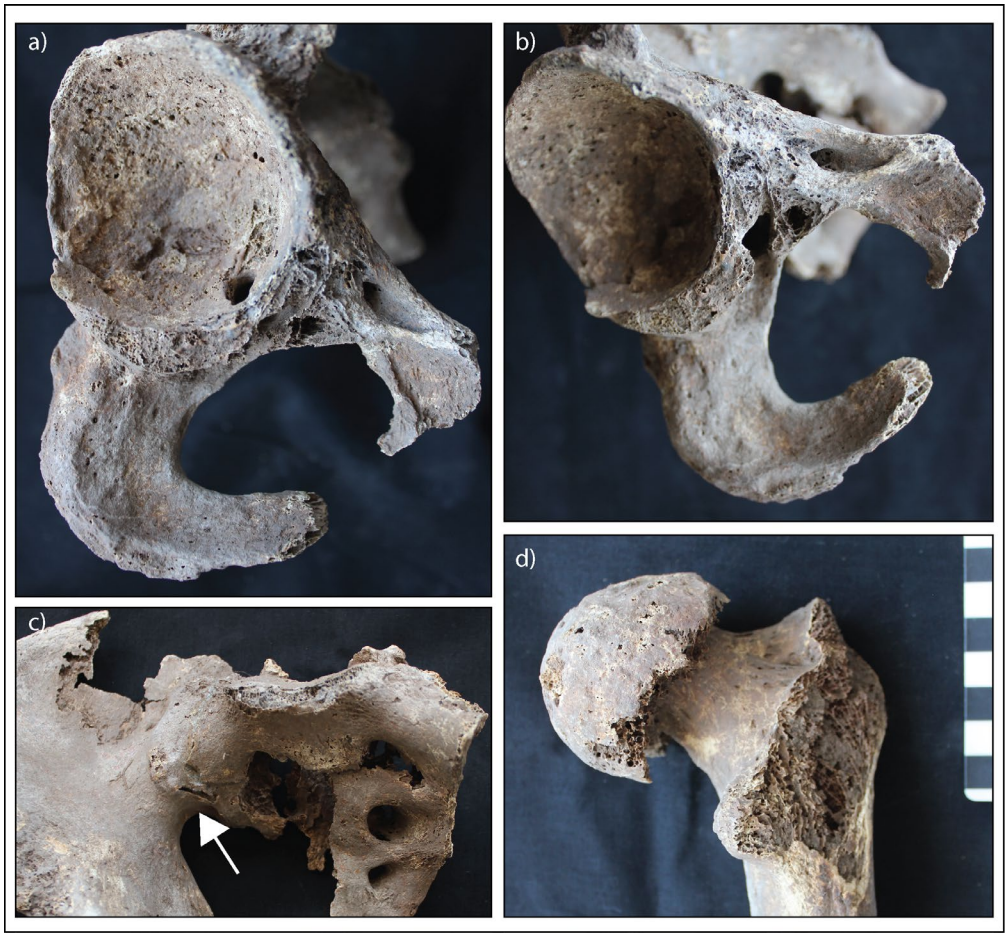

Figure 8.5: *Osteolytic lesions of AT-272, a young adult male, Slab Grave culture. a-b) Multiple channel-like osteolytic lesions within a large expanse of SPNB on the acetabulum and pubis. c) There is also ankylosis of the sacrum to the right os coxa. d) Gross osteophytes of the right femoral head. Image: author's own.*

8.4.2 Diagnosis of Infectious Disease in the Bronze Age

Only one individual (AT-233, a young adult male) exhibited diffuse SPNB across multiple elements, consistent for inclusion in the overall infectious disease criteria. Radiographs of the osteolytic lesions of AT-630 (old adult female) demonstrate multifocal cyst-like lesions resembling a "bunch of grapes" which is strongly diagnostic of infection with *Echinococcus* sp. (Figure 8.6). As such, the individual was diagnosed with probable hydatids disease. No surrounding ischemic necrosis was observed, but clear sclerosis of the margins were evident on the radiographs. Osteolytic destruction of the mastoid was also consistent with a diagnosis for probable mastoiditis in AT-630.

Figure 8.6: *Radiograph of pathology consistent with hydatids disease. The inferior margin of the acetabulum exhibits multilocular cyst-like lesions resembling a "bunch of grapes" (white arrow) strongly diagnostic for hydatids disease (AT-630, old adult female, Chemurchek culture). Image: author's own.*

The radiographs of AT-865 (middle aged adult female) demonstrated widespread erosive destruction of the acetabulae and auricular surfaces of the os coxae, with minimal sclerotic response (Figure 8.7). Osteolytic destruction of the acetabulum with minimal sclerosis and femoral head necrosis is diagnostic for tuberculosis, rendering a diagnosis of possible tuberculosis. However, femoral head necrosis is also documented in cases of brucellosis, and the skeletal lesions of the hip caused by tuberculosis and brucellosis can be indistinguishable (Al-Shahed et al. 1994; Salarvand et al. 2012; Wang et al. 2020; Zhanshui et al. 2014). Furthermore, tuberculosis of the hip is mostly commonly unilateral, and widespread osteolytic lesions throughout the skeleton are rare, but are more common in brucellosis (Al-Shahed et al. 1994; Mehmet et al. 2002). Sacroiliac involvement is one of the most common manifestations of osteoarticular brucellosis (which occurs secondary to infection within the joint), and rarely so in tuberculosis, again more suggestive of brucellosis in this case (Esmaeilnejad- Ganji and Esmaeilnejad- Ganji 2019; Hashemi et al. 2007; Ortner 2003; Rajapakse 1995). Therefore AT-865 also meets the threshold criteria for diagnosis of possible brucellosis. The bilateral pathological changes to the anatomical necks are consistent with infection in the shoulder joint capsules. Given the similar lesion pattern of the anatomical necks of the humeri, as exhibited on the pelvis and femora, it can be argued the humeral pathologies are associated with the same infectious disease, and not from another cause. Osteoarticular changes due to join infection, while non-specific, are the most common bone changes present in individuals with skeletal brucellosis (Madkour et al. 1988). In sum, tuberculosis as a cause remains a possibility. However, the widespread expression of pathology across the skeleton and the association of osteophytic response with regions of destruction does more strongly indicate brucellosis as a possible cause.

Finally, the circular osteolytic lesions associated with large expansions of SPNB are consistent with the development of an involucrum and cloacae that are strongly diagnostic for pyogenic osteomyelitis. Therefore, AT-272, was diagnosed with probable osteomyelitis. It is possible this pathology has originated from trauma. However, no signs of trauma were clearly evident on the radiographs (Figure 8.8). Overall, a low prevalence (4.6%, 4/92; Table 8.2) of infectious disease was observed in the Bronze Age.

Figure 8.7: *Radiograph of the pathology consistent with possible brucellosis or tuberculosis. a) Multiple osteolytic lesions with minimal sclerosis of the acetabulum of the right os coxa (black arrows). b) Multiple osteolytic lesions with minimal sclerosis of the acetabulum of the left os coxa (black and white arrows). c) Necrosis of the femoral head appears radiolucent on the radiograph (white arrow, AT-865, middle aged adult female, Mungun Taiga culture). Image: author's own.*

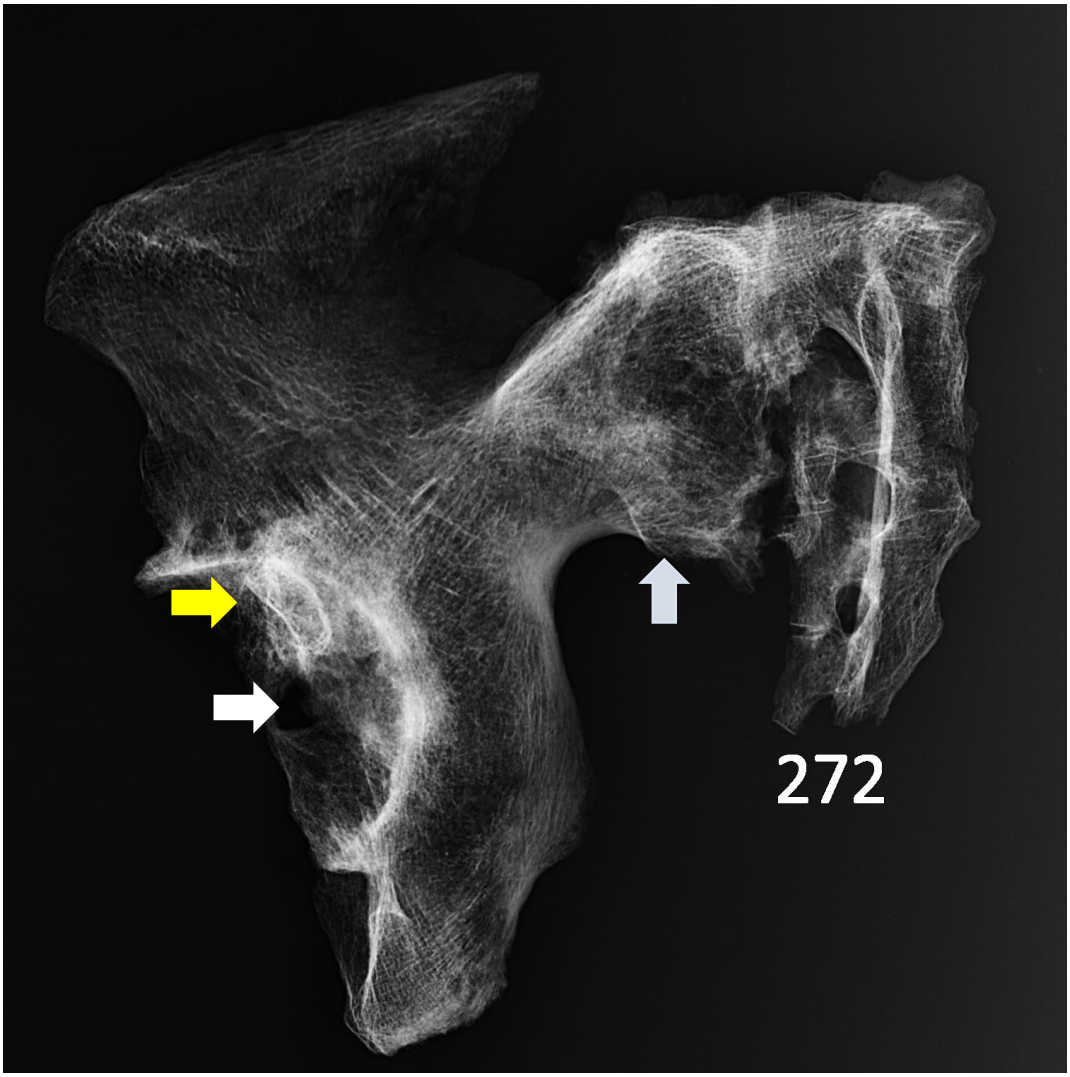

Figure 8.8: *Radiograph of the pathology consistent with probable osteomyelitis. Osteolytic destruction (white arrow) is associated with significant marginal lipping of the acetabulum (yellow arrow). Note the sacroiliac ankylosis (light blue arrow). There are no clear signs of trauma. (AT-272, young adult male, Slab Grave culture). Image: author's own.*

Table 8.2: *Summary of infectious disease in the Bronze Age*

	POSSIBLE			**PROBABLE**			**POSSIBLE AND PROBABLE**		
	Affected	***Observed***	***(%)***	***Affected***	***Observed***	***(%)***	***Affected***	***Observed***	***(%)***
Brucellosis/ Tuberculosis									
20 to 29 years	0	10	0	0	10	0	0	10	0
30 to 39 years	1	20	5	0	20	0	1	20	5
40 to 49 years	0	15	0	0	15	0	0	15	0
50+ years	0	8	0	0	8	0	0	8	0
Male	0	39	0	0	39	0	0	39	0
Female	1	28	3.6	0	28	0	1	28	3.6
Total adults	1	74	1.4	0	74	0	1	74	1.4
Total	1	92	1.1	0	92	0	1	92	1.1

	POSSIBLE			PROBABLE			POSSIBLE AND PROBABLE		
	Affected	***Observed***	***(%)***	***Affected***	***Observed***	***(%)***	***Affected***	***Observed***	***(%)***
Hydatids Disease									
20 to 29 years	0	10	0	0	10	0	0	10	0
30 to 39 years	0	20	0	0	20	0	0	20	0
40 to 49 years	0	13	0	0	13	0	0	15	0
50+ years	0	10	0	1	10	10	1	8	10
Male	0	39	0	0	39	0	0	39	0
Female	0	28	0	1	28	3.6	1	28	3.6
Total adults	0	74	0	1	74	1.4	1	74	1.4
Total	0	92	0	0	92	1.1	0	92	1.1
Otitis Media									
20 to 29 years	0	3	0	0	3	0	0	3	0
30 to 39 years	0	5	0	0	5	0	0	5	0
40 to 49 years	0	8	0	0	8	0	0	8	0
50+ years	0	6	0	1	6	16.7	1	6	16.7
Male	0	13	0	0	13	0	0	13	0
Female	0	14	0	1	14	7.1	1	14	7.1
Total adults	0	26	0	1	26	1.4	1	26	3.8
Total	0	35	0	1	35	2.8	1	35	2.8
Osteomyelitis									
20 to 29 years	0	10	0	0	10	0	0	10	0
30 to 39 years	0	20	0	0	20	0	0	20	0
40 to 49 years	0	13	0	1	13	7.7	1	13	7.7
50+ years	0	20	0	0	10	0	0	10	0
Male	0	39	0	1	39	2.6	1	39	2.6
Female	0	28	0	0	28	0	0	28	0
Total adults	0	74	0	1	74	1.4	1	74	1.4
Total	0	92	0	1	92	1.1	1	92	1.1
							CRITERIA PREVALENCE		
							Affected	*Observed*	*(%)*
Overall infectious disease criteria									
20 to 29 years							1	10	19
30 to 39 years							1	20	5
40 to 49 years							1	13	7.7
50+ years							1	10	10
Male							2	39	5.1
Female							2	28	7.1
Total adults							4	74	5.4
Total							4	92	4.3

8.4.3 Morbidity of Infectious Disease in the Bronze Age

No statistically significant differences in the morbidity across adult age and sex were observed with relative risk ratio analysis (Table 8.3). Additionally, infectious disease was observed in both Eastern and Western Mongolian cultures (Figure 8.9), and no significant differences were identified in the Fisher's exact test (n=92, p=0.625; Table 8.4). These outcomes were expected given that only four individuals exhibited signs of infectious disease.

Table 8.3: *Relative risk of infectious disease morbidity in the Bronze Age across sex and age cohorts*

EXPOSED GROUP/ CONTROL GROUP	**OUTCOME**		**RR**	**P-VALUE**	**95%CI**
	Positive: *Infection Present*	***Negative:*** *Infection Absent*			
Sex					
Female/ Male	2/2	26/37	1.3929	0.7323	0.2086- 9.3024
Adults					
<20 yrs/ >20 yrs	0/4	6/49	0.8571	0.9145	0.0514- 14.2900
<30 yrs/ >30 yrs	1/3	15/40	0.9556	0.9675	0.1074- 8.5003
<40 yrs/>40 yrs	2/2	34/21	0.6389	0.6420	0.0966- 4.2243

A relative risk (RR) >1 denotes a relationship of the exposed group with an increase in disease prevalence, whereas RR <1 denotes a relationship of the control group with an increase in disease prevalence.
**= statistically significant (p<0.10). **= statistically significant when considering size of the effect of RR.*

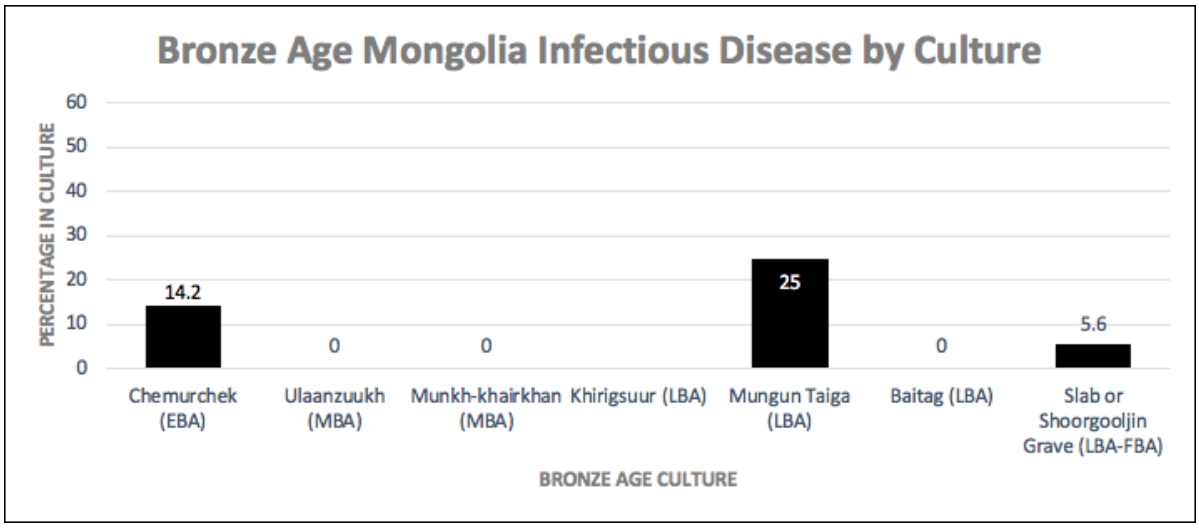

Figure 8.9: *Distribution of infectious disease prevalences across Bronze Age cultures. Image: author's own.*

Table 8.4: *Fisher's exact test for differences in morbidity of infectious disease across Eastern and Western Mongolia*

INFECTIOUS DISEASE	AFFECTED/ OBSERVED	PERCENTAGE	P-VALUE
Eastern Mongolia	2/58	3.4	0.625
Western Mongolia	2/34	5.9	

*Eastern Mongolian Bronze Age cultures include the Slab Grave and Ulaanzuukh cultures. Western Mongolian Bronze Age cultures include DSKC, Mungun Taiga, Chemruchek, Baitag, and Munkhkhairkhan cultures. *=statistically significant (p<0.05)*

8.4.4 Mortality of Infectious Disease in the Bronze Age

Relative risk ratio analysis of mortality identified no significant differences in frailty between individuals with and without skeletal signs of infectious disease (Table 8.5). This outcome was supported by Kaplan-Meier analysis (n=59, X^2=1.406, df=1, p=0.236; Table 8.6). The Kaplan-Meier survival function indicated a similar trend in mortality between those with and without skeletal evidence of infectious disease (Figure 8.10).

Table 8.5: *Relative risk of infectious disease mortality in the Bronze Age across age cohorts.*

POSITIVE OUTCOME/ NEGATIVE OUTCOME	TREATMENT		RR	P-VALUE	95%CI
	Exposed Group: *Infection Present*	***Control Group:*** *Infection Absent*			
Adults					
<20 yrs/ >20 yrs	0/4	6/49	0.8615	0.9147	0.0563- 13.1722
<30 yrs/ >30 yrs	1/3	15/40	0.9167	0.9224	0.1591- 5.2825
<40 yrs/>40 yrs	2/2	34/21	0.8088	0.6780	0.2970- 2.2025

A relative risk (RR) >1 denotes a relationship of the disease presence with the positive outcome (susceptibility to mortality), whereas RR <1 denotes a relationship of the disease absence with a negative outcome (survivorship).
**= statistically significant (p<0.10). **= statistically significant when considering size of the effect of RR.*

Table 8.6: *Statistical summary for Kaplan-Meier function of infectious disease mortality of adults in Bronze Age Mongolia.*

INFECTIOUS DISEASE	ESTIMATE	STD. ERROR	95% CI	LOG RANK (MANTEL-COX)		
				CHI SQUARE	DF	P-VALUE
Mean				1.406	1	0.236
Absent	35.262	1.434	32.452- 38.072			
Present	41.763	7.181	27.688- 55.837			
Overall	35.703	1.418	32.923- 38.482			
Median						
Absent	35.200	1.695	31.877- 38.523			
Present	34.450	9.300	16.222- 52.678			
Overall	35.200	1.610	32.044- 38.356			

**= statistical significance (p<0.15).*

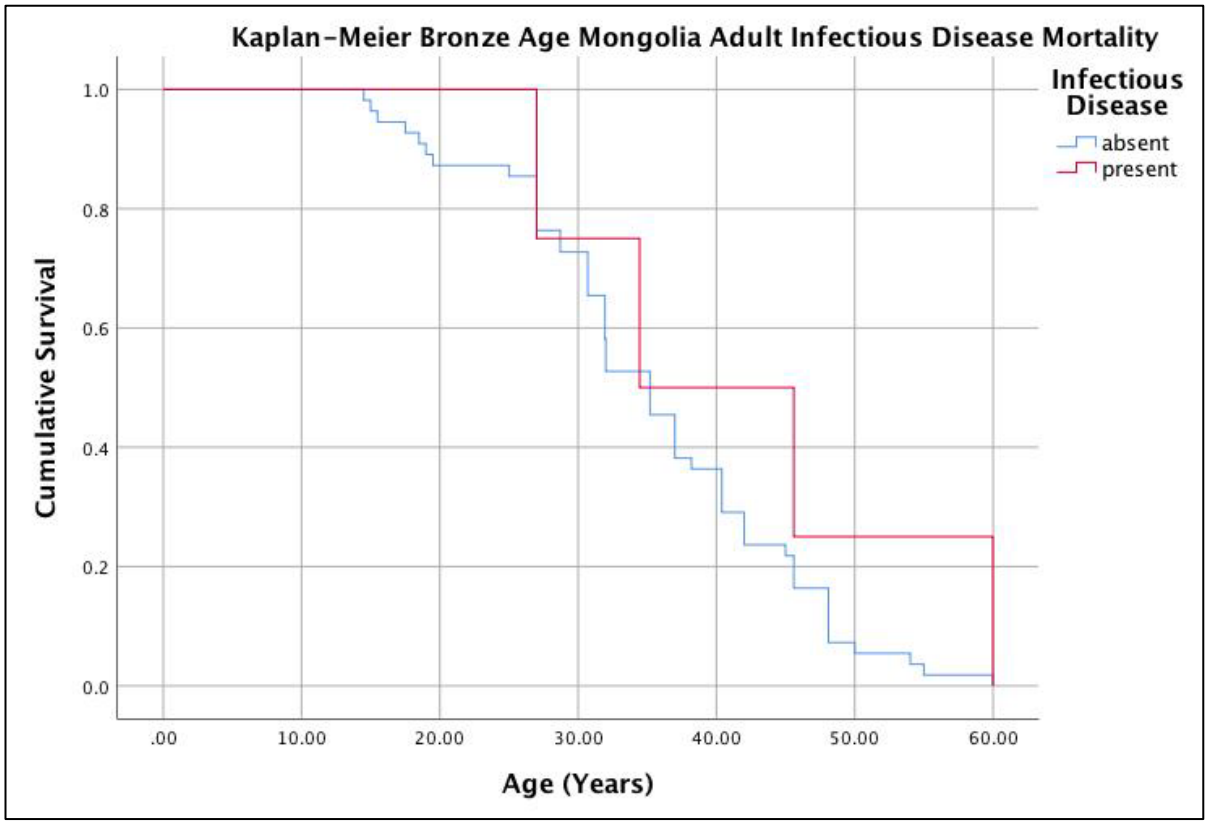

Figure 8.10: *Kaplan-Meier cumulative survival function of adult infectious disease mortality in Bronze Age Mongolia. Image: author's own.*

8.4.5 Diagnosis of Nutritional Disease in the Bronze Age

8.4.5.1 Diagnosis of Nutritional Disease in Bronze Age Nonadults

Half (50%, 9/18) of the nonadult assemblage exhibited lesions consistent with at minimum a possible diagnosis for scurvy (Table 8.7). However, only 27.8% (5/18) had lesions consistent with a probable diagnosis. Probable scurvy was predominantly identified in nonadults under the age of 10 years of age with the exception of a single adolescent (Khovd Tomb 10-5, male ~19 years of age). Lesions diagnostic for scurvy were predominantly bilateral and symmetrical discrete SPNB deposits associated with abnormal cortical porosity of the cranium including the lateral and superior greater wings of the sphenoid bones, anterior, posterior and palatal surfaces of the maxillae, superior orbital roofs and medial coronoid processes of the mandible (Figure 8.11). Additionally, lesions were also present symmetrically in the infraspinous and supraspinous fossae of the scapulae. Abnormal endochondral porosity exceeding 10mm from the metaphyseal plates was observed in the long bones of four nonadults (22.2%, 4/18). No distinct radiographic

changes attributed to scurvy were identified in preserved long bones of nonadults in the Bronze Age assemblage.

A third of nonadults (33.3%, 6/18) had lesions consistent with a diagnosis of possible or probable rickets (Table 8.7). Pathologies consistent with rickets in the Bronze Age nonadult assemblage included bending and fraying of the long bone shafts (Figure 8.12). Rib changes consistent with rickets (enlargement at the costochondral junction) was only observed in one nonadult (AT-218, male, ~15.5 years), and no cranial changes clearly associated with rickets were observed. Five individuals (27.8%, 5/18) displayed clear radiographic signs of bilateral long bone thickening, and three individuals demonstrated radiographic trabecular coarsening, both suggestive signs for rickets (Figure 8.12). Finally, one adolescent (AT-766, male, ~15 years) exhibited severe osteopenia of the vertebrae. Involvement of the axial skeleton in their mineralisation disorder is similar to that of adult osteomalacia. Given the age of the individual, pathologies similar to those in adults is expected. Osteomalacia is dealt with in more detail in the section below.

Table 8.7: *Summary of nutritional disease in the Bronze Age*

	POSSIBLE			**PROBABLE**			**POSSIBLE AND PROBABLE**		
	Affected	*Observed*	*(%)*	*Affected*	*Observed*	*(%)*	*Affected*	*Observed*	*(%)*
Scurvy									
0 to 5 months	0	2	0	2	2	100	2	2	100
6 to 11 months	0	2	0	0	2	0	0	2	0
1 to 5 years	1	2	50	1	2	50	2	2	100
6 to 10 years	1	3	33.3	1	3	33.3	2	3	66.7
11 to 14 years	1	3	33.3	0	3	0	1	3	33.3
15 to 19 years	1	6	16.7	1	6	16.7	2	6	33.3
20 to 29 years	1	10	10	0	10	0	1	10	10
30 to 39 years	0	20	0	0	20	0	0	20	0
40 to 49 years	0	13	0	0	13	0	0	13	0
50+ years	1	10	10	0	10	10	1	10	10
Total nonadults	4	18	22.2	5	18	27.8	9	18	50
Males	1	39	2.6	1	39	2.6	2	39	5.1
Females	1	28	3.6	0	28	0	1	28	3.6
Total adults	2	74	2.7	1	74	1.4	3	74	4.1
Total	6	92	6.5	6	92	6.5	12	92	13.1
Rickets/ Residual Rickets									
0 to 5 months	0	2	0	0	2	0	0	2	0
6 to 11 months	1	2	50	0	2	0	1	2	50
1 to 5 years	0	2	0	0	2	0	0	2	0
6 to 10 years	1	3	33.3	0	3	0	1	3	33.3
11 to 14 years	0	3	0	1	3	33.3	1	3	33.3
15 to 19 years	1	6	16.7	2	6	33.3	3	6	50
20 to 29 years	0	10	0	0	10	0	0	10	0
30 to 39 years	3	20	15	0	20	0	3	20	15
40 to 49 years	4	13	30.8	0	13	0	4	13	30.8
50+ years	3	10	30	1	10	10	4	10	40
Total nonadults	3	18	16.7	3	18	16.7	6	18	33.3
Males	4	39	10.3	1	39	2.6	5	39	12.8
Females	8	28	28.6	2	28	7.1	10	28	35.7
Total adults	13	74	17.6	2	74	2.7	15	74	20.3
Total	17	92	18.5	3	92	3.3	20	92	21.7
Osteomalacia									
15 to 19 years	1	6	16.7	0	6	0	1	6	16.7
20 to 29 years	0	10	0	0	10	0	0	10	0
30 to 39 years	0	20	0	1	20	5	1	20	5
40 to 49 years	2	13	15.4	1	13	7.7	3	13	23.1
50+ years	1	10	10	3	10	30	4	10	40
Males	3	39	7.7	1	39	2.6	4	39	10.3
Females	2	28	7.1	4	28	14.3	6	28	21.4
Total adults	4	74	5.4	5	74	6.8	9	74	12.2

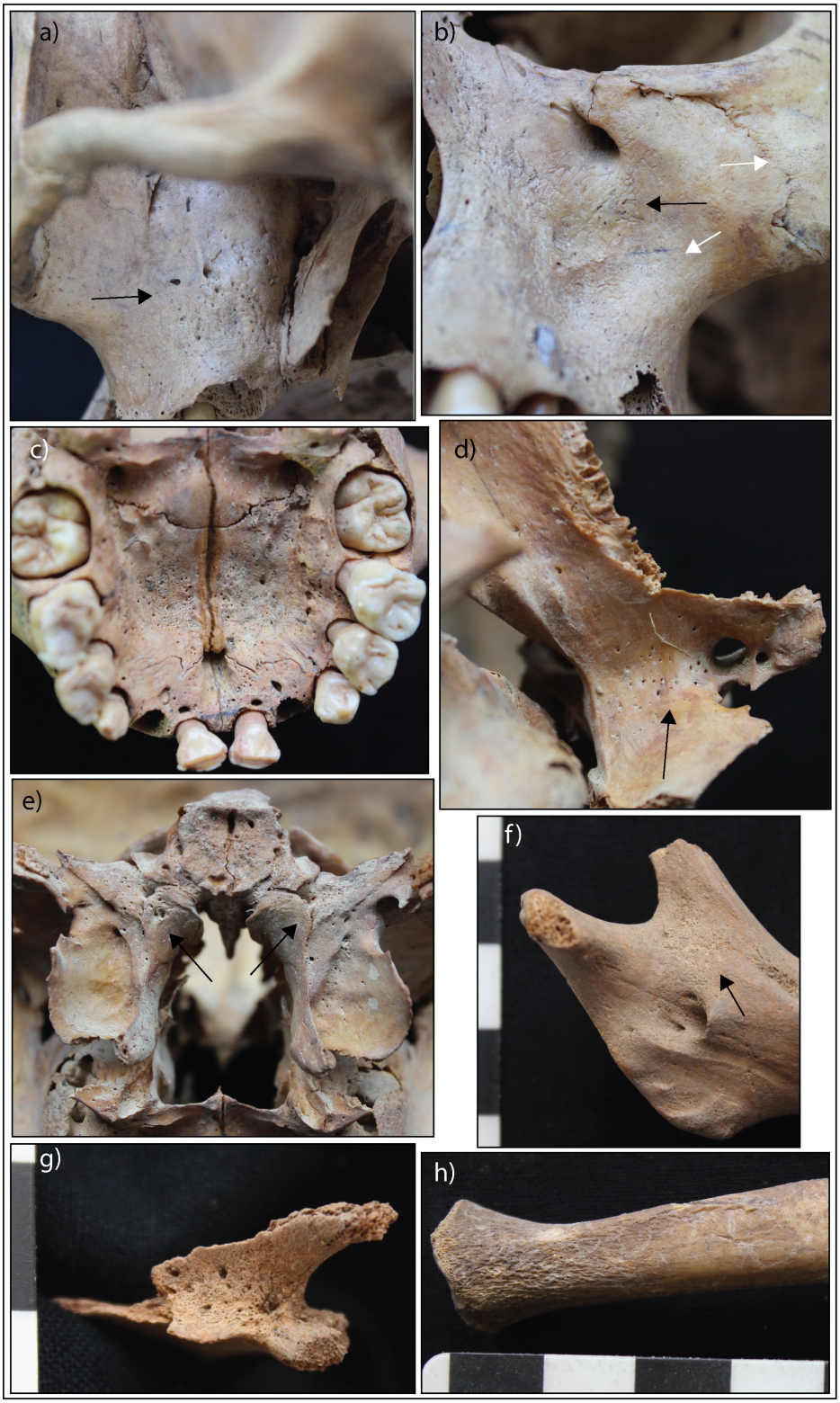

Figure 8.11: *Lesions diagnostic for scurvy in the Bronze Age Mongolian nonadults. SPNB and abnormal cortical porosity on the: a) Posterior left maxilla (black arrow, Khovd Tomb 10-5, male ~19 years, DSKC). b) Anterior left maxilla and zygoma. Note the remodelled lesion with vascular impressions (black arrow), and active lesions on the maxilla and zygoma (white arrows, Khovd Tomb 10-5, male ~19 year, DSKC). c) Palatal surface of the maxilla (AT-629, ~6.5 years, Chemurchek culture). d-e) Pterygoid plate of the left sphenoid bone and pterygoid fossae (AT-629, ~6.5 years, Chemurchek culture). f) Medial left coronoid process of the mandible (AT-232b, ~3 years, Slab Grave culture). g) Supraspinous fossa of the left scapula (Khovd Tomb 10-2, neonate, DSKC). h) Abnormal deep endochondral porosity exceeding 10mm from the distal metaphyseal plate of the right ulna (AT-981, ~13 years, Slab Grave culture). Image: author's own.*

Figure 8.12: *Lesions suggestive and diagnostic for rickets in the Bronze Age Mongolian nonadults. a-b) Fraying of the proximal and distal metaphyses of the humeri (Khovd Tomb 10-8, ~6 months, DSKC). c) Thick cortex (yellow arrow) and trabecular coarsening (white arrow, Khovd Tomb 10-8, ~6 months, DSKC). d) Osteopenia of the trabeculae of the vertebrae (AT-766,male, ~15 years, Slab Grave culture). e) Fraying of proximal metaphysis of left tibia (AT-766, male, ~15 years, Slab Grave culture), f) Enlargement of costochondral junction of the rib (AT-218, male, ~15.5 years, DSKC). g) Medial bending deformities of the tibiae (AT-766, male, ~15 years, Slab Grave culture). h) Medial bending deformities of the tibiae and cortical thickening (AT-218, male, ~15.5 years, DSKC). Image: author's own.*

8.4.5.2 Diagnosis of Nutritional Disease in Bronze Age Adults

A low prevalence (4.1%, 3/74) of possible and probable scurvy was diagnosed in the Bronze Age adults (Table 8.7). Only two individuals met the threshold criteria for possible (AT-233 a young adult male and AT-637, an old adult female), and one met the threshold criteria for probable diagnoses (AT-905, a young adult male). Diagnostic lesions included the presence of symmetrical and bilateral SPNB and/or abnormal cortical porosity on the palatal surfaces of the maxillae, posterior maxillae, pterygoid fossae of the sphenoid bones and medial coronoid processes of the mandible (Figure 8.13). Adults with abnormal cortical porosity of the palatal surfaces of the maxilla also exhibited antemortem tooth loss, that can be caused by scurvy, but is also commonly caused by periodontal disease. Therefore, palatal lesions as *diagnostic* for scurvy were considered with caution. The porosity extends symmetrically from the greater palatine foramina, that does indicate a vascular origin as in the case in scurvy (Figure 8.13e, 8.13f). Overall, 13.1% (12/92) of the Bronze Age assemblage had skeletal signs of scurvy. Infants and children (<10 years) presented with the highest prevalences, with a decline in prevalence apparent with increasing age (Figure 8.14).

As was the case in the nonadult cohort, bending deformities of the long bones, radiographic signs of trabecular coarsening of the metaphyses and thick cortices were present indicating residual rickets in the adult cohort (Figure 8.15; Table 8.7). Over 20% (20.3%, 15/74) had at minimum a possible case of residual rickets, with 2.7% (2/74) exhibiting more than two diagnostic signs consistent with probable residual rickets. Two adults also displayed coxa vara of the femoral necks, and two had alterations of the rib neck angle (Figure 8.15). One individual (AT-984, old adult female) presented with a large square shaped skull, also suggestive for residual rickets.

Additionally, overall 12.2% (9/74) of adults met the criteria for a minimum a diagnosis of possible osteomalacia, with 6.8% (5/74) diagnosed with probable osteomalacia (Table 8.7). Pathologies diagnostic for osteomalacia included buckling deformities of the sterna, scapulae, vertebrae, and sacra. Moreover, osteopenia of vertebral body cortices and trabeculae (4.1%, 3/74), loss of body height (2.7%, 2/74), and biconcavity of multiple vertebral bodies (4.1%, 3/74) were also observed on radiographs and are diagnostic for osteomalacia (Figure 8.17). The prevalence of possible or probable

osteomalacia increased with adult age, and 40% of old adults (50+ years) were diagnosed with at minimum a possible case of osteomalacia (Figure 8.18).

Eight adults (10.8%, 8/74) had lesions consistent with both possible or probable residual rickets *and* osteomalacia. The prevalence of skeletal evidence for childhood and adult mineralisation disorders can in part be attributed to shared diagnostic lesions in the criteria of the two diseases, such as coxa vara of the femoral neck and bending deformities of the femoral shaft. However, most bending deformities were of the lower leg (tibia and fibula) more consistent with residual rickets, and signs of osteomalacia were predominantly identified through axial skeletal deformities. As such there is a strong argument for multiple episodes of mineralisation disorders in these individuals (including in childhood and subsequently in adulthood).

Figure 8.13: *Lesions diagnostic for scurvy in the Bronze Age Mongolian adults. a) SPNB and abnormal cortical porosity of the pterygoid fossae (black arrows, AT-905, young adult male, DSKC). b) Abnormal cortical porosity on the left medial coronoid process of the mandible (black circle, AT-905, young adult male, DSKC). c) Abnormal cortical porosity on the left external greater wing of sphenoid (AT-905, young adult male, DSKC). d) SPNB and abnormal cortical porosity on the posterior left maxilla. Note the vascular impressions (black arrow, AT-637, old adult female, Mungun Taiga culture). e-f) Abnormal cortical porosity on the palatal surfaces of the maxillae. Note the extension of the porosity into the palatine foramina (black arrows, e: AT-905, young adult male, DSKC f: AT-233, young adult male, Slab Grave culture). Image: author's own.*

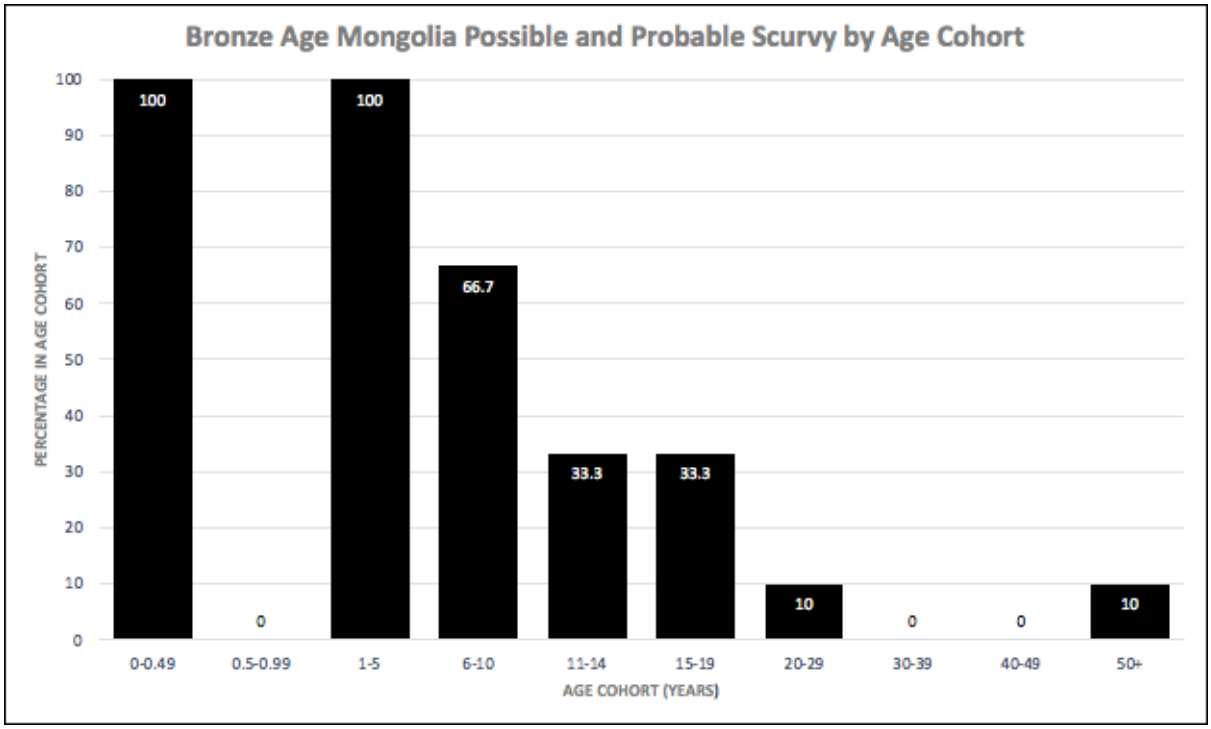

Figure 8.14: *Age-at-death distribution of possible and probable cases of scurvy in Bronze Age Mongolia. Image: author's own.*

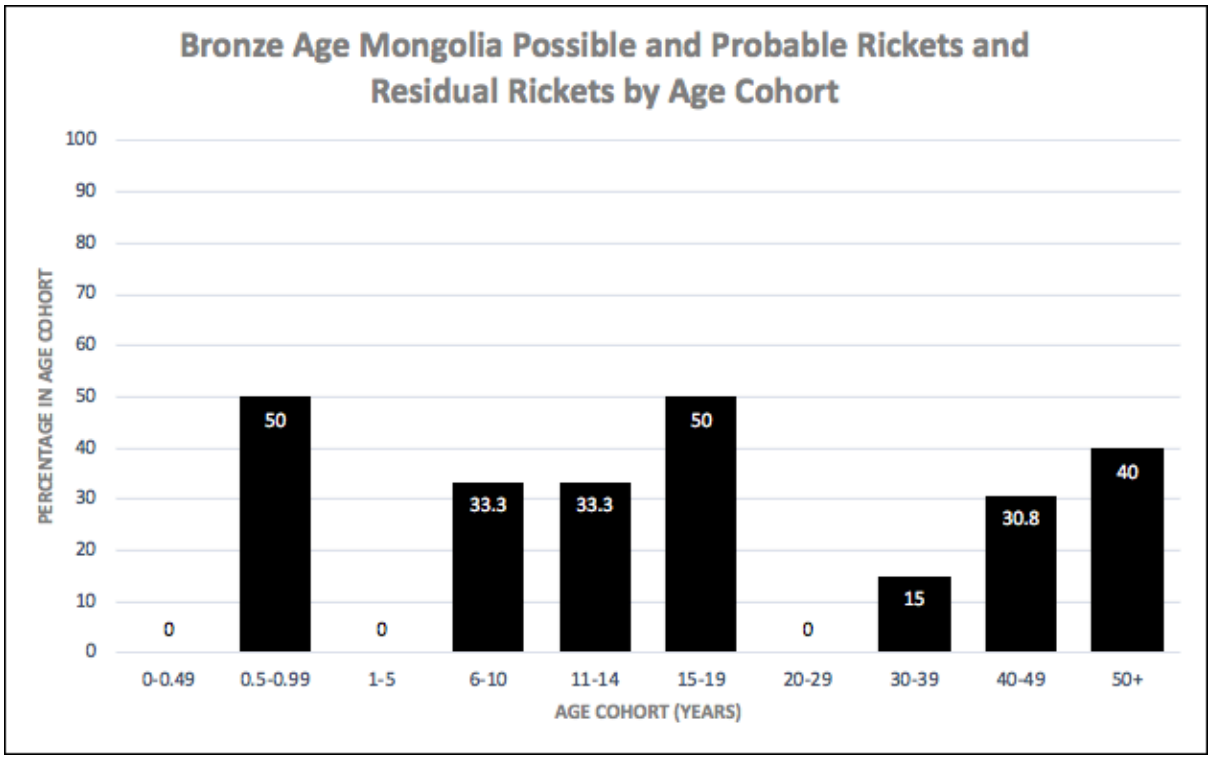

Figure 8.15: *Age-at-death distribution of possible and probable cases of rickets and residual rickets in Bronze Age Mongolia. Image: author's own.*

Figure 8.16: *Lesions suggestive and diagnostic for residual rickets in the Bronze Age adults. a) Anterior bending of the femur (AT-253, middle aged adult male, Slab Grave culture). b) Medial bending of the right tibia (AT-1001, adult male, Slab Grave culture). c) Long bone cortical thickening associated with medial bending of the left tibia (AT-676, young adult male, Baitag culture). d) Coxa vara (depression) of the right femoral neck (yellow arrow) and broad flattening of the proximal femoral shaft (white arrow, Hongio 21, young adult female, DSKC). e) Lateral bending of the tibiae and fibulae (AT-324, adult, Slab Grave culture). Image: author's own.*

Figure 8.17: *Lesions suggestive and diagnostic for osteomalacia in the Bronze Age adults. a) Anterior bending of the sternum (AT-466, middle aged adult male, DSKC). b) Severe biconcavity of multiple vertebrae (codfish sign), with anterior compression causing kyphosis (white arrows) with osteopenia of the cortex and trabeculae (AT-962, old adult female). c) Codfish sign of multiple vertebrae with osteopenia of the cortex margin and trabeculae (AT-1001, adult male, Slab Grave culture). d) Extreme ventral angulation of the sacrum (Khovd 10-11, old adult female, DSKC). e) Anterolateral bending deformities of the femora associated with genu valgum deformities (white arrow, 466- middle aged adult male, DSKC). f) Slight bucking of the left scapula (Khovd 10-11, old adult female, DSKC). g) Lateral straightening of a rib with medial indentation. Note the extreme thinning of the rib. All ribs of this individual were affected (AT-909, old adult female, DSKC). Image: author's own.*

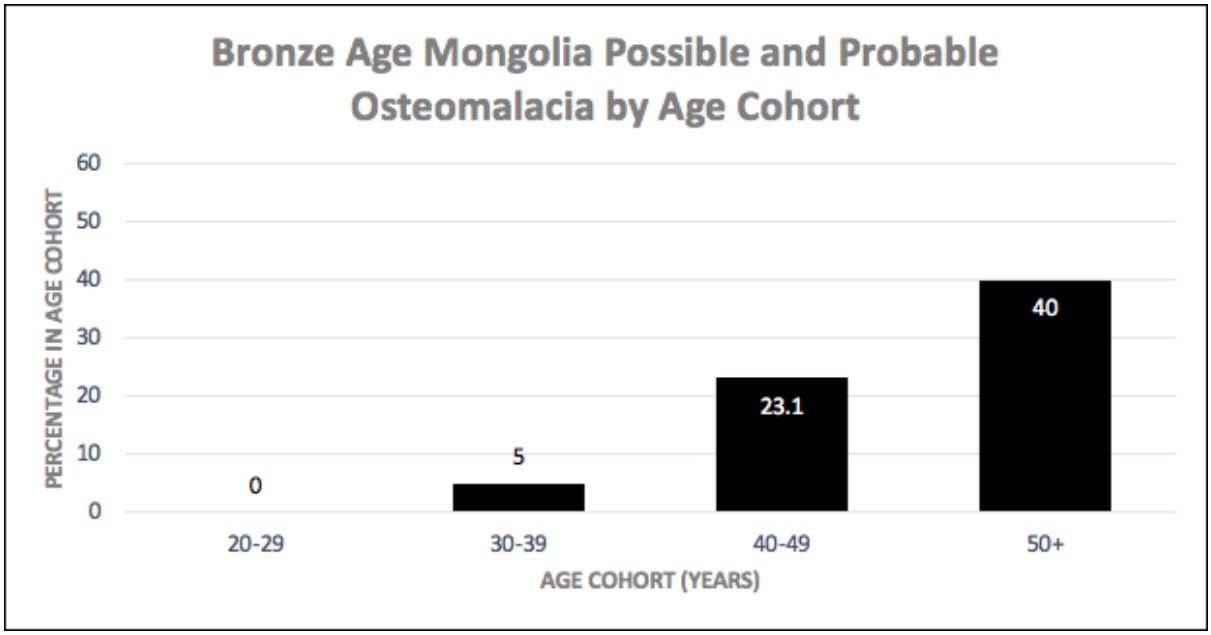

Figure 8.18: *Age-at-death distribution of possible and probable cases of osteomalacia in Bronze Age Mongolia. Image: author's own.*

8.4.6 Morbidity of Nutritional Disease in the Bronze Age

8.4.6.1 Morbidity of Scurvy in the Bronze Age

No statistically significant differences in morbidity between sex and nonadult age cohorts was identified for combined possible and probable scurvy (Table 8.8). However, Bronze Age individuals were over 17 times more likely to have possible or probable scurvy in adolescence than adulthood, which was statistically significant (n=59, RR=17.6667, p=0.0123). Similarly, Bronze Age adults were over 5 times more likely have a diagnosis of possible or probable scurvy before the age of 30 years (n=59, RR=5.3750, p=0.1573), which was statistically significant given the size of the effect. Probable scurvy was only assessed in nonadults as only one adult had lesions consistent with a probable diagnosis. No statistically significant differences in morbidity of probable scurvy was identified in nonadults (Table 8.8).

With the exception of the Chemurchek culture, scurvy prevalence was low in Early to Middle Bronze Age cultures including the Ulaanzuukh and Munkhkhairkan, and higher in the Late Bronze Age cultures (Slab Grave, DSKC and Mungun Taiga; Figure 8.19). This outcome suggests there are some differences across time within the assemblage. DSKC and Mungun Taiga, considered to possibly be extensions of a single cultural complex

(Tsybiktarov 2002), shared similar prevalences. No statistically significant differences between Eastern and Western Mongolian cultures were identified with Fishers exact (n=92, p=0.349; Table 8.9).

Table 8.8: *Relative risk of scurvy morbidity in the Bronze Age across sex and age cohorts.*

EXPOSED GROUP/ CONTROL GROUP	**OUTCOME**		**RR**	**P-VALUE**	**95%CI**
	Positive: *Disease Present*	***Negative:*** *Disease Absent*			
Possible and Probable Scurvy (combined)					
Sex					
Female/ Male	2/2	25/38	1.4815	0.6849	0.220- 9.8875
Nonadults					
<1 yr/ >1 yr	2/7	2/7	1.0000	1.0000	0.3292- 3.0380
<5 yrs/ >5yrs	4/5	2/7	1.6000	0.2933	0.6660- 3.8441
<10 yrs/ >10yrs	6/3	3/6	2.0000	0.1885	0.7119- 5.6190
Adults					
<20 yrs/ >20 yrs	2/1	4/52	**17.6667**	**0.0123***	1.8674- 167.1384
<30 yrs/ >30 yrs	2/1	14/42	**5.3750**	**0.1573****	0.5225- 55.2921
<40 yrs/>40 yrs	2/1	34/22	1.0980	0.8247	0.4800- 2.5117
Probable Only Scurvy					
Nonadults					
<1 yr/ >1 yr	2/4	2/10	1.7500	0.3926	0.4850- 6.3138
<5 yrs/ >5yrs	3/3	3/9	2.0000	0.2829	0.5644- 7.0874
<10 yrs/ >10yrs	4/2	5/7	2.0000	0.3400	0.4815- 8.3066

A relative risk (RR) >1 denotes a relationship of the exposed group with an increase in disease prevalence, whereas RR <1 denotes a relationship of the control group with an increase in disease prevalence.
**= statistically significant (p<0.10). **= statistically significant when considering size of the effect of RR.*

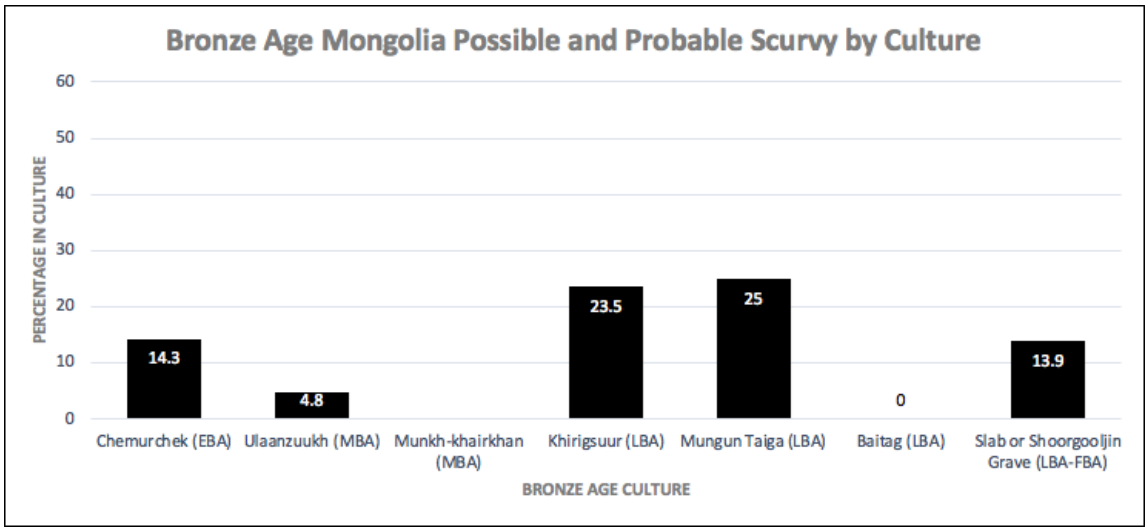

Figure 8.19: *Distribution of possible and probable scurvy prevalences across Bronze Age cultures. Image: author's own.*

Table 8.9: *Fisher's exact test for differences in morbidity of scurvy across Eastern and Western Mongolia.*

	AFFECTED/ OBSERVED	PERCENTAGE	P-VALUE
Possible and Probable Scurvy (combined)			
Eastern Mongolia	6/58	10.3	0.349
Western Mongolia	6/34	17.6	

*Eastern Mongolian Bronze Age cultures include the Slab Grave and Ulaanzuukh cultures. Western Mongolian Bronze Age cultures include DSKC, Mungun Taiga, Chemruchek, Baitag, and Munkhkhairkhan cultures. *=statistically significant (p<0.05)*

8.4.6.2 Morbidity of Rickets and Residual Rickets in the Bronze Age

No statistically significant differences in the morbidity of rickets was identified across nonadult age cohorts (Table 8.10). This was consistent for combined possible and probable; and probable only diagnoses for rickets.

In order to classify residual rickets from rickets, only individuals over the age of 20 years of age (where long bone epiphyseal fusion was completed) were included in the analysis. An active case of rickets (fraying of the long bones) in an individual over the age of 15 further supported exclusion of adolescents. Only combined possible and probable cases were assessed, as only two adults had lesions consistent with a diagnosis of probable residual rickets. Females were almost 3 times more likely to have had rickets in their childhood or adolescence than males (n=60, RR=2.7636, p= 0.0434) which was statistically significant. Similarly, age appears to have been a risk factor, with adults over the age of 40 over 3 times more likely to have had rickets in childhood (n=53, RR=0.2875, p=0.0436) which was statistically significant. Given the development of rickets in childhood, this outcome is likely a reflection of mortality on morbidity prevalence and is explored further in the next section.

The prevalence of rickets in childhood (combined rickets and residual rickets) was highest in Late Bronze Age cultures, and considerably lower in Early to Middle Bronze Age cultures (Chemurchek, Ulaanzuukh and Munkhkhairkhan; Figure 8.20). Again, this suggests some differences over time. No statistically significant differences between Eastern and Western Mongolian cultures were identified with Fishers exact (n=92, p=0.439; Table 8.11).

Table 8.10: *Relative risk of rickets/ residual rickets morbidity in the Bronze Age across sex and age cohorts.*

EXPOSED GROUP/ CONTROL GROUP	OUTCOME		RR	P-VALUE	95%CI
	Positive: *Disease Present*	***Negative:*** *Disease Absent*			
Possible and Probable Rickets (combined)					
Nonadults					
<1 yr/ >1 yr	1/5	3/9	0.7000	0.7036	0.115- 4.3950
<5 yrs/ >5yrs	1/5	5/7	0.4000	0.3472	0.0592- 2.7022
<10 yrs/ >10yrs	3/3	7/5	0.8000	0.7370	0.2175- 2.9430
Probable Only Rickets					
Nonadults					
<1 yr/ >1 yr	0/2	4/12	0.6000	0.7265	0.0343- 10.5059
<5 yrs/ >5yrs	0/2	6/10	0.3714	0.5024	0.0206- 6.7104
<10 yrs/ >10yrs	0/2	9/7	0.2000	0.2779	0.0109- 3.6609
Possible and Probable Residual Rickets (combined)					
Sex					
Female/ Male	8/5	14/33	**2.7636**	**0.0434***	1.0307- 7.4102
Adults					
<20 yrs/ >20 yrs	-	-	-	-	-
<30 yrs/ >30 yrs	0/11	10/32	0.1739	0.2131	0.0111- 2.7295
<40 yrs/>40 yrs	3/8	27/15	**0.2875**	**0.0436***	0.0857- 0.9647

A relative risk (RR) >1 denotes a relationship of the exposed group with an increase in disease prevalence, whereas RR <1 denotes a relationship of the control group with an increase in disease prevalence.
**= statistically significant (p<0.10). **= statistically significant when considering size of the effect of RR.*

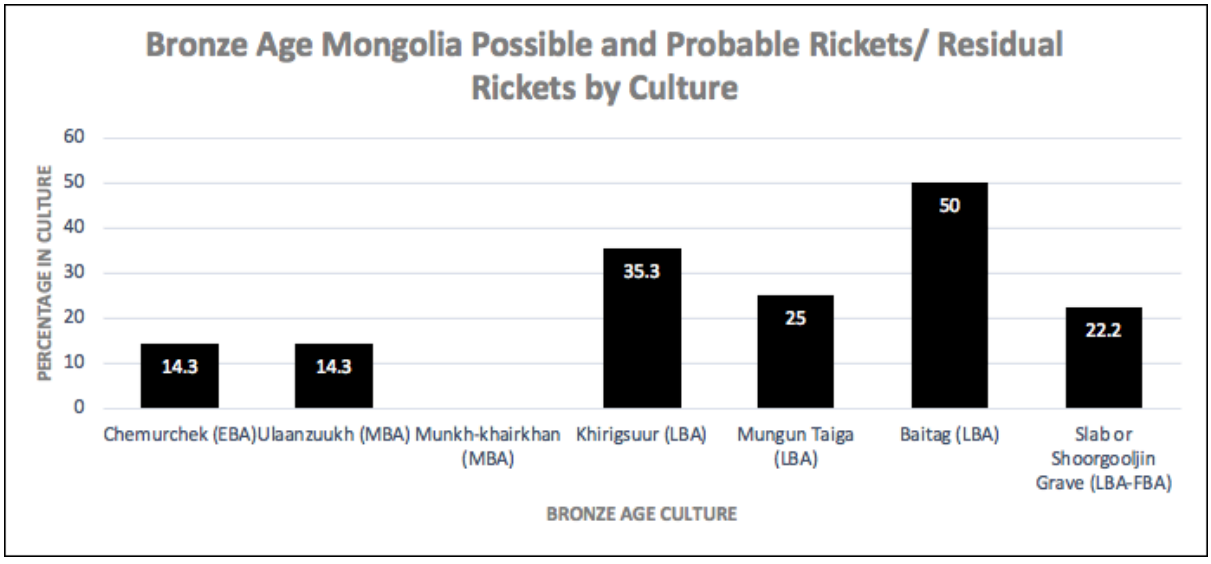

Figure 8.20: *Distribution of possible and probable rickets/residual rickets prevalences across Bronze Age cultures. Image: author's own.*

Table 8.11: *Fisher's exact test for differences in morbidity of rickets/residual rickets across Eastern and Western Mongolia.*

	AFFECTED/ OBSERVED	PERCENTAGE	P-VALUE
Possible and Probable Rickets and Residual Rickets (combined)			
Eastern Mongolia	11/58	18.9	0.439
Western Mongolia	9/34	26.5	

*Eastern Mongolian Bronze Age cultures include the Slab Grave and Ulaanzuukh cultures. Western Mongolian Bronze Age cultures include DSKC, Mungun Taiga, Chemruchek, Baitag, and Munkhkhairkhan cultures. *=statistically significant (p<0.05)*

8.4.6.3 Morbidity of Osteomalacia in the Bronze Age

A statistically significant increase in the morbidity of combined possible or probable osteomalacia was identified for adults over the age of 40 years (Table 8.12). Adults were 5.5 times more likely to exhibit signs of possible or probable osteomalacia if aged over 40 years (n=59, RR= 0.1825, p=0.0245) which was statistically significant. A similar outcome was observed when considering probable only cases of osteomalacia (n=59, RR=0.1597, p=0.0911). Females were also over 5 times more likely to exhibit probable osteomalacia than males (n=67, RR=5.5714, p=0.1151) which was statistically significant given the size of the effect.

Late and Final Bronze Ages had higher prevalences than Early to Middle Bronze Age sites (Figure 8.21). The Fishers exact test identified no significant differences in the prevalences of osteomalacia between Western and Eastern Bronze Age cultures (n=92, p=0.167, Table 8.13).

Table 8.12: *Relative risk of osteomalacia morbidity in the Bronze Age across sex and age cohorts.*

EXPOSED GROUP/ CONTROL GROUP	OUTCOME		RR	P-VALUE	95%CI
	Positive: *Disease Present*	***Negative:*** *Disease Absent*			
Possible and Probable Osteomalacia (combined)					
Sex					
Female/ Male	6/4	22/35	2.0893	0.2164	0.6495- 6.7203
Adults					
<20 yrs/ >20 yrs	1/8	5/45	1.1042	0.9186	0.1652- 7.3805
<30 yrs/ >30 yrs	1/8	14/36	0.3667	0.3242	0.0499- 2.6947
<40 yrs/>40 yrs	2/7	34/16	**0.1825**	**0.0245***	0.0415- 0.8034

EXPOSED GROUP/ CONTROL GROUP	OUTCOME		RR	P-VALUE	95%CI
	Positive: *Disease Present*	***Negative:*** *Disease Absent*			
Probable Only Osteomalacia					
Sex					
Female/ Male	4/1	24/38	**5.5714**	**0.1151****	0.6575- 47.2070
Adults					
<20 yrs/ >20 yrs	0/5	6/48	0.7013	0.8029	0.0432- 11.3721
<30 yrs/ >30 yrs	0/5	15/39	0.2557	0.3463	0.0150- 4.3690
<40 yrs/>40 yrs	1/4	35/19	**0.1597**	**0.0911***	0.0190- 1.3413

A relative risk (RR) >1 denotes a relationship of the exposed group with an increase in disease prevalence, whereas RR <1 denotes a relationship of the control group with an increase in disease prevalence.
**= statistically significant (p<0.10). **= statistically significant when considering size of the effect of RR.*

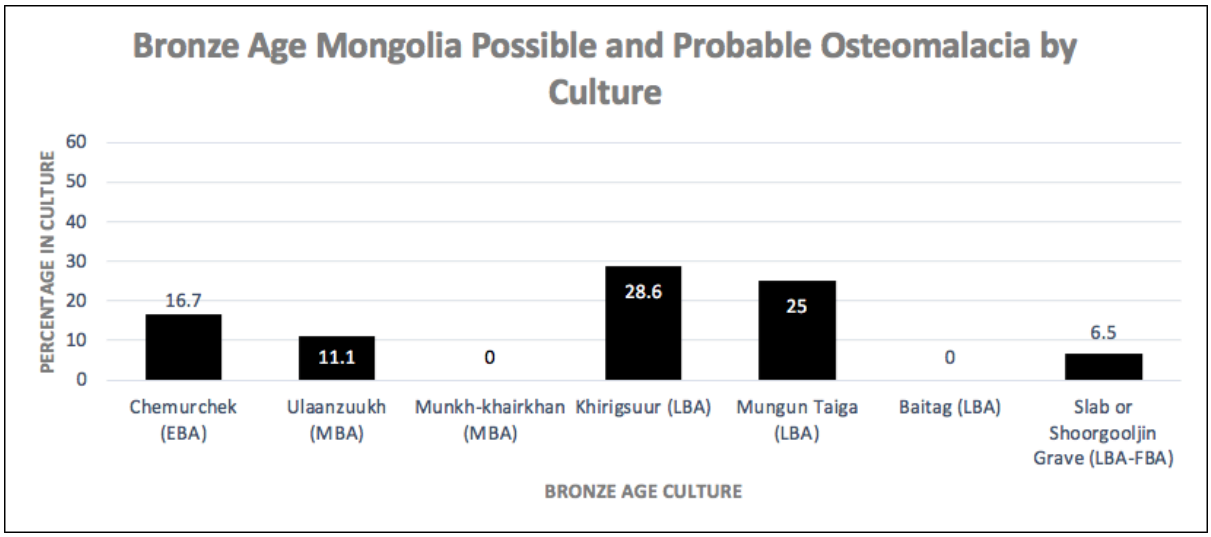

Figure 8.21: *Distribution of possible and probable osteomalacia prevalences across Bronze Age cultures. Image: author's own.*

Table 8.13: *Fisher's exact test for differences in morbidity of osteomalacia across Eastern and Western Mongolia.*

	AFFECTED/ OBSERVED	PERCENTAGE	P-VALUE
Possible and Probable Osteomalacia (combined)			
Eastern Mongolia	4/49	8.2	0.167
Western Mongolia	6/30	20	

*Eastern Mongolian Bronze Age cultures include the Slab Grave and Ulaanzuukh cultures. Western Mongolian Bronze Age cultures include DSKC, Mungun Taiga, Chemruchek, Baitag, and Munkhkhairkhan cultures. *=statistically significant (p<0.05)*

8.4.7 Mortality of Nutritional Disease in the Bronze Age

8.4.7.1 Mortality of Scurvy in the Bronze Age

Relative risk ratio analysis identified no significant increase in risk of death for nonadult age cohorts for both combined possible and probable, and probable only scurvy (Table 8.14). Similarly, Kaplan-Meier survival analysis did not identify significantly increased frailty of nonadults with skeletal signs of possible or probable scurvy (n=18, X^2=1.361, df=1, p=0.243; Table 8.15; Figure 8.22) and probable only scurvy (n=18, X^2=0.793, df=1, p=0.373; Table 8.16; Figure 8.23).

Adolescents over the age of 15 years were at a significantly increased risk of death with possible or probable scurvy than adults over 20 years of age. Adolescents were over 9 times more likely to die with possible or probable scurvy than adults (n=59, RR=9.1667, p=0.0004). Additionally, adults were still 2.8 times more likely to die with skeletal signs of possible or probable scurvy under the age of 30 years, which was statistically significant. However, Kaplan-Meier survival analysis did not identify statistically increased frailty of adults with skeletal evidence of possible or probable scurvy (n=59, X^2=0.317, df=1, p=0.573; Table 8.17; Figure 8.24). The outcome of the relative risk ratio analysis was likely a result of the increased risk of death in adolescents prior to adulthood with scurvy. Overall, while within nonadult and adult age cohorts, scurvy did not appear to increase risk of death, the presence of skeletal signs of scurvy appears to have been related to death prior to reaching adulthood.

Table 8.14: *Relative risk of scurvy mortality in the Bronze Age across age cohorts.*

POSITIVE OUTCOME/ NEGATIVE OUTCOME	**TREATMENT**		**RR**	**P-VALUE**	**95%CI**
	Exposed Group: ***Disease Present***	*Control Group:* ***Disease Absent***			
Possible and Probable Scurvy (combined)					
Nonadults					
<1 yr/ >1 yr	2/7	2/7	1.000	1.000	0.1775- 5.6325
<5 yrs/ >5yrs	4/5	2/7	2.000	0.3400	0.4815- 8.3066
<10 yrs/ >10yrs	6/3	3/6	2.000	0.1885	0.7119- 5.6190
Adults					
<20 yrs/ >20 yrs	2/1	4/51	**9.1667**	**0.0004***	2.6600- 31.5899
<30 yrs/ >30 yrs	2/1	13/42	**2.8718**	**0.0264***	1.1317- 7.2875
<40 yrs/>40 yrs	2/1	34/21	1.0784	0.8579	0.4718- 2.4650

POSITIVE OUTCOME/ NEGATIVE OUTCOME	TREATMENT		RR	P-VALUE	95%CI
	Exposed Group: ***Disease Present***	*Control Group:* ***Disease Absent***			
Probable Only Scurvy					
Nonadults					
<1 yr/ >1 yr	2/4	2/10	2.000	0.4235	0.3663- 10.9196
<5 yrs/ >5yrs	3/3	3/9	2.000	0.2829	0.5644- 7.0874
<10 yrs/ >10yrs	4/2	5/7	1.600	0.2933	0.3663- 3.8441

A relative risk (RR) >1 denotes a relationship of the disease presence with the positive outcome (susceptibility to mortality), whereas RR <1 denotes a relationship of the disease absence with a negative outcome (survivorship).
**= statistically significant (p<0.10). **= statistically significant when considering size of the effect of RR.*

Table 8.15: *Statistical summary for Kaplan-Meier function of possible and probable scurvy mortality of nonadults in Bronze Age Mongolia.*

POSSIBLE AND PROBABLE SCURVY	ESTIMATE	STD. ERROR	95% CI	LOG RANK (MANTEL-COX)		
				CHI SQUARE	DF	P-VALUE
Mean				1.361	1	0.243
Absent	11.944	2.434	7.173- 16.716			
Present	7.444	2.349	2.841- 12.048			
Overall	9.694	1.729	6.305- 13.084			
Median						
Absent	14.500	1.491	11.578- 17.422			
Present	6.500	5.217	0.000- 16.726			
Overall	8.500	5.303	0.000- 18.894			

**= statistical significance (p<0.15).*

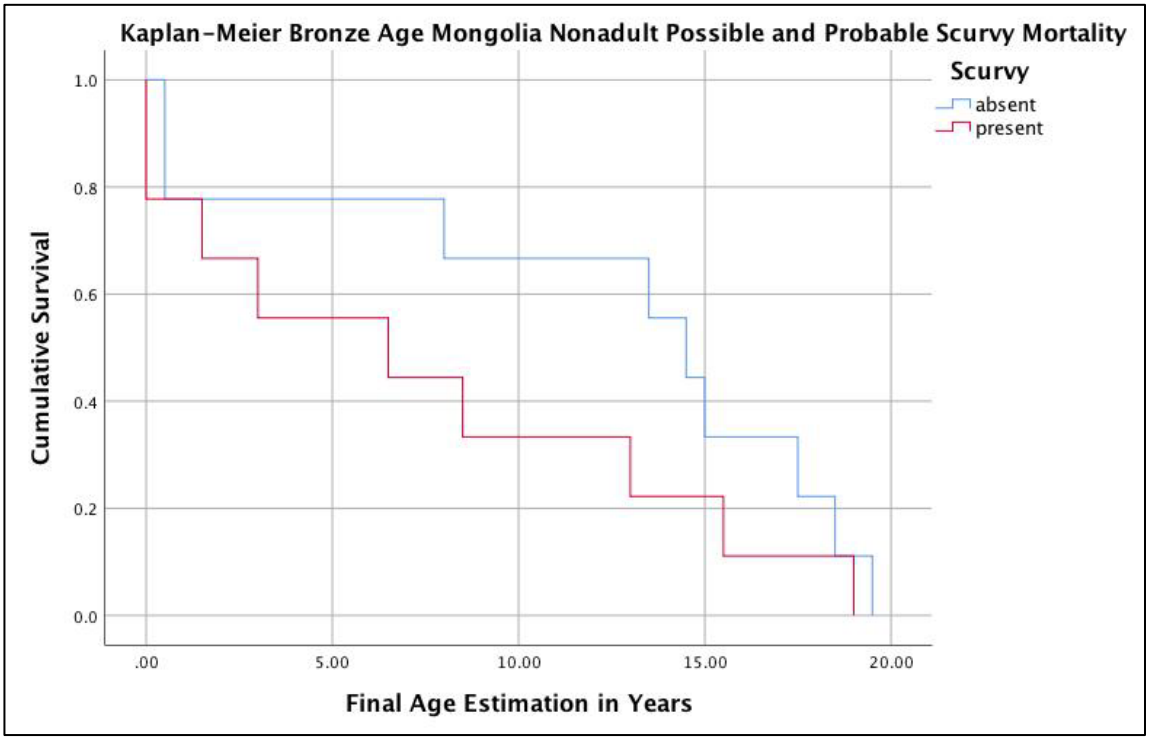

Figure 8.22: *Kaplan-Meier cumulative survival function of nonadult possible and probable scurvy mortality in Bronze Age Mongolia. Image: author's own.*

Table 8.16: *Statistical summary for Kaplan-Meier function of probable scurvy mortality of nonadults in Bronze Age Mongolia.*

PROBABLE SCURVY	ESTIMATE	STD. ERROR	95% CI	LOG RANK (MANTEL-COX)		
				CHI SQUARE	DF	P-VALUE
Mean				0.793	1	0.373
Absent	11.231	1.886	7.534- 14.927			
Present	5.700	3.534	0.000- 12.627			
Overall	9.694	1.729	6.305- 13.084			
Median						
Absent	13.500	3.595	6.454- 20.546			
Present	3.000	3.286	0.000- 9.441			
Overall	8.500	5.303	0.000- 18.894			

**= statistical significance (p<0.15).*

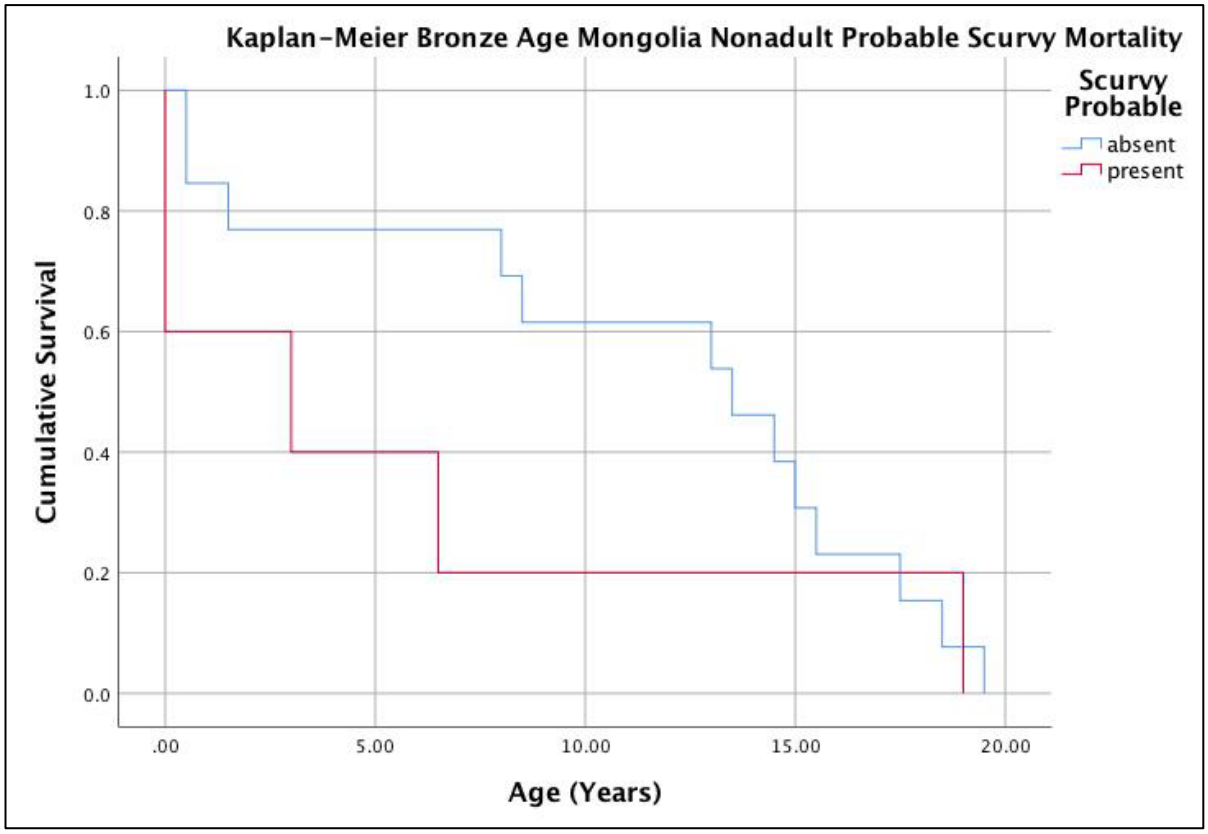

Figure 8.23: *Kaplan-Meier cumulative survival function of nonadult probable scurvy mortality in Bronze Age Mongolia. Image: author's own.*

Table 8.17: *Statistical summary for Kaplan-Meier function of possible and probable scurvy mortality of adults in Bronze Age Mongolia.*

POSSIBLE AND PROBABLE SCURVY	ESTIMATE	STD. ERROR	95% CI	LOG RANK (MANTEL-COX)		
				CHI SQUARE	DF	P-VALUE
Mean				0.317	1	0.573
Absent	36.545	1.364	33.873- 39.218			
Present	27.667	10.203	7.668- 47.665			
Overall	36.068	1.388	33.365- 38.807			
Median						
Absent	35.000	2.057	30.968- 39.032			
Present	19.000	2.449	14.199- 23.801			
Overall	35.000	2.110	30.864- 39.136			

**= statistical significance (p<0.15).*

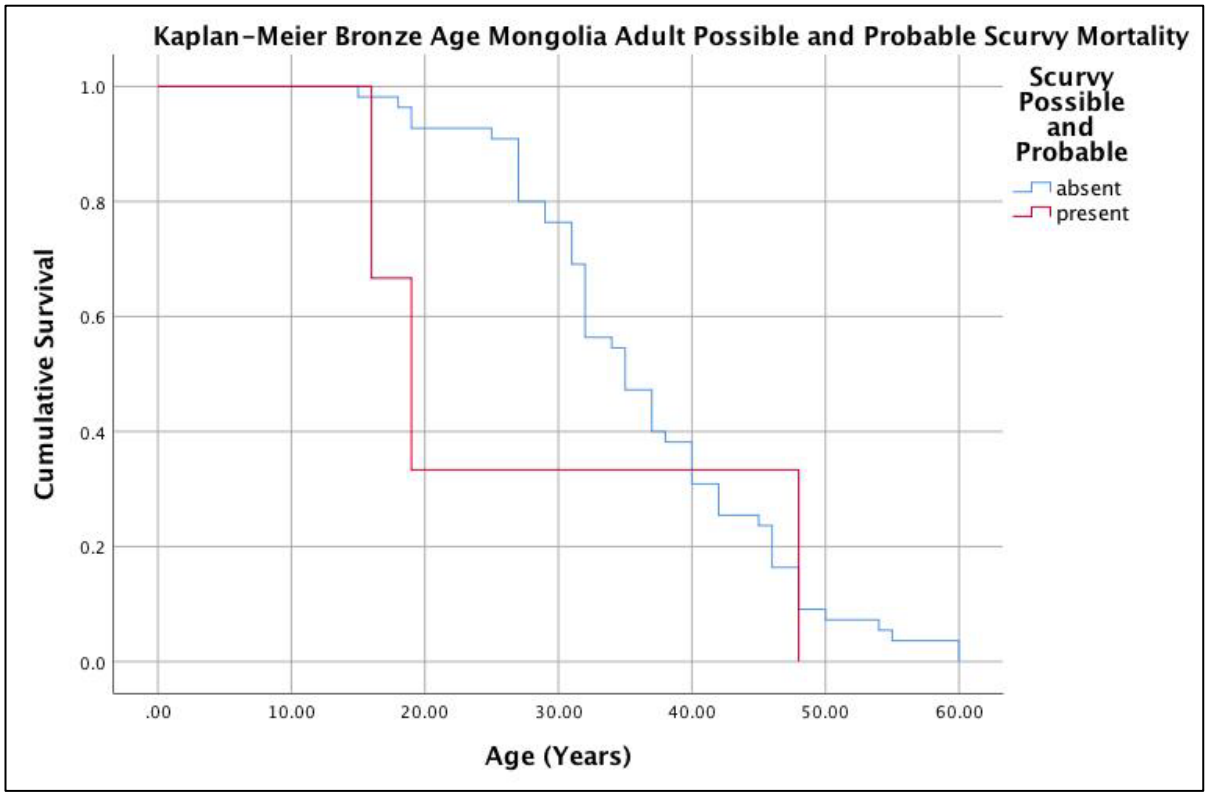

Figure 8.24: *Kaplan-Meier cumulative survival function of adult possible and probable scurvy mortality in Bronze Age Mongolia. Image: author's own.*

8.4.7.2 Mortality of Rickets and Residual Rickets in the Bronze Age

No statistically significant increases in mortality were identified in nonadults with skeletal signs of combined possible and probable or probable only rickets in both relative risk ratio analysis and Kaplan-Meier survivorship analysis (Tables 8.18- 8.20; Figures 8.25- 8.26).

A statistically significant decrease in risk of death was identified for adults over the age of 40 years of age (n=53, RR=0.4242, p=0.0899). However, Kaplan-Meier survival analysis did not produce a statistically significant result (n=53, X^2=0.978, df=1, p=0.323; Table 8.21; Figure 8.27). Overall, a weak relationship with increased survivorship of adults with skeletal signs of residual rickets to old age has been identified.

Table 8.18: *Relative risk of rickets mortality in the Bronze Age across age cohorts*

POSITIVE OUTCOME/ NEGATIVE OUTCOME	**TREATMENT**		**RR**	**P-VALUE**	**95%CI**
	Exposed Group: *Disease Present*	***Control Group:*** *Disease Absent*			
Possible and Probable Rickets (combined)					
Nonadults					
<1 yr/ >1 yr	1/5	3/9	0.5000	0.4882	0.0704- 3.5497
<5 yrs/ >5yrs	1/5	5/7	0.4000	0.3472	0.0592- 2.7022
<10 yrs/ >10yrs	3/3	7/5	0.5714	0.3719	0.1673- 1.9520
Probable Only Rickets					
Nonadults					
<1 yr/ >1 yr	0/2	4/12	0.6296	0.7324	0.0444- 8.9251
<5 yrs/ >5yrs	0/2	6/10	0.4359	0.5316	0.0323- 5.8775
<10 yrs/ >10yrs	0/2	9/7	0.2982	0.3553	0.0229- 3.8788
Possible and Probable Residual Rickets (combined)					
Adults					
<20 yrs/ >20 yrs	-	-	-	-	-
<30 yrs/ >30 yrs	0/11	10/32	0.1706	0.2099	0.0108- 2.7068
<40 yrs/>40 yrs	3/8	27/15	**0.4242**	**0.0899***	0.1575- 1.1429

A relative risk (RR) >1 denotes a relationship of the disease presence with the positive outcome (susceptibility to mortality), whereas RR <1 denotes a relationship of the disease absence with a negative outcome (survivorship).
**= statistically significant (p<0.10). **= statistically significant when considering size of the effect of RR.*

Table 8.19: *Statistical summary for Kaplan-Meier function of possible and probable rickets mortality of nonadults in Bronze Age Mongolia.*

POSSIBLE AND PROBABLE RICKETS	ESTIMATE	STD. ERROR	95% CI	LOG RANK (MANTEL-COX)		
				CHI SQUARE	DF	P-VALUE
Mean				0.018	1	0.892
Absent	8.625	2.245	4.226- 13.024			
Present	11.833	2.638	6.662- 17.005			
Overall	9.694	1.729	6.305- 13.084			
Median						
Absent	6.500	4.330	0.000- 14.987			
Present	13.000	3.980	5.198- 20.802			
Overall	8.500	5.303	0.000- 18.894			

**= statistical significance (p<0.15).*

Table 8.20: *Statistical summary for Kaplan-Meier function of probable rickets mortality of nonadults in Bronze Age Mongolia.*

PROBABLE RICKETS	ESTIMATE	STD. ERROR	95% CI	LOG RANK (MANTEL-COX)		
				CHI SQUARE	DF	P-VALUE
Mean				0.058	1	0.810
Absent	8.733	1.986	4.840- 12.626			
Present	14.500	0.764	13.003- 15.997			
Overall	9.694	1.729	6.305- 13.084			
Median						
Absent	8.000	3.542	1.057- 14.943			
Present	15.000	1.633	11.799- 18.201			
Overall	8.500	5.303	0.000- 18.894			

**= statistical significance (p<0.15).*

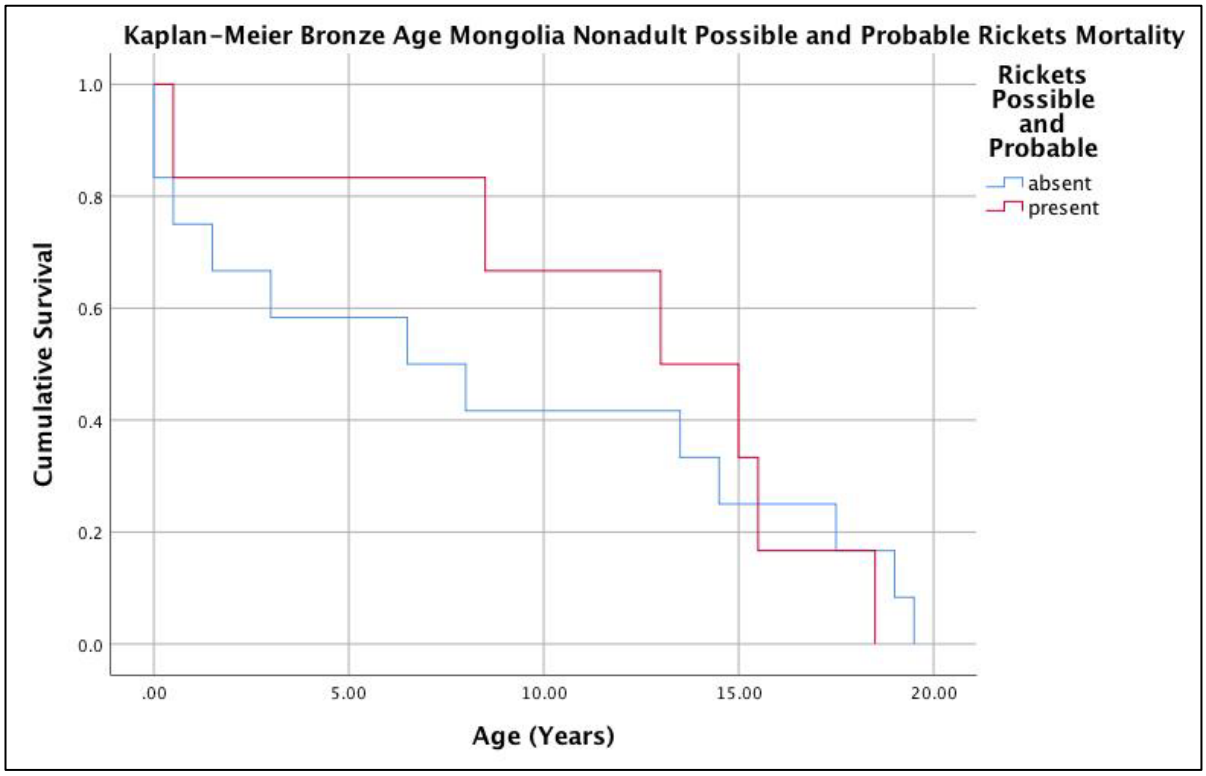

Figure 8.25: *Kaplan-Meier cumulative survival function of nonadult possible and probable rickets mortality in Bronze Age Mongolia. Image: author's own.*

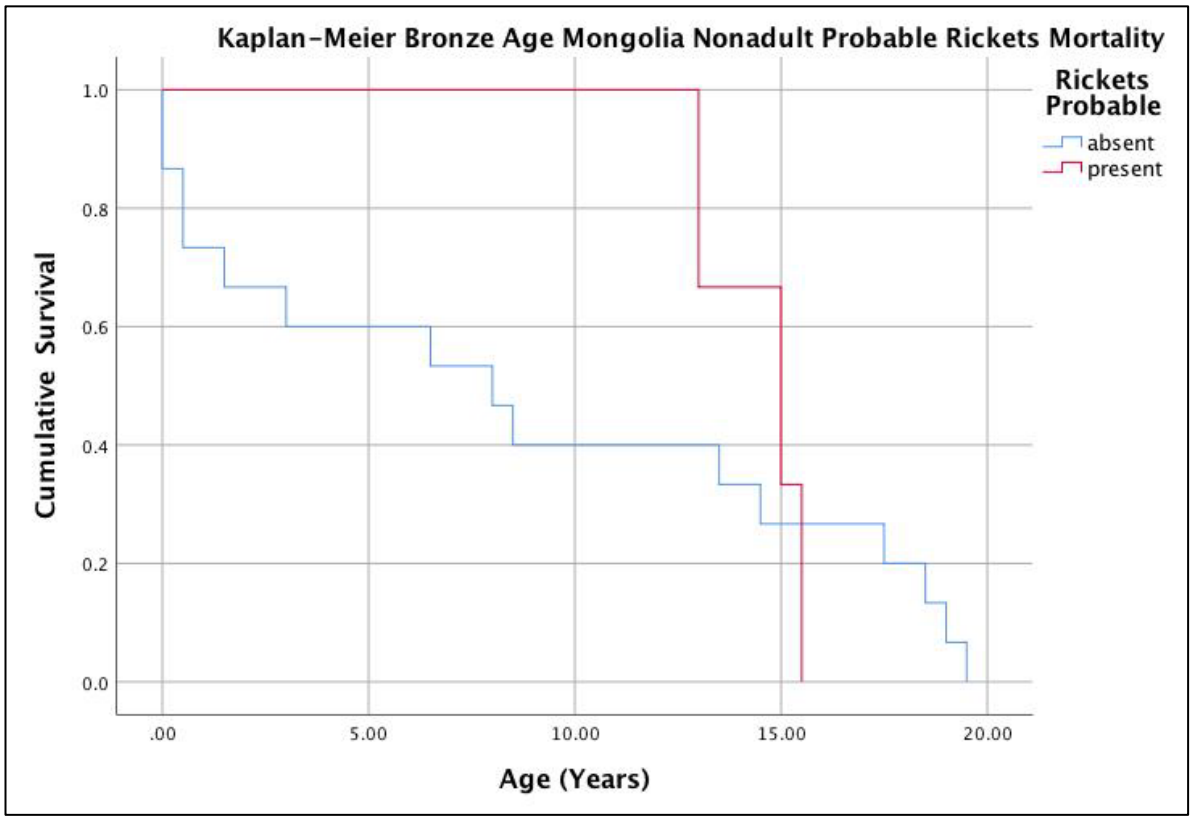

Figure 8.26: *Kaplan-Meier cumulative survival function of nonadult probable rickets mortality in Bronze Age Mongolia. Image: author's own.*

Table 8.21: *Statistical summary for Kaplan-Meier function of possible and probable residual rickets mortality of adults in Bronze Age Mongolia.*

POSSIBLE AND PROBABLE RESIDUAL RICKETS	ESTIMATE	STD. ERROR	95% CI	LOG RANK (MANTEL-COX)		
				CHI SQUARE	DF	P-VALUE
Mean				0.978	1	0.323
Absent	37.347	1.448	34.509- 40.184			
Present	41.432	2.168	37.182- 45.682			
Overall	38.211	1.243	35.774- 40.648			
Median						
Absent	33.205	1.018	33.205- 37.195			
Present	36.389	2.863	36.389- 47.611			
Overall	34.762	1.142	34.762- 39.238			

*****= *statistical significance (p<0.15).*

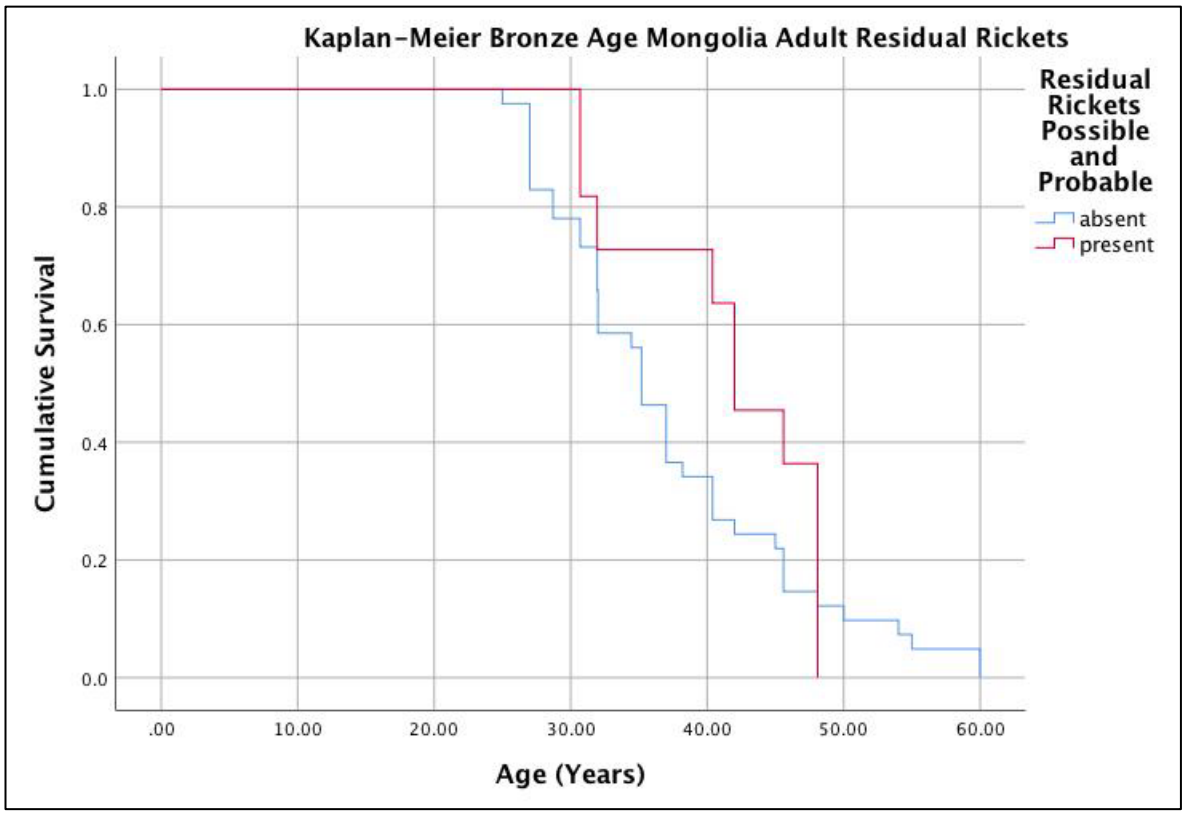

Figure 8.27: *Kaplan-Meier cumulative survival function of adult possible and probable residual rickets mortality in Bronze Age Mongolia. Image: author's own.*

8.4.7.3 Mortality of Osteomalacia in the Bronze Age

A statistically significant decreased risk of death of adults over the age of 40 years with possible and probable osteomalacia was observed with risk ratio analysis (n=59, RR=0.3268, p=0.0764; Table 8.22). Adults were over three times more likely to survive over the age of 40 years with skeletal signs of possible or probable osteomalacia. A similar

outcome was observed when only probable cases of osteomalacia were considered (n=59, RR=0.3086, p=0.1914).

However, Kapan-Meier analysis did not identify any significant increases in survivorship of those with skeletal signs of possible and probable osteomalacia (n=59, X^2=1.544, df=1, p=0.214; Table 8.23: Figure 8.28), as well as those with probable osteomalacia (n=59, X^2=1.469, df=1, p=0.225; Table 8.24: Figure 8.29). As was the case with residual rickets, a weak relationship with survivorship to old age of adults with skeletal signs of osteomalacia has been identified.

Table 8.22: *Relative risk of osteomalacia mortality in the Bronze Age across age cohorts.*

POSITIVE OUTCOME/ NEGATIVE OUTCOME	**TREATMENT**		**RR**	**P-VALUE**	**95%CI**
	Exposed Group: *Disease Present*	***Control Group:*** *Disease Absent*			
Possible and Probable Osteomalacia (combined)					
Adults					
<20 yrs/ >20 yrs	1/8	5/45	1.1111	0.9188	0.1465- 8.4296
<30 yrs/ >30 yrs	1/8	14/36	0.3968	0.3405	0.0593- 2.6548
<40 yrs/>40 yrs	2/7	34/15	**0.3268**	**0.0764***	0.0949- 1.1259
Probable Only Osteomalacia					
Adults					
<20 yrs/ >20 yrs	0/5	6/48	0.7051	0.8034	0.0451- 11.0333
<30 yrs/ >30 yrs	0/5	15/39	0.2957	0.3742	0.0201- 4.3439
<40 yrs/>40 yrs	1/4	35/19	**0.3086**	**0.1914****	0.0529- 1.8008

A relative risk (RR) >1 denotes a relationship of the disease presence with the positive outcome (susceptibility to mortality), whereas RR <1 denotes a relationship of the disease absence with a negative outcome (survivorship).
**= statistically significant (p<0.10). **= statistically significant when considering size of the effect of RR.*

Table 8.23: *Statistical summary for Kaplan-Meier function of possible and probable osteomalacia mortality of adults in Bronze Age Mongolia.*

POSSIBLE AND PROBABLE OSTEOMALACIA	**ESTIMATE**	**STD. ERROR**	**95% CI**	**LOG RANK (MANTEL-COX)**		
				CHI SQUARE	**DF**	**P-VALUE**
Mean				1.544	1	0.214
Absent	35.327	1.490	32.407- 38.246			
Present	40.222	3.670	33.030- 47.415			
Overall	36.086	1.388	33.365- 38.807			
Median						
Absent	34.000	1.166	31.714- 36.286			
Present	42.000	1.491	39.078- 44.922			
Overall	35.000	2.110	30.864- 39.136			

**= statistical significance (p<0.15).*

Table 8.24: *Statistical summary for Kaplan-Meier function of probable osteomalacia mortality of adults in Bronze Age Mongolia.*

PROBABLE OSTEOMALACIA	ESTIMATE	STD. ERROR	95% CI	LOG RANK (MANTEL-COX)		
				CHI SQUARE	DF	P-VALUE
Mean				1.469	1	0.225
Absent	35.434	1.461	32.571- 38.297			
Present	43.000	3.376	36.382- 49.618			
Overall	36.086	1.388	33.365- 38.807			
Median						
Absent	35.000	1.203	32.643- 37.357			
Present	48.000	0.000	-			
Overall	35.000	2.110	30.864- 39.136			

**= statistical significance (p<0.15).*

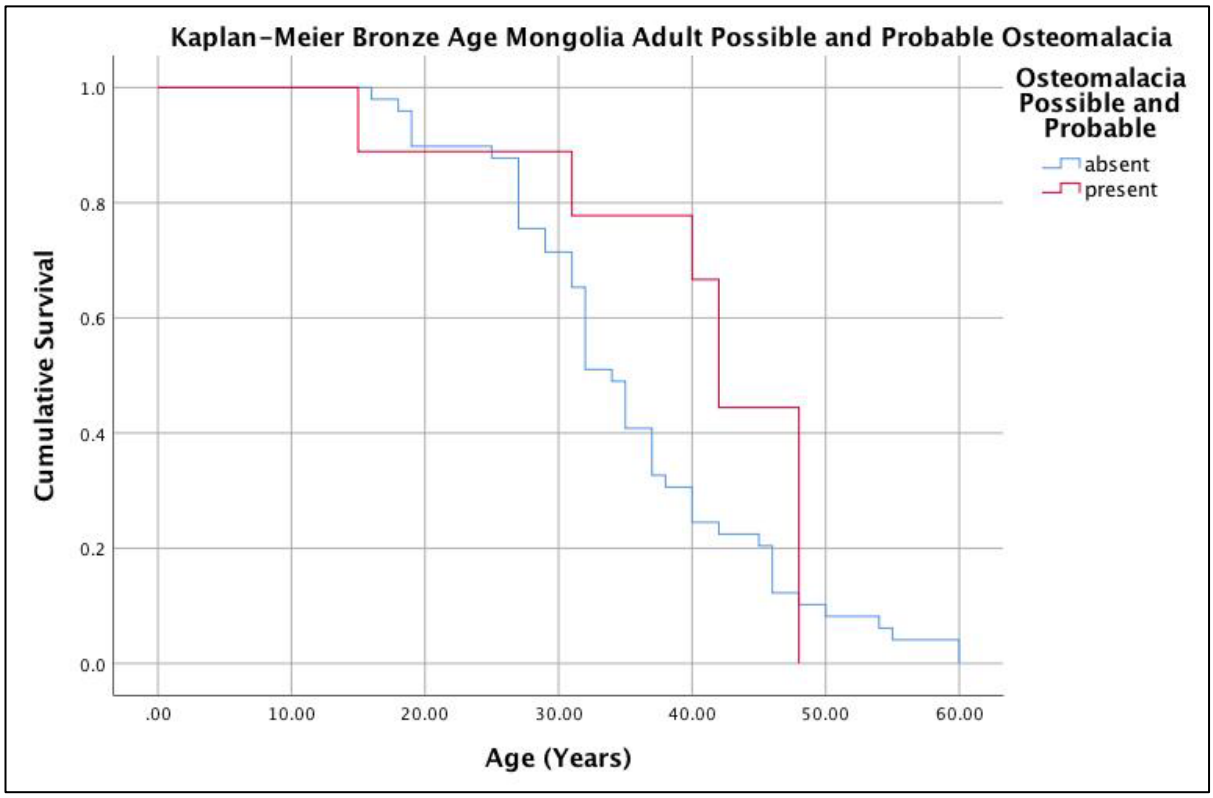

Figure 8.28: *Kaplan-Meier cumulative survival function of adult possible and probable osteomalacia mortality in Bronze Age Mongolia. Image: author's own.*

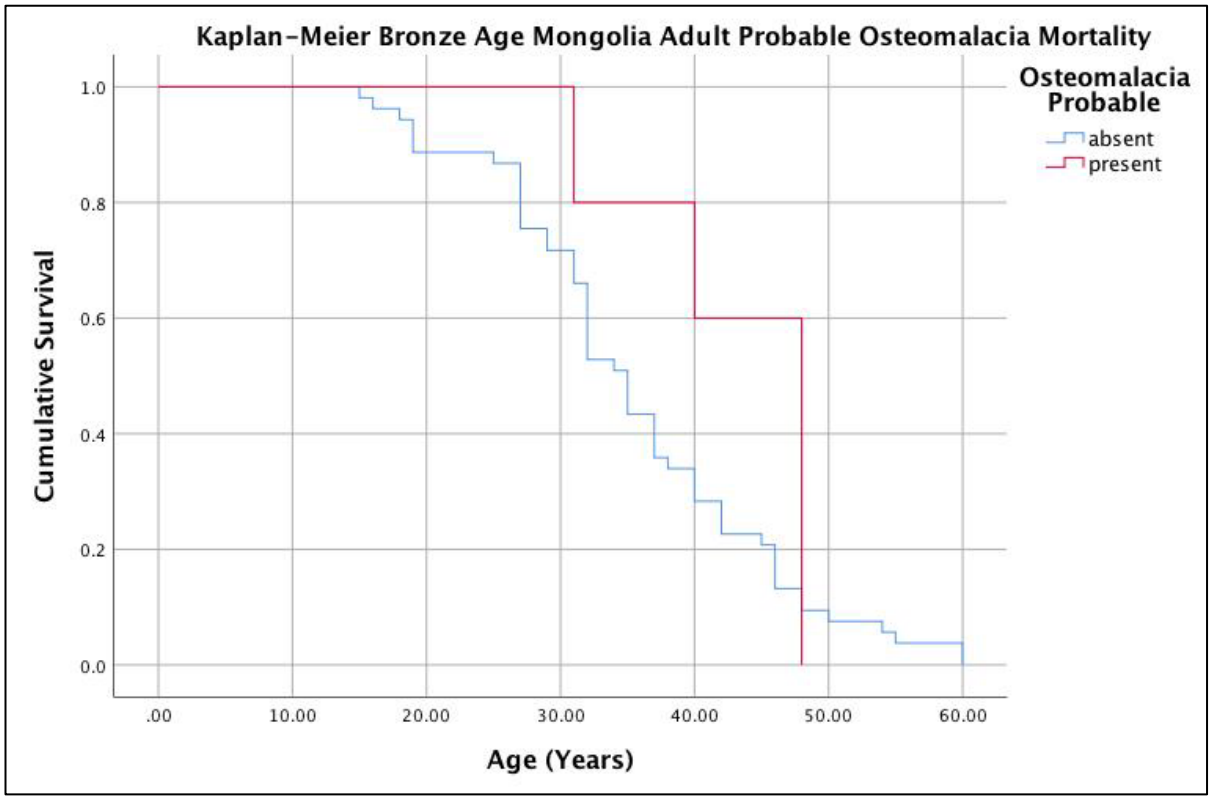

Figure 8.29: *Kaplan-Meier cumulative survival function of adult probable osteomalacia mortality in Bronze Age Mongolia. Image: author's own.*

8.4.8 Diagnosis of Anaemia in the Bronze Age

Less than one-third (30.4%, 9/30) of Bronze Age Mongolian adults, and only one individual under 20 years of age (Khovd 10-5, male, ~19 years) presented with medium or severe grade cribra orbitalia and/or porotic hyperostosis consistent with a diagnosis of anaemia (Table 8.25; Figure 8.30). Moderate or severe grade cribra orbitalia (21.7%, 5/23) was more prevalent than porotic hyperostosis (8.7%, 2/23) in the Bronze Age adults. There was no particular trend apparent in the prevalence of anaemia across adult age cohorts (Figure 8.31).

Table 8.25: *Summary of anaemia in the Bronze Age*

ANAEMIA	CO			Cranial PH			PH and/or CO		
	Affected	*Observed*	*(%)*	*Affected*	*Observed*	*(%)*	*Affected*	*Observed*	*(%)*
15 to 20 years	0	2	0	1	2	50	1	2	50
20 to 30 years	0	4	0	0	4	0	0	4	0
30 to 40 years	2	4	50	2	4	50	3	4	75
40 to 50 years	0	4	0	0	4	0	0	4	0
50+ years	4	8	50	0	8	0	4	8	50
Total nonadults	0	7	0	1	7	14.3	1	7	14.3
Males	2	10	20	3	10	30	4	10	40
Females	4	13	30.8	0	10	0	4	13	30.8
Total adults	5	23	21.7	2	23	8.7	7	23	30.4
Total	5	30	16.7	3	30	10	8	30	26.7

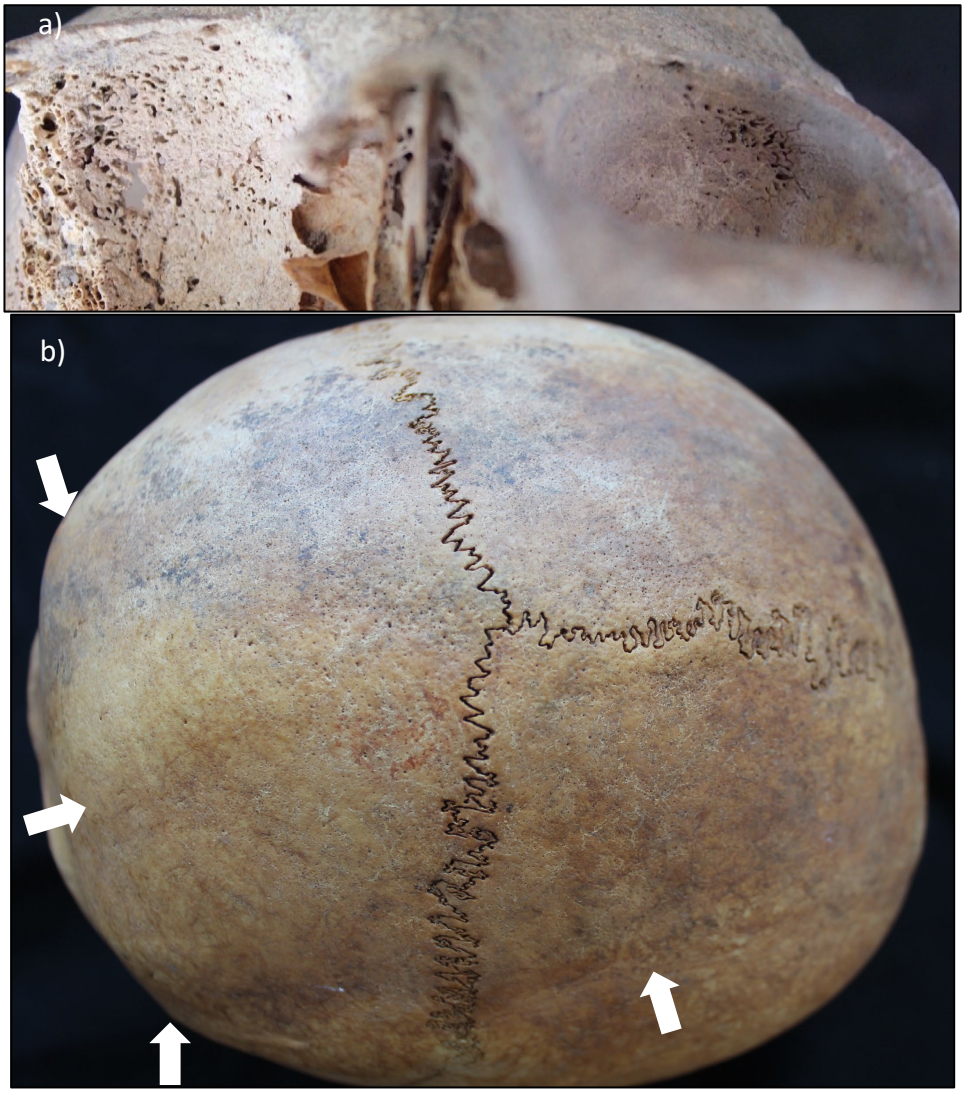

Figure 8.30: *Lesions consistent with anaemia in the Bronze Age assemblage. a) moderate cribra orbitalia. There is postmortem damage on the right orbit (AT-921, old aged adult female, Ulaanzuukh culture). b) porotic hyperostosis of the crania vault. Note the diploic expansion on the frontal and parietal bones (white arrows, Khovd 10-5, male, ~19 years).*

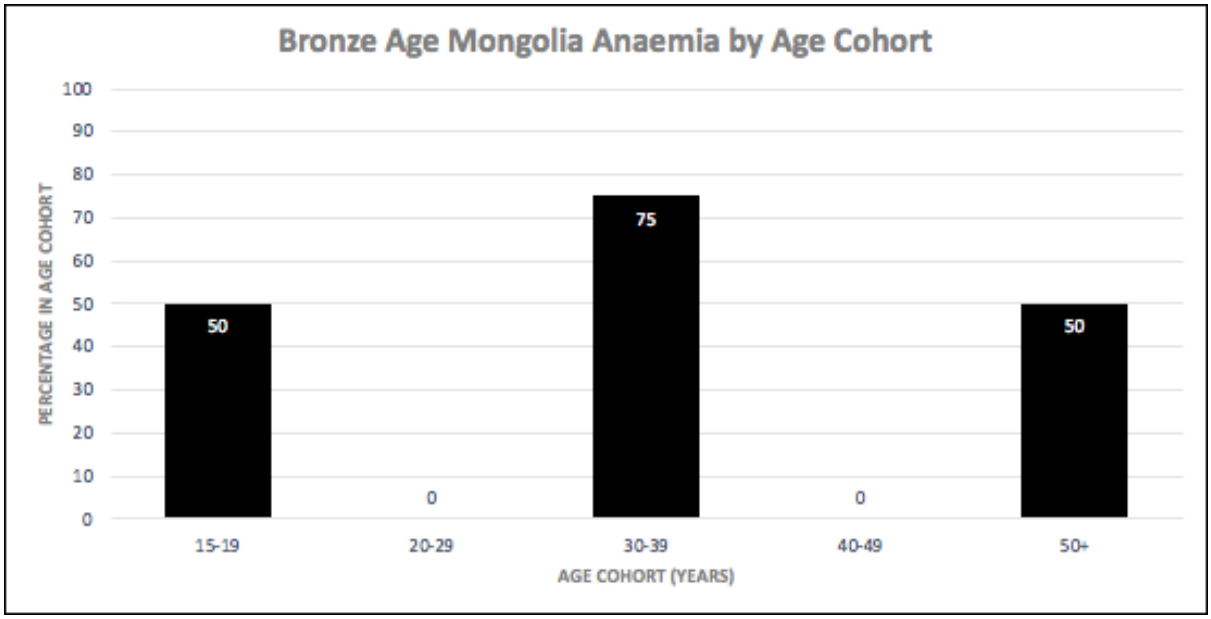

Figure 8.31: *Age-at-death distribution of anaemia in Bronze Age Mongolia. Image: author's own.*

8.4.9 Morbidity of Anaemia in the Bronze Age

No statistically significant differences in the morbidity of anaemia were identified between sex and adult age cohorts (Table 8.26). No temporal or spatial trends were apparent across the Bronze Age cultures (Figure 8.32). Additionally, Fisher's exact identified no significant differences in prevalence of anaemia between Western and Eastern Bronze Age Mongolian cultures (n=30, p=0.215; Table 8.27).

Table 8.26: *Relative risk of anaemia morbidity in the Bronze Age across sex and age cohorts*

EXPOSED GROUP/ CONTROL GROUP	**OUTCOME**		**RR**	**P-VALUE**	**95%CI**
	Positive: *Anaemia Present*	***Negative:*** *Anaemia Absent*			
Sex					
Female/ Male	4/4	9/6	0.7692	0.6444	0.2525- 2.3436
Adults					
<20 yrs/ >20 yrs	1/7	1/13	1.4286	0.6432	0.3159- 6.4612
<30 yrs/ >30 yrs	1/7	5/9	0.3810	0.3127	0.0585- 2.4804
<40 yrs/>40 yrs	4/4	6/8	1.2000	0.7459	0.3983- 3.6157

A relative risk (RR) >1 denotes a relationship of the exposed group with an increase in disease prevalence, whereas RR <1 denotes a relationship of the control group with an increase in disease prevalence.
**= statistically significant (p<0.10). **= statistically significant when considering size of the effect of RR.*

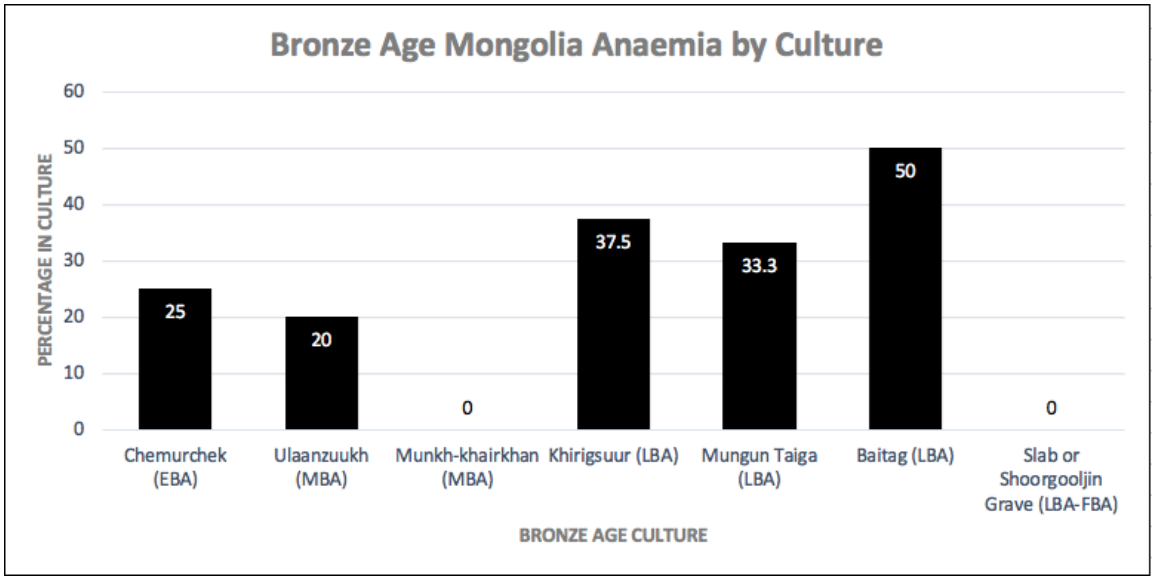

Figure 8.32: *Distribution of anaemia prevalences across Bronze Age cultures. Image: author's own.*

Table 8.27: *Fisher's exact test for differences in morbidity of anaemia across Eastern and Western Mongolia.*

INFECTIOUS DISEASE	AFFECTED/ OBSERVED	PERCENTAGE	P-VALUE
Eastern Mongolia	1/11	9.1	0.215
Western Mongolia	6/19	31.6	

*Eastern Mongolian Bronze Age cultures include the Slab Grave and Ulaanzuukh cultures. Western Mongolian Bronze Age cultures include DSKC, Mungun Taiga, Chemruchek, Baitag, and Munkhkhairkhan cultures. *=statistically significant (p<0.05)*

8.4.10 Mortality of Anaemia in the Bronze Age

Relative risk ratio analysis identified no statistically significant increases in the risk of death of adults with skeletal signs of anaemia (Table 8.28). This outcome was supported by the Kaplan-Meier survival analysis (n=22, X^2=1.665, df=1, p=0.197; Table 8.29). Similar trends in mortality of those with and without skeletal signs of childhood anaemia is apparent by the Kaplan-Meier cumulative function (Figure 8.33).

Table 8.28: *Relative risk of anaemia mortality in the Bronze Age across age cohorts.*

POSITIVE OUTCOME/ NEGATIVE OUTCOME	TREATMENT		RR	P-VALUE	95%CI
	Exposed Group: *Poss. IDA Present*	***Control Group:*** *Poss. IDA Absent*			
Adults					
<20 yrs/ >20 yrs	1/7	1/13	1.7500	0.6769	0.1259- 24.3331
<30 yrs/ >30 yrs	1/7	5/9	0.3500	0.2947	0.0491- 2.4935
<40 yrs/>40 yrs	4/4	6/8	1.1167	0.7426	0.4650- 2.9270

A relative risk (RR) >1 denotes a relationship of the disease presence with the positive outcome (susceptibility to mortality), whereas RR <1 denotes a relationship of the disease absence with a negative outcome (survivorship).
**= statistically significant (p<0.10). **= statistically significant when considering size of the effect of RR.*

Table 8.29: *Statistical summary for Kaplan-Meier function of anaemia mortality of adults in Bronze Age Mongolia.*

INFECTIOUS DISEASE	ESTIMATE	STD. ERROR	95% CI	LOG RANK (MANTEL-COX)		
				CHI SQUARE	DF	P-VALUE
Mean				1.665	1	0.197
Absent	40.458	2.225	36.098- 44.819			
Present	42.479	5.438	31.820- 53.137			
Overall	41.203	2.365	36.567- 45.839			
Median						
Absent	40.400	2.194	36.100- 44.700			
Present	48.100	7.709	32.990- 63.210			
Overall	42.000	3.700	34.748- 49.525			

**= statistical significance (p<0.15).*

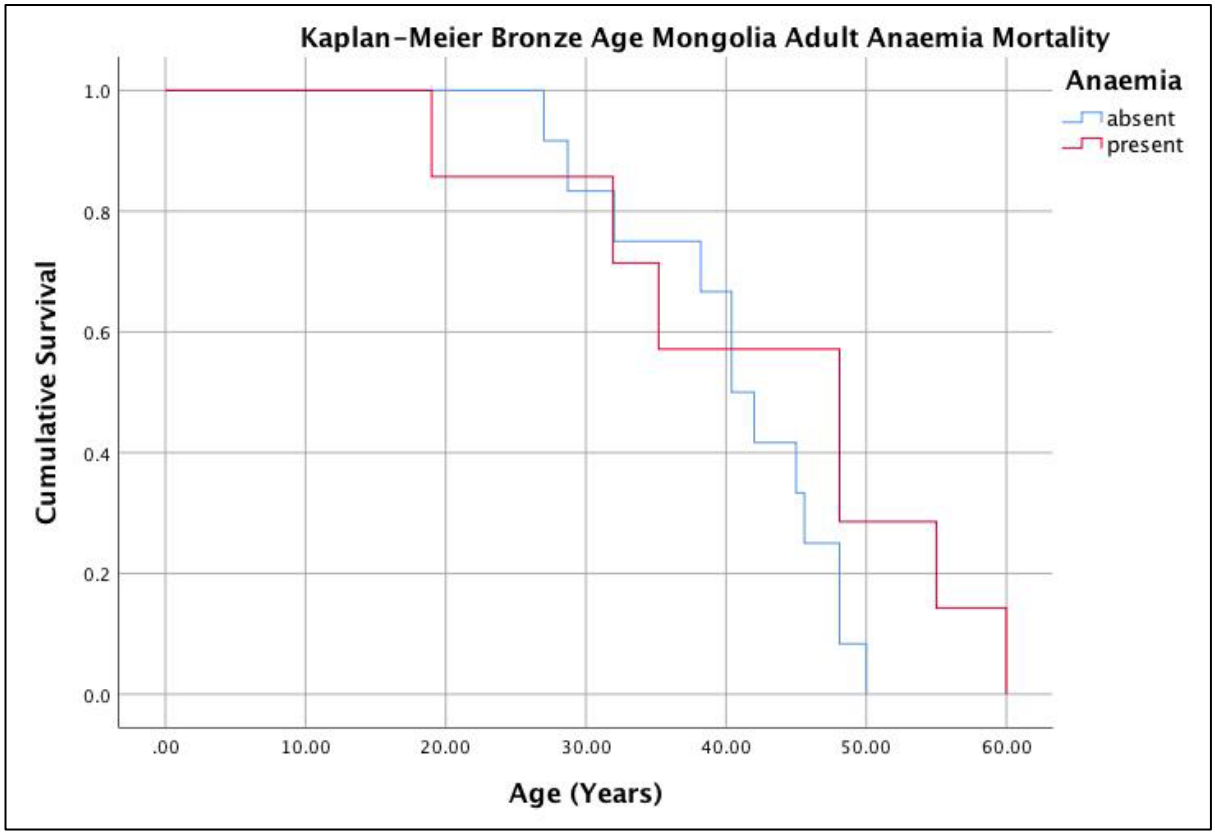

Figure 8.33: *Kaplan-Meier cumulative survival function of adult anaemia mortality in Bronze Age Mongolia. Image: author's own.*

8.4.11 Summary of Diagnosis and Context of Disease in the Bronze Age

In comparison to assemblages presented in previous chapters, a low burden of infectious disease (4.3%, 4/92), scurvy (13.1%, 12/92) and childhood anaemia (26.7%, 8/30) was observed in the Bronze Age Mongolian assemblage. However, there was also evidence

for widespread mineralisation disorders throughout the Bronze Age in the form of rickets (33.3%, 6/18), residual rickets (20.3%, 15/74) and osteomalacia (12.2%, 9/74).

8.4.11.1 Hydatids Disease in the Bronze Age

Hydatids disease is strongly linked to pastoral communities due to the intricate relationship between livestock and humans (Beggs 1985; Deplazes et al. 2017). Given that alveolar and cystic hydatids disease can cause identical bone changes it is not possible to confidently determine which disease has caused the skeletal changes observed in AT-630. Both are found in Mongolia today, although the prevalence of cystic hydatids is significantly higher (Deplazes et al. 2017). Watson-Jones et al. (1997) found 5.2% of randomly tested nomadic pastoralists from North-western Mongolia tested positive for *Echinococcus granulosis* (cystic hydatids) antibodies. Cystic hydatids disease has also been reported in the Lake Baikal region of Siberia, adjacent to the region of Northern Mongolia as early as 8000 years ago (Waters-Rist et al. 2014). Alveolar hydatids disease has a demonstrably lower relationship with pastoral livestock as it is usually restricted to infection from sylvatic hosts (Deplazes et al. 2017). However, overgrazing of pastoral livestock can make the habitat more favourable for sylvatic intermediate hosts such as pika, mole rats and voles (Wang et al. 2007).

While a number of livestock can be infected with cystic hydatids disease, the most common intermediate host for hydatids disease is sheep (Agarwal et al. 1992; Song et al. 2007). The presence of sheep dairy proteins in the dental calculus of Chemurchek individuals strongly suggests pastoral husbandry of sheep were undertaken in this population (Wilkin et al. 2020b). Given that the Chemurchek are one of the earliest pastoral cultures in the Eastern Eurasian Steppe (5000-3700 cal BP) signifies that zoonotic diseases were present even in the earliest forms of pastoralism in Mongolia (Taylor et al. 2019).

Hydatids disease does not arise without a carnivorous definitive host, and the identification of sheep livestock in the Chemurchek does not completely explain the presence of the disease in a human. Both domestic and wild canids acting as definitive hosts are a possibility. Today Mongolian livestock are often herded by dogs, and the offal of livestock fed to dogs greatly increases the risk of infection of definitive hosts (Watson-Jones et al. 1997). The possibility of domesticated dogs in Mongolian Bronze Age cultures is

intriguing. As the eggs of *Echinococcus granulosis* die within two hours of initial expulsion during defecation, the risk of transmission increases significantly with close interactions between humans and domesticated dogs (Macpherson 1995). Broderick and Houle (2013) have identified the presence of *Canis familiaris* (domesticated dog) teeth in a Khirigsuur archaeozoological assemblage from Central Mongolia. Therefore, domestic dog was present by at least the Late Bronze Age in Mongolia. Wolves and foxes raiding or scavenging infected sheep, and sharing the same water sources as humans does however, remain a possible source of infection (Deplazes et al. 2017).

While skeletal hydatids disease is often fatal, the old age of the individual is reasonable given that the cystic strain can lie dormant for decades prior to infection of bone (Agarwal et al. 1992). This is not the case for alveolar hydatids that is often fatal (Deplazes et al. 2017). Transmission of hydatids disease has been intricately tied to nomadic pastoral practices that involve the seasonal movement and interaction of both human and livestock populations. Cystic hydatids disease is found in higher prevalences in migrating compared to non-migrating pastoralists (Macpherson 1995). Persistence of hydatids disease is maintained between cross interactions of large numbers of dogs and livestock of different human groups (Macpherson 1995). In this instance, the diseases likely spread through contact between different livestock of high population densities, and then the contact of newly infected livestock to humans.

8.4.11.2 Brucellosis or Tuberculosis in the Bronze Age

As is the case with hydatids disease, brucellosis is also associated with pastoral communities as it is commonly spread to humans through infected milk (Nicoletti 2012). Therefore, it is conceivable that the disease was present in pastoral communities in Bronze Age Mongolia. Moreover, the second highest prevalence of brucellosis in the world is recorded in Mongolia today (Tsend et al. 2014). In one study, prevalence of human brucellosis was determined to be as high as 22.6% in some rural provinces and almost 40% of nomadic camps had at least one seropositive individual (Tsend et al. 2014).

Depending on the pathogen species, a wide number of ruminants including cattle, sheep, and goats, can be infected with brucellosis (Nicoletti 2012). While no individuals from the Mungun Taiga culture have been analysed for dairy proteins in dental calculus,

dairy proteins from goat and sheep milk were identified in the DSKC culture, thought to be culturally linked to the Mungun Taiga (Wilkin et al. 2020b). Additionally, cattle pastoralism was also prevalent in Western Mongolia at this time (Wilkin et al. 2020b).

Today the persistence of the disease at such a high rate is contingent on the close interactions of pastoralists to their livestock, the consumption of raw milk products, livestock population densities, herding of mixed livestock animals, and interactions of different livestock populations (Racloz et al. 2013). The fission-fusion interaction foundational to a pastoralist lifestyle is a key factor in the transmission of brucellosis from one livestock herd to another, where pastoral land or water sources are shared between herds (Smits 2013).

While the skeletal pathologies of AT-865 (middle aged adult female) are more consistent with brucellosis than tuberculosis, tuberculosis remains a possible candidate for disease. Particularly, the presence of bovine tuberculosis in the Bronze Age assemblage is reasonable. Today livestock prevalence of bovine tuberculosis in Mongolia is approximately 0.1%, compared to 2% for brucellosis (Odontsetseg et al. 2005), and a significantly lower toll on human health has been determined for bovine tuberculosis compared to brucellosis (McFadden et al. 2016). As previously mentioned, bovine tuberculosis was identified by pathological analysis and confirmed by DNA analysis in four individuals from Iron Age South Siberia (3rd to 2nd cen. BC), identifying the presence of bovine tuberculosis in the Altai region immediately following the Bronze Age (Murphy et al. 2009). It is possible bovine tuberculosis was introduced to the Eastern Eurasian region at an earlier time frame given the intense pastoral activities that have emerged in the region as early as 5000 years ago. Additionally, tuberculosis has been identified in Northern China as early as 4500 years ago, although the pathogen type has not been determined (Pechenkina et al. 2007).

8.4.11.3 Scurvy in the Bronze Age

A low prevalence of scurvy in the Bronze Age, with mortality and morbidity skewed towards nonadults indicates that scurvy likely had a negligible impact on the health of Bronze Age Mongolians. It is possible that the presence of scurvy in the Bronze Age demonstrated the extreme of malnutrition affecting few vulnerable individuals. Cyclical food restrictions such as seasonal dynamics of livestock health may have contributed to

possible food shortage at certain times. Zoonotic diseases such as brucellosis are documented to result in spontaneous abortion of animal foetuses as well as reduced fertility, significantly impacting livestock numbers and food production (Nicoletti 2012). The harsh winters of Mongolia is a large contributor to annual livestock death in Mongolia, and extreme climate events causing famine are historically common in the region, contributing to periods of malnutrition (Rao et al. 2015; Zadonina and Aptikaeva 2012).

Overall, the lack of scurvy in the Bronze Age is plausible given the sufficient quality and diversity of food types in the nomad diet. Milk, depending on the amount consumed, can provide adequate amounts of Vitamin C, particularly sheep and goats milk. Sheep milk can provide 43mg/100ml and goats milk 20mg/100ml of Vitamin C (Jandal 1996). Moreover, the fermentation processes in the production of many dairy foods produced by Mongolian nomads are purported to enrich the content of Vitamin C (Dong et al. 2015).

Additionally, it is likely that pastoralists foraged natural plant sources. Today, nomadic herdsman from Inner Mongolia, China source up to 77 species of wild plants to supplement their pastoral resources (Huai and Pei 2000). These herdsmen have been documented to collect leaves of *Allium condensatum* (cultivated garlic), *Sonchus arvensis* (field milk thistle) and *Urtica cannabina* (stinging nettles) when suffering from scurvy. The leaves of these plants contain between 64-88mg/100g of Vitamin C depending on the species (Huai and Pei 2000). Indigenous plants, such as sea buckthorn, grow naturally across 20,000 hectares in Mongolia (Singh 2003). Depending on the species, sea buckthorn juice can contribute as much as 20mg/100ml of Vitamin C (Kallio et al. 2002).

Only one out of the four individuals with infectious diseases had any skeletal signs of scurvy. AT-233 (a young adult male) exhibited both scurvy and non-specific infectious disease. It is possible that malnutrition increased the risk of systemic infection and similarly the infection depleted bodily stores of Vitamin C. However, overall there does not appear to be a link between skeletal evidence of scurvy and infection in the Bronze Age population, likely as scurvy appears to be a sporadic condition in the Bronze Age.

8.4.11.4 Mineralisation Disorders in the Bronze Age

Due to the pastoralist diet, it is highly unlikely that mineralisation disorders were caused by phosphorous or calcium deficiencies. Moreover, given the widespread prevalence of mineralisation disorders in the Bronze Age assemblage, genetically inherited parathyroid hormone imbalances leading to mineralisation disorder can similarly be ruled out. Indeed, in the present day Vitamin D deficiency in the form of rickets and osteomalacia is very prevalent in Mongolia. Over 75% of children under the age of 5 surveyed in rural and urban centres of Mongolia exhibited at least one clinical sign with 31.1% having two or more skeletal deformities due to Vitamin D deficiency (Tserendolgor et al. 1998). While Vitamin D deficiency has been strongly associated with persistent smog in the capital city of Mongolia, Ulaanbaatar (58.1% with severe rickets), a similarly high prevalence of Vitamin D deficiency in rural regions cannot be similarly linked (37.9-45.5% with severe rickets). Over 30% of women also exhibited clinical Vitamin D deficiency (Uush 2013). The long winters, where daylight hours are considerably reduced and a great many layers of clothing are worn, significantly increases the risk of Vitamin D deficiency in Mongolia (Bromage et al. 2016; Strickland 1993). Given the latitude of Mongolia (particularly regions above 40°N) low to no levels of UV-B rays are able to penetrate the atmosphere (Strickland 1993).

Little relationship between Vitamin D deficiency and mortality in the Bronze Age skeletal assemblage is then an expected result. The outcome of mortality analysis does not mean Vitamin D deficiency did not contribute to death in the Bronze Age, rather the risks of Vitamin D deficiency were not selective in terms of the age of individuals affected as all were exposed to the same seasonal effects on Vitamin D levels. Children and adults alike had skeletal signs of recent episodes of Vitamin D deficiency.

There did appear to be a weak level of survivorship of adults who suffered from rickets in childhood, surviving to old age. This outcome was associated with a similar relationship of survivorship of individuals with osteomalacia. However, it is argued here that the mortality outcome for osteomalacia is likely at least in part, a product of the severity of skeletal effects of osteomalacia in older adults. This inference is supported by an increased relative risk of morbidity (<40 years: RR=0.1746) with old age compared to mortality (<40 years: RR=0.3029). Additionally, all old adults in the assemblage who could be assessed for sex were females. Females are characteristically more affected by bone loss

than males due to post-menopausal effects of osteoporosis, increasing the severity of Vitamin D deficiency effects on bone (Holick et al. 2005; Lukert et al. 1992). Most of these old adult females were diagnosed with probable osteomalacia, indicative of an advanced form, supporting this argument. However, the increased survivorship of adults with residual rickets cannot be explained by this phenomenon. The connection of co-occurrence between residual rickets and osteomalacia in the adults is one to consider here. It is then possible, that a measure of survivorship where individuals who were able to survive multiple instances of Vitamin D deficiency in both childhood and adulthood exhibited lower frailty and lived to old age.

No individual with skeletal evidence of infectious disease exhibited skeletal signs of Vitamin D. It is possible that Vitamin D insufficiency in adulthood (rather than deficiency leading to skeletal deformity) may have contributed to the morbidity of infection. Given that 12.2% of adults had osteomalacia, a considerable percentage of individuals without skeletal signs of disease likely suffered from subclinical Vitamin D insufficiency, depending on the season at time of death. Kurtaran et al. (2016) observed considerably lower Vitamin D levels in individuals with brucellosis arguing a causal link between Vitamin D deficiency or insufficiency and infection with brucellosis. Clinically, tuberculosis has been well documented to be linked to Vitamin D deficiency (Chan 2000). Vitamin D deficiency does not appear to increase susceptibility to helminths such as hydatid disease (Berberian 1936).

8.4.11.5 Anaemia in the Bronze Age

Low levels of anaemia are expected given that infectious disease and levels of scurvy, both likely contributors to childhood anaemia are low. Vitamin D deficiency in childhood however, has been linked to iron deficiency anaemia and may have contributed to the prevalence observed in the Bronze Age (Lee et al. 2015). Close proximity to livestock may have also placed children at risk of parasitic helminths resulting in parasitic anaemia (Bechir et al. 2012). Taenia tapeworm is prevalent amongst rural Mongolian populations (Ebright et al. 2003). Additionally, human specific helminths such as Ascaris worm are also known to present but in relatively low numbers (Ebright et al. 2003). Other parasites including Cryptosporidium sp., *Giardia* sp., and *Entamoeba* sp. were also identified (Huh et al. 2006). All cause diarrhoea prompting chronic anaemia.

8.4.11.6 Intrapopulation Variation of Disease in the Bronze Age

Significant differences between males and females were observed in regards to mineralisation disorders. Females exhibited higher prevalences of both possible and probable residual rickets and probable osteomalacia. Pregnant, lactating, and as previously mentioned, menopausal women are at an increased risk for severe osteomalacia (Holick et al. 2005; Liu et al. 1941; Lukert et al. 1992). It is possible that the increased prevalence of residual rickets in females is explainable by the co-occurrence of survivors with osteomalacia (predominantly females). However, other cultural and societal differences in raising girls and boys could be at play. Social practices such as keeping children inside, swaddling, differential age of weaning (onto Vitamin D poor foods), and exclusion of supplementary foodstuffs such as Vitamin D2 rich fish all can contribute to the prevalence of rickets (Brickley and Ives 2010).

While not statistically significant, it is intriguing that with every disease prevalence observed in the Bronze Age assemblage, the rate was higher in the Western compared to the Eastern cultures. In the Late Bronze Age cultures, the Western DSKC culture also presented higher prevalences of all diseases except for infection when compared to the contemporaneous Eastern Slab Grave culture. It is possible there were regional variations in access to resources, population density across viable pastoral land, and social inequality, between the East and the West. Additionally, increased population interaction between Western cultures with human groups outside of the Mongolian steppe may also have contributed to increased disease prevalence. Similarly, disease prevalences were lower in the Early to Middle compared to the Late to Final Bronze Age assemblages. These differences were not considerable enough to have realistic influences on binomial analyses (such as presented below and in Chapter 9), but the Early to Middle and the Late to Final Bronze Age assemblages were treated separately in analyses with continuous variables in Chapter 9.

8.5 Xiongnu Period Assemblage

The historical date for the establishment of the Xiongnu Empire is 209BC, with its decline beginning in the 1st Century AD (Kradin 2011). However, expansion of the Xiongnu cultural group of pastoral herders and mounted warriors began centuries prior (Honeychurch 2015). It is thought that the Xiongnu Empire emerged as a response to either northward

expansion of the declining Chinese Qin Empire in 215BC or due to internal conflict within nomad societies, driving the consolidation of nomad groups through warfare and militarisation (Honeychurch 2015; Kradin 2011). The empire remained predominantly nomadic and pastoral, and was sustained through military raiding of the Han Chinese (206BC-220AD) for prestige goods and staple resources such as millet (Honeychurch 2015; Kradin 2011). Soon annual payments from the Han were exchanged for a peaceful frontier along the Han-Xiongnu boundaries. This conflict with the Han drove internal hierarchisation and social inequality, and differential burial practices emerged dividing the Xiongnu commoners from the elites (Wright et al. 2009). Elites were buried in terraced tombs, whereas commoners remained buried in slab-like or stone-marked graves similar to that of Eastern Bronze Age cultures (Brosseder 2009; Jones and Joseph 2008).

Expansion of the Xiongnu Empire beyond the region of modern day Mongolia also enabled control of population movement along the Silk Road and Northern China (Lee and Linhu 2011). Genetic diversity increased considerably during this period indicating more large-scale migrations in and out of the Mongolian region (Pilipenko et al. 2018). Significant geneflow within and outside of Mongolia (including genetic input from Western and Han Chinese populations) marks this period, particularly towards the later stage of the Xiongnu Period (Jeong et al. 2020).

Seasonal mobility as part of the pastoral practice continued in the Xiongnu Period (Wright et al. 2009). Strontium and oxygen isotopic data suggest such pastoral mobility occurred within local boundaries for most people, with a small proportion of individuals venturing beyond routine seasonal pastures (Machicek et al. 2019). Animal husbandry of the Xiongnu included sheep, goat, cows, horses, pigs, camels and yaks, and dairying continued (Houle and Broderick 2011; Wilkin et al. 2020b). Additionally, archaeological evidence for consumption of fish and deer, and small scale farming of crops (millet, barley and wheat) has also been found in Northern Mongolia (Houle and Broderick 2011; Makarewicz 2011; Wright et al. 2009). Pastoralism was then supplemented by a wide range of food procurement practices including hunting, fishing and farming. As previously mentioned, carbon and nitrogen isotopic data indicate an introduction of millet into the diet of Xiongnu people, albeit at a significantly lower level than in the agricultural Han, coinciding with expansion of exchange networks, consistent with historical and archaeological accounts (Ventresca Miller and Makarewicz 2019). Additionally, dietary

isotopic variation was particularly high in the Xiongnu Period indicating considerable dietary diversity within the Xiongnu population (Wilkin et al. 2020a).

The Xiongnu assemblage is an aggregate sample comprised of a number of Xiongnu Period sites throughout modern day Mongolia. The assemblage is defined by a low fertility rate (D0-14/D=0.13) (after McFadden and Oxenham 2018a), and as was the case for the Bronze Age, a natural population decrease was also observed (RNPI=-0.30) (after McFadden and Oxenham 2018b).

Analysis of trauma in a Siberian Altai Xiongnu sample identified high prevalences of perimortem cranial trauma related to interpersonal violence in males (7.3%), females (6.3%) and children (5.8%) which the authors prescribe to evidence of militarisation and testament to high levels of conflict (Tur et al. 2018). Bazarsad (2007) identified a considerable difference in the cribra orbitalia rates between males (5.3%) and females (29.4%) in a Xiongnu sample from North-Central Mongolia. Erdene (2017) identified a caries prevalence rate by individual of 17.3% in the Xiongnu Period. Almost 90% of affected individuals were from Central and Northern Mongolia indicating regionalisation. Additionally females had a significantly higher number of carious lesions by individual, as well as higher numbers of carious teeth per individual affected. The author identified no carious lesions in the Bronze Age assemblage (Erdene 2014), and argues for an increase in carbohydrate consumption such as with the introduction of millet, barley and wheat. The following section presents the results for disease diagnosis and analysis of morbidity and mortality in the same aggregated Xiongnu assemblage.

8.6 Results: Xiongnu Period Skeletal Pathology

8.6.1 Summary of Pathological Lesions in the Xiongnu Period

Of the 69 individuals included in palaeopathological assessment of the Xiongnu Period, over half (56.5%, 39/69) presented with osteoblastic lesions (Table 8.30). Similar proportions were observed in adults (54.9%, 28/51) and nonadults (61.1%, 11/18). Discrete and bilateral lesions appearing as poorly mineralised accumulations of lamellar bone on the long bones, at muscle attachment sites, were the most frequent osteoblastic lesions recorded (Figure 8.34). These poorly mineralised lesions were not similar to normal active (woven) SPNB deposits, and instead were comparable to descriptions by Brickley and Ives (2010),

in regards to deposits disrupted by metabolic abnormalities. Additionally, a large proportion of symmetrical and discrete SPNB (not appearing poorly mineralised) were observed on the crania. A combination of unilateral and bilateral discrete deposits of SPNB were also present, but less common. Diffuse SPNB lesions were infrequently observed (Figure 8.35).

Figure 8.34: *Poorly mineralised SPNB on the posterior distal femora (black arrows; AT-294, middle aged adult female, Buural Uul).These accumulations are poorly mineralised lamellar bone deposits at the attachment site of the gastrocnemius muscle rather than active SPNB Image: author's own.*

Figure 8.35: *Remodelled diffuse SPNB on the left femoral shaft (AT-154, male, ~17 years, Erdenetsagaan soum). Image: author's own.*

Seven individuals (10.1%, 7/69) exhibited osteolytic lesions in the Xiongnu Period assemblage. Most osteolytic lesions (71.4%, 5/7) were observed in adults, and the youngest individual affected was approximately 17 years of age (AT-154, male). Five different types of osteolytic lesions were observed in the assemblage. AT-2, a young adult female presented with spiculated remodelled SPNB on the anterior vertebral body of the L5 directly associated

with multifocal OL2 destruction on the superior anterior margin of the vertebral body (Figure 8.36a, 8.36b). AT-36, a middle aged adult male displayed a well remodelled unilateral focal deep OL1 lesion of the right mastoid (Figure 8.35c). AT-263, a young adult, displayed two osteolytic lesions. The first, a large circular circumscribed OL2 lesion penetrated through the sternum with sclerotic margins (Figure 8.36d, 8.36e). Remodelled SPNB is associated with the lesion on the pleural aspect, which is also larger on this aspect. The sclerosis is minimal where the lesion breaches the trabeculae. The second lesion is a unilateral OL2 focal circumscribed and well remodelled lesion on the pleural aspect of a right middle rib (Figure 8.36f). AT-292, a young adult male, exhibited a unilateral and multifocal circumscribed OL1 lesion of the distal end of the left 12^{th} rib (Figure 8.36g, 8.36h). The margins of the lesion are well defined with sclerotic response in the base. The lesion margins project beyond the distal boundaries of the 12^{th} rib indicating pathological ossification of the distal end of the rib in the disease process. Lastly, three males aged between 16 and 21 years of age presented with bilateral and/or unilateral OL1 and OL2 circumferential osteolytic lesions with sclerotic smooth margins and base (Figure 8.37). All three individuals had these lesions on the proximal fibulae, with one also exhibiting lesions of the calcanei and a left middle to lower rib (AT-146, young adult male).

Figure 8.36: *Osteolytic lesions of varying aetiologies. a-b) Multifocal osteolytic destruction associated with spiculated SPNB deposit on the anterior vertebral body (black arrows: (a) SPNB (b) osteolytic destruction on the superior margin). No other vertebrae was affected in this individual, and no lipping or osteolysis was present on other vertebrae (AT-2, young adult female, Naimaa Tolgoi). c) Remodelled focal osteolytic destruction of the right mastoid (black arrow; AT-36, middle aged adult male, Tevsh Uul). d-e) Large focal osteolytic destruction of the sternum. There is minimal sclerosis where the lesion breaches the trabeculae (black arrow; AT-263, young adult, Buural Uul). f) Remodelled focal destruction of the midshaft of a right middle rib (AT-263, young adult, Buural Uul). g-h) Multifocal circumferential osteolytic destruction with sclerotic margins and base of the distal left 12th rib (AT-292, a young adult male, Buural Uul). Image: author's own.*

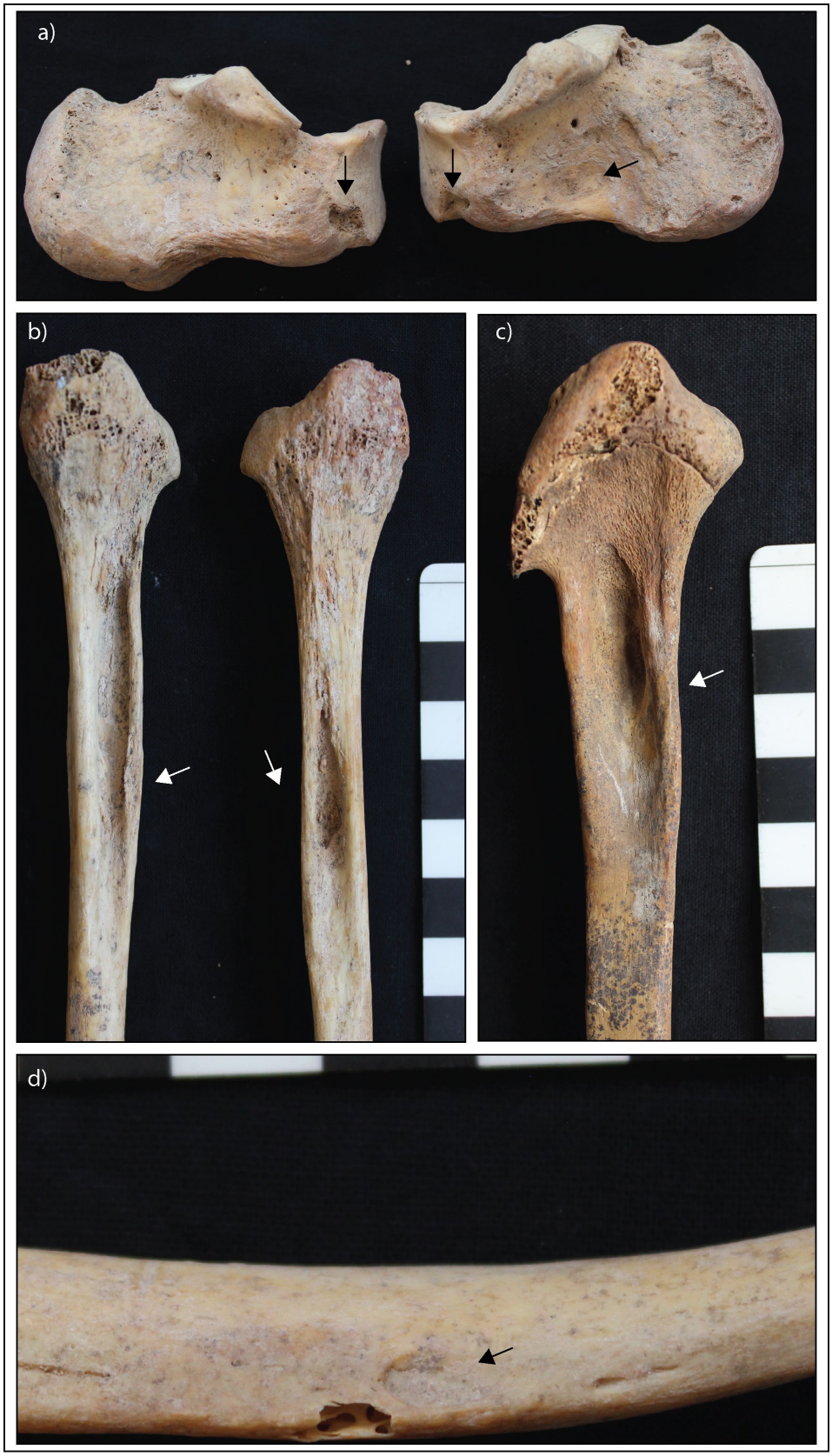

Figure 8.37: *Osteolytic lesions with smooth sclerotic margins and base. a) Three lesions of the lateral calcanei (black arrows; AT-146, young adult male, Tevsh Uul). b) Bilateral and symmetrical lesion of the proximal fibulae (white arrows; AT-146, young adult male, Tevsh Uul). c) Unilateral lesion of the proximal right fibula (white arrow; AT-154, male ~17 years, Erdenetsagaan soum). d) Lesion of the midshaft of a left middle to lower rib (black arrow; AT-146, young adult male, Tevsh Uul). Image: author's own.*

Over 17% (17.4%, 12/69) of the overall skeletal assemblage displayed bending deformities of the long bones (Table 8.30). The prevalence of long bone bending deformities were slightly higher among nonadults (22.2%, 4/18) than adults (15.7%, 12/69). Of the nonadults, three individuals (16.7%, 3/18) presented with cupping and flaring, and fraying was observed in two individuals respectively (11.1%, 2/18). Postcranial skeletal deformities other than of the long bones were observed in adults (25.5%, 18/69) and nonadults (27.8%, 5/18). These deformities included buckling and bending of the os coxae, scapulae, sterna, sacra, ribs and vertebrae. Additionally, AT-268a (female, ~15 years), exhibited hypoplasia of the 1st permanent mandibular molars, and AT-350 (young adult female) exhibited cortical enlargement of the cranium. Finally, pathological fractures consistent with pseudofractures were observed in four individuals, the youngest being approximately 17 years of age (AT-154, male).

Table 8.30: *Summary of OB and OL lesion prevalences, and skeletal deformities in the Xiongnu Period*

	NONADULT (aff/obs)	**NONADULT (%)**	**ADULT (aff/obs)**	**ADULT (%)**	**TOTAL (aff/obs)**	**TOTAL (%)**
OB Lesion	11/18	61.1	28/51	54.9	39/69	56.5
OL Lesion	2/18	11.1	5/51	9.8	7/69	10.1
Cupping	3/18	16.7	0/51	0	3/69	4.3
Flaring	2/18	11.1	0/51	0	2/69	2.9
Fraying	2/18	11.1	0/51	0	2/69	2.9
Bending of Long Bone Shafts	4/18	22.2	8/51	15.7	12/69	17.4
Cranial Deformity	0/18	0	1/51	2	1/69	1.4
Other Skeletal Deformities	5/18	27.8	13/51	25.5	18/69	2.6
Pathological Fracture	1/18	5.6	3/51	5.9	4/69	5.8

8.6.2 Diagnosis of Infectious Disease in the Xiongnu Period

Over 10% (11.6%, 8/69) of the overall assemblage met the criteria for infectious disease (Table 8.31). Overall, three adults were included in the infectious disease criteria based on the presence of two or more skeletal elements with SPNB extending beyond ¼ of the bone surface. In three individuals, one adult, one adolescent and one child, diffuse SPNB was observed on the pleural aspect of multiple ribs (Figure 8.38). As only individuals over the age of 15 years with diffuse SPNB over multiple skeletal elements are included in the infectious disease criteria, AT-538 (~7.5 years) was excluded. SPNB on the pleural aspect of ribs can be caused by respiratory infections, and infection is possible in AT-538. However, SPNB due to scurvy and other non-infections respiratory diseases are also

possible causes of osteoblastic rib lesions on the pleural aspect (Barlow 1883; Eyler et al. 1996; Roberts et al. 1994).

Additionally, AT-536 (young adult male) was excluded from the infectious disease criteria due to the likelihood of a neoplastic origin for the lesions (Figure 8.39). This individual exhibited spiculated pattern of SPNB overlying widespread trabecular destruction of the axial skeleton, scapulae and os coxae. Radiographs demonstrate focal destruction, rather than marrow hyperplasia, consistent with bone cancer, and ruling out thalassaemia as a possible cause. Differential diagnosis of the cancer is beyond the scope of this thesis, but is consistent with blood or marrow borne cancers.

Table 8.31: *Summary of infectious disease in the Xiongnu Period*

	POSSIBLE			**PROBABLE**			**POSSIBLE AND PROBABLE**		
	Affected	***Observed***	***(%)***	***Affected***	***Observed***	***(%)***	***Affected***	***Observed***	***(%)***
Brucellosis									
20 to 29 years	0	18	0	0	18	0	0	18	0
30 to 39 years	1	16	6.3	0	16	0	1	16	6.3
40 to 49 years	0	5	0	0	5	0	0	5	0
50+ years	0	9	0	0	9	0	0	9	0
Male	0	29	0	0	29	0	0	29	0
Female	1	28	3.6	0	28	0	1	28	3.6
Total adults	1	51	2	0	51	0	1	51	2
Total	1	69	1.4	0	69	0	1	69	1.4
Tuberculosis/ Mycosis									
20 to 29 years	1	18	5.6	0	18	0	1	18	5.6
30 to 39 years	0	16	0	0	16	0	0	16	0
40 to 49 years	0	5	0	0	5	0	0	5	0
50+ years	0	9	0	0	9	0	0	9	0
Male	-	-	-	0	29	0	-	-	-
Female	-	-	-	0	28	0	-	-	-
Total adults	1	51	2	0	51	0	1	51	2
Total	1	69	1.4	0	69	0	1	69	1.4
Treponemal Disease									
15 to 19 years	1	9	11.1	0	9	0	1	9	11.1
20 to 29 years	0	18	0	0	18	0	0	18	0
30 to 39 years	0	16	0	0	16	0	0	16	0
40 to 49 years	0	5	0	0	5	0	0	5	0
50+ years	0	9	0	0	9	0	0	9	0
Male	0	29	0	0	29	0	0	29	0
Female	1	28	3.6	0	28	0	1	28	3.6
Total adults	1	51	2	0	51	0	1	51	2
Total	1	69	1.4	0	69	0	1	69	1.4

	POSSIBLE			PROBABLE			POSSIBLE AND PROBABLE		
	Affected	***Observed***	***(%)***	***Affected***	***Observed***	***(%)***	***Affected***	***Observed***	***(%)***
Otitis Media									
20 to 29 years	0	8	0	0	8	0	0	8	0
30 to 39 years	0	6	0	1	6	16.7	1	6	16.7
40 to 49 years	0	2	0	0	2	0	0	2	0
50+ years	0	3	0	0	3	0	0	3	0
Male	0	12	0	1	12	8.3	1	12	8.3
Female	0	12	0	0	12	0	0	12	0
Total adults	0	21	0	1	21	4.8	1	21	4.8
Total	0	29	3.4	1	29	3.4	1	29	3.4
Hydatids Disease									
15 to 19 years	0	9	0	0	9	0	0	9	0
20 to 29 years	0	18	0	1	18	5.6	1	18	5.6
30 to 39 years	0	16	0	0	16	0	0	16	0
40 to 49 years	0	5	0	0	5	0	0	5	0
50+ years	0	9	0	0	9	0	0	9	0
Male	0	29	0	1	29	3.4	1	29	3.4
Female	0	28	0	0	28	0	0	28	0
Total adults	0	51	0	1	51	2	1	51	2
Total	0	69	0				1	69	1.4

	CRITERIA PREVALENCE		
	Affected	*Observed*	*(%)*
Overall infectious disease criteria			
15 to 19 years	3	9	33.3
20 to 29 years	3	18	16.7
30 to 39 years	2	16	12.5
40 to 49 years	0	6	0
50+ years	0	9	0
Male	4	29	13.8
Female	2	28	7.1
Total adults	6	51	11.8
Total	8	69	11.6

Figure 8.38: *Diffuse osteoblastic lesions of the pleural surface of the ribs. a) Active SPNB on multiple ribs. (AT-538, ~7.5 years, Burkhan Tolgoi). b) Active SPNB. Multiple ribs were affected. (AT-583, male, ~19 years, Emeel Tolgoi). c) Mixed active and remodelled SPNB. Only the right ribs (2 to 10) were affected (unilateral). Radiographs demonstrated cortical expansion of the pleural surface (AT-30, young adult male, Galuut soum).*

Figure 8.39: *Diffuse destruction of trabecular bone in the axial skeleton, scapulae and os coxae of AT-536 (young adult male, Burkhan Tolgoi) associated with diffuse active SPNB (black arrows). The lesions were bilateral and symmetrical. a-b) The vertebral arches and bodies were both affected. c) Right scapula. d-e) Left os coxa. Radiographs demonstrated focal destruction not consistent with thalassaemia (white arrows). f) Pleural aspect of ribs. Image: author's own.*

Osteolytic destruction with osteophytic response of the superior vertebral body is diagnostic for brucellosis (Al-Shahed et al. 1994). Therefore, the vertebral lesion observed in AT-2 (young adult female) meets the threshold criteria for possible brucellosis. Moreover, the radiographic "parrot's beak" sign suggestive for brucellosis is also observable (Figure 8.40). The lesion is consistent with the focal rather than disseminated form of brucellosis (Al-Shahed et al. 1994). While the spiculated SPNB may be an inflammatory response secondary to a cold abscess on the anterior vertebra due to tuberculosis, a combination of osteolytic and osteoblastic response is more consistent with brucellosis (Ortner 2003: 255). Additionally, lesions tend to be more severe in vertebral tuberculosis due to rapid progression of the disease (Roberts and Buikstra 2019).

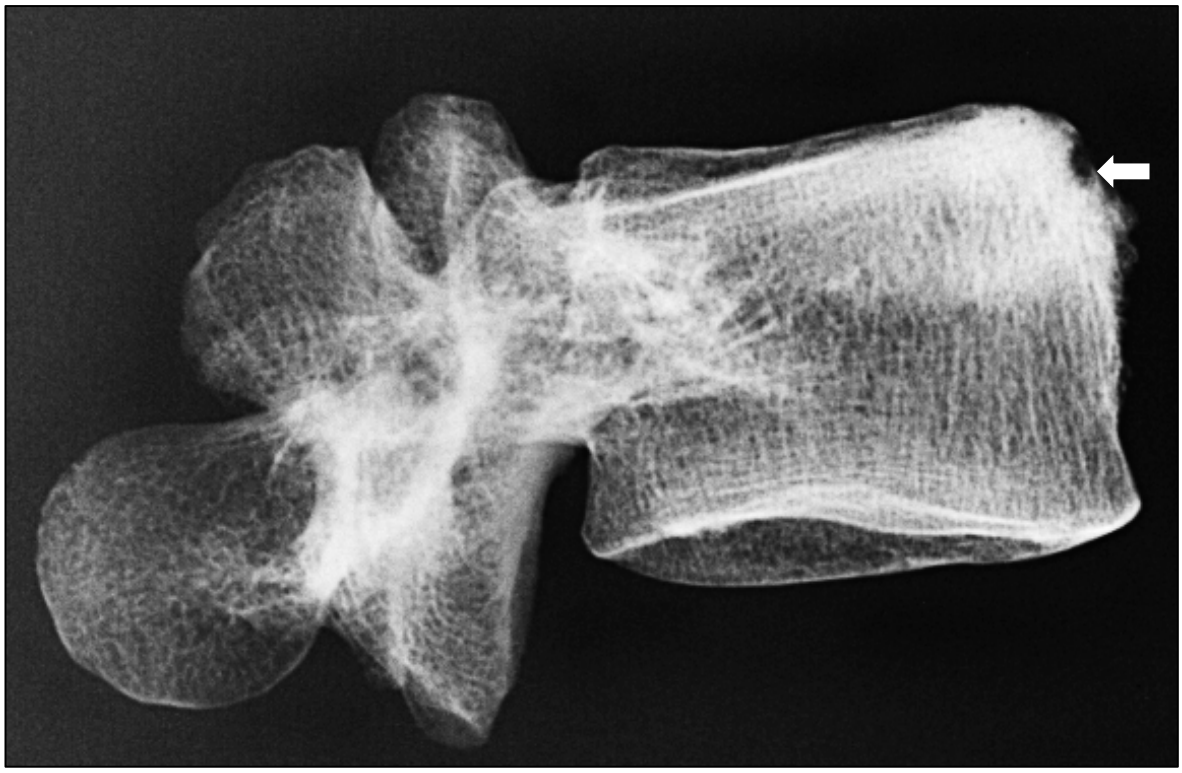

Figure 8.40: *Radiographic sign suggestive for brucellosis. Note the "parrot's beak" formation on the superior margin associated with osteolytic destruction (AT-2, young adult female, Naimaa Tolgoi). Image: author's own.*

Presence of focal lesions on the pleural surface of the ribs is diagnostic for tuberculosis (Davidson and Horowitz 1970; Kelley and Micozzi 1984; Ortner 2003: 246-247). Moreover, focal osteolysis extending from the pleural surface of the sternum is also suggestive for tuberculosis. Therefore, AT-263 (young adult) meets the threshold criteria for possible tuberculosis. The rib lesion is reminiscent of a forensic case of pulmonary tuberculosis reported by Ubelaker et al. (2000) and in anatomical collections reported by

Kelley and Micozzi (1984) where circumscribed smooth walled cavitations on the visceral surface of middle ribs were identified, although in these cases more than one lesion was identified on multiple ribs. Tuberculosis involving a single rib is reported in the literature (Kelley and Micozzi 1984; Ortner 2003: 246). The rib lesion is completely remodelled (Figure 8.41), an occurrence in some cases of tuberculosis due to the chronic progression of the disease (Ortner 2003: 230). Sclerosis is evident only on the pleural surface of the sternum, suggesting active progression of disease with a primarily osteolytic process, again consistent with tuberculosis. Perforation of the sternum in tuberculosis is uncommon, but caused by both pleural and superficial cold abscesses (Khan et al. 2007; Watts et al. 1987). However, due to the atypical expression of disease, not involving the vertebrae nor the hip, and the seeming random expression of the focal lesions throughout the thorax, AT-263 also meets the minimum criteria for respiratory mycotic infection (Jaffe 1972: 1060-1066; Ortner 2003: 325-332).

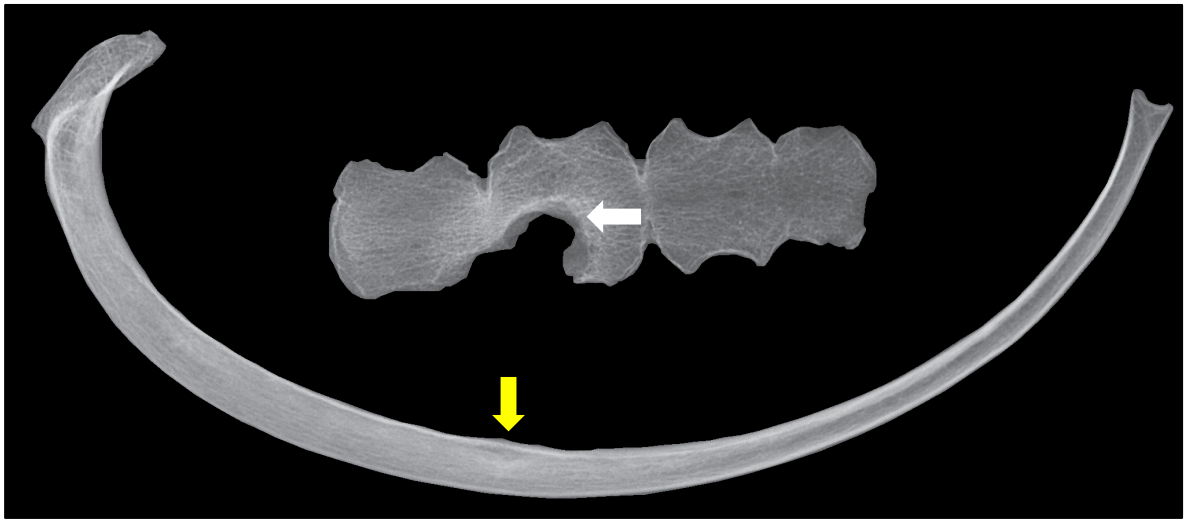

Figure 8.41: *Radiographic signs consistent with tuberculosis and mycosis. Sclerotic response is only evident on the pleural aspect (white arrow). The rib lesion has completely remodelled and was deeper than observed macroscopically (yellow arrow; AT-263, young adult, Buural Uul). Image: author's own.*

Multilocular cystic formations with sclerotic margins resembling a "bunch of grapes" is observed in the 12th rib of AT-292 (young adult male) strongly diagnostic for hydatids disease (Figure 8.42). Therefore, AT-292 meets the threshold criteria for a probable diagnosis of hydatids disease. Rib lesions are uncommon in skeletal hydatids but may occur due to adjacent infection of the surrounding viscera (Morris et al. 2002). Additionally, expansion of the surrounding bone as observed in AT-292 occurs in hydatids disease of the rib (Agarwal et al. 1992).

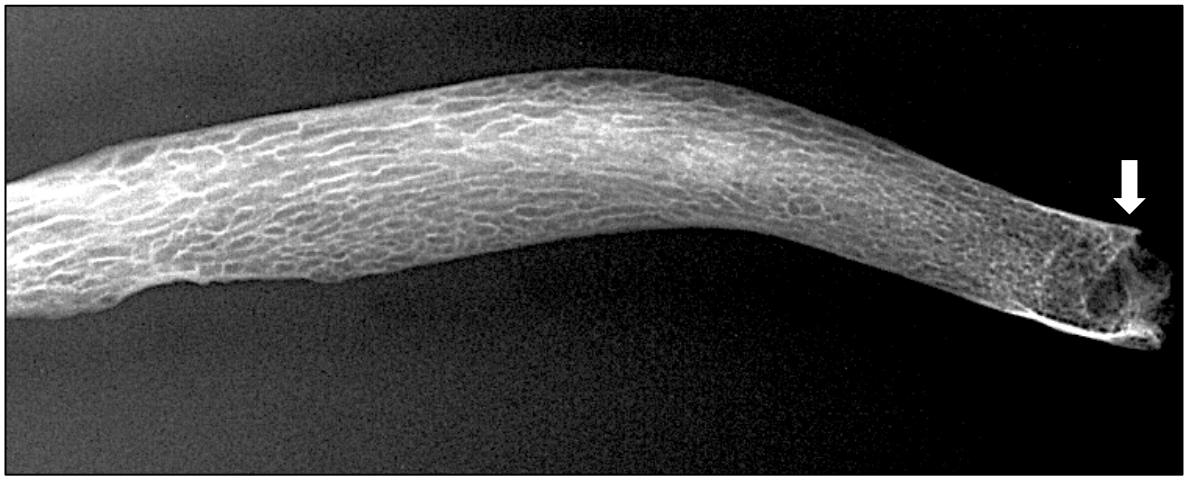

Figure 8.42: *Radiographic sign strongly diagnostic for hydatids disease. Note the multilocular cystic ("bunch of grapes") appearance (white arrow; AT-292, young adult male, Buural Uul). Image: author's own.*

The dental hypoplasia observed in AT-268a (Female, ~15 years) is consistent with descriptions of mulberry molars diagnostic for congenital treponemal disease (Figure 8.43). Therefore AT-268a, meets the threshold criteria for possible treponemal disease. Mulberry molars are predominately caused by transplacental infection of treponemal disease but can also be caused by various disruptions in-utero (Hillson et al. 1998). Only the first permanent molars are affected consistent with what is most frequently observed in congenital treponemal disease (Fiumara and Lessell 1970). Mulberry molars reported to be caused by congenital treponemal disease do tend to be more extreme than observed in AT-268a (Nissanka-Jayasuriya et al. 2016). However, the restriction of the hypoplastic defect to the occlusal surface demarcates a period of resumed normal enamel formation is at least consistent with a congenital infection (Hillson et al. 1998). While discrete symmetrical SPNB deposits were present, AT-268a lacked diffuse SPNB and any other skeletal signs of congenital treponemal disease. Again, it is not uncommon for skeletal signs of the disease to be absent, as dental defects are more common (Putkonen 1962). While mulberry molars have not been reported for Vitamin D deficiency, congenital rickets needs to be considered as a possible cause (see section below for high prevalence of Vitamin D deficiency in the Xiongnu), as enamel hypoplasias are common (Davit-Béal et al. 2014). Radiographs of the molars were taken for further assessment of infantile and childhood rickets (after D'Ortenzio et al. 2018), but proved inconclusive.

Figure 8.43: *Mulberry molars of AT-268a (female, ~15 years, Buural Uul). Note that the M2s are not affected, consistent with possible congenital treponemal disease, although generalised hypoplasia is suggested by the discolouration of the teeth.*

8.6.3 Morbidity of Infectious Disease in the Xiongnu Period

Nonadult morbidity was not assessed as only three adolescents (over the age of 15) had signs of infectious disease. Although males had a slightly higher prevalence of infectious disease, no statistically significant differences in morbidity were observed between males and females (n=57, RR=0.5179, p=0.4248). There was a statistically significant increase in the morbidity of younger adults with infectious disease. Adolescents over the age of 15 were 3.2 times (n=57, RR=3.2000, p=0.0664) at risk of infectious disease than their adult counterparts, which was statistically significant (Table 8.32). Additionally, adults under the age of 30 years were 3.3 times (n=57, RR=3.333, p=0.1190) more likely to have infectious disease than those over the age of 30 which was statistically significant give the size of the effect.

Table 8.32: *Relative risk of infectious disease morbidity in the Xiongnu Period across sex and age cohorts*

EXPOSED GROUP/ CONTROL GROUP	**OUTCOME**		**RR**	**P-VALUE**	**95%CI**
	Positive: *Infection Present*	***Negative:*** *Infection Absent*			
Sex					
Female/ Male	2/4	26/25	0.5179	0.4248	0.1029- 2.6064
Adults					
<20 yrs/ >20 yrs	3/5	6/43	**3.2000**	**0.0664***	0.9244- 11.0775
<30 yrs/ >30 yrs	6/2	21/28	**3.3333**	**0.1190****	0.7338- 15.1423
<40 yrs/>40 yrs	8/0	35/14	5.7955	0.2173	0.3555- 94.4851

A relative risk (RR) >1 denotes a relationship of the exposed group with an increase in disease prevalence, whereas RR <1 denotes a relationship of the control group with an increase in disease prevalence.
**= statistically significant (p<0.10). **= statistically significant when considering size of the effect of RR.*

8.6.4 Mortality of Infectious Disease in the Xiongnu Period

A statistically significant relationship with increased risk of death was observed for the relative risk ratio analysis of all adult age cohorts (Table 8.33). Individuals were 3.1 times (n=57, RR=3.0625, p=0.0602) more likely to die before adulthood with skeletal signs of infectious disease than without, which was statistically significant. Kaplan-Meier and Cox regression analysis both indicate a statistically significant relationship with increased frailty of adults with skeletal signs of infectious disease compared to those without. The Kaplan-Meier (n=56, X^2=6.228, df=1, p=0.013; Table 8.34) and Cox regression (n=56, Wald=5.432, df=1, p=0.020; Table 8.35) cumulative survival functions both indicate clear differences in the survival rate of adults with and without infectious disease (Figures 8.44-8.45).

Table 8.33: *Relative risk of infectious disease mortality in the Xiongnu Period across age cohorts.*

POSITIVE OUTCOME/ NEGATIVE OUTCOME	**TREATMENT**		**RR**	**P-VALUE**	**95%CI**
	Exposed Group: *Infection Present*	***Control Group:*** *Infection Absent*			
Adults					
<20 yrs/ >20 yrs	3/5	6/43	**3.0625**	**0.0602***	0.9532- 9.8391
<30 yrs/ >30 yrs	6/2	21/28	**1.7500**	**0.0330***	1.0463- 2.9271
<40 yrs/>40 yrs	8/0	35/14	**1.4000**	**0.0002***	1.1728- 1.6712

A relative risk (RR) >1 denotes a relationship of the disease presence with the positive outcome (susceptibility to mortality), whereas RR <1 denotes a relationship of the disease absence with a negative outcome (survivorship).
**= statistically significant (p<0.10). **= statistically significant when considering size of the effect of RR.*

Table 8.34: *Statistical summary for Kaplan-Meier function of infectious disease mortality of adults in the Xiongnu Period Mongolia.*

INFECTIOUS DISEASE	ESTIMATE	STD. ERROR	95% CI	LOG RANK (MANTEL-COX)		
				CHI SQUARE	DF	P-VALUE
Mean				6.228	1	**0.013***
Absent	34.180	1.926	30.406- 37.955			
Present	24.413	2.595	19.326- 29.499			
Overall	32.785	1.747	36.208- 30.700			
Median						
Absent	30.700	1.876	27.022- 34.378			
Present	21.000	4.573	12.038- 29.962			
Overall	30.700	1.721	27.328- 34.072			

**= statistical significance (p<0.15).*

Table 8.35: *Statistical summary for Cox regression function of infectious disease mortality of adults in the Xiongnu Period Mongolia.*

INFECTIOUS DISEASE	COEFFICIENT (β)	STD. ERROR	WALD	DF	P-VALUE	ODDS RATIO (Exp(β))
	-0.933	0.401	5.432	1	**0.020***	0.393

**= statistical significance (p<0.15).*

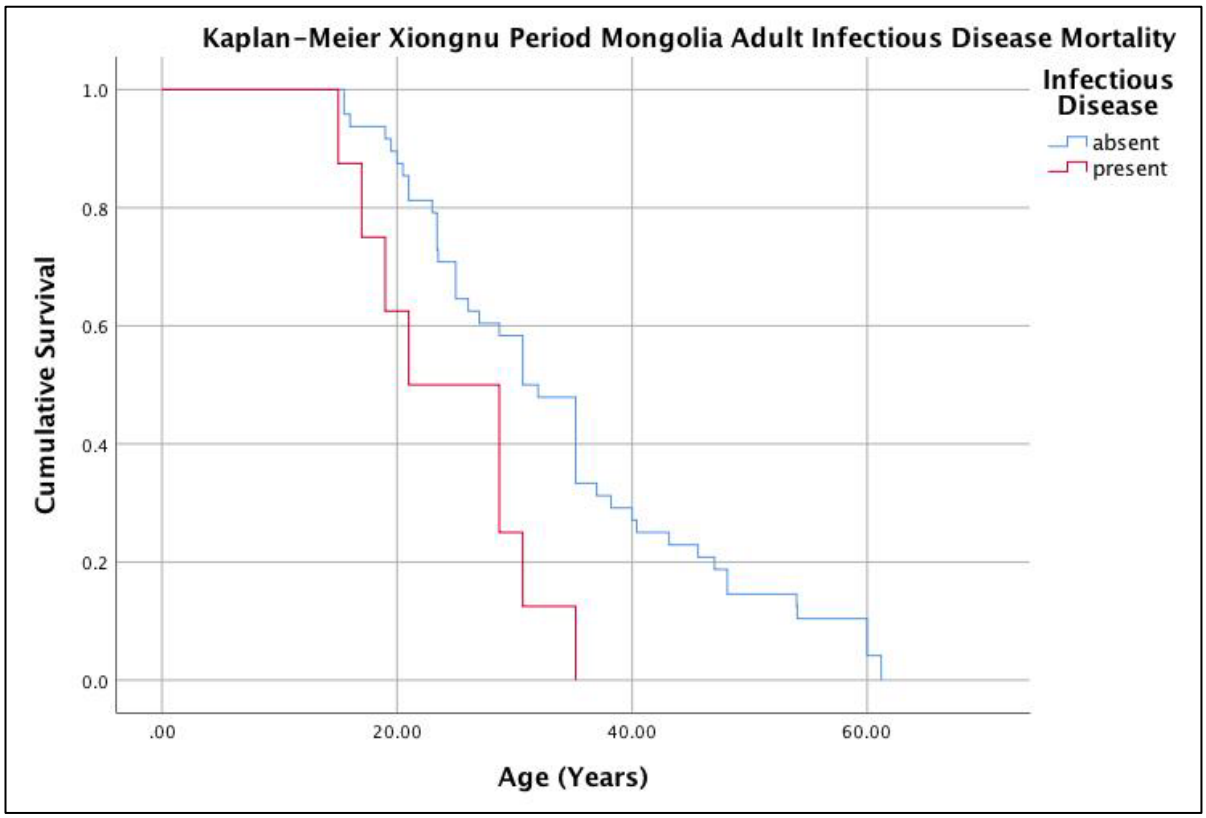

Figure 8.44: *Kaplan-Meier cumulative survival function of adult infectious disease mortality in Xiongnu Period Mongolia. Image: author's own.*

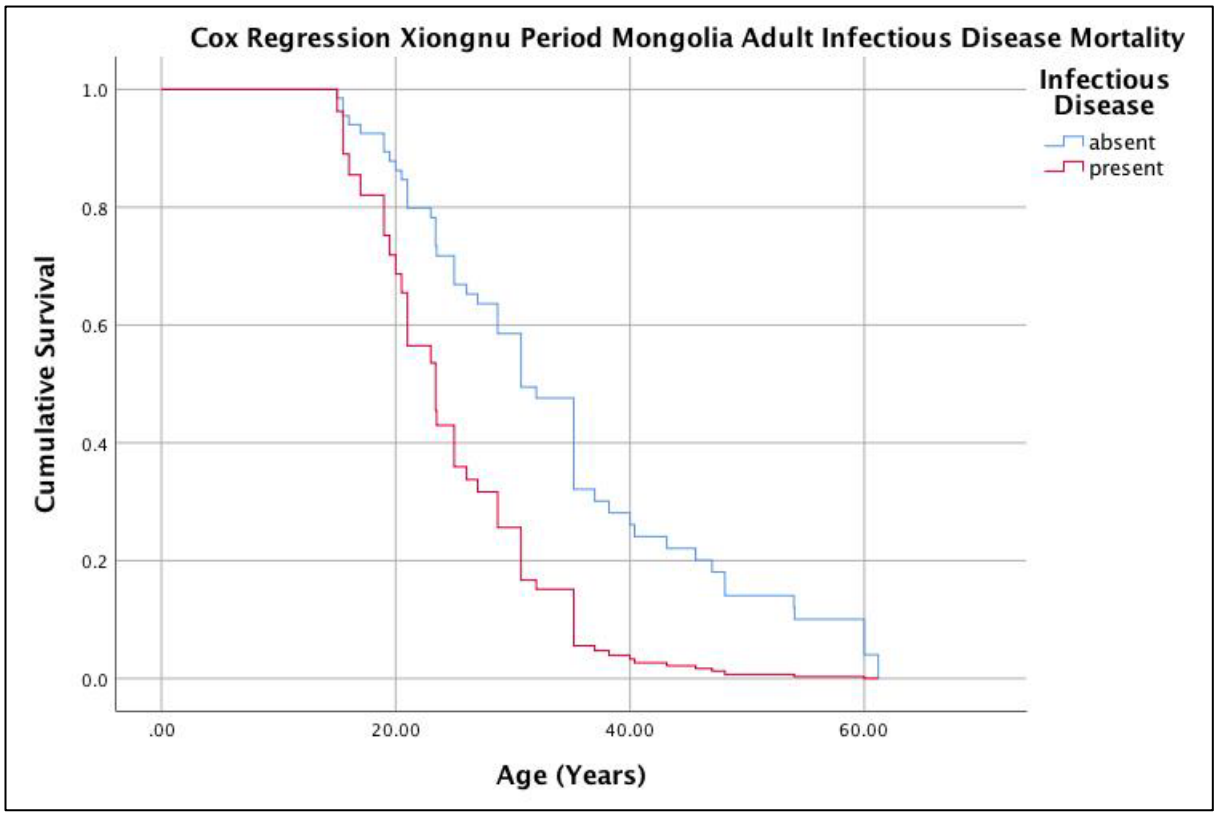

Figure 8.45: *Cox regression cumulative survival function of adult infectious disease mortality in Xiongnu Period Mongolia. Image: author's own.*

8.6.5 Diagnosis of Nutritional Disease in the Xiongnu Period

8.6.5.1 Diagnosis of Nutritional Disease in Xiongnu Period Nonadults

Over 65% of nonadults had lesions consistent with a possible or probable diagnosis of scurvy (Table 8.36). Over 50% of all nonadult age cohorts had possible or probable scurvy. Moreover, a high prevalence of nonadults were diagnosed with probable scurvy (44.4%, 8/18). Macroscopic lesions diagnostic and suggestive for scurvy were predominantly bilateral and symmetrical SPNB deposits with abnormal cortical porosity of the cranium. Cranial lesions were observed on the external greater wings and pterygoid fossae of the sphenoid bones, squamous temporal bones, anterior and posterior maxillae, anterior and posterior zygomatic bones, and orbital roofs (Figure 8.46). Macroscopic lesions were also observed on the supraspinous and infraspinous fossae of the scapulae. Abnormal endochondral porosity exceeding 10mm from the metaphyseal plate were observed in 28% (27.8%, 5/18) of nonadults. Radiographic signs diagnostic for scurvy including Trummerfeld zones, White lines of Fraenkel and Pelkan spurs were observed in three nonadults (Figure 8.46).

Almost 45% (44.4%, 8/18) of nonadults presented with skeletal lesions consistent with possible and probable rickets (Table 8.36). Fraying, a diagnostic sign of active rickets was observed in a child (AT-268b, ~7.5 years), and an adolescent (AT-154, male, ~17 years), and skeletal signs of rickets was not observed in children under the age of 5 years. Additionally, bending deformities of the long bone shafts, cupping and flaring of the metaphyseal plates, and coxa vara of the femoral necks were also observed. One adolescent (AT-365, male ~19.5 years) exhibited alterations of the rib neck angle of multiple ribs. Radiographic signs suggestive for rickets including trabecular coarsening in the distal metaphyses of long bones and appearance of thick cortex of long bones was also observed (Figure 8.47). Five nonadults between 14 and 19 years of age exhibited postcranial skeletal deformities more reminiscent of diagnostic signs for adult osteomalacia. Osteomalacia will be explored in detail below.

Table 8.36: *Summary of nutritional disease in the Xiongnu Period*

	POSSIBLE			PROBABLE			POSSIBLE AND PROBABLE		
	Affected	***Observed***	***(%)***	***Affected***	***Observed***	***(%)***	***Affected***	***Observed***	***(%)***
Scurvy									
0 to 5 months	1	1	100	0	1	0	1	1	100
6 to 11 months	0	0	0	0	0	0	0	0	0
1 to 5 years	1	3	33.3	2	3	67	3	3	100
6 to 10 years	0	5	0	4	5	80	4	5	80
11 to 14 years	0	2	0	0	1	100	0	2	0
15 to 19 years	2	9	10.5	3	9	33.3	5	9	55.6
20 to 29 years	4	18	22.2	0	18	0	4	18	22.2
30 to 39 years	0	16	0	1	16	6.3	1	16	6.3
40 to 49 years	2	5	40	0	5	0	2	5	40
50+ years	0	9	0	0	9	0	0	9	0
Total nonadults	4	18	22.2	8	18	44.4	12	18	66.7
Males	5	29	17.2	2	29	6.9	7	29	24.1
Females	2	28	10.7	2	28	7.1	5	28	17.9
Total adults	8	51	15.7	1	51	2	9	51	17.6
Total	12	69	17.4	9	69	13	21	69	30.4
Rickets/ Residual Rickets									
0 to 5 months	0	1	0	0	1	0	0	1	0
6 to 11 months	0	0	0	0	0	0	0	0	0
1 to 5 years	0	3	0	1	3	33.3	1	3	33.3
6 to 10 years	1	4	25	1	4	25	2	4	50
11 to 14 years	0	1	0	0	1	0	0	1	0
15 to 19 years	2	8	25	3	8	37.5	5	8	62.5
20 to 29 years	2	18	11.1	2	18	11.1	4	18	22.2
30 to 39 years	3	16	18.8	3	16	18.8	6	16	37.5
40 to 49 years	0	5	0	1	5	20	1	5	20
50+ years	1	9	11.1	0	9	0	1	9	11.1
Total nonadults	3	18	16.7	5	18	27.8	8	18	44.4
Males	2	24	12.5	5	24	20.8	7	24	29.2
Females	2	23	8.7	2	23	8.7	4	23	17.4
Total adults	6	51	11.8	6	51	11.8	12	51	23.5
Total	9	69	13	11	69	15.9	20	69	29
Osteomalacia									
11-14 years	1	2	50	0	2	0	1	2	50
15 to 19 years	1	8	12.5	3	8	37.5	4	8	50
20 to 29 years	2	18	11.1	4	18	22.2	6	18	33.3
30 to 39 years	1	16	6.3	4	16	25	5	16	31.3
40 to 49 years	0	5	0	2	5	0	2	5	40
50+ years	1	9	11.1	0	9	0	1	9	11.1
Males	0	29	0	11	29	37.9	11	29	37.9
*Females**	6	28	21.4	1	28	3.6	7	28	25
Total adults	4	51	7.8	10	51	19.6	14	51	27.5
Total	6	61	9.8	13	61	21.3	19	61	31.1

Figure 8.46: *Lesions diagnostic for scurvy in Xiongnu Period nonadults. SPNB and abnormal cortical porosity on a) The anterior maxilla extending from the infraorbital foramen (AT-268a, ~15 years, Buural Uul), b) Left medial coronoid process of the mandible (AT-268a, ~15 years, Buural Uul), c) Posterior maxilla. Note the vascular impressions (black arrow; AT-268b, ~7.5 years, Buural Uul), d) Palatal surface of the maxilla (AT-268b, ~7.5 years, Buural Uul) and e) lateral left sphenoid bone (AT-268b, ~7.5 years, Buural Uul). e) White line of Fraenkel (white arrow) and Trummerfeld zone (yellow arrow; AT-908, ~11 years, Biluut 2). g) SPNB in the supraspinous fossa of the left scapula (AT-844a, neonate, Atsyn Gol). h) Abnormal endochondral porosity exceeding 10mm from the metaphyseal plate of the distal right fibula. SPNB and abnormal cortical porosity on the i) infraspinous process of the left scapula (AT-575, ~4 years, Bayan Uul), and j) The posterior maxilla and zygoma. Note the vascular impressions (black arrow; AT-575, ~4 years, Bayan Uul). Image: author's own.*

Figure 8.47: *Lesions diagnostic and suggestive for rickets in Xiongnu Period nonadults. a) Cupping and flaring of the distal femora (AT-154, male, ~17 years, Erdenetsagaan soum). b) Medial bending of the fibulae shafts (AT-268b, ~7.5 years, Buural Uul). c) Coarsening trabecular of the distal left humerus (AT-268b, ~7.5 years, Buural Uul). d) Cupping the proximal tibiae (AT-268b, ~7.5 years, Buural Uul). e) cupping of the proximal radii (AT-268b, ~7.5 years, Buural Uul). f) Increased angle of a left upper rib (AT-690, male, ~19 years, Uguumur). g) Fraying and deep porosity of the distal left femoral metaphysis (AT-268b, ~7.5 years, Buural Uul). h) Coxa vara of the femoral necks. (AT-908, ~11 years, Biluut 2). i) Coxa vara of the left femora neck (AT-690, male, ~19 years, Uguumur). Image: author's own.*

8.6.5.2 Diagnosis of Nutritional Disease in Xiongnu Period Adults

Less than 20% (17.6%, 9/51) of adults presented with skeletal signs for possible or probable scurvy, with only one individual meeting the diagnostic criteria for a probable diagnosis (AT-2, young adult female). Macroscopic lesions diagnostic for scurvy were predominately on the cranium in the same regions observed in the nonadults (Figure 8.48). Lesions of the cranium involved discrete symmetrical SPNB and/or abnormal cortical porosity. Additionally bilateral and symmetrical discrete deposits of SPNB resembling haematomas of the long bones were also common. In the overall assemblage, a decline in the prevalence of scurvy with increasing age is apparent, and no old adult (50+) was observed to have any signs of scurvy (Figure 8.49).

Almost one quarter (23.5%, 12/51) of the adult assemblage had skeletal pathologies consistent with a diagnosis of possible or probable residual rickets. Residual rickets was identified in all adult age cohorts, at a considerably lower prevalence, than affected nonadult age cohorts (Figure 8.50). Skeletal pathologies consistent with residual rickets included bending deformities of the limbs, alterations in the rib neck angles, and coxa vara of the femoral necks (Figure 8.51). A young adult female also displayed cortical enlargement of the cranium that may be a result of a remodelled rachitic skull (Figure 8.51b; Brickley and Ives 2010). Additionally, radiographic signs of thickened cortices of the long bones and coarsening trabeculae in distal metaphyseal regions of the long bones was also observed.

Twenty-eight percent (27.5%, 14/51) of adults exhibited skeletal pathologies consistent with a diagnosis of possible or probable osteomalacia. As previously mentioned, a further five adolescents also had similar deformities, consistent with a diagnosis of two possible and three probable cases of osteomalacia. All males that had skeletal signs of osteomalacia were diagnosed with a probable case (Table 8.36). Bilateral and symmetrical pseudofractures of the pubic and ischial rami or spinous process of the scapulae were evident in four individuals, strongly diagnostic for osteomalacia (Figure 8.52a). Two of these also exhibited buckling of the pubic rami resulting in dislocation of the pubic symphysis (Figure 8.52b). Additionally, other postcranial skeletal deformities diagnostic for osteomalacia including buckling of the scapulae, sterna, vertebrae, and extreme lateral straightening of the ribs were observed (Figure 8.52). Coxa vara and genu valgum deformities were commonly observed alongside antero-lateral bending of the femoral shafts. No

pseudofractures of the femoral necks were identified. AT-23, a young adult male, presented with a poorly mineralised fracture callus on the left humerus, again diagnostic for active osteomalacia (Figure 8.52c). It is possible, that the discrete deposits of poorly mineralised bone at the muscles attachments sites that dominate the osteoblastic lesions in the assemblage (as described above), are manifestations of poorly mineralised remodelled lamellar bone associated with microtrauma. Consideration of new lesions contributing to the diagnostic protocols is beyond the scope of this thesis, but future investigation may demonstrate a relationship with these lesions to active osteomalacia.

Additionally, the osteolytic lesions with smooth margins and base were identified only in individuals with a probable diagnosis of osteomalacia. These lesions are reminiscent of clinical description of *Brown tumours* (fibrous cystic osteitis) consistent with development of secondary hyperparathyroidism, as a consequence of severe and chronic Vitamin D efficiency mineralisation disorder (Bereket et al. 2000; Dimitri and Bishop 2007). Brown tumours are most commonly found in childhood and adolescence (Goyal et al. 2018), as observed in this assemblage where they were restricted to individuals under 21 years of age (Figure 8.53). Overall, osteomalacia was identified in all adolescent and adult age cohorts, with an apparent decline of the prevalence with increasing age (Figure 8.54).

Ten individuals (16.4%, 10/61) exhibited co-occurrence of both possible or probable osteomalacia *and* rickets/ residual rickets. A higher prevalence (24.6%, 15/61) of individuals were observed to only exhibit signs of rickets *or* osteomalacia, not both. Therefore, unlike with the Bronze Age assemblage, there is little evidence of a clear relationship between episodes of childhood and adult mineralisation disorder.

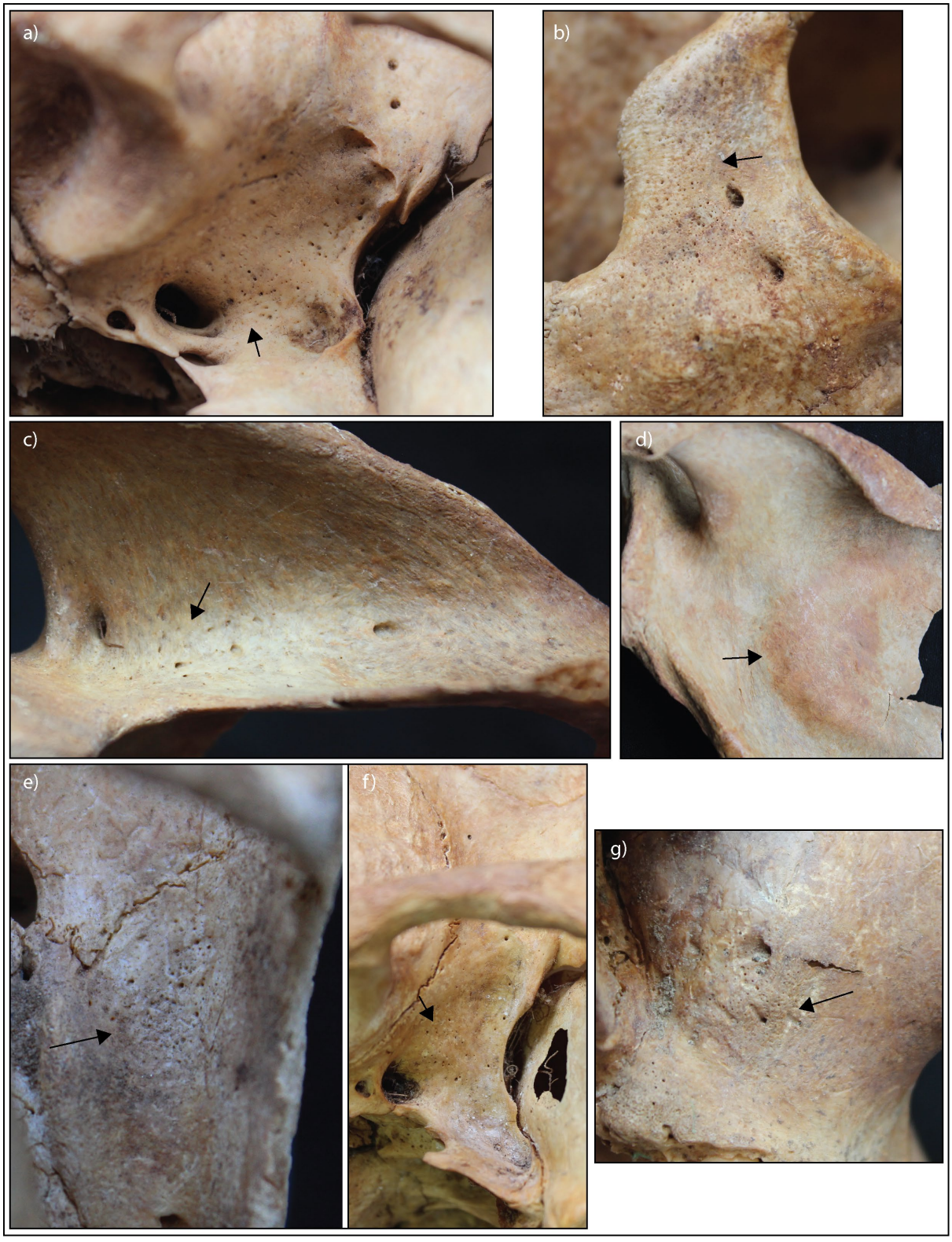

Figure 8.48: *Lesions diagnostic and suggestive for scurvy in Xiongnu Period adults. Discrete SPNB and abnormal cortical porosity on the a) Right pterygoid plate and b) Anterior right zygoma (AT-292, young adult male, Buural Uul). c-d) Abnormal cortical porosity on the supraspinous fossa, and SPNB on the infraspinous fossa of the right scapula (AT-2, young adult female, Naimaa Tolgoi). e) SPNB and abnormal cortical porosity on the on the posterior right zygoma (AT-536, young adult male, Burkhan Tolgoi). f) SPNB and abnormal cortical porosity on the right lateral sphenoid and pterygoid plate (AT-294, middle aged adult female, Buural Uul). g) SPNB and abnormal cortical porosity on the posterior maxilla (AT-747, young adult male, Uguumur). Image: author's own.*

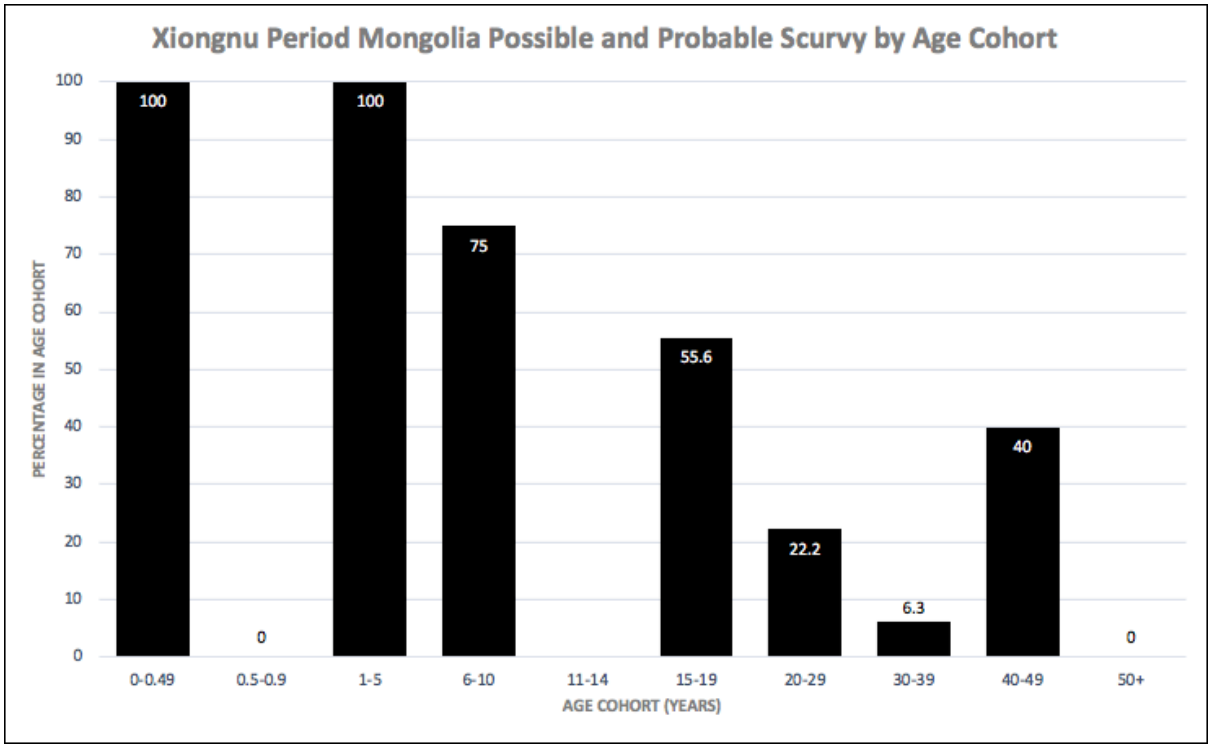

Figure 8.49: *Age-at-death distribution of possible and probable scurvy in Xiongnu Period Mongolia. Image: author's own.*

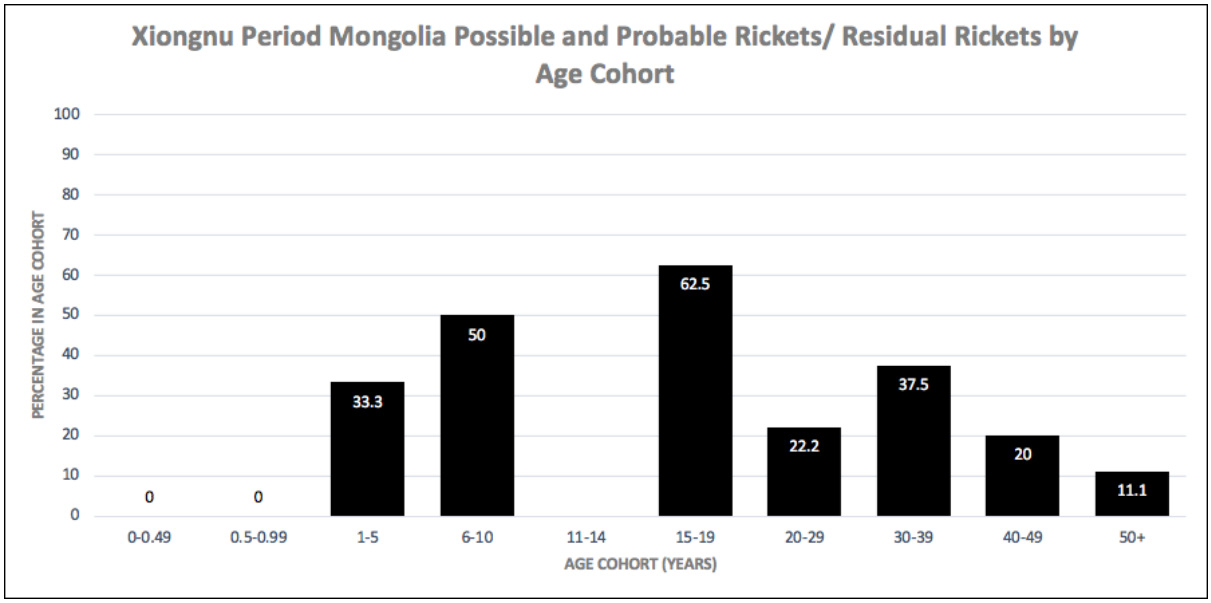

Figure 8.50: *Age-at-death distribution of possible and probable rickets and residual rickets in Xiongnu Period Mongolia. Image: author's own.*

Figure 8.51: *Lesions diagnostic and suggestive for residual rickets in Xiongnu Period adults. a) Coxa vara for the femoral necks (AT-23, young adult male, Tevsh Uul). b) Enlarged cortex of the parietal bones (AT-350, young adult female, Barzangiin Enger). c) Medial bending of the fibulae (AT-265, young adult male, Eezguutiin Khujirt). d) Medial bending deformity of the left tibia with slight cortex enlargement (AT-36, middle aged adult male, Tevsh Uul). e) Increased angulation of the rib neck (AT-23, young adult male, Tevsh Uul). f) Enlarged cortex of the right femur (AT-146, young adult male, Tevsh Uul). Image: author's own.*

Figure 8.52: *Lesions strongly diagnostic, diagnostic and suggestive for osteomalacia in Xiongnu Period adults and adolescents. a) Remodelled pseudofractures of the pubic and ischial rami (AT-259, middle aged adult male, Buural Uul) b) Buckling of the pubic and ischial rami with dislocation of the pubic symphysis (AT-365, male, ~19.5 years, Mankhan soum). c) Poorly mineralised callus on the left humerus (AT-23, young adult male, Tevsh Uul). d) Increased posterior curvature of the scapulae (AT-437, young adult male, Burkhan Tolgoi). e) Anterior- lateral bending of the femoral shafts (AT-259, middle aged adult male, Buural Uul). f) Anterior curvature of the sternum (AT-365, male, ~19.5 years, Mankhan soum) g) Curvature of the spinous process of the scapula (AT-337, middle aged adult male, Buural Uul). h) Biconcavity of the vertebra. Multiple vertebrae were affected (AT-569, middle aged adult male, Sant Uul). i) Exaggerated ventral angulation of the sacrum (AT-692, middle aged adult male, Uguumur. Image: author's own.*

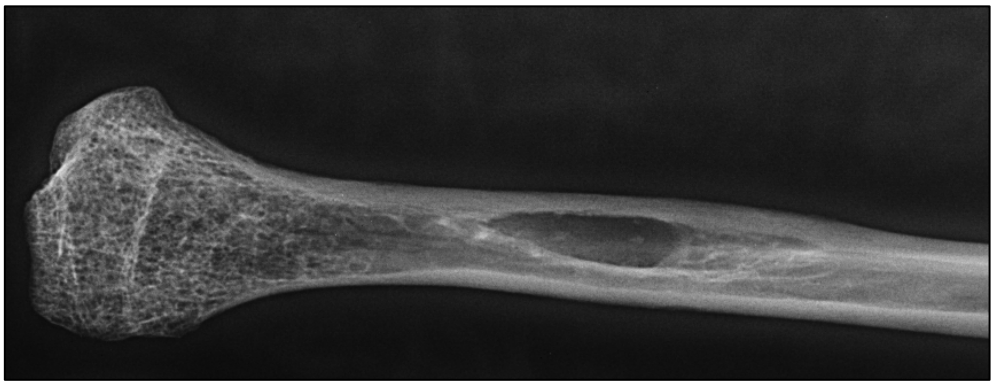

Figure 8.53: *Radiograph of osteolytic lesion consistent with a "Brown tumour" from secondary hyperparathyroidism on the proximal left fibula (AT-583, male, ~19 years. Emeel Tolgoi). Image: author's own.*

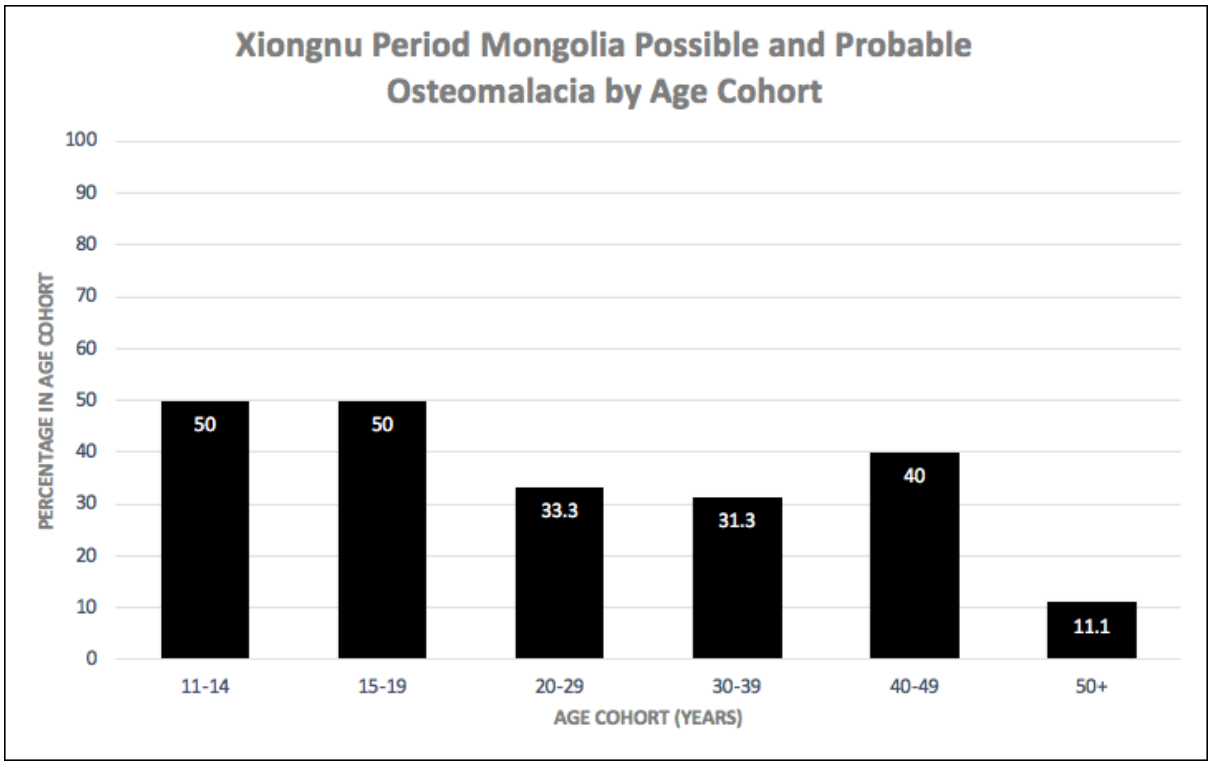

Figure 8.54: *Age-at-death distribution of possible and probable osteomalacia in Xiongnu Period Mongolia. Image: author's own.*

8.6.6 Morbidity of Nutritional Disease in the Xiongnu Period

8.6.6.1 Morbidity of Scurvy in the Xiongnu Period

No statistically significant differences were identified between males and females for both combined possible and probable and probable only scurvy (Table 8.37). However, a significant relationship was observed for nonadult age cohorts. While nonadults were only 1.5 times (n=18, RR=1.5455, p=0.0151) more likely to have scurvy before the age of 1 year

of age and 1.6 times (n=18, RR=1.6667, p=0.0154) more likely to have scurvy before the age of 5 years, both outcomes were statistically significant. Adolescents between 15-19 years were also almost 4 times (n=57, RR=3.8095, p=0.0036) more likely to present with scurvy than adults over the age of 20 years. The size of the effect was larger when considering probable only cases, where adolescents were 16 times (n=57, RR=16.000, p=0.0114) more likely to have probable scurvy. Additionally, a significant relationship between morbidity of scurvy and younger adult age was also observed with adults under the age of 30 having 3.3 times (n=57, RR=3.3333, p=0.0490) the risk of morbidity of possible or probable scurvy than adults over 30.

Table 8.37: *Relative risk of scurvy morbidity in the Xiongnu Period across sex and age cohorts.*

EXPOSED GROUP/ CONTROL GROUP	**OUTCOME**		**RR**	**P-VALUE**	**95%CI**
	Positive: *Disease Present*	***Negative:*** *Disease Absent*			
Possible and Probable Scurvy (combined)					
Sex					
Female/ Male	5/7	23/22	0.7398	0.5638	0.2658- 2.0587
Nonadults					
<1 yr/ >1 yr	1/11	0/6	**1.5455**	**0.0151***	1.0879- 2.1955
<5 yrs/ >5yrs	3/9	0/6	**1.6667**	**0.0154***	1.1025- 2.5194
<10 yrs/ >10yrs	7/5	1/5	1.7500	0.1031	0.8929- 3.4298
Adults					
<20 yrs/ >20 yrs	5/7	4/41	**3.8095**	**0.0036***	1.5486- 9.3712
<30 yrs/ >30 yrs	9/3	18/27	**3.3333**	**0.0490***	1.0052- 11.0534
<40 yrs/>40 yrs	10/2	33/12	1.6279	0.4930	0.4041- 6.5573
Probable Only Scurvy					
Sex					
Female/ Male	2/2	26/7	1.0357	0.9710	0.1565- 6.8555
Nonadults					
<1 yr/ >1 yr	0/8	1/9	0.5294	0.6109	0.0457- 6.1330
<5 yrs/ >5yrs	1/7	2/8	0.7143	0.6962	0.1319- 3.8684
<10 yrs/ >10yrs	4/4	3/7	1.5714	0.3810	0.5716-4.3202
Adults					
<20 yrs/ >20 yrs	3/1	6/47	**16.000**	**0.0114***	1.8669- 137.1264
<30 yrs/ >30 yrs	3/1	24/29	3.333	0.2840	0.3684- 30.1641
<40 yrs/>40 yrs	4/0	39/14	3.0682	0.4427	0.1753- 53.7052

A relative risk (RR) >1 denotes a relationship of the exposed group with an increase in disease prevalence, whereas RR <1 denotes a relationship of the control group with an increase in disease prevalence.
**= statistically significant (p<0.10). **= statistically significant when considering size of the effect of RR.*

8.6.6.2 Morbidity of Rickets and Residual Rickets in the Xiongnu Period

No statistically significant differences were observed in the morbidity of rickets between the nonadult age cohorts, and residual rickets in the adult age cohorts (Table 8.38). Additionally, there were no significant differences between males and females in regards to the morbidity of residual rickets. This outcome was consistent when considering combined possible and probable cases and probable only cases.

Table 8.38: *Relative risk of rickets/ residual rickets morbidity in the Xiongnu Period across sex and age cohorts.*

EXPOSED GROUP/ CONTROL GROUP	**OUTCOME**		**RR**	**P-VALUE**	**95%CI**
	Positive: *Disease Present*	***Negative:*** *Disease Absent*			
Possible and Probable Rickets (combined)					
Nonadults					
<1 yr/ >1 yr	0/8	1/9	0.5294	0.6109	0.0457- 6.1330
<5 yrs/ >5yrs	0/8	3/7	0.2353	0.2815	0.0169- 3.2754
<10 yrs/ >10yrs	3/5	5/5	0.7500	0.6044	0.2526- 2.2270
Probable Only Rickets					
Nonadults					
<1 yr/ >1 yr	0/5	1/12	0.8182	0.8750	0.0672- 9.9624
<5 yrs/ >5yrs	0/5	3/10	0.3636	0.4594	0.0249- 5.3025
<10 yrs/ >10yrs	2/3	6/7	0.8333	0.8152	0.1807- 3.8435
Possible and Probable Residual Rickets (combined)					
Sex					
Female/ Male	4/7	19/17	0.5963	0.3513	0.2010- 1.7686
Adults					
<20 yrs/ >20 yrs	-	-	-	-	-
<30 yrs/ >30 yrs	4/8	14/22	0.8333	0.7332	0.2921- 2.3775
<40 yrs/>40 yrs	10/2	24/12	2.0588	0.3067	0.5155- 8.227
Probable Only Residual Rickets					
Sex					
Female/ Male	2/5	21/19	0.4174	0.2652	0.0898- 1.9409
Adults					
<20 yrs/ >20 yrs	-	-	-	-	-
<30 yrs/ >30 yrs	2/4	16/26	0.8333	0.8226	0.1693- 4.1014
<40 yrs/>40 yrs	5/1	29/13	2.0588	0.4910	0.2638- 16.0710

A relative risk (RR) >1 denotes a relationship of the exposed group with an increase in disease prevalence, whereas RR <1 denotes a relationship of the control group with an increase in disease prevalence.
**= statistically significant (p<0.10). **= statistically significant when considering size of the effect of RR.*

8.6.6.3 Morbidity of Osteomalacia in the Xiongnu Period

While there were no significant differences between males and females when considering combined probable and possible cases (n= 57, RR=0.6591, p= 0.3026), males were over 7 times (n= 57, RR=0.1389, p= 0.0408) more likely to have probable osteomalacia than females in the Xiongnu assemblage, which was statistically significant. No statistically significant differences in the morbidity of osteomalacia between adult age cohorts was observed for both combined possible and probable and probable only cases (Table 8.39).

Table 8.39: *Relative risk of osteomalacia morbidity in the Xiongnu Period across sex and age cohorts.*

EXPOSED GROUP/ CONTROL GROUP	**OUTCOME**		**RR**	**P-VALUE**	**95%CI**
	Positive: *Disease Present*	***Negative:*** *Disease Absent*			
Possible and Probable Osteomalacia (combined)					
Sex					
Female/ Male	7/11	21/18	0.6591	0.3026	0.2983- 1.4562
Adults					
<20 yrs/ >20 yrs	4/14	4/34	1.7143	0.1984	0.7540- 3.8974
<30 yrs/ >30 yrs	10/8	16/22	1.4423	0.3494	0.6697- 3.1063
<40 yrs/>40 yrs	15/3	27/11	1.6667	0.3548	0.5648- 4.9177
Probable Only Osteomalacia					
Sex					
Female/ Male	1/11	27/18	**0.1389**	**0.0408***	0.0209- 0.9209
Adults					
<20 yrs/ >20 yrs	3/10	5/38	1.8000	0.2730	0.6293- 5.1486
<30 yrs/ >30 yrs	7/6	19/24	1.3462	0.5421	0.5177- 3.5005
<40 yrs/>40 yrs	11/2	31/12	1.8333	0.3893	0.4613- 7.2867

A relative risk (RR) >1 denotes a relationship of the exposed group with an increase in disease prevalence, whereas RR <1 denotes a relationship of the control group with an increase in disease prevalence.
**= statistically significant (p<0.10). **= statistically significant when considering size of the effect of RR.*

8.6.7 Mortality of Nutritional Disease in the Xiongnu Period

8.6.7.1 Mortality of Scurvy in the Xiongnu Period

Relative risk ratio analysis identified no statistical relationship with increased risk of death for skeletal evidence of both combined possible and probable, and probable only scurvy in the nonadult age cohorts (Table 8.40). Kaplan-Meier survival analysis similarly identified no statistical relationship for both possible and probable (n=18, X^2=0.072, df=1,

p=0.789; Table 8.41; Figure 8.55) and probable only (n=18, X^2=0.071, df=1, p=0.790; Table 8.42; Figure 8.56) cases.

Relative risk ratio analysis identified a significantly increased risk of death with scurvy in adolescents between 15-19 compared to adults over 20 years (n=57, RR=2.8571, p=0.0316), and adults under 30 years compared to those who survived past 30 years of age (n=57, RR=1.8750, p=0.0110). This outcome was supported by statistically significant results for both the Kaplan-Meier (n=57, X^2=5.600, df=1 p=0.0180; Table 8.43; Figure 8.57) and Cox regression analyses (n=57, Wald=5.013, df=1, p=0.025; Table 8.44; Figure 8.58). Similarly, a significantly increased risk of death was identified in adults who exhibited skeletal signs of probable scurvy. Individuals were more than 6.5 times (n=57, RR=6.6250, p=0.000) more likely to die before the age of 20 with skeletal signs of scurvy than survive to adulthood. Additionally, adults were 1.4 times (n=57, RR=1.3590, p=0.0002) more likely to die before the age of 40 with skeletal signs scurvy than survive to older age. While the effect is small, the outcome was statistically significant. Kaplan-Meier (n=57, X^2=8.468, df=1, p=0.004; Table 8.45; Figure 8.60) and Cox regression (n=57, Wald=6.897, df=1, p=0.009; Table 8.46; Figure 8.60) both support a significant increase in frailty of those with scurvy. Overall, while skeletal presence of scurvy did not identify significantly increased risk of mortality amongst nonadults cohorts, adolescents and adults with skeletal signs of scurvy exhibited higher frailty than those without skeletal signs of scurvy.

Table 8.40: *Relative risk of scurvy mortality in the Xiongnu Period across age cohorts.*

POSITIVE OUTCOME/ NEGATIVE OUTCOME	TREATMENT		RR	P-VALUE	95%CI
	Exposed Group: *Disease Present*	***Control Group:*** *Disease Absent*			
Possible and Probable Scurvy (combined)					
Nonadults					
<1 yr/ >1 yr	1/11	0/6	1.6154	0.7592	0.0753- 34.6573
<5 yrs/ >5yrs	3/9	0/6	3.7692	0.3559	0.2253- 63.0576
<10 yrs/ >10yrs	7/5	1/5	3.5000	0.1849	0.5492- 22.3045
Adults					
<20 yrs/ >20 yrs	5/7	4/41	**2.8571**	**0.0316***	1.0966- 7.4439
<30 yrs/ >30 yrs	9/3	18/27	**1.8750**	**0.0110***	1.1550- 3.0439
<40 yrs/>40 yrs	10/2	33/12	1.1364	0.4164	0.8349- 1.5468
Probable Only Scurvy					
Nonadults					
<1 yr/ >1 yr	0/8	1/9	0.4074	0.5673	0.0188- 8.8383
<5 yrs/ >5yrs	1/7	2/8	0.6250	0.6772	0.0683- 5.7153
<10 yrs/ >10yrs	4/4	3/7	1.6667	0.3935	0.5156- 5.3876
Adults					
<20 yrs/ >20 yrs	3/1	6/47	**6.6250**	**0.0001***	2.5820- 16.9988
<30 yrs/ >30 yrs	3/1	24/29	1.6563	0.1214	0.8746- 3.1364
<40 yrs/>40 yrs	4/0	39/14	**1.3590**	**0.0002***	1.1565- 1.5969

A relative risk (RR) >1 denotes a relationship of the disease presence with the positive outcome (susceptibility to mortality), whereas RR <1 denotes a relationship of the disease absence with a negative outcome (survivorship).
**= statistically significant (p<0.10). **= statistically significant when considering size of the effect of RR.*

Table 8.41: *Statistical summary for Kaplan-Meier function of possible and probable scurvy mortality of nonadults in Xiongnu Period Mongolia.*

POSSIBLE AND PROBABLE SCURVY	ESTIMATE	STD. ERROR	95% CI	LOG RANK (MANTEL-COX)		
				CHI SQUARE	DF	P-VALUE
Mean				0.072	1	0.789
Absent	14.667	1.563	11.602- 17.731			
Present	10.292	1.971	6.429- 14.155			
Overall	12.056	1.472	8.866- 14.634			
Median						
Absent	15.500	0.577	14.368- 16.632			
Present	8.000	2.021	4.039- 11.961			
Overall	14.500	4.243	6.184- 22.816			

**= statistical significance (p<0.15).*

Table 8.42: *Statistical summary for Kaplan-Meier function of probable scurvy mortality of nonadults in Xiongnu Period Mongolia.*

PROBABLE SCURVY	ESTIMATE	STD. ERROR	95% CI	LOG RANK (MANTEL-COX)		
				CHI SQUARE	DF	P-VALUE
Mean				0.071	1	0.790
Absent	12.700	2.135	8.516- 16.884			
Present	10.563	2.036	6.571- 14.554			
Overall	12.056	1.472	8.886- 14.634			
Median						
Absent	15.500	0.775	13.982- 17.018			
Present	8.000	0.342	7.329- 8.671			
Overall	14.500	7.425	0.000- 29.052			

*****= *statistical significance (p<0.15).*

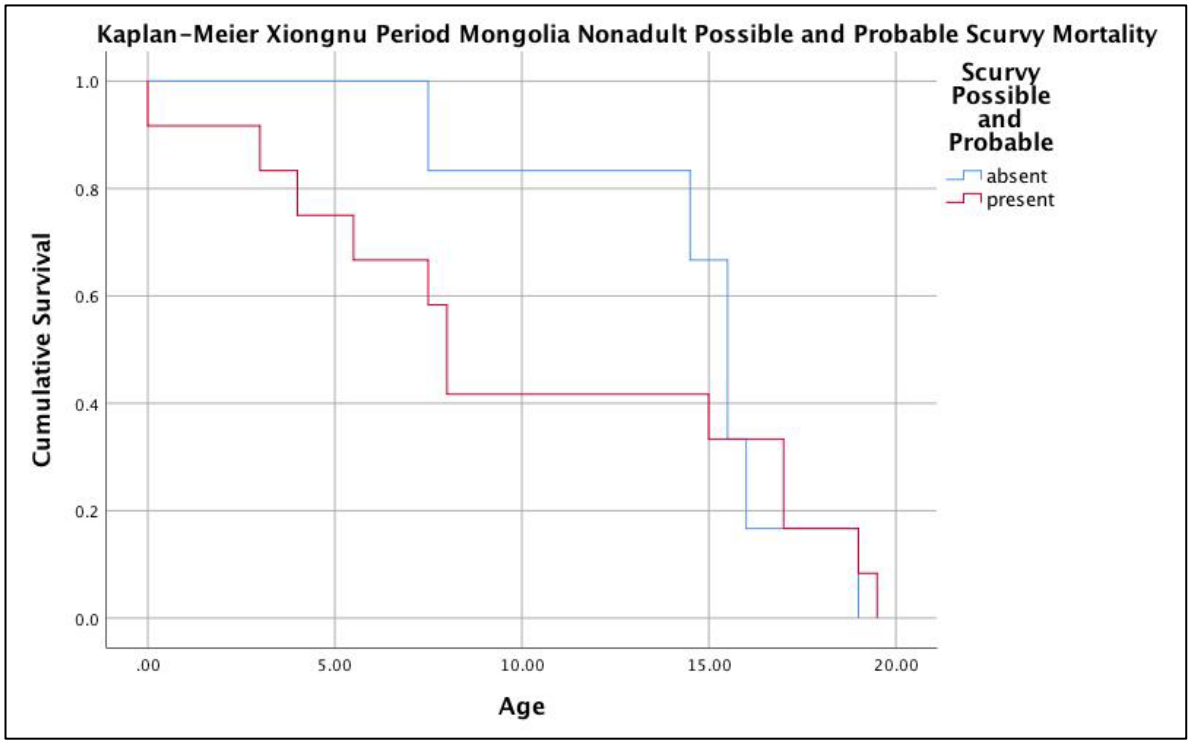

Figure 8.55: *Kaplan-Meier cumulative survival function of nonadult possible and probable scurvy mortality in Xiongnu Period Mongolia. Image: author's own.*

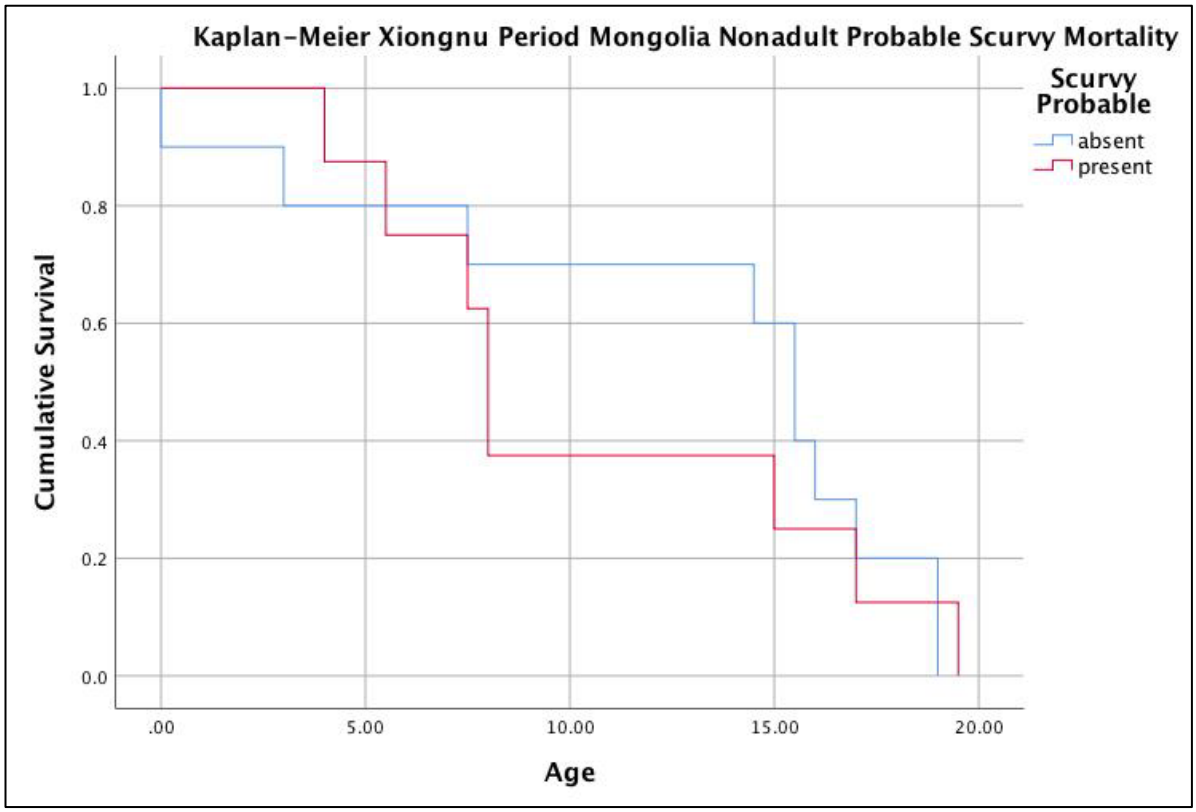

Figure 8.56: *Kaplan-Meier cumulative survival function of nonadult probable scurvy mortality in Xiongnu Period Mongolia. Image: author's own.*

Table 8.43: *Statistical summary for Kaplan-Meier function of possible and probable scurvy mortality of adults in Xiongnu Period Mongolia.*

POSSIBLE AND PROBABLE SCURVY	ESTIMATE	STD. ERROR	95% CI	LOG RANK (MANTEL-COX)		
				CHI SQUARE	DF	P-VALUE
Mean				5.600	1	**0.018***
Absent	34.227	1999	30.308- 38.145			
Present	26.062	2.883	20.412- 31.713			
Overall	32.508	1.738	29.101- 35.914			
Median						
Absent	32.000	1.677	28.714- 35.286			
Present	23.400	4.763	14.064- 32.736			
Overall	30.700	1.733	27.304- 34.096			

**= statistical significance (p<0.15).*

Table 8.44: *Statistical summary for Cox regression function of possible and probable scurvy mortality of adults in the Xiongnu Period Mongolia.*

POSSIBLE AND PROBABLE SCURVY	COEFFICIENT (β)	STD. ERROR	WALD	DF	P-VALUE	ODDS RATIO (Exp(β))
	-0.757	0.338	5.013	1	**0.025***	0.469

**= statistical significance (p<0.15).*

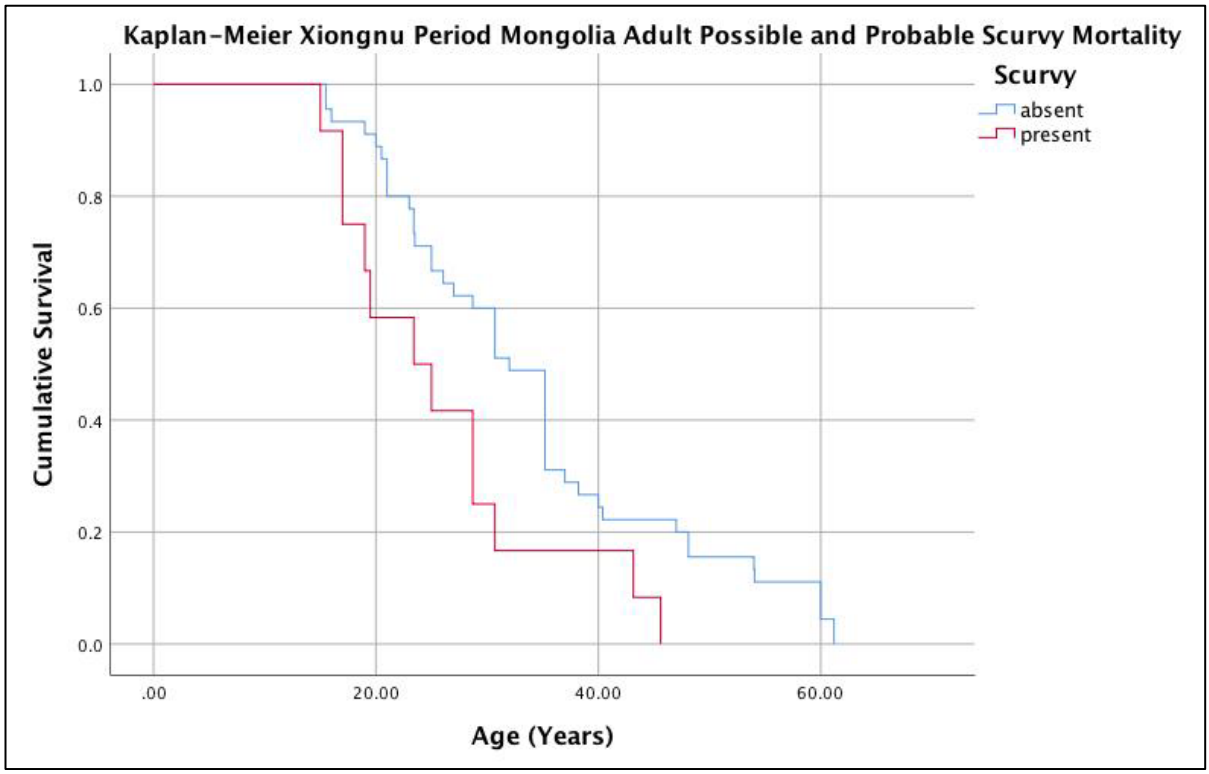

Figure 8.57: *Kaplan-Meier cumulative survival function of adult possible and probable scurvy mortality in Xiongnu Period Mongolia. Image: author's own.*

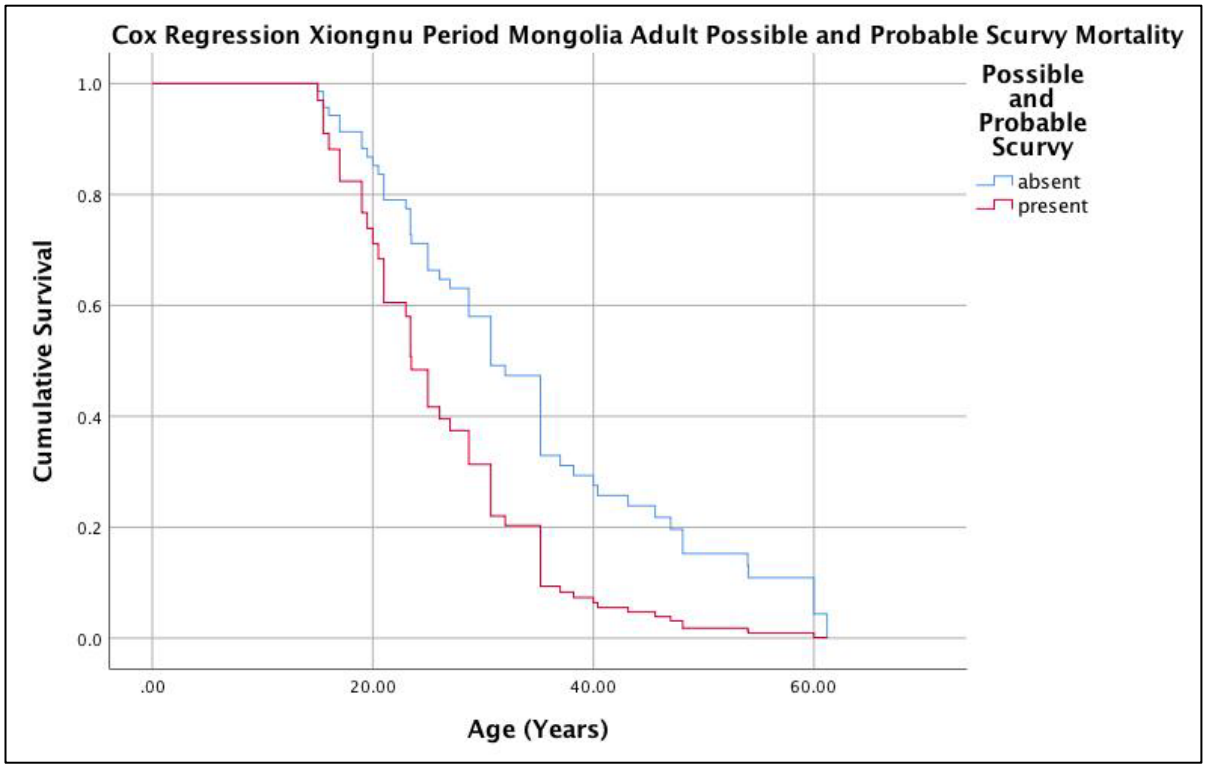

Figure 8.58: *Cox regression cumulative survival function of adult possible and probable scurvy mortality in Xiongnu Period Mongolia. Image: author's own.*

Table 8.45: *Statistical summary for Kaplan-Meier function of probable scurvy mortality of adults in Xiongnu Period Mongolia.*

PROBABLE SCURVY	ESTIMATE	STD. ERROR	95% CI	LOG RANK (MANTEL-COX)		
				CHI SQUARE	DF	P-VALUE
Mean				8.468	1	**0.004***
Absent	33.410	1.795	29.892- 36.928			
Present	20.550	3.506	13.678- 27.422			
Overall	32.508	1.738	29.101- 35.914			
Median						
Absent	30.700	1.863	27.049- 34.351			
Present	17.000	2.250	12.590- 21.410			
Overall	30.700	1.733	27.304- 34.096			

**= statistical significance (p<0.15).*

Table 8.46: *Statistical summary for Cox regression function of probable scurvy mortality of adults in the Xiongnu Period Mongolia.*

PROBABLE SCURVY	COEFFICIENT (β)	STD. ERROR	WALD	DF	P-VALUE	ODDS RATIO (Exp(β))
	1.415	0.539	6.897	1	**0.009***	4.116

**= statistical significance (p<0.15).*

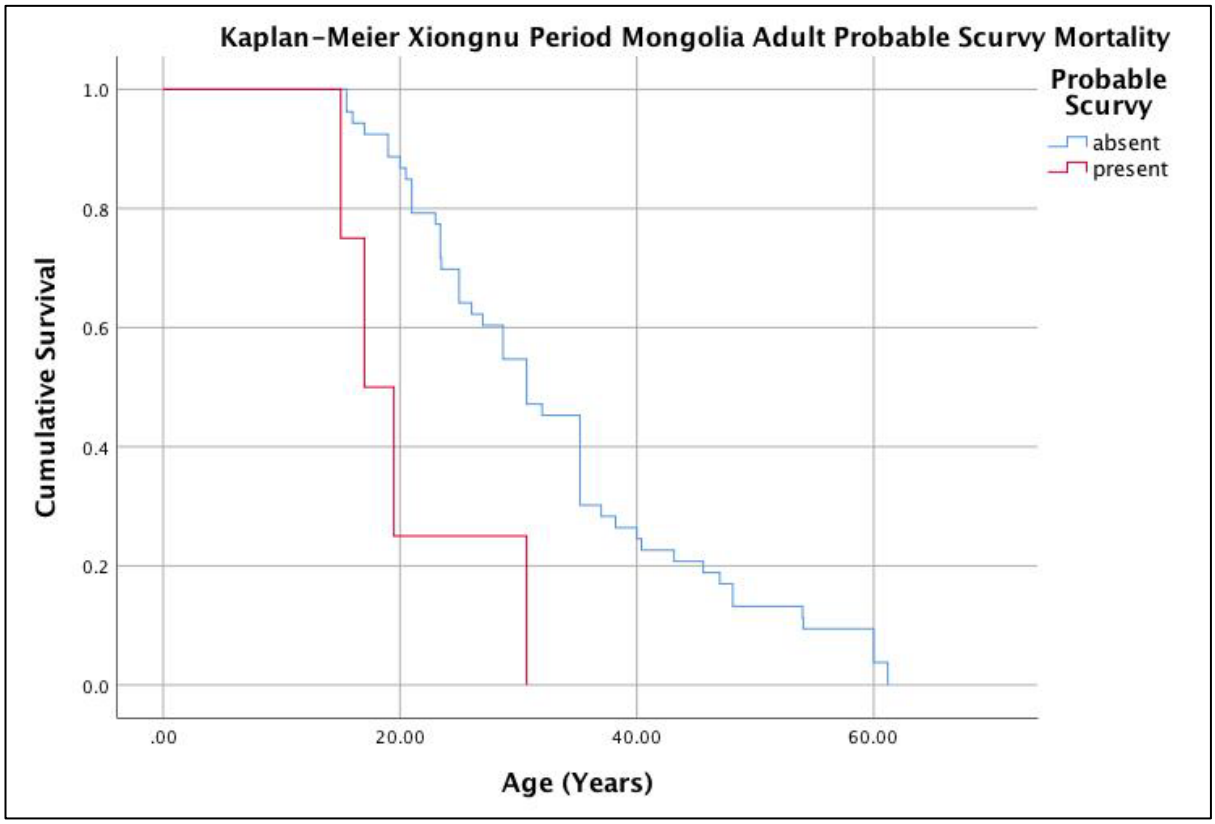

Figure 8.59: *Kaplan-Meier cumulative survival function of adult probable scurvy mortality in Xiongnu Period Mongolia. Image: author's own.*

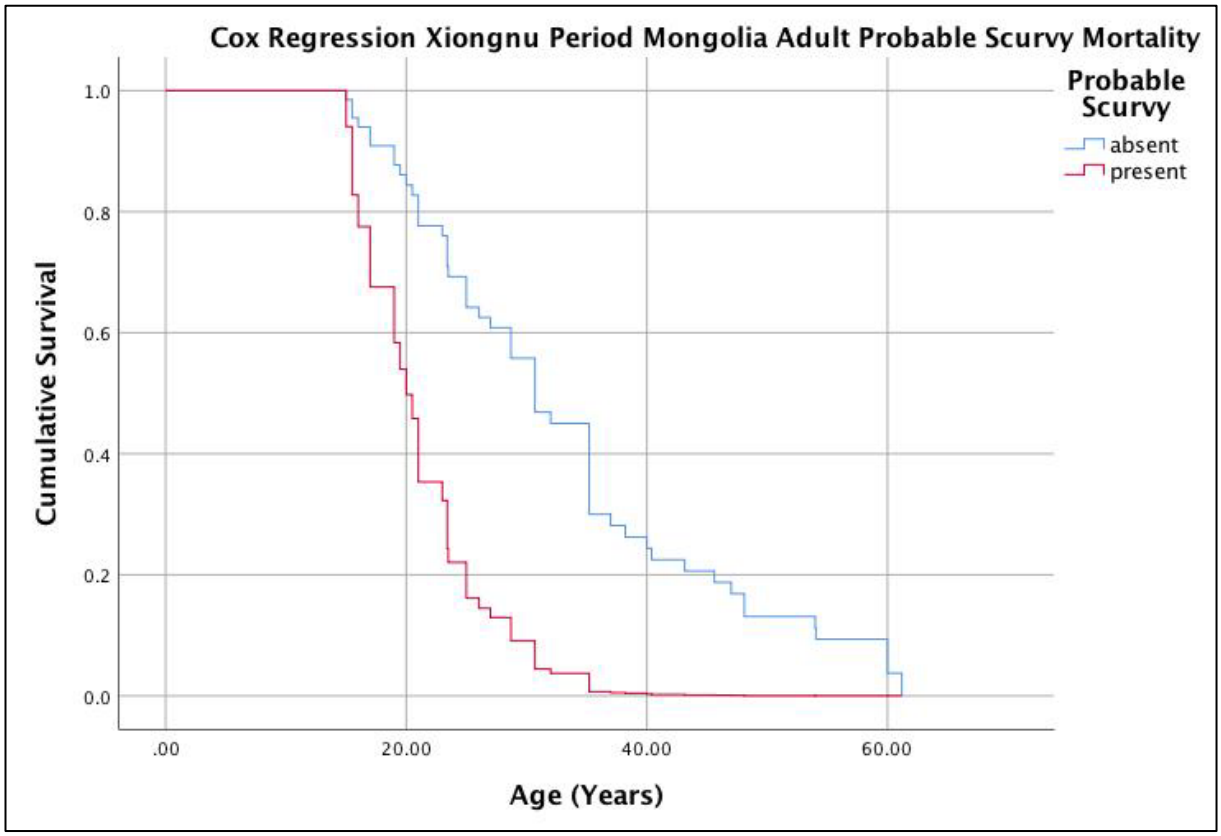

Figure 8.60: *Cox regression cumulative survival function of adult probable scurvy mortality in Xiongnu Period Mongolia. Image: author's own.*

8.6.7.2 Mortality of Rickets and Residual Rickets in the Xiongnu Period

No statistically significant increases in risk of death were observed in the relative risk ratio analysis for nonadult possible and probable, and probable only rickets (Table 8.47). However, Kaplan-Meier survival analysis (n=18, X^2=3.788, df=1, p=0.052; Table 8.48) and Cox regression (n=18, Wald=3.288, df=1, p=0.070; Table 8.49) both identified a significant relationship between the presence of combined possible and probable rickets in nonadults and increased survivorship. Clear differences in the survivorship of nonadults with and without skeletal signs of possible or probable rickets is observed in the Kaplan-Meier and Cox regression cumulative survival functions (Figures 8.61-8.62). Additionally, significantly increased survivorship was concurrently observed in probable only cases for Kaplan-Meier (n=18, X^2=2.267, df=1, p=0.132; Table 8.50; Figure 8.63) but not Cox regression analyses (n=18, Wald=1.895, df=1, p=0.169; Table 8.51; Figure 8.64), indicating a slight survivorship in probable only cases.

Relative risk ratio analysis identified no statistically significant relationship with increased risk of death of adults with combined possible and probable, as well as probable

only residual rickets (Table 8.47). Similarly, there was no statistically significant differences in the Kaplan-Meier survival analyses for both possible and probable (n=48, X^2=0.570, df=1, p=0.450; Table 8.52; Figure 8.65) and probable only (n=48, X^2=0.817, df=1, p=0.366; Table 8.53; Figure 8.66) cases of residual rickets. Overall, there was an increased relationship with survival for nonadults with skeletal signs of rickets, but there was no difference in mortality identified with adults who presented with skeletal signs of residual rickets compared to those without.

Table 8.47: *Relative risk of rickets/ residual rickets mortality in the Xiongnu Period across age cohorts.*

POSITIVE OUTCOME/ NEGATIVE OUTCOME	**TREATMENT**		**RR**	**P-VALUE**	**95%CI**
	Exposed Group: *Disease Present*	***Control Group:*** *Disease Absent*			
Possible and Probable Rickets (combined)					
Nonadults					
<1 yr/ >1 yr	0/8	1/9	0.4074	0.5673	0.0188- 8.8383
<5 yrs/ >5yrs	0/8	3/7	0.1746	0.2267	0.0100- 2.9565
<10 yrs/ >10yrs	3/5	5/5	0.7500	0.6044	0.2526-2.2270
Probable Only Rickets					
Nonadults					
<1 yr/ >1 yr	0/5	1/12	0.7778	0.8719	0.0367- 16.4961
<5 yrs/ >5yrs	0/5	3/10	0.3333	0.4426	0.0202- 5.5072
<10 yrs/ >10yrs	2/3	6/7	0.8867	0.8187	0.2549- 2.9462
Possible and Probable Residual Rickets (combined)					
Adults					
<20 yrs/ >20 yrs	-	-	-	-	-
<30 yrs/ >30 yrs	4/8	14/22	0.8571	0.7368	0.3489- 2.1058
<40 yrs/>40 yrs	10/2	24/12	1.2500	0.2018	0.8874- 1.7608
Probable Only Residual Rickets					
Adults					
<20 yrs/ >20 yrs	-	-	-	-	-
<30 yrs/ >30 yrs	2/4	16/26	0.8750	0.8267	0.2647- 2.8920
<40 yrs/>40 yrs	5/1	29/13	1.2069	0.3700	0.8000- 1.8207

A relative risk (RR) >1 denotes a relationship of the disease presence with the positive outcome (susceptibility to mortality), whereas RR <1 denotes a relationship of the disease absence with a negative outcome (survivorship).
**= statistically significant (p<0.10). **= statistically significant when considering size of the effect of RR.*

Table 8.48: *Statistical summary for Kaplan-Meier function of possible and probable rickets mortality of nonadults in Xiongnu Period Mongolia.*

POSSIBLE AND PROBABLE RICKETS	ESTIMATE	STD. ERROR	95% CI	LOG RANK (MANTEL-COX)		
				CHI SQUARE	DF	P-VALUE
Mean				3.788	1	**0.052***
Absent	10.050	1.988	6.153- 13.947			
Present	13.875	2.078	9.802- 17.948			
Overall	11.750	1.472	8.866- 14.634			
Median						
Absent	8.000	5.534	0.000- 18.847			
Present	15.500	6.364	3.027- 27.973			
Overall	14.500	7.425	0.000- 29.052			

**= statistical significance (p<0.15).*

Table 8.49: *Statistical summary for Cox regression function of possible and probable rickets mortality of nonadults in the Xiongnu Period Mongolia.*

POSSIBLE AND PROBABLE RICKETS	COEFFICIENT (β)	STD. ERROR	WALD	DF	P-VALUE	ODDS RATIO (Exp(β))
	1.023	0.564	3.288	1	**0.070***	2.782

**= statistical significance (p<0.15).*

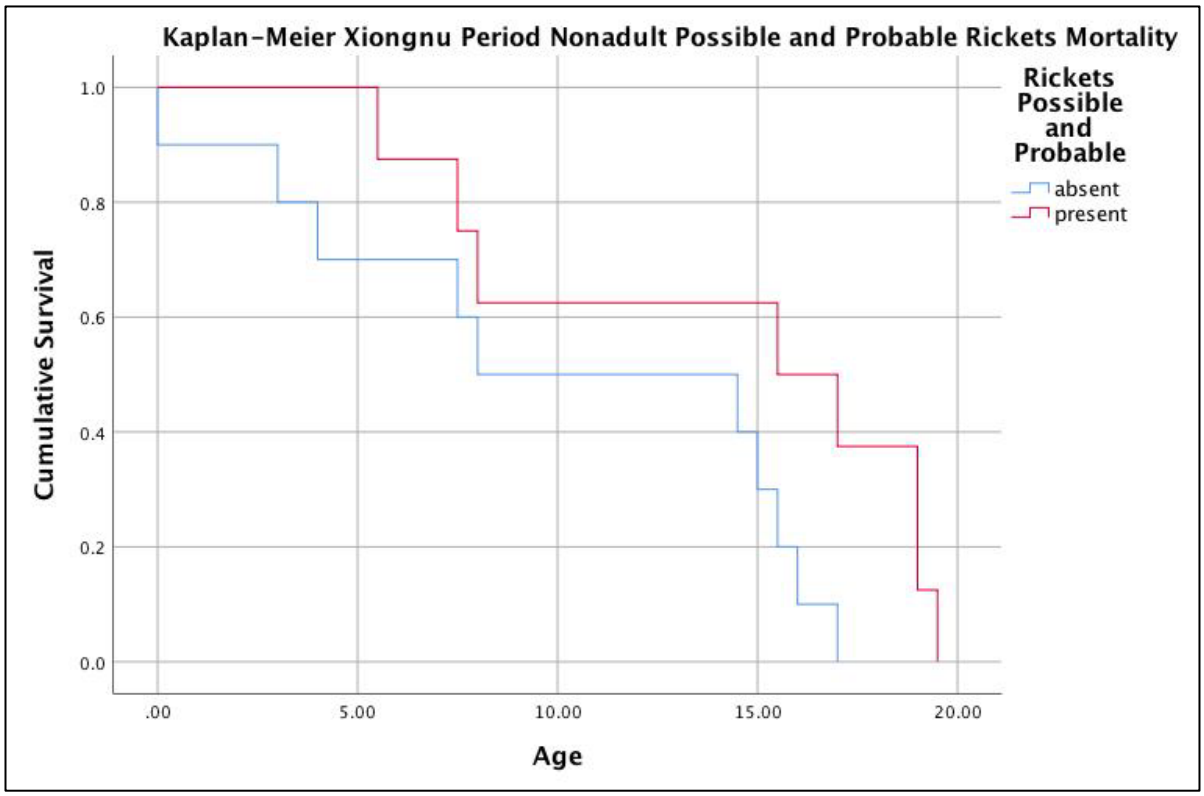

Figure 8.61: *Kaplan-Meier cumulative survival function of nonadult possible and probable rickets mortality in Xiongnu Period Mongolia. Image: author's own.*

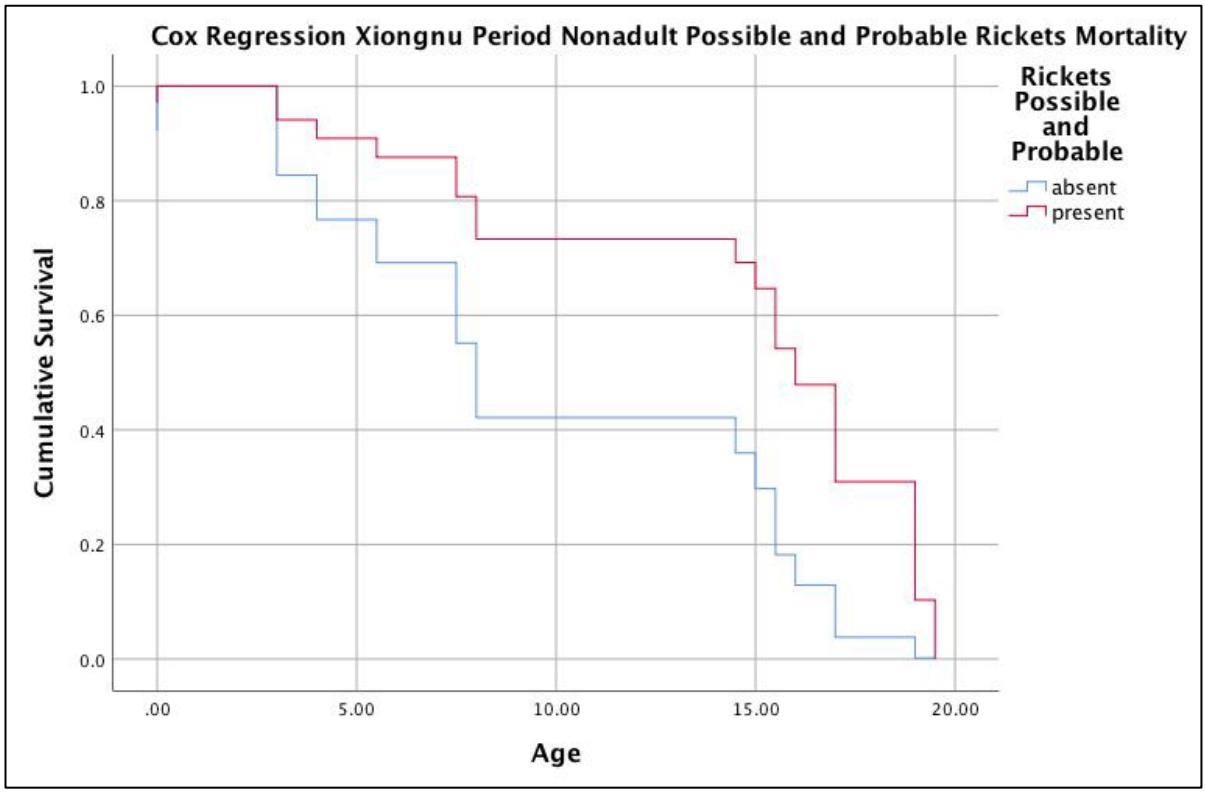

Figure 8.62: *Cox regression cumulative survival function of nonadult possible and probable rickets mortality in Xiongnu Period Mongolia. Image: author's own.*

Table 8.50: *Statistical summary for Kaplan-Meier function of probable rickets mortality of nonadults in Xiongnu Period Mongolia.*

RICKETS	ESTIMATE	STD. ERROR	95% CI	LOG RANK (MANTEL-COX)		
				CHI SQUARE	DF	P-VALUE
Mean				2.267	1	**0.132***
Absent	11.000	1.713	7.642- 14.358			
Present	13.700	2.986	7.848- 19.552			
Overall	11.750	1.472	8.866-14.634			
Median						
Absent	14.500	3.370	7.894- 21.106			
Present	17.000	10.407	0.000-37.397			
Overall	14.500	4.243	0.000-29.052			

**= statistical significance (p<0.15).*

Table 8.51: *Statistical summary for Cox regression function of probable rickets mortality of nonadults in the Xiongnu Period Mongolia.*

PROBABLE RICKETS	COEFFICIENT (β)	STD. ERROR	WALD	DF	P-VALUE	ODDS RATIO (Exp(β))
	0.819	0.595	1.895	1	0.169	2.269

**= statistical significance (p<0.15).*

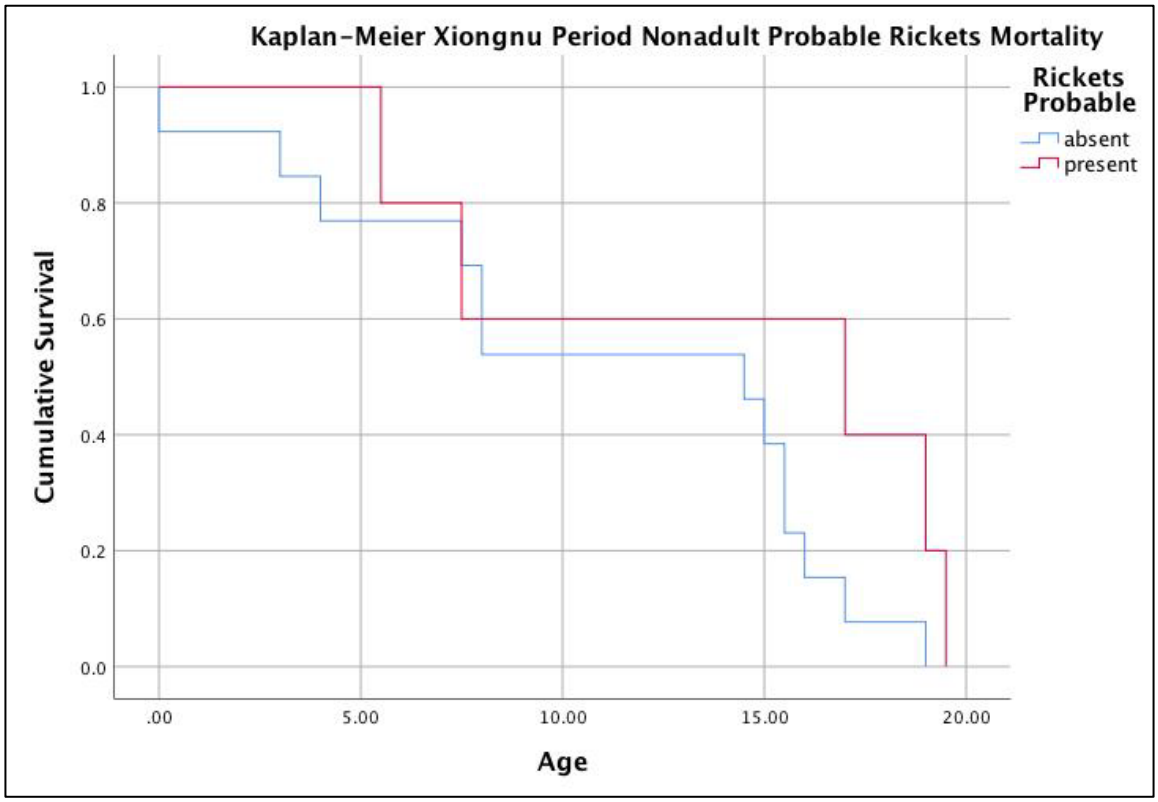

Figure 8.63: *Kaplan-Meier cumulative survival function of nonadult probable rickets mortality in Xiongnu Period Mongolia. Image: author's own.*

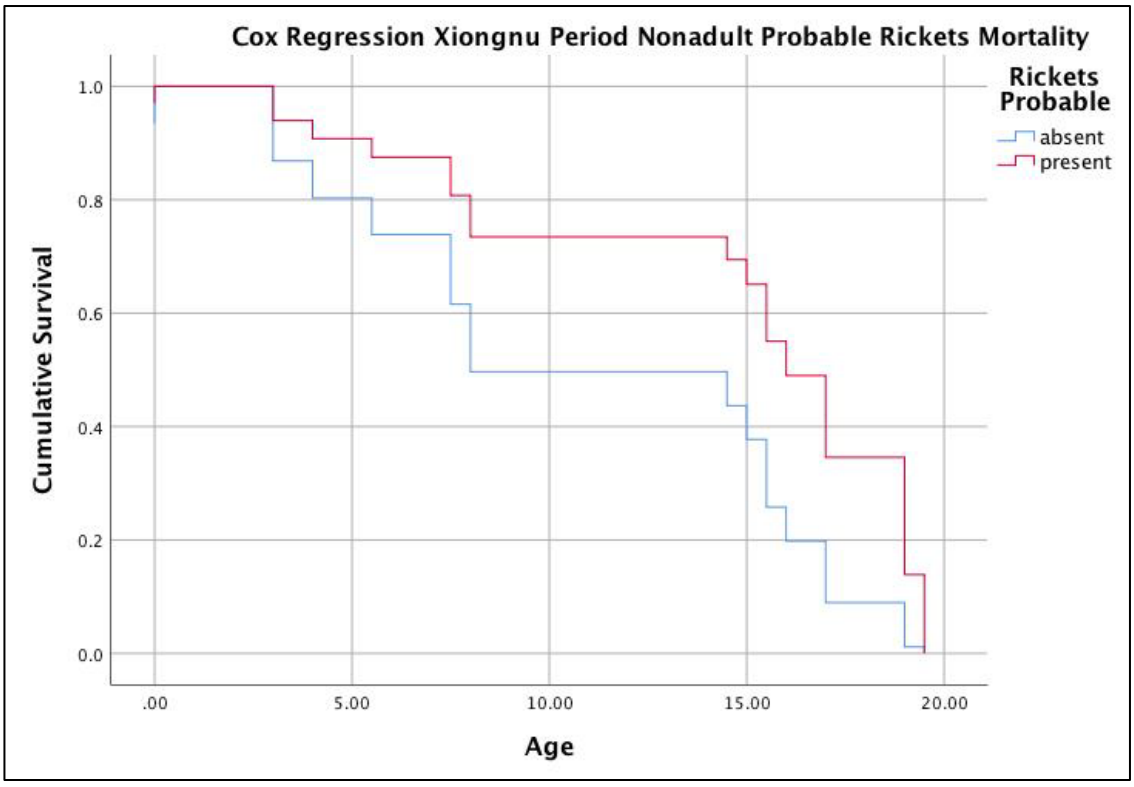

Figure 8.64: *Cox regression cumulative survival function of nonadult probable rickets mortality in Xiongnu Period Mongolia. Image: author's own*

Table 8.52: *Statistical summary for Kaplan-Meier function of possible and probable residual rickets mortality of adults in Xiongnu Period Mongolia.*

POSSIBLE AND PROBABLE RESIDUAL RICKETS	ESTIMATE	STD. ERROR	95% CI	LOG RANK (MANTEL-COX)		
				CHI SQUARE	DF	P-VALUE
Mean				0.570	1	0.450
Absent	36.157	2.111	32.020- 40.294			
Present	33.150	3.224	26.831- 39.469			
Overall	35.405	1.770	31.936- 38.874			
Median						
Absent	32.000	2.438	27.222- 36.778			
Present	30.700	2.944	24.929- 36.471			
Overall	32.000	1.608	28.848- 35.152			

**= statistical significance (p<0.15).*

Table 8.53: *Statistical summary for Kaplan-Meier function of probable residual rickets mortality of adults in Xiongnu Period Mongolia.*

POSSIBLE AND PROBABLE RESIDUAL RICKETS	ESTIMATE	STD. ERROR	95% CI	LOG RANK (MANTEL-COX)		
				CHI SQUARE	DF	P-VALUE
Mean				0.817	1	0.366
Absent	35.923	1.953	32.096- 39.750			
Present	31.783	3.703	24.526- 39.041			
Overall	35.405	1.770	31.936- 38.874			
Median						
Absent	32.000	1.915	28.247- 35.753			
Present	30.700	4.777	21.338- 40.062			
Overall	32.000	1.608	28.848- 35.152			

**= statistical significance (p<0.15).*

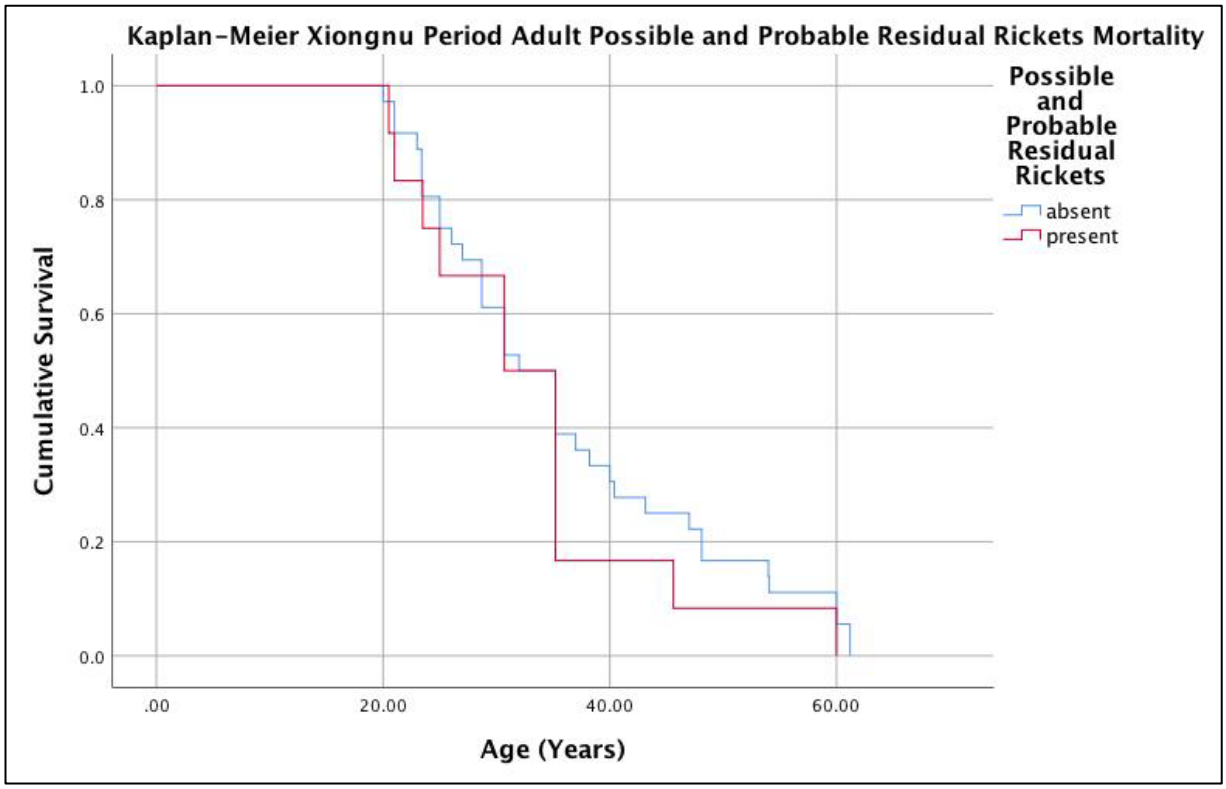

Figure 8.65: *Kaplan-Meier cumulative survival function of adult possible and probable residual rickets mortality in Xiongnu Period Mongolia. Image: author's own.*

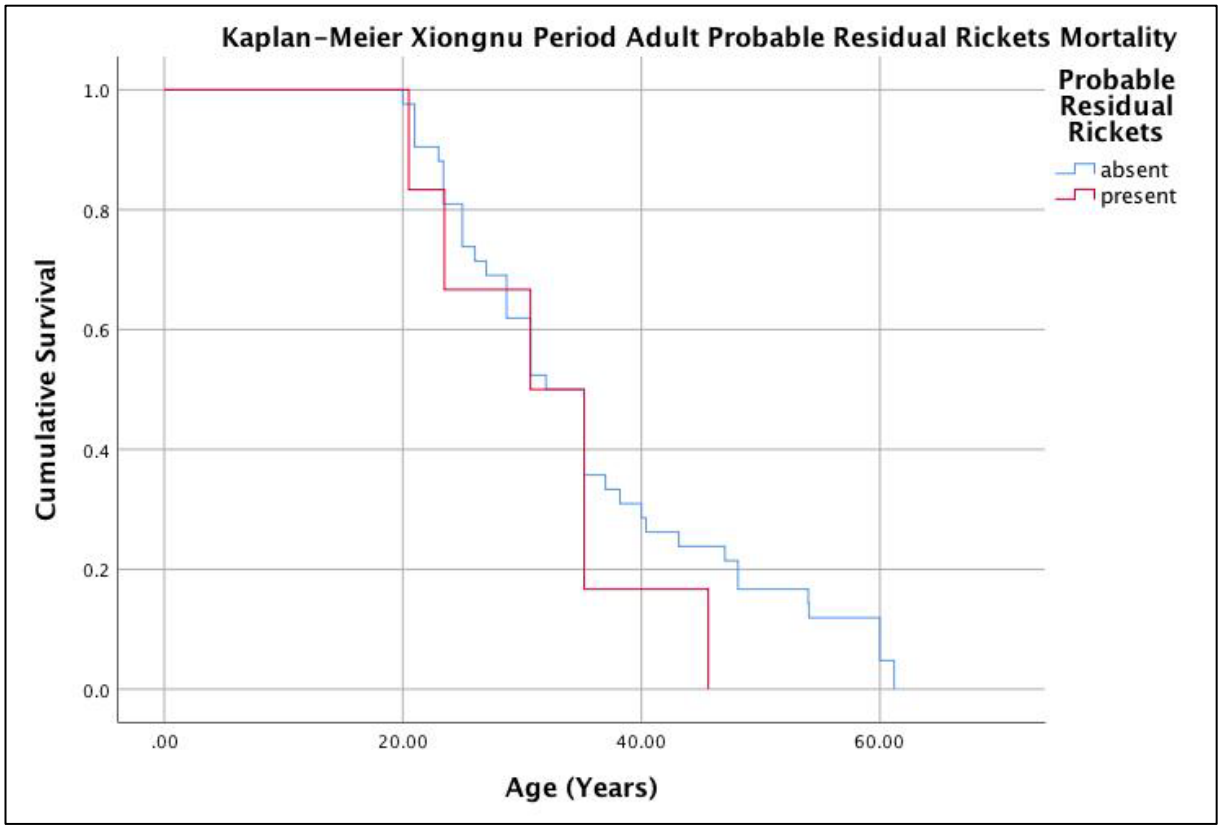

Figure 8.66: *Kaplan-Meier cumulative survival function of adult probable residual rickets mortality in Xiongnu Period Mongolia. Image: author's own.*

8.6.7.3 Mortality of Osteomalacia in the Xiongnu Period

Relative risk ratio analysis identified a statistically significant increase in risk of death of individuals with skeletal signs of possible and probable osteomalacia (Table 8.54). However, there was no relationship between increased mortality and skeletal signs of probable osteomalacia. Kaplan-Meier (n=56, X^2=4.167, df=1, p=0.041; Table 8.55; Figure 8.67) and Cox regression (n=56, Wald=3.735, df=1, p=0.053; Table 8.56; Figure 8.68) both identified significantly increased risk of death for individuals with combined possible or probable osteomalacia. However, as was the case with the relative risk ratio analysis, the Kaplan-Meier survival analysis (n=56, X^2=1.486, df=1, p=0.223; Table 8.57; Figure 8.69) identified no statistically significant increases in risk of death of individuals with probable osteomalacia.

Table 8.54: *Relative risk of osteomalacia mortality in the Xiongnu Period across age cohorts.*

POSITIVE OUTCOME/ NEGATIVE OUTCOME	**TREATMENT**		**RR**	**P-VALUE**	**95%CI**
	Exposed Group: *Disease Present*	***Control Group:*** *Disease Absent*			
Possible and Probable Osteomalacia (combined)					
Adults					
<20 yrs/ >20 yrs	4/14	4/34	**2.7083**	**0.1009****	0.8237- 8.9051
<30 yrs/ >30 yrs	10/8	16/22	**2.9537**	**0.0081***	1.3242- 6.5884
<40 yrs/>40 yrs	15/3	27/11	**1.2840**	**0.0650***	0.9846- 1.6743
Probable Only Osteomalacia					
Adults					
<20 yrs/ >20 yrs	3/10	5/38	1.6923	0.4057	0.4897- 5.8489
<30 yrs/ >30 yrs	7/6	19/24	1.4538	0.2305	0.7886- 2.6804
<40 yrs/>40 yrs	11/2	31/12	1.1635	0.3129	0.8671- 1.5612

A relative risk (RR) >1 denotes a relationship of the disease presence with the positive outcome (susceptibility to mortality), whereas RR <1 denotes a relationship of the disease absence with a negative outcome (survivorship).
**= statistically significant (p<0.10). **= statistically significant when considering size of the effect of RR.*

Table 8.55: *Statistical summary for Kaplan-Meier function of possible and probable osteomalacia mortality of adults in Xiongnu Period Mongolia.*

POSSIBLE AND PROBABLE OSTEOMALACIA	ESTIMATE	STD. ERROR	95% CI	LOG RANK (MANTEL-COX)		
				CHI SQUARE	DF	P-VALUE
Mean				4.167	1	**0.041***
Absent	34.479	2.222	30.123- 38.834			
Present	27.871	2.283	23.396- 32.345			
Overall	32.508	1.738	29.101- 35.914			
Median						
Absent	30.700	2.284	26.224- 35.176			
Present	25.000	3.567	18.008- 31.992			
Overall	30.700	1.733	27.304- 34.096			

**= statistical significance (p<0.15).*

Table 8.56: *Statistical summary for Cox regression function of possible and probable osteomalacia mortality of adults in Xiongnu Period Mongolia.*

POSSIBLE AND PROBABLE OSTEOMALACIA	COEFFICIENT (β)	STD. ERROR	WALD	DF	P-VALUE	ODDS RATIO (Exp(β))
	-0.589	0.305	3.735	1	**0.053***	0.555

**= statistical significance (p<0.15).*

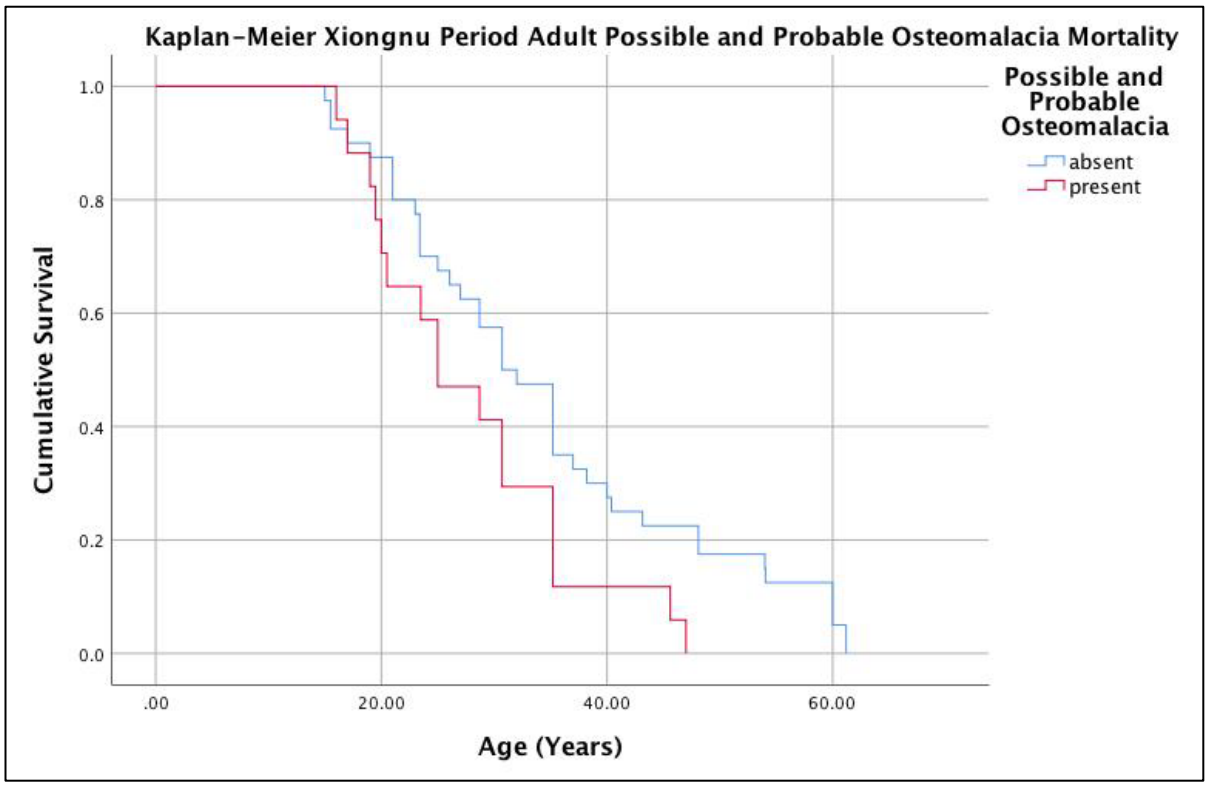

Figure 8.67: *Kaplan-Meier cumulative survival function of adult possible and probable osteomalacia mortality in Xiongnu Period Mongolia. Image: author's own.*

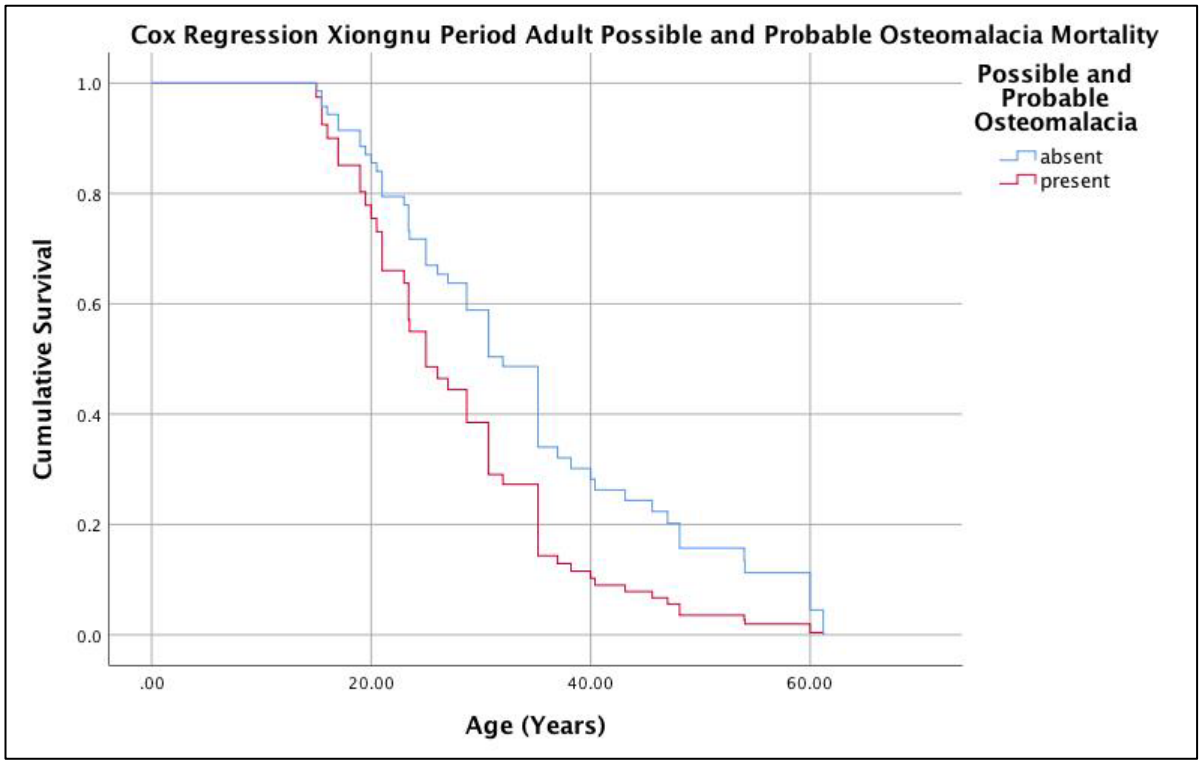

Figure 8.68: *Cox regression cumulative survival function of adult possible and probable osteomalacia mortality in Xiongnu Period Mongolia. Image: author's own.*

Table 8.57: *Statistical summary for Kaplan-Meier function of probable osteomalacia mortality of adults in Xiongnu Period Mongolia.*

PROBABLE OSTEOMALACIA	ESTIMATE	STD. ERROR	95% CI	LOG RANK (MANTEL-COX)		
				CHI SQUARE	DF	P-VALUE
Mean				1.486	1	0.223
Absent	33.428	2.096	29.321- 37.536			
Present	29.392	2.737	24.028- 34.757			
Overall	32.508	1.738	29.101- 35.914			
Median						
Absent	30.700	2.359	26.076-35.324			
Present	28.700	4.314	20.245- 37.155			
Overall	30.700	1.733	27.304- 34.096			

**= statistical significance (p<0.15).*

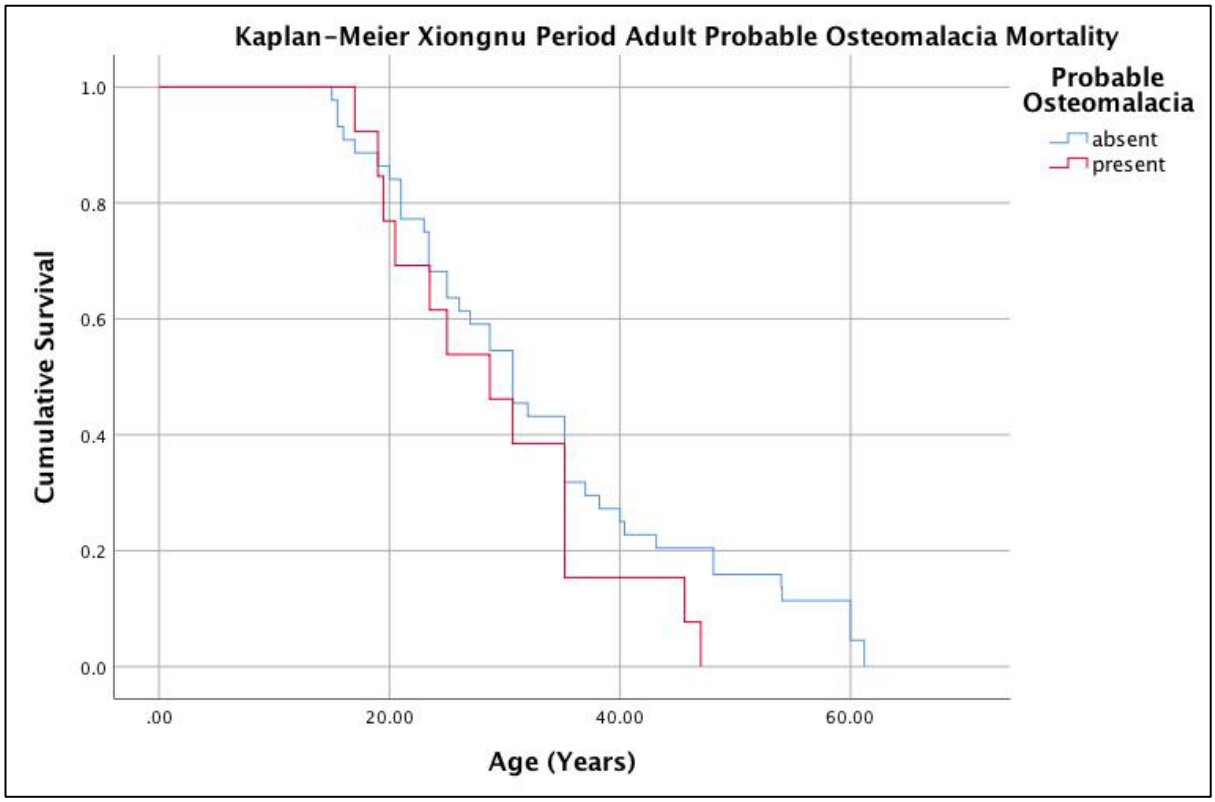

Figure 8.69: *Kaplan-Meier cumulative survival function of adult probable osteomalacia mortality in Xiongnu Period Mongolia. Image: author's own.*

8.6.8 Diagnosis of Anaemia in the Xiongnu Period

Less than 30% (27.3%, 6/22) of adults displayed skeletal signs of porotic hyperostosis and/or moderate to severe cribra orbitalia consistent with a diagnosis of anaemia (Table 8.65; Figure 8.70). Additionally, two adolescents between the ages of 15-19 were the only nonadults who had skeletal signs of anaemia. As only three nonadults under the age of 15, all aged between 4-8 years of age, had preserved crania, this outcome may be due to sample preservation. Overall, cribra orbitalia and porotic hyperostosis were present in similar prevalences and most individuals exhibited either cribra orbitalia or porotic hyperostosis. Adults aged between 30-39 years appear to have the highest prevalence of childhood anaemia amongst adult age cohorts, and no adults over the age of 40 years exhibited any skeletal signs of anaemia (Figure 8.71).

Table 8.58: *Summary of anaemia in the Xiongnu Period*

ANAEMIA	CO			Cranial PH			PH and/or CO		
	Affected	*Observed*	*(%)*	*Affected*	*Observed*	*(%)*	*Affected*	*Observed*	*(%)*
15 to 20 years	1	6	16.7	2	6	33.3	2	6	33.3
20 to 30 years	0	8	0	2	8	25	2	8	25
30 to 40 years	3	7	42.9	1	7	14.3	4	7	57.1
40 to 50 years	0	2	0	0	2	0	0	2	0
50+ years	0	3	0	0	3	0	0	3	0
Total nonadults	1	9	11.1	2	9	22.2	3	9	33.3
Males	4	13	30.8	3	13	23.1	6	13	46.2
Females	0	13	0	2	13	15.4	2	13	15.4
Total adults	3	22	13.6	3	22	13.6	6	22	27.3
Total	4	31	12.9	5	31	16.1	8	31	25.8

Figure 8.70: *Lesions consistent with anaemia in Xiongnu Period Mongolia. a) Moderate cribra orbitalia (AT-154, male, ~17 years, Erdenetsagaan soum). b) Porotic hyperostosis. Note the diploic expansion of the parietal bones and the occipital bone (AT-370, young adult female, Dolood) Image: author's own.*

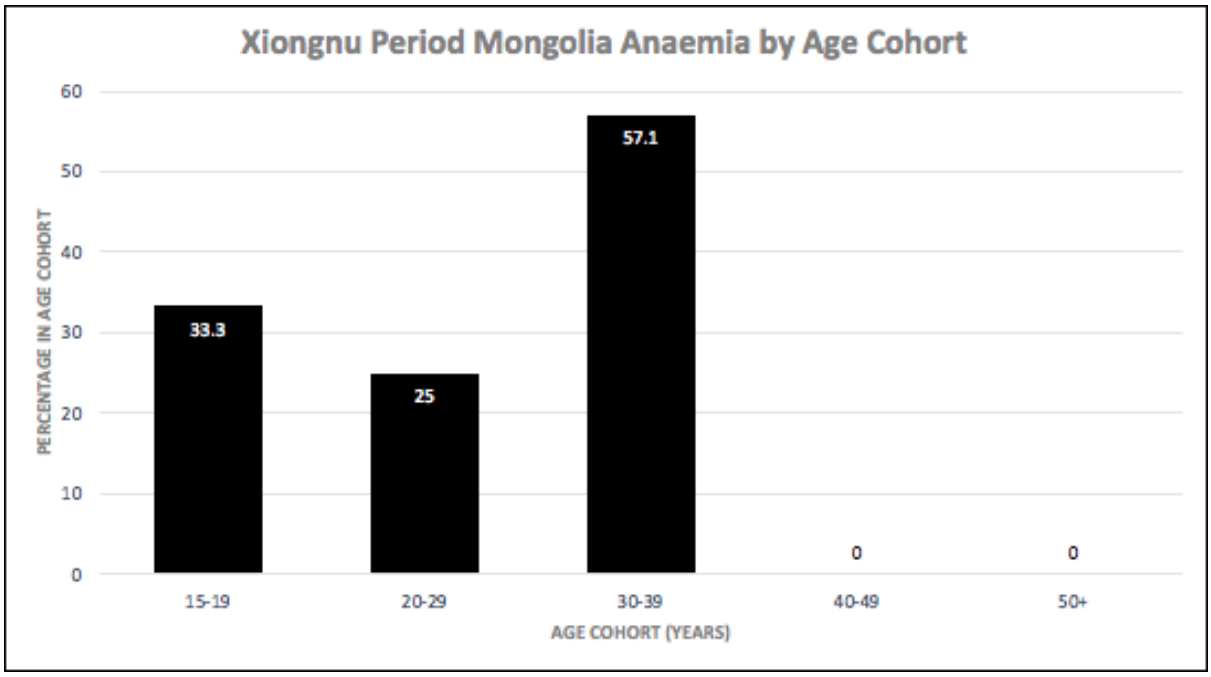

Figure 8.71: *Age-at-death distribution of anaemia in Xiongnu Mongolia. Image: author's own.*

8.6.9 Morbidity of Anaemia in the Xiongnu Period

Relative risk ratio of morbidity identified no statistically significant differences in the prevalence of anaemia across adult age cohorts (Table 8.59). However, males were 3 times (n=26, RR=0.3333, p=0.1250) more likely to exhibit skeletal evidence of childhood anaemia than females, which was statistically significant given the size of the effect.

Table 8.59: *Relative risk of anaemia morbidity in the Xiongnu Period across sex and age cohorts.*

EXPOSED GROUP/ CONTROL GROUP	**OUTCOME**		**RR**	**P-VALUE**	**95%CI**
	Positive: *Anaemia Present*	***Negative:*** *Anaemia Absent*			
Sex					
Female/ Male	2/6	4/14	**0.3333**	**0.1250****	0.0819- 1.3566
Adults					
<20 yrs/ >20 yrs	2/6	4/14	1.1111	0.8752	0.2984- 4.378
<30 yrs/ >30 yrs	4/4	10/8	0.8571	0.7930	0.2710- 2.7115
<40 yrs/>40 yrs	8/0	13/5	4.6364	0.2665	0.3098- 69.3752

A relative risk (RR) >1 denotes a relationship of the exposed group with an increase in disease prevalence, whereas RR <1 denotes a relationship of the control group with an increase in disease prevalence.
**= statistically significant (p<0.10). **= statistically significant when considering size of the effect of RR.*

8.6.10 Mortality of Anaemia in the Xiongnu Period

Relative risk ratio analysis identified an increase in risk of death of adults with skeletal signs of anaemia. Adults were 1.4 times (n=26, RR=1.3846, p=0.0260) more likely to die before the age of 40 if they had skeletal signs of childhood anaemia (Table 8.60). In contrast Kaplan-Meier (n=26 X^2=0.225, df=1, p=0.635; Table 8.61; Figure 8.72) did not identify a statistically significant increase in risk of death of adults. There may then be a slightly increased risk of death of adults who exhibited skeletal signs of childhood anaemia, but the impact may be restricted to differences in survivorship to old age.

Table 8.60: *Relative risk of anaemia mortality in the Bronze Age across age cohorts.*

POSITIVE OUTCOME/ NEGATIVE OUTCOME	**TREATMENT**		**RR**	**P-VALUE**	**95%CI**
	Exposed Group: *Poss. IDA Present*	***Control Group:*** *Poss. IDA Absent*			
Adults					
<20 yrs/ >20 yrs	2/6	4/14	1.1250	0.8730	0.2563- 4.9374
<30 yrs/ >30 yrs	4/4	10/8	0.9000	0.7980	0.4017- 2.0167
<40 yrs/>40 yrs	8/0	13/5	**1.3846**	**0.0260***	1.0397- 1.8440

A relative risk (RR) >1 denotes a relationship of the disease presence with the positive outcome (susceptibility to mortality), whereas RR <1 denotes a relationship of the disease absence with a negative outcome (survivorship).
**= statistically significant (p<0.10). **= statistically significant when considering size of the effect of RR.*

Table 8.61: *Statistical summary for Kaplan-Meier function of anaemia mortality of adults in Xiongnu Period Mongolia.*

ANAEMIA	**ESTIMATE**	**STD. ERROR**	**95% CI**	**LOG RANK (MANTEL-COX)**		
				CHI SQUARE	**DF**	**P-VALUE**
Mean				0.225	1	0.635
Absent	31.347	3.143	25.186- 37.508			
Present	27.538	3.026	21.606- 33.469			
Overall	30.175	2.359	25.551- 34.799			
Median						
Absent	27.000	3.924	9.308- 34.692			
Present	25.000	4.158	16.851- 33.149			
Overall	27.000	3.059	21.004- 32.996			

**= statistical significance (p<0.15).*

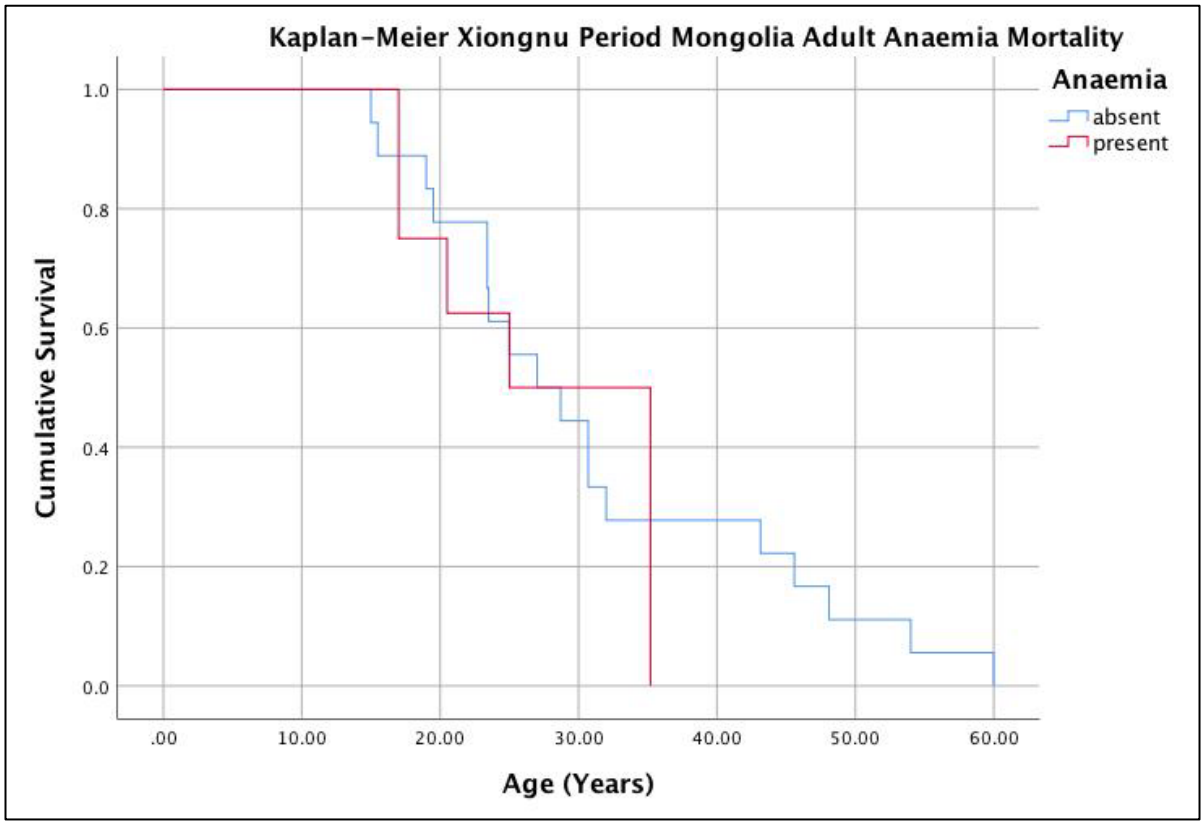

Figure 8.72: *Kaplan-Meier cumulative survival function of adult anaemia mortality in Xiongnu Period Mongolia. Image: author's own.*

8.6.11 Summary of Diagnosis and Context of Disease in the Xiongnu Period

Overall, the Xiongnu Period disease burden included infectious disease (11.6%, 8/69), scurvy (30.4%, 21/69), anaemia (25.8%, 8/31), and mineralisation disorders in the form of rickets (44.4%, 8/18), residual rickets (23.5%, 2/51), and osteomalacia (31.1%, 19/6).

8.6.11.1 Brucellosis and Hydatids Disease in the Xiongnu Period

Given the similar pastoral practices employed by the Xiongnu Period compared to the Bronze Age inhabitants of Mongolia, similar relationships with livestock likely resulted in the presence of hydatids disease and brucellosis in the Xiongnu Period.

8.6.11.2 Tuberculosis or Mycosis in the Xiongnu Period

The presence of bovine tuberculosis in the Xiongnu Period is possible given the existence of the pathogen in the region by the early Iron Age (Murphy et al. 2009). However,

human tuberculosis is similarly possible as the lesions identified in AT-263 (young adult) are restricted to the thorax and most likely were caused from adjacent cold abscesses in the plural cavity (Khan et al. 2007; Watts et al. 1987). Such skeletal expression does more strongly indicate a respiratory origin. However, haematogenous spread is still a possible origin of the lesions and therefore bovine tuberculosis cannot be ruled out as responsible for the pathology observed in AT-263. Additionally, in rare cases close proximity and inhalation of the sputum of livestock can result in respiratory transmission of bovine tuberculosis from animals to humans (Grange 2001). In Mongolia today, the prevalence of human tuberculosis is sustained through fission-fusion interactions between pastoralist groups (Mocellin and Foggin 2008). The potential presence of human tuberculosis in Mongolia during the Xiongnu Period is intriguing, particularly in relation to contact with East Asia, where tuberculosis has been identified in a number of cases from the Neolithic, Bronze and Iron Ages (Okazaki et al. 2019; Pechenkina et al. 2007; Suzuki et al. 2008; Suzuki and Inoue 2007), including a case from the Han Dynasty, China (Li et al. 2019). Pathogen DNA analysis confirms the presence of *Mycobacterium tuberculosis* in the Silk Road region of Xinjiang, China (on the border of Mongolia, and within the peripheral realms of the Xiongnu Empire) during 200BC-200AD (Fusegawa et al. 2003).

Mycosis cannot be ruled out as an alternate explanation for the lesions in AT-263. To date, there are no epidemiological reports of mycotic infections in Mongolia. However, in rare cases the spores of *Cryptococcus.* sp. can be transmitted to humans in unpasteurised milk (Sherman 2011). Additionally, contamination of water sources through faecal material similarly to hydatids disease can increase risk of transmission of fungal spores to humans (Battelli 2008).

8.6.11.3 Treponematosis in the Xiongnu Period

AT-268a (female, ~15 years) presents with a possible case of congenital treponematosis. Given the arid environment, yaws as a possible cause can be ruled out. Reported congenital cases of treponematosis are overwhelmingly due to venereal syphilis (Woods 2005). However, there are reports of possible congenital cases of endemic syphilis, the non-venereal form present in arid climates, although these are exceedingly rare, leading some to conclude that congenital endemic syphilis does not occur (Antal et al. 2002; Arslanagić et al. 1989; Grin 1956). It is possible the rarity of a congenital form is related to

predominant transmission in childhood and therefore low numbers of active cases in reproductive adults (Hudson 1965). Small communities such as in nomadic pastoralists are favourable for the spread of endemic syphilis (Grin 1953). However, transmission occurs amongst children and therefore high natural population growth is associated with endemic syphilis outbreaks, unlike the demographic conditions of the Xiongnu Period (Grin 1953). Prior to eradication, endemic syphilis was endemic to Mongolian nomadic rural populations (Antal et al. 2002; Solomon 1993). Venereal and endemic syphilis are then both possible causes for the mulberry molar malformations observed in AT-268a.

Being a single possible case of treponematosis, AT-268a does not however, present convincing evidence for treponemal disease in the prehistory of Northeast Asia (in contrast to the evidence presented in Chapter 7). While Suzuki et al. (2005) presented what they argued were a "possible" case of treponematosis in Bronze Age China, the case exhibited no diagnostic nor multiple suggestive lesions. Additionally, Zhang (1994) reported "gummatous periostitis" on a single left femur without evidence of tertiary gummatous destruction from the Han Dynasty, again not sufficient for a diagnosis of treponematosis. Zhang (1994) does report a case of possible caries sicca in a Song dynasty (960-1279AD) cranium which appears convincing. However, this case exists within the yaws tropical belt and therefore may not be related to the presence of venereal or endemic syphilis in prehistory. Machicek and Beach (2013) observed Hutchinson's incisors and Mulberry molars in an individual from the Mongol Period (1206-1368), Inner Mongolia, China which would be diagnostic for probable congenital treponematosis, but provide no accompanying photographs. As such, strong evidence for the presence of treponematosis in prehistory currently does not exist for Asia north of the tropical belt.

8.6.11.4 Scurvy, Mineralisation Disorders and Anaemia in the Xiongnu Period

The aetiology of scurvy and anaemia are likely to be very similar for the Xiongnu Period than for the Bronze Age, due to the continuation of nomadic pastoralism practices with the emergence of the Xiongnu Empire. The introduction of millet, barley and other crops may have increased the risk of scurvy, if these crops were relied on through cyclical shortages of other Vitamin C rich foods, such as during the winter time. Carbon and nitrogen isotopes indicate supplementation of the livestock diet with fodder in the winter during the Xiongnu Period, and humans may have similarly supplemented their diet during this time

of the year (Makarewicz 2017). Scurvy appears to be associated with an increased mortality in the Xiongnu Period, and in combination with low prevalences compared to assemblages from the previous chapters, suggests that individuals were afflicted with periodic food shortages.

Additionally, Vitamin D deficiency as a cause for the mineralisation disorders is also likely due to the geographic position of Mongolia. Browns tumours are also only documented in severe Vitamin D deficiency and not due to other causes of rickets (Bereket et al. 2000). Rickets was not observed in nonadults under the age of 5 years, and mortality analysis indicated survivorship of nonadults with skeletal signs of Vitamin D deficiency. In contrast, the presence of adult mineralisation disorder in the form of osteomalacia indicated increased frailty.

Out of the eight individuals with infectious disease, half (4/8) exhibited signs of possible or probable scurvy, and half (4/8) exhibited signs of mineralisation disorder. However, only one individual with infectious disease did not any exhibit skeletal signs for nutritional disease (scurvy *or* mineralisation disorder). Therefore, there may be an association between nutritional disease and infectious disease in the Xiongnu Period assemblage. AT-268a (female, ~15 years), who was diagnosed with possible congenital treponematosis, also exhibited probable scurvy. As infectious diseases are known to increase the demands of the Vitamin C in the body, a link between scurvy and treponematosis is expected (Amakye-Anim et al. 2000; Sadun et al. 1951). Historically, an association between the two diseases was not rare (Greenthal 1919). Residual rickets was also observed in AT-2 (young adult female) and AT-263 (young adult), who presented with brucellosis and tuberculosis respectively. It is not known if these two individuals experienced Vitamin D deficiency during their adulthood, but Vitamin D deficiency has been linked to the systemic spread of both infectious conditions (Kurtaran et al. 2016; Talat et al. 2010).

8.6.11.5 Intrapopulation Variation of Disease in the Xiongnu Period

Males exhibited both higher prevalences of anaemia and probable osteomalacia than females. However there were no differences between the prevalence of residual rickets nor scurvy in males compared to females. Differences in the morbidity of anaemia indicates variations in childhood stress. Boys may have had differential exposure to parasitic

infection, possibly related to division in gendered labour. Traditional gender roles exist within modern and historic nomadic households. Herding has traditionally been a male role, whereas milk production and processing of milk within the *ger* (Mongolian house) has traditionally been the role of women (Myadar 2011). Boys may then have been at an increased risk of parasitism due to direct contact with raw meat and faecal matter due to herding. Additionally, young male roles in conflict may have increased their risk of nutritional stress if they were involved in warfare, where food is rationed (Honeychurch 2013).

While males exhibited significantly higher prevalences of probable osteomalacia than females, combined possible and probable cases of osteomalacia had a higher relationship with frailty than probable cases. This may indicate that females while exhibiting less advanced forms of Vitamin D deficiency, were the most vulnerable to Vitamin D deficiency in terms of mortality. Severe Vitamin D deficiency can increase mortality due to co-morbidity with infectious diseases but also increase the risk of non-communicable diseases such as type II diabetes and heart failure (Cubbon et al. 2019; Ozfirat and Chowdhury 2010). Vitamin D deficiency also exacerbates pregnancy related conditions such as pre-eclampsia increasing the risk of maternal mortality (Bodnar et al. 2007). Additionally, even slight pelvic distortion can increase the risk of maternal mortality during labour, the effects of which can be a result of both residual rickets and osteomalacia (Strickland 1993). Given that the prevalences of residual rickets were not different between males and females, this gendered differences in morbidity and mortality may have not extended into childhood.

8.7 Regional Level Results: Bronze Age to Xiongnu Period Mongolia

8.7.1 Diachronic Assessment of Morbidity of Infectious Disease from the Bronze Age to Xiongnu Period

There were no significant differences in the morbidity of infectious diseases between the Bronze Age and Xiongnu Period adults (Table 8.62). However, Xiongnu Period nonadults were 7 times (n=36, RR=7.000, p=0.1876) more likely to have infectious disease than Bronze Age nonadults, which was statistically significant given the size of the effect.

Table 8.62: *Relative risk of infectious disease morbidity from the Bronze Age to Xiongnu Period Mongolia.*

EXPOSED GROUP/ CONTROL GROUP	**OUTCOME**		**RR**	**P-VALUE**	**95%CI**
	Positive: *Infectious Disease Present*	***Negative:*** *Infectious Disease Absent*			
Nonadults					
Xiongnu/Bronze	3/0	15/18	**7.0000**	**0.1876****	0.3874- 126.4839
Adults					
Xiongnu/Bronze	6/4	45/70	2.1765	0.2092	0.6465- 7.3269

A relative risk (RR) >1 denotes a relationship of the exposed group with an increase in disease prevalence, whereas RR <1 denotes a relationship of the control group with an increase in disease prevalence.
**= statistically significant (p<0.10). **= statistically significant when considering size of the effect of RR.*

8.7.2 Diachronic Assessment of Morbidity of Nutritional Disease from the Bronze Age to Xiongnu Period

Xiongnu Period adults exhibited 4.4 times (n=125, RR=4.3529, p=0.0218) the risk of morbidity of possible and probable scurvy compared to Bronze Age adults (Table 8.63). Xiongnu Period nonadults did not exhibit any statistically significant differences in both combined possible and probable and probable only cases of scurvy. As there was only one case of probable scurvy in the Xiongnu assemblage and the Bronze Age assemblage respectively, similarly no differences were observed.

No statistically significant differences in the morbidity of rickets were observed between the Xiongnu nonadults compared to the Bronze Age adults (Table 8.64). Similarly, there were no statistically significant differences in the prevalences of residual rickets between the two assemblages. However, Xiongnu adults were 4.4 times (n=125, RR=4.3529, p=0.0646) more likely to exhibit probable residual rickets than Bronze Age adults, which was statistically significant. Xiongnu adults were 2.3 times (n=125, RR=2.2571, p=0.0352) more likely to exhibit possible or probable osteomalacia and 3 times (n=125, RR=2.9020, p=0.0392) more likely to exhibit probable osteomalacia than Bronze Age adults (Table 8.65).

Table 8.63: *Relative risk of scurvy morbidity from the Bronze Age to Xiongnu Period Mongolia.*

EXPOSED GROUP/ CONTROL GROUP	**OUTCOME**		**RR**	**P-VALUE**	**95%CI**
	Positive: *Scurvy Present*	***Negative:*** *Scurvy Absent*			
Possible and Probable (combined) Scurvy					
Nonadults					
Xiongnu/Bronze	12/6	9/9	1.3333	0.3190	0.7572- 2.3478
Adults					
Xiongnu/Bronze	9/3	42/71	**4.3529**	**0.0218***	1.2384- 16.3005
Probable Scurvy					
Nonadults					
Xiongnu/Bronze	8/5	10/13	1.6000	0.3095	0.6463- 3.9609
Adults					
Xiongnu/Bronze	1/1	50/73	1.4510	0.7907	0.0929- 22.6702

A relative risk (RR) >1 denotes a relationship of the exposed group with an increase in disease prevalence, whereas RR <1 denotes a relationship of the control group with an increase in disease prevalence.
**= statistically significant (p<0.10). **= statistically significant when considering size of the effect of RR.*

Table 8.64: *Relative risk of rickets/residual rickets morbidity from the Bronze Age to Xiongnu Period Mongolia.*

EXPOSED GROUP/ CONTROL GROUP	**OUTCOME**		**RR**	**P-VALUE**	**95%CI**
	Positive: *Rickets Present*	***Negative:*** *Rickets Absent*			
Possible and Probable (combined) Rickets					
Nonadults (Rickets) *Xiongnu/Bronze*	8/6	10/12	1.3333	0.4984	0.5798- 3.0665
Adults (Residual Rickets)					
Xiongnu/Bronze	12/15	39/59	1.1608	0.6628	0.5939- 2.2686
Probable Rickets					
Nonadults (Rickets)					
Xiongnu/Bronze	5/3	13/15	1.6667	0.4318	0.4664- 5.9560
Adults (Residual Rickets)					
Xiongnu/Bronze	6/2	45/72	**4.3529**	**0.0646***	0.9146- 20.7164

A relative risk (RR) >1 denotes a relationship of the exposed group with an increase in disease prevalence, whereas RR <1 denotes a relationship of the control group with an increase in disease prevalence.
**= statistically significant (p<0.10). **= statistically significant when considering size of the effect of RR.*

Table 8.65: *Relative risk of osteomalacia morbidity from the Bronze Age to Xiongnu Period Mongolia.*

EXPOSED GROUP/ CONTROL GROUP	OUTCOME		RR	P-VALUE	95%CI
	Positive: *Osteo. Present*	***Negative:*** *Osteo. Absent*			
Possible and Probable (combined) Osteomalacia					
Adults					
Xiongnu/Bronze	14/9	37/65	**2.2571**	**0.0352***	1.0581- 4.8148
Probable Osteomalacia					
Adults					
Xiongnu/Bronze	10/5	41/69	**2.9020**	**0.0392***	1.0543- 7.9879

A relative risk (RR) >1 denotes a relationship of the exposed group with an increase in disease prevalence, whereas RR <1 denotes a relationship of the control group with an increase in disease prevalence.
**= statistically significant (p<0.10). **= statistically significant when considering size of the effect of RR.*

8.7.3 Diachronic Assessment of Morbidity of Anaemia from the Bronze Age to Xiongnu Period

There were no statistically significant differences in the morbidity of anaemia between Xiongnu Period and Bronze Age nonadults and adults (Table 8.66).

Table 8.66: *Relative risk of anaemia morbidity from the Bronze Age to Xiongnu Period Mongolia.*

EXPOSED GROUP/ CONTROL GROUP	OUTCOME		RR	P-VALUE	95%CI
	Positive: *Anaemia Present*	***Negative:*** *Anaemia Absent*			
Nonadults					
Xiongnu/Bronze	3/1	6/6	2.3333	0.4148	0.3045- 17.8784
Adults					
Xiongnu/Bronze	8/7	23/16	0.8479	0.7067	0.3591- 2.0020

A relative risk (RR) >1 denotes a relationship of the exposed group with an increase in disease prevalence, whereas RR <1 denotes a relationship of the control group with an increase in disease prevalence.
**= statistically significant (p<0.10). **= statistically significant when considering size of the effect of RR.*

8.7.4 Diachronic Assessment of Overall Mortality from the Bronze Age to Xiongnu Period

Relative risk ratio analysis identified a significant but slight increase in mortality of Xiongnu Period adults (Table 8.67). The Xiongnu adults were 1.8 times (n=115, RR=1.8316, p=0.0212) more likely to die before the age of 30 years than Bronze Age adults. However, Kaplan-Meier survival analysis (n=115, X^2=0.0613, df=1, p=0.434; Table 8.68; Figure 8.73) did not identify a significant increase in the overall mortality rate of Xiongnu adults compared to Bronze Age adults.

Table 8.67: *Relative risk of overall mortality from the Bronze Age to Xiongnu Period Mongolia across age cohorts.*

POSITIVE OUTCOME/ NEGATIVE OUTCOME	TREATMENT		RR	P-VALUE	95%CI
	Exposed Group: *Xiongnu*	***Control Group:*** *Bronze*			
<20 yrs/ >20 yrs	9/48	6/52	1.5263	0.3910	0.5808- 4.0109
<30 yrs/ >30 yrs	27/30	15/43	**1.8316**	**0.0212***	1.0949- 3.0640
<40 yrs/>40 yrs	43/14	36/22	1.2154	0.1259	0.9467- 1.5604

A relative risk (RR) >1 denotes a relationship of the disease presence with the positive outcome (susceptibility to mortality), whereas RR <1 denotes a relationship of the disease absence with a negative outcome (survivorship).
**= statistically significant (p<0.10). **= statistically significant when considering size of the effect of RR.*

Table 8.68: *Statistical summary for Kaplan-Meier function of overall mortality of adults from the Bronze Age to Xiongnu Period of Mongolia.*

OVERALL MORTALITY	ESTIMATE	STD. ERROR	95% CI	LOG RANK (MANTEL-COX)		
				CHI SQUARE	DF	P-VALUE
Mean				0.613	1	0.434
Absent	36.086	1.388	33.365- 38.807			
Present	32.500	1.734	29.102- 35.898			
Overall	34.309	1.116	32.121- 36.496			
Median						
Absent	35.000	2.110	30.864- 39.136			
Present	31.000	1.873	27.329- 34.671			
Overall	32.000	1.021	29.999- 34.001			

**= statistical significance (p<0.15).*

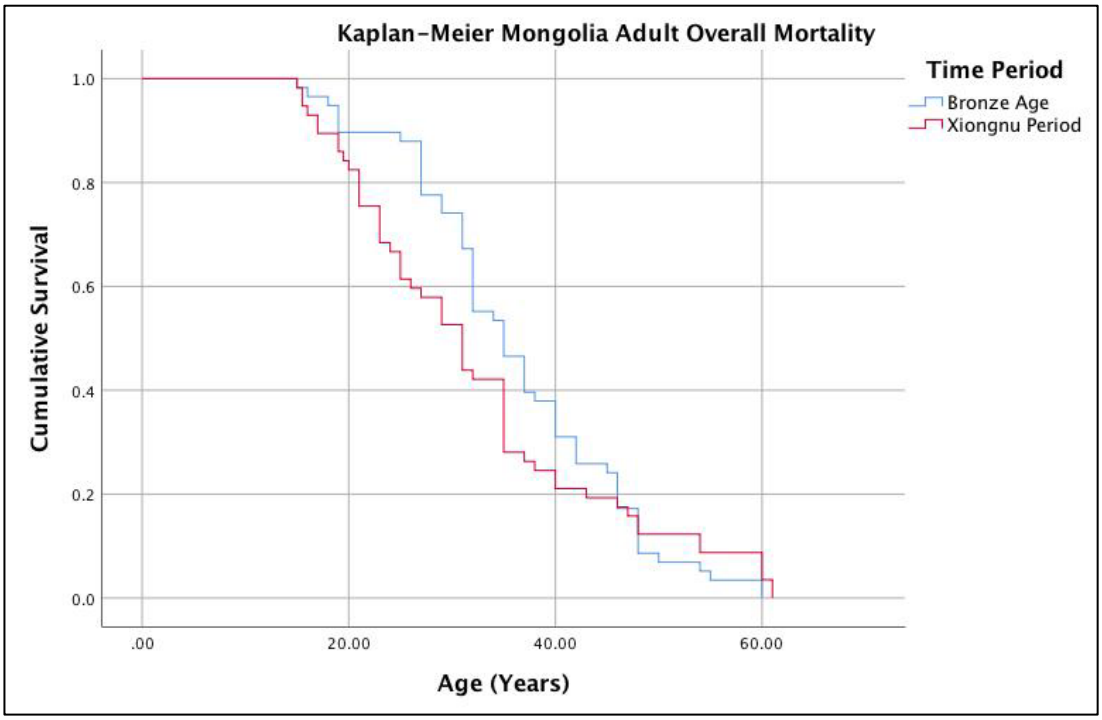

Figure 8.73: *Kaplan-Meier cumulative survival function of adult overall mortality from the Bronze Age to Xiongnu Period Mongolia. Image: author's own*

8.8 Discussion: Diachronic Changes in Disease from the Bronze Age to Xiongnu Period Mongolia

The results presented in this chapter report significant increases in the morbidity of nonadult infectious disease and adult nutritional disease (scurvy and osteomalacia) from the Bronze Age to the Xiongnu Period. Additionally, there was a significant increase in adults who had survived childhood rickets. However, no significant changes were found in the patterns of adult infectious disease, nonadult nutritional disease (scurvy and rickets) and childhood anaemia.

A slight increase in the mortality of Xiongnu Period adults before the age of 30 was observed compared to adults. This difference in mortality may be related to age specific changes to risk of death. For example, increased maternal mortality and/or conflict during the Xiongnu Period may have increased the mortality rates of young adult males and females (Chamberlain 2006; Högberg and Broström 1985). However, overall, no increase in the mortality rate was observed with an increase in the level of population interaction. Both assemblages exhibited a similar level of natural population decline (RNPI= -0.3), and therefore appear to have shared similar fertility and mortality rates.

8.8.1 Changes in Infectious Disease with Increasing Population Interaction Mongolia

While there was no statistical increase in the morbidity of infectious diseases in adults, there was a significant increase in the morbidity of infectious disease in nonadults from the Bronze Age to the Xiongnu Period. This outcome was a result of the presence of infectious disease in Xiongnu Period adolescents, whereas no cases of nonadult infectious disease were observed in the Bronze Age. As such there is some evidence to support an increase in the prevalence of infectious disease with increasing interaction levels during the Xiongnu Period. The high diversity of infectious disease present in both Mongolian assemblages is of interest as a moderate level of interaction was prevalent from the Bronze Age onwards. It is likely the fission-fusion interactions foundational to nomadic pastoralism coupled with migration from external groups enabled the introduction of a number of infectious diseases in the Bronze Age and Xiongnu Period. However, all infectious diseases in the Bronze Age can be explained by zoonotic disease, whereas there remains tentative evidence for human to human transmission of infectious disease in the Xiongnu Period, in

the possible cases of respiratory tuberculosis and treponematosis. Possible brucellosis and probable hydatids disease, zoonotic diseases associated with livestock, were identified in both the Bronze Age and the Xiongnu Period assemblage, indicating persistence of zoonotic diseases through pastoral group interactions. External migrations, trade or conflict likely introduced new infectious diseases, that then persisted in low population density communities due to the seasonal fission-fusion interactions of pastoral groups.

While there were no differences in overall mortality of the two assemblages, the relationship between the presence of infectious disease and increased mortality in the Xiongnu Period was higher than in the Bronze Age. Increased risk of mortality to infectious diseases with increased population interaction is then a likely factor. It is possible that the increased interpopulation interactions experienced by the Xiongnu Period population also increased the risk of transmission of infectious diseases with a high mortality rate such as tuberculosis.

8.8.2 Changes in Specific Nutritional Disease with Increasing Population Interaction in Mongolia

An increase in adult possible and probable scurvy was observed for the Xiongnu Period compared to the Bronze Age. In both assemblages the presence of scurvy signified increased risk of death in adults and indicated that scurvy reflected extremes of malnutrition. A number of factors likely underlie the increase in micronutrient deficiency during the Xiongnu Period. Firstly, the introduction of millet initiated a slight subsistence change wherein a complex form of pastoralism supplemented with crops emerged. As previously mentioned, periods of food scarcity during the winter time may have been supplemented by crop foods, and frost and snowfall likely restricted access to indigenous plants encouraging the development of scurvy. As an increase in millet consumption was associated with increased economic diversification and population interaction (Ventresca Miller and Makarewicz 2019), the outcome of scurvy was indirectly affected by increased population interaction during the Xiongnu Period. An increase in conflict, particularly during the Han frontier wars may have also driven periods of malnutrition. Han warriors are historically documented to have suffered scurvy during the conflict (Barbieri-Low 2011), and Xiongnu warriors may have similarly suffered during this time. The first Century AD saw invasion

of Xiongnu territory by the Han that likely exacerbated any malnutrition in pastoralist groups (Psarras 2004).

It is unclear why the morbidity of residual rickets and osteomalacia increased from the Bronze Age to the Xiongnu Period. It is possible this reflects differing cultural practices, such as a shift in time spent indoors or clothes worn. Hierarchical stratification may play a role in this difference with an increased prevalence of individuals who may have spent less time performing communal labour outside (Di Cosmo 2011), or Vitamin D rich foods such as fish may not have comprised a considerable part of the diet of some Xiongnu nomadic groups or classes. The percentage of Xiongnu elites in this assemblage is not known and is beyond the scope of this thesis. Increase in population interaction does not appear to be associated with an increase in mineralisation disorders observed in Xiongnu Period adults.

8.8.3 Changes in Anaemia with Increasing Population Interaction in Mongolia

There were no changes between the prevalences of anaemia from the Bronze Age to the Xiongnu Period. The conditions responsible for childhood anaemia in both assemblages were likely similar and tied to pastoralist practices and interactions with animals. As such, there is no evident relationship between the prevalence of anaemia and an increase in human population interaction.

8.9 Chapter Summary

This chapter explored differences in the prevalences of infectious and nutritional diseases in the Bronze Age and Xiongnu Period of Mongolia. Nomadic pastoralism was introduced as a subsistence practice in the Bronze Age, and was sustained by a system of seasonally mediated interactions between pastoral groups known as fission-fusion interaction. Pastoral nomadism continued as a way of life with the emergence of the Xiongnu Empire in Mongolia, where conflict, trade and migration from Siberia, Central Asia and East Asia increased. A high diversity of zoonotic diseases including brucellosis and hydatids disease was identified in both the Bronze Age and Xiongnu Period. Possible tuberculosis and treponematosis was additionally identified in the Xiongnu Period indicating a possible introduction of human to human transmissive diseases following the Bronze Age. An increase in the mortality of infectious diseases was also observed for the Xiongnu Period, although the overall mortality rate did not significantly change from the Bronze Age to the

Xiongnu Period. Both assemblages exhibited scurvy, mineralisation disorders (including rickets, residual rickets and osteomalacia), and anaemia. The Xiongnu Period presented with higher levels of scurvy, possibly due to the introduction of millet that was associated with increased economic efforts by the Xiongnu through trade, and by conflict particularly with the Han Empire of China. Additionally, the prevalence of mineralisation disorders also significantly increased over time. However, the reasons for this are ambiguous and likely not related to increasing population interaction levels. Overall, there is evidence for significant influence of increasing population interaction levels on the dynamics of infectious and nutritional diseases from the Bronze Age to Xiongnu Period of Mongolia.

CHAPTER 9:
FACTORS OF DISEASE DYNAMICS IN CONTINENT LEVEL ANALYSIS

9.1 Introduction

The final objective of this thesis is to develop a model using statistical techniques to assess the role of human population interaction levels on infectious and nutritional disease while also considering other interplaying factors. The statistical outcomes to inform the model (discussed in Chapter 10) are presented in this chapter. Different approaches to addressing the research question from a statistical perspective are discussed before the methodology and outcomes are presented.

Variations in *interpopulation interaction* only is assessed here, as the potential for newly introduced infectious diseases influencing the disease dynamics, discussed in Chapter 2, are likely to have larger influences on health visible through statistical means at a continent scale. As intrapopulation interaction occurs at a smaller scale, it is more fitting to observe these impacts at a site or regional level (see the model presented in Chapter 6). Additionally, variations in the prevalence of scurvy are also assessed here. Scurvy was the only nutritional disease identified in all of the sites and is more directly related to factors of food instability than rickets and osteomalacia, and therefore more reflects potential influences of human population interaction processes on nutrition. Anaemia is also not assessed here due to the complex aetiology of anaemic lesions. At a site and regional level there was no clear evidence that anaemia was related to variations in population interaction in any of the three case studies.

9.2 Statistical Approaches in Continent Level Analysis

9.2.1 Univariate Compared to Multivariate Methods: What is the Best Approach?

Both multivariate and univariate methods are routinely employed in palaeoepidemiological studies. Univariate approaches (e.g. linear or logistic regression models, Fisher's exact and Chi square tests) are usually performed as intra- or inter-site comparisons, whereas multivariate approaches (ANOVAs, ANCOVAS, GLMs or multiple regression) are often applied in larger regional studies (Cheverko and Hubbe 2017; Steckel

2005; Steckel and Rose 2002; Willis and Oxenham 2013). Multivariate analysis allows for statistical comparisons of interactions between multiple variables. Therefore, confounding factors or interplays between more than one factor can be explored. Major limitations to multivariate analysis include sample size to account for the number of statistical interactions and independence of variables (Spicer 2005). When multivariate analysis is completed in palaeoepidemiology, often this is a result of a meta-analysis where the statistics are employed by a researcher who has not themselves collected the data. The pitfalls of such an approach is that biases within the skeletal assemblage observed by the recorder do not translate in the data and become hidden within the interactions of the multivariate analysis. This problem relates to the expectation of internal consistency within the data that are often not met in skeletal populations (Spicer 2005). In contrast, relationships that are realistic may not be reflected in the output of multivariate analysis. For example, Steckel (2005) assessed multiple social, ecological and geographical variables potentially influencing health across pre-Columbian American sites. Univariate regression identified significant relationships between compromised health and domesticated plants, higher elevation, forest and grassland regions and inland regions. In the multivariate regression only elevation remained statistically significant, and therefore instead of revealing complexity, the statistical test eliminated it. Multivariate analysis may then provide outcomes that do not reflect the true interactions within the data in an archaeological context.

Univariate analyses have their own limitations. They do not allow for the consideration of confounding factors, and each factor needs to be statistically assessed independently. Judgement of the context of the data is essential for the interpretation of the outcomes of univariate analysis, particularly when the actual picture is more complex, such as in the context of infectious disease dynamics.

Multiple regression and ANOVAs were both attempted with the data compiled for this thesis. However, these techniques proved to mask data artefacts such as sample bias, as was the case where there were suspected biases in collection of skeletons in the Jomon and Con Co Ngua samples. The sample sizes available were also too small for multiple regression. Overall, the samples presented in this thesis were then not suitable for these approaches. Additionally, there were interactions which obscured the data that were reliant on the limitations of the selection of samples in this thesis. Such problems included where some samples represented the same ratio across two different tested variables. For example,

mobile populations were also the only populations represented in arid/arctic regions, influencing the interaction between infection, climate and residential mobility.

With univariate analysis, significant outcomes as a result of data artefacts instead of realistic trends could be removed from interpretation, while interactions between factors could still be assessed. It is argued here, that while multivariate analysis remains a potentially powerful tool for interpreting palaeoepidemiological data (see Baten et al. 2018; Steckel et al. 2002), caution should be taken in their application to archaeological data, and critical consideration of the fit of sample data is required prior to the employment of such techniques. For this reason, univariate techniques were only applied to the data presented below.

9.2.2 Methods of Continent Level Statistical Analysis

Only individuals over the age of 15 years were included in the analysis (n=343), as the preservation of the nonadults was too variable across each assemblage. Relative risk ratio analyses were applied to nominal and ordinal variables. In order to perform relative risk ratio analysis, nominal and ordinal variables were coded within a binary. Statistical significance was considered at $p<0.10$. However, the size of the effect was also taken into account. Continuous variables were assessed with Pearson correlation. This statistical test is a simple test to describe the linear correlation of two continuous variables (Sedgwick 2012). A correlation co-efficient of 1 is considered a perfect positive correlation, -1 a perfect negative correlation, 0 is considered no correlation. A coefficient higher than 0.7, or -0.7 is considered a strong correlation, whereas a correlation higher than 0.5 or -0.5 is considered a moderate correlation

The Pearson correlation is calculated by:

$$r = \frac{\sum (x - \bar{x})(y - \bar{y})}{\sqrt{\sum (x - \bar{x})^2 \sum (y - \bar{y})^2}}$$

r= correlation coefficient
$\bar{x}$ =mean of variable *x*
$\bar{y}$= mean of variable *y*

Table 9.1 presents the factors that were assessed in this analysis, and their rationale as a potential factor in disease dynamics. These factors are explored as possible co-variates with human population interaction levels, and are well described in palaeopathology as influential to disease prevalence. As such, the statistical analysis presented here directly addresses the second research question pertaining to this thesis: *How did population interaction interplay with a range of other sociocultural, biological and ecological factors to influence the health of populations in prehistoric Asia?*

As a univariate approach is taken, a direct covariation between population interaction and other factors is not assessed here. Instead each factor is independently explored in relation to its strength of influence on the disease prevalence. Where interesting trends have been identified further, statistical tests were applied to subsamples and this has allowed the assessment of interplay between two factors (e.g. statistically assessing interaction levels separately in mobile versus sedentary populations).

The dependant variables assessed in this chapter include infectious disease prevalence, infectious disease diversity, and combined possible and probable scurvy prevalence. Infectious disease diversity pertains to the number of infectious diseases observed in the assemblages. An *infectious disease diversity index (IDDI)* was produced for each assemblage wherein a percentage of the number of infectious diseases out of the seven diagnosed was produced for each site (e.g. Man Bac exhibited two identified infectious diseases: yaws and otitis media. Ratio=2/7. IDDI=28.6). A similar index was not applied to nutritional disease as only scurvy and mineralisation disorders were observed.

Table 9.1: *Factors Assessed in the Continent Level Statistical Analysis*

VARIABLE	COMPARISONS	DESCRIPTION	POTENTIAL INTERPLAYS WITH HUMAN POPULATION INTERACTION	REFERENCES
Human Population Interaction	High-Medium/ Very Low-Low (see Table 9.2)	Main topic of research in this thesis	N/A	See Chapter 2
Residential Mobility	Mobile/Sedentary	Sedentary populations considered to have higher levels of infectious disease, but mobility influences disease transmission	Potential differential effects of human population interaction between mobile and sedentary populations.	(Armelagos and Cohen 1984; Armelagos et al. 1991; Larsen 2006)
Rate of Natural Population Increase (RNPI)	Continuous Variable	RNPI as a proxy for population density. Increased population density is a recognised factor of infectious disease transmission.	Higher population density increases the potential for contact between individuals.	(Hu et al. 2013; Larsen 2006; McFadden and Oxenham 2018)
Climate	Non-Tropical/ Tropical	Tropical regions considered to be a risk area for infectious diseases. A significantly higher vector burden is identified for the tropics.	Impact of population interaction could be influenced by the nature of disease types. e.g. tropical vs. non-tropical diseases.	(Rohr et al. 2011; Steckel 2005)
Time Period	Continuous Variables	Possible introductions of new diseases or new disease pressures in Asia over time. A compound product of a number of socioeconomic and environmental changes.	Increase in population interaction and other factors with time	N/A
Subsistence	Cereals/ No Cereals	Domestication considered a possible factor in the influence of health.	Population interaction, population density and sedentism may be driven by agricultural efforts. Increased malnutrition due to cereal agriculture may increase susceptibility it newly introduced infectious diseases.	(Armelagos and Cohen 1984; Larsen 2006; Steckel 2005)

9.2.3 Measuring Human Population Interaction Levels

In order to assess varying levels of human population interaction, a definition for classification is required. The definition for human population interactions are provided in Table 9.2. A site is classified as having a particular interaction level if they meet at least *one* of the criteria provided. The outcomes of the variables for each of the sites is presented in Appendix 3. While binary variables are applied to the statistics below, these categories

enable ordinal ranking which may be employed in various statistical approaches in the future.

Table 9.2: *Parameters for the classification of human population interaction levels. A site is designated a human population interaction level based on meeting at least one of the criteria for each level.*

HUMAN POPULATION INTERACTION LEVELS		SITES
Very Low	No existing evidence for interpopulation interaction. The population is geographically isolated.	Middle and Final Jomon
Low	1) Isotopic, morphometric, and/or DNA evidence demonstrates few migrants. 2) There is some archaeological or proteomic evidence of trade and cultural exchange networks. 3) The population exists within a geographical space where some interaction with adjacent populations cannot be excluded. 4) There is historical evidence of minimal interaction.	Pre-Neolithic Vietnam
Medium	1) Isotopic, morphometric, historic and/or DNA evidence demonstrates migration, or trade. However, migration is not extensive to the degree wherein the population comprises clearly of a mixture of migrants and locals. 2) There is archaeological evidence to indicate established trade or cultural exchange, but this is not associated with connections to established routes of trade.	Bronze Age Mongolia
High	1) The site is a conflict zone. 2) There is clear DNA, isotopic, historic and/or morphometric evidence of large migration (the site is clearly a mixture of locals or migrants). 3) The site is an urban or trade centre with connections to established trade routes. 4) The interaction is directly related with significant social or cultural change.	Neolithic Vietnam; Xiongnu Period Mongolia

9.3 Results: Variable Factors in Infectious Disease Prevalence in Prehistoric Asia

9.3.1 Infectious Disease Prevalence and Human Population Interaction

When considering variation in population interaction levels and the relationship to infectious disease levels, relative risk ratios identified no statistical relationship (Table 9.3).

Table 9.3: *Relative risk of infectious disease prevalence across human population interaction levels.*

EXPOSED GROUP/ CONTROL GROUP	OUTCOME		RR	P-VALUE	95%CI
	Positive: *Infectious Disease Present*	***Negative:*** *Infectious Disease Absent*			
Human Pop. Interaction *High-Medium/ Low-Very Low*	23/33	147/140	0.7093	0.1681	0.4352- 1.1560

A relative risk (RR) >1 denotes a relationship of the exposed group with an increase in disease prevalence, whereas RR <1 denotes a relationship of the control group with an increase in disease prevalence.
**= statistically significant (p<0.10). **= statistically significant when considering size of the effect of RR.*

9.3.2 Infectious Disease Prevalence and Residential Mobility

The risk of infectious disease was almost 2.3 times (n=343, RR=2.2812, p=0.0055) higher in sedentary than mobile populations, which was statistically significant (Table 9.4).

Table 9.4: *Relative risk of infectious disease prevalence across human population interaction levels.*

EXPOSED GROUP/ CONTROL GROUP	**OUTCOME**		**RR**	**P-VALUE**	**95%CI**
	Positive: *Infectious Disease Present*	***Negative:*** *Infectious Disease Absent*			
Residential Mobility *Sedentary/ Mobile*	43/13	160/127	**2.2812**	**0.0055***	1.2749- 4.0816

A relative risk (RR) >1 denotes a relationship of the exposed group with an increase in disease prevalence, whereas RR <1 denotes a relationship of the control group with an increase in disease prevalence.
**= statistically significant (p<0.10). **= statistically significant when considering size of the effect of RR.*

9.3.3 Infectious Disease Prevalence and Human Population Interaction Across Residential Mobilities

Given the statistically significant differences between mobile and sedentary samples, variation in population interaction levels were assessed separately in mobile and sedentary subsamples. Statistically significant differences in population interaction levels were observed for both mobile and sedentary subsamples. It is noted here that mobile groups were only represented by Mongolian sites, therefore interpretations within the mobile subsample are limited. Sedentary populations with high to medium interactions were nearly 1.8 times (n=343, RR=1.7475, p=0.0645) more at risk of infectious disease than low or very low levels of human population interaction (Table 9.5).

Table 9.5: *Relative risk of infectious disease prevalence across human population interaction levels for sedentary and mobile subsamples.*

EXPOSED GROUP/ CONTROL GROUP	**OUTCOME**		**RR**	**P-VALUE**	**95%CI**
	Positive: *Infectious Disease Present*	***Negative:*** *Infectious Disease Absent*			
Human Pop. Interaction (Sedentary Only) *High/ Low-Very Low*	10/33	20/140	**1.7475**	**0.0645***	0.9669- 3.1583
Human Pop. Interaction (Mobile Only) *High/ Medium*	9/4	51/76	**3.000**	**0.0565***	0.9698- 9.2800

A relative risk (RR) >1 denotes a relationship of the exposed group with an increase in disease prevalence, whereas RR <1 denotes a relationship of the control group with an increase in disease prevalence.
*= statistically significant (p<0.10). **= statistically significant when considering size of the effect of RR.

9.3.4 Infectious Disease Prevalence and Rate of Natural Population Increase

The rate of natural population increase (RNPI) is here used as a proxy to estimate relative population density. As the D0-14/D ratio, a requirement for RNPI estimation, could not be estimated for the Jomon samples they were excluded from analysis. A comparison between RNPI and infectious disease prevalences are presented in Table 9.6. A strong positive linear correlation between RNPI values and infectious disease prevalence was observed (r= 0.9030). It is noted here that the sites with high RNPI are sedentary, whereas those with negative RNPI are mobile. There is a known association between population density and sedentary residential mobility (Armelagos and Cohen 1984; Armelagos et al. 1991).

Table 9.6: *Data for consideration in the Pearson correlation between RNPI and infectious disease prevalence*

TIME PERIOD	RNPI	PREVALENCE (%)
Neolithic Vietnam	4.32	33.3
Pre-Neolithic Vietnam	1.37	11.1
EBA-MBA Mongolia	-0.3	3.6
LBA Mongolia	-0.3	5.8
Xiongnu Period Mongolia	-0.3	15

9.3.5 Infectious Disease Prevalence and Climate

No statistically significant relationship to increased risk of infectious disease was observed for the tropical cohort (Table 9.7).

Table 9.7: *Relative risk of infectious disease prevalence across tropical and non-tropical climates.*

EXPOSED GROUP/ CONTROL GROUP	OUTCOME		RR	P-VALUE	95%CI
	Positive: *Infectious Disease Present*	***Negative:*** *Infectious Disease Absent*			
Climate *Tropical/ Non-Tropical*	16/52	132/141	0.9183	0.7319	0.5639- 1.4954

A relative risk (RR) >1 denotes a relationship of the exposed group with an increase in disease prevalence, whereas RR <1 denotes a relationship of the control group with an increase in disease prevalence.
*= statistically significant (p<0.10). **= statistically significant when considering size of the effect of RR.

9.3.6 Infectious Disease Prevalence and Time Period

There is a weak negative correlation with time period (in years BP) with infection (r=-0.2874). However, as observed in Figure 9.1, there are different trends for sedentary and mobile groups. There is a strong negative correlation with time period when considering sedentary only (r=-0.9275), and mobile only (r=-0.9702) subsamples.

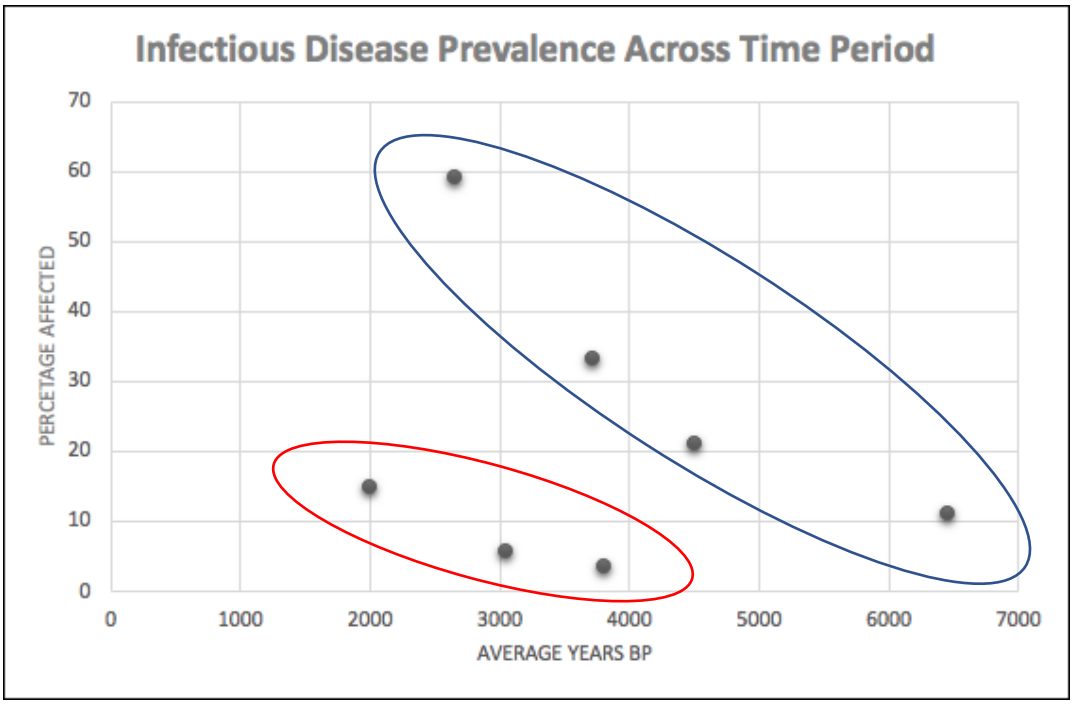

Figure 9.1: *Graphical representation of infectious disease prevalence across time period. Sites are represented in average years BP. The blue circle denotes the sedentary populations whereas the red circle denotes the mobile populations.*

9.3.7 Infectious Disease Prevalence and Subsistence

There was no statistically significant relationship between subsistence and infectious disease prevalence (Table 9.8).

Table 9.8: *Relative risk of infectious disease prevalence across subsistence types.*

EXPOSED GROUP/ CONTROL GROUP	**OUTCOME**		**RR**	**P-VALUE**	**95%CI**
	Positive: *Infectious Disease Present*	***Negative:*** *Infectious Disease Absent*			
Cereal Agriculture *Cereals/ No Cereals*	19/37	71/216	1.4435	0.1486	0.8772- 2.3756

A relative risk (RR) >1 denotes a relationship of the exposed group with an increase in disease prevalence, whereas RR <1 denotes a relationship of the control group with an increase in disease prevalence.
*= statistically significant (p<0.10). **= statistically significant when considering size of the effect of RR.

9.4 Results: Variable Factors in Infectious Disease Diversity in Prehistoric Asia

9.4.1 Infectious Disease Diversity and Human Population Interaction

Table 9.9 depicts the overall disease diversity across the sites included in analysis. A general trend in higher disease diversity with higher levels of human population interaction are apparent. However, no statistically significant relationship in the levels of human population interaction and disease diversity was identified (Table 9.10).

Table 9.9: *The presence of diagnosed possible and probable infectious diseases, nutritional diseases and anaemias across the sites studied in this thesis.*

SITE	**HUMAN POPULATION INTERACTION LEVEL**	**DISEASES DIAGNOSED**											
		Treponemal Disease	*TB*	*Otitis Media/ Mastoiditis*	*Mycosis*	*Brucellosis*	*Osteomyelitis*	*Hydatids*	*Anaemia*	*Thalassaemia*	*Scurvy*	*Rickets*	*Osteomalacia*
Middle Jomon Japan	Very Low	-	-	4/18 (22.2%)	1/34 (2.9%)	-	-	-	12/19 (63.2%)	-	11/32 (34.4%)	-	-
Final Jomon Japan	Very Low	-	-	4/22 (18.1%)	-	-	1/30 (3.3%)	-	18/28 (69.2%)	-	28/30 (93.3%)	-	-
Con Co Ngua Vietnam	Low	-	-				1/155 (0.6%)	13/155 (8.4%)	95/128 (74.2%)	1/155 (0.6%)	10/155 (6.5%)	-	-
Bronze Age Mongolia	Medium	-	1/92* (1.1%)	1/38 (2.6%)	-	1/92* (1.1%)	1/92 (1.1%)	1/92 (1.1%)	8/30 (26.7%)	-	12/92 (13.1%)	20/92 (21.7%)	10/80 (12.5%)
Man Bac Vietnam	High	6/70 (8.5%)	-	1/58 (1.7%)	-	-	-	-	28/58 (48%)	8/70 (11.4%)	54/70 (77.1%)	22/70 (31.4%)	-
Xiongnu Period Mongolia	High	1/69 (1.4%)	1/69* (1.4%)	1/31 (3.2%)	1/69* (1.4%)	1/69 (1.4%)	-	1/69 (1.4%)	8/31 (25.8%)	-	21/69 (30.4%)	20/69 (29%)	19/61 (31.1%)

***** denotes an individual with more than one possible diagnosis for infectious disease

Table 9.10: *Relative risk of infectious disease diversity across human population interaction levels.*

EXPOSED GROUP/ CONTROL GROUP	**OUTCOME**		**RR**	**P-VALUE**	**95%CI**
	Positive: *Infectious Disease Identified*	***Negative:*** *Infectious Disease Not Identified*			
Human Pop. Interaction					
High-Medium/ Low-Very Low	11/6	10/15	1.8333	0.1325	0.8323- 4.0384

A relative risk (RR) >1 denotes a relationship of the exposed group with an increase in disease prevalence, whereas RR <1 denotes a relationship of the control group with an increase in disease prevalence.
*= statistically significant (p<0.10). **= statistically significant when considering size of the effect of RR.

9.4.2 Infectious Disease Diversity and Residential Mobility

Mobile groups were almost 2.3 times (n=42, RR=2.2500, p=0.0239) at risk of a greater number of infectious diseases than sedentary groups (Table 9.11).

Table 9.11: *Relative risk of infectious disease diversity across residential mobility*.

EXPOSED GROUP/ CONTROL GROUP	**OUTCOME**		**RR**	**P-VALUE**	**95%CI**
	Positive: *Infectious Disease Identified*	***Negative:*** *Infectious Disease Not Identified*			
Residential Mobility					
Mobile/Sedentary	9/8	5/20	**2.2500**	**0.0239***	1.1130- 4.5485

A relative risk (RR) >1 denotes a relationship of the exposed group with an increase in disease prevalence, whereas RR <1 denotes a relationship of the control group with an increase in disease prevalence.
*= statistically significant (p<0.10). **= statistically significant when considering size of the effect of RR.

9.4.3 Infectious Disease Diversity and Human Population Interaction Across Residential Mobilities

There were no statistically significant differences in the number of infectious diseases with increased human population interaction levels in mobile only and sedentary only subsamples (Table 9.12).

Table 9.12: *Relative risk of infectious disease diversity across human population interaction levels for sedentary and mobile subsamples.*

EXPOSED GROUP/ CONTROL GROUP	**OUTCOME**		**RR**	**P-VALUE**	**95%CI**
	Positive: *Infectious Disease Identified*	***Negative:*** *Infectious Disease Not Identified*			
Human Pop. Interaction (Sedentary Only) *High/ Low-Very Low*	2/6	3/15	1.4000	0.6032	0.3936- 4.9791
Human Pop. Interaction (Mobile Only) *High/Medium*	5/4	2/3	1.2500	0.5820	0.5648- 2.7665

A relative risk (RR) >1 denotes a relationship of the exposed group with an increase in disease prevalence, whereas RR <1 denotes a relationship of the control group with an increase in disease prevalence.
*= statistically significant (p<0.10). **= statistically significant when considering size of the effect of RR.

9.4.4 Infectious Disease Diversity and Rate of Natural Population Increase

A comparison between RNPI and infectious disease prevalences are presented in Table 9.13. A weak negative linear correlation between RNPI values and infectious disease diversity index was observed (correlation coefficient= -0.3087).

Table 9.13: *Data for consideration in the Pearson correlation between RNPI and infectious disease diversity (IDDI)*

TIME PERIOD	**RNPI**	**IDDI**
Neolithic Vietnam	4.32	28.6
Pre-Neolithic Vietnam	1.37	28.6
EBA-MBA Mongolia	-0.3	14.30
LBA Mongolia	-0.3	42.9
Xiongnu Period Mongolia	-0.3	71.4

9.4.5 Infectious Disease Diversity and Climate

No statistically significant relationship with increased infectious disease diversity was observed for tropical cohorts (Table 9.14).

Table 9.14: *Relative risk of infectious disease diversity across human population interaction levels for tropical compared to non-tropic cohorts.*

EXPOSED GROUP/ CONTROL GROUP	**OUTCOME**		**RR**	**P-VALUE**	**95%CI**
	Positive: *Infectious Disease Present*	***Negative:*** *Infectious Disease Absent*			
Climate *Tropical/ Non-Tropical*	4/13	10/15	0.6154	0.3004	0.2455- 1.5424

A relative risk (RR) >1 denotes a relationship of the exposed group with an increase in disease prevalence, whereas RR <1 denotes a relationship of the control group with an increase in disease prevalence.
*= statistically significant (p<0.10). **= statistically significant when considering size of the effect of RR.

9.4.6 Infectious Disease Diversity and Time Period

Figure 9.2 presents the representation of infectious disease diversity index across time period. Like with infectious disease prevalence there are clear differences between mobile and sedentary populations. A moderate negative correlation was observed overall (r=-0.5385). A strong negative correlation was observed for mobile groups (r=-0.9953) whereas no correlation (r=0) was observed for sedentary groups.

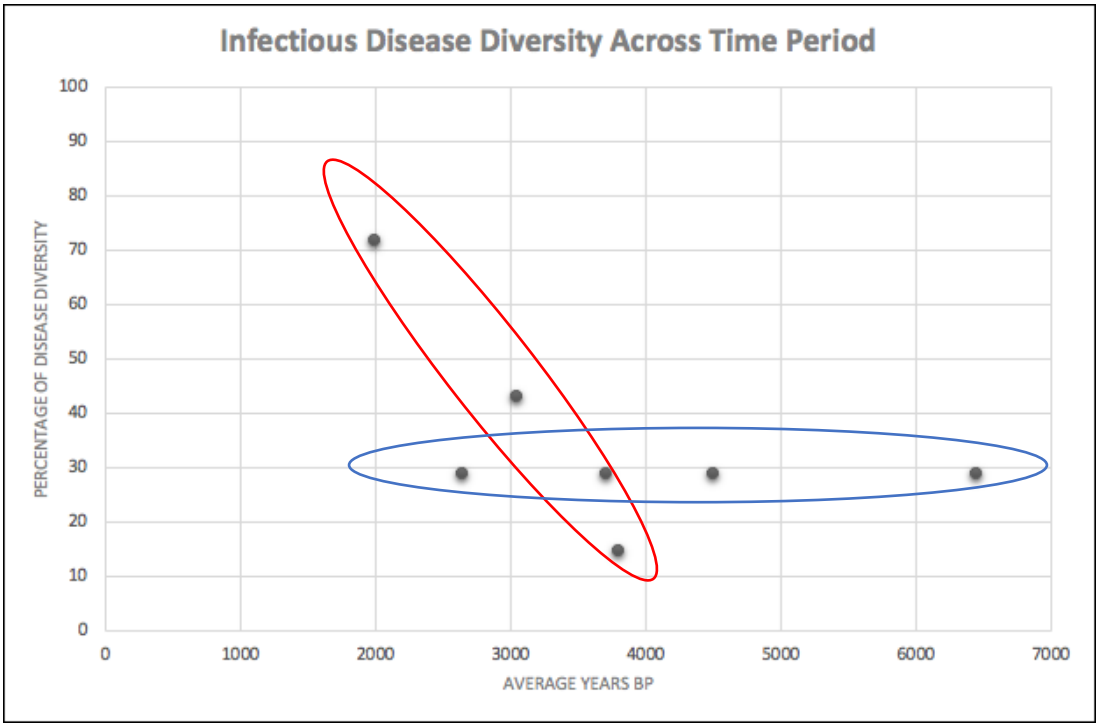

Figure 9.2: *Graphical representation of infectious disease diversity across time period. Sites are represented in average years BP. The blue circle denotes the sedentary populations whereas the red circle denotes the mobile populations.*

9.4.7 Infectious Disease Diversity and Subsistence

No significant differences in infectious disease diversity were observed among different subsistence bases (Table 9.15).

Table 9.15: *Relative risk of infectious disease diversity across different subsistence.*

EXPOSED GROUP/ CONTROL GROUP	**OUTCOME**		**RR**	**P-VALUE**	**95%CI**
	Positive: *Infectious Disease Present*	***Negative:*** *Infectious Disease Absent*			
Cereal Agriculture					
Cereals/ No Cereals	12/10	15/6	0.7636	0.2584	0.4784- 1.2189

A relative risk (RR) >1 denotes a relationship of the exposed group with an increase in disease prevalence, whereas RR <1 denotes a relationship of the control group with an increase in disease prevalence.
*= statistically significant (p<0.10). **= statistically significant when considering size of the effect of RR.

9.5 Summary of Factors in Infectious Disease Dynamics

Human population interaction appears to have influenced mobile and sedentary populations separately in terms of infectious disease prevalence but not in infectious disease diversity. Sedentary populations had significantly higher infectious disease prevalences, whereas mobile populations had significantly higher infectious disease diversity. High population density also influenced the prevalence rate. Subsistence and climate did not significantly affect infectious disease prevalences nor diversity. Time periods closer to the present had higher infectious disease prevalences, whereas high infectious disease diversity closer to present day was observed for mobile groups. Caution is noted here in regards to a relationship between infectious disease and mobile populations as all of the samples come from Mongolia and therefore may reflect a regional trend.

9.6 Results: Variable Factors in Scurvy Prevalence in Prehistoric Asia

9.6.1 Scurvy Prevalence and Human Population Interaction

No statistically significant differences in scurvy prevalence was observed between different human population interaction levels (Table 9.16). The relative risk was near identical for the two variables (n=343, RR=1.0059, p=0.9784).

Table 9.16*: *Relative risk of scurvy prevalence across human population interaction levels.

EXPOSED GROUP/ CONTROL GROUP	OUTCOME		RR	P-VALUE	95%CI
	Positive: *Scurvy Present*	***Negative:*** *Scurvy Absent*			
Human Pop. Interaction *High-Medium/ Low-Very Low*	34/34	136/137	1.0059	0.9784	0.6574- 1.5391

A relative risk (RR) >1 denotes a relationship of the exposed group with an increase in disease prevalence, whereas RR <1 denotes a relationship of the control group with an increase in disease prevalence.
*= statistically significant (p<0.10). **= statistically significant when considering size of the effect of RR.

9.6.2 Scurvy Prevalence and Residential Mobility

Sedentary populations were almost 2.3 times (n=343, RR=2.2812, p=0.0055) at an increased risk for scurvy than mobile populations which was statistically significant (Table 9.17).

***Table 9.17:** Relative risk of scurvy prevalence across human population interaction levels.*

EXPOSED GROUP/ CONTROL GROUP	OUTCOME		RR	P-VALUE	95%CI
	Positive: *Scurvy Present*	***Negative:*** *Scurvy Absent*			
Residential Mobility *Sedentary/ Mobile*	43/13	160/127	**2.2812**	**0.0055***	1.2749- 4.0816

A relative risk (RR) >1 denotes a relationship of the exposed group with an increase in disease prevalence, whereas RR <1 denotes a relationship of the control group with an increase in disease prevalence.
*= statistically significant (p<0.10). **= statistically significant when considering size of the effect of RR.

9.6.3 Scurvy Prevalence and Human Population Interaction Across Residential Mobilities

When assessed separately there was a significant difference in scurvy prevalence across varying human population interaction levels in mobile and sedentary subsamples (Table 9.18). Sedentary groups with high to medium interactions were over 2.5 times (n=343, RR=2.5147, p=0.0001) more at risk of scurvy than low or very low levels of human population interaction.

Table 9.18: *Relative risk of scurvy prevalence across human population interaction levels for sedentary and mobile subsamples.*

EXPOSED GROUP/ CONTROL GROUP	**OUTCOME**		**RR**	**P-VALUE**	**95%CI**
	Positive: *Scurvy Present*	***Negative:*** *Scurvy Absent*			
Human Pop. Interaction (Sedentary Only) *High/ Low-Very Low*	15/34	15/137	**2.5147**	**0.0001***	1.5756- 4.0136
Human Pop. Interaction (Mobile Only) *High/ Medium*	14/5	46/75	**3.7333**	**0.0074***	1.4227- 9.7964

A relative risk (RR) >1 denotes a relationship of the exposed group with an increase in disease prevalence, whereas RR <1 denotes a relationship of the control group with an increase in disease prevalence.
*= statistically significant (p<0.10). **= statistically significant when considering size of the effect of RR.

9.6.4 Scurvy Prevalence and Rate of Natural Population Increase

Table 9.19 provides data for Pearson correlation between RNPI and scurvy prevalence. A strong positive linear correlation between RNPI values and scurvy prevalence was observed (r= 0.7574).

Table 9.19: *Data for consideration in the Pearson correlation between RNPI and scurvy prevalence*

TIME PERIOD	**RNPI**	**PREVALENCE (%)**
Neolithic Vietnam	4.32	50
Pre-Neolithic Vietnam	1.37	0.8
EBA-MBA Mongolia	-0.3	0
LBA Mongolia	-0.3	9.6
Xiongnu Period Mongolia	-0.3	23.3

9.6.5 Scurvy Prevalence and Climate

Non-tropical populations were at almost 2.5 times (n=343, RR=0.4012, p=0.0005) the increased risk of scurvy than tropical populations, which was statistically significant (Table 9.20).

Table 9.20: *Relative risk of scurvy prevalence across tropical and non-tropical climates.*

EXPOSED GROUP/ CONTROL GROUP	**OUTCOME**		**RR**	**P-VALUE**	**95%CI**
	Positive: *Scurvy Present*	***Negative:*** *Scurvy Absent*			
Climate					
Tropical/ Non-Tropical	16/52	132/141	**0.4012**	**0.0005***	0.2391- 0.6734

A relative risk (RR) >1 denotes a relationship of the exposed group with an increase in disease prevalence, whereas RR <1 denotes a relationship of the control group with an increase in disease prevalence.
*= statistically significant (p<0.10). **= statistically significant when considering size of the effect of RR.

9.6.6 Scurvy Prevalence and Time Period

Different trends for mobile and sedentary groups were once again observed across time period (Figure 9.3). While overall, a weak negative correlation was observed (r=-0.41421), strong correlations were observed within sedentary (r=-0.9638) and mobile (r=-0.9999) only subsamples.

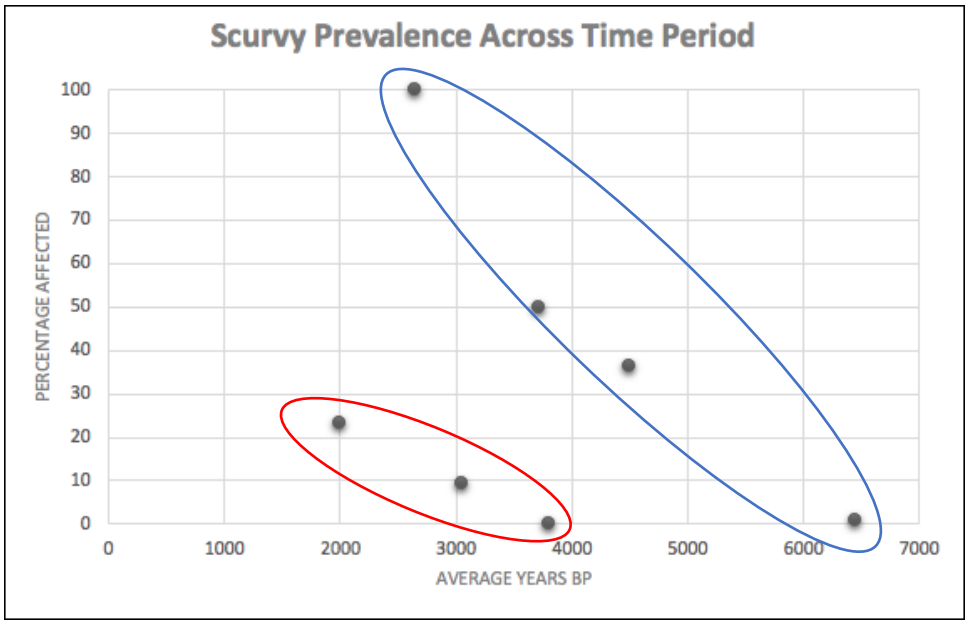

Figure 9.3: *Graphical representation of scurvy prevalence across time period. Sites are represented in average years BP. The blue circle denotes the sedentary populations whereas the red circle denotes the mobile populations.*

9.6.7 Scurvy Prevalence and Subsistence

Populations with cereal agriculture as part of their subsistence base were at over 2 times at risk for scurvy than populations without cereal agriculture, which was statistically significant (Table 9.21).

Table 9.21: *Relative risk of scurvy prevalence across subsistence types.*

EXPOSED GROUP/ CONTROL GROUP	**OUTCOME**		**RR**	**P-VALUE**	**95%CI**
	Positive: *Scurvy Present*	***Negative:*** *Scurvy Absent*			
Cereal Agriculture					
Cereals/ No Cereals	29/39	61/212	**2.0738**	**0.0006***	1.3682- 3.1433

A relative risk (RR) >1 denotes a relationship of the exposed group with an increase in disease prevalence, whereas RR <1 denotes a relationship of the control group with an increase in disease prevalence.
*= statistically significant (p<0.10). **= statistically significant when considering size of the effect of RR.

9.7 Summary of Factors in Scurvy Prevalence in Prehistoric Asia

Human population interaction was not observed to be a factor in scurvy prevalence. While there seems to be a statistically significant difference in scurvy prevalence across human population interaction levels when considering sedentary and mobile only subsamples; this outcome co-occurs with crop subsistence. That is, all samples with high levels of population interaction also had cereal crop subsistence. Overall samples with cereal crop subsistence presented significantly higher prevalences of scurvy, than those without domesticated crops. Sedentary populations had higher prevalences than mobile samples and different patterns in scurvy prevalences between sedentary and mobile samples were observed across time period. Scurvy levels increased alongside time periods closer to the present, indicating considerable biosocial and environment change over time in Asia's prehistory. Tropical populations had significantly lower prevalences of scurvy than non-tropical populations.

9.8 Chapter Summary

This chapter presented the continent level statistics employing all samples explored in chapters 6 to 8, to assess how human population interaction levels in Asia have interplayed with other important socioeconomic and environmental factors to influence prehistoric health. Statistically, considerable variation in the prevalences of mobile and sedentary groups were observed. In terms of infectious disease, a higher prevalence was observed in sedentary groups, whereas an increase in infectious disease diversity was observed in mobile groups. Human

population interaction levels significantly impacted the prevalence of infectious disease, albeit differently in mobile and sedentary groups. Subsistence base was a significant factor in scurvy prevalence, with a higher prevalence in populations with staple cereal crops in their diet. There is no considerable evidence to associate population interaction levels with scurvy prevalence. These results will be discussed in the following chapter.

CHAPTER 10:
DISCUSSION AND CONCLUSIONS

10.1 Introduction

The results of this investigation have been outlined in the preceding chapters (Chapters 6 to 9). These chapters addressed the skeletal evidence of infectious disease, nutritional disease and anaemia at site, regional and continent levels across Asia's prehistory.

The first aim of this chapter is to summarise the results and discuss the findings in relation to current epidemiological and palaeopathological literature. The second aim is to present the epidemiological model of human population interaction and its consequences on disease dynamics in prehistoric populations. The presentation of this model achieves the final objective of this thesis. The third aim of this chapter is to discuss the proposed model in light of the osteological paradox and to critically assess the methodology applied in this thesis. Finally this chapter addresses the significance, opportunities for future research and the conclusions of the thesis.

The conclusions directly address the two research questions of this thesis:

1. *Did increasing levels of population interaction over time significantly affect the health of populations in prehistoric Asia?*

2. *How did population interaction interplay with a range of other sociocultural, biological and ecological factors to influence the health of populations in prehistoric Asia?*

10.2 Results Summary

In order to evaluate the impacts of human interaction on health in prehistoric Asia, discussion on *regional* level and *continent* level characteristics of disease are necessary, as they explore different elements of disease dynamics. In doing so, the research questions of this thesis can be properly addressed, as varying levels of analyses acknowledge the complexities of disease transmission and the importance of biosocial context. The following

section investigates trends of human interaction at these two levels of analyses. *Site* level disease dynamics were discussed in detail in the respective case study chapters (Chapters 6 to 8). It is acknowledged that intrapopulation variation in disease dynamics concerning factors such as age, gender, socio-economic status, among others, are not captured in the analysis at a regional or continent level. Additionally, site level analysis enabled discussion of the overall impact of disease, whether or not they directly pertained to human population interaction. Table 10.1 summarises intrapopulation variations of age and sex observed at the site level.

10.2.1 Human Interaction Disease Dynamics at a Regional Level

Comparisons of the outcomes of the three case studies are necessary to understand variation in the role of human interaction at a regional level. Table 10.2 summarises changes in the prevalences of diagnosed diseases at regional levels, as well as overall impact on mortality. The table identifies whether higher or lower prevalences of diseases, or overall changes to mortality were observed with increasing levels of human population interaction. Across the three case studies it is apparent that disease prevalences were generally higher in the sites with an increase in population interaction. However, there remains variation as to the degree of influence on disease patterns across the case studies. As an increase in human population interaction levels often accompany or are driven by a host of socio-economic or environmental changes, the relationship between an increase in the prevalence of diseases with increasing levels of population interaction need to be critically considered (Gushulak and MacPherson 2004; MacPherson and Gushulak 2001). It is clear from the previous chapters (6 to 8) that multiple factors influenced the prevalence of diseases, of which population interaction was one element driving change in disease dynamics. The following section summarises and discusses the results of the regional level analyses.

Table 10.1: *Intrapopulation variation in the risk of diseases across sites in this thesis. Statistically significant variations across different cohorts of age and sex factors are presented.*

REGION	**SITES**	**INFECTIOUS DISEASE**		**SCURVY**		**RICKETS/ OSTEOMALACIA**		**ANAEMIA**	
Significant Change Across Cohorts		***Morbidity***	***Mortality***	***Morbidity***	***Mortality***	***Morbidity***	***Mortality***	***Morbidity***	***Mortality***
Japan	*Ota*	-	-	Adult Age	Adult Age	-	-	Sex, Adult Age	Adult Age
	Tsukumo	-	-	Adult Age	Adult Age	-	-	Sex, Nonadult Age, Adult Age	Nonadult Age, Adult Age
Vietnam	*Con Co Ngua*	-	-	Nonadult Age	Nonadult Age	-	-	Adult Age	Adult Age
	Man Bac	Nonadult Age	Nonadult Age	Adult Age	Adult Age	Nonadult Age	Nonadult Age	Nonadult Age, Adult Age	Nonadult Age, Adult Age
Mongolia	*Bronze Age*	-	-	Adult Age	Adult Age	Sex, Adult Age	Adult Age	-	-
	Xiongnu Period	Adult Age	Adult Age	Nonadult Age, Adult Age	Adult Age	Sex	Adult Age	Sex	-

Table 10.2: *Regional changes in the prevalence of diseases across each region (Japan, Mongolia and Vietnam) with increasing human population interaction levels. * = statistically significant change.*

		JAPAN	VIETNAM	MONGOLIA
Infectious Disease (Prevalence)	*Nonadult*	-	Higher	Higher*
	Adult	Higher*	Higher*	Higher
Scurvy (Prevalence)	*Nonadult*	-	Higher*	Similar
	Adult	Higher*	Higher*	Higher*
Rickets (Prevalence)	*Nonadult*	-	Higher*	Similar
	Adult	-	-	Higher*
Osteomalacia (Prevalence)	*Adult*	-	-	Higher*
Anaemia (Prevalence)	*Nonadult*	-	Higher*	Higher
	Adult	Higher*	Higher*	Similar
Thalassaemia (Prevalence)	*Nonadult*	-	Higher	-
	Adult	-	Similar	-
Overall Mortality	*Adult*	Higher*	Similar	Similar

10.2.1.1 Infectious Disease at a Regional Level

As addressed in Chapter 2, the pathogen's mechanism for transmission partially mediates the conditions of disease transmission. Therefore, it is important to consider that the disease contexts differ across these three case studies, and this influences the degree of impact of human population interaction on disease transmission. Each of the three case studies had different types of infectious diseases. Climatic variations contributed to this difference. For example, tropical specific yaws was the likely cause for treponematosis at Man Bac, and would therefore not be expected to have been identified in Japanese and Mongolian sites. Additionally, evidence of tuberculosis in Mongolia can also be linked to the relationship of respiratory diseases with colder climates and decreased humidity, where the bacteria can remain airborne for longer periods of time (Shaman and Kohn 2009; Sloan et al. 2011).

Moreover, the ecological relationship between human groups, animals and the surrounding environment also influenced the presence of particular infectious diseases.

While the identification of hydatids disease at Con Co Ngua was an unusual finding, given the lack of evidence for clear domestication at the site, this disease, and other zoonotic diseases, are expected findings in the Mongolian assemblages (Beggs 1985; Deplazes et al. 2017). Hydatids disease then highlighted different relationships to animals in Vietnam compared to Mongolia. In the case of Con Co Ngua, the prevalence of hydatids disease had no relationship with human population interaction and was a product of environmental exposure. In contrast, the movement of livestock and interaction of people was likely an essential component of the spread of hydatids disease in Mongolia, as it is today (Macpherson 1995). That is, not all infectious diseases, even when considering the same pathogen, can be attributed to human population interaction. As explained in Chapter 1, interaction between two populations results in a combination of 1) environmental exposure to diseases, 2) continued spread of pre-existing diseases within the population, and 3) the introduction of new diseases via population interaction. The presence of possible mycotic infection in the Ota Jomon assemblage may also reflect environmental exposure to the pathogen rather than an increase in population interaction, as infection occurs with soil contamination (Goodwin et al. 1981; Oberoi et al. 2012). Therein lies the difficulty in determining what infectious diseases may be attributed to human population interaction and what infectious diseases are products of the immediate environment.

Micro-changes in climate were also observed across the time periods, likely influencing the ecological niches of environmental pathogens (Estrada-Peña et al. 2014). Climate cooling appears to be a primary factor in the displacement and depopulation of the Jomon people, whereas this same climate cooling event likely led to the adoption of agriculture in Southeast Asia (Koyama 1979; Oxenham et al. 2018; Temple 2007). It can then be assumed that an increase in overall infectious disease levels encompass both the environmental exposure to pathogens and changes in human population interaction levels. However, the findings of all three case studies consistently demonstrated an association between increasing human population interaction levels and an increase in infectious disease prevalence.

What is of particular interest, is that in the two case studies assessing interpopulation interaction (Vietnam and Mongolia), human specific infectious diseases were observed only in the populations with increased human population interaction. Treponematosis was identified in Man Bac, and treponematosis and tuberculosis were possibly identified in the

Xiongnu Period of Mongolia. These diseases are not related to environmental exposure and were either pre-existing infections within the population (but not observable in the earlier skeletal assemblages) or introduced by the interaction event. The interaction events driving transmission of human specific infectious diseases in these two cases remains a possibility.

There were not considerable increases in the diversity of infectious diseases observed across the three case studies. That is, the number of infectious diseases did not greatly increase across the time periods. Additionally, with the exception of the Mongolian case, the types of infectious diseases observed in earlier time periods, were not diagnosed in the later time periods. This outcome highlights the difficulty in identifying infectious diseases in the skeletal record, but also identifies shifting environmental, socio-cultural and biological contexts influencing the impacts of particular infectious diseases in a region over time.

10.2.1.2 Nutritional Disease at a Regional Level

The prevalence of scurvy was higher in all post-interaction sites. Additionally, where rickets and/or osteomalacia were identified (Vietnam and Mongolia), prevalences were also higher in the post-interaction sites. However, as discussed in the results chapters, human population interaction often had an indirect influence on nutritional status. In regards to scurvy, an increase in the Late to Final Jomon compared to the Middle Jomon was likely associated with ecological decline following climate change, driving both nutritional stress and human population interaction simultaneously. In Vietnam and Mongolia, the processes of population interaction initiated subsistence changes that influenced micronutrient deficiencies. A subsistence change was also likely the primary factor in the prevalence of rickets in children under the age of 10 years at Man Bac. In contrast, there was no apparent correlation between human interaction levels and the increase in rickets and osteomalacia from the Bronze Ages to the Xiongnu Period in Mongolia. Instead, other socio-cultural changes in association with the emergence of a confederate empire likely contributed to an increase in the prevalences of mineralisation disorders.

Overall, it is evident that in contrast to infectious disease prevalences, population interaction levels did not necessarily influence nutritional status. A relationship between nutritional disease and population interaction levels were dependent on the context of the

interaction processes and the pre-existing socio-economic and environmental conditions of the affected populations. As mentioned in Chapter 2, modern epidemiological studies demonstrate that there is not necessarily a direct relationship between migration and poor nutritional status. Instead, the impacts are dependent on the migrants' original health status and socio-economic standing (Karamba et al. 2011; Sharghi et al. 2011). The results of the regional analysis of nutritional diseases in this thesis supports the outcomes of modern studies on migrant health.

Trends in co-morbidities between skeletal evidence of infectious diseases and nutritional diseases were variable across the assemblages. That is, there was no clear relationship at site level between skeletal evidence for infectious disease and skeletal evidence for nutritional disease. Roberts and Brickley (2018) reported on an 18th Century British cemetery where skeletal evidence of tuberculosis was low in a sample of eleven rachitic individuals. However, biomolecular analysis identified evidence for co-morbidity of Vitamin D deficiency and tuberculosis in a number of individuals. As nutritional stress is likely to also increase the risk of death to infectious disease, a complex relationship between skeletal presence of co-morbid infectious and nutritional diseases is an expected outcome. Interestingly, overall, in the assemblages with high prevalences of infectious diseases (Ota, Tsukumo and Man Bac), there were also high prevalences of nutritional diseases. For this reason a synergy between nutritional and infectious diseases was observed in the skeletal remains analysed in this thesis. This trend was only visible when all cases were considered, and sample size is likely an influencing factor when considering co-morbidity. Therefore, while a direct relationship between human population interaction levels and nutritional disease was not observed, underlying nutritional status was likely an important aspect of susceptibility to infectious pathogens in the three case studies.

10.2.1.3 Anaemia at a Regional Level

The prevalences of anaemia were higher in Man Bac compared to Con Co Ngua, higher in the nonadults of the Xiongnu Period compared to the Bronze Age in Mongolia, and higher in the adults from Tsukumo compared to Ota. However, overall there appears to be a weak association between human population interaction levels and anaemia prevalences. It is important to note that non-specific stress markers such as anaemia, may not be particularly valuable in identifying regional level changes to disease when addressing

specific research questions such as in this thesis. The multitude of factors that contribute to the formation of anaemia lesions are likely the reason for this. However, the identification of anaemia remains useful in understanding the overall stress of a site, not necessarily captured by the identification of specific disease (McIlvaine 2015). For example, the diagnosis of scurvy only identifies micronutrient deficiency of Vitamin C, whereas anaemic lesions are more sensitive indicators of interacting factors of malnutrition, parasitism and pathogen load in childhood (Gowland and Western 2012; Oxenham and Cavill 2010; Walker et al. 2009). As such, skeletal markers of anaemia are essential contributors in identifying whether particular elements of specific disease contributed greatly to the overall burden of health. For example, while scurvy was significantly higher in Tsukumo than in Ota with a considerable increase in relative risk of morbidity, the relative risk of anaemia was only slightly higher in Tsukumo, indicating there were other factors with deleterious health outcomes beyond nutritional and infectious diseases in Jomon childhood.

Thalassaemia was only diagnosed in Vietnam, which is an expected outcome given the distribution of thalassaemia alleles in Asia today (see Chapter 3). Given the relationship in Southeast Asia between the high prevalence of malaria and haemoglobinopathies including alpha and beta thalassaemias (Weatherall 2008), the identification of thalassaemia may be beneficial in assessing the potential of malaria presence in the prehistory of this region. In sites such as Man Bac, where there is direct evidence of genetic admixture between two populations, the role that human interaction plays in the prevalence of malaria and thalassaemia, is an avenue to explore. However, as mentioned in Chapter 7, the direct relationship between malaria and thalassaemia presence should be considered with caution as genetic admixture can occur in absence of the malarial parasite. For example, Lewis (2012) identified thalassaemia in infants from the Romano-British site Poundbury Camp. The author attributes the presence of the disease to immigration from Mediterranean regions where thalassaemia is endemic, and there is no clear relationship with malaria at the site.

10.2.1.4 Mortality at a Regional Level

Whether there was an increase in the mortality rate across time periods was in part dependant on the pathogen specific impact on mortality. For example, there was no increase in mortality across the Vietnamese sites. However, the mortality rates of hydatids disease and endemic treponematosis were low, and expected to not have significantly contributed to

mortality at a young age within and between the sites (Beggs 1985; Hook III and Marra 1992; Peeling and Hook III 2006). Where infectious diseases with high mortality rates were present (e.g. possible tuberculosis in Mongolia) this influenced the site level mortality, while significant impact on the overall mortality across time periods was not observed.

The only case study where there was a significant influence on overall mortality rate over time, was that of Jomon Japan. There was no shift in the levels of interpopulation interaction from the Middle to Late-Final Jomon Periods, that could be expected to have a dramatic influence on health. As such, the change in mortality was likely an overall product of climatic cooling leading to nutritional stress, significant social change, and population decline. Population interaction was therefore but a minor factor in changes to mortality. Overall, there is not considerable evidence to suggest that an increase in human population interaction was associated with substantial changes to population mortality across the three case studies.

10.2.5 Interpopulation versus Intrapopulation Human Interaction Impacts on Health

The case study of Jomon Japan explored intrapopulation interaction in the absence of interpopulation interaction, therefore comparisons could be made to the other case studies where interpopulation interactions were key factors. Indeed it is noted here that extrapolations made are restricted by the comparisons of only three case studies, and again the context of the diseases proved to differ considerably across the case studies. While the prevalences of infectious diseases did increase with intrapopulation interaction in the Jomon, the effects of interpopulation interaction on infectious disease were more noticeable. As previously mentioned, only with an increase in interpopulation interaction was the introduction of human specific infectious diseases observed. Additionally, in the case of intrapopulation interaction in the Jomon, a significant proportion of the infectious diseases were non-specific, whereas a larger proportion of identified specific diseases were observed in the Vietnamese and Mongolian samples. When considering the impacts of epidemiological bridging (discussed in Chapter 2) this outcome is expected as there is a greater genetic and demographic difference between interacting populations, increasing the probability of the introduction of new pathogens (Cui et al. 2013; Kodaman et al. 2014). The potential for newly introduced diseases to have significant impact on the overall prevalence of infectious disease within an assemblage can be largely attributed to the susceptibility of

naïve populations to new pathogens (Bansal et al. 2010). Overall, it is clear that considerable influences of human population interaction on disease dynamics can be observed at a regional level.

10.2.2 Human Interaction Disease Dynamics at a Continental Level

10.2.2.1 Summary of Significant Factors Identified in Continent Level Analysis

Human population interaction was only a statistically significant factor in infectious disease prevalence when mobile and sedentary populations were separately analysed. An increase in overall infectious disease prevalences were also significantly related to sedentary populations, high population density and more recent time periods, regardless of population interaction levels. Increased infectious disease diversity was significantly related with mobile populations only. In contrast, human population interaction did not have a significant relationship with increased nutritional status (in the form of scurvy). Instead, non-tropical climates, cereal crop subsistence, sedentary residential mobility and more recent time periods were related to increased nutritional stress.

10.2.2.2 The Epidemiological Bridge

Strong statistical relationships between infectious disease prevalences, high population densities and sedentary residence is supported by a number of palaeopathological studies (Armelagos and Cohen 1984; Eshed et al. 2010; Larsen 1995; Larsen et al. 2015). Higher population densities enable more frequent community transmission of pathogens as probabilities of interactions between individuals increases (Dalziel et al. 2013). Higher population densities then increase the *intensity* of local interaction networks. Sedentary residence increases the *dwelling time* of interactions between individuals in local networks (Belik et al. 2011). Therefore, while mobility at a community level is practically invisible in an archaeological context (as argued by Clark 2001), local interaction networks clearly leave palaeoepidemiologically visible markers in a skeletal assemblage.

However, larger scale interactions, that are less frequent but are visible in the archaeological record do appear to affect the nature of disease transmission. Introduction of a new pathogen through interpopulation interaction, greatly influenced the prevalence of infectious diseases in sedentary populations, particularly those with high population

densities. The conditions of these factors are favourable for the spread of a new pathogen throughout a population with relative ease. The fact that higher population interaction levels drove higher prevalences of infectious diseases in these populations indicates the size of the interacting (migrant) population is also an aspect of increased *intensity* of disease transmission through epidemiological bridging (discussed in Chapter 2). Overall, the size of both the *migrant* population and the *local* population appeared to influence the risk of disease spread at an interaction zone. Again this trend is observed in modern day epidemiological studies (Gushulak and MacPherson 2004).

What is of great interest is that the mobile populations in this thesis were observed to have considerably different epidemiological complications from interpopulation interaction than sedentary populations. As these mobile populations also had low population densities, it is likely that again residential mobility *and* population density contributed to the disease patterns observed. Instead of affecting the prevalence rate of infectious diseases, a greater number of infectious disease types were observed. The mobile populations assessed in this thesis were all exposed to medium or high levels of human population interaction. Therefore, the disease prevalences of low density mobile populations with low population interactions were not assessed. However, research into those populations in archaeological and modern contexts demonstrate low burdens of infectious diseases (Cassidy 1984; Lieverse 2005; Webb 2009). Lieverse (2005) observed subperiosteal new bone deposits in 0-4% of individuals from Mid-Holocene mobile hunter-gatherer sites from the Cis-Baikal region of Siberia, all were non-specific. Therefore, the diversity of the infectious diseases in the mobile population in this thesis may then be a product of episodic interactions increasing the *frequency* of contact leading to disease transmission. Mobility then in of itself was not likely the factor driving disease transmission, without considerable levels of population interaction. Overall, human population interaction then appears to be the causal factor for driving disease transmission between populations. However, the epidemiological impact of population interaction, as observed in the archaeological record, is greatly mediated by population density and patterns of residential mobility.

10.2.2.3 Environmental Considerations of Disease

While climate did not significantly influence the prevalences of infectious diseases in the continent level analysis, this is likely related to the climatic variations that drive

pathogen prevalence. Many pathogens or their vectors are geographically restricted, with climate and ecology contributing to this restriction. As overall infectious disease prevalences were produced in this thesis, encompassing all skeletal evidence for infectious diseases regardless of mode of transmission, this nuance in environmental variation was lost in the continent level analysis. However, as previously mentioned, these variations were visible at a regional level where the contexts of specific diseases were considered. For some pathogens or vectors (such as yaws, endemic syphilis, leprosy and malaria) the suitability of the climate will influence the transmission of disease (Martens et al. 1999; Mitjà et al. 2013; Willcox 1974). In these cases, if the pathogen or vector is not viable within a geographical region, the level of human interaction has little to no effect on disease transmission and the pathogen will fail to proliferate in the population (Kazadi et al. 2014). If there are some ecological factors that negatively impact disease transmission but the pathogen is still viable, it will spread but at a lower rate, or give rise to selected outbreaks not experienced by the majority of the population (Kazda 2000). For example, prior to improvement in hygiene conditions and antibiotic treatment, leprosy had global distribution, and therefore the pathogen could spread in many climatic conditions. Today, it remains endemic in tropical regions (Ramos-e-Silva and Rebello 2001). It is recognised that increased humidity encourages transmission of leprosy, and variations in global humidity may underlie problems of eradication of leprosy in tropical countries (Kazda 2000). In contrast, if a pathogen is well suited to the climate and ecology of a region, the pathogen is able to spread with relative ease (Noor et al. 2009). Therefore, the geography, climate and overall ecology of the interaction zone can be an initial barrier in the potential of transmission of new pathogens through epidemiological bridging (addressed in Chapter 2).

In contrast to infectious disease prevalences, climate was a significant factor in the prevalence of scurvy. Overall, higher prevalences of scurvy were observed in sites outside of the tropical zone. Tropical regions contain an abundance of indigenous sources of fruits, nuts, vegetables and tubers that are not affected by seasonal fluctuations of availability (Buckley et al. 2014; Halcrow et al. 2014), and this may underlie this statistical trend. It was observed however, that even in tropical regions, high levels of scurvy (at Man Bac) could form in the context of cereal crop introduction or due to frequent tropical storms disrupting access to resources. A similar argument for resource disruption due to extreme weather events was made for a high burden of scurvy at the tropical Lapita (Neolithic) site of Teouma in Vanuatu (Buckley et al. 2014).

10.2.2.4 Diachronic Changes in Disease Prevalences at a Continent Level

Prevalences of infectious diseases and scurvy were observed to increase with time periods closer to present day. The reasons for these linear relationships are likely multifactorial and capture general trends of increase in social inequality, territorial conflict, climate change, population density, agricultural efforts, and human interaction intensification over time in Asia's prehistory (Glover et al. 2004; Habu et al. 2017; Higham 1989). A general increase in morbidity of infectious and nutritional diseases across time cannot be directly attributed to a 'decline' in health, but does suggest disease dynamics became more complex and favoured higher burdens of disease over time.

10.2.2.4 Hypothesis

In Chapter 1, it was hypothesised that human population interaction would have a significant influence on the diversity and the prevalence of infectious and nutritional diseases, but that other factors would determine the degree of influence. In regards to infectious disease, the hypothesis was supported. At a regional and a continent level, statistical analysis demonstrated that human population interaction had a significant influence on the prevalence and diversity of infectious diseases. However, this was dependent on the type of residential mobility and level of population density. In contrast, an increase in nutritional disease with increasing human population interaction levels was only supported at the regional level. While nutritional disease did increase over time in each case study, the impacts of population interaction were secondary, and factors of subsistence transition and climate change played more significant roles in determining the nutritional status of individuals. *Therefore, the hypothesis was supported in regards to infectious diseases, but not nutritional diseases*.

10.2.2.5 A New Synthesised Model for Disease Transmission

The outcomes of the site, regional and continent level analyses can be synthesised into a palaeoepidemiological model for the introduction of new pathogens into prehistoric populations (Figure 10.1). It is noted here that this model was derived from outcomes related to Asian archaeological sites only. However, given the generality of the model it may be valuable to test these outcomes in other contexts. As nutritional disease did not serve to be primarily affected by human population interaction, the model was only produced for

infectious diseases. However, the interaction between migrants and locals as a factor influencing nutritional status should still be considered where appropriate. Additionally, underlying nutritional status is recognised to be a contributing factor to the expression of overall infectious disease burden (Figure 10.1).

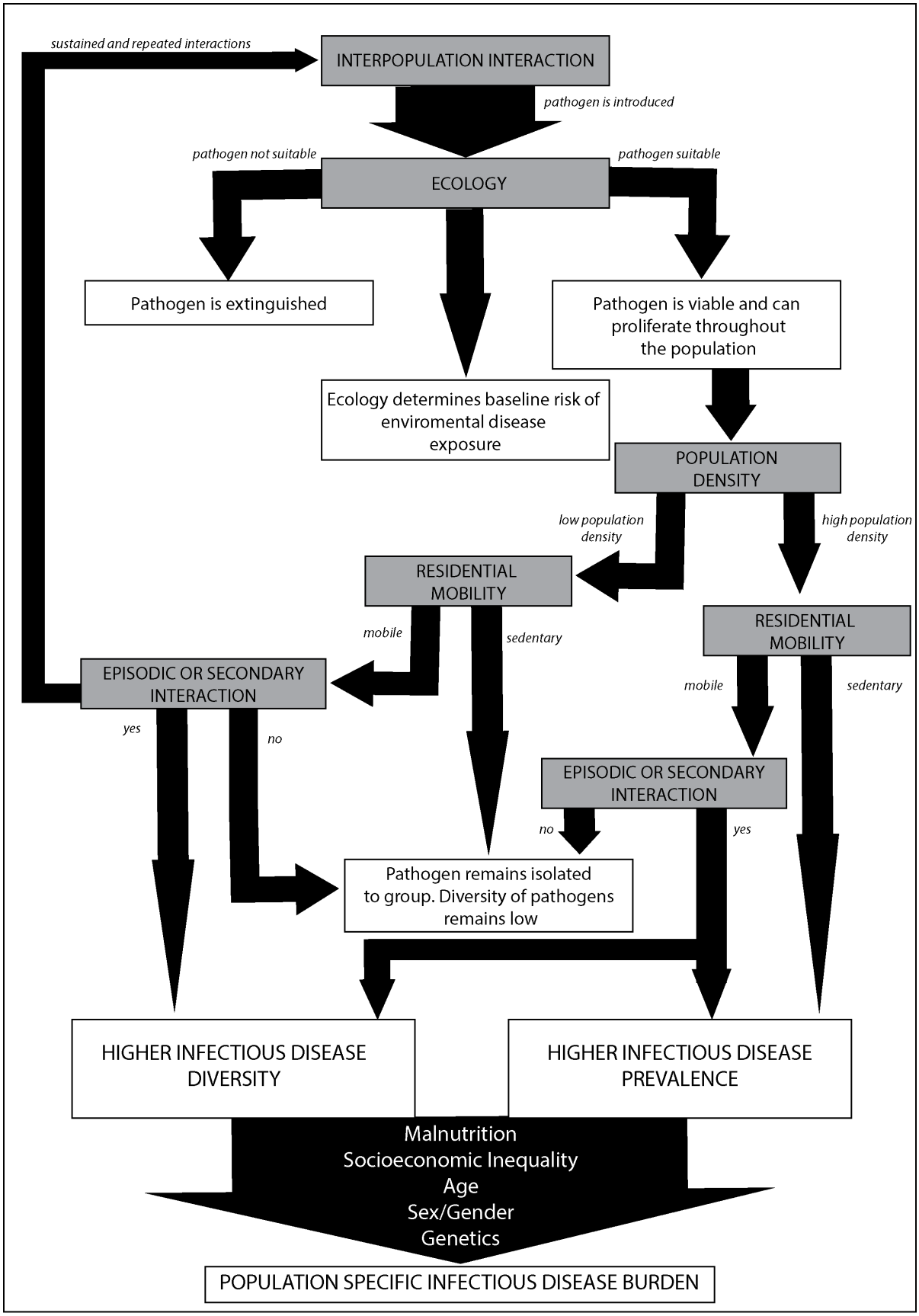

Figure 10.1: *A new palaeoepidemiological model for the introduction of infectious diseases in prehistoric populations. Image: author's own.*

10.3 The Osteological Paradox

Issues in interpretation of skeletal evidence of disease as they pertain to the osteological paradox was addressed in Chapter 1. Nonetheless, the problems of demographic non-stationarity, selective mortality and hidden heterogeneity in risk need to be cautiously considered in light of the three phases of analysis implemented in this thesis and the palaeoepidemiological model presented above.

10.3.1 Prehistoric Samples and the Problem of Demographic Non-stationarity

It is recognised here that issues in the assessment of disease in prehistoric assemblages are affected by demographic non-stationarity. While this factor of the osteological paradox particularly addressed approaches in palaeodemography, rather than palaeopathology of the time, issues of non-stationarity do in part influence the interpretation of diseases in the past (as mentioned in Chapter 1). The cases presented here would have had fluctuations in population growth, fertility, and mortality which all affect the skeletal interpretation of disease (DeWitte and Stojanowski 2015). Additionally migration, a primary focus of this study, affects the underlying age-at-death distribution and therefore the interpretation of disease (Wood et al. 1992). While stationary outcomes of disease are subsequently presented in this thesis, as in all palaeopathological research, fluctuations in disease prevalences would have occurred.

10.3.2 The Morbidity and Mortality Continuum

The comparisons of the relative risk ratio analysis of morbidity and mortality across age groups indicated similar outcomes. This similarity is in part a product of the statistical method that does not consider age of onset. The underlying assumption in any statistical analysis of mortality or relationship to age in archaeological samples is that individuals have operated under the same conditions and timing of exposure to disease than others in the assemblage. That is, the relationship between age at death and the presence of disease is the same across the entire population. In skeletal assemblages this cannot be controlled for. However, the strength of the relative risk was particularly useful in determining to what degree the process was a factor of morbidity or mortality. For example, in the Bronze Age Mongolian assemblage, individuals with osteomalacia were considered survivors in the mortality analysis. However, as discussed in Chapter 8, bone metabolism in post-

menopausal females is a significant confounding factor in the expression of osteomalacia. Indeed the relative risk of morbidity in older age groups was higher than that of mortality. Wood et al. (1992) outlined the impacts of mortality on the expression of morbidity (in the form selective mortality and hidden heterogeneity of risk) in skeletal assemblages. However, it is clear that morbidity also influences the distribution of disease when assessing mortality in the past, a factor not addressed by Wood et al. (1992). The essential element of morbidity in this relationship is likely why research in the volumes by Armelagos and Cohen (1984) and Cohen and Crane-Kramer (2007), demonstrated considerable increases in morbidity as reflective of a decline in health during the transition to agriculture. Additionally, consistent increases in morbidity of infectious and nutritional diseases were observed in this thesis regardless of the relationship of mortality to disease in each assemblage.

It is proposed here that given the limitations of assessment of population health from skeletal assemblages, that morbidity and mortality should be considered along a continuum, with each component influencing the presence of the other (Figure 10.2). That is, the prevalence within a particular age group should be considered both in terms of selective mortality, but also in terms of the association with that age group to age of onset *and* age dependent immunological and bone remodelling parameters for skeletal expression. While this is difficult to interpret in relation to non-specific markers of stress or disease, the epidemiological and clinical contexts of specific diseases can be readily considered. For example, in the Tsukumo Jomon assemblage, 100% of adults exhibited skeletal signs of possible scurvy. However, when considering the relationships to mortality of probable cases compared to combined possible and probable cases, it was apparent that scurvy lesions were associated with survivorship. An increase in morbidity and a decrease in mortality likely underlies the exceptionally high prevalence observed.

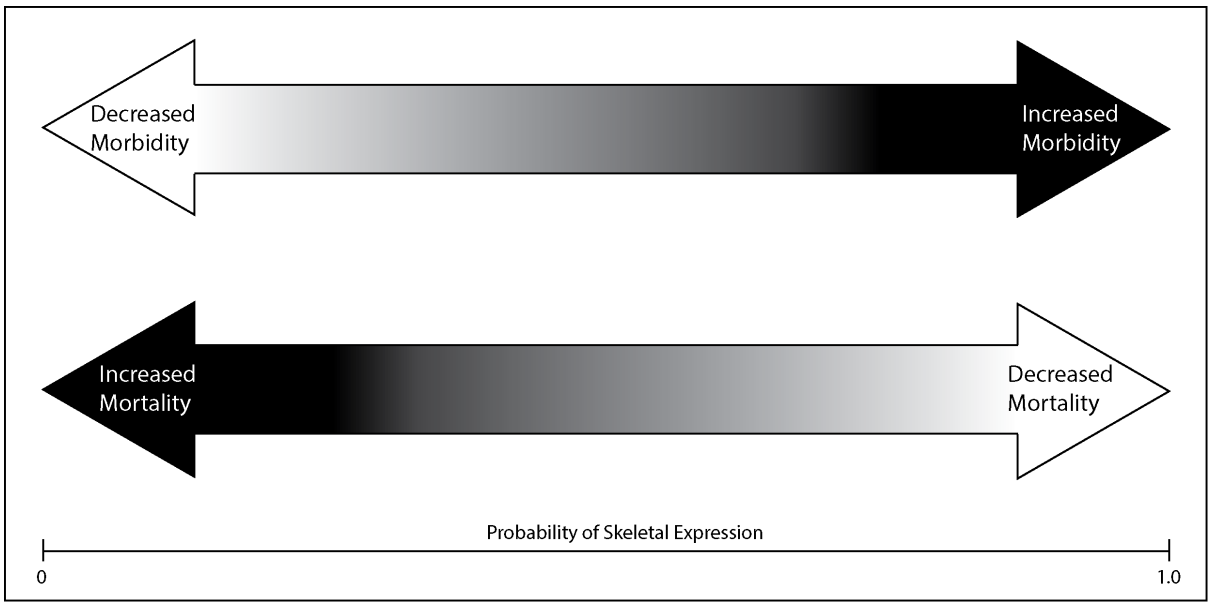

Figure 10.2: *The morbidity-mortality continuum. An inverse relationship between morbidity and mortality exists in the skeletal expression of disease. With an increase in morbidity and decrease in mortality the probability of skeletal expression of disease will increase. Image: author's own.*

In light of the morbidity-mortality continuum, diachronic changes in the prevalence of diseases need to be considered in relation to the biosocial context of both sites, as was discussed in Chapters 6 to 8. For example, in the Jomon, a statistically significant increase in scurvy was observed from the Middle to the Late and Final Jomon Periods. However, in the Middle Jomon site of Ota, the presence of scurvy was associated with increased frailty, whereas in the Late to Final Jomon site of Tsukumo, the presence of scurvy indicated increased survivorship. The higher relationship with mortality at Ota may underlie a lower skeletal presence of scurvy. However, it is apparent that scurvy was not the only disease that increased in morbidity, as the prevalences of anaemia and infectious diseases increased over time as well, indicating a general decline in health. Additionally, the archaeological context indicated ecological and social change thought to have had a negative influence on health.

10.3.3 Variations in Disease Patterns between Adults and Nonadults

For the most part, changing trends in disease prevalences across time within each region were consistently observed between adults and nonadults. However, some variations do exist (Table 10.2), which is an expected outcome given the differences in disease susceptibility between adults and nonadults (Lewinsohn and Lewinsohn 2008). For example, an increase in the prevalence of scurvy was observed in the Xiongnu Period compared to the Bronze Age Mongolian adults, whereas no change was observed in the

nonadults. A strong relationship between the presence of skeletal signs of scurvy and increased frailty in both assemblages likely underlies this trend as nonadults represented the most susceptible cohort to death from nutritional stress. Differences between the two assemblages in terms of exposure to nutritional stress were then only clear amongst the adult cohorts.

Overall, nonadults did not appear to be sensitive barometers to infectious disease. This may be due to the susceptibility of nonadults to death prior to development of skeletal lesions from infection (Wood et al. 1992). Skeletal lesions diagnostic of specific diseases with high mortality rates such as tuberculosis are documented in children in the palaeopathological literature but are far rarer than the reports of adult cases (Dawson and Brown 2012; Hlavenková et al. 2015; Lewis 2017; Tkalčec et al. 2015; Weber et al. 2004). Nonadults, particularly infants under 2 years of age, are at a far greater risk of developing primary and secondary tuberculosis than adults (see Chapter 3), and have a considerably higher mortality rate (Mueller et al. 2011). Research demonstrates lower monocyte recruitment in the innate immune system, and lower naïve T cell response in active immunity in children compared to adults (Newton et al. 2008). Therefore, while children are more susceptible to infection with most pathogens, this may not necessarily translate well into skeletal evidence of infectious diseases. When considering the issue of hidden heterogeneity of risks and selective mortality, it can be assumed that those who died prior to adulthood were the most susceptible to death from disease. With the exception of Man Bac, where possible endemic treponematosis (a disease with a very low mortality rate) was observed in nonadults as young as 18 months of age, all evidence of infectious disease in other assemblages was not observed until at least from 15 years of age.

In contrast to infectious disease, nonadults were more sensitive to skeletal expression of nutritional disease. The bone response rate of children is most likely the primary factor in this visibility, and a more direct relationship between morbidity and skeletal expression is observed than in adults (Brickley et al. 2016). It is possible that evidence of nutritional disease in nonadults, particularly infants and children may be accepted as a product of both nutritional and pathogen stress. Such an argument has previously been postulated by Buckley (2000) in regards to scurvy in a prehistoric Pacific assemblage. The morbidity-mortality continuum, as described above, underlies differences in adult and nonadult skeletal expression of disease, with a stronger influence of mortality assumed for nonadults, as they

represent non-survivors (Lewis 2017). Given the variation in skeletal presence of disease in adults and nonadults, an overall disease prevalence for an assemblage is likely to be strongly influenced by the proportion of nonadults to adults. The need to assess both adults and nonadults in a skeletal assemblage separately is clear from the outcomes of morbidity and mortality in this thesis.

10.3.4 Applying the Palaeoepidemiological Model in Light of the Osteological Paradox

As mentioned above, an increase in morbidity of infectious diseases was consistent across the case studies in this thesis. However, the proposed model does also need to be critically considered in relation to selective mortality and hidden heterogeneity of risks. The model above pertains to theoretical exploration of disease spread in the populations while they were living, that may be reflected in the skeletal record. As the continent analysis focused on morbidity, so does the model. However, as addressed in the model, exogenous and endogenous variations in risk to disease (including nutritional status, genetics, age, sex, gender and socioeconomic status) influence the final outcome of infectious disease prevalence. It is recognised that the majority of infectious diseases within an assemblage cannot be diagnosed in the skeletal record (Ortner 2009). However, as demonstrated in this thesis, factors of disease transmission do leave significant markers in the skeletal record that are statistically observable, enabling discussion of diachronic and spatial variations in disease. Additionally, non-specific indicators of stress including linear enamel hypoplasia, porotic hyperostosis, cribra orbitalia and variation in stature are useful for determining general parameters of overall health in the population that include the burden of infectious diseases that cannot be directly diagnosed. These skeletal indicators are similarly limited by the relationship between skeletal development of stress and mortality (Temple and Goodman 2014; Wood et al. 1992). The application of this model should then include consideration of the context of overall disease burdens at the site, as well as environmental, biological and social parameters derived from archaeological, geographical, and ecological research.

10.4 Methodological Considerations

The outcomes of this thesis relied on a three level statistical approach. This approach enabled analysis of disease dynamics at both nuanced and more generalised levels. Fundamental to this approach was the threshold method of differential diagnosis and the

inclusion criteria for population level analysis of infectious disease morbidity and mortality. The limitations of these methodological approaches as they relate to the outcomes are discussed here.

10.4.1 The Threshold Approach to Differential Diagnosis

A call for standardised and rigorous approaches to differential diagnosis have been well addressed in the palaeopathological literature (Buikstra et al. 2017; Klaus 2017; Snoddy et al. 2020). However, threshold approaches whereby diagnosis is determined through weighted diagnostic criteria have only emerged over the last decade (see Brickley and Ives 2010; Harper et al. 2011), with application of this methodological approach as a new standard in diagnosis in recent years (Baker et al. 2020; Snoddy et al. 2018; Vlok et al. 2020). It is argued here that threshold approaches are particularly useful in palaeoepidemiological studies as they enable consistent diagnostic protocols applicable across multiple individuals in a population, thereby standardising diagnosis for statistical purposes. Moreover, the benefit of threshold approaches are that they enable transparent diagnosis of diseases whose origins and antiquity remain contested. In debates such as those surrounding the origins of syphilis, threshold approaches enable consideration of weighted diagnosis of previously reported cases. An example in this thesis includes the *possible* case of treponematosis observed in Xiongnu Period Mongolia assemblage. As mentioned in Chapter 8, this case remains tentative as to date most evidence of treponematosis prior to pre-Columbian contact in East and Northeast Asia is scant and would not fulfil the requirements of even a *possible* case following the diagnostic criteria in this thesis (Vlok et al. 2020). In contrast, there is stronger evidence for treponematosis in tropical regions of the Asia-Pacific including the *probable* cases reported for Man Bac (Chapter 7).

However, there remain limitations to the threshold approaches that require consideration in future palaeopathological studies. Severity of lesions are not considered in current diagnostic protocols, nor are they considered here in this thesis. Considerations of slight changes that may be within the realms of normal variation compared to more severe and clearly observable changes require further discussion in the palaeopathological literature. For example following the current Snoddy et al. (2018) criteria for scurvy, an individual with slight changes to two regions associated with scurvy diagnosis is consistent with a probable case, whereas an individual with well delineated discrete SPNB lesions with

vascular impressions in one region would be considered a possible case. Issues of *specificity* compared to *sensitivity* are recognised as problems in palaeopathological research (Boldsen and Milner 2012). Palaeopathologists must deliberate whether their research approach increases the accuracy of diagnosis (which increases the proportion of true positives), or whether they choose to capture a more representative disease burden (which increases the proportion of true negatives). Considerations of *clear cut* lesions in the diagnosis is a more conservative approach, but are also likely to underdiagnose cases especially that of individuals who exhibit well remodelled lesions that may be difficult to observe. As such, a level of interobserver error remains in the determination of skeletal changes considered to be *abnormal*.

Additionally, in infants the factor of normal growth also requires further consideration in the expression of infantile scurvy (although see Snoddy et al. (2017) and Vlok et al. (in review); Appendix 5 for discussion on perinatal scurvy). Challenges to the diagnosis of scurvy in infants were highlighted in Chapter 7, where discrete SPNB formations were present in perinates from Con Co Ngua, although abnormal cortical porosity was not, casting doubt on the diagnosis of scurvy in these individuals. In contrast, Man Bac infants exhibited clear associations of abnormal cortical porosity and vascular impressions with discrete deposits of SPNB.

As such, the threshold approaches have room for future adaptation. However, they do provide a fundamental basis for consideration of what lesions should be considered to be more suitable for diagnosis over others. More importantly, they currently remain the most appropriate approaches to standardisation in differential diagnosis of disease.

10.4.2 Application of Infectious Disease Criteria

Inclusion criteria for infectious disease was presented in Chapter 5. This inclusion criteria enabled the combination of specific and non-specific infectious disease. This approach enabled valuable statistical comparisons as the identification of specific infectious diseases are relatively rare in the palaeopathological literature (Boldsen and Milner 2012). However, statistical analysis of a general infectious disease prevalence is limited in that it does not encompass the variation in disease morbidity and mortality of the underlying infectious diseases. The general infectious disease prevalence then only assesses an average

effect of infection on morbidity and mortality in a population. The epidemiological circumstances of the specific diseases then were not explicitly addressed in this research. While there were some cases where the prevalences of specific diseases were sufficient for statistical analysis (hydatids disease in Con Co Ngua, and treponemal disease in Man Bac) for the most part the prevalences of diagnosed specific diseases were too low for any valuable statistical comparisons. The epidemiological impact of these diseases were instead qualitatively addressed in the appropriate results chapters (Chapter 6 to 8) in light of clinical and epidemiological research on the specific diseases. The overall trend of mortality for infectious diseases in each assemblage did reflect the known relationship between the specific infectious diseases and mortality. For example, the relationship between mortality and overall infectious disease was low in the Northern Vietnamese samples where hydatids disease and endemic treponemal diseases were diagnosed. These diseases have negligible impacts on mortality. Similarly, in Bronze Age Mongolia, the low mortality rates of hydatids disease and brucellosis was reflected in the trend in mortality of the combined infectious diseases. In contrast, in the Xiongnu Period assemblage, where possible tuberculosis was identified, the overall infectious disease criteria had a significant association with increased frailty. As only one case of specific infection was diagnosed for the Jomon samples (mycotic infection at Ota), similar extrapolations cannot be made for the Jomon assemblages.

As mentioned in Chapter 5, individuals with diffuse SPNB across two skeletal elements were included in the infectious disease criteria. While more diffuse lesions of multiple elements are more likely due to systemic infection (Buckley and Tayles 2003; Ortner 1991; Weston 2008), the unintentional inclusion of individuals with SPNB related to nutritional stress, trauma or other pathologies remains a possibility. Additionally, the inclusion of otitis media and osteomyelitis in the infectious disease criteria needs to also be considered. Osteomyelitis can occur secondary to trauma (Dubey et al. 1988), and therefore may not necessarily be a useful indicator for the identification of pathogens related to human interaction. Otitis media in adults is most commonly a product of the occurrence of the disease in childhood (Lewis 2017). Therefore, the inclusion of otitis media in the morbidity and mortality analysis of infectious disease in adults is not directly reflective of the relationship between mortality and age at death, although disease and stress in childhood has been related to susceptibility to early death later on in life (Armelagos et al. 2009).

Overall, the combination of specific and non-specific infection is a sound approach given that the research questions of this thesis focused on overall impact on health. Nevertheless, issues in nuanced variations in disease trends are noted here, and do influence the interpretations made from the outcomes of statistical analysis.

10.4.3 Statistical Determinants of Disease in an Absent-Present Binary

Morbidity and mortality analysis of disease was restricted to disease presence and absence. However, the remodelling of lesions are important for interpreting the relationship of diseases to mortality. Active lesions indicate the disease remained active at or near time of death whereas, remodelled or remodelling lesions indicate recovery from disease (Mays et al. 2002; Wood et al. 1992). The statistical relationship of individuals with active, mixed and remodelled lesions can further contribute to discussion on the relationship between lesion healing and mortality. DeWitte (2014) demonstrated that individuals with active SPNB lesions exhibited lower survivorship than those with remodelled lesions. Additionally, those with remodelled lesions also exhibited better survivorship than those without any evidence of lesions. The sample sizes employed in this thesis however, do not allow for the assessment of mortality across four different variables (active, mixed, healed and absent), therefore analysis of morbidity and mortality was restricted to absence and presence of disease.

Additionally, while the remodelling of lesions are readily observable (woven bone vs. lamellar bone) the same cannot be said for the recovery from disease. For example, there is difficulty in establishing active versus healing cases of scurvy, particularly regarding lesions present in different age groups. An infant with evidence of remodelling may have had scurvy for as long as an adolescent with active lesions, with the remodelling rate being a confounding factor. The role of the periosteum in growth in infancy underlies this potential issue (Dwek 2010). Additionally, repeated episodes of scurvy are expected as the presence of discrete SPNB deposits indicate cyclical return of Vitamin C to the system (Crandall and Klaus 2014). As such, there is difficulty in determining the difference between a healing versus a newly active case with prior episodes of scurvy. Both conditions would result in the presence of mixed active and remodelled lesions. Therefore, simple statements of active, mixed or healed are simplistic narratives that may confound understanding of the impact of scurvy on mortality.

Similar issues in relation to documenting healing of rickets exist. Active cases of rickets were identified through fraying and porosity (see Chapter 7 and 8). However, the absence of fraying does not necessarily represent a healing or healed case, and most diagnostic lesions for rickets do not provide a basis for determining the level of healing (Brickley and Mays 2019). The presence of thickened long bones has been considered as indicative of heling or healed cases of rickets by Brickley et al. (2018). However, thickened long bones (synonymous with cortical enlargement) is a common pathological change in infectious diseases and thalassaemia. Therefore, long bone thickening may be a useful criterion for identifying healing or healed cases of rickets in Mongolian assemblages, but the complex co-morbidity with other diseases at Man Bac, means this pathology cannot be applied in the discussion of disease healing. Additionally, co-morbidity with scurvy and anaemia further complicates the matter as these are known to cause 'thinning' of the cortex in an individual with healing or healed rickets (Cambouris 1989; Gupta et al. 2020; Ortner 2003).

There remain similar issues with identifying recovery from infectious diseases that cause osteolytic lesions. A healing osteolytic lesion often cannot be differentiated from an active osteolytic lesion of slow formation. Both conditions are accompanied by sclerotic response (Ortner 2003). The exception is in the case where the specific disease diagnosed is one known to elicit a rapid lytic destruction. In this case, sclerotic response would be associated with healing. For example, sclerotic response of gummatous lesions in treponemal disease is an essential component in the progression of the active lesion and does not suggest that the individual is recovering from the pathogen, only that the progression of destruction is slow enough to allow an osteoblastic response (Hackett 1976; Ortner 2003). In contrast, where tuberculosis has been identified, sclerotic response on the margins of the osteolytic lesions can suggest a level of recovery of the disease (Holloway et al. 2013). Given the difficulties in determining the recovery from diseases, especially if the aetiology cannot be identified, the application of an absent-present binary to statistical analysis of morbidity and mortality is sound. However, it is recognised that investigation of differences in activity of disease to the relationship of mortality is an area for further research.

10.4.4 The Application of Binaries in Continent Level Analysis

Binaries of residential mobility, climate, and human population interaction were employed in the statistical analysis. While this was necessary given the sample size, the existence of these factors along a continuum is a recognised limitation given the statistical approach, and an area for further research. Residential mobility is complex and variations in mobility occur. Even the most mobile groups have some level of static rest in an area, particularly when they arrive in area abundant with resources (Wendrich and Barnard 2008). Defining a site as 'sedentary' or 'mobile' does require an arbitrary distinction amongst groups that does not strictly exist. For example, the Jomon are described as being sedentary (Habu 1996). However, places of residence were not occupied throughout the year, and some level of residential mobility was essential particularly in light of seasonal availability of resources (Habu 1996). Wendrich and Barnard (2008) argue that residential mobility is best described in terms of length of time, mobility pattern over time, motivation for movement, and segment of the population involved in mobility, rather than a sedentary or mobile binary. Future exploration of disease dynamics, considering more complex patterns of mobility may be more valuable in assessing the role of mobile behaviours contributing to disease transmission.

Additionally, climate has been used in this thesis as a proxy for variations in ecological impact of disease. As climate contributes only partially to the overall ecology of a region, further research into geography (e.g. inland vs. coastal), latitude, and faunal and floral diversity, will contribute to assessment of ecological variation in disease dynamics. Additionally, year-round variations in climatic factors such as rainfall and temperature also influence disease transmission (Wilcox and Colwell 2005). These factors are highly context specific, best studied within a region, and therefore not suited to assessment in continent analysis. Consequently, climate remained the best proxy available for analysis of environmental variation in this thesis at a continent level. The considerations of more nuanced ecological aspects were addressed in the results chapters and were essential elements for contextualising the diseases diagnosed.

Finally, human population interaction was statistically assessed as a binary. However the classification of human population across four different levels enables ordinal statistical analysis, that may be valuable for future research. Valuable outputs were extrapolated from

the binary analysis presented in Chapter 9. However, the limitations of binaries in the continent analysis demonstrates that regional and site level analysis must accompany generalised models.

10.5 Areas for Future Research

10.5.1 Human Interaction as a Key Element in Studies of Infectious Disease Origins

The outcomes of this thesis clearly demonstrate that a shift in the theoretical thinking of disease transmission in the prehistoric past is required. While residential mobility did play a role in disease transmission, exploration of disease contexts at interaction zones enable more comprehensive understanding of complex disease patterns in the past. However, given the restrictions of the sample size and the number of assemblages assessed, further research is necessary to continue to explore the implications of population interaction and disease transmission in Asia. Inclusion of more sites with variation in geographic, biological, environmental and socio-cultural backgrounds will enable assessment of whether the outcomes in this thesis stand. To date, palaeopathological research in Asia remains in its infancy. However, as demonstrated in this thesis the continent of Asia has significant potential to address major questions in regards to the origins and antiquity of infectious diseases in the past. The number of previously unrecognised diseases diagnosed in this thesis stand testament to what remains unknown in the region. Additionally, analysis of the possible epidemiological implications of human population interaction, as defined in this thesis, may also indicate whether the trends observed in the continent analysis are universal. Palaeopathological research has been intensive in other regions of the world such as in Europe and North America, and may provide a platform for further research. As sedentism and high population density are recognised to have been major contributors to disease in other parts of the world (Armelagos and Cohen 1984) so too can the aspect of human population interaction be similarly investigated.

Additionally, further theoretical considerations of human population interaction, and the application of disease studies in assemblages within interaction zones, is an avenue for further exploration and refinement. For example, consideration of the many types of mobility processes that occur within interaction zones, and how they influence disease dynamics was not explored in this thesis. Where archaeological data allows for detailed analysis of mobility and migration patterns of an archaeological site, considerations of the

potential of pathogen mediated factors of disease transmission, including the mode of transmission, may be further investigated. Questions that remain include: do specific types of mobility processes influence which infectious diseases are spread within interaction zones? And does the demography of migrants (e.g. average age and gender) influence which pathogens are spread from one population to another? Such questions may only be answered where significant contextual data (including isotopes, DNA, archaeological and historical data) exists.

Lastly, how the three degrees of interaction (community interaction, intrapopulation interaction, and interpopulation interaction) interweave to influence transmission of a newly introduced pathogen is not modelled in this thesis and provides an opportunity for future research. Moreover, whether factors of mobility and population density mediate disease transmission differently at each degree of interaction remains to be explored. Overall, it is apparent that consideration of population interaction in the dynamics of disease transmission in prehistory has opened up a new avenue to explore in palaeoepidemiological research.

10.5.2 Multilevel Analyses in the Theoretical Considerations of Disease Dynamics in Prehistoric Assemblages

This thesis introduced a three stage holistic approach to the study of infectious diseases in skeletal assemblages (Figure 10.3). While palaeopathological research to date has focused on a range of issues regarding health at site, regional or continent levels, these have been produced in isolation. Generalised trends across continents have been produced through the employment of skeletal data collected for the Global History of Health Projects (GHHP) for Europe and the Americas (McFadden and Oxenham 2020; Steckel et al. 2018; Steckel and Rose 2002). As addressed in Chapter 9, these studies identified major factors that influenced health in past populations. However, the outcomes did not consider the confounding impacts of nuanced trends of disease in tandem. The outcomes of multivariate statistical analyses are then accepted as convention, and critical consideration of biases within the data pertaining to skeletal material are not considered. This thesis demonstrated that generalised continent level analyses (such as by the GHHP) are indeed valuable. However, with the above caveats in mind the site and regional level analyses in this thesis provided significant context to the disease trends observed across the Asian assemblages employed in the continent analysis. While site, regional and continent level analyses were

produced here, similar models may be appropriate for future palaeopathological research that enable addressing larger theoretical questions such as those posed by this thesis. Again, the employment of more assemblages, with larger sample sizes and consideration of more variables provides an avenue for future research. Additionally, there is room for revision of the model produced in this thesis, encompassing a more synergistic structure including site, regional and continent level analysis in investigation of disease trends in the past.

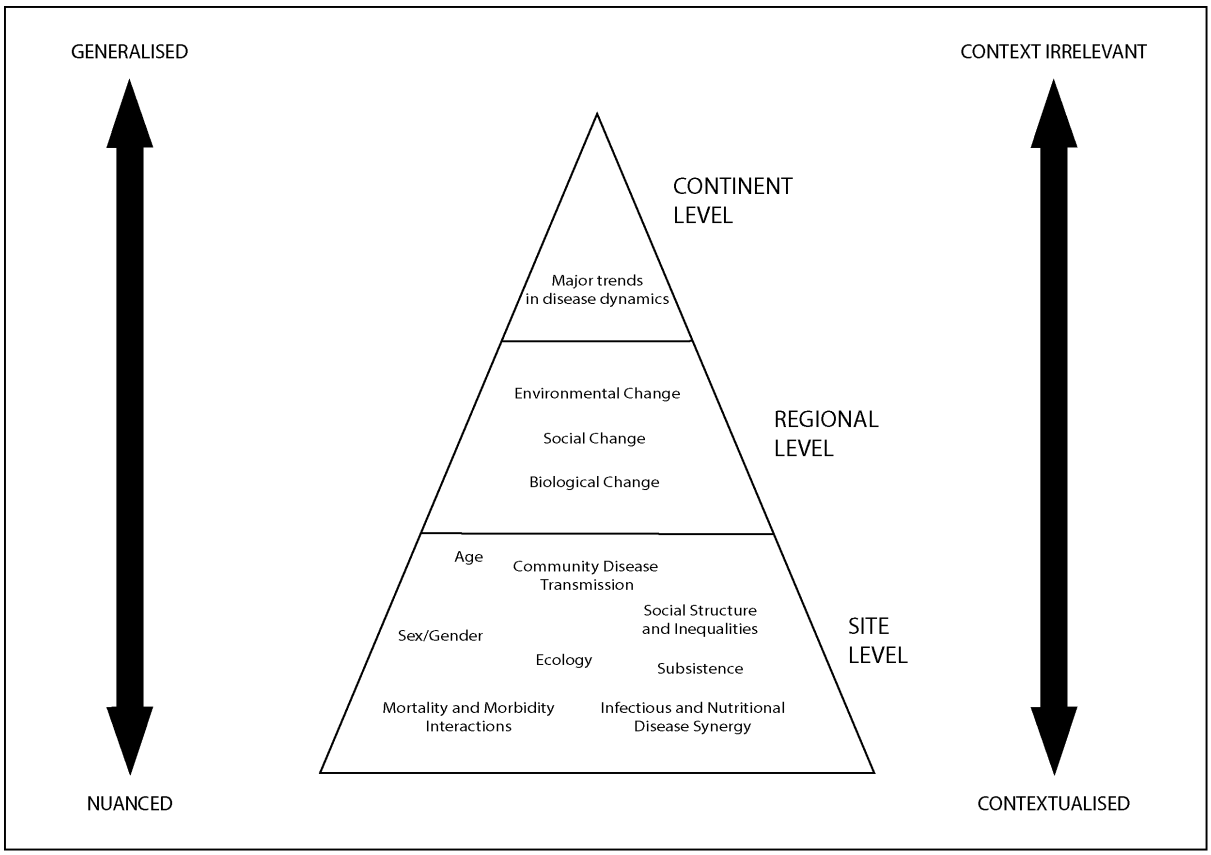

Figure 10.3: *The hierarchy of information extrapolated from the three-stage approach to statistics applied in this thesis. The approach enables consideration of disease patterns in nuanced as well as generalised trends. Image: author's own.*

10.6 Significance

This thesis has demonstrated that the process of interactions between human populations have distinct epidemiological impacts, and should be differentially defined from *mobility*. Therefore, simplistic accounts of mobility and disease transmission are not entirely valid when considering the complexity of disease transmission in prehistory. While chemical analysis such as isotopic and DNA research are useful in defining mobility and migration, how these processes relate to the interactions between human groups and the

spread of infectious diseases requires cautious consideration. It is instead argued here that disease transmission should be assessed at the zones of population interaction, rather than tied to specific processes of mobility. Moreover, the relationships between major factors including population density, residential mobility and population interaction defined the epidemiological impact of the introduction of new pathogens. Additionally, new threshold criteria for differential diagnosis were produced for a number of infectious diseases and thalassaemia. These standards may be employed in future palaeopathological research and initiate further discussion on the standardisation of differential diagnosis. Moreover, as mentioned above, this thesis also presented a novel statistical approach that enabled consideration of disease dynamics at site, regional and continent levels.

10.7 Conclusions

This thesis has made a significant and new contribution to the discussion on the impacts of infectious and nutritional diseases in prehistoric populations. This thesis explored the impact of *human population interaction*, a process that occurs following mobility of human groups due to migration, trade and conflict, on the spread of infectious diseases and the prevalence of nutritional diseases. Taking a palaeoepidemiological approach, this research explored two different impacts of disease on overall health of past populations: morbidity and mortality. Additionally, it considered not only prevalence but the diversity of diseases within an assemblage.

10.7.1 Research Question 1: Did increasing levels of population interaction over time significantly affect the health of populations in prehistoric Asia?

The outcomes of the site and regional level analyses were particularly valuable to addressing research question 1. Site level analysis enabled consideration of intrapopulation variation in disease susceptibility in regards to morbidity *and* mortality, and demonstrated that the impacts of disease were not uniformly shared between different groups of age and sex. This outcome was expected as demographic variations to the vulnerability of disease and death are well documented in epidemiological and palaeopathological literature. While each of the three cases studies exhibited notably different biosocial and epidemiological contexts, an increase in human population interaction was consistently associated with an increase in the prevalence of infectious diseases. In two of the cases studies assessing interpopulation interaction (Vietnam and Mongolia), the process of two exogenous

populations interacting, the increase in interaction coincided with the introduction of human specific infectious diseases. Additionally, an increase in human population interaction also initiated economic and social changes that contributed to an increase in micronutrient deficiencies in the two case studies associated with interpopulation interaction. However, the outcomes for regional changes in mortality were variable, and direct associations between increasing human population levels and increased mortality were not supported. Overall, it is apparent that population interaction over time did significantly impact the health of past populations in Asia in terms of increased morbidity of infectious and at times nutritional diseases, but did not necessarily influence the overall mortality of these populations. Additionally, it appears that interpopulation interaction, had a more direct epidemiological impact on disease dynamics than intrapopulation interaction, the processes of interaction within one distinct population. A summary of the findings of the three cases studies are presented below.

10.7.1.1 Case Study 1: Middle to Late and Final Jomon Japan

Case study 1 assessed whether an increase in intrapopulation interaction alongside climate cooling from the Middle to the Late and Final Jomon Periods in Japan significantly increased morbidity and mortality from infectious and nutritional diseases. The prevalence of infectious diseases, scurvy and anaemia were significantly higher in the Late and Final Jomon site of Tsukumo than in the Middle Jomon site of Ota. Additionally, a significant increase in mortality of the Tsukumo population compared to the Ota population was observed. However, when considered in context it is apparent that the increase in nutritional stress was likely related to ecological change driving population decline and dispersal. Nevertheless, the increase in infectious disease prevalences may at least in part be attributed to increase in intrapopulation interaction following population movements during this climate cooling period. The epidemiological effects of intrapopulation interaction were then embedded within a number of consequential factors that led to a decline in health from the Middle to Late and Final Jomon Periods.

10.7.1.2 Case Study 2: Pre-Neolithic to Neolithic Vietnam

Case study 2 assessed whether a large migration from Southern China, and subsequent interpopulation interaction between local foragers and migrant farmers, significantly impacted the health of prehistoric populations in Northern Vietnam. Infectious

disease prevalences, and nutritional diseases in the form of scurvy and calcium deficiency rickets significantly increased with increasing population interaction. The migration was associated with the earliest cases of human specific infectious diseases in the Southeast Asian region in the form of treponematosis. Additionally, a significant increase in micronutrient deficiencies were initiated by a subsistence transition induced by the interaction between foragers and farmers. However, there was no significant increase in mortality over time.

10.7.1.3: Case Study 3: Bronze Age to Xiongnu Period Mongolia

Case study 3 assessed whether increased migration, trade and conflict from the Bronze Age to the formation of the Xiongnu Empire in Mongolia was associated with a decline in health. Infectious disease and scurvy prevalences significantly increased with increasing population interaction. The prevalences of rickets and osteomalacia also increased, but these were likely unrelated to population interaction levels. The increase in population interaction also was associated with the presence of possible treponematosis and respiratory tuberculosis indicating possible emergence of human specific infectious disease in the region during this time.

10.7.2 Research Question 2: How did population interaction interplay with a range of other sociocultural, biological and ecological factors to influence the health of populations in prehistoric Asia?

The continent level analysis was the final objective in this thesis and was particularly important to addressing research question 2. While regional level analysis demonstrated that diachronic increases in population interaction were associated with an impact on health, the continent level analysis assessed to what degree did human population interaction influence disease dynamics given that other social, biological and environmental factors were also important in disease proliferation. Human population interaction levels significantly influenced the prevalences of infectious diseases levels. However, only when mobile and sedentary populations were assessed separately. Therefore, residential mobility was recognised to play a major role in disease prevalence. This outcome was expected as sedentary residential mobility increased the duration of interaction between individuals facilitating disease transmission. In contrast, where mobile populations exhibited multiple

episodes of interaction with external populations, a significant increase in the number of infectious disease types was observed. Additionally, infectious disease prevalences were also significantly associated with an increase in population density. Overall residential mobility and population density mediated the role that human population interaction played in the disease dynamics across prehistoric Asia. In sum, it was determined that sedentary populations with high population densities and high levels of interpopulation interaction were at a significantly increased risk of infectious disease outbreaks following the introduction of new pathogens through processes of interaction.

At a continent level, human population interaction did not significantly influence the prevalences of nutritional disease. Instead factors such as climate, cereal crop subsistence and sedentary residential mobility, served to have more primary roles. This outcome was expected given that nutritional quality of diet is well known to be contingent on available resources within the local ecology and the role of staple crops in the diet. Therefore, as observed in the case studies, human population interaction only indirectly influenced the nutritional status of underlying populations where significant social or dietary change was initiated. In sum, the impact of population interaction on nutritional stress was deeply contextual with generalised trends not observed.

The interaction between human populations in the prehistoric past enabled the transmission of infectious diseases, significantly influencing the health of past populations. Additionally, these processes of interaction initiated shifts in subsistence, social structure, and economical engagement, that influenced the nutritional status of some prehistoric populations. These processes of interaction and exchange amongst prehistoric populations initiated irreversible change to the epidemiology of populations within the continent of Asia. This deep history of co-existence with pathogens continues to have significant impacts on the health of populations in Asia today.

REFERENCES CITED

1995. Stedman's Medical Dictionary (26th Edition). Baltimore, USA: Williams and Wilkins.

Abt AF, Farmer CJ, and Topper YJ. 1940. Influence of Catharsis and Diarrhea on Gastrointestinal Absorption of Ascorbic Acid in Infants. Proceedings of the Society for Experimental Biology and Medicine 43(1):24-26.

Abulafia J, and Vignale RA. 1999. Leprosy: Pathogenesis Updated. International Journal of Dermatology 38(5):321-334.

Achtman M. 2016. How Old are Bacterial Pathogens? Proceedings of the Royal Society B: Biological Sciences 283(1836):20160990.

Acosta FL, Chin CT, Quiñones-Hinojosa A, Ames CP, Weinstein PR, and Chou D. 2004. Diagnosis and Management of Adult Pyogenic Osteomyelitis of the Cervical Spine. Neurosurgical Focus 17(6):1-9.

Acsádi G, Nemeskéri J, and Balás K. 1970. History of Human Life Span and Mortality. Budapest, Hungary: Akademiai kiado.

Adachi N, Shinoda Ki, Umetsu K, Kitano T, Matsumura H, Fujiyama R, Sawada J, and Tanaka M. 2011. Mitochondrial DNA Analysis of Hokkaido Jomon Skeletons: Remnants of Archaic Maternal Lineages at the Southwestern Edge of Former Beringia. American Journal of Physical Anthropology 146(3):346-360. 10.1002/ajpa.21561

Adamopoulos SG, and Petrocheilou GM. in press. Skeletal Radiological Findings in Thalassemia Major. Journal of Research and Practice on the Musculoskeletal System.

Agarwal S, Shah A, Kadhi S, and Rooney RJ. 1992. Hydatid Bone Disease of the Pelvis. A Report of Two Cases and Review of the Literature. Clinical Orthopaedics and Related Research(280):251-255.

Al Dahouk S, Sprague L, and Neubauer H. 2013. New Developments in the Diagnostic Procedures for Zoonotic Brucellosis in Humans. Scientific Technical Review 32(1):177-188.

Al-Shahed MS, Sharif HS, Haddad MC, Aabed MY, Sammak BM, and Mutairi MA. 1994. Imaging Features of Musculoskeletal Brucellosis. Radiographics 14(2):333-348.

Alam MK, Hamza MA, Khafiz MA, Rahman SA, Shaari R, and Hassan A. 2014. Multivariate Analysis of Factors Affecting Presence and/or Agenesis of Third Molar Tooth. PLoS One 9(6):e101157.

Albert P, and Davies P. 2008. Tuberculosis and Migration. In: Barnes P, Davies PD, and Gordon SB, editors. Clinical Tuberculosis. Boca Raton, USA: CRC Press. p 367-384.

Aldred O. 2014. Past Movements, Tomorrow's Anchors. On the Relational Entanglements between Archaeological Mobilities. In: Leary J, editor. Past Mobilities: Archaeological Approaches to Movement and Mobility. Surry, England: Asgate Publishing Limited. p 21-48.

Allard F, and Erdenebaatar D. 2005. Khirigsuurs, Ritual and Mobility in the Bronze Age of Mongolia. Antiquity 79(305):547-563.

Almaghamsi A, Almalki MH, and Buhary BM. 2018. Hypocalcemia in Pregnancy: A Clinical Review Update. Oman Medical Journal 33(6):453.

Altman DG. 1990. Practical Statistics for Medical Research. New York, USA: CRC Press.

Amakye-Anim J, Lin T, Hester P, Thiagarajan D, Watkins B, and Wu C. 2000. Ascorbic Acid Supplementation Improved Antibody Response to Infectious Bursal Disease Vaccination in Chickens. Poultry Science 79(5):680-688.
Ammerman AJ. 1973. A Population Model for the Diffusion of Early Farming in Europe. In: Renfrew C, editor. The Explanation of Culture Change: Models in Prehistory. London: Duckworth. p 343-357.
Andersen JG, and Manchester K. 1992. The Rhinomaxillary Syndrome in Leprosy: A Clinical, Radiological and Palaeopathological Study. International Journal of Osteoarchaeology 2(2):121-129.
Anderson HC. 1989. Mechanism of Mineral Formation in Bone. Laboratory Investigation; A Journal of Technical Methods and Pathology 60(3):320-330.
Anderson PH, Atkins GJ, Turner AG, Kogawa M, Findlay DM, and Morris HA. 2011. Vitamin D Metabolism within Bone Cells: Effects on Bone Structure and Strength. Molecular and Cellular Endocrinology 347(1-2):42-47.
Angel JL. 1966. Porotic Hyperostosis, Anemias, Malarias, and Marshes in the Prehistoric Eastern Mediterranean. Science 153(3737):760-763.
Anglewicz P. 2012. Migration, Marital Change, and HIV Infection in Malawi. Demography 49(1):239-265.
Annibale B, Capurso G, Martino G, Grossi C, and Delle Fave G. 2000. Iron Deficiency Anaemia and Helicobacter pylori Infection. International Journal of Antimicrobial Agents 16(4):515-519.
Anstead GM, and Graybill JR. 2020. Coccidioidomycosis. In: Ryan E, Hill D, Solomon T, and Aronson N, editors. Hunter's Tropical Medicine and Emerging Infectious Diseases. North York, Canada: Elsevier. p 666-670.
Antal GM, Lukehart SA, and Meheus AZ. 2002. The Endemic Treponematoses. Microbes and Infection 4(1):83-94.
Aparicio ED. 2013. Epidemiology of Brucellosis in Domestic Animals Caused by Brucella melitensis, Brucella suis and Brucella abortus. Scientific Technical Review 32(1):53-60.
Apostolopoulos Y, and Sönmez S. 2007. Demographic and Epidemiological Perspectives of Human Movement. Population Mobility and Infectious Disease: Springer. p 1-16.
Armelagos GJ, and Cohen MN. 1984. Paleopathology at the Origins of Agriculture. Orlando, USA: Academic Press.
Armelagos GJ, Goodman AH, Harper KN, and Blakey ML. 2009. Enamel Hypoplasia and Early Mortality: Bioarcheological Support for the Barker Hypothesis. Evolutionary Anthropology: Issues, News, and Reviews: Issues, News, and Reviews 18(6):261-271.
Armelagos GJ, Goodman AH, and Jacobs KH. 1991. The Origins of Agriculture: Population Growth during a Period of Declining Health. Population and Environment 13(1):9-22.
Arslanagić N, Bokonjić M, and Macanović K. 1989. Eradication of Endemic Syphilis in Bosnia. Sexually Transmitted Infections 65(1):4-7.
Assis S, Santos AL, and Roberts CA. 2011. Evidence of Hypertrophic Osteoarthropathy in Individuals from the Coimbra Skeletal Identified Collection (Portugal). International Journal of Paleopathology 1(3-4):155-163.
Aufderheide AC, Rodríguez-Martín C, and Langsjoen O. 1998. The Cambridge Encyclopedia of Human Paleopathology: Cambridge University Press Cambridge.
Aydinok Y. 2012. Thalassemia. Hematology 17(S1):s28-s31.

Baccino E, Ubelaker DH, Hayek L-A, and Zerilli A. 1999. Evaluation of Seven Methods of Estimating Age at Death from Mature Human Skeletal Remains. Journal of Forensic Science 44(5):931-936. 10.1520/JFS12019J

Bagnall K, Harris P, and Jones P. 1982. A Radiographic Study of the Longitudinal Growth of Primary Ossification Centers in Limb Long Bones of the Human Fetus. The Anatomical Record 203(2):293-299.

Bailey SM, Gershoff SN, McGandy RB, Nondasuta A, Tantiwongse P, Suttapreyasri D, Miller J, and McCree P. 1984. A Longitudinal Study of Growth and Maturation in Rural Thailand. Human Biology:539-557.

Baker BJ, Crane-Kramer G, Dee MW, Gregoricka LA, Henneberg M, Lee C, Lukehart SA, Mabey DC, Roberts CA, and Stodder AL. 2020. Advancing the Understanding of Treponemal Disease in the Past and Present. American Journal of Physical Anthropology.

Balcan D, Colizza V, Gonçalves B, Hu H, Ramasco JJ, and Vespignani A. 2009. Multiscale Mobility Networks and the Spatial Spreading of Infectious Diseases. Proceedings of the National Academy of Sciences 106(51):21484-21489.

Bansal S, Read J, Pourbohloul B, and Meyers LA. 2010. The Dynamic Nature of Contact Networks in Infectious Disease Epidemiology. Journal of Biological Dynamics 4(5):478-489.

Barbieri-Low A. 2011. Model Legal and Administrative Forms from the Qin, Han, and Tang and their Role in the Facilitation of Bureaucracy and Literacy. Oriens Extremus:125-156.

Baten J, Steckel RH, Larsen CS, and Roberts CA. 2018. Multidimensional Patterns of European Health, Work, and Violence over the Past Two Millennia. In: Steckel RH, Larsen CS, Roberts C, and Baten J, editors. The Backbone of Europe: Health, Diet, Work and Violence over Two Millennia. Cambridge, UK: Cambridge University Press. p 381.

Bathurst RR. 2005. Archaeological Evidence of Intestinal Parasites from Coastal Shell Middens. Journal of Archaeological Science 32(1):115-123.

Battelli G. 2008. Zoonoses as Occupational Diseases. Veterinaria Italiana 44(4):601-609.

Bazarsad N. 2007. Iron-Deficiency Anemia in Early Mongolian Nomads. In: Cohen M, and Crane-Kramer G, editors. Ancient Health: Skeletal Indicators of Agricultural and Economic Intensification. Gainesville: University Press Florida. p 250-254.

Bechir M, Schelling E, Hamit M, Tanner M, and Zinsstag J. 2012. Parasitic Infections, Anemia and Malnutrition among Rural Settled and Mobile Pastoralist Mothers and their Children in Chad. Ecohealth 9(2):122-131.

Becker I, Woodley SJ, and Stringer MD. 2010. The Adult Human Pubic Symphysis: A Systematic Review. Journal of Anatomy 217(5):475-487.

Beggs I. 1985. The Radiology of Hydatid Disease. American Journal of Roentgenology 145(3):639-648.

Behrman RE, Masci JR, and Nicholas P. 1990. Cryptococcal Skeletal Infections: Case Report and Review. Reviews of Infectious Diseases 12(2):181-190.

Belik V, Geisel T, and Brockmann D. 2011. Natural Human Mobility Patterns and Spatial Spread of Infectious Diseases. Physical Review X 1(1):011001.

Bell LS, Cox G, and Sealy J. 2001. Determining Isotopic Life History Trajectories using Bone Density Fractionation and Stable Isotope Measurements: A New Approach. American Journal of Physical Anthropology 116(1):66-79.

Bellwood P. 2001. Early Agriculturalist Population Diasporas? Farming, Languages, and Genes. Annual Review of Anthropology 30(1):181-207.

Bellwood P. 2008. First Farmers: The Origins of Agricultural Societies. Oxford, UK: Blackwell Publishing.
Bellwood P, and Oxenham M. 2008. The Expansions of Farming Societies and the Role of the Neolithic Demographic Transition. In: Bocquet-Appel J-P, and Bar-Yosef O, editors. The Neolithic Demographic Transition and its Consequences: Springer Science. p 13-34.
Belyi A, Bojic I, Sobolevsky S, Sitko I, Hawelka B, Rudikova L, Kurbatski A, and Ratti C. 2017. Global Multi-Layer Network of Human Mobility. International Journal of Geographical Information Science 31(7):1381-1402.
Bendich A, Machlin L, Scandurra O, Burton G, and Wayner D. 1986. The Antioxidant Role of Vitamin C. Advances in Free Radical Biology & Medicine 2(2):419-444.
Bentley GR, Aunger R, Harrigan AM, Jenike M, Bailey RC, and Ellison PT. 1999. Women's Strategies to Alleviate Nutritional Stress in a Rural African Society. Social Science & Medicine 48(2):149-162.
Bentley RA. 2006. Strontium Isotopes from the Earth to the Archaeological Skeleton: A Review. Journal of Archaeological Method and Theory 13(3):135-187.
Berberian D. 1936. Some Observations on the Effect of Digestive Juices on Scolices of Echinococcus granulosus (Batsch). Journal of Helminthology 14(1):21-40.
Bereket A, Casur Y, Firat P, and Yordam N. 2000. Brown Tumour as a Complication of Secondary Hyperparathyroidism in Severe Long-Lasting Vitamin D Deficiency Rickets. European Journal of Pediatrics 159(1-2):70-73.
Bhan A, Rao AD, and Rao DS. 2010. Osteomalacia as a Result of Vitamin D Deficiency. Endocrinology and Metabolism Clinics 39(2):321-331.
Bhat RM, and Prakash C. 2012. Leprosy: An Overview of Pathophysiology. Interdisciplinary Perspectives on Infectious Diseases 2012.
Binford LR. 1980. Willow Smoke and Dogs' Tails: Hunter-Gatherer Settlement Systems and Archaeological Site Formation. American Antiquity 45(1):4-20.
Black FL. 2004. Disease Susceptibility among New World Peoples. In: Salzano F, and Hurtado M, editors. Lost Paradises and the Ethics of Research and Publication. Oxford, UK: Oxford University Press. p 146-163.
Blau S, and Yagodin V. 2005. Osteoarchaeological Evidence for Leprosy from Western Central Asia. American Journal of Physical Anthropology 126(2):150-158.
Bloem M, Wedel M, Egger RJ, Speek AJ, Schrijver J, Saowakontha S, and Schreurs W. 1989. Iron Metabolism and Vitamin A Deficiency in Children in Northeast Thailand. The American Journal of Clinical Nutrition 50(2):332-338.
Bocquet-Appel J-P, Naji S, Vander Linden M, and Kozlowski J. 2012. Understanding the Rates of Expansion of the Farming System in Europe. Journal of Archaeological Science 39(2):531-546.
Bodey G, and Vartivarian S. 1989. Aspergillosis. European Journal of Clinical Microbiology and Infectious Diseases 8(5):413-437.
Bodnar LM, Catov JM, Simhan HN, Holick MF, Powers RW, and Roberts JM. 2007. Maternal Vitamin D deficiency Increases the Risk of Preeclampsia. The Journal of Clinical Endocrinology & Metabolism 92(9):3517-3522.
Boelaert JR, Vandecasteele SJ, Appelberg R, and Gordeuk VR. 2007. The Effect of the Host's Iron Status on Tuberculosis. The Journal of Infectious Diseases 195(12):1745-1753.
Bogin BA, and MacVean RB. 1978. Growth in Height and Weight of Urban Guatemalan Primary School Children of Low and High Socioeconomic Class. Human Biology 50(4):477.

Bokhary M, and Phung TL. 2016. Molecular Pathogenesis of Leprosy. Current Tropical Medicine Reports 3(4):127-130.
Boldsen JL, and Milner GR. 2012. An Epidemiological Approach to Paleopathology. In: Grauer A, editor. A Companion to Paleopathology. Oxford, UK: Wiley-Blackwell. p 114-132.
Bouguila J, Besbes G, and Khochtali H. 2015. Skeletal Facial Deformity in Patients with β Thalassemia Major: Report of One Tunisian Case and a Review of the Literature. International Journal of Pediatric Otorhinolaryngology 79(11):1955-1958.
Bouis HE, and Welch RM. 2010. Biofortification—A Sustainable Agricultural Strategy for Reducing Micronutrient Malnutrition in the Global South. Crop Science 50(Supplement 1):S20-S32.
Brackett WJ, and Standley TB. 2019. Simulating Non-Accidental Trauma with Worsening Findings: Congenital Syphilis. SN Comprehensive Clinical Medicine 1(8):571-574.
Bradsher RW, Chapman SW, and Pappas PG. 2003. Blastomycosis. Infectious Disease Clinics of North America 17(1):21-40, vii.
Brickley M, and Ives R. 2010. The Bioarchaeology of Metabolic Bone Disease. Oxford, UK: Academic Press.
Brickley MB. 2018. Cribra Orbitalia and Porotic Hyperostosis: A Biological Approach to Diagnosis. American Journal of Physical Anthropology 167(4):896-902.
Brickley MB, and Mays S. 2019. Metabolic Disease. In: Buikstra JE, editor. Ortner's Identification of Pathological Conditions in Human Skeletal Remains. 3rd ed. Cambridge, USA: Elsevier. p 531-566.
Brickley MB, Mays S, George M, and Prowse TL. 2018. Analysis of Patterning in the Occurrence of Skeletal Lesions used as Indicators of Vitamin D Deficiency in Subadult and Adult Skeletal Remains. International Journal of Paleopathology 23:43-53.
Brickley MB, Schattmann A, and Ingram J. 2016. Possible Scurvy in the Prisoners of Old Quebec: A Re-evaluation of Evidence in Adult Skeletal Remains. International Journal of Paleopathology 15:92-102.
Broderick LG, and Houle J-L. 2013. More than Just Horse: Dietary Breadth and Subsistence in Bronze Age Central Mongolia. Mongolian Journal of Anthropology, Archaeology and Ethnology 9:149-157.
Bromage S, Rich-Edwards JW, Tselmen D, Baylin A, Houghton LA, Baasanjav N, and Ganmaa D. 2016. Seasonal Epidemiology of Serum 25-hydroxyvitamin D Concentrations among Healthy Adults Living in Rural and Urban Areas in Mongolia. Nutrients 8(10):592.
Brooks S, and Suchey JM. 1990. Skeletal Age Determination Based on the Os Pubis: A Comparison of the Acsádi-Nemeskéri and Suchey-Brooks Methods. Human Evolution 5(3):227-238. DOI: 10.1007/BF02437238
Brosseder U. 2009. Xiongnu Terrace Tombs and Their Interpretation as Elite Burials. Current Archaeological Research in Mongolia. Bonn, Germany: Rheinische Friedrich-Wilhelms-Universität. p 247-280.
Brothwell DR. 1981. Digging Up Bones: The Excavation, Treatment, and Study of Human Skeletal Remains. New York: Cornell University Press.
Brown M, and Ortner DJ. 2011. Childhood Scurvy in a Medieval Burial from Mačvanska Mitrovica, Serbia. International Journal of Osteoarchaeology 21(2):197-207.
Brunetti E, Kern P, and Vuitton DA. 2010. Expert Consensus for the Diagnosis and Treatment of Cystic and Alveolar Echinococcosis in Humans. Acta Tropica 114(1):1-16.

Bruzek J. 2002. A Method for Visual Determination of Sex, Using the Human Hip Bone. American Journal of Physical Anthropology 117(2):157-168.
Buckberry JL, and Chamberlain AT. 2002. Age Estimation from the Auricular Surface of the Ilium: A Revised Method. American Journal of Physical Anthropology 119(3):231-239.
Buckley H, Oxenham M, Domett K, Willis A, and Hiep TH. 2018. Osteolytic Metaphyseal Lesions and a Calcified Cyst in a Pre-Farming Skeletal Assemblage from Northern Vietnam. 22nd European Meeting of the Paleopathology Association. Zagreb, Croatia.
Buckley HR. 2000. Subadult Health and Disease in Prehistoric Tonga, Polynesia. American Journal of Physical Anthropology 113(4):481-505.
Buckley HR. 2016. Health and Disease in the Prehistoric Pacific Islands. Oxford, UK: British Archaeological Reports Ltd.
Buckley HR, and Dias GJ. 2002. The Distribution of Skeletal Lesions in Treponemal Disease: Is the Lymphatic System Responsible? International Journal of Osteoarchaeology 12(3):178-188.
Buckley HR, Kinaston R, Halcrow SE, Foster A, Spriggs M, and Bedford S. 2014. Scurvy in a Tropical Paradise? Evaluating the Possibility of Infant and Adult Vitamin C Deficiency in the Lapita Skeletal Sample of Teouma, Vanuatu, Pacific islands. International Journal of Paleopathology 5:72-85.
Buckley HR, and Oxenham M. 2016a. Bioarchaeology in the Pacific Islands: a Temporal and Geographical Examination of Nutritional and Infectious Disease. The Routledge handbook of bioarchaeology in Southeast Asia and the Pacific London: Routledge p:363-388.
Buckley HR, and Oxenham MF. 2016b. Bioarchaeology in the Pacific islands: A Temporal and Geographical Examination of Nutritional and Infectious Disease. In: Oxenham MF, and Buckley H, editors. The Routledge Handbook of Bioarchaeology in Southeast Asia and the Pacific. London: Routledge. p 363-388.
Buckley HR, and Tayles N. 2003. Skeletal Pathology in a Prehistoric Pacific Island Sample: Issues in Lesion Recording, Quantification, and Interpretation. American Journal of Physical Anthropology 122(4):303-324.
Buikstra JE. 2019. Ortner's Identification of Pathological Conditions in Human Skeletal Remains. London, UK: Academic Press.
Buikstra JE, Cook DC, and Bolhofner KL. 2017. Introduction: Scientific Rigor in Paleopathology. International Journal of Paleopathology 19:80-87.
Buikstra JE, Konigsberg LW, and Bullington J. 1986. Fertility and the Development of Agriculture in the Prehistoric Midwest. American Antiquity 51(3):528-546.
Buikstra JE, and Ubelaker DH. 1994. Standards for Data Collection from Human Skeletal Remains: Proceedings of a Seminar at the Field Museum of Natural History, Arkansas Archaeological Survey Research Series No. 44. Fayetteville, USA: Arkansas Archaeological Survey.
Bupp MRG. 2015. Sex, the Aging Immune System, and Chronic Disease. Cellular Immunology 294(2):102-110.
Burkle FM. 2007. War, Refugees, Migration, and Public Health: Do Infectious Diseases Matter? In: Apostolopoulos Y, and Sönmez SF, editors. Population Mobility and Infectious Disease: Springer. p 159- 179.
Butte NF, Lopez-Alarcon MG, and Garza C. 2002. Nutrient Adequacy of Exclusive Breastfeeding for the Term Infant during the First Six Months of Life.
Caffey J. 1939. Syphilis of the Skeleton in Early Infancy: The Nonspecificity of Many of the Roentgenographic Changes. American Journal of Roentgenology 42:637.

Camaschella C. 2015. Iron-Deficiency Anemia. New England Journal of Medicine 372(19):1832-1843.
Cambouris T. 1989. Radiological Bone Changes in Thalassemia Major. In: Papavasiliou C, editor. Radiology of Thalassemia: Springer Science & Business Media. p 21-43.
Cameron CM, Kelton P, and Swedlund AC. 2015. Beyond Germs: Native Depopulation in North America: University of Arizona Press.
Campbell G, Adams L, and Sowa B. 1994. Mechanisms of Binding of *Brucella abortus* to Mononuclear Phagocytes from Cows Naturally Resistant or Susceptible to Brucellosis. Veterinary Immunology and Immunopathology 41(3-4):295-306.
Campbell J. 1983. Smallpox in Aboriginal Australia, 1829–31. Historical Studies 20(81):536-556.
Capasso L. 2007. Infectious Diseases and Eating Habits at Herculaneum (1st century AD, southern Italy). International Journal of Osteoarchaeology 17(4):350-357.
Carlson AK. 1996. Lead Isotope Analysis of Human Bone for Addressing Cultural Affinity: A Case Study from Rocky Mountain House, Alberta. Journal of Archaeological Science 23(4):557-567.
Carragee EJ. 1997. Pyogenic Vertebral Osteomyelitis. The Journal of Bone and Joint Surgery 79(6):874-880.
Cartmill M, Hylander WL, and Shafland J. 1987. Human Structure: Harvard University Press.
Cassidy CM. 1984. Skeletal Evidence for Prehistoric Subsistence Adaptation in the Central Ohio River Valley. In: Armelagos GJ, and Cohen MN, editors. Paleopathology at the Origins of Agriculture. Orlando, USA: Academic Press. p 307-345.
Castillo C. 2011. Rice in Thailand: The Archaeobotanical Contribution. Rice 4(3):114.
Castillo C, Higham CF, Miller K, Chang N, Douka K, Higham TF, and Fuller DQ. 2018. Social Responses to Climate Change in Iron Age north-east Thailand: New Archaeobotanical Evidence. Antiquity 92(365):1274-1291.
Chamberlain AT. 2006. Demography in Archaeology. Cambridge, UK: Cambridge University Press.
Chan T. 2000. Vitamin D Deficiency and Susceptibility to Tuberculosis. Calcified Tissue International 66(6):476-478.
Chang Q, Su Mh, Chen Qx, Zeng By, Li Hh, and Wang W. 2017. Physicochemical Properties and Antioxidant Capacity of Chinese Olive (Canarium album L.) Cultivars. Journal of Food Science 82(6):1369-1377.
Cheverko CM, and Hubbe M. 2017. Comparisons of Statistical Techniques to Assess Age-Related Skeletal Markers in Bioarchaeology. American Journal of Physical Anthropology 163(2):407-416.
Chowdhury A, and Chen LC. 1977. The Interaction of Nutrition, Infection, and Mortality during Recent Food Crises in Bangladesh. Food Research Institute Studies 16(1387-2016-115954):47-61.
Clark JJ. 2001. Tracking Prehistoric Migrations: Pueblo Settlers among the Tonto Basin Hohokam: University of Arizona Press.
Clark SF. 2008. Iron Deficiency Anemia. Nutrition in Clinical Practice 23(2):128-141.
Coburn BJ, Wagner BG, and Blower S. 2009. Modeling Influenza Epidemics and Pandemics: Insights into the Future of Swine Flu (H1N1). BMC Medicine 7(1):30.
Codeço CT. 2001. Endemic and Epidemic Dynamics of Cholera: The Role of the Aquatic Reservoir. BMC Infectious Diseases 1(1):1.

Cohen MN, and Crane-Kramer GMM. 2007. Ancient Health: Skeletal Indicators of Agricultural and Economic Intensification. Gainesville, USA: University Press of Florida.
Colavita N, Orazi C, Danza S, Falappa P, and Fabbri R. 1987. Premature Epiphyseal Fusion and Extramedullary Hematopoiesis in Thalassemia. Skeletal Radiology 16(7):533-538.
Cole G, and Waldron T. 2019. Cribra Orbitalia: Dissecting an Ill-Defined Phenomenon. International Journal of Osteoarchaeology 29(4):613-621.
Collier L, and Primeau C. 2019. A Tale of Two Cities: A Comparison of Urban and Rural Trauma in Medieval Denmark. International Journal of Paleopathology 24:175-184.
Comas I, and Gagneux S. 2009. The Past and Future of Tuberculosis Research. PLoS Pathogens 5(10):e1000600.
Corbel MJ. 1989. Brucellosis: Epidemiology and Prevalence Worldwide. In: Young EJ, and Corbel MJ, editors. Brucellosis: Clinical and Laboratory Aspects. Boca Raton, USA: CRC Press. p 25-40.
Corbel MJ. 2006. Brucellosis in Humans and Animals: World Health Organization.
Corr PD. 2011. Musculoskeletal Fungal Infections. Seminars in Musculoskeletal Radiology 15(5):506-510.
Cox E, Meynell M, Northam B, and Cooke W. 1967. The Anaemia of Scurvy. The American Journal of Medicine 42(2):220-227.
Crandall JJ, and Klaus HD. 2014. Advancements, Challenges, and Prospects in the Paleopathology of Scurvy: Current Perspectives on Vitamin C Deficiency in Human Skeletal Remains. International Journal of Paleopathology 5:1-8.
Crist TA, and Sorg MH. 2014. Adult Scurvy in New France: Samuel de Champlain's “Mal de la Terre” at Saint Croix Island, 1604–1605. International Journal of Paleopathology 5:95-105.
Cubbon RM, Lowry JE, Drozd M, Hall M, Gierula J, Paton MF, Byrom R, Kearney LC, Barth JH, and Kearney MT. 2019. Vitamin D Deficiency is an Independent Predictor of Mortality in Patients with Chronic Heart Failure. European Journal of Nutrition 58(6):2535-2543.
Cui Y, Yu C, Yan Y, Li D, Li Y, Jombart T, Weinert LA, Wang Z, Guo Z, and Xu L. 2013. Historical Variations in Mutation Rate in an Epidemic Pathogen, Yersinia pestis. Proceedings of the National Academy of Sciences 110(2):577-582.
Cummings P. 2009. The Relative Merits of Risk Ratios and Odds Ratios. Archives of Pediatrics & Adolescent Medicine 163(5):438-445.
Cuong NL. 1986. Two Early Hoabinhian Crania from Thanh Hoa province, Vietnam. Zeitschrift für Morphologie und Anthropologie 77(1):11-17.
Cuong NL. 2007. Paleoanthropology in Vietnam. Khao Co Hoc (Vietnamese Archaeology) 2:23-41.
Currarino G, and Erlandson M. 1964. Premature Fusion of Epiphyses in Cooley’s Anaemia. Radiology 93:656-664.
Czermak BV, Unsinn KM, Gotwald T, Waldenberger P, Freund MC, Bale RJ, Vogel W, and Jaschke WR. 2001. Echinococcus multilocularis Revisited. American Journal of Roentgenology 176(5):1207-1212.
d'Anastasio R, Staniscia T, Milia M, Manzoli L, and Capasso L. 2011. Origin, Evolution and Paleoepidemiology of Brucellosis. Epidemiology & Infection 139(1):149-156.
D’Andrea AC. 1995. Later Jomon Subsistence in Northeastern Japan: New Evidence from Palaeoethnobotanical Studies. Asian Perspectives 34(2):195-227.

D'Ortenzio L, Ribot I, Kahlon B, Bertrand B, Bocaege E, Raguin E, Schattmann A, and Brickley M. 2018. The Rachitic Tooth: The Use of Radiographs as a Screening Technique. International Journal of Paleopathology 23:32-42.
Dahiru T. 2008. P-value, a True Test of Statistical Significance? A Cautionary Note. Annals of Ibadan Postgraduate Medicine 6(1):21-26.
Dalziel BD, Pourbohloul B, and Ellner SP. 2013. Human Mobility Patterns Predict Divergent Epidemic Dynamics Among Cities. Proceedings of the Royal Society B: Biological Sciences 280(1766):20130763.
Dashtseveg T. 2013. Mongolian Origins and Cranio-Morphometric Variability: Neolithic to Mongolian Period. In: Pechenkina K, and Oxenham MF, editors. Bioarchaeology of East Asia: Movement, Contact, Health. Gainesville, FL: University Press of Florida. p 85-109.
Dashtseveg T, Dorjpurev K, and Myagmar E. 2013. Bronze Age Graves in the Delgerkhaan Mountain Area of Eastern Mongolia and the Ulaanzuukh Culture. Asian Archaeology 2:40-49.
Davidson PT, and Horowitz I. 1970. Skeletal Tuberculosis: A Review with Patient Presentations and Discussion. The American Journal of Medicine 48(1):77-84.
Davit-Béal T, Gabay J, Antoniolli P, Masle-Farquhar J, and Wolikow M. 2014. Dental Complications of Rickets in Early Childhood: Case Report on 2 Young Girls. Pediatrics 133(4):e1077-e1081.
Dawson H, and Brown KR. 2012. Childhood Tuberculosis: A Probable Case from Late Mediaeval Somerset, England. International Journal of Paleopathology 2(1):31-35.
Dax EC, and Stewart R. 1939. The Sign of the Clavicle. British Medical Journal 1(4084):771-772.
de Haan K, Groeneveld AJ, de Geus HR, Egal M, and Struijs A. 2014. Vitamin D Deficiency as a Risk Factor for Infection, Sepsis and Mortality in the Critically Ill: Systematic Review and Meta-Analysis. Critical Care 18(6):660.
De la Rua-Domenech R. 2006. Human Mycobacterium bovis Infection in the United Kingdom: Incidence, Risks, Control Measures and Review of the Zoonotic Aspects of Bovine Tuberculosis. Tuberculosis 86(2):77-109.
de Vizia B, Poggi V, Conenna R, Fiorillo A, and Scippa L. 1992. Iron Absorption and Iron Deficiency in Infants and Children with Gastrointestinal Diseases. Journal of Pediatric Gastroenterology and Nutrition 14(1):21-26.
Dean M. 2000. Incremental Markings in Enamel and Dentine: What They Can Tell Us About the Way Teeth Grow. In: Teaford M, Smith M, and Fergusion M, editors. Development, Function and Evolution of Teeth. Cambridge, UK: Cambridge University Press. p 119-130.
Delanghe JR, Langlois MR, De Buyzere ML, and Torck MA. 2007. Vitamin C Deficiency and Scurvy are Not Only a Dietary Problem but are Codetermined by the Haptoglobin Polymorphism. Clinical Chemistry 53(8):1397-1400.
DeLoughery TG. 2014. Microcytic Anemia. New England Journal of Medicine 371(14):1324-1331.
Demirjian A, and Levesque G-Y. 1980. Sexual Differences in Dental Development and Prediction of Emergence. Journal of Dental Research 59(7):1110-1122.
Denning DW. 1998. Invasive Aspergillosis. Clinical Infectious Diseases 26(4):781-803.
Deplazes P, Rinaldi L, Rojas CA, Torgerson P, Harandi M, Romig T, Antolova D, Schurer J, Lahmar S, and Cringoli G. 2017. Global Distribution of Alveolar and Cystic Echinococcosis. Advances in Parasitology: Elsevier. p 315-493.
Derlacki EL, and Clemis JD. 1965. Congenital Cholesteatoma of the Middle Ear and Mastoid. Annals of Otology, Rhinology & Laryngology 74(3):706-727.

Dervenis C, Delis S, Avgerinos C, Madariaga J, and Milicevic M. 2005. Changing Concepts in the Management of Liver Hydatid Disease. Journal of Gastrointestinal Surgery 9(6):869-877.
Desenclos J-C, Berry A, Padt R, Farah B, Segala C, and Nabil A. 1989. Epidemiological Patterns of Scurvy Among Ethiopian Refugees. Bulletin of the World Health Organization 67(3):309.
DeWitte SN. 2014a. Differential Survival Among Individuals with Active and Healed Periosteal New Bone Formation. International Journal of Paleopathology 7:38-44.
DeWitte SN. 2014b. Mortality Risk and Survival in the Aftermath of the Medieval Black Death. PloS one 9(5):e96513.
DeWitte SN. 2016. Archaeological Evidence of Epidemics Can Inform Future Epidemics. Annual Review of Anthropology 45:63-77.
DeWitte SN, and Hughes-Morey G. 2012. Stature and Frailty During the Black Death: The Effect of Stature on Risks of Epidemic Mortality in London, AD 1348–1350. Journal of Archaeological Science 39(5):1412-1419.
DeWitte SN, and Stojanowski CM. 2015. The Osteological Paradox 20 Years Later: Past Perspectives, Future Directions. Journal of Archaeological Research 23(4):397-450.
Di Cosmo N. 2011. Ethnogenesis, Coevolution and Political Morphology of the Earliest Steppe Empire: The Xiongnu Question Revisited. In: Brosseder U, and Miller B, editors. Xiongnu Archaeology: Multidisciplinary Perspectives of the First Steppe Empire in Inner Asia. Bonn, Germany: Rheinische Friedrich-Wilhelms-Universität p35-48.
Dickson EC, and Gifford MA. 1938. Coccidioides Infection (Coccidioidomycosis): II. The Primary Type of Infection. Archives of Internal Medicine 62(5):853-871.
Dimitri P, and Bishop N. 2007. Rickets. Paediatrics and Child Health 17(7):279-287.
Domett KM, and Oxenham MF. 2011. The Demographic Profile of the Man Bac Cemetery Sample. In: Oxenham MF, Matsumura H, and Kim Dung N, editors. Man Bac: The Excavation of a Neolithic Site in Northern Vietnam, The Biology Terra Australis 33: ANU ePress. p 9-20.
Dong J, Zhang Y, and Zhang H. 2015. Health Properties of Traditional Fermented Mongolian Milk Foods. In: Liong M, editor. Beneficial Microorganisms in Food and Nutraceuticals. Cham, Switzerland: Springer. p 37-61.
Donoghue HD, Taylor GM, Marcsik A, Molnár E, Pálfi G, Pap I, Teschler-Nicola M, Pinhasi R, Erdal YS, and Velemínsky P. 2015. A Migration-Driven Model for the Historical Spread of Leprosy in Medieval Eastern and Central Europe. Infection, Genetics and Evolution 31:250-256.
Dubey L, Krasinski K, and Hernanz-Schulman M. 1988. Osteomyelitis Secondary to Trauma or Infected Contiguous Soft Tissue. The Pediatric Infectious disease Journal 7(1):26-34.
Duggan AT, Harris AJ, Marciniak S, Marshall I, Kuch M, Kitchen A, Renaud G, Southon J, Fuller B, and Young J. 2017. Genetic Discontinuity between the Maritime Archaic and Beothuk Populations in Newfoundland, Canada. Current Biology 27(20):3149-3156. e3111.
Duintjer Tebbens RJ, Pallansch MA, Kew OM, Cáceres VM, Sutter RW, and Thompson KM. 2005. A Dynamic Model of Poliomyelitis Outbreaks: Learning from the Past to Help Inform the Future. American Journal of Epidemiology 162(4):358-372.
Dwek JR. 2010. The Periosteum: What is It, Where is It, and What Mimics It in its Absence? Skeletal Radiology 39(4):319-323.

Ebright JR, Altantsetseg T, and Oyungerel R. 2003. Emerging Infectious Diseases in Mongolia. Emerging Infectious Diseases 9(12):1509.
Eichelmann K, González SG, Salas-Alanis J, and Ocampo-Candiani J. 2013. Leprosy. An Update: Definition, Pathogenesis, Classification, Diagnosis, and Treatment. Actas Dermo-Sifiliográficas (English Edition) 104(7):554-563.
Ekiz C, Agaoglu L, Karakas Z, Gurel N, and Yalcin I. 2005. The Effect of Iron Deficiency Anemia on the Function of the Immune System. The Hematology Journal 5(7):579-583.
Eng JT. 2016. A Bioarchaeological Study of Osteoarthritis Among Populations of Northern China and Mongolia during the Bronze Age to Iron Age Transition to Nomadic Pastoralism. Quaternary International 405:172-185.
Eng JT, and Quanchao Z. 2013. Conflict and Trauma among Nomadic Pastoralists on China's Northern Frontier. In: Pechenkina K, and Oxenham MF, editors. Bioarchaeology of East Asia: Movement, Contact, Health. Gainesville, FL: University Press of Florida. p 213-245.
Engelhardt HK. 1959. A Study of Yaws (Does Congenital Yaws Occur?). Journal of Tropical Medicine and Hygiene 62(10):238-240.
Erdene M. 2014. Распространение некоторых Зүбных Патологий среди Населения Бронзовой Эпохи Монголии (Distribution of some Dental Pathologies among the Bronze Age Populations of Mongolia). Ancient Cultures of Mongolia and Baikalian Siberia 15-19 September, 2014. Kyzyl, Russia. (In Mongolian).
Erdene M. 2017. Dental Caries Prevalence in Xiongnu Populations from Mongolia: Age, Sex, and Regional Variation. Asian Journal of Paleopathology: The Official Journal of Japanese Society of Paleopathology 1:19-29.
Eshed V, Gopher A, Pinhasi R, and Hershkovitz I. 2010. Paleopathology and the Origin of Agriculture in the Levant. American Journal of Physical Anthropology 143(1):121-133.
Eslami A, and Hosseini SH. 1998. Echinococcus granulosus Infection of Farm Dogs of Iran. Parasitology Research 84(3):205-207.
Esmaeilnejad- Ganji SM, and Esmaeilnejad- Ganji SMR. 2019. Osteoarticular Manifestations of Human Brucellosis: A Review. World Journal of Orthopedics 10(2):54-62.
Estrada-Peña A, Ostfeld RS, Peterson AT, Poulin R, and de la Fuente J. 2014. Effects of Environmental Change on Zoonotic Disease Risk: An Ecological Primer. Trends in Parasitology 30(4):205-214.
Ewald PW. 1994. Evolution of Infectious Disease. New York: Oxford University Press.
Ewald PW. 2000. Plague Time: How Stealth Infections Cause Cancers, Heart Disease, and Other Deadly Ailments. New York: Simon and Schuster.
Faerman M, Bar-Gal GK, Filon D, Greenblatt CL, Stager L, Oppenheim A, and Smith P. 1998. Determining the Sex of Infanticide Victims from the Late Roman Era Through Ancient DNA Analysis. Journal of Archaeological Science 25(9):861-865.
Fain O. 2005. Musculoskeletal Manifestations of Scurvy. Joint Bone Spine 72(2):124-128.
Fan CC, and Huang Y. 1998. Waves of Rural Brides: Female Marriage Migration in China. Annals of the Association of American Geographers 88(2):227-251.
Fanning A. 1999. Tuberculosis: 6. Extrapulmonary Disease. CMAJ: Canadian Medical Association Journal 160(11):1597.
Favereau A, and Bellina B. 2016. Thai-Malay Peninsula and South China Sea Networks (500 BC–AD 200), Based on a Reappraisal of "Sa Huynh-Kalanay"-Related Ceramics. Quaternary International 416:219-227.

Fazekas I, and Kosa F. 1978. Determination of the Body Length and Age of Foetuses on the Basis of the Diaphyseal Size of the Extremity Bones. In: Fazekas I, and Kosa F, editors. Forensic Foetal Osteology. Budapest, Hungary: Akademiai-Kiado. p 232-277.

Feldman M, Master DM, Bianco RA, Burri M, Stockhammer PW, Mittnik A, Aja AJ, Jeong C, and Krause J. 2019. Ancient DNA Sheds Light on the Genetic Origins of Early Iron Age Philistines. Science Advances 5(7):eaax0061.

Ferembach D. 1980. Recommendations for Age and Sex Diagnosis of Skeletons. Journal of Human Evolution 9:517-549.

Field CJ. 2005. The Immunological Components of Human Milk and their Effect on Immune Development in Infants. The Journal of Nutrition 135(1):1-4.

Fincher CL, Thornhill R, Murray DR, and Schaller M. 2008. Pathogen Prevalence Predicts Human Cross-Cultural Variability in Individualism/Collectivism. Proceedings of the Royal Society of London B: Biological Sciences 275(1640):1279-1285.

Fischer PR, Thacher TD, Pettifor JM, Jorde LB, Eccleshall TR, and Feldman D. 2000. Vitamin D Receptor Polymorphisms and Nutritional Rickets in Nigerian Children. Journal of Bone and Mineral Research 15(11):2206-2210.

Fitzgerald F. 1978. Clinical Hypophosphatemia. Annual Review of Medicine 29(1):177-189.

Fiumara NJ, and Lessell S. 1970. Manifestations of Late Congenital Syphilis: An Analysis of 271 Patients. Archives of Dermatology 102(1):78-83.

Flint J, Hill A, Bowden D, Oppenheimer S, Sill P, Serjeantson S, Bana-Koiri J, Bhatia K, Alpers M, and Boyce A. 1986. High Frequencies of α-Thalassaemia are the Result of Natural Selection by Malaria. Nature 321(6072):744-750.

Flohr S, and Schultz M. 2009. Osseous Changes due to Mastoiditis in Human Skeletal Remains. International Journal of Osteoarchaeology 19(1):99-106.

Flynn JL, and Chan J. 2001. Immunology of Tuberculosis. Annual Review of Immunology 19(1):93-129.

Foldenauer A, Vossbeck S, and Pohlandt F. 1998. Neonatal Hypocalcaemia Associated with Rotavirus Diarrhoea. European Journal of Pediatrics 157(10):838-842.

Foss NT, and Motta ACF. 2012. Leprosy, A Neglected Disease that Causes a Wide Variety of Clinical Conditions in Tropical Countries. Memórias do Instituto Oswaldo Cruz 107:28-33.

Foy H, and Nelson GS. 1963. Helminths in the Etiology of Anemia in the Tropics, with Special Reference to Hookworms and Schistosomes. Experimental Parasitology 14(2):240-262.

Frachetti MD. 2009. Pastoralist Landscapes and Social Interaction in Bronze Age Eurasia: Univ of California Press.

Frachetti MD, Anthony DW, Epimakhov A, Hanks BK, Doonan R, Kradin NN, Lamberg-Karlovsky C, Olsen SL, Potts D, and Rogers JD. 2012. Multiregional Emergence of Mobile Pastoralism and Nonuniform Institutional Complexity across Eurasia. Current Anthropology 53(1):2-38.

Franco MP, Mulder M, Gilman RH, and Smits HL. 2007. Human Brucellosis. The Lancet Infectious Diseases 7(12):775-786.

Frangos CC, Lavranos GM, and Frangos CC. 2011. Higoumenakis' Sign in the Diagnosis of Congenital Syphilis in Anthropological Specimens. Medical Hypotheses 77(1):128-131.

Frieman C, Piper P, Nguyen K, Tran T, and Oxenham M. 2017. Ground Stone Technology in Coastal Neolithic Settlements of Southern Vietnam: Grinding Stones and Adzes from Rach Nui. Antiquity 91(358):933-946.

Fu X. 2002. The Dingsishan Site and the Prehistory of Guangxi, South China. Bulletin of the Indo-Pacific Prehistory Association 22:63-72.
Fujita H. 1997. Ritual Tooth Ablation of the Jomon Skeletal Remains of Atsumi Peninsula, Aichi Prefecture: Evalution of Age of Tooth Ablation Kodai 104:42-63. (In Japanese).
Fusegawa H, Wang B-H, Sakurai K, Nagasawa K, Okauchi M, and Nagakura K. 2003. Outbreak of Tuberculosis in a 2000-year-old Chinese Population. Kansenshogaku Zasshi The Journal of the Japanese Association for Infectious Diseases 77(3):146-149.
Gagneux S. 2012. Host–Pathogen Coevolution in Human Tuberculosis. Proceedings of the Royal Society of London B: Philosophical Transactions 367(1590):850-859.
Galanello R, and Cao A. 2011. Alpha-Thalassemia. Genetics in Medicine 13(2):83-88.
Galinska EM, and Zagórski J. 2013. Brucellosis in Humans- Etiology, Diagnostics, Clinical Forms. Annals of Agricultural and Environmental Medicine 20(2):233-238.
Galvani AP, and Slatkin M. 2003. Evaluating Plague and Smallpox as Historical Selective Pressures for the CCR5-Δ32 HIV-Resistance Allele. Proceedings of the National Academy of Sciences 100(25):15276-15279.
Garn SM, Lewis AB, and Kerewsky RS. 1965. Genetic, Nutritional, and Maturational Correlates of Dental Development. Journal of Dental Research 44(1):228-242.
Garvin HM, and Passalacqua NV. 2012. Current Practices by Forensic Anthropologists in Adult Skeletal Age Estimation. Journal of Forensic Sciences 57(2):427-433.
Gayer M, Legros D, Formenty P, and Connolly MA. 2007. Conflict and Emerging Infectious Diseases. Emerging Infectious Diseases 13(11):1625-1631.
Geber J, and Murphy E. 2012. Scurvy in the Great Irish Famine: Evidence of Vitamin C Deficiency from a mid-19th century Skeletal Population. American Journal of Physical Anthropology 148(4):512-524.
Giaccai L, and Idriss H. 1952. Osteomyelitis Due to Salmonella Infection. The Journal of Pediatrics 41(1):73-78.
Giffin K, Lankapalli AK, Sabin S, Spyrou MA, Posth C, Kozakaitė J, Friedrich R, Miliauskienė Ž, Jankauskas R, and Herbig A. 2020. A Treponemal Genome from an Historic Plague Victim Supports a Recent Emergence of Yaws and its Presence in 15th Century Europe. Scientific Reports 10(1):1-13.
Gilbert BM, and McKern TW. 1973. A Method for Aging the Female Os Pubis. American Journal of Physical Anthropology 38(1):31-38.
Gilles H. 1968. Gastrointestinal Helminthiasis. British Medical Journal 2(5603):475-477.
Ginde AA, Mansbach JM, and Camargo CA. 2009. Vitamin D, Respiratory Infections, and Asthma. Current Allergy and Asthma Reports 9(1):81-87.
Gip LS. 1989. Yaws Revisited. Medical Journal of Malaysia 44(4):307-311.
Glover I, Bellwood P, and Bellwood PS. 2004. Southeast Asia: From Prehistory to History. London: Psychology Press.
Gocha TP, Ingvoldstad ME, Kolatorowicz A, Cosgriff-Hernandez M-TJ, and Sciulli PW. 2015. Testing the Applicability of Six Macroscopic Skeletal Aging Techniques on a Modern Southeast Asian Sample. Forensic Science International 249:318. e311-318. e317.
Godde K, Pasillas V, and Sanchez A. 2020. Survival Analysis of the Black Death: Social Inequality of Women and the Perils of Life and Death in Medieval London. American Journal of Physical Anthropology:e24081.
Goh BT. 2005. Syphilis in Adults. Sexually Transmitted Infections 81(6):448-452.

González PN, Bernal V, Perez SI, and Barrientos G. 2007. Analysis of Dimorphic Structures of the Human Pelvis: Its Implications for Sex Estimation in Samples without Reference Collections. Journal of Archaeological Science 34(10):1720-1730.
Goodman AH. 1993. On the Interpretation of Health from Skeletal Remains. Current Anthropology 34(3):281-288.
Goodman AH, and Leatherman TL. 2010. Building a New Biocultural Synthesis: Political-Economic Perspectives on Human Biology: University of Michigan Press.
Goodwin RA, Loyd JE, and Des Prez RM. 1981. Histoplasmosis in Normal Hosts. Medicine 60(4):231-266.
Gowland RL, and Western A. 2012. Morbidity in the Marshes: Using Spatial Epidemiology to Investigate Skeletal Evidence for Malaria in Anglo-Saxon England (AD 410–1050). American Journal of Physical Anthropology 147(2):301-311.
Goyal A, Boro H, and Khadgawat R. 2018. Brown Tumor as an Index Presentation of Severe Vitamin D Deficiency in a Teenage Girl. Cureus 10(5).
Grange J. 2001. Mycobacterium bovis Infection in Human Beings. Tuberculosis 81(1-2):71-77.
Grant WB. 2002. An Ecologic Study of Dietary and Solar Ultraviolet-B Links to Breast Carcinoma Mortality Rates. Cancer 94(1):272-281.
Grauer AL. 2011. Introduction: The scope of Paleopathology. A Companion to Paleopathology. Oxford, UK: Wiley-Blackwell. p 1-14.
Green MH. 2017. The Globalisations of Disease. In: Boivin N, Crassard R, and Petraglia MD, editors. Human Dispersals and Species Movement: From Prehistory to Present. Cambridge, UK: Cambridge University Press. p 494-520.
Green MH, and Jones L. 2020. The Evolution and Spread of Major Human Diseases in the Indian Ocean World. In: Campbell G, and Knoll E-M, editors. Disease Dispersion and Impact in the Indian Ocean World: Springer. p 25-57.
Greenthal RM. 1919. Infantile Scurvy Associated with Hereditary Syphilis: Report on a Breast Fed Infant with Multiple Fractures. American Journal of Diseases of Children 17(6):440-443.
Greenwood MJ. 1985. Human Migration: Theory, Models, and Empirical Studies. Journal of Regional Science 25(4):521-544.
Grin EI. 1953. Epidemiology and Control of Endemic Syphilis: Report on a Mass-Treatment Campaign in Bosnia: World Health Organization.
Grin EI. 1956. Endemic Syphilis and Yaws. Bulletin of the World Health Organization 15(6):959-973.
Groube LM. 1993. Contradictions and Malaria in Melanesian and Australian Prehistory. In: Spriggs M, and Yen D, editors. A Community of Culture: the People and Prehistory of the Pacific. Canberra, Australia: The Australian National University. p 164-186.
Grove NJ, and Zwi AB. 2006. Our Health and Theirs: Forced Migration, Othering, and Public Health. Social Science & Medicine 62(8):1931-1942.
Grupe G, Marx M, Schellerer P-M, Bemmann J, Brosseder U, Yeruul-Erdene C, and Gantulga J. 2019. Bioarchaeology of Bronze and Iron Age Skeletal Finds from a Microregion in Central Mongolia. Anthropologischer Anzeiger 76(3):233-243.
Guimarães FN. 1953. Yaws in Brazil. Bulletin of the World Health Organization 8(1-3):225.
Gunson N. 1997. Great Families of Polynesia: Inter-island Links and Marriage Patterns. The Journal of Pacific History 32(2):139-179.

Gupta N, Toteja N, Sasidharan R, and Singh K. 2020. Childhood Scurvy: A Nearly Extinct Disease Posing a New Diagnostic Challenge, A Case Report. Journal of Tropical Pediatrics 66(2):231-233.
Gupta S. 2007. The Bay of Bengal Interaction Sphere (1000 BC-AD 500). Bulletin of the Indo-Pacific Prehistory Association 25:21-30.
Gushulak BD, and MacPherson DW. 2004. Globalization of Infectious Diseases: The Impact of Migration. Clinical Infectious Diseases 38(12):1742-1748.
Habu J. 1996. Jomon Sedentism and Intersite Variability: Collectors of the Early Jomon Moroiso Phase in Japan. Arctic Anthropology:38-49.
Habu J. 2004. Ancient Jomon of Japan. Cambridge, UK: Cambridge University Press.
Habu J. 2008. Growth and Decline in Complex Hunter-Gatherer Societies: A Case Study from the Jomon Period Sannai Maruyama Site, Japan. antiquity 82(317):571-584.
Habu J, Lape PV, and Olsen JW. 2017. Handbook of East and Southeast Asian Archaeology: Springer.
Hackett CJ. 1936. A Critical Survey of Some References to Syphilis and Yaws among the Australian Aborigines. Medical Journal of Australia 1(22).
Hackett CJ. 1946. The Clinical Course of Yaws in Lango, Uganda. Transactions of the Royal Society of Tropical Medicine and Hygiene 40(3):205-227.
Hackett CJ. 1951. Bone Lesions of Yaws in Uganda. Oxford, UK: Blackwell Scientific Publications.
Hackett CJ. 1953a. Extent and Nature of the Yaws Problem in Africa. Bulletin of the World Health Organization 8(1-3):127-182.
Hackett CJ. 1953b. The Natural History of Yaws. Transactions of the Royal Society of Tropical Medicine and Hygiene 47(4):318- 320.
Hackett CJ. 1975. An Introduction to Diagnostic Criteria of Syphilis, Treponarid and Yaws (Treponematoses) in Dry Bones, and Some Implications. Virchows Archive A 368(3):229-241.
Hackett CJ. 1976. Diagnostic Criteria of Syphilis, Yaws and Treponarid (Treponematoses) and of Some Other Diseases in Dry Bones. Berlin, Germany: Springer.
Hackett CJ. 1978. Treponematoses (Yaws and Treponarid) in Exhumed Australian Aboriginal Bones. Records of the South Australian Museum Adelaide 17(27):307-406.
Hadjidakis DJ, and Androulakis II. 2006. Bone Remodeling. Annals of the New York Academy of Sciences 1092(1):385-396.
Hakim DN, Pelly T, Kulendran M, and Caris JA. 2015. Benign Tumours of the Bone: A Review. Journal of Bone Oncology 4(2):37-41.
Halcrow S, Harris N, Beavan N, and Buckley H. 2014. First Bioarchaeological Evidence of Probable Scurvy in Southeast Asia: Multifactorial Etiologies of Vitamin C Deficiency in a Tropical Environment. International Journal of Paleopathology 5:63-71.
Halcrow S, Tayles N, and King CL. 2016. Infant and Child Health and Disease with Agricultural Intensification in Mainland Southeast Asia. In: Oxenham M, and Buckley H, editors. The Routledge Handbook of Bioarchaeology in Southeast Asia and the Pacific Islands: Routledge. p 186-214.
Halcrow SE, Tayles N, and Buckley HR. 2007. Age Estimation of Children from Prehistoric Southeast Asia: Are the Dental Formation Methods Used Appropriate? Journal of Archaeological Science 34(7):1158-1168.
Hammer MF, Karafet TM, Park H, Omoto K, Harihara S, Stoneking M, and Horai S. 2006. Dual Origins of the Japanese: Common Ground for Hunter-Gatherer and Farmer Y Chromosomes. Journal of Human Genetics 51(1):47-58.

Hanihara T, and Ishida H. 2009. Regional Differences in Craniofacial Diversity and the Population History of Jomon Japan. American Journal of Physical Anthropology 139(3):311-322.
Haque AK. 1990. The Pathology and Pathophysiology of Mycobacterial Infections. Journal of Thoracic Imaging 5(2):8-16.
Harney É, Nayak A, Patterson N, Joglekar P, Mushrif-Tripathy V, Mallick S, Rohland N, Sedig J, Adamski N, and Bernardos R. 2019. Ancient DNA from the Skeletons of Roopkund Lake Reveals Mediterranean Migrants in India. Nature Communications 10(1):1-10.
Harper K, and Armelagos G. 2010. The Changing Disease-Scape in the Third Epidemiological Transition. International Journal of Environmental Research and Public Health 7(2):675-697.
Harper KN, Zuckerman MK, Harper ML, Kingston JD, and Armelagos GJ. 2011. The Origin and Antiquity of Syphilis Revisited: An Appraisal of Old World Pre-Columbian Evidence for Treponemal Infection. American Journal of Physical Anthropology 146(S53):99-133. DOI: 10.1002/ajpa.21613
Hashemi SH, Keramat F, Ranjbar M, Mamani M, Farzam A, and Jamal-Omidi S. 2007. Osteoarticular Complications of Brucellosis in Hamedan, an Endemic Area in the West of Iran. International Journal of Infectious Diseases 11(6):496-500.
Hawkes K, O'Connell JF, and Jones NGB. 2014. More Lessons from the Hadza About Men's Work. Human Nature 25(4):596-619.
He G, Chen P, Wu J, Luo L, Gao H, Wang M, Zou X, Luo H, Yu L, and Han Y. 2019. Population Genetic Analysis of Modern and Ancient DNA Variations Yields New Insights into the Formation, Genetic Structure and Phylogenetic Relationship of Northern Han Chinese. Frontiers in Genetics 10:1045.
Hemilä H. 2017. Vitamin C and Infections. Nutrients 9(4):339.
Henrich J, and Henrich N. 2010. The Evolution of Cultural Adaptations: Fijian Food Taboos Protect Against Dangerous Marine Toxins. Proceedings of the Royal Society B: Biological Sciences 277(1701):3715-3724.
Hens SM, and Godde K. 2016. Auricular Surface Aging: Comparing Two Methods that Assess Morphological Change in the Ilium with Bayesian Analyses. Journal of Forensic Sciences 61:S30-S38.
Hernández-Mora G, Palacios-Alfaro J, and González-Barrientos R. 2013. Wildlife Reservoirs of Brucellosis: Brucella in Aquatic Environments. Rev Sci Tech 32(1):89-103.
Hess KR. 1995. Graphical Methods for Assessing Violations of the Proportional Hazards Assumption in Cox Regression. Statistics in Medicine 14(15):1707-1723.
Hiep T. 2004. Di Tich Man Bac va Moi Quan he cua no Voi Cac di Tich Tien Dong Son o Dong Bang Song Hong (in Vietnamese). Hanoi, Vietnam: Hanoi National University.
Higham C. 1989. The Archaeology of Mainland Southeast Asia: from 10,000 BC to the Fall of Angkor. Cambridge, UK: Cambridge University Press.
Higham C. 2007. The Origins of the Civilization of Angkor Volume 2: The Excavation of Noen U-Loke and Non Muang Kao: Fine Arts Department of Thailand.
Higham C, Guangmao X, and Qiang L. 2011. The Prehistory of a Friction Zone: First Farmers and Hunters-Gatherers in Southeast Asia. Antiquity 85(328):529-543.
Higham C, and Thosarat R. 2005. Excavation of Khok Phanom Di, 7: Summary and Conclusions: Fine Arts Department of Thailand.

Higham CF, Cameron J, Chang N, Castillo C, Halcrow S, O'Reilly D, Petchey F, and Shewan L. 2014. The Excavation of Non Ban Jak, Northeast Thailand-A Report on the First Three Seasons. Journal of Indo-Pacific Archaeology 34:1-41.
Hill KR. 1953. Non-Specific Factors in the Epidemiology of Yaws. Bulletin of the World Health Organization 8(1-3):17.
Hillson S, Grigson C, and Bond S. 1998. Dental Defects of Congenital Syphilis. American Journal of Physical Anthropology 107(1):25-40.
Hirschmann J, and Raugi GJ. 1999. Adult Scurvy. Journal of the American Academy of Dermatology 41(6):895-910.
Hlavenková L, Teasdale M, Gábor O, Nagy G, Beňuš R, Marcsik A, Pinhasi R, and Hajdu T. 2015. Childhood Bone Tuberculosis from Roman Pécs, Hungary. Homo 66(1):27-37.
Hodges RE, Hood J, Canham JE, Sauberlich HE, and Baker EM. 1971. Clinical Manifestations of Ascorbic Acid Deficiency in Man. The American Journal of Clinical Nutrition 24(4):432-443.
Högberg U, and Broström G. 1985. The Demography of Maternal Mortality-Seven Swedish Parishes in the 19th century. International Journal of Gynecology & Obstetrics 23(6):489-497.
Holick MF, Siris ES, Binkley N, Beard MK, Khan A, Katzer JT, Petruschke RA, Chen E, and de Papp AE. 2005. Prevalence of Vitamin D Inadequacy among Postmenopausal North American Women Receiving Osteoporosis Therapy. The Journal of Clinical Endocrinology & Metabolism 90(6):3215-3224.
Hollander D, and Turner T. 1954. The Role of Temperature in Experimental Treponemal Infection. American Journal of Syphilis 38(6):489-505.
Holloway KL, Link K, Rühli F, and Henneberg M. 2013. Skeletal Lesions in Human Tuberculosis May Sometimes Heal: An Aid to Palaeopathological Diagnoses. PloS one 8(4).
Honda H, and McDonald JR. 2009. Current Recommendations in the Management of Osteomyelitis of the Hand and Wrist. The Journal of Hand Surgery 34(6):1135-1136.
Honeychurch W. 2013. The Nomad as State Builder: Historical Theory and Material Evidence from Mongolia. Journal of World Prehistory 26(4):283-321.
Honeychurch W. 2015. Inner Asia and the Spatial Politics of Empire: Archaeology, Mobility, and Culture Contact. New York, USA: Springer.
Hook EW, and Marra CM. 1992. Acquired Syphilis in Adults. New England Journal of Medicine 326(16):1060-1069.
Hoover KC, and Hudson MJ. 2016. Resilience in Prehistoric Persistent Hunter–Gatherers in Northwest Kyushu, Japan as Assessed by Population Health and Archaeological Evidence. Quaternary International 405:22-33.
Hoover KC, and Matsumura H. 2008. Temporal Variation and Interaction between Nutritional and Developmental Instability in Prehistoric Japanese Populations. American Journal of Physical Anthropology 137(4):469-478.
Hoppa RD. 1999. Modeling the Effects of Selection Bias on Palaeodemographic Analyses. Homo 50(3):228-243.
Hoppa RD, and Gruspier KL. 1996. Estimating Diaphyseal Length from Fragmentary Subadult Skeletal Remains: Implications for Palaeodemographic Reconstructions of a Southern Ontario Ossuary. American Journal of Physical Anthropology 100(3):341-354.

Höuffding J, Maeda M, Yamaguchi K, Tsuji H, Kuwabara S, Nohara Y, and Yoshida S. 1984. Emergence of Permanent Teeth and Onset of Dental Stages in Japanese children. Community Dentistry and Oral Epidemiology 12(1):55-58.
Houle J-L. 2016. Bronze Age Mongolia. Oxford Handbooks Online. Oxford, UK: University of Oxford.
Houle J-L, and Broderick LG. 2011. Settlement Patterns and Domestic Economy of the Xiongnu in Khanui Valley, Mongolia. In: Brosseder U, and Miller BK, editors. Xiongnu Archaeology: Multidisciplinary Perspectives of the First Steppe Empire in Inner Asia. Bonn, Germany: Rheinische Friedrich-Wilhelms-Universität. p 137-152.
Hsia CC. 1998. Respiratory Function of Hemoglobin. New England Journal of Medicine 338(4):239-248.
Hu H, Nigmatulina K, and Eckhoff P. 2013. The Scaling of Contact Rates with Population Density for the Infectious Disease Models. Mathematical Biosciences 244(2):125-134.
Huai KH-Y, and Pei S-J. 2000. Wild Plants in the Diet of Arhorchin Mongol Herdsmen in Inner Mongolia. Economic Botany 54(4):528-536.
Hudson EH. 1965. Treponematosis in Perspective. Bulletin of the World Health Organization 32(5):735.
Huffer D, Bentley A, and Oxenham M. in press. Community and Kinship during the Transition to Agriculture in Northern Vietnam. In: Higham C, and Kim Dung N, editors. The Oxford Handbook of Southeast Asian Archaeology. Oxford, UK: Oxford University Press.
Huffer D, and Oxenham M. 2015. Investigating Activity and Mobility Patterns during the Mid-Holocene in Northern Vietnam. The Routledge Handbook of Bioarchaeology in Southeast Asia and the Pacific Islands:110.
Hughes PJ, Sullivan ME, and Hiscock P. 2017. Palaeoclimate and Human Occupation in Southeastern Arid Australia. Quaternary Science Reviews 163:72-83.
Huh S, Yu J-R, Kim J-I, Gotov C, Janchiv R, and Seo J-S. 2006. Intestinal Protozoan Infections and Echinococcosis in the Inhabitants of Dornod and Selenge, Mongolia (2003). The Korean Journal of Parasitology 44(2):171.
Hume DA. 2006. The Mononuclear Phagocyte System. Current Opinion in Immunology 18(1):49-53.
Hung H-C, Nguyen KD, Bellwood P, and Carson MT. 2013. Coastal Connectivity: Long-Term Trading Networks Across the South China Sea. The Journal of Island and Coastal Archaeology 8(3):384-404.
Huss-Ashmore R. 1980. Fat and Fertility: Demographic Implications of Differential Fat Storage. American Journal of Physical Anthropology 23(S1):65-91.
Ikehara-Quebral RM, Stark MT, Belcher W, Vuthy V, Krigbaum J, Bentley RA, Douglas MT, and Pietrusewsky M. 2017. Biocultural Practices during the Transition to History at the Vat Komnou Cemetery, Angkor Borei, Cambodia. Asian Perspectives 56(2):191-236. DOI: 10.1353/asi.2017.0008
Ikpeme I, Ngim N, and Ikpeme A. 2010. Diagnosis and Treatment of Pyogenic Bone Infections. African Health Sciences 10(1):82.
Inada T. 2001. Yuudoru suru Kyuu-Sekki Jin. Tokyo: Iwanami Shoten (in Japanese).
Isanaka S, Mugusi F, Urassa W, Willett WC, Bosch RJ, Villamor E, Spiegelman D, Duggan C, and Fawzi WW. 2011. Iron Deficiency and Anemia Predict Mortality in Patients with Tuberculosis. The Journal of Nutrition 142(2):350-357.

Izuho M, Hayashi K, Nakazawa Y, Soda T, Oda N, Yamahara T, Kitazawa M, and Buvit I. 2014. Investigating the Eolian Context of the Last Glacial Maximum Occupation at Kawanishi-C, Hokkaido, Japan. Geoarchaeology 29(3):202-220.
Jaffe HL. 1972. Metabolic, Degenerative, and Inflammatory Diseases of Bones and Joints. London: Lea and Febiger.
Jandal JM. 1996. Comparative Aspects of Goat and Sheep Milk. Small Ruminant Research 22(2):177-185.
Janz L, Odsuren D, and Bukhchuluun D. 2017. Transitions in Palaeoecology and Technology: Hunter-gatherers and Early Herders in the Gobi Desert. Journal of World Prehistory 30(1):1-80.
Jeanty P. 1983. Fetal Limb Biometry. Radiology 147(2):601-602.
Jeong C, Wang K, Wilkin S, Taylor WTT, Miller B, Ulziibayar S, Stahl R, Chiovelli C, Bemmann JH, and Knolle F. 2020. A Dynamic 6,000-Year Genetic History of Eurasia's Eastern Steppe. bioRxiv.
Jeong C, Wilkin S, Amgalantugs T, Bouwman AS, Taylor WTT, Hagan RW, Bromage S, Tsolmon S, Trachsel C, and Grossmann J. 2018. Bronze Age Population Dynamics and the Rise of Dairy Pastoralism on the Eastern Eurasian Steppe. Proceedings of the National Academy of Sciences 115(48):E11248-E11255.
Johansson SR, and Horowitz S. 1986. Estimating Mortality in Skeletal Populations: Influence of the Growth Rate on the Interpretation of Levels and Trends during the Transition to agriculture. American Journal of Physical Anthropology 71(2):233-250.
Johns D. 1970. Syphilitic Disorders of the Spine: Report of Two Cases. The Journal of Bone and Joint Surgery British Volume 52(4):724-731.
Jones B. 1972. Doigt en Lorgnette and Concentric Bone Atrophy Associated with Healed Yaws Osteitis: Report of Two Cases. The Journal of Bone and Joint Surgery British Volume 54(2):341-345.
Jones J, and Joseph V. 2008. Excavation of a Xiongnu Satellite Burial. The Silk Road 5(2):36-41.
Jones RK. 2017. Transitions to Animal Domestication in Southeast Asia: Zooarchaeological Analysis of Cồn Cổ Ngựa and Mán Bạc, Vietnam. Canberra, Australia: Australian National University.
Jones RK, Piper PJ, Groves CP, Anh TN, Thi MHN, Thị HN, Hoang TH, and Oxenham MF. 2019. Shifting Subsistence Patterns from the Terminal Pleistocene to Late Holocene: A Regional Southeast Asian Analysis. Quaternary International 529:47-56.
Junqueira L, and Carneiro J. 1980. Basic Histology Los Altos, Califronia: Lange Medical Publication.
Kaestle FA, and Horsburgh KA. 2002. Ancient DNA in Anthropology: Methods, Applications, and Ethics. American Journal of Physical Anthropology 119(S35):92-130.
Kaidonis JA. 2008. Tooth Wear: The View of the Anthropologist. Clinical Oral Investigations 12(1):21-26.
Kalinova K, Proichev V, Stefanova P, Tokmakova K, and Poriazova E. 2005. Hydatid Bone Disease: A Case Report and Review of the Literature. Journal of Orthopaedic Surgery 13(3):323-325.
Kallio H, Yang B, and Peippo P. 2002. Effects of Different Origins and Harvesting Time on Vitamin C, Tocopherols, and Tocotrienols in Sea Buckthorn (Hippophaë rhamnoides) Berries. Journal of Agricultural and Food Chemistry 50(21):6136-6142.

Kalra S, Kumar A, Jarhyan P, and Unnikrishnan AG. 2015. Endemic or Epidemic? Measuring the Endemicity Index of Diabetes. Indian Journal of Endocrinology and Metabolism 19(1):5-7.
Kanehara M. 1995. In the Forefront of Research, Jomon People Suffered from Parasites. Gekkan Rekishi Kaido 84.
Kanthawang T, Pattamapaspong N, and Louthrenoo W. 2016. Acute Bone Infarction: A Rare Complication in Thalassemia. Skeletal Radiology 45(7):1013-1016.
Karamba WR, Quiñones EJ, and Winters P. 2011. Migration and Food Consumption Patterns in Ghana. Food policy 36(1):41-53.
Karstens S, Littleton J, Frohlich B, Amgaluntugs T, Pearlstein K, and Hunt D. 2018. A Palaeopathological Analysis of Skeletal Remains from Bronze Age Mongolia. HOMO 69(6):324-334.
Kawahata H. 2019. Climatic Reconstruction at the Sannai-Maruyama Site between Bond Events 4 and 3—Implication for the Collapse of the Society at 4.2 ka Event. Progress in Earth and Planetary Science 6(1):63.
Kawahata H, Yamamoto H, Ohkushi Ki, Yokoyama Y, Kimoto K, Ohshima H, and Matsuzaki H. 2009. Changes of Environments and Human Activity at the Sannai-Maruyama Ruins in Japan during the Mid-Holocene Hypsithermal Climatic Interval. Quaternary Science Reviews 28(9-10):964-974.
Kawashima T. 2013. Social Change at the End of the Middle Jomon: A Perspective From Resilience Theory. Documenta Praehistorica 40:227-232.
Kawashima T. 2016. Food Processing and Consumption in the Jōmon. Quaternary International 404:16-24.
Kazadi WM, Asiedu KB, Agana N, and Mitjà O. 2014. Epidemiology of Yaws: An Update. Clinical Epidemiology 6:119.
Kazda J. 2000. The Ecological Approach to Leprosy: Non-Cultivable Acid-Fast Bacilli and Environmentally-Derived M. leprae. The Ecology of Mycobacteria: Springer. p 40-47.
Keenan S, Mitts KG, and Kurtz CA. 2002. Scurvy Presenting as a Medial Head Tear of the Gastrocnemius. Orthopedics 25(6):689-691.
Kelley MA, and Micozzi MS. 1984. Rib Lesions in Chronic Pulmonary Tuberculosis. American Journal of Physical Anthropology 65(4):381-386.
Kelly D, and Coutts A. 2000. Early Nutrition and the Development of Immune Function in the Neonate. Proceedings of the Nutrition Society 59(2):177-185.
Key JA. 1940. The Pathology of Tuberculosis of the Spine. The Journal of Bone and Joint Surgery 22(3):799-806.
Keyser-Tracqui C, Crubézy E, Pamzsav H, Varga T, and Ludes B. 2006. Population Origins in Mongolia: Genetic Structure Analysis of Ancient and Modern DNA. American Journal of Physical Anthropology 131(2):272-281.
Khan S, Varshney M, Hasan A, Kumar A, and Trikha V. 2007. Tuberculosis of the Sternum: A Clinical Study. The Journal of Bone and Joint Surgery British Volume 89(6):817-820.
Kharbanda Y, and Dhir R. 1991. Natural Course of Hematogenous Pyogenic Osteomyelitis (A Retrospective Study of 110 Cases). Journal of Postgraduate Medicine 37(2):69.
Khaw K-T, and Woodhouse P. 1995. Interrelation of Vitamin C, Infection, Haemostatic Factors, and Cardiovascular Disease. Bmj 310(6994):1559-1563.
Khoach NB. 1980. Phung Nguyen. Asian Perspectives 23(1):23-54.
Killgrove K. 2010. Migration and Mobility in Imperial Rome: University of North Carolina at Chapel Hill.

Killip S, Bennett JM, and Chambers MD. 2007. Iron Deficiency Anemia. American Family Physician 20:671-678.
Kim K, Brenner CH, Mair VH, Lee KH, Kim JH, Gelegdorj E, Batbold N, Song YC, Yun HW, and Chang EJ. 2010. A Western Eurasian Male is Found in 2000-year-old Elite Xiongnu Cemetery in Northeast Mongolia. American Journal of Physical Anthropology 142(3):429-440.
King CL, Bentley RA, Higham C, Tayles N, Viðarsdóttir US, Layton R, Macpherson CG, and Nowell G. 2014. Economic Change after the Agricultural Revolution in Southeast Asia? Antiquity 88(339):112-125.
King CL, Halcrow SE, Tayles N, and Shkrum S. 2017. Considering the Palaeoepidemiological Implications of Socioeconomic and Environmental Change in Southeast Asia. Archaeological Research in Asia 11:27-37.
Kirch PV. 1997. The Lapita Peoples: Ancestors of the Oceanic World. The Peoples of South-East Asia and the Pacific: Blackwell, Cambridge, MA.
Kivisild T. 2017. The Study of Human Y Chromosome Variation through Ancient DNA. Human Genetics 136(5):529-546.
Kiyono K. 1969. Nihon Kaizuka no Kenkyu (In Japanese). Tokyo, Japan: Iwanami Shoten.
Kiyono K, Shimada S, and Hamada K. 1920. The Excavation of the Shell-Drive at Tsukumo, a Neolithic Cemetery in the Province of Bitchu. Report Upon Archaeological Research. Kyoto: Department of Literature, Kyoto Imperial University (in Japanese).
Klaus HD. 2014. Frontiers in the Bioarchaeology of Stress and Disease: Cross-Disciplinary Perspectives from Pathophysiology, Human Biology, and Epidemiology. American Journal of Physical Anthropology 155(2):294-308.
Klaus HD. 2017. Paleopathological Rigor and Differential Diagnosis: Case Studies involving Terminology, Description, and Diagnostic Frameworks for Scurvy in Skeletal Remains. International Journal of Paleopathology 19:96-110.
Klaus HD, and Lynnerup N. 2019. Abnormal Bone: Considerations for Documentation, Disease Process Identification, and Differential Diagnosis. In: Buikstra JE, editor. Ortner's Identification of Pathological Conditions in Human Skeletal Remains. London, UK: Academic Press. p 59-89.
Klein GL, and Simmons DJ. 1993. Nutritional Rickets: Thoughts About Pathogenesis. Annals of Medicine 25(4):379-384.
Klein JO. 1994. Otitis Media. Clinical Infectious Diseases 19(5):823-832.
Klein SL, and Flanagan KL. 2016. Sex Differences in Immune Responses. Nature Reviews Immunology 16(10):626.
Knechel NA. 2009. Tuberculosis: Pathophysiology, Clinical Features, and Diagnosis. Critical Care Nurse 29(2):34-43.
Kodaman N, Sobota RS, Mera R, Schneider BG, and Williams SM. 2014. Disrupted Human–Pathogen Co-evolution: A Model for Disease. Frontiers in Genetics 5:290.
Koletsi D, and Pandis N. 2017. Survival Analysis, Part 2: Kaplan-Meier Method and the Log-Rank Test. American Journal of Orthodontics and Dentofacial Orthopedics 152(4):569-571.
Komar D, and Buikstra JE. 2003. Differential Diagnosis of a Prehistoric Biological Object from the Koster (Illinois) Site. International Journal of Osteoarchaeology 13(3):157-164.
Kontuly T, and Smith KR. 1995. Culture as a Determinant of Reasons for Migration. The Social Science Journal 32(2):179-193.
Koudou B, Tano Y, Doumbia M, Nsanzabana C, Cissé G, Girardin O, Dao D, N'goran E, Vounatsou P, and Bordmann G. 2005. Malaria Transmission Dynamics in Central

Côte d'Ivoire: The Influence of Changing Patterns of Irrigated Rice Agriculture. Medical and Veterinary Entomology 19(1):27-37.
Kovalev AA, and Erdenebaatar D. 2009. Discovery of New Cultures of the Bronze Age in Mongolia according to the Data Obtained by the International Central Asian Archaeological Expedition. In: Bemmann J, Parzinger H, Pohl E, and Tseveendorzh D, editors. Current Archaeological Research in Mongolia. Bonn, Germany: Rheinische Friedrich-Wilhelms-Universität. p 149-170.
Koyama S. 1979. Jomon Subsistence and Population. Senri Ethnological Studies 2:1-65.
Kradin N. 2011. Stateless Empire: The Structure of the Xiongnu Nomadic Super-Complex Chiefdom. Xiongnu Archaeology: Multidisciplinary Perspectives of the First Steppe Empire in Inner Asia. Bonn, Germany: Rheinische Friedrich-Wilhelms-Universität. p 77-96.
Krishan K, Chatterjee PM, Kanchan T, Kaur S, Baryah N, and Singh R. 2016. A Review of Sex Estimation Techniques during Examination of Skeletal Remains in Forensic Anthropology Casework. Forensic Science International 261:165. e161-165. e168.
Kumar SS, Nasidze I, Walimbe S, and Stoneking M. 2000. Brief Communication: Discouraging Prospects for Ancient DNA from India. American Journal of Physical Anthropology 113(1):129-133.
Kurtaran B, Akyildiz O, Ulu AC, Inal SA, Komur S, Seydaoglu G, Arslan YK, Yaman A, Kibar F, and Aksu HSZ. 2016. The Relationship between Brucellosis and Vitamin D. The Journal of Infection in Developing Countries 10(02):176-182.
Kusaka S, Ando A, Nakano T, Yumoto T, Ishimaru E, Yoneda M, Hyodo F, and Katayama K. 2009. A Strontium Isotope Analysis on the Relationship Between Ritual Tooth Ablation and Migration among the Jomon People in Japan. Journal of Archaeological Science 36(10):2289-2297.
Kusaka S, Hyodo F, Yumoto T, and Nakatsukasa M. 2010. Carbon and Nitrogen Stable Isotope Analysis on the Diet of Jomon Populations from Two Coastal Regions of Japan. Journal of Archaeological Science 37(8):1968-1977.
Kusaka S, Nakano T, Morita W, and Nakatsukasa M. 2012. Strontium Isotope Analysis to Reveal Migration in Relation to Climate Change and Ritual Tooth Ablation of Jomon Skeletal Remains from Western Japan. Journal of Anthropological Archaeology 31(4):551-563.
Kusaka S, Nakano T, Yumoto T, and Nakatsukasa M. 2011. Strontium Isotope Evidence of Migration and Diet in Relation to Ritual Tooth Ablation: A Case Study from the Inariyama Jomon Site, Japan. Journal of Archaeological Science 38(1):166-174.
Kusaka S, Uno KT, Nakano T, Nakatsukasa M, and Cerling TE. 2015. Carbon Isotope Ratios of Human Tooth Enamel Record the Evidence of Terrestrial Resource Consumption during the Jomon Period, Japan. American Journal of Physical Anthropology 158(2):300-311.
Kuzmina EE. 1998. Cultural Connections of the Tarim Basin People and Pastoralists of the Asian Steppes in the Bronze Age. In: Mair VH, editor. The Bronze Age and early Iron Age peoples of Eastern Central Asia: Institute for the Study of Man. p 63-93.
LaFond EM. 1958. An Analysis of Adult Skeletal Tuberculosis. The Journal of Bone and Joint Surgery 40(2):346-364.
Lamberg-Allardt C. 2006. Vitamin D in Foods and as Supplements. Progress in Biophysics and Molecular Biology 92(1):33-38.
Lane WR, Looney SW, and Wansley JW. 1986. An Application of the Cox Proportional Hazards Model to Bank Failure. Journal of Banking & Finance 10(4):511-531.

Larsen CS. 1995. Biological Changes in Human Populations with Agriculture. Annual Review of Anthropology 24(1):185-213. DOI: 10.1146/annurev.an.24.100195.001153
Larsen CS. 2006. The Agricultural Revolution as Environmental Catastrophe: Implications for Health and Lifestyle in the Holocene. Quarternary International 150(1):12-20. DOI: 10.1016/j.quaint.2006.01.004
Larsen CS, Hillson SW, Boz B, Pilloud MA, Sadvari JW, Agarwal SC, Glencross B, Beauchesne P, Pearson J, and Ruff CB. 2015. Bioarchaeology of Neolithic Çatalhöyük: Lives and Lifestyles of an Early Farming Society in Transition. Journal of World Prehistory 28(1):27-68.
Larson G, Cucchi T, Fujita M, Matisoo-Smith E, Robins J, Anderson A, Rolett B, Spriggs M, Dolman G, and Kim T-H. 2007. Phylogeny and Ancient DNA of Sus Provides Insights into Neolithic Expansion in Island Southeast Asia and Oceania. Proceedings of the National Academy of Sciences 104(12):4834-4839.
Lawson JP, Ablow RC, and Pearson HA. 1981. The Ribs in Thalassemia. II. The Pathogenesis of the Changes. Radiology 140(3):673-679.
Lawson JP, Ablow RC, and Pearson HA. 1983. Premature Fusion of the Proximal Humeral Epiphyses in Thalassemia. American Journal of Roentgenology 140:239-244.
Leder K, and Newman D. 2005. Respiratory Infections During Air Travel. Internal Medicine Journal 35(1):50-55.
Lee C. 2013. The Population History of China and Mongolia from the Bronze Age to the Medieval Period (2500 BC-AD 1500). In: Pechenkina K, and Oxenham M, editors. Bioarchaeology of East Asia: Movement, Contact, Health. Gainesville: University Press of Florida. p 61-84.
Lee C, and Linhu Z. 2011. Xiongnu Population History in Relation to China, Manchuria, and the Western Regions. Xiongnu Archaeology:193-200.
Lee JA, Hwang JS, Hwang IT, Kim DH, Seo J-H, and Lim JS. 2015. Low Vitamin D Levels are Associated with Both Iron Deficiency and Anemia in Children and Adolescents. Pediatric Hematology and Oncology 32(2):99-108.
Léger D. 2008. Scurvy: Reemergence of Nutritional Deficiencies. Canadian Family Physician 54(10):1403-1406.
Lentz RD, Brown DM, and Kjellstrand CM. 1978. Treatment of Severe Hypophosphatemia. Annals of Internal Medicine 89(6):941-944.
Lew DP, and Waldvogel FA. 2004. Osteomyelitis. The Lancet 364(9431):369-379.
Lewinsohn DA, and Lewinsohn DM. 2008. Immunologic Susceptibility of Young Children to Mycobacterium tuberculosis. Pediatric Research 63(2):115.
Lewis M. 2011a. The Osteology of Infancy and Childhood: Misconceptions and Potential. (Re)thinking the Little Ancestor: New Perspectives on the Archaeology of Infancy and Childhood. Oxford, UK: Archaeopress. p 1-13.
Lewis M. 2012. Thalassaemia: Its Diagnosis and Interpretation in Past Skeletal Populations. International Journal of Osteoarchaeology 22(6):685-693.
Lewis ME. 2011b. Tuberculosis in the Non-Adults from Romano-British Poundbury Camp, Dorset, England. International Journal of Paleopathology 1(1):12-23.
Lewis ME. 2017. Paleopathology of Children: Identification of Pathological Conditions in the Human Skeletal Remains of Non-Adults. London: Academic Press.
Lewis ME, and Gowland R. 2007. Brief and Precarious Lives: Infant Mortality in Contrasting Sites from Medieval and post-Medieval England (AD 850–1859). American Journal of Physical Anthropology 134(1):117-129.

Lewis SJ, Mcdowell I, and Hawthorne AB. 1998. Vitamin C Deficiency in Asian Women. Nutrition (Burbank, Los Angeles County, Calif) 14(2):231.
Li M, Roberts CA, Chen L, and Zhao D. 2019. A Male Adult Skeleton from the Han Dynasty in Shaanxi, China (202 BC–220 AD) with Bone Changes that Possibly Represent Spinal Tuberculosis. International Journal of Paleopathology 27:9-16.
Lieverse AR. 2005. Bioarchaeology of the Cis-Baikal: Biological Indicators of mid-Holocene Hunter-Gatherer Adaptation and Cultural Change: Cornell University.
Linster CL, and Van Schaftingen E. 2007. Vitamin C. The FEBS journal 274(1):1-22.
Lipson M, Cheronet O, Mallick S, Rohland N, Oxenham M, Pietrusewsky M, Pryce TO, Willis A, Matsumura H, and Buckley H. 2018. Ancient Genomes Document Multiple Waves of Migration in Southeast Asian Prehistory. Science 361(6397):92-95. DOI: 10.1126/science.aat3188
Littleton J, Floyd B, Frohlich B, Dickson M, Amgalantögs T, Karstens S, and Pearlstein K. 2012. Taphonomic Analysis of Bronze Age Burials in Mongolian Khirigsuurs. Journal of Archaeological Science 39(11):3361-3370.
Liu L. 2018. Heart Failure: Epidemiology and Research Methods. Elsevier Health Sciences.
Liu S, Chu H, Hsu H, Chao H, and Cheu S. 1941. Calcium and Phosphorus Metabolism in Osteomalacia. XI. The Pathogenetic Role of Pregnancy and Relative Importance of Calcium and Vitamin D Supply. The Journal of Clinical Investigation 20(3):255-271.
Liu X, Hunt HV, and Jones MK. 2009. River Valleys and Foothills: Changing Archaeological Perceptions of North China's Earliest Farms. Antiquity 83(319):82-95.
Llorente MG, Jones ER, Eriksson A, Siska V, Arthur K, Arthur J, Curtis M, Stock JT, Coltorti M, and Pieruccini P. 2015. Ancient Ethiopian Genome Reveals Extensive Eurasian Admixture in Eastern Africa. Science 350(6262):820-822.
Lockwood DN. 2004. Commentary: Leprosy and Poverty. International Journal of Epidemiology 33(2):269-270.
Lombardi GP, and García Cáceres U. 2000. Multisystemic Tuberculosis in a Pre-Columbian Peruvian Mummy: Four Diagnostic Levels, and a Paleoepidemiological Hypothesis. Chungará (Arica) 32(1):55-60.
Lopez A, Cacoub P, Macdougall IC, and Peyrin-Biroulet L. 2016. Iron Deficiency Anaemia. The Lancet 387(10021):907-916.
Lovejoy CO, Meindl RS, Pryzbeck TR, and Mensforth RP. 1985. Chronological Metamorphosis of the Auricular Surface of the Ilium: A New Method for the Determination of Adult Skeletal Age at Death. American Journal of Physical Anthropology 68(1):15-28.
Lovell WG. 1992. “Heavy Shadows and Black Night”: Disease and Depopulation in Colonial Spanish America. Annals of the Association of American Geographers 82(3):426-443.
Loyer J, Murphy E, Ruppe M, Moiseyev V, Khartanovich V, Zammit J, Rottier S, Potrakhov N, Bessonov V, and Obodovskiy A. 2019. Co-Morbidity with Hypertrophic Osteoarthropathy: A Possible Iron Age Sarmatian Case from the Volga Steppe of Russia. International Journal of Paleopathology 24:66-78.
Luck MR, Jeyaseelan I, and Scholes RA. 1995. Ascorbic Acid and Fertility. Biology of Reproduction 52(2):262-266.
Lukacs JR. 1992. Dental Paleopathology and Agricultural Intensification in South Asia: New Evidence from Bronze Age Harappa. American Journal of Physical Anthropology 87(2):133-150.

Lukert B, Higgins J, and Stoskopf M. 1992. Menopausal Bone Loss is Partially Regulated by Dietary Intake of Vitamin D. Calcified Tissue International 51(3):173-179.
Lummaa V, and Clutton-Brock T. 2002. Early Development, Survival and Reproduction in Humans. Trends in Ecology & Evolution 17(3):141-147.
Maat G. 2004. Scurvy in Adults and Youngsters: The Dutch Experience. A Review of the History and Pathology of a Disregarded Disease. International Journal of Osteoarchaeology 14(2):77-81.
Machicek M, and Beach J. 2013. Stress of Life: A Preliminary Study of Degenerative Joint Disease and Dental Health among Ancient Populations of Inner Asia. In: Pechenkina K, and Oxenham M, editors. Bioarchaeology of East Asia: Movement, Contact, Health: University Press of Florida. p 246-264.
Machicek M, Chenery C, Evans J, Cameron A, and Chamberlain A. 2019. Pastoralist Strategies and Human Mobility: Oxygen (δ 18 O p) and Strontium (87 Sr/86 Sr) Isotopic Analysis of Early Human Remains from Egiin Gol and Baga Gazaryn Chuluu, Mongolia. Archaeological and Anthropological Sciences 11(12):6649-6662.
Mackie E, Ahmed Y, Tatarczuch L, Chen K-S, and Mirams M. 2008. Endochondral Ossification: How Cartilage is Converted into Bone in the Developing Skeleton. The International Journal of Biochemistry & Cell Biology 40(1):46-62.
Macpherson C. 1995. The Effect of Transhumance on the Epidemiology of Animal Diseases. Preventive Veterinary Medicine 25(2):213-224.
MacPherson DW, and Gushulak BD. 2001. Human Mobility and Population Health: New Approaches in a Globalizing World. Perspectives in Biology and Medicine 44(3):390-401.
MacPherson DW, Gushulak BD, Baine WB, Bala S, Gubbins PO, Holtom P, and Segarra-Newnham M. 2009. Population Mobility, Globalization, and Antimicrobial Drug Resistance. Emerging Infectious Diseases 15(11):1727-1731.
Madkour MM, Sharif H, Abed M, and Al-Fayez M. 1988. Osteoarticular Brucellosis: Results of Bone Scintigraphy in 140 Patients. American Journal of Roentgenology 150(5):1101-1105.
Mai Huong NT. 2013. Neolithic Vegetation in Northern Vietnam: An Indication of Early Agricultural Activities. Journal of Austronesian Studies 4:1.
Mai Huong NT. 2016. Burnt Rice from Four Archaeological Sites in Northern Vietnam. Vietnam Social Sciences(3):64-77.
Makarewicz C. 2011. Xiongnu Pastoral Systems: Integrating Economies of Subsistence and Scale. Xiongnu Archaeology: Multidisciplinary Perspectives of the First Steppe Empire in Inner Asia. Bonn, Germany: Rheinische Friedrich-Wilhelms-Universität. p 181-192.
Makarewicz CA. 2017. Winter is Coming: Seasonality of Ancient Pastoral Nomadic Practices Revealed in the Carbon (δ 13 C) and Nitrogen (δ 15 N) Isotopic Record of Xiongnu Caprines. Archaeological and Anthropological Sciences 9(3):405-418.
Manchester K. 1984. Tuberculosis and Leprosy in Antiquity: An Interpretation. Medical History 28(2):162-173.
Manchester K, and Roberts C. 1989. The Palaeopathology of Leprosy in Britain: A Review. World Archaeology 21(2):265-272.
Mao S, and Huang S. 2014. Vitamin D Receptor Gene Polymorphisms and the Risk of Rickets among Asians: a Meta-Analysis. Archives of Disease in Childhood 99(3):232-238.
Marais BJ, Loennroth K, Lawn SD, Migliori GB, Mwaba P, Glaziou P, Bates M, Colagiuri R, Zijenah L, and Swaminathan S. 2013. Tuberculosis Comorbidity with

Communicable and Non-Communicable Diseases: Integrating Health Services and Control Efforts. The Lancet Infectious Diseases 13(5):436-448.
Marangoni F, Cetin I, Verduci E, Canzone G, Giovannini M, Scollo P, Corsello G, and Poli A. 2016. Maternal Diet and Nutrient Requirements in Pregnancy and Breastfeeding. An Italian Consensus Document. Nutrients 8(10):629.
Maresh M. 1970. Measurements from Roentgenograms, Heart Size, Long Bone Lengths, Bone, Muscles and Fat Widths, Skeletal Maturation. Human Growth and Development:155-200.
Mari L, Bertuzzo E, Righetto L, Casagrandi R, Gatto M, Rodriguez-Iturbe I, and Rinaldo A. 2012. Modelling Cholera Epidemics: The Role of Waterways, Human Mobility and Sanitation. Journal of the Royal Society Interface 9(67):376-388.
Marks M, Solomon AW, and Mabey DC. 2014. Endemic Treponemal Diseases. Transactions of the Royal Society of Tropical Medicine and Hygiene 108(10):601-607.
Martens P, Kovats R, Nijhof S, De Vries P, Livermore M, Bradley D, Cox J, and McMichael A. 1999. Climate Change and Future Populations at Risk of Malaria. Global Environmental Change 9:S89-S107.
Martin DL, and Goodman AH. 2002. Health Conditions before Columbus: Paleopathology of Native North Americans. Western Journal of Medicine 176(1):65-68.
Masaki T, Qu J, Cholewa-Waclaw J, Burr K, Raaum R, and Rambukkana A. 2013. Reprogramming Adult Schwann Cells to Stem Cell-like Cells by Leprosy Bacilli Promotes Dissemination of Infection. Cell 152(1-2):51-67.
Mathews DM, John R, Verghese V, Parmar H, Chaudhary N, Mishra S, and Mathew L. 2016. Histoplasma Capsulatum Infection with Extensive Lytic Bone Lesions Mimicking LCH. Journal of Tropical Pediatrics 62(6):496-499.
Matisoo-Smith E. 2009. The Commensal Model for Human Settlement of the Pacific 10 Years On—What Can We Say and Where to Now? The Journal of Island and Coastal Archaeology 4(2):151-163.
Matsui A, and Kanehara M. 2006. The Question of Prehistoric Plant Husbandry during the Jomon Period in Japan. World Archaeology 38(2):259-273.
Matsumoto N, Habu J, and Matsui A. 2017. Subsistence, Sedentism, and Social Complexity among Jomon Hunter-Gatherers of the Japanese Archipelago. Handbook of East and Southeast Asian Archaeology: Springer. p 437-450.
Matsumura H. 2006. The Population History of Southeast Asia Viewed from Morphometric Analyses of Human Skeletal and Dental remains. Bioarchaeology of Southeast Asia Cambridge University Press, Cambridge:33-58.
Matsumura H, Hung H-C, Cuong NL, Zhao Y-f, He G, and Chi Z. 2017. Mid-Holocene Hunter-Gatherers 'Gaomiao' in Hunan, China: The First of the Two-Layer Model in the Population History of East/Southeast Asia. New Perspectives in Southeast Asian and Pacific Prehistory. Canberra, Australia: ANU ePress. p 61-78.
Matsumura H, Nguyen LC, Nguyen KT, and Anezake T. 2001. Dental Morphology of the Early Hoabinian, the Neolithic Da But and the Metal Age Dong Son Civilized Peoples in Vietnam. Zeitschrift für Morphologie und Anthropologie 83(1):59-73.
Matsumura H, and Oxenham M. 2013. Population Dispersal from East Asia into Southeast Asia: Evidence from Cranial and Dental Morphology. In: Pechenkina EA, and Oxenham M, editors. Bioarchaeology of East Asia: Movement, Contact, Health. Gainesville, USA: University Press of Florida. p 179-212.
Matsumura H, and Oxenham M. 2014. Demographic Transitions and Migration in Prehistoric East/Southeast Asia Through the Lens of Nonmetric Dental Traits.

American Journal of Physical Anthropology 155(1):45-65. DOI: 10.1002/ajpa.22537
Matsumura H, Oxenham MF, Dodo Y, Domett K, Thuy NK, Cuong NL, Dung NK, Huffer D, and Yamagata M. 2008. Morphometric Affinity of the Late Neolithic Human Remains from Man Bac, Ninh Binh Province, Vietnam: Key Skeletons with Which to Debate the 'Two Layer' Hypothesis. Anthropological Science 116(2):135-148.
Mays S. 2014. The Palaeopathology of Scurvy in Europe. International Journal of Paleopathology 5:55-62.
Mays S, Fysh E, and Taylor GM. 2002. Investigation of the Link between Visceral Surface Rib Lesions and Tuberculosis in a Medieval Skeletal series from England using Ancient DNA. American Journal of Physical Anthropology 119(1):27-36.
Mays SA. 2005. Paleopathological Study of Hallux Valgus. American Journal of Physical Anthropology 126(2):139-149.
McColl H, Racimo F, Vinner L, Demeter F, Gakuhari T, Moreno-Mayar JV, Van Driem G, Wilken UG, Seguin-Orlando A, and De la Fuente Castro C. 2018. The Prehistoric Peopling of Southeast Asia. Science 361(6397):88-92. DOI: 10.1126/science.aat3628
McDonell A, and Oxenham MF. 2014. Localised Primary Canine Hypoplasia: Implications for Maternal and Infant Health at Man Bac, Vietnam, 4000–3500 years BP. International Journal of Osteoarchaeology 24(4):531-539. DOI: 10.1002/oa.2239
McEvoy BP, and Visscher PM. 2009. Genetics of Human Height. Economics & Human Biology 7(3):294-306.
McFadden A, Muellner P, Baljinnyam Z, Vink D, and Wilson N. 2016. Use of Multicriteria Risk Ranking of Zoonotic Diseases in a Developing Country: Case Study of Mongolia. Zoonoses and Public Health 63(2):138-151.
McFadden C, Buckley H, Halcrow SE, and Oxenham MF. 2018. Detection of Temporospatially Localized Growth in Ancient Southeast Asia Using Human Skeletal Remains. Journal of Archaeological Science 98:93-101. DOI: 10.1016/j.jas.2018.08.010
McFadden C, and Oxenham M. 2020. A Paleoepidemiological Approach to the Osteological Paradox: Investigating Stress, Frailty and Resilience through Cribra Orbitalia. American Journal of Physical Anthropology.
McFadden C, and Oxenham MF. 2016. Revisiting the Phenice Technique Sex Classification Results Reported by MacLaughlin and Bruce (1990). American Journal of Physical Anthropology 159(1):182-183.
McFadden C, and Oxenham MF. 2018a. The D0-14/D Ratio: A New Paleodemographic Index and Equation for Estimating Total Fertility Rates. American Journal of Physical Anthropology 165(3):471-479. DOI: 10.1002/ajpa.23365
McFadden C, and Oxenham MF. 2018b. Rate of Natural Population Increase as a Paleodemographic Measure of Growth. Journal of Archaeological Science: Reports 19:352-356.
McGrath J. 2001. Does 'Imprinting' with Low Prenatal Vitamin D Contribute to the Risk of Various Adult Disorders? Medical Hypotheses 56(3):367-371.
McGrath R, and Boyd WE. 2001. The Chronology of the Iron Age 'Moats' of Northeast Thailand. Antiquity 75(288):349-360.
McIlvaine BK. 2015. Implications of Reappraising the Iron-Deficiency Anemia Hypothesis. International Journal of Osteoarchaeology 25(6):997-1000.

McKern TW, and Stewart TD. 1957. Skeletal Age Changes in Young American Males Analysed from the Standpoint of Age Identification. Quartermaster Research and Engineering Command Natick MA
McKillup S. 2006. Statistics Explained: An Introductory Guide for Life Scientists. Cambridge UK: Cambridge University Press. 2006 p.
Mehmet F, Ali G, Kemal N, Remzi Ç, Jale S, Bunyamin D, and Celal A. 2002. Musculoskeletal Involvement in Brucellosis in Different Age Groups: A Study of 195 Cases. Swiss Medical Weekly 132(0708).
Mehta AB, and Hoffbrand AV. 2009. Haematology at a Glance. Oxford, UK: John Wiley & Sons.
Meindl RS, and Lovejoy CO. 1985. Ectocranial Suture Closure: A Revised Method for the Determination of Skeletal Age at Death based on the Lateral-Anterior Sutures. American Journal of Physical Anthropology 68(1):57-66.
Mejia LA. 1993. Role of Vitamin A in Iron Deficiency Anemia. Nestle Nutrition Workshop Series: Rowen Press. p 93-93.
Meltzer E, Sidi Y, Smolen G, Banai M, Bardenstein S, and Schwartz E. 2010. Sexually Transmitted Brucellosis in hHumans. Clinical Infectious Diseases 51(2):e12-e15.
Menendez C, Fleming A, and Alonso P. 2000. Malaria-Related Anaemia. Parasitology Today 16(11):469-476.
Menger D-J, Fokkens WJ, Lohuis PJ, Ingels KJ, and Trenité GJN. 2007. Reconstructive Surgery of the Leprosy Nose: A New Approach. Journal of Plastic, Reconstructive & Aesthetic Surgery 60(2):152-162.
Merkle E, Kramme E, Vogel J, Krämer S, Schulte M, Usadel S, Kern P, and Brambs H-J. 1997. Bone and Soft Tissue Manifestations of Alveolar Echinococcosis. Skeletal Radiology 26(5):289-292.
Merler S, and Ajelli M. 2010. The Role of Population Heterogeneity and Human Mobility in the Spread of Pandemic Influenza. Proceedings of the Royal Society B: Biological Sciences 277(1681):557-565.
Micarelli I, Paine RR, Tafuri MA, and Manzi G. 2019. A Possible Case of Mycosis in a Post-Classical Burial from La Selvicciola (Italy). International Journal of Paleopathology 24:25-33.
Miles AEW. 2001. The Miles Method of Assessing Age from Tooth Wear Revisited. Journal of Archaeological Science 28(9):973-982.
Miller G, Ridley M, and Medd W. 1963. Typhoid Osteomyelitis of the Spine. British Medical Journal 1(5337):1068.
Miller LH, Good MF, and Milon G. 1994. Malaria Pathogenesis. Science 264(5167):1878-1883.
Milner GR, and Boldsen JL. 2012. Estimating Age and Sex from the Skeleton, a Paleopathological Perspective. In: Grauer A, editor. A Companion to Paleopathology: John Wiley & Sons. p 268-284.
Milner GR, and Boldsen JL. 2017. Life Not Death: Epidemiology from Skeletons. International Journal of Paleopathology 17:26-39.
Mitchell PD. 2006. Trauma in the Crusader Period City of Caesarea: A Major Port in the Medieval Eastern Mediterranean. International Journal of Osteoarchaeology 16(6):493-505.
Mitchell PD. 2012. Integrating Historical Sources with Paleopathology. In: Grauer AL, editor. A Companion to Paleopathology. New York: Wiley-Blackwell. p 310-338.
Mitjà O, Asiedu K, and Mabey D. 2013. Yaws. The Lancet 381(9868):763-773.
Mocellin J, and Foggin P. 2008. Health Status and Geographic Mobility Among Semi-Nomadic Pastoralists in Mongolia. Health & Place 14(2):228-242.

Moe SM, Zidehsarai MP, Chambers MA, Jackman LA, Radcliffe JS, Trevino LL, Donahue SE, and Asplin JR. 2011. Vegetarian Compared with Meat Dietary Protein Source and Phosphorus Homeostasis in Chronic Kidney Disease. Clinical Journal of the American Society of Nephrology 6(2):257-264.
Møller-Christensen V. 1961. Bone Changes in Leprosy. Copenhagen, Denmark: Munksgaard.
Møller-Christensen V. 1978. Leprosy Changes of the Skull. Odense, Denmark: Odense University Press.
Møller-Christensen V, Bakke SN, Melsom RS, and Waaler E. 1952. Changes in the Anterior Nasal Spine and the Alveolar Process of the Maxillary Bone in Leprosy. International Journal of Leprosy 20:335-340.
Molnar P. 2011. Extramasticatory Dental Wear Reflecting Habitual Behavior and Health in Past Populations. Clinical Oral Investigations 15(5):681-689.
Molnar S. 1971. Human Tooth Wear, Tooth Function and Cultural Variability. American Journal of Physical Anthropology 34(2):175-189.
Molto JE, Kirkpatrick CL, and Keron J. 2019. The Paleoepidemiology of Sacral Spina Bifida Occulta in Population Samples from the Dakhleh Oasis, Egypt. International Journal of Paleopathology 26:93-103.
Moon M-S, Kim S-S, Lee S-R, Moon Y-W, Moon J-L, and Moon S-I. 2012. Tuberculosis of Hip in Children: A Retrospective Analysis. Indian Journal of Orthopaedics 46(2):191-199.
Moore J, and Koon HE. 2017. Basilar Portion Porosity: A Pathological Lesion Possibly Associated with Infantile Scurvy. International Journal of Paleopathology.
Moorrees CF, Fanning EA, and Hunt EE. 1963. Formation and Resorption of Three Deciduous Teeth in Children. American Journal of Physical Anthropology 21(2):205-213.
Morein B, Blomqvist G, and Hu K. 2007. Immune Responsiveness in the Neonatal Period. Journal of Comparative Pathology 137:S27-S31.
Morris BS, Madiwale CV, Garg A, and Chavhan GB. 2002. Hydatid Disease of Bone: A Mimic of Other Skeletal Pathologies. Australasian Radiology 46(4):431-434.
Morris HA, and Anderson PH. 2010. Autocrine and Paracrine Actions of Vitamin D. The Clinical Biochemist Reviews 31(4):129.
Mueller H, Fae KC, Magdorf K, Ganoza CA, Wahn U, Guhlich U, Feiterna-Sperling C, and Kaufmann SH. 2011. Granulysin-Expressing CD4+ T Cells as Candidate Immune Marker for Tuberculosis during Childhood and Adolescence. PloS one 6(12).
Muir BJ. 2019. Mortuary Ritual and Social Differentiation at Con Co Ngua, Vietnam: Australian National University.
Munson PL. 1955. Studies on the Role of the Parathyroids in Calcium and Phosphorus Metabolism. Annals of the New York Academy of Sciences 60(5):776-796.
Murphy E, Chistov Y, Hopkins R, Rutland P, and Taylor G. 2009. Tuberculosis among Iron Age Individuals from Tyva, South Siberia: Palaeopathological and Biomolecular Findings. Journal of Archaeological Science 36(9):2029-2038.
Myadar O. 2011. Imaginary Nomads: Deconstructing the Representation of Mongolia as a Land of Nomads. Inner Asia 13(2):335-362.
Nakamura T, Taniguchi Y, Tsuji S, and Oda H. 2001. Radiocarbon Dating of Charred Residues on the Earliest Pottery in Japan. Radiocarbon 43:1129-1148.
Nakashima A, Ishida H, Shigematsu M, Goto M, and Hanihara T. 2010. Nonmetric Cranial Variation of Jomon Japan: Implications for the Evolution of Eastern Asian Diversity. American Journal of Human Biology 22(6):782-790.

Navarra T. 2014. The Encyclopedia of Vitamins, Minerals, and Supplements: Infobase Publishing.
Nawrocki SP. 1995. Taphonomic Processes in Historic Cemeteries. In: Grauer A, editor. Bodies of Evidence: Reconstructing History Through Skeletal Analysis. New York, USA: John Wiley & Sons. p 49-66.
Newton SM, Brent AJ, Anderson S, Whittaker E, and Kampmann B. 2008. Paediatric Tuberculosis. The Lancet Infectious Diseases 8(8):498-510.
Nguyen KD. 2008. The Scientific Cooperation Program at Man Bac (2004–2007): Results and Questions. International Forum on the Prehistoric Man Bac Site. The Institute of Archaeology, Vietnam Academy of Social Sciences Institute, Hanoi.
Nguyen V. 2005. The Da But Culture: Evidence for Cultural Development in Vietnam during the Middle Holocene. Bulletin of the Indo-Pacific Prehistory Association 25:89-94.
Nhamoyebonde S, and Leslie A. 2014. Biological Differences between the Sexes and Susceptibility to Tuberculosis. The Journal of Infectious Diseases 209(Supplement 3):S100-S106.
Nicoletti P. 2012. Brucellosis in Animals. In: Madkour MM, editor. Madkour's Brucellosis. Berlin, Germany: Springer Science & Business Media. p 267-275.
Nieburg P, Person-Karell B, and Toole MJ. 1992. Malnutrition-Mortality Relationships Among Refugees. Journal of Refugee Studies 5(3-4):247-256.
Nissanka-Jayasuriya EH, Odell EW, and Phillips C. 2016. Dental Stigmata of Congenital Syphilis: A Historic Review with Present Day Relevance. Head and Neck Pathology 10(3):327-331.
Nnoaham KE, and Clarke A. 2008. Low Serum Vitamin D Levels and Tuberculosis: A Systematic Review and Meta-Analysis. International Journal of Epidemiology 37(1):113-119.
Noor AM, Gething PW, Alegana VA, Patil AP, Hay SI, Muchiri E, Juma E, and Snow RW. 2009. The Risks of Malaria Infection in Kenya in 2009. BMC Infectious Diseases 9(1):180.
Noordeen SK. 1998. Epidemiology of Leprosy. In: Gangadharam PRJ, and Jenkins PA, editors. Mycobacteria. New York, USA: Chapman & Hall. p 379-397.
Ntagiopoulos PG, Moutzouris DA, and Manetas S. 2007. The “fish-vertebra” sign. Emergency Medicine Journal 24(9):674-675.
Núñez-Rocha G, Bullen-Navarro M, Castillo-Treviño B, and Solís-Pérez E. 1998. Malnutrition in Pre-School Infants in Migrant Families. Salud Publica de Mexico 40(3):248-255.
Oberoi J, Wattal C, Aggarwal P, Khanna S, Basu A, and Verma K. 2012. Pulmonary Coccidiomycosis in New Delhi, India. Infection 40(6):699-702.
Odontsetseg N, Mweene AS, and Kida H. 2005. Viral and Bacterial Diseases in Livestock in Mongolia. Japanese Journal of Veterinary Research 52(4):151-162.
Oh R, and Brown DL. 2003. Vitamin B12 Deficiency. American Family Physician 67(5):979-986.
Okazaki K, Takamuku H, Yonemoto S, Itahashi Y, Gakuhari T, Yoneda M, and Chen J. 2019. A Paleopathological Approach to Early Human Adaptation for Wet-Rice Agriculture: The First Case of Neolithic Spinal Tuberculosis at the Yangtze River Delta of China. International Journal of Paleopathology 24:236-244.
Olausson H, Goldberg GR, Laskey MA, Schoenmakers I, Jarjou LM, and Prentice A. 2012. Calcium Economy in Human Pregnancy and Lactation. Nutrition Research Reviews 25(1):40-67.

Ong ST, Ho JZS, Ho B, and Ding JL. 2006. Iron-Withholding Strategy in Innate Immunity. Immunobiology 211(4):295-314.
Ortner DJ. 1991. Theoretical and Methodological Issues in Paleopathology. In: Ortner DJ, and Aufderheide AC, editors. Human Paleopathology: Current Syntheses and Future Options. Washington DC, USA: Smithsonian Institution Press. p 5-11.
Ortner DJ. 2003. Identification of Pathological Conditions in Human Skeletal Remains. San Diego, USA: Academic Press.
Ortner DJ. 2009. Issues in Paleopathology and Possible Strategies for Dealing with Them. Anthropologischer Anzeiger 67(4):323-340.
Ortner DJ. 2011. Human Skeletal Paleopathology. International Journal of Paleopathology 1(1):4-11.
Ortner DJ. 2012. Differential Diagnosis and Issues in Disease Classification. In: Grauer A, editor. A Companion to Paleopathology. Oxford, UK: Wiley-Blackwell. p 250-267.
Ortner DJ, Butler W, Cafarella J, and Milligan L. 2001. Evidence of Probable Scurvy in Subadults from Archeological Sites in North America. American Journal of Physical Anthropology 114(4):343-351.
Ortner DJ, and Ericksen MF. 1997. Bone Changes in the Human Skull Probably resulting from Scurvy in Infancy and Childhood. International Journal of Osteoarchaeology 7(3):212-220.
Ortner DJ, Kimmerle EH, and Diez M. 1999. Probable Evidence of Scurvy in Subadults from Archeological Sites in Peru. American Journal of Physical Anthropology 108(3):321-331.
Overbury RS, Cabo LL, Dirkmaat DC, and Symes SA. 2009. Asymmetry of the Os Pubis: Implications for the Suchey-Brooks Method. American Journal of Physical Anthropology: 139(2):261-268.
Oxenham M. 2006. Biological Responses to Change in Prehistoric Viet Nam. Asian Perspectives 45(2):212-239.
Oxenham M, and Buckley H. 2016a. The Population History of Mainland and Island Southeast Asia. In: Oxenham MF, and Buckley H, editors. The Routledge Handbook of Bioarchaeology in Southeast Asia and the Pacific. London: Routledge. p 9-23.
Oxenham M, and Buckley H. 2016b. The Routledge Handbook of Bioarchaeology in Southeast Asia and the Pacific Islands. New York, USA: Routledge.
Oxenham M, Matsumura H, Domett K, Thuy NK, Dung NK, Cuong NL, Huffer D, and Muller S. 2008. Health and the Experience of Childhood in Late Neolithic Viet Nam. Asian Perspectives:190-209.
Oxenham M, and Tayles N. 2006. Synthesising Southeast Asian Population History and Palaeohealth. In: Oxenham M, and Tayles N, editors. Bioarchaeology of Southeast Asia. Cambridge, UK: Cambridge University Press. p 335-349.
Oxenham MF. 2000. Health and Behaviour: During the Mid-Holocene and Metal Period of Northern Viet Nam: Northern Territory University.
Oxenham MF, and Cavill I. 2010. Porotic Hyperostosis and Cribra Orbitalia: The Erythropoietic Response to Iron-deficiency Anaemia. Anthropological Science 118(3):199-200.
Oxenham MF, and Matsumura H. 2008. Oral and Physiological Paleohealth in Cold Adapted Peoples: Northeast Asia, Hokkaido. American Journal of Physical Anthropology 135(1):64-74.
Oxenham MF, Matsumura H, and Kim Dung N. 2011. Man Bac: The Excavation of a Neolithic Site in Northern Vietnam The Biology, Terra Australis 33. Canberra, Australia: ANU ePress.

Oxenham MF, Piper PJ, Bellwood P, Bui CH, Nguyen KTK, Nguyen QM, Campos F, Castillo C, Wood R, and Sarjeant C. 2015. Emergence and Diversification of the Neolithic in Southern Vietnam: Insights from Coastal Rach Nui. The Journal of Island and Coastal Archaeology 10(3):309-338.
Oxenham MF, Thuy NK, and Cuong NL. 2005. Skeletal Evidence for the Emergence of Infectious Disease in Bronze and Iron age Northern Vietnam. American Journal of Physical Anthropology 126(4):359-376. DOI: 10.1002/ajpa.20048
Oxenham MF, Trinh HH, Willis A, Jones RK, Domett K, Castillo C, Wood R, Bellwood P, Tromp M, and Kells A. 2018. Between Foraging and Farming: Strategic Responses to the Holocene Thermal Maximum in Southeast Asia. Antiquity 92(364):940-957. DOI: 10.15184/aqy.2018.69
Ozfirat Z, and Chowdhury TA. 2010. Vitamin D Deficiency and Type 2 Diabetes. Postgraduate Medical Journal 86(1011):18-25.
Pace J, and Csonka G. 1984. Endemic Non-Venereal Syphilis (Bejel) in Saudi Arabia. Sexually Transmitted Infections 60(5):293-297.
Paine RR, and Brenton BP. 2006. The Paleopathology of Pellagra: Investigating the Impact of Prehistoric and Historical Dietary Transitions to Maize. Journal of Anthropological Sciences 84:125-135.
Palubeckaitė Ž, Jankauskas R, Ardagna Y, Macia Y, Rigeade C, Signoli M, and Dutour O. 2006. Dental Status of Napoleon's Great Army's (1812) Mass Burial of Soldiers in Vilnius: Childhood Peculiarities and Adult Dietary Habits. International Journal of Osteoarchaeology 16(4):355-365.
Papavasiliou C. 2012. Radiological Aspects of Marrow Heterotopia in Thalassemia. In: Papavasiliou C, Cambouris T, and Fessas P, editors. Radiology of Thalassemia: Springer Science & Business Media. p 105-112.
Pappas PG, Threlkeld MG, Bedsole GD, Cleveland KO, Gelfand MS, and Dismukes WE. 1993. Blastomycosis in Immunocompromised Patients. Medicine 72(5):311-325.
Parfitt A, Travers R, Rauch F, and Glorieux F. 2000. Structural and Cellular Changes during Bone Growth in Healthy Children. Bone 27(4):487-494.
Parker GJ, Yip JM, Eerkens JW, Salemi M, Durbin-Johnson B, Kiesow C, Haas R, Buikstra JE, Klaus H, and Regan LA. 2019. Sex Estimation using Sexually Dimorphic Amelogenin Protein Fragments in Human Enamel. Journal of Archaeological Science 101:169-180.
Pavithran K. 1987. Acquired Syphilis in a Patient with Late Congenital Syphilis. Sexually Transmitted Diseases 14(2):119-121.
Pearson R. 2006. Jomon Hot Spot: Increasing Sedentism in South-Western Japan in the Incipient Jomon (14,000–9250 cal. BC) and Earliest Jomon (9250–5300 cal. BC) Periods. World Archaeology 38(2):239-258.
Pearson R. 2007. Debating Jomon Social Complexity. Asian Perspectives 46(2):361-388.
Pechenkina EA, Benfer Jr RA, and Ma X. 2007. Diet and Health in the Neolithic of the Wei and Middle Yellow River Basins, Northern China. In: Cohen MN, and Crane-Kramer G, editors. Ancient Health: Skeletal Indicators of Agricultural and Economic Intensification University Press of Florida, Gainesville. Gainesville, Florida: University Press of Florida. p 255-272.
Pechenkina K, and Oxenham M. 2013. Human Ecology in Continental and Insular Asia. In: Pechenkina K, and Oxenham M, editors. Bioarchaeology of East Asia: Movement, Contact, Health: University Press of Florida. p 28-57.
Peeling RW, and Hook EW. 2006. The Pathogenesis of Syphilis: The Great Mimicker, Revisited. The Journal of Pathology: A Journal of the Pathological Society of Great Britain and Ireland 208(2):224-232.

Perfect JR, and Casadevall A. 2002. Cryptococcosis. Infectious Disease Clinics of North America 16(4):837-874, v-vi.
Perine PL, Hopkins DR, Niemel PL, St John R, Causse G, and Antal G. 1984. Handbook of Endemic Treponematoses: Yaws, Endemic Syphilis and Pinta: World Health Organization.
Perrotta S, Nobili B, Rossi F, Criscuolo M, Iolascon A, Di Pinto D, Passaro I, Cennamo L, Oliva A, and Della Ragione F. 2002. Infant Hypervitaminosis A Causes Severe Anemia and Thrombocytopenia: Evidence of a Retinol-Dependent Bone Marrow Cell Growth Inhibition. Blood 99(6):2017-2022.
Pessoa L, and Galvão V. 2011. Clinical Aspects of Congenital Syphilis with Hutchinson's Triad. Case Reports 2011:bcr1120115130.
Pettifor J, Ross F, Travers R, Glorieux F, and DeLuca H. 1981. Dietary Calcium Deficiency: A Syndrome Associated with Bone Deformities and Elevated Serum 1, 25-Dihyroxyvitamin D Concentrations. Metabolic Bone Disease and Related Research 2(5):301-305.
Pettifor JM. 2004. Nutritional Rickets: Deficiency of Vitamin D, Calcium, or Both? The American Journal of Clinical Nutrition 80(6):1725S-1729S.
Pettifor JM, Thandrayen K, and Thacher TD. 2018. Vitamin D Deficiency and Nutritional Rickets in Children. Vitamin D: Elsevier. p 179-201.
Phenice TW. 1969. A Newly Developed Visual Method of Sexing the Os Pubis. American Journal of Physical Anthropology 30(2):297-301.
Pietrusewsky M, and Douglas MT. 2001. Intensification of Agriculture at Ban Chiang: Is there Evidence from the Skeletons? Asian Perspectives 40(2):157-178.
Pietrusewsky M, Douglas MT, Ikehara-Quebral RM, and Kadohiro Lauer K. 2019. Skeletal and Dental Health of Early Tongans: The Bioarchaeology of the Human Skeletons from the To-At-36 Site, Ha 'ateiho, Tongatapu, Tonga. The Journal of Island and Coastal Archaeology:1-40.
Pilipenko AS, Cherdantsev SV, Trapezov RO, Zhuravlev AA, Babenko VN, Pozdnyakov DV, Konovalov PB, and Polosmak NV. 2018. Mitochondrial DNA Diversity in a Transbaikalian Xiongnu Population. Archaeological and Anthropological Sciences 10(7):1557-1570.
Pinhasi R, and Stock JT. 2011. Human Bioarchaeology of the Transition to Agriculture. Sussex, UK: John Wiley & Sons.
Piper P, Campos F, Ngoc Kinh D, Amano N, Oxenham M, Chi Hoang B, Bellwood P, and Willis A. 2014. Early Evidence for Pig and Dog Husbandry from the Neolithic Site of An Son, Southern Vietnam. International Journal of Osteoarchaeology 24(1):68-78.
Poolsuwan S. 1995. Malaria in Prehistoric Southeastern Asia. Southeast Asian Journal of Tropical Medicine and Public Health 26:3-22.
Poulin R, and Randhawa HS. 2015. Evolution of Parasitism along Convergent Lines: From Ecology to Genomics. Parasitology 142(S1):S6-S15.
Powell ML, and Cook DC. 2005. The Myth of Syphilis: The Natural History of Treponematosis in North America. Gainesville, USA: University Press of Florida.
Prentice A. 1995. Calcium Requirements of Children. Nutrition Reviews 53(2):37-40.
Prothero RM. 1977. Disease and Mobility: A Neglected Factor in Epidemiology. International Journal of Epidemiology 6(3):259-267.
Psarras S-K. 2003. Han and Xiongnu a Reexamination of Cultural and Political Relations (I). Monumenta Serica 51(1):55-236.
Psarras S-K. 2004. Han and Xiongnu: A Reexamination of Cultural and Political Relations (II). Monumenta Serica 52(1):37-93.

Putkonen T. 1962. Dental Changes in Congenital Syphilis. Relationship to Other Syphilitic Stigmata. Acta Dermato-venereologica 42:44-62.
Quinn TC. 1994. Population Migration and the Spread of Types 1 and 2 Human Immunodeficiency Viruses. Proceedings of the National Academy of Sciences 91(7):2407-2414.
Racloz V, Schelling E, Chitnis N, Roth F, and Zinsstag J. 2013. Persistence of Brucellosis in Pastoral Systems. OIE Revue Scientifique et Technique 32(1):61-70.
Raggatt LJ, and Partridge NC. 2010. Cellular and Molecular Mechanisms of Bone Remodeling. Journal of Biological Chemistry 285(33):25103-25108.
Rajapakse C. 1995. Bacterial Infections: Osteoarticular Brucellosis. Bailliere's Clinical Rheumatology 9:161-177.
Ramos-e-Silva M, and Rebello PFB. 2001. Leprosy. American Journal of Clinical Dermatology 2(4):203-211.
Rao MP, Davi NK, D D'Arrigo R, Skees J, Nachin B, Leland C, Lyon B, Wang S-Y, and Byambasuren O. 2015. Dzuds, Droughts, and Livestock Mortality in Mongolia. Environmental Research Letters 10(7):074012.
Rasmussen S, Allentoft ME, Nielsen K, Orlando L, Sikora M, Sjögren K-G, Pedersen AG, Schubert M, Van Dam A, and Kapel CMO. 2015. Early Divergent Strains of Yersinia pestis in Eurasia 5,000 years ago. Cell 163(3):571-582.
Rasool M, and Govender S. 1989. The Skeletal Manifestations of Congenital Syphilis. A Review of 197 Cases. The Journal of Bone and Joint Surgery British Volume 71(5):752-755.
Ratledge C. 2004. Iron, Mycobacteria and Tuberculosis. Tuberculosis 84(1-2):110-130.
Ratnam I, Leder K, Black J, and Torresi J. 2013. Dengue Fever and International Travel. Journal of Travel Medicine 20(6):384-393.
Rausch RL, and D'Alessandro A. 1999. Histogenesis in the Metacestode of Echinococcus vogeli and Mechanism of Pathogenesis in Polycystic Hydatid Disease. Faculty Publications from the Harold W Manter Laboratory of Parasitology:400-418.
Raviglione MC, Snider DE, and Kochi A. 1995. Global Epidemiology of Tuberculosis: Morbidity and Mortality of a Worldwide Epidemic. JAMA 273(3):220-226.
Raynaud-Simon A, Cohen-Bittan J, Gouronnec A, Pautas E, Senet P, Verny M, and Boddaert J. 2010. Scurvy in Hospitalized Elderly Patients. The Journal of Nutrition, Health & Aging 14(6):407-410.
Redfern RC, and DeWitte SN. 2011. A New Approach to the Study of Romanization in Britain: A Regional Perspective of Cultural Change in Late Iron Age and Roman Dorset using the Siler and Gompertz–Makeham Models of Mortality. American Journal of Physical Anthropology 144(2):269-285.
Reitsema LJ, and McIlvaine BK. 2014. Reconciling "Stress" and "Health" in Physical Anthropology: What can Bioarchaeologists Learn from the Other Subdisciplines? American Journal of Physical Anthropology 155(2):181-185.
Rendall J, and McDougall A. 1976. Reddening of the Upper Central Incisors Associated with Periapical Granuloma in Lepromatous Leprosy. British Journal of Oral Surgery 13(3):271-277.
Renssen H, Seppä H, Crosta X, Goosse H, and Roche DM. 2012. Global Characterization of the Holocene Thermal Maximum. Quaternary Science Reviews 48:7-19.
Resnick D. 1995a. Diagnosis of Bone and Joint Disorders. Philadelphia, USA: Saunders.
Resnick D. 1995b. Hypervitaminosis and Hypovitaminosis. Diagnosis of Bone and Joint Disorders. Philadelphia, USA: W.B Saunders Company. p 3343-3352.

Roberts C. 2012. Re-Emerging Infections: Developments in Bioarchaeological Contributions to Understanding Tuberculosis. In: Grauer A, editor. A Companion to Paleopathology. Oxford, UK: Wiley-Blackwell. p 434-457.
Roberts C, Boylston A, Buckley L, Chamberlain A, and Murphy E. 1998. Rib Lesions and Tuberculosis: The Palaeopathological Evidence. Tubercle and Lung Disease 79(1):55-60.
Roberts C, Millard A, Nowell G, Gröcke D, Macpherson C, Pearson D, and Evans D. 2013. Isotopic Tracing of the Impact of Mobility on Infectious Disease: The Origin of People with Treponematosis Buried in Hull, England, in the Late Medieval Period. American Journal of Physical Anthropology 150(2):273-285.
Roberts CA. 2015. Old World Tuberculosis: Evidence from Human Remains with a Review of Current Research and Future Prospects. Tuberculosis 95:S117-S121.
Roberts CA, and Brickley M. 2018. Infectious and Metabolic Diseases: a Synergistic Relationship. In: Katzenberg MA, and Grauer AL, editors. Biological Anthropology of the Human Skeleton. p 415-446.
Roberts CA, and Buikstra JE. 2003. The Bioarchaeology of Tuberculosis: A Global Perspective on a Re-Emerging Disease. Gainesville, USA: University Press of Florida.
Roberts CA, and Buikstra JE. 2019. Bacterial Infections. Ortner's Identification of Pathological Conditions in Human Skeletal Remains: Elsevier. p 321-439.
Roberts CA, and Connell B. 2004. Guidance on Recording Palaeopathology. British Association for Biological Anthropology and Osteoarchaeology.
Roberts CA, and Manchester K. 2012. The Archaeology of Disease: Cornell University Press.
Rogers JD. 2017. Inner Asian Polities and their Built Environment. Archaeological Research in Asia:1-14.
Rohr JR, Dobson AP, Johnson PT, Kilpatrick AM, Paull SH, Raffel TR, Ruiz-Moreno D, and Thomas MB. 2011. Frontiers in Climate Change–Disease Research. Trends in Ecology & Evolution 26(6):270-277.
Rokkas T, Papatheodorou G, Karameris A, Mavrogeorgis A, Kalogeropoulos N, and Giannikos N. 1995. Helicobacter pylori Infection and Gastric Juice Vitamin C Levels. Digestive Diseases and Sciences 40(3):615-621.
Rowbotham SK. 2016. Anthropological Estimation of Sex. Handbook of Forensic Anthropology and Archaeology:261-272.
Rowland M, and Nosten F. 2001. Malaria Epidemiology and Control in Refugee Camps and Complex Emergencies. Annals of Tropical Medicine & Parasitology 95(8):741-754.
Rumm-Kreuter D, and Demmel I. 1990. Comparison of Vitamin Losses in Vegetables Due to Various Cooking Methods. Journal of Nutritional Science and Vitaminology 36(4):S7-S15.
Sadé J, and Berco E. 1974. Bone Destruction in Chronic Otitis Media: a Histopathological Study. The Journal of Laryngology & Otology 88(5):413-422.
Sadun EH, Bradin Jr JL, and Faust EC. 1951. The Effect of Ascorbic Acid Deficiency on the Resistance of Guinea-Pigs to Infection with Endamoeba Histolytica of Human Origin1, 2. The American Journal of Tropical Medicine and Hygiene 1(4):426-437.
Saggurti N, Mahapatra B, Sabarwal S, Ghosh S, and Johri A. 2012. Male Out-Migration: A Factor for the Spread of HIV Infection Among Married Men and Women in Rural India. PloS one 7(9):e43222.

Saha R, Sarkar S, Majumder M, and Banerjee G. 2019. Bacteriological Profile of Aerobic and Anaerobic Isolates of Trophic Ulcer in Leprosy: A Study from Eastern India. Indian Journal of Dermatology 64(5):372.

Sakaguchi T. 2009. Storage Adaptations among Hunter–Gatherers: A Quantitative Approach to the Jomon Period. Journal of Anthropological Archaeology 28(3):290-303.

Saker L, Lee K, Cannito B, Gilmore A, and Campbell-Lendrum DH. 2004. Globalization and Infectious Diseases: A review of the Linkages. Geneva: World Health Organization.

Salarvand S, Nazer M, Shokri S, Bazhvan S, and Pournia Y. 2012. Brucellosis-Induced Avascular Necrosis of the Hip in a Middle-aged Person. Iranian Journal of Public Health 41(12):86-88.

Salzano FM. 2011. The Prehistoric Colonization of the Americas: Evidence and Models. Evolution: Education and Outreach 4(2):199.

Saonere JA. 2011. Leprosy: An Overview. Journal of Infectious Diseases and Immunity 3(14):233-243.

Saraf SK, and Tuli SM. 2015. Tuberculosis of Hip: A Current Concept Review. Indian Journal of Orthopaedics 49(1):1-9.

Satter EK, and Tokarz VA. 2010. Secondary Yaws: An Endemic Treponemal Infection. Pediatric Dermatology 27(4):364-367.

Saunders SR, Fitzgerald C, Rogers T, Dudar C, and McKillop H. 1992. A Test of Several Methods of Skeletal Age Estimation using a Documented Archaeological Sample. Canadian Society of Forensic Science Journal 25(2):97-118.

Sawada J, Thuy NK, and Tuan NA. 2011. Faunal Remains at Man Bac. In: Oxenham MF, Matsumura H, and Kim Dung N, editors. Man Bac: The Excavation of a Neolithic Site in Northern Vietnam, The Biology Terra Australis 33. Canberra, Australia: ANU ePress. p 105-116.

Saxoni F, Lapatsanis P, and Pantelakis SN. 1967. Congenital Syphilis: A Description of 18 Cases and Re-examination of an Old but Ever-Present Disease. Clinical Pediatrics 6(12):687-691.

Scaffidi BK. 2020. Spatial Paleopathology: A Geographic Approach to the Etiology of Cribrotic Lesions in the Prehistoric Andes. International Journal of Paleopathology 29:102-116.

Schaefer M, Black SM, and Scheuer L. 2009. Juvenile Osteology: A Laboratory and Field Manual: Elsevier, Academic Press.

Schattmann A, Bertrand B, Vatteoni S, and Brickley M. 2016. Approaches to Co-occurrence: Scurvy and Rickets in Infants and Young Children of 16–18th Century Douai, France. International journal of paleopathology 12:63-75.

Scheuer JL, Musgrave JH, and Evans SP. 1980. The Estimation of Late Fetal and Perinatal Age from Limb Bone Length by Linear and Logarithmic Regression. Annals of Human Biology 7(3):257-265.

Scheuer L, and Black S. 2000. Developmental Juvenile Osteology. Oxford, UK: Academic Press.

Schmidt CO, and Kohlmann T. 2008. When to Use the Odds Ratio or the Relative Risk? International Journal of Public Health 53(3):165.

Schmidt M, Leipe C, Becker F, Goslar T, Hoelzmann P, Mingram J, Müller S, Tjallingii R, Wagner M, and Tarasov PE. 2019. A Multi-Proxy Palaeolimnological Record of the Last 16,600 years from Coastal Lake Kushu in Northern Japan. Palaeogeography, Palaeoclimatology, Palaeoecology 514:613-626.

Schmitt A. 2004. Age-at-Death Assessment using the Os Pubis and the Auricular Surface of the Ilium: A Test on an Identified Asian Sample. International Journal of Osteoarchaeology 14(1):1-6.
Scott EC. 1979. Dental Wear Scoring Technique. American Journal of Physical Anthropology 51(2):213-217.
Scott RM, Buckley HR, Domett K, Tromp M, Trinh HH, Willis A, Matsumura H, and Oxenham MF. 2019. Domestication and Large Animal Interactions: Skeletal Trauma in Northern Vietnam during the Hunter-gatherer Da But Period. PloS one 14(9).
Scutellari P, Franceschini F, and O'rzincolo C, D.J.W. 1989. A Reappraisal of Some Skeletal Changes in Currently Treated β-Thalassemia. In: Papavasiliou C, Cambouris T, and Fessas P, editors. Radiology of Thalassemia. Berlin, Germany: Springer p50-61.
Sedgwick P. 2012. Pearson's Correlation Coefficient. BMJ 345:e4483.
Seguchi N, Quintyn CB, Yonemoto S, and Takamuku H. 2017. An Assessment of Postcranial Indices, Ratios, and Body Mass versus Eco-Geographical Variables of Prehistoric Jomon, Yayoi Agriculturalists, and Kumejima Islanders of Japan. American Journal of Human Biology.
Seitsonen O, Houle J-L, and Broderick LG. 2014. GIS Approaches to Past Mobility and Accessibility: An Example from the Bronze Age Khanuy Valley, Mongolia. In: Leary J, editor. Past Mobilities: Archaeological Approaches to Movement and Mobility. Surry, England: Ashgate Publishing Ltd. p 79-110.
Semba RD, and Bloem M. 2002. The Anemia of Vitamin A Deficiency: Epidemiology and Pathogenesis. European Journal of Clinical Nutrition 56(4):271-281.
Sequeira W. 1994. The Neuropathic Joint. Clinical and Experimental Rheumatology 12(3):325-337.
Sevilla-Casas E. 1993. Human Mobility and Malaria Risk in the Naya River Basin of Colombia. Social Science & Medicine 37(9):1155-1167.
Sfikakis P. 1989. Osseous X-Ray Findings in Thalassemia Minor. In: Papavasiliou C, Cambouris T, and Fessas P, editors. Radiology of Thalassemia. Berlin, Germany: Springer. p 44-49.
Shah AR, Zeitler D, and Wise JB. 2009. Nasal Reconstruction of the Leprosy Nose Using Costal Cartilage. Otolaryngologic Clinics of North America 42(3):547-555.
Shaman J, and Kohn M. 2009. Absolute Humidity Modulates Influenza Survival, Transmission, and Seasonality. Proceedings of the National Academy of Sciences 106(9):3243-3248.
Shapland F, and Lewis ME. 2013. Brief Communication: A Proposed Osteological Method for the Estimation of Pubertal Stage in Human Skeletal Remains. American Journal of Physical Anthropology 151(2):302-310.
Sharghi A, Kamran A, and Faridan M. 2011. Evaluating Risk Factors for Protein-Energy Malnutrition in Children Under the Age of Six Years: A Case-Control study from Iran. International Journal of General Medicine 4:607-611.
Sheppard PJ, Bedford S, Bellwood P, Burley DV, Chiu S, Irwin G, Kirch PV, Lilley I, Matisoo-Smith L, and Pawley A. 2011. Lapita Colonization across the Near/Remote Oceania Boundary. Current Anthropology 52(6):799-840.
Sherman D. 2011. The Spread of Pathogens Through Trade in Small Ruminants and Their Products. Revue Scientifique et Technique-OIE 30(1):207.
Shiomi H, Kawagoshi T, and Kawase M. 1971. Report on the Excavation of Ota Shell Mound of the Onomichi City, Hiroshima Prefecture In: Shiomi H, editor. Report

on the Research of Cultural Heritage of Hiroshima Prefecture (In Japanese). Hiroshima, Japan: Educational Board of Hiroshima Prefecture.
Singh V. 2003. Geographical Adaptation and Distribution of Seabuckthorn (Hippophae L.) Resources. In: Singh V, Kallio H, Sawney R, Gupta R, RongSen L, Eliseev I, Khabarov S, Korovina M, Skuridin G, and Shchapov N, editors. Seabuckthorn (*Hippophae L)*: A Multipurpose Wonder Plant. New Delhi, India: Indus Publishing. p 21-34.
Skaf G, Domloj N, Fehlings M, Bouclaous C, Sabbagh A, Kanafani Z, and Kanj S. 2010. Pyogenic Spondylodiscitis: An Overview. Journal of Infection and Public Health 3(1):5-16.
Sloan C, Moore ML, and Hartert T. 2011. Impact of Pollution, Climate, and Sociodemographic Factors on Spatiotemporal Dynamics of Seasonal Respiratory Viruses. Clinical and Translational Science 4(1):48-54.
Smith RJ. 2020. P>. 05: The Incorrect Interpretation of "Not Significant" Results is a Significant Problem. American Journal of Physical Anthropology:e24092.
Smith-Guzmán NE. 2015. The Skeletal Manifestation of Malaria: An Epidemiological Approach using Documented Skeletal Collections. American Journal of Physical Anthropology 158(4):624-635.
Smits H. 2013. Brucellosis in Pastoral and Confined Livestock: Prevention and Vaccination. Rev Sci Tech 32:219-228.
Snoddy AM, Buckley H, King C, Kinaston R, Nowell G, Gröcke D, Duncan W, and Petchey P. 2020a. 'Captain of All These Men of Death': An Integrated Case Study of Tuberculosis in Nineteenth-Century Otago, New Zealand. Bioarchaeology International 3(4):217-237.
Snoddy AME, Beaumont J, Buckley HR, Colombo A, Halcrow SE, Kinaston RL, and Vlok M. 2020b. Sensationalism and Speaking to the Public: Scientific Rigour and Interdisciplinary Collaborations in Palaeopathology. International Journal of Paleopathology 28:88-91.
Snoddy AME, Buckley HR, Elliott GE, Standen VG, Arriaza BT, and Halcrow SE. 2018. Macroscopic Features of Scurvy in Human Skeletal Remains: A Literature Synthesis and Diagnostic Guide. American Journal of Physical Anthropology 167(4):876-895. DOI: 10.1002/ajpa.23699
Snoddy AME, Halcrow SE, Buckley HR, Standen VG, and Arriaza BT. 2017. Scurvy at the Agricultural Transition in the Atacama Desert (ca 3600–3200 BP): Nutritional Stress at the Maternal-Foetal Interface? International Journal of Paleopathology 18:108-120. DOI: 10.1016/j.ijpp.2017.05.011
Søe MJ, Nejsum P, Seersholm FV, Fredensborg BL, Habraken R, Haase K, Hald MM, Simonsen R, Højlund F, and Blanke L. 2018. Ancient DNA from Latrines in Northern Europe and the Middle East (500 BC–1700 AD) Reveals Past Parasites and Diet. PLoS One 13(4).
Sohler A. 2017. Nutritional Factors in the Paleoepidemiology of Infectious Disease in the Ancient Atacama Desert: University of Otago.
Solomon SG. 1993. The Soviet-German Syphilis Expedition to Buriat Mongolia, 1928: Scientific Research on National Minorities. Slavic Review 52(2):204-234.
Somily A, Robinson JL, Miedzinski LJ, Bhargava R, and Marrie TJ. 2005. Echinococcal Disease in Alberta, Canada: More than a Calcified Opacity. BMC Infectious Diseases 5(1):34.
Song X, Ding L, and Wen H. 2007. Bone Hydatid Disease. Postgraduate Medical Journal 83(982):536-542.

Spengler RN, Frachetti MD, and Fritz GJ. 2013. Ecotopes and Herd Foraging Practices in the Steppe/Mountain Ecotone of Central Asia during the Bronze and Iron Ages. Journal of Ethnobiology 33(1):125-147.
Spicer J. 2005. Making Sense of Multivariate Data Analysis: An Intuitive Approach. Thousand Oaks, CA: Sage.
Steckel RH. 2005. Health and Nutrition in Pre-Columbian America: The Skeletal Evidence. The Journal of Interdisciplinary History 36(1):1-32.
Steckel RH, Larsen CS, Roberts CA, and Baten J. 2018. The Backbone of Europe: Health, Diet, Work and Violence over Two Millennia. Cambridge, UK: Cambridge University Press.
Steckel RH, Larsen CS, Sciulli PW, and Walker PL. 2011. Data Collection Codebook: The Global History of Health.
Steckel RH, and Rose JC. 2002. The Backbone of History: Health and Nutrition in the Western Hemisphere. Cambridge, UK: Cambridge University Press.
Steckel RH, Rose JC, Spencer Larsen C, and Walker PL. 2002. Skeletal Health in the Western Hemisphere from 4000 BC to the Present. Evolutionary Anthropology: Issues, News, and Reviews: Issues, News, and Reviews 11(4):142-155.
Steinbock R. 1976. Paleopathological Diagnosis and Interpretation: Bone Diseases in Ancient Human Populations. Springfield, Illinois: Charles C Thomas Pub Limited.
Steinmann G. 1986. Changes in the Human Thymus During Aging. The Human Thymus. Berlin: Springer. p 43-88.
Stephensen CB. 2001. Vitamin A, Infection, and Immune function. Annual Review of Nutrition 21(1):167-192.
Steyn M, and Patriquin M. 2009. Osteometric Sex Determination from the Pelvis—Does Population Specificity Matter? Forensic Science International 191(1-3):113. e111-113. e115.
Stokes JH, and Gardner BS. 1923. The Demonstration of Unerupted Hutchinson's Teeth by the Roentgen Ray. Journal of the American Medical Association 80(1):28-29.
Stoneking M, and Krause J. 2011. Learning About Human Population History from Ancient and Modern Genomes. Nature Reviews Genetics 12(9):603-614.
Storey AA, Clarke AC, Ladefoged T, Robins J, and Matisoo-Smith E. 2013. DNA and Pacific Commensal Models: Applications, Construction, Limitations, and Future Prospects. The Journal of Island and Coastal Archaeology 8(1):37-65.
Storey AA, Spriggs M, Bedford S, Hawkins SC, Robins JH, Huynen L, and Matisoo-Smith E. 2010. Mitochondrial DNA from 3000-Year Old Chickens at the Teouma site, Vanuatu. Journal of Archaeological Science 37(10):2459-2468.
Stout SD, and Crowder C. 2012. Bone Remodeling, Histomorphology, and Histomorphometry. Bone Histology–An Anthropological Perspective. Boca Raton, Florida: CRC Press. p 1-21.
Straus LG. 1991. Human Geography of the Late Upper Paleolithic in Western Europe: Present State of the Question. Journal of Anthropological Research 47(2):259-278.
Strickland SS. 1993. Human Nutrition in Mongolia: Maternal Mortality and Rickets. Nomadic Peoples:231-239.
Stuart-Macadam P. 1985. Porotic Hyperostosis: Representative of a Childhood Condition. American Journal of Physical Anthropology 66(4):391-398.
Su X, Sun K, Cui F, and Landis W. 2003. Organization of Apatite Crystals in Human Woven Bone. Bone 32(2):150-162.
Subbarao K. 1987. Periosteal Reactions in Pediatrics. Indian Journal of Pediatrics 54(1):45-52.

Suzuki T. 1998. Indicators of Stress in Prehistoric Jomon Skeletal Remains in Japan. Anthropological Science 106(Supplement):127-137.
Suzuki T, Fujita H, and Choi JG. 2008. Brief Communication: New Evidence of Tuberculosis from Prehistoric Korea—Population Movement and Early Evidence of Tuberculosis in Far East Asia. American Journal of Physical Anthropology 136(3):357-360. DOI: 10.1537/ase.040831
Suzuki T, and Inoue T. 2007. Earliest Evidence of Spinal Tuberculosis from the Aneolithic Yayoi Period in Japan. International Journal of Osteoarchaeology 17(4):392-402.
Suzuki T, Matsushita T, and Han K. 2005. On the Possible Case of Treponematosis from the Bronze Age in China. Anthropological Science 113(3):253-258. DOI: 10.1537/ase.040831
Swezey RL, Bjarnason DM, Alexander SJ, and Forrester D. 1972. Resorptive Arthropathy and the Opera-glass Hand Syndrome. Seminars in Arthritis and Rheumatism 2(3):191-244.
Szulc P, Seeman E, and Delmas P. 2000. Biochemical Measurements of Bone Turnover in Children and Adolescents. Osteoporosis International 11(4):281-294.
Tague RG. 1992. Sexual Dimorphism in the Human Bony Pelvis, with a Consideration of the Neandertal Pelvis from Kebara Cave, Israel. American Journal of Physical Anthropology 88(1):1-21.
Takahashi R. 2001. Soron: Sonraku to Shakai no Kokogaku (General Remarks: The Archaeology of Settlement and Society). In: Takahashi R, editor. Sonraku to Shakai no Kokogaku (The Archaeology of Settlement and Society). Tokyo: Asakura Shoten.
Takahashi R, and Hosoya LA. 2016. Nut Exploitation in Jomon Society. Hunter-Gatherer Archaeobotany: Perspectives from the Northern Temperate Zone.
Talat N, Perry S, Parsonnet J, Dawood G, and Hussain R. 2010. Vitamin D Deficiency and Tuberculosis Progression. Emerging Infectious Diseases 16(5):853.
Tanabe S, Saito Y, Vu QL, Hanebuth TJ, Ngo QL, and Kitamura A. 2006. Holocene Evolution of the Song Hong (Red River) Delta System, Northern Vietnam. Sedimentary Geology 187(1-2):29-61.
Tao W, Huijun W, and Dabang J. 2010. Mid-Holocene East Asian Summer Climate as Simulated by the PMIP2 Models. Palaeogeography, Palaeoclimatology, Palaeoecology 288(1-4):93-102.
Tatem AJ, Rogers DJ, and Hay S. 2006. Global Transport Networks and Infectious Disease Spread. Advances in Parasitology 62:293-343.
Tatem AJ, and Smith DL. 2010. International Population Movements and Regional Plasmodium falciparum Malaria Elimination Strategies. Proceedings of the National Academy of Sciences 107(27):12222-12227.
Tayles N. 1996. Anemia, Genetic Diseases, and Malaria in Prehistoric Mainland Southeast Asia. American Journal of Physical Anthropology 101(1):11-27.
Tayles N, and Buckley HR. 2004. Leprosy and Tuberculosis in Iron Age Southeast Asia? American Journal of Physical Anthropology 125(3):239-256. DOI: 10.1002/ajpa.10378
Tayles N, and Halcrow S. 2016. Age-at-Death Estimation in a Sample of Prehistoric Southeast Asian Adolescents and Adults. In: Oxenham MF, and Buckley HR, editors. The Routledge Handbook of Bioarchaeology in Southeast Asia and the Pacific Islands. New York: Taylor and Francis. p 286-307.
Taylor W, Wilkin S, Wright J, Dee M, Myagmar E, Clark J, Tuvshinjargal T, Bayarsaikhan J, Fitzhugh W, and Boivin N. 2019. Radiocarbon Dating and

Cultural Dynamics across Mongolia's Early Pastoral Transition. PloS one 14(11):e0224241.
Taylor WTT, Clark J, Jamsranjav B, Tumurbaatar T, Jobe JT, Fitzhugh W, Kortum R, Spengler III RN, Svetlana S, and Valeur SF. 2020. Early Pastoral Economies and Herding Transitions in Eastern Eurasia. Scientific Reports 10(1):1-15.
Temple DH. 2007a. Dietary Variation and Stress among Prehistoric Jomon Foragers from Japan. American Journal of Physical Anthropology 133(4):1035-1046.
Temple DH. 2007b. Human Biological Variation During the Agricultural Transition in Prehistoric Japan: The Ohio State University.
Temple DH. 2008. What Can Variation in Stature Reveal about Environmental Differences between Prehistoric Jomon Foragers? Understanding the Impact of Systemic Stress on Developmental Stability. American Journal of Human Biology 20(4):431-439.
Temple DH. 2010. Patterns of Systemic Stress During the Agricultural Transition in Prehistoric Japan. American Journal of Physical Anthropology 142(1):112-124. DOI: 10.1002/ajpa.21208
Temple DH. 2018. Persistence of Time: Resilience and Adaptability in Prehistoric Jomon Hunter-Gatherers from the Inland Sea Region of Southwestern Honshu, Japan. In: Temple DH, and Stojanowski CM, editors. Hunter-Gatherer Adaptation and Resilience: a Bioarchaeological Perspective. Cambridge, UK: Cambridge University Press. p 85-109.
Temple DH, Bazaliiskii VI, Goriunova OI, and Weber AW. 2014. Skeletal Growth in Early and Late Neolithic Foragers from the Cis-Baikal Region of Eastern Siberia. American Journal of Physical Anthropology 153(3):377-386.
Temple DH, and Goodman AH. 2014. Bioarcheology has a "Health" Problem: Conceptualizing "Stress" and "Health" in Bioarcheological Research. American Journal of Physical Anthropology 155(2):186-191.
Temple DH, Kusaka S, and Sciulli PW. 2011. Patterns of Social Identity in Relation to Tooth Ablation among Prehistoric Jomon Foragers from the Yoshigo site, Aichi pPefecture, Japan. International Journal of Osteoarchaeology 21(3):323-335.
Temple DH, and Matsumura H. 2011. Do Body Proportions among Jomon Foragers from Hokkaido Conform to Ecogeographic Expectations? Evolutionary Implications of Body Size and Shape among Northerly Hunter-Gatherers. International Journal of Osteoarchaeology 21(3):268-282.
Temple DH, Nakatsukasa M, and McGroarty JN. 2012. Reconstructing Patterns of Systemic Stress in a Jomon Period Subadult using Incremental Microstructures of Enamel. Journal of Archaeological Science 39(5):1634-1641.
Teo HE, and Peh WC. 2004. Skeletal Tuberculosis in Children. Pediatric Radiology 34(11):853-860.
Thein SL, and Menzel S. 2009. Discovering the Genetics Underlying Foetal Haemoglobin Production in Adults. British Journal of Haematology 145(4):455-467.
Tiemersma EW, van der Werf MJ, Borgdorff MW, Williams BG, and Nagelkerke NJ. 2011. Natural History of Tuberculosis: Duration and Fatality of Untreated Pulmonary Tuberculosis in HIV Negative Patients: A Systematic Review. PloS one 6(4):e17601.
Tilley L, and Oxenham M. 2016. Reflections on Life and Times in Neolithic Vietnam: One Person's Story. In: Oxenham MF, and Buckley H, editors. The Routledge Handbook of Bioarchaeology in Southeast Asia and the Pacific. London: Routledge. p 95-113.

Tizzoni M, Bajardi P, Decuyper A, King GKK, Schneider CM, Blondel V, Smoreda Z, González MC, and Colizza V. 2014. On the Use of Human Mobility Proxies for Modeling Epidemics. PLoS Computational Biology 10(7):e1003716.
Tkalčec T, Vyroubal V, Bedić Ž, and Šlaus M. 2015. A Case of Childhood Tuberculosis from Modern Period Burial from Crkvari, Northern Croatia. Podravina: Časopis za Multidisciplinarna Istraživanja 14(28).
Todd TW. 1920. Age Changes in the Pubic Bone. I. The Male White Pubis. American Journal of Physical Anthropology 3(3):285-334.
Toizumi T, Thuy NK, and Sawada J. 2011. Fish Remains at Man Bac. In: Oxenham MF, Matsumura H, and Kim Dung N, editors. Man Bac: The Excavation of a Neolithic Site in Northern Vietnam The Biology, Terra Australis 33. Cannerra, Australia: ANU ePress. p 117-126.
Tolley H, Barnes J, and Freeman M. 2016. Survival Analysis. In: Freeman M, and Zeegers M, editors. Forensic Epidemiology: Elsevier. p 261-284.
Tontisirin K, Nantel G, and Bhattacharjee L. 2002. Food-Based Strategies to Meet the Challenges of Micronutrient Malnutrition in the Developing World. Proceedings of the Nutrition Society 61(2):243-250.
Toussaint F, Pere P, Le Chaffotec L, Grandhaye P, Pourel J, and Chary-Valckenaere I. 2001. Alveolar Echinococcosis of the Spine. JCR: Journal of Clinical Rheumatology 7(4):248-251.
Trembly DL. 1995. On the Antiquity of Leprosy in Western Micronesia. International Journal of Osteoarchaeology 5(4):377-384.
Tsend S, Baljinnyam Z, Suuri B, Dashbal E, Oidov B, Roth F, Zinstag J, Schelling E, and Dambadarjaa D. 2014. Seroprevalence Survey of Brucellosis among Rural People in Mongolia. Western Pacific Surveillance and Response Journal: WPSAR 5(4):13.
Tserendolgor U, Mawson J, MacDonald A, and Oyunbileg M. 1998. Prevalence of Rickets in Mongolia. Asia Pacific Journal of Clinical Nutrition 7:325-328.
Tsuda T, and Baker BJ. 2015. Conclusion: Migration and Disruptions from Prehistory to the Present. In: Baker BJ, and Tsuda T, editors. Migration and Disruptions: Toward a Unifying Theory of Ancient and Contemporary Populations. Gainesville, Florida: University Press of Florida. p 296-331.
Tsuda T, Baker BJ, Eder JF, Knudson KJ, Maupin J, Meierotto L, and Scott RE. 2015. Unifying Themes in Studies of Ancient and Contemporary Migrations. In: Baker BJ, and Tsuda T, editors. Migration and Disruptions: Toward a Unifying Theory of Ancient and Contemporary Populations. Gainesville, Florida: University Press of Florida. p 15-30.
Tsybiktarov A. 2002. Khereksury i Pamiatniki Mongun-Taiginskogo Tipa. In: Piotrovskii I, editor. Stepi Evrazii v Drevnosti i Srednevekov'e (in Russian). Saint Petersburg, Russia: Institute of History of Material Culture and the State Hermitage Museum. p 173-176.
Tunacı M, Tunacı A, Engin G, Özkorkmaz B, Dinçol G, Acunaş G, and Acunaş B. 1999. Imaging Features of Thalassemia. European Radiology 9(9):1804-1809.
Tung T. 2012. The Bioarchaeology of Migration. SAA Archaeological Record:42-45.
Tung TA. 2008. Life on the Move: Bioarchaeological Contributions to the Study of Migration and Diaspora Communities in the Andes. In: Silverman H, and Isbell WH, editors. The Handbook of South American Archaeology. New York: Springer. p 671-680.
Tur S, Matrenin S, and Soenov V. 2018. Armed Violence Among the Altai Mountains Pastoralists of the Xiongnu-Sarmatian Age. Archaeology, Ethnology & Anthropology of Eurasia 46(4):132-139.

Turgut M. 2001. Spinal Tuberculosis (Pott's Disease): Its Clinical Presentation, Surgical Management, and Outcome. A Survey Study on 694 Patients. Neurosurgical Review 24(1):8-13.

Turner BL, Zuckerman MK, Garofalo EM, Wilson A, Kamenov GD, Hunt DR, Amgalantugs T, and Frohlich B. 2012. Diet and Death in Times of War: Isotopic and Osteological Analysis of Mummified Human Remains from Southern Mongolia. Journal of Archaeological Science 39(10):3125-3140.

Tykot RH, and Chia S. 1996. Long-Distance Obsidian Trade in Indonesia. MRS Online Proceedings Library Archive 462:175.

Ubelaker D, Jones E, Donoghue HD, and Spigelman M. 2000. Skeletal and Molecular Evidence for Tuberculosis in a Forensic Case. Anthropologie (1962-) 38(2):193-200.

Ubelaker DH. 1987. Estimating Age at Death from Immature Human Skeletons: An Overview. Journal of Forensic Science 32(5):1254-1263. DOI: 10.1520/JFS11176J

US Department of Agriculture. 2019. FoodData Central. https://fdc.nal.usda.gov.

Uush T. 2013. Prevalence of Classic Signs and Symptoms of Rickets and Vitamin D Deficiency in Mongolian Children and Women. The Journal of Steroid Biochemistry and Molecular Biology 136:207-210.

van der Bij AK, and Pitout JD. 2012. The Role of International Travel in the Worldwide Spread of Multiresistant Enterobacteriaceae. Journal of Antimicrobial Chemotherapy 67(9):2090-2100.

van der Mei IA, Ponsonby A-L, Blizzard L, and Dwyer T. 2001. Regional Variation in Multiple Sclerosis Prevalence in Australia and its Association with Ambient Ultraviolet Radiation. Neuroepidemiology 20(3):168-174.

Vatankhah A, Halász J, Piurkó V, Barbai T, Rásó E, and Tímár J. 2015. Characterization of the Inflammatory Cell Infiltrate and Expression of Costimulatory Molecules in Chronic Echinococcus granulosus Infection of the Human Liver. BMC Infectious Diseases 15(1):530.

Vazquez-Prokopec GM, Bisanzio D, Stoddard ST, Paz-Soldan V, Morrison AC, Elder JP, Ramirez-Paredes J, Halsey ES, Kochel TJ, and Scott TW. 2013. Using GPS Technology to Quantify Human Mobility, Dynamic Contacts and Infectious Disease Dynamics in a Resource-Poor Urban Environment. PloS one 8(4):e58802.

Ventresca Miller AR, and Makarewicz CA. 2019. Intensification in Pastoralist Cereal use Coincides with the Expansion of Trans-Regional Networks in the Eurasian Steppe. Scientific Reports 9(1):8363.

Verge CF, Lam A, Simpson JM, Cowell CT, Howard NJ, and Silink M. 1991. Effects of Therapy in X-linked Hypophosphatemic Rickets. New England Journal of Medicine 325(26):1843-1848.

Viswanath B, Shastry V, Ramamurty U, and Ravishankar N. 2010. Effect of Calcium Deficiency on the Mechanical Properties of Hydroxyapatite Crystals. Acta Materialia 58(14):4841-4848.

Vlok M, Oxenham M, Domett K, Tran MT, Mai Huong NT, Matsumura H, Trinh HH, Higham T, Higham CF, Huu NT et al. . 2020. Two Probable Cases of Infection with *Treponema pallidum* during the Neolithic Period in Northern Vietnam (ca. 2000-1500B.C.). Bioarchaeology International 4(1):15-39.

Vlok M, Oxenham MF, Domett K, Hiep TH, Minh TT, Mai Huong NT, Matsumura H, McFadden C, Huu NT, and Buckley H. in review. Subadult Nutritional Stress during the Agricultural Transition in Southeast Asia: Perspectives from a Neolithic site in Northern Vietnam. International Journal of Paleopathology.

Vohra R, Kang HS, Dogra S, Saggar RR, and Sharma R. 1997. Tuberculous Osteomyelitis. The Journal of Bone and Joint Surgery British Volume 79(4):562-566.
Waguespack NM. 2002. Colonization of the Americas: Disease Ecology and the Paleoindian Lifestyle. Human Ecology 30(2):227-243.
Waldholtz BD, and Andersen AE. 1988. Hypophosphatemia During Starvation in Anorexia Nervosa. International Journal of Eating Disorders 7(4):551-555.
Waldron T. 1991a. Rates for the Job. Measures of Disease Frequency in Palaeopathology. International Journal of Osteoarchaeology 1(1):17-25.
Waldron T. 1991b. Variations in the Rates of Spondylolysis in Early Populations. International Journal of Osteoarchaeology 1(1):63-65.
Waldron T. 2008. Palaeopathology: Cambridge University Press.
Walker PL, Bathurst RR, Richman R, Gjerdrum T, and Andrushko VA. 2009. The Causes of Porotic Hyperostosis and Cribra Orbitalia: A Reappraisal of the Iron-Deficiency-Anemia Hypothesis. American Journal of Physical Anthropology 139(2):109-125.
Walrath DE, Turner P, and Bruzek J. 2004. Reliability Test of the Visual Assessment of Cranial Traits for Sex Determination. American Journal of Physical Anthropology 125(2):132-137.
Walter BS, and DeWitte SN. 2017. Urban and Rural Mortality and Survival in Medieval England. Annals of Human Biology 44(4):338-348.
Wang M, He Y, Shi L, and Shi C. 2011. Multivariate Analysis by Cox Proportional Hazard Model on Prognosis of Patient with Epithelial Ovarian Cancer. European Journal of Gynaecological Oncology 32(2):171-177.
Wang M-C, Liu C-Y, Shiao A-S, and Wang T. 2005. Ear Problems in Swimmers. Journal of the Chinese Medical Association 68(8):347-352.
Wang P, Sun W, Shi L, and Li T. 2020. Osteonecrosis of the Femoral Head due to Brucellosis: A Case Report. BMC Infectious Diseases 20(1):1-4.
Wang Q, Xiao Y-f, Vuitton DA, Schantz PM, Raoul F, Budke C, Campos-Ponce M, Craig PS, and Giraudoux P. 2007. Impact of Overgrazing on the Transmission of Echinococcus multilocularis in Tibetan Pastoral Communities of Sichuan Province, China. Chinese Medical Journal (Beijing English Edition) 120(3):237.
Ward SM. 2019. The Health Impacts of Increasing Social Inequality in Late Prehistoric Northeast Thailand: University of Otago.
Wärmländer SK, and Sholts SB. 2011. Sampling and Statistical Considerations for the Suchey–Brooks Method for Pubic Bone Age Estimation: Implications for Regional Comparisons. Science & Justice 51(3):131-134.
Watanabe F. 2007. Vitamin B12 sources and bioavailability. Experimental Biology and Medicine 232(10):1266-1274.
Watanabe H. 1966. Jomonjin no Seitai: Jukyo no Anteisei to Sono Seibutsugakuteki Minzokushiteki Igi (Ecology of the Jomon People: Stability of Habitation and its Biological and Ethnohistorical Implications). Jinruigaku Zasshi 74(749):73-84.
Watanabe H. 1986. Community Habitation and Food Gathering in Prehistoric Japan: An Ethnographic Interpretation of the Archaeological Evidence. In: Pearson R, Barnes G, and Hutterer K, editors. Windows on the Japanese Past: Studies in Archaeology and Prehistory. Ann Arbor, Michigan: University of Michigan Center for Japanese Studies.
Waters-Rist AL, Faccia K, Lieverse A, Bazaliiskii VI, Katzenberg MA, and Losey RJ. 2014. Multicomponent Analyses of a Hydatid Cyst from an Early Neolithic Hunter–Fisher–Gatherer from Lake Baikal, Siberia. Journal of Archaeological Science 50:51-62.

Watson-Jones D, Craig P, Badamochir D, Rogan M, Wen H, and Hind B. 1997. A Pilot, Serological Survey for Cystic Echinococcosis in North-Western Mongolia. Annals of Tropical Medicine & Parasitology 91(2):173-177.
Watts R, Paice E, and White A. 1987. Spontaneous Fracture of the Sternum and Sternal tuberculosis. Thorax 42(12):984-985.
Weatherall D. 2008. Genetic Variation and Susceptibility to Infection: The Red Cell and Malaria. British Journal of Haematology 141(3):276-286.
Webb S. 2009. Palaeopathology of Aboriginal Australians: Health and Disease across a Hunter-gatherer Continent. Cambridge, UK: Cambridge University Press.
Weber J, Czarnetzki A, and Pusch CM. 2004. Paleopathological Examination of Medieval Spines with Exceptional Thoracic Kyphosis most likely Secondary to Spinal Tuberculosis: Historical Vignette. Journal of Neurosurgery: Spine 1(2):238-242.
Weber S, Lehman H, Barela T, Hawks S, and Harriman D. 2010. Rice or Millets: Early Farming Strategies in Prehistoric Central Thailand. Archaeological and Anthropological Sciences 2(2):79-88.
Webster JP, and McConkey GA. 2010. Toxoplasma gondii-Altered Host Behaviour: Clues as to Mechanism of Action. Folia parasitologica 57(2):95-104.
Wells CR, Sah P, Moghadas SM, Pandey A, Shoukat A, Wang Y, Wang Z, Meyers LA, Singer BH, and Galvani AP. 2020. Impact of International Travel and Border Control Measures on the Global Spread of the Novel 2019 Coronavirus Outbreak. Proceedings of the National Academy of Sciences 117(13):7504-7509.
Wendrich W, and Barnard H. 2008. The Archaeology of Mobility: Definitions and Research Approaches. In: Barnard H, and Wendrich W, editors. The Archaeology of Mobility: Old World and New World Nomadism. Los Angeles, CA: ISD LLC. p 1-24.
Wesolowski A, Qureshi T, Boni MF, Sundsøy PR, Johansson MA, Rasheed SB, Engø-Monsen K, and Buckee CO. 2015. Impact of Human Mobility on the Emergence of Dengue Epidemics in Pakistan. Proceedings of the National Academy of Sciences 112(38):11887-11892.
Weston DA. 2008. Investigating the Specificity of Periosteal Reactions in Pathology Museum Specimens. American Journal of Physical Anthropology 137(1):48-59.
Weston DA. 2012. Nonspecific Infection in Paleopathology: Interpreting Periosteal Reactions. In: Grauer AL, editor. A Companion to Paleopathology. p 492-512.
Wharton B, and Bishop N. 2003. Rickets. The Lancet 362(9393):1389-1400.
White NJ, Pukrittayakamee S, Hien TT, Faiz MA, Mokuolu OA, and Dondorp AM. 2014. Malaria. The Lancet 383:723-735.
White TD. 1992. Prehistoric Cannibalism at Mancos 5MTUMR-2346. Princeton, USA: Princeton University Press.
White TD, Black MT, and Folkens PA. 2012. Human Osteology: Academic Press.
WHO. 2000. WHO Report on Global Surveillance of Epidemic-Prone Infectious Diseases.
Wiessner P. 2002. Hunting, Healing, and Hxaro Exchange: A Long-Term Perspective on !Kung (Ju/'hoansi) Large-Game Hunting. Evolution and Human Behavior 23(6):407-436.
Wilcox BA, and Colwell RR. 2005. Emerging and Reemerging Infectious Diseases: Biocomplexity as an Interdisciplinary Paradigm. EcoHealth 2(4):244.
Wilkin S, Miller AV, Miller BK, Spengler RN, Taylor WT, Fernandes R, Hagan RW, Bleasdale M, Zech J, and Ulziibayar S. 2020a. Economic Diversification Supported the Growth of Mongolia's Nomadic Empires. Scientific Reports 10(1):1-12.
Wilkin S, Miller AV, Taylor WT, Miller BK, Hagan RW, Bleasdale M, Scott A, Gankhuyg S, Ramsøe A, and Uliziibayar S. 2020b. Dairy Pastoralism Sustained

Eastern Eurasian Steppe Populations for 5,000 years. Nature Ecology & Evolution 4(3):346-355.
Willcox R. 1974. Changing Patterns of Treponemal Disease. British Journal of Venereal Diseases 50(3):169.
Willis A, and Oxenham MF. 2013. The Neolithic Demographic Transition and Oral Health: The Southeast Asian Experience. American Journal of Physical Anthropology 152(2):197-208.
Wilson ME. 1995. Travel and the Emergence of Infectious Diseases. Emerging Infectious Diseases 1(2):39-46.
Wilson ME. 2007. Population Mobility and the Geography of Microbial Threats. Population Mobility and Infectious Disease: Springer Online. p 21-39.
Winichagoon P, Fucharoen S, Weatherall D, and Wasi P. 1985. Concomitant Inheritance of α-Thalassemia in β°-Thalassemia/Hb E Disease. American Journal of Hematology 20(3):217-222.
Wintergerst ES, Maggini S, and Hornig DH. 2006. Immune-Enhancing Role of Vitamin C and Zinc and Effect on Clinical Conditions. Annals of Nutrition and Metabolism 50(2):85-94.
Wood JW, Milner GR, Harpending HC, Weiss KM, Cohen MN, Eisenberg LE, Hutchinson DL, Jankauskas R, Cesnys G, and Česnys G. 1992. The Osteological Paradox: Problems of Inferring Prehistoric Health from Skeletal Samples [And Comments and Reply]. Current Anthropology 33(4):343-370.
Woods CR. 2005. Syphilis in Children: Congenital and Acquired. Seminars in Pediatric Infectious Diseases: Elsevier. p 245-257.
Woolhouse ME, Webster JP, Domingo E, Charlesworth B, and Levin BR. 2002. Biological and Biomedical Implications of the Co-evolution of Pathogens and their Hosts. Nature Genetics 32(4):569-577.
World Health Organization. 1998. WHO Expert Committee on Leprosy: Seventh Report.
World Health Organization. 2013. Global Tuberculosis Report 2013.
Wright J. 2012. Landscapes of Inequality?: A Critique of Monumental Hierarchy in the Mongolian Bronze Age. Asian Perspectives 51(2):139-163.
Wright J, Honeychurch W, and Amartuvshin C. 2009. The Xiongnu Settlements of Egiin Gol, Mongolia. Antiquity 83(320):372-387.
Wright LE, and Yoder CJ. 2003. Recent Progress in Bioarchaeology: Approaches to the Osteological Paradox. Journal of Archaeological Research 11(1):43-70.
WWF. 2016. Living Planet: Report 2016: Risk and Resilience in a New Era: World Wide Fund for Nature.
Yamaguchi Y. 2010. Sanyo Chiho ni Okeru Jomon Jidai Ko-Banki no Shuraku (Late and Final Jomon Settlements in the Sanyo Region). Kokogaku Kenkyukai Okayama Reikai (Okayama Section of the Quarterly of Archaeological Studies). Okayama: Kokogaku Kenkyukai. p 7-23. (In Japanese).
Yamazaki Y, Okazaki R, Shibata M, Hasegawa Y, Satoh K, Tajima T, Takeuchi Y, Fujita T, Nakahara K, and Yamashita T. 2002. Increased Circulatory Level of Biologically Active Full-Length FGF-23 in Patients with Hypophosphatemic Rickets/Osteomalacia. The Journal of Clinical Endocrinology & Metabolism 87(11):4957-4960.
Yang K. 1940. Clavicle Sign of Late Congenital Syphilis: Review of Literature and Report of Six Cases. Archives of Dermatology and Syphilology 41(6):1060-1065.
Yeh H-Y, Mao R, Wang H, Qi W, and Mitchell PD. 2016. Early Evidence for Travel with Infectious Diseases along the Silk Road: Intestinal Parasites from 2000 year-old

Personal Hygiene Sticks in a Latrine at Xuanquanzhi Relay Station in China. Journal of Archaeological Science: Reports 9:758-764.
Yoneda M. 2008. Dietary Reconstruction of Ancient Vietnamese based on Carbon and Nitrogen Isotopes. Man Bac Symposium. Institute of Archaeology, Hanoi, Vietnam.
Zadonina N, and Aptikaeva O. 2012. Rhythms in Occurrence of Epidemics and Epizootics in Siberia and Mongolia. Izvestiya, Atmospheric and Oceanic Physics 48(8):818-822.
Zasloff M. 2006. Fighting Infections with Vitamin D. Nature Medicine 12(4):388-390.
Zezza A, Carletto C, Davis B, and Winters P. 2011. Assessing the Impact of Migration on Food and Nutrition Security. Food Policy 36(1):1-6.
Zhang C, and Hung H-C. 2012. Later Hunter-Gatherers in Southern China, 18 000–3000 BC. Antiquity 86(331):11-29.
Zhang Z. 1994. The Skeletal Evidence of Human Leprosy and Syphilis in Anciet China. Acta Anthropologica Sinica 4.
Zhanshui Y, Cheng D, Chen X, Xie F, and Fuxing L. 2014. Relationship between Brucellosis Arthritis of the Hip and Femoral Head Necrosis. Chinese Journal of Endemiology 33(1):93-95.
Zhao Z. 2011. New Archaeobotanic Data for the Study of the Origins of Agriculture in China. Current Anthropology 52(S4):S295-S306.
Zhou Y, Ma Z, and Brauer F. 2004. A Discrete Epidemic Model for SARS Transmission and Control in China. Mathematical and Computer Modelling 40(13):1491-1506.
Zlitni M, Ezzaouia K, Lebib H, Karray M, Kooli M, and Mestiri M. 2001. Hydatid Cyst of Bone: Diagnosis and Treatment. World Journal of Surgery 25(1):75-82.
Zuckerman MK, Turner BL, and Armelagos GJ. 2012. Evolutionary Thought in Paleopathology and the Rise of the Biocultural Approach. In: Grauer A, editor. A Companion to Paleopathology. Oxford, UK: Wiley-Blackwell. p 34-57.

APPENDICES

APPENDIX 1:
SEX AND AGE ESTIMATION METHODS

Ota: Middle Jomon Japan

Approximately two-thirds of the assemblage could be estimated for sex with the crania, and two-thirds with the pelvis (Table A1.1), reflective of preservation issues in this assemblage.

Table A1.1: *Number of individuals from Ota estimated with each sex estimation method.*

ESTIMATION TECHNIQUE	# INDIVIDUALS ESTIMATED
Cranial Estimation	21
Pelvic Estimation	20

The pubic symphysis was poorly preserved for most individuals, therefore adult age estimation predominantly relied on the auricular surface method (Table A1.2). Four adult individuals did not have pubic symphyses nor auricular surfaces; therefore an age category was assigned to these individuals based on tooth wear seriation. When these individuals are removed from the age distribution, the distribution varies minimally.

Table A1.2: *Number of individuals from Ota estimated with each age estimation method.*

AGE COHORT	# INDIVIDUALS ESTIMATED
Long Bone Length	2
Primary Elements	0
Dental Eruption (supplemented by formation of loose teeth)	1
Epiphysial Fusion Timing	2
Auricular Surface	17
Pubic Symphysis	6
Tooth Wear Seriation	4

Tsukumo: Late to Final Jomon Japan

Pelvic and cranial estimates were available for 20 individuals, with one individual estimated with cranial features only, and one individual with pelvic features only (Table A1.3).

Table A1.3: *Number of individuals from Tsukumo estimated with each sex estimation method.*

ESTIMATION TECHNIQUE	# INDIVIDUALS ESTIMATED
Cranial Estimation	21
Pelvic Estimation	21

Dental eruption was the primary method of age estimation for nonadults as most were between the ages of 1 and 5 years of age (Table A1.4). All adult individuals presented with either an auricular surface or a pubic symphysis, and therefore estimate of age with dental wear seriation was not necessary for this assemblage.

Table A1.4: *Number of individuals from Tsukumo estimated with each age estimation method.*

AGE COHORT	# INDIVIDUALS ESTIMATED
Long Bone Length	2
Primary Elements	4
Dental Eruption (supplemented by formation of loose teeth)	8
Epiphysial Fusion Timing	5
Auricular Surface	18
Pubic Symphysis	16
Tooth Wear Seriation	0

Bronze Age Mongolia

All individuals wherein sex could be estimated with the exception of one individual, had pelvic elements preserved for estimation and a significantly higher present of pelvic than cranial elements were present in this assemblage (Table A1.5). Therefore confident estimates of sex could be presented, and where individuals were considered *probable male* or *probable female* this was due to intermediate traits of the pelvis, or poor preservation of the pelvis where only single features such as the greater sciatic notch or preauricular sulcus were present. The exception is of one individual estimated as a *probable male* due to the availability of a cranial estimate only. However, there were a number of individuals where neither pelvis nor cranial estimates were possible due to missing elements, resulting in the high number of indeterminate estimates in this assemblage.

Table A1.5: *Number of individuals from Bronze Age Mongolia estimated with each sex estimation method.*

ESTIMATION TECHNIQUE	# INDIVIDUALS ESTIMATED
Cranial Estimation	25
Pelvic Estimation	62

Crania and teeth were missing for most nonadults, therefore nonadult age estimation was reliant on long bone length, primary elements and for older nonadults, epiphysial fusion timing (Table A1.6). In adults, the auricular surfaces were better preserved than pubic symphyses. All individuals estimated with pubic symphyses also had auricular surfaces present for estimation. Two adults were estimated with tooth seriation, one a young adult with fused epiphyses and minimal tooth wear, another an old adult with severe tooth wear, advanced osteoporosis of the bones and advanced degeneration of all preserved joints.

Table A1.6**:** *Number of individuals from Bronze Age Mongolia estimated with each age estimation method.*

AGE COHORT	# INDIVIDUALS ESTIMATED
Long Bone Length	6
Primary Elements	3
Dental Eruption (supplemented by formation of loose teeth)	4
Epiphysial Fusion Timing	10
Auricular Surface	56
Pubic Symphysis	35
Tooth Wear Seriation	2

Xiongnu Period (Iron Age) Mongolia

All individuals with the exception of five individuals could be estimated from the pelvis. Of these five, one had cranial estimates only, with the further four missing both cranial and pelvic estimates. The presence of pelvic elements available for sex estimation were considerably higher than the presence of cranial elements, as most individuals in the assemblage had missing crania (Table A1.7). The high number of individuals who could be confidently identified as *male* and *female* is attributed to excellent preservation of pelvic elements in this assemblage.

Table A1.7: *Number of individuals from Xiongnu Period Mongolia estimated with each sex estimation method.*

ESTIMATION TECHNIQUE	# INDIVIDUALS ESTIMATED
Cranial Estimation	29
Pelvic Estimation	54

As was the case with the Bronze Age Mongolian assemblage, crania and teeth were missing for most nonadults, therefore nonadult age estimation was reliant on long bone length, primary elements and for older nonadults, epiphysial fusion timing (Table A1.8). In adults, the auricular surfaces were only slightly better preserved than pubic symphyses. This was due to excellent preservation of the pelvis.

Table A1.8: *Number of individuals from Xiongnu Period Mongolia estimated with each age estimation method.*

AGE COHORT	# INDIVIDUALS ESTIMATED
Long Bone Length	5
Primary Elements	2
Dental Eruption (supplemented by formation of loose teeth)	3
Epiphysial Fusion Timing	12
Auricular Surface	45
Pubic Symphysis	38
Tooth Wear Seriation	0

APPENDIX 2:
INDIVIDUAL CATALOGUE

Skeletal profile for individuals assessed by M. Vlok is presented here.

Ota (Middle Jomon Period, Japan)

Skeletal ID: 666A

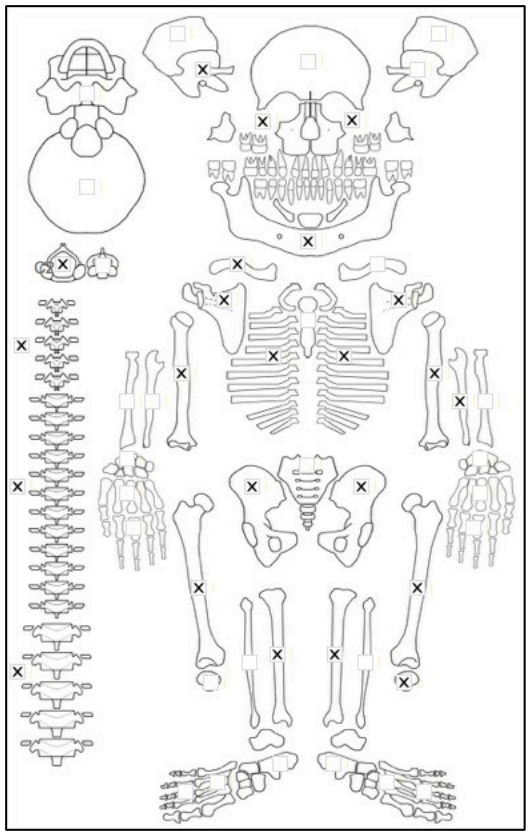

Completeness: Near Complete (66 to 75%). Represented by 47% of long bones, 6% of hands and feet, 54% of vertebrae and approx. 33% of ribs.
Preservation/ Taphonomy: Was originally labelled as 666. Could be clearly separated as two individuals (666A and 666B). Some of the vertebrae are represented only by broken fragments of vertebral body. Many ribs were represented, but all fragmented.
Age: 40- 49, *Middle Aged Adult*
Sex: Male
Macroscopic Lesion Summary:
- enlarged posterior foramen on the posterior left zygomatic
- unilateral fine cortical porosity on the anterior surface of the zygoma more laterally towards the temporal process and inferior to the foramen. The surface makes it difficult to determine where the extent of the lesion is but is directly under the foramen. Appears to be associated with a thin deposit of remodelled new bone.
- Remodelled new bone response and porosity across the posterior aspect of the right maxilla body superior to the alveolar margin. Porosity is less than 1mm in diameter. The margin of the bone deposition is defined. There is severe lytic and blastic process to the right maxillary including the maxillary sinus (and alveolar lesion of tooth). Left side missing.
- Bilateral mixed remodelled porosity and new bone deposition across the palatal surfaces of the maxillae. There is a tooth abscess of the right maxillary M1. This is associated with severe lytic and blastic process to the right maxillary including the maxillary sinus (and abscess of tooth), and the left and right palatal region of the maxillae. There is severe alveolar resorption indicating gum disease (remodelled erosion of the anterior alveolar bone of the left and right maxilla leading to antemortem tooth loss of the left central incisor).

- Remodelled lytic destruction in the right maxillary sinus. There are deep circular and irregular cavitations in the remodelled bone surface particularly noticeable on the anterior margin of the sinus suggestive of infectious process. There is deep penetration and subsequent remodelling of the root are of the M3. Lesion max diameter: 34mm
- Localised unilateral remodelled porosity inferior to the infraorbital foramen likely an extension of the sinus lytic destruction penetrating the cortical bone.
- Lytic channel on the inferior nasal surface, margins are sharp and bilateral and lateral to the anterior nasal spine. May be anatomical variant.
- Unilateral remodelled deposit of new bone on the anterior and medial middle third shaft of the left tibia.
- Unilateral diffuse mixed active and remodelled new bone on the medial middle third shaft of the left femur. The lesion terminates medial to the linea aspera. There is some associated cortical porosity. Remodelling proximally and active more distally.

Radiographic Lesion Summary:
No radiographs taken
Differential Diagnosis Outcome:
No specific disease diagnosed

Skeletal ID: 666B.

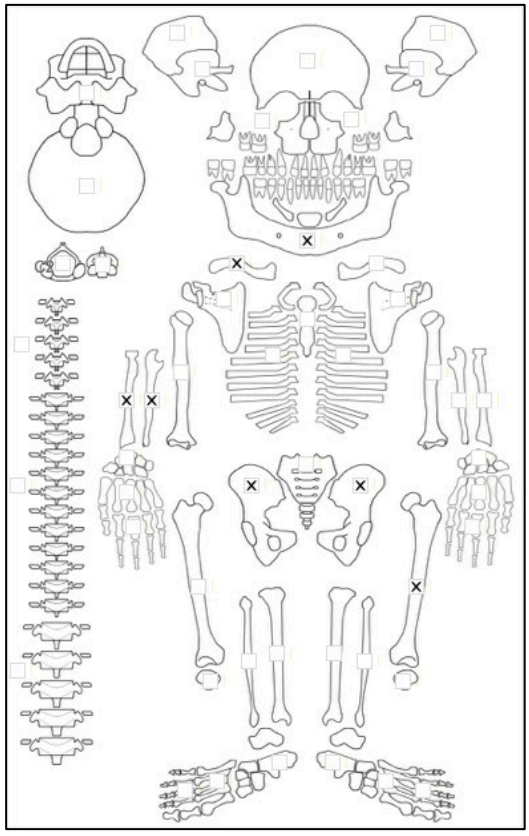

Completeness: Fragmented. Only represented by mandible, right radius and ulna, left femur, other fragments of long bones, 2 metacarpals, partial os coxae and right clavicle.
Preservation/ Taphonomy: Was originally labelled as 666. Could be clearly separated as two individuals (666A and 666B).
Age: 30-39, *Middle Aged Adult*
Sex: Male
Macroscopic Lesion Summary:
- Bilateral oval lytic lesions on the posterior border of the ischial tuberosities with defined margins, and sclerotic reaction on the base. Lesion diameters: 10mm (left) and 11.5mm (right). The is considerable remodelling.

Radiographic Lesion Summary:
No radiographs taken
Differential Diagnosis Outcome:
No specific disease diagnosed

Skeletal ID: 707

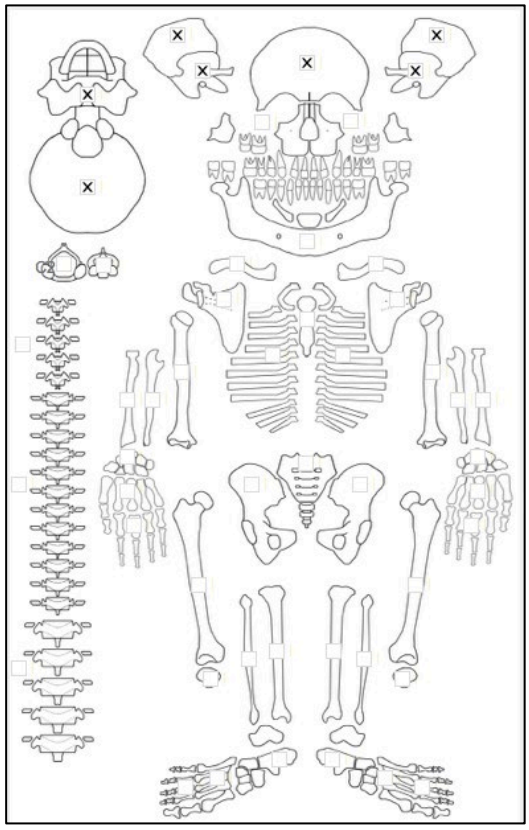

Completeness: Fragmented. Cranium only. Basioccipital missing.
Preservation/ Taphonomy: Surfaces in good condition.
Age: Adult
Sex: Male
Macroscopic Lesion Summary:
- Fine diffuse porosity across the occipital planum of the occipital and posterior halves of the parietals. Consistent with porotic hyperostosis.
Radiographic Lesion Summary:
No radiographs taken
Differential Diagnosis Outcome:
Anaemia

Skeletal ID: 697

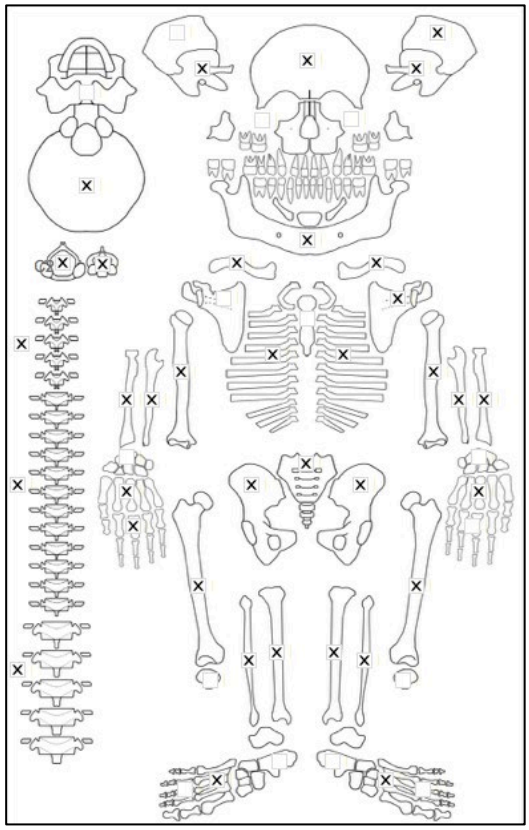

Completeness: Complete (min 75%). 78% of long bones, 21% of hands and feet, 100% of vertebrae, 62.5% of cranium, Approx. 33% of ribs represented.
Preservation/ Taphonomy: Some of surfaces are blackened with severe damage to the endocranial surface of the skull. Ribs are fragmented. Vertebrae are mostly intact. Some commingling of hand bones.
Age: 30-39, *Young Adult*
Sex: Female
Macroscopic Lesion Summary:
- Diffuse porosity in the process of remodelling on the occipital planum and left parietal with the exception of the anterior third. remodelled more anteriorly and more active towards the lambdoid suture on the parietal. occipital porosity remodelled close to the lambdoid but more active towards the nuchal crest. possibly consistent with remodelling mild porotic hyperostosis.
- Lateral bending of the distal third of the shaft. There does not seem to be a corresponding bending that is marked on the radius. Appears bilateral but the distal end of the right ulna is damaged and less clear (no associated bending of the lower leg)
- Bilateral exacerbated lateral curvature at the midshaft of the 5th metatarsals
Radiographic Lesion Summary:
- Ulna radiographed due to slight bending. No abnormal pathology observed. Normal variant.
Differential Diagnosis Outcome:
Anaemia

Skeletal ID: 683

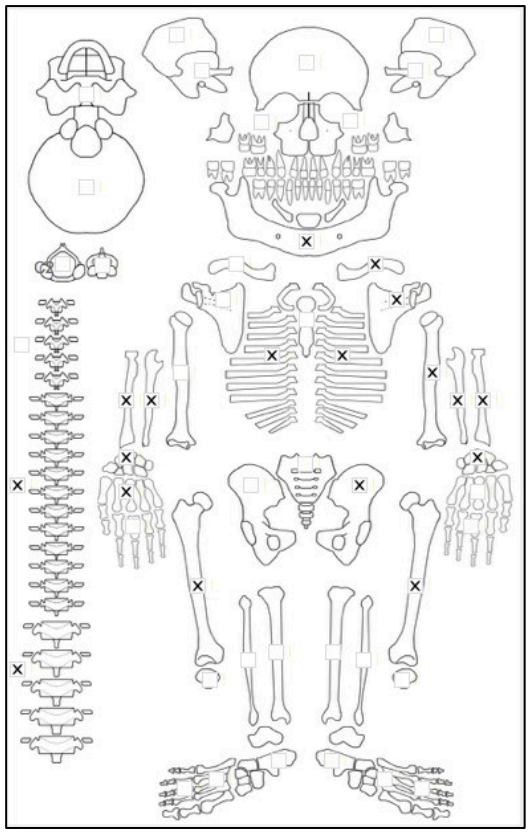

Completeness: Incomplete (33 to 50%). 52% of long bones, 12% of hands and feet, 21% of vertebrae, and one cranial fragment present. Approx. 50% of ribs present.
Preservation/ Taphonomy: Ribs most fragmented but 50% are partially complete.
Age: 20-29, *Young Adult*
Sex: Male
Macroscopic Lesion Summary:
- unilateral defined oval lytic lesion with clear defined margins, with remodelling in the base on the distal posterior shaft of the right radius. The lesion has raised margins. Lesion max diameter: 9.5mm
- a posterior parietal fragment with the lambdoid suture demonstrating fine diffuse porosity throughout the ectocranial aspect of the fragment. The fragment appears to demonstrate mild expansion of the diploe. There is some filling in of the region suggesting the process of remodelling. Consistent with mild porotic hyperostosis.
- remodelled new bone in the formation of striations superior to the costal groove along the internal ribs (likely due to robusticity- normal variant)
Radiographic Lesion Summary:
- lytic lesion on the distal right radius is superficial (does not go deeper than the cortex), with clear sclerotic reaction, localised around the lytic action. There is endosteal expansion of the proximal third posterior aspect of the shaft, possibly similar infectious response.
Differential Diagnosis Outcome:
No specific disease diagnosed

Skeletal ID: 673

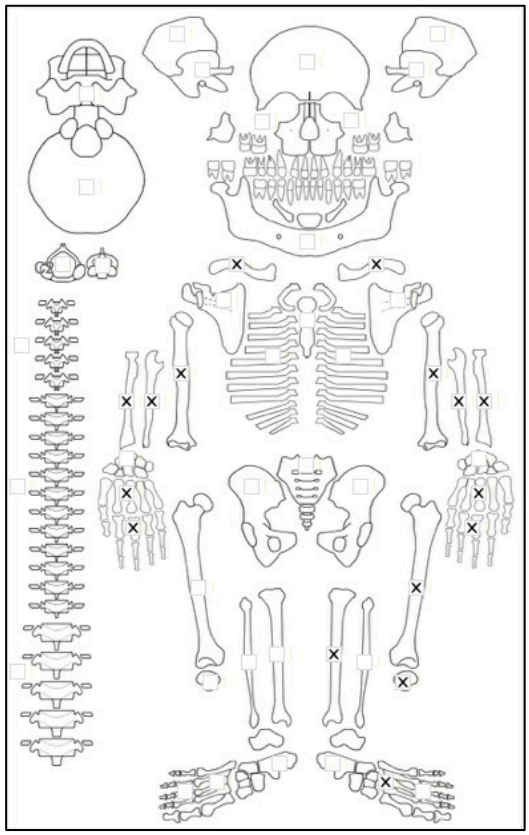

Completeness: Partially Complete (50 to 66%). 78% of long bones, and 39% of hands and feet, no cranium.
Preservation/ Taphonomy: 673 and 672 have commingled ribs and vertebrae, these were not included in analysis (no pathology identified on the vertebrae and ribs)
Age: Adult
Sex: Indeterminate
Macroscopic Lesion Summary:
- Very thick deposit of new bone on the medial portion of the anterior crest of the left tibia. Well healed. Button and circular- consistent with an ulcer.
Radiographic Lesion Summary:
No radiographs taken
Differential Diagnosis Outcome:
No specific disease diagnosed

Skeletal ID: 672

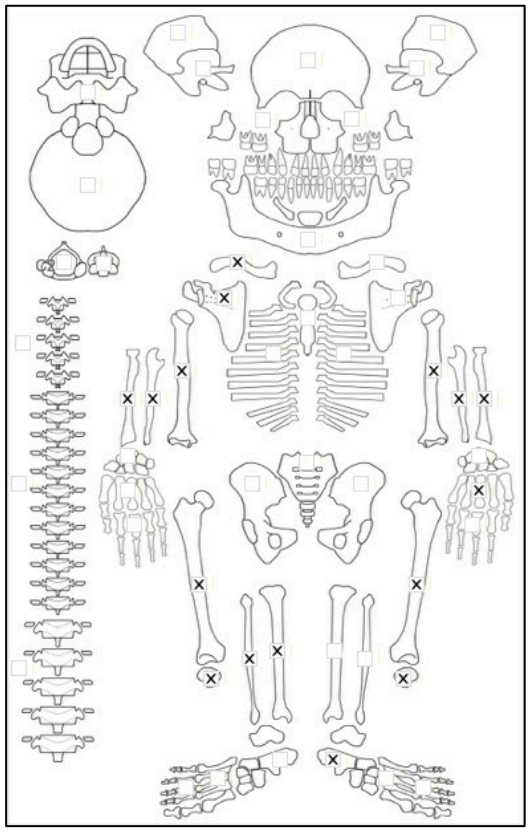

Completeness: Partially Complete (50 to 66%). 78% of long bones and 12.3% of hands and feet, no cranium.
Preservation/ Taphonomy: 673 and 672 have commingled ribs and vertebrae, these were not included in analysis (no pathology identified on the vertebrae and ribs)
Age: Adult.
Sex: Indeterminate
Macroscopic Lesion Summary:
- small remodelled deposit of new bone localised to the middle anterior crest, on the lateral portion, the margins are defined from the lateral view. Appears haematoma-like, but also at region of anterior crest where trauma is common. (left side missing)
- unilateral very thin and small/ poorly defined deposition of remodelled bone anterior to the margin of the deltoid tuberosity, directly inferior to the crest of the lesser tubercle. May be associated with muscle attachments.

Radiographic Lesion Summary:
No radiographs taken.
Differential Diagnosis Outcome:
No specific disease diagnosed

Skeletal ID: 718

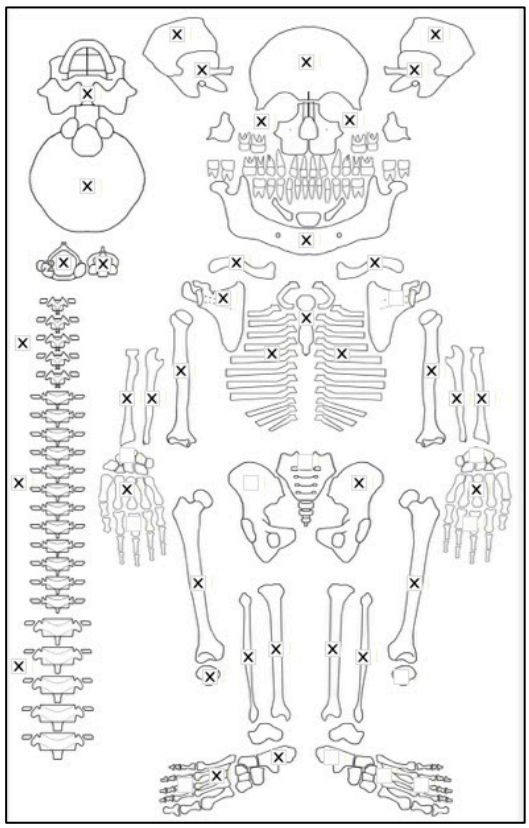

Completeness: Complete (min 75%). 97% of long bones, 25% of hands and feet, 83% of vertebrae, and 87.5% of cranium is present. Approx. 90% of ribs represented.
Preservation/ Taphonomy: Almost all ribs are present, but they are fragmented. Surfaces in good condition.
Age: 40-49, *Middle Aged Adult*
Sex: Indeterminate
Macroscopic Lesion Summary:
- Diffuse fine porosity across the parietals and frontal bone. Appears to be trabecular expansion in form. It is particularly marked around the area of the bregma. The porosity is round and well remodelled but still present suggesting process of remodelling.
- bilateral remodelled cribra orbitalia
- bilateral diffuse fine porosity of unknown aetiology across the anterior left zygomatic.
- unilateral remodelling fine cortical porosity less than 1mm in size on the coronoid process, on the medial surface and superior to the mandibular foramen. Does not involve the foramen.
- two elongated lytic channels with sharp margins in the shape of a channel lateral to the anterior nasal spine on the inferior surface of the nasal region (nasal floor). bilateral but the right maxilla is more marked. possibly a normal anatomical variant
- large deformity with remodelling, a possible lytic lesion, trauma or both on the lateral epicondyle of the right humerus. A notch has formed on the inferior portion of the epicondyle. Margins are irregular due to the bone response; the lesion has formed a channel in the bone. Possibly erosive arthropathy.
- unilateral thick deposit of remodelled new bone on the posteromedial aspect of the proximal to middle third of the right tibia. associated with a possible vascular impression. Possibly trauma to a muscle attachment
- possible remodelled erosive lesion or trauma on the superior margin of a left rib sternal end. Crescent shaped.
- bilateral remodelling cortical porosity localised to the incisive fossae of the mandible
Radiographic Lesion Summary:
No radiographs taken.
Differential Diagnosis Outcome:
Anaemia

Skeletal ID: 687

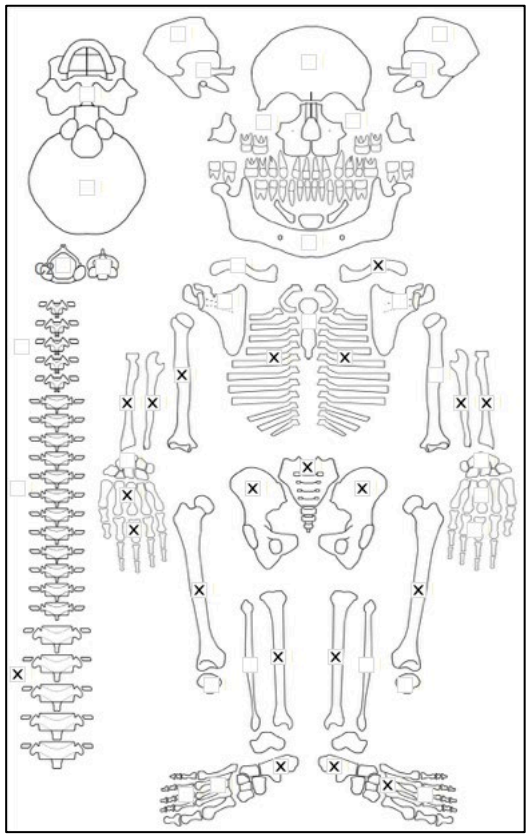

Completeness: Partially Complete (50 to 66%). 60% of long bones, 17% of vertebrae (lumbar only), 178% of hands and feet, and approximately 50% of ribs are represented.
Preservation/ Taphonomy: There is commingling and the skeletal elements are from at least two people (particularly the ribs) there is a gracile and a robust individual. The robust bones: a femur, ulna, left os coxae and mandible were excluded. The mandible may belong to this individual but it is heavily robust, so it has been excluded. The bones are discoloured black. The ribs are partially complete to complete.
Age: Adult
Sex: Indeterminate
Macroscopic Lesion Summary:
- unilateral deposition of new bone on the anterior crest. the deposit is remodelled. The margins more medially can be defined. Continues from proximal third to the midshaft. More marked on the medial surface. Haematoma like- but also at region where trauma is common.
Radiographic Lesion Summary:
No radiographs taken
Differential Diagnosis Outcome:
No specific disease diagnosed

Skeletal ID: 715A

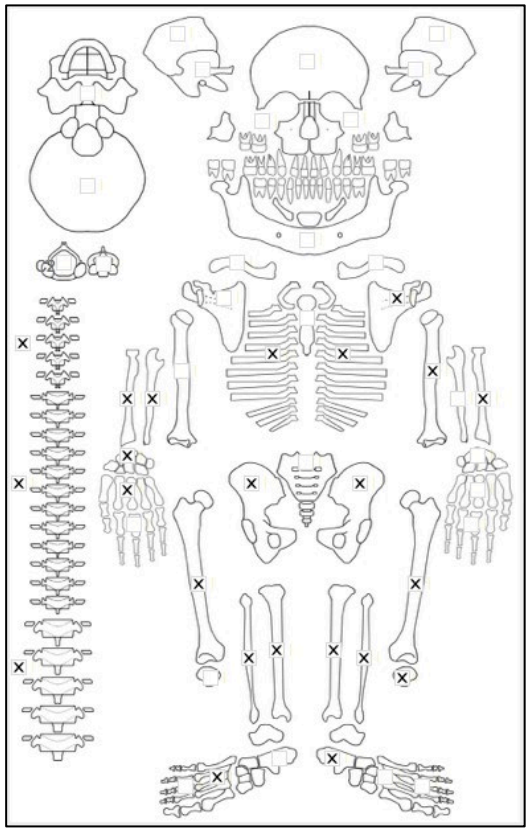

Completeness: Near Complete (66 to 75%). 73% of long bones, 21% of hands and feet, 67% of vertebrae, no cranium, and approximately 50% of ribs represented.
Preservation/ Taphonomy: The bones are chalky have lichen on the surface and also the lower long bones have significant animal scavenging marks on the surface. - gnaw marks on cranium and postcranium (some identified as belonging to rat species endemic to Japan). The ribs are heavily fragmented.
Age: 20-29, Young *Aged Adult*
Sex: Male
Macroscopic Lesion Summary:
- possible remodelled circular lytic lesion on the superior vertebral body of the T11 (or instead is blastic action in the trabecular bone). There is considerable taphonomic damage to the vertebrae therefore it is difficult to determine the original margins of the lesion. The base shows bone filling of the trabecular.
- active lytic expansion horizontal vascular channel, coalescing trabecular expansion on the anterior and lateral vertebral body. (possible normal variation)
- diffuse cortical porosity across the external aspect of multiple fragments of left and right ribs, may be associated with new bone but may also be taphonomic damage to the surface
Radiographic Lesion Summary:
No radiographs taken
Differential Diagnosis Outcome:
No specific disease diagnosed

Skeletal ID: 710

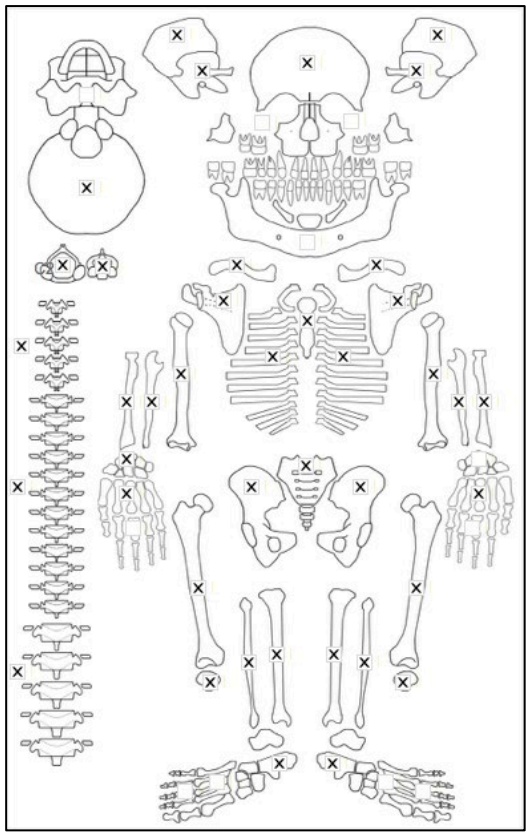

Completeness: Complete (min 75%). 95% of long bones, 28.3% of hands and feet, 100% of vertebrae, 75% of cranium and approximately 66% of ribs represented.
Preservation/ Taphonomy: Intrusive ulna, scapular body, fibula and facial bones of a larger individual, intrusive larger capitate. Mandible too large for individual and male in appearance- these bones were excluded. The basal portion of the skull is missing and the maxillae are fragmented. Ribs are fragmented.
Age: 30- 39, *Young Adult*
Sex: Female
Macroscopic Lesion Summary:
- retained non-closure of the tympanic regions of the temporals.
- bilateral remodelled fine porosity anterior to the carotid canal
- remodelled diffuse porosity across the cranium involving all cranial bones except for the temporal, focus on the parietal eminences, and some focus on the temporal lines and supercilliary arches. no porosity appears active. diploic expansion present.
- bilateral localised fine porosity (likely restricted to the cortical bone only) extending from the supraorbital notches
- remodelled unilateral possible mild cribra orbitalia on the right superior orbital roof. appears as shallow striations on the lateral superior region of the orbit.
- deep arachnoid grooves of the endocranial parietals
- abnormal manubrial porosity
- small focal lytic lesion on the right lateral iliac body inferior to the iliac crest. the outer margins are circular and defined with no sclerotic response. lesion max diameter is 4.5mm
- deep porosity of the sacral alae
- small round lytic lesion with some penetration into the trabecular bone underneath on the posterior aspect of the L1 arch between the spinous process and the superior articular facet. Lesion is well remodelled with 5mm max diameter.
- two circular coalesced depressions on the popliteal surface superior to the medial condyle on the posterior metaphysis of the right femur. The two lesions cover an area of 11mm. Possibly due to trauma.
- diffuse porosity across external ribs (may be robusticity related- seems population specific)
Radiographic Lesion Summary:
No radiographs taken

Differential Diagnosis Outcome:
Anaemia
Possible Scurvy

Skeletal ID: 695

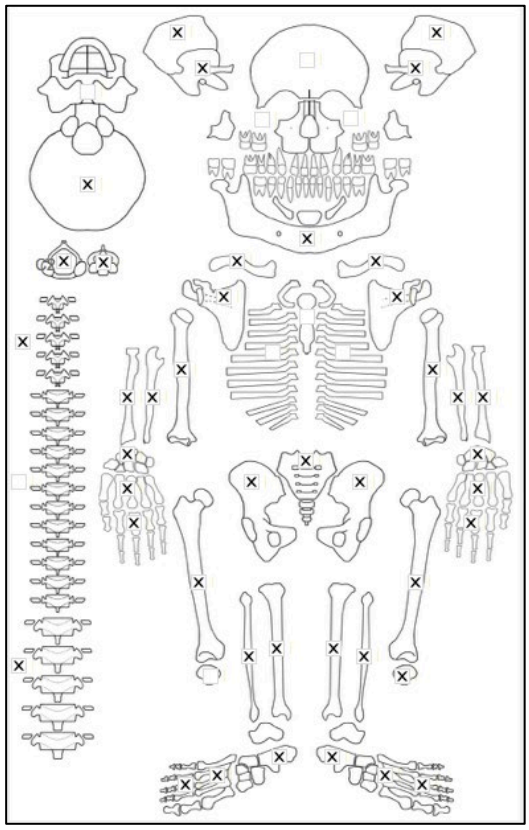

Completeness: Complete (min 75%). 83% of long bones, 59% of hands and feet, 96% of vertebrae, 63% of cranium and no ribs represented.
Preservation/ Taphonomy: Intrusive patellae, radius and ulna of a smaller individual- excluded. The basioccipital is missing.
Age: 40- 49, *Middle Aged Adult*
Sex: Male
Macroscopic Lesion Summary:
- mixed active and remodelled porosity extending from the suprameatal triangle of the right temporal (left missing). Along the suprameatal crest. Associated with a remodelled region of new bone.
- unilateral extensive cortical expansion of the distal end of the left fibula leading to expansion and disfigurement of the surface. Well remodelled.
Radiographic Lesion Summary:
No radiographs taken
Differential Diagnosis Outcome:
No specific disease diagnosed

Skeletal ID: 724

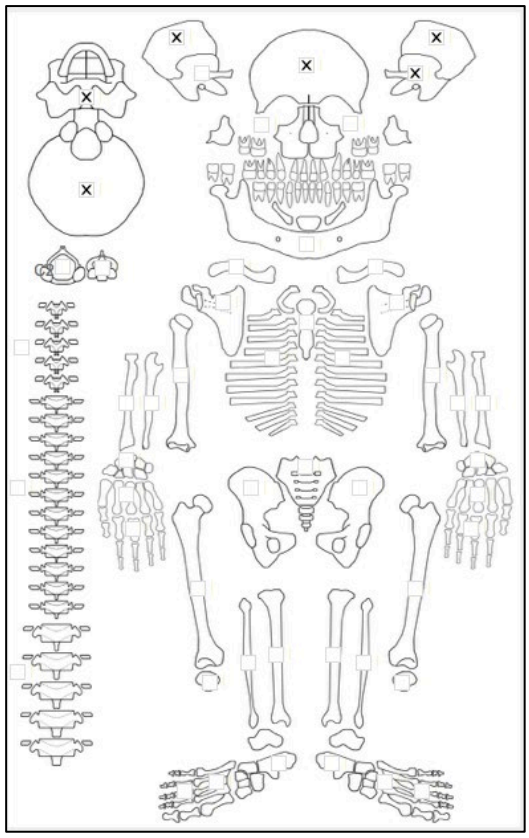

Completeness: Fragmented. Represented by cranium only (75% represented).
Preservation/ Taphonomy: Parietals are incomplete, and left greater wing of sphenoid is only partially complete.
Age: Adult
Sex: Male
Macroscopic Lesion Summary:
- diffuse remodelled new bone and cortical porosity across the endocranial frontal and parietals, with vascular impressions. Some arachnoid granulations.
- remodelled moderate cribra orbitalia
Radiographic Lesion Summary:
No radiographs taken
Differential Diagnosis Outcome:
Anaemia

Skeletal ID: 717

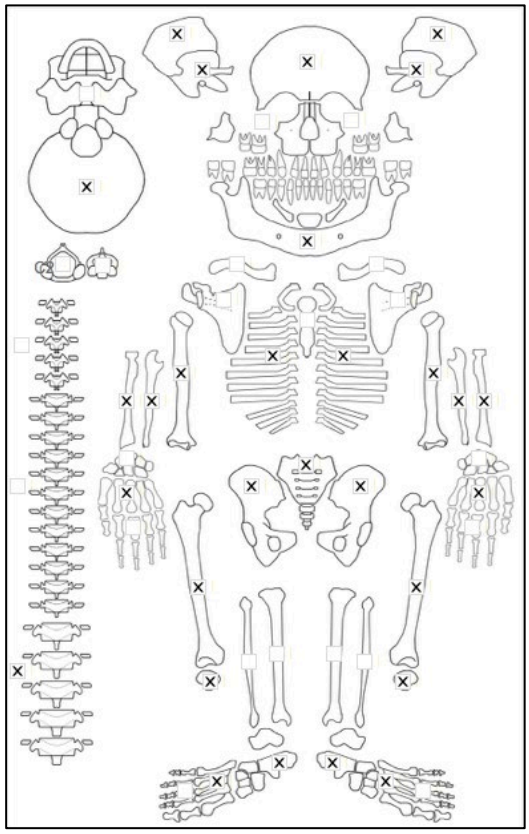

Completeness: Partially Complete (50 to 66%). 62% of long bones, 31% of hands and feet, 21% of vertebrae, 75% of cranium, and approximately 50% of ribs represented.
Preservation/ Taphonomy: There is commingling between a gracile female and a robust male (commingling of ribs, pelvis and vertebrae)- due to the strong sexual dimorphism present between these individuals it was possible to separate most elements. Only fragments of ribs, vertebrae and pelvis that could be identified as belonging to the gracile individual (the recorded individual) were considered in the analysis. Ribs are fragmented with some incomplete ribs.
Age: 30-39. *Middle Aged Adult*
Sex: Female
Macroscopic Lesion Summary:
- deep vascular grooves and arachnoid granulations on the endocranial parietals
- lytic and blastic osteoarticular changes to the posterior left patella
- biconcavity of an upper lumbar vertebral body
- 'U' shaped remodelling expansion on the greater tubercle and lateral to the humeral head (possible erosive arthropathy)

Radiographic Lesion Summary:
No radiographs taken
Differential Diagnosis Outcome:
No specific disease diagnosed

Skeletal ID: 728

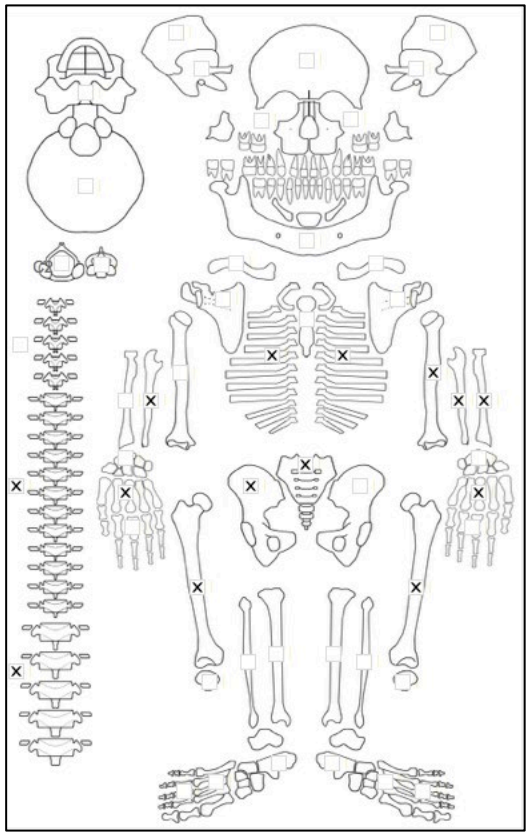

Completeness: Incomplete (33 to 50%). 32% of long bones, 8% of hands and feet, 33% of vertebrae, approximately 50% of ribs and no cranium is represented.
Preservation/ Taphonomy: Intrusive ischium, rib and proximal femur of a larger individual- excluded. Ribs are mostly fragmented with some incomplete elements.
Age: 30-39, *Middle Aged Adult*
Sex: Male
Macroscopic Lesion Summary:
None
Radiographic Lesion Summary:
No radiographs taken
Differential Diagnosis Outcome:
No specific disease diagnosed

Skeletal ID: 725

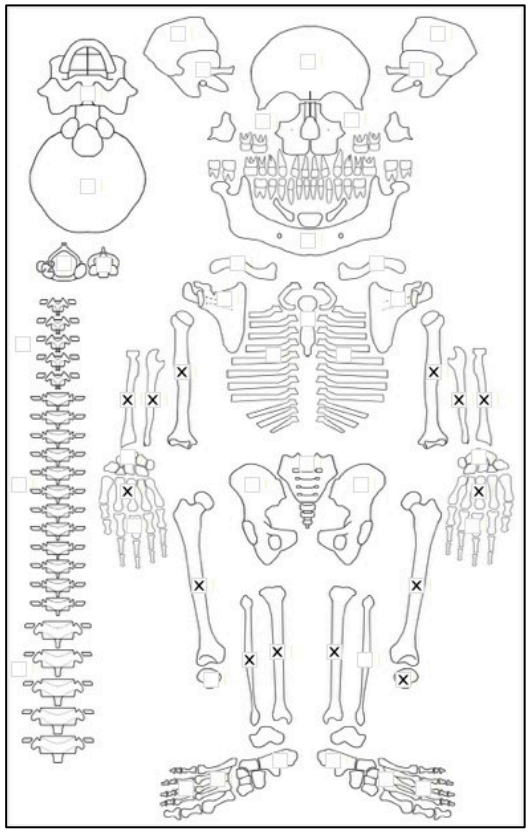

Completeness: Incomplete (33 to 50%). 70% of long bones, 10% of hands and feet and no ribs, vertebrae and cranium represented.
Preservation/ Taphonomy: Long bones mostly complete with exception of a fragmented left fibula.
Age: Adult
Sex: Indeterminate
Macroscopic Lesion Summary:
No pathology
Radiographic Lesion Summary:
No radiographs taken
Differential Diagnosis Outcome:
No specific disease diagnosed

Skeletal ID: 678A

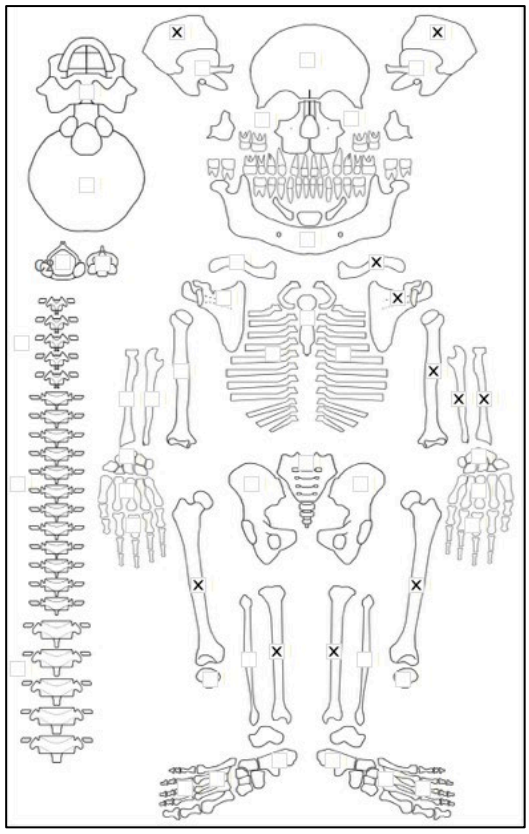

Completeness: Incomplete (33 to 66%). 32% of long bones, 1% of hands and feet, no vertebrae, 25% of cranium, and no ribs represented.
Preservation/ Taphonomy: There is commingling of two individuals: a possible male (A) and a female (B) both could be separated with confidence.
Age: Adult
Sex: Male
Macroscopic Lesion Summary:
- bilateral mild remodelling cribra orbitalia
- unilateral remodelled new bone deposition on the proximal anterior crest of the left tibia. Occurs as a thick expansion and uneven margins on the crest. In a region where trauma is common.

Radiographic Lesion Summary:
No radiographs taken
Differential Diagnosis Outcome:
No specific disease identified

Skeletal ID: 678B

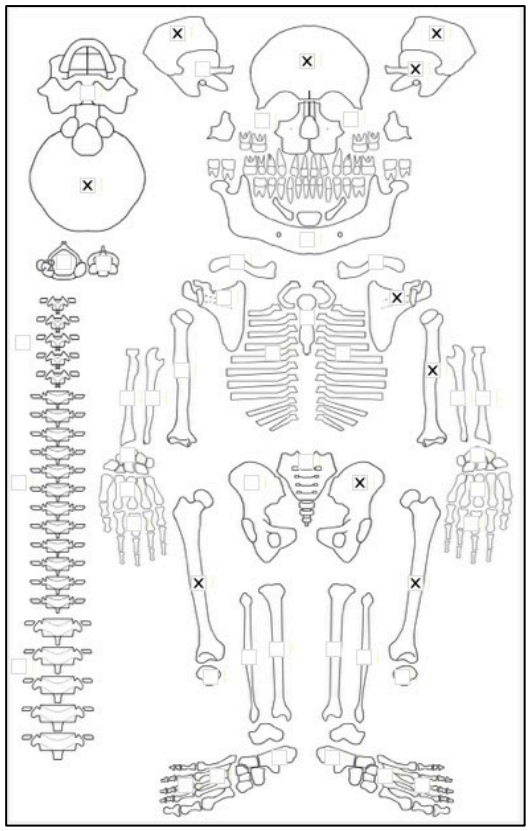

Completeness: Incomplete (33 to 50%). 12% of long bones and 63% of cranium represented.
Preservation/ Taphonomy: There is commingling of two individuals: a possible male (A) and a female (B) both could be separated with confidence. There is severe gnaw marking 58mm long gnaw mark on the endocranium of the right parietal. this may have had some pathology (recorded as a lesion just in case). Confirmed to be a rodent species endemic to Japan by K. Sakaue. Some blackened discolouration of cranial fragments.
Age: 20-29, *Young Adult*
Sex: Female
Macroscopic Lesion Summary:
- well remodelled channel inferior to the glenoid fossa on the lateral infraglenoid tubercle of the left scapula.
- increased cortical density resulting in densification of diploic region on superior frontal and parietals (according to K. Sakaue- common in the Jomon, possibly due to carrying of goods on head)
Radiographic Lesion Summary:
- xrays confirm sclerosis in the superior region of the cranium
Differential Diagnosis Outcome:
No specific disease diagnosed

Skeletal ID: 668A

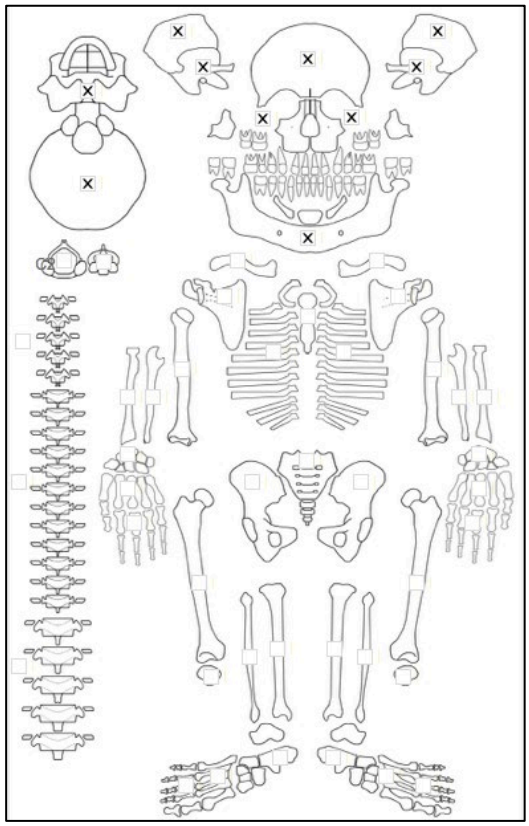

Completeness: Incomplete (33 to 50%). Skull only.
Preservation/ Taphonomy: Sphenoid body missing and basioccipital missing otherwise skull is intact,
Age: Male
Sex: 30-39, *Middle Aged Adult*
Macroscopic Lesion Summary:
- diffuse porosity across the frontal, superior parietals and occipital of the ectocranium. consistent with remodelling porotic hyperostosis.
- cranial deformation (depression of anterior parietal in relation to posterior with occipital flattening)
- localised deposit of new bone and porosity that has remodelled across the palatal surface, associated with alveolar resorption
- bilateral symmetrical mixed active and remodelling porosity superior to the mandibular foramen on the coronoid process of the mandible (could be within normal range)
Radiographic Lesion Summary:
No radiographs taken
Differential Diagnosis Outcome:
Probable Scurvy

Skeletal ID: 668B

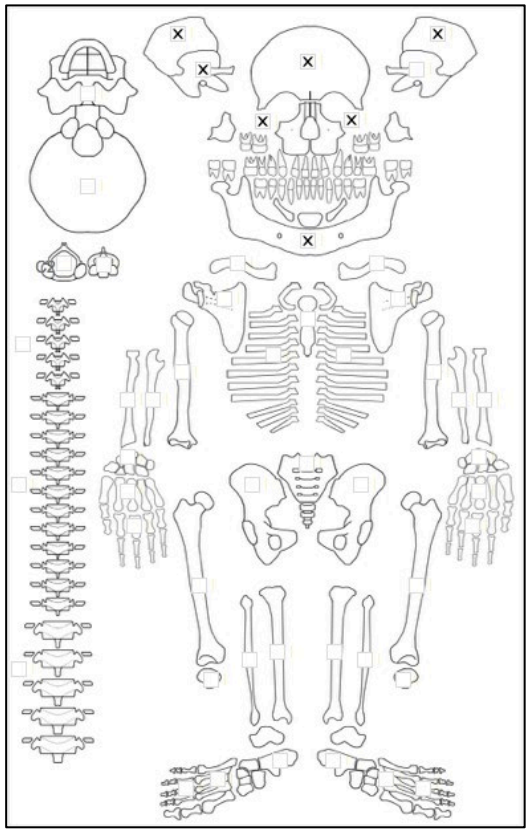

Completeness: Fragmented. Skull only. 63% of cranium represented.
Preservation/ Taphonomy: Posterior and basioccipital missing. Partially complete parietals present.
Age: 40-49, *Middle Aged Adult*
Sex: Male
Macroscopic Lesion Summary:
- focal lesion with smooth margins lateral and sharp margins medial on the posterior mastoid of the right temporal. The lesion is oval in shape and there is removal of the air cells. The lesion has a maximum diameter of 7mm
- bilateral moderate cribra orbitalia
- large thin deposition of diffuse remodelled new bone and cortical porosity across the endocranial frontal parietals and right temporal (left missing)- associated with many vascular impressions
- remodelled deposition of new bone and porosity on the palatal surfaces of the maxilla
Radiographic Lesion Summary:
No radiographs taken
Differential Diagnosis Outcome:
Possible Scurvy
Anaemia

Skeletal ID: 688

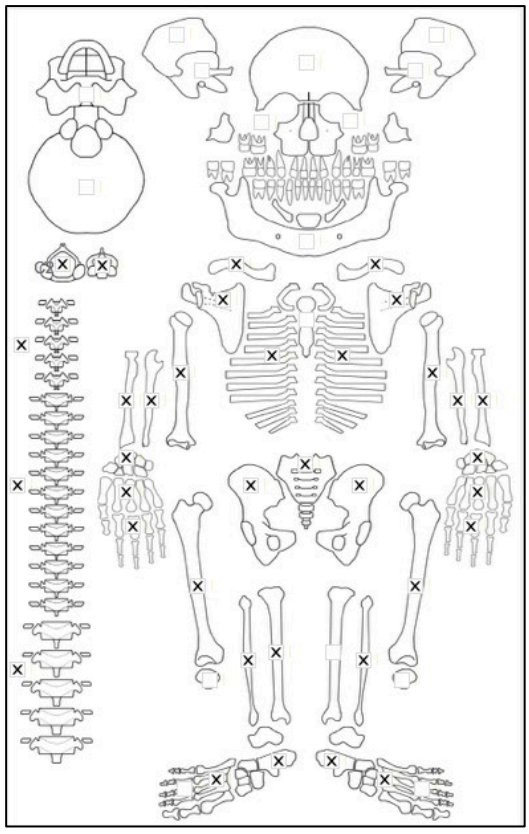

Completeness: Near Complete (66 to 75%). 83% of long bones, 39% hands and feet, 87.5% vertebrae, no ribs and cranium represented.
Preservation/ Taphonomy: Commingled with non-adult and larger adult remains (hand bones and ribs). only bones that could be confidently attributed to this individual was included.
Age: 50+, *Old Adult*
Sex: Female
Macroscopic Lesion Summary:
- well remodelled circular lytic expansions inferior to the superior articular processes of the L2 and L4. May be anatomical variants
Radiographic Lesion Summary:
No radiographs taken.
Differential Diagnosis Outcome:
No specific disease diagnosed.

Skeletal ID: 708A

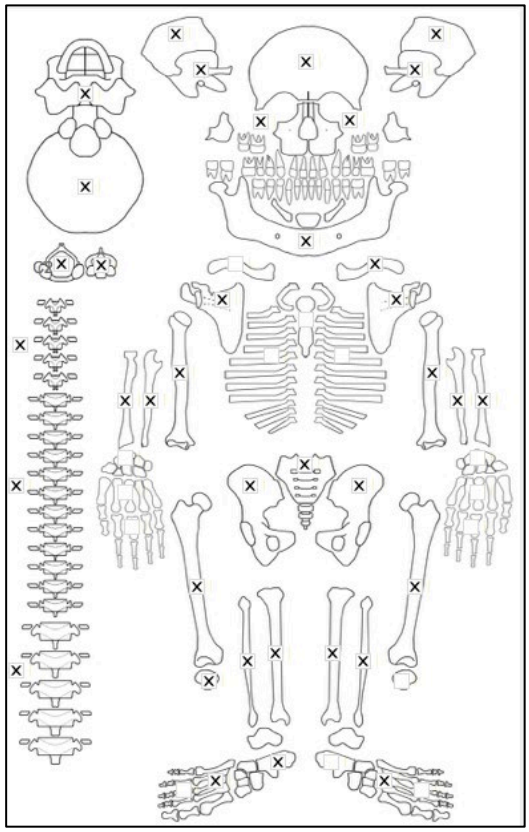

Completeness: Near Complete (66 to 75%). 8% of long bones, 14% of hands and feet, 87.5% vertebrae and approx. 30% of ribs are represented.
Preservation/ Taphonomy: Commingled remains with a smaller and younger individual- excluded.
Age: 30-39, *Young Adult*
Sex: Male
Macroscopic Lesion Summary:
- thick remodelled deposit of new bone with cortical fine porosity across the palatal surfaces of the maxillae. Associated with thick deposit of new bone across the alveolar margin and resorption.
- unilateral localised cortical porosity on the anterior region of the lateral aspect of the right temporal squama.
- diffuse porosity in the process of remodelling across the ectocranium involving the frontal, parietals and occipital. Consistent with mild porotic hyperostosis.
- remodelled mild cribra orbitalia
- bilateral diffuse remodelled new bone deposition thin and continuous with underlying cortical margin associated with cortical porosity on the posterior shaft of the ulna.
- bilateral thin deposit of remodelled new bone on the proximal third anterior crest of the tibiae
- expanded foramina on a T4-6.
Radiographic Lesion Summary:
No radiographs taken
Differential Diagnosis Outcome:
Possible Scurvy
Anaemia

Skeletal ID: 719

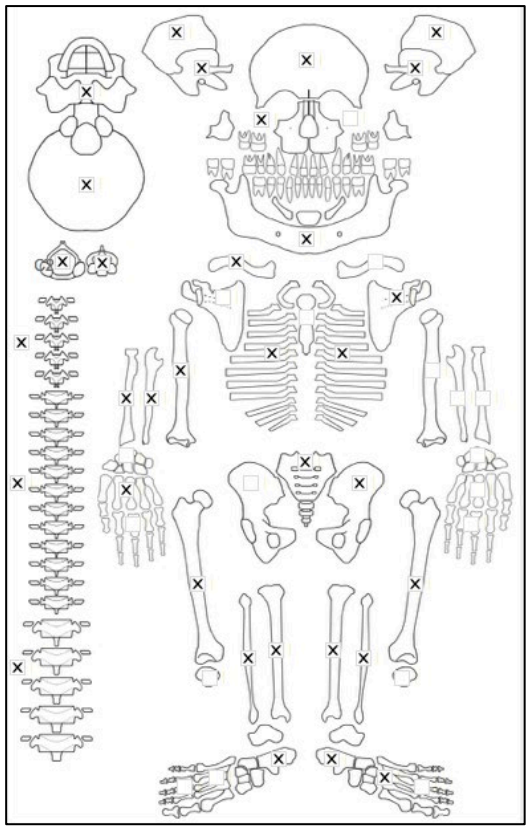

Completeness: Near Complete (66 to 75%). 72% of long bones, 26% of hands and feet, 54% of vertebrae, 87.5% of the cranium, and approx. 50% of ribs are represented.
Preservation/ Taphonomy: Ribs are mixture of fragmented to partially complete. The skull is fragmented but most is represented.
Age: 30-39, *Middle Aged Adult*
Sex: Male
Macroscopic Lesion Summary:
- bilateral remodelled cribra orbitalia
- porotic hyperostosis of the parietals and occipital planum
- bilateral symmetrical mixed active and remodelled deposition of new bone with porosity extending superiorly on the mastoid and from the superior margin of the external auditory canal at the region of the auditory triangle and the temporal squama. Continues superiorly to the junction of the zygomatic process where there is still unorganised bone.
- mixed active and remodelled localised new bone deposition with vascular impressions in the sulcus junction between superior petrous and endocranial squama of right temporal (left missing).
- small localised deposition of active new bone and cortical porosity on the superior surface of the left scapula in the supraspinous fossa. The piece is fragmented. (right missing)
- localised mixed active and remodelled but slightly diffuse new bone deposit and cortical porosity across the lateral and pterygoid fossa of right greater wing of sphenoid and continues with the lesion on the temporal squama.
- Active and remodelled new bone on the endocranial sphenoid associated with vascular impressions.
- bilateral porosity of unknown aetiology on the anterior zygomatics (possibly cortically restricted)
- diffuse active and remodelled cortical porosity and remodelled new bone deposition on the palatal surfaces of the maxilla (porosity extending from the foramina)
- bilateral symmetrical small localised mixed active and remodelled deposition of new bone appearing as a layer of plaque overlying the cortical bone with vascular impressions. Inferior to the mandibular notch on the lateral rami of the mandible
- bilateral symmetrical localised mixed active and remodelled deposition of new bone appearing as a layer of plaque overlying the cortical bone inferior to the oblique lines, incisive fossae, inferior body, mylohyoid lines (with vascular impressions), coronoid processes (and around foramen) on the mandible

- localised thick deposition of new bone inferior to alveolar bone at the region of the left mandibular premolars on the posterior aspect of the mandibular body
- diffuse active new bone on the medial ilium (fragmented)- right os coxa missing
- localised active bone deposition and cortical porosity anterior and lateral to the radial tuberosity on right radius. attachment site of the biceps brachii. left radius missing. May be a haematoma.
- active new bone deposition and cortical porosity on the posterior middle third related to the attachment site of the medial head of the triceps brachii of the right humerus. follows along medial to the radial sulcus. left humerus missing
- small remodelled lytic depression on the anterior aspect of the inferior trochlear of the right talus (left missing). circular in shape with sharp margins penetrating only the cortical bone. (adjacent to articular surface- may be articular variant)
- unilateral remodelled new bone with porosity on the anterior crest on the lateral edge of the right tibia
- bilateral diffuse mixed active and remodelled new bone and porosity across the entire shaft of the femora, more marked in new bone response posteriorly.
- shallow circular depression medial to the intertrochanteric crest on the posterior right femoral neck
- diffuse thick mixed active and remodelled new bone and porosity on the internal and external surfaces of left and right rib fragments. Appears more severe closer to spine and more severe in the inferior ribs. Most of the ribs affected (ribs are heavily fragmented).
- mostly active with some remodelling new bone on the vertebral arches of mid to lower thoracic and lumbar. New bone becomes spiculated projections posteriorly from the bone surface and more severe on the lower thoracic and lumbar spine increasing in severity the further down the spine. Vertebral bodies appear unaffected.
- abnormal vascular impressions on the endocranium of the frontal bone indicating diffuse remodelled new bone across the endocranial surface of the frontal and parietals

Radiographic Lesion Summary:

- no signs of radiodensity or radiolucency of the vertebral bodies. The vertebral arches are radiodense. Vertical spiculations radiating outwards is clear on the radiographs.
- biconcavity of multiple vertebrae (codfish sign)
- no clear cortical expansion of the os coxae
- fibrosis in some of the rib shafts.

Differential Diagnosis Outcome:

Anaemia
Probable Scurvy

Skeletal ID: 664

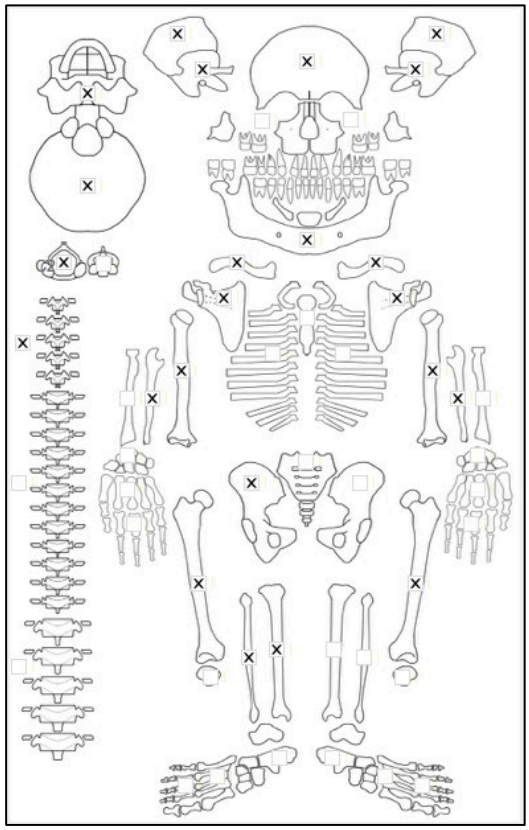

Completeness: Partially Complete (50 to 66%). 33% of long bones, no hands and feet, 25% of vertebrae, approx. 50% of ribs and 88% of cranium are represented.
Preservation/ Taphonomy: The bones are discoloured black. Ribs are fragmented. Skull is in large fragments.
Age: 40-49, *Middle Aged Adult*
Sex: Female
Macroscopic Lesion Summary:
- fine diffuse porosity across the posterior parietals and occipital remodelled consistent with mild porotic hyperostosis.
- one remodelled semilunar lytic lesion on the posterior mastoid with expansion of the internal air cells on the left temporal, changes external morphology of the left mastoid.
Radiographic Lesion Summary:
No radiographs taken
Differential Diagnosis Outcome:
Anaemia
Probable Otitis Media/ Mastoiditis

Skeletal ID: 703

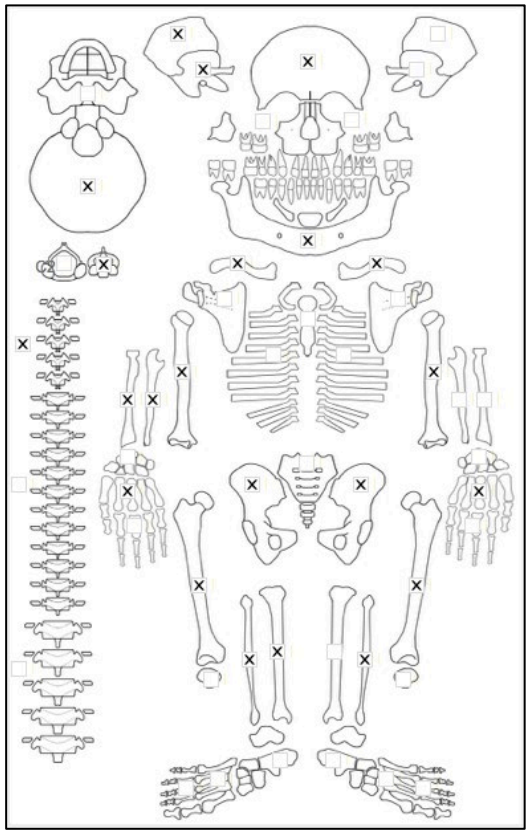

Completeness: Incomplete (33 to 50%). 50% of long bones, 15% of hands and feet, 13% of vertebrae, 63% of cranium and approx. 40% of ribs are represented.
Preservation/ Taphonomy: Ribs heavily fragmented.
Age: 50+, *Old Adult*
Sex: Male
Macroscopic Lesion Summary:
- large lytic channel superior to the petrous bone on the endocranial squama of the right temporal. Impacts cortical bone only. Likely expanded mastoid foramen associated with remodelled new bone around the canal with vascular impressions. Foramen is expanded on the external surface as well.
- small remodelled circular lytic defect on the endocranial mastoid region of the right temporal, impacts the trabecular- may be associated to the channel
- remodelled circular lytic lesion inferior to the external auditory meatus of the tight temporal
- remodelled cortical fine porosity on the meatal triangle and extending from the superior external auditory meatus border to the suprameatal crest of the right temporal.
- arachnoid granulations around the sagittal suture of the endocranium
- thick localised deposit of remodelled new bone on the internal margin of the shaft of a middle left rib shaft fragment- may be microtrauma.
- localised remodelled deposition of new bone on the superior margin of the left 3rd metatarsal, may be muscle strain or haematoma (right MT3 missing).
Radiographic Lesion Summary:
No radiographs taken
Differential Diagnosis Outcome:
Possible Otitis Media/ Mastoiditis

Skeletal ID: 670A

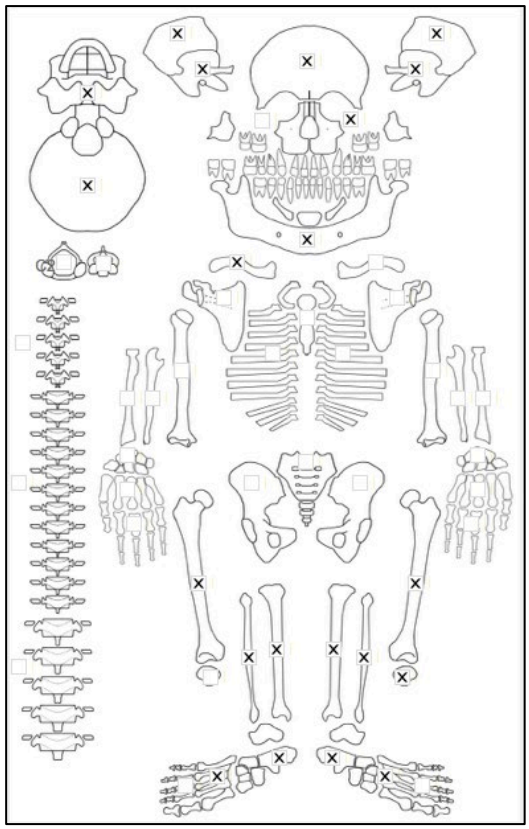

Completeness: Incomplete (33 to 50%). 40% of long bones, 88% of cranium, no vertebrae, no hands and feet, and no ribs represented.
Preservation/ Taphonomy: Commingled remains of two individuals. Could be easily separated.
Age: 30-39, *Middle Aged Adult*
Sex: Indeterminate
Macroscopic Lesion Summary:
- localised very fine cortical porosity lateral to the nasal margin on the left maxilla (right missing).
- small circular focal lytic lesion sclerotic reaction in and around the margins of the lytic lesion on the medial left nasal margin. Lesion max diameter is 4mm. Another circular remodelled erosion of the left anterior surface of the inferior nasal border (less than 10mm in size).
- thick deposition of new bone and cortical porosity well remodelled on the palatal surface
- large cystic resorption on the sphenoidal side at the sphenoid occipital synchondrosis point. Appears remodelled but this is hard to define as no margins are present due to taphonomic breakage. lesion max diameter is 16mm. Maybe a fusion defect.
- large expansion of the right condylar foramen resulting in a double foramen and oval lytic area with remodelled bone linking the two foramen. Remodelled. Associated with expansion of the right hypoglossal canal on the endocranial surface, a notch is present with remodelled slightly spiculated bone response. Another lytic channel extends anteriorly parallel to the foramen magnum margin.
- two small circular lesions with some sclerotic response in the base on the left lateral and also inferior aspects of the pars basilaris with considerable remodelled bone response
- bilateral remodelling moderate cribra orbitalia
- diffuse remodelled new bone deposition and cortical porosity with abnormal vascular impressions throughout the endocranium.
- small focal very fine porosity and remodelled new bone inferior to the foramen on the anterior left zygomatic towards the lateral margin (right zygomatic missing).
- small circular remodelled lytic expansion of the foramen on the inferior orbital margin of the left zygoma. Lesion max diameter is 5mm.
- active lytic circular expansion of the carotid canals on the external surface. margins of canals are very sharp.

- localised bilateral remodelled new bone and porosity remodelled extending from the superior border of the external auditory canal onto the suprameatal crest and triangle, associated with two small remodelled shallow lytic defects (max diameters of 6 and 4mm) on the right side.
- Expansion of the mastoid foramen resulting in two lytic channels in the endocranial sigmoid sulcus potentially as drainage points through the ectocranium, one lytic opening on the ectocranium present on the left temporal. (endocranial expansion cannot be measured, external max diameter is 4mm).
- very large lytic expansion on the inferior right mastoid, with complete destruction of the internal air cells in the mastoid. Appears completely remodelled (the largest air cell is 21mm in max diameter)
- bilateral remodelled deposit of new bone on the proximal to middle the anterior crests of the tibia resulting in protrusion of the anterior crest (slight pseudobending)

Radiographic Lesion Summary:
No radiographs taken
Differential Diagnosis Outcome:
Probable Scurvy
Possible Mycosis
Probable Otitis/Media
Anaemia

Skeletal ID: 670B

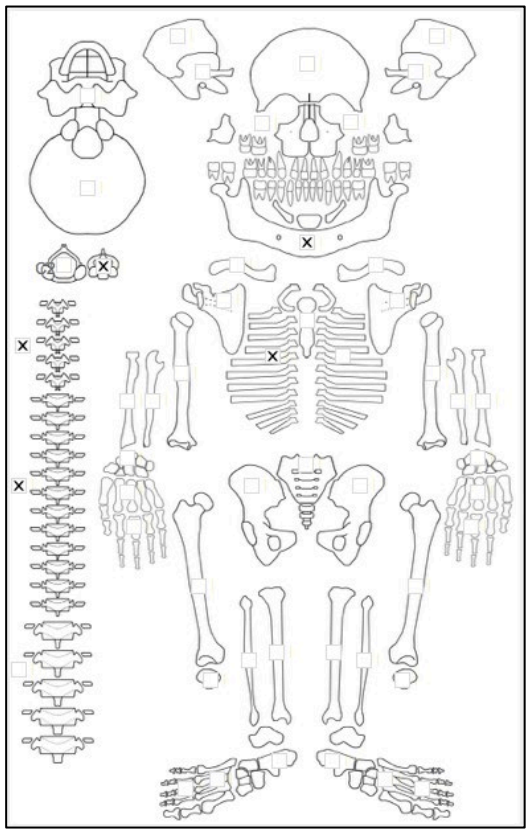

Completeness: Fragmented. Represented by 46% of vertebrae, mandible and approx. 25% of ribs.
Preservation/ Taphonomy: Commingled remains of two individuals. Could be easily separated. 670B is older individual. Ribs are heavily fragmented.
Age: 40-49, *Middle Aged Adult*
Sex: Indeterminate
Macroscopic Lesion Summary:
None
Radiographic Lesion Summary:
No radiographs taken
Differential Diagnosis Outcome:
No specific disease diagnosed

Skeletal ID: 674

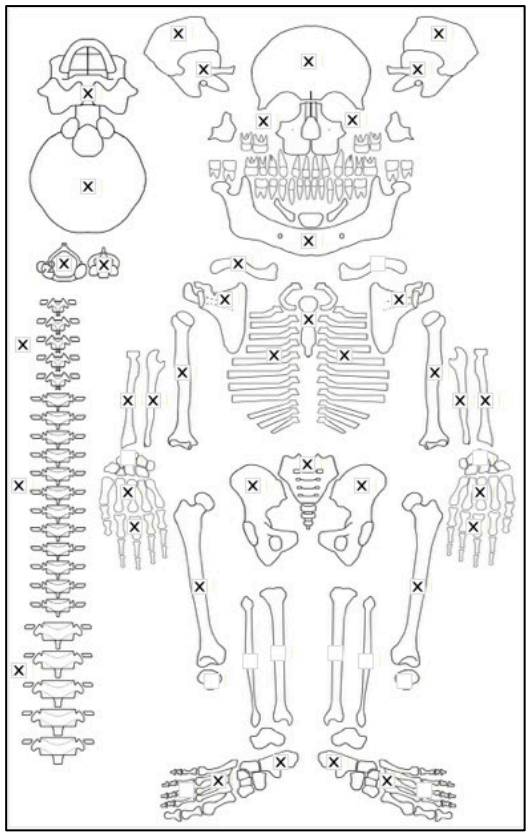

Completeness: Complete (min 75%). 65% of long bones, 36% of hands and feet, 92% of vertebrae, 88% of the cranium, and approx. 90% of ribs are represented.
Preservation/ Taphonomy: There are intrusive metacarpals and a pelvis of an older and larger individual (excluded). There is some moderate damage to the long bone surfaces.
Age: 30-39, *Young Adult*
Sex: Male
Macroscopic Lesion Summary:
- bilateral moderate remodelling cribra orbitalia
- small deep fine porosity diffuse throughout the ectocranial temporals and lateral sphenoid bones, associated with remodelled new bone as surface is rugose.
- bilateral discrete patches of new bone and fine cortical porosity on the zygomatic processes of the temporals adjacent to the temporal lines.
- abnormal vascular impressions throughout entire endocranium particularly visible on the parietals. Remodelled deep lytic vascular channels lateral to the mid sagittal suture on the endocranial surface of the parietals.
- fine diffuse porosity inferior to the foramen on the anterior left zygomatic (right missing). Not possible to determine whether the porosity is cortically restricted.
- bilateral remodelled new bone with vascular impressions on the base of the maxillary sinuses. There is resorption of the alveolar margin with remodelled possible gum disease which may relate with the sinus infection and the palatal porosity.
- Remodelled new bone and cortical porosity of the palatal surfaces of the maxillae.
- bilateral slightly diffuse active very fine cortical porosity across the anterior maxillae concentrated around the inferior and medial nasal margin.
- unilateral localised very fine cortical porosity in the left incisive fossa and extending from the incisive foramen of the mandible
- localised very fine cortical porosity across the inferior mandibular body.
- bilateral remodelled new bone and cortical porosity around the regions of the mandibular foramen and coronoid processes.
- unilateral remodelled vascular impressions inferior to the right mylohyoid line of the mandible.
- abnormal manubrial porosity

- Oval lytic lesion has sharp margins but this has taphonomic damage, with sclerotic response on the base although it is on the internal surface only which makes this unlikely. Lesion diameter is 5mm. Does not have the morphology of a sternal foramen.
- deep porosity on the S2 alae and of the thoracic and lumbar vertebral bodies.

Radiographic Lesion Summary:
No radiographs taken
Differential Diagnosis Outcome:
Probable Scurvy
Anaemia

Skeletal ID: 904

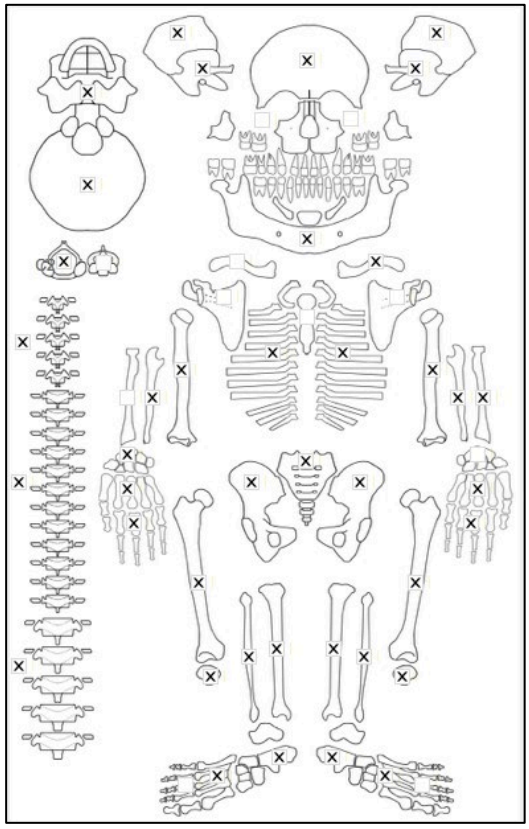

Completeness: Complete (min 75%). 82% of long bones, 43% of hands and feet, 50% of vertebrae, 88% of cranium and approx. 60% of ribs are represented.
Preservation/ Taphonomy: Ribs are fragmented to partially complete. Severe damage to vertebral bodies with fragmentation of the arches of the middle thoracic vertebrae.
Age: 40-49, *Middle Aged Adult*
Sex: Female
Macroscopic Lesion Summary:
- remodelled diffuse new bone deposition with porosity and severe abnormal vascular impressions on the entire endocranial surface with arachnoid granulations and some deep channels.
- bilateral discrete deposits of new bone and fine cortical porosity on the anterior zygomatics, extending from the foramina
- bilateral deposits of localised plaque like deposition of new bone inferior to the alveolar margin at the anterior terminal of the oblique lines of the mandible.
- bilateral remodelling localised cortical porosity on the incisive fossae of the mandible
- bilateral localised remodelled fine deposits of new bone and cortical porosity on the muscle attachment sites inferior to the oblique lines on the mandibular rami.
- remodelled deposit of new bone and porosity on the inferior mandibular body
- bilateral very fine remodelled localised cortical porosity on the attachment site on the lateral superior rami inferior to the mandibular notch

- bilateral remodelled fine cortical porosity on the coronoid processes and around the region of the mandibular foramina of the mandible
- bilateral remodelled thin new bone deposition with vascular impressions and fine cortical porosity inferior to the mylohyoid lines of the mandible
- bilateral remodelling mild cribra orbitalia
- fine cortical porosity at the attachment site of the supinator anterior to the radial tuberosity of the left radius (right radius missing)
- unilateral small region of localised remodelled bone on the anterior distal shaft of the left femur
- unilateral region of localised remodelled bone along the lateral proximal/medial crest of the femur, associated with cortical porosity (haematoma like)

Radiographic Lesion Summary:
No radiographs taken
Differential Diagnosis Outcome:
Possible Scurvy
Anaemia

Skeletal ID: 709

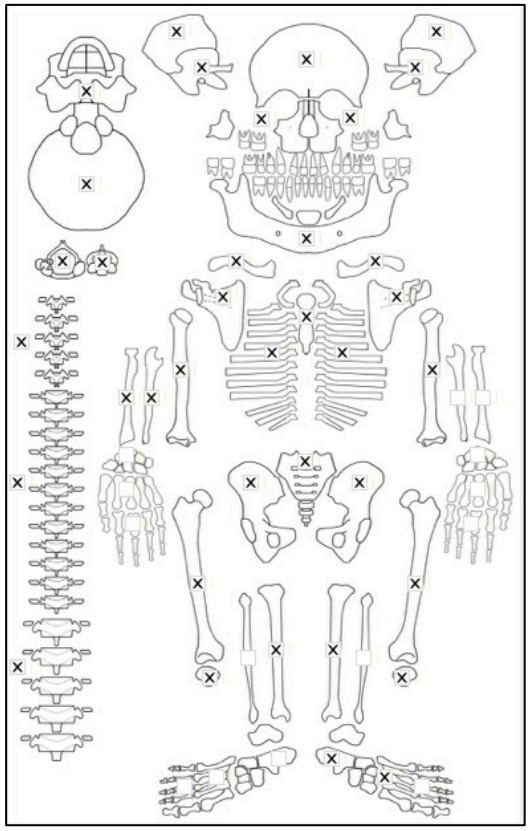

Completeness: Complete (min 75%). 83% of long bones, 19% of hands and feet, 100% of vertebrae, 88% of cranium and approx. 80% of ribs are represented.
Preservation/ Taphonomy: Ribs are partially fragmented, with predominantly incomplete to near complete ribs.
Age: 20-29, *Young Adult*
Sex: Male
Macroscopic Lesion Summary:
- bilateral moderate remodelled cribra orbitalia.
- remodelling porotic hyperostosis of the frontal, superior and posterior parietals and occipital bone.
- arachnoid granulations of the endocranium
- fine cortical porosity extending from the foramen on the on the anterior left zygomatic (right missing)
- bilateral very fine remodelling localised cortical porosity and new bone on the incisive fossae of the mandible
- remodelled new bone and fine cortical porosity on the inferior mandibular body
- bilateral remodelled new bone on the medial coronoid processes of the mandible

- bilateral remodelled new bone with vascular impressions inferior to the mylohyoid lines of the mandible
- bilateral remodelled thick diffuse deposit of new bone and porosity on the palatal surfaces of the maxillae
- deep manubrial porosity
- bilateral lytic destruction of the costal facets on the lateral sternal body (erosion of the articular surfaces)
- unilateral large arthritic change to the right proximal ulna and radius and distal humerus with focal destructive lesion of the lateral olecranon (lesion is 9mm in max diameter. has sclerotic response in the base and subchondral) (infectious arthritis?)
- remodelled new bone deposition likely involving endosteal change leading to circumferential expansion on the distal third end of the left radius.
- expanded foramina of the left ilium
- bilateral mixed remodelling lytic expansions with sclerotic reaction on the mid left and right acetabulae appears to be articular erosive changes
- bilateral mixed remodelling multifocal pitting lytic expansions with sclerotic reaction on the auricular surfaces. Is not normal density associated with older individuals as this individual is still young and is consistent with all the other pathologic articular changes on this individual.
- deep porosity of the anterior sacra bodies
- remodelling deep focal lytic expansion on the anterior sacral body of the S5. Margins are defined- likely associated with the other deep porosity of the sacrum.
- small circular remodelled lytic lesion on the transverse process articular facet of multiple middle ribs.
- thick remodelled deposition of bone distorting the rib shape on the external posterior surface of the 10th right rib and a right 5th or 6th rib (left missing), results in articular change, there is shape distortion of the distal end.

Radiographic Lesion Summary:

-The articular changes to the right ulna, radius and humerus: Slight cortical expansion of the right ulnar shaft (no visible macroscopic changes to the shaft) this is more prominent on the posterior aspect, there are not lytic focal changes consistent with tuberculosis arthritis.
- parrot's beak sign on multiple vertebrae, but this is not associated with macroscopic observance of lytic changes (not consistent with an infectious aetiology)- lacks the surrounding sclerosis noted on parrot's beak sign of brucellosis (likely an anterior osteophyte). Also clear burst fractures (Schmorl's nodes) on the superior and inferior vertebrae indicating high activity.
- cortical expansion of the ribs macroscopically observed to have pathological change.
- slight biconcavity of the vertebrae, but likely within normal range. No associated signs of osteopenia.

Differential Diagnosis Outcome:

Probable Scurvy
Anaemia

Skeletal ID: 704

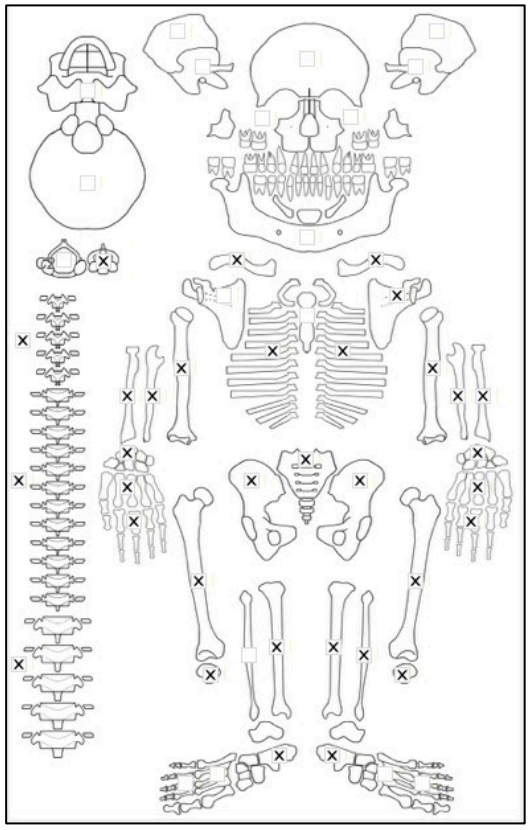

Completeness: Near Complete (66 to 75%). 77% of long bones, 39% of hands and feet, 75% of vertebrae and no cranium present. Approx. 75% of ribs represented.
Preservation/ Taphonomy: Ribs partially fragmented. Intrusive right talus and scapula (comingling), easily separated as belongs to a juvenile.
Age: 20-29, *Young Adult*
Sex: Male
Macroscopic Lesion Summary:
- Deep porosity on the inferior S1 ala and on the sacral tuberosities between 2 and 9mm in diameter. (possibly normal variant)
- Deep porosity creating channels on the anterior and lateral vertebral bodies, between 5 and 20 mm of 3 middle to lower thoracic vertebrae. Lesions are mostly remodelled with considerable bone filling. (possibly normal variant)
- Deep porosity on the anterior body of the S5 between 2 and 7.5mm in diameter. (possibly normal variant)
- bilateral fine cortical porosity across the external surface of the ribs (may be normal variant- robusticity related)
- thick and thin active diffuse new bone across the internal margins of 6 rib fragments representing both left and right ribs including 1st ribs
Radiographic Lesion Summary:
- some of the rib shafts show evidence of endosteal expansion of the cortex (appears to be from lower ribs)
Differential Diagnosis Outcome:
No specific disease diagnosed

Skeletal ID: 708B

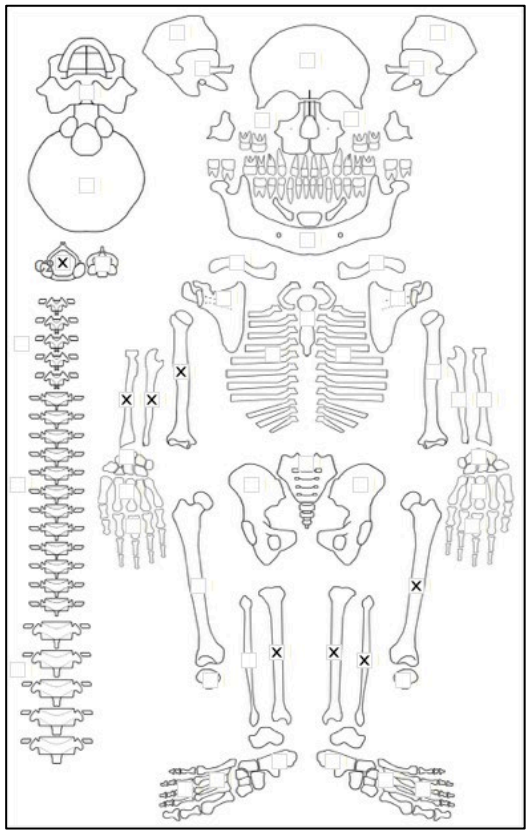

Completeness: Incomplete (33 to 50%). Approx. 50% of ribs, 42% of long bones, 2% of hands and feet, 8% of vertebrae and no cranium represented.
Preservation/ Taphonomy: Distal half of right radius missing, only distal end of left humerus present, distal half of lower long bones missing except left fibula where there is an end only.
Age: 1.5 to 6 months, *Infant*
Sex: Indeterminate
Macroscopic Lesion Summary:
No lesions observed
Radiographic Lesion Summary:
No radiographs taken
Differential Diagnosis Outcome:
No Diagnosis

Skeletal ID: 708C

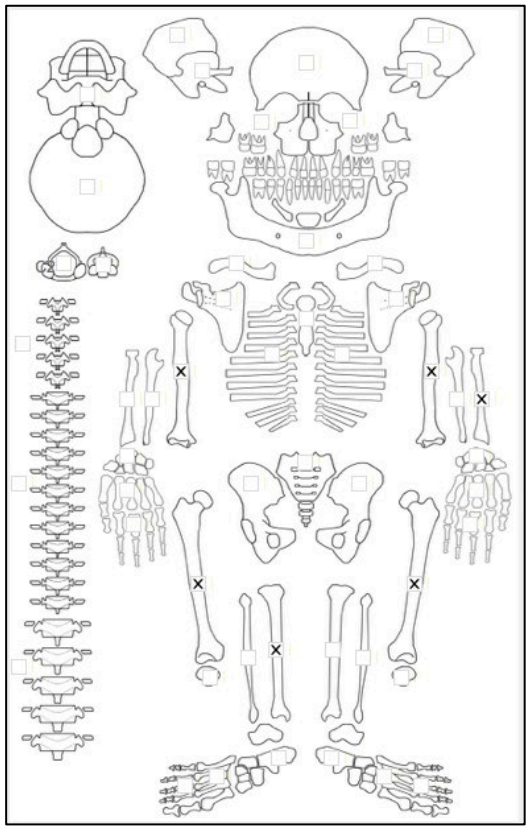

Completeness: Fragmented. 39% of long bones.
Preservation/ Taphonomy: All long bone ends are missing. represented.
Age: 1.5 months (+/- 1.5 months), *Infant*
Sex: Indeterminate
Macroscopic Lesion Summary:
- unilateral active diffuse new bone across the medial aspect of the proximal and middle two-thirds shaft of the left femur
Radiographic Lesion Summary:
No radiographs taken
Differential Diagnosis Outcome:
No Diagnosis

Skeletal ID: 715B

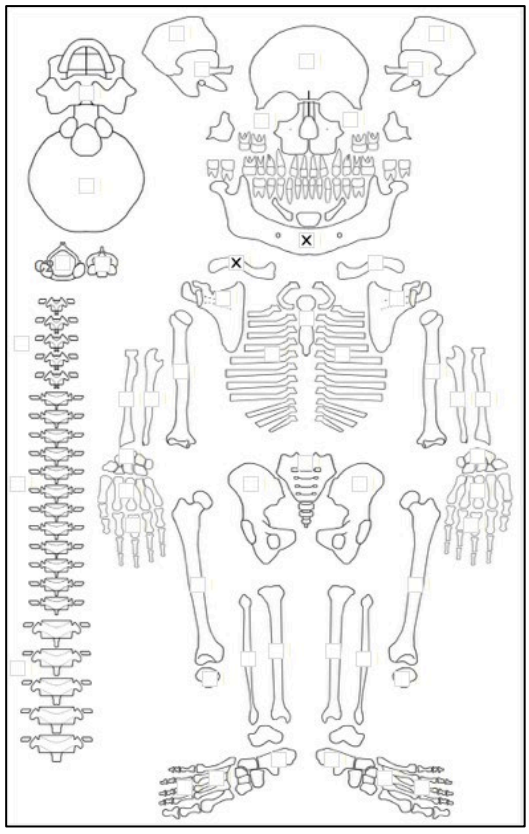

Completeness: Fragmented. Represented by skull fragment, right zygoma, right clavicle and right hemimandible only
Preservation/ Taphonomy: Surfaces well preserved
Age: 15-23, *Adolescent*
Sex: Indeterminate
Macroscopic Lesion Summary:
- remodelled thin localised deposit of new bone on the right sublingual fossa extending from the alveolar margin, inferior to the mylohyoid line (with vascular impressions), the right medial aspect of the coronoid process and along the inferior aspect of the mandibular body (with cortical porosity)
- remodelled diffuse fine scattered porosity across the anterior right zygomatic with some striations likely resulting from mild porotic hyperostosis
- localised remodelling fine cortical porosity and new bone deposition on the right incisive fossa extending to the alveolar margin
Radiographic Lesion Summary:
No radiographs taken
Differential Diagnosis Outcome:
Possible Scurvy

Tsukumo (Late to Final Jomon Period, Japan)

Skeletal ID: 21

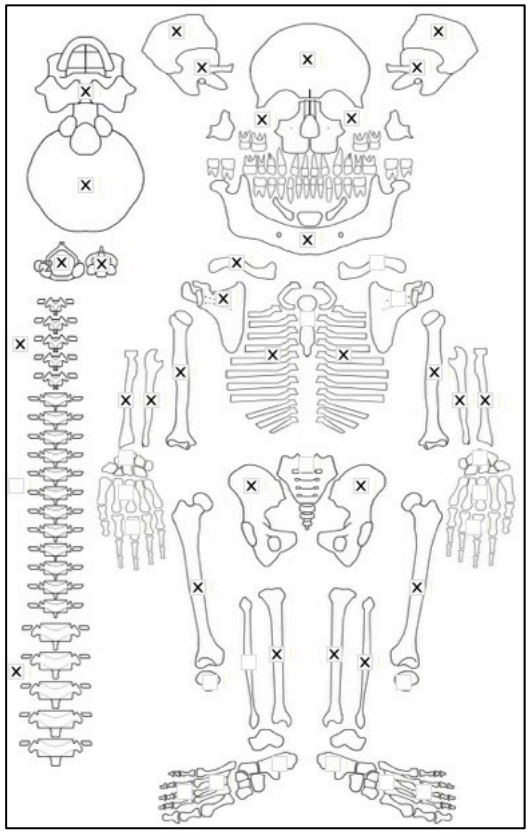

Completeness: Near Complete (66 to 75%). All long bones present with exception of right fibula and left clavicle. 8 vertebrae from cervical and lumbar spine with only 2 presenting with vertebral bodies. All cranium except ethmoid present. Minimum 6 right 7 left ribs represented.
Preservation/ Taphonomy: Surfaces well preserved. All metaphyseal ends complete with the exception of distal left radius and ulna.
Age: 3 (+/- 1 year), *Child*
Sex: Indeterminate
Macroscopic Lesion Summary:
- diffuse remodelling fine scattered porosity consistent with mild porotic hyperostosis on the occipital planum
- localised mixed active and remodelling fine cortical porosity and a deposit of new bone on the left pars lateralis
- localised active porosity and localised mixed active and remodelling new bone on the right zygomatic process of the frontal bone with multiple expanded foramina
- localised remodelling fine cortical porosity and remodelling new bone on the left superior orbit with vascular impressions
- very fine active porosity supero-medial to the supercillary arches with unknown aetiology
- bilateral remodelling localised fine cortical porosity and new bone around the region of the nasal and infraorbital foramen of the anterior maxillae. There is new bone and vascular impressions extending from within the foramen.
- bilateral active diffuse new bone and cortical porosity across the palatal surface of the maxillae, with vascular impressions extending along the palatal sutures
- bilateral remodelling localised active cortical porosity and new bone on the inferior orbital surface of the superior maxillae and left zygomatic
- remodelling new bone and cortical porosity on the posterior left zygomatic
- remodelling new bone and cortical porosity in the right pterygoid region
- bilateral active new bone and cortical porosity on the medial coronoid processes of the mandible
- bilateral active new bone on the lateral ramus directly inferior to the mandibular notch

- bilateral active and remodelling new bone and cortical porosity on the incisive fossae of the mandible
- remodelled deposit of localised new bone and cortical porosity in the supraspinous fossa of the right scapula
- bilateral and symmetrical active deposit of localised new bone and cortical porosity inferior to the radial notch on the lateral ulnae
- deep endochondral porosity extending beyond 10mm on the metaphyseal end of the proximal humeri metaphyses (the left is accompanied by an oval cortical defect on the anterior aspect), proximal and distal metaphyses of the tibiae, proximal and distal femora (with circular cortical defects on the posterior distal metaphyses which may be a normal stress trait exacerbated by the weakened bone)
- bilateral symmetrical active localised circular deposit of new bone on the patellar surfaces of the femora
- bilateral and symmetrical localised remodelling new bone and porosity on the superior margin of the olecranon fossae of the posterior humeri
- unilateral localised deposition of new bone on the posterior to medial middle third around the foramen of the left humerus.

Radiographic Lesion Summary:
- White line of Fraenkle on proximal and distal fibula, tibiae, femur, distal radius and proximal humeri
- generalised osteopenia in the metaphyses of all limb bones with ground glass appearance. Severe radiolucency of the distal radius
- faint Harris lines of the distal and proximal metaphyses of the tibiae, femur, fibula and radius
- ulnae thickened medial laterally at the proximal third region with loss of cortico-medullary distinction.

Differential Diagnosis Outcome:
Probable Scurvy

Skeletal ID: 31

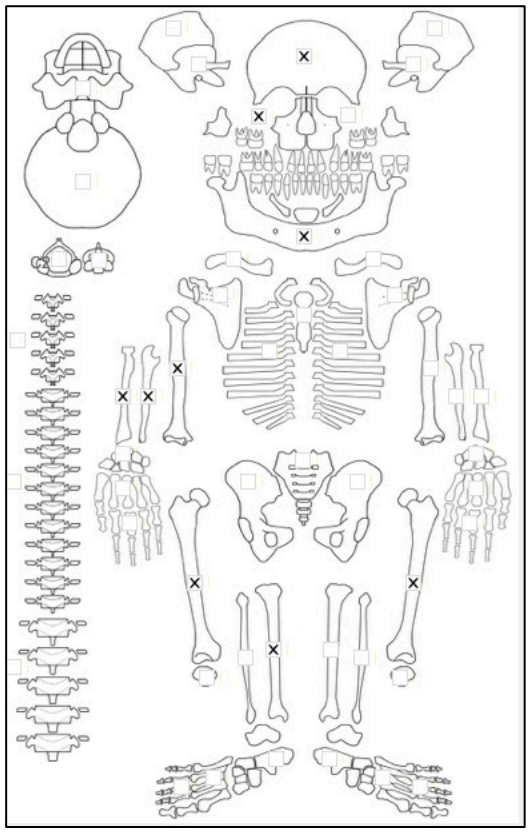

Completeness: Incomplete (33 to 50%). All right limb bones with exception of fibula present plus left femur. Frontal bone, sphenoid and right facial bones present with remainder of cranium fragmented. Mandible present. 3 vertebrae.
Preservation/ Taphonomy: distal metaphyseal ends of femurs damaged, middle shaft of right tibia missing and distal ends of right ulna damaged. Surfaces well preserved.
Age: 2 (+/- 0.5 years), *Child*
Sex: Indeterminate
Macroscopic Lesion Summary:
- bilateral active cortical porosity and new bone across the lateral (external) right greater wing of the sphenoid

- layered active new bone deposition with vascular impressions and cortical porosity on the endocranial surface on the lateral left frontal bone
- active new bone and cortical porosity on the right zygomatic process of the frontal bone
- bilateral and symmetrical active new bone and cortical porosity localised to the left medial supraorbital ridge around the region of the supraorbital notch
- active fine porosity superior and medial to the supercillary arches. Unknown aetiology.
- bilateral layered and plaque like active new bone and cortical porosity on the superior orbital roofs
- deep vessel channels with sharp margins on the endocranium of the frontal protruding into the underlying diploic bone extending bilaterally from the metopic suture region, there are 5 circular expanded vessels on the ectocranium.
- localised fine cortical porosity and new bone on the anterior right maxilla extending from the infraorbital foramen to the nasal margin associated with a vascular impression medial to the infraorbital foramen
- active fine cortical porosity and new bone diffuse throughout the right palatal surface
- active localised cortical porosity, new bone and vascular impressions on the medial nasal surface and nasal floor of the right maxilla. There is a concentration of new bone in the lacrimal groove
- remodelling fine cortical porosity and new bone localised to the inferior orbital surface on the superior right zygomatic associated with vascular impressions.
- active cortical porosity across the right posterior zygomatic
- bilateral mixed active and remodelling new bone and fine cortical porosity on the incisive fossae extending towards the alveolar bone
- localised active cortical porosity and new bone on the inferior mandibular body
- active endochondral porosity extending beyond 10mm but on the medial aspect of the right humerus. This is associated with an oval cortical defect 6mm in maximum diameter
- small localised active cortical porosity across the anterior orbital surface of the right greater wing of the sphenoid with associated vascular impressions

Radiographic Lesion Summary:

- generalised osteopenia at the metaphyses of the humerus and femora. Distal humerus demonstrates severe osteopenia

Differential Diagnosis Outcome:

Probable Scurvy

Skeletal ID: 26

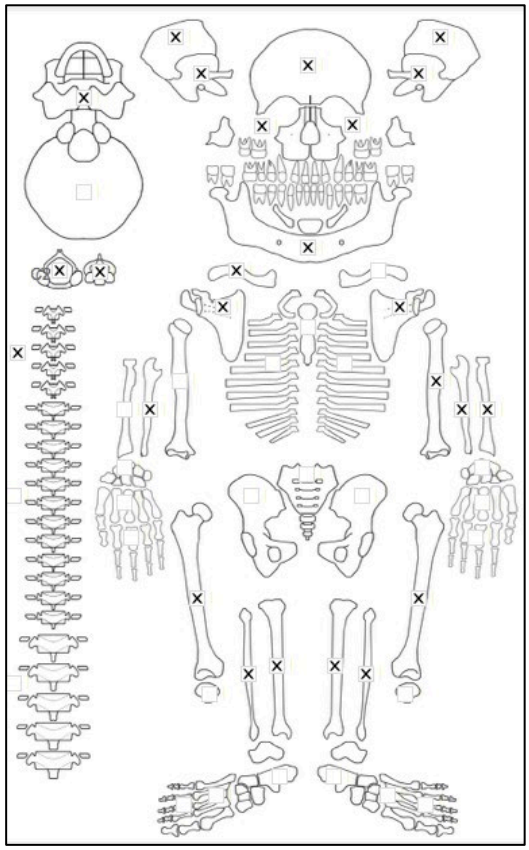

Completeness: Partially Complete (50 to 66%). All limb bones except right radius and humerus present. All cranium except occipital and ethmoid present. At least 3 right 2 left ribs present.
Preservation/ Taphonomy: Cranium is partially fragmented. Sphenoid body missing. Surfaces well preserved. Multiple broken metaphyseal ends but the metaphyses are still partially represented for all long bones with the exception of the proximal half of left fibula and humerus, proximal third of right fibula, and posterior portion of ulna.
Age: 1.5 (+/- 6 months), *Child*
Sex: Indeterminate
Macroscopic Lesion Summary:
- remodelled new bone diffuse across the endocranial surface of the left parietal with capillary formations (Lewis type 3) and across the endocranium of the frontal with deep vascular channels
- small localised active new bone deposition on the endocranial aspect of the pars basilaris with small capillary formations (Lewis type 3)
- active new bone and cortical porosity on the pars basilaris near the attachment site of the capitalis muscle.
- three different localised lesion processes on the superior aspect of the greater wings of the sphenoid: bilateral localised active new bone on the superior greater wings of the sphenoid toward the lateral margin, bilateral localised remodelled new bone lateral to the foramen rotundum on the superior greater wings of the sphenoid, and remodelling new bone and cortical porosity around the margins of the foramen rotundum.
- bilateral mixed active and remodelling fine cortical porosity and new bone across the lateral (external greater wing) greater wing
- bilateral mixed active and remodelling localised deposit of new bone and cortical porosity on the pterygoid regions inferior aspect) of the sphenoid. Right pterygoid fossa has preserved foramen ovale and demonstrates new bone extending from the foramen
- mixed active and remodelling cortical porosity and new bone across the posterior left zygomatic
- mixed remodelled and active cortical porosity and new bone on the right zygomatic process of the frontal bone with vascular impressions.
- mixed remodelled and active cortical porosity and new bone on the posterior maxilla superior to the alveolar margin with vascular impressions
- unilateral mixed remodelled and active cortical porosity and new bone on the anterior maxilla extending laterally from the infraorbital foramen.
- diffuse thin active woven new bone lateral to the auricular surface and inferior to the iliac spine on the visceral aspect of the left ilium. The nature of the new bone makes it difficult to determine if strictly pathological.
- localised active woven new bone on the medial aspect of the distal third fibula shaft following the interosseous border.
- bilateral mixed active and remodelling cortical porosity and new bone deposition on the ulnar tuberosity and around the foramen on the anterior proximal third ulnae.
- remodelled cortical porosity and new bone deposition anterior to the radial tuberosity of the left radius
- bilateral diffuse heavy active new bone deposition across the anterior, and medial tibial shaft, may be normal physiological process. linear discontinuity with underlying cortical bone on the distal end.
- deep endochondral porosity extending beyond 10mm on the proximal and distal metaphyses of the tibiae, distal right femur
- bilateral but not symmetrical diffuse new bone across the diaphyses of the femora: active new bone on across the middle third shaft of the right femur, and remodelling new bone on the proximal to middle third shaft of the left femur sparing the anterior aspect
- large elongated channel-like focal trabecular expansion across the anterior body of a lumbar vertebra. The margins are sharp and there is no bone filling, but internal surfaces of the lesion have a layer of cortical bone suggesting a slow formation process. The cavitation extends deep and almost half of the internal vertebral body is compromised. The channel extends 14mm in length.
Radiographic Lesion Summary:
- severe postmortem damage, but distinct white line of Frankel of posterior tibia and distal femur is present
- periosteal new bone on medial tibiae present on radiographs, and middle third of the right femur
Differential Diagnosis Outcome:
Probable Scurvy

Skeletal ID: 8

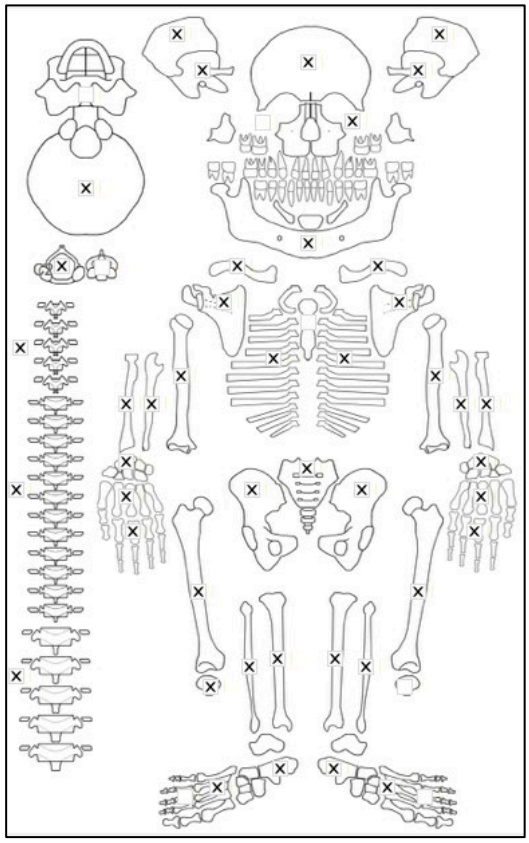

Completeness: Complete (min 75%). All long bones present. All skull with exception of the ethmoid and sphenoid present. 16 vertebrae present. 62% of hand and feet bones presented including both calcanei and left talus. 10 right and 9 left ribs.
Preservation/ Taphonomy: Distal half of right radius missing. Surfaces well preserved.
Age: 15 (+/- 1 year), *Adolescent*
Sex: Male
Macroscopic Lesion Summary:
- small remodelled deposit of new bone on the internal proximal third shaft of a left rib (3-9)
- mixed remodelling very fine cortical porosity and new bone on the supraspinous fossa of the right scapula.
- deep endochondral porosity extending beyond 10mm. There is some bone filling of some of the bone ends indicating a remodelling process: remodelling proximal and distal right (with 9mm oval cortical defect on the proximal aspect and 6 mm cortical defect on the distal aspect of right fibula) and remodelling distal left fibula, active proximal humeri (with three cortical defects on the posterior aspect-one circular defect directly inferior to the metaphyseal plate and two on the proximal third), proximal and distal tibiae (right side has 7mm circular cortical defect directly inferior to the metaphyseal plate on the posterior aspect), deep endochondral porosity extending beyond 10mm from the distal metaphyses of the femora. Associated with 11mm circular cortical defects on the posterior aspect (a known normal variant but may be exacerbated by the compromised bone)
- bilateral localised remodelled new bone deposit with cortical porosity on the middle third posterior and medial surface of the tibiae
- unilateral localised deposit of remodelling new bone as a plaque overlying the cortical bone on the distal medial and posterior end of the right tibia
- bilateral cribra femoris or Allen's fossa
- remodelling new bone across the anterior and lateral vertebra bodies across all lumbar and two thoracic (10-12) vertebral bodies. These are associated with minor vascular expansions, but these are mild and within normal range of variation.
- Mandible: localised active bilateral new bone deposition and cortical porosity on the medial coronoid processes, bilateral localised remodelling new bone and cortical porosity inferior to the mylohyoid lines (with vascular impressions), remodelling cortical porosity around the mental spines, mixed active and remodelling new bone across the inferior mandibular body, bilateral mixed active and remodelling new bone continuing along the oblique lines from posterior to the molar to the inferior mandibular body (more active superiorly closer to the alveolar bone).

- localised small region of active new bone and porosity superior to the alveolar margin on the lateral and posterior left maxilla inferior to the zygomatic process
- diffuse remodelled new bone and porosity on the palatal surface of the left maxilla
- fine diffuse remodelling porosity on the posterior parietals and occipital planum consistent with mild porotic hyperostosis
- bilateral symmetrical remodelled cortical porosity and new bone extending from the superior external auditory canal and suprameatal crest with extension onto the suprameatal triangle region and a portion of the mastoid.
- fine cortical porosity and remodelled new bone on the lateral left greater wing of the sphenoid and in the pterygoid region associated with porosity and new bone on the anterior temporal squama. The new bone and porosity of the temporal squama is bilateral suggesting that although the right greater wing is missing, this lesion was likely bilateral and symmetrical.
- mixed remodelling bilateral mild cribra orbitalia

Radiographic Lesion Summary:
- severe osteopenia of the metaphyses of the tibia and 'ground glass' appearance of the metaphyses

Differential Diagnosis Outcome:
Anaemia
Probable Scurvy

Skeletal ID: 25

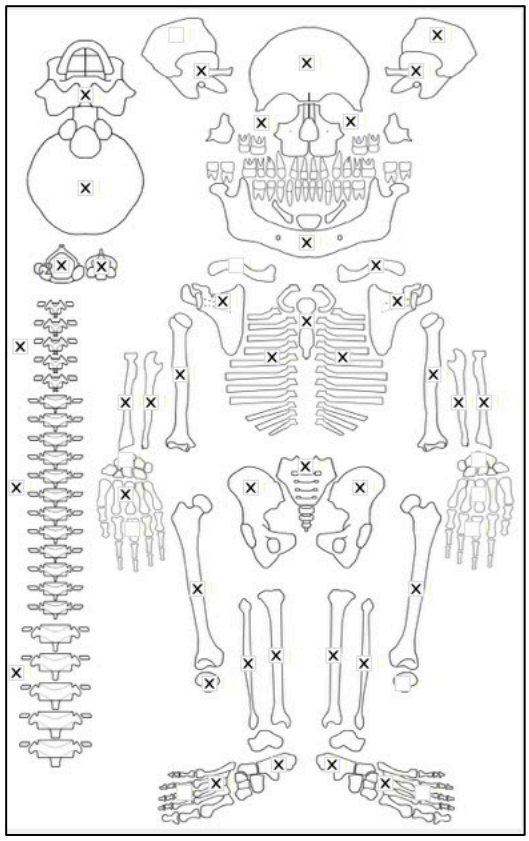

Completeness: Complete (min 75%). All long bones present. Skull present except for ethmoid. 83% of vertebra present. 18% of hands and feet present.
Preservation/ Taphonomy: Distal ulna and proximal fibula ends missing. Right sphenoid wing missing. Surfaces well preserved.
Age: 12 (+/- 3 years), *Adolescent*
Sex: Indeterminate

Macroscopic Lesion Summary:
- bilateral symmetrical localised mixed remodelling porosity on the superior margin of the external auditory meatus on the suprameatal crest, suprameatal triangle and anterior temporal squama
- bilateral mixed active and remodelled new bone with pin prick porosity on the superior lateral border of the superior orbital roofs. The porosity aetiology is difficult to discern. It may be cortically restricted, or consistent with mild cribra orbitalia, or both. The new bone is associated with vascular impressions.

- mandible: remodelling deposit of new bone and fine cortical porosity on the right medial aspect of the coronoid processes including the region of the mandibular foramen, bilateral remodelled deposit of new bone and fine cortical porosity extending from the inferior point of the right oblique line to around the mental foramen and incisive fossa with vascular impressions (both mental foramina are expanded circumferentially), remodelled new bone and cortical porosity on the inferior mandibular body.
- circular vascular trabecular expansions on the anterior and lateral vertebral bodies of the T10 to L2 from 3 to 17mm in maximum diameter.
- localised small deposit of remodelling new bone on the internal aspect of the angle of a left 3rd or 4th rib
- mixed diffuse active and remodelling new bone and fine cortical porosity across the external aspect of selected ribs extending distally along the shaft from the rib neck: left 3rd or 4th and 10th rib, and right ribs 1 to 10.
- bilateral and symmetrical localised mixed small deposit of new bone on lateral olecranon extending onto the articular surface
- unilateral small circular localised active deposit of new bone on the ulnar tuberosity of the left ulna
- bilateral symmetrical localised deposit of new bone on the medial olecranon of the ulnae around the region of foramen
- unilateral active localised deposit of new bone around the foramen on the proximal third anterior right radius
- unilateral remodelled new bone deposit with cortical porosity on the anterior aspect at the radial tuberosity of the right radius
- deep endochondral porosity extending beyond 10mm from the metaphyses: distal radii proximal humeri, proximal fibulae, proximal and distal tibiae, distal femora
- unilateral remodelled new bone and some cortical porosity across the anterior aspect of the distal third shaft superior to and extending into the coronoid fossa of the right humerus
- bilateral mixed active and remodelling cortical porosity on the superior border of the olecranon fossa
- large bone projection on the medial aspect of the left tibia directly inferior to the proximal metaphyseal plate likely to be an osteochondroma
- bilateral cribra femoris or Allen's fossa

Radiographic Lesion Summary:

- Multiple growth arrest lines proximal and distal tibia, distal radius
- generalised osteopenia and radiolucency at the distal tibia, humerus and radius
- radiographs of vertebrae demonstrate considerable internal vascular expansion of the vertebral bodies, with some radio-dense bone filling of these vascular channels

Differential Diagnosis Outcome:

Probable Scurvy

Skeletal ID: 46(2)B

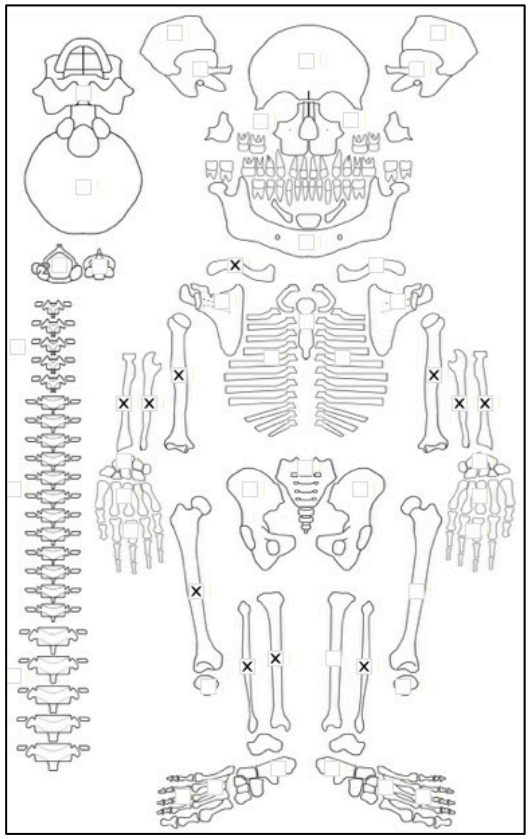

Completeness: Incomplete (33 to 50%). Represented by long bones only. Right clavicle and all long bones with the exception of the left femur and tibia.
Preservation/ Taphonomy: Surfaces well preserved.
Age: 1-5 years, *Child*
Sex: Indeterminate
Macroscopic Lesion Summary:
- bilateral diffuse active new bone with some porosity on the posterior to lateral distal third region of the fibulae
- bilateral localised active cortical porosity and new bone inferior to the radial notch and in the ulnar tuberosity of the ulnae
- plaque of active new bone on the distal third posterior left radius
- diffuse mixed active and remodelled woven bone and porosity on the middle third medial aspect of the right tibia

Radiographic Lesion Summary:
No radiographs taken
Differential Diagnosis Outcome:
Non Diagnostic

Skeletal ID: 56

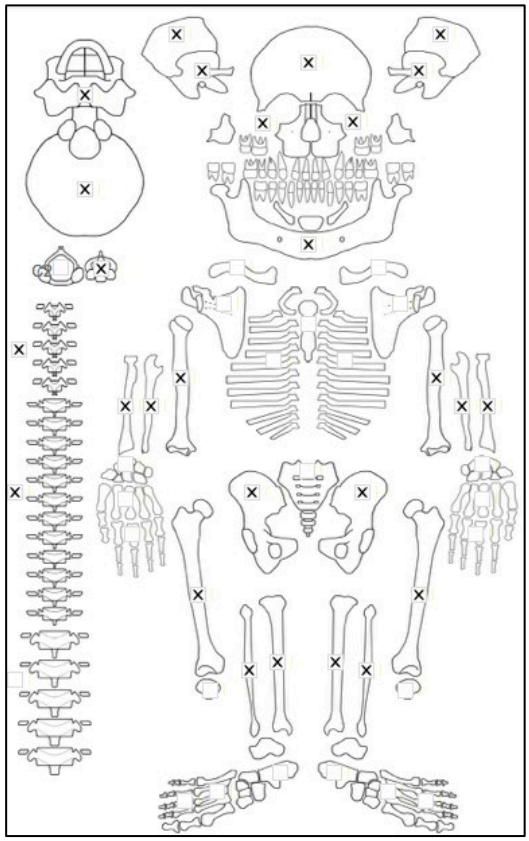

Completeness: Near Complete (66 to 75%). Cranium complete with exception of ethmoid. 10 cervical and thoracic vertebrae with 7 represented by vertebral bodies. All long bones except clavicles present. Ribs heavily fragmented.
Preservation/ Taphonomy: Post-mortem damage to internal surfaces impact radiographic diagnosis.
Age: 3 (+/- 1 year), *Child*
Sex: Indeterminate
Macroscopic Lesion Summary:
- fine active cortical porosity on the external shaft of two unsided rib fragments.
- localised very fine cortical porosity and remodelling deposit of new bone on the anterior distal shaft directly superior to the coronoid and radial fossae on the anterior right humerus
- mixed active and remodelling fine cortical porosity and new bone on the superior portion of the olecranon fossa of the posterior right humerus
- diffuse active new bone and porosity on the medial middle third of the right tibia. The new bone is continuous with the underlying cortical bone.
- mandible: bilateral active new bone and cortical porosity on the incisive fossae, remodelled new bone and cortical porosity on the mental spines, bilateral mixed active and remodelled new bone and cortical porosity on the medial coronoid processes extending from the mandibular foramina
- bilateral mixed active and remodelled fine cortical porosity and new bone across the entire anterior aspect of both maxillae. The new bone is concentrated towards the nasal margin. Some porosity is large and likely caused expanded foramina indicative of haematoma.
- bilateral fine cortical porosity on the inferior orbital surfaces of the maxillae
- mixed active and remodelled fine cortical porosity and new bone on the palatal surface of the left maxilla
- bilateral active fine cortical porosity and new bone deposition on the posterior and lateral maxillae (undercutting the zygomatic process) with vascular impressions on the posterior aspect. This connects with porosity on the posterior and inferior zygomatics.
- mixed cortical porosity concentrated more laterally on the anterior zygomatics towards the temporal process
- bilateral fine cortical porosity with diffuse new bone across the temporal squama. There is porosity extending across the preserved anterior squama with particular concentration of porosity on the suprameatal crest. It is clear that these lesions are continuous with the external sphenoid and follows the region of the temporalis muscles. The lateral and inferior (pterygoid region) external sphenoid is affected by active cortical porosity.
- mixed active and remodelled fine cortical porosity with new bone and vascular impressions medial and

superior to the superciliary arches.
- bilateral active moderate cribra orbitalia
- fine diffuse pin prick porosity on the left parietal eminence and mid lambdoid region of the occipital of unknown aetiology consistent with mild porotic hyperostosis or cortical porosity.

Radiographic Lesion Summary:
- post-mortem damage too severe for any observations

Differential Diagnosis Outcome:
Probable Scurvy

Skeletal ID: 71

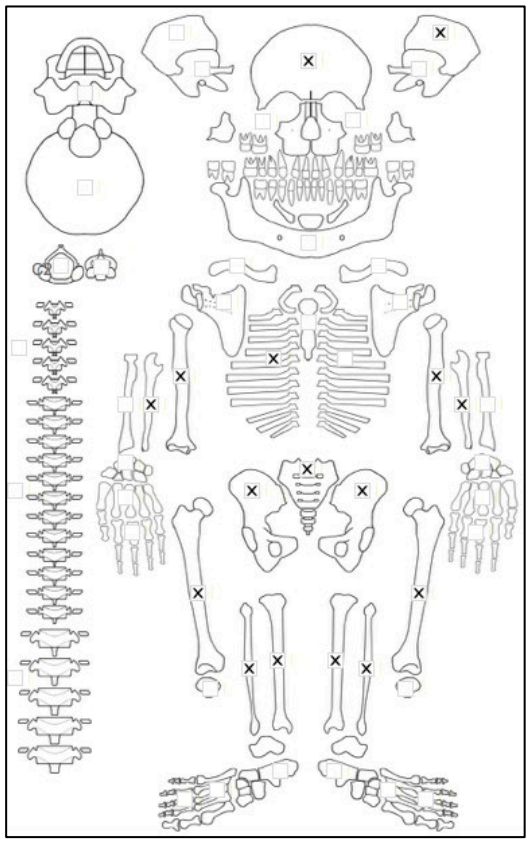

Completeness: Incomplete (33 to 50%). Fragmented skull with identifiable frontal and left parietal bone fragments. 5 partially complete right ribs. All long bones present with exception of radii. 1 vertebra.
Preservation/ Taphonomy: Surfaces well preserved. Midshaft of ulnae only, proximal ends of fibulae damaged, distal end of left femur missing, proximal third of left humerus missing.
Age: 1-5 years, *Child*
Sex: Indeterminate

Macroscopic Lesion Summary:
- unilateral diffuse woven bone on the lateral middle third of the fibula continuous with the cortical bone
- deep endochondral porosity extending beyond 10mm from the metaphyseal plate: proximal and distal tibiae (with a slight cupping indentation on the proximal metaphyseal plate, distal right femur
- bilateral cribra femoris
- bilateral active diffuse woven bone across the medial shafts of the tibiae

Radiographic Lesion Summary:
- white line of Fraenkel on the distal femur and proximal and distal tibiae
- ground glass sign in the distal femur and proximal and distal tibia
- multiple arrest lines of the distal femur and proximal and distal tibia
- generalised radiolucency (osteopenia) of the proximal and distal femur and tibia
- Trummerfeld line: the proximal and distal tibia

Differential Diagnosis Outcome:
Probable Scurvy

Skeletal ID: 29

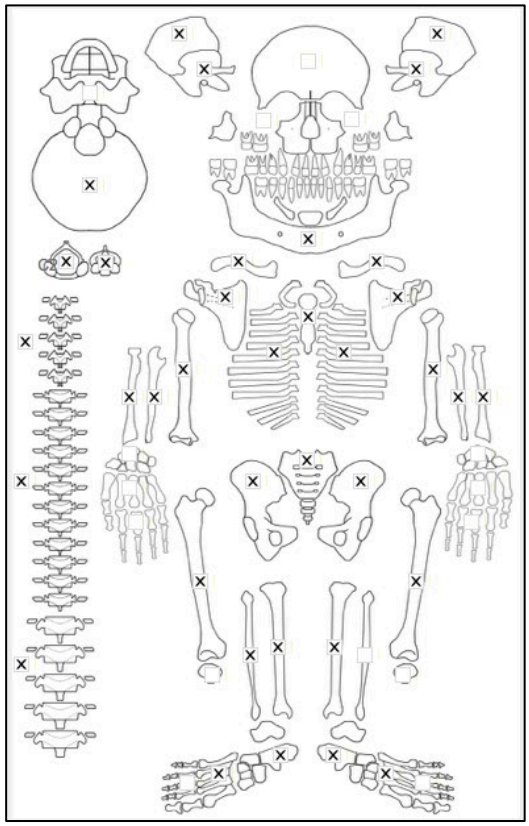

Completeness: Complete (min 75%). 92% of long bones, 19% of hands and feet, 100% of vertebrae and 63% of neurocranium present. Facial bones absent. Ribs complete.
Preservation/ Taphonomy: Well preserved surfaces. Long bone ends intact. Scapula bodies missing. Postmortem breakage of some vertebrae and ribs, minimal.
Age: 16 (+/- 2 years), *Adolescent*
Sex: Female
Macroscopic Lesion Summary:
- bilateral remodelled porosity and new bone extending from the superior margin of the superior external auditory canal towards the suprameatal crest.
- bilateral diffuse remodelled deposit of new bone as indicated by deep vascular channels with sharp margins on the superior endocranium (inferior surface of the parietals), and on the transverse sulcus of the occipital
- mixed remodelling thin diffuse pinprick porosity on the occipital planum and posterior parietals close to the lambdoid suture. Consistent with mild porotic hyperostosis.
- bilateral mixed remodelling porosity and localised new bone on the medial coronoid processes not inclusive of the mandibular foramen, small deposit of unilateral localised remodelled new bone around the region of the left mental foramen, bilateral mixed remodelling new bone and cortical porosity on the inferior margin of the oblique lines, remodelled new bone and cortical porosity on the inferior mandibular ramus
- unilateral diffuse mixed remodelling and active new bone on the anterior crest and more distally on the lateral aspect of the right fibula. Remodelled more proximally and still active distally.
- bilateral large striations on the anterior crest, lateral and medial aspect throughout the shaft of the tibia consistent with a diffuse remodelled deposit of new bone. Left side is more profuse.
- unilateral localised deposit of new bone on the lateral midshaft of the femur, not presence of woven bone but there is continued disorganised nature consistent with remodelling in process.
- deep vertebral and sacral body porosity
Radiographic Lesion Summary:
Radiographs not taken
Differential Diagnosis Outcome:
Possible Scurvy
Anaemia

Skeletal ID: 161

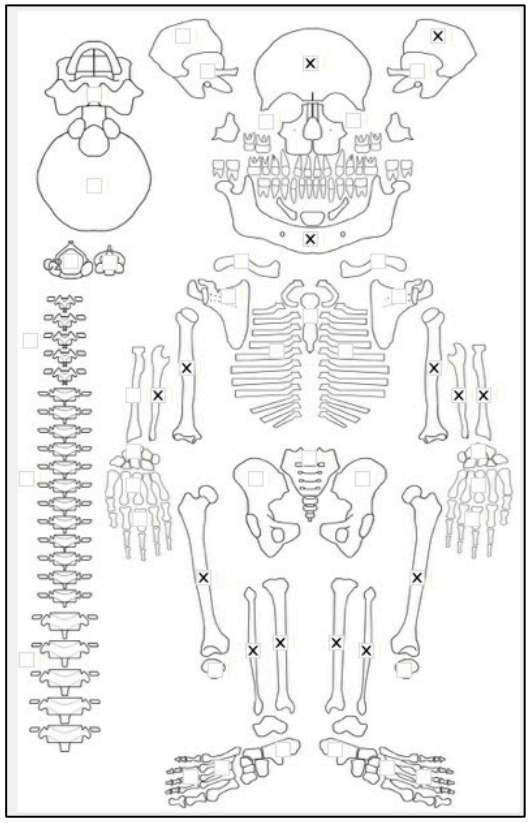

Completeness: Incomplete (33 to 50%). 80% of long bones, and 25% of neurocranium. No vertebrae. No hands and feet, No ribs.
Preservation/ Taphonomy: Surfaces well preserved. Proximal left humerus, femur and ulna metaphyses missing. Fibulae and right femora represented by middle shafts only. The skull is fragmented.
Age: 15 (+/- 3 years), *Adolescent*.
Sex: Indeterminate.
Macroscopic Lesion Summary:
- Remodelling moderate cribra orbitalia in the left eye orbit (right orbit missing).
- diffuse cortical pin prick porosity on the left anterior zygoma (right side missing).
small thin active plaque deposit of new bone inferior to the right oblique line of the mandible (left side missing)
- small thin remodelling plaque like deposit on the lateral ramus attachment site directly inferior to the right mandibular notch (left side missing).
- Mixed active and remodelling cortical porosity and new bone on the right medial coronoid process of the mandible (left side missing)
- remodelled new bone and porosity on the mental spines on the posterior mandibular body
- unilateral small remodelled deposit of new bone on the distal lateral left fibular shaft
Radiographic Lesion Summary:
No radiographs taken
Differential Diagnosis Outcome:
Possible Scurvy
Anaemia

Skeletal ID: 151

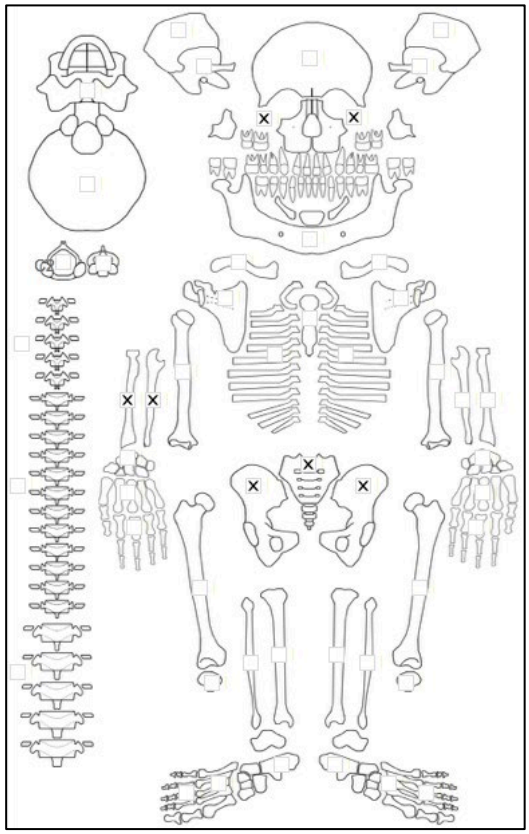

Completeness: Fragmented. Facial bones. Left radius and ulna. Left calcaneus. 7 incomplete unsided ribs. 1 thoracic, 1 lumbar and 2 cervical vertebrae. Pelvis and sacrum present.
Preservation/ Taphonomy: Surfaces well preserved. Ulna distal metaphyses damaged.
Age: 2 (+/- 0.5 years), *Child*
Sex: indeterminate
Macroscopic Lesion Summary:
- mixed active and remodelling small fine cortical porosity and localised new bone inferior to the radial notch on the right ulna
- circumferential trabecular expansions on the anterior and lateral vertebral body of a middle to lower thoracic, and a lumbar vertebra ranging from 5 to 11m in maximum diameter.
- bilateral localised fine cortical porosity and new bone on the inferior orbital floor (superior maxillae). The heavy apposition of new bone is indicated through the presence of vascular impressions.
Radiographic Lesion Summary:
No radiographs taken
Differential Diagnosis Outcome:
Non Diagnostic

Skeletal ID: 55

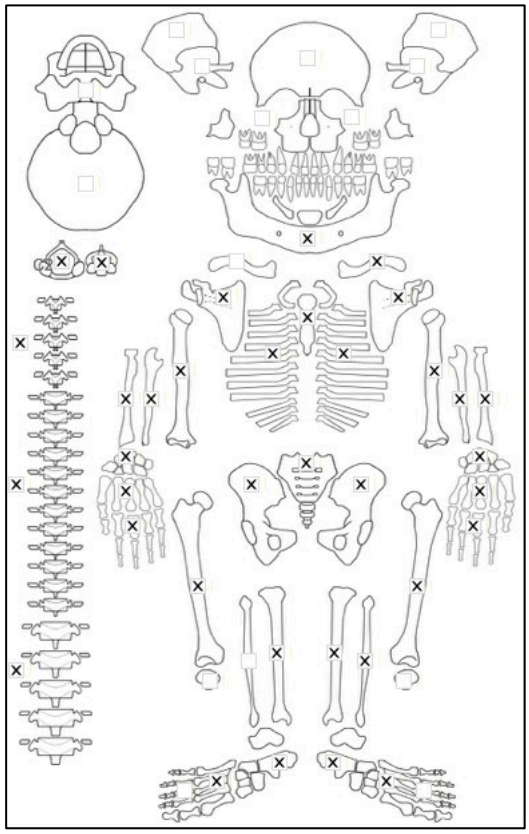

Completeness: Near Complete (66 to 75%). 90% of long bones, 61% of hands and feet, 92% of vertebrae and skull is missing. Ribs complete.
Preservation/ Taphonomy: Surfaces well preserved. All preserved long bones complete except for proximal left tibia. Scapula bodies missing. Postmortem breakage of ribs.
Age: 20-29, *Young Adult*
Sex: Male
Macroscopic Lesion Summary:
- bilateral symmetrical remodelled small localised deposit of new bone and very fine cortical porosity anterior to the mandibular foramen superior to the mylohyoid line around the coronoid process region, on the medial coronoid process, around the mental spines and sublingual fossa, the inferior aspect of the mandibular body, and new bone with vascular impression inferior to the mylohyoid regions of the mandible.
- bilateral active deposits of woven bone on the anterior scapulae directly medial to the scapular neck, and the supraspinous fossa of the left scapula (right missing), appears diffuse.
- deep manubrial porosity
- bilateral active diffuse and thick woven new bone on the lateral anterior iliac blades extending from the iliac spine to the superior margin of the acetabulae
- active new bone on the iliopubic rami, bilateral but not symmetrical as the right is on the ramus and the left is directly lateral to the pubic symphysis and also bilaterally on the ischial tuberosities.
- Dactylitis: bilateral remodelled deposit of new bone on the plantar surface proximal to the metatarsal head of the right MT1, mixed active and remodelled deposit of woven bone on the medial and dorsal midshaft of the right MT5 (left missing).
- remnant of active new bone on the internal surface of the right 11th rib directly distal to the rib head.
- bilateral diffuse active new bone on the posterior and lateral aspects of the upper 2/3 of the ulnae
- bilateral diffuse active new bone on the radii: proximal to middle third of the right shaft, and distal end and metaphysis of the left radius.
- bilateral diffuse remnants of active new bone on the posterior distal ends and lateral proximal ends of the humeri suggesting that there was more diffuse periosteal reaction that has since worn away.
- diffuse new woven bone across the distal half shaft of the left fibula (right missing), more spread on the medial aspect but the lesion is more severe on the lateral distal end.
- bilateral diffuse new bone on the tibial shafts: mixed remodelled and woven new bone on the left tibial shaft, more remodelled on the anterior crest whereas active on the medial surface, active thick woven new bone

across the entire right tibia with exception of the epiphysis, the reaction is more marked on the bone ends. There are areas of the shaft where no lesion is present but this is likely due to taphonomic destruction. Lesion spread is consistent with having been across the entire shaft.
- bilateral thick active woven new bone across the upper 2/3 of the femur. The lesion is concentrated on the upper 1/3 but continues further on the posterior aspect. The degree of severity is worse on the anterior aspect on the right femur and the lateral and medial aspects of the left femur. There is a remnant of new bone on the distal metaphysis of the left femur suggest the entire shaft may have been compromised.
- Diffuse mixed active and remodelling new bone on the internal margins of the lamina and on the right superior articular facet of the C1.
- Remodelling deep vertebral body porosity.

Radiographic Lesion Summary:
No radiographs taken
Differential Diagnosis Outcome:
Possible Scurvy

Skeletal ID: 1

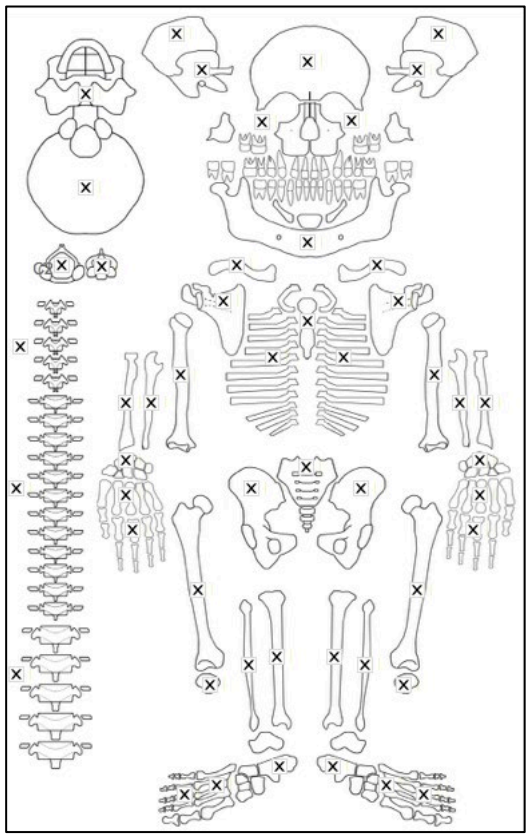

Completeness: Complete (min 75%). 110% of long bones, 62% of hands and feet. 100% of vertebrae, 88% of neurocranium. Ribs complete.
Preservation/ Taphonomy: Surfaces well preserved.
Age: 40-49, *Middle Aged Adult*
Sex: Female
Macroscopic Lesion Summary:
- bilateral remodelled diffuse new bone across the ectocranial occipital squama of the temporals.
- fine diffuse pin prick porosity with bone filling consistent with remodelled mild porotic hyperostosis on the occipital planum and posterior parietals with diploic expansion.
- bilateral remodelled cortical porosity and new bone on the on the lateral greater wing and pterygoid fossa of the sphenoid
- diffuse remodelled new bone as identified through partially unorganised porous structure and abnormal vascular channel throughout the visible endocranial surface (skull is closed).
- remodelling porosity on the middle inferior mandible body
- bilateral remodelled thin depositions of new bone with very fine cortical porosity inferior to the mylohyoid lines of the mandible with vascular impressions.

- bilateral remodelled new bone and cortical porosity on the medial coronoid processes of the mandible
- bilateral remodelled fine cortical porosity on the superior orbital roofs

Radiographic Lesion Summary:
No radiographs taken

Differential Diagnosis Outcome:
Anaemia
Probable Scurvy

Skeletal ID: 3

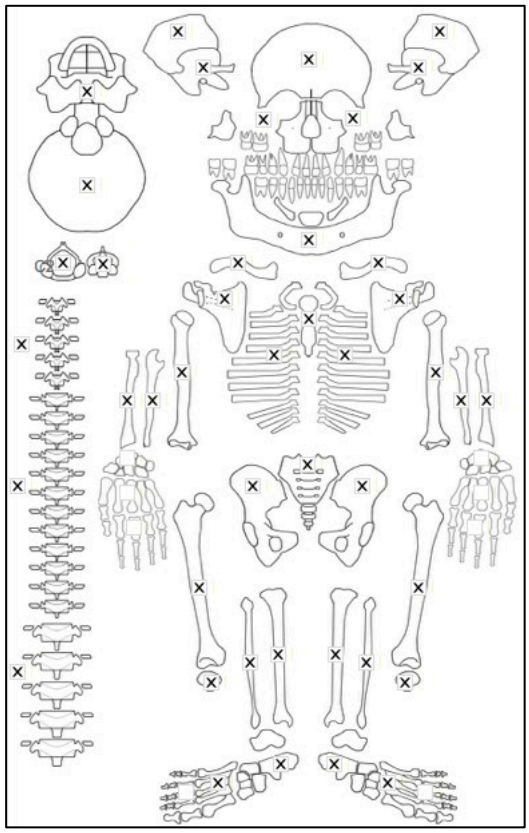

Completeness: Complete (min 75%). 100% of long bones, 20% of hands and feet, 88% of neurocranium. Ribs complete.
Preservation/ Taphonomy: Surfaces well preserved and bones intact.
Age: 20-29, *Young Adult*
Sex: Male

Macroscopic Lesion Summary:
- bilateral remodelling moderate cribra orbitalia
- bilateral fine remodelled pinprick diffuse cortical porosity on the supercilliary arches, temporal lines and superior frontal- porosity superior and posterior parietals and occipital planum consistent with mild remodelling porotic hyperostosis.
- bilateral remodelled cortical porosity on the superior margin of the external auditory meatus and suprameatal crest of the temporal, anterior squama, lateral greater wings and pterygoid region of the sphenoid
- bilateral symmetrical mixed active and remodelling new bone and cortical porosity on the anterior lateral and posterior maxillae superior to the alveolar margin and around the region of the infraorbital foramen. Vascular impressions on the lateral aspect and inferior to the foramen and near the nasal margin. There is significant alveolar resorption.
- remodelled new bone and fine cortical porosity on the palatal surface of the maxillae. Porosity is extending from the foramina.
bilateral cortical porosity of the anterior zygomatics
- bilateral symmetrical remodelled cortical porosity with thin remodelled new bone on the posterior zygomatic bones with vascular impressions
- mixed active and remodelled cortical porosity with new bone on the medial coronoid processes of the mandible including anterior to the mandibular foramen and extending towards the alveolar bone

- bilateral remodelled cortical porosity and new bone on the inferior oblique lines of the mandible
- remodelled cortical porosity on the incisive fossae of the mandible
- bilateral and symmetrical localised remodelling new bone deposition inferior to the humeral heads on the medial and posterior aspect, appears poorly mineralised
- unilateral thick remodelled projection of new bone on the anterior shaft of the left tibia- likely myositis ossificans
- bilateral remodelled cortical porosity on the superior acromion ends of the clavicles
- unilateral localised active new bone with associated cortical porosity on the inferior acromion at the deltoid attachment of the left clavicle
- unilateral localised deposit of active woven new bone inferior to the coracoid process on the anterior scapula
- unilateral remodelling deposit of new bone on the dorsal and medial right calcaneal tuberosity.
- remodelling deep vertebral body porosity
- remodelled striated new bone on the internal ribs (likely normal variant)
- porosity on the external rib shafts (likely normal variants)
- unilateral remnant of diffuse woven new bone on the external iliac blade. Remnants extend from the posterior superior iliac spine to the anterior superior iliac spine.
- bilateral diffuse woven bone on the ischial body directly superior to the ischial tuberosities and posterior margin of the acetabulae.
- unilateral active bone on the proximal end of the femur with a region of active clustered pits on the medial aspect in a region of 54mm. clusters are between 1-2mm in size and multifocal and coalesced.
- diffuse active cortical porosity on the external aspect of the rib shaft from the rib neck onwards of the 5th left rib, and 10th left and right ribs. Large clustered pits on the external shaft, similar to on the right proximal femur (most severe on the 10th left rib).

Radiographic Lesion Summary:
No radiographs taken
Differential Diagnosis Outcome:
Anaemia
Probable Scurvy

Skeletal ID: 11

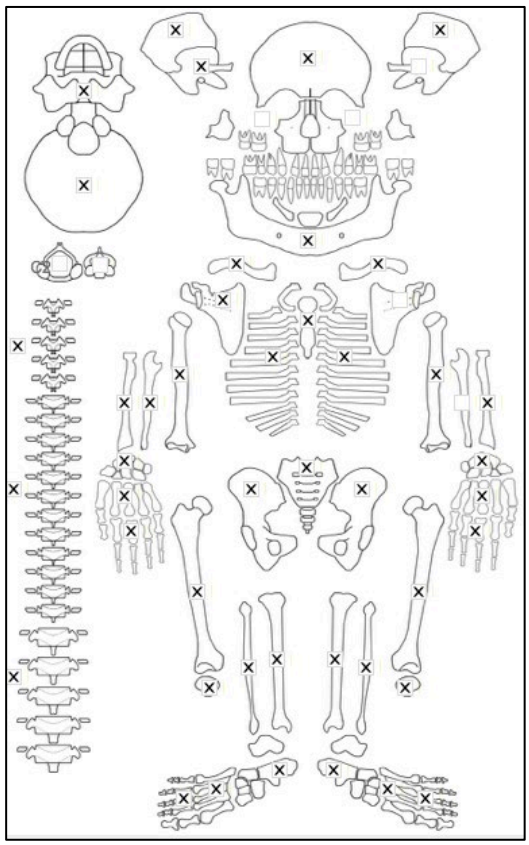

Completeness: Complete (min 75%). 90% of long bones, 68% of hands and feet, 100% of vertebrae, 75% of neurocranium. Near complete ribs.

Preservation/ Taphonomy: Scapular bodies missing. Postmortem breakage of ribs. Left proximal humerus missing, all other preserved long bones complete.
Age: 30-39, *Middle Aged Adult*
Sex: Female
Macroscopic Lesion Summary:
- mixed active and remodelling new bone and cortical porosity on the medial right coronoid process of the mandible (left side missing)
- mixed active and remodelling very fine cortical porosity on the inferior mandibular body
- moderate cribra orbitalia of the left orbit (right side missing)
- remodelling porotic hyperostosis of the frontal, superior and posterior parietals and the squamal occiptial.
- remodelled concentrated focal fine cortical porosity extending from the superior external auditory meatus to the suprameatal crest of the right temporal (left side missing).
- deep manubrial porosity
- remodelled localised new bone extending from the foramen superior to the radial notch onto the articular surface of the trochlea notch on the right ulna.
- bilateral localised thin remodelled deposition of new bone on the anterior proximal third shaft of the femora. More marked on the right femur
Radiographic Lesion Summary:
No radiographs taken
Differential Diagnosis Outcome:
Anaemia
Possible Scurvy

Skeletal ID: 6

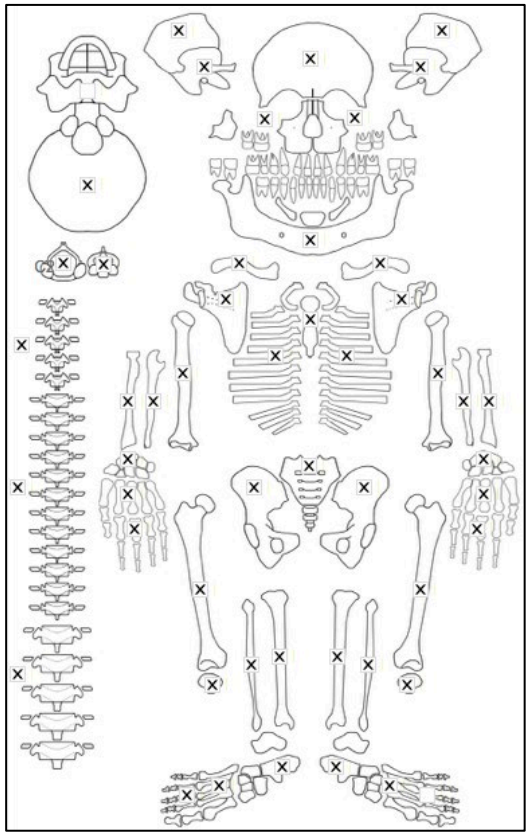

Completeness: Complete (min 75%). 100% of long bones, 58% of hands and feet, 96% of vertebrae, 100% of neurocranium. Ribs complete.
Preservation/ Taphonomy: Surfaces well preserved.
Age: 20-29, *Young Adult*
Sex: Female
Macroscopic Lesion Summary:
- remodelling bilateral moderate cribra orbitalia

- remodelling porotic hyperostosis of the of the occipital squama, superior and posterior parietals and the frontal
- bilateral remodelled new bone and cortical porosity on the suprameatal triangle extending from the superior margin of external auditory canal to the suprameatal crest. There is also the same deposit of new bone and porosity in the right mastoid notch extending from the inferior margin of the external auditory meatus.
- bilateral symmetrical remodelled fine cortical porosity on the lateral external left greater wing of sphenoid and into the pterygoid fossa and lateral sphenoid. Mixture of fine and very fine porosity. Continues onto the anterior margin of the temporal squama superior to the zygomatic process.
- diffuse remodelled new bone and vascular impressions on the endocranial parietals and frontal
- bilateral remodelled cortical porosity on the anterior zygomatic bones
- bilateral symmetrical very fine active cortical porosity extending from the infraorbital foramen to the nasal margin and remodelled thin deposit of new bone with vascular impressions on the anterior maxilla.
- remodelled porosity and new bone on the posterior maxilla with vascular impressions superior to the alveolar bone. on the right side this continues onto the posterior zygomatic not on the left.
- bilateral remodelled diffuse cortical porosity and remodelled deposition of new bone on the palatal surface
- bilateral symmetrical remodelled deposit of new bone and very fine and mild cortical porosity inferior to the left oblique line on the ramus.
- bilateral symmetrical remodelled deposit of new bone and porosity on the right medial coronoid extending to include the region of the mandibular foramen and directly anterior to the foramen
- bilateral symmetrical remodelled deposit of new bone and porosity inferior to the mylohyoid lines. The deposit is thin but identified through the presence of vascular impressions.
- remodelled deposit of new bone and porosity on the left sublingual fossa extending towards the mental spines and onto the inferior mandibular body
- remodelling deposit of new bone and very fine cortical porosity on the costoclavicular impression of the clavicles, may be related to muscle trauma. is bilateral.
- remodelled small deposit of new bone on the palmar surface directly proximal to the phalangeal head of the left 5th proximal hand phalanx.
- multiple foramen expansions of the palmar surfaces of the left 2nd, 5th and 4th intermediate hand phalanges
- expanded foramen inferior to the radial notch on the left ulna
- bilateral symmetrical remodelled localised deposit of new bone with very fine cortical porosity on the anterior distal end shaft and metaphysis of the humeri.
- unilateral focal oval lytic lesion with sclerotic response on the margins and base on the distal metaphysis of the anterior left humerus (less than 10mm in diameter)
- possible retained deep endochondral porosity in the proximal tibial metaphysis (may or may not be abnormal)
- remodelled striations on the superior left ala of the S1, may be related to some sort of development failure of the bone. may have included hypervascularisation of the trabecular bone of the alae (i.e remodelled deep porosity)
- bilateral new bone depositions with cortical porosity on the superior aspect of the inferior articular facet region on the pedicles of C2.
- deep vertebral body porosity in the process of remodelling
- large channel like lytic lesion on the inferior vertebral body of the L1 penetrating into the posterior aspect through the vascular channels. the margins are well defined with sclerotic response. Lesion max diameter: 17mm. May also be a result of trauma. Associated with expanded foramina on the arches. There are burst fractures on multiple vertebrae.
- large multifocal and coalesced lesion with some sclerotic response covering an area over 1cm on posterior margin of the superior vertebral body of the L2.
- multifocal and coalesced lytic lesion with some sclerotic response on the anterior region of the superior body of the L4. There is slightly osteophytic response with anterior project of bone. There is also a Schmorl's node in the central endplate. The lesion creates a circular cavity on the anterior margin.
- extension of remodelled bone from the proximal plantar end of a 4th or 5th distal phalanx, may likely be related to trauma.
- expansion of foramina on the left 4th and 2nd proximal hand phalanges

Radiographic Lesion Summary:

- the lytic lesions on the vertebra show some sclerotic response on the margins. There appears to be internal destruction of the anterior vertebral bodies (likely in the vascular channels).
- osteopenia of the metaphyses of the tibia
- fibrosis and some endosteal expansion at the midshaft of the left tibia, which endosteal expansion of the anterior crest (there was no macroscopic change visible)

Differential Diagnosis Outcome:

Probable Osteomyelitis

Probable Scurvy
Anaemia

Skeletal ID: 23

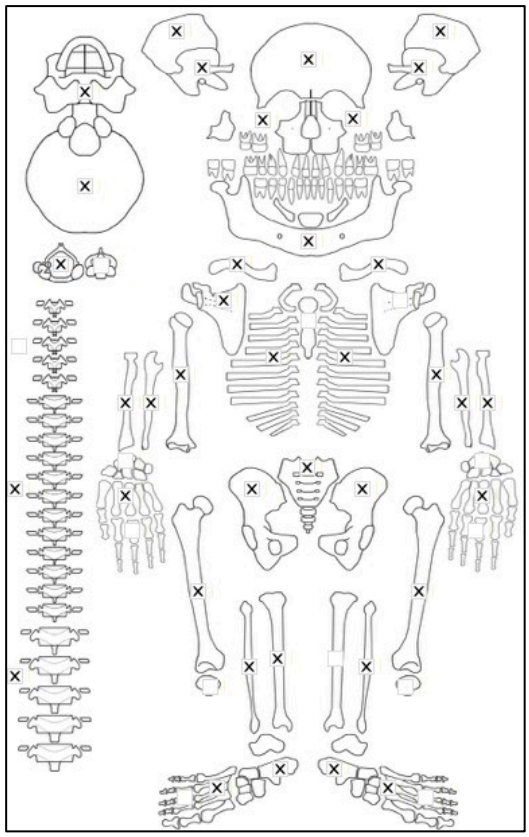

Completeness: Near Complete (66 to 75%). 90% of long bones, 35% of hands and feet, 58% of vertebrae, 88% of neurocranium. Ribs partially complete.
Preservation/ Taphonomy: Surfaces well preserved. Ribs heavily fragmented and many postmortem breaks to long bones and vertebrae. Surfaces well preserved.
Age: 50+, *Old Adult*
Sex: Male
Macroscopic Lesion Summary:
- remodelling bilateral moderate cribra orbitalia
- remodelling porotic hyperostosis of the superior frontal, superior and posterior parietals and occipital squama
- bilateral and symmetrical remodelled cortical porosity on the lateral left greater wing and pterygoid fossa continuing onto the anterior squama of the temporal bone.
- bilateral remodelled new bone and cortical porosity extending from the superior margin of the external auditory canal onto the suprameatal crest region.
- bilateral symmetrical remodelled fine cortical porosity on the inferior mastoid notch and continuing onto the pars lateralis regions.
- remodelled oval cleft on the inferior right mastoid with circular margins. Lesion max diameter: 10mm
- remodelled deposit of new bone on the superior endocranium and superior portion of the occipital cranium. Identified through irregular surface and abnormal vascular impressions. A thicker deposit of new bone is present on the sagittal sulcus region of the endocranial occiput.
- bilateral symmetrical remodelled deposit of new bone and cortical porosity on the medial coronoid processes of the mandible. The porosity extends from within the mandibular foramen
- unilateral remodelled deposit of new bone and cortical porosity inferior to the right mylohyoid line.
- active deposit of localised new bone on the supraspinous fossa of the right scapula (left missing)
- bilateral symmetrical small deposit of remodelling new bone and porosity on the medial calcaneus
- diffuse mixed remodelled new bone with overlying active woven bone on the medial aspect and interosseous crest of the left fibula. The two stages of bone suggest long term chronic activity. Makes trauma unlikely. (right side missing)

- expanded foramen on the distal metaphyseal palmar surface of an unsided 2nd to 4th proximal hand phalanx.
Radiographic Lesion Summary:
No radiographs taken
Differential Diagnosis Outcome:
Probable Otitis Media/ Mastoiditis
Probable Scurvy
Anaemia

Skeletal ID: 19

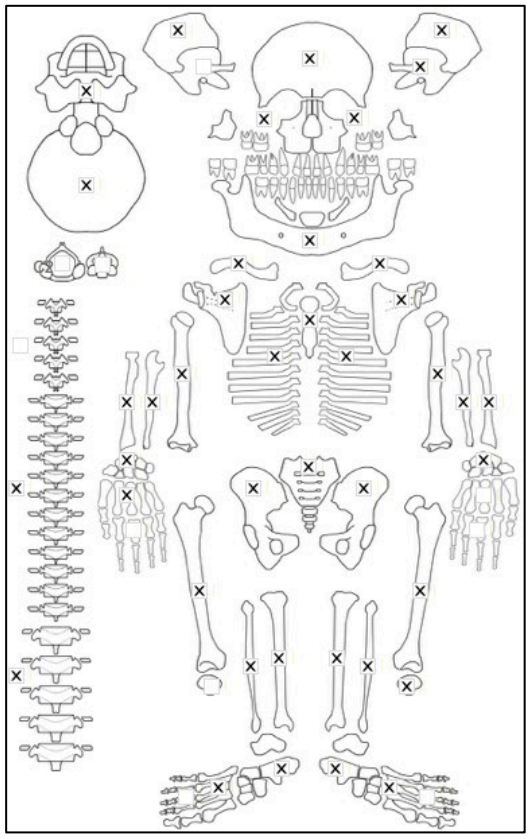

Completeness: Complete (min 75%). 92% of long bones, 50% of hands and feet, 71% of vertebrae, and 75% of neurocranium. Ribs complete.
Preservation/ Taphonomy: Surfaces well preserved. Extra auricular surface of another individual, was easily removed. Scapular bodies missing. Postmortem breakage of ribs.
Age: 40-49, *Middle Aged Adult*
Sex: Male
Macroscopic Lesion Summary:
- thick deposit of remodelled new bone and porosity across the non articular bone on an unsided 1st proximal phalanx
- thick deposit of remodelled new bone on the proximal medial and plantar surface of an unsided 2nd proximal pedal phalanx possibly related to trauma or muscle strain.
- small localised active deposit of new bone on the medial midshaft of the left MT2
- bilateral symmetrical localised remodelling new bone plaque deposit on the distal anterior fibular ends
- unilateral thin localised well remodelled deposit of new bone on the middle anterior crest of the right tibia.
- mixed active and remodelled diffuse deposit of new bone on the medial and posterior distal end of the left tibia. Bilateral but right tibia extends more extensively to the midshaft.
- bilateral remodelled moderate cribra orbitalia
- well remodelled fine diffuse pin prick porosity with diploic expansion on the frontal (more marked on the superciliary arches), superior and posterior parietals and the occipital. Consistent with mild porotic hyperostosis
- small deposit of remodelled new bone and cortical porosity on the right medial nasal margin (left side missing)
- bilateral remodelled deposit of new bone and cortical porosity on the palatal surfaces of the maxillae

- remodelled fine cortical porosity on the anterior left zygoma (right missing)
- deposit of remodelled new bone around the left incisive foramen of the mandible lifting the margins of the foramen (right missing)
- deposit of remodelled new bone and cortical porosity on the inferior mandibular body
- deposit of remodelled new bone and cortical porosity remodelled on the left coronoid extends towards the mandibular foramen and also towards the alveolar margin, with remodelled new bone and vascular impressions inferior to the mylohyoid line (right side missing)
- deposit of remodelled new bone and very fine cortical porosity on the medial left mandible inferior to the alveolar margin at the
P4, there is evidence of alveolar bone loss

Radiographic Lesion Summary:
No radiographs taken

Differential Diagnosis Outcome:
Probable Scurvy
Anaemia

Skeletal ID: 16

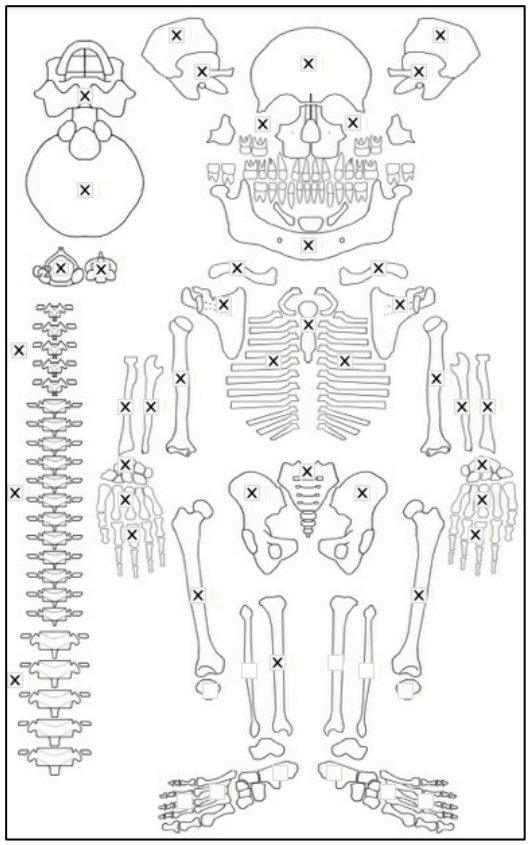

Completeness: Complete (min 75%). 67% long bones, 25% hands and feet, 96% vertebrae, 88% neurocranium. Ribs complete.
Preservation/ Taphonomy: Surfaces well preserved. Long bones mostly intact with damage to distal left femur. Vertebrae intact. Scapular bodies missing.
Age: 20-29, *Young Adult*
Sex: Female
Macroscopic Lesion Summary:
- remodelling new bone localised to the inferior aspect of the pars basilaris region.
- bilateral remodelling moderate cribra orbitalia
- small pin prick porosity mixed sharp margins and bone filling restricted to the occipital planum and on the posterior and superior parietals. Consistent with porotic hyperostosis.
- remodelled deposit of new bone with abnormal vascular impressions on the endocranial frontal and superior endocranial parietals.
- bilateral remodelled deposit of new bone and porosity on the superior external auditory meatal margin to the suprameatal crest

- destruction of internal air cells of the left mastoid. The margins of the opening demonstrate taphonomic damage so it is not possible to determine the extent or the level of remodelling. The air cell pockets appear remodelled suggesting that the lesion is at least not active in the preserved bone area. Size of lytic lesion could not be recorded due to taphonomic destruction. There is very little of the right mastoid preserved but the remnant demonstrates smaller and normal air cells on this side.
- delayed closure of the left tympanic foramen.
- bilateral remodelled pin prick porosity and vascular impressions indicating new bone on the anterior zygomatic bones around the foramen region.
- bilateral symmetrical remodelled cortical porosity on the mid posterior temporal process of the zygomatic bones.
- bilateral remodelled cortical porosity and thick diffuse new bone across the palatal surface. thick diffuse bone at the intermaxillary suture.
- bilateral symmetrical remodelled cortical porosity and localised deposit of new bone on the mandibular rami and incisive fossae
- bilateral symmetrical remodelled cortical porosity and localised deposit of new bone inferior to the oblique lines of the mandible.
- bilateral symmetrical remodelling cortical porosity and localised deposit of new bone on the medial coronoid processes of the mandible with finer porosity anterior to the mandibular foramen
- remodelled cortical porosity and localised deposit of new bone on the inferior mandibular body
- unilateral right foramen expansion on the C1 (may be normal anatomical variant)
- deep vertebral body porosity
- unilateral foramen with remodelled bone deposit indicating well healed with a remodelled lytic channel on the ectocranium posterior to the mastoid foramen, continues through the cranium. Appears to be a sinus drainage channel (max lesion length 17mm).

Radiographic Lesion Summary:
No radiographs taken
Differential Diagnosis Outcome:
Probable Otitis Media/Mastoiditis
Probable Scurvy
Anaemia

Skeletal ID: 27

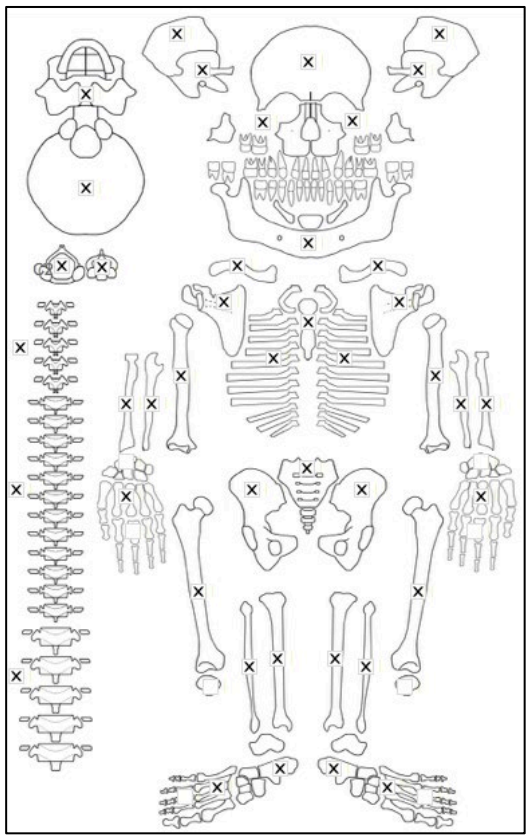

Completeness: Complete (min 75%). 93% of long bones, 46% of hands and feet, 100% of vertebrae, and 88% of neurocranium. Ribs complete.
Preservation/ Taphonomy: Surfaces well preserved. Proximal left tibia, distal half left femur and distal end of left fibula are missing, other long bones intact. Ribs have postmortem breakage.
Age: 20-29, *Young Adult*
Sex: Male
Macroscopic Lesion Summary:
- diffuse remodelled new bone on the frontal endocranium and antero-superior parietals identified by abnormal vascular impressions.
- bilateral remodelling moderate cribra orbitalia
- bilateral remodelled deposit of new bone and cortical porosity extending from the superior external auditory margin onto the suprameatal crest and triangle on the superior mastoid (may be within normal variation)
- bilateral delayed closure of the tympanic foramina remnant of a thin line of unfused bone.
- bilateral remodelled cortical porosity on the anterior zygomatics
- thick deposit of remodelled new bone and cortical porosity on the palatal surfaces of the maxillae
- remodelled porosity on the medial aspect of the mandibular coronoid processes (relatively mild, but localised pin prick porosity is clear on the right side)
- remodelled porosity and thin deposition of localised new bone on the inferior mandible
- bilateral thin localised deposit of remodelled new bone on the anterior crest extending onto the medial aspect of the tibiae
- thin localised deposit of remodelled new bone on the posterior third medial aspect of the right femur. not bilateral.
- deep posterior manubrial porosity
- deep vertebral body porosity
Radiographic Lesion Summary:
No radiographs taken
Differential Diagnosis Outcome:
Possible Scurvy
Anaemia

Skeletal ID: 30

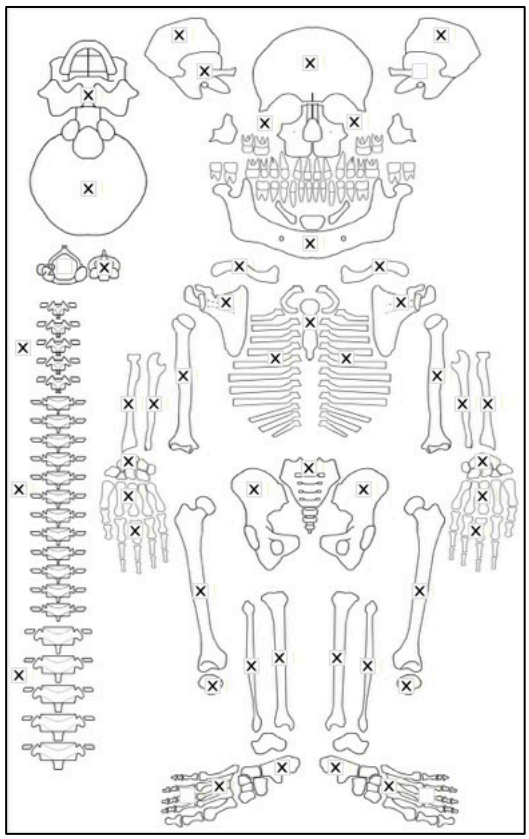

Completeness: Complete (min 75%). 95% of long bones, 66% of hands and feet, 71% of vertebrae, and 88% of neurocranium. Ribs partially complete.
Preservation/ Taphonomy: Surfaces well preserved. Ribs heavily fragmented. Epiphyses of left ulna, distal epiphysis of left fibula and proximal epiphysis of right fibula missing, other long bones intact. Scapular bodies missing.
Age: 30-39, *Young Adult*
Sex: Male
Macroscopic Lesion Summary:
- deep vertebral and sacral body porosity (mild)
- pin prick porosity on the superciliary arches (remodelling), superior and posterior parietal (well remodelled) and occipital planum (remodelling) consistent with porotic hyperostosis.
- bilateral mild remodelling cribra orbitalia
- bilateral small remodelled projection of new bone on the superior external auditory margins. Some porosity around the region
- bilateral localised region of remodelled cortical porosity on the right lateral greater wing and pterygoid region, associated with a small deposit of remodelled new bone and porosity on the anterior squama of the temporal.
- remodelled new bone on the frontal and superior endocranium of the parietals identified through the presence of abnormal vascular impressions.
- bilateral localised deposit of remodelled new bone and cortical porosity on the anterior zygomatic bones. There is a vascular impression of the right side
- remodelled diffuse cortical porosity and new bone across the palatal surfaces of the maxillae
- localised remodelled new bone on the medial right nasal margin surrounded by remodelled vascular impressions.
- bilateral symmetrical localised remodelled new bone and fine cortical porosity on the incisive fossae, oblique lines, medial coronoid processes, inferior body of the mandible
- deep manubrial porosity
- bilateral remodelled rugose surface on the posterior fibular shafts
- small thin remodelled unilateral deposit of new bone on the medial proximal right femur.
Radiographic Lesion Summary:
No radiographs taken
Differential Diagnosis Outcome:
Probable Scurvy
Anaemia

Skeletal ID: 32

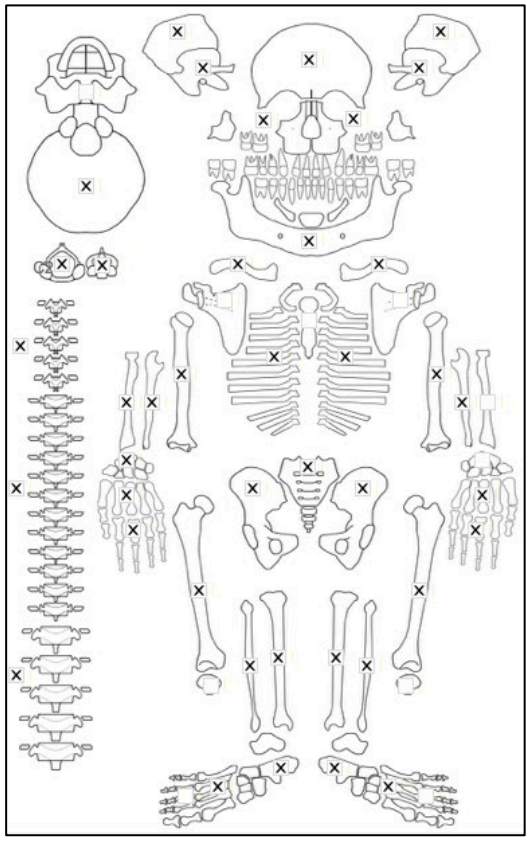

Completeness: Complete (min 75%). 80% of long bones, 62% of hands and feet, 100% of vertebrae, and 75% of neurocranium. Ribs near complete.
Preservation/ Taphonomy: Surfaces well preserved. Intrusive sacrum, left fibula and vertebra, was easily removed. Ribs fragmented. All vertebrae intact.
Age: 20-29, *Young Adult*
Sex: Male
Macroscopic Lesion Summary:
-remodelling pin prick porosity across the frontal, superior and posterior parietals and occipital planum, consistent with porotic hyperostosis.
- remodelled new bone deposition on the frontal and superior parietal and occipital endocranial surface identified through the presence of abnormal vascular impressions.
- bilateral remodelled new bone deposition and cortical porosity around the ear canal region, extends superiorly from the superior external auditory margin to the suprameatal crest, as well as from the infer canal margin onto the tympanic region and into the mastoid notch.
- bilateral symmetrical remodelled fine cortical porosity and new bone on the posterior zygomatic process of the maxillae and temporal process of the zygomatic bones. With vascular impressions. More cortical porosity and new bone superior to the alveolar margin of the maxilla
- bilateral symmetrical remodelled new bone and cortical porosity on the anterior zygomatic bones- vascular impressions
- bilateral remodelled deposit of new bone and cortical porosity across the palatal surfaces of the maxillae
- bilateral and symmetrical remodelled deposit of new bone and cortical porosity on the incisive fossae, oblique lines, lateral mandibular notches, medial coronoids, inferior to the mylohyoid lines, inferior body, mental spines, and sublingual fossae of the mandible.
- bilateral symmetrical remodelled new bone localised across the anterior crests of the tibiae
- bilateral symmetrical remodelled thick new bone across the posterior and lateral fibulae encompasses the region of the foramen.
- Dactylitis: mixed active and remodelling new bone of the right MT4 across the dorsal shaft appears to be chronic inflammation. New bone is not plaque like and continuous with the cortical bone. Endosteal involvement on the medial aspect likely. Mixed active and remodelling new bone of the right MT2 on the medial aspect of the shaft. Encompasses superior and posterior area. Bone enlargement suggests endosteal activity.

- remodelled projection of new bone on the distal medial region of the right 5th proximal phalanx.
- bilateral symmetrical remodelled thin new bone and fine cortical porosity on the medial calcanei. Left calcaneus has bony extensions from the lateral and inferior calcaneus.
- deep vertebral body porosity

Radiographic Lesion Summary:
No radiographs taken

Differential Diagnosis Outcome:
Probable Scurvy
Anaemia

Skeletal ID: 37

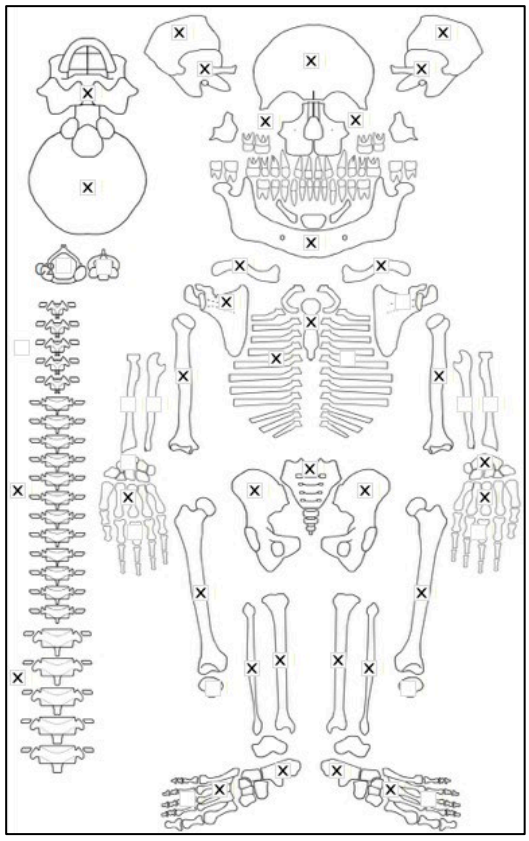

Completeness: Partially Complete (50 to 66%). $8% of long bones, 48% of hands and feet, 50% of vertebrae and 88% of neurocranium.
Preservation/ Taphonomy: Surfaces well preserved. Face fragmented, scapular bodies missing, ribs and vertebrae highly fragmented.
Age: 30-39, *Middle Aged Adult*
Sex: Female

Macroscopic Lesion Summary:
- remodelling mild cribra of the right orbit (left missing)
- bilateral symmetrical localised cortical porosity on lateral greater wings of the sphenoid and anterior squama of the temporals.
- unilateral remodelled cortical localised porosity extending from the superior border of the left external auditory meatus onto the suprameatal crest.
- remodelled new bone across the entire preserved endocranium. Abnormal vascular impressions and associated arachnoid granulations
- diffuse pin prick porosity and remodelled new bone across the anterior right zygomatic (left missing)
- small localised deposit of remodelled new bone on the inferior orbital margin on the superior right zygoma (left missing)
- bilateral remodelled deposit of new bone and porosity on the inferior floor of the maxillary sinuses.
- bilateral remodelled deposit of new bone and porosity on the anterior maxillae inferior to the infraorbital foramen (that was not preserved) and extending to the alveolar margin

- bilateral but not symmetrical remodelled deposit of new bone and porosity throughout the palatal surface, more cortical porosity on the left than the right.
- remodelled deposit of new bone anterior to the right incisive fossa and continuing to the alveolar border, may be part of alveolar resorption (left side missing)
- remodelled diffuse new bone across the posterior preserved shaft including the region of the foramen of the left fibula (right missing)
- bilateral but not symmetrical remodelled diffuse new bone on the middle anterior crest and medial/posterior middle third of the left tibia, and medial proximal, middle anterior crest and medial middle third right tibia.
- bilateral near symmetrical remodelled localised oval deposit of new bone on the medial towards posterior proximal right femoral shaft, and extending to the middle shaft of the left femur. There are vascular impressions on the right femur. Deposits appear haematoma-like.
- remodelled new bone on the anterior pubic bones may suggest remodelled hypervascularity or remodelled poor bone development
- remodelled new bone and cortical porosity localised to the medial left calcaneus (right missing).

Radiographic Lesion Summary:
No radiographs taken
Differential Diagnosis Outcome:
Possible Scurvy

Skeletal ID: 42

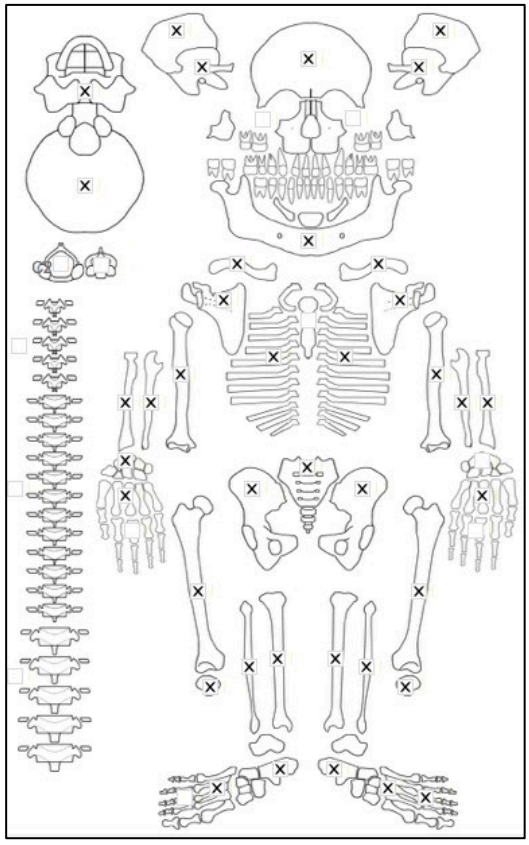

Completeness: Near Complete (66 to 75%). 95% of long bone, 58% of hands and feet, 0% of vertebrae, and 88% of neurocranium. Ribs near complete.
Preservation/ Taphonomy: Surfaces well preserved. Vertebrae were commingled with another individual and therefore was excluded. Some postmortem breakage of ribs. Scapular bodies missing.
Age: 20-29, *Young Adult*
Sex: Female
Macroscopic Lesion Summary:
- remodelled new bone deposition with abnormal vascular impressions on the endocranial frontal bone only
- remodelling pin prick porosity consistent with mild cribra orbitalia.

- bilateral symmetrical remodelled localised new bone and cortical porosity around the ear canal region: extending superior for the canal to the suprameatal crest and inferior on to the tympanic region. The right temporal tympanic has delayed tympanic foramen closure
- remodelled cortical porosity across the lateral right greater wing, pterygoid region and on the anterior squama of the right temporal (may be within normal range- left side missing)
- thick deposit of remodelled new bone on the inferior pars basilaris region near the spheno-occipital synchondrosis.
- bilateral symmetrical thin localised deposit of new bone and cortical porosity on the incisive fossae extending to medial to the mental foramen, oblique lines, inferior mandibular body of the mandible
- bilateral medial curvature of the proximal third shaft of the humeri at the deltoid (likely activity related)
- bilateral symmetrical remodelled new bone deposition diffuse across the posterior shafts and middle third anterior border of the fibulae
- bilateral symmetrical remodelled new bone deposition slightly diffuse and thin across the posterior middle to distal thirds of the tibiae
- bilateral remodelled diffuse new bone across the lateral medial and posterior shafts of the femora. note: left femur also has an active region on the anterior margin of this lesion but they have been recorded separately as this is very well remodelled, possibly two processes or two stages to the disease in the region, suggests this is disease not trauma related.
- a small region of highly active woven new bone on the medio-anterior midshaft of the left femur in the same region as well remodelled diffuse bone. it is likely this new bone used to extend further. This active bone surrounds the foramen.
- remodelled new bone and cortical porosity on the anterior and posterior left zygoma (right missing)

Radiographic Lesion Summary:
No radiographs taken
Differential Diagnosis Outcome:
Probable Scurvy

Skeletal ID: 58

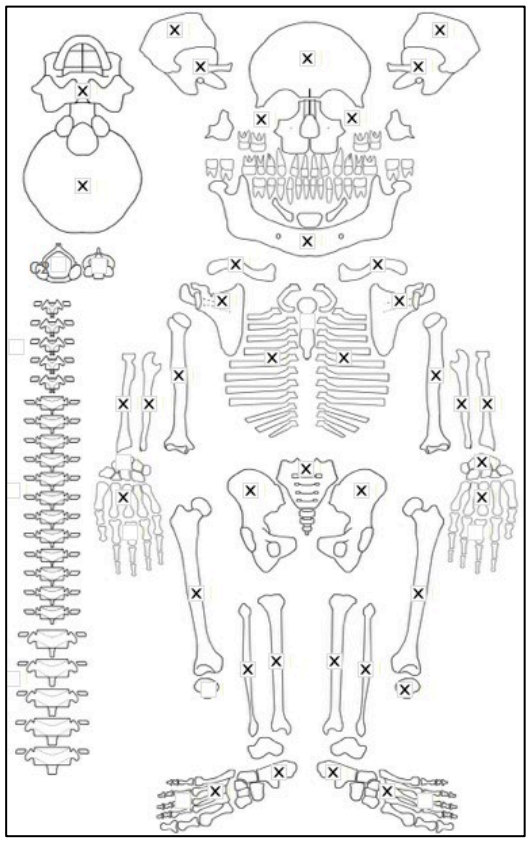

Completeness: Near Complete (66 to 75%). 98% of long bones, 33% of hands and feet, 0% of vertebrae and 88% of neurocranium. Ribs partially complete.
Preservation/ Taphonomy: Surfaces well preserved. Vertebrae commingled therefore excluded. Postmortem breakage of ribs, scapular bodies missing, distal end of left radius missing.

Age: 40-49, *Middle Aged Adult*
Sex: Male
Macroscopic Lesion Summary:
- Right mandibular M1 and 2 tooth loss with associated alveolar resorption
- bilateral remodelled moderate cribra orbitalia
- porotic hyperostosis of the occipital, frontal and parietals with diploic expansion
- bilateral symmetrical localised remodelled new bone on the pterygoid fossa, plate and part of the lateral greater wing sphenoid. The porosity appears deep as if it extends into the trabecular bone (age related?) but there is also smaller porosity on the anterior squama of the temporal. Some of the porosity is large more than 1mm in size. The left temporal also has remodelled thin deposit of localised new bone. The inferior sphenoid appears to have a thick deposit of remodelled new bone and this may be why the porosity appears deep
- bilateral remodelled cortical porosity extending from the superior margin of the external auditory canals to the suprameatal crests and from the inferior margin onto the tympanic regions. There are some remodelled deposits of new bone. The cortical porosity and new bone continues along anterior to the carotid canal and may be associated with similar new bone and porosity on the pars basilaris and sphenoid
- unilateral localised remodelled thick new bone overlying the mastoid notch and part of a remodelled crescent shaped lytic depression on the inferior left mastoid possibly indicative of well remodelled mastoiditis (approx. 14mm in max diameter)
- localised remodelled new bone with lytic channels posterior to the left and right mastoids, possibly fistula drainage areas
- remodelled new bone and cortical porosity across the pars basilaris inferior aspect. may be associated with the sphenoid and temporal porosities. Associated with a small lytic circular depression
- remodelled diffuse new bone across the endocranium frontal parietals temporals and occipital identified through abnormal vascular impressions. The bone deposition is most thick on the superior occipital.
- bilateral symmetrical remodelled new bone and cortical porosity with vascular impressions on the anterior zygomatic bones, with cortical porosity on the posterior (with vascular impressions) and superior zygomatic bones.
- remodelled cortical porosity and new bone across the palatal surfaces of the maxillae
- remodelled new bone with vascular impressions across the inferior nasal floor
- bilateral symmetrical remodelled new bone and cortical porosity on the oblique lines, inferior to the lateral mandibular notch, medial coronoid processes, with vascular impressions inferior to the mylohyoid line, and inferior body of the mandible.
- bilateral remodelled diffuse new bone across the external iliac blades
- dactylitis: remodelled localised thick new bone with some endosteal expansion on the medial mid to distal shaft of the right M2
- bilateral symmetrical remodelled diffuse new bone across the posterior and lateral shafts including the posterior foramen of the fibulae
- bilateral symmetrical localised remodelled new bone on the medial proximal femora
- localised remodelled localised new bone deposition on the proximal anterior crest of the right tibia (left missing)
- remodelled striae on the internal ribs and cortical porosity of the external ribs
- arachnoid granulations on the endocranium
- bilateral fine cortical porosity on the medial nasal margins with vascular impressions
Radiographic Lesion Summary:
No radiographs taken
Differential Diagnosis Outcome:
Probable Otitis Media/ Mastoiditis
Probable Scurvy
Anaemia

Skeletal ID: 24

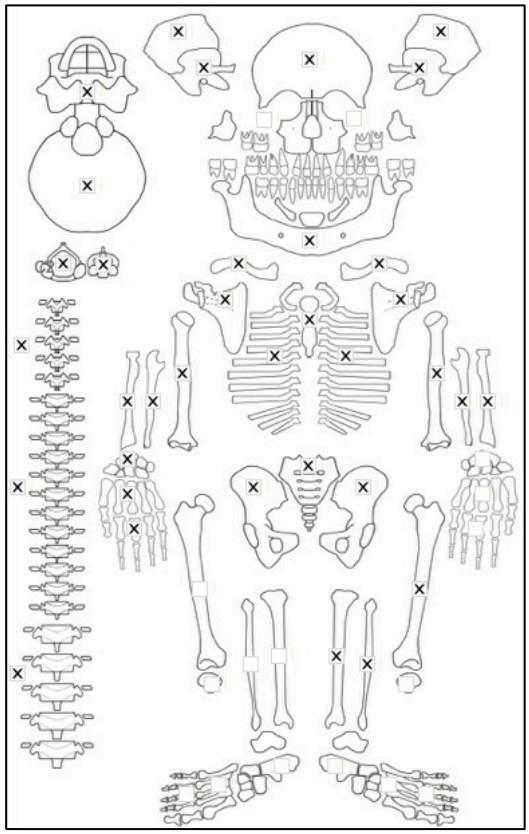

Completeness: Complete (min 75%). 67% long bones, 17% hands and feet, 100% vertebrae, 88% neurocranium. Ribs complete.
Preservation/ Taphonomy: All present long bones, vertebrae and ribs intact. Surfaces well preserved.
Age: 30-39, *Young Adult*
Sex: Male
Macroscopic Lesion Summary:
- button osteoma on right mastoid
- aplasia of the C2 dens
- remodelled bilateral moderate cribra orbitalia
- diffuse remodelled pin prick porosity across the temporal line and superior margin of the frontal, the superior and posterior parietals (medial to the temporal line) and the occipital planum. consistent with porotic hyperostosis
- bilateral localised remodelled new bone and cortical porosity superior to the external auditory canal and onto the suprameatal crest
- remodelled new bone and cortical porosity slightly diffuse but localised intermediate between the inferior nuchal line and the foramen magnum on the occipital squama
- bilateral symmetrical remodelled cortical porosity and new bone on the lateral greater wings of the sphenoid, pterygoid plate and the anterior region of the temporal squama.
- diffuse remodelled deposit of new bone across the visible endocranial surface as identified by the presence of abnormal vascular impressions
- diffuse remodelled deposit of new bone and cortical porosity across the palatal surfaces of the maxillae
- localised remodelled new bone and fine cortical porosity, with vascular impressions on the lateral and posterior left maxilla. Superior to the alveolar bone (right side missing)
- unilateral localised remodelled new bone and fine cortical porosity extending superiorly from the right mental foramen to the alveolar margin of the mandible
- bilateral remodelled new bone and cortical porosity in the incisive fossae, inferior to the oblique lines, inferior to the lateral mandibular notch (with vascular impressions), inferior mandibular body, medial coronoid processes, inferior to the mylohyoid line (with vascular impressions) of the mandible
- bilateral lateral bending at the deltoid tuberosities of the humeri (likely activity related)
- localised remodelled deposit of very thin bone on the lateral proximal left femoral shaft (right missing)

- localised remodelled deposit of new bone on the mid anterior crest of the left tibia with associated slight pseudo bowing. The periosteal activity is not marked suggesting that this involves possible endosteal activity. (right side missing- right leg may have been lost in shark attack (trauma recorded by A. Donnan, University of Oxford)
- remodelled diffuse new bone across the posterior middle third shaft of the left fibula including the region of the foramen (right side missing).
- unilaterally smaller left clavicle. The right clavicle sternal end may also be abnormally enlarged
- small oval lytic depression on the posterior aspect of the vertebral body bordering the inferior endplate of the T5. due to compression or remodelled fracture?
- bilateral small localised remodelled new bone and fine cortical porosity extending from the supraorbital notches with some vascular impressions
- alae of sacrum are striated- remodelled deep porosity
- compression fractures in C4 to C7 posterior vertebral bodies.

Radiographic Lesion Summary:
No radiographs taken
Differential Diagnosis Outcome:
Probable Scurvy
Anaemia

Skeletal ID: 65

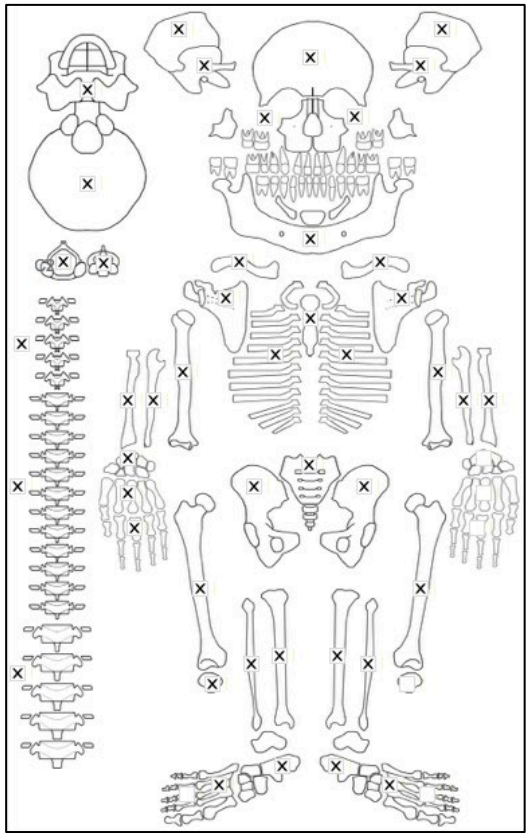

Completeness: Complete (min 75%). 98% long bones, 26% of hands and feet, 96% of vertebrae, 88% of neurocranium, ribs near complete.
Preservation/ Taphonomy: Surfaces well preserved. Vertebrae and long bones intact except for proximal third shaft of left humerus. Ribs have some postmortem breakage.
Age: 20-29, *Young Adult*
Sex: Male
Macroscopic Lesion Summary:
- remodelled new bone and cortical porosity diffuse across the inferior basial cranium including the basio-occipital, petrous bone of the temporal
- bilateral remodelled new bone and cortical porosity around the margins of the external auditory meatuses and extend to the suprameatal crests and superior mastoids

- bilateral symmetrical remodelled new bone and cortical porosity on the left lateral sphenoid and pterygoid plate as well as the anterior squama of the temporals.
- remodelling pin prick porosity and diploic expansion across the frontal, occipital and superior and posterior parietals consistent with porotic hyperostosis.
- remodelled new bone across the endocranial frontal, superior parietals and superior half of the endocranial occipital planum
- bilateral remodelled moderate cribra orbitalia
- bilateral symmetrical remodelled new bone and cortical porosity on the anterior zygomatic bones
- bilateral symmetrical remodelled cortical porosity on the posterior zygomatic bones
- bilateral symmetrical remodelled new bone and very fine cortical porosity on the anterior maxillae following the medial and inferior nasal border meets the alveolar bone
- remodelled new bone and very fine cortical porosity on the mental eminence and incisive fossae of the mandible
- bilateral symmetrical remodelled new bone and fine cortical porosity extending superiorly from the mental foramina to the alveolar margin, inferior to the oblique lines, the inferior mandibular body, the medial coronoid processes, lateral ramus inferior to mandibular notch (with vascular impressions), and inferior to the mylohyoid lines (with vascular impressions) on the mandible
- bilateral symmetrical remodelled new bone thin and localised with active cortical porosity on the lateral acromion spine near the scapular neck and extending into the supraspinous fossa
- deep manubrial porosity
- remodelled new bone and cortical porosity on the mid posterior shaft at the area of the foramen of the left clavicle (right missing).
- possible erosive arthropathy of the right proximal humerus
- bilateral symmetrical remodelled diffuse new bone across the posterior crest shaft of the fibulae
- bilateral symmetrical remodelled diffuse new bone across the proximal to middle anterior crest of the tibiae
- bilateral symmetrical remodelled deposit of new bone localised to the posterior medial midshaft region of the tibiae
- bilateral symmetrical remodelled deposit of new bone localised to the medial proximal third of the femora, anterior to the spiral line. Associated with cortical porosity
- deep vertebral and sacral porosity

Radiographic Lesion Summary:
No radiographs taken
Differential Diagnosis Outcome:
Probable Scurvy
Anaemia

Skeletal ID: 60

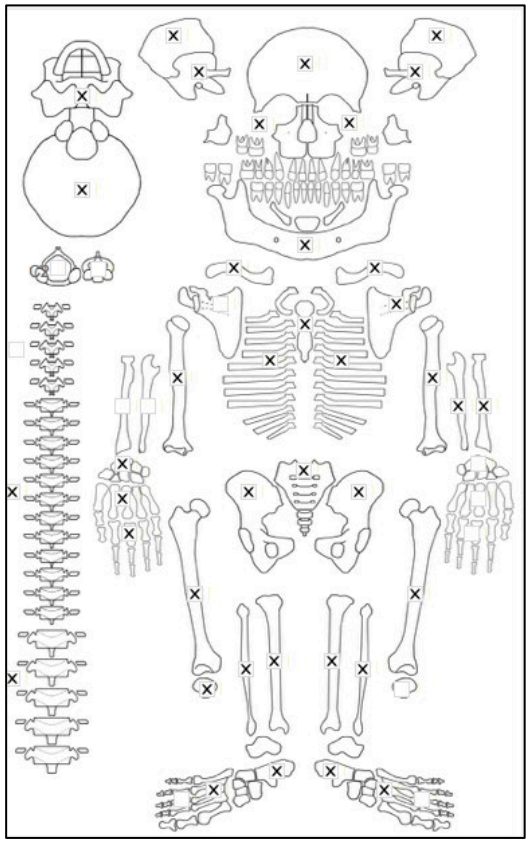

Completeness: Near Complete (66 to 75%). 70% of long bones, 44% of hands and feet, 46% of vertebrae, 88% of neurocranium. Ribs near complete.
Preservation/ Taphonomy: Some surfaces of cranium are black in colour and therefore could not be properly observed for pathology. Some intrusive metatarsals from younger individual, easily removed. Right scapula fragmented, left scapula body is missing. Some postmortem breakage of ribs.
Age: 20-29, *Young Adult*
Sex: Female
Macroscopic Lesion Summary:
- diffuse pin prick porosity in the process of remodelling across the frontal (particularly marked medial to the temporal line), superior and posterior parietals and the occipital planum with diploic expansion
- bilateral remodelling moderate cribra orbitalia
- bilateral symmetrical remodelled localised new bone and cortical porosity extending from the superior margin of the external auditory canal to the suprameatal crest.
- bilateral symmetrical remodelled fine cortical porosity and new bone on the lateral greater wings of sphenoid, pterygoid plates and anterior squama of the temporal where remodelled new bone has also pooled at the superior junction of the zygomatic process (where the new bone deposit is clear)
- remodelled diffuse new bone across the endocranial surface of the frontal, posterior superior parietals and superior occipital it is likely it continues further but the endocranium of the parietals is stained black.
- bilateral symmetrical localised remodelled new bone and cortical porosity on the anterior and posterior zygomatic bones
- localised remodelled new bone on the right maxillary sinus floor.
- remodelling localised cortical porosity on the inferior orbital surface of the right maxilla (superior maxilla orbital surface) as well as the inferior orbital margin (left side missing)
- bilateral symmetrical remodelled localised cortical porosity and remodelled new bone with vascular impressions on the anterior maxilla, intermediate from the infraorbital foramen to the nasal margin. This is inferred for the left as the same porosity is present but the infraorbital foramen is not preserved.
- bilateral symmetrical active new bone on the anterior middle third crest of the fibulae. Most of the new bone is still highly unorganised but minimal remodelling process has begun. There are also vascular impressions on the right fibula lesion.
- bilateral remodelled and symmetrical new bone on the middle to distal posterior third of the fibulae incorporating the region of the foramen.

- bilateral symmetrical mixed remodelling new bone and cortical porosity on the lateral and posterior maxilla inferior to the zygomatic process and superior to the alveolar margin
- bilateral symmetrical localised new bone and cortical porosity on the medial coronoid processes, and inferior body of the mandible.
- localised active new bone on the medial and lateral proximal third shaft sites of the right MT2, medial is more marked, medial and superior proximal third shaft of the right MT3, and remodelled new bone on the mid lateral shaft of the MT5 (left side missing).
- diffuse remodelled cortical porosity across the superior acromion and extending to midshaft of the clavicles (possible normal variant)
- active remnants of diffuse new bone on the proximal to mid anterior shaft encompassing region of the foramen. Inferior to the radial tuberosity
- active remnants of diffuse new bone on the proximal to mid lateral shaft facing the radius
- bilateral symmetrical mixed active and remodelled new bone across the anterior to lateral posterior to middle third shaft of the femora. More active proximally where the extent onto the anterior surface is more marked. The new bone is associated with cortical porosity.
- bilateral symmetrical remodelled new bone across the anterior crests of the tibiae
- bilateral symmetrical remodelled new bone localised to the posterior middle shafts of the tibiae
- mixed active and remodelled new bone on the distal medial aspect and distal end of the tibial shaft. Symmetrical and bilateral.
- mixed active and remodelled new bone diffuse across the dorsal and lateral surfaces of the calcanei. Bilateral but the right side lateral aspect is damaged and only superior aspect can be observed
- mixed active and remodelled new bone across the dorsal surface of the cuboid
- bilateral symmetrical mixed active and remodelled new bone diffuse across the external iliac blade
- bilateral mixed active and remodelled new bone diffuse across the internal and external margins of the ribs. Some of the ribs are more active while others more remodelled. The fragmented nature of the ribs makes it not possible to determine a pattern of activity. New bone is faint and has mostly been lost postmortem
- Thick remodelled new bone on the anterior right patella (left side missing).
- deep porosity of the sacral alae and of the posterior manubrium

Radiographic Lesion Summary:

No radiographs taken

Differential Diagnosis Outcome:

Probable Scurvy

Anaemia

Skeletal ID: 61

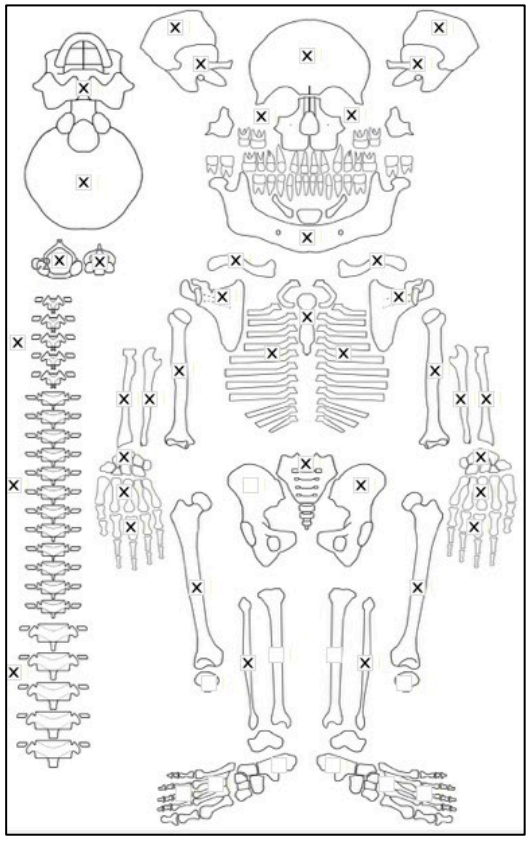

Completeness: Complete (min 75%).
Preservation/ Taphonomy:
Age: 40-49, *Middle Aged*
Sex: Male
Macroscopic Lesion Summary:
- bilateral mild remodelling cribra orbitalia
- remodelled pin prick porosity diffuse across the frontal, superior and posterior parietals and occipital planum consistent with remodelled porotic hyperostosis.
- bilateral symmetrical remodelled cortical porosity and new bone extending from the superior margin of the external auditory meatus onto he suprameatal crest and the superior mastoid
- remodelled lytic oval destruction of the mastoid right. Through a broken fragment it is possible to determine that the air cells have been destroyed. extent of lesion then cannot be measured. There is a fistula draining posterior and superior to the mastoid. There is a similar lytic remodelled oval lesion of the left mastoid.
- bilateral remodelled new bone and cortical porosity on the inferior petrous bones anterior to the carotid canal and on the inferior pars basilaris region.
- remodelled new bone identified through the presence of abnormal vascular impressions on the posterior endocranium including the parietals and occipital
- remodelled new bone and cortical porosity on the anterior zygomatic bones.
- bilateral symmetrical remodelled localised thin deposit of new bone intermediate to the infraorbital foramen to the medial nasal margin, there is some fine cortical porosity and new bone involvement along the inferior nasal margin.
- bilateral symmetrical remodelled new bone with cortical porosity across the palatal surface of the maxillae.
- bilateral symmetrical remodelled localised thin new bone on the lateral coronoid processes, and medial coronoid processes of the mandible.
- bilateral symmetrical remodelled localised thin new bone and very fine cortical porosity on the supraspinous fossae of the scapula around the region of the foramen, the new bone is clearer toward the lateral margin of the acromion.
- remodelled localised small deposit of new bone on the infraspinous fossa region of the left scapula (right missing). More superiorly near the spine. Much of the scapula body is damaged.
- deep vertebral porosity

- remodelled thick new bone deposit of the posterior shaft of the right fibula accompanied by a semilunar remodelled erosive lesion (max diameter 20mm) on the posterior proximal third shaft. Endosteal action and medullary canal closing can be identified through the broken shaft. Medullary closure is 3/4 complete at the midshaft. Prolific enough to incorporate the medial and lateral aspects. There is a thin diffuse new bone lesion on the middle to distal posterior shaft of the left fibula.
- bilateral symmetrical remodelled new bone localised anterior to the spiral line on the medial proximal femora, with cortical porosity
- remodelled striae on the internal ribs and porosity on the external ribs (likely normal variant)
- bone is striated on the sacral alae- possible remodelled deep porosity.

Radiographic Lesion Summary:
- the endosteal expansion in the right fibula is exceptionally thick, there is no evidence of sequestra.

Differential Diagnosis Outcome:
Probable Scurvy
Anaemia
Probable Otitis Media/ Mastoiditis

Skeletal ID: 70

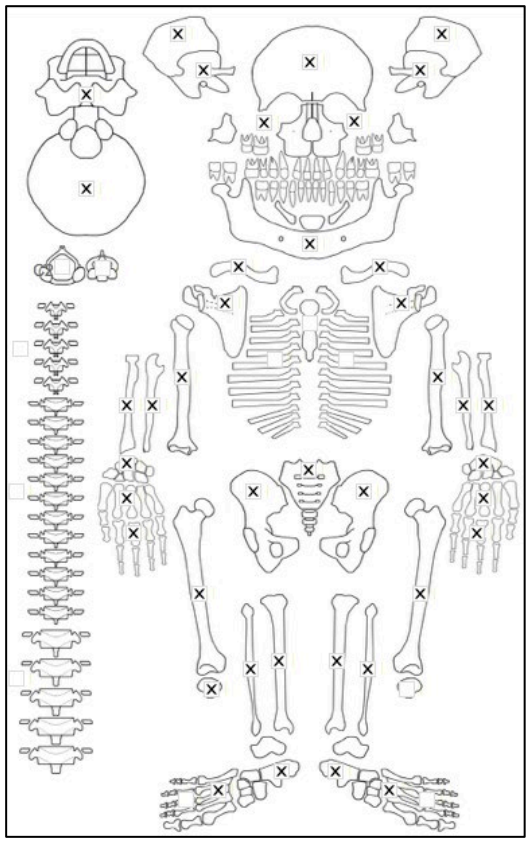

Completeness: Partially Complete (50 to 66%). 98% long bones, 56% hands and feet, 0% vertebrae, 88% neurocranium. Ribs absent.
Preservation/ Taphonomy: Bleaching of the cranium and mandible. Proximal third shafts of both tibiae damaged with epiphyses present. The proximal shafts are incomplete but still present. Distal end of left femur missing.
Age: 20-29, *Young Adult*
Sex: Female
Macroscopic Lesion Summary:
- bilateral mild remodelled cribra orbitalia
- bilateral symmetrical remodelled cortical porosity across the lateral greater wing and pterygoid plates of the sphenoid and anterior squama of temporals. Temporal bone surface on left side damaged and cannot be
- diffuse new bone and cortical porosity on the basiocranium including the pars basilaris and laterali regions, petrous bones of the of the temporals.

- remodelled diffuse new bone with clear abnormal vascular channels on the frontal, occipital, left parietal, left temporal and superior endocranium of the right parietal. The lesion is then predominantly to the left side of the cranium. it remains bilateral but not symmetrical.
- remodelled new bone and cortical porosity with vascular impressions on the anterior and posterior right zygoma (left missing)
- bilateral remodelled new bone with vascular impressions along the medial margin of the nasal.
- bilateral symmetrical remodelled new bone with vascular impressions on the anterior maxilla around the region of the infraorbital foramen and onto the medial nasal margin of the right side, there is a vascular impression along the infraorbital foramen which extends onto the orbital floor. Left side is missing infraorbital foramen and superior maxilla.
- circular depression of the posterior right maxilla.
- bilateral symmetrical remodelled new bone and cortical porosity on the medial coronoid processes extending towards the alveolar margin, inferior to the mylohyoid lines (with vascular impressions), mental eminence and incisive fossae, and inferior body of the mandible.
- thin localised remodelled new bone and cortical porosity on the supraspinous fossae of the scapula.
- fine cortical porosity across the superior acromion of the clavicle (may be normal variant at muscle attachment site)
- enlarged foramen of an unsided 5th proximal phalanx
- unilateral localised remodelling new bone on the posterior distal third of the right humeral shaft
- bilateral diffuse remodelled new bone on the lateral, medial and posterior aspects of the femora from the proximal and middle third shafts.
- bilateral symmetrical remodelled localised new bone on the middle anterior aspect on the crest of the fibulae
- diffuse highly active new bone on the distal third of both fibulae. There is expansion of the distal ends of the fibulae.
- bilateral thick diffuse mixed active and remodelling new bone across the tibial shafts. More remodelled towards the middle medial aspect and active more distally. There appears endosteal expansion of the distal end

Radiographic Lesion Summary:

- endosteal expansion of the tibiae and fibulae are clear on the radiographs

Differential Diagnosis Outcome:

Probable Scurvy

Con Co Ngua (Pre-Neolithic Vietnam)

Skeletal ID: CCN13M36a

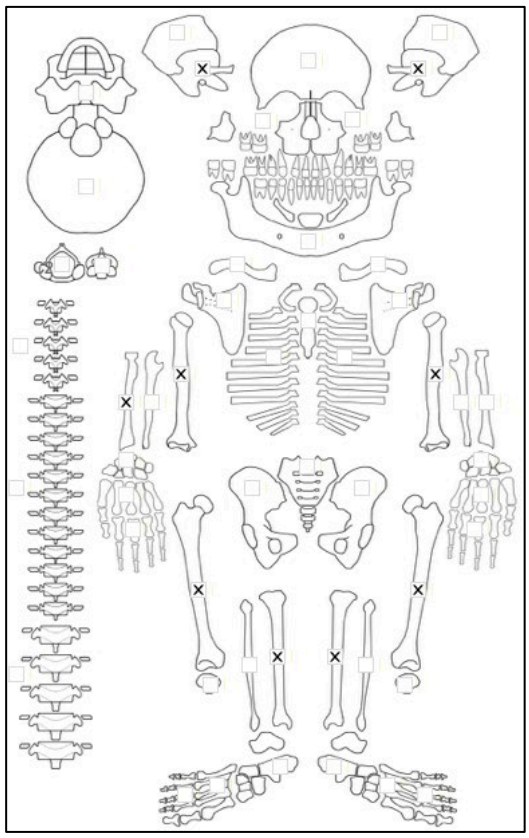

Completeness: Fragmented. 1 rib fragment, 2 possible fibula fragments, 1 lumbar vertebra, distal halves of humeri, shafts of femora, shafts of tibia. Left and right petrous with left have partial squama attached. Left orbit only of frontal.
Preservation/ Taphonomy: Moderate damage to surfaces
Age: ~37 weeks in utero, *Infant*
Sex: indeterminate
Macroscopic Lesion Summary:
- active layer of new bone on the left superior orbital roof and zygomatic process (right side missing)
- bilateral active new bone on the preserved temporal squama and the petrous processes
- bilateral diffuse active new bone across the preserved shafts of the humeri (proximal ends missing), lateral and posterior right ulna (left missing), anterior and lateral shafts of the femora, medial and posterior tibiae, and shafts of unsided fibular or ulna fragments.
- abnormal endochondral porosity exceeding 10mm from the metaphyseal plate of the proximal right tibia (left missing)

Radiographic Lesion Summary:
No radiographs taken
Differential Diagnosis Outcome:
Possible Scurvy

Skeletal ID: CCN13M60a

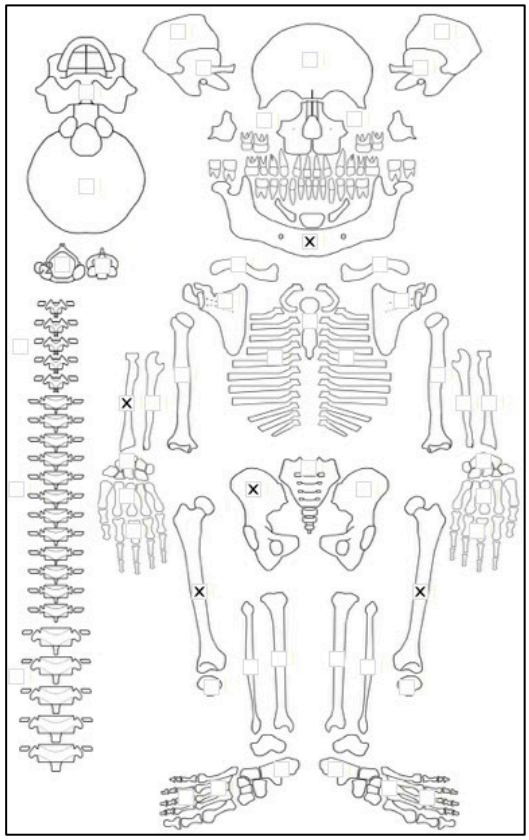

Completeness: Fragmented. Some commingled long bone pieces (extra femur and ulna fragment). Right petrous, two orbits, Partial mandible. Two rib fragments. Right ilium and radius. Both femora.
Preservation/ Taphonomy: Moderate surface damage.
Age: 0 years, *Infant*
Sex: Indeterminate
Macroscopic Lesion Summary:
- bilateral diffuse layer of new bone across all surfaces of the preserved femoral shafts. The new bone is more marked around the linea aspera but this could be a result of preservation of the new bone.
Radiographic Lesion Summary:
No radiographs taken
Differential Diagnosis Outcome:
No diagnosis

Skeletal ID: CCN13M149a

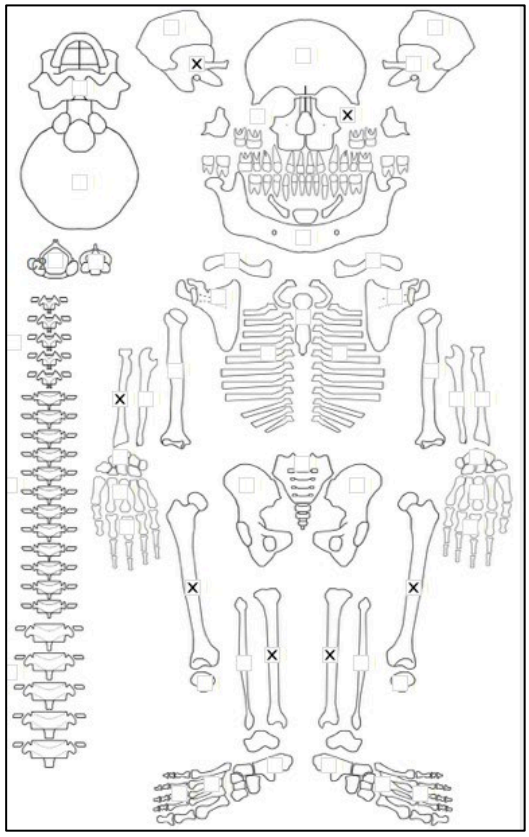

Completeness: Fragmented. Right petrous process, femora, tibiae, radii, pars basilaris, left pars lateralis, left orbit, ilia, 3 rib fragments.
Preservation/ Taphonomy: Moderate damage to surfaces. Long bone shafts only.
Age: ~37 weeks in utero, *Infant*
Sex: Indeterminate
Macroscopic Lesion Summary:
- active new bone and cortical porosity on the inferior pars basilaris and left pars lateralis (right missing)
- active new bone on the medial possible proximal third shaft of the right tibia (left side not observable)
- active new bone on two possible fibular fragments, one has new bone on the same aspect as a foramen.
- active new bone on the posterior left zygoma (right missing)

Radiographic Lesion Summary:
No radiographs taken
Differential Diagnosis Outcome:
Possible Scurvy

Skeletal ID: CCN13M143a

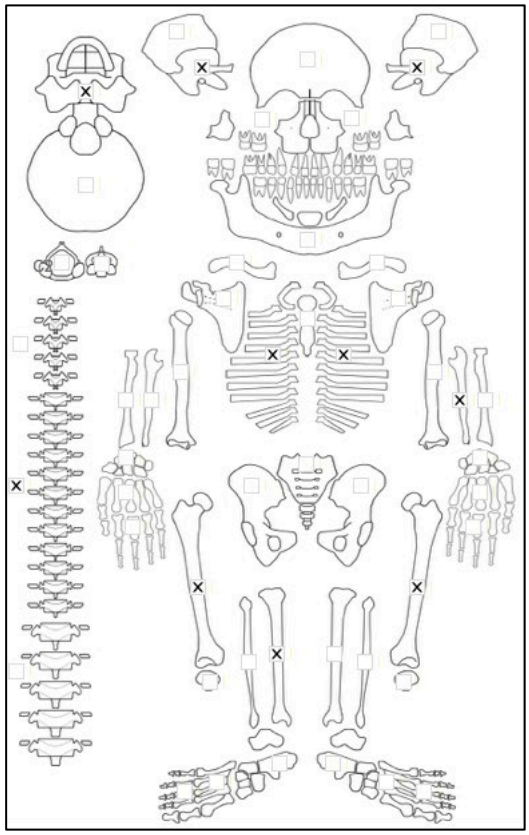

Completeness: Fragmented. 25% long bones, 0% hands and feet, 17% vertebrae, and 38% neurocranium. Ribs incomplete. Fragments of right orbit and mental prominence region of mandible present.
Preservation/ Taphonomy: Moderate damage to surfaces.
Age: 0 years, *Infant*
Sex: Indeterminate
Macroscopic Lesion Summary:
- active new bone on the right zygomatic process of the frontal (left side missing)
- active new bone on the external left greater wing of sphenoid (right missing)
- bilateral symmetrical active new bone on the anterior incisive fossae of the mandible

Radiographic Lesion Summary:
No radiographs taken
Differential Diagnosis Outcome:
Possible Scurvy

Skeletal ID: CCN13M151a

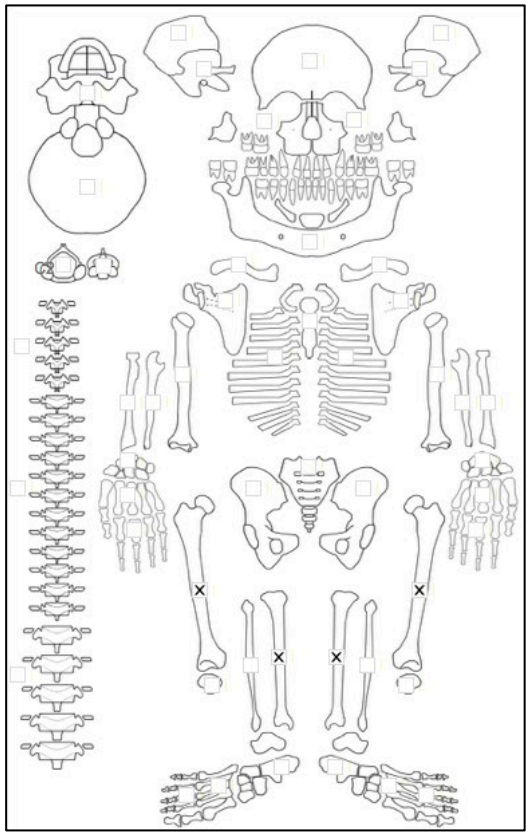

Completeness: Fragmented. Represented by femora and tibia only.
Preservation/ Taphonomy: Moderate damage to surfaces. Metaphyseal ends present but severely damaged.
Age: 0 years, *Infant*
Sex: Indeterminate
Macroscopic Lesion Summary:
- bilateral symmetrical diffuse new bone across the medial shafts of the tibiae and the anterior shafts of the femora
Radiographic Lesion Summary:
No radiographs taken
Differential Diagnosis Outcome:
No Diagnosis

Skeletal ID: CCN13M137a

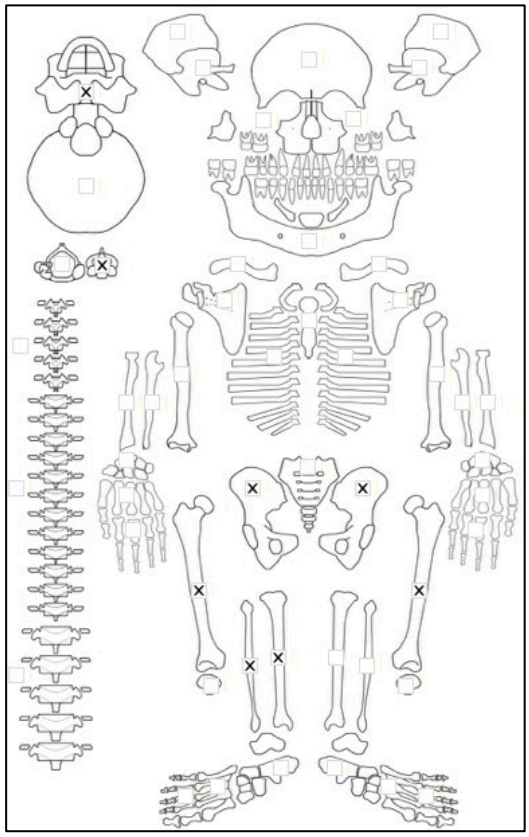

Completeness: Fragmented. 31% of long bones, 0% of hands and feet, 8.3% of vertebrae, and 12.5% of neurocranium. Ribs fragmented.
Preservation/ Taphonomy: Moderate damage to surfaces. Shafts of long bones preserved only.
Age: 0 years, *Infant*
Sex: Indeterminate
Macroscopic Lesion Summary:
- active new bone on the external and endocranial left greater and lesser wing of sphenoid (right missing)
Radiographic Lesion Summary:
No radiographs taken
Differential Diagnosis Outcome:
Possible Scurvy

Skeletal ID: CCN13M156a

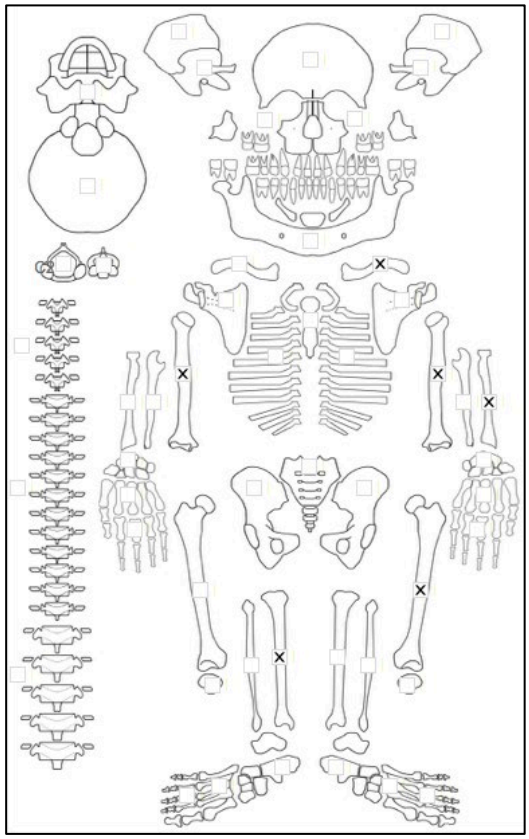

Completeness: Fragmented. Left orbit of frontal, distal halves of humeri, shaft of left femur, middle third shaft of right tibia, middle shaft of left radius and left clavicle shaft only.
Preservation/ Taphonomy: Charring on the tibia.
Age: ~32 weeks in utero, *Infant*
Sex: Indeterminate
Macroscopic Lesion Summary:
- active layered new bone on the left superior orbital roof and on the left zygomatic process of the frontal (right side missing)
- active diffuse new bone on the posterior preserved middle third shaft of the right tibia. The medial aspect cannot be assessed due to charring. (left tibia missing)

Radiographic Lesion Summary:
No radiographs taken
Differential Diagnosis Outcome:
Possible Scurvy

Skeletal ID: CCN13M167a

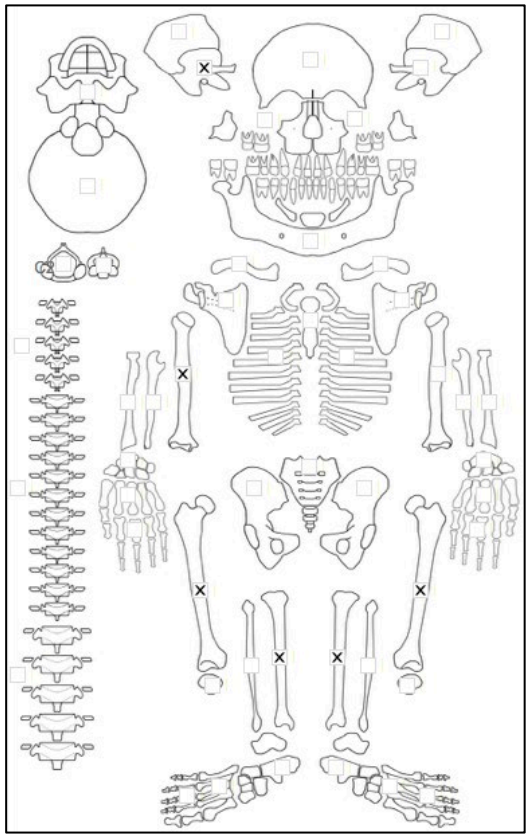

Completeness: Fragmented. 36% of long bones and 12% of neurocranium.
Preservation/ Taphonomy: Moderate surface damage. Distal ends of preserved long bones missing.
Age: ~37 weeks in utero, *Infant*
Sex: Indeterminate
Macroscopic Lesion Summary:
- active layered new bone on the right superior orbital roof and new bone on the right zygomatic process of the frontal (left side missing)
- active new bone on a small preserved fragment of the external right temporal squama (left missing)
- diffuse new bone on the endocranium of an unidentified cranial fragment
- bilateral symmetrical active diffuse new bone on the medial aspect of the preserved proximal half shafts of the tibiae

Radiographic Lesion Summary:
No radiographs taken
Differential Diagnosis Outcome:
Possible Scurvy

Skeletal ID: CCN13M145a

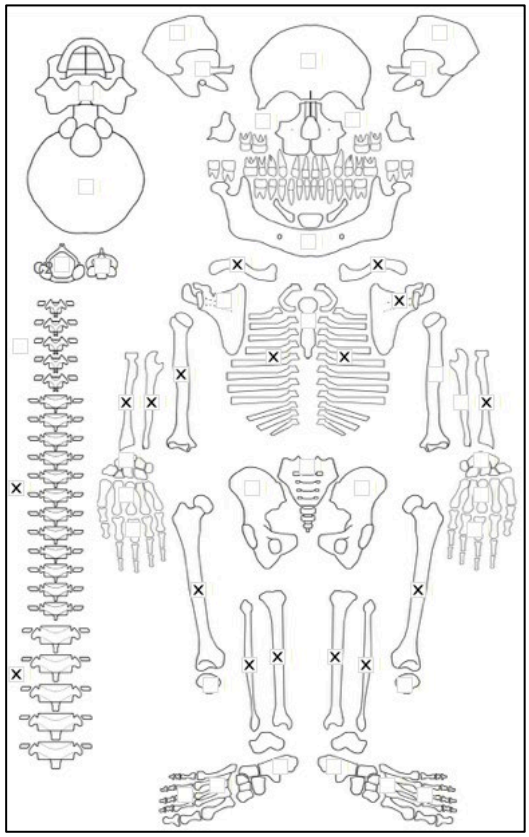

Completeness: Incomplete (33 to 50%). 75% of long bones, 0% of hands and feet, 21% of vertebrae and 0% of neurocranium. Ribs incomplete.
Preservation/ Taphonomy: Moderate surface damage. Many postmortem breakages of long bones. Most long bones have preserved metaphyses.
Age: 8.5 years (+/- 9 months), *Child*
Sex: Indeterminate
Macroscopic Lesion Summary:
- abnormal deep endochondral porosity exceeding 10mm from the metaphyseal plate of the proximal humeri, left distal femur (right missing), proximal tibiae and right distal fibula (left missing).
Radiographic Lesion Summary:
No radiographs taken
Differential Diagnosis Outcome:
Possible Scurvy

Skeletal ID: CCN13M110a

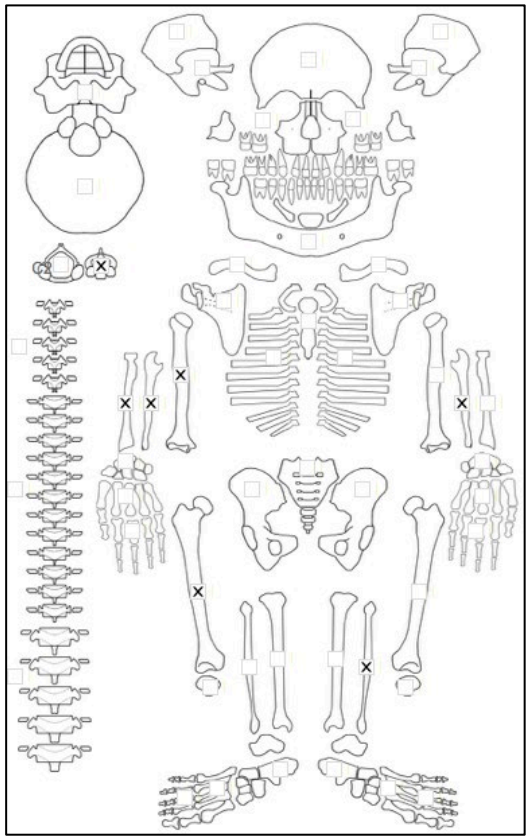

Completeness: Fragmented. 47% of long bones, 8% of vertebrae, 0% of hands and feet, and 0% of neurocranium. Fragmented ribs.
Preservation/ Taphonomy: Moderate surface damage. All long bones that are present are represented by their entire shafts except right radius which is missing the proximal third but the metaphyses are missing. Vertebrae severely fragmented.
Age: 10.5 years (+/- 9 months), *Child*
Sex: Indeterminate
Macroscopic Lesion Summary:
No lesions observed.
Radiographic Lesion Summary:
No radiographs taken
Differential Diagnosis Outcome:
No Diagnosis

Skeletal ID: CCN13M146a

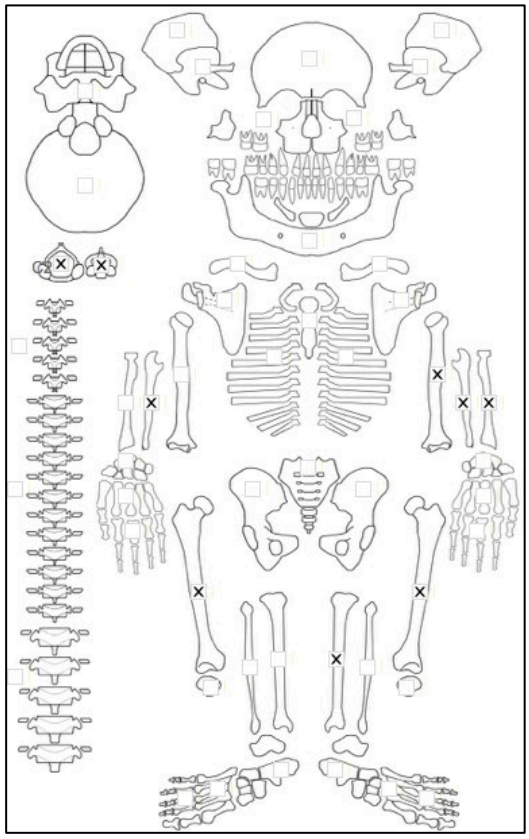

Completeness: Fragmented. 44% of long bones, 0% of hands and feet, 13% of vertebrae, 0% of neurocranium.
Preservation/ Taphonomy: Moderate surface damage. Left orbit and pars basilaris of cranium only. Fragmented long bones, shafts only except for distal left metaphysis of humerus present.
Age: 7.5 months (+/- 1.5 months), *Infant*
Sex: Indeterminate
Macroscopic Lesion Summary:
- active new bone on the endocranium and ectocranium with cortical porosity on the ectocranium of the pars basilaris.
- diffuse active new one on the distal half of the anterior left humerus (right missing)
- bilateral symmetrical active diffuse new bone on the anterior and medial proximal ulnae directly inferior and medial to the ulnar notch including the region of the foramen on the anterior aspect.
- bilateral symmetrical diffuse new bone across entire of the preserved shaft (distal half) of the femora
- localised new bone on the anterior and lateral proximal third shaft of left radius encompassing the area of the foramen (right side missing)
Radiographic Lesion Summary:
No radiographs taken
Differential Diagnosis Outcome:
Possible Scurvy

Skeletal ID: CCN13M109a

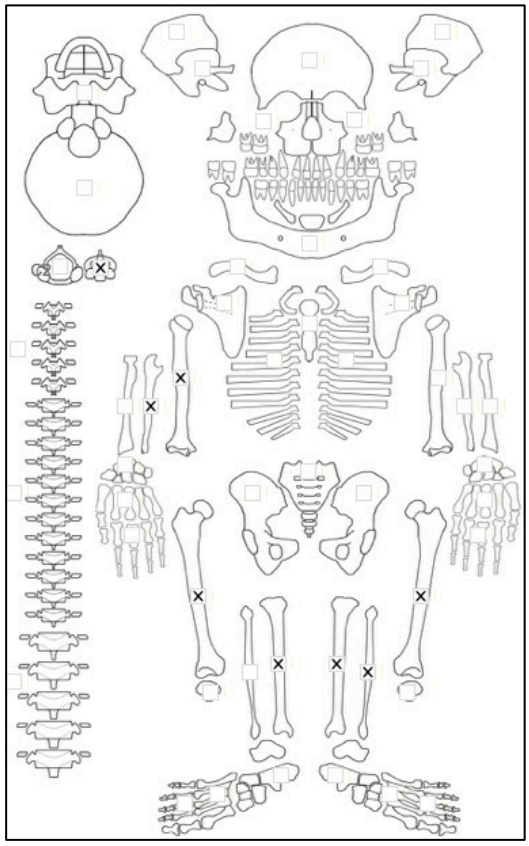

Completeness: Fragmented. 44% of long bones, 0% of hands and feet, 13% of vertebrae, and 0% of neurocranium.
Preservation/ Taphonomy: Moderate surface damage. Long bones and ribs significant postmortem breakage,
Age: 6 months (+/- 6 months), *Infant*
Sex: Indeterminate
Macroscopic Lesion Summary:
- bilateral symmetrical active woven new bone on the medial and posterior margins of the tibial shafts. More marked on the posterior aspect.
- diffuse woven bone on the anterior and lateral aspects of the preserved proximal third right ulna including the region of the radial and ulnar fossae. (left missing)
- abnormal deep endochondral porosity exceeding 10mm from the metaphyseal plate of the distal metaphysis of the right femur (left missing)
Radiographic Lesion Summary:
No radiographs taken
Differential Diagnosis Outcome:
No Diagnosis

Skeletal ID: CCN13M111a

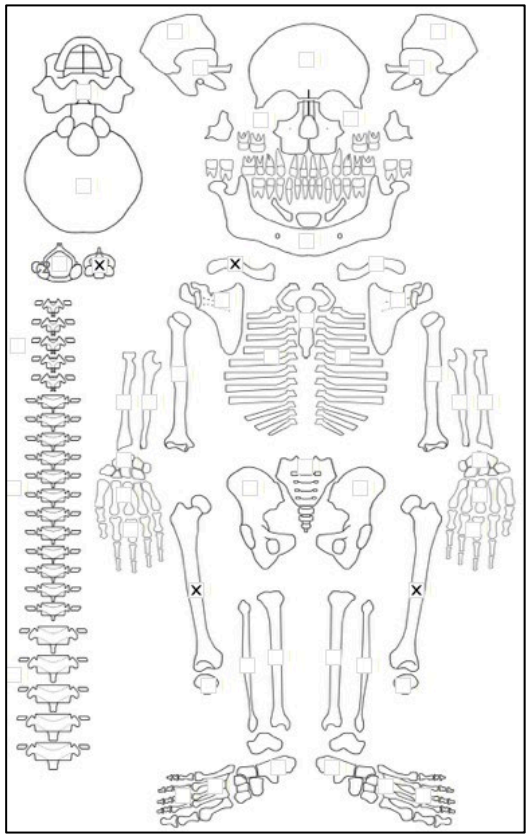

Completeness: Fragmented. 17% long bones, 2% hands and feet, 13% vertebrae, and 0% neurocranium. Ribs fragmented.
Preservation/ Taphonomy: Moderate surface damage. Many postmortem breakages to long bones.
Age: 1.75 years (+/- 6 months), *Child*
Sex: Indeterminate
Macroscopic Lesion Summary:
- deep lytic defect on the inferior side of the acromial end = just marginal to the acromial joint. Lesion Diameter: 6.7x6.4mm
Radiographic Lesion Summary:
No radiographs taken
Differential Diagnosis Outcome:
No Diagnosis

Skeletal ID: CCN13M18a

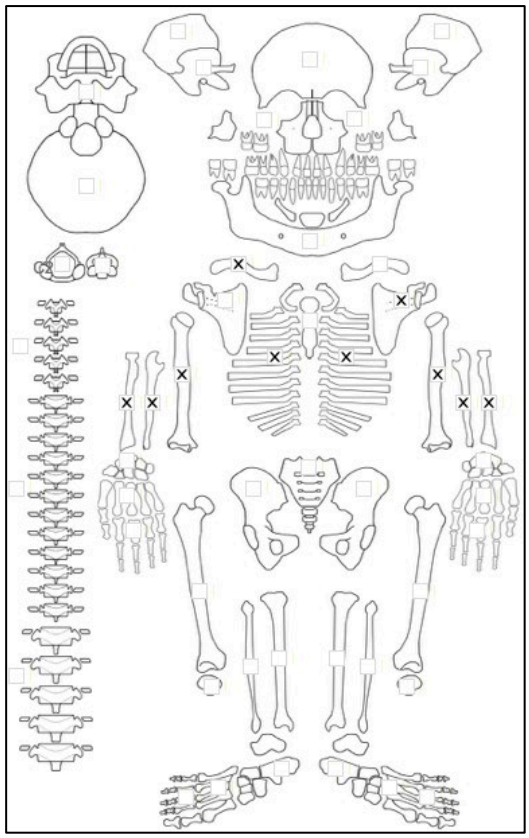

Completeness: Fragmented. 42% long bones, 6% hands and feet, 135 vertebrae, 0% neurocranium. Ribs incomplete.
Preservation/ Taphonomy: Moderate surface damage. Severe postmortem breakage of ribs and long bones.
Age: 8 years (+/- 9 months), *Child*
Sex: Indeterminate
Macroscopic Lesion Summary:
- porotic hyperostosis of the anterior distal metaphysis of the right humerus (left side missing). Some of the margins appear to be healing.
Radiographic Lesion Summary:
No radiographs taken
Differential Diagnosis Outcome:
No Diagnosis

Skeletal ID: CCN13M75a

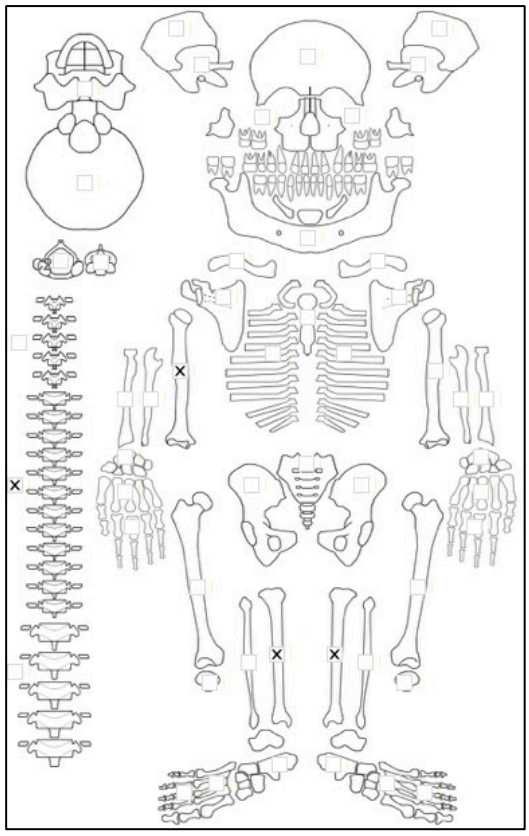

Completeness: Fragmented. 19% long bones, 0% hands and feet, 17% vertebrae survival, and 0% neurocranium. Ribs fragmented.
Preservation/ Taphonomy: Moderate surface damage. Shafts of long bones only.
Age: 3.5 years (+/- 9 months), *Child*
Sex: Indeterminate
Macroscopic Lesion Summary:
No lesions observed
Radiographic Lesion Summary:
No radiographs taken
Differential Diagnosis Outcome:
No Diagnosis

Man Bac (Neolithic Vietnam)

Skeletal ID: MB05M1

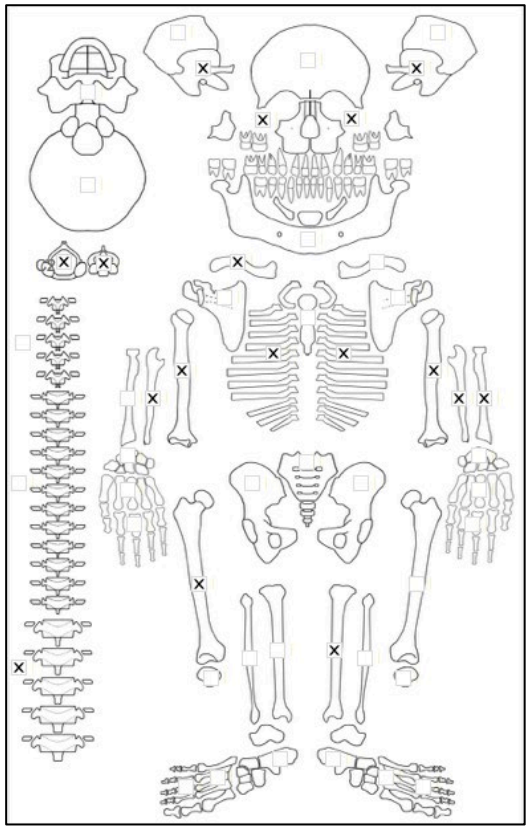

Completeness: Incomplete (33 to 50%). 39% long bones, 0% hands and feet, 25% vertebrae, 25% neurocranium. Ribs incomplete.
Preservation/ Taphonomy: Surfaces well preserved**.** Skull heavily fragmented and cranium unidentifiable with the exception of the pars basilaris, temporals and right zygomatic process of the frontal (orbit). No complete long bones. Proximal half of right ulna and humerus, distal two third of left humerus, proximal and distal thirds of left radius, middle third of left tibia and middle third of right femur. Intrusive humerus of younger age.
Age: 1.5 years (+/- 6 months), *Child*
Sex: Indeterminate
Macroscopic Lesion Summary:
- abnormal endochondral porosity exceeding 10mm from the proximal metaphyseal plate of the right humerus (left side missing)
- discrete mixed active and remodelled new bone and cortical porosity on the right zygomatic process of the frontal.
- discrete mixed active and remodelled new bone and cortical porosity on the inferior pars basilaris

Radiographic Lesion Summary:
No radiographs taken
Differential Diagnosis Outcome:
Possible Scurvy

Skeletal ID: MB05M2

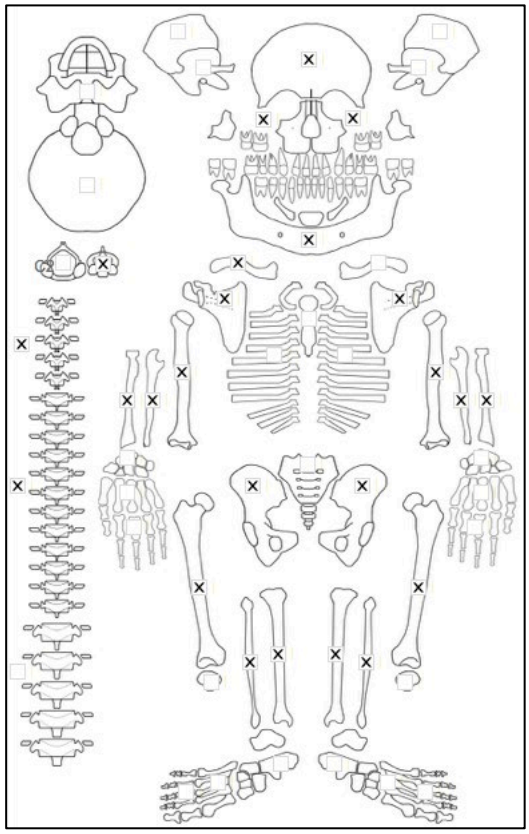

Completeness: Near Complete (66 to 75%). 100% long bones, 7% hands and feet, 46% vertebrae, 13% neurocranium, ribs fragmented.
Preservation/ Taphonomy: Surfaces well preserved. Long bones intact. Skull fragmented- frontal bone identifiable only.
Age: 0 years, *Infant*
Sex: Indeterminate
Macroscopic Lesion Summary:
- Discrete active new bone on the right superior orbital roof
- Discrete bilateral active new bone and cortical porosity on the anterior maxillae around the region of the infraorbital foramen.
- Symmetrical active new bone on the palatal surfaces of the maxillae
- Discrete symmetrical active new bone deposit with cortical porosity on the medial right coronoid process of the mandible, left missing
- Discrete unilateral active new bone deposit with cortical porosity on the left incisive fossa of the mandible
- Discrete active new bone deposit on the right mylohyoid line of the mandible. left side is missing
- Discrete active new bone deposit and cortical porosity on the posterior right zygomatic, left zygomatic is missing
- Bilateral symmetrical discrete active new bone deposit on the posterior distal humeri superior and extending into the olecranon fossa
- Bilateral symmetrical discrete active new bone deposit on the anterior proximal radii
- Bilateral symmetrical diffuse active new bone deposit across the medial shafts of the tibiae
- Abnormal endochondral porosity exceeding 10mm from metaphyseal plate on the proximal left tibial metaphysis, right side is broken.
- Discrete active new bone on the supraspinous fossa of the right scapula, left side obscured by concretions
- Symmetrical heavy appositional woven new bone on the external ilia
Radiographic Lesion Summary:
- distinct radiolucent end with thick radiodense lines in the metaphyses
Differential Diagnosis Outcome:
Probable Scurvy

Skeletal ID: MB05M3

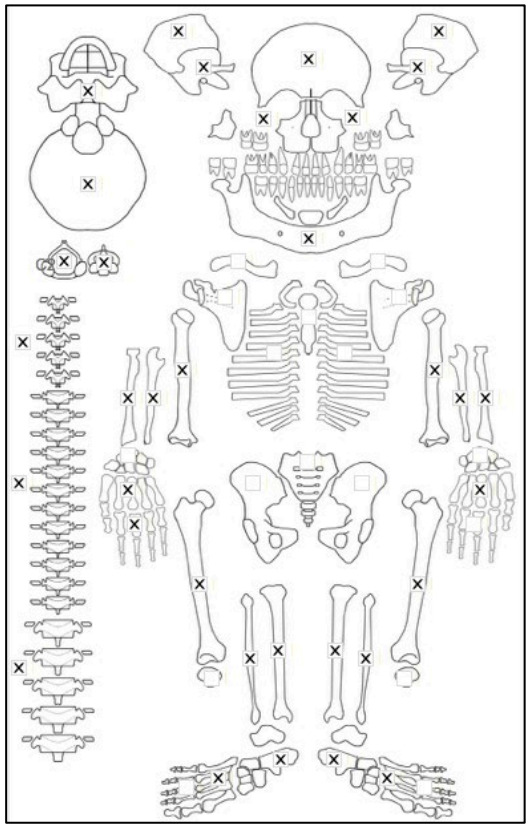

Completeness: Complete (>75%). 100% long bones, 32% hands and feet, 79% vertebrae, 88% neurocranium, ribs partially complete.
Preservation/ Taphonomy: Surfaces excellently preserved.
Age: 6 months (+/- 2 months), *Infant*
Sex: Indeterminate
Macroscopic Lesion Summary:
- layered spiculated new bone on the sutural margins of the cranial bones and extending onto the posterior parietals and occipital squama and across the temporal squama and inferior petrous portion. The temporal squama new bone is associated with porosity.
- bilateral symmetrical discrete deposit of new bone and cortical porosity on the zygomatic processes of the frontal
- bilateral symmetrical discrete deposit of layered new bone and cortical porosity on the superior orbits of the frontal
- bilateral symmetrical discrete deposit of layered new bone on the inferior pars lateralis and new bone and cortical porosity on the inferior pars basilaris
- bilateral symmetrical discrete deposit of layered new bone and cortical porosity on the external greater wings of the sphenoid
- bilateral symmetrical active new bone and cortical porosity on the supraspinous fossae of the scapulae
- bilateral symmetrical diffuse mixed active and remodelled new bone possibly with endosteal expansion (radiographs needed for confirmation) across the shafts and metaphyses of the humeri, radii, ulnae, tibiae, femora and fibulae.
- Both humeri have lateral bending deformities at the midshaft, left ulna appears to have a mild lateral bending deformity at the midshaft (right is broken and deformity cannot be observed)
- femoral necks appear to be slightly depressed with swelling of the distal metaphyses anterior posteriorly with mild cupping (cupping may be within normal range)
- there is an indented defect on the lateral distal metaphyseal plate (right distal metaphyses not preserved)
- circumferential expansion of the a preserved sternal end of a right rib. Post mortem damage means comments cannot be made on whether there is active fraying or not.
- discrete deposit of active new bone and cortical porosity on the medial right coronoid fossa (left side missing)

- bilateral bulging of the zygomatics, particularly anterior- posteriorly. There appears to be an extra bar of new bone at the frontal suture area on the posterior margin of the orbital surface
- medial bending deformity at the proximal third shaft of the rib (rib neck) associated with active new bone on the superior aspect of a right rib
- bilateral symmetrical active new bone and cortical porosity on the posterior zygomatic bones

Radiographic Lesion Summary:
- thick and clear white line (may be more than scorbutic- healing rickets?) , ground glass osteopenia, trummerfeld zone
- cortex thick at regions of bending deformities
- metaphyseal plates of the long bones are thick and comprise of a series of radiolucent, and radiodense lines
- marrow hyperplasia of the zygomatic bones
- rib within a rib sign

Differential Diagnosis Outcome:
Probable Scurvy
Probable Rickets
Probable Thalassaemia

Skeletal ID: MB05M4

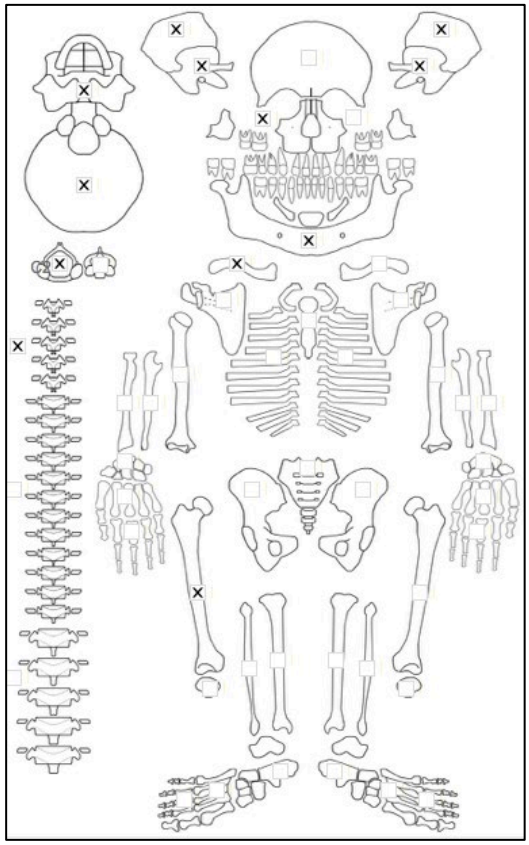

Completeness: Fragmented. 6% long bones, 8% vertebrae, 0% hands and feet, 63% neurocranium.
Preservation/ Taphonomy: Surfaces well preserved. Skull fragmented- occipital, sphenoid temporals, and parietals are identified. Few rib fragments.
Age: 2 years (+/- 6 months), *Child*
Sex: Indeterminate

Macroscopic Lesion Summary:
- discrete localised active cortical porosity on the inferior right pars lateralis lateral to the occipital condyle (left side missing)
- discrete localised mixed active and remodelled new bone on the left external greater wing of the sphenoid, and more inferiorly towards the pterygoid region. (right side missing)
- diffuse mixed active and remodelled new bone with vascular impressions (Lewis Grade 3) of the occipital and right temporal squama (left squama missing) endocranium.
- diffuse very thin mixed active and remodelled new bone across the ectocranial right temporal squama (left squama missing) following the contours of the temporalis muscle.

- discrete localised remodelling cortical porosity on the posterior right zygomatic (left side missing)
Radiographic Lesion Summary:
No radiographs taken
Differential Diagnosis Outcome:
Probable Scurvy

Skeletal ID: MB05M5

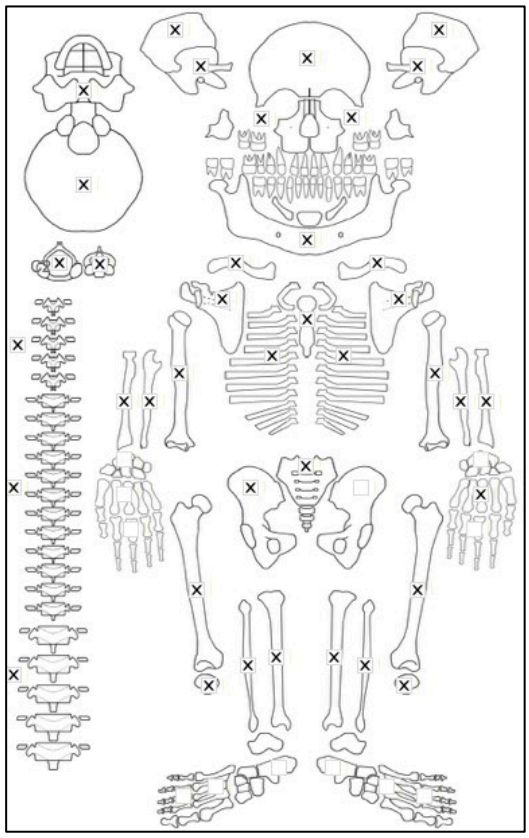

Completeness: Complete (>75%). 81% long bones, 9% hands and feet, 79% vertebrae, 88% neurocranium, ribs complete.
Preservation/ Taphonomy: Surfaces excellently preserved. Distal half of left radius and ulna missing.
Age: 1.5 years (+/- 3 months), *Child*
Sex: Indeterminate
Macroscopic Lesion Summary:
- large carious lesions of the maxillary incisors
- bilateral mild cribra orbitalia
- unilateral discrete deposit of active new bone and cortical porosity superior to the mastoid of the right temporal
- abnormal vertebral porosity of two anterior thoracic bodies. Margins are sharp. Resulting in Kyphosis?
- bilateral symmetrical discrete mixed active and remodelled deposit of new bone and cortical porosity of the supraspinous and infraspinous fossae of the scapulae
- circular lytic defect on the superior metaphyseal area of the superior right clavicle. There is sclerotic reaction present but the outer margins are sharp and slightly scalloped lesion diameter= 3.02x3.02mm.
- bilateral symmetrical discreet mixed active and remodelled new bone deposit on the superior margin of the olecranon processes of the posterior humeri
- bilateral expanded foramina of the anterior proximal third ulnae
- discreet remodelled deposit of new bone on the lateral middle third shaft of the right femur (left femur missing)
- remodelled deposit of new bone on the anterior distal third of the femur, appears to be associated with a slight anterior bulge which may indicate endosteal involvement. Associated with some cortical porosity.
- bilateral mixed active and remodelled deposit of thick new bone with endosteal action on the tibiae. There are two bilaterally symmetrical nodes (localised endosteal expansions) on the posterolateral proximal and

distal thirds, the proximal bulges extend superiorly from the posterior foramina, with no active subperiosteal reaction at these sites. For both tibiae the postero-lateral midshaft remains the most active.
- active discrete new bone and cortical porosity extending from the condylar foramen on the left pars lateralis
- bilateral remodelled endosteal expansions of the proximal third humeri
- bilateral and symmetrical remodelled deposit of new bone with thick endosteal expansion of the distal thirds of the fibulae, the endosteal expansions are more pronounced laterally.
- active diffuse deposit of new bone around the shaft of the 1st left metatarsal, associated with an expanded foramen on the plantar aspect.
- active diffuse deposit of new bone on the palmar surface of an unidentified right metacarpal associated with an expanded foramen
- active diffuse deposit of new bone across all aspects of an unidentified right proximal hand phalanx
- bilateral remodelled endosteal expansions (nodes) of the proximal third humeri. Right side has a remodelled focal lytic oval lesion with rounded margins, which may be a possible gummatous lesion on the medial aspect of the distal metaphysis. lesion diameter= 3.9x 1.73mm. Radiographs show expansion throughout entire shafts
- discrete remodelled new bone and cortical porosity posterior and inferior to the radial notch of the right ulna (cannot observe left)

Radiographic Lesion Summary:
- white line of Fraenkel with Trummerfeld zone
- thick subperiosteal deposition along the shafts of the long bones
- sclerotic margins around the clavicle and humerus superficial lesions
- coarsened trabeculae

Differential Diagnosis Outcome:
Probable Scurvy
Possible Rickets
Possible Treponematosis

Skeletal ID: MB05M6

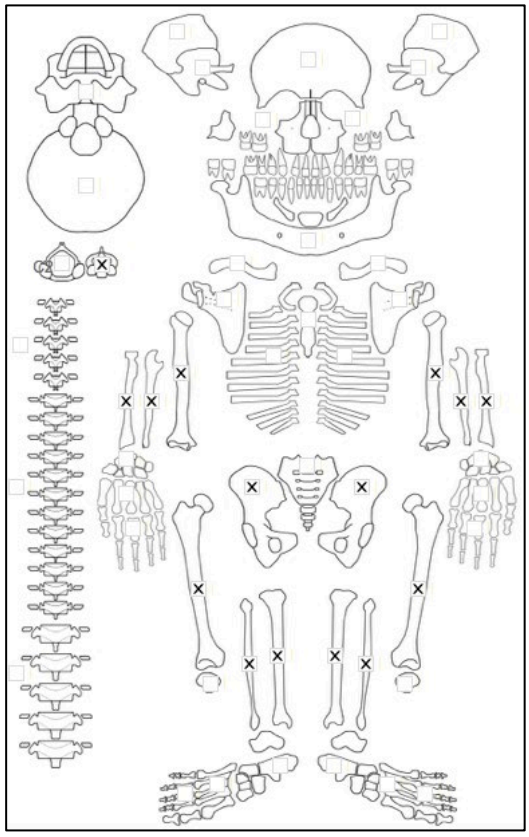

Completeness: Incomplete (33 to 50%). 69% long bones, 2% hands and feet, 4% vertebrae, 0% neurocranium. Ribs fragmented.
Preservation/ Taphonomy: Surfaces well preserved. All metaphyses missing except distal right femur and proximal tibiae, middle third left radius only. Three small cranial fragments.
Age: 1.5 years, *Child*
Sex: Indeterminate
Macroscopic Lesion Summary:
- mixed active and remodelled discrete deposit of new bone and cortical porosity on the inferior pars basilaris
- bilateral symmetrical diffuse mixed active and remodelled new bone across the medial shafts of the tibiae
Radiographic Lesion Summary:
- Pelkan spur of the distal femur
- ground glass osteopenia
Differential Diagnosis Outcome:
Possible Scurvy

Skeletal ID: MB05M7

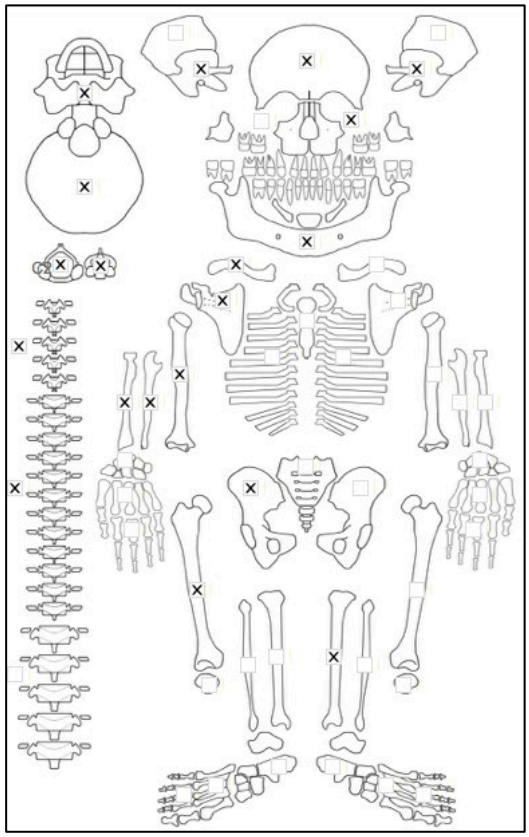

Completeness: Incomplete (33 to 50%). 36% long bones, 1% hands and feet, 50% vertebrae, 63% neurocranium. Ribs fragmented.
Preservation/ Taphonomy: Surfaces well preserved. Right side long bones only with exception of left tibia. Skull fragmented, parietal and frontal fragments unidentifiable with exception of orbital region. Sphenoid complete.
Age: 0 years, *infant*
Sex: Indeterminate
Macroscopic Lesion Summary:
- discrete deposit of active new bone and cortical porosity across the inferior pars basilaris
- bilateral discrete deposit of active new bone and cortical porosity across the inferior left pars laterali extending from the hypoglossal canal
- bilateral diffuse deposit of active new bone across the petrous processes of the temporal bones
- bilateral discrete deposits of new bone and cortical porosity in the pyramidal processes of the palatine bones
- bilateral symmetrical diffuse active new bone and cortical porosity across the external greater wings of sphenoid involving pterygoid region and orbital surface.
- bilateral symmetrical discrete active new bone and cortical porosity in the endocranial aspect of the greater wings of sphenoid, there is cortical porosity concentrated around the foramen rotundum.
- bilateral symmetrical discrete active new bone on the left lesser wings of the sphenoid
- discrete active new bone superior sphenoid body
- bilateral symmetrical discrete active new bone and cortical porosity on the zygomatic processes of the frontal bone
- bilateral symmetrical discrete layered active new bone on the superior orbits (the layered new bone may suggest normal appositional growth)
- active new bone across the posterior and superior, and new bone with cortical porosity on the anterior left zygomatic bone (right side not preserved)
- active diffuse new bone across the superior acromial end of the right clavicle (left clavicle not preserved)
- active new bone and cortical porosity on the medial right coronoid fossa (left side not preserved)
- active new bone and cortical porosity inferior to the right oblique line of the mandible
- bilateral symmetrical active new bone and cortical porosity on the incisive fossae of the mandible
- discrete active new bone on the supraspinous fossa of the right scapula (left scapula missing)

- active new bone on the distal posterior right humerus extending onto the superior olecranon fossa (may be normal appositional growth)
- diffuse active new bone across the medial shaft and extending anteriorly on the distal third shaft of the left tibia (right tibia not preserved).

Radiographic Lesion Summary:
- white line of Fraenkel and Trummerfeld zone
Differential Diagnosis Outcome:
Probable Scurvy

Skeletal ID: MB05M8

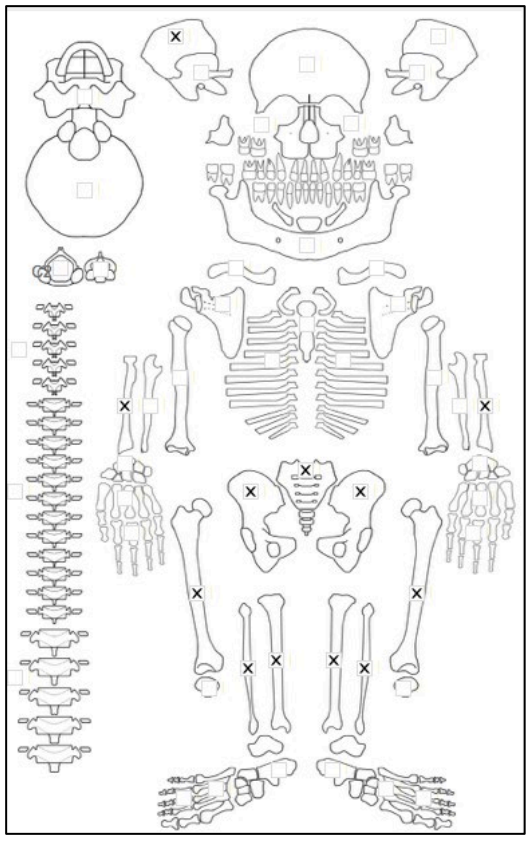

Completeness: Incomplete (33 to 50%). 59% long bones, 5% hands and feet, 8% vertebrae, 13% neurocranium. Ribs fragmented
Preservation/ Taphonomy: Surfaces well preserved. Cranial bones present but none are identifiable except right parietal. Proximal ends of femora missing. Ends of right radius and proximal end of left radius missing and proximal ends of fibulae missing.
Age: 6 months, *Infant*
Sex: Indeterminate
Macroscopic Lesion Summary:
- abnormal endochondral porosity exceeding 10mm from the metaphyseal plate on the proximal right humerus (left side missing), proximal and distal tibiae, and distal femora.
- bilateral diffuse woven bone across the entire shafts of the femora
- bilateral diffuse woven bone across the entire medial and distal third anterior aspects of the tibiae.
Radiographic Lesion Summary:
- Trummerfeld zone and white line of Fraenkel
Differential Diagnosis Outcome:
Probable Scurvy

Skeletal ID: MB05M9

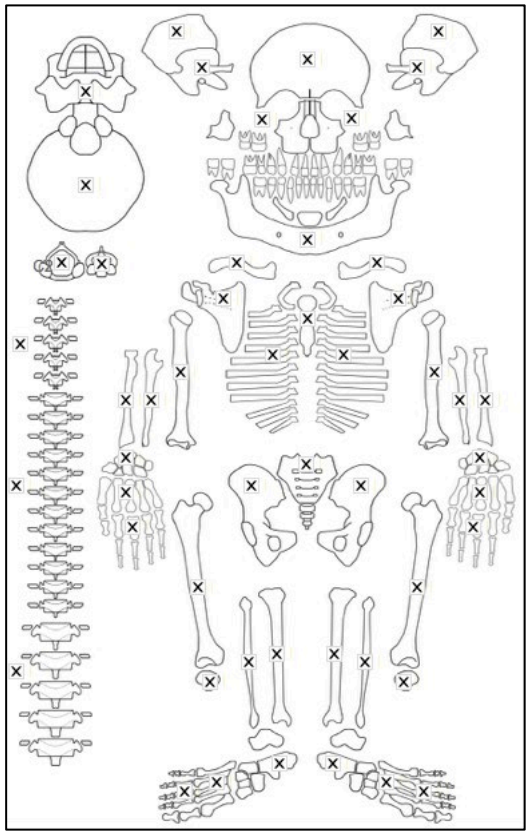

Completeness: Complete (>75%). 99% long bones, 85% hands and feet, 100% vertebrae, 100% neurocranium, ribs partially complete.
Preservation/ Taphonomy: Surfaces well preserved with some concretions.
Age: 40-49, *Middle Aged Adult*
Sex: Female
Macroscopic Lesion Summary:
- Asymmetric concentric shaft thinning directly inferior to the radial head of the right radius
- Symmetrical discreet bilateral remodelled new bone deposit with cortical porosity inferior to the radial notch and anterior to the supinator crest on the proximal lateral ulnae. Right side is more severe than the left.
- Asymmetric enlarged foramen on the lateral left third metatarsal
- Discrete localised remodelled new bone and cortical porosity around the foramen of the posterior right maxilla
- Symmetrical remodelled cortical porosity inferior to the mylohyoid lines of the mandible

Radiographic Lesion Summary:
No radiographs taken
Differential Diagnosis Outcome:
Possible Scurvy

Skeletal ID: MB05M10

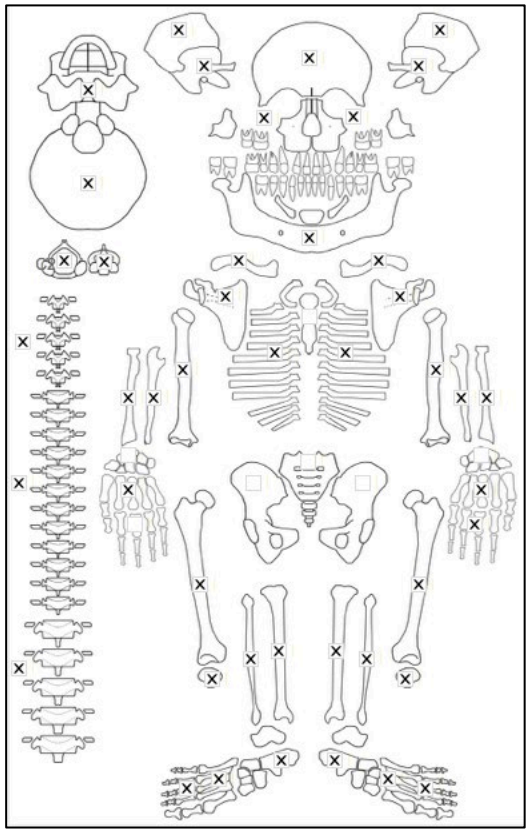

Completeness: Complete (>75%). 89% long bones, 43% hands and feet, 100% vertebrae, 88% neurocranium, ribs complete.
Preservation/ Taphonomy: Surfaces excellently preserved. Proximal thirds of right radius and ulna only, right femoral head missing.
Age: 9 (+/- 9 months), *Child*
Sex: Indeterminate
Macroscopic Lesion Summary:
- active mild cribra orbitalia of the left orbit (right missing)
- bilateral remodelled new bone deposit and cortical porosity on the temporal squama extending superior to the zygomatic arch and continuing across the superior margin of the external auditory canal. The left temporal lesion is more profuse than the right.
- bilateral remodelled new bone deposit and cortical porosity on the posterior zygomatic bones
- bilateral symmetrical remodelled new bone deposit and cortical porosity on the medial coronoid fossae of the mandible
- bilateral symmetrical remodelled new bone deposit inferior to the mylohyoid lines accompanied by vascular impressions
- bilateral symmetrical mixed active and remodelled new bone on the supraspinous and infraspinous fossae of the scapulae. The infraspinous lesions are diffuse across the posterior scapular body.
- Unilateral mixed active and remodelled new bone on the anterior left scapular body
- Abnormal deep endochondral porosity exceeding 10mm from the metaphyseal plates of the proximal humeri, distal femora, proximal and distal tibiae and proximal fibulae.
- Bilateral symmetrical well remodelled diffuse new bone on the distal third shafts and metaphyses of the humeri sparing only the posterior aspects.
- well remodelled thick diffuse new bone of the distal third ulna shaft (right side missing)
- Thick well remodelled new bone deposit with endosteal expansion of the proximal half of the left MC2, MC4 and possibly MC3 (very slight if any), endosteal expansions of the proximal and distal thirds of the MC5.
- Bilateral symmetrical well remodelled diffuse new bone on the distal third shafts and metaphyses of the humeri sparing only the proximal aspects.
- Bilateral symmetrical moderate porotic hyperostosis of the distal metaphysis of the humeri

- Bilateral symmetrical mixed active and remodelled diffuse new bone across the posterior and lateral shafts of the femora
- Bilateral symmetrical thick mixed active and remodelled diffuse new bone across all aspects of the tibial shafts. The lesions are more active across the medial and posterior aspects. There is endosteal inflammation resulting in alteration of the medial midshaft shape of both tibiae. Possible endosteal aspect of the distal tibiae as well, radiographs required for confirmation.
- Bilateral symmetrical thick mixed active and remodelled diffuse new bone across all aspects of the fibular shafts and distal metaphysis. The lesions are more active across the medial aspects. There is endosteal inflammation resulting in alteration of the lateral middle third and medial distal third shape of both tibiae resulting in a pseudobowing effect laterally.
- Abnormal vertebral porosity on the anterior T4-8 bodies, anterior and lateral T9-12 and lateral lumbar
- Diffuse bilateral active new bone across all non-articular surfaces of the calcanei, associated with endosteal expansion on the medial aspects. The periosteal lesion on the right calcaneus is associated with an oval lytic defect directly inferior to the 9.38x5.85mm. sustentaculum tali, margins are rounded with sclerotic reaction.
- Diffuse bilateral mixed active and remodelled new bone across the superior tali
- bilateral thick mixed active and remodelled new bone across all aspects of the 1st metatarsals and inferior 1st proximal phalanges. Infection has resulted in bilateral early fusion of the distal epiphyses 1st metatarsals and 1st proximal phalanges. Lateral aspect of left M1 includes an expanded foramen.
- bilateral diffuse active new bone across all aspects except medial of the 2nd metatarsals. Right 2nd metatarsal has endosteal expansion of the distal third.
- Bilateral diffuse active new bone across the 3rd metatarsals with endosteal expansion of the middle third shafts. The right MT3 has active bone across all aspects. The left MT3 is active on the medial and inferior aspects with a large foramen on the medial aspect.
- Bilateral diffuse mixed active and remodelled new bone across all aspects of the 4th metatarsals with endosteal expansion of the distal third shafts.
- Bilateral diffuse mixed active and remodelled new bone across all aspects of the 5th metatarsals with endosteal expansion of the distal third shaft of the right and the entire length of the superior shaft of the left.
- Large remodelled endosteal expansion of the proximal halves of the right 2nd and 5th proximal pedal phalanges (left side missing)
- Small focal circular lytic lesion with a defined margin on the mastoid. There are no signs of remodelling. The internal air cells appear enlarged.

Radiographic Lesion Summary:
- Pelkan spur on distal left femur
- Wimberger's ring sign of proximal tibia
- Trummerfeld zones and white line of Fraenkel of long bones

Differential Diagnosis Outcome:
Probable Scurvy
Possible Treponematosis

Skeletal ID: MB05M11

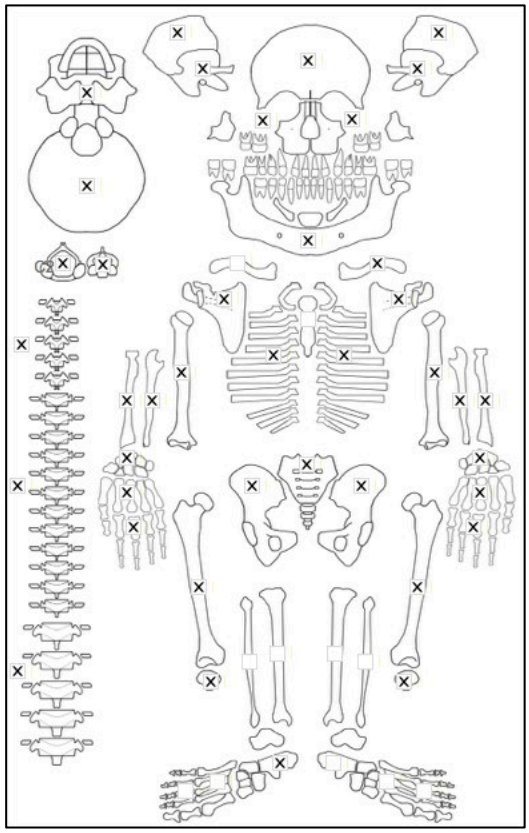

Completeness: Complete (>75%). 67% long bones, 47% hands and feet, 100% vertebrae, 88% neurocranium, ribs complete.
Preservation/ Taphonomy: Surfaces excellently preserved with exception of endocranium covered by concretion. Tibiae, fibulae and feet missing since excavation
Age: 20-29, *Young Adult*
Sex: Male
Macroscopic Lesion Summary:
- bilateral remodelled moderate cribra orbitalia
- severe remodelled porotic hyperostosis with hair on end pattern on the mid ectocranial occipital, across the superior frontal and parietals (medial to the temporal line) and the occipital planum.
- bilateral remodelled diffuse porosity consistent with mild porotic hyperostosis on the anterior zygomatic bones
- discrete remodelled new bone and cortical porosity on the mental eminence of the mandible
- discrete unilateral remodelled new bone lateral to the incisive fossae on the right oblique line of the mandible
- discrete bilateral symmetrical remodelled new bone identifiable through vascular impressions and cortical porosity on the anterior maxillae around the infraorbital foramina
- discrete bilateral symmetrical remodelled new bone associated with vascular impressions and cortical porosity on the posterior maxillae
- deep and large porosity on the proximal metaphyseal regions of the proximal humeri, possibly consistent with remodelled porotic hyperostosis. The porosity penetrates into the trabecular bone and coalesces at areas.
- bilateral deep and large porosity on non-articular surfaces of the carpals. May be a form of porotic hyperostosis.
- bilateral deep and large porosity on costal demi facet areas of the lateral aspects of the body of the T1, may be some form of porotic hyperostosis.
- deep and large porosity on non-articular surfaces of the right talus (left missing) May be a form of porotic hyperostosis.
- expanded foramen on the palmar proximal thirds of the right 4th proximal, 2nd to 5th right and left intermediate, and 3rd left and right distal hand phalanges.
- two bilateral haematomas on the proximal medial and lateral aspects of the femoral shafts. The haematomas on the left side are marked.

Radiographic Lesion Summary:
No radiographs taken
Differential Diagnosis Outcome:
Probable Scurvy
Anaemia

Skeletal ID: MB05M12

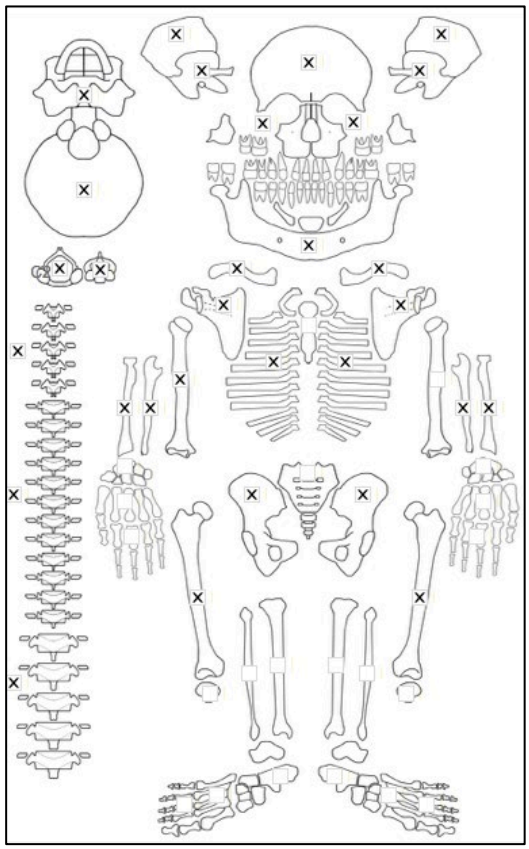

Completeness: Near Complete (66 to 75%). 56% long bones, 2% hands and feet, 96% vertebrae, 88% neurocranium, ribs complete.
Preservation/ Taphonomy: Surfaces well preserved except for endocranium covered by soil concretions. Distal half of left femur missing.
Age: 2 years (+/- 1 year), *Child*
Sex: Indeterminate
Macroscopic Lesion Summary:
- bilateral severe cribra orbitalia
- bilateral symmetrical active new bone and cortical porosity on the external left greater wing of sphenoid, pterygoid region and on the zygomatic processes of the frontal, with bilateral cortical porosity on the inferior margin of the ectocranial parietals. The right temporal demonstrated the sphenoid new bone and cortical porosity continues onto the temporal squama but the left side is missing.
- remodelled new bone with possible lytic process involving the diploic bone consistent with Lewis Grade 4 on the right parietal endocranium (the rest of the endocranium could not be observed). This is accompanied by diploic thickening of the parietal cranial vault.
- bilateral bulging zygomatic bones particularly anteriorly with rounding of the infraorbital margin, associated with mixed active and remodelled new bone on the anterior and superior surfaces.
- bilateral symmetrical active new bone with cortical porosity on the posterior zygomatic bones
- bilateral symmetrical active new bone with cortical porosity on the anterior, lateral and posterior maxillae
- maxillae are bulging anteriorly
- active new bone and cortical porosity on the palatal surface of the right maxilla (left palatal surface missing)
- bilateral symmetrical active new bone and cortical porosity on the medial coronoid processes of the mandible

- possible enlargement of the clavicles (radiographs needed to determine whether due to cortical or trabecular expansion)
- bilateral depression of the femoral heads compared to H2M12
- possible bilateral expansion of the ilia of the pelvis
- bilateral symmetrical discrete mixed active and remodelling new bone across the supraspinous fossae of the scapulae
- discrete active new bone and cortical porosity on the superior margin of the olecranon fossa of the right humerus (left missing)
- abnormal endochondral porosity exceeding 10mm from the distal metaphyseal plate of the right femur (left distal end missing), associated with cupping of the metaphyseal plate and flaring (possible erlenmeyer flask deformity of the distal third shaft and metaphysis radiographs required for confirmation). Distal end appears demineralised.
- expansion of the costal ends of 4 preserved right and 2 left rib ends circumferentially, possibly associated with fraying suggesting active.
- discrete deposit of active new bone and cortical porosity on the anterior frontal superior to the superciliary arches

Radiographic Lesion Summary:

- pelkan spur of the left distal femur
- possible white line of Fraenkel but definition is not clear
- Ground glass osteopenia with regions of coarsened trabeculae
- marrow hyperplasia of the facial bones with crowding of the maxillae, but the maxillary sinus has properly pneumatised
- There is marrow hyperplasia within the cranial bones which are presenting as a 'hair on end' appearance, but is not macroscopically visible.

Differential Diagnosis Outcome:

Anaemia
Probable Scurvy
Probable Rickets
Probable Thalassaemia

Skeletal ID: MB05M13

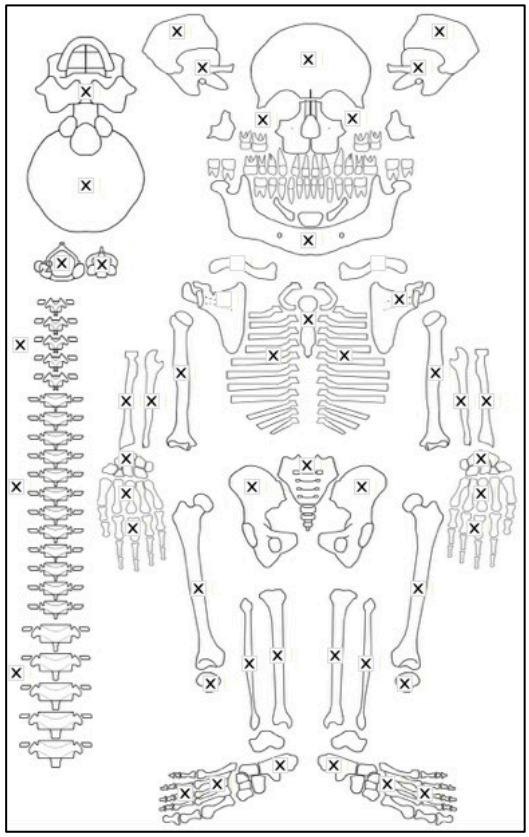

Completeness: Complete (>75%). 100% long bones, 88% hands and feet, 83% vertebrae, 100% neurocranium, ribs complete.
Preservation/ Taphonomy: Surfaces in excellent condition. PM breakage of some vertebrae.
Age: ~16 years, *Adolescent*
Sex: Indeterminate
Macroscopic Lesion Summary:
- bilateral remodelled discrete new bone identified through the presence of vascular impressions on the anterior maxillae
- the left maxilla has an abnormal indentation on the anterior aspect
- bilateral mixed active and remodelled discrete new bone and cortical porosity on the posterior maxillae and zygomatic bones
- bilateral mixed active and remodelled discrete new bone on the medial coronoid processes of the mandible
- remodelled discrete new bone identified through the presence of vascular impressions inferior to the mylohyoid lines (left side unobservable) of the mandible
- remodelled cortical porosity on the left supraspinous fossa (right side could not be observed)
- bilateral symmetrical remodelled diffuse new bone on the posterior distal half shafts of the ulnae
- bilateral symmetrical mixed active and remodelled new bone and cortical porosity on the medial proximal third and olecranon process of the ulnae
- bilateral symmetrical mixed active and remodelled new bone on the anterior distal third of the humeri superior to the lateral epicondyles
- bilateral symmetrical mixed active and remodelled new bone on all aspects of the distal end of the radii including metaphyses and distal shaft
- bilateral new bone on the medial, anterior and lateral aspects of the shafts of the tibiae. The right side is well remodelled with enlarged striations, the left tibia remains active on the medial aspect.
- bilateral remodelled diffuse new bone across the lateral aspects of the fibulae with enlarged striations.
Radiographic Lesion Summary:
No radiographs taken
Differential Diagnosis Outcome:
Probable Scurvy

Skeletal ID: MB05M14

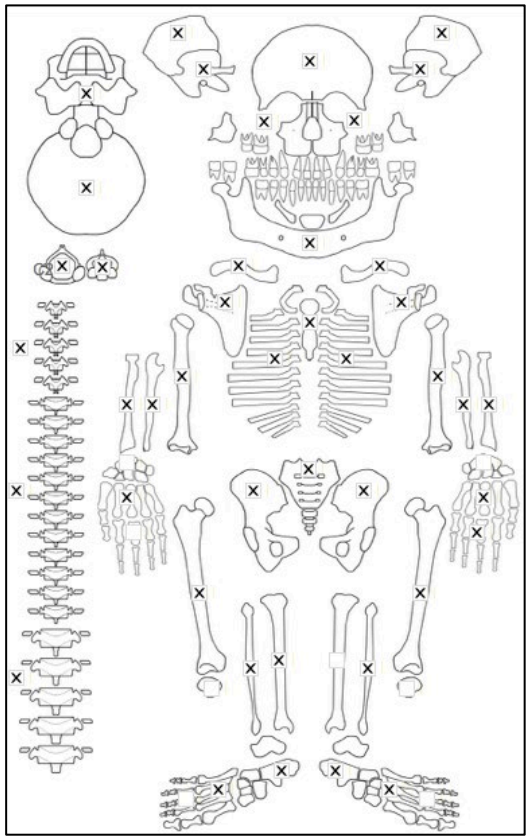

Completeness: Complete (>75%). 84% long bones, 37% hands and feet, 96% vertebrae, 75% neurocranium, ribs complete.
Preservation/ Taphonomy: Surfaces excellently preserved except endocranium that could not be observed due to soil concretions. Skeleton mostly intact.
Age: 3.5 Years (+/- 1.5 years), *Child*
Sex: Indeterminate
Macroscopic Lesion Summary:
Radiographic Lesion Summary:
Differential Diagnosis Outcome:
Probable Scurvy
Possible Rickets

Skeletal ID: MB05M15

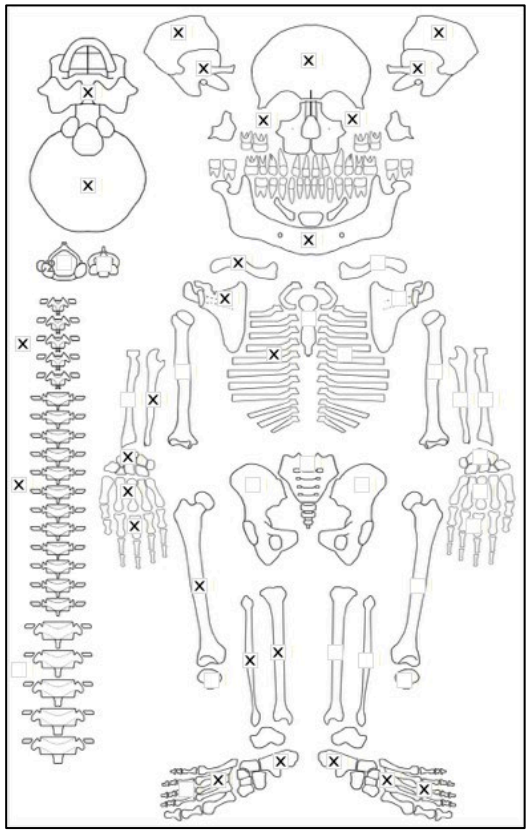

Completeness: Partially Complete (50 to 66%). 27% long bones, 40% hands and feet, 42% vertebrae, 88% neurocranium, ribs partially complete.
Preservation/ Taphonomy: Surfaces well preserved. Right side of postcranium present only with exception of foot.
Age: 17.5 years (+/- 6 months), *Adolescent*
Sex: Female
Macroscopic Lesion Summary:
- moderate remodelled cribra orbitalia of the right orbit (left missing)
- mixed active and remodelled diffuse porosity consistent with porotic hyperostosis on the superior and posterior parietals, and occipital planum
- bilateral remodelled new bone with vascular impressions inferior to the left mylohyoid line of the mandible
- remodelled lytic erosion and tapering of the distal ends of the 2nd proximal and intermediate right hand phalanges. Possible antemortem loss of the distal 2nd hand phalanx as a result of the pathology. There is some sclerotic response which may be related to changes to the articular surface.

Radiographic Lesion Summary:
Radiographs not taken.
Differential Diagnosis Outcome:
Anaemia

Skeletal ID: MB05M16a

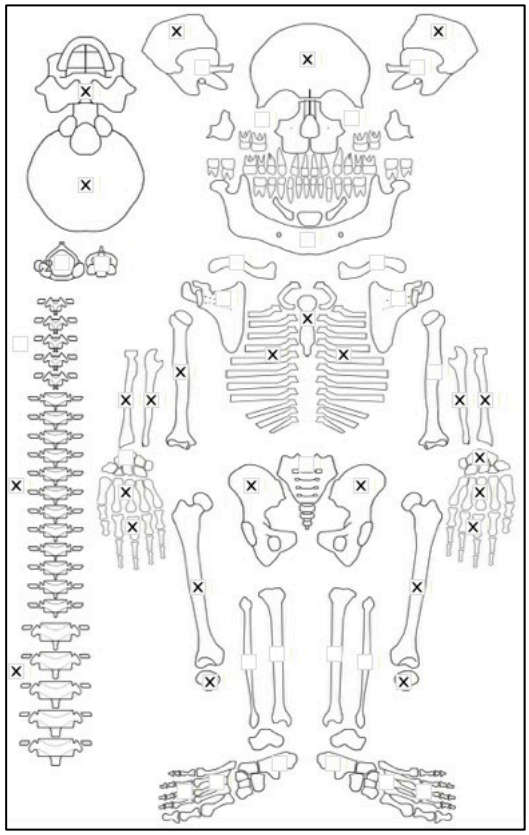

Completeness: Near Complete (66 to 75%). 55% long bones, 35% hands and feet, 42% vertebrae, 63% neurocranium, ribs incomplete.
Preservation/ Taphonomy: Concretions and dirt present and severe, cannot be removed. Especially pelvis.
Age: 40-49, *Middle Aged Adult*
Sex: Indeterminate
Macroscopic Lesion Summary:
No pathology
Radiographic Lesion Summary:
No radiographs taken
Differential Diagnosis Outcome:
No diagnosis

Skeletal ID: MB05M18

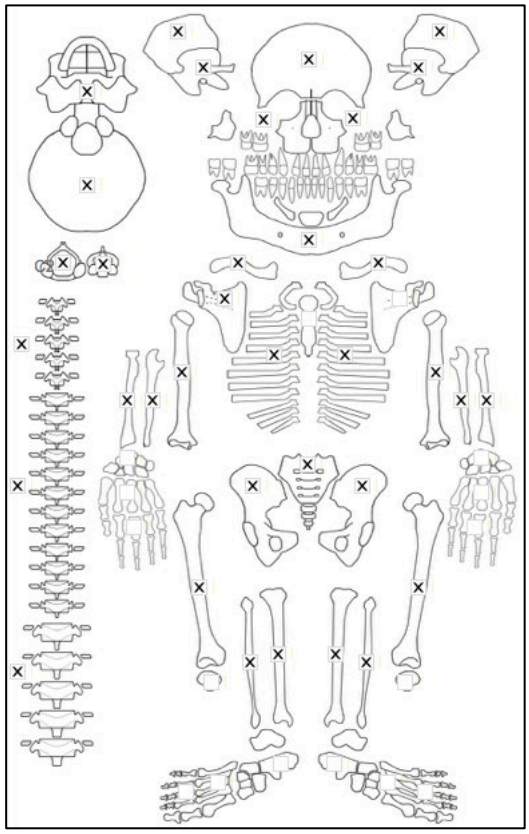

Completeness: Complete (>75%). 97% long bones, 0% hands and feet, 71% vertebrae, 88% neurocranium, ribs complete.
Preservation/ Taphonomy: Surfaces well preserved. Skull has major postmortem breakage but bones are predominantly present and identifiable. Most metaphyses very well preserved.
Age: 1.5 years (+/- 3 months), *Child*
Sex: Indeterminate
Macroscopic Lesion Summary:
- severe dental caries to the right central and left lateral maxillary incisors.
- unilateral diffuse active bone across the posterior right parietal
- diffuse active bone on the inferior margin of the occipital squama
- bilateral active new bone on the left zygomatic process of the frontal. Bilateral but the right zygomatic process new bone is associated with a thickened layered cortex and disruption of the normal suture morphology as a result of the thick new bone deposit.
- bilateral symmetrical layered new bone and cortical porosity of the superior orbital roofs
- bilateral symmetrical diffuse active bone on the external temporal squama and inferior petrous portion
- active new bone on the inferior left pars lateralis (right missing)
- mixed active and remodelling new bone and cortical porosity on the inferior right pars basilaris
- active layered new bone and cortical porosity on the external left greater wing of sphenoid (right missing)
- bilateral active layered new bone and cortical porosity on the posterior zygomatic bones
- bilateral mixed active and remodelled layered new bone with marked vascular impressions on the superior orbital surface of the zygomatic bones (orbital floor)
- bilateral symmetrical active new bone and cortical porosity on the palatal surfaces of the maxillae
- biconcavity of the lumbar vertebrae, with deformity of the inferior plate of one lumbar vertebrae resulting in anterior 'slipping' and protrusion of the margin. May have resulted in kyphosis.
- bilateral symmetrical active new bone and cortical porosity on the anterior and lateral aspects inferior to the radial notch and in the ulnar tuberosity
- fraying, flaring and cupping of the proximal humeri, proximal and right femur (left missing), proximal and distal (right missing) tibiae and distal right fibula (left missing). Fraying identifies activity.
- there is also a mild lateral bending deformity at the proximal third of the left humerus.
Radiographic Lesion Summary:
- white lines of Fraenkel and Trummerfeld zones

- ground glass osteopenia
Differential Diagnosis Outcome:
Probable Scurvy
Probable Rickets

Skeletal ID: MB05M20

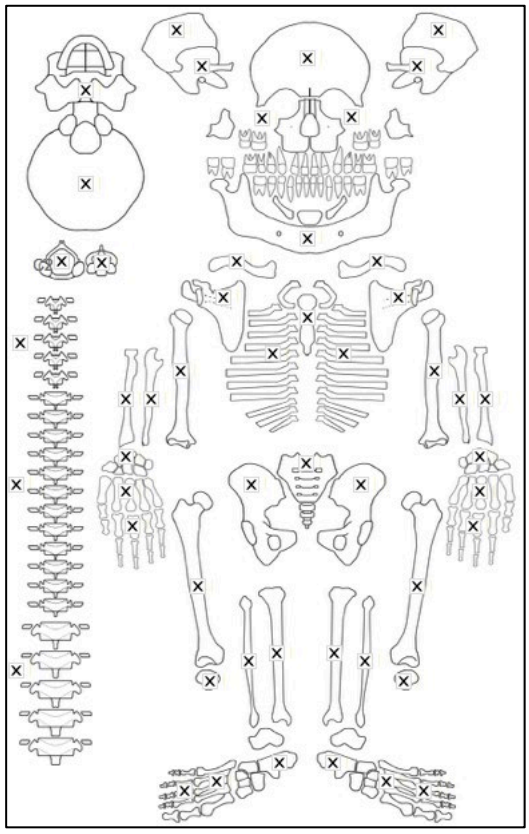

Completeness: Complete (>75%). 98% long bones, 79& hands and feet, 67% vertebrae, 88% neurocranium, and ribs near complete.
Preservation/ Taphonomy: Surfaces well preserved. Left 3rd and unknown metacarpal intrusive. Facial region is fragmented.
Age: 20-29, *Young Aged Adult*
Sex: Male
Macroscopic Lesion Summary:
- Discrete remodelled deposit of new bone inferior to the humeral head on the anterior aspect of the left humerus
- Remodelled deposit of new bone on the distal lateral humerus superior to the lateral epicondyle associated with two lytic lesions (possible gummatous lesions) (2b). Radiographs show there is a thick deposit of new bone across the entire shaft and distal metaphyses. associated with two lytic lesions (possible gummatous lesions). One lesion is anterior and lateral to the radial notch, oval in form with sclerotic base but sharp margins. Lesion is superficial. (17.6x 7.5mm). The second lesion is posterior oval in shape with sclerotic reaction, slightly rounded margins and also superficial (6.7x 3.5mm).
- unilateral remodelled discreet deposit of new bone on the medial proximal third left femur- the lesion appears haematoma-like.
- Large bilateral remodelled new bone across the entire shafts of the tibiae with endosteal expansion of shaft. On the right tibia is a distinctive node on the medial middle third of the shaft. Radiographs demonstrate considerable endosteal thickening with medullary constriction but not complete closure, and slight sabre shin of both tibiae.
- Remodelled localised plaques of new bone on the medial and lateral proximal thirds of the tibiae.
- Symmetrical proliferative new bone with gummatous lesions on the distal fibulae: Bilateral and symmetrical remodelled new bone with endosteal expansion associated with 3 gummatous like lesions on the distal two thirds of the right fibula and 2 gummatous like lesions on the distal left fibula. The new bone forms distinct nodes on the distal third shafts. The cross section demonstrates pathological involvement of

the distal two thirds and medullary closure on the distal end. The lesions are oval in shape with sclerotic response on the margins. With postmortem damage on the base of the two larger lesions of the right fibula, the third smaller lesion is clearly superficial with both lesions on the left appearing superficial. The lesion diameters are: 9.9x7.1mm, 10.5x6.7mm, and 6.4x3.7mm for the right and 12.7x7mm and 12.6x5.9mm for the left. The bone directly surrounding the margins of the lesions appear more active than the surrounding node.
- Multifocal (2 lesions) superficial cavitations on the posterior proximal metaphysis of the right fibula, may be consistent with the gummatous lesions seen elsewhere. However, there is an absence of proliferative new bone. Margins are sharp and defined with sclerotic reaction present in the base. Circular in shape. The lesion diameters are 8x4.8mm and 6.45x2.5mm.
- 2 superficial cavitations. on the left calcaneus with defined margins with sclerotic reaction in the base. One on the lateral midbody, another antero-medial on the medial border of the articular facet for the cuboid. There is remodelled new bone response overhanging the lytic region of the lateral lesion. The pattern is consistent with the lytic lesions seen elsewhere on the individual, without proliferative periosteal reaction associated. The margins are sharp and the lesion is oval in shape. The antero-medial lesion is circular in shape with sclerotic response in the base. The lesion diameters are 18.48x9.45mm (lateral), and 7.71x 6.13mm (antero-medial)
- Bilateral mixed remodelling moderate cribra orbitalia
- Mixed remodelling porotic hyperostosis across the ectocranium of the frontal, occipital and parietals (medial to the temporal lines)
- Remodelled bilateral symmetrical discrete new bone deposit and cortical porosity around the foramen on the posterior zygomatic bones.
- Mixed remodelling porosity of unknown aetiology across the anterior zygomatic bones and zygomatic arch of the right temporal (left missing)
- Remodelled bilateral symmetrical new bone deposit and cortical porosity on the external greater wings of sphenoid, continuing onto the external squama of the temporals and extending across the superior auditory area onto the mastoids. New bone is pooling superior to the zygomatic arch attachments
- Remodelled symmetrical discrete new bone deposit and cortical porosity superior to the mental foramina extending medially from the oblique lines.

Radiographic Lesion Summary:
- Right humerus shows thin radiolucent cloak of remodelled new bone across the shaft and distal metaphysis. Not sure if bilateral as left was not radiographed
- large and small gummatous lesions on the right humerus have radiodense sclerotic margins.
- very fine ring of sclerosis on the lesions of the lateral left calcaneus, not distinct on the antero-medial lesion.
- formation of a slight sabre shin with excessive thick deposit of new bone on the anterior crests of the tibia with medullary constriction at the middle third shafts. Endosteal and periosteal expansion clear on the radiographs.
- distal nodes of the fibulae are associated with complete closure of the medullary canals
- generalised osteopenia of the long bone ends

Differential Diagnosis Outcome:
Probable Scurvy
Probable Treponematosis
Anaemia

Skeletal ID: MB05M21

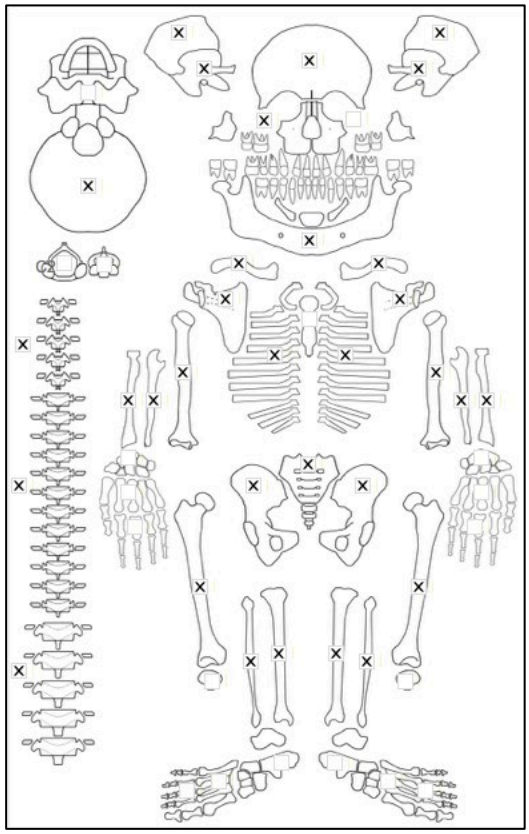

Completeness: Complete (>75%). 95% long bones, 4% hands and feet, 50% vertebrae, 88% neurocranium and ribs partially complete.
Preservation/ Taphonomy: Surfaces well preserved. Middle third of left fibula only, PM breakage to radii, tibiae and fibulae. Maxillae missing.
Age: 6 months, *Infant*
Sex: Indeterminate
Macroscopic Lesion Summary:
- poor mineralisation of new bone growth at the cranial bone ends, sutural margins of all of the cranial bones, continues as layered spiculated new bone with porosity on the endocranial and ectocranial occiptial planum.
- frontal bone is thickened
- bilateral discrete layered active new bone with cortical porosity on the superior orbits
- bilateral symmetrical active new bone and cortical porosity on the external left greater wing, pterygoid region and superior endocranial region including the foramen rotundum.
- discrete active new bone and cortical porosity on the posterior right zygomatic (left side missing)
- discrete active new bone on the right mylohyoid line of the mandible (left side missing)
- discrete active new bone and cortical porosity on the right incisive fossa of the mandible (left side missing)
- bilateral mixed active and remodelling cortical thickening of the shafts and metaphyses of the humeri. Accompanied by unilateral lateral bending deformity of the midshaft of the left humerus
- bilateral abnormal endochondral porosity exceeding 10mm from the metaphyseal plates of the proximal humeri, distal femora and proximal tibiae.
- bilateral mixed active and remodelling cortical thickening of the shafts and metaphyses of the ulnae, expansion is thick towards the posterior aspect.
- bilateral femoral neck depression, flaring and cupping of the distal ends of the femora
- bilateral thick diffuse mixed active and remodelled new bone across the shaft and metaphyses of the tibiae with endosteal expansion of the medial aspect. Associated with lateral bending of the tibial shaft, with the endosteal expansion on the concave aspect of the bending deformity.
- bilateral abnormal endochondral porosity exceeding 10mm from the sternal ends of ribs. Accompanied by circumferential expansion of 1 right and 2 left preserved costal ends of the ribs.
Radiographic Lesion Summary:
- white line of Fraenkel and Trummerfeld zones
- ground glass osteopenia

- coarsened trabeculae and cortical expansion at regions of bending deformities on the humeri
Differential Diagnosis Outcome:
Probable Scurvy
Probable Rickets

Skeletal ID: MB05M22

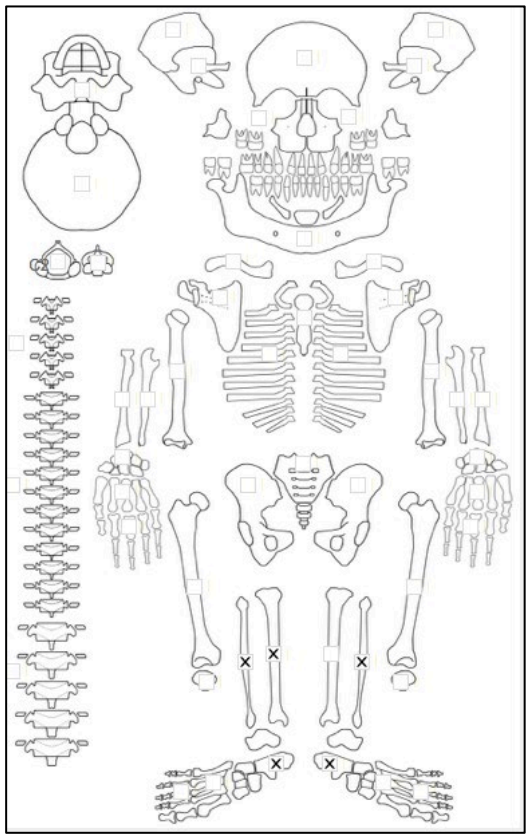

Completeness: Fragmented. 17% long bones, 9% hands and feet, 0% vertebrae, 0% neurocranium.
Preservation/ Taphonomy: Surfaces well preserved. Distal half of right tibia, distal metaphysis of left tibia, distal half of left fibula, middle half of right fibula only
Age: 1.5 years, *Child*
Sex: Indeterminate
Macroscopic Lesion Summary:
- mixed active and remodelled deposit of new bone across the lateral and plantar aspects of the 1st left metatarsal, accompanied by an enlarged foramen on the lateral midshaft.
Radiographic Lesion Summary:
Radiographs Not taken
Differential Diagnosis Outcome:
No diagnosis

Skeletal ID: MB05M23

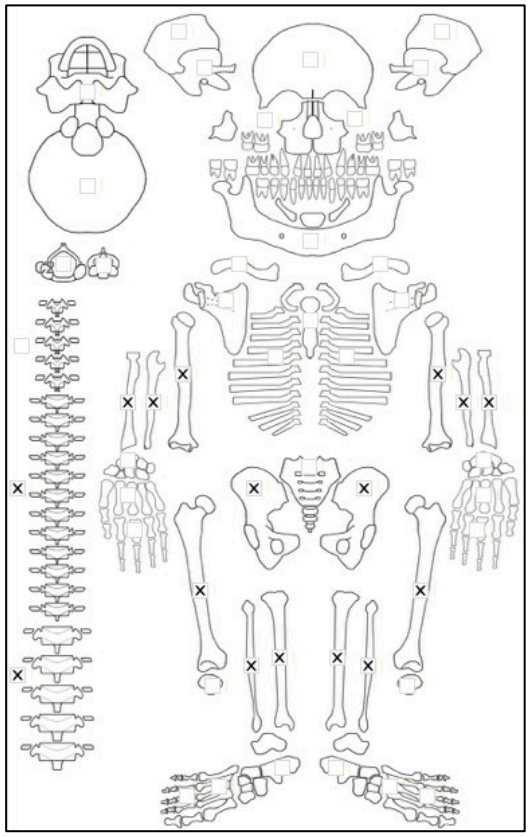

Completeness: Partially Complete (50 to 66%). 97% long bones, 6% hands and feet, 54% vertebrae, 0% neurocranium, ribs incomplete.
Preservation/ Taphonomy: Surfaces well preserved. Some cranial fragments.
Age: 1.25 years, *Child*
Sex: Indeterminate
Macroscopic Lesion Summary:
- Bilateral symmetrical localised discrete new bone deposit with cortical porosity inferior to the trochlea notch on the anterior proximal ulnae
- Bilateral abnormal endochondral porosity exceeding beyond 10mm on the proximal metaphyses of the tibiae
- Bilateral symmetrical diffuse mixed remodelling new bone on the medial shafts of the tibiae.

Radiographic Lesion Summary:
- multiple Harris lines in the limb bones
- expanded cortex of the femoral shafts
- osteopenia with ground glass appearance
- possible white line of Fraenkel, no clear scurvy zone as the entire metaphysis and shaft is radiolucent

Differential Diagnosis Outcome:
Possible Scurvy

Skeletal ID: MB05M24

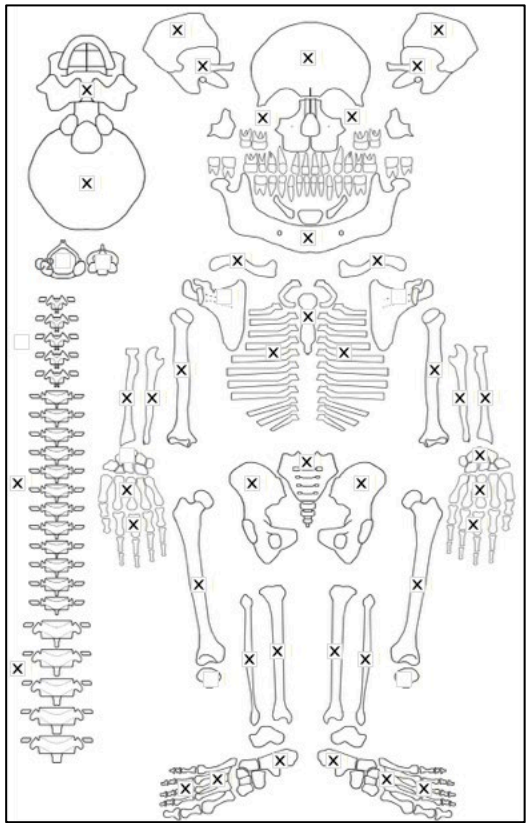

Completeness: Complete (>75%). 100% long bones, 59% hands and feet, 67% vertebrae, 88% neurocranium, ribs partially complete.
Preservation/ Taphonomy: Scapulae covered in concretions, other surfaces well preserved. Bones mostly intact.
Age: 8 years (+/- 9 months).
Sex: Indeterminate
Macroscopic Lesion Summary:
- bilateral active moderate cribra orbitalia
- localised remodelling porosity of unknown aetiology on the anterior frontal medial and superior to the superciliary arches
- localised remodelling porosity of unknown aetiology on the posterior occipital planum. Based on location it is plausible that this is mild porotic hyperostosis.
- bilateral symmetrical mixed active and remodelled new bone and cortical porosity on the external greater wings of sphenoid, the right greater wing presents with new bone and cortical porosity as well on the external pterygoid plate and the pterygoid fossa (left not preserved). The new bone and cortical porosity continues on the anterior margin of the temporal squama.
- bilateral symmetrical localised remodelling cortical porosity on the anterior maxillae around the regions of the infraorbital foramina
- bilateral symmetrical localised mixed active and remodelled new bone and cortical porosity on the posterior and lateral maxillae continuing onto the posterior zygomatic bones.
- bilateral symmetrical localised mixed active and remodelled new bone on the palatal surfaces of the maxillae
- bilateral symmetrical localised mixed active and remodelled new bone and cortical porosity on the medial coronoid processes of the mandible
- bilateral symmetrical localised mixed active and remodelled new bone and cortical porosity inferior to the mylohyoid lines of the mandible, associated with vascular impressions
- bilateral symmetrical remodelling diffuse new bone across the lateral shafts of the ulnae
- bilateral and symmetrical active localised new bone deposit on the proximal metaphyseal plate and on the posterior necks of the femora. There is also a bilateral and symmetrical depression deformity on the proximal femoral head metaphyseal plate. Located on the posterior margin.

- bilateral and mixed active and remodelled new bone on the medial and anterior shafts of the tibiae. The new bone is more active on the medial midshaft. The left tibia new bone also continues onto the posterior midshaft.
- mild cupping of the proximal metaphyseal plates of the tibiae
- unilateral active new bone on the lateral and anterior distal half shaft of the left fibula.
- bilateral symmetrical localised mixed active and remodelled new bone on the medial aspects of the calcanei
- bilateral symmetrical abnormal deep endochondral porosity exceeding 10mm from the metaphyseal plate of the proximal humeri, distal radii and ulnae, and proximal and distal femora, tibiae and fibulae.
- bilateral and mixed active and remodelled new bone on the medial/ posterior middle third shafts of the femora. There appear to be vascular impressions on the new bone.

Radiographic Lesion Summary:
- White line of Fraenkel and Trummerfeld zones
- Harris lines of long bones
- ground glass osteopenia
- pelkan spur of distal left fibula
- coarse trabeculae and thick cortex

Differential Diagnosis Outcome:
Anaemia
Probable Scurvy
Possible Rickets

Skeletal ID: MB05M25

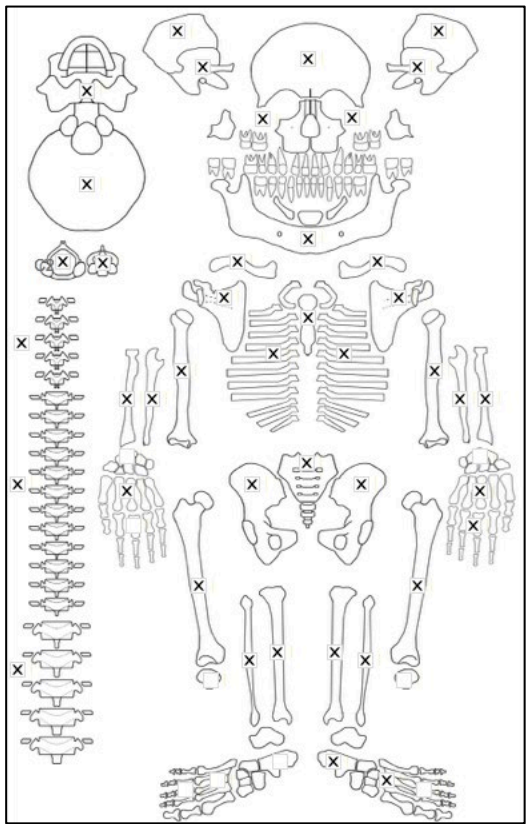

Completeness: Complete (>75%).
Preservation/ Taphonomy: Surfaces excellently preserved and bones mostly intact. 92% long bones, 29% hands and feet, 100% vertebrae, 100% neurocranium, ribs complete.
Age: 5 years (+/- 9 months), *Child*
Sex: Indeterminate
Macroscopic Lesion Summary:
- bilateral severe cribra orbitalia
- diffuse porosity of unknown aetiology intermediate to the superciliary arches on the anterior frontal bone
- mild active porotic hyperostosis of the occipital planum and on the posterior parietals directly anterior to the lambdoid suture

- bilateral symmetrical mixed active and remodelling new bone and cortical porosity on the temporal squama directly superior to the zygomatic processes and extending along the superior margins of the external auditory canals.
- bilateral symmetrical discrete mixed active and remodelling new bone and cortical porosity on the pterygoid region, and the pterygoid fossa of the left greater wing of sphenoid
- bilateral symmetrical discrete mixed active and remodelling new bone and cortical porosity on the palatal surfaces of the maxillae
- bilateral symmetrical discrete remodelled new bone and cortical porosity on the anterior maxillae, medial and extending from the infraorbital foramina
- bilateral symmetrical discrete remodelled new bone and cortical porosity on the incisive fossae of the mandible
- bilateral symmetrical discrete mixed active and remodelled new bone and cortical porosity on the oblique lines of the mandible directly inferior to the molar region
- bilateral symmetrical discrete active new bone on the medial coronoid fossae of the mandible
- bilateral symmetrical discrete mixed active and remodelled new bone and cortical porosity on the supraspinous fossa of the scapulae
- Abnormal endochondral porosity extending >10mm from the metaphyseal plates of the distal femora, proximal tibiae, left distal tibia (right side missing), distal fibulae and left proximal fibula (right side missing)
- mild cupping of the distal femora, proximal tibiae and distal left tibia (right missing)

Radiographic Lesion Summary:
- White line of Fraenkel and Trummerfeld zones of the long bones

Differential Diagnosis Outcome:
Anaemia
Probable Scurvy
Possible Rickets

Skeletal ID: MB05M28

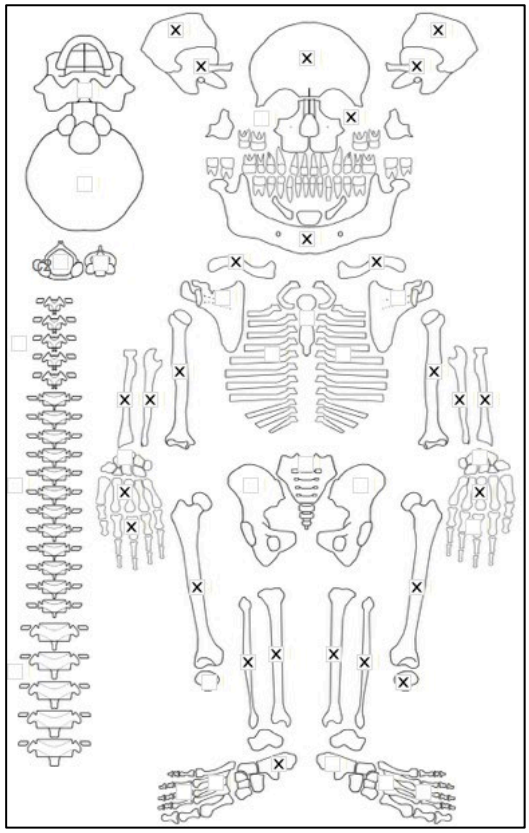

Completeness: Fragmented. 30% long bones, 26% hands and feet, 0% vertebrae, 75% neurocranium.
Preservation/ Taphonomy: All bones have heavy PM breakage. Although represented not well preserved. Only a portion of right fibula shaft, right proximal tibia epiphysis, proximal to mid left femoral shaft, proximal

and distal epiphysis of right femur, complete right radius, midshaft of left radius, mid to distal shaft of right ulna, proximal metaphysis of left ulna and proximal to middle shaft of right humerus, proximal left and distal right clavicles out of the long bones are identifiable. Few fragments of pelvis and ribs.
Age: 20-29, *Young Adult*
Sex: Female
Macroscopic Lesion Summary:
- bilateral mild remodelled porotic hyperostosis of the superior parietals. Associated with thickened diploe of the frontal, parietals and temporals
- remodelled new bone deposit on the superior endocranial surface of the left greater wing of sphenoid fragment
Radiographic Lesion Summary:
No radiographs taken
Differential Diagnosis Outcome:
Anaemia

Skeletal ID: MB05M29

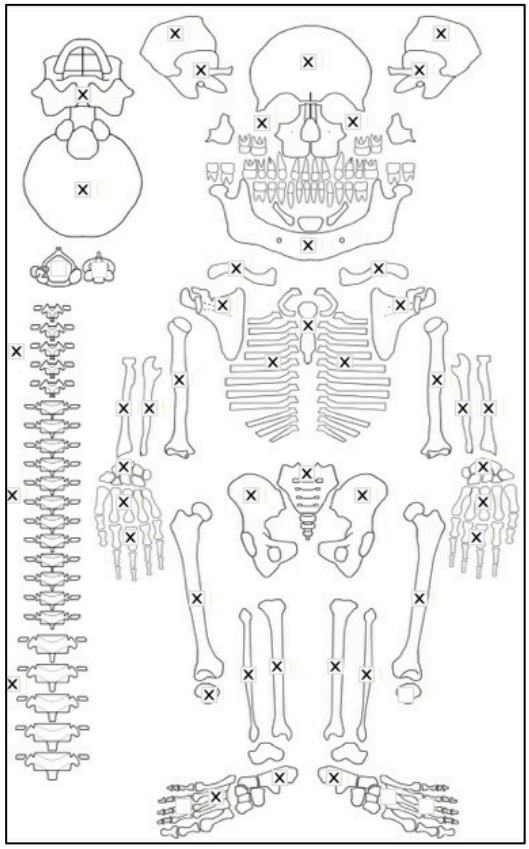

Completeness: Complete (>75%). 95% long bones, 66% hands and feet, 83% vertebrae, 88% neurocranium,
Preservation/ Taphonomy: Ribs heavy PM breakage. Surfaces excellently preserved except endocranium that could not be observed due to soil concretions.
Age: 30-39 years, *Middle Aged Adult*
Sex: Male
Macroscopic Lesion Summary:
- bilateral remodelling moderate cribra orbitalia
- Diffuse remodelled porosity with hair on end pattern at the occipital crest consistent with severe porotic hyperostosis on the superior frontal, superior and posterior parietals (medial to the temporal lines) and occipital planum
- Bilateral symmetrical remodelled deposit of discrete new bone on the posterior maxillae associated with vascular impressions
- unilateral remodelled deposit of cortical porosity on the posterior left zygomatic
- bilateral symmetrical remodelled cortical porosity on the incisive fossae of the mandible

- bilateral symmetrical remodelled discrete new bone with vascular impressions inferior to the mylohyoid lines of the mandible
- bilateral symmetrical active discrete new bone on the inferior margin of the scapular spine in the infraspinous fossae of the scapulae
- bilateral active discrete new bone across the superior margin of the anterior scapular bodies
- active discrete new bone across the supraspinous fossa of the left scapula (right not observable)
- circular focal lytic lesion on the left lateral vertebral body on the posterior margin of a lower thoracic vertebra (likely T11). There is sclerotic reaction on the margin. Lesion diameter 2.91x3.16mm.
- multifocal and coalesced lytic destruction on the superior S1 body. This may be age related degeneration. largest lesion diameter 12.03x 4.83. Erosion covers a diameter of 19.13x 16.83mm
- bilateral diffuse new bone on either side of the interosseous crests on the shafts of the ulnae
- unilateral discrete active new bone deposit inferior to the radial tuberosity of the left radius
- bilateral symmetrical discrete active new bone deposit on the anterior distal metaphyses of the radii
- bilateral active new bone on the palmar shafts of the 1st metacarpals (with new bone also on the dorsal surface of left), lateral aspects of the 2nd metacarpals, and thick unilateral mixed active and new bone on the palmar distal third shaft of the right 3rd metacarpal.
- bilateral symmetrical mixed active and new bone across the femora sparing only the epiphysis and the anterior 2/3rds of the shafts. The lesion is more active around the linea aspera and more proximally on the shaft.
- bilateral mixed active and remodelled new bone across all aspects of the preserved tibiae sparing only the epiphyses. The lesion is more active on the proximal and distal ends (right missing), with a marked active deposit without apparent endosteal thickening on the medial distal left tibia (right side not preserved)
- bilateral symmetrical thick mixed active and remodelled new bone across all aspects of the preserved fibulae sparing only the epiphyses. The lesion is more active towards the distal end. The new bone is particularly marked along the interosseous crest and there appears to be endosteal expansion of the distal ends. The right fibula new bone is associated with superficial cavitation lesions with irregular margins on the medial distal epiphysis, which may be consistent with gummatous lesions. There is sclerotic reaction and the new bone surround the lytic lesions is well remodelled. The margins are well defined and sharp suggesting active. The lesion diameters are 11.47x7.1mm and 4.65x2.95mm respectively
- unusually enlarged sesamoid bone on the inferior right 1st metatarsal.

Radiographic Lesion Summary:

- sclerotic margin around the lytic lesion of the fibula
- sabre shin of the tibia

Differential Diagnosis Outcome:

Anaemia
Probable Scurvy
Possible Treponematosis

Skeletal ID: MB05M30

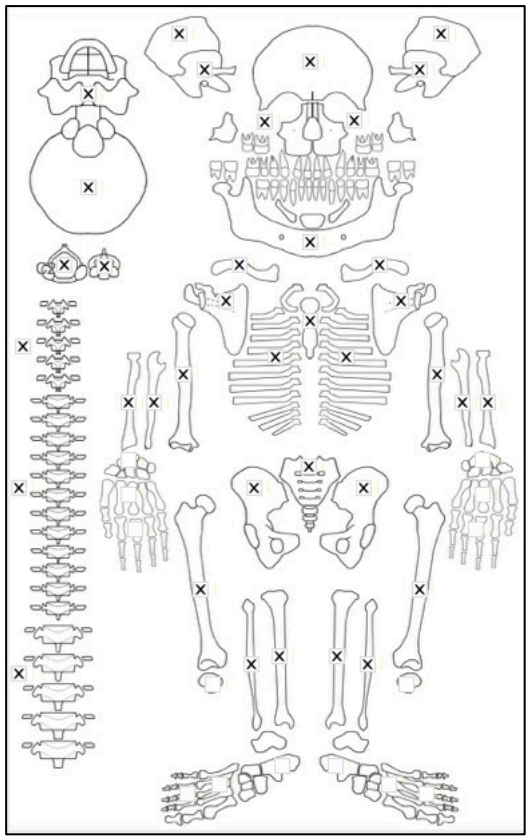

Completeness: Complete (>75%). 100% long bones, 6% hands and feet, 79% vertebrae, 88% neurocranium and ribs near complete.
Preservation/ Taphonomy: Surfaces excellently preserved. Bones mostly intact.
Age: 6 months (+/- 3 months), *Infant*
Sex: Indeterminate
Macroscopic Lesion Summary:
- anterior displacement of the lower table of the growing the vertebrae of the lower thoracic and lumbar vertebrae which may have resulted in kyphosis of the lower spine.
- unilateral discrete deposit of active new bone and cortical porosity on the superior margin of the external auditory canal of the left temporal
- bilateral symmetrical diffuse active new bone on the external greater wings of the sphenoid and the temporal squama
- diffuse deep porosity and grooves on the occipital planum which may be porotic hyperostosis, but is also associated within a layer of active new bone on the posterior occipital. The grooves follow the cranial plate growth trajectory.
- The active new bone continues on the sutural margins of the ectocranial occipital (with concentration on the pars laterali), parietals and frontal
- discrete active new bone and cortical porosity on the inferior pars basilaris
- discrete active new bone on the anterior right maxilla (left not preserved) around the region of the infraorbital foramen
- discrete active new bone and cortical porosity on the posterior right zygomatic and maxilla (left side missing)
- bilateral symmetrical discrete active new bone on the palatal surfaces of the maxillae
- bilateral symmetrical discrete active new bone on the orbital roofs
- bilateral symmetrical discrete active new bone on the medial coronoid processes of the mandible
- discrete active new bone on the left mylohyoid line (right missing)
- bilateral discrete active new bone and cortical porosity on the incisive fossae to mental foramen region of the mandible
- bilateral discrete active new bone on the supraspinous fossae of the scapulae
- bilateral discrete active cortical porosity on the infraspinous fossae around the foramina of the scapulae

- thick layered mixed active and remodelled new bone resulting in cortical thickening and some medullary constriction apparent in postmortem breaks on the shaft and metaphyses of the humeri, radii, ulnae, femora, tibiae and fibulae.
- slight lateral bending deformity and the mid to distal third shaft of the left humerus, and medial bending of the metaphyseal proximal and distal (right only left missing) plates of the tibia.
- mild depression of the femoral necks, cupping of the distal metaphyseal plates of the femora
- initiation of fraying on the proximal tibiae suggests active

Radiographic Lesion Summary:
- white line of Fraenkel and Trummerfeld zones
- ground glass osteopenia
- pelkan spurs of the distal femora
- coarse trabeculae

Differential Diagnosis Outcome:
Probable Scurvy
Probable Rickets

Skeletal ID: MB05M31

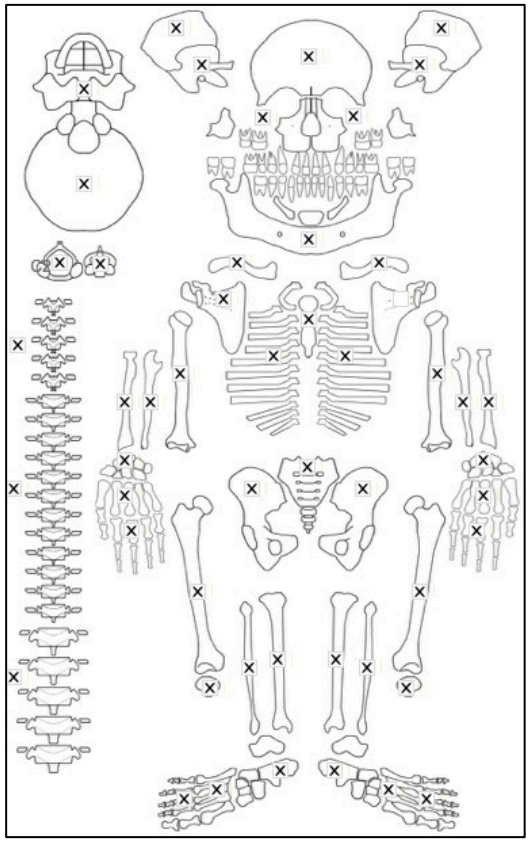

Completeness: Complete (>75%). 98% long bones, 79% hands and feet, 100% vertebrae, 88% neurocranium and ribs complete.
Preservation/ Taphonomy: Surfaces excellently preserved.
Age: 20-29, *Young Aged Adult*
Sex: Male

Macroscopic Lesion Summary:
- remodelled bilateral mild cribra orbitalia
- diffuse porosity consistent with porotic hyperostosis on the superior frontal, superior and posterior parietals and the occipital planum. The occipital planum also presents with thickened cranial vault.
- bilateral symmetrical remodelled new bone and cortical porosity on the external greater wing of sphenoid bones, and along the superior margin of the zygomatic arch and superior auditory canals of the temporals.
- localised unilateral remodelling cortical porosity on the lateral anterior right zygomatic.
- bilateral symmetrical remodelled new bone in the shape of haematomas on the medial proximal shaft of the tibiae.

- remodelled new bone in the shape of a haematoma on the middle third anterior tibia on the crest (right side is not observable)

Radiographic Lesion Summary:
Radiographs not taken.

Differential Diagnosis Outcome:
Anaemia
Probable Scurvy

Skeletal ID: MB05M32

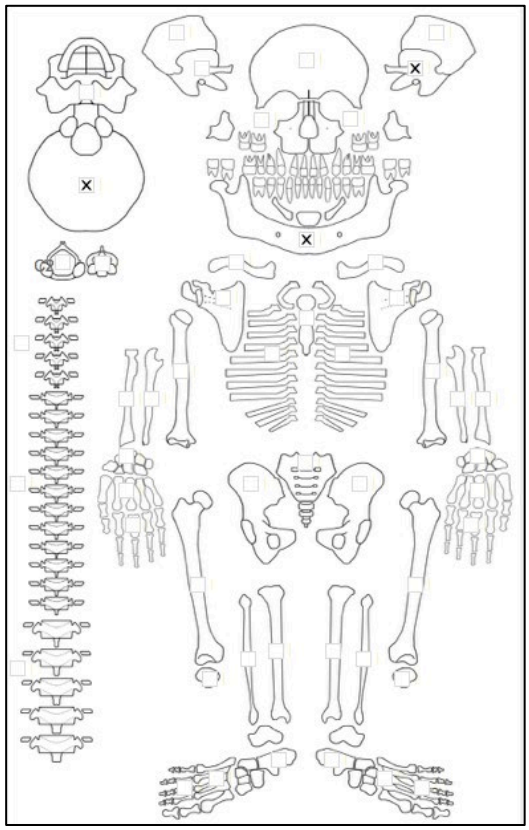

Completeness: Fragmented. 0% long bones, 1% hands and feet, 0% vertebrae, 38% neurocranium.
Preservation/ Taphonomy: Many PM breaks but surfaces well preserved.
Age: 20-29, *Young Adult*
Sex: Male

Macroscopic Lesion Summary:
- remodelled discrete deposit of new bone and cortical porosity on the inferior mandibular body

Radiographic Lesion Summary:
No radiographs taken

Differential Diagnosis Outcome:
No diagnosis

Skeletal ID: MB05M34

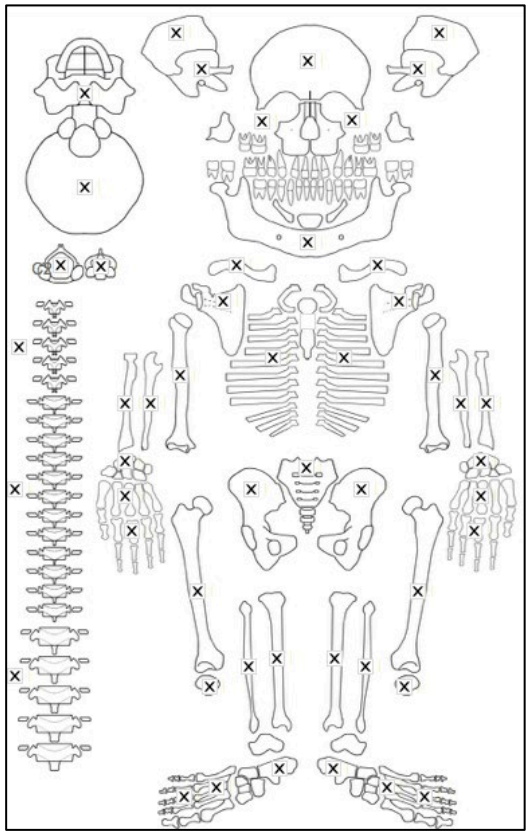

Completeness: Complete (>75%). 92% long bones, 75% hands and feet, 92% vertebrae, 88% neurocranium and ribs partially complete.
Preservation/ Taphonomy: Surfaces well preserved. PM breakage of ribs.
Age: 400-49, *Middle Aged Adult*
Sex: Female
Macroscopic Lesion Summary:
- Bilateral remodelled mild cribra orbitalia
- Remodelled porotic hyperostosis on the posterior and superior parietals, and the occipital planum
- Bilateral symmetric discrete remodelled cortical porosity and new bone deposition on the lateral calcanei. May not be pathological.
- Enlarged nutrient foramen on the plantar surface of the left 1st metatarsal. Asymmetric.
- Small circular lytic defect on the superior vertebral body of the C6, located more posteriorly and towards the lateral right. Margins are rounded and well remodelled. Lesion diameter: 2.63x 2.63mm

Radiographic Lesion Summary:
No radiographs taken
Differential Diagnosis Outcome:
Anaemia

Skeletal ID: MB05M36

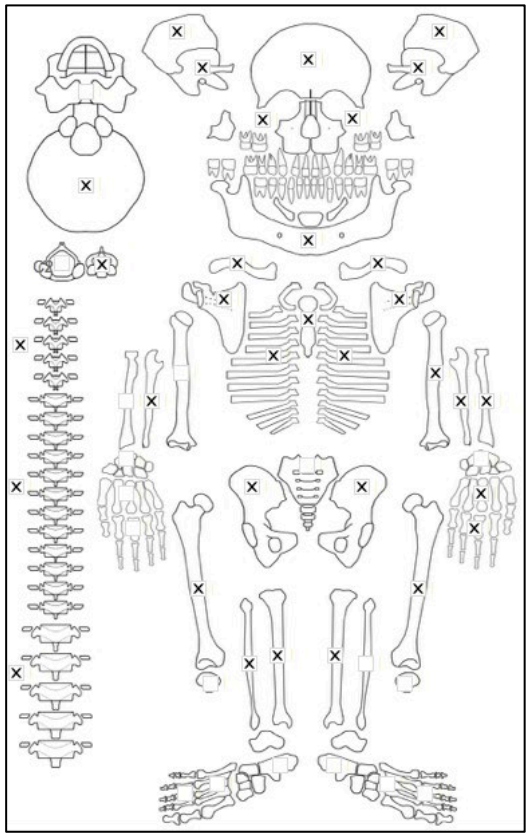

Completeness: Near Complete (66 to 75%). 61% long bones, 8% hands and feet, 79% vertebrae, 88% neurocranium, ribs near complete.
Preservation/ Taphonomy: Surfaces well preserved. Skull severely fragmented, only some could be reconstructed. Mostly complete sphenoid bone with exception of external right greater wing, mostly complete frontal and partial to incomplete parietals, mostly complete occipital, partial complete temporals. Many PM breaks of ribs.
Age: 3 years (+/- 6 months), *Child*
Sex: Indeterminate
Macroscopic Lesion Summary:
- Endocranial remodelled new bone deposit with accompanied lytic destruction penetrating into the inner diploe, but with sclerotic remodelling of the margins minimally on the endocranial aspect of the occipital and parietal, and frontal. 1 region of abnormal bone occurs left right lateral to the cruciform eminence and inferior to the transverse sulcus. Single bilateral lesions occur in the central-posterior endocranium of the parietals and lesion on the central frontal. The new bone lesions are consistent with Lewis Grade 4
Extent of frontal of parietal lesions unknown. Lesion diameter of the occipital:
32.58x12.12mm
- Diffuse cortical porosity and active new bone across the external left greater wing of sphenoid (right missing) and bilateral cortical porosity and new bone across the squama of the temporals. The left side new bone and porosity is continuous across the external sphenoid and left temporal.
- Unilateral active discrete deposit of new bone on the left medial coronoid process of the mandible
- Bilateral discrete deposit of active new bone and cortical porosity across the palatal surfaces of the maxillae
- Bilateral symmetrical discrete deposit of active new bone and cortical porosity across the anterior maxillae and around the regions of the infraorbital foramina. The porosity is notably severe inferior to the foramina, and result in a coalescing region of lytic destruction.
- Bilateral mixed remodelling new bone deposit across the medial and posterior aspects of the preserved proximal middle right tibia and posterior middle third of the left tibia.
- Bilateral mixed remodelling active new bone deposit and cortical porosity across the temporal lines and zygomatic processes of the frontal
- Bilateral active discrete deposit of new bone and cortical porosity on the superior orbital roofs
- Bilateral active discrete deposit of new bone and cortical porosity on the anterior zygomatic bones around the regions of the foramina

- Bilateral symmetrical mixed remodelling discrete deposit of new bone and cortical porosity on the posterior zygomatic bones
- Unilateral discrete deposit of mixed remodelling new bone and cortical porosity in the pterygoid region of the left greater wing of sphenoid

Radiographic Lesion Summary:
No remarkable changes
Differential Diagnosis Outcome:
Probable Scurvy

Skeletal ID: MB07H1M1

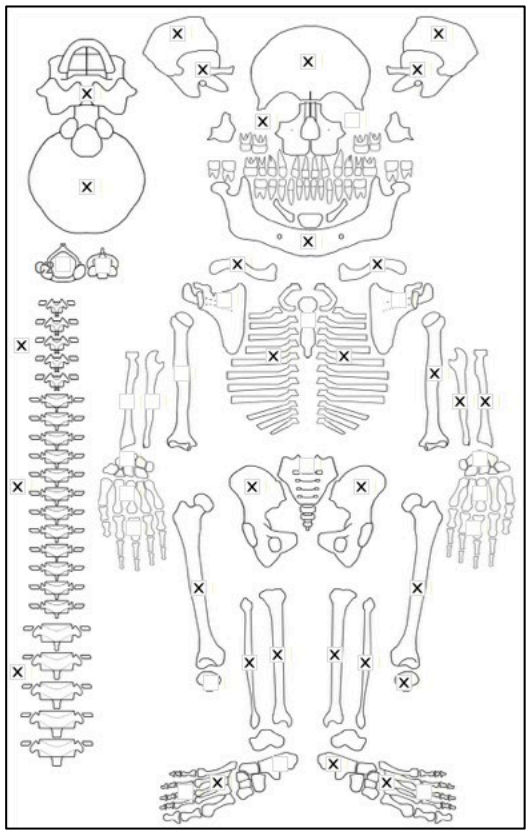

Completeness: Partially Complete (66 to 75%). 61% long bones, 24% hands and feet, 50% vertebrae, 75% neurocranium, ribs partially complete.
Preservation/ Taphonomy: Long bones have heavy PM breakage. Many surfaces caked in concretions and cannot be studied. Right tarsals caked in soil concretion and considered absent.
Age: 12 years (6 months), *Adolescent*
Sex: Indeterminate
Macroscopic Lesion Summary:
- Diffuse remodelled new bone consistent with Lewis Grade 4 on the frontal, parietals and occipital endocranium. The impressions are deep and intrude into the trabecular bone.
- Bilateral severe cribra orbitalia
- Bilateral symmetrical porosity of unknown aetiology on the posterior parietals adjacent to the lambdoid suture
- Bilateral symmetrical mixed active and remodelled new bone and cortical porosity with vascular impressions on the lateral anterior zygomatic bones particularly on the frontal process.
- possible anterior bulging with rounding of the orbital margins
- Bilateral symmetrical mixed active and remodelled new bone and cortical porosity with vascular impressions on the posterior zygomatic bones
- mixed active and remodelled cortical porosity on the anterior right maxilla round the region of the infraorbital foramen (left missing)
- anterior teeth appear to be protruding anteriorly and there is mild anterior bulging of the maxilla
- bilateral symmetrical mixed active and remodelled new bone and cortical porosity of the medial coronoid processes of the mandible

- diffuse woven bone on the medial middle third left tibia (right obscured cannot be observed)
- there appears to be no development of a frontal sinus with noticeably thickened diploe of the cranial vault (maxillary sinuses damaged and unobservable)
- very thick diploic bone of cranium

Radiographic Lesion Summary:

- no pneumatisation of the frontal sinuses
- extensive marrow proliferation of the zygomatic bones and maxilla, with crowding of teeth and no pneumatisation of the maxillary sinuses
- marrow hyperplasia of the frontal bone, and the hair on end pattern from the severe cribra orbitalia is prevalent on the radiographs.
- Thin cortices of the long bones, but there is heavy PM damage and concretions on the surfaces of the bone
- Clear and extensive marrow hyperplasia of the ribs and thinning of the cortices

Differential Diagnosis Outcome:

Anaemia
Possible Scurvy
Probable Thalassaemia

Skeletal ID: MB07H1M2

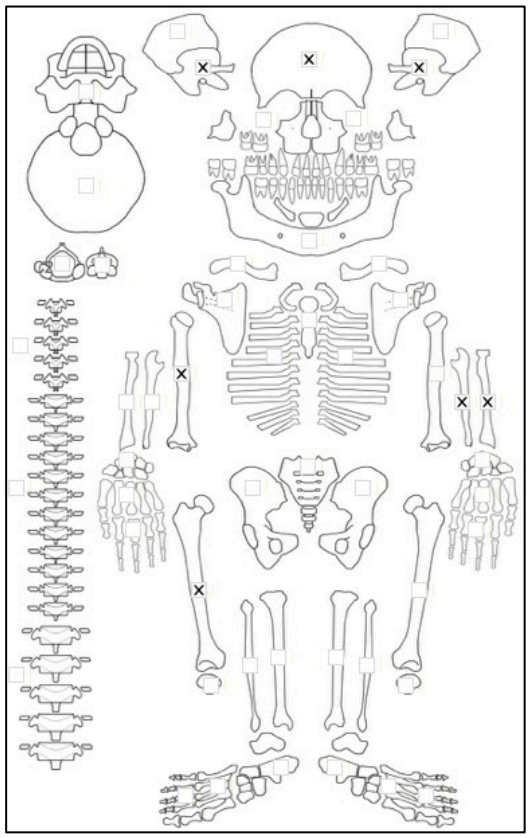

Completeness: Fragmented. 25% long bones, 0% hands and feet, 0% vertebrae, 38% neurocranium.
Preservation/ Taphonomy: Surfaces well preserved. Cranium is heavily fragmented and fragments are difficult to identify. Distal 2/3rds of right humerus, proximal to mid 2/3 shaft of left ulna and radius, right femur with distal metaphysis missing and an unsided middle third fibula only.
Age: 0 years, *Infant*
Sex: Indeterminate

Macroscopic Lesion Summary:

- active diffuse new bone on the endocranium of the frontal
- active diffuse new bone on the endocranium and ectocranium of unidentified cranial fragments
- bilateral symmetrical diffuse new bone across the ectocranium and endocranium of the temporals including the petrous process
- diffuse active new bone across all preserved shafts of the long bones associated with a thickened trabecular region restricting the medullary area but not associated with a thickened cortex. The long bones include the

right humerus (left missing), left ulna and radius (right missing), right femur (left missing) and an unsided fibula.
Radiographic Lesion Summary:
No distinct features observed.
Differential Diagnosis Outcome:
Possible Scurvy

Skeletal ID: MB07H1M3

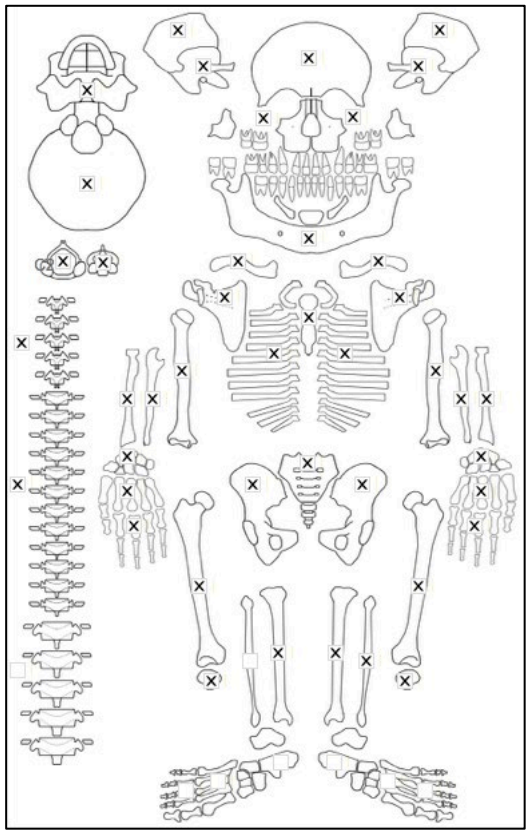

Completeness: Complete (>75%). 100% long bones, 72% hands and feet, 83% vertebrae, 88% neurocranium, ribs complete.
Preservation/ Taphonomy: Surfaces excellently preserved, and most bones intact.
Age: 14.5 years (+/- 6 months), *Adolescent*
Sex: Indeterminate
Macroscopic Lesion Summary:
- bilateral severe cribra orbitalia, some new remodelled new bone deposits as well.
- bilateral symmetrical remodelled new bone and cortical porosity on the external greater wing of sphenoid, and extending from the foramen ovale onto the pterygoid plate and fossa, continuing across the superior margin of the zygomatic arch and external auditory canal on the temporal squama.
- bilateral symmetrical remodelled new bone and cortical porosity on pars laterali around the condylar foramen with associated vascular impressions.
- bilateral symmetrical mixed active and remodelled new bone and cortical porosity on the posterior maxillae and zygomatic
- bilateral symmetrical mixed active and remodelled cortical porosity on the palatal surfaces of the maxillae
- bilateral symmetrical mixed active and remodelled new bone cortical porosity on the medial coronoid processes of the mandible
- bilateral symmetrical active new bone superior to the mylohyoid lines and remodelled new bone with vascular impressions inferior to the mylohyoid lines of the mandible.
- coalesced active trabecular expansions on the posterior sternum and manubrium (sternal and manubrial porosity)

- abnormal trabecular expansion (vertebral porosity) on 8 anterior and lateral middle to lower thoracic bodies, 2 lateral lower lumbar bodies, and S1 to 5 sacral anterior bodies and lateral alae with increasing severity of the porosity on the sacrum from S1 to 5.
- bilateral symmetrical well remodelled discrete new bone with slight changes in matrix organisation on the medial to posterior proximal third femora.
- deep endochondral porosity exceeding 10mm from the metaphyseal plates of the proximal humeri, distal radii and ulnae, distal femora, and proximal and distal tibiae and fibulae.
- mixed active and remodelled discrete deposit of new bone and cortical porosity on the medial and lateral calcanei
- discrete active new bone around the foramina of the medial 1st metatarsals

Radiographic Lesion Summary:
Ground glass osteopenia of the long bones
Differential Diagnosis Outcome:
Anaemia
Probable Scurvy

Skeletal ID: MB07H1M4

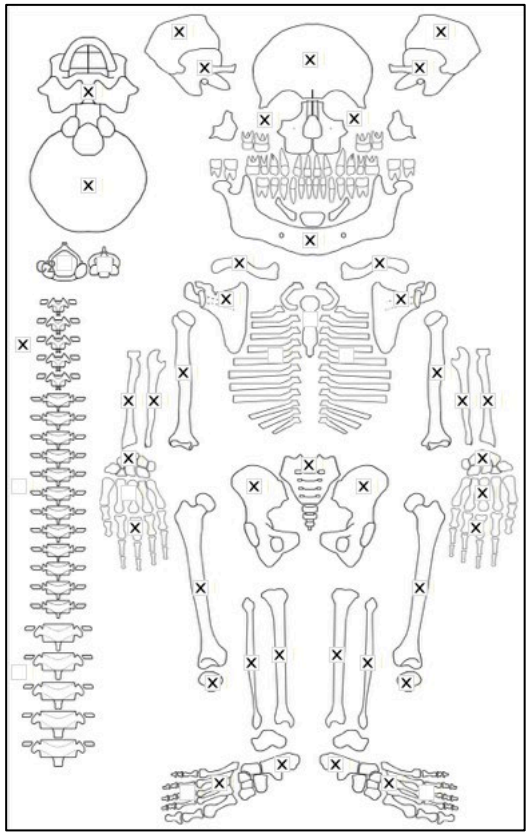

Completeness: Near Complete (66 to 75%). 70% long bones, 52% hands and feet, 8% vertebrae, 88% neurocranium, ribs fragmented.
Preservation/ Taphonomy: Bones of the axial skeleton are severely fragmented, but a lot of the long bones surfaces are well represented. Femora, tibiae, fibulae, radii and ulnae shafts are mostly intact.
Age: 40-49, *Middle Aged Adult*
Sex: Female
Macroscopic Lesion Summary:
- bilateral symmetrical remodelled new bone on the left external greater wing of sphenoid extending from the eternal foramen ovale and onto the anterior squama of the temporals
- remodelled moderate cribra orbitalia
- remodelled abnormal vascular impressions on the endocranial frontal and parietal

Radiographic Lesion Summary:
No radiographs taken
Differential Diagnosis Outcome:

Anaemia
Possible Scurvy

Skeletal ID: MB07H1M5

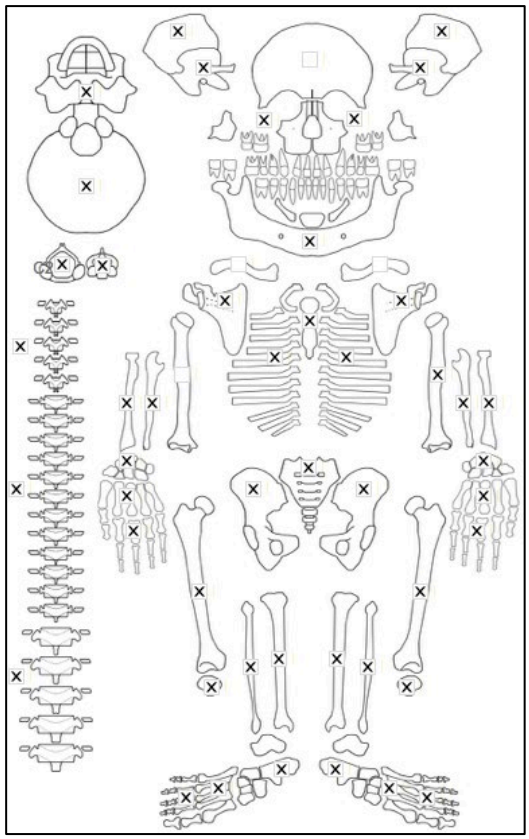

Completeness: Complete (>75%). 100% long bones, 84% hands and feet, 100% vertebrae, 100% neurocranium, ribs complete.
Preservation/ Taphonomy: Surfaces in excellent condition but endocranium could not be observed (some concretions).
Age: 40-49, *Middle Aged Adult*
Sex: Male
Macroscopic Lesion Summary:
- Bilateral symmetrical remodelled discrete new bone and cortical porosity on the superior external auditory meatus extending onto the meatal triangle and the mastoid
- Bilateral symmetrical remodelled discrete haematoma like new bone deposits on the medial proximal tibiae directly medial to the tibial tuberosity
- Bilateral symmetrical remodelled haematoma like new bone deposits on the medial to posterior middle third tibiae
- Bilateral symmetrical remodelled new bone deposits on all aspects of the distal metaphyseal regions of the tibiae
- Bilateral symmetrical remodelled new bone deposits on the entire medial aspect and continuing on the posterior aspect on the proximal third and distal metaphyseal region of the fibulae
- Bilateral symmetrical discrete remodelled new bone with very fine cortical porosity on the medial calcaneus inferior to the sustemtaculum tali.
- Circular erosive destruction of the posterior spinous process of the C1, some sclerotic reaction inside the lesion. 8.98x8.67mm.
- Remodelled bilateral moderate cribra orbitalia
- Remodelled diffuse porosity consistent with porotic hyperostosis across the superior frontal, superior and posterior parietals (medial to the temporal lines) and the occipital squama
Radiographic Lesion Summary:
No radiographs taken
Differential Diagnosis Outcome:

Anaemia

Skeletal ID: MB07H1M7

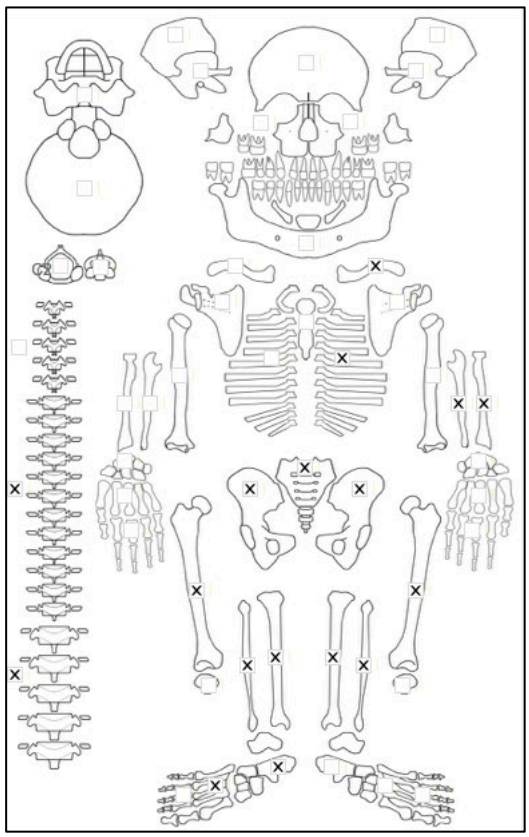

Completeness: Incomplete (33 to 50%). 67% long bones, 11% hands and feet, 33% vertebrae, 0% neurocranium, ribs fragmented.
Preservation/ Taphonomy: Surfaces well preserved. Some left facial fragments.
Age: 1 year (+/- 3 months), *Child*
Sex: Indeterminate
Macroscopic Lesion Summary:
- discrete active new bone and cortical porosity on the superior orbital surface (orbital floor) of the left maxilla (right missing)
- discrete active new bone on the lateral and posterior aspect of the left maxilla with deep vascular impression (right missing)
- discrete active new bone on the palatal surface of the left maxilla (right missing)
- discrete mixed active and remodelled new bone and cortical porosity on the posterior left zygomatic. (right missing)
- expanded foramen on the palmar aspect of an unsided intermediate hand phalanx
- diffuse active new bone on the lateral shaft of the left ulna (right missing)
- diffuse active new bone on the medial proximal metaphysis and shaft of the left radius along the border of the interosseous crest and on the radial tuberosity (right missing)
- bilateral symmetrical diffuse active new bone on the medial posterior proximal to mid shaft of the femora adjacent to the linea aspera. This is connected to a region on the proximal posterior of growth initiation and muscle attachment rugosity and may be related to normal childhood growth.
- bilateral symmetrical diffuse active new bone on the medial and posterior shafts of the tibiae
- unilateral remodelled cortical expansion of the distal third left fibula. The expansion is more marked anterior-posteriorly
- abnormal endochondral porosity exceeding 10mm from the metaphyseal plate of the distal left ulna and radius (right missing), proximal and distal femora, tibiae and fibulae.
- mild cupping of the distal femora
Radiographic Lesion Summary:
- white line of Fraenkel and Trummerfeld zones

- ground glass osteopenia
Differential Diagnosis Outcome:
Probable Scurvy
Possible Rickets

Skeletal ID: MB07H1M8

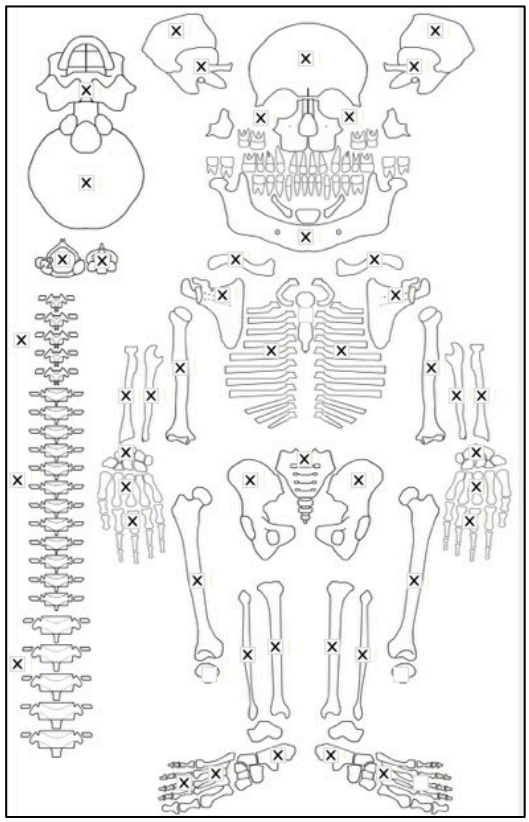

Completeness: Complete (>75%). 100% long bones, 67% hands and feet, 75% vertebrae, 88% neurocranium, ribs near complete.
Preservation/ Taphonomy: Surfaces excellently preserved and most bones intact.
Age: 30-39, *Middle Aged Adult*
Sex: Male

Macroscopic Lesion Summary:
- Bilateral symmetrical remodelled porotic hyperostosis of the superior parietals
- Bilateral moderate remodelling cribra orbitalia
- Remodelled discrete deposit of new bone and cortical porosity in the pterygoid region of the left greater wing of sphenoid extending from the foramen ovale
- Unilateral enlarged foramina on the plantar aspect of the left 4th proximal and right 3rd proximal hand phalanges.

Radiographic Lesion Summary:
- rib within a rib appearance
- marrow hyperplasia of the hands, an associated cyst like luciencies

Differential Diagnosis Outcome:
Anaemia
Possible Scurvy
Possible Thalassaemia

Skeletal ID: MB07H1M9

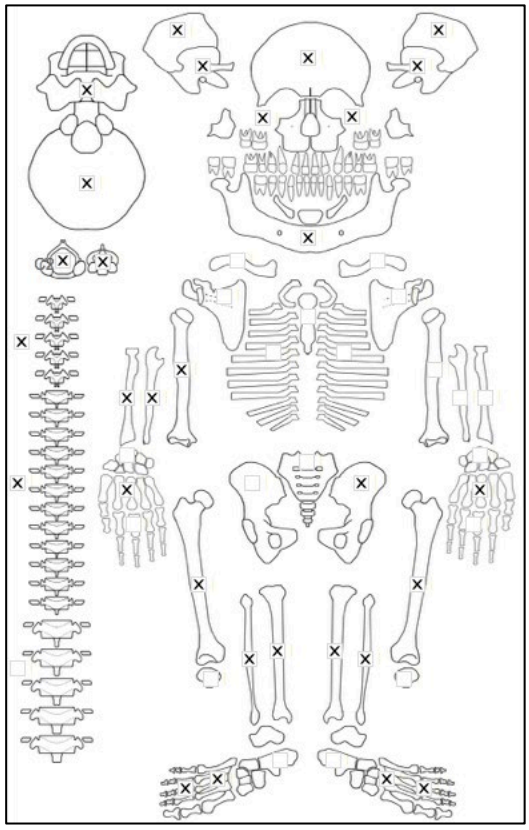

Completeness: Partially Complete (50 to 66%). 63% long bones, 33% hands and feet, 38% vertebrae, 88% neurocranium and ribs fragmented.
Preservation/ Taphonomy: Surfaces well preserved but long bone ends are missing.
Age: 20-29, *Young Adult*
Sex: Male
Macroscopic Lesion Summary:
- Localised circular rounded and thick deposit of remodelled bone consistent with a button osteoma on the lateral left ramus of the mandible
- Abnormal enlargement of the occipital protuberance, the protuberance is also accompanied by a vertical crest continuing inferiorly consistent with developmental abnormalities at the closure of the pars supra occipitalis. The abnormal protuberance is also slanted to the lateral right. The occipital bone is exceptionally thick at this region.
- Severe atrophy of the cortex and internal trabecular bone of the right humerus, radius and ulna (left missing) and the tibiae, fibulae and femora involving the entirety of the preserved bone. The bones are also considerably and abnormally shorter. Consistent with long term non- use of the limbs.
- Severe atrophy of the shafts of multiple proximal and distal phalanges of the feet. Including a left and right possible 4th proximal phalanx, unsided possible 3rd phalanx, left and right possible 2nd proximal phalanx and left and right possible 1st, 4th and 5th distal phalanges.
- The possible unsided 3rd pedal phalanx has an expanded foramen on the plantar aspect.
- Severe atrophy of the shafts of 4 unsided and unidentified metatarsals (2 to 5), no identifiable elements for siding.
- Severe atrophy of the shafts of 8 left and right metacarpals (2 to 5). Disfigurement (anterior- posterior compression) of the proximal end of one of the metacarpals (unsided and unidentified due to level of atrophy). Some with curvature of the shafts.
- Severe atrophy of the shafts and distal end of a proximal hand phalanx, the atrophy is more severe anterior posteriorly. 2 other unsided proximal phalanges appear shortened but do not present with severe shaft atrophy.
- Thinning and abnormal reduction in size of the ilium (only left side preserved).
- Bilateral remodelled mild cribra orbitalia
- Ankylosis of the preserved cervical and thoracic neural arches (minimum 14 ankylosed). Further ankylosis of the lumbar vertebrae, but too fragmented to determine more detail. C1 to 4 minimum are completely fused

including body and neural arches. Probable spinal constriction at the C2 to 3, some rotation and complete ankylosis. The C1 is fused rotated right laterally in relation to the C2 and subsequent spine. A portion of the occipital condyle is fused to the right superior articular facet of the superior C1 (atlanto-occipital fusion). C2 to C3 fused by vertebral body, articular facets, and across the lamina. Possible ossified connective tissue connecting anteriorly from the C2 dens to the C1. Recording consistent with description by Oxenham et.al in 2009.
- Remodelled diffuse porosity consistent with porotic hyperostosis across the superior and posterior parietals and the occipital planum
Radiographic Lesion Summary:
No radiographs taken
Differential Diagnosis Outcome:
Klippel-Feil Syndrome (see Tilley and Oxenham, 2011).

Skeletal ID: MB07H1M10

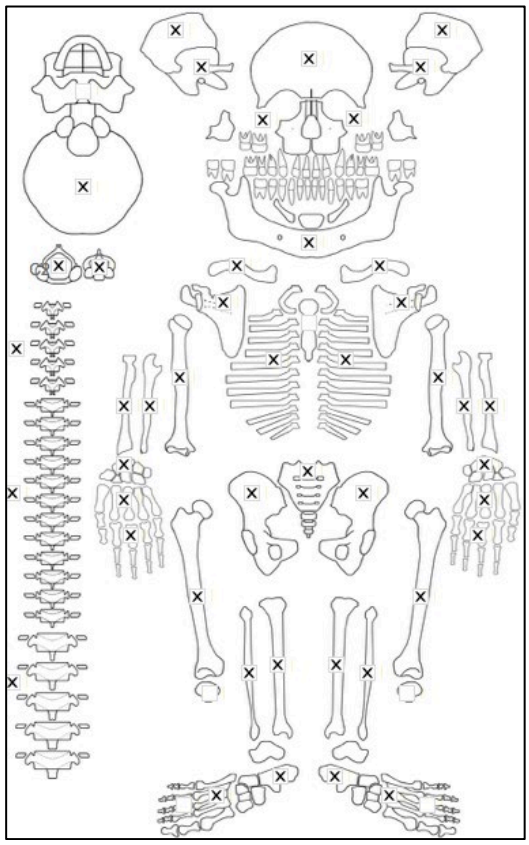

Completeness: Near Complete (60 to 75%). 85% long bones, 63% hands and feet, 63% vertebrae, 75% neurocranium, ribs incomplete.
Preservation/ Taphonomy: Surfaces well preserved but many PM breakages particularly to the axial skeleton.
Age: 40-49, *Middle Aged Adult*
Sex: Male
Macroscopic Lesion Summary:
- unilateral thick remodelled new bone with slight cortical expansion on the posterior and later proximal to middle third of the left femur.
Radiographic Lesion Summary:
No radiographs taken
Differential Diagnosis Outcome:
No diagnosis

Skeletal ID: MB07H1M11

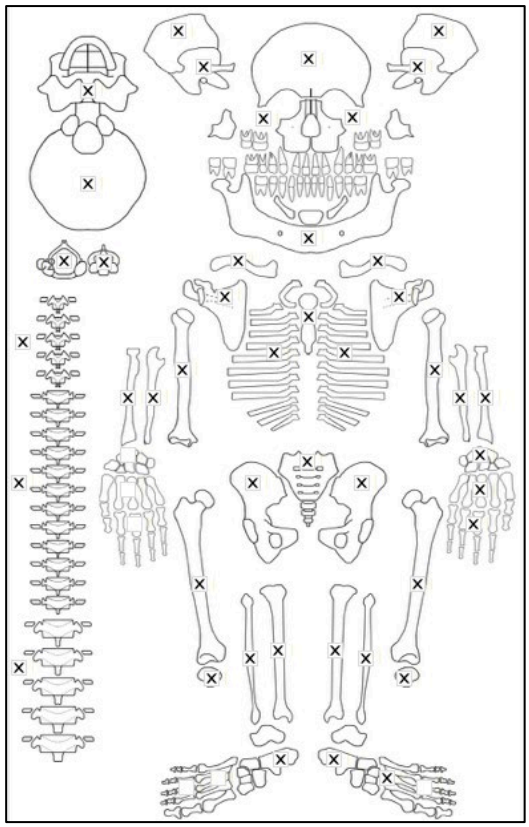

Completeness: Complete (>75%). 97% long bones, 38% hands and feet, 100% vertebrae, 88% neurocranium, ribs partially complete.
Preservation/ Taphonomy: Surfaces excellently preserved and most bones intact.
Age: 50+, *Old Adult*
Sex: Female
Macroscopic Lesion Summary:
- bilateral mixed active and remodelled cortical porosity and new bone on the external greater wings and pterygoid plates of the sphenoid, with continuation along the superior margin of the zygomatic arch and external auditory canal of the temporal squama. Right pterygoid fossa also affected (left missing)
- remodelled diffuse new bone and cortical porosity with abnormal vascular impressions on the endocranium of the frontal, parietals and superior occipital squama
- bilateral symmetrical discrete deposit of mixed active and remodelled new bone on the lateral margin of the anterior zygomatic bones
- bilateral symmetrical discrete deposit of mixed active and remodelled new bone on palatal surfaces of the maxillae

Radiographic Lesion Summary:
No radiographs taken
Differential Diagnosis Outcome:
Probable Scurvy

Skeletal ID: MB07H1M12

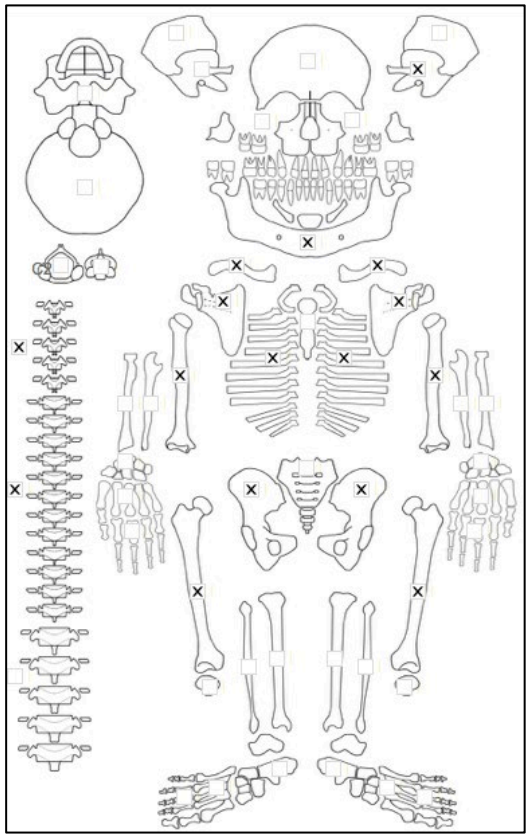

Completeness: Fragmented. 22% long bones, 0% hands and feet, 25% vertebrae, 13% neurocranium, ribs partially complete.
Preservation/ Taphonomy: Many PM breakages but the surfaces are well preserved.
Age: 0 years, *Infant*
Sex: Indeterminate
Macroscopic Lesion Summary:
- Diffuse active new bone across all aspect of the left pars lateralis, left temporal and other identified cranial bones, associated with diploic thickening. There is no porosity of the outer table identified, but the cranium is heavily fragmented.
- Discrete active new bone and cortical porosity on the left medial coronoid process of the mandible (left side missing)
- Bilateral diffuse active new bone across the entire surfaces of the scapulae and pelvic bones associated with marked expansion of the trabecular bone and increase in thickness of the bones as a result. Cortex appears to remain thin but layered on the subperiosteal surfaces.
- Bilateral diffuse active very thick new bone deposit with endosteal expansion apparent in the postmortem breakages of the clavicles, humeri (proximal third humeri are reminiscent of Erlenmeyer flask deformity), ribs and femora. Bones are thick compared to bones of a similar aged infant (05MBM7).
Radiographic Lesion Summary:
Alteration of the trabecular structures in the ilia and the scapulae
Loss of distinction between cortex and medullary canal of the humeri and the femora
Thick temporal squama and apparent marrow hyperplasia but this is not resulting in macroscopic ectocranial porosity
Differential Diagnosis Outcome:
Possible Scurvy
Possible Thalassaemia

Skeletal ID: MB07H1M13a

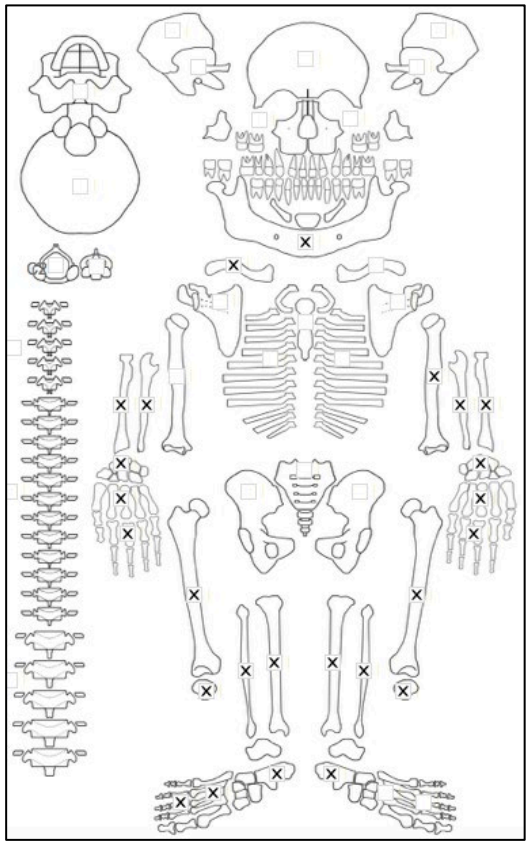

Completeness: Incomplete (33 to 50%). 58% long bones, 64% hands and feet, 4% vertebrae, 0% neurocranium.
Preservation/ Taphonomy: Surfaces well preserved. Some PM breakages of the axial skeleton and flat bones.
Age: 40-49, *Middle Aged Adult*
Sex: Indeterminate
Macroscopic Lesion Summary:
- bilateral symmetrical mixed active and remodelled cortical porosity on the temporal squama superior to the zygomatic arch and auditory canal
Radiographic Lesion Summary:
No radiographs taken
Differential Diagnosis Outcome:
No diagnosis

Skeletal ID: MB07H2M1

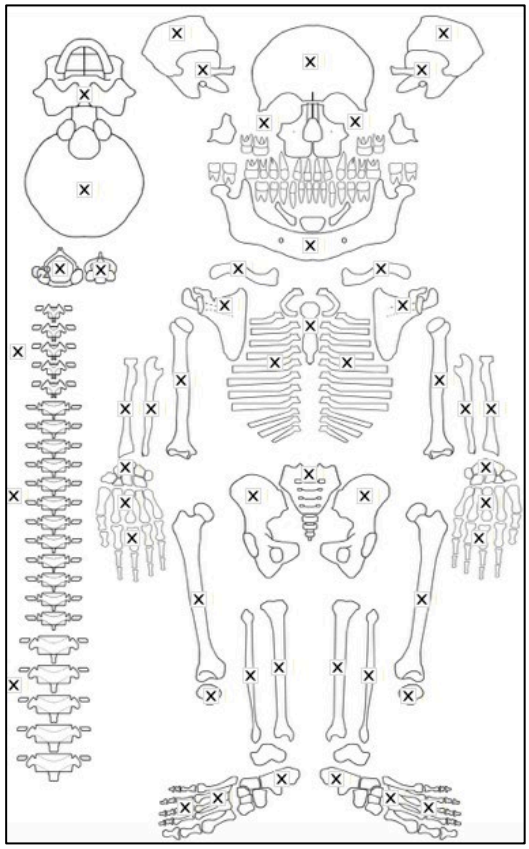

Completeness: Complete (>75%). 95% long bones, 87% hands and feet, 100% vertebrae, 88% neurocranium, ribs complete.
Preservation/ Taphonomy: Surfaces excellent preserved. Basioccipital missing other most bones intact.
Age: 40-49*, Middle Aged Adult*
Sex: Male
Macroscopic Lesion Summary:
- unilateral remodelled vascular impressions on the posterior right maxilla
- bilateral symmetrical mixed active and remodelled cortical porosity on the temporal squama superior to the zygomatic arch and auditory canal
- bilateral symmetrical marked remodelled new bone and cortical porosity on the palatal surfaces of the maxillae
- bilateral symmetrical mixed active and remodelled new bone and cortical porosity on the lateral margin of the anterior zygomatic bones.
- bilateral symmetrical remodelled localised bone deposits on the proximal third medial femora, lateral distal third tibiae and medial distal third fibulae
- remodelled diffuse new bone with possible vascular impressions on the superior margin of the costal grooves of preserved middle to lower ribs
- remodelled oval lytic defect on the proximal third visceral surface of the right 12th rib. This is not associated with new bone response. Margins are well rounded. lesion diameter: 8.20x4.38mm
Radiographic Lesion Summary:
No radiographs taken
Differential Diagnosis Outcome:
Probable Scurvy

Skeletal ID: MB07H2M2

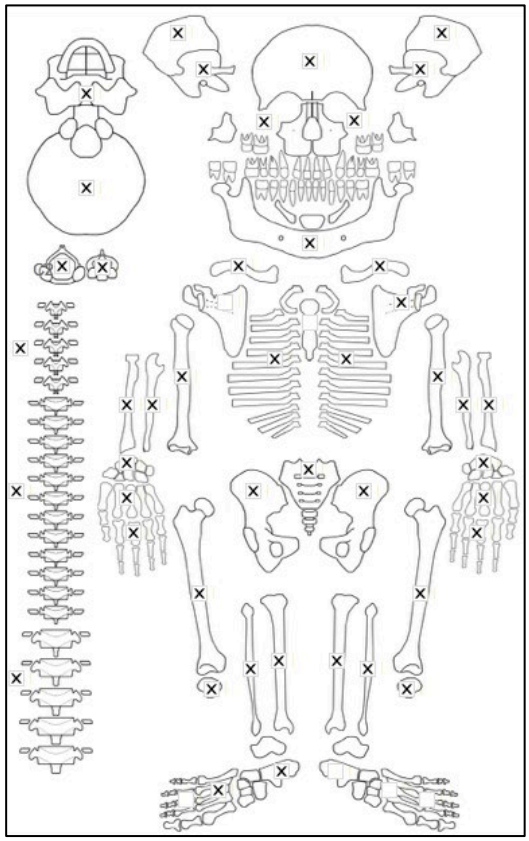

Completeness: Complete (>75%). 100% long bones, 58% hands and feet, 96% vertebrae, 88% neurocranium, ribs incomplete.
Preservation/ Taphonomy: Ribs, cervical and thoracic spine caked in soil concretions and many surfaces unobservable. Unaffected surfaces are well preserved.
Age: 15 years (+/- 3 years), *Adolescent*
Sex: Indeterminate
Macroscopic Lesion Summary:
- bilateral active moderate cribra orbitalia
- mild remodelled porotic hyperostosis of the superior parietals, medial to the temporal line
- active discrete new bone on the posterior right maxilla (left side missing)
- bilateral mixed active and remodelled new bone and cortical porosity on the palatal surfaces of the maxillae.
- bilateral symmetrical discrete mixed active and remodelled new bone superior to the medial epicondyle on the medial and anterior aspects of the humeri
- bilateral symmetrical discrete mixed active and remodelled cortical porosity inferior to the radial notch of the ulnae
- bilateral symmetrical discrete active new bone on the superior and posterior femoral necks
- bilateral symmetrical diffuse mixed active and remodelled new bone on the proximal 2/3rds of the posterior (around the linea aspera), medial and lateral aspects of the femora
- deep endochondral porosity exceeding 10mm from the metaphyseal plates of the proximal humeri, distal radii, ulnae and femora, and proximal and distal tibiae and fibulae.
- bilateral symmetrical discrete active new bone and cortical porosity on the medial coronoid processes of the mandible
- bilateral symmetrical discrete active new bone on the lateral rami inferior to the mandibular notch
Radiographic Lesion Summary:
- ground glass osteopenia
Differential Diagnosis Outcome:
Anaemia
Probable Scurvy

Skeletal ID: MB07H2M3

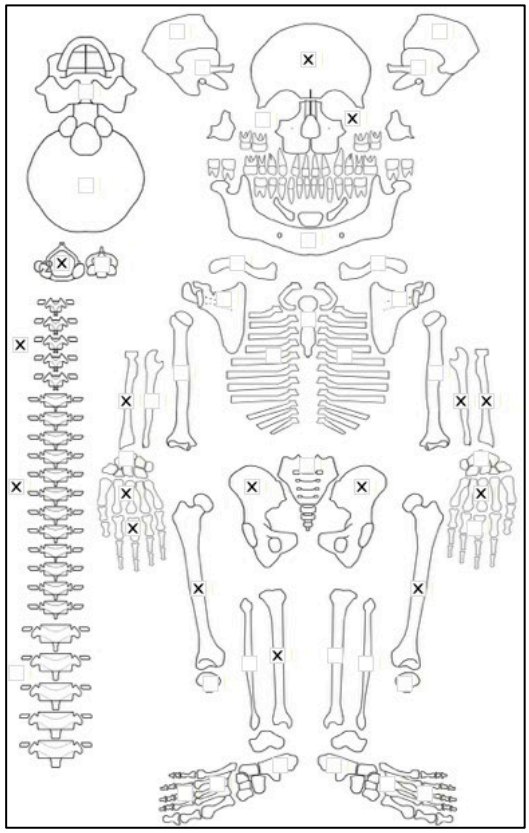

Completeness: Incomplete (33 to 50%). 44% long bones, hands and feet bones not counted but hands are well preserved, 38% vertebrae, 13% neurocranium.
Preservation/ Taphonomy: Surfaces well preserved.
Age: 0 years, *Infant*
Sex: Indeterminate
Macroscopic Lesion Summary:
- abnormal endochondral porosity extending beyond 10mm from the metaphyseal plate of the distal radii, proximal and distal femora, and the proximal and distal right tibia (left side missing)
- diffuse active new bone across the medial left tibial shaft (right side missing)
- mixed active and remodelling new bone and cortical porosity on the inferior right pars lateralis (left side missing)
- active cortical porosity across the anterior and posterior left zygomatic bone (right side missing)
- enlarged bony defect with a sinus like channel on the medial aspect of the right superior eye orbit (left side missing) at the point of the metopic suture. This may be a developmental defect.
Radiographic Lesion Summary:
No distinct changes observed.

Differential Diagnosis Outcome:
Possible Scurvy

Skeletal ID: MB07H2M5

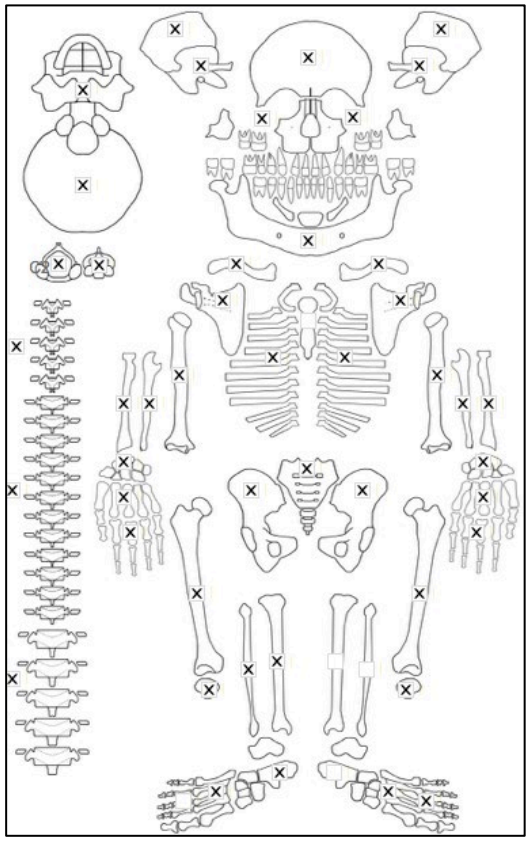

Completeness: Complete (>75%). 80% long bones, 56% hands and feet, 92% vertebrae, 100% neurocranium and ribs complete.
Preservation/ Taphonomy: Surfaces well preserved. Fragmentation of the lower leg and scapular bodies.
Age: 20-29, *Young Adult*
Sex: Female
Macroscopic Lesion Summary:
- bilateral remodelled moderate cribra orbitalia
Radiographic Lesion Summary:
No radiographs taken
Differential Diagnosis Outcome:
Anaemia

Skeletal ID: MB07H2M6

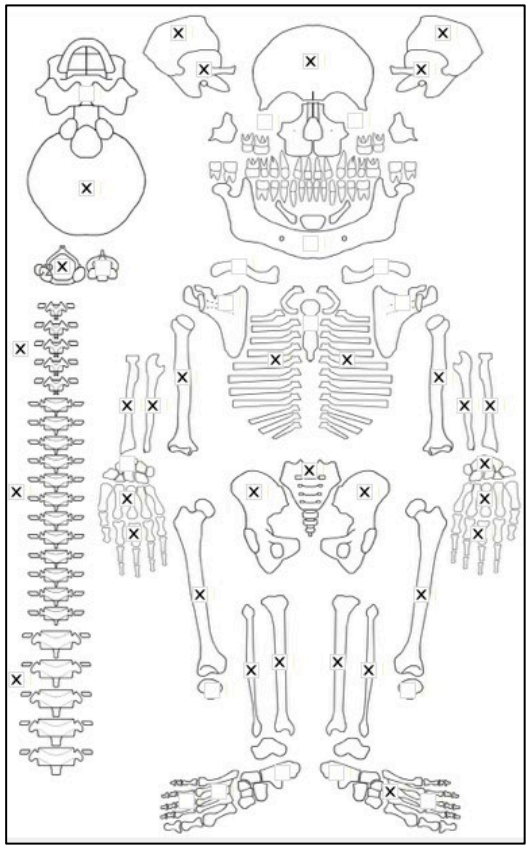

Completeness: Complete (>75%). 97% long bones 41% hands and feet, 67% vertebrae, 75% neurocranium, ribs complete.
Preservation/ Taphonomy: Basiocranium and sphenoid bone missing. Surfaces well preserved.
Age: 2 years (+/- 6 months), *Child*
Sex: Indeterminate
Macroscopic Lesion Summary:
- abnormal endochondral porosity exceeding 10mm from the metaphyseal plate of the distal femora, proximal tibiae and proximal fibula. This is associated with mild cupping on the distal femur, proximal tibiae and distal fibulae.

Radiographic Lesion Summary:
- Ground glass osteopenia
- white line of Fraenkel and Trummerfeld zones
- pelkan spur of distal right femur
- clear coarsened trabeculae
- lateral bending deformities of the distal third shafts are visible on the radiographs

Differential Diagnosis Outcome:
Probable Scurvy
Probable Rickets

Skeletal ID: MB07H2M7

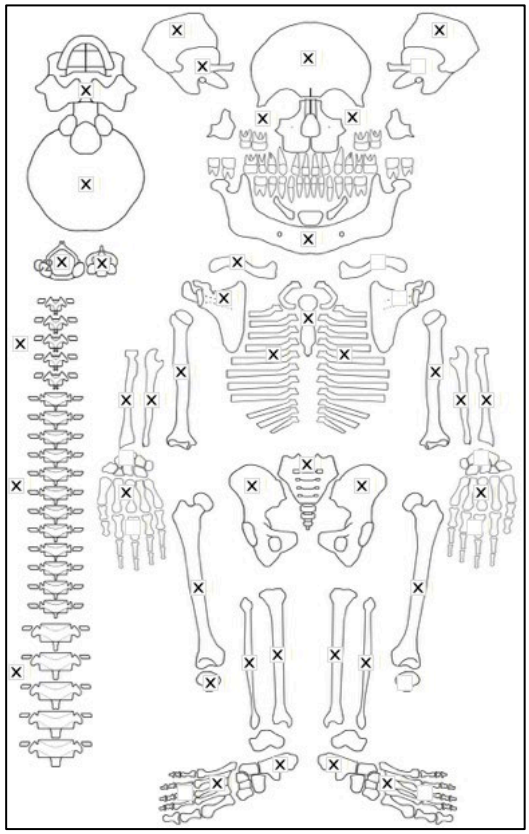

Completeness: Complete (>75%). 72% long bones, 31% hands and feet, 100% vertebrae, 75% neurocranium, ribs complete.
Preservation/ Taphonomy: Some of the spine is unobservable due to soil concretions. Other surfaces excellently preserved. Most bones intact.
Age: 1.5 years (+/- 6 months), *Child*
Sex: Indeterminate
Macroscopic Lesion Summary:
- diffuse mixed active and remodelling new bone and cortical porosity across the squama of the right temporal, concentrated on the superior margin of the external auditory canal (left temporal missing)
- diffuse mixed active and remodelling new bone on the endocranial right temporal squama adjacent to the petrous bone (left temporal missing)
- discrete bilateral active new bone and cortical porosity on the zygomatic processes of the frontal
- discrete bilateral active new bone and cortical porosity on the superior orbits. There may also be mild cribra orbitalia.
- discrete active new bone and cortical porosity on the inferior pars basilaris
- bilateral symmetrical discrete active new bone and cortical porosity on the posterior zygomatic bones.
- bilateral symmetrical discrete mixed active and remodelled new bone and cortical porosity on the anterior maxillae extending from the infraorbital foramen
- bilateral symmetrical discrete active new bone and cortical porosity on the palatal surfaces of the maxillae
- discrete active new bone and cortical porosity on the lateral and posterior left maxilla (right not preserved)
- bilateral symmetrical discrete active new bone and cortical porosity on the medial coronoid processes of the mandible
- bilateral symmetrical discrete mixed active and remodelled new bone and cortical porosity on the incisive fossae of the mandible
- discrete mixed active and remodelled new bone and cortical porosity on the supraspinous fossa of the right scapula (left side missing)
- abnormal vertebral porosity on the anterior aspect of 3 lumbar vertebrae
- bilateral abnormal endochondral porosity exceeding 10mm from the metaphyseal plate of the proximal humeri, distal femora, proximal and distal tibiae and proximal and distal fibulae. Associated with mild cupping of the distal femurs and proximal tibiae, may be within normal range

- bilateral symmetrical diffuse active bone across medial aspect of the middle to distal third shafts of the tibiae
- bilateral circumferential expansion of 1 right and 1 left middle rib costal end, other rib ends unaffected

Radiographic Lesion Summary:
- white line of Fraenkel and Trummerfeld zones
- ground glass osteopenia
- pelkan spur of the medial distal femora
- coarsened trabeculae

Differential Diagnosis Outcome:
Probable Scurvy
Probable Rickets

Skeletal ID: MB07H2M8

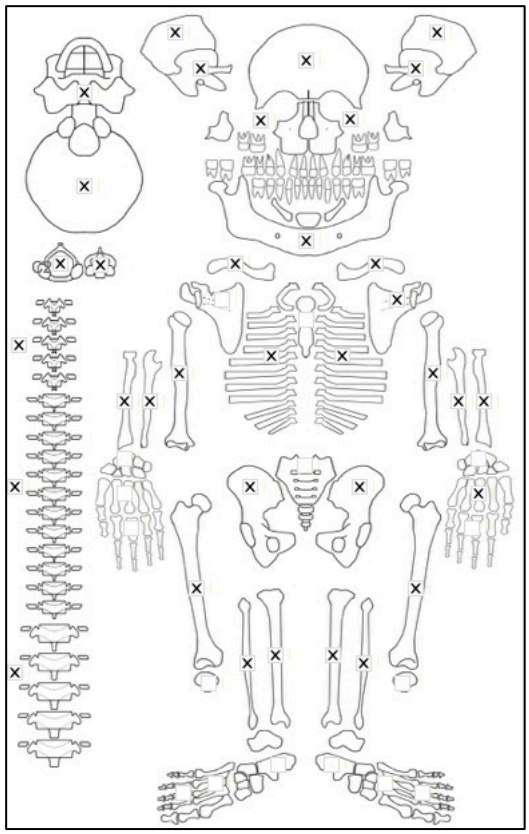

Completeness: Complete (>75%). 100% long bones, 5% hands and feet, 100% vertebrae, 88% neurocranium, ribs complete.
Preservation/ Taphonomy: Surfaces well preserved and bones mostly intact.
Age: 1.5 years (+/- 6 months), *Child*
Sex: Indeterminate

Macroscopic Lesion Summary:
- bilateral discrete active new bone and cortical porosity
- bilateral discrete active and remodelled new bone and cortical porosity on the posterior parietals
- Lewis Grade 3 (capillary formations) diffuse active new bone on the endocranial occipital squama around the cruciform eminence.
- mixed diffuse active and remodelled new bone and cortical porosity on the temporal squama, right external greater wing of sphenoid including the pterygoid plates and fossae.
- bilateral symmetrical discrete active bone around the left foramen rotundum on the endocranial sphenoid
- bilateral symmetrical discrete mixed active and remodelling new bone and cortical porosity on the posterior zygomatic bones
- bilateral symmetrical discrete mixed active and remodelling new bone and cortical porosity on the posterior, lateral, superior, and anterior (around the region of the infraorbital foramen) with vascular impressions on the anterior and posterior aspects.

- bilateral symmetrical discrete active new bone and cortical porosity on the palatal surfaces of the maxillae
- bilateral symmetrical discrete mixed active new bone and cortical porosity on the incisive fossae of the mandible
- bilateral symmetrical discrete mixed active new bone and cortical porosity in the olecranon fossae of the humeri
- bilateral mixed active and remodelled diffuse new bone on all aspects of the shafts and metaphyses of the femora with vascular impressions, including on the superior and posterior femoral necks.
- cupping of the distal metaphyseal plates of the femora
- bilateral mixed active and remodelled diffuse new bone on the lateral and posterior aspects of the tibial shafts with vascular impressions
- enlarged foramina on the posterior tibiae
- maxillary and frontal sinuses appear normal
- abnormal deep endochondral porosity exceeding 10mm from the proximal tibial and distal femoral metaphyseal plates
- discrete mixed active new bone and cortical porosity on the inferior pars basilaris

Radiographic Lesion Summary:
- white line of Fraenkel, Trummerfeld zone
- ground glass osteopenia but also coarsening of some of the trabeculae

Differential Diagnosis Outcome:
Probable Scurvy
Possible Rickets

Skeletal ID: MB07H2M9

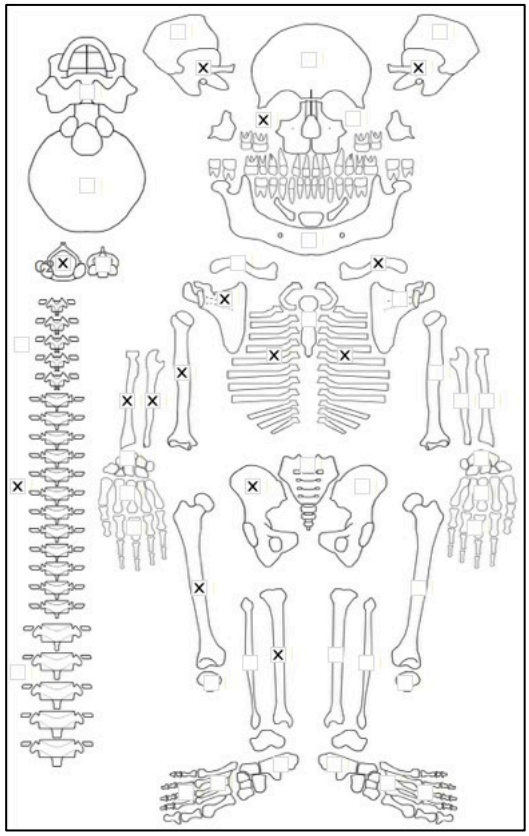

Completeness: Incomplete (33 to 50%). 33% long bones, 0% hands and feet, 29% vertebrae, 38% neurocranium, ribs incomplete.
Preservation/ Taphonomy: Surfaces well preserved. Cranium is largely present but many fragments unidentifiable. Right femur proximal third only, right radius distal half only
Age: 0 years, *Infant*
Sex: Indeterminate
Macroscopic Lesion Summary:

- diffuse active new bone across the squama of the temporal and external right greater wing of the sphenoid and anterior right lesser wing (left side missing)
- discrete active new bone and cortical porosity on the inferior pars basilaris and right pars lateralis (left missing)
- discrete active new bone and cortical porosity on the palatal surface, anterior (around the infraorbital foramen) and posterior right maxilla (left missing)
- discrete active new bone and cortical porosity on the posterior left zygomatic (right missing)
- diffuse active new bone across the posterior shaft of the right ulna (left missing)
- diffuse active new bone across the distal half shaft and metaphysis of the right humerus (left missing)
- thick diffuse active new bone without apparent endosteal involvement on the medial shaft of the tibia.
- slight cupping, fraying and flaring of the proximal and some fraying and swelling of the distal end of the tibia
- slight lateral bending deformities at the midshaft of the right humerus and ulna
- abnormal porosity and fraying of a sternal rib end

Radiographic Lesion Summary:
- thick cortex at region of bending deformity

Differential Diagnosis Outcome:
Probable Scurvy
Probable Rickets

Skeletal ID: MB07H2M10

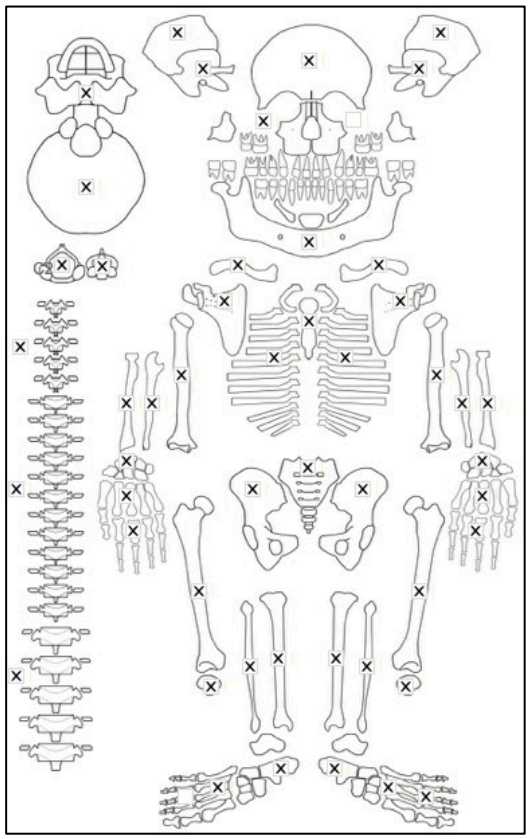

Completeness: Complete (>75%). 100% long bones, 82% hands and feet, 100% vertebrae, 100% neurocranium and ribs complete.
Preservation/ Taphonomy: Surfaces excellently preserved. Partial PM breakages of scapulae, and missing facial bones, otherwise bones intact.
Age: 30-39, *Middle Aged Adult*
Sex: Male
Macroscopic Lesion Summary:
- unilateral diffuse new bone on the lateral posterior distal half of the right ulna
- bilateral symmetrical remodelled new bone on the medial margin of the linea aspera on the posterior middle third of the femora

- bilateral symmetrical diffuse remodelled new bone on all aspects of the shafts of the tibiae. The lesions are more marked on the lateral midshaft
- bilateral symmetrical diffuse mixed active and remodelled new bone on the medial distal third shafts of the fibulae
- bilateral symmetrical remodelled new bone on the lateral proximal third shafts of the fibulae
- bilateral symmetrical remodelled new bone with apparent vascular impressions on the superior margins of the costal grooves of middle ribs
- remodelled porotic hyperostosis across the superior frontal, superior and posterior parietals (medial to the temporal line) and occipital squama
- remodelled new bone and cortical porosity on the palatal surface of the right maxilla (left missing)
- bilateral remodelled new bone around the condylar foramina on the inferior occipital

Radiographic Lesion Summary:
Radiographs not taken
Differential Diagnosis Outcome:
Anaemia
Possible Scurvy

Skeletal ID: MB07H2M12

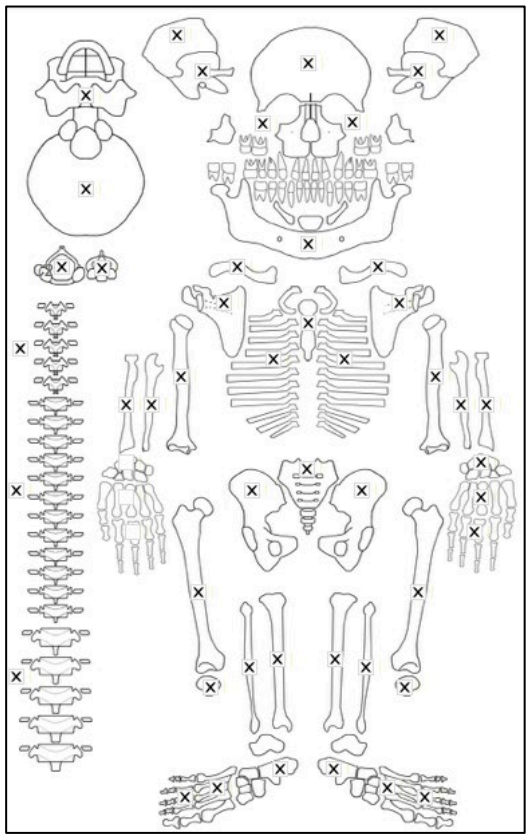

Completeness: Complete (>75%). 92% long bones, 62% hands and feet, 96% vertebrae, 88% neurocranium, ribs partially complete.
Preservation/ Taphonomy: Intrusive right zygoma. Surfaces well preserved.
Age: 50+, *Old Adult*
Sex: Female
Macroscopic Lesion Summary:
- slight lateral bending deformity at the midshaft of the right humerus, there is an oblique fracture of the midshaft of the left ulna which means the right humerus may be a result of trauma.

Radiographic Lesion Summary:
No radiographs taken
Differential Diagnosis Outcome:
No diagnosis.

Skeletal ID: MB07H2M13

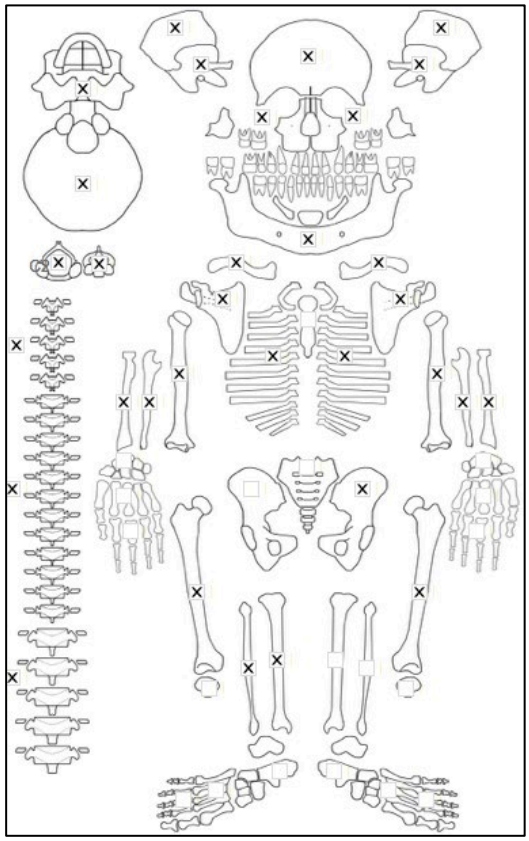

Completeness: Complete (>75%). 67% long bones, 5% hands and feet, 92% vertebrae, 88% neurocranium, ribs complete.
Preservation/ Taphonomy: Surfaces excellently preserved and bones mostly intact.
Age: 4 years (+/- 9 months), *Child*
Sex: Indeterminate
Macroscopic Lesion Summary:
- bilateral symmetrical discrete remodelled new bone deposit with cortical porosity of the superior orbits
- discrete mixed active and remodelled new bone deposit with cortical porosity on the external pterygoid bone of the left greater wing of the sphenoid (right side missing)
- bilateral symmetrical discrete mixed active and remodelled new bone deposit with cortical porosity on posterior maxillae
- bilateral symmetrical discrete remodelled new bone deposit with cortical porosity on incisive fossae of the mandible
- bilateral symmetrical discrete remodelled new bone deposit with the presence of vascular impressions on the mylohyoid lines of the mandible
- bilateral symmetrical discrete mixed active and remodelled new bone deposit on the medial coronoid processes of the mandible
- bilateral symmetrical discrete mixed active and remodelled new bone deposit with cortical porosity on palatal surfaces of the maxillae
- abnormal large vertebral porosity of 10 upper middle and lower thoracic and all 5 lumbar anterior vertebral bodies. Margins are sharp and appear to be erythropoietic activity.
- unilateral discrete remodelled haematoma-like deposit of new bone on the posterior olecranon of the proximal right ulna
- bilateral abnormal endochondral porosity exceeding more than 10mm from the proximal metaphyseal plate of the humeri, proximal and distal left tibia and fibula (right tibia missing), and proximal and distal femora. The distal femora and proximal left tibia is associated with mild cupping of the metaphyseal plate.
- bilateral symmetrical discrete remodelled new bone deposit with cortical porosity on supraspinous fossae of the scapulae
- mixed active and remodelled diffuse new bone across the medial shaft of the left tibia (right tibia missing)
- deep depression of the acetabular surface of the left ilium (right not preserved)
Radiographic Lesion Summary:

- White line of Fraenkel and Trummerfeld zones of the long bones (thick dense zone)
- Ground glass osteopenia with regions of coarsened trabeculae

Differential Diagnosis Outcome:
Probable Scurvy
Possible Rickets

Skeletal ID: MB07H2M14

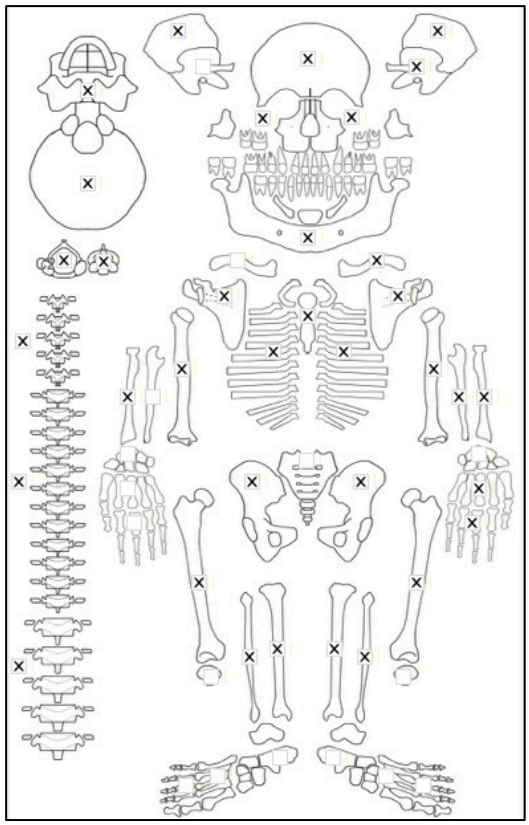

Completeness: Near Complete (66 to 75%). 75% long bones, 17% hands and feet, 67% vertebrae, 75% neurocranium, ribs partially complete.
Preservation/ Taphonomy: Surfaces well preserved. PM breakage of ribs and scapulae.
Age: 0 years, *Infant*
Sex: Indeterminate

Macroscopic Lesion Summary:
- diffuse layered, spiculated and porous new bone across the entire ectocranial surfaces of the parietals, left temporal (right missing), occipital, and the sutural margins of the frontal.
- cranial plates are markedly thin
- discrete active new bone and cortical porosity on the superior and inferior pars basilaris
- active new bone on the endocranial petrous process of the left temporal (right missing).
- bilateral symmetrical active new bone on the external greater wings of sphenoid, pterygoid fossa and plates
- bilateral symmetrical active new bone and cortical porosity on the posterior maxillae
- bilateral symmetrical active new bone and cortical porosity on the posterior and superior zygomatic bones.
- bilateral symmetrical active new bone and cortical porosity on the medial coronoid processes of the mandible
- bilateral symmetrical active new bone on the mylohyoid lines of the mandible
- bilateral symmetrical active new bone and cortical porosity posterior to the oblique lines of the mandible
- bilateral symmetrical active new bone and cortical porosity on the incisive fossae of the mandible
- active new bone on the inferior mandibular body.
- bilateral symmetrical active new bone on the supraspinous fossae and posterior aspects of the spines of the scapulae
- diffuse new bone on the anterior left clavicle shaft (right missing)
- bilateral symmetrical diffuse layered active new bone with endosteal expansion and medullary constriction (as seen in post mortem break) of the shafts and metaphyses of the humeri.

- fraying and porosity of the proximal metaphyses of the humeri
- diffuse active new bone across all aspects of the proximal two-thirds metaphysis and shaft of the left ulna (right missing)
- bilateral symmetrical diffuse new bone on the lateral shafts of the radii
- swelling and fraying/porosity of left and right costal rib ends
- diffuse active new bone on the metaphyses and shafts of the femora. The new bone appears poorly mineralised.
- fraying of the distal ends and porosity of the proximal and distal ends that are not reminiscent of endochondral porosity in scurvy.
- fraying of the distal ends and porosity of the proximal ends of the tibiae (distal ends damaged). Metaphyseal plate of the right tibia is characteristically 'velvet' in appearance.
- Slight anterior bending deformity of the left tibia (right is incomplete)
- bilateral symmetrical diffuse active layered new bone on the medial, anterior and posterior shafts of the tibiae with the new bone most marked on the medial aspect. New bone appears poorly mineralised.
- bilateral symmetrical diffuse active layered new bone on the lateral and anterior distal two-thirds of the shafts of the fibulae
- bilateral symmetrical layered new bone on the superior orbital roofs

Radiographic Lesion Summary:
- Thick white line of Fraenkel and Trummerfeld zone
- Thick cortex

Differential Diagnosis Outcome:
Probable Scurvy
Probable Rickets

Skeletal ID: MB07H2M15

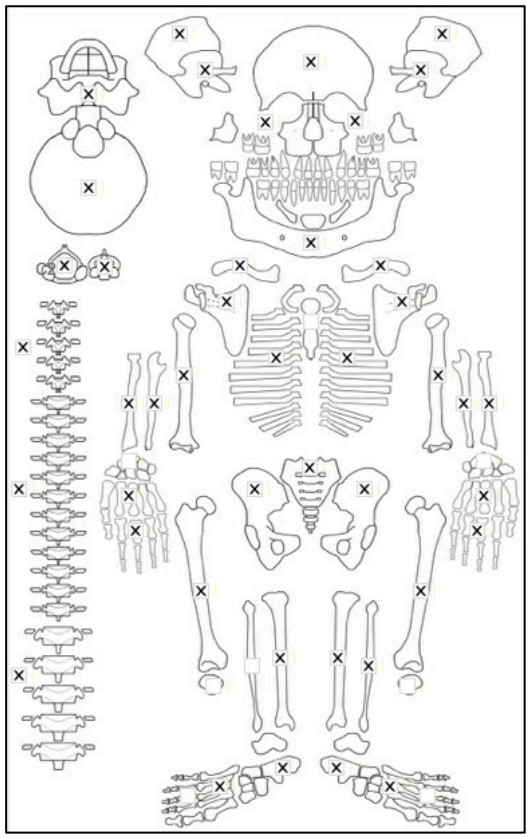

Completeness: Complete (>75%). 89% long bones, 32% hands and feet, 75% vertebrae, 88% neurocranium, ribs near complete.
Preservation/ Taphonomy: Surfaces well preserved, and bones mostly intact except for fragmented basioccipital.
Age: 4 years (+/- 9 months), *Child*
Sex: Indeterminate

Macroscopic Lesion Summary:
- diffuse remodelled new bone across the endocranium with Lewis Grade 3 capillary formations including the frontal, parietals and superior to the cruciform eminence of the occipital
- bilateral cortical porosity on the temporal squama on the superior margin of the zygomatic arch and auditory canal. However the left side is remodelled the right side is active and associated with active new bone.
- bilateral mixed active and remodelled discrete deposit of new bone and cortical porosity on the posterior maxillae and zygomatic bones associated with vascular impressions
- mixed active and remodelled discrete deposit of new bone on the right zygomatic process of the frontal inferior to the temporal line (left side missing)
- bilateral moderate cribra orbitalia
- bilateral symmetrical active new bone and cortical porosity on the palatal surfaces of the maxillae
- bilateral symmetrical remodelled new bone with vascular impressions on the inferior pars laterali
- mixed discrete active new bone and cortical porosity in the inferior pars basilaris
- bilateral symmetrical discrete deposit of remodelled new bone as identified through the presence of vascular impressions inferior to the left mylohyoid line of the mandible
- bilateral symmetrical discrete deposit of mixed active and remodelled new bone and cortical porosity on the supraspinous fossae of the scapulae
- deep abnormal vertebral trabecular porosity on the anterior and lateral vertebral bodies of 4 mid to lower thoracic and 1 lumbar body
- bilateral and symmetrical thick deposit of mixed active and new bone with endosteal expansion on the palmar, medial and lateral surfaces of the metacarpals 2-5 and entire shaft of mc1. Expansion of foramen on the left mc4, left mc5, and right mc5 is associated with the inflammatory changes to the metacarpal shaft.
- depression of the femoral necks and cupping of the distal metaphyseal plates of the femora
- Deep vascular impressions on the posterior distal metaphyses of the femora and posterior proximal tibiae may suggest well remodelled new bone in the region.
- slight cupping of the proximal distal metaphyseal plates of the tibia
- remodelled haematoma like new bone deposit on the anterior distal third shaft of the left fibula (right missing)

Radiographic Lesion Summary:
- Wimberger's ring sign of the proximal tibial epiphyses
- white line of Fraenkel and Trummerfeld zone
- ground glass osteopenia

Differential Diagnosis Outcome:
Anaemia
Probable Rickets
Probable Scurvy

Skeletal ID: MB07H2M16

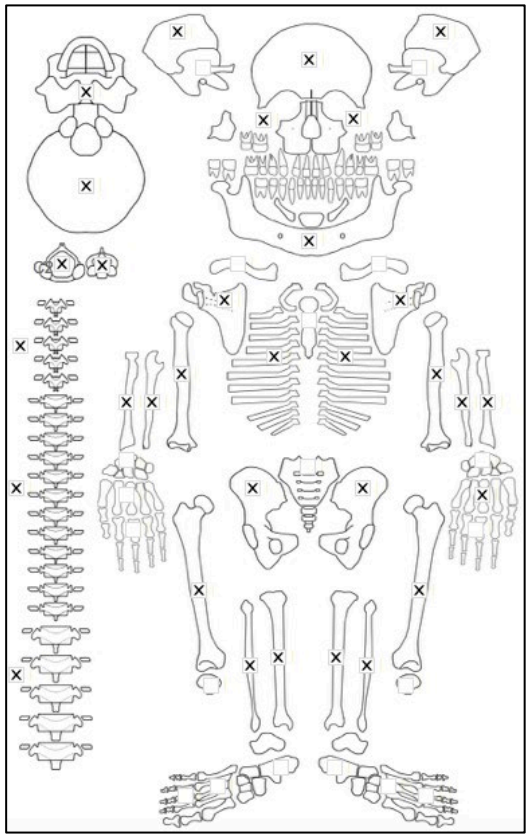

Completeness: Complete (>75%). 81% long bones, 4% hands and feet, 96% vertebrae, 75% neurocranium, ribs complete.
Preservation/ Taphonomy: Surfaces excellently preserved and most bones intact.
Age: 1.5 years (+/- 6 months), *Child*
Sex: Indeterminate
Macroscopic Lesion Summary:
- bilateral moderate cribra orbitalia
- bilateral mixed active and remodelled cortical porosity on the zygomatic processes of the frontal, inferior and following the contours of the temporal line
- mixed active and remodelled cortical porosity on an unsided temporal squama fragment
- bilateral mixed active and remodelled cortical porosity on the anterior maxillae around the regions of the infraorbital foramina
- bilateral active discrete new bone and cortical porosity on the posterior maxillae
- bilateral mixed active and remodelled discrete new bone and cortical porosity on the palatal surfaces of the maxillae
- bilateral mixed active and remodelled cortical porosity on the posterior zygomatic bones
- bilateral mixed active and remodelled discrete new bone and cortical porosity on the incisive fossae of the mandible
- bilateral mixed active and remodelled cortical porosity inferior to the lateral mandibular notches
- bilateral mixed active and remodelled new bone and cortical porosity on the medial aspect of the coronoid processes of the mandible
- unilateral mixed active and remodelled new bone on the lateral proximal third shaft of the right radius.
- abnormal endochondral porosity exceeding 10mm from the proximal metaphyseal plates of the humeri and the distal left femur (right side missing). The distal femur is associated with mild cupping which may be within normal range.
- bilateral mixed active and remodelled cortical porosity around the foramen rotunda and the external pterygoid regions of the greater wings of sphenoid
- remodelled new bone and cortical porosity on the inferior pars basilaris and lateralis (extending laterally from the condyles)
- remodelled new bone and cortical porosity on the supraspinous fossae of the scapulae
Radiographic Lesion Summary:
- pelkan spur of the distal femur

- ground glass osteopenia with some regions of coarsening trabeculae

Differential Diagnosis Outcome:

Anaemia
Probable Scurvy
Possible Rickets

Skeletal ID: MB07H2M17

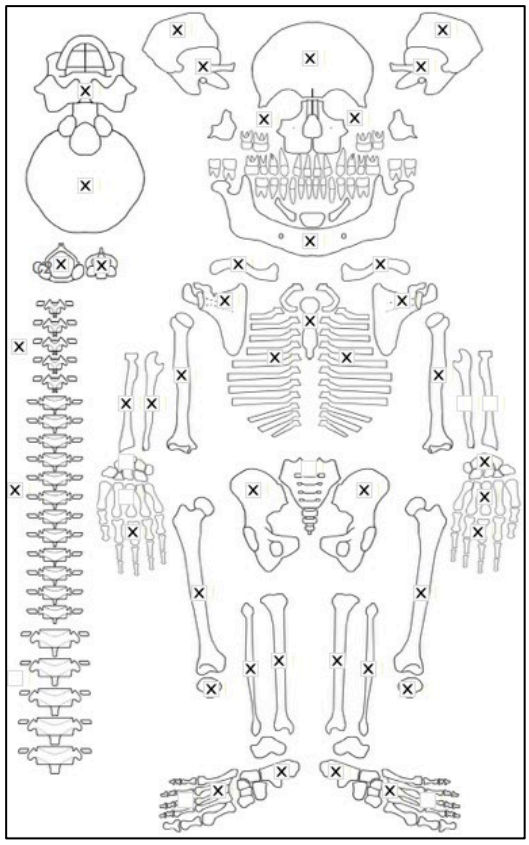

Completeness: Complete (>75%). 83% long bones, 56% hands and feet, 79% vertebrae, 100% neurocranium, ribs partially complete.
Preservation/ Taphonomy: Surfaces well preserved. PM breakage of axial skeleton, scapulae and pelvis.
Age: 13 years (+/- 2 years), *Adolescent*
Sex: Indeterminate
Macroscopic Lesion Summary:
- bilateral remodelling cribra orbitalia (left orbit moderate, right orbit mild)
- bilateral symmetrical remodelled new bone and cortical porosity on the external greater wings of sphenoid and the pterygoid plates and fossae.
- bilateral symmetrical remodelled new bone and cortical porosity on the pars laterali and the pars basilaris
- localised remodelled cortical porosity medial and superior to the superciliary arches
- bilateral remodelled new bone on the superior orbital roofs as indicated by abnormal vascular impressions
- bilateral remodelled symmetrical new bone on the posterior maxillae and zygomatic bones
- bilateral diffuse porosity of unknown aetiology on the posterior parietals (the pattern is consistent with porotic hyperostosis but also of cortical porosity)
- bilateral symmetrical mixed active and remodelled new bone and cortical porosity on the medial coronoid processes of the mandible
- bilateral symmetrical remodelled new bone with vascular impressions inferior to the mylohyoid lines of the mandible
- remodelled new bone and cortical porosity on the posterior mandible directly inferior to the anterior teeth
- bilateral symmetrical active porosity on the supraspinous fossae of the scapulae
- diffuse mixed active and remodelled new bone on the anterior medial and lateral distal shaft and metaphysis of the left humerus (right side missing).

- diffuse mixed active and remodelled new bone across the metaphyses and shaft of the right ulna sparing only the posterior crest. The new bone is more marked around the interosseous crest (left ulna missing)
- deep endochondral porosity exceeding 10mm from the metaphyseal plate on the distal femora
- bilateral mixed active and remodelled diffuse new bone on all aspects of the shaft of the metatarsals. The 5th metatarsals have symmetrical thick layered active new bone on the lateral aspects.
- diffuse mixed active and remodelled new bone across the plantar, medial and lateral aspects of the left metacarpals associated with an expanded foramen of the left mc5 on the medial aspect (right metacarpals missing)
- remodelled discrete deposit of new bone and cortical porosity with vascular impressions on the superior and posterior femoral neck of the left femur (right femoral neck missing)
- bilateral symmetrical diffuse mixed active and remodelled new bone across the posterior, medial and lateral proximal two-thirds shaft of the femora. The new bone is more active towards the midshaft and more marked posteriorly.
- bilateral symmetrical diffuse mixed active and remodelled new bone across the entire shaft of the tibiae. The new bone is more active on the posterior middle third.
- bilateral symmetrical diffuse mixed active and remodelled new bone across the entire shaft of the fibulae sparing only the posterior crests. The new bone is more marked on the interosseous crests.

Radiographic Lesion Summary:
Radiographs not taken
Differential Diagnosis Outcome:
Anaemia
Probable Scurvy

Skeletal ID: MB07H2M18

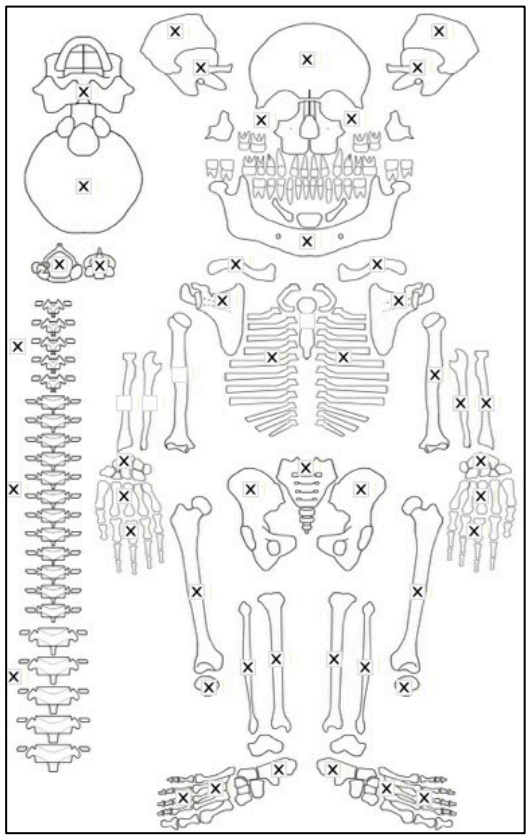

Completeness: Complete (75%). 100% long bones, 80% hands and feet, 92% vertebrae, 100% neurocranium, ribs complete.
Preservation/ Taphonomy: Surfaces excellently preserved except for endocranium that could not be preserved because of soil concretions.
Age: 16 years (+/- 2 years), *Adolescent*
Sex: Female
Macroscopic Lesion Summary:

- Bilateral abnormal vascular impressions in the superior orbits indicating discrete remodelled new bone
- Bilateral remodelled mild cribra orbitalia
- Mostly remodelled porotic hyperostosis across the posterior parietals and occipital planum
- Active moderate porotic hyperostosis on the radial fossa of the anterior left humerus (right cannot be observed)
- Remodelled localised cortical porosity on the posterior left zygomatic (right side missing)
- Bilateral deposit of remodelled new bone and cortical porosity on the palatal surfaces of the maxillae
- Bilateral symmetrical deposit of remodelled new bone and cortical porosity on the medial coronoid processes of the mandible
- Bilateral symmetrical deposit of remodelled new bone indicated by abnormal vascular impressions inferior to the mylohyoid lines of the mandible
- Bilateral symmetrical discrete deposit of remodelled new bone and cortical porosity on the superior-anterior acromial end of the clavicles
- Bilateral symmetrical thick diffuse deposit of active new bone across all aspects of the distal third (with apparent expansion of the distal region) and across the interosseous crest (medial and anteriorly) of the radii.
- Bilateral symmetrical mixed remodelling diffuse new bone on the posterior and lateral aspects of the proximal metaphysis and shaft directly inferior to the heads and mixed remodelling diffuse new bone on all aspects of the distal metaphyses and distal third shaft of the humeri.
- Bilateral mostly active diffuse new bone on all aspects of the ulnae with the exception of the medial shafts
- Bilateral mixed active and remodelled diffuse new bone deposit across the entirety of the femora sparing only the epiphyses. The distal end appears to have endosteal action, new bone thickest on distal end and across the posterior shaft.
- Bilateral remodelled thick diffuse new bone deposit across the entirety of the tibiae, including the non-articular surfaces of distal epiphysis with the exception of the preserved proximal epiphyses with endosteal expansion of the distal end
- Bilateral remodelled thick diffuse new bone deposit across the entirety of the fibulae shafts and metaphyses with endosteal expansion
- Bilateral mixed active and remodelled new bone deposit across the anterior patellae
- Bilateral mixed active and remodelled new bone deposit with endosteal thickening on all aspects except for the dorsal aspects of the metacarpal shafts and metaphyses (the exception is the 1st left metacarpal which also has new bone on the dorsal aspect).
- Unilateral mixed active and remodelled new bone deposit with endosteal thickening on all aspects of the shafts and metaphyses of the left proximal hand phalanx.
- Bilateral mixed active and remodelled new bone deposit without endosteal thickening on the distal third palmar aspects of the 3rd proximal hand phalanges.
- Expanded foramen on the proximal palmar aspect of the 3rd, 4th and 5th intermediate left hand phalanges.
- Diffuse bilateral mixed active and remodelled new bone across all non-articular surfaces of the calcanei, tali and cuboids
- Bilateral mixed active and remodelled new bone deposit with endosteal thickening on all aspects of all the metatarsals. Left 2nd metatarsal includes an abnormally large expansion of the foramen on the lateral aspect proximal region, indicative of intrusion of the infectious process into the foramen.
- Bilateral mixed active and remodelled new bone deposit without endosteal thickening on all aspects of all the 1st pedal proximal phalanges
- Bilateral mixed active and remodelled new bone deposit without endosteal thickening on the proximal thirds of the preserved proximal 2nd to 5th pedal phalanges (includes left 2nd, 3rd, 4th and 5th, and right 3rd and 4th).

Upper limb affected predominantly in the distal third humeri, distal third radii and proximal third ulna. Lower limb affected predominantly in the distal third femur and distal tibiae and fibulae. Subperiosteal deposit also more prevalent at points of the interosseous crests of the radii and ulnae, and tibiae and fibulae.

Radiographic Lesion Summary:

- periosteal reactions on long bones and feet clear on radiographs- with cortical expansions of the long bones
- slight coarsening trabeculae

Differential Diagnosis Outcome:

Anaemia
Probable Scurvy
Possible Treponematosis

Skeletal ID: MB07H2M19

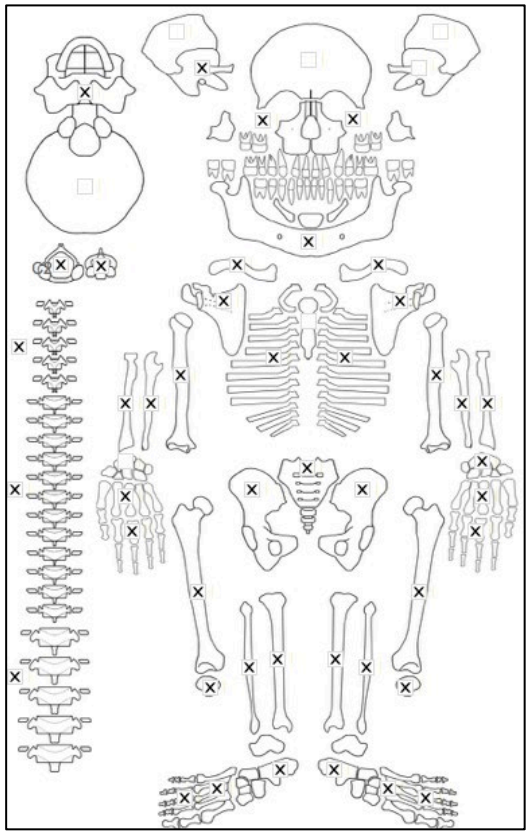

Completeness: Complete (>75%). 100% long bones, 80% hands and feet, 100% vertebrae, 35% neurocranium, ribs complete.
Preservation/ Taphonomy: Some axial elements encased in concretions, other surfaces were well preserved.
Age: 20-29, *Young Adult*
Sex: Male
Macroscopic Lesion Summary:
- Unilateral discrete deposit of remodelled new bone and cortical porosity on the left medial coronoid process
- Bilateral symmetrical discrete deposit of remodelled new bone and cortical porosity across the oblique lines and extending onto the regions of the mental foramina of the mandible
- Bilateral symmetrical discrete deposit of remodelled new bone and cortical porosity in the incisive fossa regions of the mandible
- Bilateral symmetrical discrete deposit of remodelled new bone inferior to the mylohyoid lines of the mandible indicated by the presence of vascular impressions
- Remodelled new bone deposit and cortical porosity across the inferior mandibular body
- Bilateral symmetrical remodelled new bone deposit and cortical porosity on the anterior maxillae. The preserved right infraorbital foramen is included in the right lesion.
- Remodelled new bone and cortical porosity on the posterior right maxilla, right side not preserved.
- Bilateral symmetrical remodelled new bone and cortical porosity on the palatal surfaces of the maxillae.
- Remodelled new bone and cortical porosity on the posterior right zygomatic bone, the left side is not preserved.
- Diffuse remodelled porosity across the anterior right zygomatic bone of unknown aetiology, may be consistent with mild porotic hyperostosis.
- Diffuse remodelled new bone and cortical porosity across the external right greater wing of sphenoid, the pterygoid region of the sphenoid and continuing on the anterior squama of the right temporal bone. Left side not preserved.
- Remodelled discrete deposit of new bone with vascular impressions on the endocranial aspect of the right greater wing of sphenoid left side, not preserved.
- Remodelled unilateral localised porosity inferior to the radial notch on the proximal left ulna
Radiographic Lesion Summary:
No radiographs taken

Differential Diagnosis Outcome:
Probable Scurvy

Skeletal ID: MB07H2M20

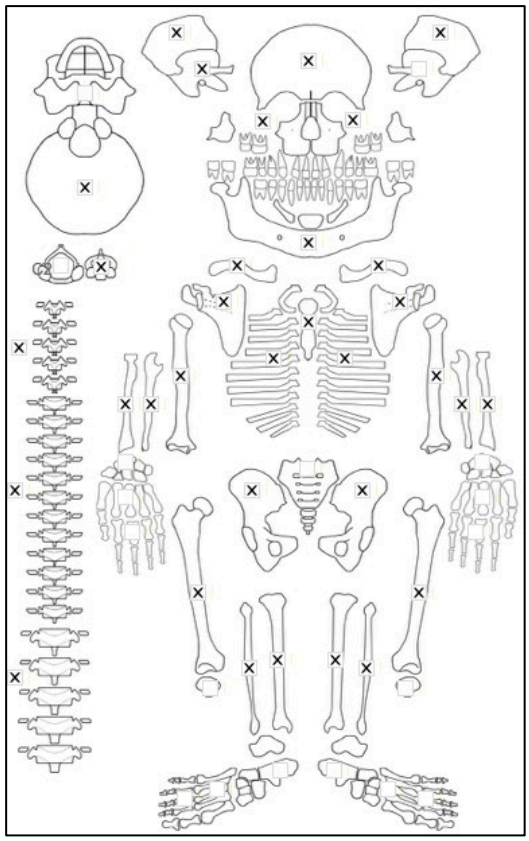

Completeness: Complete (>75%). 100% long bones, 9% hands and feet, 83% vertebrae, 63% neurocranium, ribs near complete.
Preservation/ Taphonomy: Surfaces mostly excellent with spots of concretions. Bones mostly intact.
Age: 7 months (+/- 2 months), *Infant*
Sex: Indeterminate
Macroscopic Lesion Summary:
- Endochondral porosity exceeding 10mm at the costochondral end of the ribs, associated with concentric expansion of the ends.
- Active symmetrical discrete localised new bone deposit with cortical porosity on the supraspinous fossae of the scapulae
- Active symmetrical discrete localised new bone deposit with cortical porosity on the infraspinous fossa of the left scapula
- Active symmetrical discrete localised new bone deposit with cortical porosity on the coronoid processes of the mandible
- Active symmetrical discrete localised new bone deposit with cortical porosity on the left mylohyoid line. Right line is not preserved
- Abnormal endochondral porosity of the proximal and distal metaphyses of the femora, tibiae, proximal humeri and distal radii exceeding 10mm in length. from metaphyseal plate
- Diffuse active new bone across the medial shaft of the left tibia.
- Discrete active new bone and cortical porosity on the left external greater wing of sphenoid.
- Discrete active new bone and cortical porosity on the inferior and superior pars basilaris
- Diffuse symmetrical active new bone across the distal posterior shafts of the humeri extending into the olecranon fossae
- Discrete active new bone and cortical porosity inferior to the trochlear notch on the anterior proximal left ulna, right side obscured by concretion
Radiographic Lesion Summary:
- Clear white line of Fraenkel, Trummerfeld zones of the limb bones and sternal ends of ribs.

- Bilateral lateral bending deformities of the midshaft and clear cortical expansion of the shafts of the humeri
- Regions of coarsened trabeculae

Differential Diagnosis Outcome:
Probable Scurvy
Probable Rickets

Skeletal ID: MB07H2M21

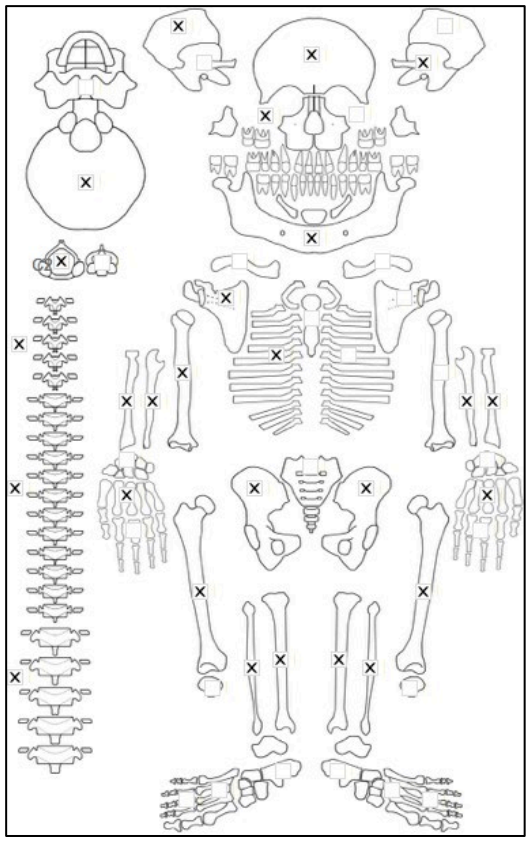

Completeness: Near Complete (66 to 75%). 89% long bones, 8% hands and feet, 67% vertebrae, 50% neurocranium, ribs incomplete.
Preservation/ Taphonomy: Preserved bones are mostly intact and surfaces in good condition.
Age: 9 months (+/- 2 months), *Infant*
Sex: Indeterminate
Macroscopic Lesion Summary:
- diffuse spiculated and layered new bone on the sutural margins of the ectocranium and endocranium of the frontal, right parietal (left parietal missing), and occipital bones
- active layered new bone and cortical porosity on the right superior orbital roof (left side missing)
- mixed active and remodelled discrete new bone and cortical porosity on the superior margin of the external auditory canal.
- mixed active and remodelled discrete new bone and cortical porosity on the anterior right maxilla associated with a vascular impression (left maxilla missing)
- active discrete new bone and cortical porosity on the posterior right maxilla (left side missing)
- active discrete new bone and cortical porosity on the medial right coronoid process of the mandible (left side missing)
- active discrete new bone on an unsided external greater wing fragment
- active discrete new bone on the supraspinous and infraspinous fossae of the right scapula (left scapula missing)
- active thick diffuse new bone and endosteal thickening across all long bone shafts and metaphyses: right humerus (left missing), radii, ulnae, femora, tibiae and fibulae. Thick new bone has multiple layers which can be seen in postmortem breaks of the shafts. New bone appears undulating and poorly mineralised.
- Femora appear to have depressed femoral necks and the distal end of left femur is flared medial- laterally and flared anterior-posteriorly, with mild cupping (distal half of right femur missing)

- abnormal endochondral porosity exceeding 10mm from the metaphyseal plates of the distal left femur (right distal half missing), and the proximal tibiae
- diffuse active new bone across the lateral shaft of the right 3rd metacarpal
- diffuse active thick new bone without endosteal expansion across the entire shaft of the left 1st metacarpal (right mc1 missing)
- diffuse active thick new bone without endosteal expansion across the external ilia
- diffuse active new bone across all aspects across all preserved vertebral archs representing cervical, thoracic and lumbar vertebrae

Radiographic Lesion Summary:
- white line of Fraenkel with very distinct radiolucent zones in the metaphyses of the long bones

Differential Diagnosis Outcome:
Probable Scurvy
Probable Rickets

Skeletal ID: MB07H2M22

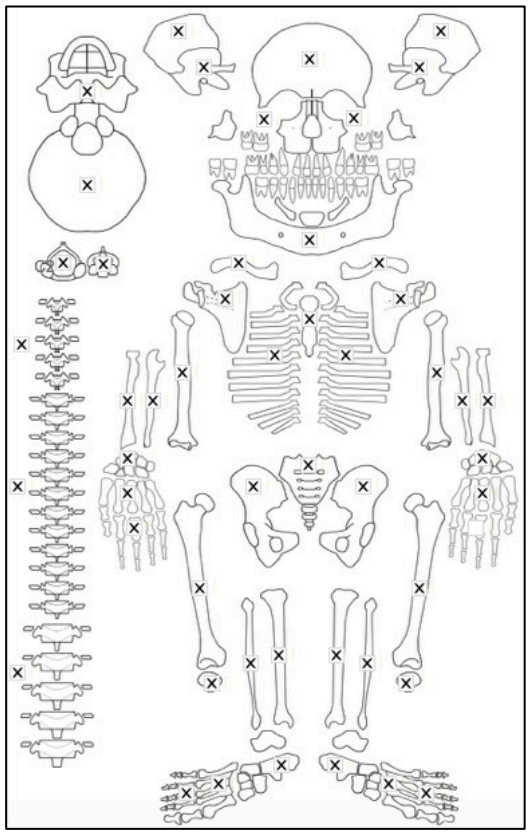

Completeness: Complete (>75%). 95% long bones, 36% hands and feet, 100% vertebrae, 100% neurocranium, near complete.
Preservation/ Taphonomy: Surfaces excellently preserved. Some PM breakage of the ribs, most bones intact.
Age: 30-39, *Middle Aged Adult*
Sex: Female
Macroscopic Lesion Summary:
- bilateral remodelled moderate cribra orbitalia
- diffuse remodelled porotic hyperostosis of the superior and posterior parietals (medial to the temporal line) and the occipital squama. The porosity is more marked posteriorly.
- diffuse layers of remodelled but porous new bone across the entire shaft of humeri, (can see layers in a proximal metaphyseal break of left humerus), entire shaft of left radius, proximal third shaft of the right radius, entire shafts and distal metaphyses of the femora (with bilateral exaggerated patellar grooves), both metaphyses and entire shafts of the tibiae (with enlarged foramen on the posterior left tibia), and lateral and posterior shafts of the fibulae

Radiographic Lesion Summary:
No radiographs taken

Differential Diagnosis Outcome:
Anaemia

Skeletal ID: MB07H2M24

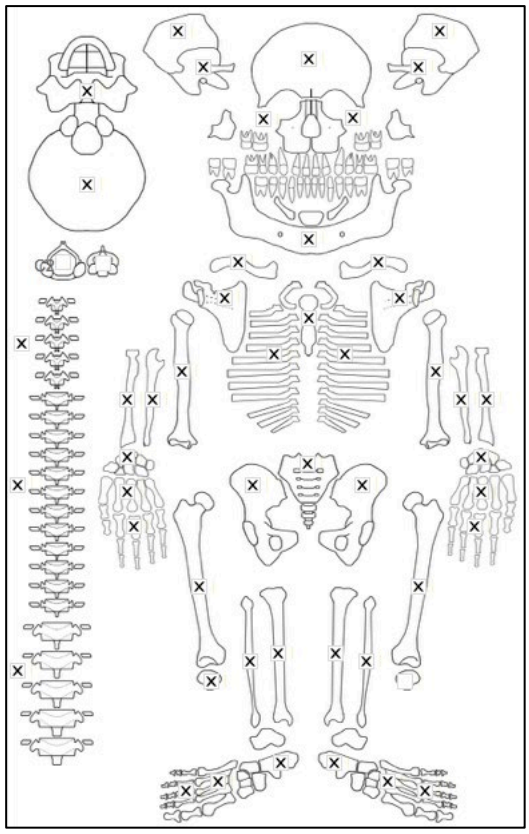

Completeness: Complete (>75%). 88% long bones, 99% hands and feet, 92% vertebrae, 88% neurocranium, ribs fragmented.
Preservation/ Taphonomy: Surfaces are well preserved, but there is PM breakage to the epiphyses and scapular bodies. The ribs are crushed.
Age: 50+, *Old Adult*
Sex: Female
Macroscopic Lesion Summary:
- unilateral enlarged foramen on the plantar aspect of the left 1st metatarsal. May be within normal limits.
Radiographic Lesion Summary:
No radiographs taken
Differential Diagnosis Outcome:
No diagnosis

Skeletal ID: MB07H2M26

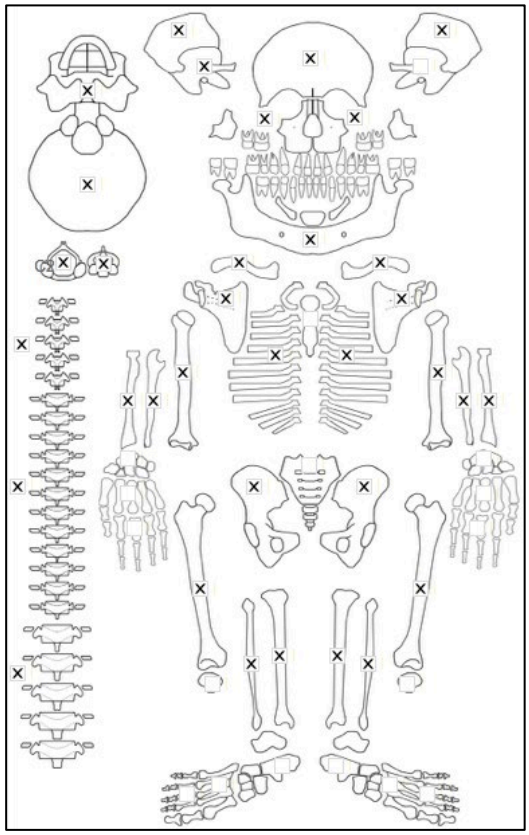

Completeness: Complete (>75%). 81% long bones, 0% hands and feet, 71% vertebrae, 75% neurocranium, ribs partially complete.
Preservation/ Taphonomy: Surfaces well preserved. Some PM breakage.
Age: 1.5 years (+/- 6 months), *Child*
Sex: Indeterminate
Macroscopic Lesion Summary:
- bilateral bulging zygomatic bones particularly anterior posteriorly, resulting in an anterior curvature of the zygomatic
- discrete deposit of mixed active new bone and cortical porosity on the posterior zygomatic bones (left side could not be observed)
- bulging and enlargement of the entire mandible, particularly pronounced medially at the molar area. It has resulted in considerable crowding of the teeth. Possible delayed growth of teeth as the long bones are considerably longer than similar aged individuals in this collection.
- bilateral symmetrical mixed active and remodelled new bone on the medial coronoid processes of the mandible
- discrete mixed active and remodelled new bone and cortical porosity on the supraspinous fossa of the right scapula (left not observable)
- bilateral enlarged clavicles. Radiographs required to decide whether cortical or trabecular.
- diffuse unilateral mixed active and remodelled new bone on the medial- posterior aspect of the left tibia
- bilateral abnormal endochondral porosity extending beyond 10mm from the distal metaphyseal plates of the femora. Associated with flaring and cupping of the distal end.
- bilateral expansion of the zygomatic process regions posterior to the superior orbits of the frontal
- possible bilateral thickening of the pelvis due to trabecular expansion (radiographs needed for confirmation)
Radiographic Lesion Summary:
- very dense metaphyseal plates
- coarsened trabeculae particularly of the distal humeri
- multiple Harris lines of the distal right femur
- clear crowding of the maxillae and hyperplasia of the facial and maxillary bones with poor (incomplete) pneumatisation of the maxillary sinus
- loss of distinction between cortex and medullary canal of the radii and ulnae
- radiolucency of the preserved metaphyseal ends and clear cupping and swelling of the distal femora

- rib within a rib sign
Differential Diagnosis Outcome:
Probable Scurvy
Probable Rickets
Probable Thalassaemia

Skeletal ID: MB07H2M27

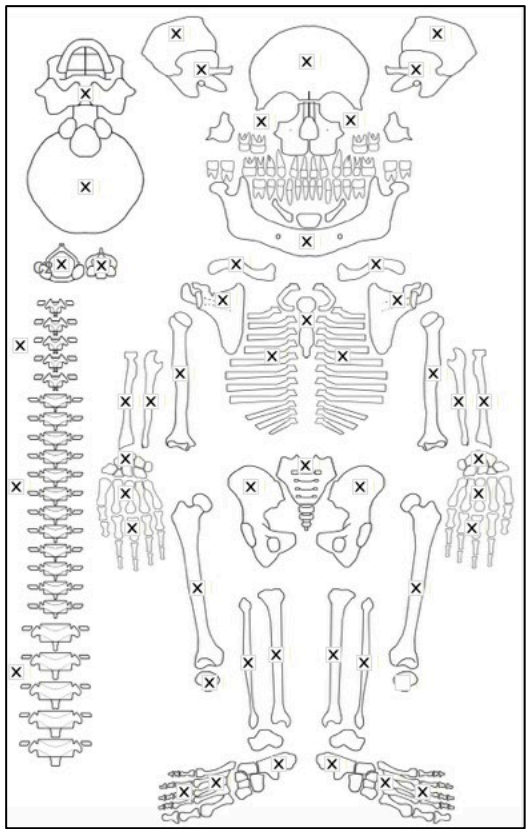

Completeness: Complete (>75%). 100% long bones, 77% hands and feet, 100% vertebrae, 100% neurocranium, ribs complete.
Preservation/ Taphonomy: Surfaces excellently preserved and bones mostly intact.
Age: 30-39, *Middle Aged Adult*
Sex: Male
Macroscopic Lesion Summary:
- bilateral remodelled mild cribra orbitalia
- remodelled diffuse porotic hyperostosis across the majority of the frontal where it is most marked, the parietals (medial to the temporal line) and the occipital squama
- remodelling deep trabecular expansions on the posterior manubrium.
- bilateral discrete haematoma like lesions on the lateral olecranon and proximal shaft of the ulnae. The left ulna lesion is more pronounced.
- unilateral discrete haematoma like lesion on the lateral olecranon and proximal shaft of the right ulna posterior and inferior to the radial fossa.
- two bilateral symmetrical well remodelled haematoma like lesions on the middle third anterior crest continuing on the lateral and medial aspects, and on the posterior third shaft of the tibiae.
- bilateral remodelled diffuse new bone on the latero-posterior shafts of the fibulae. The left fibula lesion is focused on the middle third shaft, with the right fibula extending on the middle to distal third shaft.
- bilateral symmetrical remodelled diffuse new bone on the lateral and posterior calcanei
Radiographic Lesion Summary:
No radiographs taken
Differential Diagnosis Outcome:
Anaemia

Skeletal ID: MB07H2M28

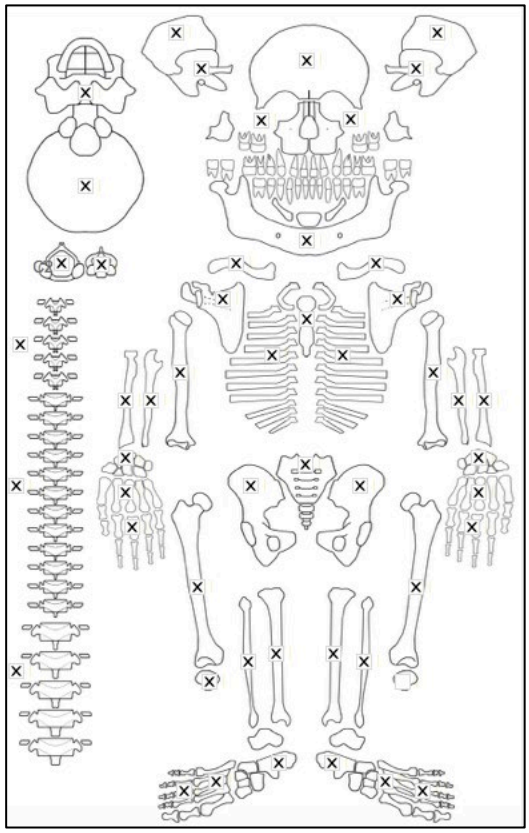

Completeness: Complete (>75%). 100% long bones, 6% hands and feet, 75% vertebrae, 63% neurocranium, ribs complete.
Preservation/ Taphonomy: Surfaces excellently preserved and most bones intact except for fragmented cranium.
Age: 0 years, *Infant*
Sex: Indeterminate
Macroscopic Lesion Summary:
- Active diffuse new bone across the ectocranial temporals, right pars lateralis (left side missing), pars basilaris, and unidentified cranial fragments.
- active diffuse new bone on the endocranium of an unidentified possible parietal fragment.
- active diffuse new bone on the external ectocranial and superior endocranial right wing of the sphenoid (left side not preserved)
- bilateral active symmetrical discrete new bone and cortical porosity on the right zygomatic process of the frontal bone
- active discrete new bone and cortical porosity on the posterior right zygomatic bone (left side missing)
- bilateral symmetrical active discrete new bone and cortical porosity on the medial coronoid processes of the mandible
- bilateral symmetrical active discrete new bone and cortical porosity on the incisive fossae of the mandible
- bilateral symmetrical active discrete new bone on the supraspinous fossae of the scapulae
- bilateral symmetrical mixed active and remodelling discrete new bone and cortical porosity on the infraspinous fossae of the scapulae
- bilateral symmetrical diffuse abnormal active new bone on the preserved external ribs
- bilateral symmetrical discrete active new bone and cortical porosity at the deltoid attachment of the anterior distal third clavicles
- bilateral symmetrical thick diffuse new bone deposit resulting in cortical expansion of the medial and posterior aspects of the ulnae. Cortical expansion can be seen in a postmortem shaft break.
- bilateral symmetrical thick diffuse new bone deposit resulting in cortical expansion of the proximal third anterior aspects of the radii. Cortical expansion can be seen in a postmortem shaft break.
- bilateral symmetrical diffuse new bone deposit across all aspects except the lateral shafts of the tibia (radiographs are required to determine if there is cortical expansion)

- bilateral symmetrical diffuse new bone deposit across all aspects except the anterior distal third shafts of the femur (radiographs are required to determine if there is cortical expansion)

Radiographic Lesion Summary:

- White line of Fraenkel and Trummerfeld zones of the long bones

Differential Diagnosis Outcome:

Probable Scurvy

Skeletal ID: MB07H2M29

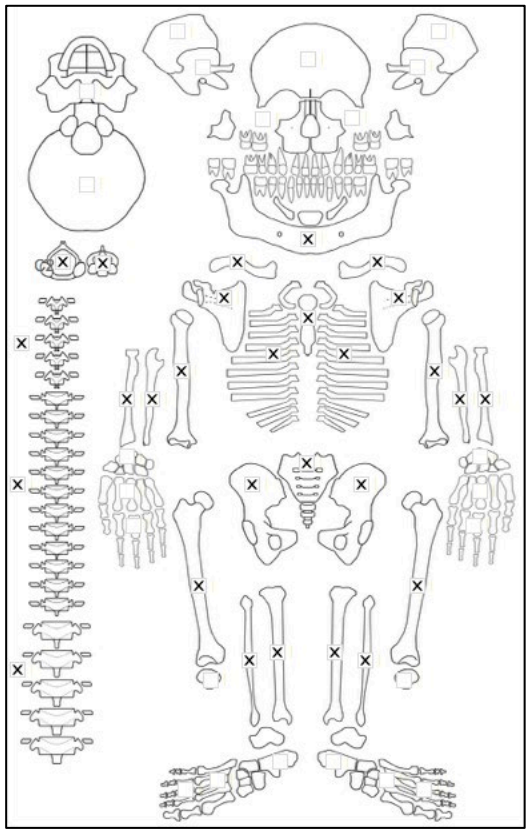

Completeness: Near Complete (66 to 75%). 100% long bones, 1% hands and feet, 71% vertebrae, 0% neurocranium, ribs complete.

Preservation/ Taphonomy: Long bones complete. Surfaces in good condition except for gnaw and puncture marks from scavenging of the lower limbs. Concretions of the spine impact observation.

Age: 7 years (+/- 9 months), *Child*

Sex: Indeterminate

Macroscopic Lesion Summary:

- remodelled cortical porosity on the right medial coronoid process of the mandible (left side missing)
- mixed active and remodelled cortical porosity superior to the right incisive fossa but not including the fossa itself. The lesion is adjacent to the 1st right mandibular deciduous molar which has a large posterior interproximal carious lesion involving the enamel and the root (photo 3846-48).
- bilateral symmetrical mixed active and remodelled new bone and cortical porosity on the supraspinous fossae of the scapulae.
- unilateral remodelled discrete deposit of new bone lateral to the deltoid tuberosity on the left humerus
- bilateral symmetrical diffuse active new bone across all aspects of the distal shafts of the humeri
- bilateral symmetrical diffuse thick and layered new bone with endosteal expansion particularly at the midshaft across all aspects of the shafts and metaphyses of the ulnae. The right ulna is a mixed of active and remodelled with the left ulna remaining mostly active. The new bone on the right ulna is associated with an oval gummatous (superficial cavitation) lesion on the antero-lateral midshaft, where there is a node produced by the endosteal expansion associated with the new bone. The superior margin has been damaged postmortem but the inferior margin is intact. Sclerotic reaction is prevalent but margins remain well defined suggesting continued activity. The lesion diameters are: 9.31x4.01mm. The gummatous lesion is associated to a gummatous lesion on the right radius anterior midshaft. Both lesions border the interosseous crest.

- There is a small (<10mm) oval gummatous lesion on the posterior olecranon process of the left ulna with some sclerotic reaction present on the margins as identified on the radiographs. There is also sclerotic reaction at the base of the lesion. The margins remain sharp. The gummatous lesion is associated with a node of expanded bone on the posterior and lateral aspect of the olecranon process. Diameter of lesion is under 1mm. (recorded upon return from field)
- bilateral symmetrical diffuse thick and layered new bone with endosteal expansion across all aspects of the shafts and metaphyses of the radii. . The right radius is mixed active and remodelled with the left ulna remaining mostly active. The new bone on the right radius is associated with an oval gummatous (superficial cavitation) lesion on the antero-medial midshaft. The inferior margin has been damaged postmortem but the superior margin is intact. Sclerotic reaction is prevalent but margins remain well defined suggesting continued activity. The new bone around the gummatous lesion remains active. The lesion diameters are: 12.03x4.6.7mm. The gummatous lesion is associated to a gummatous lesion on the right ulna anterior midshaft. Both lesions border the interosseous crest.
- bilateral remodelled symmetrical diffuse thick new bone on the shafts and metaphyses of the femora with endosteal expansion particularly marked anterior-posteriorly on the distal third of the femora. The new bone also appear more marked on the posterior shafts along the linea aspera. Radiographs demonstrate thickened cortex continuing throughout the entire shaft.
- There is slight cupping and swelling of the distal femora which may be in relation to the thickened cortex of the distal third shaft of the femora
- bilateral symmetrical diffuse thick mixed active and remodelled new bone on the shafts of the tibiae with endosteal expansion particularly marked on the medial and posterior aspects where they remain active. Radiographs demonstrate proliferative new bone on the anterior crest as well that may be remodelled new bone not identified macroscopically.
- There is slight medial true bowing of both tibiae confirmed by radiographs, with a slight posterior exaggeration of the angle of the proximal metaphyseal plates of the tibiae
- bilateral symmetrical diffuse thick mixed active and remodelled new bone on the distal third shafts of the fibulae with endosteal expansion. This is associated with a gummatous lesion on the anterior distal third left fibula and posterior distal third right fibula. Both lesions are oval with remodelling on the margins and appear to penetrate into the medullary canal as the cortex is particularly thin at this region and no bone in the area appears to be unaffected by a pathological process. Left fibula lesion diameter: 9.07x3.94mm. Right fibula lesion diameter: 12.32x3.29 Both are associated with marked sclerotic activity. There is closure of the medullary canals distal to the lytic lesions.
- Bilateral symmetrical deposit of active new bone on the posterior and superior femoral necks that appears as a separate lesion from the larger new bone deposits on the femora. There is also active new bone on the epiphyseal plate of the femoral heads and distal right femoral epiphyseal plate (left missing)
- thick and layered diffuse active new bone resulting in pathological change throughout the preserved bone of a damaged left unidentified metacarpal. Original cortex is heavily porous.
- unilateral expansion of the sternal end of the left clavicle. The metaphyseal plate also seems to be bulging compared to the right.
- there is mild bilateral lateral bending deformities of the proximal third shafts of the humeri at the position of the deltoid tuberosities, and mild depression with deformity of the proximal metaphyseal plates.

Radiographic Lesion Summary:

- the femoral shaft cortices are thick throughout except on the distal third where the cortices are thinned, even though macroscopically this region is abnormally enlarged.
- osteopenia with ground glass appearance is present in the metaphyses of the long bones
- white line of Fraenkel present with Trummerfeld zones in the metaphyses
- enlargement of the medial left clavicle is associated with a large region of radiolucency, as well as a small oval lesion within the cortex on the inferior aspect of the medial end without noticeable sclerotic reaction identified, possibly indicating an initiating gummatous lesion. This lesion does not penetrate to the outer surface of the cortex. The enlargement is associated with a slight increase in radiodensity of the cortex than the right clavicle but no profuse new bone is identifiable indicative of Higoumenakis sign.
- there is a lack of discernible differentiation between cortex and medullary canal of the radii and ulnae.
- cortex is radiolucent on the lateral aspect of the posterior third humeri where the mild bending deformities are
- radiodensity around the oval gummatous lesions on the midshafts of the right ulna and radius
- multiple Harris lines on the proximal and distal tibiae and distal femora
- medullary canal closure of the distal fibulae
- noticeable endosteal thickness of the anterior crests of the tibiae
- the slight medial tibial bowing and lateral bowing of the humeri appears to be true bowing
- unidentified metacarpal is radiolucent throughout the preserved shaft

Differential Diagnosis Outcome:
Probable Scurvy
Probable Rickets
Probable Treponematosis

Skeletal ID: MB07H2M30

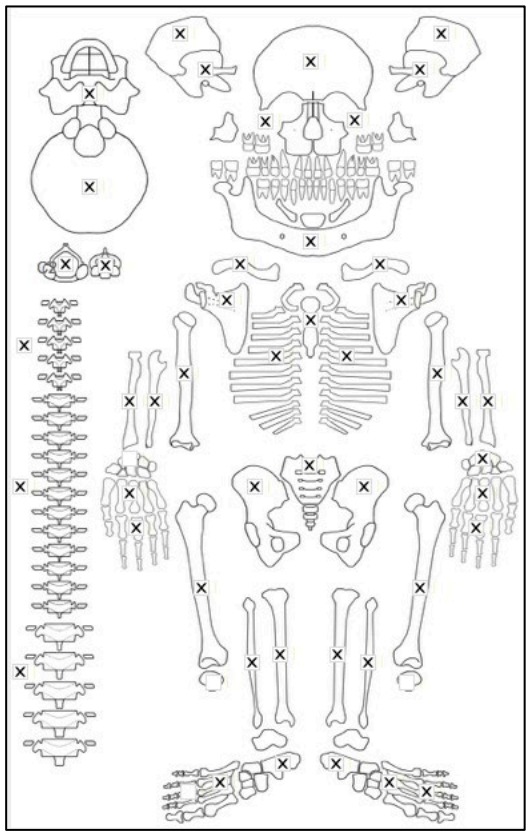

Completeness: Complete (>75%). 95% long bones, 74% hands and feet, 88% vertebrae, 100% neurocranium, ribs near complete.
Preservation/ Taphonomy: Surfaces well preserved except right hand phalanges encased in soil concretions. PM breakage of ribs, and scapular bodies.
Age: 30-39, *Middle Aged Adult*
Sex: Male
Macroscopic Lesion Summary:
- remodelled porotic hyperostosis on the superior and posterior parietals (medial to the temporal line) and the occipital squama
- bilateral remodelled moderate cribra orbitalia
Radiographic Lesion Summary:
No radiographs taken
Differential Diagnosis Outcome:
Anaemia

Skeletal ID: MB07H2M31

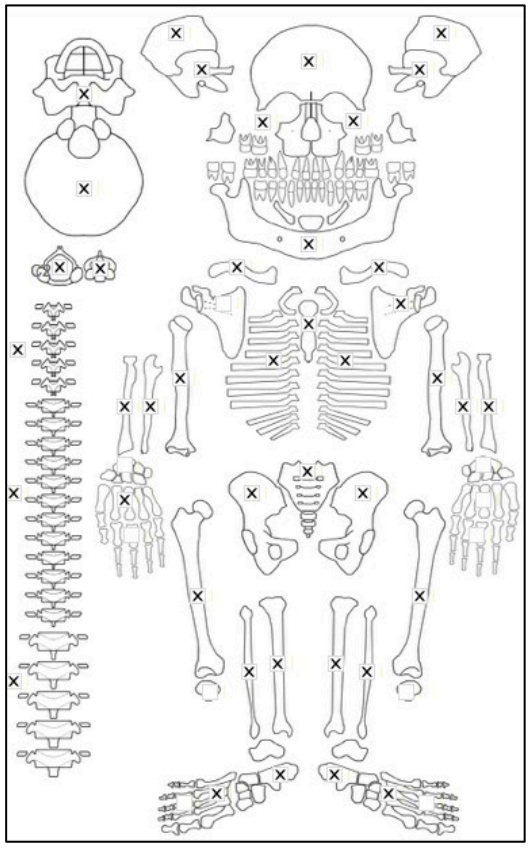

Completeness: Complete (>75%). 100% long bones, 17% hands and feet, 83% vertebrae, 88% neurocranium, ribs near complete.
Preservation/ Taphonomy: Long bones are covered in concretions making them difficult to observe. Some PM breakage of the ribs. Metaphyses of distal tibiae, distal and proximal fibulae, proximal left femur, and proximal left ulna are missing. Metaphyses of distal femora are crushed.
Age: 4 years (+/- 9 months), *Child*
Sex: Indeterminate
Macroscopic Lesion Summary:
diffuse fine active porosity on the occipital squama and posterior parietals which may be porotic hyperostosis
- mixed active new bone and cortical porosity superior to the external auditory canal of the right temporal (left side canal not preserved)
- remodelled discrete new bone and cortical porosity with vascular impressions on the left zygomatic process of the frontal (right side missing)
- active localised cortical porosity medial and superior to the superciliary arches of the frontal bone
- active new bone with capillary formations (Lewis Grade 3) around the frontal crest on the endocranium of the frontal.
- bilateral active moderate cribra orbitalia
- remodelled new bone and cortical porosity on the inferior pars basilaris
- bilateral symmetrical remodelled cortical porosity on the external greater wings of sphenoid (the porosity is slight)
- remodelled porosity on the anterior maxillae and zygomatic bones
- mixed active and remodelled new bone and cortical porosity on the posterior maxillae and zygomatic bones
- active cortical porosity on the superior maxillae and zygomatic bones (orbital floor)
- active new bone and cortical porosity on the palatal surfaces of the maxillae
- mixed active and remodelled new bone and cortical porosity on the medial coronoid processes of the mandible
- localised deposit of remodelled new bone on the posterior mandible inferior to the anterior teeth
- bilateral symmetrical remodelled new bone and cortical porosity on the incisive fossae extending to the incisive foramen of the mandible
- deep endochondral porosity exceeding 10mm from the metaphyseal plate on the distal femora and proximal tibiae

- bilateral symmetrical diffuse active new bone on the medial aspects and mixed active and remodelled new bone on the posterior aspects of the shafts of the tibiae.

Radiographic Lesion Summary:
Radiographs not taken

Differential Diagnosis Outcome:
Anaemia
Probable Scurvy

Skeletal ID: MB07H2M32

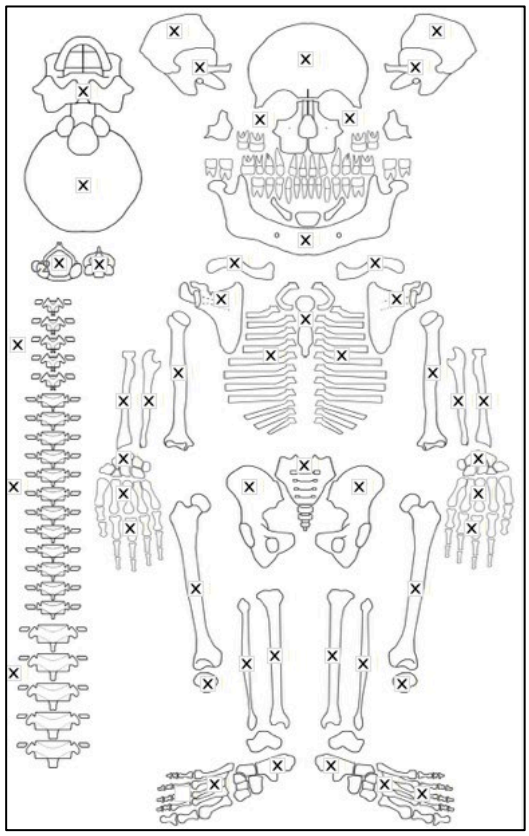

Completeness: Complete (>75%). 98% long bones, 78% hands and feet, 100% vertebrae, 88% neurocranium, ribs complete.

Preservation/ Taphonomy: PM breakage of the axial skeleton (except vertebrae that are mostly intact) and scapular bodies. Surfaces well preserved,

Age: 20-29, *Young Adult*

Sex: Male

Macroscopic Lesion Summary:
- diffuse remodelling porotic hyperostosis on the superior frontal and along the temporal line, superior and posterior parietals (medial to the temporal line) and the occipital squama. The porosity is more marked on the posterior cranium.
- bilateral remodelling mild cribra orbitalia
- remodelled new bone deposit and cortical porosity with abnormal vascular impressions on the entire endocranium, sparing the petrous process of the temporals (sphenoid unobservable)
- localised bilateral symmetrical remodelled cortical porosity and new bone on the nasal margins of the maxillae (the infraorbital foramen regions are damaged so extent not known)
- vascular impressions suggesting remodelled new bone on the endonasal margins of the medial maxillae
- bilateral symmetrical mixed active and remodelled discrete deposit of new bone and cortical porosity on the posterior maxillae
- bilateral symmetrical remodelled discrete deposit of new bone and cortical porosity on medial coronoid process of the mandible
- bilateral symmetrical remodelled discrete deposit of new bone with vascular impressions inferior to the mylohyoid lines on the mandible

- unilateral discrete haematoma-like new bone deposit on the right oblique line of the mandible.
- bilateral symmetrical discrete new bone and cortical porosity extending from the external hypoglossal canals
- abnormal vascular impressions on the anterior sternum suggesting diffuse remodelled new bone.

Radiographic Lesion Summary:
No radiographs taken
Differential Diagnosis Outcome:
Anaemia
Probable Scurvy

Bronze Age Mongolia

Skeletal ID: AT-921

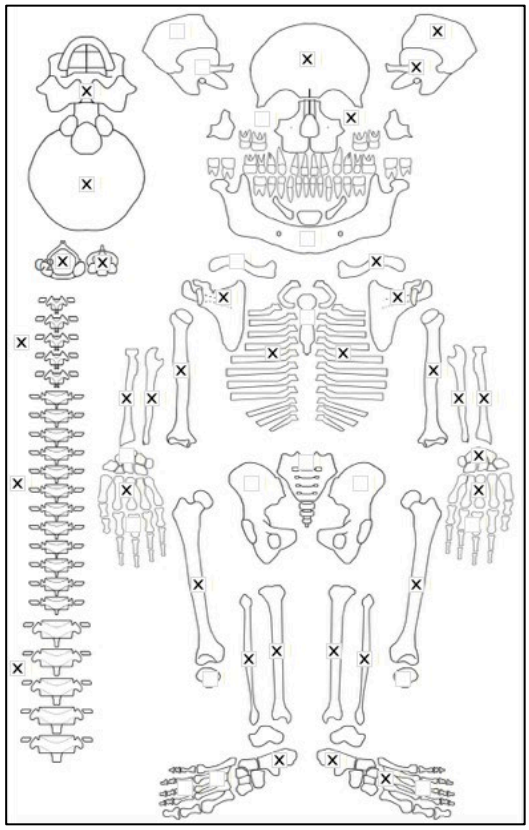

Completeness: Complete (>75%). 92% long bones, 33% hands and feet, 100% vertebrae, 88% neurocranium, and ribs complete.
Preservation/ Taphonomy: Surfaces are in good condition with exception of fibula with severe gnaw marks, some gnaw marks on the tibiae. Anterior middle right femur taken for sampling. Bones mostly intact.
Age: 50+, *Old Adult*
Sex: Female
Macroscopic Lesion Summary:
- bilateral remodelling moderate cribra orbitalia
- bilateral mixed active and remodelled cortical porosity of the palatal surfaces of the maxillae (note there is association with tooth loss of the posterior teeth).

Radiographic Lesion Summary:
No radiographs taken
Differential Diagnosis Outcome:
Anaemia

Skeletal ID: AT-448

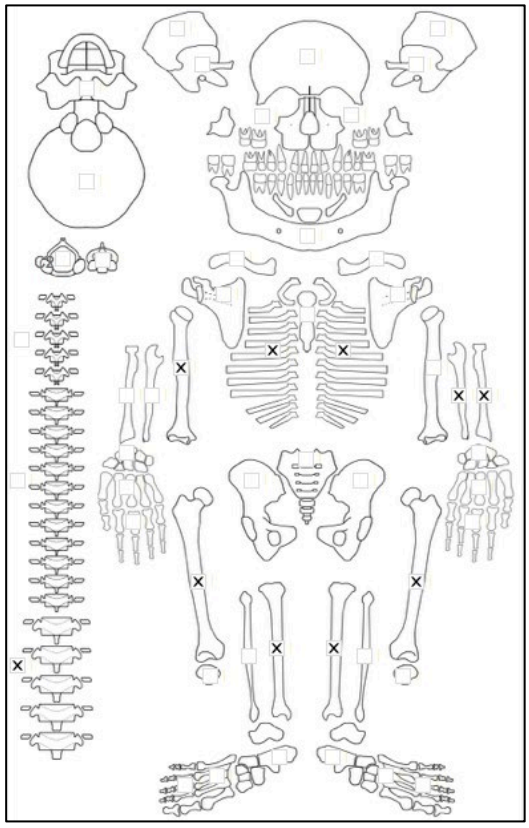

Completeness: Incomplete (33 to 50%). 47% long bones, 0% hands and feet, 17% vertebrae, 0% neurocranium, ribs incomplete.
Preservation/ Taphonomy: Long bones have severe animal scavenging on the surface- rodent like. Proximal third of right femur, left femur complete, shafts of both tibiae with proximal metaphyses of right tibia, midshaft of left radius, left ulna with damage to metaphyses, and shaft of right ulna present.
Age: 8 years (+/- 2), *Child*
Sex: Indeterminate
Macroscopic Lesion Summary:
No pathology
Radiographic Lesion Summary:
No radiographs taken
Differential Diagnosis Outcome:
No diagnosis

Skeletal ID: AT-250

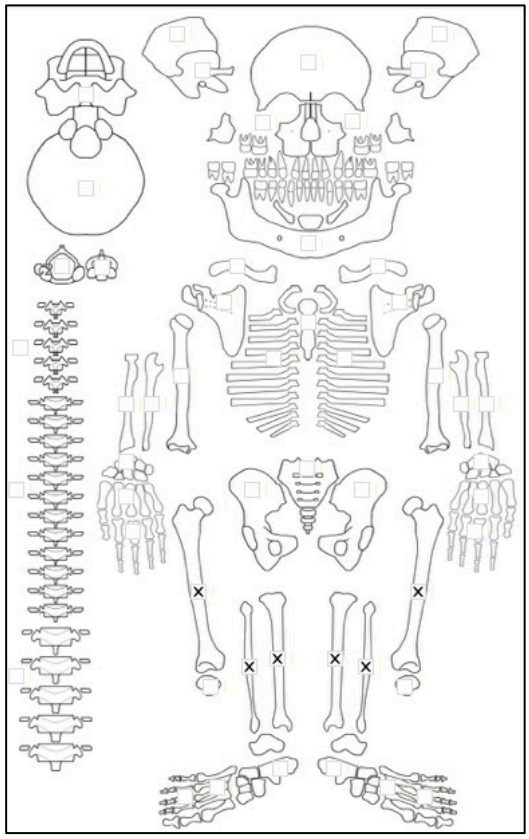

Completeness: Incomplete (33 to 50%). 47% long bones, 0% hands and feet, 0% vertebrae, 0% neurocranium, no ribs.
Preservation/ Taphonomy: Right anterior femur has been taken for isotope analysis. Intrusive fibulae of a more gracile individual- this individual was not assessed. Proximal fibulae epiphysis missing- all other preserved long bones are intact. surfaces excellent with a few areas of minimal rodent scavenging
Age: *Adult*
Sex: Indeterminate
Macroscopic Lesion Summary:
No pathology
Radiographic Lesion Summary:
No radiographs taken
Differential Diagnosis Outcome:
No diagnosis

Skeletal ID: AT-249

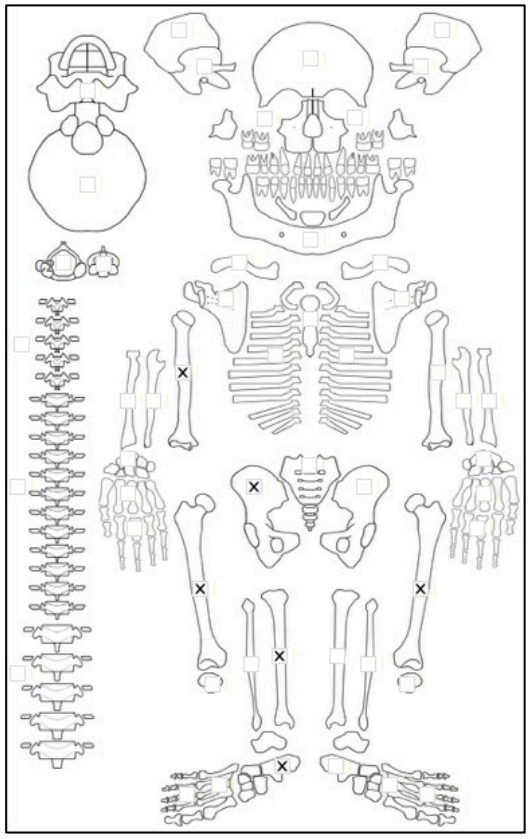

Completeness: Incomplete (33 to 50%). 32% long bones, 2% hands and feet, 4% vertebrae, 0% neurocranium, no ribs.
Preservation/ Taphonomy: Long bones complete except proximal epiphysis of humerus missing, but femora have anterior portions taken for isotopes. Some surfaces have weathering.
Age: 20-29, *Young Adult*
Sex: Male
Macroscopic Lesion Summary:
No pathology
Radiographic Lesion Summary:
No radiographs taken
Differential Diagnosis Outcome:
No diagnosis

Skeletal ID: AT-233

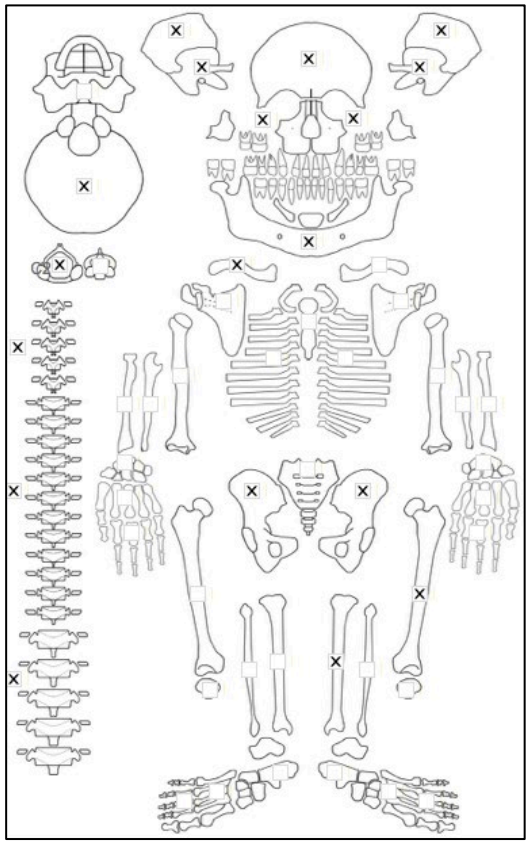

Completeness: Partially Complete (50 to 66%). 13% long bones, 0% hands and feet, 46% vertebrae, 75% neurocranium, and ribs partially complete.
Preservation/ Taphonomy: Some surface damage, rodent scavenging and weathering- ribs are sheared in half due to weathering, vertebrae bodies and arches are in separate fragments with the exception of an upper thoracic. Portion of proximal tibia and whole distal femur epiphyses are missing. Left pelvis consists of large fragments which do not reconstruct. Left anterior femur taken for sampling.
Age: 20-29, *Young Adult*
Sex: Male
Macroscopic Lesion Summary:
- diffuse, thick and proliferative mixed periosteal reaction on the shafts of the left femur and tibia (right missing) and the lateral os coxa extending from superior to the acetabulum. The new bone is most proliferative on the tibia where there is cortical expansion particularly on the medial aspect associated. On the femur the new bone is more prolific on the posterior extending across the linea aspera and the mid to distal anterior aspect appears to be relatively spared (but most of this region has been removed for sampling so difficult to tell extent). The new bone appears more active on the os coxa where there is a spiculated contour (possible rapid expansion of the periosteum?)
- bilateral symmetrical remodelled new bone and cortical porosity on the palatal surfaces of the maxillae
Radiographic Lesion Summary:
No radiographs taken
Differential Diagnosis Outcome:
Possible Scurvy

Skeletal ID: AT-324

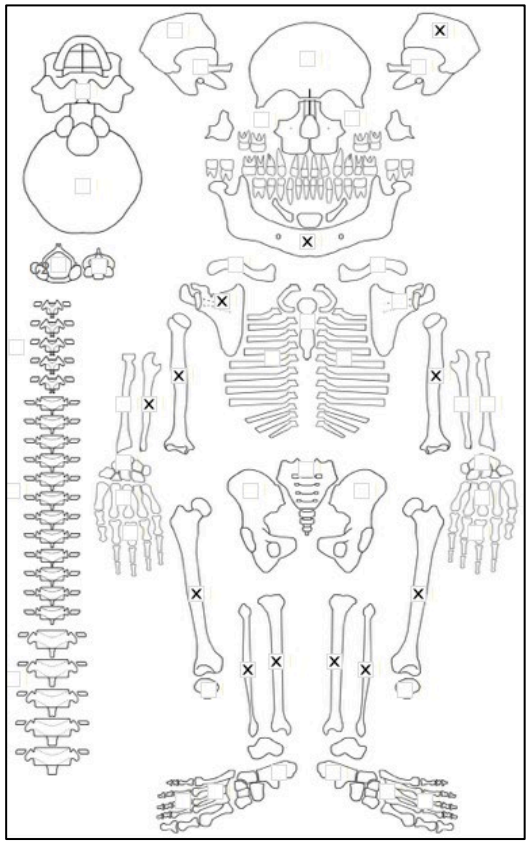

Completeness: Partially Complete (50 to 66%). 62% long bones, 0% hands and feet, 0% vertebrae, 13% neurocranium, no ribs.
Preservation/ Taphonomy: Some rodent gnawing on the long bones but otherwise surfaces are excellently preserved. Epiphyses of right femur, distal epiphysis of right ulna and humerus and left femur and proximal epiphyses of fibulae and left tibia are missing.
Age: *Adult*
Sex: Indeterminate
Macroscopic Lesion Summary:
- lateral bending of the shafts of the tibiae with posterior bending of the shafts of the fibulae. The fibulae are more severe
- some porosity and vascular channels suggesting diffuse remodelled new bone on the endocranium of the parietal
Radiographic Lesion Summary:
No radiographs taken
Differential Diagnosis Outcome:
Possible Residual Rickets

Skeletal ID: AT-126

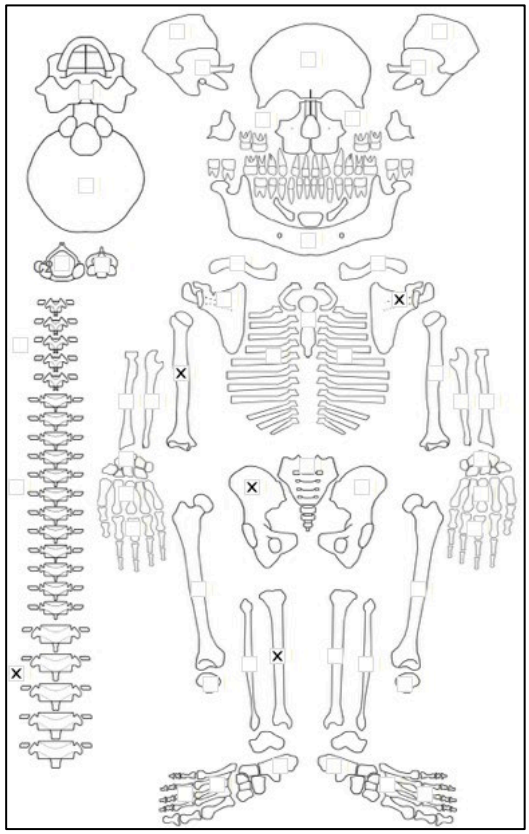

Completeness: Incomplete (33 to 50%). 17% long bones, 0% hands and feet, 13% vertebrae, 0% neurocranium, and no ribs.
Preservation/ Taphonomy: All bones that are preserved are in excellent condition and not fragmented. There is intrusion of other bones including a few fragmented long bones from a child (not assessed)
Age: 30-39, *Middle Aged Adult*
Sex: Male
Macroscopic Lesion Summary:
No pathology
Radiographic Lesion Summary:
No radiographs taken
Differential Diagnosis Outcome:
No diagnosis

Skeletal ID: AT-322

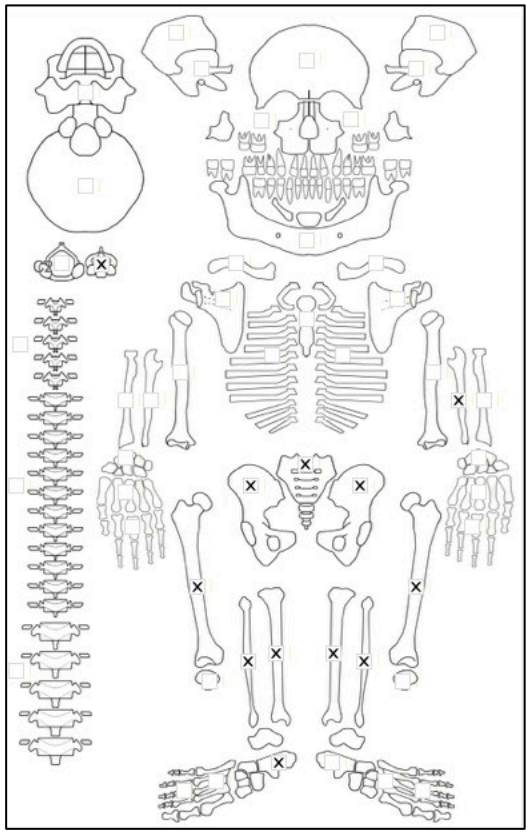

Completeness: Partially Complete (50 to 66%). 53% long bones, 11% hands and feet, 4% vertebrae, 0% neurocranium, ribs fragmented.
Preservation/ Taphonomy: Surfaces are in good condition with minimal to moderate rodent damage. Lower limbs have considerable rodent damage. Proximal half left femur taken for sampling. only distal epiphyses of tibiae and right fibula and proximal epiphysis of left tibia are spared. shafts complete of long bones present.
Age: 35 to 49, *Middle Aged Adult*
Sex: Female
Macroscopic Lesion Summary:
No pathology
Radiographic Lesion Summary:
No radiographs taken
Differential Diagnosis Outcome:
No diagnosis

Skeletal ID: AT-251

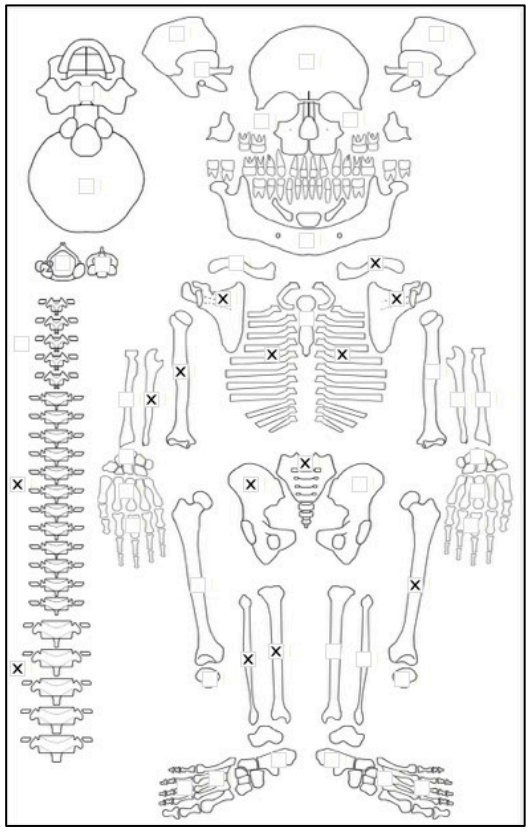

Completeness: Partially Complete (50 to 66%). 35% long bones, 2% hands and feet, 25% vertebrae, 0% neurocranium, ribs partially complete.
Preservation/ Taphonomy: Some rodent gnawing damage particularly to the fibula but other surfaces are well preserved. Distal epiphysis of femur and ulna and epiphyses of fibula missing. Severe PM damage to the vertebral bodies.
Age: 50+, *Old Adult*
Sex: Female
Macroscopic Lesion Summary:
No pathology
Radiographic Lesion Summary:
No radiographs taken
Differential Diagnosis Outcome:
No diagnosis

Skeletal ID: AT-232a

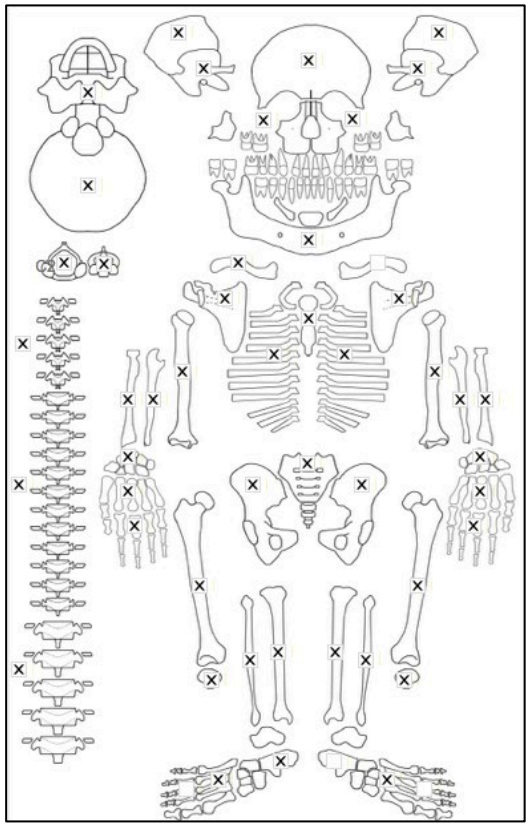

Completeness: Complete (>75%). 98% long bones, 31% hands and feet, 100% vertebrae, 88% neurocranium, ribs complete.
Preservation/ Taphonomy: All preserved bones are intact with minimal pm damage, some gnaw marks on the fibulae. distal third shaft of right femur taken for sampling. Intrusive left humerus of a more gracile individual (not assessed).
Age: 20-29, *Young Adult*
Sex: Male
Macroscopic Lesion Summary:
- remodelled unilateral discrete remodelled deposit of new bone and fine cortical porosity on the infraspinous fossa around the foramen
Radiographic Lesion Summary:
No radiographs taken
Differential Diagnosis Outcome:
No diagnosis

Skeletal ID: AT-253

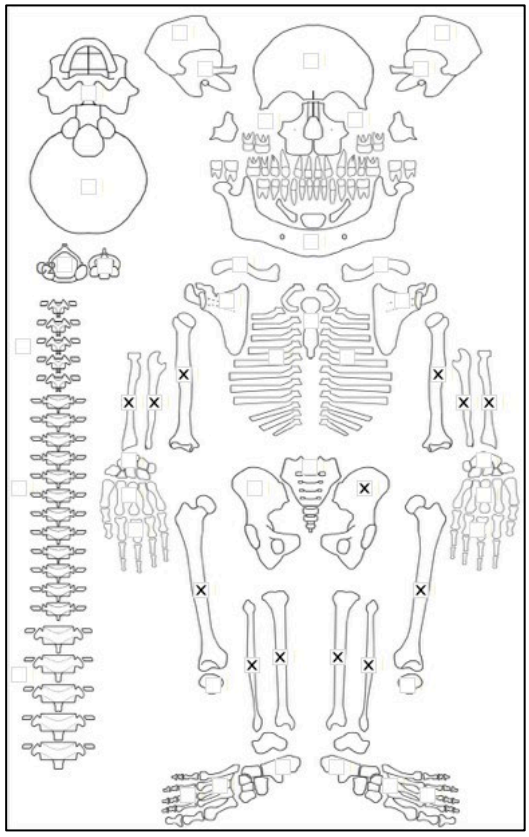

Completeness: Incomplete (33 to 50%). 8-% long bones, 0% hands and feet, 0% vertebrae, 0% neurocranium, no ribs.
Preservation/ Taphonomy: Scavenging marks across the long bones moderate damage to the surfaces. Long bones and left os coxa only, but long bones intact with distal epiphyses of right radius, proximal epiphysis of right femur, distal epiphysis of left fibula and ulna and epiphyses of right fibula are missing. Middle third anterior shaft of the left femur has been removed for sampling
Age: 40-49, *Middle Aged Adult*
Sex: Male
Macroscopic Lesion Summary:
Anterior bowing of the femora with knocked knees
Radiographic Lesion Summary:
Radiographs not taken
Differential Diagnosis Outcome:
Possible Osteomalacia
Possible Residual Rickets

Skeletal ID: AT-248

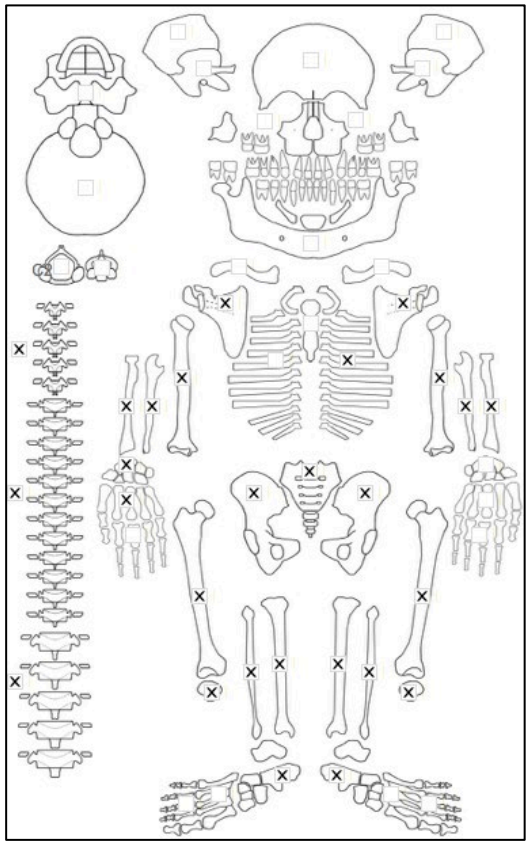

Completeness: Near Complete (66 to 75%). 100% long bones, 12% hands and feet, 50% vertebrae, 0% neurocranium, incomplete ribs.
Preservation/ Taphonomy: Surfaces in good condition but there is some pm damage particularly to the axial skeleton and weathering. severe damage to the vertebral bodies.
Age: 20-29, *Young Adult*
Sex: Male
Macroscopic Lesion Summary:
No pathology
Radiographic Lesion Summary:
No radiographs taken
Differential Diagnosis Outcome:
No diagnosis

Skeletal ID: AT-463

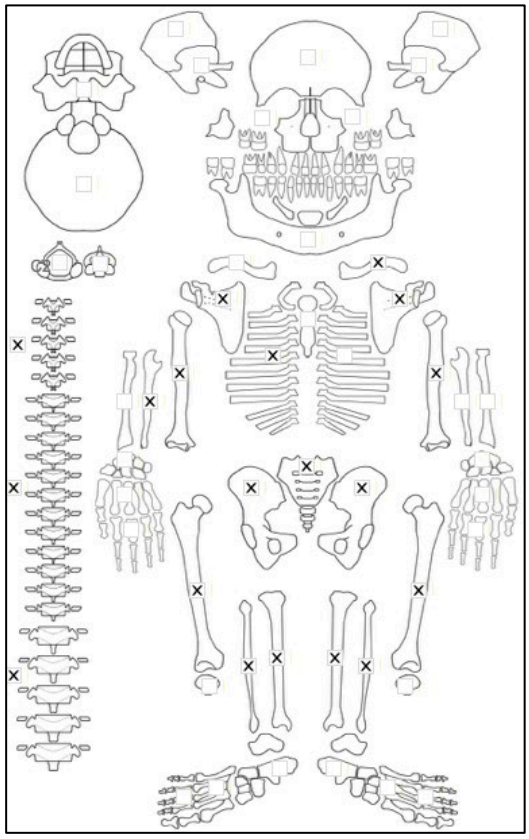

Completeness: Near Complete (66 to 75%). 65% long bones, 1% hands and feet, 91% vertebrae, 0% neurocranium, ribs incomplete.
Preservation/ Taphonomy: Bone surfaces are excellently preserved and bones intact. Anterior middle third of left femur removed for sampling.
Age: 30-39, *Young Adult*
Sex: Female
Macroscopic Lesion Summary:
No pathology
Radiographic Lesion Summary:
No radiographs taken
Differential Diagnosis Outcome:
No diagnosis

Skeletal ID: AT-821

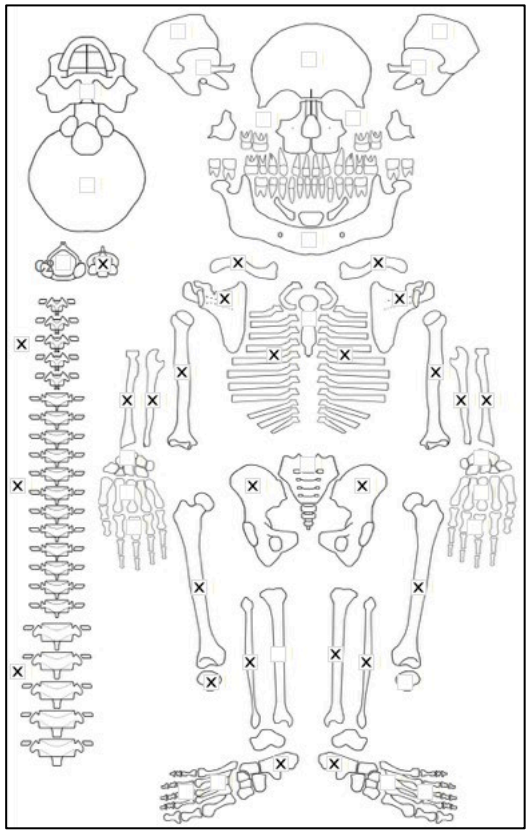

Completeness: Near Complete (66 to 75%). 68% long bones, 19% hands and feet, 75% vertebrae, 0% neurocranium, ribs near complete.
Preservation/ Taphonomy: Intrusive femoral head and lateral cuneiform- not assessed.
Bones covered in soil but surfaces can still be assessed. Anterior middle third of right femur has been sampled. Vertebral bodies of upper spine are preserved, but lower bodies are not.
Age: 30-39, *Middle Aged Adult*
Sex: Male
Macroscopic Lesion Summary:
No pathology
Radiographic Lesion Summary:
No radiographs taken
Differential Diagnosis Outcome:
No diagnosis

Skeletal ID: AT-825

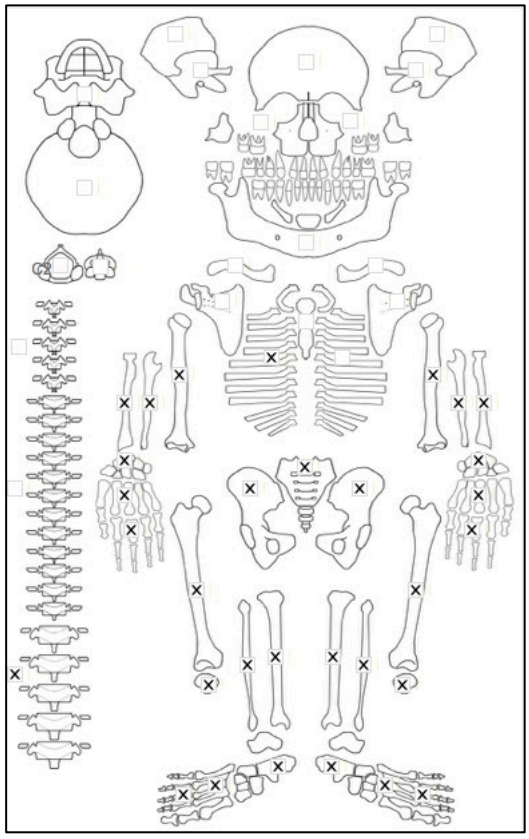

Completeness: Near Complete (66 to 75%). 100% long bones, 65% hands and feet, 13% vertebrae, 0% neurocranium, ribs incomplete.
Preservation/ Taphonomy: All long bones intact. middle third anterior left femur sampled. Surfaces are in excellent condition and preservation is excellent
Age: 20-29, *Young Adult*
Sex: Female
Macroscopic Lesion Summary:
No pathology
Radiographic Lesion Summary:
No radiographs taken
Differential Diagnosis Outcome:
No diagnosis

Skeletal ID: AT-822

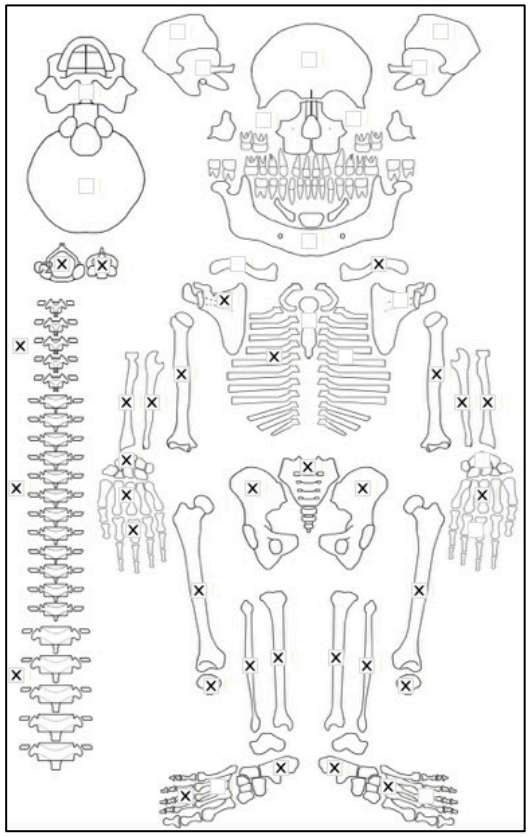

Completeness: Near Complete (66 to 75%). 95% long bones, 37% hands and feet, 42% vertebrae, 0% neurocranium, ribs partially complete.
Preservation/ Taphonomy: some intrusive hand and feet bones, excluded. Distal epiphysis of right ulna, proximal epiphysis of eft femur and fibula are missing. Anterior middle third of left femur taken for sampling. surfaces are intact and there is no animal scavenging. Soil on surface but surfaces can still be assessed.
Age: 20-29, *Young Adult*
Sex: Male
Macroscopic Lesion Summary:
No pathology
Radiographic Lesion Summary:
No radiographs taken
Differential Diagnosis Outcome:
No diagnosis

Skeletal ID: AT-823

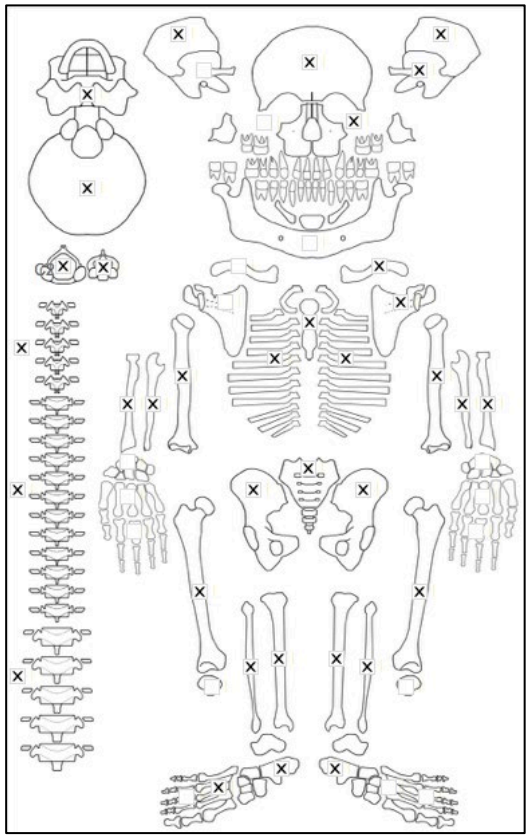

Completeness: Complete (>75%). 67% long bones, 18% hands and feet, 50% vertebrae, 75% neurocranium, ribs partially complete.
Preservation/ Taphonomy: all bone surfaces excellently preserved, epiphyses are well represented. some dust covering the surfaces but surfaces are still visible. Vertebrae are in good condition and mostly intact with some PM breakage of bodies and arches.
Age: 13.5 years (+/- 2.5 years), *Adolescent*
Sex: Indeterminate
Macroscopic Lesion Summary:
No pathology
Radiographic Lesion Summary:
No radiographs taken
Differential Diagnosis Outcome:
No diagnosis

Skeletal ID: AT-824

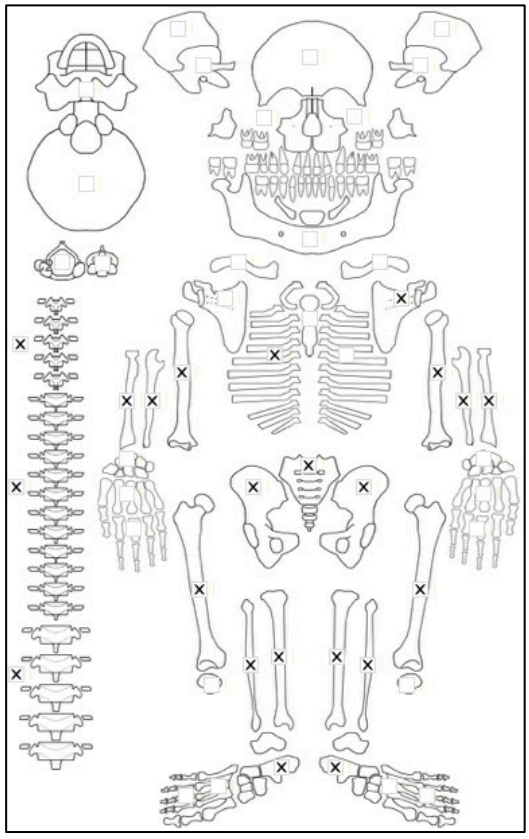

Completeness: Near Complete (66 to 75%). 78% long bones, 6% hands and feet, 33% vertebrae, 0% neurocranium, ribs incomplete.
Preservation/ Taphonomy: Right femur has medial middle third removed for sampling. Epiphyses of lower leg and distal femora, left radius and left and right ulna missing, right radial midshaft only present.
Age: 1.4 years (+/- 6 months). *Adolescent*
Sex: Female
Macroscopic Lesion Summary:
No pathology
Radiographic Lesion Summary:
No radiographs taken
Differential Diagnosis Outcome:
No diagnosis

Skeletal ID: AT-826

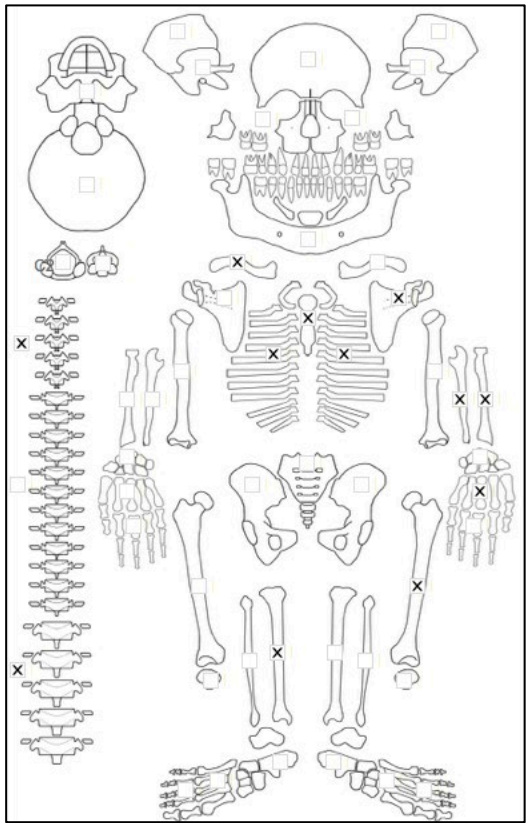

Completeness: Partially Complete (50 to 66%). 32% long bones, 7% hands and feet, 33% vertebrae, 0% neurocranium, ribs near complete.
Preservation/ Taphonomy: Distal end of tibia missing. Surfaces are well represented but a slight layer of soil covers, surfaces are still visible. Vertebrae preserved are mostly intact, most lumbar vertebrae only represented by arches though
Age: 30-39, *Young Adult*
Sex: Female
Macroscopic Lesion Summary:
No pathology
Radiographic Lesion Summary:
No radiographs taken
Differential Diagnosis Outcome:
No diagnosis

Skeletal ID: AT-880

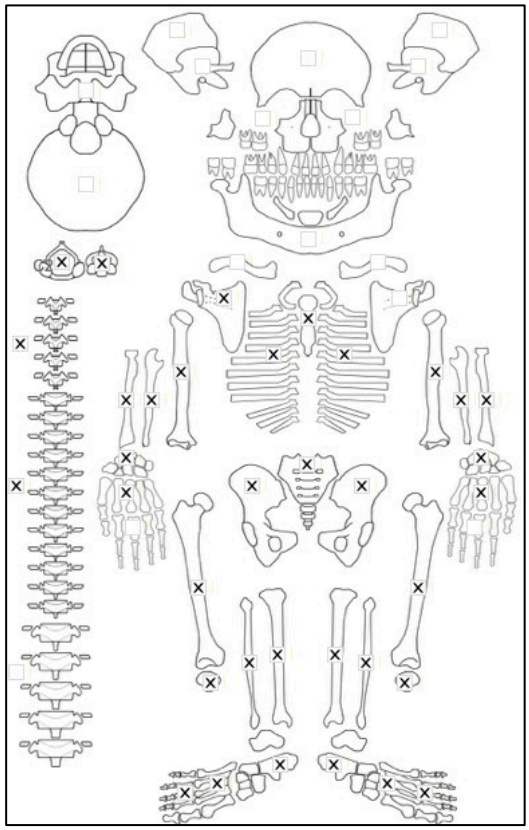

Completeness: Near Complete (66 to 75%). 93% long bones, 62% hands and feet, 100% vertebrae, 0% neurocranium, ribs complete.
Preservation/ Taphonomy: Surfaces are in excellent condition with a thin layer of soil.
Distal epiphysis of left radius and proximal epiphysis of left fib, proximal 1/2s of right ulna are missing.
Vertebrae intact and in excellent condition and all present
Age: 30-39, *Middle Aged Adult*
Sex: Male
Macroscopic Lesion Summary:
No pathology
Radiographic Lesion Summary:
No radiographs taken
Differential Diagnosis Outcome:
No diagnosis

Skeletal ID: AT-881

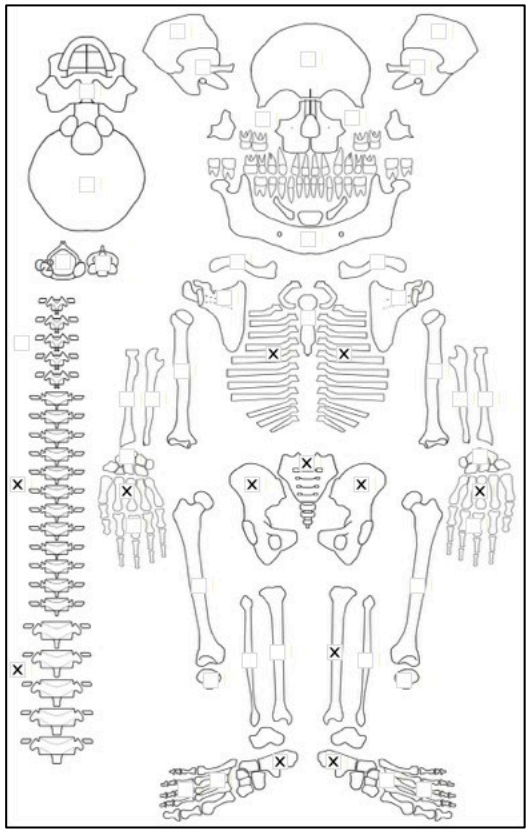

Completeness: Incomplete (33 to 50%). 8% long bones, 19% hands and feet, 58% vertebrae, 0% neurocranium, ribs near complete.
Preservation/ Taphonomy: Surfaces in good condition but covered with thin layer of soil. All vertebrae that are preserved are intact. Only left tibia of the long bones is present but intact.
Age: 50+, *Old Adult*
Sex: Female
Macroscopic Lesion Summary:
No pathology
Radiographic Lesion Summary:
No radiographs taken
Differential Diagnosis Outcome:
No diagnosis

Skeletal ID: AT-885b

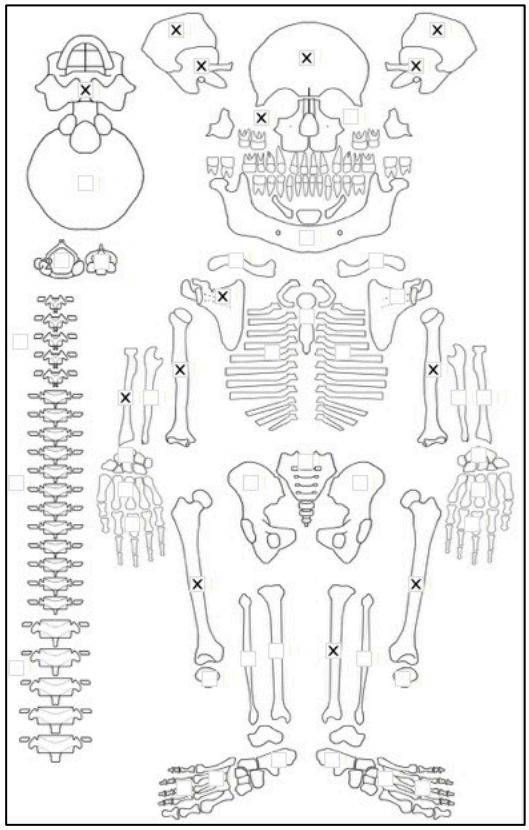

Completeness: Partially Complete (50 to 66%). 50% long bones, 0% hands and feet, 0% vertebrae, 75% neurocranium, ribs fragmented.
Preservation/ Taphonomy: Bones and surfaces have excellent preservation and most metaphyseal plates are intact.
Age: 0 years (+/- 1.5 months). *Infant*
Sex: Indeterminate
Macroscopic Lesion Summary:
- bilateral discrete deposit of new bone and cortical porosity on the superior orbital roofs.
- bilateral diffuse active new bone on the external squamous of the temporal bones
- diffuse new bone on the right external great wing, around the region of the foramen rotundum and lesser wing of the sphenoid
- diffuse new bone and cortical porosity on the right maxilla: palatal surface, posterior, infraorbital surface and anterior maxilla
- discrete active new bone on the endocranial and ectocranial left pars lateralis
- discrete active deposits of new bone on the supraspinous and infraspinous fossae of the right scapula
- bilateral diffuse active new bone across the entire shafts of the humeri and the femora
- bilateral abnormal deep endochondral porosity exceeding 10mm from the distal metaphyseal plates of the femora
- diffuse new bone on the medio-posterior and lateral aspects of the shaft of the left tibia

Radiographic Lesion Summary:
Possible white line of Fraenkel and Trummerfeld zone but not that radiodense. Line of radiolucency is very clear.
Differential Diagnosis Outcome:
Probable Scurvy

Skeletal ID: AT-885a

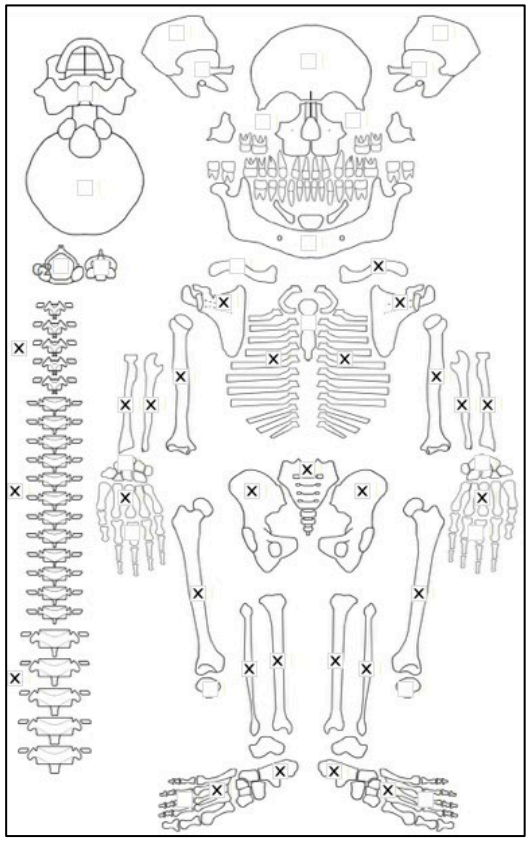

Completeness: Near Complete (66 to 75%). 10% long bones, 52% hands and feet, 79% vertebrae, 0% neurocranium, ribs complete.
Preservation/ Taphonomy: Bones surfaces are excellently preserved. All preserved bones intact.
Age: 18.5 years (+/- 6 months), *Adolescent*
Sex: Female
Macroscopic Lesion Summary:
- medial bending of the shafts of the tibiae and fibulae
Radiographic Lesion Summary:
- very mild cortical thickness of the tibiae and fibulae but associated with clear bending of the shafts
Differential Diagnosis Outcome:
Possible Rickets

Skeletal ID: AT-886

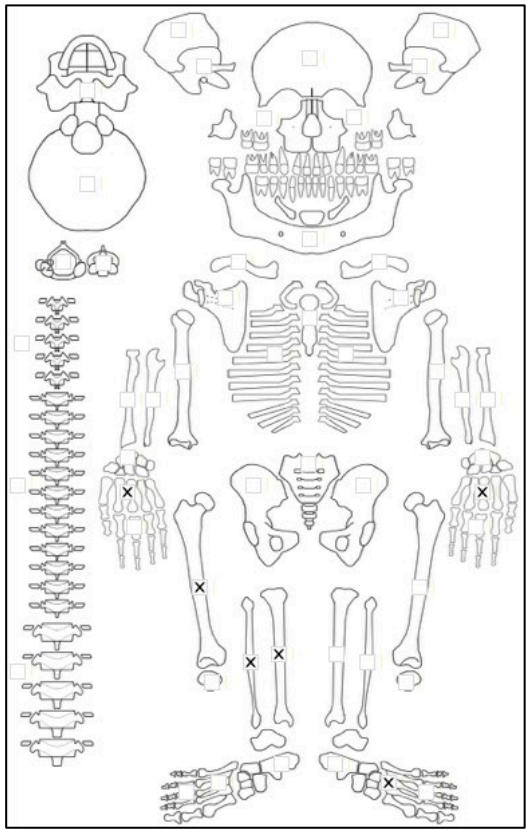

Completeness: Incomplete (33 to 50%). 20% long bones, 11% hands and feet, 13% vertebrae, 0% neurocranium, ribs fragmented.
Preservation/ Taphonomy: Femur intact, proximal tibia missing, both epiphyses of fibula missing. 1 cervical 1 thoracic and 1 lumbar vertebrae intact.
Age: *Adult*
Sex: Indeterminate
Macroscopic Lesion Summary:
No pathology
Radiographic Lesion Summary:
No radiographs taken
Differential Diagnosis Outcome:
No diagnosis

Skeletal ID: AT-992

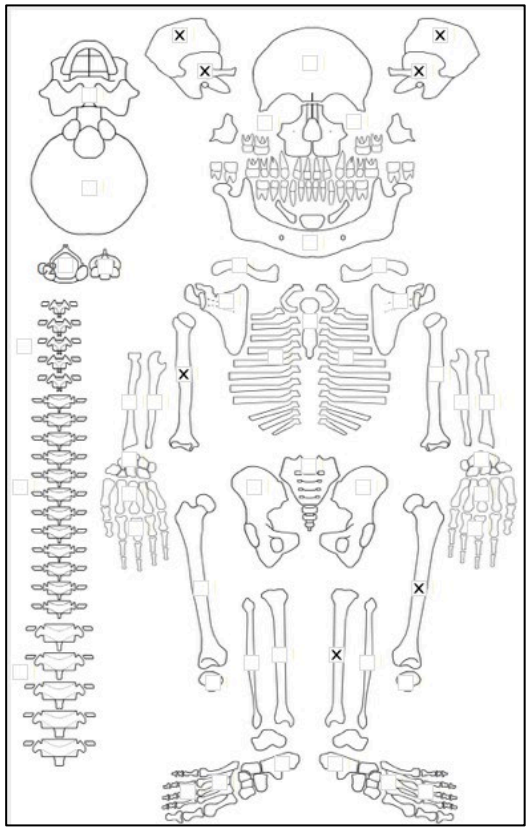

Completeness: Fragmented. 15% long bones, 0% hands and feet, 0% vertebrae, 0% neurocranium, no ribs.
Preservation/ Taphonomy: Surfaces are severely damaged by weathering. No epiphyses preserved. Lateral third tibia taken for sampling
Age: *Adult*
Sex: Indeterminate
Macroscopic Lesion Summary:
No pathology
Radiographic Lesion Summary:
No radiographs taken
Differential Diagnosis Outcome:
No diagnosis

Skeletal ID: AT-923

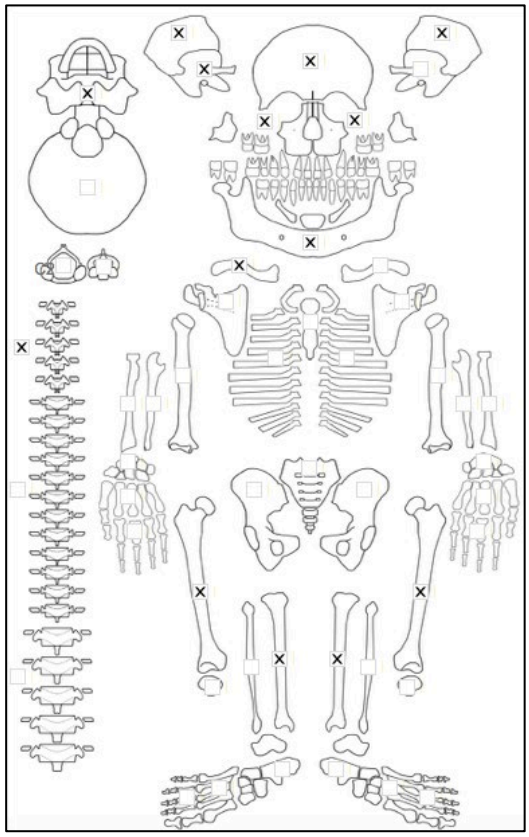

Completeness: Incomplete (33 to 50%). 23% long bones, 5% hands and feet, 13% vertebrae, 63% neurocranium, no ribs.
Preservation/ Taphonomy: Severe weathering and fragmentation, but the shafts of the femora and tibiae can be observed, right fibula middle anterior third taken for sampling. Left femur medial shaft only. Only the right femoral epiphyses are preserved.
Age: 50+, *Old Adult*
Sex: Indeterminate
Macroscopic Lesion Summary:
- bilateral remodelled deep vascular impressions on the endocranium of the parietals around the sagittal suture
Radiographic Lesion Summary:
No radiographs taken
Differential Diagnosis Outcome:
No diagnosis

Skeletal ID: AT-931

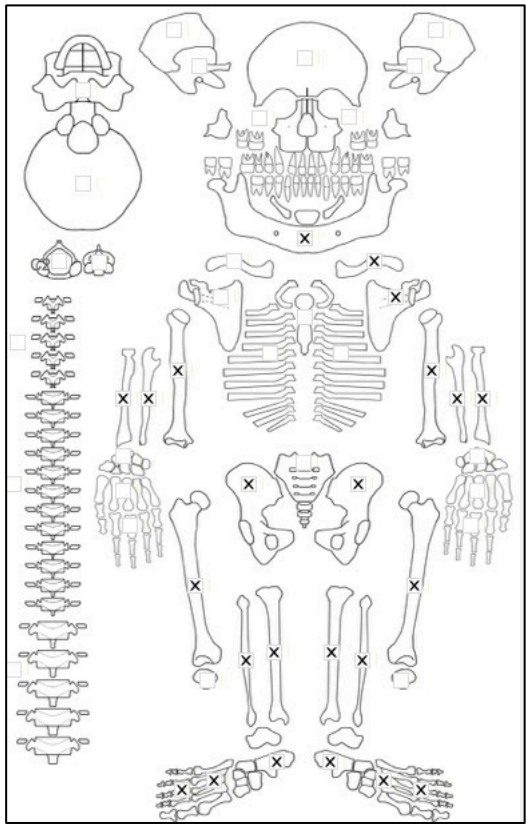

Completeness: Near Complete (66 to 75%). 90% long bones, 30% hands and feet, 0% vertebrae, 0% neurocranium, no ribs.
Preservation/ Taphonomy: Surfaces in good condition except for weathering on the right humerus, left radius. surfaces have a layer of soil but can still be observed. Both epiphyses of right humerus, distal epiphyses of left humerus and ulna, and proximal epiphysis of left radius and right fibula are missing. Anterior right middle third femur sampled for isotopes
Age: 30-39, *Young Adult*
Sex: Male
Macroscopic Lesion Summary:
No pathology
Radiographic Lesion Summary:
No radiographs taken
Differential Diagnosis Outcome:
No diagnosis

Skeletal ID: AT-951

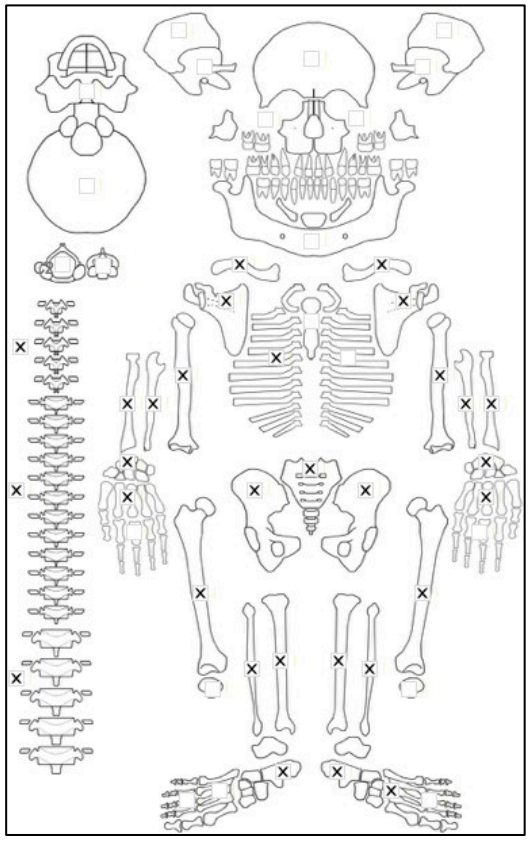

Completeness: Near Complete (66 to 75%). 93% long bones, 39% hands and feet, 63% vertebrae, 0% neurocranium, ribs incomplete.
Preservation/ Taphonomy: soil is covering the bones but the surfaces can still be observed. some animal gnaw marks on the long bone, right scapula body mostly intact. Both epiphyses of the left radius, distal epiphyses of the left ulna, and proximal epiphysis of left fibula is missing. Vertebrae mixed preservation, some are severely fragmented while others are intact. fragmentation more common of the upper spine. Two mandibles present both severely damaged, do not appear to belong to this individual anyway so was excluded.
Age: 30-39, *Young Adult*
Sex: Male
Macroscopic Lesion Summary:
No pathology
Radiographic Lesion Summary:
No radiographs taken
Differential Diagnosis Outcome:
No diagnosis

Skeletal ID: AT-952

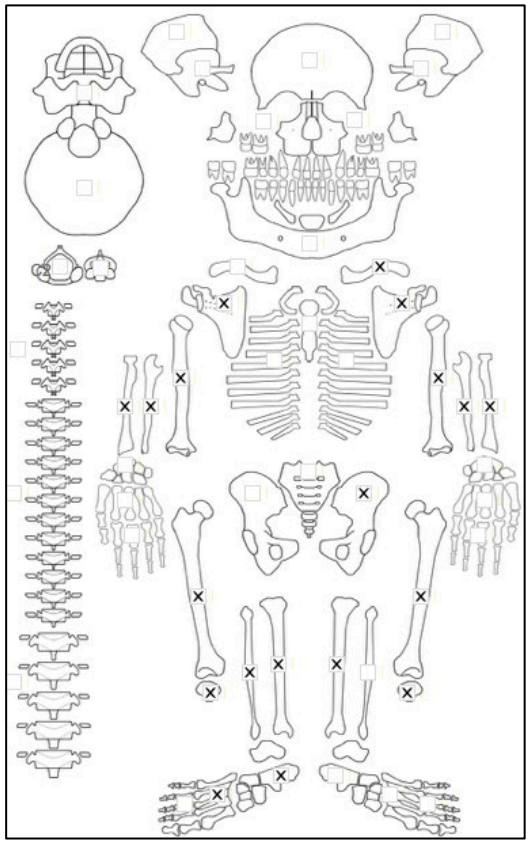

Completeness: Partially Complete (50 to 66%). 75% long bones, 5% hands and feet, 4% vertebrae, 0% neurocranium, no ribs.
Preservation/ Taphonomy: Moderate to severe scavenging of the long bones (gnaw marks) scapula blades missing. Both epiphyses of radii left ulna, proximal epiphysis of fibula, and distal 2/3rd of right ulna missing.
Age: 30-39, *Middle Aged Adult*
Sex: Male
Macroscopic Lesion Summary:
No pathology
Radiographic Lesion Summary:
No radiographs taken
Differential Diagnosis Outcome:
No diagnosis

Skeletal ID: AT-961

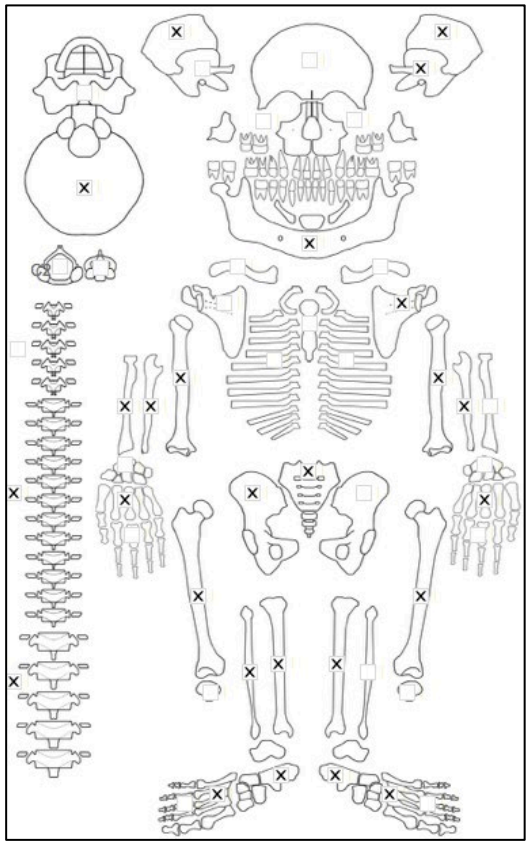

Completeness: Near Complete (66 to 75%). 67% long bones, 15% hands and feet, 29% vertebrae, 0% neurocranium, no ribs.
Preservation/ Taphonomy: Some gnaw marks on long bones, and soil on the surfaces. All vertebrae have pm breakage between arches and bodies except 3. Both epiphyses of right humerus and right radius, distal epiphysis of left and right ulna and left femur and proximal epiphysis of right fibula and left tibia missing. Skull cap except frontal, left temporal, near complete mandible present. Covered in thick grey soil. Difficult to assess the surfaces. Severe weathering of the mandible.
Age: 40-49, *Middle Aged Adult*
Sex: Female
Macroscopic Lesion Summary:
- medial bending of the shafts of the tibiae
- anterior bending of the right femur with some gena valgum (knocked knees). Left femur too damaged to assess.

Radiographic Lesion Summary:
- some mild cortical thickness in the concave aspect of the tibial bending deformities.

Differential Diagnosis Outcome:
Possible Osteomalacia
Possible Residual Rickets

Skeletal ID: AT-962

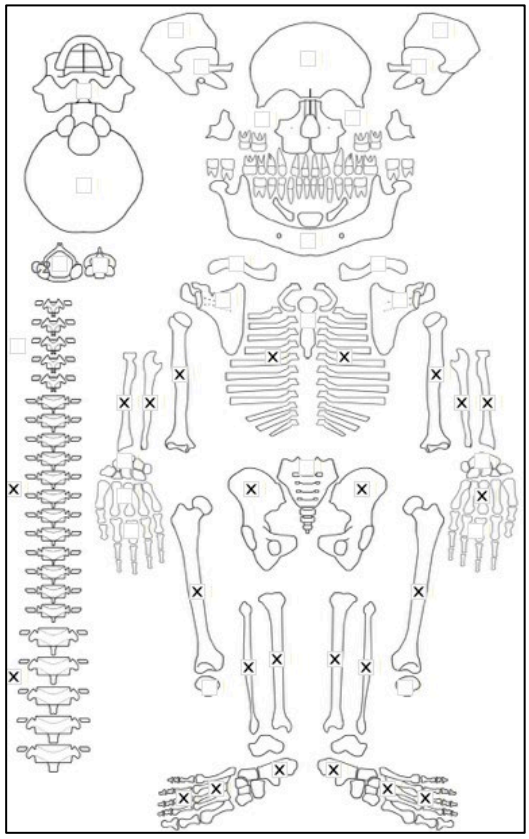

Completeness: Complete (>75%). 80% long bones, 43% hands and feet, 42% vertebrae, 0% neurocranium, ribs partially complete.
Preservation/ Taphonomy: Surfaces in good condition but covered in dark soil. Breakage of the pelvis and bone ends. proximal epiphysis tibiae and fibulae, distal epiphysis of radii and ulnae and right femur, both epiphyses of left humerus missing. All preserved vertebrae are intact
Age: 50+, *Old Aged Adult*
Sex: Female
Macroscopic Lesion Summary:
- Biconcavity of the vertebrae (T8 to L5), resulting in severe kyphosis at the T10 to 12 region. There is no lytic destruction in this region just depression of the vertebral bodies
- medial bending of the shafts of the tibiae
Radiographic Lesion Summary:
- vertical trabecular coarsening with loss of horizontal trabeculae of the vertebrae (but there is severe compression making it difficult to study), cortical margins of the vertebrae are thin, codfish vertebrae
- no clear cortical thickening of the tibiae
Differential Diagnosis Outcome:
Probable Osteomalacia
Probable Residual Rickets

Skeletal ID: AT-963

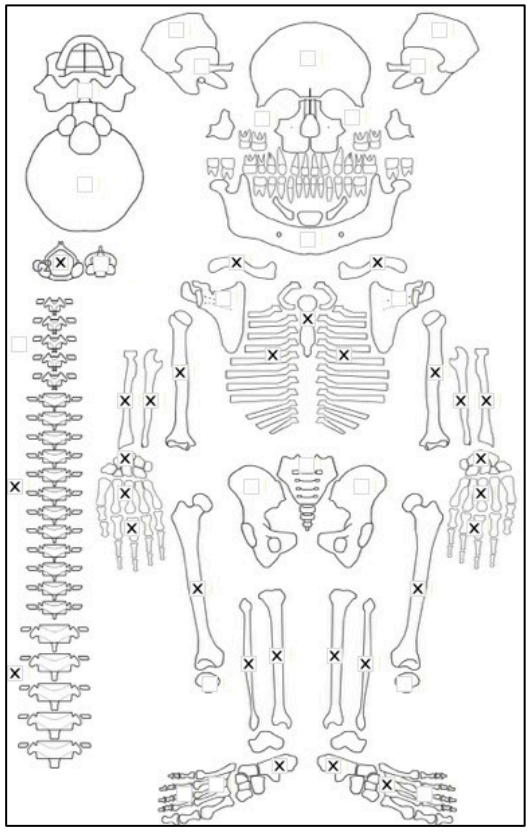

Completeness: Near Complete (66 to 75%). 98% long bones, 48% hands and feet, 46% vertebrae, 0% neurocranium, ribs partially complete.
Preservation/ Taphonomy: Surfaces in excellent condition but covered in a thin layer of soil. Vertebrae preserved are mostly intact with few fragmented.
Age: 40-49, *Middle Aged Adult*
Sex: Male
Macroscopic Lesion Summary:
- Foramen expansion on the anterior body of an upper lumbar vertebra
Radiographic Lesion Summary:
No radiographs taken
Differential Diagnosis Outcome:
No diagnosis

Skeletal ID: AT-965

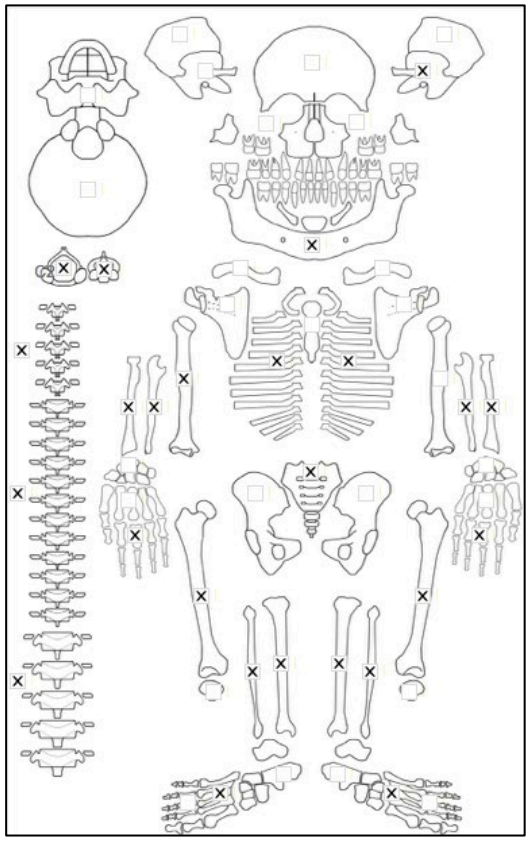

Completeness: Near Complete (66 to 75%). 90% long bones, 23% hands and feet, 96% vertebrae, 13% neurocranium, ribs near complete.
Preservation/ Taphonomy: Surfaces in good condition, covered in thin layer of soil but surfaces are still visible.
Age: *Adult*
Sex: Male
Macroscopic Lesion Summary:
- localised discrete deposit of remodelled new bone on the left medial coronoid fossa of the mandible (right missing)
- localised vascular impressions indicating remodelled deposit of new bone inferior to the left mylohyoid line of the mandible (right side missing).
- unilateral remodelled discrete deposit of new bone on the medial proximal aspect of the right femur

Radiographic Lesion Summary:
No radiographs taken
Differential Diagnosis Outcome:
No diagnosis

Skeletal ID: AT-232b

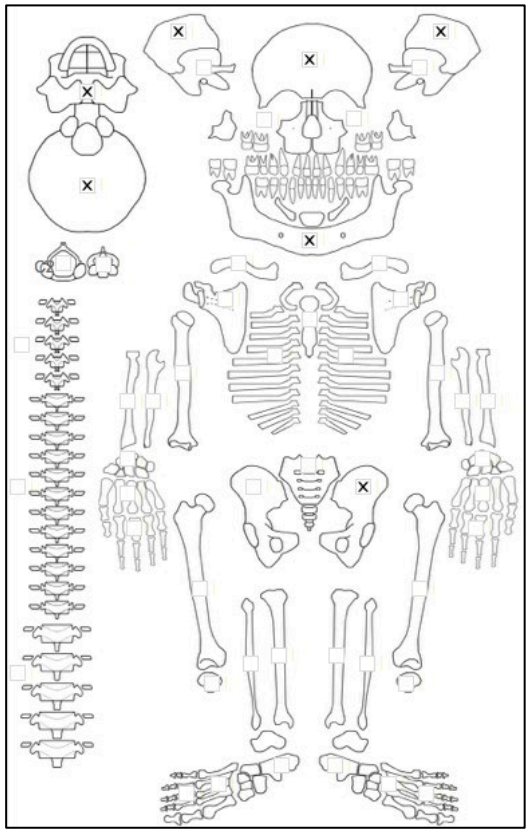

Completeness: Incomplete (33 to 50%). 0% long bones, 0% vertebrae, 0% hands and feet, 75% neurocranium, ribs fragmented.

Preservation/ Taphonomy: Skull, ilium, rib fragment only. Parietals, frontal, mandible, occipital and right wing sphenoid and ethmoid preserved.

Age: 3 years (+/- 1 year). *Child*

Sex: Indeterminate

Macroscopic Lesion Summary:

- remodelled bilateral discrete new bone deposits and cortical porosity on the incisive fossae of the mandible
- bilateral mixed active and remodelled discrete new bone deposits on the external ramii of the mandible inferior to the oblique line
- bilateral discrete active new bone deposits on the medial coronoid processes of the mandible
- remodelling porosity of unknown aetiology on the occipital planum
- remodelling bilateral fine porosity of unknown aetiology on superior orbits
- remodelling bilateral discrete deposit of remodelled cortical porosity and vascular impressions on the zygomatic processes of the frontal
- mixed active and remodelled new bone on the external right greater wing of sphenoid, on the right lesser wing and around the region of the foramen rotundum.

Radiographic Lesion Summary:

Radiographs not taken

Differential Diagnosis Outcome:

Probable Scurvy

Skeletal ID: AT-176

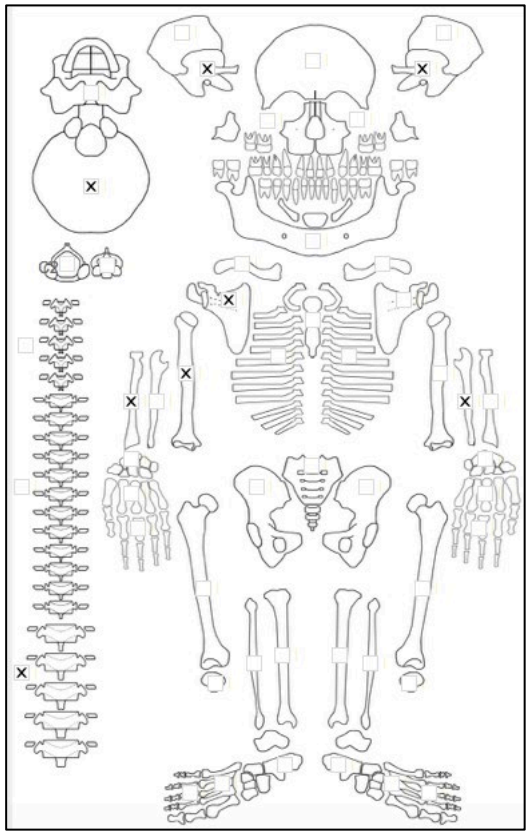

Completeness: Incomplete (33 to 50%). 25% long bones, 0% hands and feet, 13% vertebrae, 38% neurocranium.
Preservation/ Taphonomy: Metaphyses of radius and distal humerus not preserved, proximal plate of ulna not preserved and metaphyses of distal end of ulna not preserved. moderate weathering of the bones.
Age: Approx. 6-10 years, *Child*
Sex: Indeterminate
Macroscopic Lesion Summary:
- abnormal endochondral porosity exceeding 10mm from the proximal metaphyseal plate of the right humerus
- slight posterior bending with lateral rotation of the distal shaft leading to protrusion of the distal end anteriorly.
- enlarged sternal ends of ribs

Radiographic Lesion Summary:
- Coarsening trabeculae in the metaphyses of the humeri
- Long bone cortices appear thickened

Differential Diagnosis Outcome:
Possible Rickets
Possible Scurvy

Skeletal ID: AT-177

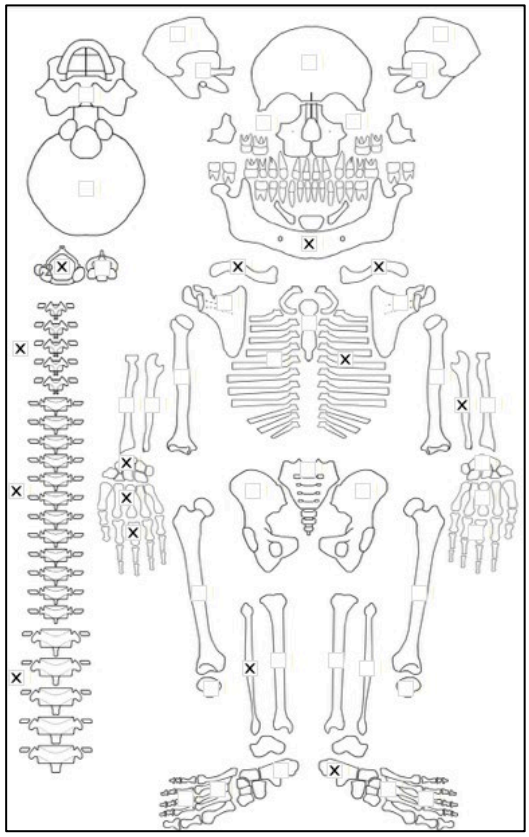

Completeness: Incomplete (33 to 50%). 20% long bones, 12% hands and feet, 71% vertebrae, 0% neurocranium, ribs incomplete.
Preservation/ Taphonomy: Surfaces well preserved. Some long bones, calcanei, talus and lumbar vertebrae of a second smaller individual. Not assessed. Mandible body and palatal portion of maxillae present. All preserved vertebrae intact.
Age: 20-29, *Young Adult*
Sex: Male
Macroscopic Lesion Summary:
- vertebral porosity and expanded foramen on the anterior bodies of T8, T9 and T12
Radiographic Lesion Summary:
- some possible mild osteopenia of the vertebrae.
- no sclerotic processes detected in vertebrae
Differential Diagnosis Outcome:
No diagnosis

Skeletal ID: AT-218

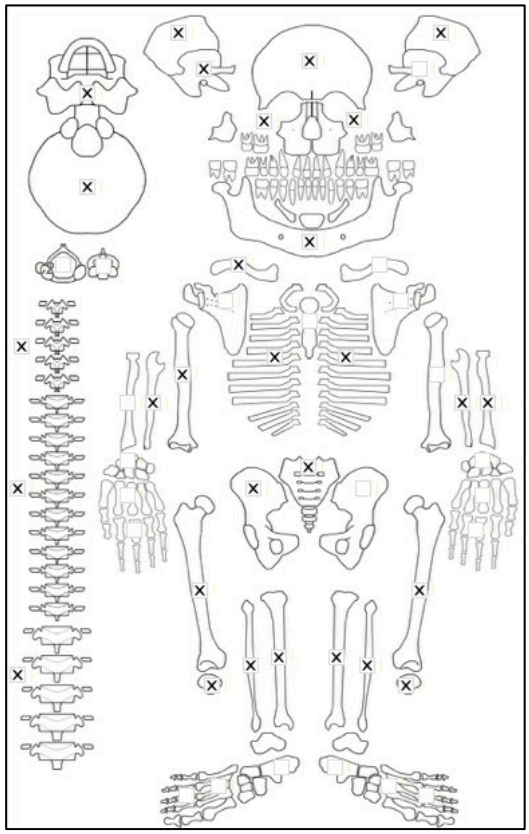

Completeness: Complete (>75%). 81% long bones, 3% hands and feet, 54% vertebrae, 100% neurocranium, ribs complete.
Preservation/ Taphonomy: Surfaces moderately damaged by weathering. Epiphyses and metaphyses present and in good condition. Anterior left femur middle third taken for isotope studies. Proximal 2/3s of left fibula missing. Preserved vertebrae in excellent condition.
Age: 15.5 (+/- 6 months), *Adolescent*
Sex: Female
Macroscopic Lesion Summary:
- bilateral medial bending of the tibiae
- lateral bending deformity at the proximal third shaft of the right humerus
- bilateral mild active cribra orbitalia
- unilateral cortical porosity on the right greater wing of sphenoid, left has cortical porosity as well but this is slight and within normal limits
- bilateral discrete new bone deposit and cortical porosity on the left coronoid process of the mandible. The left new bone is active whereas there is some remodelling on the right.

Radiographic Lesion Summary:
- clear thickening of the shafts of the tibiae and right femur and right humerus.
- right femur has lateral broadening and flattening of the proximal shafts
- clear true bending of the tibiae with multiple stress lines present in the proximal and distal metaphyses.
- ground glass osteopenia of the metaphyses
- no clear evidence of osteopenia in the vertebrae (one vertebrae show very mild osteopenia)
- multiple stress lines in the long bones shafts
- coarsened trabeculae in the distal humeri

Differential Diagnosis Outcome:
Probable Rickets
Possible Scurvy

Skeletal ID: AT-271

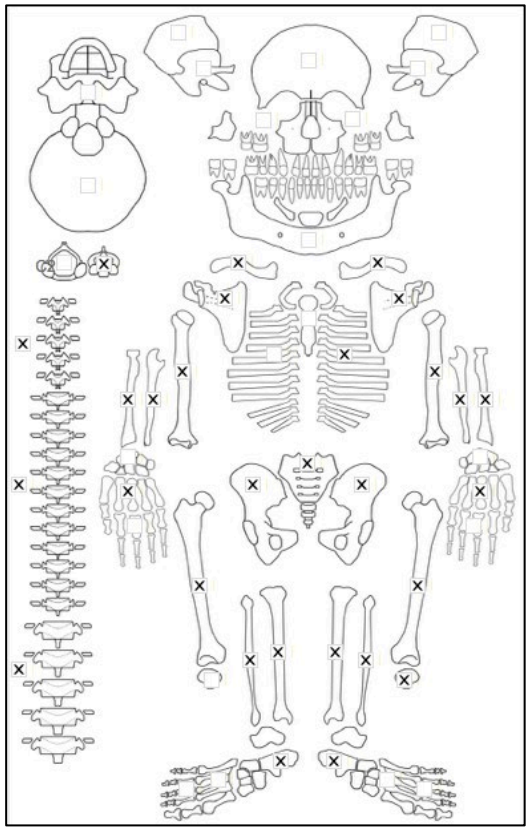

Completeness: Near Complete (66 to 75%). 95% long bones, 11% hands and feet, 79% vertebrae, 0% neurocranium, ribs partially complete.
Preservation/ Taphonomy: Long bone surfaces in excellent condition. Proximal epiphysis of left fib, and both epiphysis of right fib missing. Anterior middle third of right femur taken for sampling. Most vertebrae that are preserved are intact and surfaces in excellent condition.
Age: 19.5 years (+/- 1.5 years). *Adolescent*
Sex: Female
Macroscopic Lesion Summary:
- small discrete unilateral deposit of remodelled new bone on the posterior middle third of the left tibia
Radiographic Lesion Summary:
No radiographs taken
Differential Diagnosis Outcome:
No diagnosis

Skeletal ID: AT-276

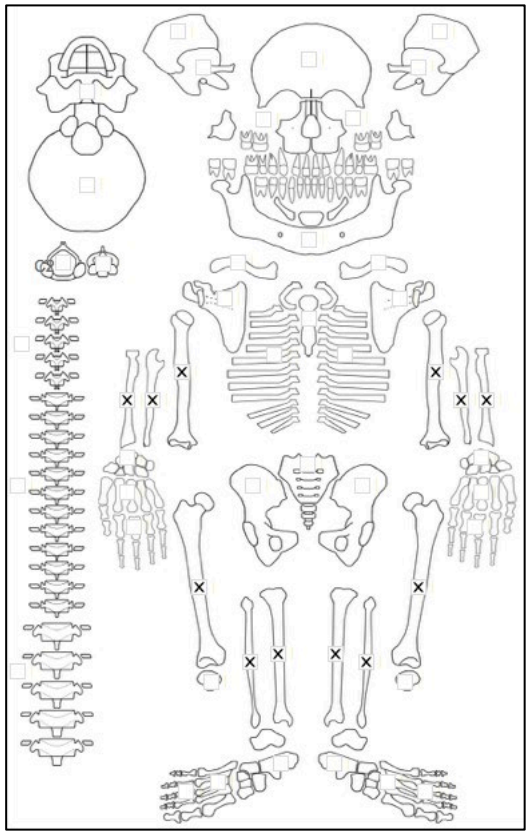

Completeness: Partially Complete (50 to 66%). 72% long bones, 0% hands and feet, 0%vertebrae, 0% neurocranium, no ribs.
Preservation/ Taphonomy: Intrusive clavicle and fibula from smaller individual- not assessed. Long bones only- both epiphysis of right fibula, proximal epiphyses of tibiae and left humerus missing. proximal 2/3rds of left fibula missing. Moderate damage by gnaw marks and soil on the surfaces
Age: *Adult*
Sex: Indeterminate
Macroscopic Lesion Summary:
No pathology
Radiographic Lesion Summary:
No radiographs taken
Differential Diagnosis Outcome:
No diagnosis

Skeletal ID: AT-275

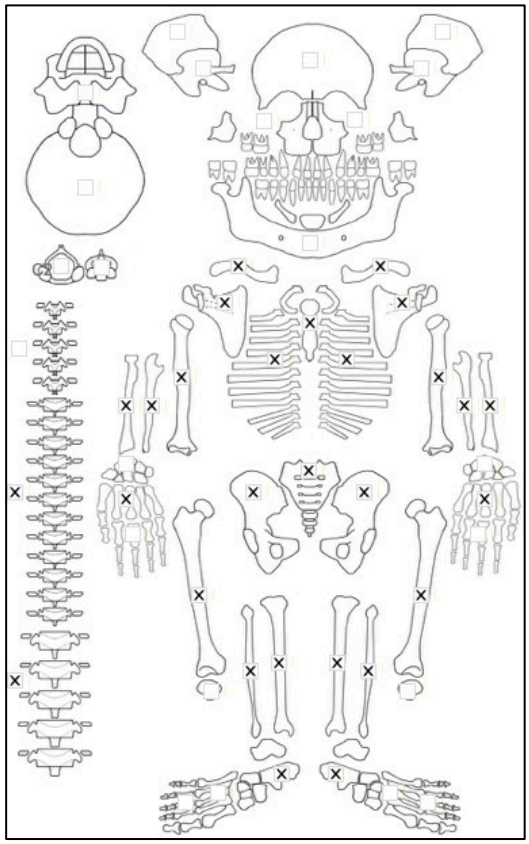

Completeness: Near Complete (66 to 75%). 98% long bones, 16% hands and feet, 46% vertebrae, 0% neurocranium, ribs partially complete.
Preservation/ Taphonomy: Surfaces in good condition with some soil covering the bones. Proximal epiphysis of left fibula missing. Anterior distal third shaft of right femur taken for sampling.
Age: 30-39, *Middle Aged Adult*
Sex: Male
Macroscopic Lesion Summary:
No pathology
Radiographic Lesion Summary:
No radiographs taken
Differential Diagnosis Outcome:
No diagnosis

Skeletal ID: AT-273

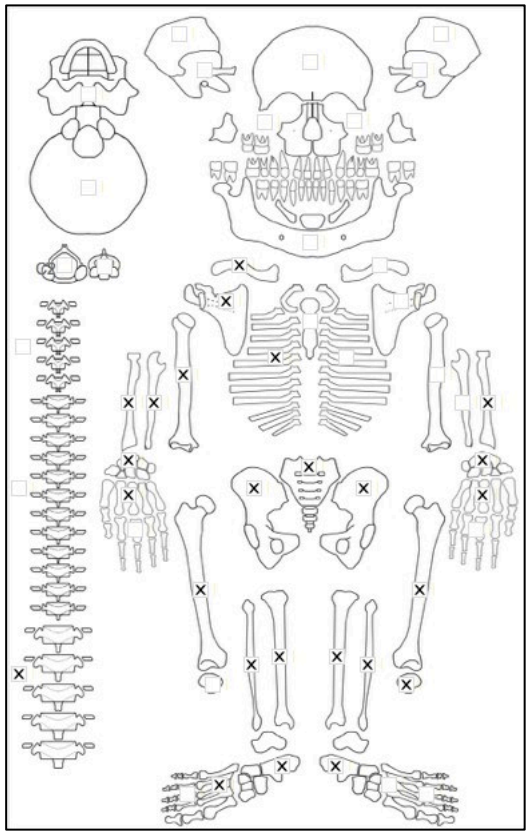

Completeness: Near Complete (66 to 75%). 82% long bones, 24% hands and feet, 8% vertebrae, 0% neurocranium, ribs incomplete.
Preservation/ Taphonomy: Surfaces in excellent condition. All long bones intact except for proximal epiphysis of left radius. Anterior middle third of right femur taken for sampling
Age: 30-39, *Middle Aged Adult*
Sex: Male
Macroscopic Lesion Summary:
No pathology
Radiographic Lesion Summary:
No radiographs taken
Differential Diagnosis Outcome:
No diagnosis

Skeletal ID: AT-466

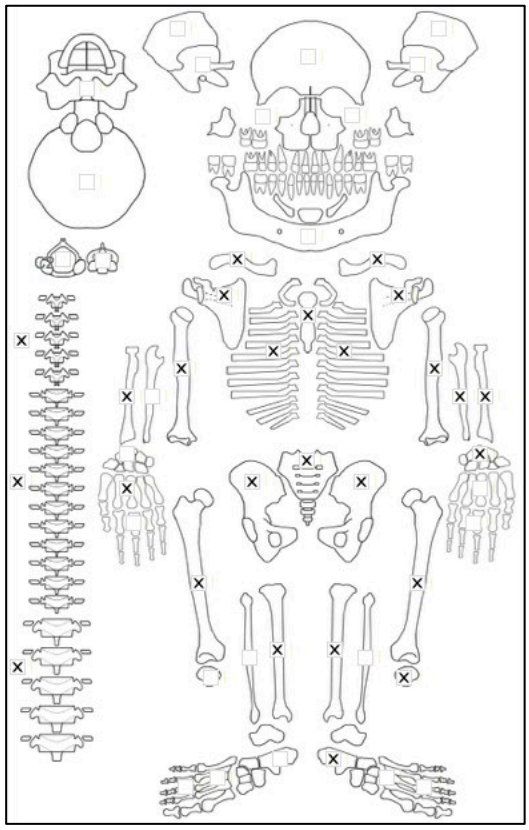

Completeness: Near Complete (66 to 75%). 68% long bones, 8% hands and feet, 100% vertebrae, 0% neurocranium, ribs partially complete.
Preservation/ Taphonomy: Surfaces in excellent condition with weathering of the distal humeri. Anterior middle third of femur taken for sampling.
Age: 40-49, *Middle Aged Adult*
Sex: Male
Macroscopic Lesion Summary:
- anterior bending deformity of the sternum
- bilateral anterior and slight lateral bending deformities of the femoral shafts
- bilateral medial bending deformities of the tibial shafts. right side more severe than the left

Radiographic Lesion Summary:
- There may be very slight vertical trabecular coarsening of the vertebrae
- multiple stress lines in the proximal and distal shafts of the metaphyses
- clear cortical thickness of the tibial shafts particularly at region of bending

Differential Diagnosis Outcome:
Probable Osteomalacia
Possible Residual Rickets

Skeletal ID: AT-484

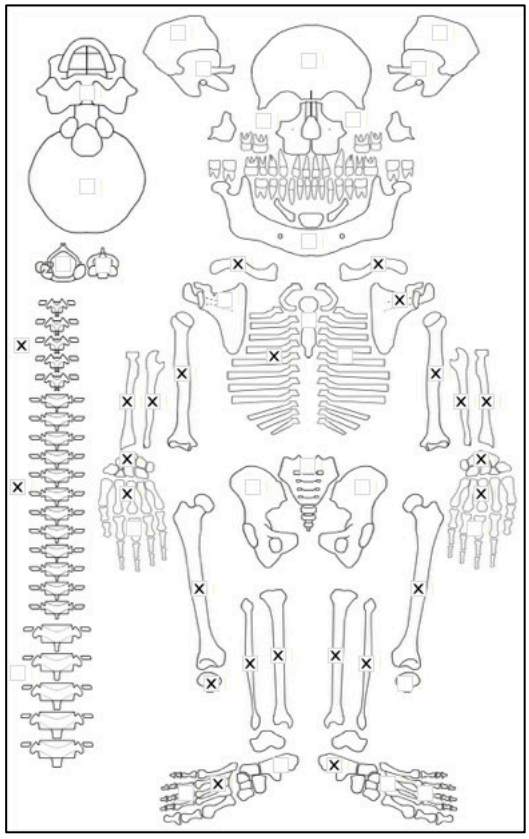

Completeness: Partially Complete (50 to 66%). 75% long bones, 25% hands and feet, 25% vertebrae, 0% neurocranium, partially complete ribs.
Preservation/ Taphonomy: Surfaces have some weathering and many of the bone ends are damaged, epiphyses of humeri and left radius, distal epiphysis of tibiae and right radius, proximal epiphyses of the ulnae are preserved. Partial distal epiphysis of left femur preserved. Distal third shafts of fibulae only are present
Age: *Adult*
Sex: Indeterminate
Macroscopic Lesion Summary:
- bilateral medial bending deformities of the femoral shaft
Radiographic Lesion Summary:
No radiographs taken
Differential Diagnosis Outcome:
Possible Residual Rickets

Skeletal ID: AT-534

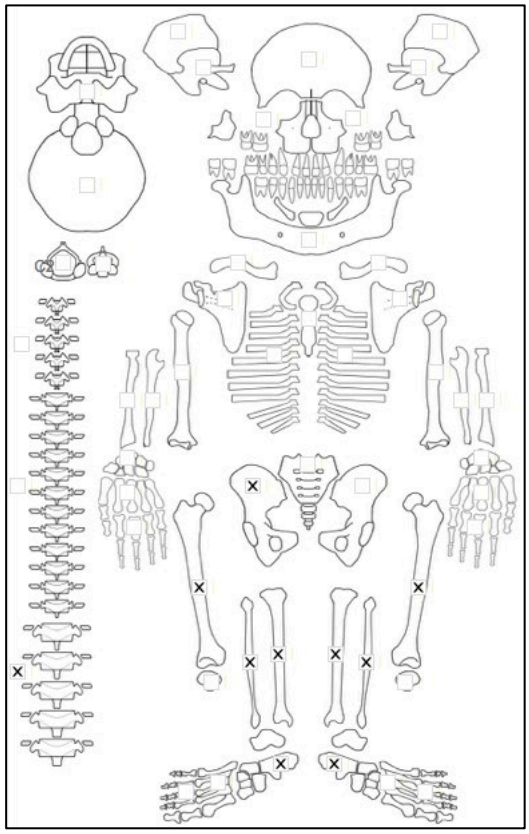

Completeness: Partially Complete (50 to 66%). 25% long bones, 5% hands and feet, 8% vertebrae, 0% neurocranium, no ribs.
Preservation/ Taphonomy: Surfaces covered in dark soil and considerable damage to bone ends, only proximal femur and distal fibulae and tibiae epiphyses preserved. Distal half of right femur missing. only distal third of left fibula.
Age: *Adult*
Sex: Female
Macroscopic Lesion Summary:
- bilateral medial bending deformities of the tibial shafts
Radiographic Lesion Summary:
No radiographs taken
Differential Diagnosis Outcome:
Possible Residual Rickets

Skeletal ID: AT-565

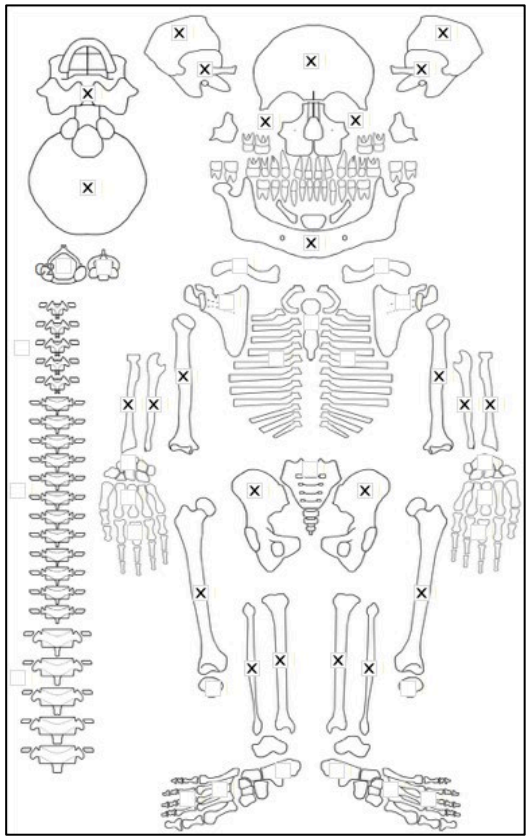

Completeness: Near Complete (66 to 75%). 77% long bones, 0% hands and feet, 0% vertebrae, 88% neurocranium, no ribs.
Preservation/ Taphonomy: Surfaces in good condition but covered in dark soil. Proximal epiphyses of humeri, distal epiphyses of radii and ulnae, and both epiphyses of fibulae missing. only distal third shaft of right radius and left fibula present.
Age: 40-49, *Middle Aged Adult*
Sex: Female
Macroscopic Lesion Summary:
No pathology
Radiographic Lesion Summary:
No radiographs taken
Differential Diagnosis Outcome:
No diagnosis

Skeletal ID: AT-608

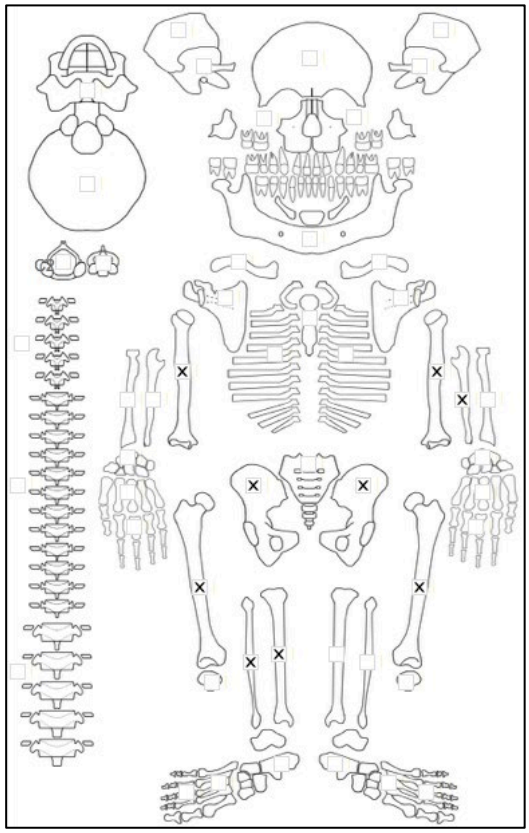

Completeness: Incomplete (33 to 50%). 45% long bones, 0% hands and feet, 0% vertebrae, 0% neurocranium, no ribs
Preservation/ Taphonomy: Long bones and pelvis only. surfaces have dark soil and moderate to severe weathering of the humeri. Epiphyses of humeri and ulna and proximal tibia and fibula missing. Anterior middle third of left humerus taken for sampling.
Age: *Adult*
Sex: Male
Macroscopic Lesion Summary:
No pathology
Radiographic Lesion Summary:
No radiographs taken
Differential Diagnosis Outcome:
No diagnosis

Skeletal ID: AT-609

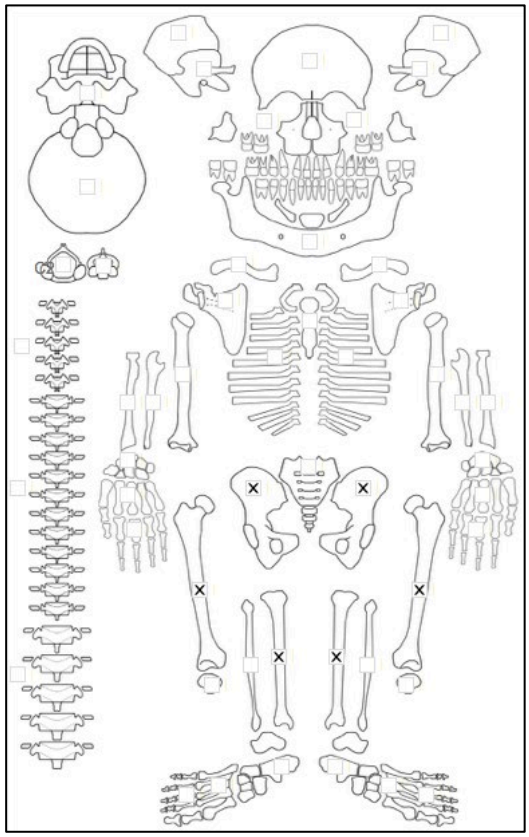

Completeness: Incomplete (33 to 50%). 20% long bones, 0% hands and feet, 0% vertebrae, 0% neurocranium, no ribs
Preservation/ Taphonomy: Long bones are severely weathered. No epiphyses preserved.
Age:
Sex:
Macroscopic Lesion Summary:
No pathology
Radiographic Lesion Summary:
No radiographs taken
Differential Diagnosis Outcome:
No diagnosis

Skeletal ID: AT-630

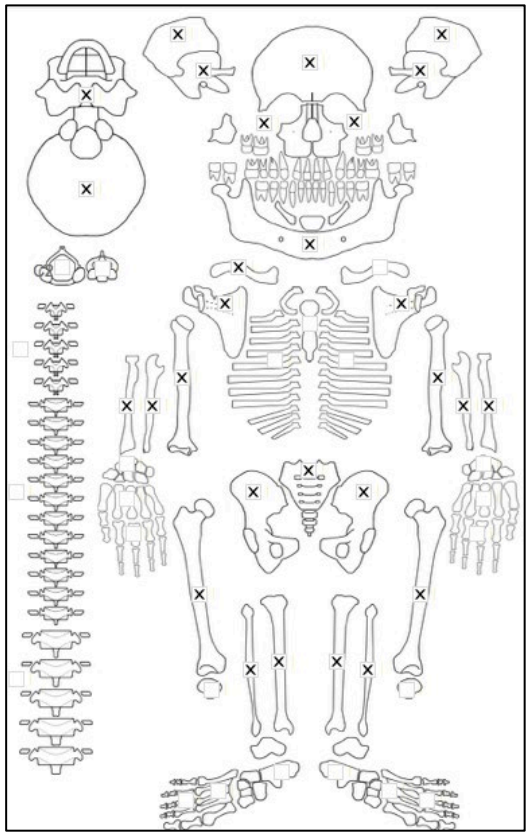

Completeness: Near Complete (66 to 75%). 98% long bones, 0% hands and feet, 0% vertebrae, 100% neurocranium, no ribs.
Preservation/ Taphonomy: Surfaces in excellent condition. Scapula bodies partially damaged. Medial middle third of left femur has been sampled. Proximal epiphysis of right radius missing. Cranium intact
Age: 50+, *Old Adult*
Sex: Female
Macroscopic Lesion Summary:
- large and deep circumscribed lytic lesion with sharp defined margins but sclerotic response in the base infero-lateral to the acetabulum of the right os coxa. Lesion diameter: 11.78x9.11mm. Another small circumscribed lesion extends into the acetabular fossa and appears to extend behind the articular surface of the inferior acetabulum through a channel. Lesion diameter: 6.05x4.47mm. There is lipping (articular changes) to the inferior acetabulum as a result of the lesion. There is no associated response on the femoral head. The iliac blade appears porous.
- bilateral but not symmetrical lytic destruction on the superior greater tubercles of the humeri. The lesion runs adjacent to the margin of the articular surface of the head of the humerus. There is minimal sclerotic response and margins are sharp. The larger lesion is circumscribed. There is associated arthritic changes on the lesser tubercle of the left humerus. There is another unilateral circumscribed lesion with sclerotic response on the lateral margin of the olecranon process of the left humerus
Left humerus proximal lesion diameter: 7.92x4.11mm, Left humerus distal lesion diameter: 9.30x5.79mm, Right humerus proximal lesion diameter: 15.97x7.50mm
- 3 small unilateral circumscribed lesions on the inferior articular surface of the left ulna. There is sclerotic response in the base, but the margins are well defined. Lesion diameters: 2.86x1.88mm, 1.54x1.31mm, 3.96x3.337mm.
- bilateral remodelling cribra orbitalia. The right side is moderate (due to some coalescing) whereas the left is mild
- remodelled circular deep focal lesion extending into the trabecular bone directly superior to the mastoid process of the left temporal. X-ray required to investigate the extent. Lesion diameter is 2.54x1.85mm.
Radiographic Lesion Summary:
Lytic lesions appear to be three large overlapping cystic lesions with sclerotic margins on the inferior border of the acetabulum. All three appear to have a focal channel extending deeper into the underlying trabeculae.
- the right os coxa appears to be have some generalised internal bone loss.

Differential Diagnosis Outcome:
Probable Hydatids Disease
Anaemia

Skeletal ID:AT-627

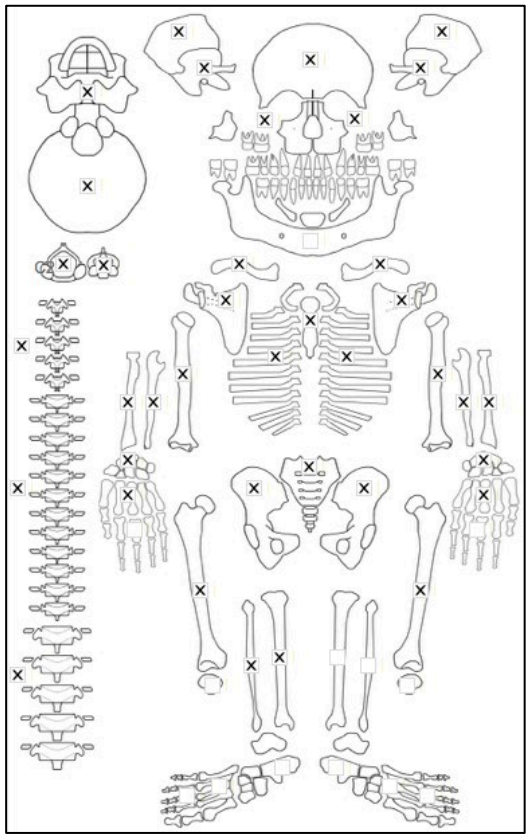

Completeness: Complete (>75%). 83% long bones, 19% hands and feet, 71% vertebrae, 88% neurocranium, ribs near complete.
Preservation/ Taphonomy: Surfaces in excellent condition. anterior middle third of right femur taken for sampling. Intrusive vertebrae, radius and carpals from younger small individual. easily separated.
Age: 40-49, *Middle Aged Adult*
Sex: Male
Macroscopic Lesion Summary:
- small discrete deposit of remodelled new bone on the lateral proximal third of the left tibia on the interosseous crest extending onto the posterior aspect (left tibia missing)
Radiographic Lesion Summary:
No radiographs taken
Differential Diagnosis Outcome:
No diagnosis

Skeletal ID: AT-628

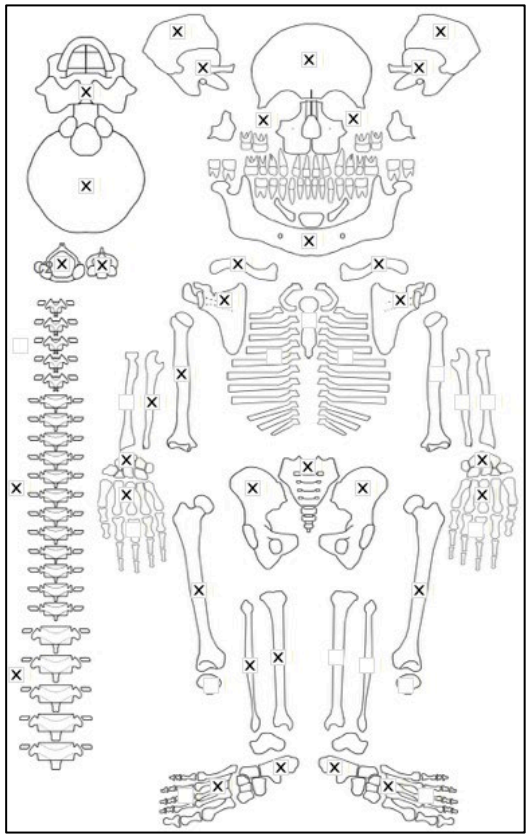

Completeness: Complete (>75%). 52% long bones, 34% hands and feet, 54% vertebrae, 88% neurocranium, no ribs.
Preservation/ Taphonomy: Surfaces in good condition but covered in grey dust. Proximal epiphysis of left tibia, both epiphyses of left fibula present only. Vertebrae half have arches separated from bodies. Anterior middle third of right femur taken for sampling
Age: 30-39, *Young Adult*
Sex: Female
Macroscopic Lesion Summary:
- bilateral discrete remodelled cortical porosity on the left lateral greater wings of sphenoid extending from the foramen ovale. Not associated with any clear new bone.
- bilateral discrete remodelled cortical porosity on the palatal surfaces of the maxillae. There is antermortem tooth loss associated
- remodelled new bone extending from the incisive foramen into the nasal cavity of the left maxilla may indicate continuation of oral infection.
Radiographic Lesion Summary:
No radiographs taken
Differential Diagnosis Outcome:
No diagnosis

Skeletal ID: AT-632

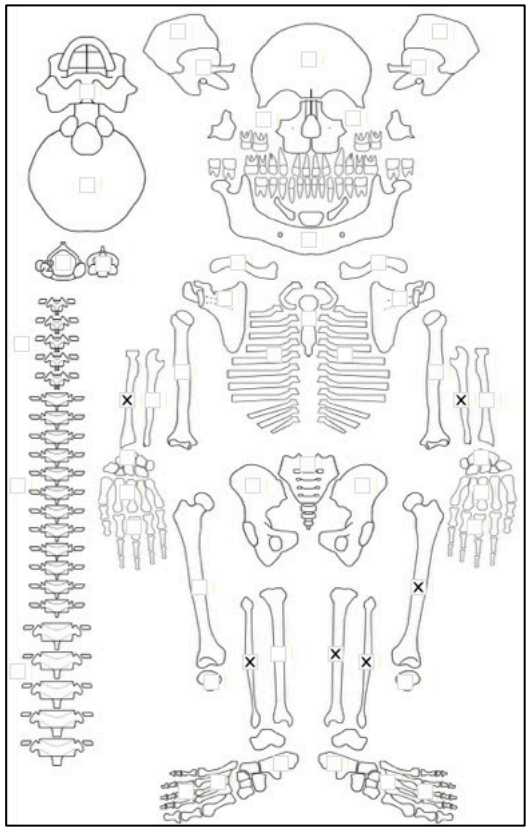

Completeness: Incomplete (33 to 50%). 37% long bones, 2% hands and feet, 0% vertebrae, 0% neurocranium, ribs fragmented.
Preservation/ Taphonomy: Proximal third of left femur taken for sampling. Distal epiphysis of ulna, proximal epiphysis of right fibula and left tibia, and both epiphyses of left fibula and right radius missing. Surfaces in excellent condition.
Age: *Adult*
Sex: Indeterminate
Macroscopic Lesion Summary:
No pathology
Radiographic Lesion Summary:
No radiographs taken
Differential Diagnosis Outcome:
No diagnosis

Skeletal ID: AT-633

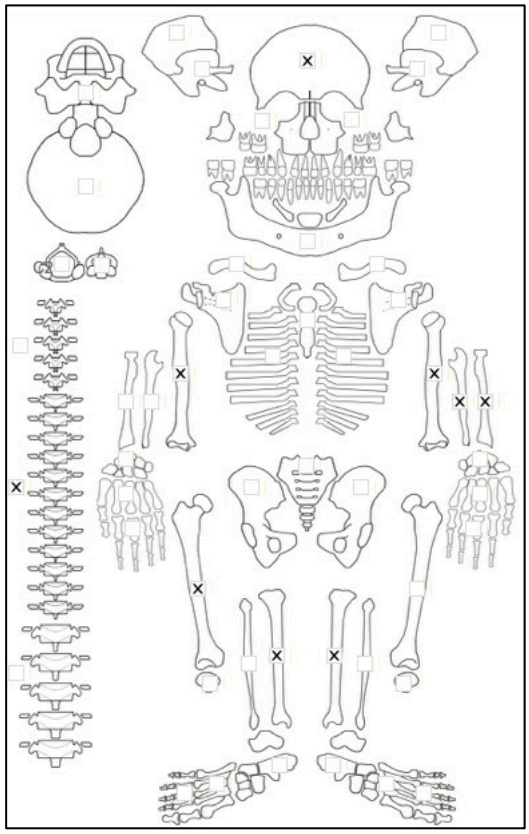

Completeness: Incomplete (33 to 50%). 38% long bones, 7% hands and feet, 21% vertebrae, 13% neurocranium, no ribs.
Preservation/ Taphonomy: Lower limb shafts only. Right femur posterior shaft only preserved. Surfaces of axial skeleton in excellent condition. Long bones has many PM breakage and weathering. Spots of red staining on some of the bones (not lesions).
Age: *Adult*
Sex: Indeterminate
Macroscopic Lesion Summary:
No pathology
Radiographic Lesion Summary:
No radiographs taken
Differential Diagnosis Outcome:
No diagnosis

Skeletal ID: AT-635

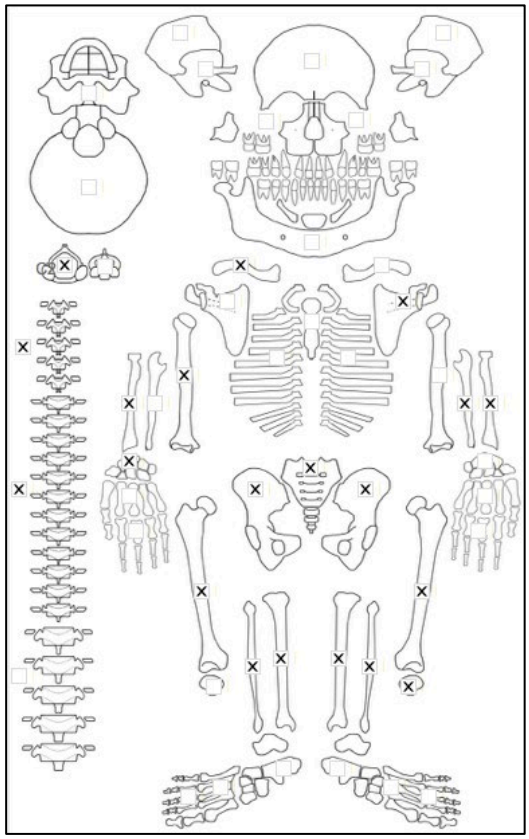

Completeness: Near Complete (66 to 75%). 80% long bones, 4% hands and feet, 38% vertebrae, 0% neurocranium, ribs fragmented.
Preservation/ Taphonomy: Surfaces are excellent. Proximal fibulae epiphysis missing. Posterior middle third femur taken for sampling. Intrusive humerus.
Age: 30-39, *Young Adult*
Sex: Female
Macroscopic Lesion Summary:
- unilateral lateral bending deformity of the shafts of the left tibia with bilateral medial bending of the fibulae
Radiographic Lesion Summary:
- concave thickening of the left tibial bend and the bilateral bends of the fibulae
- thickened trabeculae with osteopenia of the long bone ends
Differential Diagnosis Outcome:
Possible Residual Rickets

Skeletal ID: AT-637

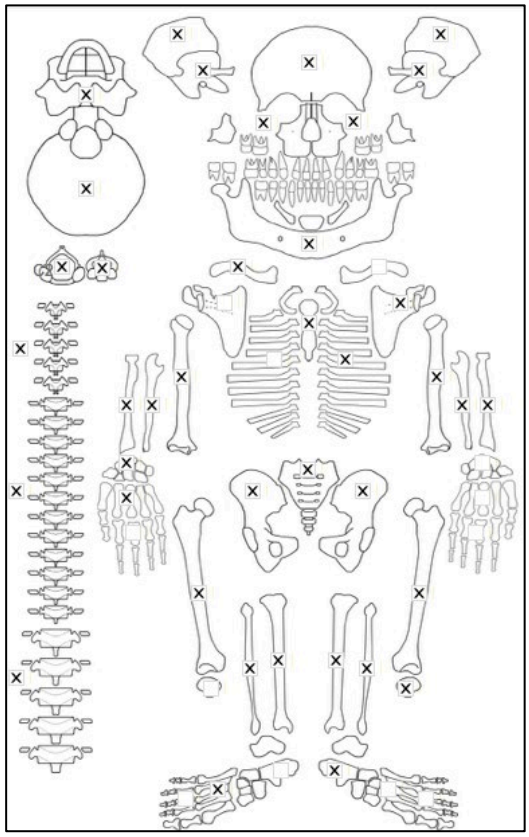

Completeness: Complete (>75%). 98% long bones, 14% hands and feet, 88% vertebrae, 100% neurocranium, ribs incomplete.
Preservation/ Taphonomy: Surfaces in excellent condition. Some taphonomic damage to shafts of the ulnae. Proximal epiphysis of right humerus missing.
Age: 50+, *Old Adult*
Sex: Female
Macroscopic Lesion Summary:
small unilateral discrete deposit of active new bone on the medial distal shaft of the left tibia
- bilateral medial bending deformities of the fibulae
- bilateral remodelled cortical porosity on the greater wings of sphenoid and pterygoid fossa region. Individual is old. No evidence of new bone.
- discrete mixed active and remodelled new bone, cortical porosity and vascular impressions on the posterior left maxilla (right missing). This individual is edentulous and lesion may be related to antemortem tooth loss.
- abnormally deep vascular impressions across the entire endocranium. May suggest remodelled diffuse new bone across the endocranium.
Radiographic Lesion Summary:
- thickened medial shafts of the tibiae not related to apparent macroscopically observed bending, slightly more thickened on the concave surfaces of the bends of the fibulae
- undulating pattern of the cortex of the long bones due to gnaw marks of the tibiae and fibulae
- tibiae and fibulae have multiple stress lines
- osteopenia that appears 'ground glass' like
- codfish appearance with osteopenia of the vertebrae, and some loss of body height
Differential Diagnosis Outcome:
Probable Osteomalacia
Possible Residual Rickets
Possible Scurvy

Skeletal ID: AT-638

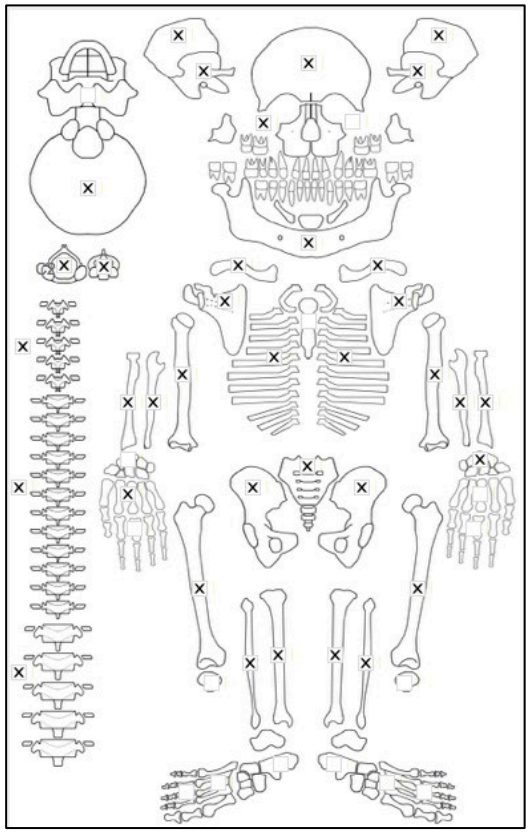

Completeness: Complete (>75%). 100% long bones, 8% hands and feet, 83% vertebrae, 75% neurocranium, ribs near complete.
Preservation/ Taphonomy: Surfaces in excellent condition. Left anterior middle third femur taken for sampling.
Age: 30-39, *Middle Aged Adult*
Sex: Male
Macroscopic Lesion Summary:
- small unilateral discrete deposit of remodelled new bone on the medial proximal shaft of the left tibia
- moderate remodelling cribra orbitalia of the left orbit (right missing)

Radiographic Lesion Summary:
Differential Diagnosis Outcome:
Anaemia

Skeletal ID: AT-639

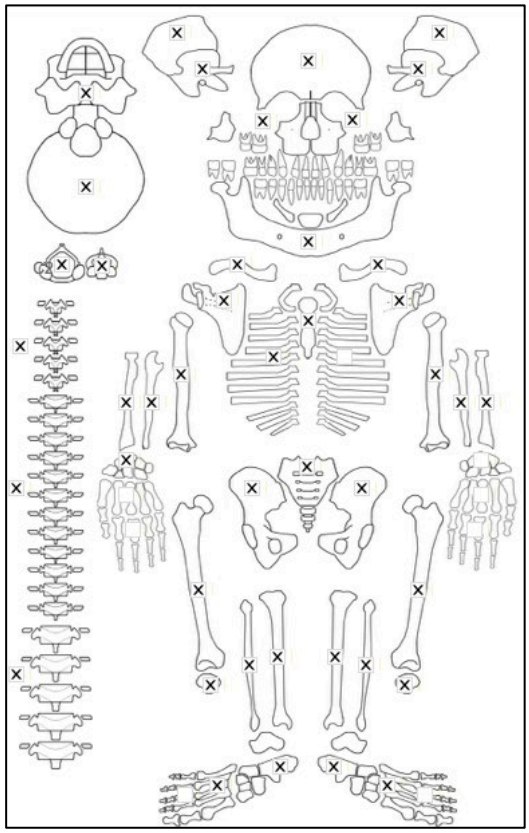

Completeness: Complete (>75%). 100% long bones, 27% hands and feet, 100% vertebrae, 100% neurocranium, ribs incomplete.
Preservation/ Taphonomy: Surfaces in excellent condition with slight layer of dust but surface is visible. All preserved bones intact.
Age: 40-49, *Middle Aged Adult*
Sex: Male
Macroscopic Lesion Summary:
- small bilateral and symmetrical discrete deposit of remodelled new bone on the lateral aspect of the interosseous crest on the proximal shafts of the fibulae
- small unilateral discrete deposit of remodelled new bone on the anterior aspect of the interosseous crest on the distal shaft of the right fibula
Radiographic Lesion Summary:
No radiographs taken
Differential Diagnosis Outcome:
No diagnosis

Skeletal ID: AT-674

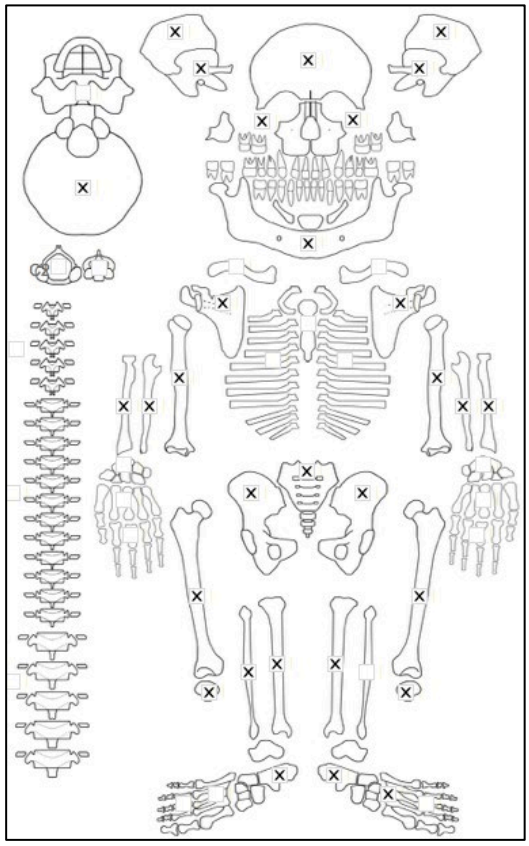

Completeness: Near Complete (66 to 75%). 78% long bones, 14% hands and feet, 0% vertebrae, 100% neurocranium, ribs fragmented.
Preservation/ Taphonomy: Bone surfaces clean and in excellent condition. Middle shaft of left humerus, distal third of right humerus, distal epiphysis of right ulna, proximal epiphysis of left fibula, radius and ulna, and both epiphyses of right fibula are missing.
Age:
Sex:
Macroscopic Lesion Summary:
- bilateral remodelled new bone and cortical porosity extending from the mental foramen onto the incisive fossa. Clearer on the left side.
- bilateral remodelling mild cribra orbitalia
Radiographic Lesion Summary:
No radiographs taken
Differential Diagnosis Outcome:
No diagnosis

Skeletal ID: AT-676

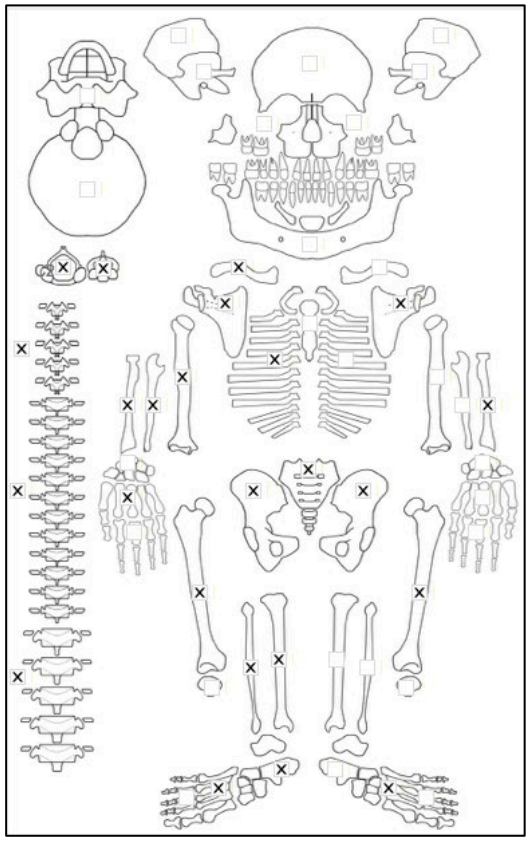

Completeness: Near Complete (66 to 75%). 67% long bones, 17% hands and feet, 95% vertebrae, 0% neurocranium, ribs partially complete.
Preservation/ Taphonomy: Intrusive left clavicle and distal end of right humerus. All surfaces clean and in excellent condition.
Age: 30-39, *Young Adult*
Sex: Male
Macroscopic Lesion Summary:
- medial bending deformity of the upper shaft of the right tibia associated with latero-anterior bending deformity of the upper shaft of the right fibula (left side missing)
- bilateral remodelled mild porotic hyperostosis on the posterior parietals and around sagittal crest and occipital planum
- bilateral remodelled moderate cribra orbitalia

Radiographic Lesion Summary:
No radiographs taken
Differential Diagnosis Outcome:
Possible Residual Rickets
Anaemia

Skeletal ID: AT-828

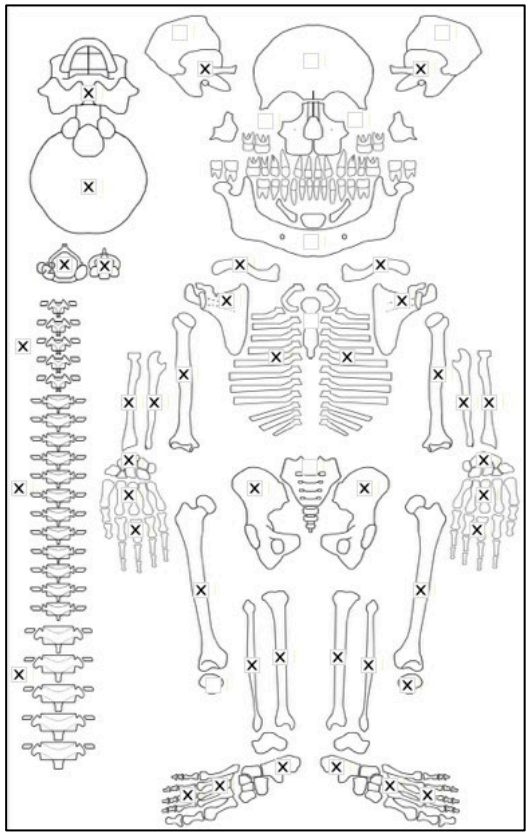

Completeness: Complete (>75%). 85% long bones, 64% hands and feet, 100% vertebrae, 50% neurocranium,
Preservation/ Taphonomy: Surfaces are in excellent condition with some PM breaks of fragile margins. Cranium has many PM breakages.
Age: 30-39, *Middle Aged Adult*
Sex: Male
Macroscopic Lesion Summary:
- discrete deposit of mixed active and remodelled new bone with vascular grooves in the transverse sulcus of the occipital endocranium
- fine diffuse remodelling porosity on the occipital planum consistent with mild porotic hyperostosis
Radiographic Lesion Summary:
No radiographs taken
Differential Diagnosis Outcome:
Anaemia

Skeletal ID: AT-837

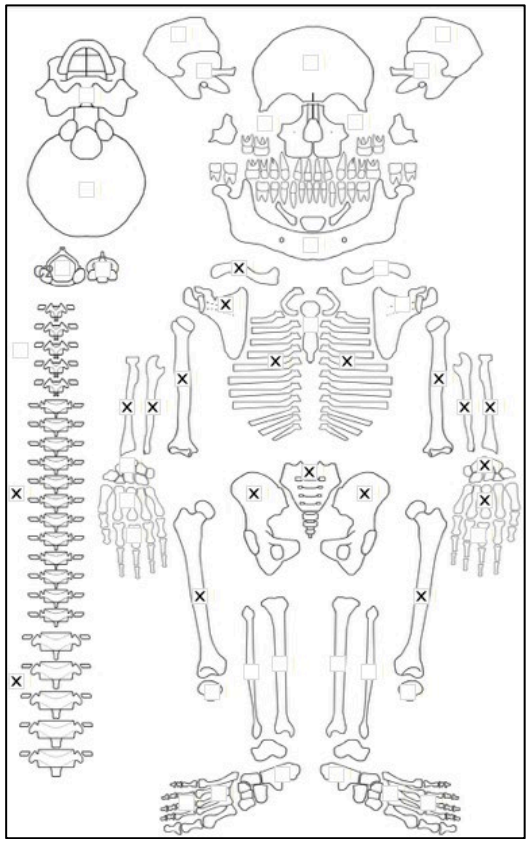

Completeness: Partially Complete (50 to 66%). 48% long bones, 11% hands and feet, 42% vertebrae, 0% neurocranium, ribs near complete.
Preservation/ Taphonomy: Bones have lots of PM breakages, surfaces have reddish soil but are visible for analysis. Proximal third shaft of left radius and right humerus, distal half of ulnae, and distal epiphyses of femora missing. Only middle third shaft and distal epiphysis of right radius present.
Age: 30-39, *Young Adult*
Sex: Male
Macroscopic Lesion Summary:
No pathology
Radiographic Lesion Summary:
No radiographs taken
Differential Diagnosis Outcome:
No diagnosis

Skeletal ID: AT-838

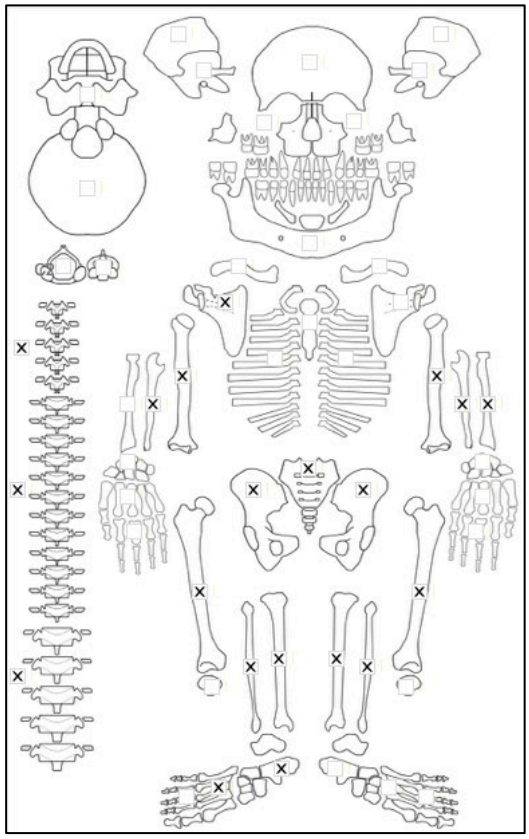

Completeness: Near Complete (66 to 75%). 67% long bones, 9% hands and feet, 75% vertebrae, 0% neurocranium,
Preservation/ Taphonomy: Proximal epiphysis of humeri, and right tibia missing. Distal epiphysis of right femur, distal half of left ulna, distal 2/3rds of right ulna and right fibula, and both epiphyses of left radius missing. While most surfaces are excellent, some are blackened
Age: 40-49, *Middle Aged Adult*
Sex: Male
Macroscopic Lesion Summary:
- diffuse remodelled new bone on the medial middle third shaft of the left tibia, it is associated with some myositis ossificans therefore is likely to be trauma related rather than disease
- bilateral bending deformities of the humeral shafts, and medial bending deformity of the left fibula shaft (right missing
Radiographic Lesion Summary:
No radiographs taken
Differential Diagnosis Outcome:
Possible Residual Rickets

Skeletal ID: AT-839

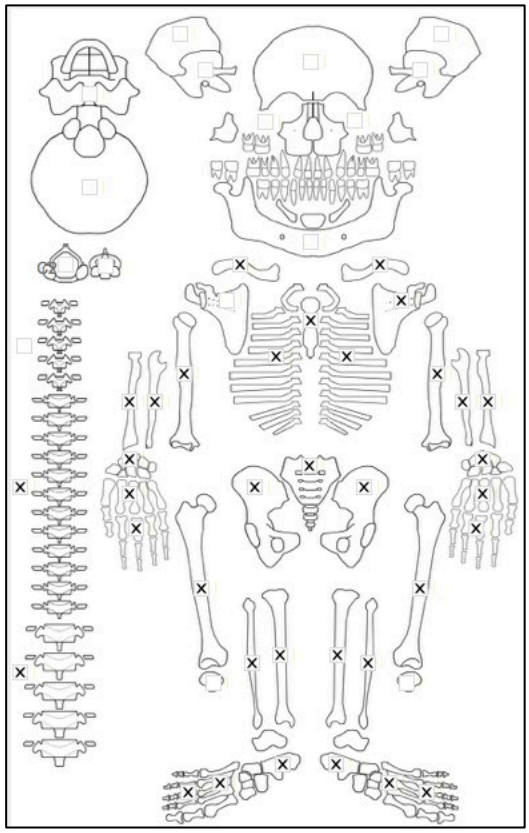

Completeness: Near Complete (66 to 75%). 97% long bones, 55% hands and feet, 63% vertebrae, 0% neurocranium, ribs complete.
Preservation/ Taphonomy: Proximal epiphysis of left fibula and radius is missing. Surfaces in excellent condition.
Age: 30-39, *Young Adult*
Sex: Male
Macroscopic Lesion Summary:
No pathology
Radiographic Lesion Summary:
No radiographs taken
Differential Diagnosis Outcome:
No diagnosis

Skeletal ID: AT-861

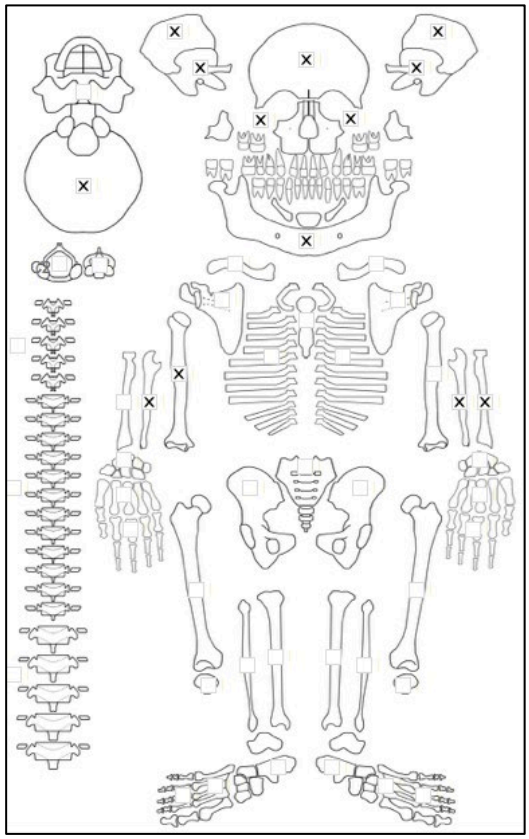

Completeness: Incomplete (33 to 50%). 33% long bones, 0% hands and feet, 0% vertebrae, 75% neurocranium, no ribs.
Preservation/ Taphonomy: Moderate damage to the surfaces- scavenging.
Age: 17.5 (+/- 3) years, *Adolescent*
Sex: Female
Macroscopic Lesion Summary:
No pathology
Radiographic Lesion Summary:
No radiographs taken
Differential Diagnosis Outcome:
No diagnosis

Skeletal ID: AT-862

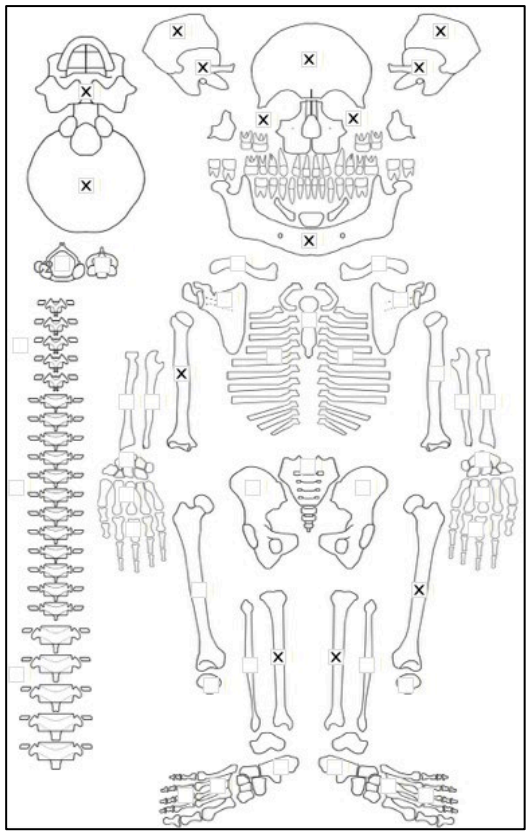

Completeness: Incomplete (33 to 50%). 20% long bones, 0% hands and feet, 0% vertebrae, 100% neurocranium, no ribs.
Preservation/ Taphonomy: Moderate gnawing damage to the surfaces. No epiphyses preserved.
Age: *Adult*
Sex: Intermediate
Macroscopic Lesion Summary:
No pathology
Radiographic Lesion Summary:
No radiographs taken
Differential Diagnosis Outcome:
No diagnosis

Skeletal ID: AT-945
Completeness: Incomplete (33 to 50%). 24% long bones, 0% hands and feet, 0% vertebrae, 0% neurocranium, no ribs.

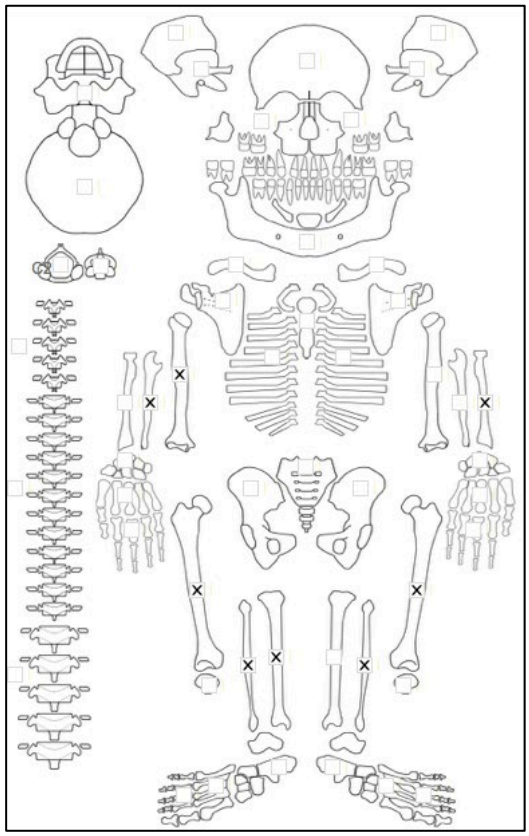

Preservation/ Taphonomy: No epiphyses present. Long bones only. Moderate gnawing of the surfaces some longitudinal splitting of the shafts, severe gnawing of the fibulae.
Age: *Adult*
Sex: Intermediate
Macroscopic Lesion Summary:
No pathology
Radiographic Lesion Summary:
No radiographs taken
Differential Diagnosis Outcome:
No diagnosis

Skeletal ID: AT-865

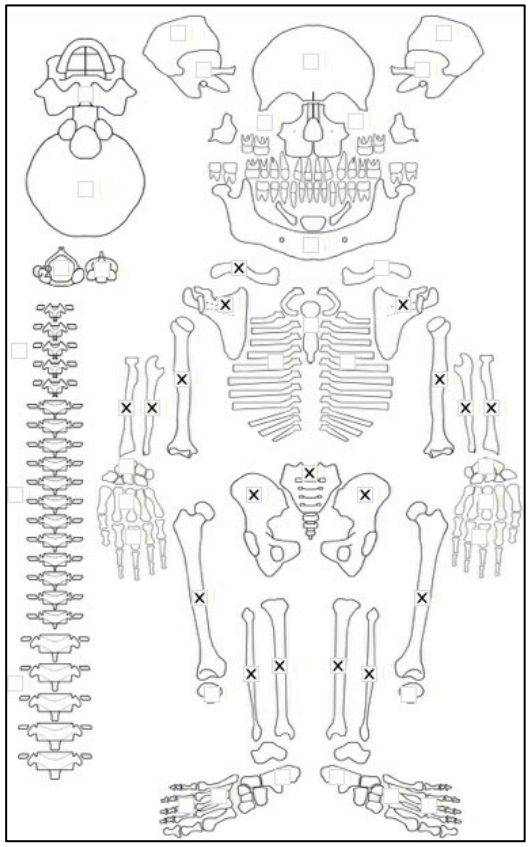

Completeness: Partially Complete (50 to 66%). 100% long bones, 1% hands and feet, 0% vertebrae, no ribs.
Preservation/ Taphonomy: Bone surfaces in excellent condition
Age: 30-39, *Middle Aged Adult*
Sex: Female
Macroscopic Lesion Summary:
- bilateral deep multifocal and coalesced lytic destruction in the acetabulum and of the femoral heads. There is no evidence of remodelling and there is considerable articular change associated on the acetabular margins. The left side has considerably more destruction than the right. There is also remodelled reactive new bone on the superior and posterior margins of the acetabulum on the ilium. There is also bilateral abnormal macroporosity on the left auricular surface. X-rays confirm this is multifocal lytic destruction. The lytic destruction covers almost the entire articular surface of the left acetabulum (diameter: 45.81x40.91). The left femoral head has considerable lipping, osteophytic and erosive changes associated with a large active focal destruction on the anterior superior aspect of the femoral head, this may be necrotic but xrays are necessary to confirm this. The focal destruction on the left femoral head is: 41.81x22.98mm in diameter. The destruction on the right acetabulum is localised to a region on the anterior border that is 11.45x6.95 in diameter. The left femoral head destruction is also localised but very deep into the femoral head. There is some lipping and erosive changes but this is minimal. Diameter of area on left femoral head affected is: 18.95x12.33mm.
The lytic lesions are not circumscribed, except for the macroporosity. The shape of the destruction is irregular.
- focal active destruction on the left lateral superior portion of the S1 sacrum. The destruction appear superficial and recent, there is no evidence of any response or remodelling. diameter: 15.94x8.87mm. There is also destruction in the right auricular surface of the sacrum (where there is adjacent destruction on the auricular surfaces of the os coxae- left auricular surface of sacrum is missing postmortem).
- bilateral very slight medial bending deformities of the tibiae and fibulae
Radiographic Lesion Summary:
- multifocal circumscribed lesions of the acetabulae, and in the iliosacral region are clear on the radiographs (lytic lesions are present on the sacrum and the ilia- auricular surface)- more severe on the left acetabulum and auricular surface. There is also multifocal radiolucent regions bilaterally on the mid iliac blades.
- no distinct change in the thickness of the shafts of the tibiae and fibulae, but thick femoral cortex, with broad and flat proximal third shaft

- multiple stress lines in the distal tibial metaphyses.
- clear avascular necrosis of the left femoral head

Differential Diagnosis Outcome:
Possible Brucellosis
Possible Tuberculosis

Skeletal ID: AT-902

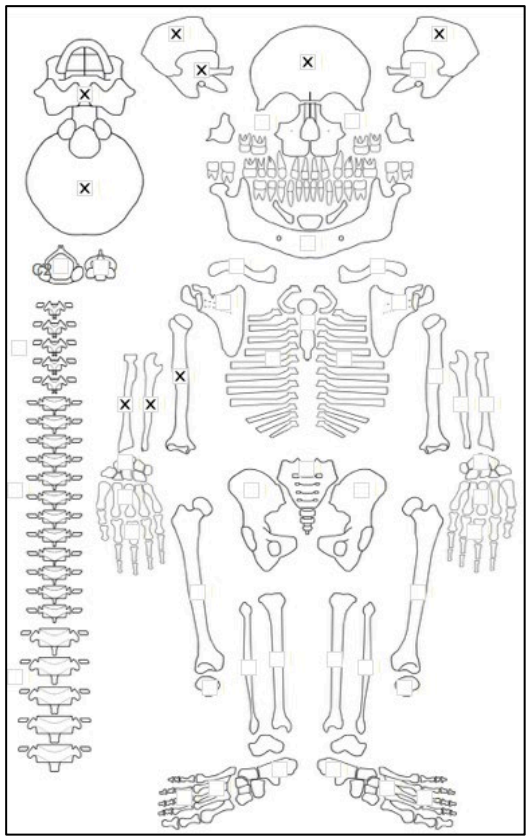

Completeness: Incomplete (33 to 50%). 10% long bones, 0% hands and feet, 0% vertebrae, 63% neurocranium, no ribs.
Preservation/ Taphonomy: Surfaces are darkened but visible. Moderate gnawing on some of the cranial bone. On proximal third shaft of humerus, proximal 2/3 of ulna and proximal third of radius present for long bones.
Age: *Adult*
Sex: Male
Macroscopic Lesion Summary:
- remodelled mild cribra orbitalia of the right superior orbit (left missing)

Radiographic Lesion Summary:
No radiographs taken
Differential Diagnosis Outcome:
No diagnosis

Skeletal ID: AT-903

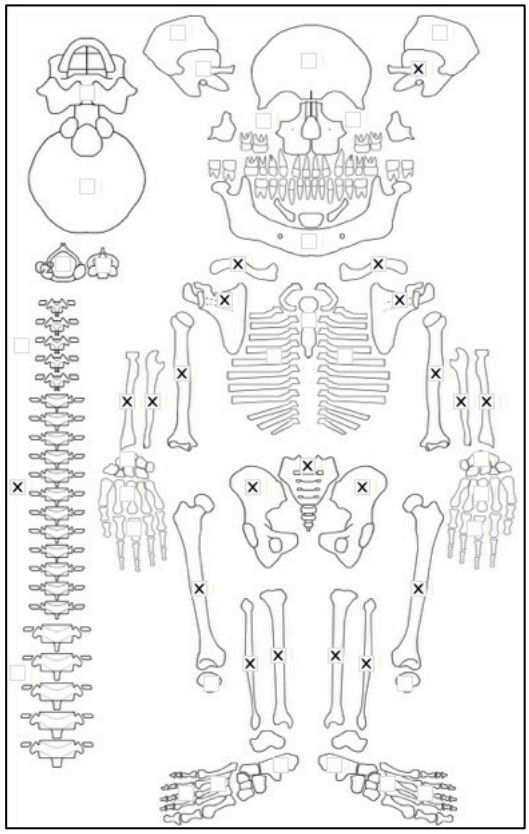

Completeness: Near Complete (66 to 75%). 92% long bones, 0% hands and feet, 17% vertebrae, 13% neurocranium, no ribs.
Preservation/ Taphonomy: All preserved bones intact. Surfaces in excellent condition except skull, that has moderate surface damage. Intrusive portion of a femur.
Age: 40-49, *Middle Aged Adult*
Sex: Male
Macroscopic Lesion Summary:
- bilateral symmetrical discrete deposits of new bone on the anterior crest and medal to the crest on the proximal shafts of the tibiae
Radiographic Lesion Summary:
No radiographs taken
Differential Diagnosis Outcome:
No diagnosis

Skeletal ID: AT-905

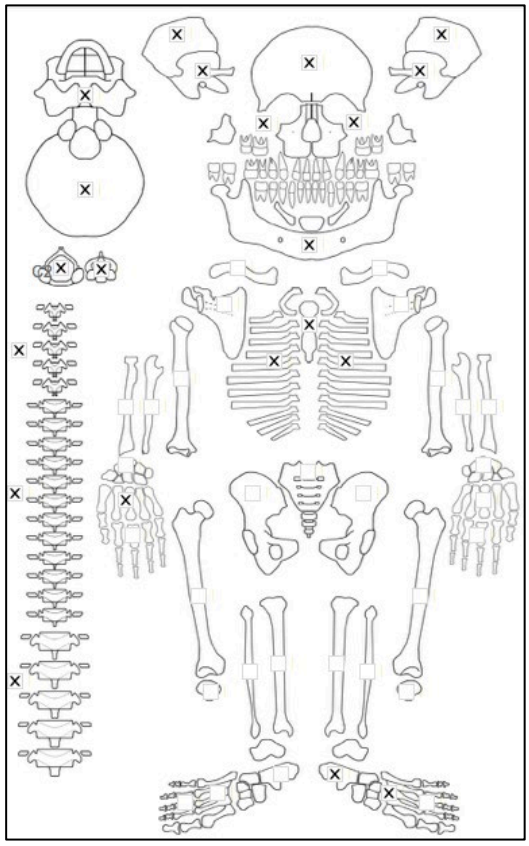

Completeness: Partially Complete (50 to 66%), 0% long bones, 9% hands and feet, 88% vertebrae, 100% neurocranium, ribs complete.
Preservation/ Taphonomy: All surfaces intact and in excellent condition
Age: *Young Adult*
Sex: Male
Macroscopic Lesion Summary:
- bilateral remodelled new bone and cortical porosity on the pterygoid fossae and on the lateral pterygoid region extending from the foramen ovale.
- thick remodelled new bone and cortical porosity on the palatal surfaces of the maxillae. There is associated alveolar antemortem tooth loss.
- bilateral thick remodelled new bone resulting in closure of the condylar foramina
- bilateral mixed active and remodelled cortical porosity on the medial coronoid processes of the mandible
- bilateral remodelled mild cribra orbitalia
Radiographic Lesion Summary:
No radiographs
Differential Diagnosis Outcome:
Probable Scurvy

Skeletal ID: AT-904

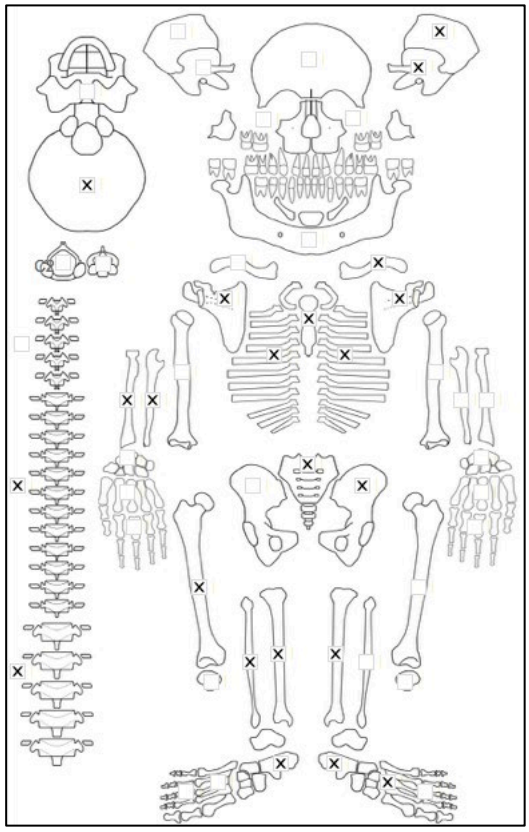

Completeness: Partially Complete (50 to 66%). 50% long bones, 11% hands and feet, 50% vertebrae, 38% neurocranium, ribs partially complete.
Preservation/ Taphonomy: Postcranial surfaces intact and in excellent condition. Left tibia middle anterior third taken for sampling.
Age: 30-39, *Young Adult*
Sex: Male
Macroscopic Lesion Summary:
No pathology
Radiographic Lesion Summary:
No radiographs taken
Differential Diagnosis Outcome:
No diagnosis

Skeletal ID: AT-909

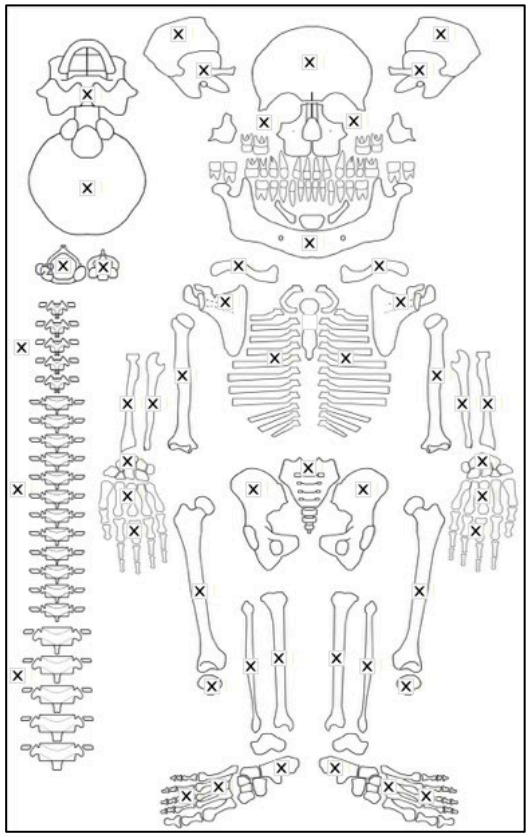

Completeness: Complete (>75%). 100% long bones, 75% hands and feet, 100% vertebrae, 100% neurocranium, ribs complete.
Preservation/ Taphonomy: Surfaces in excellent condition, surfaces are dark red but surfaces are clearly visible.
Age: 50+, *Old Adult*
Sex: Female
Macroscopic Lesion Summary:
- bilateral exaggerated angle of the middle ribs with lateral straightening of the shafts and some medial indentation
- There is also a remodelled fracture at the midshaft of an upper right rib, and anterior bending of the shaft on one of the right middle ribs with affected rib angulation
- bilateral remodelled moderate cribra orbitalia
Radiographic Lesion Summary:
No radiographs taken
Differential Diagnosis Outcome:
Possible Osteomalacia
Possible residual Rickets
Anaemia

Skeletal ID: AT-960

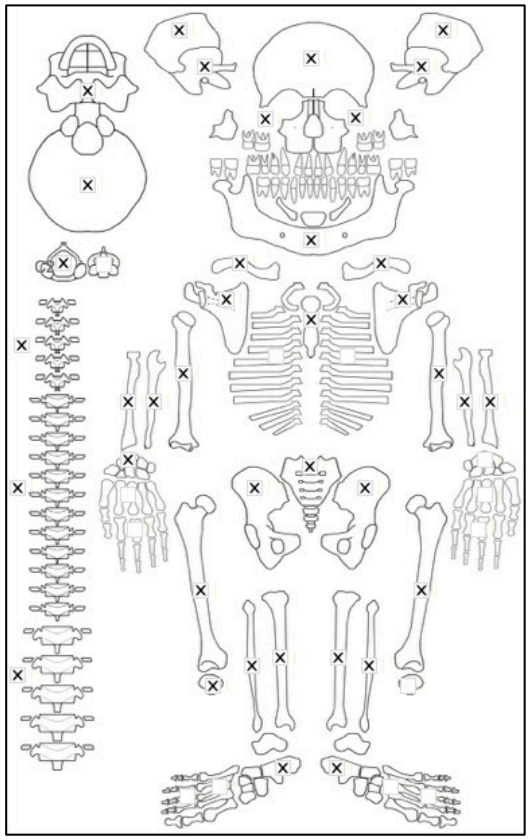

Completeness: Complete (>75%). 90% long bones, 14% hands and feet, 83% vertebrae, 100% neurocranium, no ribs.
Preservation/ Taphonomy: Surfaces in good condition except for severe surface gnawing of right radius only represented by middle third shaft, and some moderate gnawing on the lower limbs. Proximal epiphysis of right fibula, and distal epiphysis of right ulna missing.
Age: 40-49, *Middle Aged Adult*
Sex: Male
Macroscopic Lesion Summary:
No pathology
Radiographic Lesion Summary:
No radiographs taken
Differential Diagnosis Outcome:
No diagnosis

Skeletal ID: AT-976

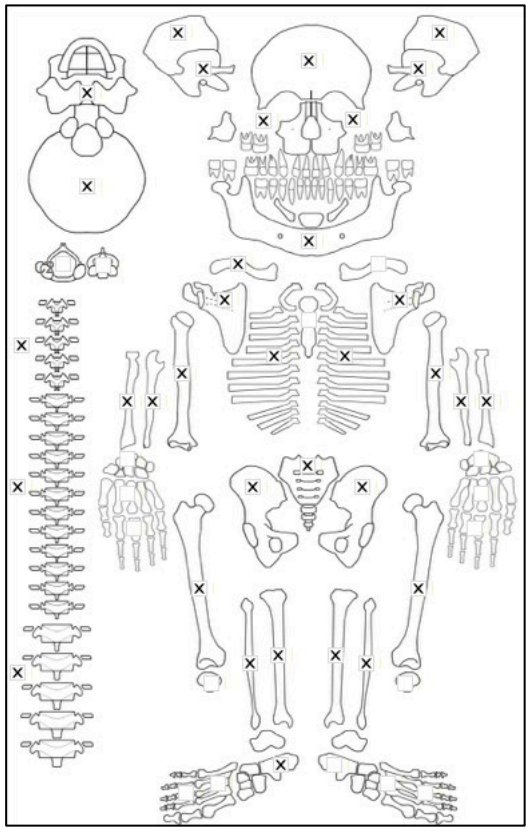

Completeness: Complete (>75%). 100% long bones, 4% hands and feet, 80% vertebrae, 100% neurocranium, ribs near complete.
Preservation/ Taphonomy: Surfaces in great condition just with grey discolouration
Age: 20-29, *Young Adult*
Sex: Female
Macroscopic Lesion Summary:
No pathology
Radiographic Lesion Summary:
No radiographs taken
Differential Diagnosis Outcome:
No diagnosis

Skeletal ID: AT-977

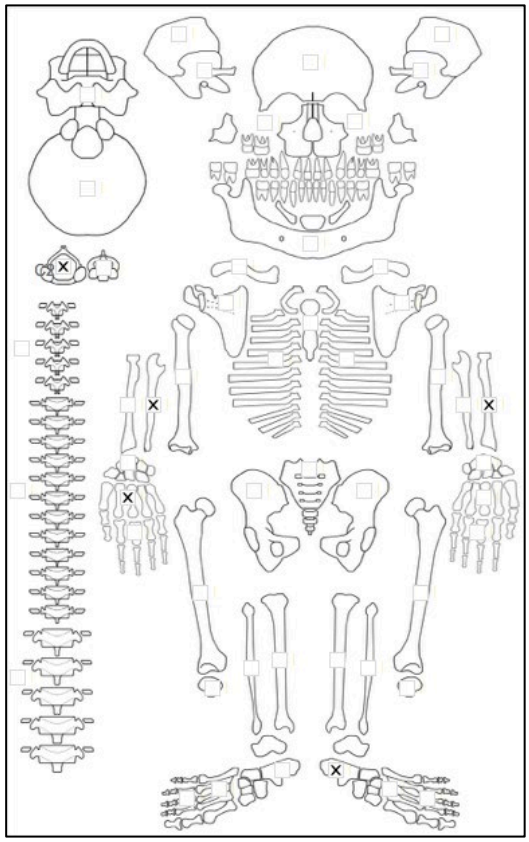

Completeness: Fragmented. 15% long bones, 14% hands and feet, 17% vertebrae, 0% neurocranium, no ribs.
Preservation/ Taphonomy: Distal epiphysis of left radius missing. Surfaces in good condition.
Age: *Adult*
Sex: Indeterminate
Macroscopic Lesion Summary:
No pathology
Radiographic Lesion Summary:
No radiographs taken
Differential Diagnosis Outcome:
No diagnosis

Skeletal ID: AT-980

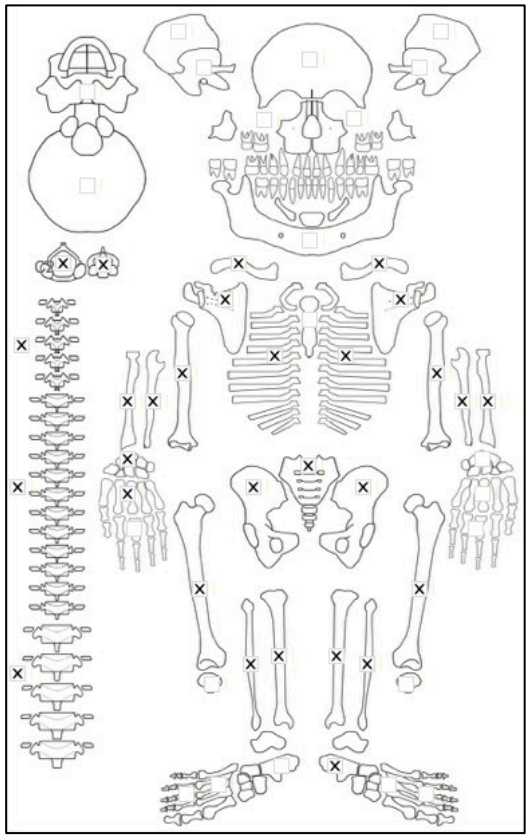

Completeness: Near Complete (66 to 75%). 95% long bones, 9% hands and feet, 54% vertebrae, 0% neurocranium, ribs near complete.
Preservation/ Taphonomy: Margins of bones have PM damage. Surfaces are grey and bone ends are also damaged. Proximal epiphyses of fibulae and distal epiphysis of right femur missing.
Age: *Adult*
Sex: Indeterminate
Macroscopic Lesion Summary:
No pathology
Radiographic Lesion Summary:
No radiographs taken
Differential Diagnosis Outcome:
No diagnosis

Skeletal ID: AT-981

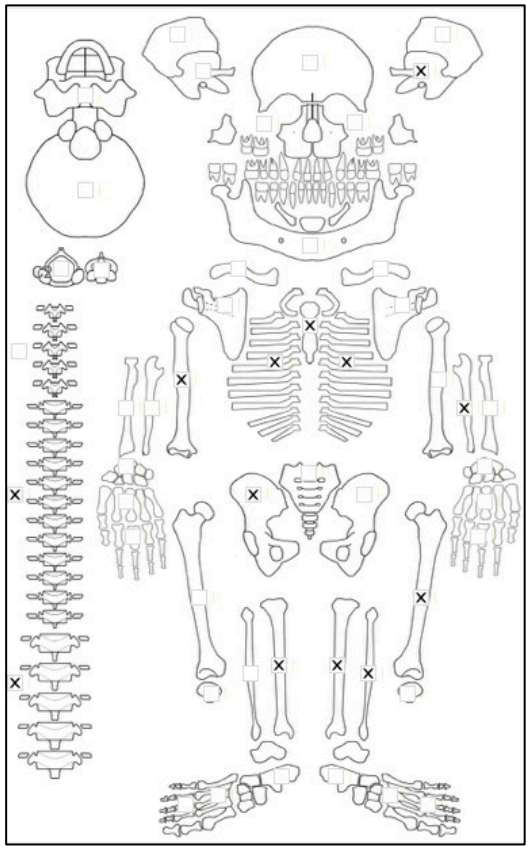

Completeness: Partially Complete (50 to 66%). 58% long bones, 2% hands and feet, 33% vertebrae, 13% neurocranium, ribs incomplete.
Preservation/ Taphonomy: All preserved long bones intact with some damage to distal metaphysis of the femur. Distal femur and proximal tibiae and humerus epiphysis present. Right ischium and pubis.
Age: 13 (+/- 2) years.
Sex: Indeterminate
Macroscopic Lesion Summary:
- small discrete deposit of remodelled new bone on the anterior squama of the left temporal at the margin with the sphenoid under the zygomatic arch
- abnormal endochondral porosity exceeding 10mm from metaphyseal plate on the distal right ulna (left missing). 17.5mm in length
- mixed active and remodelled diffuse new bone on the posterior left femur extending from the superior femoral next to the posterior midshaft. There is a large remodelled deposit of bon o the posterior third that is consistent with myositis ossificans (likely as a result of trauma). However, the remodelled new bone is not smooth possibly suggesting fast periosteal response due to infection, or poorly mineralised bone.
- bilateral medial bending deformities of the tibiae and slight medial bending of the fibulae
Radiographic Lesion Summary:
- White line of Fraenkel with Trummerfeld zones of the lower limb bones (femur too damaged to assess), multiple stress lines and ground glass osteopenia, humerus has very coarsened trabeculae in the distal metaphysis. No change to the cortex thickness of the long bones, but the bending deformities in the tibiae are particularly distinct on the x-rays (there is slightly more thickening on the medial aspect of the shaft of the right tibia compared to the lateral aspect. Both tibiae do have slight periosteal apposition on the shafts.
- there is cupping of the distal left fibula.
Differential Diagnosis Outcome:
Probable rickets
Possible Scurvy

Skeletal ID: AT-984

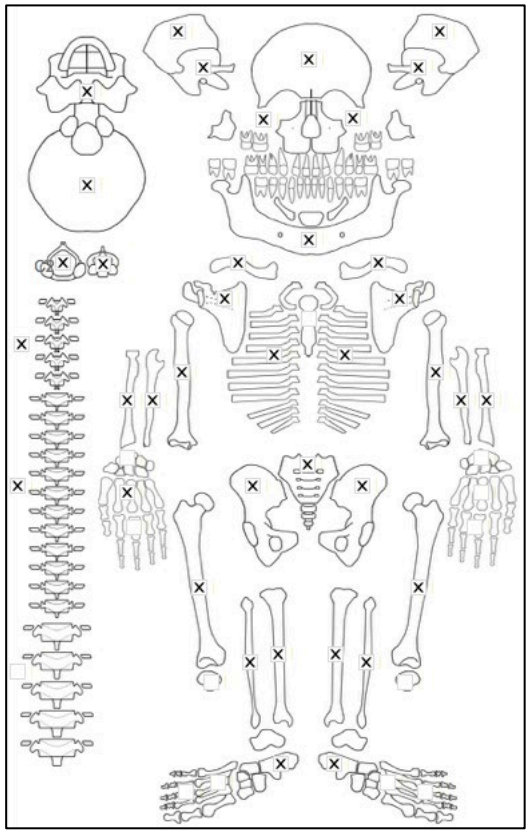

Completeness: Complete (>75%). 97% long bones, 9% hands and feet, 100% vertebrae, 100% neurocranium, ribs complete.
Preservation/ Taphonomy: Surfaces are covered in grey soil and difficult to observe but otherwise surfaces in good condition. Proximal epiphysis and distal third of left fibula missing.
Age:50+, *Old Adult*
Sex: Female
Macroscopic Lesion Summary:
- increase acute rib angle angulation of multiple right upper to middle ribs. This does not seem to occur on the left side. One of the right upper ribs appears to be a bifid rib. May be within normal variation.
- skull is brachycephalic and square shaped
Radiographic Lesion Summary:
Differential Diagnosis Outcome:
Possible Residual Rickets

Skeletal ID: AT-985

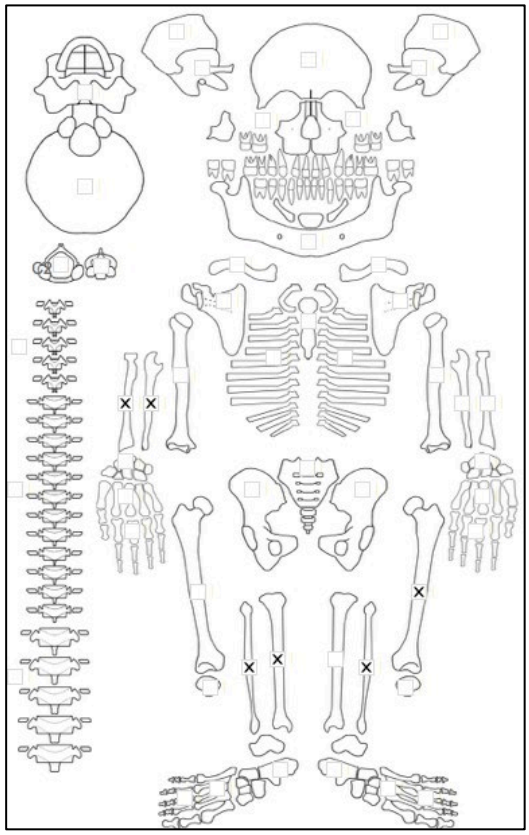

Completeness: Incomplete (33 to 50%). 43% long bones, 0% hands and feet, 0% vertebrae, 0% neurocranium, no ribs.
Preservation/ Taphonomy: Long bones only. Surfaces of thinner long bones such as forearm and fibula have moderate gnawing. Some grey soil on surfaces. Proximal third of femur only, proximal epiphysis of left fibula is missing
Age: *Adult*
Sex: Indeterminate
Macroscopic Lesion Summary:
No pathology
Radiographic Lesion Summary:
No radiographs taken
Differential Diagnosis Outcome:
No diagnosis

Skeletal ID: AT-986

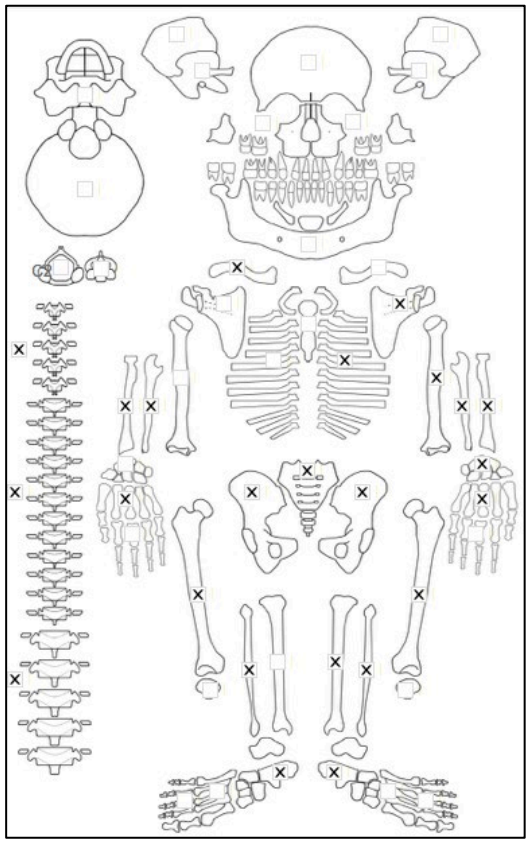

Completeness: Near Complete (66 to 75%). 90% long bones, 32% hands and feet, 50% vertebrae, 0% neurocranium, ribs incomplete.
Preservation/ Taphonomy: Grey soil on the surfaces. Moderate gnawing on feet bones. Proximal left fibula epiphysis missing.
Age: 20-29, *Young Adult*
Sex: Male
Macroscopic Lesion Summary:
No pathology
Radiographic Lesion Summary:
No radiographs taken
Differential Diagnosis Outcome:
No diagnosis

Skeletal ID: AT-988

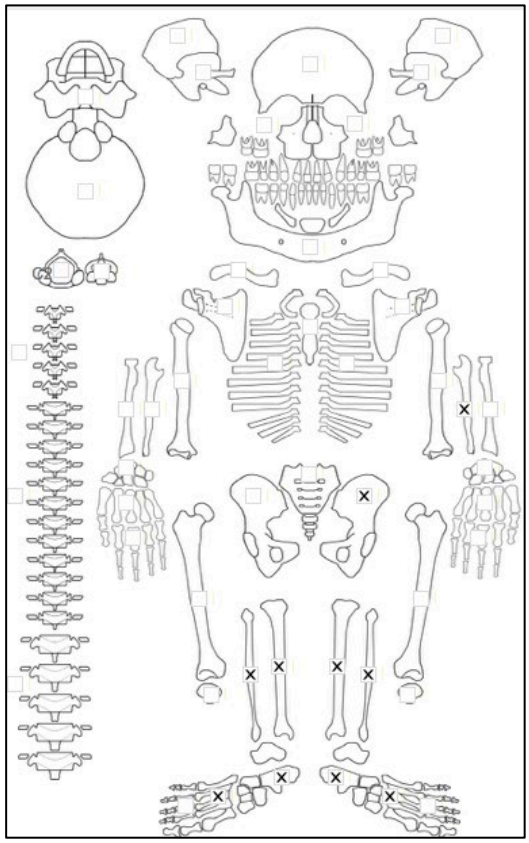

Completeness: Incomplete (33 to 50%). 35% long bones, 14% hands and feet, 17% vertebrae, 0% neurocranium, no ribs.
Preservation/ Taphonomy: Surfaces are moderately to severely weathered with gnaw marks and covered in dark soil. A lot of damage to the bone neds, only distal epiphyses of fibula and left tibia, proximal epiphysis of ulna and both epiphyses of tibia present.
Age: *Adult*
Sex: Male
Macroscopic Lesion Summary:
No pathology
Radiographic Lesion Summary:
No radiographs taken
Differential Diagnosis Outcome:
No diagnosis

Skeletal ID: AT-998

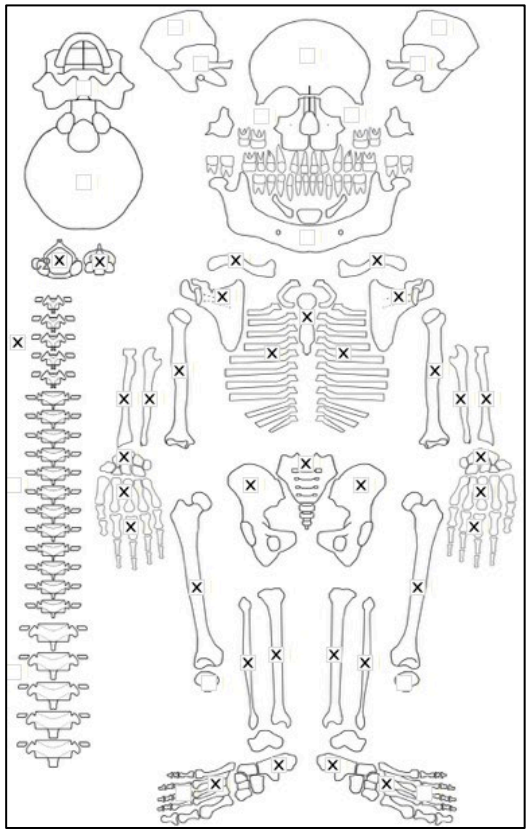

Completeness: Near Complete (66 to 75%). 93% long bones, 61% hands and feet, 33% vertebrae, 0% neurocranium, ribs complete.
Preservation/ Taphonomy: Surfaces in good condition. Proximal epiphysis of right fibula missing.
Age: 20-29, *Young Adult*
Sex: Male
Macroscopic Lesion Summary:
No pathology
Radiographic Lesion Summary:
No radiographs taken
Differential Diagnosis Outcome:
No diagnosis

Skeletal ID: AT-1000

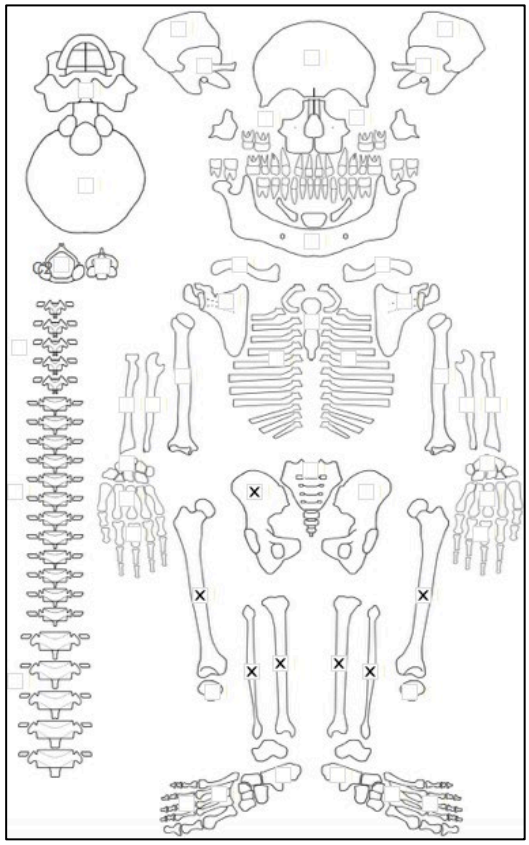

Completeness: Incomplete (33 to 50%). 50% long bones, 0% hands and feet, 13% vertebrae, 0% neurocranium, no ribs.
Preservation/ Taphonomy: Surfaces have moderate gnaw marking. no metaphyseal plates have been preserved.
Age: 1.5 years (+/- 6 months), *Child*
Sex: Indeterminate
Macroscopic Lesion Summary:
- bilateral abnormal endochondral porosity extending beyond 10mm from the metaphyseal plate (>15mm) of the proximal tibiae
- mixed active and remodelled diffuse new bone across the medial aspects of the tibiae (there is considerable gnaw marks on the surface but new bone is still visible).
Radiographic Lesion Summary:
No radiographs taken
Differential Diagnosis Outcome:
Possible Scurvy

Skeletal ID: AT-1001

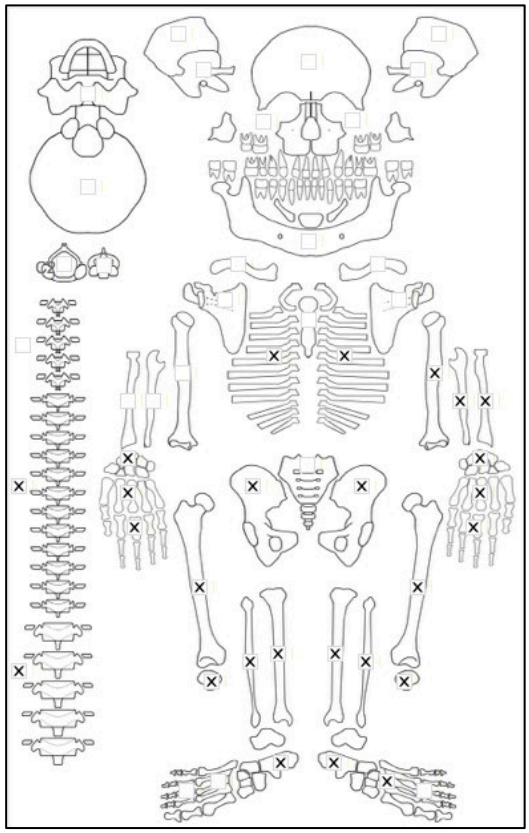

Completeness: Near Complete (66 to 75%). 93% long bones, 38% hands and feet, 38% vertebrae, 0% neurocranium, ribs incomplete.
Preservation/ Taphonomy: Surface in excellent condition but covered in grey soil- surfaces still visible. The shaft of the left tibia is shattered, all pieces are present.
Age: *Adult*
Sex: Male
Macroscopic Lesion Summary:
- bilateral coxa vara of the femoral heads, there is no associated trauma of the proximal femur.
- medial bending of the right tibia shaft (left side is too damaged for comparison)
Radiographic Lesion Summary:
- severe osteopenia of the margins and internal trabeculae of the vertebrae, codfish appearance on multiple vertebrae,
- long bone thickening of the tibiae, the cortex is thin on the concave aspect and thick on the convex aspect
Differential Diagnosis Outcome:
Possible Osteomalacia
Probable Residual Rickets

Skeletal ID: AT-629

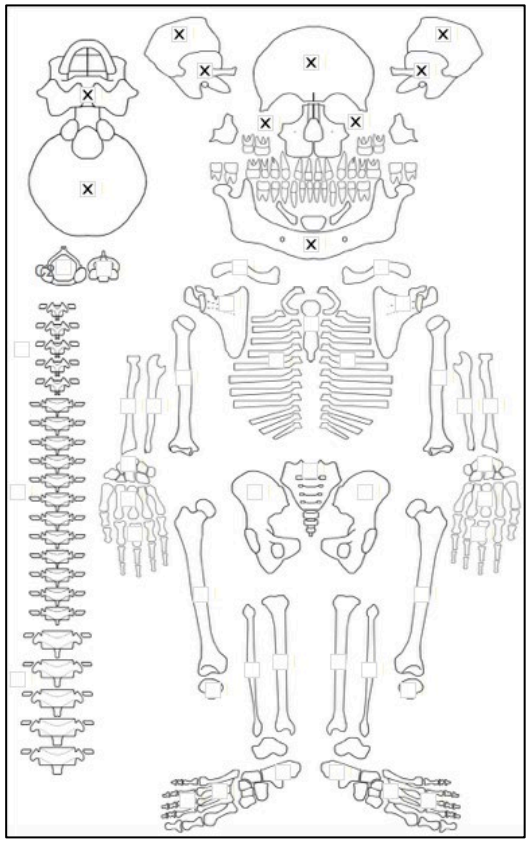

Completeness: Incomplete (33 to 50%). 0% long bones, 0% hands and feet, 0% vertebrae, 88% neurocranium, no ribs,
Preservation/ Taphonomy: Skull only intact except ethmoid.
Age: 6.5 (+/- 2) years, *Child*
Sex: Indeterminate
Macroscopic Lesion Summary:
- bilateral remodelled cortical porosity extending from the foramen ovale on the inferior lateral left greater wing of sphenoid at the pterygoid region and the pterygoid fossa
- bilateral discrete active new bone and cortical porosity on the posterior maxillae. The new bone is associated with the eruption of the 1st permanent molars but there are also remodelled vascular impressions visible.
- bilateral discrete mixed active and remodelled new bone and cortical porosity on the palatal surfaces of the maxillae
- bilateral fine diffuse porosity on the left superior orbit of unknown aetiology. However this is associated with remodelled vascular impressions.
- bilateral discrete mixed active and remodelled new bone and cortical porosity on the coronoid processes of the mandible
- bilateral discrete remodelled deposit of new bone, cortical porosity and vascular impressions inferior to the mylohyoid lines of the mandible
- bilateral discrete remodelled deposit of new bone, and cortical porosity on the mastoids of the temporals
- bilateral discrete remodelled cortical porosity on the incisive fossae of the mandible
Radiographic Lesion Summary:
No radiographs taken
Differential Diagnosis Outcome:
Probable Scurvy

Skeletal ID: AT-766

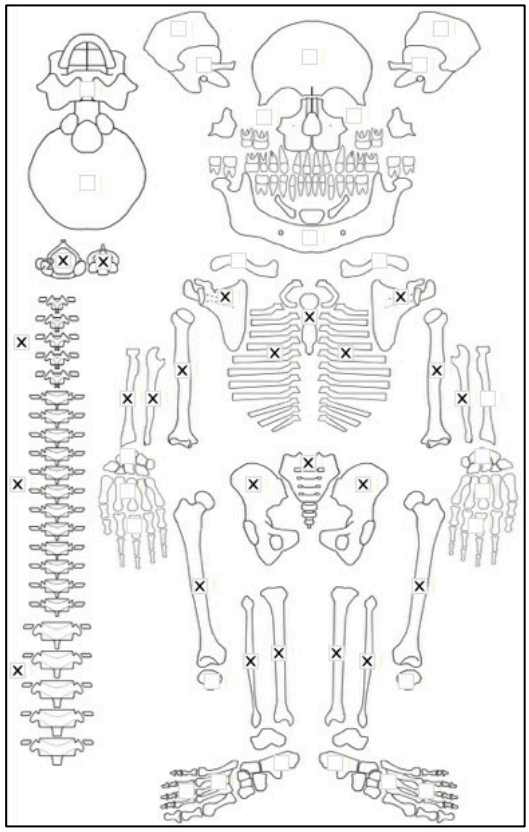

Completeness: Near Complete (66 to 75%). 92% long bones, 0% hands and feet, 83% vertebrae, 0% neurocranium, ribs near complete.
Preservation/ Taphonomy: Surfaces minimally to moderately damaged with light dust coverage, damage to metaphyseal plates of the tibiae some PM breakage of ribs.
Age: 15 years, *Adolescent*
Sex: Male
Macroscopic Lesion Summary:
- abnormal endochondral porosity exceeding 10mm from metaphyseal plate on the proximal humeri, distal left femur (right missing), distal tibiae (proximal missing) and distal fibulae. May be poorly mineralised bone. (not reminiscent of scorbutic porosity rather poor mineralisation at attachment sites)
- there is fraying at the tibial tuberosity and bilateral medial bending of the tibial shafts
- bilateral poorly mineralised new bone on the proximal linea aspera of the femora

Radiographic Lesion Summary:
- osteopenia of the vertebrae
- thickened cortex at the concave aspect of the bending deformities of the tibia
- fraying of the proximal tibiae is clear on the radiographs
- coarsening trabeculae of the distal metaphyses of the tibiae

Differential Diagnosis Outcome:
Possible Osteomalacia
Probable Rickets

Skeletal ID: Khovd Tomb 10-11

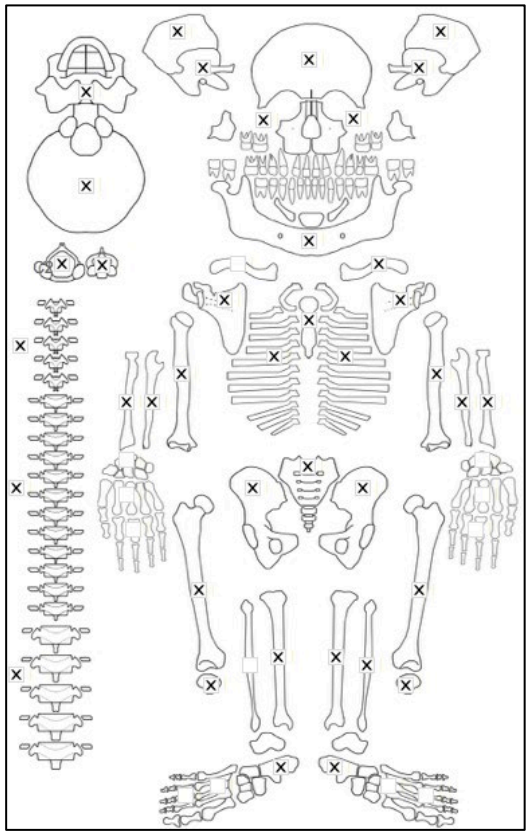

Completeness: Complete (>75%). 98% long bones, 10% hands and feet, 100% vertebrae, 100% neurocranium, ribs near complete.
Preservation/ Taphonomy: Surfaces are in good condition, skull intact, minimal breakage of the vertebrae. Some damage to proximal ends of the tibiae. Distal end of left fibula missing.
Age: 50+, *Old Adult*
Sex: Female
Macroscopic Lesion Summary:
- antemortem tooth loss but individual is old
- moderate anterior bending of the sternum (border line abnormal)
- bilateral slight posterior bending of the scapular blades (borderline abnormal)
- exaggerated anterior bending at the S2 to 3 region
- bilateral moderate remodelled cribra orbitalia

Radiographic Lesion Summary:
No radiographs taken
Differential Diagnosis Outcome:
Probable Osteomalacia
Anaemia

Skeletal ID: Khovd Tomb 10-5

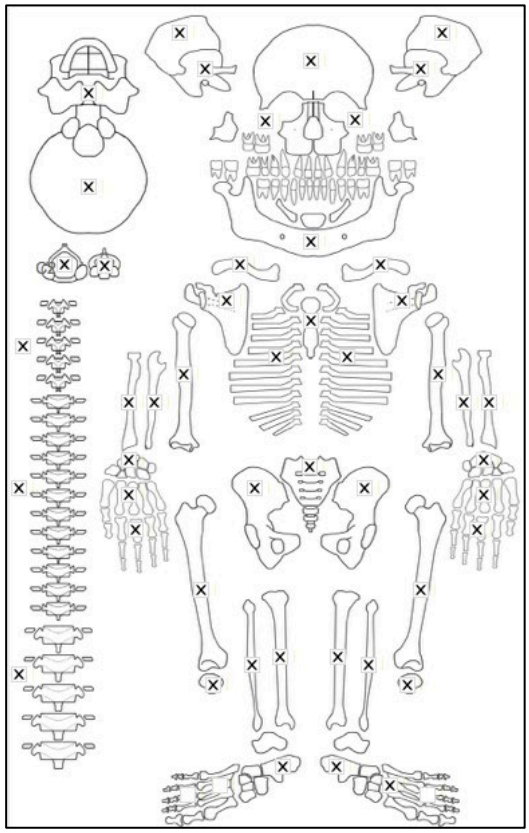

Completeness: Complete (>75%). 100% long bones, 64% hands and feet, 95% vertebrae, 100% neurocranium, ribs complete.
Preservation/ Taphonomy: The right side of cranium and mandible, and right lower limb has root damage which means surfaces are not observable. Left side is in excellent condition.
Age: 19 (+/1) years, *Adolescent*
Sex: Male
Macroscopic Lesion Summary:
- antemortem tooth loss
- discrete mixed active and remodelled new bone on the left medial coronoid processes, inferior to the mylohyoid line (with vascular impressions), on the oblique line extending from the alveolar margin (all right side surfaces damaged), bilaterally on the incisive fossae and on the sublingual fossae.
- discrete mixed active and remodelled new bone on the left anterior lateral portion of the left zygomatic, posterior zygomatic and maxilla, and vascular impressions around the left infraorbital foramen
- bilateral remodelling mild cribra orbitalia
- remodelled new bone and porosity around the superior margin of the left ear canal and onto the zygomatic arch (right side missing)
- remodelling porotic hyperostosis of the superior frontal, parietals (medial to the temporal line) and on the occipital planum
- bilateral symmetrical remodelled haematoma like new bone on the proximal medial shafts of the tibiae close to the anterior crest
Radiographic Lesion Summary:
Radiographs not taken
Differential Diagnosis Outcome:
Probable Scurvy
Anaemia

Skeletal ID: Khovd Tomb 10-2

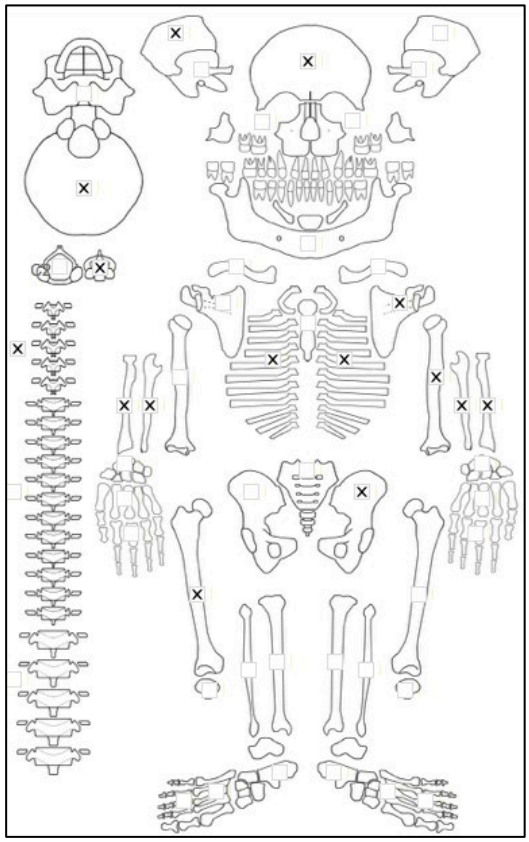

Completeness: Incomplete (33 to 50%). 39% long bones, 0% hands and feet, 17% vertebrae, 38% neurocranium, ribs partially complete.
Preservation/ Taphonomy: Proximal half od left humerus missing, only distal metaphysis of left humerus and proximal right ulna and left radius relatively preserved the plates themselves are damaged. Surfaces are covered in a thin layer of dust and some surface damage.
Age: *Neonate*
Sex: Indeterminate
Macroscopic Lesion Summary:
- active layered new bone in the left superior orbit (right missing)
- active layered new bone and cortical porosity on supraspinous fossa of the left scapula (right missing)
Radiographic Lesion Summary:
- periosteal reactions on shaft are visible on x-rays- not distinct endosteal expansion
Differential Diagnosis Outcome:
Probable Scurvy

Skeletal ID: Khovd Tomb 10-8

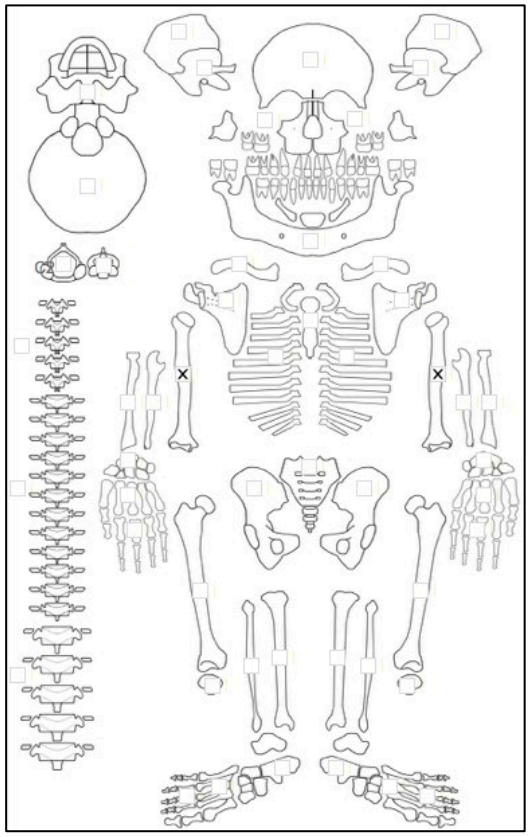

Completeness: Fragmented. 17% long bones.
Preservation/ Taphonomy: Represented only by two humeri complete and 1 left rib (complete).
Age: ~6 months, *Infant*
Sex: Indeterminate
Macroscopic Lesion Summary:
- bilateral symmetrical diffuse active new bone on the shafts of the humeri this is associated with fraying and porosity of the proximal and distal metaphyses.
Radiographic Lesion Summary:
- coarsened trabeculae
- thick periosteal deposit on the shafts
- metaphyseal plates of proximal humeri are not present, distal end there are thin remnants
- cortex is radiolucent
Differential Diagnosis Outcome:
Possible Rickets

Skeletal ID: Khovd Tomb 10-7

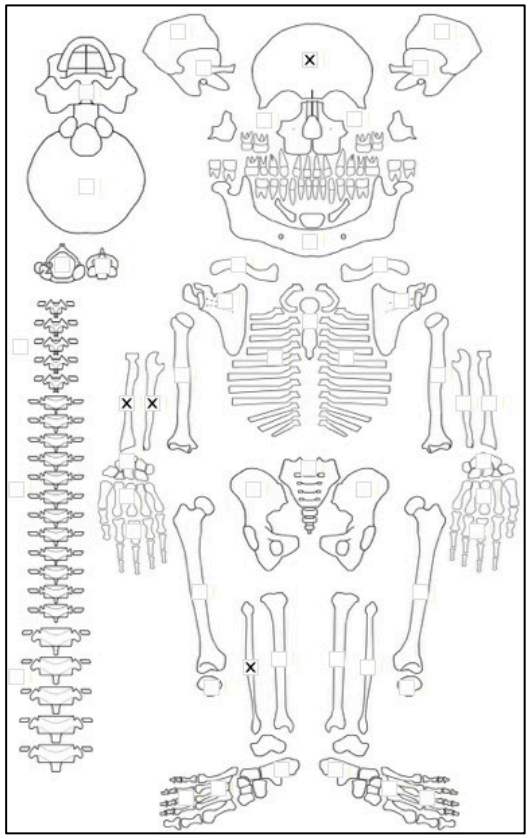

Completeness: Fragmented. 25% long bones, 2% hands and feet, 0% vertebrae, 13% neurocranium.
Preservation/ Taphonomy:
Age: 6 months (+/- 3 months), *Infant*
Sex: Indeterminate
Macroscopic Lesion Summary: Preserved bone intact and surfaces in good condition.
- active layered new bone in the right superior orbit (left missing)
- active diffuse new bone on the anterior shaft of the right radius and medial shaft of the right ulna (left missing)
Radiographic Lesion Summary:
- periosteal reactions on shaft are visible on x-rays- not distinct endosteal expansion
Differential Diagnosis Outcome:
No diagnosis

Skeletal ID: Hongio 21

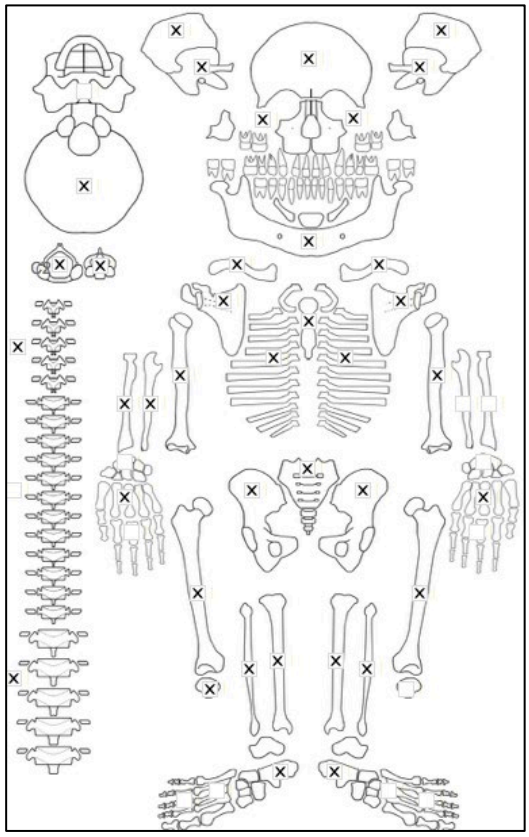

Completeness: Complete (>75%). 73% long bones, 15% hands and feet, 100% vertebrae, 100% neurocranium, ribs complete.
Preservation/ Taphonomy: Surfaces are in good condition but there is dark staining. PM breakage of many long bones. Epiphyses of left ulna and radius only (no shaft), midshaft of left fibula only. Proximal epiphysis of right tibia missing. Damage to distal end of left femur.
Age: 30-39, *Young Adult*
Sex: Female
Macroscopic Lesion Summary:
- bilateral coxa vara of the femoral neck and broadening of the proximal shafts of the femora. Slight genu valgum is noticeable on the right femur
Radiographic Lesion Summary:
No radiographs taken
Differential Diagnosis Outcome:
Probable Osteomalacia
Possible Residual Rickets

Skeletal ID: AT-272

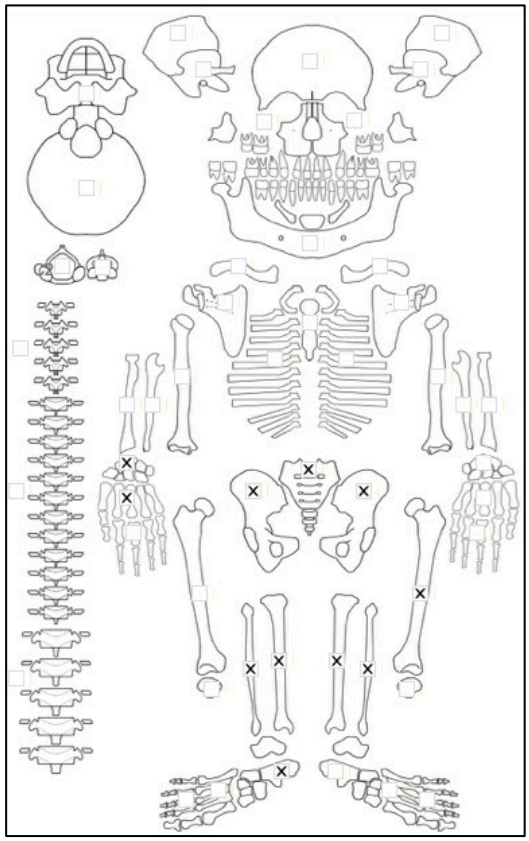

Completeness: Incomplete (33 to 50%). 47% long bones, 12% hands and feet, 4% vertebrae, 0% neurocranium, no ribs.
Preservation/ Taphonomy: Moderate weather and gnaw marks and bones are covered in soil. Anterior middle third of right femur taken for sampling.
Age: 40-49, *Middle Aged Adult*
Sex: Male
Macroscopic Lesion Summary:
- large and deep remodelled multifocal oval lytic destruction, medial to the antero-medial border of the acetabulum and extend into behind the acetabulum of the right os coxa The larger lytic lesion also penetrates into the acetabular surface itself Opening is 16.79x15.57mm on the border of the acetabulum and 19.3x17.68mm in the acetabular surface. The smaller lesion is circular and consistent with a cloacae (8.12x6.33mm). There are two superficial irregular shaped lesions with sclerotic response on the superior margin of the acetabulum (27.20x8.53mm) and inferior to the medial aspect of the anterior inferior iliac spine, superomedial to the acetabular rim (16.58x15.65). The acetabulum has erosive changes, is larger to accommodate the right femoral head with has severe articular changes (the femoral head is considerably larger due to arthritic changes). There is articular changes to the distal right tibia, fibula and superior articular surface of the talus. There is pitting on the articular surface of the right femoral head. There is also fusion of the sacrum to the right os coxa. The region of lytic lesion is in remodelled expanded bone. There are two small lytic cavities on the anterior (distal) border of the lateral articular surface of the right talus. These penetrate into the underlying trabecular bone. The superior one is channel like (10.91x 2.79mm), whereas the inferior one is oval (5.57x4.67). Both have sharp defined margins but sclerotic reaction in the base. The knee joint is spared.
Radiographic Lesion Summary:
- sclerotic ring around the cloacae- appears to be channel like
- the erosive changes are very radiodense, including the acetabular rim.
- there is internal lytic destruction with minimal sclerotic damage on the superior acetabular region. This appears to be multifocal and coalesced lesions. There are very small macroscopic perforations in this region which are obscured by PM damage. The radiographs indicate lytic destruction. Extent of destruction is beyond what is macroscopically visible and involved the entire acetabular region. These smaller lesions are not cyst like.

- although clear remodelling and rounding of the borders, there is no density change between the margins and surrounding bone of the large lytic lesions
Differential Diagnosis Outcome:
Probable Osteomyelitis

Xiongnu Period Mongolia

Skeletal ID: AT-568

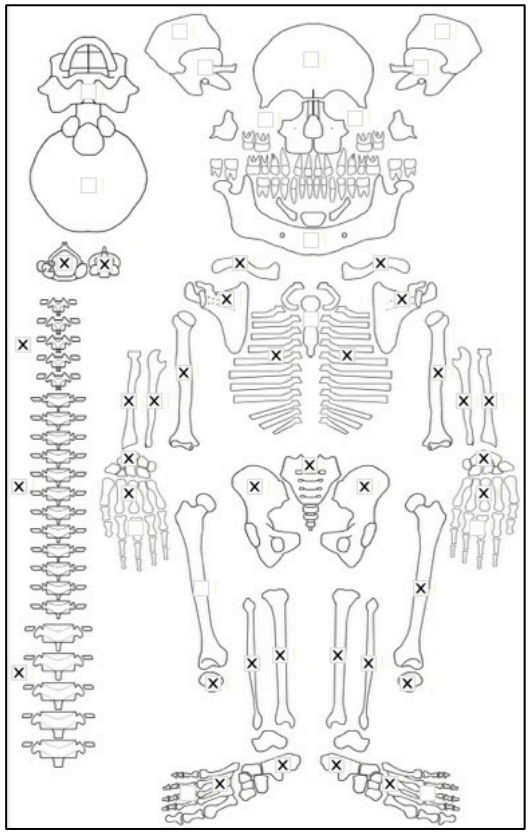

Completeness: Near Complete (66 to 75%). 87% long bones, 29% hands and feet, 67% vertebrae, 0% neurocranium, near complete ribs.
Preservation/ Taphonomy: Surfaces are clean and in excellent condition. Proximal epiphysis of right fibula and left humerus and both epiphyses of left fibula are missing.
Age: 50+, *Old Adult*
Sex: Female
Macroscopic Lesion Summary:
- unilateral remodelled deposit of discrete new bone on the posterior neck of the right humerus
Radiographic Lesion Summary:
No radiographs taken
Differential Diagnosis Outcome:
No diagnosis

Skeletal ID: AT-589

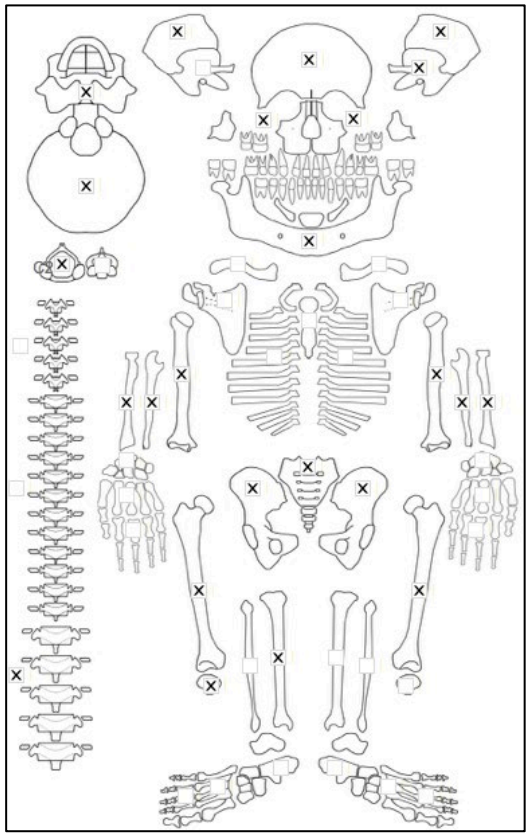

Completeness: Near Complete (66 to 75%). 52% long bones, 0% hands and feet, 29% vertebrae, 75% neurocranium, ribs fragmented.
Preservation/ Taphonomy: Severe gnawing of the surfaces with many bone ends chewed off. anterior shaft of right femur taken for sampling. Distal epiphysis of left humerus, left radius and femora, proximal epiphysis of tibia and ulnae are the only ones preserved. Distal third shaft of right humerus missing. Surfaces of the skull are severely gnawed whereas surfaces of face are in good condition. left side of mandible is missing.
Age: 20-29, *Young Adult*
Sex: Female
Macroscopic Lesion Summary:
No pathology
Radiographic Lesion Summary:
No radiographs taken
Differential Diagnosis Outcome:
No diagnosis

Skeletal ID: AT-259

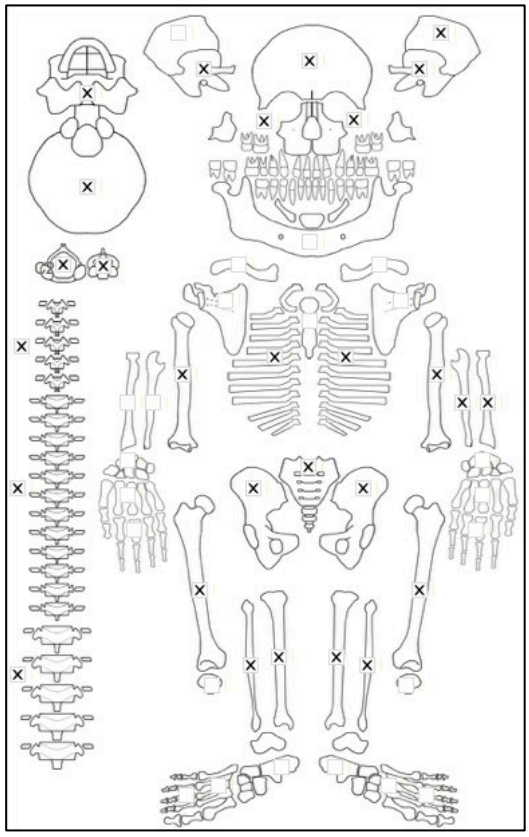

Completeness: Complete (>75%). 77% long bones, 0% hands and feet, 79% vertebrae, 88% neurocranium, ribs near complete.
Preservation/ Taphonomy: Surfaces are in excellent condition with the exception of some gnaw marks of the long bones. Proximal epiphysis of left humerus, distal epiphysis of left ulna and both epiphyses of right fibula missing.
Age: 40-49, *Middle Aged Adult*
Sex: Male
Macroscopic Lesion Summary:
- abnormal cortical porosity extending from the foramen ovale of the right greater wing of sphenoid onto the pterygoid region (left side missing)
- bilateral posterior bending of the distal third shaft of the humeri
- bilateral extreme anterior bending of the femoral shafts, with slight lateral associated bending. There is also coxa vara of the femoral necks with no associated trauma
- fusion of the S1 to S2 on the left sacral ala. There is a aplasia of the right transverse process of the S1.
- possible remodelled bilateral pseudofractures of the superior and inferior rami. However, the calluses are at primary ossification sites
Radiographic Lesion Summary:
- biconcavity of vertebrae with osteopenia (both slight but in multiple vertebrae), individual is older in age
Differential Diagnosis Outcome:
Probable Osteomalacia
Probable Residual Rickets
Possible Scurvy

Skeletal ID: AT-841

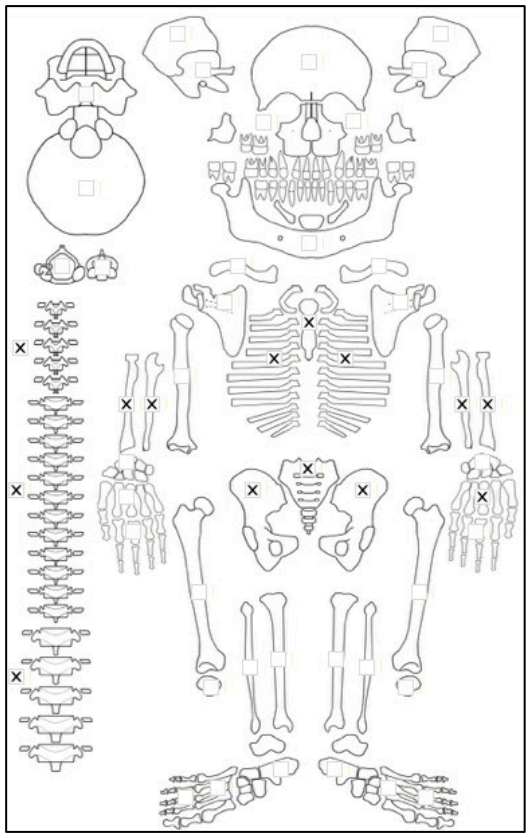

Completeness: Partially Complete (50 to 66%). 32% long bones, 8% hands and feet, 83% vertebrae, 0% neurocranium, ribs partially complete.
Preservation/ Taphonomy: Bone surfaces of long bones are moderately to severely damaged. Epiphyses and fragments of shaft only present for the femora. Severely gnawed parietal fragment.
Age: 50+, *Old Adult*
Sex: Female
Macroscopic Lesion Summary:
No pathology
Radiographic Lesion Summary:
No radiographs taken
Differential Diagnosis Outcome:
No diagnosis

Skeletal ID: AT-438

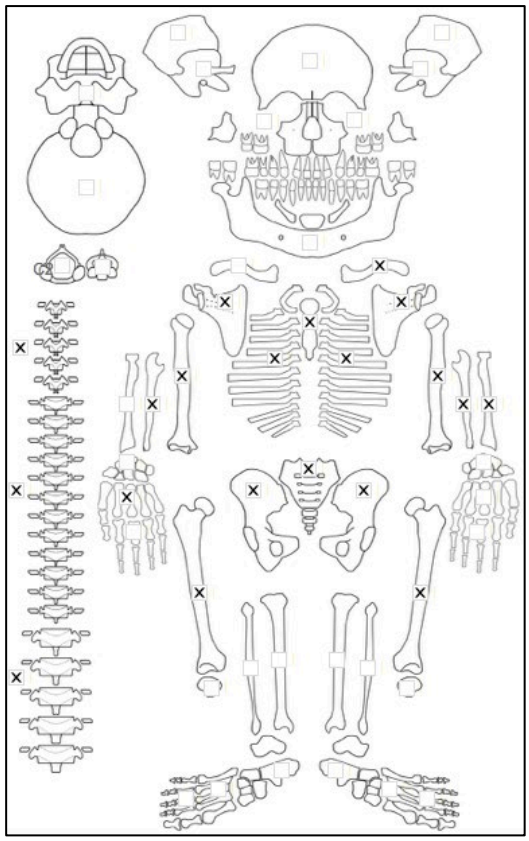

Completeness: Near Complete (66 to 75%). 68% long bones, 5% hands and feet, 54% vertebrae, 0% neurocranium, ribs near complete.

Preservation/ Taphonomy: Surfaces are clean and in excellent condition and all preserve bones are intact (except some PM breakage of ribs and sternum).

Age: 30-39, *Middle Aged Adult*

Sex: Male

Macroscopic Lesion Summary:

No pathology

Radiographic Lesion Summary:

No radiographs taken

Differential Diagnosis Outcome:

No diagnosis

Skeletal ID: AT-452

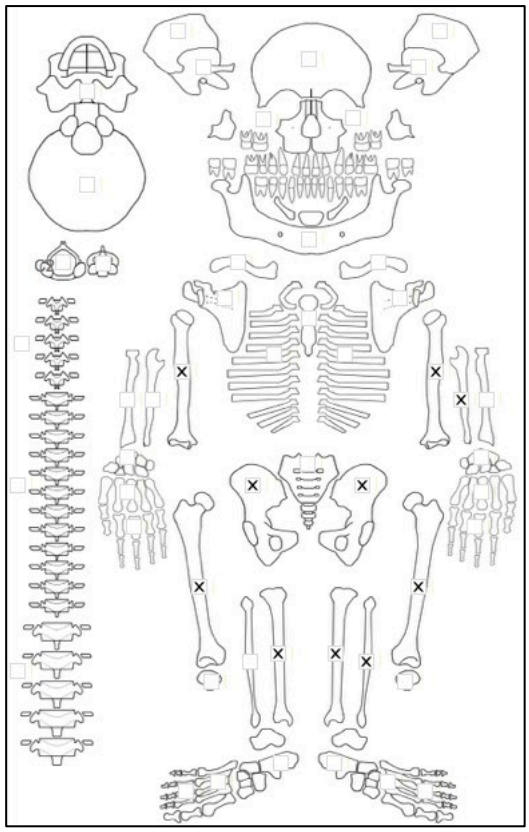

Completeness: Partially Complete (50 to 66%). 65% long bones, 0% hands and feet, 0% vertebrae,)% neurocranium, no ribs.
Preservation/ Taphonomy: Surfaces in excellent condition.
Age: 30-39, *Middle Aged Adult*
Sex: Male
Macroscopic Lesion Summary:
No pathology
Radiographic Lesion Summary:
No radiographs taken
Differential Diagnosis Outcome:
No diagnosis

Skeletal ID: AT-268a

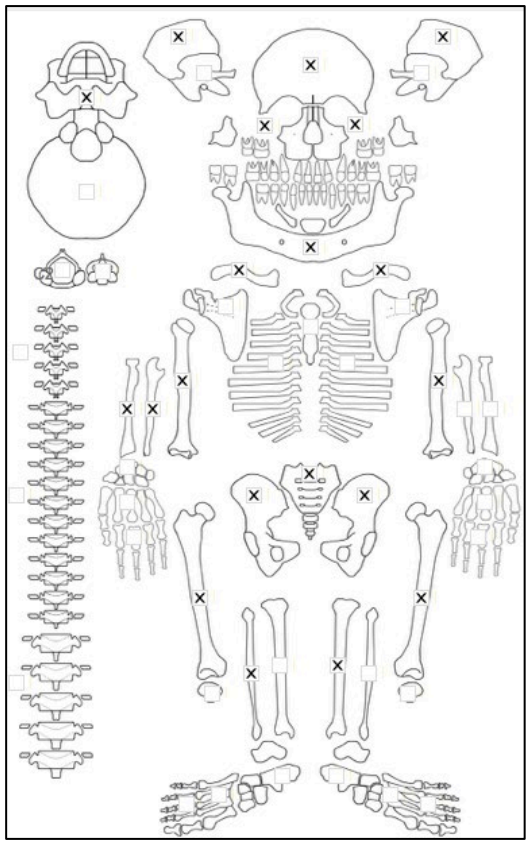

Completeness: Near Complete (66 to 75%). 63% long bones, 0% hands and feet, 0% vertebrae, 63% neurocranium, no ribs.
Preservation/ Taphonomy: Surfaces in excellent condition except for some margins with weathering- lower limb bones have moderate weathering on the edges. Lateral middle third femur taken for sampling. shaft of fibula only
Age: 15 (+/- 1) year, *Adolescent*
Sex: Female
Macroscopic Lesion Summary:
- mineralisation new bone on the distal posterior femora (record lesion)
- Permanent mandibular M1s appear to have mulberry molars, severe carious lesions
- bilateral symmetrical active new bone and cortical porosity superior to the oblique lines from the alveolar margin, coronoid fossae, mylohyoid lines and in the sublingual fossae of the mandibles and unilaterally on the lateral left condylar neck
- active discrete deposits of new bone on the supraorbital tori and medial superior margins of the orbits
- bilateral symmetrical active discrete deposits of new bone and cortical porosity on the inferior orbital surface (includes zygomatic bones and maxillae) with vascular impressions, posterior zygomatic bones and maxillae, anterior maxillae around the infraorbital foramen, palatal surfaces of the maxillae, and anterior zygomatic bones
- bilateral symmetrical active discrete deposits of new bone on the pterygoid regions and fossae, lateral greater wings, lesser wings, and endocranial sphenoid
- active diffuse new bone across the frontal and parietal endocranium
Radiographic Lesion Summary:
- radiolucent M2, with abnormal pulp chamber
Differential Diagnosis Outcome:
Probable Scurvy
Possible Treponematosis

Skeletal ID: AT-262

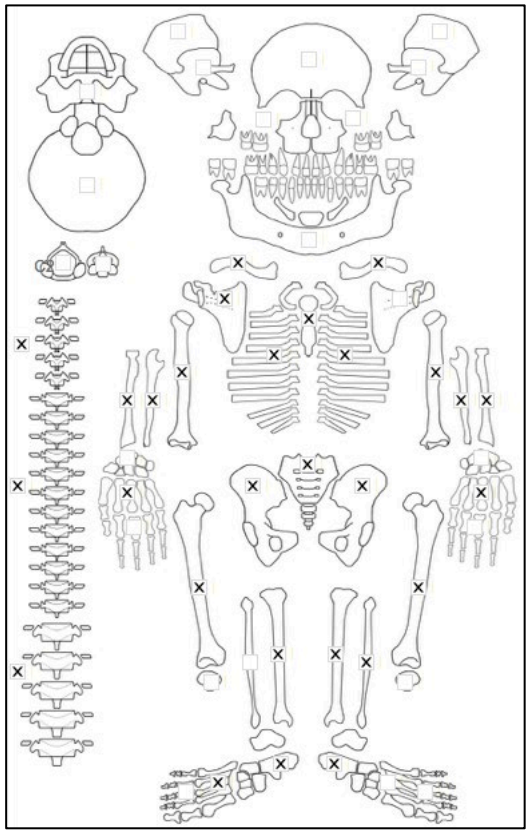

Completeness: Near Complete (66 to 75%). 92% long bones, 22% hands and feet, 63% vertebrae, 0% neurocranium, ribs complete.
Preservation/ Taphonomy: All surfaces in excellent condition. Right distal third anterior femur taken for sampling.
Age: 30-39, *Young Adult*
Sex: Female
Macroscopic Lesion Summary:
- small discrete region of cortical porosity extending from the foramen on the supraspinous fossa of the right scapula (left missing)
- bilateral decreased angle (more acute) of multiple upper to middle ribs. The left side is more exacerbated than the left. A left upper rib also demonstrates increased curvature throughout entire length and increased inferior angulation on the distal end. There is also a remodelled complete fracture of the 2nd left rib.
- bilateral symmetrical focal remodelled poorly mineralised bone on the medial humeral necks
- bilateral coxa vara of the femoral necks with no associated trauma
- bilateral medial bending deformities of the tibiae and left fibula (right missing)
- bilateral symmetrical focal remodelled poorly mineralised bone inferior to the tibial tuberosities
Radiographic Lesion Summary:
- very clear osteopenia and codfish appearance of multiple vertebrae with loss of body height in one vertebra
- concave thickening of the right tibia, where there is concave thinning of the left tibia, the anterior crests are pulled laterally past the lateral margins of the tibiae
- some coarsening of trabeculae in the tibiae
Differential Diagnosis Outcome:
Probable Osteomalacia
Probable Residual Rickets

Skeletal ID: AT-536

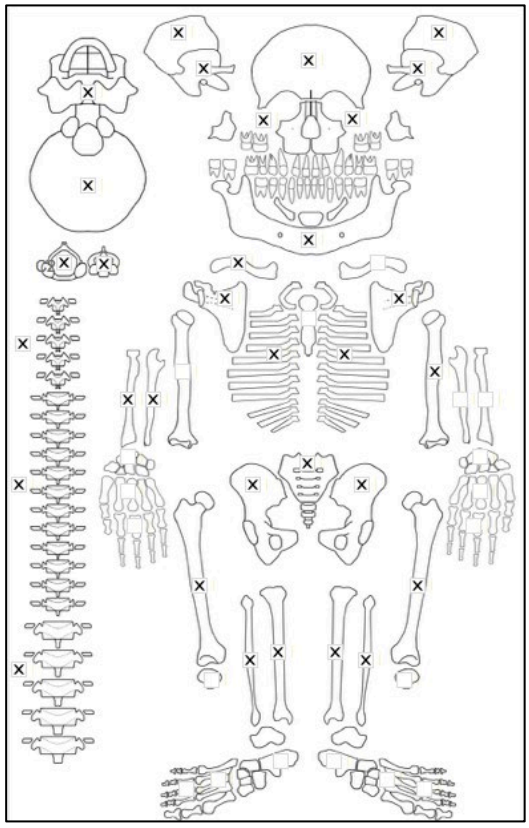

Completeness: Complete (>75%). 70% long bones, 0% hands and feet, vertebrae 100%, neurocranium 100%, and ribs complete.
Preservation/ Taphonomy: All surfaces are in excellent condition and intact.
Age: 20-29, *Young Adult*
Sex: Male
Macroscopic Lesion Summary:
- bilateral and symmetrical diffuse lytic porosity associated with diffuse active new bone on the superior half of the scapulae. The pathological process is concentrated around the glenoid coracoid and acromion regions where there is more trabecular bone. Active new bone continues across the anterior and posterior aspects of the blades
- bilateral diffuse porotic destruction on one left and one right inferior ribs. The remaining ribs appear spared. The left rib (a distal third fragment- likely a lower rib) has diffuse porosity across the entirety of the distal inferior portion with damage close to the sternal margin. The right rib (a lower rib) has porosity and new bone across the distal half shaft in the costal groove, with porosity and new bone more concentrated at the sternal end. There are also 2 circular remodelled masses on the superior proximal third shafts of the 2nd ribs which may be muscular or trauma related.
- Diffuse deep lytic porosity across all surfaces of the vertebrae seeming to spare the superior and inferior aspects of the vertebral bodies of T2-4, 10-12, L5, S1 and adjacent to the right superior articular facet of the C1. The destruction has resulted in complete loss of the cortical bone in most regions that are affected. posterior sacrum fragment shows lower sacrum also affected.
- bilateral diffuse deep porotic destruction associated with diffuse active new bone across the entirety of the os coxa, sparing the acetabulum, auricular surface and medial region of the posterior ilium. The porosity and new bone is more concentrated in thick trabecular rich areas such as the ischium and around the acetabulum. The active bone on the more intact left ilium is thick and spiculated, as well as on the right ischium posterior to the acetabulum suggesting rapid periosteal stripping more in line with a malignant source for the pathological insult.
- the appendicular skeleton appears unaffected
Radiographic Lesion Summary:
- widespread bone loss in all of the affected bones (affected vertebrae, sacrum, os coxae. No clear radiographic signs of bone changes in the affected ribs. Some multifocal lytic destruction seen from a superior view of the T2.
- coarsened trabeculae on the right humerus

- possible Wilson's metaphyseal band in the distal left tibia (Leukaemia band), not present in the proximal metaphysis of the tibia
- multiple stress lines in the distal metaphysis of the left tibia, possible focal lesion of the medial malleolus of the left tibia (not observable macroscopically), focal radiolucent region also on the proximal metaphysis may also be a focal lesions.
- bilateral remodelling mild cribra orbitalia
- unilateral fine cortical porosity on the posterior left zygomatic
- fine abnormal porosity on the palatal surfaces of the maxillae
- the anterior aspect of the maxillae are sunken in
- diffuse porous lytic destruction of the petrous process of the left temporal (right is missing)

Differential Diagnosis Outcome:
No diagnosis

Skeletal ID: AT-538

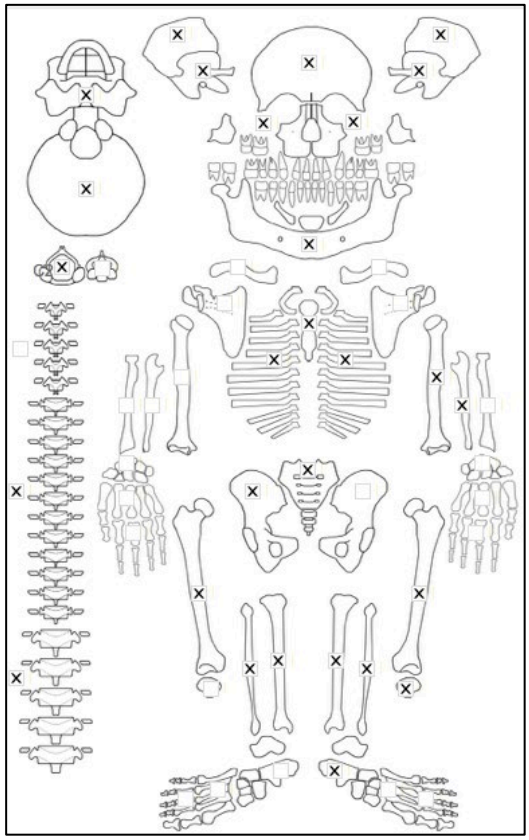

Completeness: Complete (>75%). 61% long bones, 7% hands and feet, 63% vertebrae, 100% neurocranium, near complete.
Preservation/ Taphonomy: Surfaces of axial skeleton moderately damaged, severe damage to surfaces of long bones particularly the lower limb. Cranium and mandible intact but severe damage to the surface of the cranium.
Age: 7.5 (+/- 2.5) years
Sex: Indeterminate
Macroscopic Lesion Summary:
- diffuse active new bone across the interior surface of 3 left upper to middle incomplete ribs (proximal third present). It is not possible to determine whether it is bilateral due to significant surface taphonomic damage to the right side.
- remodelled poorly mineralised bone on the posterior proximal third of the femur at the linea aspera (surface of right side too damaged to observe).
- mixed active and remodelled discrete deposit of new bone on the medial aspect of the left calcaneus (right missing)

Radiographic Lesion Summary:
No radiographs taken

Differential Diagnosis Outcome:
No diagnosis

Skeletal ID: AT-1

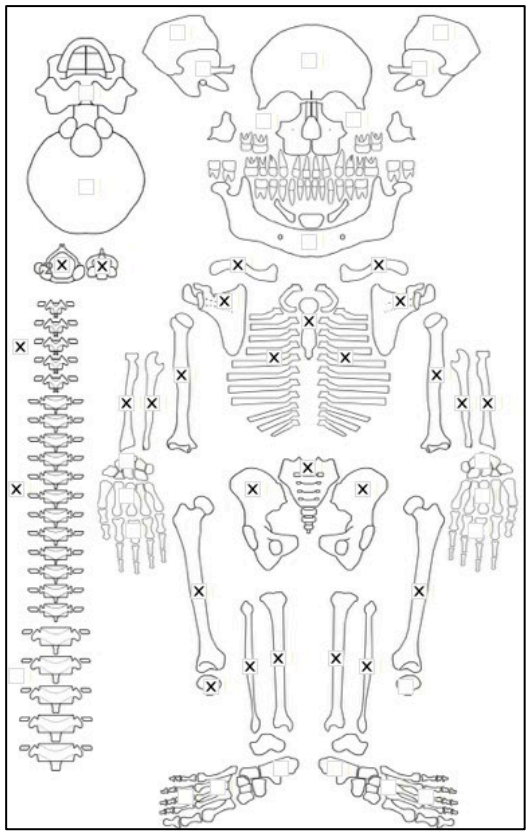

Completeness: Near Complete (660 to 75%). 97% long bones, 0% hands and feet, 96% vertebrae, 0% neurocranium, ribs complete.
Preservation/ Taphonomy: Surfaces are in excellent condition. Long bones intact except proximal third of right tibia missing. Anterior distal third of right femur taken for sampling.
Age: 20-29, *Young Adult*
Sex: Male
Macroscopic Lesion Summary:
No pathology
Radiographic Lesion Summary:
No radiographs taken
Differential Diagnosis Outcome:
No diagnosis

Skeletal ID: AT-294

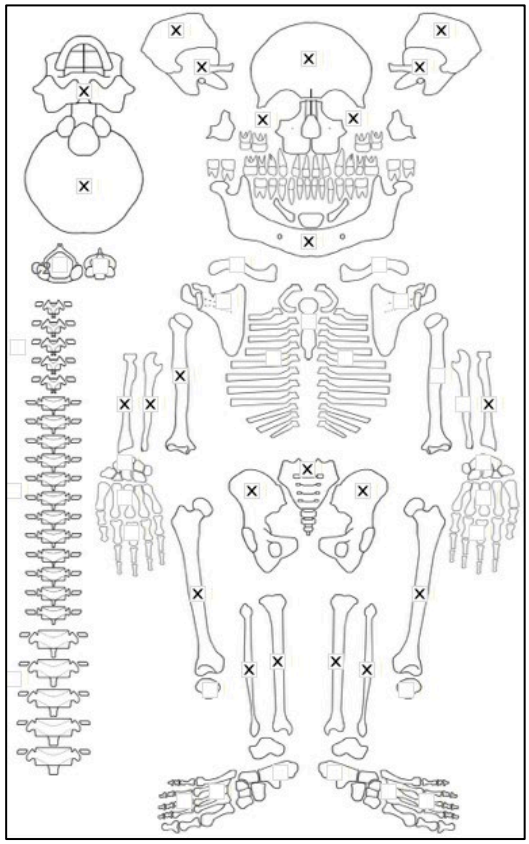

Completeness: Near Complete (66 to 75%). 83% long bones, 0% hands and feet, 0% vertebrae, 100% neurocranium,
Preservation/ Taphonomy: Middle third medial shaft of left femur taken for sampling, rest of long bones intact.
Age: 40-49, *Middle Aged Adult*
Sex: Female
Macroscopic Lesion Summary:
- remodelled poorly mineralised new bone on the medial humeral neck of the left humerus (right side missing)
- bilateral remodelled poorly mineralised new bone on the posterior distal metaphyses of the femora
- aplasia of the right ala of the S1 leading to angulation of the sacral body
- bilateral symmetrical fine cortical porosity not associated with new bone extending from the pterygoid region, foramen oval onto the lateral wing of sphenoid across the superior margin of the zygomatic arch on the squama of the temporals.
- bilateral symmetrical fine cortical porosity and mixed active and remodelled new bone extending from the hypoglossal canals on the inferior occipital
- bilateral symmetrical remodelled new bone, cortical porosity and vascular impressions on the posterior zygomatic bones
Radiographic Lesion Summary:
No radiographs taken
Differential Diagnosis Outcome:
Possible Scurvy

Skeletal ID: AT-338

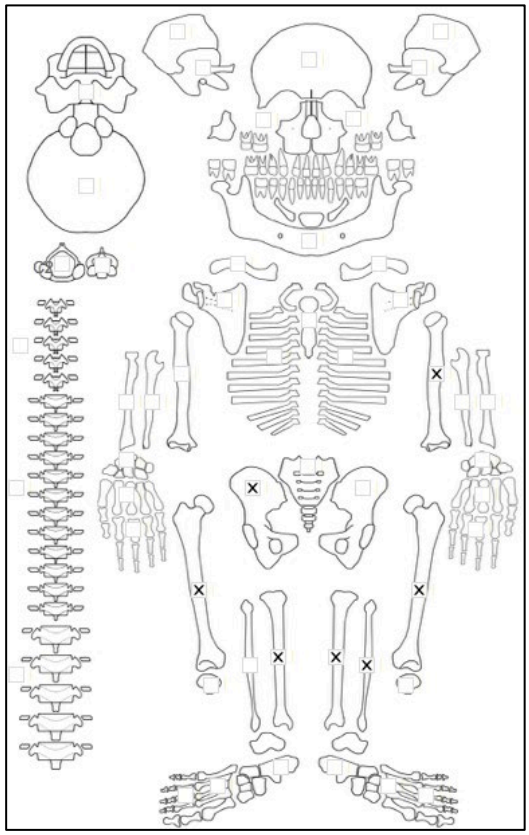

Completeness: Incomplete (33 to 50%). 42% long bones, 0% hands and feet, 0% vertebrae, 0% neurocranium, no ribs.
Preservation/ Taphonomy: Left femur distal anterior third shaft taken for sampling. Intrusive long bones from adolescent (severe damage to surfaces not recorded)
Age: 30-39, *Young Adult*
Sex: Female
Macroscopic Lesion Summary:
No pathology
Radiographic Lesion Summary:
No radiographs taken
Differential Diagnosis Outcome:
No diagnosis

Skeletal ID: AT-689

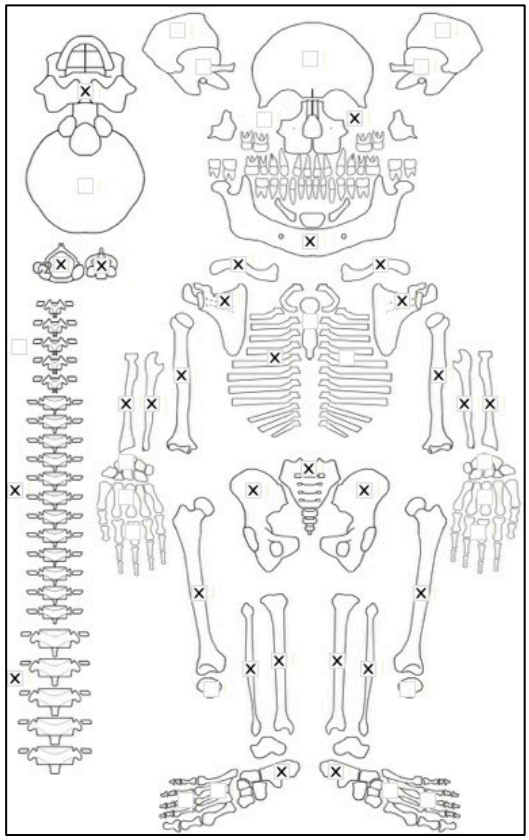

Completeness: Near Complete (66 to 75%). 78% long bones, 5% hands and feet, 50% vertebrae, 13% neurocranium, partially complete.
Preservation/ Taphonomy: Surfaces are moderately to severely damaged. Proximal third of left fibula and right radius and proximal half of left ulna only, proximal epiphysis of right fibula and tibiae, both of right humerus, distal epiphysis of right ulna missing
Age: 30-39, *Middle Aged Adult*
Sex: Female
Macroscopic Lesion Summary:
- remodelled vascular impressions extending from the foramen on the posterior right zygomatic bone (left side missing)
Radiographic Lesion Summary:
No radiographs taken
Differential Diagnosis Outcome:
No diagnosis

Skeletal ID: AT-692

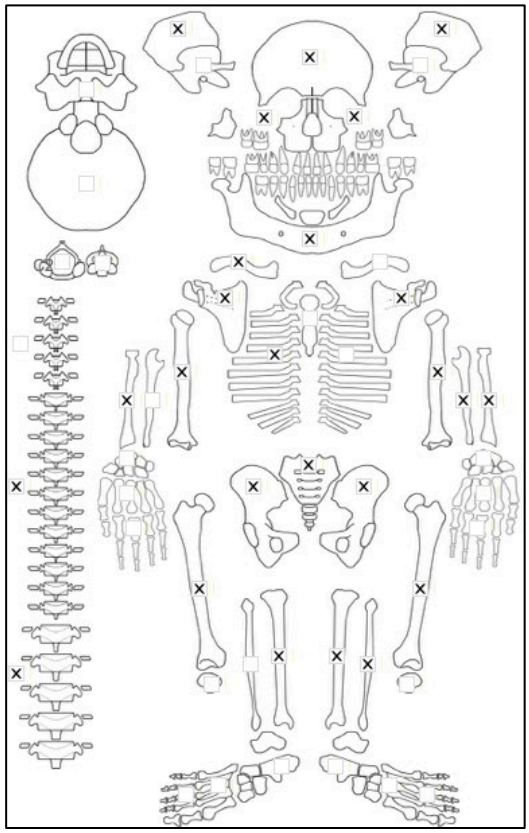

Completeness: Complete (>75%). 72% long bones, 2% hands and feet, 33% vertebrae, 38% neurocranium, ribs incomplete.
Preservation/ Taphonomy:
Age: 30-39, *Middle Aged Adult*
Sex: Male
Macroscopic Lesion Summary:
- Exaggerated anterior protrusion of the sacrum at the site of the S3. Possible fracture at the region of angulation on the S3 body and some calcification around the S3 region around the possible fracture suggests antemortem with attempts at healing), there is another possible fracture on the left ala of the S4 but difficult to determine if this is a postmortem fracture, no calcification on the radiograph. There is a fracture of different pattern directly beneath the S3 fracture that appears a true post-mortem fracture, suggesting the others are true fractures.
- bilateral well remodelled moderate cribra orbitalia
Radiographic Lesion Summary:
- calcification around the possible fracture of the S3, the sacrum appears to have some general osteopenia
- osteopenia of the vertebrae, but codfish appearance of only one of the vertebra, but bucking of another vertebra with some calcification on the anterior portion at region of buckling (possible remodelled pseudofracture)
Differential Diagnosis Outcome:
Probable Osteomalacia
Anaemia

Skeletal ID: AT-583

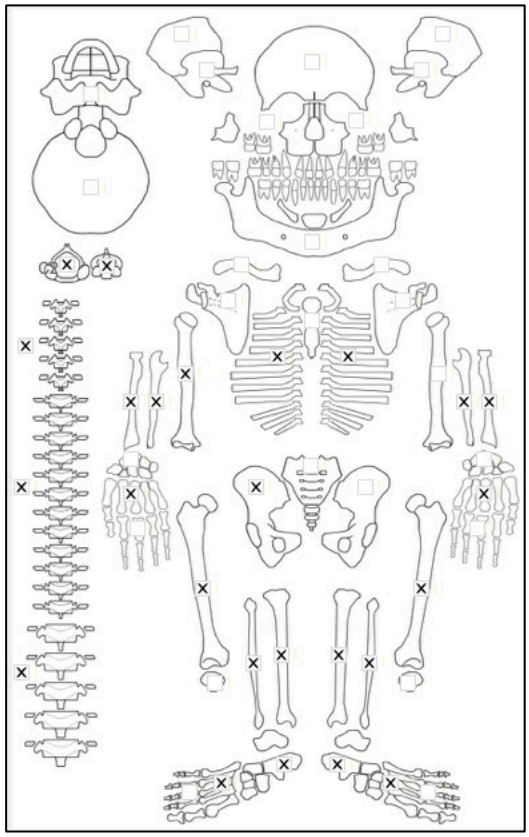

Completeness: Near Complete (66 to 75%). 92% long bones, 38% hands and feet, 80% vertebrae, 0% neurocranium, ribs complete.
Preservation/ Taphonomy: Surfaces are intact, clean and excellent. There is commingling of hands and feet of another individual but the size and taphonomy meant they could easily be separated. Some commingling is still possible of some of the phalanges. PM breakage of midshaft of right tibia and anterior distal third of right femur taken for sampling otherwise intact.
Age: 19 (+/-1) year, *Adolescent*
Sex: Male
Macroscopic Lesion Summary:
- bilateral mixed remodelling diffuse new bone deposits visible on 3 left and 1 right middle rib
- poorly mineralised new bone on the medial neck of the right humerus
- bilateral poorly mineralised new bone on the distal posterior metaphyses of the femora
- genu valgum of the right femur (unilateral)
- bilateral poorly mineralised new bone on the posterior apexes of the patellae, there is associated destruction of the superior aspect of the left patella due to poor mineralisation
- bilateral poorly mineralised new bone on the proximal posterior shafts of the fibulae at the site of muscle attachment
- unilateral medial bending of the shaft of the left fibula
- bilateral poorly mineralised new bone on the proximal medial metaphyses of the tibiae at the site of muscle attachment
- Severe medial bending deformities of the shafts of the tibiae
- bilateral poorly mineralised new bone on the superior calcaneal tuber
- bilateral mixed active and remodelled new bone on the coronoid processes of the mandible. surface is severely damaged.
- abnormal cortical porosity on the right lateral wing of sphenoid continuing onto the right zygomatic process of the frontal
Radiographic Lesion Summary:
- no clear osteopenia of the vertebrae, there is loss of horizontal trabeculae, but slight codfish appearance on multiple vertebrae.
- left fibula is thick on the concave aspect, the anterior crest has lateral bending as it is present on the radiographs more lateral than the lateral shaft of the tibia, the bone ends have coarse trabeculae.

- cystic lesion on the proximal shaft of the left fibula (may be Brown's tumour- hyperparathyroidism)
- Multiple stress lines present in the distal ends of the tibiae.

Differential Diagnosis Outcome:
Possible Rickets
Probable Osteomalacia

Skeletal ID: AT-370

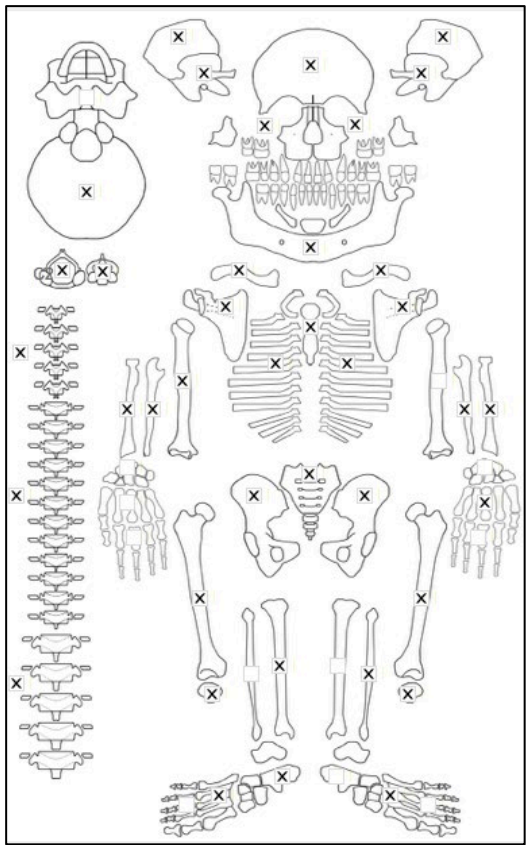

Completeness: Complete (>75%). 52% long bones, 17% hands and feet, 96% vertebrae, 75% neurocranium, ribs partially complete.
Preservation/ Taphonomy: Surfaces of axial skeleton are in good condition but there is moderate to severe buckling and scavenging of the surfaces of the long bones. Many post mortem breakages of the long bones: right radius, left fibula only represented by shafts (fibula is proximal third shaft only), distal epiphyses of femora, humerus and right ulna, proximal epiphysis of left ulna and both epiphyses of tibiae are missing.
Age: 20-29, *Young Adult*
Sex: Female
Macroscopic Lesion Summary:
- focal destruction with osteoarticular response of the left inferior articular surface of the T1. There is some sclerotic response. Destruction is confined to the articular surface. There is minimal adjacent erosive response of the superior articular facet of the T2. Lesion diameter: 3.78x1.88mm.
- unilateral remodelled thin discrete deposit of new bone on the distal to middle posterior shaft of the femur medial to the linea aspera
- unilateral remodelled thick and irregular new bone without apparent cortical expansion on the posterior medial and later surfaces of the shaft of the left femur. It is most severe along the linea aspera.
- unilateral remodelled discrete deposit of new bone inferior to the left mylohyoid line of the mandible
- remodelling porotic hyperostosis with marked diploic expansion on the superior frontal, superior and posterior parietals medial to the temporal line, and the occipital planum

Radiographic Lesion Summary:
No radiographs taken
Differential Diagnosis Outcome:
Anaemia

Skeletal ID: AT-36

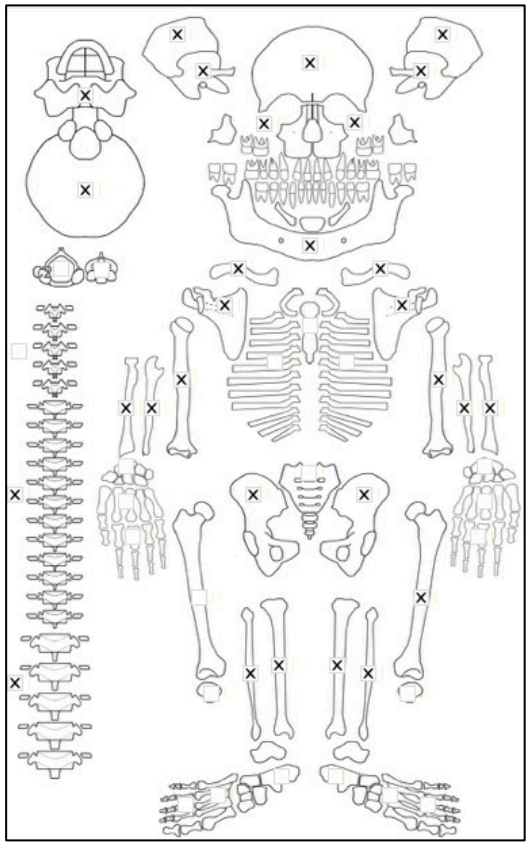

Completeness: Complete (>75%). 100% long bones, 0% hands and feet, 46% vertebrae, 100% neurocranium, ribs fragmented.
Preservation/ Taphonomy: Surfaces are in excellent condition with all preserved remains intact and clean. Middle anterior third of left femur taken for sampling.
Age: 30-39, *Middle Aged Adult*
Sex: Male
Macroscopic Lesion Summary:
- acute angulation of the rib next with lateral straightening of the ribs shafts of 2 preserved left middle ribs.
- unilateral discrete deposit of remodelled new bone on the medial midshaft of the right fibula
- unilateral discrete deposit of remodelled new bone around the foramen on the posterior proximal third shaft of the right tibia
- bilateral severe medial bending deformities of the tibial shafts. Shafts are extremely thin medial laterally.
- remodelled discrete deposit of new bone and cortical porosity extending from the anterior alveolar margin to the mental eminence of the mandible. there is antemortem tooth loss.
- unilateral remodelled mild cribra orbitalia of the left orbit
- bilateral remodelled new bone and cortical porosity extending posterior from the ear canal onto the mastoids. There is unilateral remodelled circular lytic destruction of the right mastoid resulting in shape change to the mastoid. The lesion is 8.11x5.59mm
- diffuse remodelled porotic hyperostosis on the superior frontal, parietals and occipital planum
Radiographic Lesion Summary:
- codfish appearance of multiple vertebrae without clear osteopenia
- thickened cortex of the concave aspect of the fibulae, without clear thickening of the tibial shaft, but the true bending deformity in the tibia is clear on the radiograph.
Differential Diagnosis Outcome:
Probable Osteomalacia
Probable Residual Rickets
Anaemia
Probable Otitis Media/Mastoiditis

Skeletal ID: AT-292

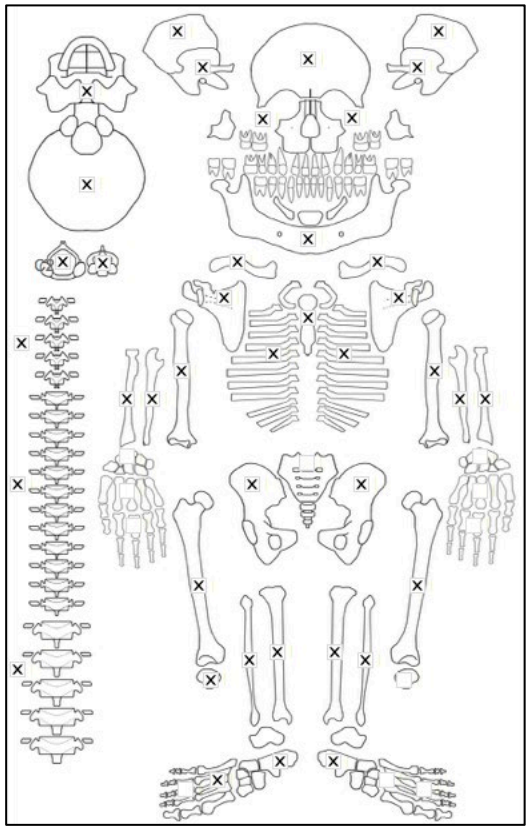

Completeness: Complete (>75%). 100% long bones, 11% hands and feet, 83% vertebrae, 100% neurocranium, ribs complete.
Preservation/ Taphonomy: All preserved surfaces intact clean and in excellent condition. Anterior distal half of right femur taken for sampling.
Age: 20-29, *Young Adult*
Sex: Male
Macroscopic Lesion Summary:
- Unilateral focal circumferential lesion on the internal margin of the distal end of the left 12th rib. The margins are sharp and well defined but there is some sclerotic response in the base more distally. There is a secondary lytic channel extending from the lesions potentially a continuation of the lytic destruction to the sternal end. lesion diameter is 9.51x8.6mm. The lytic lesion is actually in a portion of ossified cartilage.
- bilateral symmetrical discrete mixed active and remodelled new bone deposit on the anterior-medial aspect of the proximal shafts to the fibulae. Lesions appear haematoma-like.
- unilateral discrete mixed active and remodelled new bone deposit on the lateral metaphysis lateral to the tibial tuberosity of the left tibia.
- bilateral symmetrical remodelled discrete deposits of new bone and cortical porosity on the oblique lines of the mandible
- bilateral symmetrical remodelled discrete deposits of new bone and cortical porosity on the pterygoid regions of the sphenoid extending from the foramen ovale
- bilateral symmetrical remodelled cortical porosity on the posterior zygomatic bones
- bilateral symmetrical remodelled cortical porosity on the lateral margin of the anterior zygomatic bones
Radiographic Lesion Summary:
- left 12th rib: minimal sclerosis in the cyst, margins of the calcified region is radiodense. Multilocular cystic appearance.
Differential Diagnosis Outcome:
Probable Hydatids Disease

Skeletal ID: AT-537

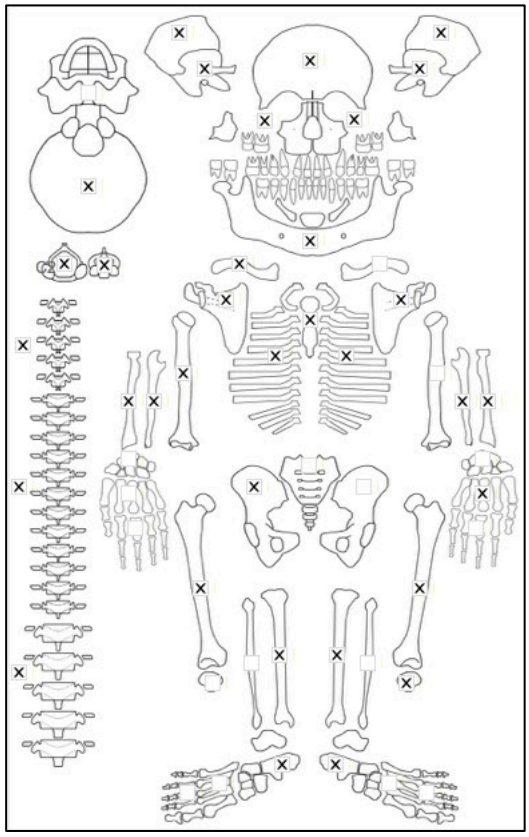

Completeness: Complete (>75%). 67% long bones, 11% hands and feet, 50% vertebrae, 100% neurocranium, ribs incomplete.
Preservation/ Taphonomy: Surfaces of lower limb bones are severely damaged but upper limbs have minimal scavenging. some post mortem damage to surfaces of the pelvis. preserved vertebrae are intact except two lumbar with damage of the body. Most of anterior shaft of right femur taken for sampling.
Age: 50+, *Old Adult*
Sex: Female
Macroscopic Lesion Summary:
- bilateral discrete remodelled deposit of new bone and cortical porosity on the incisive fossae of the mandible
Radiographic Lesion Summary:
No radiographs taken
Differential Diagnosis Outcome:
No diagnosis

Skeletal ID: AT-907

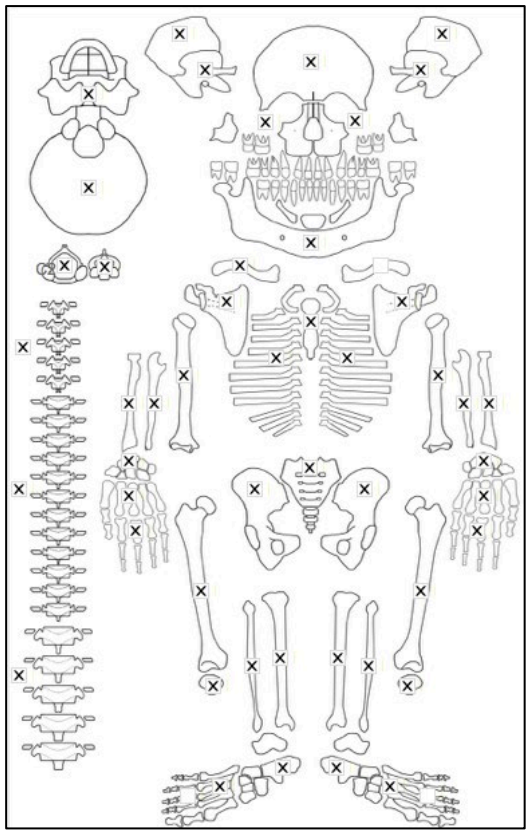

Completeness: Complete (>75%). 97% long bones, 64% hands and feet, 100% vertebrae, 100% neurocranium, ribs near complete.
Preservation/ Taphonomy: Individual is very old so bones are fragile. Surfaces have minimal to moderate scavenging.
Age: 50+, *Old Adult*
Sex: Female
Macroscopic Lesion Summary:
- unilateral moderate medial bending of the right fibula shaft
Radiographic Lesion Summary:
- very slight cortical expansion on the concave right fibula shaft bend (concave thicker than convex side) but this is not very distinct
Differential Diagnosis Outcome:
Possible Residual Rickets

Skeletal ID: AT-908

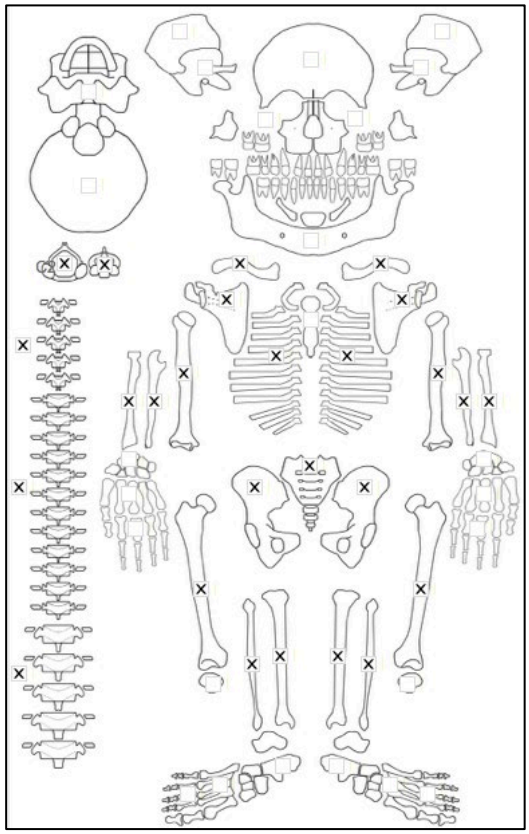

Completeness: Near Complete (66 to 75%). 100% long bones, 0% hands and feet, 100% vertebrae, 0% neurocranium, ribs complete.
Preservation/ Taphonomy: Surfaces are covered by dust and there is root etching affecting the surfaces. All preserved bones are intact.
Age: ~5-6 years, *Child*
Sex: Indeterminate
Macroscopic Lesion Summary:
- bilateral genu valgum of the distal femora with medial bending of the shaft
Radiographic Lesion Summary:
- white line of Fraenkel with associated Trummerfeld zones of the long bones
- there is unilateral compression of the left femoral neck (possible coxa vara)
- ground osteopenia and coarsened trabeculae
- cupping of the proximal tibiae and this a particularly radiodense metaphyseal plate
Differential Diagnosis Outcome:
Probable Rickets
Probable Scurvy

Skeletal ID: AT-154

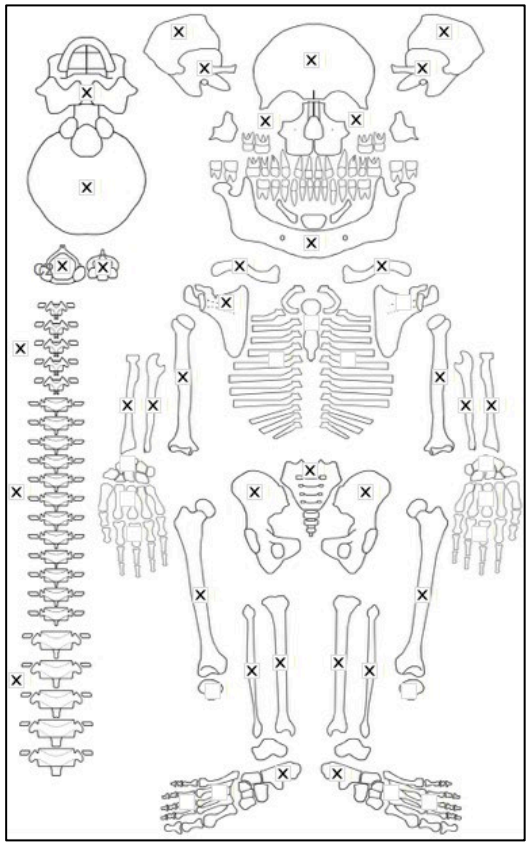

Completeness: Complete (>75%). 100% long bones, 4% hands and feet, 100% vertebrae, 0% neurocranium, ribs incomplete.
Preservation/ Taphonomy: All surfaces are intact and excellently preserved, distal epiphyses of ulna and radii and proximal epiphyses of left fibula missing. Some copper (bronze) staining on the radii. Anterior middle third of right femur taken for sampling.
Age: 17 (+/-1) years, *Adolescent*
Sex: Male
Macroscopic Lesion Summary:
- bilateral abnormal endochondral porosity exceeding 10mm from the metaphyseal plate on the proximal humeri, distal radii, distal femora, proximal tibia and distal fibulae. The porosity on the femora is severe and may be related to poor mineralisation.
- bilateral lateral bending of the humeral shafts
- bilateral flaring of the distal metaphysis and genu valgum of the femora
- moderate medial bending of the shafts of the tibiae
- extensive remodelled new bone deposit on the anterior aspect of the left fibula shaft, with diffuse active bone on the posterior aspect. There is a transverse fracture associated on the proximal third shaft and likely the cause of the infection. There is anterior pseudobending occurring. There is also flaring of the proximal metaphysis of the left fibula. Much of the new bone can be attributed to a remodelled callus, but the active bone suggests pathology.
- very deep remodelled oval lytic depression on the poster-lateral proximal shaft of the right fibula. there is a peak of bone on the posterior aspect of the proximal metaphysis which may be remnants of metaphyseal flaring which has fused to the epiphyseal plate. margins are defined but rounded with no evidence of activity. lesion diameter: 38.86x9.01mm. (this lesion may be a Brown tumour- hyperparathyroidism)
-focal deep circumferential lytic lesion in the right acetabulum. The margins are slightly rounded and there is no sign of activity. Minimal sclerotic response. Lesion diameter: 9.35x9.35mm. iliac blade is thin
- mostly remodelled diffuse new bone on the posterior shafts of the tibiae and femora associated with patches of active new bone
- remodelled new bone and cortical porosity on the mental eminence, inferior mandibular rami and extending medially from the incisive foramina of the mandible. Severe antemortem tooth loss.
- unilateral diffuse new bone and cortical porosity on the right lateral greater wing of sphenoid and right temporal squama.

- bilateral remodelled new bone and cortical porosity on the nasal margin of the maxillae and on the nasals, this appears to be related to trauma of the nasal region
- bilateral remodelling moderate cribra orbitalia
- remodelled porotic hyperostosis of the frontal, parietals (medial to temporal line) and occipital planum
- bilateral thick remodelled new bone and cortical porosity on the palatal surfaces of the maxillae

Radiographic Lesion Summary:
- no clear changes between margin and surrounding bone of the focal lytic lesion on the right acetabulum, possibly a normal variant
- codfish sign of multiple vertebrae
- bending deformities of the tibiae are clear without cortical expansion
- coarsened trabeculae of the distal metaphyses of the tibiae and humeri. Ground glass form of the distal tibiae.
- multiple stress lines of the tibial metaphyses.
- A fracture can be identified in the expanded bone of the left fibula (there the new bone is likely a result of a remodelled callus). Though there is angulation at this site, the bending deformity does not appear to be a direct result of the fracture.

Differential Diagnosis Outcome:
Probable Rickets
Probable Osteomalacia
Probable Scurvy
Anaemia

Skeletal ID: AT-23

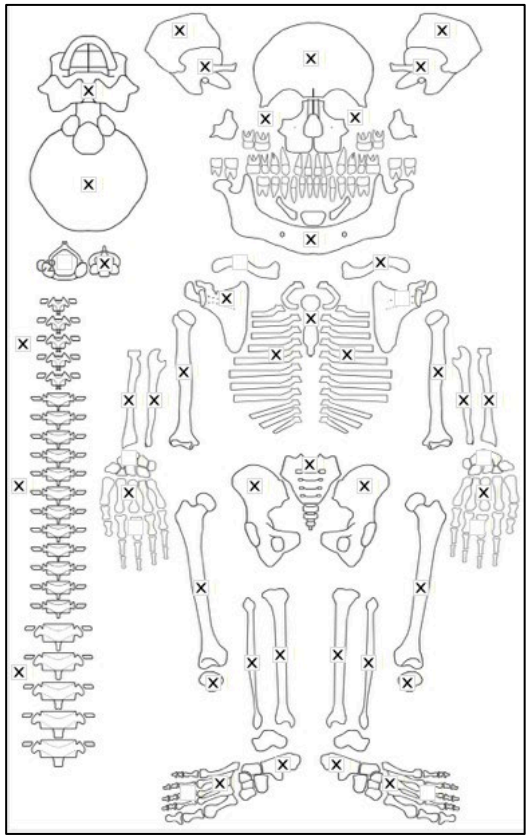

Completeness: Complete (>75%). 100% long bones, 15% hands and feet, 88% vertebrae, 100% neurocranium, ribs complete.
Preservation/ Taphonomy: Surfaces are clean in excellent condition and bones are completely intact. Small sample of anterior distal femur taken and missing
Age: 20-29, *Young Adult*
Sex: Male
Macroscopic Lesion Summary:

- Unilateral discrete but extensive deposit of new bone projecting from the surface of the lateral distal third humerus. The new bone is remodelled but poorly mineralised. Unlike other deposits in this assemblage this resembles Brickley and Ives as a potential poorly mineralised fracture callus.
- bilateral coxa vara of the femoral neck
- exaggerated angle of the ribs particularly at the rib neck. the right side appears more severe
- focal deep circumferential lytic lesion in the right acetabulum. The margins are slightly rounded and there is no sign of activity. Minimal sclerotic response. Lesion diameter: 9.35x9.35mm
- remodelled new bone and cortical porosity on the mental eminence and incisive fossae of the mandible
- bilateral symmetrical remodelled pseudo fractures with proper mineralisation of the superior and inferior rami of the os coxae.

Radiographic Lesion Summary:
- osteopenia of the vertebrae, no codfish or loss of body height

Differential Diagnosis Outcome:
Probable Osteomalacia
Probable Residual Rickets

Skeletal ID: AT-2

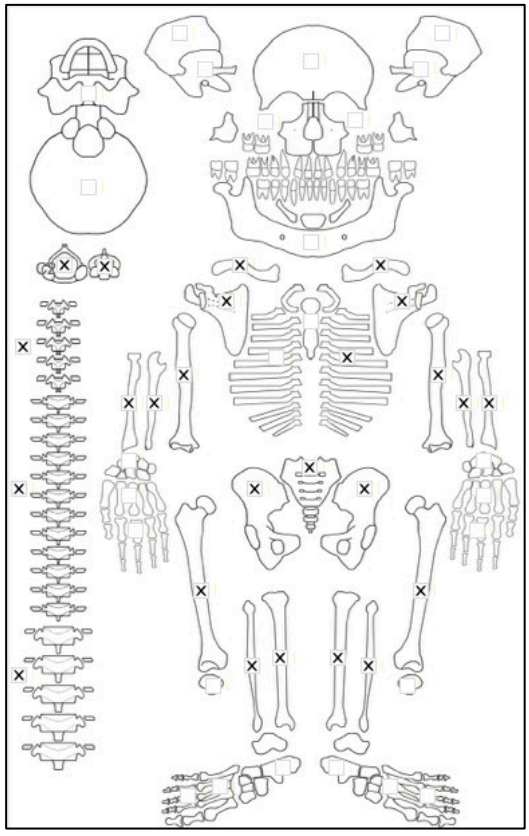

Completeness: Near Complete (>75%). 100% long bones, 0% hands and feet, 88 vertebrae, 0% neurocranium, ribs incomplete.
Preservation/ Taphonomy: Surfaces are excellent and intact. Medial proximal half of right femur taken for sampling.
Age: 30-39, *Young Adult*
Sex: Female
Macroscopic Lesion Summary:
- bilateral symmetrical remodelled new bone and cortical porosity on the supraspinous fossae of the scapulae
- left scapula also has discrete deposit of new bone in the shape of a haematoma on the infraspinous fossa (right side missing)
- unilateral discrete remodelled deposit of new bone on the posterior distal third shaft of the right tibia
- poorly mineralised bone deposit on the posterior distal metaphyses of the femora
- bilateral exaggerated acute angulation of the rib necks

- spiculated remodelled new bone on the anterior vertebral body of the L5 associated with diffuse porotic destruction on the superior anterior margin of the vertebral body. No other vertebrae show any signs of erosive destruction.

Radiographic Lesion Summary:

- slight biconcavity of the radiographed vertebra, radiodensity of the superior anterior margin of the vertebral body.

Differential Diagnosis Outcome:

Possible Brucellosis
Possible Residual Rickets
Probable Scurvy

Skeletal ID: AT-930

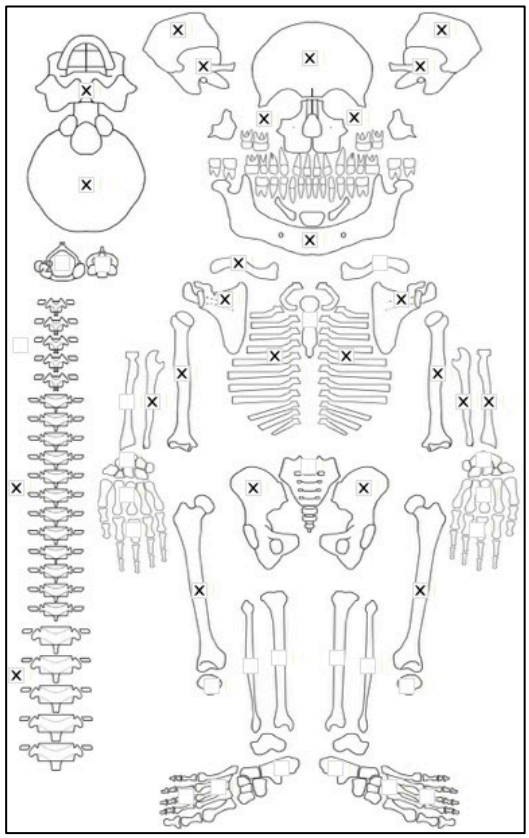

Completeness: Partially Complete (5o to 66%). 58% long bones, 3% hands and feet, 58% vertebrae, 88% neurocranium, ribs incomplete.
Preservation/ Taphonomy: Surfaces covered in dark soil and there is considerable post mortem breakage.
Age: 15.5 (+/-1.5) years, *Adolescent*
Sex: Female
Macroscopic Lesion Summary:

- coxa vara of the left femur (right femur missing)

Radiographic Lesion Summary:

No radiographs taken

Differential Diagnosis Outcome:

Possible Residual Rickets

Skeletal ID: AT-265

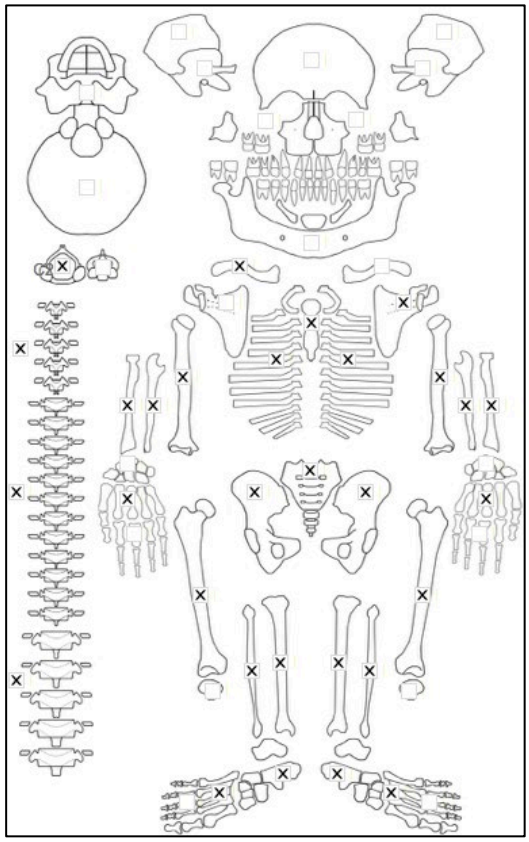

Completeness: Near Complete (66 to 75%). 100% long bones, 31% hands and feet, 88% vertebrae, 0% neurocranium, ribs complete.
Preservation/ Taphonomy: All surfaces are excellent and intact. Medial middle third of tibia has been taken for sampling.
Age: 20-29, *Young Adult*
Sex: Male
Macroscopic Lesion Summary:
No pathology
Radiographic Lesion Summary:
No radiographs taken
Differential Diagnosis Outcome:
No diagnosis

Skeletal ID: AT-267

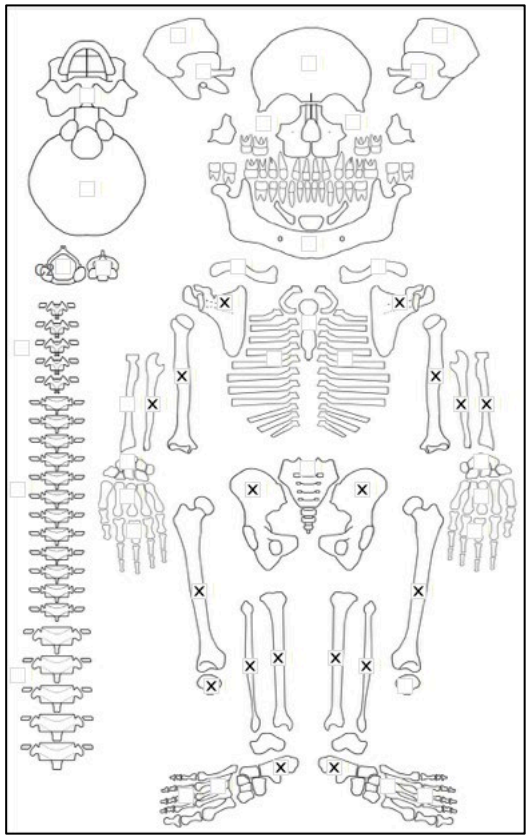

Completeness: Partially Complete (50 to 66%). 98% long bones, 4% hands and feet, 0% vertebrae, 0% neurocranium, no ribs.
Preservation/ Taphonomy: Surfaces are in excellent condition. Distal epiphysis of the right ulna is missing. humeral head of right humerus is detached. Anterior distal third of left femur has been taken for sampling.
Age: 50+, *Old Adult*
Sex: Female
Macroscopic Lesion Summary:
- bilateral abnormal vascular impressions on the shafts of the posterior, medial and lateral femora indicating the presence of remodelled diffuse new bone.
Radiographic Lesion Summary:
No radiographs taken
Differential Diagnosis Outcome:
No diagnosis

Skeletal ID: AT-268b

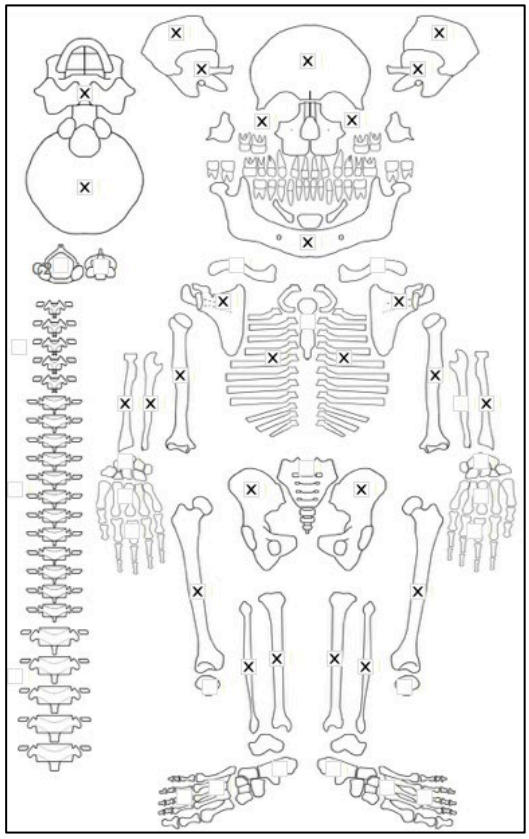

Completeness: Complete (>75%). 92% long bones, 0% hands and feet, 8% vertebrae, 88% neurocranium, ribs partially complete.
Preservation/ Taphonomy: Surfaces are complete and in excellent condition
Age: 7.5 (+/-2) years, *Child*
Sex: Indeterminate
Macroscopic Lesion Summary:
- small bilateral discrete symmetrical mixed active and remodelled deposit of new bone on the medial midshafts of the humeri
- small bilateral discrete symmetrical mixed active and remodelled deposit of new bone on the anterior lateral middle shafts of the radii extending from the foramen.
- flaring of the proximal metaphyses of the radii
- deep porosity of the distal ends of the femora. The porosity is more consistent with mineralisation problems than scorbutic deep endochondral porosity. Metaphyseal plate is thin and there may be initial fraying occurring. There is also slight cupping of the distal ends with medial bending of the shafts and slight genu valgum. There is marked cupping of the proximal greater trochanter metaphyseal plate. The right femoral neck is associated with coxa vara
- bilateral symmetrical mixed active and remodelled diffuse new bone deposit on the medial shafts of the tibiae.
- bilateral marked medial bending of the fibulae. The peak of the bend is more distal and severe on the right than the left. Both have cupping on the distal end with flaring of the proximal right end.
- bilateral discrete deposits of new bone on the pars laterali and basilaris, extending from the hypoglossal canals
- bilateral discrete deposits of remodelled new bone and cortical porosity on the superior orbits
- bilateral discrete deposits of mixed active and remodelled new bone on the anterior temporal squama, associated with active new bone on the lateral aspect of the left greater wing, lesser wing and pterygoid region and fossa of the left sphenoid (right side missing)
- bilateral active new bone on the posterior zygomatics continuing onto the posterior left maxilla where is porosity and deep vascular impressions, there is also new bone and cortical porosity on the palatal surface as well as the inferior orbital surface where vascular grooves are also identified.
- bilateral symmetrical discrete deposits of new bone and cortical porosity on the coronoid processes of the mandible

- bilateral abnormal flaring of the rami
- bilateral symmetrical discrete deposits of mixed active and remodelled new bone and cortical porosity around the regions of the oblique line. The bone is more remodelled near the alveolar margins.

Radiographic Lesion Summary:
- cupping of the long bones are very clear on the radiographs
- no white line of Fraenkel, but ground glass osteopenia
- tibiae femora and radius show thick periosteal deposits on the shaft
- multiple stress lines in the long bones with coarsened trabeculae
- distal ends of femora are radiolucent, but fraying isn't clear on the radiographs

Differential Diagnosis Outcome:
Probable Rickets
Probable Scurvy

Skeletal ID: AT-690

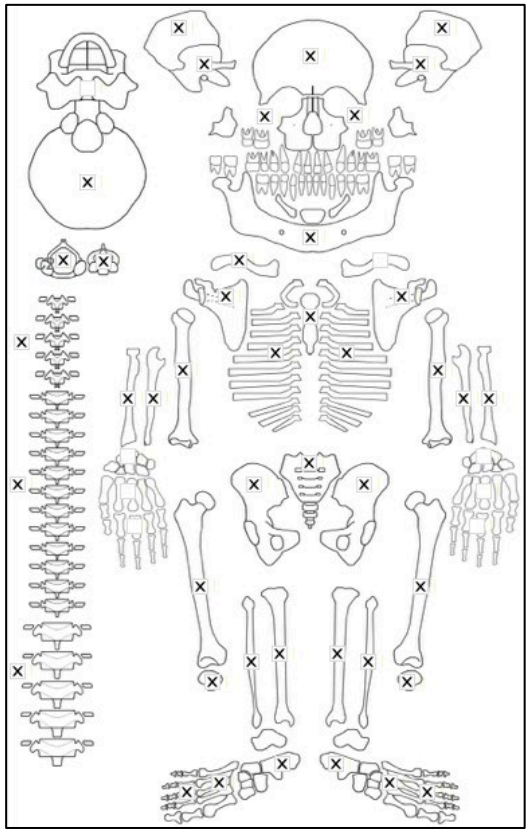

Completeness: Complete (>75%). 90% long bones, 30% hands and feet, 96% vertebrae, 75% neurocranium, ribs incomplete.
Preservation/ Taphonomy: Surfaces are moderately to severely weathered with lower limb bones surfaces in good condition. Some dark soil covering surfaces.
Age: 19 (+/- 1) years, *Adolescent*
Sex: Male
Macroscopic Lesion Summary:
- exaggerated acute angle of multiple upper to middle left ribs (right missing).
- unilateral medial bending of the left fibula, there is slight bilateral lateral bending of the anterior crest of the tibiae
- discrete remodelled deposit of new bone and cortical porosity on the posterior left zygomatic bone (right zygomatic bone missing)
- bilateral symmetrical discrete mixed active and remodelled deposit of new bone and cortical porosity on the posterior maxillae

Radiographic Lesion Summary:
No radiographs taken
Differential Diagnosis Outcome:

Probable Residual Rickets
Possible Scurvy

Skeletal ID: AT-747

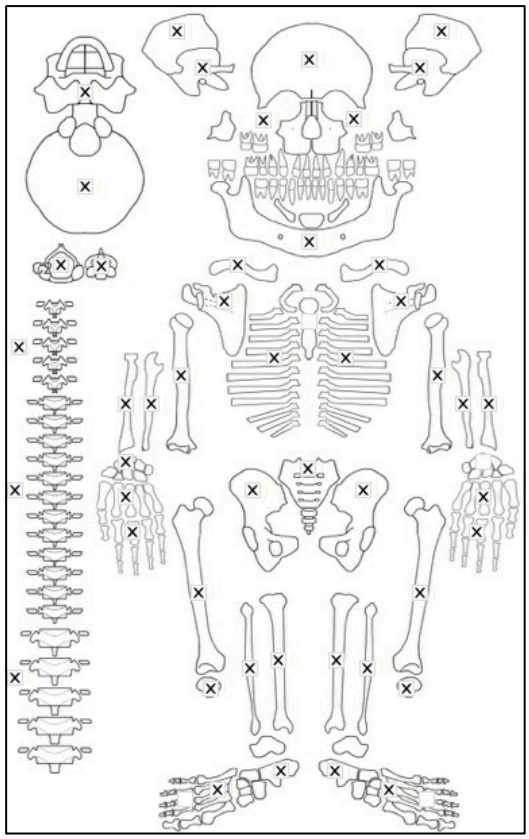

Completeness: Complete (>75%). 92% long bones, 36% hands and feet, 83% vertebrae, 0% neurocranium, ribs near complete.
Preservation/ Taphonomy: Surfaces are mostly in good condition except for spine and scapula where there is severe damage to the cortical surfaces and trabecular bone is exposed, damage to some of the trabecular bone in the bone end. Distal 2/3rds of left fibula, shaft of right radius only. distal epiphyses of ulnae and proximal epiphysis of right fibula is missing Partial damage to the proximal epiphysis of the humeri.
Age: 20-29, *Young Adult*
Sex: Male
Macroscopic Lesion Summary:
- bilateral remodelling mild cribra orbitalia
- unilateral new bone and cortical porosity superior to the zygomatic arch on the left temporal
- bilateral symmetrical discrete cortical porosity on the posterior maxillae

Radiographic Lesion Summary:
No radiographs taken
Differential Diagnosis Outcome:
Possible Scurvy

Skeletal ID: AT-545

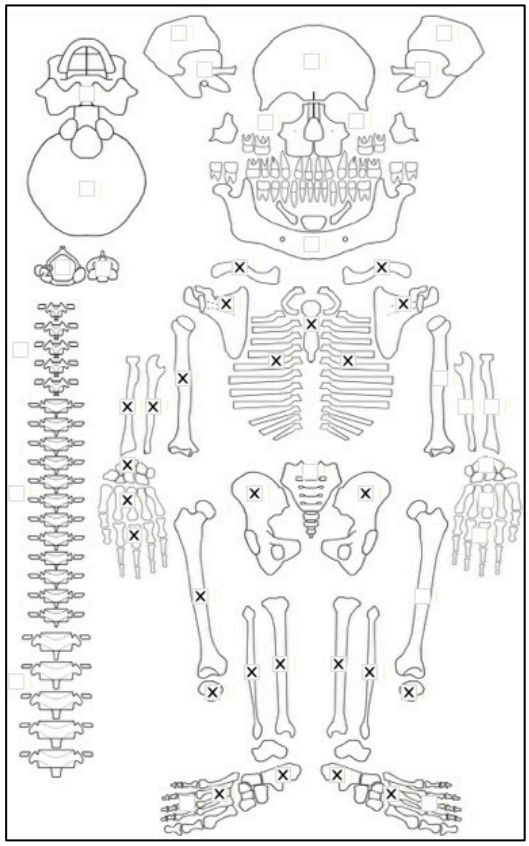

Completeness: Near Complete (66 to 75%). 65% long bones, 37% hands and feet, 4% vertebrae, 0% neurocranium, ribs near complete.
Preservation/ Taphonomy: Surfaces are excellent and intact except proximal epiphysis of right fibula is missing. Anterior distal half of right femur has been taken for sampling.
Age: 50+, *Old Adult*
Sex: Male
Macroscopic Lesion Summary:
No pathology
Radiographic Lesion Summary:
No radiographs taken
Differential Diagnosis Outcome:
No diagnosis

Skeletal ID: AT-465

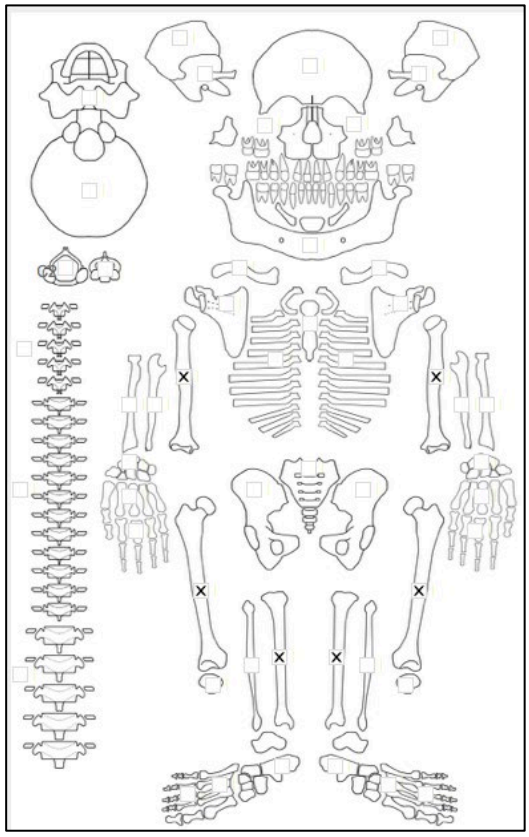

Completeness: Incomplete (33 to 50%). 40% long bones, 0% hands and feet, 0% vertebrae, 0% neurocranium, no ribs.
Preservation/ Taphonomy: Long bones only- proximal epiphysis of left humerus and right tibia, distal epiphysis of femora, and both epiphyses of left tibia are missing. Surfaces are excellent and clean.
Age: *Adult*
Sex: Indeterminate
Macroscopic Lesion Summary:
- remodelled discrete deposit of new bone, appears haematoma like on the proximal lateral third of the left femur (right side missing)
Radiographic Lesion Summary:
No radiographs taken
Differential Diagnosis Outcome:
No diagnosis

Skeletal ID: AT-435

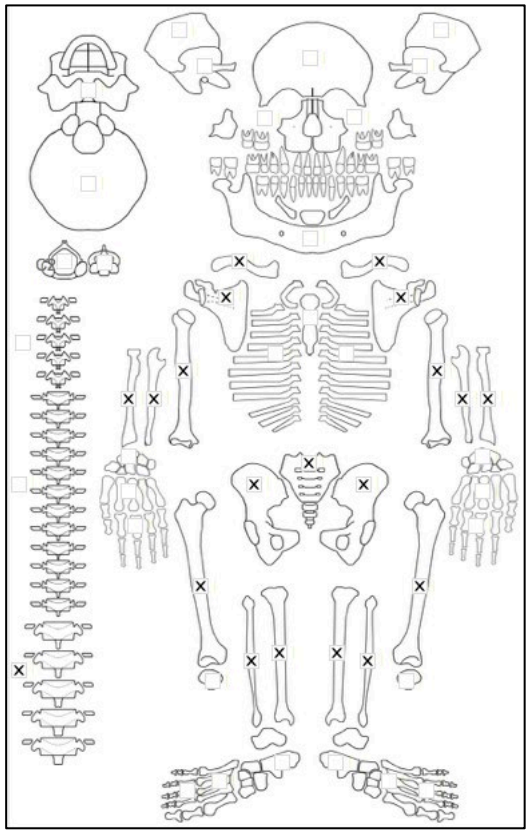

Completeness: Partially Complete (50 to 66%). 100% long bones, 0% hands and feet, 21% vertebrae, 0% neurocranium, no ribs.
Preservation/ Taphonomy: Surfaces are clean and in excellent condition. Anterior distal half of the right femur was taken for sampling.
Age: 30-39, *Middle Aged Adult*
Sex: Male
Macroscopic Lesion Summary:
- discrete poorly mineralised new bone on the posterior neck of the left humerus and bilaterally/ symmetrically lateral to the tibial tuberosities, and the medial distal shaft of the right fibula
Radiographic Lesion Summary:
No radiographs taken
Differential Diagnosis Outcome:
No diagnosis

Skeletal ID: AT-844a

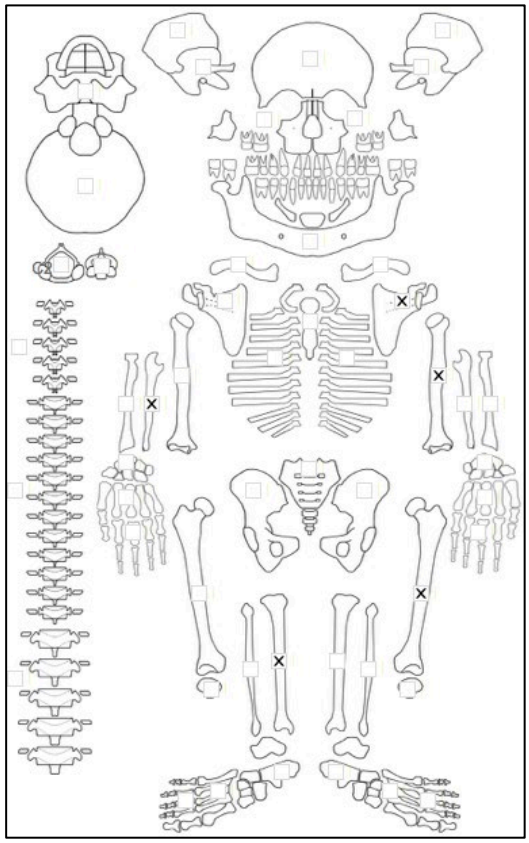

Completeness: Incomplete (33 to 50%). 33% long bones, 0% hands and feet, 0% vertebrae, 0% neurocranium.
Preservation/ Taphonomy: Surfaces are in good condition with damage to the metaphyseal plates.
Age: 35 foetal weeks (+/- 1 week), *Infant*
Sex: Indeterminate
Macroscopic Lesion Summary:
- diffuse active new bone across the anterior, medial and lateral shaft and distal metaphysis of the left humerus (right missing). The new bone is most active and concentrated around the medial foramen.
- diffuse active new bone across the anterior shaft of the left femur (right side missing).
- diffuse active new bone across the medial shaft of the right ulna (left side missing).
- diffuse active new bone across the anterior and medial shaft of the right tibia (left side missing).
discrete deposit of active new bone on the supraspinous fossa of the left scapula (right missing).
Radiographic Lesion Summary:
- radiolucency of the long bone ends
Differential Diagnosis Outcome:
Possible Scurvy

Skeletal ID: AT-844b

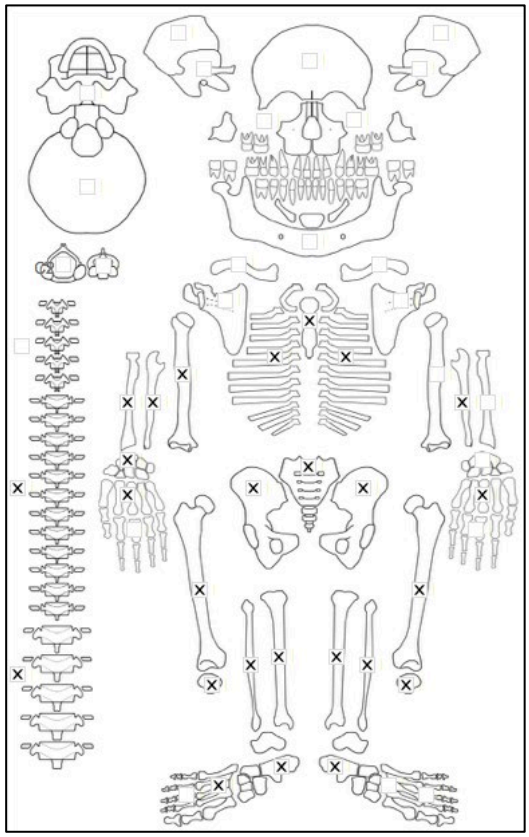

Completeness: Near Complete (50 to 66%). 83% long bones, 27% hands and feet, 33% vertebrae, 0% neurocranium, ribs incomplete.
Preservation/ Taphonomy: All preserved bones are clean and in excellent condition.
Age: 16 (+/- 1) years, *Adolescent*
Sex: Female
Macroscopic Lesion Summary:
- bilateral genu valgum (knocked knees) of the femora. The left side is slight whereas the right femur is more severe in medial angulation. There is associated slight antero-medial shaft bending
Radiographic Lesion Summary:
- vertebrae appear normal.
Differential Diagnosis Outcome:
Possible Osteomalacia

Skeletal ID: AT-441

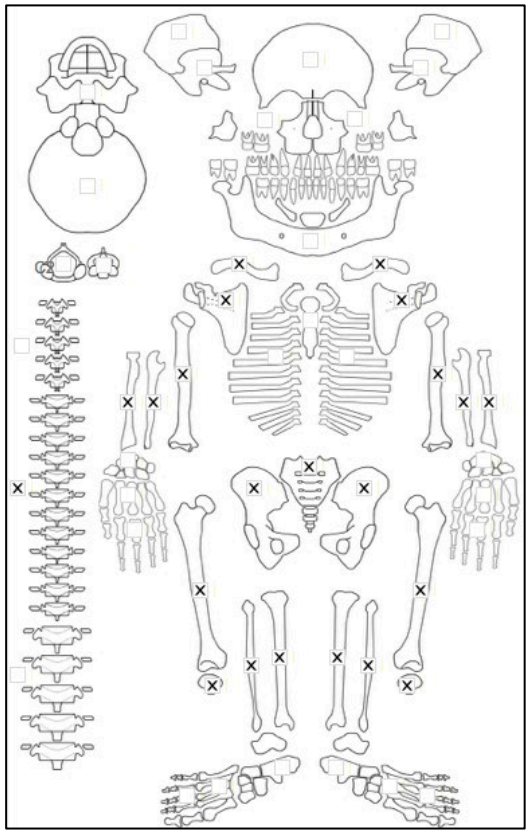

Completeness: Near Complete (66 to 75%). 100% long bones, 0% hands and feet, 29% vertebrae, 0% neurocranium, no ribs.
Preservation/ Taphonomy: Surfaces are excellent and all preserved bones are intact surfaces are excellent and all preserved bones are intact. Anterior distal half of left femur is missing.
Age: 20-29, *Young Adult*
Sex: Female
Macroscopic Lesion Summary:
- bilateral symmetrical deposit of poorly mineralised bone on the medial neck of the humeri, and the posterior distal metaphyses of the femora
- aplasia of the left ala of the S1- possibly a genetic trait
Radiographic Lesion Summary:
- codfish appearance on one vertebra. Horizontal trabecular structure intact (no clear osteopenia)
Differential Diagnosis Outcome:
No diagnosis

Skeletal ID: AT-459

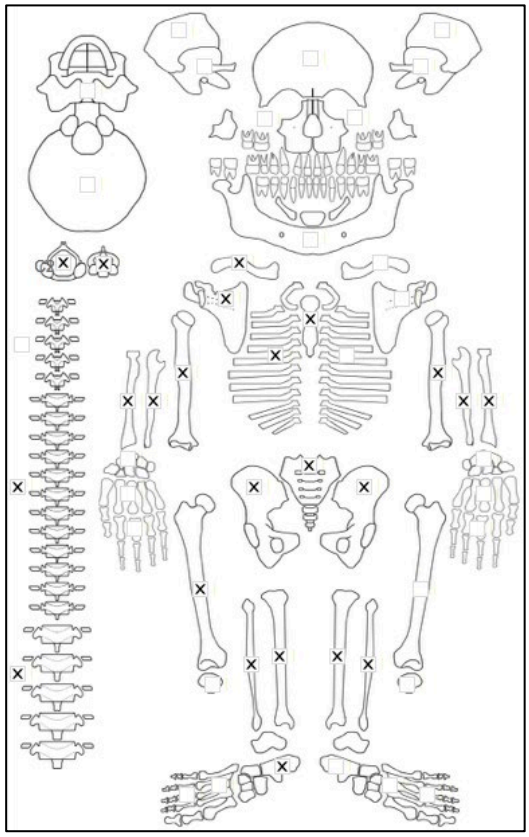

Completeness: Near Complete (60 to 75%). 93% long bones, 5% hands and feet, 50% vertebrae, 0% neurocranium, ribs incomplete.
Preservation/ Taphonomy: Surfaces are in excellent condition and preserved bones are intact except for right scapula which has the blade missing. Intrusive hand and feet bones from a larger and older individual- was easily separated. This individual was not recorded.
Age: 20-29, *Young Adult*
Sex: Female
Macroscopic Lesion Summary:
- unilateral small discrete deposit of remodelled new bone on the proximal medial shaft of the right fibula
Radiographic Lesion Summary:
No radiographs taken
Differential Diagnosis Outcome:
No diagnosis

Skeletal ID: AT-587

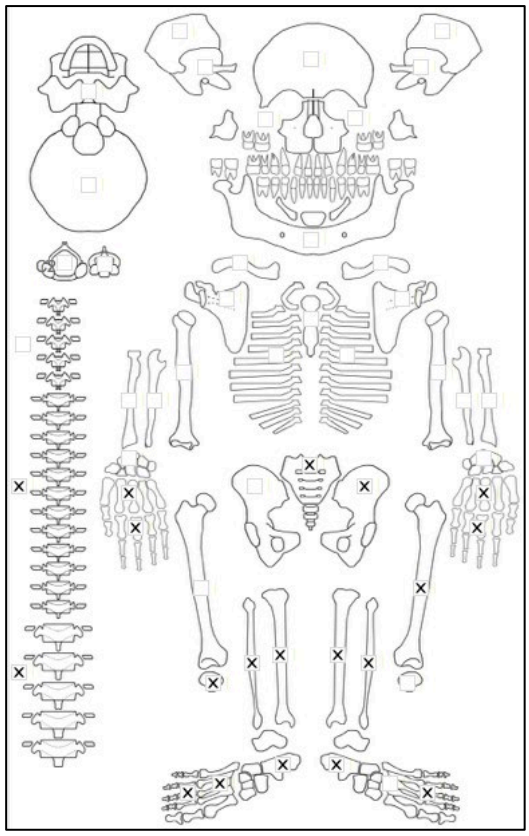

Completeness: Partially Complete (50 to 66%). 38% long bones, 44% hands and feet, 54% vertebrae, 0% neurocranium, no ribs.
Preservation/ Taphonomy: Surfaces of long bones are moderately damaged, pelvis has severe weathering, remaining axial skeleton is intact. Some damage to trabecular ends of the hands and feet with moderate to severe damages of the surfaces of metacarpals, metatarsals and phalanges.
Age: 50+, *Old Adult*
Sex: Male
Macroscopic Lesion Summary:
No pathology
Radiographic Lesion Summary:
No radiographs taken
Differential Diagnosis Outcome:
No diagnosis

Skeletal ID: AT-179

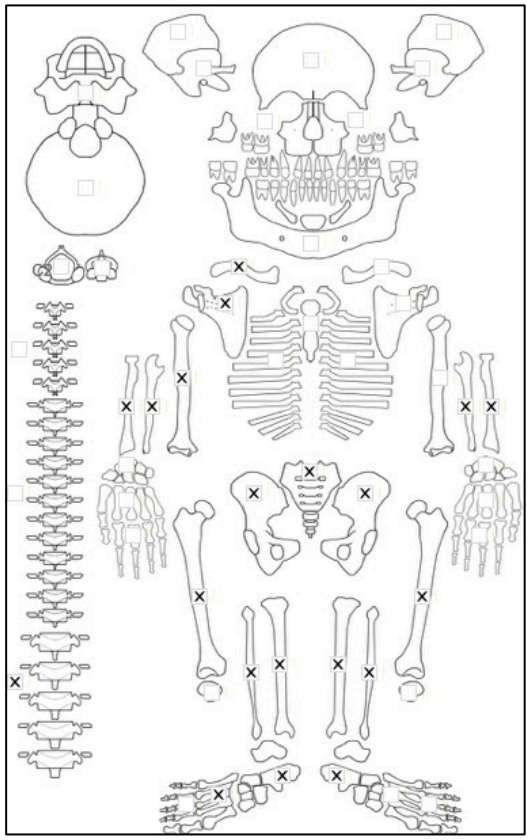

Completeness: Partially Complete (50 to 66%). 78% long bones, 11% hands and feet, 25% vertebrae, 0% neurocranium, no ribs.
Preservation/ Taphonomy: Surfaces are moderately damaged by root etching. Edges of bones are broken. Only epiphyses of femora, left radius and right humerus, distal epiphyses of fibulae and tibiae, proximal epiphyses of ulna are present.
Age: 50+, *Old Adult*
Sex: Female
Macroscopic Lesion Summary:
No pathology
Radiographic Lesion Summary:
No radiographs taken
Differential Diagnosis Outcome:
No diagnosis

Skeletal ID: AT-437

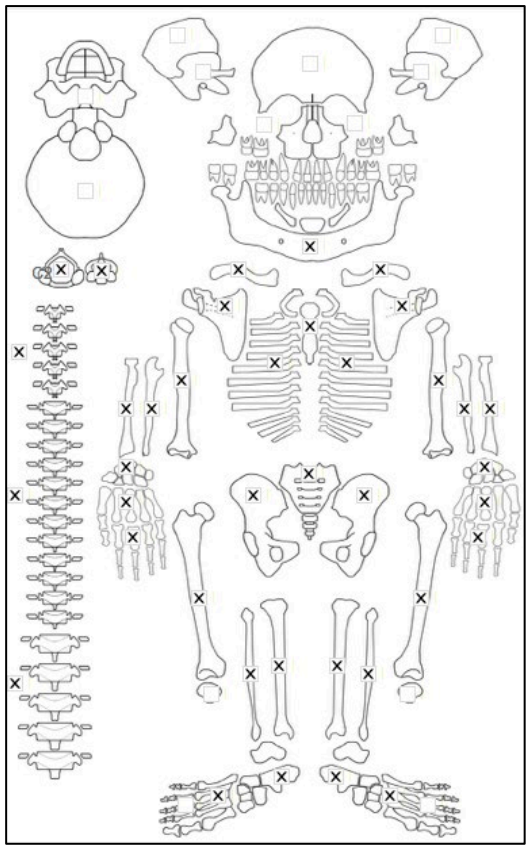

Completeness: Near Complete (66 to 75%). 100% long bones, 52% hands and feet, 100% vertebrae, 0% neurocranium, ribs complete.
Preservation/ Taphonomy: Surfaces are clean, intact and in excellent condition. Anterior middle third of left femur taken for sampling.
Age: 20-29, *Young Adult*
Sex: Male
Macroscopic Lesion Summary:
- bilateral symmetrical remodelled new bone with cortical porosity from the alveolar margin to the incisive foramina and incisive fossae on the mandible
- discrete remodelled new bone on the posterior mandibular body extending from the alveolar margin at the incisors to the mental spines, his new bone extends to bilaterally and inferiorly to the mylohyoid lines where there is slight vascular impressions
- bilateral and symmetrical abnormal 'V' shaped cupping of the medial (sternal) ends of the clavicle
- unilateral abnormal posterior bending of the superior third region of the right scapula compared to the left
- bilateral and symmetrical deposits of new bone which appear haematoma like on the lateral proximal to middle third shafts of the femora
- small discrete remodelled plaque of new bone on the anterior midshaft of the right fibula
Radiographic Lesion Summary:
- biconcavity and loss of height of one of the radiographed vertebrae, but all three radiographed vertebrae have clear osteopenia of the trabeculae and cortical margins.
Differential Diagnosis Outcome:
Probable Osteomalacia
Possible Scurvy

Skeletal ID: AT-658

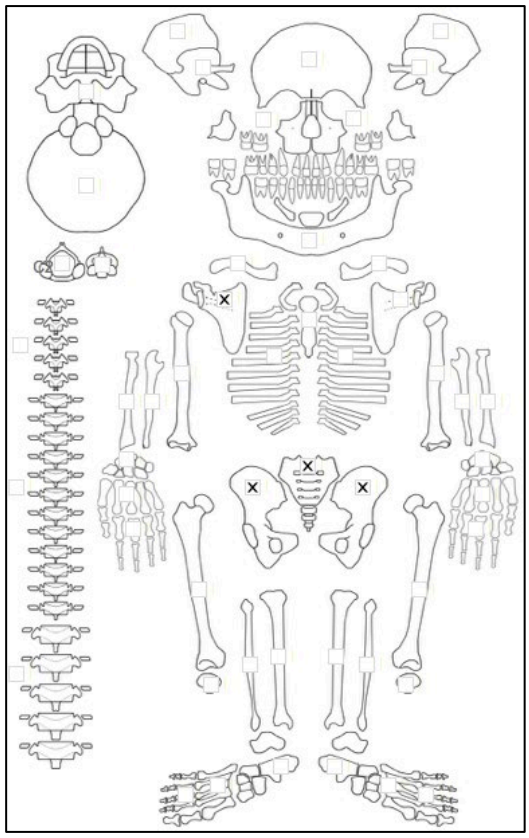

Completeness: Fragmented. 0% long bones, 0% vertebrae, 0% hands and feet, 0% neurocranium, no ribs.
Preservation/ Taphonomy: There are remains of 1 robust adult, 1 gracile adult and 1 juvenile. Only the nonadult was recorded as their remains could be successfully separated.
Age: 15.5 (+/- 6 months) years
Sex: Male
Macroscopic Lesion Summary:
No pathology
Radiographic Lesion Summary:
No radiographs taken
Differential Diagnosis Outcome:
No diagnosis

Skeletal ID: AT-657

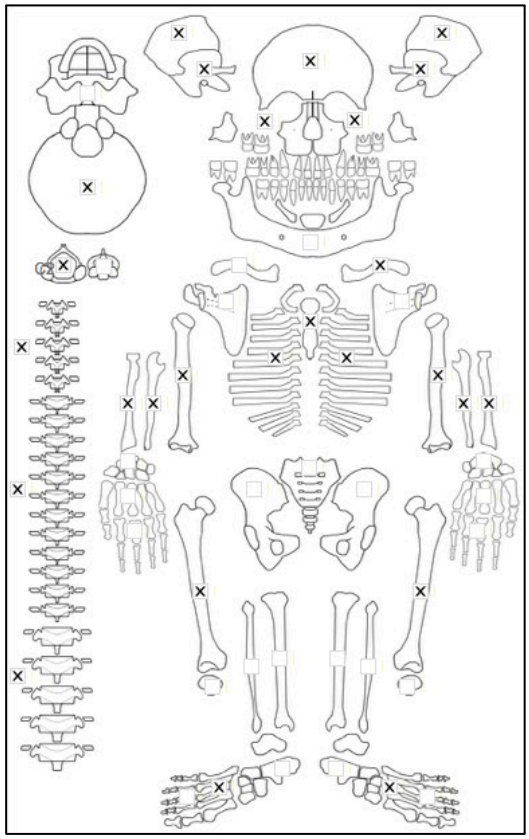

Completeness: Near Complete (66 to 75%). 55% long bones, 19% hands and feet, 92% vertebrae, 75% neurocranium, ribs near complete.
Preservation/ Taphonomy: Surfaces are in excellent condition but there is some PM breakage to trabecular heavy areas.
Age: *Adult*
Sex: Indeterminate
Macroscopic Lesion Summary:
- remodelled vascular impressions in remodelled new bone on the proximal third shaft directly lateral to the linea aspera of the femora
Radiographic Lesion Summary:
No radiographs taken
Differential Diagnosis Outcome:
No diagnosis

Skeletal ID: AT-261

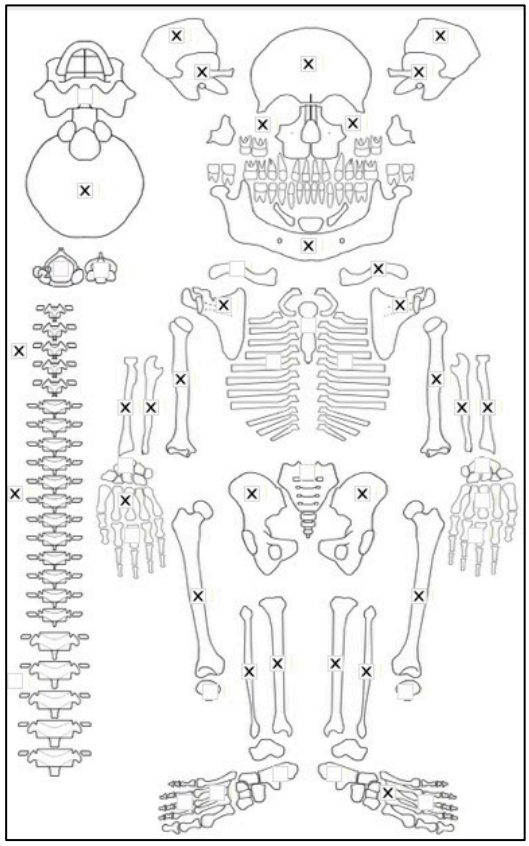

Completeness: Near Complete (66 to 75%). 82% long bones, 7% hands and feet, 25% vertebrae, 100% neurocranium, ribs fragment.
Preservation/ Taphonomy: Surfaces are in good condition with damage to bone ends. Preserved vertebrae and os coxae are intact. Scapula bodies missing. Proximal epiphysis of left humerus, right radius and ulna, right fibula and tibiae, distal epiphysis of right femur and both epiphyses of left fibula missing. Only distal half of right humerus is present.
Age: 50+, *Old Adult*
Sex: Female
Macroscopic Lesion Summary:
- unilateral remodelled discrete deposit of new bone on the right oblique line of the mandible
- unilateral remodelling moderate cribra orbitalia of the left orbit

Radiographic Lesion Summary:
No radiographs taken
Differential Diagnosis Outcome:
Anaemia

Skeletal ID: AT-263

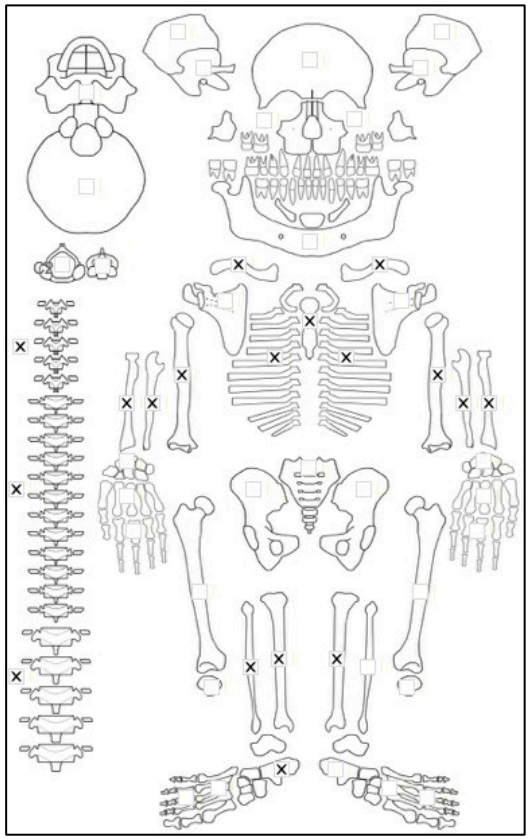

Completeness: Partially Complete (50 to 66%). 70% long bones, 8% hands and feet, 75% vertebrae, 0% neurocranium, ribs near complete.
Preservation/ Taphonomy: All preserved bones are intact, except distal third of right tibia only.
Age: 20-29, *Young Adult*
Sex: Indeterminate
Macroscopic Lesion Summary:
- circular circumscribed lesion on the posterior sternum associated with remodelled new bone. There is postmortem damage, meaning the extent is unknown. However, there is some sclerotic response present. Reminiscent of a case by Orther (3rd edition- page 425). Lesion diameter: 15.06x11.4 mm
- circular circumscribed remodelled lesion on the internal midshaft of a right middle rib. The lesion would have penetrated to the trabeculae. No signs of activity. Lesion diameter: 10.47x7.9mm
- medial angulation of the proximal epiphysis of the left tibia) right missing)
Radiographic Lesion Summary:
- sternal lesions has a clear sclerotic ring
- rib lesions cortex is well remodelled, but there is a focal radiolucent regent underlying the cortex that demonstrates prior to healing the lesion was deeper.
Differential Diagnosis Outcome:
Possible Tuberculosis
Possible Mycosis
Possible Residual Rickets

Skeletal ID: AT-146

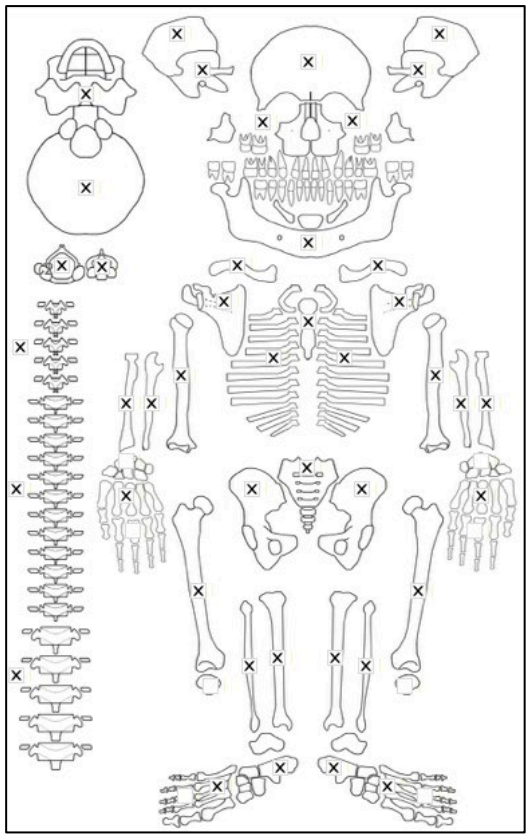

Completeness: Complete (>75%). 100% long bones, 24% hands and feet, 100% vertebrae, 100% neurocranium, ribs complete.
Preservation/ Taphonomy: All preserved surfaces are intact, clean and in excellent condition. Medial middle third of right femur taken for sampling.
Age: 20-29, *Young Adult*
Sex: Male
Macroscopic Lesion Summary:
- bilateral slight medial bending of the tibial shafts with unilateral medial bending of the shaft of the right fibula
- unilateral depression on the medial aspect of the right calcaneus, may be related to trauma
- bilateral coxa vara of the femoral heads
- focal remodelled oval lytic lesion with defined margins on the distal third inferior shaft of a left mid to lower rib. Lesion diameter: 7.93x3.65mm (similar to the depression on the fibulae)
- bilateral symmetrical deep remodelled depressions on the posterior proximal third shafts of the fibulae
- unilateral active moderate cribra orbitalia of the left orbit
- remodelled porotic hyperostosis of the frontal, parietals medial to the temporal line and occipital planum
Radiographic Lesion Summary:
- very thick cortex of the femur, tibiae and left fibula.
- focal lesion in the right femoral neck has a sclerotic margin- suggesting remodelled. approx. 10mm in size
- clear osteopenia with horizontal trabeculae missing and thickened vertical trabeculae, codfish appearance and loss of body height of multiple vertebrae
- multiple stress lines in the long bones with coarsened trabeculae
Differential Diagnosis Outcome:
Probable Residual Rickets
Probable Osteomalacia
Anaemia

Skeletal ID: AT-566

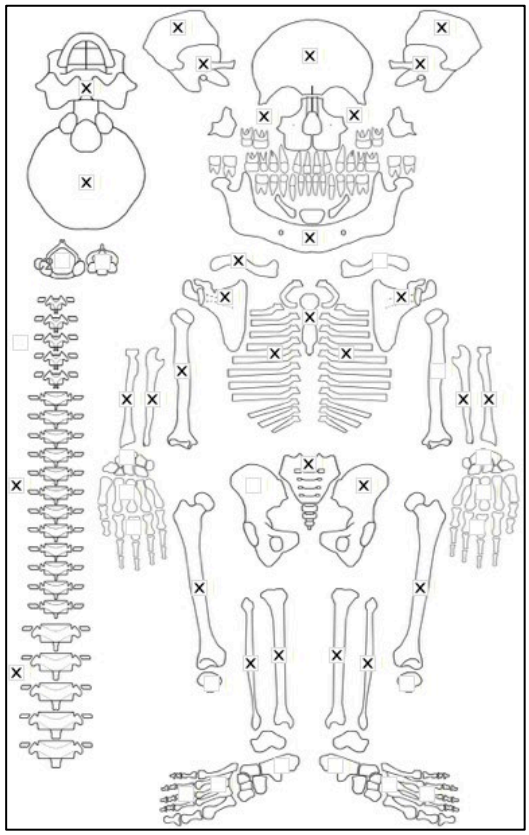

Completeness: Complete (>75%). 92% long bones, 0% hands and feet, 58% vertebrae, 100% neurocranium, ribs complete.
Preservation/ Taphonomy: Some surfaces covered in some dark dust but the surfaces are still visible. All surfaces in excellent condition and all preserved bones are intact.
Age: 20-29, *Young Adult*
Sex: Female
Macroscopic Lesion Summary:
- bilateral genu valgum of the femora
- small deposit of poorly mineralised new bone on the medial neck of the right humerus and unilaterally on the distal posterior metaphysis of the right femur
- bilateral remodelled cortical porosity on either side of the nasals and anterior maxillae- there is some deformation to the nose shape
- bilateral remodelling mild cribra orbitalia
- diffuse active new bone on the endocranium of the frontal and parallel to the sagittal crest

Radiographic Lesion Summary:
- Osteopenia of the vertebrae

Differential Diagnosis Outcome:
Probable Osteomalacia

Skeletal ID: AT-584

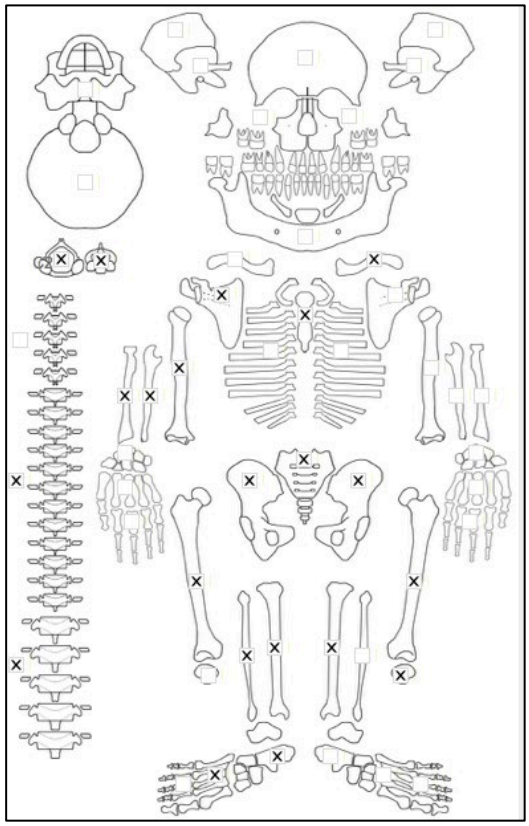

Completeness: Partially Complete (50 to 66%). 68% long bones, 7% hands and feet, 71% vertebrae, 0% neurocranium, ribs incomplete.
Preservation/ Taphonomy: Surfaces of long bones are moderately to severely weathered, no right scapula body, left scapula represented by coracoid only, proximal epiphysis of right tibia and right fibula are missing. Distal half of left humerus is missing.
Age: 40-49, *Middle Aged Adult*
Sex: Male
Macroscopic Lesion Summary:
No pathology
Radiographic Lesion Summary:
No radiographs taken
Differential Diagnosis Outcome:
No diagnosis

Skeletal ID: AT-297

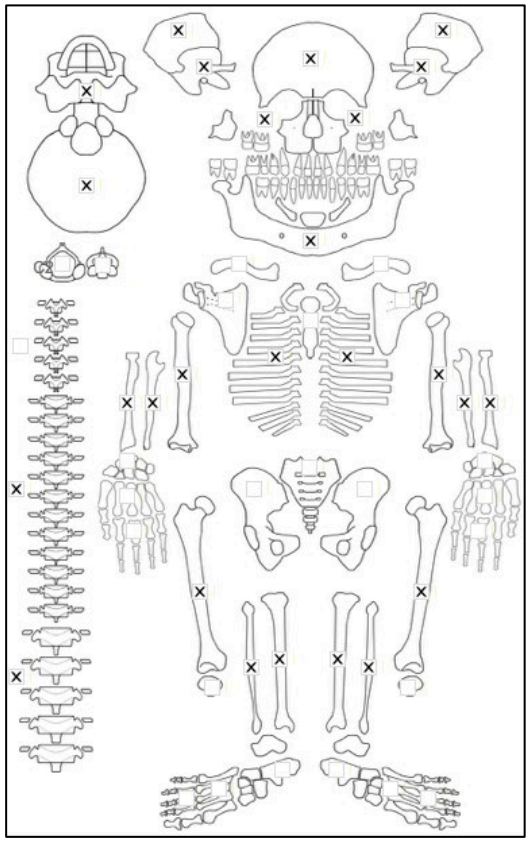

Completeness: Near Complete (66 to 75%).100% long bones, 0% hands and feet, 50% vertebrae, 100% neurocranium, near complete ribs.
Preservation/ Taphonomy: All preserved surfaces are intact, clean and in excellent condition. Some copper (bronze) staining. Anterior middle third of right femur taken for sampling.
Age: *Adult*
Sex: Indeterminate
Macroscopic Lesion Summary:
- unilateral discrete deposit of remodelled bone on the antero-medial proximal shaft of the right ulna
- unilateral discrete deposit of remodelled bone on the medial proximal shaft of the right tibia. Margins are not visible but bone is raised compared to the left side.
- diffuse active new bone across the endocranium of the frontal, extent can't be determined due to soil coverage. Could not be photographed due to position in the endocranium

Radiographic Lesion Summary:
No radiographs taken
Differential Diagnosis Outcome:
No diagnosis

Skeletal ID: AT-260

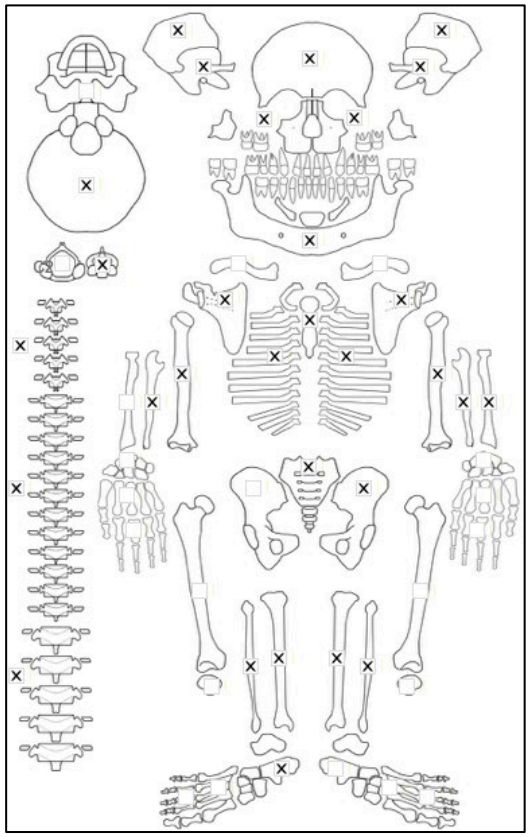

Completeness: Near Complete (66 to 75%). 73% long bones, 3% hands and feet, 54% vertebrae, 100% neurocranium, ribs near complete.
Preservation/ Taphonomy: surfaces present are intact and excellent except for some PM breakage of the ribs and left scapula body is partially damaged.
Age: 30-39, *Young Adult*
Sex: Female
Macroscopic Lesion Summary:
- unilateral discrete deposit of remodelled bone on the posterior distal third shaft of the left humerus
- bilateral symmetric discrete cortical porosity on the posterior maxillae and zygomatic bones, no apparent associated new bone
- large square shaped head
No radiographs taken
Differential Diagnosis Outcome:
No diagnosis

Skeletal ID: AT-575

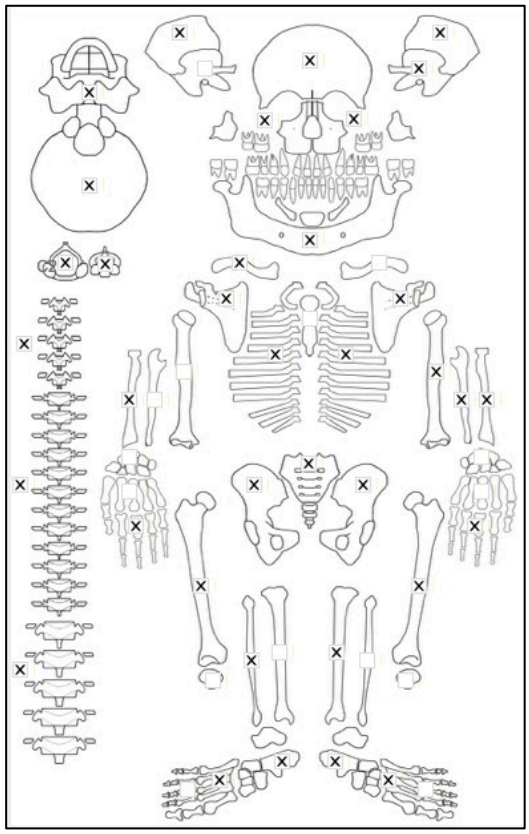

Completeness: Complete (>75%). 67% long bones, 24% hands and feet, 83% vertebrae, 88% neurocranium, ribs complete.
Preservation/ Taphonomy: Surfaces are in excellent condition but there is many PM breaks. proximal third of right fibula is missing, partial present of distal end of left femur, distal end of left ulna missing, and right humerus is only represented by the distal end.
Age: 4 (+/-1) years
Sex: Indeterminate
Macroscopic Lesion Summary:
- bilateral symmetrical discrete active new bone and cortical porosity on the infraspinous and supraspinous fossae of the scapula
- bilateral symmetrical discrete active new bone and cortical porosity on the inferior pars laterali extending from the hypoglossal canal and the pars basilaris. There are vascular impressions on the pars laterali
- abnormal deep endochondral porosity exceeding 10mm from the metaphyseal plate on the distal femora, proximal left tibia (right missing) and distal right fibula (left missing).
- mixed active and remodelled discrete deposit of new bone on the anterior distal third of the right femur (left is missing)
- diffuse active new bone across the medial aspect of the left tibia (right missing)
active new bone on the right lesser wing of sphenoid
- diffuse active new bone on the endocranium of the parietals, frontal, left temporal (right missing) and occipital, and sphenoid
- discrete patch of active new bone on the posterior inferior right corner of occipital squama
- discrete patch of mixed active and remodelled new bone and cortical porosity directly anterior to the squamosal sutures of the parietals
- active new bone on the lesser wings of sphenoid, and with new bone and cortical porosity on the lateral left greater wing and pterygoid region and fossa (right side missing), associated with mixed active and remodelled new bone on the left temporal squama (right missing)
- bilateral symmetrical discrete deposits of mixed active and remodelled new bone and cortical porosity on the superior orbits, with active new bone and porosity on the zygomatic processes, and mixed new bone and porosity superior around the region of the supraorbital ridge

- bilateral symmetrical discrete deposits of active new bone and cortical porosity on the anterior and posterior maxillae (with vascular impressions), palatal surfaces of the maxillae, in the maxillary sinuses (possible sinus infection), medial margin of anterior zygomatics (extending from new bone on the maxillae which is focused around the infraorbital foramen), infraorbital surfaces (including maxillae and zygomatic surfaces with vascular impressions), posterior palatines and zygomatics (continuation of new bone on posterior maxillae),
- bilateral symmetrical discrete deposits of active new bone and cortical porosity on the incisive fossae, around the oblique lines, on the lateral superior margin of the rami, medial coronoid process, inferior to the mylohyoid lines (with vascular impressions), on the inferior body and around the mental spines.

Radiographic Lesion Summary:
- No white line of Fraenkel or scurvy lines, but multiple intermittent stress lines of the metaphyseal ends of all long bones
- coarsened trabeculae and osteopenia (not ground glass in appearance)
- cortices of the long bones are thin

Differential Diagnosis Outcome:
Probable Scurvy

Skeletal ID: AT-337

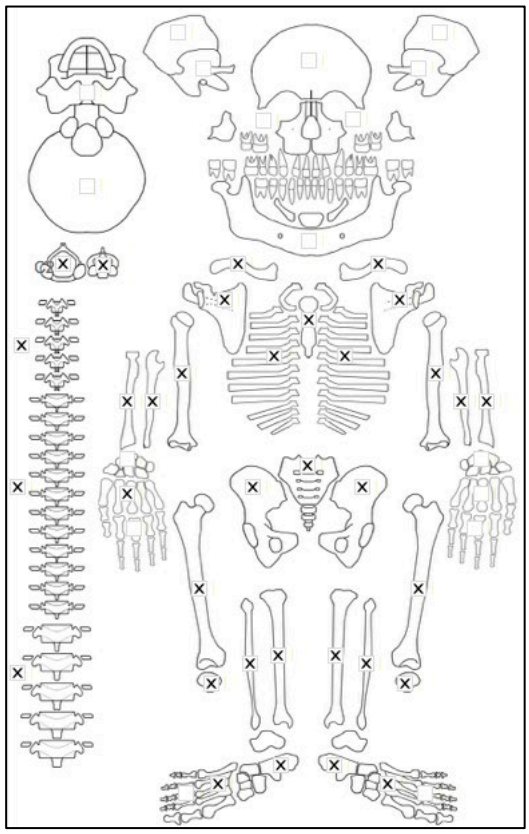

Completeness: Near Complete (66 to 75%). 97% long bones, 28% hands and feet, 96% vertebrae, 0% neurocranium, ribs complete.
Preservation/ Taphonomy: surfaces are intact and in excellent condition except most of scapula blades are missing, some PM breakage of rib ends but all present and proximal epiphyses of fibulae are missing. Anterior middle third of right femur has been taken for sampling.
Age: 40-49, *Middle Aged*
Sex: Male
Macroscopic Lesion Summary:
- V shaped cupping, invagination of the medial sternal ends of the clavicles
- bilateral increased 'S' shaped curve of the scapula spines
- there appears to be a remodelled unilateral pseudo fracture inferior to the glenoid fossa of the left scapula (identified on photographs. The picture is blurry, but the callus is still clear)

Radiographic Lesion Summary:

Radiographs not taken
Differential Diagnosis Outcome:
Probable Osteomalacia

Skeletal ID: AT-30

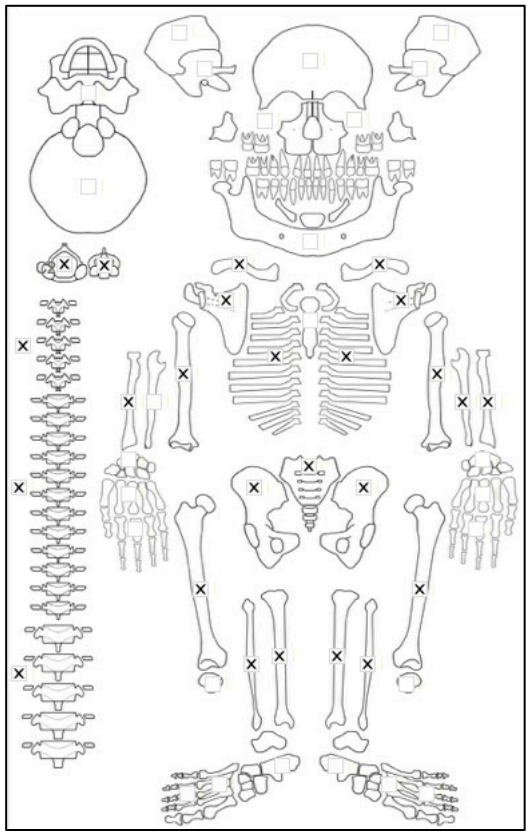

Completeness: Near Complete (66 to 75%). 92% long bones, 0% hands and feet, 100% vertebrae, 0% neurocranium, ribs near complete.
Preservation/ Taphonomy: All surfaces are in excellent condition, there is a thin film on the left femur which appears to be desiccated periosteum. Anterior middle third of left femur has been taken for sampling.
Age: 20-29, *Young Adult*
Sex: Male
Macroscopic Lesion Summary:
bilateral thick remodelled cortical expansion of the sternal ends of the clavicles
- Unilateral very thick mixed active and remodelled new bone with cortical expansion across all surfaces of the all the 9 right preserved ribs (ribs 2 to 10). The new bone is more active on the internal aspect, but the bone is expanded across all aspects. There is no sign of any new bone to the left ribs. There is no associated pathology on the thoracic spine.
- expanded foramina on L1 and L2
- mostly active new bone on the medial olecranon of the left ulna
- bilateral mixed active and diffuse new bone on the posterior femur, the right femur has new bone continuing on medial, lateral and partially anteriorly. The left side has been sampled and therefore much of the surface is missing- extent cannot be determined. Lesion is more active around the linea aspera
- bilateral patches of remodelled bone on the posterior proximal third tibia and anterior proximal third fibula shafts.
Radiographic Lesion Summary:
- the enlarged clavicles appear to be both thick periosteal appositions, particularly on the anterior aspect, but also enlarged trabecular region. the enlargement is bilateral and symmetrical.
- the periosteal reactions on the internal right ribs are observed as very thick on the radiographs. The underlying cortex of all of the ribs are thin and in places radiolucent not very distinguishable on the radiographs from the internal trabeculae.
Differential Diagnosis Outcome:

No diagnosis

Skeletal ID: AT-35

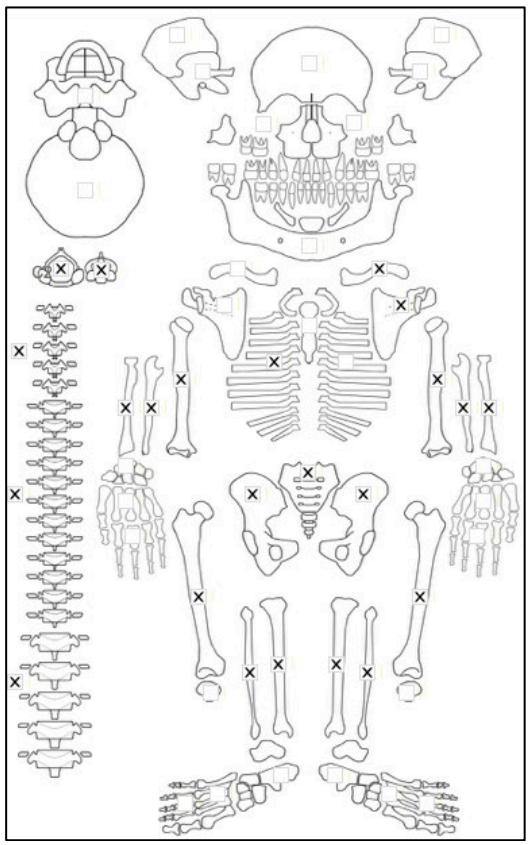

Completeness: Near Complete (66 to 75%). 100% long bones, 3% hands and feet, 92% vertebrae, 0% neurocranium, ribs incomplete.
Preservation/ Taphonomy: Surfaces are clean and in excellent condition except for moderate to severe weathering of the right forelimb shafts, all preserved bones intact.
Age: 20-29, *Young Adult*
Sex: Female
Macroscopic Lesion Summary:
- bilateral symmetrical poorly mineralised bone on the medial humeral necks
- bilateral symmetrical poorly mineralised bone on the medial, posterior and lateral metaphyses of the femora
- there is also a bilateral symmetrical remodelled deposit of new bone in the shape of a haematoma on the medial proximal shafts of the femora
- bilateral symmetrical poorly mineralised bone on medial to the tibial tuberosities on the proximal tibiae
- bilateral moderate medial bending deformities of the tibial shafts
Radiographic Lesion Summary:
- slight codfish sign of multiple vertebrae (biconcavity)
Differential Diagnosis Outcome:
Possible Residual Rickets
Possible Osteomalacia
Possible Scurvy

Skeletal ID: AT-683

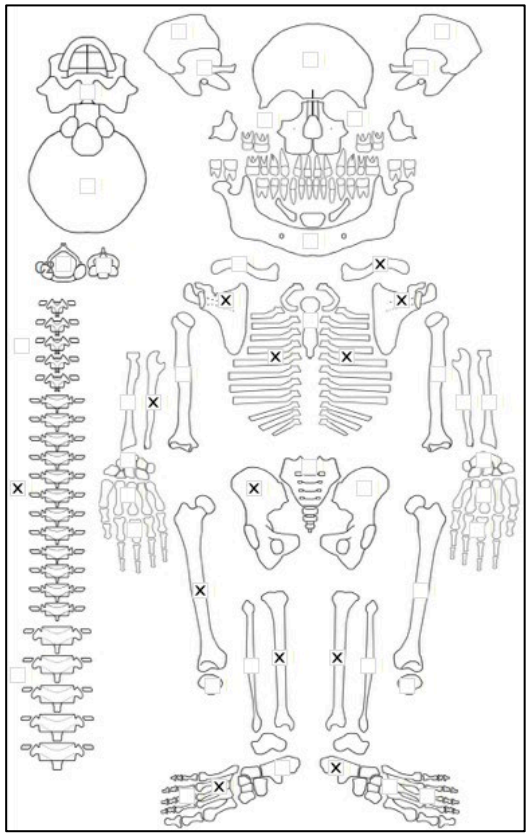

Completeness: Incomplete (33 to 50%). 33% long bones, 6% hands and feet, 33% vertebrae, 0% neurocranium, ribs incomplete.
Preservation/ Taphonomy: Long bones have severe weathering. Only proximal epiphysis of left tibia, distal of right tibia and both of femur and ulna have survived. Right ulna shaft is split and warped.
Age: 14.5 (+/- 5) years
Sex: Indeterminate
Macroscopic Lesion Summary:
- unilateral 'S' shaped bucking of the medial border of the right scapula
Radiographic Lesion Summary:
No radiographs taken
Differential Diagnosis Outcome:
Possible Osteomalacia

Skeletal ID: AT-546B

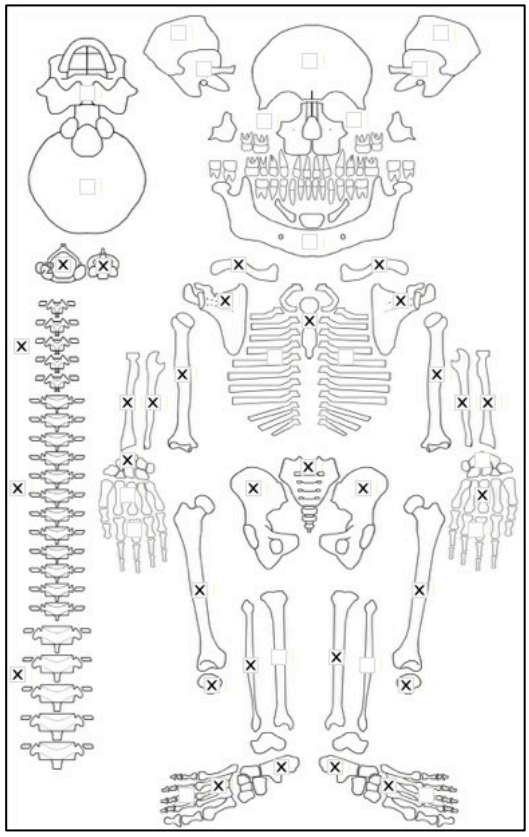

Completeness: Near Complete (66 to 75%). 82% long bones, 24% hands and feet, 100% vertebrae, 0% neurocranium, ribs fragmented.
Preservation/ Taphonomy: Surfaces are in good condition all bone intact except ribs and partial breakage to the scapula bodies but all of the surface is present. Proximal epiphysis of the right fibula missing.
Age: 40-49, *Middle Aged Adult*
Sex: Male
Macroscopic Lesion Summary:
- large node of remodelled new bone on the middle anterior crest and medial aspect of the left tibia (right tibia missing).
Radiographic Lesion Summary:
- Cortical expansion of the medial and lateral margins of the tibia. Consistent with osteoid osteoma. (not infectious origin). No other bones affected.
Differential Diagnosis Outcome:
No diagnosis

Skeletal ID: AT-365

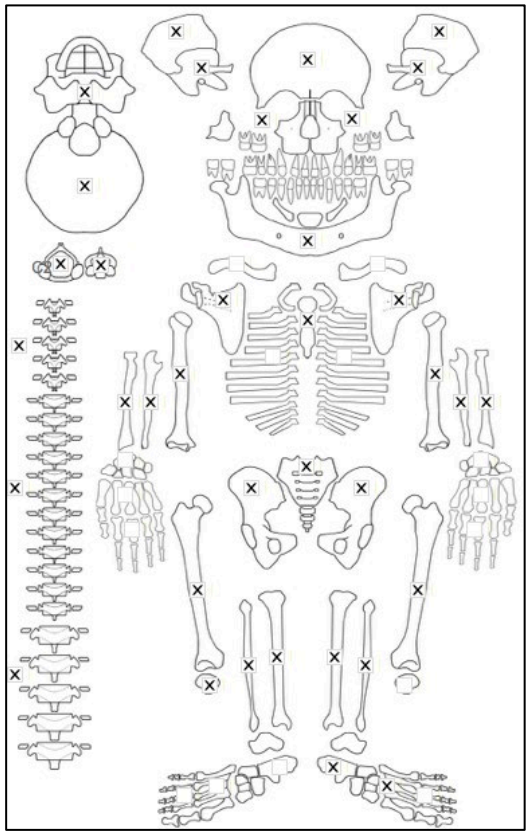

Completeness: Complete (>75%). 90% long bones, 8% hands and feet, 96% vertebrae, 100% neurocranium, ribs incomplete.
Preservation/ Taphonomy: Surfaces are in excellent condition except ribs. there is copper staining on the right os coxa and femur. Right femur has middle anterior third taken for sampling.
Age: 19.5 (+/-5) years
Sex: Male
Macroscopic Lesion Summary:
- severe anterior protrusion of the sternum
- lateral straightening of a rib (others are fragmented)
- unilateral lateral bending of the right humeral shaft
- biconcavity of the superior and inferior vertebral bodies of L2-5
- considerable medio-lateral broadening with anterior-posterior thinning of the proximal third shafts of the femora
- Depression of the patellar surfaces and coxa vara of the femoral necks
- bilateral moderate medial bending of the tibial shafts associated with severe medial bending of the fibular shafts
- bilateral and symmetrical mixed active and remodelled new bone and cortical porosity on the lateral margin of the anterior aspect of the zygomatics
- discrete mixed active and remodelled new bone and cortical porosity on the pterygoid region of the right greater wing of sphenoid (left side is damaged)
- discrete bilateral and symmetrical remodelled new bone and cortical porosity with vascular impressions on anterior maxillae extending from the nasals
- bilateral symmetrical remodelled (properly mineralised) pseudofractures of the inferior pubic rami, with bilateral posterior buckling of the pubic symphysis (dislocation) and inferior rami
Radiographic Lesion Summary:
- Clear codfish sign of vertebrae and osteopenia, and loss of height of vertebrae
- thinning trabeculae in distal metaphyses of tibiae
- thickened concave surface of bending deformities in the tibiae and fibulae
- horizontal radioculcent lines (are these hairline stress fractures?)
Differential Diagnosis Outcome:
Probable Rickets

Probable Osteomalacia
Probable Scurvy

Skeletal ID: AT-583b

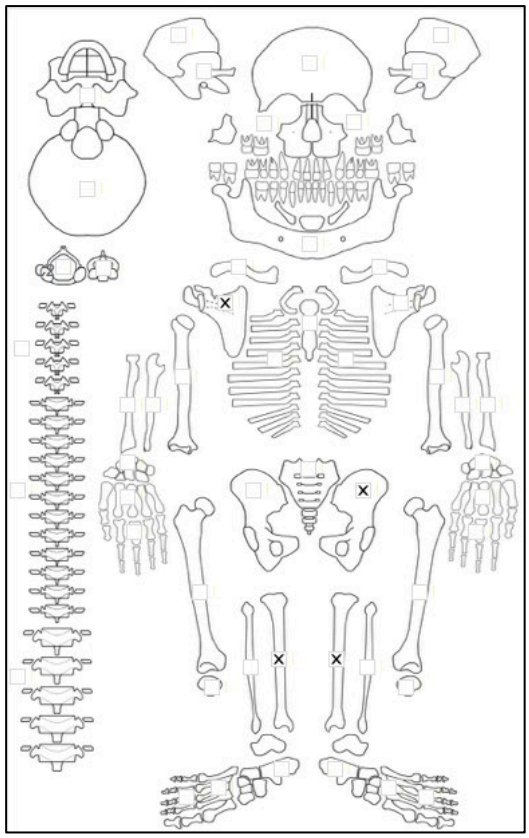

Completeness: Fragmented. 17% long bones, 0% hands and feet, 0% vertebrae, 0% neurocranium, no ribs.
Preservation/ Taphonomy: Multiple commingled individuals, but could sort a portion of the juvenile out. left os coxa right scapula and tibiae only. largest of the 3 juveniles
surface of long bones moderately damaged but metaphyseal plates are present
Age: ~9-10 years, *Child*
Sex: Indeterminate
Macroscopic Lesion Summary:
- abnormal endochondral porosity exceeding 10mm from the proximal metaphyseal plates of the tibiae
- slight cupping of the proximal metaphyseal plates

Radiographic Lesion Summary:
- multiple stress lines and radiodense metaphyseal plate, but this is not associated with a Trummerfeld zone
- cupping of proximal tibia is clear on the radiographs

Differential Diagnosis Outcome:
Possible Rickets
Probable Scurvy

Skeletal ID: AT-583c

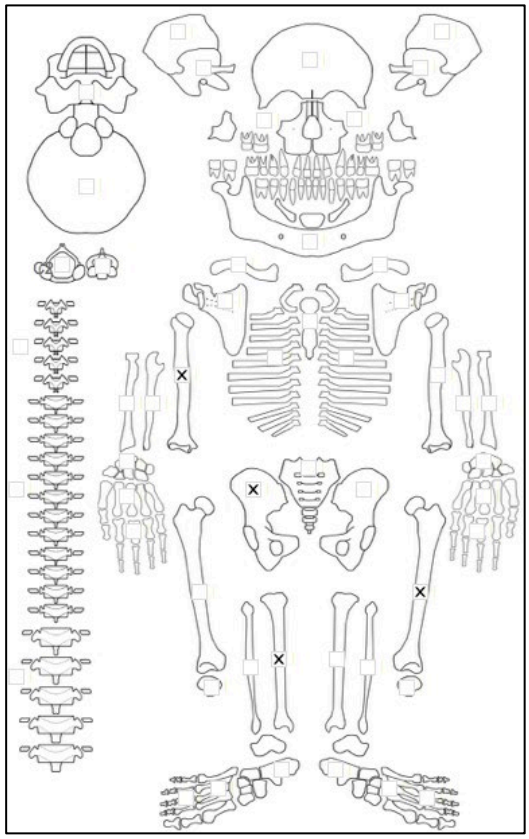

Completeness: Fragmented. 25% long bones, 0% hands and feet, 0% vertebrae, 0% neurocranium, no ribs.
Preservation/ Taphonomy:
Age: ~6-7 years, *Child*
Sex: Indeterminate
Macroscopic Lesion Summary: Multiple commingled individuals, but could sort a portion of the juvenile out. Right os coxa and right tibia and humerus and left femur only. Surface of long bones moderately to severely damaged but metaphyseal plates are present
- abnormal endochondral porosity exceeding 10mm from the proximal metaphyseal plate of the right humerus, proximal and distal plates of the right tibia and the distal plate of the left femur (opposite sides are missing)
- possible Pelkan spur on the lateral aspect of distal tibia
Radiographic Lesion Summary:
- Pelkan spur of the distal tibia present on radiographs (but not within a dense zone of calcification)
- no clear white line of Fraenkel, but metaphyseal region is radiolucent with ground glass osteopenia and coarsened trabeculae (noticeable on the distal humerus)
Differential Diagnosis Outcome:
Probable Scurvy

Skeletal ID: AT-583d

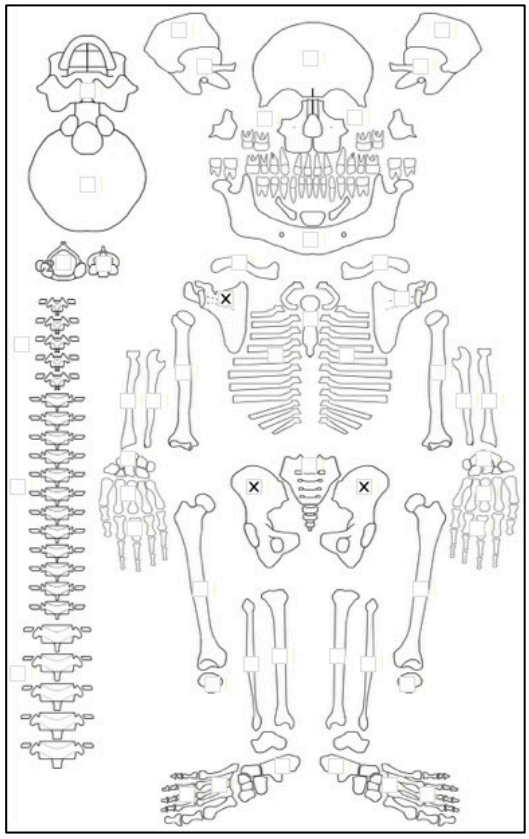

Completeness: Fragmented.
Preservation/ Taphonomy: Os coxae and right scapula only.
Age: <6 years, *Child*
Sex: Indeterminate
Macroscopic Lesion Summary:
- discrete remodelled new bone and cortical porosity on the supraspinous fossa of the right scapula (left missing)
Radiographic Lesion Summary:
No radiograph taken
Differential Diagnosis Outcome:
Possible Scurvy

Skeletal ID: AT-544

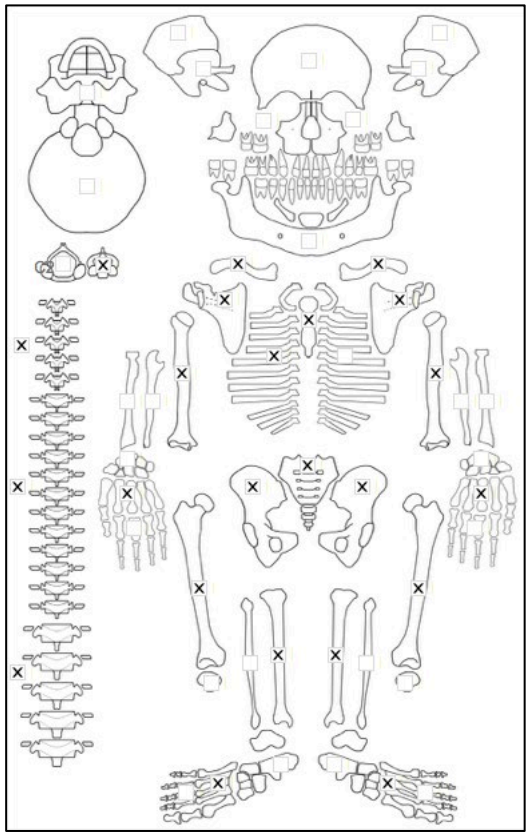

Completeness: Near Complete (66 to 75%). 48% long bones, 20% hands and feet, 75% vertebrae, 0% neurocranium, ribs incomplete.
Preservation/ Taphonomy: Surfaces are in good condition but there is some PM breakage. Partial breakage of scapula. Lower thoracic and lumbar are missing their vertebral bodies. Distal epiphysis of right tibia is missing. Anterior third of left femur taken for sampling.
Age: 30-39, *Middle Aged Adult*
Sex: Male
Macroscopic Lesion Summary:
- complete ankylosis of at least T12-S1 spine and fusion of the S1 to the os coxae. Unknown whether vertebral bodies were affected as they are missing. S1 sacral body does not appear to be ankylosed. Cervical and upper thoracic are unaffected
- bilateral lateral bending of the humeral shafts at the region of the deltoid tuberosities so it may be activity related.
- exaggerated acute angle of a left middle rib (right side missing)

Radiographic Lesion Summary:
No radiographs taken
Differential Diagnosis Outcome:
Possible Rickets

Skeletal ID: AT-350

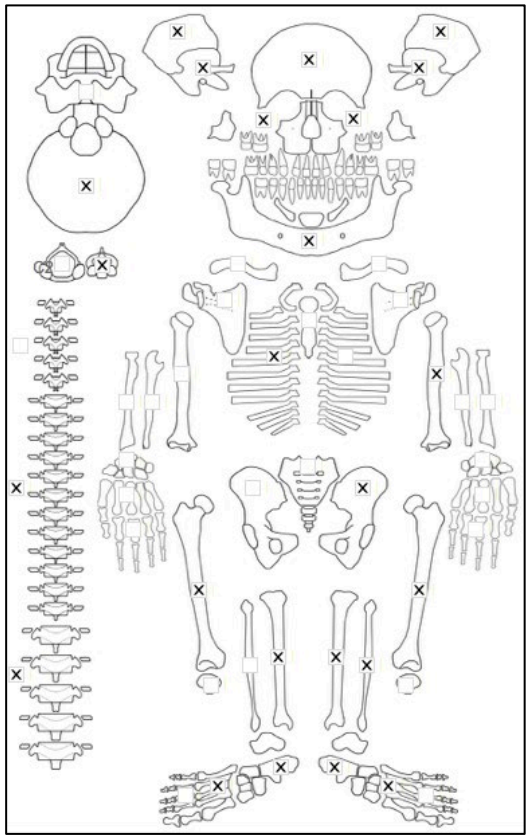

Completeness: Complete (>75%). 48% long bones, 12% hands and feet, 63% vertebrae, 100% neurocranium, incomplete ribs.
Preservation/ Taphonomy: All surfaces in excellent condition. Bone intact except pubis only of right os coxa and pubis missing from left os coxa, left scapula acromion only. Partially maxillae (oral and nasal region).
Age: 30-39, *Young Adult*
Sex: Female
Macroscopic Lesion Summary:
- posterior bending of the distal third shaft of the left humerus resulting in anterior angulation of the distal end (right humerus missing)
- bilateral genu valgum of the distal femora
- diffuse mixed active and remodelled new bone across the endocranium of the parietals and frontal
- diploic expansion of the frontal, parietals and occipital planum

Radiographic Lesion Summary:
No pathology
Differential Diagnosis Outcome:
Possible Osteomalacia

Skeletal ID: AT-530

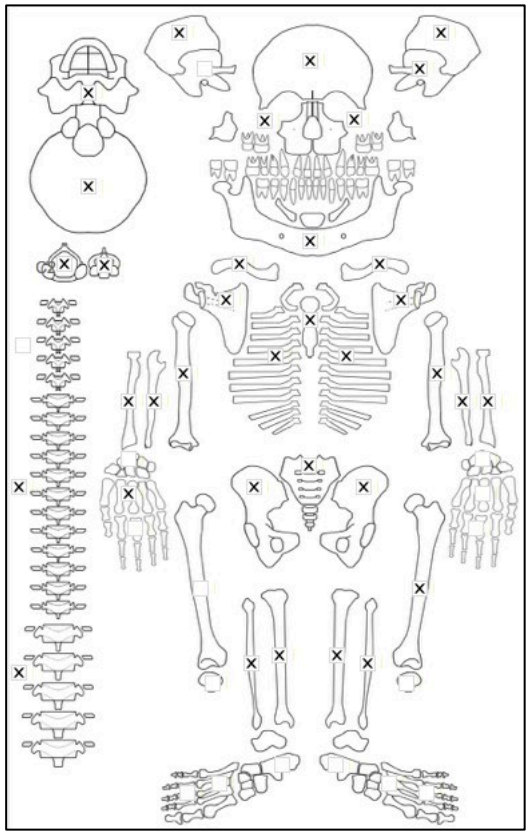

Completeness: Complete (>75%). 73% long bones, 14% hands and feet, 67% vertebrae, 75% neurocranium, ribs partially complete.
Preservation/ Taphonomy: Surfaces are moderately damaged. Distal shaft of left fibula only, both epiphyses of right fibula, and proximal epiphyses of humeri, tibiae and left radius is missing. Intrusive femora of smaller individual
Age: 30-39, *Middle Aged Adult*
Sex: Male
Macroscopic Lesion Summary:
- bilateral medial bending of the tibiae
- bilateral remodelled moderate cribra orbitalia
Radiographic Lesion Summary:
No radiographs taken
Differential Diagnosis Outcome:
Possible Residual Rickets
Anaemia

Skeletal ID: AT-569

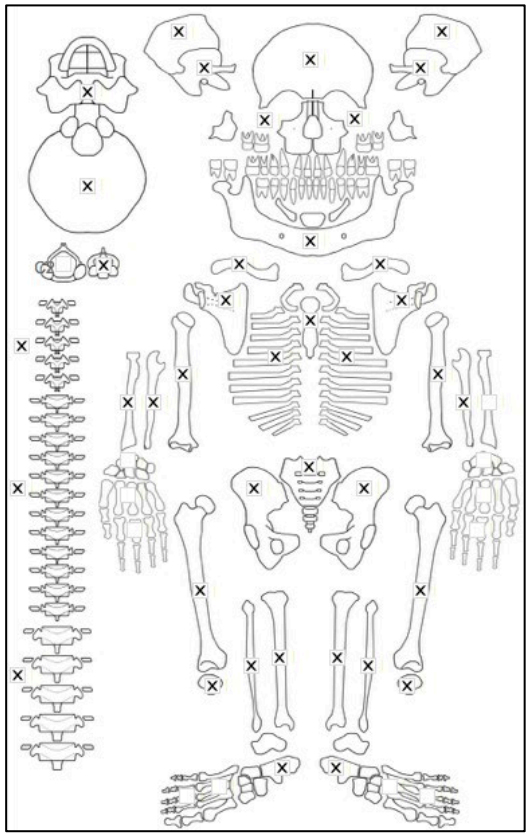

Completeness: Complete (>75%). 10% hands and feet, 83% vertebrae, 0% neurocranium. Ribs complete.
Preservation/ Taphonomy: Most surfaces are in excellent condition with distal epiphysis of left tibia and femur missing and damage to many epiphyses, 2/3 shafts of right and left fibulae only.
Age: 30-39, *Middle Aged Adult*
Sex: Male
Macroscopic Lesion Summary:
- biconcavity of vertebrae from T10 to L6, there is ankylosis of the vertebral bodies of L4-5 and ankylosis of the arches of T10-11. There is kyphosis of T12-L5
- unilateral lateral bending of the left femoral shaft. The shaft is also very broad. There is also coxa vara of left femoral neck
- inwards depression of bone on either side of the tibial tuberosity of the left tibia (right missing)
- bilateral remodelled cribra orbitalia, right is mild, left is moderate
Radiographic Lesion Summary:
- very thick cortex of the right femur
- biconcave depression (codfish sign), osteopenia and loss of body height of multiple vertebrae. There is spondylosis and ankylosis of the vertebrae. The concavity with result in kyphosis with slight scoliosis
Differential Diagnosis Outcome:
Probable Rickets
Probable Osteomalacia
Anaemia

Skeletal ID: AT-730

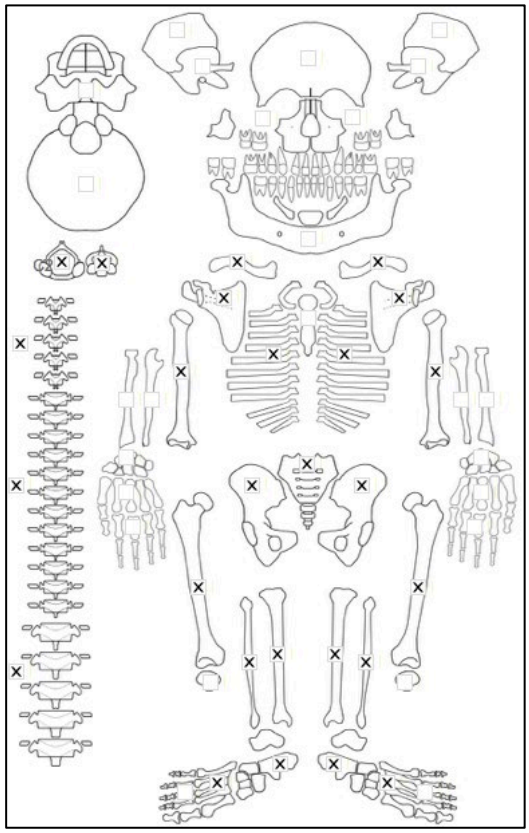

Completeness: Near Complete (66 to 75%). 67% long bones, 17% hands and feet, 92% vertebrae, 0% neurocranium, ribs complete.

Preservation/ Taphonomy: Surfaces are moderately to severely damaged.

Age: 30-39, *Middle Aged Adult*

Sex: Female

Macroscopic Lesion Summary:

No pathology

Radiographic Lesion Summary:

No radiographs taken

Differential Diagnosis Outcome:

No diagnosis

Skeletal ID: AT-736

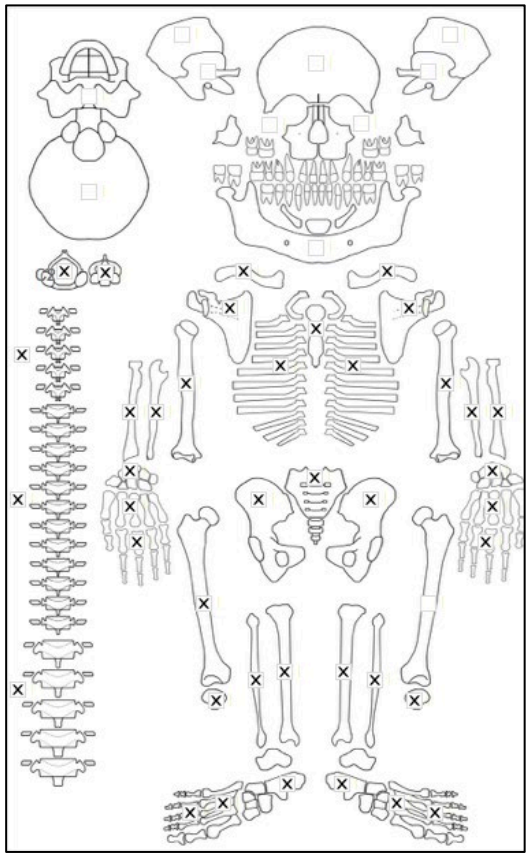

Completeness: Near Complete (66 to 75%). 98% long bones, 57% hands and feet, 83% vertebrae, 0% neurocranium, ribs complete.
Preservation/ Taphonomy: Surfaces in excellent condition except for severe surface damage to distal humerus and shaft of left femur.
Age: 20-29, *Young Adult*
Sex: male
Macroscopic Lesion Summary:
No pathology
Radiographic Lesion Summary:
No radiographs taken
Differential Diagnosis Outcome:
No diagnosis

Skeletal ID: AT-751

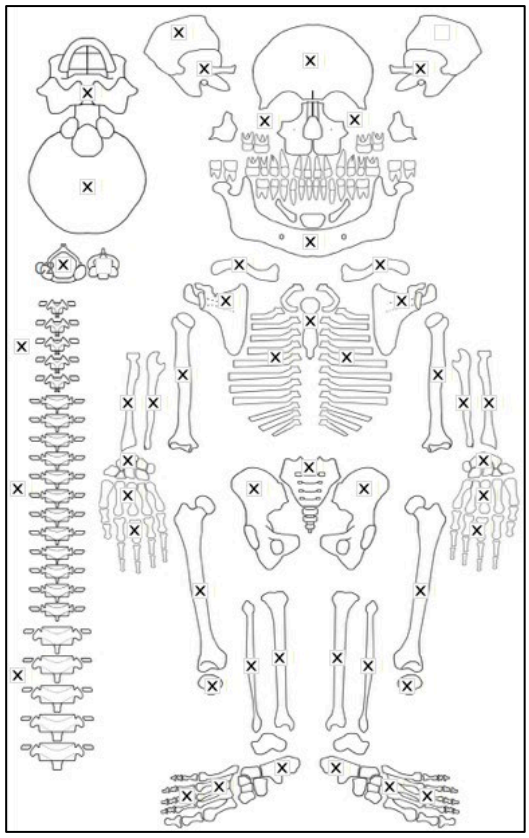

Completeness: Complete (>75%). 97% long bones, 56% hands and feet, 79% vertebrae, 100% neurocranium, ribs complete.
Preservation/ Taphonomy: Most surfaces are in excellent condition with exception of right lower and upper limb which has moderate damage. Proximal epiphysis of right fibula. Right humerus and partial of left tibia is missing. all preserved vertebrae are intact.
Age: 30-39, *Young Adult*
Sex: Female
Macroscopic Lesion Summary:
- bilateral remodelled plaques of new bone on the inferior nasal surfaces of the maxillae
- active patch of new bone on the orbital surface of the left zygomatic bone (right missing)
- active diffuse new bone on the endocranium of the frontal and the ethmoid
- remodelled new bone on the pterygoid region of the left greater wing of sphenoid (right missing)

Radiographic Lesion Summary:
No radiographs taken
Differential Diagnosis Outcome:
No diagnosis

Skeletal ID: AT-30b

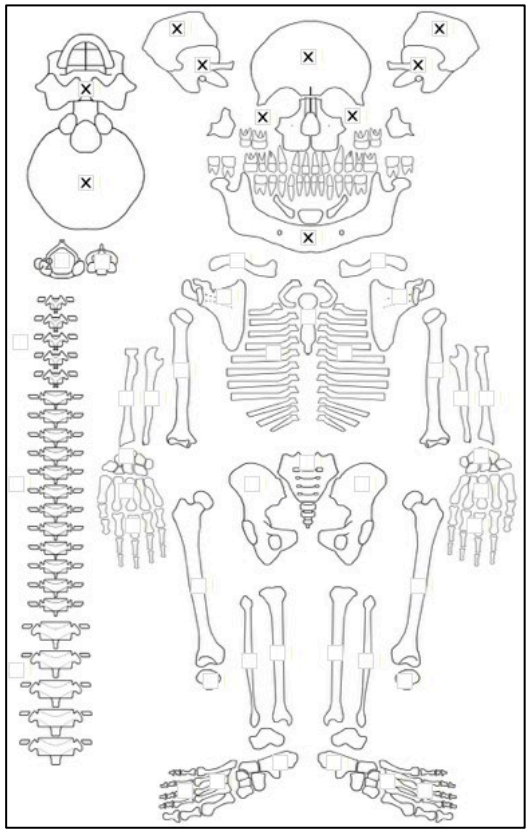

Completeness: Incomplete (33 to 50%).100% neurocranium.
Preservation/ Taphonomy: Skull only which is intact.
Age: *Adolescent*
Sex: Female
Macroscopic Lesion Summary:
- bilateral symmetrical discrete active new bone and cortical porosity on the coronoid fossae and inferior to the mylohyoid lines of the mandible.
- bilateral symmetrical discrete remodelled new bone and cortical porosity on the sublingual fossae of the mandible
- bilateral symmetrical discrete active new bone and cortical porosity on the palatal surfaces and posterior maxillae, there are vascular impressions on the posterior
- bilateral symmetrical discrete mixed active and remodelled new bone on the pterygoid region extending from the foramen ovale and lesser wings which are associated with new bone on the superior orbits
- bilateral symmetrical discrete active new bone on the superior orbits there is also cortical porosity of unknown aetiology possibly mild cribra orbitalia, there is also active new bone superior to the orbits on the ridge
- remodelled porotic hyperostosis on the on the frontal, superior parietals and occipital planum, with diploic expansion
- active diffuse new bone on the endocranial parietals (cannot be photographed)

Radiographic Lesion Summary:
No radiographs taken
Differential Diagnosis Outcome:
Possible Scurvy
Anaemia

Skeletal ID: AT-767

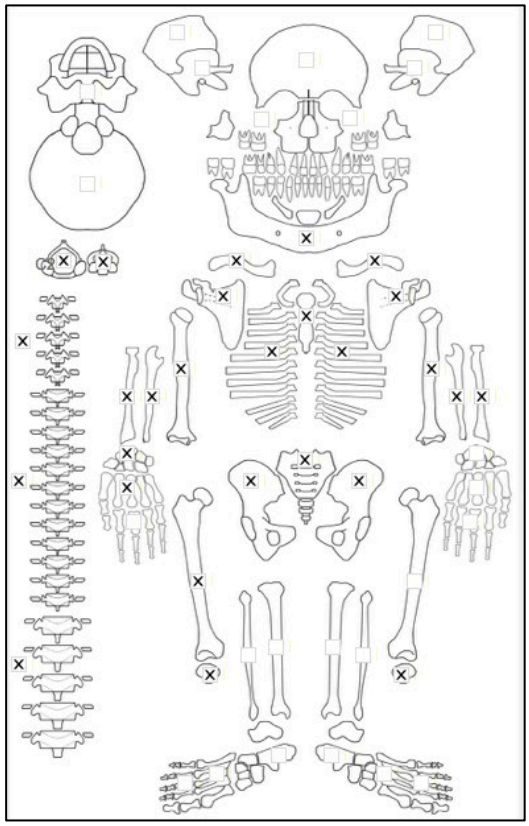

Completeness: Near Complete (66 to 75%). 48% long bones, 21% hands and feet, 100% vertebrae, 0% neurocranium.
Preservation/ Taphonomy: Most surfaces intact and in excellent condition except for partial damage of the scapula blades and distal epiphysis missing of right femur. Some long bones were excluded as they were severely damaged and no longer recognisable or useful for study: this included tibiae
Age: 20-29, *Young Adult*
Sex: Female
Macroscopic Lesion Summary:
- genu valgum and slight anterior bending of the right femur (left missing)
Radiographic Lesion Summary:
- no cortex thickness of long bones There is some coarsening trabeculae particularly visible in the distal humerus shaft.
Differential Diagnosis Outcome:
Possible Osteomalacia

APPENDIX 3:

DATA FOR CONTINENT STATISTICAL ANALYSIS

Time Period	Degree of Interaction	Interaction Zone	Time Period BP	Climate	RNPI	Subsistence	Crop Domestication	Residential Mobility	Infection Present	Infection Absent	Infectious Disease Prevalence	Scurvy Present	Scurvy Absent	Scurvy Prevalence	Infectious Disease Index
Middle Jomon	Very Low	None	4500	Temperate	N/A	Forager	No	Sedentary	7	26	21.2	12	20	36.4	28.6
Late/Final Jomon	Very Low	None	2650	Temperate	N/A	Forager	No	Sedentary	13	9	59.1	21	0	100	28.6
Pre-Neolithic Vietnam	Low	None	6450	Tropical	1.37	Forager	No	Sedentary	13	105	11.1	1	117	0.8	28.6
Neolithic Vietnam	High	Migration	3714	Tropical	4.32	Mixed	Yes	Sedentary	10	20	33.3	15	15	50	28.6
Early/Middle Bronze Age Mongolia	Medium	Fission-Fusion	3800	Arid	-0.3	Farmer	No	Mobile	1	27	3.6	0	28	0	14.30
Late/Final Bronze Age Mongolia	Medium	Fission-Fusion	3050	Arid	-0.3	Farmer	No	Mobile	3	49	5.8	5	47	9.6	42.9
Xiongnu Period Mongolia	High	Commerce	2000	Arid	-0.3	Farmer	Yes	Mobile	9	51	15	14	46	23.3	71.4

APPENDIX 4:

BIOARCHAEOLOGY INTERNATIONAL PAPER

Bioarchaeology International
Volume 4, Number 1: 15–39
DOI: 10.5744/bi.2020.1000

Two Probable Cases of Infection with *Treponema pallidum* during the Neolithic Period in Northern Vietnam (ca. 2000–1500 B.C.)

Melandri Vlok,[a]* Marc Fredrick Oxenham,[b,c] Kate Domett,[d] Tran Thi Minh,[e] Nguyen Thi Mai Huong,[e] Hirofumi Matsumura,[f] Hiep Hoang Trinh,[e] Thomas Higham,[g] Charles Higham,[h] Nghia Truong Huu,[e] and Hallie Ruth Buckley[a]

[a]Department of Anatomy, University of Otago, Dunedin, New Zealand
[b]School of Archaeology and Anthropology, The Australian National University, Canberra, Australia
[c]School of Archaeology, University of Aberdeen, Scotland, UK
[d]College of Medicine and Dentistry, James Cook University, Townsville, Australia
[e]Institute of Archaeology, Hanoi, Vietnam
[f]School of Health Sciences, Sapporo Medical University, Sapporo, Japan
[g]Oxford Radiocarbon Accelerator Unit, University of Oxford, Oxford OX1 3QY, UK
[h]School of Social Sciences, University of Otago, Dunedin, New Zealand
*Correspondence to: Melandri Vlok, Department of Anatomy, University of Otago, 270 Great King Street, Dunedin 9016, New Zealand
e-mail: Melandri.vlok@postgrad.otago.ac.nz

This research was supported by a National Geographic Early Career Grant (EC-54332R-18), a Royal Society of New Zealand Skinner Fund Grant, and a University of Otago Doctoral Scholarship.

ABSTRACT Skeletal evidence of two probable cases of treponematosis, caused by infection with the bacterium *Treponema pallidum*, from the northern Vietnamese early Neolithic site of Man Bac (1906–1523 cal B.C.) is described. The presence of nodes of subperiosteal new bone directly associated with superficial focal cavitations in a young adult male and a seven-year-old child are strongly diagnostic for treponemal disease. Climatic and epidemiological contexts suggest yaws *(Treponema pallidum pertenue)* as the most likely causative treponeme. This evidence is the oldest discovered in the Asia-Pacific region and is the first well-established pre-Columbian example in this region in terms of diagnosis and secure dating. The coastal ecology, sedentary settlement, and high fertility at the site of Man Bac all provided a biosocial context conducive to the spread of treponemal disease among inhabitants of the site. Co-morbidity with scurvy in both individuals demonstrates that malnutrition during the agricultural transition may have exacerbated the expression of treponematosis in this community.

Man Bac is a site of great regional importance owing to its role during the Neolithic transition of Mainland Southeast Asia. During this transition, approximately 4,000 years ago, farmers migrating from southern China into Southeast Asia influenced a number of changes in subsistence and demography and potentially introduced new infectious diseases such as treponematosis to indigenous forager communities. The findings presented here may encourage reevaluation of existing Southeast Asian skeletal samples and demonstrate the importance of using weighted diagnostic criteria for future reporting of treponematosis cases.

Keywords: agricultural transition; Southeast Asia; yaws

Received 8 August 2019
Revised 24 February 2020
Accepted 24 February 2020

Hai trường hợp nhiều khả năng mắc bệnh ghẻ cóc do nhiễm vi khuẩn *Treponema pallidum*, thuộc di chỉ Mán Bạc sơ kì đá mới Việt Nam (cal 1906–1523 B.C.) được mô tả trên bằng chứng di cốt. Sự có mặt của các hạt xương mới dưới màng xương trực tiếp liên quan đến các lỗ ổ bề mặt ở một nam trẻ tuổi trưởng thành và một trẻ em 7 tuổi là chẩn đoán nhiều khả năng cho bệnh này. Bối cảnh khí hậu và dịch tễ học cho thấy bệnh ghẻ cóc do nhiễm xoắn khuẩn *Treponema pallidum pertenue* là nguyên nhân phổ biến nhất. Bằng chứng trên được phát hiện muộn nhất ở khu vực Châu Á-Thái Bình Dương và là một ví dụ điển hình đầu tiên giai đoạn tiến Columbia trong khu vực này dựa vào chẩn đoán và định niên đại chính xác. Sinh thái biển, lối sống ít di động, và tỷ lệ sinh sản cao ở di chỉ Mán Bạc, tất cả đã tạo ra sự tương tác giữa các yếu tố sinh học và xã hội thuận lợi cho việc lây lan bệnh ghẻ cóc giữa các cư dân thuộc di chỉ này. Cùng với đó là sự mắc bệnh thiếu vitamin C (scurvy) ở cả hai cá thể trên chỉ ra rằng sự suy dinh dưỡng trong suốt quá trình chuyển tiếp nông nghiệp có thể trầm trọng hơn và biểu hiện bệnh ghẻ cóc ở cộng đồng này.

Mán Bạc là một di chỉ vùng quan trọng bởi vì nó nằm trong ranh giới giai đoạn chuyển tiếp Đá Mới của Đông Nam Á lục địa. Trong suốt bước chuyển này, khoảng 4000 năm cách đây, các cư dân nông nghiệp di cư từ miền nam Trung Quốc vào Đông Nam Á đã ảnh hưởng nhiều thay đổi trong phương thức sinh kế, dân số, và mang theo bệnh nhiễm trùng mới tiềm ẩn như là bệnh ghẻ cóc vào các cộng đồng nông nghiệp bản địa . Các phát hiện trình bày trên đây hi vọng sẽ là khởi đầu đánh giá lại về sự tồn tại các di cốt Đông Nam Á và minh họa tầm quan trọng của việc sử dụng tiêu chí chẩn đoán tin cậy về các trường hợp bệnh ghẻ cóc cho nghiên cứu tiếp theo.

In recent years, intensive archaeological and bioarchaeological research in Mainland Southeast Asia (MSEA) has described a unique agricultural transition that had a significant impact on the region's genetics, demographics, social organization, and subsistence base (Lipson et al. 2018; Matsumura and Oxenham 2014; Oxenham and Buckley 2016). Strong morphological evidence for the admixture of local indigenous populations and migrants from southern China (Matsumura and Oxenham 2013a, 2013b, 2014; Matsumura et al. 2008, 2019) has been supported by recent genome-wide ancient DNA analyses (Lipson et al. 2018; McColl et al. 2018). The evidence indicates that co-habitation and genetic admixture of agriculturalists and local foragers resulted in considerable social and demographic change at this time in MSEA (Lipson et al. 2018; McColl et al. 2018; Oxenham et al. 2011). While there remains a considerable focus on subsistence transitions and its impact on general health worldwide (Armelagos and Cohen 1984; Cohen and Crane-Kramer 2007; Snoddy et al. 2017; Temple 2010), less attention has been given to the mechanisms of infectious disease transmission from one population to another where substantial levels of mobility (including migration) have been demonstrated. In these circumstances, interaction between two or more populations in so-called friction zones transpires (Bellwood and Oxenham 2008). Here genetic admixture and social transition occurs between foragers and farmers. Epidemiological transitions may follow population interactions, as subsistence transitions can cause micronutrient deficiencies, and contact between populations (as evidenced in MSEA) encourages the spread of infectious disease from one group to another. The identification of specific infectious diseases (such as leprosy, tuberculosis [TB], and treponemal disease) and the consequent epidemiological impact within the chronological, social, and environmental context of friction zones offers important information on human and pathogen co-evolution in the changing biosocial contexts of Southeast Asia over time. An example of the possible introduction of infectious disease with increased population interaction has been suggested in the case of leprosy and TB at a late Iron Age site in northeast Thailand (Tayles and Buckley 2004) but has not been explored in other regions or during periods of agricultural transitions in this region.

This article describes two cases of specific infectious and nutritional disease from the site of Man Bac in northern Vietnam and explores the social, biological, and ecological contexts that may have encouraged the spread of infectious disease during the Neolithic demographic transition in MSEA.

Materials and Methods

The site

Man Bac is a Phung Nguyen period early Neolithic habitation site with an associated cemetery located in Ninh Binh province in northern Vietnam, known for complex incised designs on pottery vessels, intricate stone craftwork, and interaction with Chinese Neolithic farming societies (Oxenham et al. 2011). Cultural material reflects both foraging and agricultural subsistence (Oxenham et al. 2011). Excavated in 1999, 2001, 2004/5, and 2007, the cemetery component of the

Fig. 1. The burial position and associated artifacts of M20 (*left*) and M29 (*right*). Both individuals were buried extended and supine. The burials are in excellent skeletal condition with the exception of the cranium of M29, which was not present during excavation. (Image: M. Oxenham)

site consists of 101 individuals of exceptional skeletal preservation. Rib samples from four individuals from Man Bac have been dated to 1906–1523 cal B.C. (IntCal13, 95% CI, with marine reservoir effect applied; Online Supplement). While insufficient collagen yield meant direct dates could not be derived from the two individuals of focus in this paper, all burials were found within a secure single stratigraphic layer (Oxenham et al. 2011). The burial layer was found below two occupation layers. Cultural material from all layers are contemporaneous, suggesting an association between the three layers. Charcoal from the occupation layers dates to 2016–1524 cal B.C. (95% CI; Oxenham et al. 2011). As such, Man Bac is the only well-documented example of an early Neolithic settlement in Southeast Asia where local indigenous people coexisted with migrants from southern China who introduced agricultural practices to the region approximately 4,500 to 3,500 years ago (Bellwood and Oxenham 2008; Matsumura 2011a, 2011b).

It is not possible to estimate the population density of the Man Bac community, because the number of burials is not likely representative of the numbers in the living population and the full extent of the site has not been excavated. However, the Man Bac cemetery sample is characterized by a high fertility ratio and high rate of natural population growth, with 47.5% of individuals under the age of five years (McFadden et al. 2018). All burials, with the exception of three flexed inhumations, were in a supine extended position (Fig. 1), which is the normative pattern of burial at this time throughout Southeast Asia (Higham et al. 2011). Grave goods and ritual tooth removal (ablation) suggest age-based social hierarchy and affinal relationships

that may have affected the distribution of resources within the community (Tilley and Oxenham 2016). Archaeological remains reveal a mixed or transitional subsistence based on foraging and agricultural practices, similar to other Phung Ngyuen period settlements. A diet of both terrestrial and aquatic protein resources is indicated by stable isotope collagen values, with more than 50% from aquatic resources (Oxenham et al. 2011). The presence of domesticated pig (*Sus scrofa*) dominates the zooarchaeological assemblage (R. K. Jones et al. 2019; Oxenham et al. 2011).

Today, Man Bac is situated approximately 25 km from the coast (Oxenham et al. 2011). However, given high sea levels in the mid-Holocene, Man Bac was likely much closer to the coast within an estuarine zone (Tanabe et al. 2006). The variety of faunal sources indicate that the inhabitants of Man Bac were exploiting a number of ecological zones, including forests, grasslands, lowlands, and marine and estuarine environments (Sawada et al. 2011; Toizumi et al. 2011). The site forms part of the Phung Nguyen complex, a series of sites found within the Ninh Binh region along the Red River Delta. The presence of contemporaneous pottery suggests extensive interaction between the sites farther inland along the river, as well as shared archaeological material with agricultural sites in southern China (Bellwood 2005; Nguyen 2008). The type site of Phung Nguyen is approximately 160 km from today's coastline, which represents the possible extent of interaction of farming settlements within northern Vietnam, although this site is dated to slightly later at around 1500 B.C. (Khoach 1980). Evidence of housing styles was not excavated at Man Bac. However, they may have been similar to other Phung Nguyen habitation sites where large houses on stilts (see Oxenham et al. [2015] for a discussion of built structures in the slightly later site of Rach Nui in southern Vietnam) appear to have been built, possibly for similar reasons as constructed in mountainous regions of Vietnam today, to keep out snakes and small animals (Khoach 1980).

Concerning the general health of people buried at Man Bac, previous research has demonstrated high levels of non-specific stress; 92.3% of males and 53.8% of females presented with cribra orbitalia, and 64.9% of the total assemblage presented with linear enamel hypoplasia of the incisors or canines (Oxenham et al. 2011). Forty-two percent of individuals had localized primary canine hypoplasia, which may be related to deficiencies of calcium, Vitamin A, or Vitamin D during gestation (McDonell and Oxenham 2014). Therefore, stress from parasitic, dietary, or infectious origin was commonplace during childhood for many of the individuals from Man Bac. The detailed paleopathology analysis of the total sample will be presented in forthcoming publications.

Methods for age and sex estimation

The age and sex of individuals from Man Bac were previously reported by Domett and Oxenham (2011). Adult sex estimations were based on standard methods for qualitative morphological estimates from the skull and pelvis (Acsádi et al. 1970; Buikstra and Ubelaker 1994; Phenice 1969). Non-adult age estimates were based on standards for the timing of dental calcification and eruption (Moorrees et al. 1963; Ubelaker 1999). Where teeth were not available for age assessment in non-adults, long bone lengths were compared to non-adults with dental estimates available, as well as to standards for long bone estimates in non-adults by Scheuer and Black (2000). Adult age estimation followed Suchey-Brooks standards for the pubic symphysis (Brooks and Suchey 1990).

Recording methods for abnormal variation (pathological changes)

Proliferative (lamellar and woven bone) and lytic lesions as well as bone deformities were recorded in the entire preserved skeleton. Lesions with the potential to contribute to diagnosis were also radiographed. A differential diagnosis was performed with the basis drawn from seminal literature in paleopathology (Brickley and Ives 2008; Lewis 2017; Ortner 2003; Snoddy et al. 2018; Weston 2012) as well as clinical literature concerning specific diseases (Hackett 1976; Jaffe 1972; Resnick 1995a). Lesions were characterized as diagnostic and suggestive of specific disease based on recommendations by Snoddy et al. (2018). A clinical basis for diagnosis of specific disease has also been championed by Mays (2012), Ortner (2011), Snoddy et al. (2020), Zuckerman et al. (2016), and others (for treponemal disease, Powell and Cook advocated such criteria in their 2005 book, as do Baker et al. [2020]). In the Snoddy et al. (2018) criteria, lesions are only considered to be *diagnostic* (D) if there is strong clinical basis or considerable body of paleopathological work supporting the diagnostic weight of the lesion. Lesions where there is no consensus in the clinical or paleopathological literature, but remain anatomically intuitive, were designated a *suggestive* (S) value. In addition, lesions that have been considered elsewhere as pathognomonic for disease are here scored as *strongly diagnostic* (SD) (after Brickley and Ives 2008). For a probable case of disease at least one strongly diagnostic and/or two diagnostic lesions are required (Brickley and Ives 2008; Snoddy et al. 2018). A possible case of disease requires a minimum of one diagnostic lesion and/or two suggestive lesions (Snoddy et al. 2018).

Clinically documented associated pathology was also considered in discussion of the disease expression, but it was not a primary deciding factor in the

differential diagnosis due to their poor diagnostic strength in dry bone. These included generalized proliferative bone changes which can be caused by multiple diseases. (See Online Table S5 for summary of diagnostic strength of lesions.)

Results

The lesions at Man Bac were predominantly bilateral, symmetrical, and discrete and affected both the postcranial and cranial remains. As the focus of this paper is the identification of specific infectious disease at Man Bac, the causes of the more generalized pattern of proliferative lesions at Mac Bac will be reported at a later date but are likely a result of a number of etiologies.

A total of seven individuals (10%, 7/70) from Man Bac—two adults, two adolescents, and three children—share a similar skeletal pattern of diffuse proliferative new bone lesions consistent with systemic disease. Two of these seven individuals presented with widespread subperiosteal new bone, endosteal enlargements in the long bone shafts, *and* focal superficial lytic lesions within nodes of subperiosteal new bone (localized enlargements of subperiosteal new bone). These two individuals are the focus here due to the diagnostic potential of their lesions, with a brief discussion of a further five cases with lower diagnostic strength. A differential diagnosis was conducted on MB05 M20 and MB07 H2 M29, which includes systemic conditions known to produce lesions similar to those observed here: osteomyelitis (non-specific bone infection), leprosy, tuberculosis, brucellosis, mycosis, treponematosis, rickets/osteomalacia, and scurvy. A description of the bone pathology in these two individuals and a full differential diagnosis are presented. Detailed descriptions of lesions in all seven individuals are found in Online Table S5. Descriptions of skeletal lesions consistent with possible and probable treponemal disease in all affected Man Bac individuals can be found in Online Table S6.

M20

MB05 M20 (herein called M20) is a young adult male (15–29 years old). The individual was buried east to west in a supine position with three ceramic pots characteristic of the Phung Ngyuen period (Fig. 1). The skeleton is excellently represented, with all limbs, skull (and teeth), hands, and feet complete and 60% representation of the ribs and vertebrae. The surfaces of the bones are in excellent condition. M20 presented with diffuse thick and remodeled new bone with endosteal enlargement of the entire shafts of the right humerus, tibiae, and fibulae (Fig. 2). Discrete nodes of new bone are present on the medial midshaft of the right tibia and on the distal third of both fibulae symmetrically. The new bone is present on the metaphyses and shafts of the tibiae and fibulae and the distal metaphysis of the right humerus. There are pathological pseudo-bowing deformities in the tibiae similar to bowing in a saber shin. While new bone is macroscopically only visible on the distal metaphysis of the right humerus, radiographs reveal endosteal enlargement of the entire shaft, suggesting prior osteoblastic activity that has since remodeled. Further discrete deposits of new bone can also be observed on the medial proximal left femur and medial and lateral proximal tibiae. Multiple superficial focal lytic lesions are present on the distal fibulae shafts, proximal right fibula, lateral metaphysis of the left humerus, and the lateral aspect of the left calcaneus. The focal lytic lesions of the fibulae are associated with discrete nodes of new bone and active new bone is observed around the margins of the lytic lesions. Two focal lesions of the right distal fibula have been damaged postmortem, so it is not possible to determine whether the lesions are superficial or extend into the medulla. However, a small focal superficial lesion is present adjacent to the larger two lesions (Fig. 2f), supporting the interpretation that the lesions with postmortem damage do not extend beyond the external cortical bone surface. The two focal lesions of the left distal fibula are clearly superficial, within a node of new bone and with smooth sclerotic margins (Fig. 2g).

No lytic or diffuse proliferative lesions were present on the cranial vault. Bilateral and symmetrical discrete deposits of remodeled new bone and abnormal cortical porosity are present on the external greater wings of the sphenoid bones, temporal bone squama, and posterior and anterior zygomatic bones. The lesions are clearly discrete and do not represent diffuse inflammatory changes in the skull. There are also porotic lesions across the ectocranium (frontal bone, occipital bone, and parietal bones medial to the temporal lines) consistent with porotic hyperostosis, although the diploe is not exposed so this cannot be confirmed. Medium-grade cribra orbitalia was also observed (after Stuart-Macadam 1985:392).

M29

MB07 H2 M29 (herein called M29) is a non-adult approximately seven years of age at death (Oxenham et al. 2011). M29 was buried supine; no clear grave goods were identified, but pottery sherds were present around the region of the sacrum (Fig. 1). The cranium was not present, and only the right side of the mandible (including teeth), remained. The individual's postcranial axial skeleton is very well preserved, but the hands and feet were virtually absent (with the exception of a single preserved metacarpal). There were some hardened soil concretions on the surfaces of the

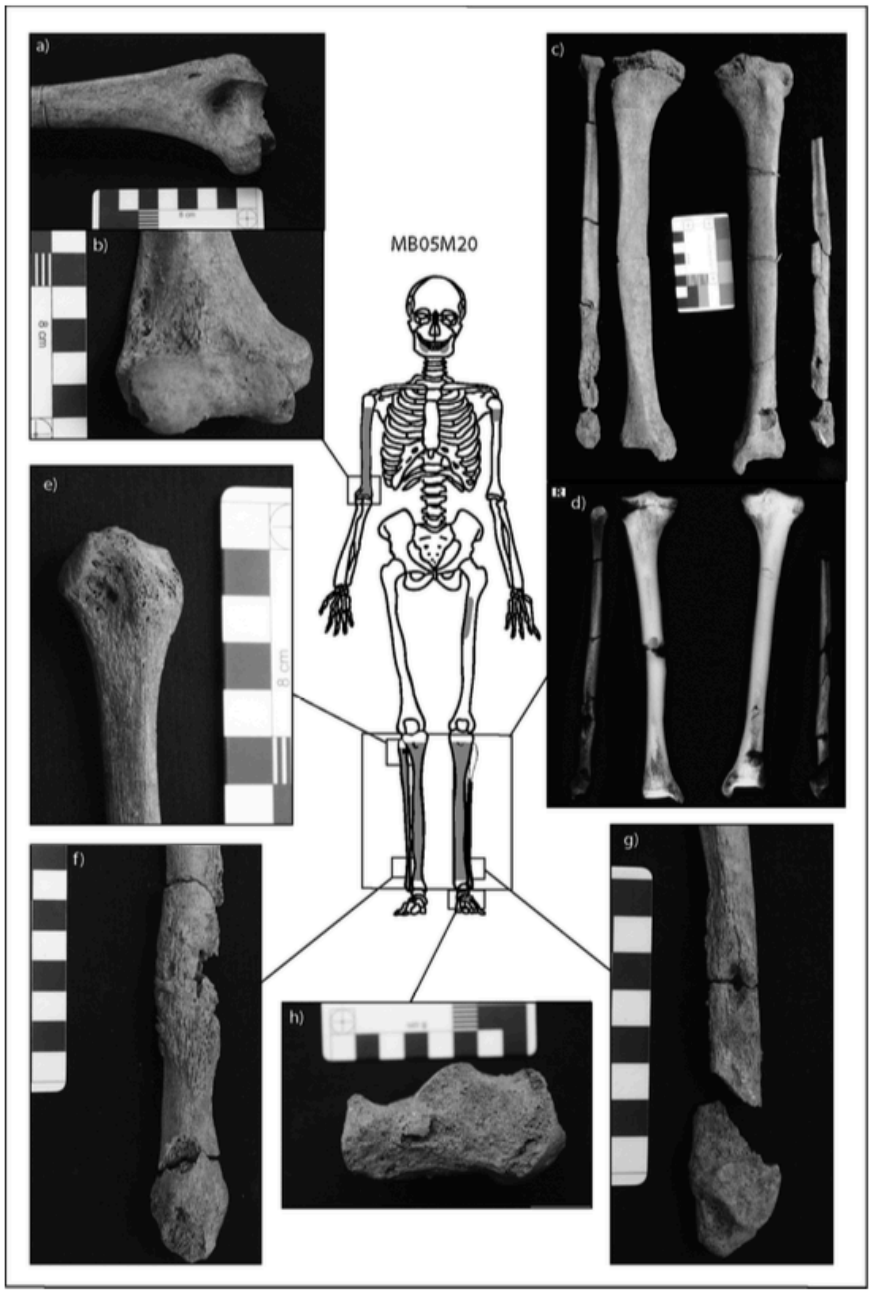

Fig. 2. Expression of lesions related to infectious disease in M20. Preserved bones are outlined in black, with absent bones outlined in light gray. The skeletal extent of osteoblastic lesions is indicated by dark gray fill. (a) and (b) Superficial focal cavitations with smooth sclerotic margins not within distinct nodes of new bone on the anterior and posterior lateral epicondyle of the right humerus. (c) Remodeled cortical enlargements throughout the shafts of the tibiae with striated nodes of new bone on the distal fibulae. (d) Radiographs of the tibiae and fibulae: a distinct node of new bone with medullary intrusion is present on the medial middle shaft of the right tibia. The nodes of new bone of the distal fibulae are radiolucent due to the extent of pathological change to the internal cortex of the bone. (e) Superficial focal cavitation not within a distinct node of new bone on the proximal right fibula. (f) Two focal superficial cavitations on the lateral aspect of the right distal fibula within a distinct node of striated new bone. (g) Focal superficial cavitation on the medial aspect of the right distal fibula within a distinct node of striated new bone. (h) Focal superficial cavitation on the medial left calcaneal body, not within a distinct node of new bone. (Image: M. Vlok)

long bones and vertebrae, but this was minimal. Animal gnaw and puncture marks were observed on some of the lower limb bones.

M29 presents with diffuse multi-layered new bone across the diaphyses of all limb bones bilaterally, and on the single preserved metacarpal (Fig. 3). Nodes of subperiosteal new bone are present at the midshafts of the right radius and ulna, proximal left ulna, entire shafts of tibiae, and distal fibulae. Multiple lytic lesions with sclerotic margins, observed radiographically, are present on the proximal left ulna, midshafts of the right radius and ulna, and inferior medial left clavicle. The lytic lesions of the midshaft of the right ulna and radius have some postmortem damage to the floor and margins. However, the preserved margins of the lesions indicate they did not penetrate the cortex. The lytic lesions on the distal fibulae do penetrate the cortex to the medullary canal. Radiographs also show well-remodeled proliferative new bone on the anterior crest of the tibiae, indicating so-called saber shin. A unilateral enlargement of the sternal end of the left clavicle without any macroscopic presence of thick subperiosteal new bone deposit is evident, and a thin cortex is appreciated from the radiograph. Symmetrical mixed active and remodeled new bone and abnormal cortical porosity is present in the supraspinous fossae of the scapulae. Although the cranium is absent, remodeled abnormal cortical porosity of the right coronoid process of the mandible is observed. Radiographically, all the long bones present with radiodense metaphyseal plates in association with zones of radiolucency in the metaphyseal region.

Deformity of some long bones is also present in M29. Symmetrical swellings of the distal metaphyses and slight cupping of the femora occur (Fig. 4c). There is slight bilateral medial "true" bowing of both tibiae confirmed by radiographs with slight posterior protrusion of proximal metaphyseal plates, suggesting depression and deformity (Fig. 4g). Further, there is lateral bowing of the proximal third of the humeral shafts, and depression and deformity of the metaphyses of the humeral heads (Fig. 4d).

Discussion

Differential diagnosis

The differential diagnosis of the types and skeletal pattern of the lesions in these Man Bac individuals included bone cancers, osteomyelitis, tuberculosis, brucellosis, mycosis, leprosy, and treponematosis. These diseases are included in the differential diagnosis due to the combination of proliferative and destructive lesions in the disease pathophysiology. The bone response to metastatic cancers may produce a combination of extensive subperiosteal and lytic response. However, these conditions are less likely to cause such widespread involvement of the skeleton as that observed here and are not known to cause multiple and widespread superficial cavitations (Ortner 2003:363–382, 503–544). Cancers such as multiple myeloma or Langerhan's cell histiocytosis (LCH), which can result in systemic multifocal destruction of the skeleton, most often appear as punched-out lytic lesions without sclerosis and can be ruled out (Ortner 2003:362, 377). M20 and M29 do not appear similar to a possible case of multiple myeloma or LCH identified by Domett and Buckley (2012) in pre-Angkorian Cambodia, and marginal sclerosis of the lytic lesions are rare and subperiosteal new bone deposits are not characteristic of these diseases (Ortner 2003:363, 377). Because bone cancer in archaeological contexts is extremely rare (Ortner 2003:363–382, 503–544), the presence of two individuals in the collection with similar bone lesions (M20 and M29) further demonstrates that cancer can be ruled out as a possible cause.

While subperiosteal and endosteal enlargement are non-specific inflammatory responses to various diseases and trauma (Weston 2012), the widespread and non-uniform nature of the enlargements in the Man Bac cases are more consistent with that of a systemic infection than metabolic or traumatic etiologies. The subperiosteal new bone lesions of metabolic disease tend to be uniform and symmetrical, unlike the majority of the lesions of M20 and M29 (Brickley and Ives 2008; Pitt 1995; Resnick 1995b; Snoddy et al. 2018). Furthermore, subperiosteal new bone from trauma is most often localized, also unlike that observed in M20 and M29 (Rana et al. 2009). However, some of the subperiosteal lesions in both M20 and M29 are symmetrical, and a metabolic etiology contributing to the overall expression of subperiosteal lesions in both individuals is not ruled out and is discussed further below.

Pyogenic osteomyelitis is a non-specific infection of the bone producing a characteristic suite of lesions of bone death from loss of blood supply (sequestrum), combining a lytic lesion (circular pus-draining cloaca) and a proliferative healing response (involucrum) (Ikpeme et al. 2010). The major causative agents are *Staphylococcus* or *Streptococcus* bacterial species, although other pathogens can infect bone (Acosta et al. 2004; Ikpeme et al. 2010). Initial transmission generally occurs through soft tissue infection of open wounds and, less frequently, secondary to respiratory, food-borne or water-borne diseases (Giaccai and Idriss 1952; Honda and McDonald 2009; Jaffe 1972:1015–1046; Miller et al. 1963; Vohra et al. 1997). The pathogenic agent enters the bone through the bloodstream and

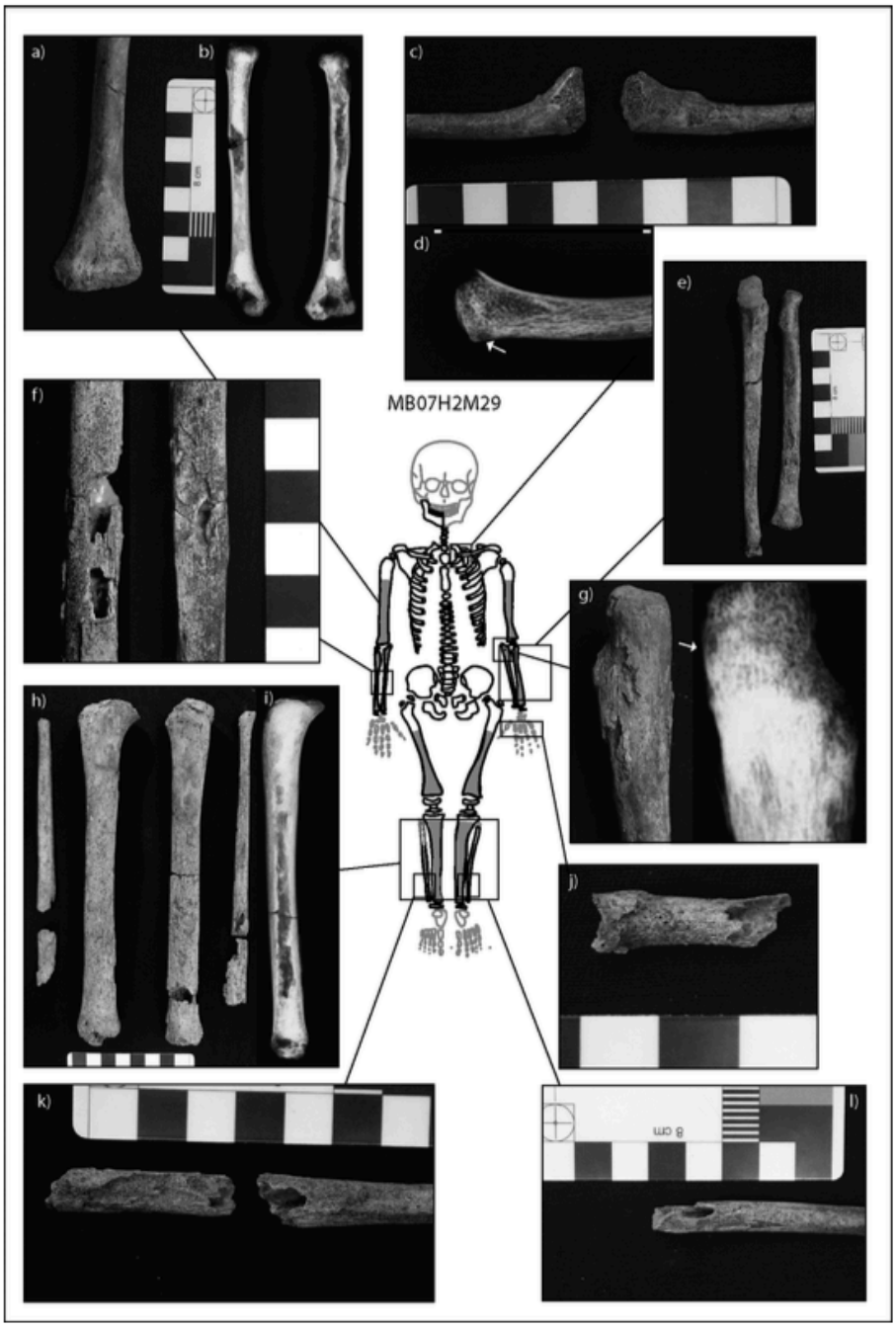

Fig. 3. Expression of lesions related to infectious disease in M29. Preserved bones are outlined in black, with absent bones outlined in light gray. An undetermined metacarpal is also present but not demonstrated in the figure, as its skeletal position is unknown. The skeletal extent of osteoblastic lesions is indicated by dark gray fill. (a) Subperiosteal new bone deposit on the distal shafts and metaphyses of the humeri. (b) There are slight cortical enlargements visible on radiographs throughout the humeral shafts. (c) Remodeled enlargement of the medial left clavicle. The metaphyseal plate is bulging. (d) Radiographs do not demonstrate a distinct cortical enlargement of the left medial clavicle. The internal trabeculae appear radiolucent, and a distinct oval lytic lesion with a radiodense sclerotic margin is present on the inferior margin of the medial metaphysis. Some increased calcification is present on the medial metaphyseal plate. (e) Diffuse subperiosteal new bone deposit across the radii and ulnae. (f) Two oval cavitations within nodes of new bone on the midshafts of the right radius and ulna. While significant damage has occurred to the lesion floor, the margins of the lesion are preserved and indicate superficial cavitation. (g) Large node of new bone on the proximal left ulna. Radiographs demonstrate a small oval lytic lesion with sclerotic margins within the node. (h) Prolific subperiosteal new bone across the tibiae and fibulae. Fibular cortical enlargements are thickest toward the distal shaft. Note the rounded margins of the anterior shaft of the tibiae indicating saber shin deformity. (i) Radiograph of the right tibia demonstrating cortical enlargement of the anterior crest indicating saber shin. (j) An unknown metacarpal with significant postmortem damage. However, it is clear that the entire shaft of the metacarpal has undergone prolific pathological change indicative of dactylitis. The internal margins of the cortex are porous. (k) and (l) Focal cavitations of the right and left distal fibulae. Margins of the lesions are smooth and within nodes of new bone. The surrounding bone has undergone complete prolific pathological change with the internal cortex appearing porous. Osteoblastic lesions considered in the diagnosis of nutritional disease are presented in Figure 4. (Image: M. Vlok)

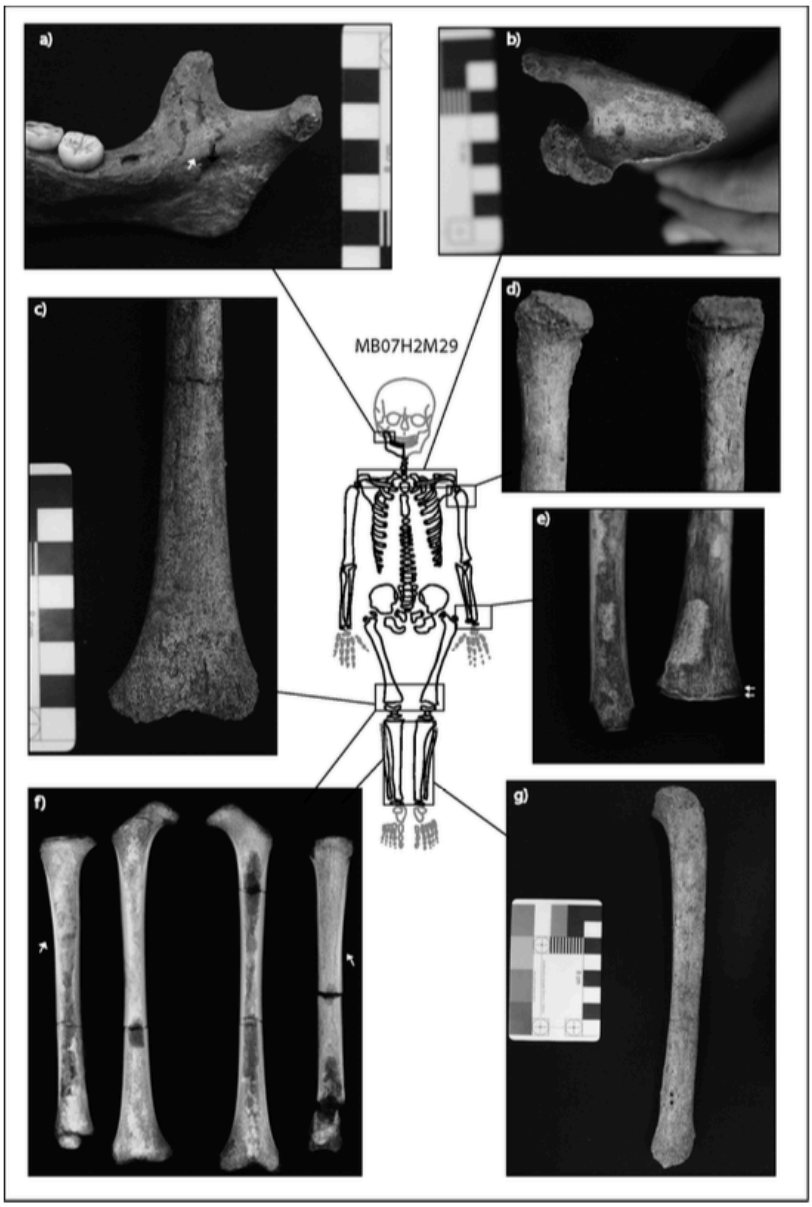

Fig. 4. Expressions of lesions related to nutritional disease in M29. Preserved bones are outlined in black, with absent bones outlined in light gray. An undetermined metacarpal is also present but not demonstrated in the figure, as its skeletal position is unknown. The skeletal extent of osteoblastic lesions possibly related to nutritional disease is indicated by dark gray fill. (a) Mixed active and remodeled discrete deposit of subperiosteal new bone and abnormal cortical porosity medial to the coronoid process of the mandible. (b) Symmetrical mixed active and remodeled discrete deposit of subperiosteal new bone in the supraspinous fossa of the scapulae. (c) Bilateral swelling and slight cupping of the distal femur. (d) Depression of the humeral heads which are reminiscent of coxa vara deformities of the femoral heads (see Brickley and Ives 2008:102). (e) Trummerfeld (scurvy) line and white line of Frankle on the distal radius and ulna. These radiographic changes were identified in all metaphyses of long bones. (f) Slight medial bending deformities of the tibial shafts. (g) Posterior bending of the proximal metaphyseal plate of the tibia. (Image: M. Vlok)

infiltrates through nutrient arteries (Jaffe 1972:1015–1020). Proliferation within bone generally begins in the metaphyseal region, eventually spreading to the cortex through the Haversian canals (Ikpeme et al. 2010; Jaffe 1972:1020). Osteomyelitis can result in nodes of new bone only, like treponemal disease (Hackett 1976:424). However, it is particularly diagnostic in its pyogenic form. Substantial deposits of subperiosteal new bone occur particularly in the long bones, resulting in a shell of new bone termed the involucrum (Ikpeme et al. 2010; Kharbanda and Dhir 1991). Disruption to blood supply by the involucrum results in bone death (sequestrum) (Ikpeme et al. 2010; Kharbanda and Dhir 1991). Finally, cloacae develop within the involucrum in order to drain pus that has accumulated within the medullary canal (Ikpeme et al. 2010; Kharbanda and Dhir 1991). Dactylitis, as observed in M29, is known to occur in osteomyelitis, but it is frequently associated with direct infection to the surrounding soft tissue due to trauma or localized infection (Jaffe 1972:1018). Osteomyelitis is rare in adults but can result from reoccurrence of infection from adolescence (Ortner 2003:187; Resnick and Niwayama 1995). However, the superficial focal cavitations on the external cortex as observed in the left fibula of M20 are unknown to occur in osteomyelitis and are incompatible with the pathophysiology of cloacae in pyogenic bone infection. While necrotic abscesses have been observed in osteomyelitis, they occur within the medullary canal and not the external cortex (Jaffe 1972:1020). Although two lesions in the distal fibulae of M29 penetrate to the medullary canal and are reminiscent of cloacae, such lesions have also been observed in cases of treponemal disease where gummatous lesions are associated with advanced endosteal enlargement (Hackett 1975). It is clear the entire bone of the fibulae shafts has been involved in this child with the inner cortex appearing porous. There is a lack of association of involucrum or sequestrae with the lytic lesions in M29, as would be expected with osteomyelitis, and more extensive proliferative new bone response also would be expected (Hackett 1976:92). Furthermore, it would be unusual for cloacae to occur symmetrically, such as observed in M29, as formation of cloacae is determined by the nature of the involucrum development and therefore they do not appear in predictable patterns (Jaffe 1972:1018; Roberts 2019:298). Systemic non-localized skeletal expression of both the lytic and proliferative lesions in M20 and M29 without focus of the infection in the metaphyseal regions of bone make osteomyelitis as the underlying cause extremely unlikely. However, given the non-specificity of osteomyelitis, particularly the non-pyogenic form, a secondary bacterial, viral, or fungal infection cannot be ruled out.

The *Mycobacterium tuberculosis* complex (MTBC) is a group of infectious slow-growing gram-positive bacteria that can cause granulomatous necrotizing abscesses throughout the entire body, including bone (Flynn and Chan 2001; Haque 1990; Knechel 2009). The MTBC consists of *Mycobacterium* strains that infect a number of mammalian primary hosts but can all cause infection of humans. These include: *M. tuberculosis* (humans), *M. bovis* (domestic livestock), *M. canetti* (humans), *M. microti* (voles, hyrax, llama, rarely humans), *M. caprae* (goats), *M. pinnipedii* (seals and sea lions, rarely humans), and *M. africanum* (humans) (Roberts 2012). The most common form is *M. tuberculosis,* which is primarily a respiratory disease affecting the lungs (De la Rua-Domenech 2006; World Health Organization 2013). *M. tuberculosis* is most often spread through air droplets from coughing, sneezing, and talking (Knechel 2009; World Health Organization 2013), whereas zoonotic forms such as *M. bovis* tend to spread to humans through ingestion of meat or dairy (De la Rua-Domenech 2006).

In its chronic form, tuberculosis can cause systemic granulomatous skeletal destruction with minimal new bone response, predominantly in regions of trabecular bone and articular surfaces, such as the vertebral bodies (Jaffe 1972:956; Key 1940; LaFond 1958; Ortner 2003:228). Therefore, bone destruction in tuberculosis most commonly affects the spine above all other skeletal elements, followed in frequency by involvement of the hip and knee joints (Jaffe 1972:956; LaFond 1958; Ortner 2003:228). In the most advanced form, destruction of the vertebral bodies results in collapse referred to as gibbus formation (or structural kyphosis) seen in Pott's disease, which has been considered pathognomonic for tuberculosis (Davidson and Horowitz 1970; Jaffe 1972:958–961; Turgut 2001). While circumferential deep focal destruction can occur in the long bones in tuberculosis, it is more characteristic of childhood tuberculosis, and even then it is focused in long bone ends rather than shafts (Lewis 2017:161; Ortner 2003:245; Teo and Peh 2004). Sclerotic margins of the superficial focal lesions on the external shafts of the long bones of M20 and M29 accompanied by cortical enlargement is not reminiscent of the destruction of tuberculosis, which, while chronic, elicits minimal remodeling of the lesion margins (Jaffe 1972:976). Proliferative new bone response is known to occur, particularly in the early stages of disease, as a systemic inflammatory response to the pathogen or due to psoas abscess formation adjacent to the lumbar spine, but is infrequently found in direct association with the destructive lesions in adults (Davidson and Horowitz 1970; Ortner 2003:232; Ridley et al. 1998). In the case of tuberculosis, dactylitis is rare but can occur in juveniles such as that observed in the single

metacarpal of M29 (Teo and Peh 2004). However, in M29 the degree of expression is not severe and lacks the cystic destructive form more common to childhood tuberculosis (Lewis 2017:162; Teo and Peh 2004). As there is no evidence of spinal, trabecular, or joint involvement of which pathogens in the MTBC complex are selective for, tuberculosis is ruled out as a possible cause for the lesions in M20 and M29.

Brucellosis is a bacterial zoonotic disease commonly associated with animal husbandry. Human disease is mainly caused by four species of *Brucella: B. abortus, B. suis, B. canis,* and *B. melitensis* (Al-Shahed et al. 1994; Franco et al. 2007). The bacteria are transmitted mostly through consumption of animal products such as dairy, but they can be transmitted through skin lesions in circumstances of close contact with animals (d'Anastasio et al. 2011; Franco et al. 2007; Mehmet et al. 2002). The *Brucella* bacteria bind to cells of the mononuclear phagocyte system, a group of cells that includes bone marrow progenitors, blood monocytes, and macrophages found in hematopoietic regions of the body including in bone (Campbell et al. 1994; Hume 2006). Once chronic, brucellosis can affect the skeleton in focal or diffuse forms (Al-Shahed et al. 1994). Less has been described about the skeletal pathology of brucellosis than of tuberculosis, and questions remain about how to differentiate definitively between the two, and whether this is even possible in many cases (Al-Shahed et al. 1994). As is the case in tuberculosis, focal destruction of the spine is a primary characteristic of this disease (Al-Shahed et al. 1994). Brucellosis can cause widespread destruction of the skeleton, and skeletal involvement is common (Al-Shahed et al. 1994; Mehmet et al. 2002). Destructive lesions are often but not always accompanied by sclerotic reaction due to their slow development, which is not characteristic of tuberculosis (Roberts and Buikstra 2019: 421). Remodeling can result in the presence of parrot's beak osteophytes on the superior margin of the anterior vertebral bodies (Al-Shahed et al. 1994). While collapse of the spine can occur, it is unusual for the destruction to advance to the severity seen in tuberculosis (Roberts and Buikstra 2019). Similar to tuberculosis, osteolytic lesions develop in regions of hematopoiesis, including the hip, knee, and ankle joints (Al-Shahed et al. 1994; Mehmet et al. 2002). Unlike in tuberculosis, following the spine, the sacroiliac joint and knee are most commonly affected (Al-Shahed et al. 1994). For reasons similar to those stated in the consideration of tuberculosis, it is unlikely that brucellosis is responsible for the skeletal appearance of disease observed in M20 and M29. Although brucellosis is known to result in focal lesions with sclerotic response, superficial lesions of the external cortex, particularly in relation to cortical enlargements of long bone shafts, have not been observed in the pathophysiology of this disease.

Various fungal infections are known to result in skeletal involvement. Diseases including coccidioidomycosis, blastomycosis, histoplasmosis, aspergillosis, and cryptococcosis rarely infect the musculoskeletal system but are more common in immunocompromised individuals (Corr 2011). Transmission often occurs through open wounds or through the respiratory tract whereby hematogenous spread occurs (Corr 2011). Infection is more common in the spine, but it can occur in any region of the skeleton, particularly in regions of hematopoiesis (Corr 2011; Toone and Kelly 1956). For this reason there is a predilection for axial skeletal involvement (Taljanovic and Adam 2011). When long bones are involved the metaphyses are more commonly affected, with joints affected if destruction is extensive, at times resulting in septic arthritis (Taljanovic and Adam 2011). The pathological response is primarily in the form of focal punched-out or deep granulomatous osteolytic lesions with or without sclerotic margins (Corr 2011; R. C. Jones and Goodwin 1981; Taljanovic and Adam 2011; Toone and Kelly 1956). Proliferative new bone response to the extent observed in M20 and M29 has not been reported for mycotic infections. However, given the systemic inflammatory response observed in fungal infections such as coccidioidomycosis, the potential for subperiosteal involvement in mycotic infections cannot be ruled out (Corr 2011; Taljanovic and Adam 2011). Finally, clinical reports of skeletal mycotic infections describe lesions that tend to be unilateral and asymmetrical throughout the skeleton (R. C. Jones and Goodwin 1981; Taljanovic and Adam 2011; Toone and Kelly 1956). Given the predilection for the axial skeleton such as in the case of tuberculosis and brucellosis, destruction is associated with hematopoiesis in the skeleton, whereby deep osteolysis is more consistent with the pathophysiology of this disease group rather than superficial lytic lesions in the appendicular skeleton as observed in M20 and M29. The symmetrical lytic lesion pattern in the Man Bac individuals is also not consistent with clinical reports of mycosis. Mycosis is therefore ruled out as a possible cause.

Leprosy is a bacterial infection caused by *Mycobacterium leprae or M. lepromatosis* that affects the skin, nasal mucosa, and peripheral nerves (Eichelmann et al. 2013; Saonere 2011). The symptoms of the disease vary along a spectrum and are highly dependent on individual immune response (Eichelmann et al. 2013). Tuberculoid leprosy is a milder form that is often noncontagious, whereas lepromatous leprosy is more systemic, infectious, and results in more severe symptoms (Eichelmann et al. 2013; Saonere 2011). Major skeletal changes in leprosy involve naso-facial destruction

with inflammatory pitting, and resorption of the terminal phalanges of the hands and feet secondary to loss of sensation from peripheral nerve or circulatory degeneration caused by the pathogen (Møller-Christensen 1961, 1978; Ortner 2003:264–265). Slow progression of resorption of the naso-palatal margins, including the anterior nasal spine, and alveolar process of the maxillary incisor area, with associated proliferative subperiosteal new bone and cortical pitting, are considered strongly diagnostic features of this disease (Møller-Christensen 1961, 1978; Møller-Christensen et al. 1952). While new bone can occur in leprosy, particularly in the lower legs, and skin granulomas can also occur, leprosy is not known to cause focal granulomatous-like lytic lesions of the long bones such as that observed in M20 and M29 (Faget and Mayoral 1944). Osteomyelitis secondary to peripheral nerve destruction in advanced stages of the disease is well documented, but as described above, the superficial lytic lesions of M20 and M29 are not characteristic of osteomyelitis (Faget and Mayoral 1944; Maas et al. 2002). The suite of cranial lesions observed in M20 is not characteristic of leprosy, as neither destructive lesions of the cranium nor proliferative or cortical pitting lesions of the nasal region were observed. Furthermore, no destructive changes to the preserved tubular hand and feet bones of M20 and M29 were observed. The absence of the cranium and the presence of only one metacarpal means leprosy cannot be ruled out as a co-morbidity in the case of the child. However, it is improbable that leprosy is responsible for lesions observed in both M20 and M29.

Treponematosis

Treponemal disease is a group of infections caused by a spirochete bacterium that primarily affects the skin but can also affect bones and other organs (Hook and Marra 1992). Four diseases, including yaws (*Treponema pallidum pertenue),* pinta (*T. carateum),* venereal syphilis (*T. pallidum pallidum),* and endemic syphilis *(T. pallidum endemicum),* have similar bacterium morphology and share similar pathogenesis (Hook and Marra 1992; Marks et al. 2014; Willcox 1974). Pinta is the only treponemal disease that does not affect bone (Willcox 1974). Each treponeme occupies a different ecological niche (Marks et al. 2014). For example, endemic syphilis is restricted to warm, arid regions of the world, whereas yaws thrives in subtropical and tropical regions (Willcox 1974). Yaws, pinta, and endemic syphilis are non-venereal treponemal diseases that are transmitted primarily by skin contact, whereas venereal syphilis has evolved to be spread primarily through sexual contact (Willcox 1974). A primary skin lesion forms at the site of inoculation within a few weeks of initial infection and subsequently resolves itself (Peeling and Hook 2006). If left untreated, the disease almost always progresses to a secondary phase. In the secondary phase, the skin rash reappears, becoming more diffuse and is associated with swelling of lymph nodes (lymphadenopathy) (Peeling and Hook 2006). The secondary phase is then followed by an asymptomatic latent phase, where the infection is contained within granulomas by the immune system (Hackett 1953b). Latency can last from three to 10 years beyond the initial infection (Hackett 1953b). Following the period of latency, except in the case of pinta, a tertiary stage begins, where necrosis of the granulomas occurs, resulting in *gummatous* lesions of skin, internal organs, and bones (Hackett 1953b; Powell and Cook 2005:15–51). Formation of the tertiary stage has been historically documented to occur in one in three untreated cases (Hackett 1953b). The tertiary stage is distinctive for its gross destruction of the face, skull, limbs, and, in the case of venereal syphilis, arterial vessels and organs (Hackett 1951; Peeling and Hook 2006). During the tertiary stage, secondary lesions stop forming (Hackett 1953b). While early treponemal lesions can heal within a few months, the late (tertiary stage) lesions can last for more than a year and leave permanent changes in bone (Hackett 1978).

These granulomatous, gummatous lesions are distinctive and specific to all treponemal diseases, and are universally accepted as strongly diagnostic in paleopathology (Harper et al. 2011; Ortner 2003:286). The so-called *caries sicca* lesions on the skull are the most well recognized lesions of the disease and are clinically and paleopathologically documented in all skeletal forms of treponemal disease (Hackett 1951:159–165, 1974; Sandison 1980). Gumma outside of the cranium can develop as focal lesions termed "superficial cavitations" within proliferative new bone on outer surfaces of long bones (Hackett 1976:362–396, 429–433). All tertiary lesions of treponemal disease are also associated with a sclerotic smoothing of the margins and base of the lesion (Hackett 1976:362–396, 429–433). Gross destruction of the palate and the nasal aperture can also occur (Hackett 1946). In the case of venereal syphilis, transplacental transmission, congenital syphilis, causes distinctive bone and dental deformations in infants and young children up until puberty (Jaffe 1972:908–910; Lewis 2017:176–177). Congenital forms are rarer in the endemic treponemes but have been reported in endemic syphilis from the Ramadi District of Iraq, and in yaws in central Java, Indonesia (Akrawi 1949; Csonka 1953; Engelhardt 1959). The three treponemes that affect bone cannot be distinguished by their skeletal expression (Harper et al. 2011).

As the above diseases are unlikely causes of the lesions, the presence of superficial cavitations within

nodes of new bone in M20 and M29 strongly suggests that the etiology of the lesions expressed is treponematosis (Fig. 5). The presence of saber shin and dactylitis supports this diagnosis. We also note here that the lytic lesions and distinct nodes of new bone in M20 and M29 correspond with dissemination through lymph nodes argued by Buckley and Dias (2002) to be the primary form of noncranial dissemination of the *Treponema pallidum* spirochete into bone. Unilateral enlargement of the sternal end of the clavicle, as observed in M29, has been noted in cases of late-onset congenital syphilis (Dax and Stewart 1939; Frangos et al. 2011; Harper et al. 2011; Lewis 2017:179; Yang 1940). This so-called Higoumenakis sign presents as layers of proliferative new bone on the sternal end of the clavicle unilaterally (Frangos et al. 2011). The lack of macroscopic or radiographic trace of proliferative subperiosteal new bone or cortical enlargement on the sternal end of M29's left clavicle makes the identification of this pathology as a clear Higoumenakis sign difficult. However, a rationale for this is explained below in consideration of co-morbidity with nutritional stress.

To allow for standardization of diagnosis of treponemal diseases, we here present threshold criteria for the designation of possible and probable cases (Table 1). Standard criteria have been presented previously by Harper et al. (2011) using a five-point system for inclusion or exclusion of cases. This system attributes a score between 1 and 5, dependent on the specificity of the lesion to treponemal disease. Non-specific lesions such as subperiosteal new bone deposit are classified as a score of 1, and lesions specific to treponemal disease, such as gummatous lesions and late stage caries sicca of multiple skeletal elements, are provided a score of 5. However, the authors do not give a minimum point score required for a sufficient diagnosis of treponemal disease in dry bone. The standardization presented here builds upon work by Harper et al. (2011) by introducing a "threshold approach" to diagnosis as recommended by Brickley and Ives (2008) for their criteria for diagnosis of scurvy, rickets, and osteomalacia and by Snoddy et al. (2018) for their criteria for scurvy diagnosis. As described above, we have employed the minimum criteria of one strongly diagnostic or two diagnostic lesions for a probable diagnosis of treponemal disease, which both of these cases demonstrate.

A recent review of global evidence for treponemal disease by Baker et al. (2020) includes a diagnostic protocol similar to the one presented here. The Baker et al. (2020) protocol divides lesions into three diagnostic strengths, consistent with treponemal infection but not diagnostic (C), strongly suggestive (ST), and pathognomonic (P). The criteria presented by Baker et al. (2020) illustrate the consensus among paleopathologists to work toward standards of diagnosis of treponemal disease. Each of the two cases presented here would score 5 out of 5 using the Harper et al. (2011) criteria for diagnosis and would be scored as having pathognomonic lesions using the Baker et al. (2020) criteria, all consistent with probable diagnoses using the threshold criteria presented here.

Nutritional disease

Not all lesions of M20 and M29 are consistent with infectious disease only (Online Table S5). The discrete deposits of new bone and cortical porosity on the posterior and anterior aspects of the zygomatic bones, and the external greater wings of the sphenoid bones and the temporal bone squama in M20 are more consistent with repeated microtrauma and hematoma formation characteristic of scurvy and not of treponemal infection, where diffuse subperiosteal new bone across the face and cranium would be expected (Samarkos et al. 2011; Snoddy et al. 2018). This individual also has evidence of anemia in the form of cribra orbitalia and porotic hyperostosis of the ectocranial vault, which may be a consequence of parasitic, infectious, and/or nutritional stress in childhood. A synergistic relationship between infectious and nutritional diseases is well documented (Chan 2000; Larsen 1995; Mata 1975; Nussenblatt and Semba 2002; Pelletier et al. 1995; Roberts 2000; Roberts and Brickley 2018; Ruiz et al. 1994), and co-morbidity between these would not be unexpected at Man Bac given the biosocial context of subsistence transition occurring at the site (Larsen 1995; Oxenham et al. 2011).

Similar to M20, there are lesions present in M29 that are more likely to result from metabolic or developmental defects than infection (Fig. 4). As outlined above, various deformities are present in the long bones of M29. While it is possible that the swelling of the distal femora is a result of the infection, the combination of bending deformities, cupping, and swelling of distal ends of multiple long bones suggests alternative etiologies for these pathologies and is particularly indicative of a demineralization disorder, such as rickets (Brickley and Ives 2008:103–107). Interactions between infectious and nutritional diseases during childhood growth is an area of ongoing study in paleopathology, and it is possible that a combination of these factors caused the long bone bowing identified in M29. The described porotic and new bone lesions of the mandible and scapulae are all diagnostic macroscopic signs of scurvy (Snoddy et al. 2018). The radiographs also revealed ground-glass osteopenia, and Trummerfeld zones (radiolucent bands within the metaphyses) in association with white lines of Frankel

Fig. 5. Strongly diagnostic and diagnostic macroscopic lesions for treponemal disease in M20 and M29. (a) Superficial focal cavitation of the medial left calcaneus (M20, diagnostic). (b) Superficial focal cavitation of the anterior lateral epicondyle of the right humerus (M20, diagnostic). (c) Superficial focal cavitation of the posterior lateral epicondyle of the right humerus (M20, diagnostic). (d) Superficial focal cavitations within a distinct node of new bone of the right distal fibular shaft (M20, strongly diagnostic). (e) Superficial focal cavitations within a distinct node of new bone of the right distal fibular shaft (M20, strongly diagnostic). (f) Focal cavitation of the right distal fibular shaft with sclerotic margins within a distinct node of new bone (M29, strongly diagnostic). (g) Superficial focal cavitation of the proximal right fibula (M20, diagnostic). (h) Focal cavitation of the right distal fibular shaft with sclerotic margins within a distinct node of new bone, same lesion as 5f. (M29, strongly diagnostic). (i) Focal cavitations of the right mid-ulnar and radial shafts with sclerotic margins within a distinct node of new bone (M29, strongly diagnostic). (Image: M. Vlok)

Table 1. Diagnostic criteria for identification of treponematosis (SD = strongly diagnostic, D = diagnostic, and S = suggestive). One SD lesion or two D lesions are required for diagnosis consistent with a probable case. One D lesion or two S lesions are required for diagnosis consistent with a possible case. Some lesions are provided for congenital cases and have been observed only in infants and children. The final column indicates which lesions were present in M20 and M29.

Lesion	Diagnostic Strength	Differential Diagnosis	Clinical Reference	Paleopathological Reference	Lesion Present
Caries sicca sequence stages 4–8: circumvallate cavitation, radial scars, serpiginous cavitation, nodular cavitation, and *caries sicca* of the ectocranium	SD		Hackett 1975, 1976:362–396	Harper et al. 2011	–
Gummatous lesions on any skeletal element: focal superficial cavitations in direct relation with nodes or expansions (enlargements) of new bone	SD		Hackett 1975, 1976:429–433	Harper et al. 2011	M20 M29
Hutchinson's incisors (congenital)	SD	Normal morphology	Hackett 1976:441; Pessoa and Galvão 2011; Stokes and Gardner 1923	Harper et al. 2011; Hillson et al. 1998; Lewis 2017:179	–
Moon's Molars (congenital)	SD	Growth disruption	Hackett 1976:441	Harper et al. 2011; Hillson et al. 1998; Lewis 2017:179	–
Congenital syphilis (Caffey's) triad: osteochondritis, bilateral thick periosteal reaction of the long bones, *and* osteomyelitis of metaphyseal ends (early congenital)	D	Non-specific osteomyelitis, infantile cortical hyperostosis, Paget's disease	Caffey 1939; Jaffe 1972:910	Lewis 2017:178	–
Caries sicca sequence stages 1–3: clustered pits, confluent clustered pits, focal superficial cavitation of the ectocranium *or* focal superficial cavitation of the cortex of long bones not within a distinct node or expansion (enlargement)	D	Mycosis, tuberculosis, Langerhans's cell histiocytosis, multiple myeloma, and other metastatic neoplasms	Hackett 1975, 1976:362–396		M20
Gross rhinomaxillary and palatal destruction (gangosa)	D	Leprosy, tuberculosis, mycosis, destructive neoplasms, trauma, leishmaniasis	Fiumara and Lessell 1970; Hackett 1951:164–168, 1975, 1976:399–401	Lewis 2017:175	–
Wimberger's corner sign (congenital): bilateral widening band of decreased calcification of the metaphyses leading to destruction	D	Non-specific osteomyelitis, trauma, scurvy	Brackett and Standley 2019; Rasool and Govender 1989	Harper et al. 2011; Lewis 2017:178	–
Mulberry (Fournier's) molars	D	Mercury use, growth disruption		Harper et al. 2011; Hillson et al. 1998; Lewis 2017:179	–
Thick periosteal new bone deposition and exostoses on the maxillae (goundou)	S	Scurvy, osteomyelitis, leprosy, infantile cortical hyperostosis, Paget's disease, genetic anemias		Buckley 2016:30; Harper et al. 2011; Lewis 2017:175	–
Higoumenakis sign: unilateral enlargement of the sternal end of the clavicle (congenital)	S	Trauma, non-specific osteomyelitis, normal variant	Dax and Stewart 1939; Yang 1940	Frangos et al. 2011; Harper et al. 2011; Lewis 2017:179	M29
Saber shin (pseudobowing of the tibia without bowing of the medullary canal)	S	Leprosy, osteomyelitis, various benign and malignant bone tumors, Paget's disease, hyperflourosis	Hackett 1951:28	Harper et al. 2011	M20 M29
Boomerang leg: true tibial bowing with bowing of medullary canal (until adolescence)	S	Rickets, skeletal dysplasias, osteogenesis imperfecta, fracture		Harper et al. 2011; Lewis 2017:175	–
Dactylitis (subperiosteal new bone enlargement of the hand and feet bones)	S	Tuberculosis, non-specific osteomyelitis, genetic anemias	Hackett 1951:30; Rasool and Govender 1989	Harper et al. 2011; Lewis 2017:178–179	M20 M29
Charcot's joint (resorption of weight bearing joints)	S	Septic arthritis, diabetes, osteoarthritis, syringomyelia, tuberculosis	Hackett 1976; Johns 1970; Sequeira 1994	Harper et al. 2011; Lewis 2017:179	–

(*continued*)

Table 1. (*continued*).

Lesion	Diagnostic Strength	Differential Diagnosis	Clinical Reference	Paleopathological Reference	Lesion Present
Opera glass fingers: diaphyseal tapering of the bone	S	Leprosy, rheumatoid arthritis, syringomyelia, diabetes, osteomyelitis, erosive osteoarthritis	Hackett 1951:153–154; B. S. Jones 1972; Swezey et al. 1972	Ortner 2003:277	–
Radiographic: saw tooth appearance of metaphyseal ends *or* macroscopic symmetrical destruction of metaphyses attributed to osteochondritis (early congenital)	S	Rickets, scurvy, trauma, tuberculosis	Jaffe 1972:910–912; Rasool and Govender 1989	Harper et al. 2011; Lewis 2017:178	–
Thick deposit of mixed active and remodeled new bone on the long bones, thickest at the midshaft (congenital), or long bone endosteal nodes or expansions (enlargements) with medullary canal intrusion	S	Paget's disease, non-specific osteomyelitis, metastatic bone tumors, tuberculosis	Hackett 1951, 1975, 1976:411–433	Harper et al. 2011; Lewis 2017:178–180	M20 M29
Saddle nose (congenital)	S	Leprosy, trauma, non-specific osteomyelitis	Fiumara and Lessell 1970; Pavithran 1987	Harper et al. 2011; Lewis 2017:177	–
High palatal arch (congenital)	S	Various congenital deformities, including Turner's syndrome and Klippel-Feil syndrome	Pavithran 1987	Lewis 2017:177	–

(radiodense lines on the metaphyseal plates of the long bones) (Fig. 4), which are further diagnostic signs of Vitamin C deficiency (Brickley and Ives 2008; Snoddy et al. 2017, 2018).

The likelihood of co-morbidity of treponemal disease with nutritional deficiency in M29, including scurvy as well as deficiency of hormones, minerals, and/or vitamins related to the mineralization process (Vitamin D, calcium, phosphorus, and/or parathyroid hormones), may be causing the concurrent thinning of cortices impacting the visibility of a clear Higoumenakis sign of congenital syphilis. As gummatous lesions usually form within localized nodes of new bone, the presence of a small lytic process on the medial end of M29's left clavicle may suggest a well-remodeled new bone deposit in a child with a high bone turnover rate also undergoing nutritional stress. The presence of a congenital expression of treponemal disease at Man Bac is then possible. In summary, M29 probably suffered from tertiary treponemal disease in association with multiple nutrient deficiencies affecting both osteoid formation and mineralization at various points in the child's lifetime. In light of more definitive evidence of nutritional stress in M29, an argument could be made for a co-morbidity of treponemal disease and Vitamin C deficiency in M20 as well.

Possible treponemal disease?

Lesions in five other individuals are also consistent with treponemal disease. However, the skeletal expression of their lesions does not provide enough diagnostic strength to allow a probable diagnosis. MB05 M5 is an infant approximately 18 months of age with endosteal enlargement of the long bones associated with superficial lytic lesions. While the radiographs demonstrate a superficial focal sclerotic response in the distal metaphysis of the left humerus and superior acromial end of the clavicle, these lesions are small (lesion is 3.9 × 1.7 mm on humerus and 3 × 3 mm on clavicle), impeding confidence that these lesions are superficial focal cavitations as described by Hackett (1976:429–433). MB05 M29 is a middle-aged adult male with dactylitis and diffuse new bone in the forearms and legs associated with endosteal enlargements. Two focal superficial lesions with sclerotic response are present on the medial distal right fibula. However, these lesions are not within a distinct node of new bone and therefore do not strictly fit the definition of superficial cavitation by Hackett. A further three individuals present with endosteal nodes/enlargements, and/or dactylitis, which are also consistent with treponemal disease (see Online Table S6). All lesions follow a postcranial pattern of lymphatic dissemination consistent with treponemal disease (Buckley and Dias 2002).

Pathophysiology of treponemal disease in M20 and M29

The presence of gummatous lesions in M20 and M29 is strongly diagnostic for treponemal disease in this early Neolithic community and, therefore, is sufficient evidence for pre-Columbian treponemal disease outside of the Americas, and represent the oldest cases in

the Asia-Pacific region. The presence of a possible Higoumenakis sign in M29 attributed to the late-onset congenital form of treponemal disease does suggest the possibility of transplacental transmission in this case. Transplacental transmission of yaws has been known to occur, albeit rarely (Engelhardt 1959). Children infrequently develop gummatous lesions, but they also have been documented to occur in yaws (Hackett 1951). Given the age of M20 it is possible that initial infection occurred in late childhood to adolescence, which is epidemiologically consistent with all treponemal diseases.

Which treponemal disease was present in Neolithic Man Bac?

We offer no attempt to diagnose which treponemal disease is responsible based solely on skeletal expression. Discussion on the uniformity of skeletal lesions of different treponemes has been dealt with elsewhere (Buckley and Dias 2002). However, the epidemiological, social, and environmental contexts of the disease do allow some discussion on the treponeme responsible. Climatically, Vietnam is within latitudinal boundaries where yaws has been historically documented (Mitjà et al. 2013). Prior to the eradication attempts of yaws by the World Health Organization in the 1950s, yaws was endemic to Vietnam, and reports as late as the 1990s demonstrate a recent history of the disease in the region (Meheus and Antal 1992). With consideration of all possible and probable cases at Man Bac, it is clear the lesions are predominantly in non-adults, with only two adults presenting lesions consistent with treponematosis and only one of these with strongly diagnostic lesions (Online Table S6). The epidemiological distribution in terms of age does suggest a non-venereal form such as yaws, where initial infection most often occurs between the ages of two and 15 years (Mitjà et al. 2013). Therefore, yaws is a possible candidate for the treponemal disease present at Man Bac. However, the climate of this region is marginal for the successful maintenance of yaws in a community. Yaws thrives in regions with average yearly temperatures of 27°C but can persist in areas of, at minimum, 21°C yearly average temperature (Hill 1953). While northern Vietnam fits into this range, in regions where temperatures are not consistent year round, yaws is even less likely to thrive (Hill 1953). In January the minimum average temperature in northern Vietnam is 12°C, and 14.3°C specifically for Ninh Binh province where Man Bac is situated (Oxenham et al. 2011). The temperature during the early Neolithic of Vietnam may have been slightly elevated compared to the present day due to the termination of the mid-Holocene Thermal Maximum at around 3000 B.C., which was marked by higher temperatures and rainfall (Oxenham et al. 2018). While there are no historic reports of endemic syphilis in the region, northern Vietnam becomes cold and dry during the winter months, which is more suitable for the endemic form. In summary, the ecological and climatic context of Man Bac allowed for the presence of all of the treponemal conditions. However, given the age of the site and epidemiology in regard to the ages of affected individuals, it is more likely a non-venereal rather than venereal form.

Social and biological conditions promoting treponemal disease at Man Bac

The ecological and social contexts of Man Bac fostered an environment that was advantageous to the spread of non-venereal treponemal disease in the community. Agricultural transitions such as that which occurred at Man Bac have been universally documented to have resulted in epidemiological transitions as farming practices encouraged sedentism, population growth, and increased susceptibility to infection due to nutritional stress (Armelagos and Cohen 1984; Cohen and Crane-Kramer 2007; Larsen 2006). In northern Vietnam this subsistence change may have led to different epidemiological pressures in the communities with no distinct decline in health, as pre-Neolithic sedentary foragers also had high disease burdens (Oxenham et al. 2018). Signs of multi-nutrient deficiency throughout the life of M20 and M29 is further supported by considerably high levels of stress identified in other dental and skeletal evidence from the site (McDonell and Oxenham 2014; Oxenham and Domett 2011).

Coastal habitations such as prehistoric Man Bac have been associated with higher yaws incidence in historical contexts due to the abundance of water and vegetation, increasing population density (Hackett 1953a:135; Kazadi et al. 2014). Furthermore, pre-industrialized agricultural communities have also been associated with increased incidence of yaws (Guimarães 1953; Hackett 1953a:135). The coastal region is also slightly warmer and more humid than inland northern Vietnam and therefore more conducive to the spread of yaws (Hill 1953).

The increase in fertility and population growth at Man Bac was likely associated with an increase in the number of infants and children within the community, who are known to be the primary transmitters of yaws (McFadden et al. 2018; Mitjà et al. 2013). Given the age-based hierarchy, possible relocation of resources to older individuals in the community may have promoted malnutrition in younger individuals, further encouraging disease transmission in children (Hill 1953; Oxenham et al. 2011). A degree of social

group cohesiveness may have further encouraged the transmission of a non-venereal form of treponematosis spread through close skin contact. The presence of a profoundly disabled individual with quadriparesis following Klippel-Feil syndrome, who required continuous and intensive care, highlights that the community was one in which individuals were highly cooperative (Oxenham et al. 2009; Tilley and Oxenham 2011).

Origins of treponemal disease at Man Bac

It is not possible at this point to determine confidently whether treponemal disease was introduced by the farmers from southern China. However, the spread of treponemal disease into MSEA with migrant farmers during the Neolithic is plausible when considering the extent of the migration and the sedentary agricultural contexts they brought with them (Bellwood and Oxenham 2008). There is no archaeological evidence for contact with other groups apart from southern Chinese farmers outside of MSEA at this time. Admixture with indigenous foragers in northern Vietnam may have enabled further transmission of treponemal disease throughout MSEA, although currently no further evidence for prehistoric treponemal disease exists in Southeast Asian skeletal collections. While we recognize that absence of evidence is not evidence of absence, and a deep antiquity of treponemal disease in MSEA is possible prior to the agricultural transition, there is no identification of human-to-human transmissive diseases (such as tuberculosis, treponematosis, or leprosy) prior to this time in MSEA despite intensive bioarchaeological research in the region (Buckley and Oxenham 2016). The evidence of infectious disease in MSEA considerably increases from the Bronze and Iron Ages (Oxenham et al. 2005; Tayles and Buckley 2004). If the treponemal disease at Man Bac is in fact yaws, the route of transmission throughout the continent would be restricted to tropical and subtropical zones. Although Man Bac is positioned at the present-day upper geographical limit of the survival of yaws, documented cases of yaws existed in southern China and Taiwan prior to worldwide eradication attempts where the climate is similar to northern Vietnam's (Hill 1953). In light of pre-eradication, clinical evidence of yaws in this region, a possible origin for the spread of treponemal disease into MSEA from farmers originating in southern China from approximately 4,000 years ago is plausible. Given the presence of treponemal disease at Man Bac, regional interactions throughout the Red River delta also present possible routes of transmission to and from other Phung Nguyen sites where archaeological material indicates contact with agricultural groups of southern China (Khoach 1980; Nguyen 2008). The implications of migration and human population interaction on the potential spread of treponemal disease into northern Vietnam is an area for further research, particularly with regard to the broader context of the timing of the introduction of treponemal disease into MSEA. Further investigation of existing and newly excavated skeletal assemblages in southern China and MSEA may provide further insight into the origins and antiquity of this disease within the region.

It can be hypothesized that, with the demographic and subsistence transition resulting in nutritional instability, and possibly the introduction of new infectious diseases with migration, the social and environmental contexts of Man Bac were suitable for the spread of treponematosis. The high rate of natural population increase at Man Bac was likely fueled by the supplementation of agricultural foods, enabling larger groups to thrive, increasing the number of individuals in the community, and further encouraging the spread of treponematosis (McFadden et al. 2018). The identification of two cases of probable tertiary treponemal disease in a northern Vietnamese Neolithic community further supports the contextual evidence for a population undergoing accelerated growth, significant social change, necessitating the navigation of interaction between two populations and one of a unified and close community wherein a treponeme could spread with relative ease.

Acknowledgments

We would like to thank Dr. Ngo Anh Son, Mr. Bui Van Khanh, and Ms. Nellissa Ling for their assistance with the radiographs, and Dr. Anne Marie E. Snoddy for input on the application of a standardized approach to treponemal disease. We thank the associate editor of *Bioarchaeology International* and three anonymous reviewers for their comments and advice in revising the manuscript.

Author Contributions

MV wrote majority of the manuscript and performed data collection and processing. HRB contributed to research design, assisted in data processing, and contributed substantially to the manuscript. MFO and KD contributed to research design, provided preliminary data, and contributed to the manuscript. TTM facilitated access to collections, assisted with the data collection, and provided Vietnamese translation of the abstract. NTM, HM, HHT, and NTH facilitated access to collections and provided essential background

knowledge for the production of this publication. TH and CH contributed radiocarbon dates for the publication and produced the supplementary information on the radiocarbon dates. All authors critically reviewed, revised, and edited the content of the manuscript.

References

Acosta, Frank L., Cynthia T. Chin, Alfredo Quiñones-Hinojosa, Christopher P. Ames, Philip R. Weinstein, and Dean Chou. 2004. Diagnosis and management of adult pyogenic osteomyelitis of the cervical spine. *Neurosurgical Focus* 17(6):1–9.

Acsádi, György, János Nemeskéri, and Kornél Balás. 1970. *History of Human Life Span and Mortality*. Akademiai kiado, Budapest, Hungary.

Akrawi, Fathallah. 1949. Is bejel syphilis? *British Journal of Venereal Diseases* 25(3):115–123.

Al-Shahed, Mona S., Hassan S. Sharif, Maurice C. Haddad, Mohamed Y. Aabed, Bassam M. Sammak, and Mohamed A. Mutairi. 1994. Imaging features of musculoskeletal brucellosis. *Radiographics* 14(2):333–348.

Armelagos, George J., and Mark Nathan Cohen. 1984. *Paleopathology at the Origins of Agriculture*. Academic Press, New York, USA.

Baker, Brenda J., Gillian Crane-Kramer, Michael W. Dee, Lesley A. Gregoricka, Maciej Henneberg, Christine Lee, Sheila A. Lukehart, David C. Mabey, Charlotte A. Roberts, and Ann L. W. Stodder. 2020. Advancing the understanding of treponemal disease in the past and present. *Yearbook of Physical Anthropology*. DOI: Early view.

Bellwood, Peter. 2005. *First Farmers: The Origins of Agricultural Societies*. Blackwell Publishing, Oxford, UK.

Bellwood, Peter, and Marc Oxenham. 2008. The expansions of farming societies and the role of the neolithic demographic transition. In *The Neolithic Demographic Transition and Its Consequences*, edited by Jean-Pierre Bocquet-Appel and Ofer Bar-Yosef. Springer Science+Business Media, Berlin, pp. 13–34.

Brackett, William Janika, and Todd B. Standley. 2019. Simulating non-accidental trauma with worsening findings: Congenital syphilis. *SN Comprehensive Clinical Medicine* 1(8):571–574.

Brickley, Megan, and Rachel Ives. 2008. *The Bioarchaeology of Metabolic Bone Disease*. Academic Press, Oxford, UK.

Brooks, Sheilagh, and Judy M. Suchey. 1990. Skeletal age determination based on the os pubis: A comparison of the Acsádi-Nemeskéri and Suchey-Brooks methods. *Human Evolution* 5(3):227–238. DOI: 10.1007/BF02437238.

Buckley, Hallie R. 2016. *Health and Disease in the Prehistoric Pacific Islands*. BAR International Series 2792. British Archaeological Reports Ltd, Oxford, UK.

Buckley, Hallie R., and George J. Dias. 2002. The distribution of skeletal lesions in treponemal disease: Is the lymphatic system responsible? *International Journal of Osteoarchaeology* 12(3): 178–188.

Buckley, Hallie R., and Marc F. Oxenham. 2016. Bioarchaeology in the Pacific islands: A temporal and geographical examination of nutritional and infectious disease. In *The Routledge Handbook of Bioarchaeology in Southeast Asia and the Pacific*, edited by Marc Fredrick Oxenham and Hallie Buckley. Routledge, London, pp. 363–388.

Buikstra, Jane E., and Douglas H. Ubelaker. 1994. *Standards for Data Collection from Human Skeletal Remains: Proceedings of a Seminar at the Field Museum of Natural History, Arkansas Archaeological Survey Research Series No. 44*. Arkansas Archaeological Survey, Fayetteville, USA.

Caffey, John. 1939. Syphilis of the skeleton in early infancy: The nonspecificity of many of the roentgenographic changes. *American Journal of Roentgenology* 42:637–655.

Campbell, G. A., L. G. Adams, and B. A. Sowa. 1994. Mechanisms of binding of *Brucella abortus* to mononuclear phagocytes from cows naturally resistant or susceptible to brucellosis. *Veterinary Immunology and Immunopathology* 41(3–4):295–306.

Chan, T. Y. K. 2000. Vitamin D deficiency and susceptibility to tuberculosis. *Calcified Tissue International* 66(6):476–478.

Cohen, Mark Nathan, and Gillian Margaret Mountford Crane-Kramer. 2007. *Ancient Health: Skeletal Indicators of Agricultural and Economic Intensification*. University Press of Florida, Gainesville.

Corr, Peter D. 2011. Musculoskeletal fungal infections. *Seminars in Musculoskeletal Radiology* 15(5):506–510.

Csonka, G. W. 1953. Clinical aspects of bejel. *British Journal of Venereal Diseases* 29(2):95–103.

d'Anastasio, Ruggero, T. Staniscia, M. L. Milia, Lamberto Manzoli, and Lorenzo Capasso. 2011. Origin, evolution and paleoepidemiology of brucellosis. *Epidemiology & Infection* 139(1): 149–156.

Davidson, Paul T., and Isaac Horowitz. 1970. Skeletal tuberculosis: A review with patient presentations and discussion. *The American Journal of Medicine* 48(1):77–84.

Dax, E. Cunningham, and R. M. Stewart. 1939. The sign of the clavicle. *British Medical Journal* 1(4084):771–772.

De la Rua-Domenech, Ricardo. 2006. Human *Mycobacterium bovis* infection in the United Kingdom: Incidence, risks, control measures and review of the zoonotic aspects of bovine tuberculosis. *Tuberculosis* 86(2):77–109.

Domett, Kate M., and Hallie R. Buckley. 2012. Large lytic cranial lesions: A differential diagnosis from pre-Angkorian Cambodia. *International Journal of Osteoarchaeology* 22(6):731–739. DOI: 10.1002/oa.1234.

Domett, Kate M., and Marc F. Oxenham. 2011. The demographic profile of the Man Bac Cemetery sample. In *Man Bac: The Excavation of a Neolithic Site in Northern Vietnam, The Biology. Terra Australis 33*, edited by Marc Fredrick Oxenham, H. Matsumura, and Nguyen Kim Dung. ANU ePress, Canberra, Australia, pp. 9–20.

Eichelmann, K., S. E. González González, J. C. Salas-Alanis, and J. Ocampo-Candiani. 2013. Leprosy. An update: Definition, pathogenesis, classification, diagnosis, and treatment. *Actas Dermo-Sifiliográficas (English Edition)* 104(7):554–563.

Engelhardt, H. K. 1959. A study of yaws (Does congenital yaws occur?). *Journal of Tropical Medicine and Hygiene* 62(10): 238–240.

Faget, G. H., and A. Mayoral. 1944. Bone changes in leprosy: A clinical and roentgenologic study of 505 cases. *Radiology* 42(1):1–13.

Fiumara, Nicholas J., and Simmons Lessell. 1970. Manifestations of late congenital syphilis: An analysis of 271 patients. *Archives of Dermatology* 102(1):78–83.

Flynn, JoAnne L., and John Chan. 2001. Immunology of tuberculosis. *Annual Review of Immunology* 19(1):93–129.

Franco, María Pía, Maximilian Mulder, Robert H. Gilman, and Henk L. Smits. 2007. Human brucellosis. *The Lancet Infectious Diseases* 7(12):775–786.

Frangos, Constantinos C., Giagkos M. Lavranos, and Christos C. Frangos. 2011. Higoumenakis' sign in the diagnosis of congenital syphilis in anthropological specimens. *Medical Hypotheses* 77(1):128–131.

Giaccai, L., and H. Idriss. 1952. Osteomyelitis due to salmonella infection. *The Journal of Pediatrics* 41(1):73–78.

Guimarães, F. Nery. 1953. Yaws in Brazil. *Bulletin of the World Health Organization* 8(1–3):225.
Hackett, Cecil John. 1946. The clinical course of yaws in Lango, Uganda. *Transactions of the Royal Society of Tropical Medicine and Hygiene* 40(3):205–227.
Hackett, Cecil John. 1951. *Bone Lesions of Yaws in Uganda*. Blackwell Scientific Publications, Oxford, UK.
Hackett, Cecil John. 1953a. Extent and nature of the yaws problem in Africa. *Bulletin of the World Health Organization* 8(1–3):127–182.
Hackett, Cecil John. 1953b. The natural history of yaws. *Transactions of the Royal Society of Tropical Medicine and Hygiene* 47(4):318–320.
Hackett, Cecil John. 1974. Possible treponemal changes in a Tasmanian skull. *Man* 9(3):436–443.
Hackett, Cecil John. 1975. An introduction to diagnostic criteria of syphilis, treponarid and yaws (treponematoses) in dry bones, and some implications. *Virchows Archive A* 368(3):229–241.
Hackett, Cecil John. 1976. *Diagnostic Criteria of Syphilis, Yaws and Treponarid (Treponematoses) and of Some Other Diseases in Dry Bones*. Springer, Berlin.
Hackett, Cecil John. 1978. Treponematoses (yaws and treponarid) in exhumed Australian Aboriginal bones. *Records of the South Australian Museum Adelaide* 17(27):307–406.
Haque, Abida K. 1990. The pathology and pathophysiology of mycobacterial infections. *Journal of Thoracic Imaging* 5(2):8–16.
Harper, Kristin N., Molly K Zuckerman, Megan L. Harper, John D. Kingston, and George J. Armelagos. 2011. The origin and antiquity of syphilis revisited: An appraisal of Old World pre-Columbian evidence for treponemal infection. *American Journal of Physical Anthropology* 146(S53):99–133. DOI: 10.1002/ajpa.21613.
Higham, C. F. W, Xie Guangmao, and Lin Qiang. 2011. The prehistory of a friction zone: First farmers and hunters-gatherers in Southeast Asia. *Antiquity* 85(328):529–543.
Hill, Kenneth R. 1953. Non-specific factors in the epidemiology of yaws. *Bulletin of the World Health Organization* 8(1–3):17.
Hillson, Simon, Caroline Grigson, and Sandra Bond. 1998. Dental defects of congenital syphilis. *American Journal of Physical Anthropology* 107(1):25–40.
Honda, Hitoshi, and Jay R. McDonald. 2009. Current recommendations in the management of osteomyelitis of the hand and wrist. *The Journal of Hand Surgery* 34(6):1135–1136.
Hook, Edward W., III, and Christina M. Marra. 1992. Acquired syphilis in adults. *New England Journal of Medicine* 326(16):1060–1069.
Hume, David A. 2006. The mononuclear phagocyte system. *Current Opinion in Immunology* 18(1):49–53.
Ikpeme, I. A., N. E. Ngim, and A. A. Ikpeme. 2010. Diagnosis and treatment of pyogenic bone infections. *African Health Sciences* 10(1):82–88.
Jaffe, Henry Lewis. 1972. *Metabolic, Degenerative, and Inflammatory Diseases of Bones and Joints*. Lea and Febiger, London.
Johns, David. 1970. Syphilitic disorders of the spine: Report of two cases. *The Journal of Bone and Joint Surgery. British Volume* 52(4):724–731.
Jones, B. S. 1972. Doigt en lorgnette and concentric bone atrophy associated with healed yaws osteitis: Report of two cases. *The Journal of Bone and Joint Surgery. British Volume* 54(2):341–345.
Jones, Rebecca K., Philip J. Piper, Colin P. Groves, Tuấn Nguyễn Anh, Mai Huong Nguyễn Thi, Hảo Nguyễn Thị, Trinh Hiep Hoang, and Marc F. Oxenham. 2019. Shifting subsistence patterns from the terminal Pleistocene to late Holocene: A regional Southeast Asian analysis. *Quaternary International* 529:47–56.
Jones, Roger C., and Robert A. Goodwin Jr. 1981. Histoplasmosis of bone. *The American Journal of Medicine* 70(4):864–866.
Kazadi, Walter M., Kingsley B. Asiedu, Nsiire Agana, and Oriol Mitjà. 2014. Epidemiology of yaws: An update. *Clinical Epidemiology* 6:119.
Key, J. Albert. 1940. The pathology of tuberculosis of the spine. *The Journal of Bone and Joint Surgery* 22(3):799–806.
Kharbanda, Y., and R. S. Dhir. 1991. Natural course of hematogenous pyogenic osteomyelitis (A retrospective study of 110 cases). *Journal of Postgraduate Medicine* 37(2):69.
Khoach, Nguyen Ba. 1980. Phung Nguyen. *Asian Perspectives* 23(1):23–54.
Knechel, Nancy A. 2009. Tuberculosis: Pathophysiology, clinical features, and diagnosis. *Critical Care Nurse* 29(2):34–43.
LaFond, Edward M. 1958. An analysis of adult skeletal tuberculosis. *The Journal of Bone and Joint Surgery* 40(2):346–364.
Larsen, Clark S. 1995. Biological changes in human populations with agriculture. *Annual Review of Anthropology* 24(1):185–213. DOI: 10.1146/annurev.an.24.100195.001153.
Larsen, Clark S. 2006. The agricultural revolution as environmental catastrophe: Implications for health and lifestyle in the Holocene. *Quarternary International* 150(1):12–20. DOI: 10.1016/j.quaint.2006.01.004.
Lewis, Mary E. 2017. *Paleopathology of Children: Identification of Pathological Conditions in the Human Skeletal Remains of Non-adults*. Academic Press, London.
Lipson, Mark, Olivia Cheronet, Swapan Mallick, Nadin Rohland, Marc Oxenham, Michael Pietrusewsky, Thomas Oliver Pryce, Anna Willis, Hirofumi Matsumura, and Hallie Buckley. 2018. Ancient genomes document multiple waves of migration in Southeast Asian prehistory. *Science* 361(6397):92–95. DOI: 10.1126/science.aat3188.
Maas, Marioo, Erik J. Slim, Agnes F. Heoksma, Ad J. van der Kleij, Erik M. Akkerman, Gerardd J. den Heeten, and William R. Faber. 2002. MR imaging of neuropathic feet in leprosy patients with suspected osteomyelitis. *International Journal of Leprosy and Other Mycobacterial Diseases* 70(2):97–103.
Marks, Michael, Anthony W. Solomon, and David C. Mabey. 2014. Endemic treponemal diseases. *Transactions of the Royal Society of Tropical Medicine and Hygiene* 108(10):601–607.
Mata, Leonardo J. 1975. Malnutrition-infection interactions in the tropics. *The American Journal of Tropical Medicine and Hygiene* 24(4):564–574.
Matsumura, Hirofumi. 2011a. Quantitative and qualitative dental-morphology at Man Bac. In *Man Bac: The Excavation of a Neolithic Site in Northern Vietnam, The Biology. Terra Australis 33*, edited by Marc Fredrick Oxenham, Hirofumi Matsumura and Nguyen Kim Dung. ANU ePress, Canberra, Australia, pp. 43–63.
Matsumura, Hirofumi. 2011b. Quantitative cranio-morphology at Man Bac. In *Man Bac: The Excavation of a Neolithic Site in Northern Vietnam. The Biology, Terra Australis 33*, edited by Marc Fredrick Oxenham, Hirofumi Matsumura, and Nguyen Kim Dung. ANU ePress, Canberra, Australia, pp. 21–32.
Matsumura, Hirofumi, Hsiao-chun Hung, Charles Higham, Chi Zhang, Mariko Yamagata, Lan Cuong Nguyen, Zhen Li, Xuechun Fan, Truman Simanjuntak, and Adhi Agus Oktaviana. 2019. Craniometrics reveal "two layers" of prehistoric human dispersal in Eastern Eurasia. *Scientific Reports* 9(1):1451.
Matsumura, Hirofumi, and Marc Oxenham. 2013a. Eastern Asia and Japan: Human biology. In *The Encyclopedia of Global Human Migration*, edited by Immanuel Ness. Wiley-Blackwell, Chichester, UK, pp. 217–223.
Matsumura, Hirofumi, and Marc Oxenham. 2013b. Population dispersal from East Asia into Southeast Asia: Evidence from cranial and dental morphology. In *Bioarchaeology of East Asia: Movement, Contact, Health*, edited by Ekaterina A. Pechenkina and M. F. Oxenham. University Press of Florida, Gainesville, pp. 179–212.

Matsumura, Hirofumi, and Marc Oxenham. 2014. Demographic transitions and migration in prehistoric East/Southeast Asia through the lens of nonmetric dental traits. *American Journal of Physical Anthropology* 155(1):45–65. DOI: 10.1002/ajpa.22537.

Matsumura, Hirofumi, Marc F. Oxenham, Yukio Dodo, Kate Domett, Nguyen Kim Thuy, Nguyen Lan Cuong, Nguyen Kim Dung, Damien Huffer and Mariko Yamagata. 2008. Morphometric affinity of the Late Neolithic human remains from Man Bac, Ninh Binh Province, Vietnam: Key skeletons with which to debate the "two layer" hypothesis. *Anthropological Science* 116(2):135–148. DOI: 10.1537/ase.070405

Mays, Simon. 2012. The relationship between paleopathology and the clinical sciences. In *A Companion to Paleopathology*, edited by Anne L. Grauer. Wiley-Blackwell, Oxford, UK, pp. 285–309.

McColl, Hugh, Fernando Racimo, Lasse Vinner, Fabrice Demeter, Takashi Gakuhari, J Víctor Moreno-Mayar, George Van Driem, Uffe Gram Wilken, Andaine Seguin-Orlando, and Constanza De la Fuente Castro. 2018. The prehistoric peopling of Southeast Asia. *Science* 361(6397):88–92. DOI: 10.1126/science.aat3628.

McDonell, Amy, and Marc F. Oxenham. 2014. Localised primary canine hypoplasia: implications for maternal and infant health at Man Bac, Vietnam, 4000–3500 years BP. *International Journal of Osteoarchaeology* 24(4):531–539. DOI: 10.1002/oa.2239.

McFadden, Clare, Hallie Buckley, Sian E. Halcrow, and Marc F. Oxenham. 2018. Detection of temporospatially localized growth in ancient Southeast Asia using human skeletal remains. *Journal of Archaeological Science* 98:93–101. DOI: 10.1016/j.jas.2018.08.010.

Meheus, André, and G. M. Antal. 1992. The endemic treponematoses: Not yet eradicated. *World Health Statistics Quarterly* 45:228–228.

Mehmet, F. G., G. Ali, N. Kemal, Ç. Remzi, S. Jale, D. Bunyamin, and A. Celal. 2002. Musculoskeletal involvement in brucellosis in different age groups: A study of 195 cases. *Swiss Medical Weekly* 132(0708).

Miller, G. A. H., Mark Ridley, and W. E. Medd. 1963. Typhoid osteomyelitis of the spine. *British Medical Journal* 1(5337):1068.

Mitjà, Oriol, Kingsley Asiedu, and David Mabey. 2013. Yaws. *The Lancet* 381(9868):763–773. DOI: 10.1016/S0140-6736(12)62130-8.

Møller-Christensen, Vilhelm. 1961. *Bone Changes in Leprosy*. Munksgaard, Copenhagen.

Møller-Christensen, Vilhelm. 1978. *Leprosy Changes of the Skull*. Odense University Press, Odense, Denmark.

Møller-Christensen, Vilhelm, Sigvald N. Bakke, Reider S. Melsom, and Erik Waaler. 1952. Changes in the anterior nasal spine and the alveolar process of the maxillary bone in leprosy. *International Journal of Leprosy* 20:335–340.

Moorrees, Coenraad F. A., Elizabeth A. Fanning, and Edward E. Hunt Jr. 1963. Age variation of formation stages for ten permanent teeth. *Journal of Dental Research* 42(6):1490–1502.

Nguyen, Kim Dung. 2008. The scientific cooperation program at Man Bac (2004–2007): Results and questions. Paper presented at the International Forum on the Prehistoric Man Bac Site, The Institute of Archaeology, Vietnam Academy of Social Sciences Institute, Hanoi.

Nussenblatt, Veronique, and Richard D. Semba. 2002. Micronutrient malnutrition and the pathogenesis of malarial anemia. *Acta Tropica* 82(3):321–337.

Ortner, Donald J. 2003. *Identification of Pathological Conditions in Human Skeletal Remains*. Academic Press, San Diego, USA.

Ortner, Donald J. 2011. Human skeletal paleopathology. *International Journal of Paleopathology* 1(1):4–11.

Oxenham, Marc, and Hallie Buckley. 2016. *The Routledge Handbook of Bioarchaeology in Southeast Asia and the Pacific Islands*. Routledge, New York.

Oxenham, Marc F., and Kate M. Domett. 2011. Palaeohealth at Man Bac. In *Man Bac: The Excavation of a Neolithic Site in Northern Vietnam. The Biology, Terra Australis 33*. edited by Marc Fredrick Oxenham, Hirofumi Matsumura, and Nguyen Kim Dung. ANU ePress, Canberra, Australia, pp. 77–93.

Oxenham, Marc Fredrick, Hirofumi Matsumura, and Nguyen Kim Dung, eds. 2011. *Man Bac: The Excavation of a Neolithic Site in Northern Vietnam. The Biology, Terra Australis 33*. ANU ePress, Canberra, Australia.

Oxenham, Marc F., Philip J. Piper, Peter Bellwood, Chi Hoang Bui, Khanh Trung Kien Nguyen, Quoc Manh Nguyen, Fredeliza Campos, Cristina Castillo, Rachel Wood, and Carmen Sarjeant. 2015. Emergence and diversification of the neolithic in southern Vietnam: Insights from coastal Rach Nui. *The Journal of Island and Coastal Archaeology* 10(3):309–338.

Oxenham, Marc F., Nguyen Kim Thuy, and Nguyen Lan Cuong. 2005. Skeletal evidence for the emergence of infectious disease in Bronze and Iron Age northern Vietnam. *American Journal of Physical Anthropology* 126(4):359–376. DOI: 10.1002/ajpa.20048.

Oxenham, Marc F., Lorna Tilley, Hirofumi Matsumura, Lan Cuong Nguyen, Kim Thuy Nguyen, Kim Dung Nguyen, Kate Domett, and Damien Huffer. 2009. Paralysis and severe disability requiring Intensive care in neolithic Asia. *Anthropological Science* 117(2):107–112. DOI: 10.1537/ase.081114.

Oxenham, Marc F., Hiep Hoang Trinh, Anna Willis, Rebecca K Jones, Kathryn Domett, Cristina Castillo, Rachel Wood, Peter Bellwood, Monica Tromp, and Ainslee Kells. 2018. Between foraging and farming: Strategic responses to the holocene thermal maximum in Southeast Asia. *Antiquity* 92(364):940–957. DOI: 10.15184/aqy.2018.69.

Pavithran, Kuyyalil. 1987. Acquired syphilis in a patient with late congenital syphilis. *Sexually Transmitted Diseases* 14(2):119–121.

Peeling, Rosanna W., and Edward W. Hook III. 2006. The pathogenesis of syphilis: The great mimicker, revisited. *The Journal of Pathology: A Journal of the Pathological Society of Great Britain and Ireland* 208(2):224–232.

Pelletier, David L., Edward A. Frongillo Jr., Dirk G. Schroeder, and Jean-Pierre Habicht. 1995. The effects of malnutrition on child mortality in developing countries. *Bulletin of the World Health Organization* 73(4):443.

Pessoa, Larissa, and Virgilio Galvão. 2011. Clinical aspects of congenital syphilis with Hutchinson's triad. *Case Reports* 2011: bcr1120115130.

Phenice, Terrell Wayne. 1969. A newly developed visual method of sexing the os pubis. *American Journal of Physical Anthropology* 30(2):297–301.

Pitt, Michael J. 1995. Rickets and osteomalacia. In *Diagnosis of Bone and Joint Disorders*, edited by Donald Resnick. Saunders, Philadelphia, pp. 1885–1922.

Powell, Mary Lucas, and Della Collins Cook. 2005. *The Myth of Syphilis: The Natural History of Treponematosis in North America*. University Press of Florida, Gainesville.

Rana, Rich S., Jim S. Wu, and Ronald L. Eisenberg. 2009. Periosteal reaction. *American Journal of Roentgenology* 193(4):259–272.

Rasool, M. N., and S. Govender. 1989. The skeletal manifestations of congenital syphilis. A review of 197 cases. *The Journal of Bone and Joint Surgery. British Volume* 71(5):752–755.

Resnick, Donald, ed. 1995a. *Diagnosis of Bone and Joint Disorders*. Saunders, Philadelphia.

Resnick, Donald. 1995b. Hypervitaminosis and hypovitaminosis. In *Diagnosis of Bone and Joint Disorders*, edited by Donald Resnick. Saunders, Philadelphia, pp. 3343–3352.

Resnick, Donald, and Gen Niwayama. 1995. Osteomyelitis, septic arthritis and soft tissue infection: Organisms. In *Diagnosis of Bone and Joint Disorders*, edited by Donald Resnick. Saunders, Philadelphia, pp. 2448–2558.

Ridley, N., M. I. Shaikh, D. Remedios, and R. Mitchell. 1998. Radiology of skeletal tuberculosis. *Orthopedics* 21(11):1213–1220.

Roberts, Charlotte. 2000. Infectious disease in biocultural perspective: Past, present and future work in Britain. In *Human Osteology in Archaeology and Forensic Science*, edited by Margaret Cox and Simon Mays. Greenwich Medical Media, London, pp. 145–162.

Roberts, Charlotte. 2012. Re-emerging infections: Developments in bioarchaeological contributions to understanding tuberculosis. In *A Companion to Paleopathology*, edited by Anne L. Grauer. Wiley-Blackwell, Oxford, UK, pp. 434–457.

Roberts, Charlotte. 2019. Infectious disease: Introduction, periostosis, periostitis, osteomyelitis, and septic arthritis. In *Ortner's Identification of Pathological Conditions in Human Skeletal Remains,* edited by Jane E. Buikstra. 3rd ed. Elsevier, San Diego, pp. 285–319.

Roberts, Charlotte A., and Megan Brickley. 2018. Infectious and metabolic diseases: A synergistic relationship. In *Biological Anthropology of the Human Skeleton*, edited by M. Anne Katzenberg and Anne L. Grauer. John Wiley & Sons, New York, pp. 415–446.

Roberts, Charlotte A., and Jane E. Buikstra. 2019. Bacterial infections. In *Ortner's Identification of Pathological Conditions in Human Skeletal Remains,* edited by Jane E. Buikstra. 3rd ed. Elsevier, San Diego, pp. 321–439.

Ruiz, Bernardo, Jennifer Carlton Rood, Elizabeth T. H. Fontham, Gray T. Malcom, Fred M. Hunter, Mahboob Sobhan, William D. Johnson, and Pelayo Correa. 1994. Vitamin C concentration in gastric juice before and after anti–*Helicobacter pylori* treatment. *American Journal of Gastroenterology* 89(4):533–539.

Samarkos, Michael, Charis Giannopoulou, Eleni Karantoni, Vassileios Papastamopoulos, Ioannis Baraboutis, and Athanassios Skoutelis. 2011. Syphilitic periostitis of the skull and ribs in a HIV positive patient. *Sexually Transmitted Infections* 87(1): 44–45.

Sandison, A. T. 1980. Notes on some skeletal changes in pre-European contact Australian aborigines. *Journal of Human Evolution* 9(1):45–47.

Saonere, Jyotsna A. 2011. Leprosy: An overview. *Journal of Infectious Diseases and Immunity* 3(14):233–243.

Sawada, Junmei, Nguyen Kim Thuy, and Nguyen Anh Tuan. 2011. Faunal remains at Man Bac. In *Man Bac: The Excavation of a Neolithic Site in Northern Vietnam, The Biology. Terra Australis 33*, edited by Marc Fredrick Oxenham, Hirofumi Matsumura, and Nguyen Kim Dung. ANU ePress, Canberra, Australia, pp. 105–116.

Scheuer, Louise, and Sue Black. 2000. *Developmental Juvenile Osteology.* Academic Press, Oxford, UK.

Sequeira, W. 1994. The neuropathic joint. *Clinical and Experimental Rheumatology* 12(3):325–337.

Snoddy, Anne Marie E., Julia Beaumont, Hallie R. Buckley, Antony Colombo, Siân E Halcrow, Rebecca L. Kinaston, and Melandri Vlok. 2020. Sensationalism and speaking to the public: Scientific rigour and interdisciplinary collaborations in palaeopathology. *International Journal of Paleopathology* 28:88–91.

Snoddy, Anne Marie E., Hallie R. Buckley, Gail E. Elliott, Vivien G. Standen, Bernardo T. Arriaza, and Siân E. Halcrow. 2018. Macroscopic features of scurvy in human skeletal remains: A literature synthesis and diagnostic guide. *American Journal of Physical Anthropology* 167(4):876–895. DOI: 10.1002/ajpa.23699.

Snoddy, Anne Marie E., Siân E. Halcrow, Hallie R. Buckley, Vivien G. Standen, and Bernardo T. Arriaza. 2017. Scurvy at the agricultural transition in the Atacama Desert (ca 3600–3200 BP): Nutritional stress at the maternal-foetal interface? *International Journal of Paleopathology* 18:108–120. DOI: 10.1016/j.ijpp.2017.05.011.

Stokes, John H., and Boyd S. Gardner. 1923. The demonstration of unerupted Hutchinson's teeth by the roentgen ray. *Journal of the American Medical Association* 80(1):28–29.

Stuart-Macadam, Patty. 1985. Porotic hyperostosis: Representative of a childhood condition. *American Journal of Physical Anthropology* 66(4):391–398.

Swezey, Robert L., David M. Bjarnason, Stanley J. Alexander, and D. B. Forrester. 1972. Resorptive arthropathy and the operaglass hand syndrome. *Seminars in Arthritis and Rheumatism* 2(3):191–244.

Taljanovic, Mihra S., and Rodney D. Adam. 2011. Musculoskeletal coccidioidomycosis. *Seminars in Musculoskeletal Radiology* 15(5):511–526.

Tanabe, Susumu, Yoshiki Saito, Quang Lan Vu, Till J. J. Hanebuth, Quang Lan Ngo, and Akihisa Kitamura. 2006. Holocene evolution of the Song Hong (Red River) delta system, northern Vietnam. *Sedimentary Geology* 187(1–2):29–61.

Tayles, Nancy, and Hallie R. Buckley. 2004. Leprosy and tuberculosis in Iron Age Southeast Asia? *American Journal of Physical Anthropology* 125(3):239–256. DOI: 10.1002/ajpa.10378.

Temple, Daniel H. 2010. Patterns of systemic stress during the agricultural transition in prehistoric Japan. *American Journal of Physical Anthropology* 142(1):112–124. DOI: 10.1002/ajpa.21208.

Teo, Harvey E. L., and Wilfred C. G. Peh. 2004. Skeletal tuberculosis in children. *Pediatric Radiology* 34(11):853–860.

Tilley, Lorna, and Marc F. Oxenham. 2011. Survival against the odds: Modeling the social implications of care provision to seriously disabled individuals. *International Journal of Paleopathology* 1(1):35–42. DOI: 10.1016/j.ijpp.2011.02.003.

Tilley, Lorna, and Marc F. Oxenham. 2016. Reflections on life and times in Neolithic Vietnam: One person's story. In *The Routledge Handbook of Bioarchaeology in Southeast Asia and the Pacific*, edited by Marc Fredrick Oxenham and Hallie Buckley. Routledge, London, pp. 95–113.

Toizumi, Takeji, Nguyen Kim Thuy, and Junmei Sawada. 2011. Fish remains at Man Bac. In *Man Bac: The Excavation of a Neolithic Site in Northern Vietnam. The Biology, Terra Australis 33*, edited by Marc Fredrick Oxenham, Hirofumi Matsumura, and Nguyen Kim Dung. ANU ePress, Canberra, Australia, pp. 117–126.

Toone, Elam C., Jr., and John Kelly. 1956. Joint and bone disease due to mycotic infection. *Transactions of the American Clinical and Climatological Association* 67:91–103.

Turgut, Mehmet. 2001. Spinal tuberculosis (Pott's disease): Its clinical presentation, surgical management, and outcome. A survey study on 694 patients. *Neurosurgical Review* 24(1):8–13.

Ubelaker, Douglas H. 1999. *Human Skeletal Remains: Excavation, Analysis, Interpretation*. 3rd ed. Aldine Manuals on Archaeology. Taraxacum Press, Washington, D.C.

Vohra, Rajeev, Harinder S. Kang, Sameer Dogra, Radha R. Saggar, and Rajan Sharma. 1997. Tuberculous osteomyelitis. *The Journal of Bone and Joint Surgery. British Volume* 79(4):562–566.

Weston, Darlene A. 2012. Nonspecific infection in paleopathology: Interpreting periosteal reactions. In *A Companion to Paleopathology*, edited by Anne L Grauer. John Wiley & Sons, Chichester, UK, pp. 492–512.

Willcox, R. R. 1974. Changing patterns of treponemal disease. *British Journal of Venereal Diseases* 50(3):169.

World Health Organization. 2013. *Global Tuberculosis Report 2013.*

Yang, K. L. 1940. Clavicle sign of late congenital syphilis: Review of literature and report of six cases. *Archives of Dermatology and Syphilology* 41(6):1060–1065.

Zuckerman, Molly K., Kristin N. Harper, and George J. Armelagos. 2016. Adapt or die: Three case studies in which the failure to adopt advances from other fields has compromised paleopathology. *International Journal of Osteoarchaeology* 26(3):375–383.

APPENDIX 5:

INTERNATIONAL JOURNAL OF PALEOPATHOLOGY PAPER

Subadult nutritional stress during the agricultural transition in Southeast Asia: perspectives from a Neolithic site in Northern Vietnam

Vlok, M. Oxenham, M.F. Domett, K. Hiep, H.T. Minh, T.T. Mai Huong, N.T, Matsumura, H. McFadden, C, Nghia, T.H and Buckley, H.R.

Abstract

Objective: Nutritional diseases including scurvy and rickets in subadults were assessed at the Neolithic site of Man Bac to investigate nutritional stress during the agricultural transition in Mainland Southeast Asia (MSEA).

Materials: Forty-four human skeletons under the age of 20 years were assessed.

Methods: Lesions were recorded macroscopically and radiographically. Differential diagnosis using prior established palaeopathological diagnostic criteria on the identification of nutritional disease was completed.

Results: Seventy-nine percent of subadults met the criteria for probable scurvy and 32% met the criteria for probable rickets. All individuals with rickets presented with co-morbidity of scurvy. Scurvy levels were high across all subadult age cohorts, whereas rickets was especially high between 6 months to 1 year of age.

Conclusions: High levels of micronutrient deficiency in subadults at Man Bac were likely due to a combination of decreased dietary diversity, high pathogen load and increased population stress. Calcium stores in breastmilk were likely insufficient to prevent calcium deficiency resulting in a peak of rickets following 6 months of age.

Significance: This is the first subadult investigation of specific nutritional disease in MSEA and demonstrates an increase in nutritional stress during the Neolithic transition in Northern Vietnam.

Limitations: Subperiosteal new bone deposits can also be part of the normal growth process in infants, therefore identification of levels of scurvy in young infants needs further consideration.

Suggestions for further research: Man Bac does not represent the entire Neolithic transition of MSEA. Further work in diagnosing nutritional disease in other subadult cohorts throughout MSEA is required.

Keywords: health, agriculture, nutritional disease, scurvy, rickets, diet

1. Introduction

An increase in the prevalence of infectious and nutritional diseases with the agricultural transition is well recognised in bioarchaeology. However, the effect of this transition globally has demonstrated considerable regional variation (Bocquet-Appel et al. 2008; Eshed et al. 2010; Oxenham 2006; Snoddy et al. 2017; Temple and Larsen 2013). Specifically, work by Tayles et al. (2000), Halcrow et al. (2013), Oxenham (2006) and Oxenham et al. (2018) have shown that in Mainland Southeast Asia (MSEA) the intensification of agriculture was not associated with a distinct decline in health. However, previous research has focused on non-specific stress markers and the systematic study of specific nutritional disease during the agricultural transition has not been attempted. Regional differences in the impact of agricultural transitions on health may be related to variations in climate, the types of domesticated food produced, social structure, and whether the subsistence shift occurred through local innovation or was introduced from other human groups (Bellwood and Oxenham 2008; Larsen 1995).

Subadults are the most sensitive indicators of health in a population and due to their rapid bone development, disease is likely to be more visible in this cohort than in adults (Halcrow et al. 2016; Lewis 2017). The subadult cohort of a skeletal sample also represents those individuals who did not survive the general disease pressures affecting the wider population (Lewis 2017).

1.1 Nutritional stress with the introduction of agricultural foods

Reduction of dietary diversity, coupled with a reliance on domesticated cereals for energy requirements may have also led to deficiencies of many micronutrients in prehistoric agricultural societies (Brickley and Ives 2010; Larsen 2006). Depending on the cereal, insufficient levels in micronutrients may have caused associated clinical deficiencies (Bouis and Welch 2010; Larsen 2006; Pettifor 2004; Snoddy et al. 2017).

The bioavailability of these micronutrients is further reduced by other *antinutrient* compounds in crops. Compounds such as phytates, tannins and other polyphenolics inhibit

absorption (Bouis and Welch 2010). In contrast, compounds including certain organic acids, fatty acids and beta carotene from diverse food types such as fruits, vegetables, meat, human breast milk, seafoods and tropical nuts promote the bioavailability of micronutrients from cereals (Bouis and Welch 2010). However, the interaction of micronutrient deficiency and agricultural dependency is complex, particularly in light of mixed subsistence bases or where foraging has been supplemented by agricultural efforts. Micronutrient depleted crops may be supplemented by diverse foraged and hunted foods. Finally, the threshold for micronutrient intake sufficiency in the body is further impacted by pathogen load, where the body's requirement for micronutrients increases in order to fight infection (Carr and Maggini 2017; Ekiz et al. 2005).

Only a certain number of micronutrient deficiencies affect the skeleton macroscopically. These include scurvy (Vitamin C deficiency), rickets (Vitamin D, calcium or phosphate deficiency), hypovitaminosis A (Vitamin A deficiency), pellagra (Vitamin B3 deficiency) as well as the iron deficiency, folate and B12 deficiency anaemias. Scurvy and rickets have well established methods for diagnosis in palaeopathology (Brickley and Ives 2010; Ortner 2003; Ortner and Ericksen 1997; Snoddy et al. 2018), and are therefore useful for investigating micronutrient deficiency in prehistory.

1.2 The Agricultural Transition in South East Asia

Over 4000 years ago, farmers from Southern China migrated to MSEA and interacted with local indigenous foragers (Bellwood and Oxenham 2008). This migration prompted a subsistence transition with the introduction of domesticated pigs and dogs, and rice and/or millet farming (Castillo 2011; Jones et al. 2019; Piper et al. 2014; Weber et al. 2010). However, variation within MSEA as to the degree of adoption of agriculture likely led to a heterogenous impact on health (King et al. 2017; Oxenham and Tayles 2006). Foraging supplemented farming at many, if not all, sites in the region, which may have provided a buffer to nutritional deficiencies caused by a reliance on a single staple (Castillo et al. 2018; Higham and Thosarat 2005; Jones et al. 2019; Oxenham 2015; Oxenham et al. 2011). Indeed, full agricultural dependence did not perhaps occur until as late as the Iron Age (500BC to 500AD; see Table 1 for time periods in MSEA) with the intensification of wet rice agriculture and the construction of moated settlements (Halcrow et al. 2016; Higham 2007; Higham et al. 2014; King et al. 2014; McGrath and Boyd 2001). Intensification and eventual agricultural dependency in MSEA occurred gradually which is thought to have ameliorated

the impact of agriculture on health compared to other regions of the world (Newton et al. 2013; Oxenham and Tayles 2006).

***Table 1**: Approximate dates for time periods in MSEA. Note that there is considerable intraregional variation in the timing of these periods.*

Time Period	Approximate Dates	References
Pre-Neolithic	Before 2300 BC	(Oxenham et al. 2018)
Neolithic	2300-1000 BC	(Bellwood et al. 2011; Higham et al. 2019b; Higham et al. in press; Vlok et al. in press)
Bronze Age (Metal Age)	1000-500BC	(Higham et al. 2011; Higham et al. 2019b; Higham et al. in press)
Iron Age (Metal Age)	500BC-500AD	(Higham et al. 2019a; Higham et al. 2019b)

It is important to recognise that initial adoption and subsequent intensification of rice agriculture are two distinct processes, with adoption occurring in the Neolithic, and intensification leading to dependence on rice as a staple occurring through the Metal Ages. While significant research describes the health impacts of intensification, the impacts on health of the initial adoption has not been comprehensively assessed, with the exception of Neolithic Khok Phanom Di in Southern Thailand (Tayles 1999). Neolithic sites in MSEA are marked by extraordinarily high fertility and rate of natural population increase, demonstrating significant demographic changes during the initial agricultural transition in the region that likely impacted health (McFadden et al. 2018). Given the importance of this period for understanding the impacts of subsistence transition in the past, further research into health at Neolithic sites in MSEA may elucidate potential variation of the initial transition and eventual dependence on agriculture in the region.

The site of Man Bac, an early Neolithic site in Northern Vietnam, is characterised by a high fertility rate, a high rate of natural population increase and well preserved subadults in the assemblage (McFadden et al. 2018). Over 60% of the total skeletal assemblage (n=101) is under the age of 20, an expected prevalence for a population undergoing demographic transition (Oxenham et al. 2011). The habitation of Man Bac captures the initial stages of the adoption of agriculture and is the only site in MSEA with direct evidence for cohabitation of local foragers with migrant farmers (Lipson et al. 2018; Matsumura and Oxenham 2013; Matsumura and Oxenham 2014; McColl et al. 2018). Assessment of the subadults from the Man Bac assemblage therefore provides a unique lens through which to view the initial

ecological, social and biological conditions of the adoption of agriculture in MSEA and any impact on health.

This paper aims to explore the nutritional impact of the initial adoption of farming in a subtropical community from Neolithic Northern Vietnam. In order to achieve this, we analyse the skeletal evidence of rickets and scurvy in the subadult cohort of Man Bac.

2. Methods and Materials

2.1 The site: Man Bac

Man Bac is a habitation and burial site in Ninh Binh province of Northern Vietnam, dating to 3906-3523 cal BP, excavated in 1999, 2005 and 2007 (Oxenham et al. 2011; Vlok et al. in press). Today the site is on a lowland coastal plain surrounded by limestone karsts. The climate is subtropical, with two distinct seasons, a hot and cold season, where high levels of humidity are sustained year-round. In the past, the surrounding ecology likely included riverine, coastal and estuarine flora and fauna (Tanabe et al. 2006). Storms including large typhoons are common in the region today and likely also occurred in prehistory, probably disrupting agricultural efforts (Oxenham 2006). The site is associated with the Phung Ngyuen period known for early agriculture, distinct pottery designs, and interactions with Southern Chinese farmers (Hiep and Phung 2004; Oxenham et al. 2011). Long grain rice phytoliths were found within the cultural layers of Man Bac, similarly identified at other Phung Nguyen sites (Bellwood and Oxenham 2008; Jones et al. 2019; Mai Huong 2013; Mai Huong 2016; Willis and Oxenham 2013). The remains of domesticated pigs and a lower diversity of faunal taxa when compared to pre-Neolithic forager sites of Northern Vietnam, has been noted (Jones et al. 2019; Oxenham et al. 2018; Sawada et al. 2011). However, preliminary carbon isotope results suggest a lower reliance on C3 plants, such as rice, than subsequent Bronze and Iron Age assemblages in Vietnam (Oxenham et al. 2011; Yoneda 2008). Along with faunal evidence demonstrating a continued exploitation of marine, freshwater, estuarine and terrestrial resources, a mixed subsistence base of foraging and farming is proposed for Man Bac (Jones 2017; Jones et al. 2019; Sawada et al. 2011; Toizumi et al. 2011).

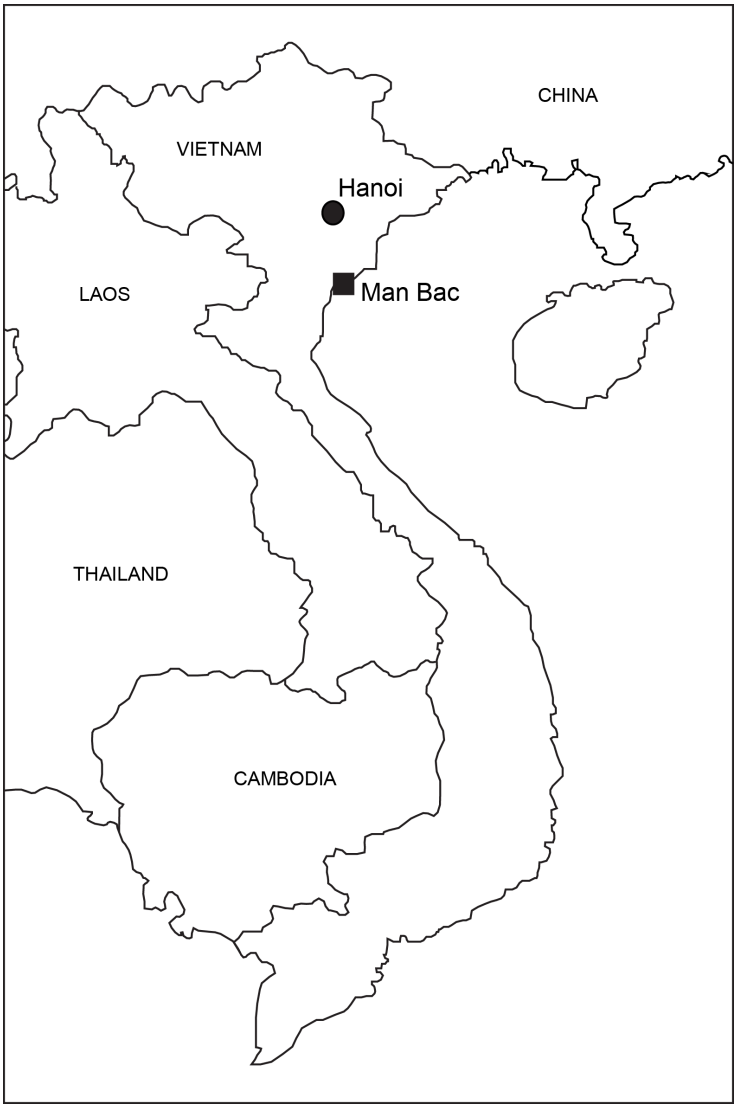

Figure 1: *Location of Man Bac. The present day capital city of Hanoi is provided for comparison.*

2.2 The sample

Forty-four subadults under the age of 20 years were assessed for this study. Individuals up to the age of 20 were considered as subadults on the grounds of continued biological development of the skeleton until this age (Scheuer and Black 2000). Unless stated otherwise, the term assemblage refers to the subadult portion of the Man Bac assemblage. More than half of the assemblage had a minimum of 75% completeness of the skeleton, unlike most Southeast Asian sites where skeletons are often poorly preserved.

Skeletal surfaces exhibited minimal to slight surface erosion (Grade 0 to 1 of McKinley (2004)). Beetle chewing and rodent gnawing was identified in one individual, and concretions of solid soil matrix was present in some individuals but had minimal impact on

pathological observations. Infrequently, endocranial surfaces were unobservable due to concretions inside the cranium.

2.3 Age and Sex Estimation

Estimation of subadult ages for Man Bac were previously reported by Domett and Oxenham (2011). Dental eruption and calcification methods were used and compared to standards presented by Moorrees et al. (1963) and Ubelaker (1989) published in Buikstra and Ubelaker (1994) and White et al. (2000). Where dentition was not available, long bone diaphyseal lengths were compared to other children within the assemblage with a recorded dental age. For individuals over the age of approximately 12 years, standards for epiphyseal fusion methods were used based on Scheuer and Black (2000). Individuals were assessed in age categories organised according to life stages in association with immune system development (Lewis 2017). These age categories are: preterm to 6 months post-natal, 6 months to 1 year, 1 to 5 years, 5 to 10 years, 10 to 15 years and 15 to 20 years of age (Figure 2). Only four individuals over the age of 15 were present, therefore sex was not assessed in this investigation. Over 75% of the assemblage were 5-years of age or younger. A high fertility rate is likely the cause of this age demographic and this distribution strongly suggests that differential burial of adults and nonadults was not practiced (McFadden et al. 2018; McFadden and Oxenham 2018).

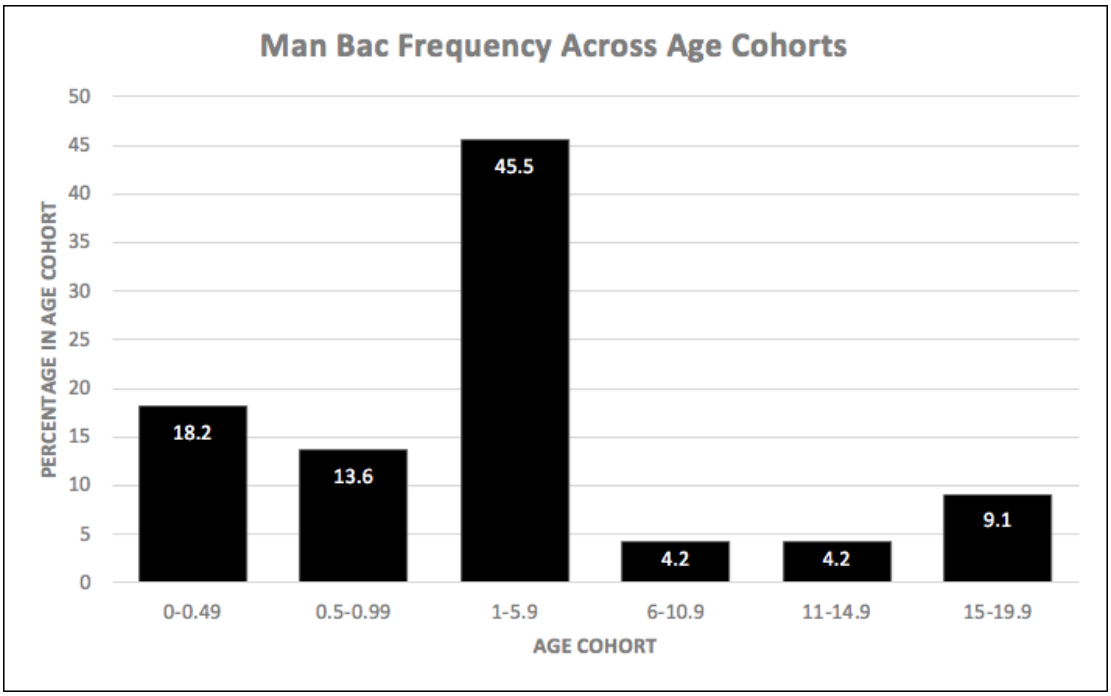

Figure 2: *Distribution of Man Bac subadults across age categories assessed for pathology*

2.4 Pathophysiology of Nutritional Diseases

Skeletal changes in subadult scurvy result from both direct and indirect impacts of malproduction of collagen on skeletal tissue (Fain 2005). Regions of association between blood vessels in contact with bone that underlie habitually used muscles cause repeated episodes of weakened vessel rupture and elicit subperiosteal new bone (SPNB) production as an part of an inflammatory response (Brickley and Ives 2010). Abnormal cortical porosity can also develop due to increased capillary formation as a consequence of the repeated microtrauma to weakened blood vessels (Ortner and Ericksen 1997). The diagnosis of scurvy is therefore based on these 'anatomically intuitive' associations between bone to soft tissue known as the 'Ortner criteria' (Ortner et al. 2001; Ortner and Ericksen 1997). These criteria were supplemented by Brickley and Ives (2010), and more recently by Snoddy et al. (2018), who incorporated clinical reports of lesions in specific bones, further standardising the diagnostic strength of the Ortner criteria.

Radiographic diagnostic signs for scurvy include a translucent zone in the metaphyses called a 'Trummerfeld' or 'Scurvy' line (Jaffe 1972; Resnick 1995). This radiolucency is often accompanied by a radiodense metaphyseal plate due to poor resorption of calcified cartilage, termed a 'White line of Fraenkel'. A similar radiodense line around the epiphyseal plate (Wimberger ring sign) can also occur (Snoddy et al. 2018). Given the disruption to osteoid formation, the structural integrity of the bone is compromised and fractures at the corners of the metaphyseal plates termed Pelkan spurs are also clinically reported (Snoddy et al. 2018).

Disruption to the balance of minerals and hormones which regulate mineralisation of osteoid (calcium, phosphate, parathyroid hormone and Vitamin D) interrupts the normal modelling and remodelling processes of bone causing rickets in children. The pathophysiology and skeletal expression of rickets has been recently reviewed by Brickley and Mays (2019).

2.5 Lesion Recording and Differential Diagnosis

All cranial and postcranial non-articular pathologies were recorded macroscopically. The long bones were also radiographed. Differential diagnosis of nutritional diseases in this investigation were as follows. Standardised methods for scurvy diagnosis by Snoddy et al. (2018) and methods for diagnosis of rickets by Brickley and Ives (2010) were employed for this analysis (Table 2). Diagnosis of disease was determined as consistent with a *possible* or a *probable* diagnosis following these standards. A minimum of one *diagnostic* or two

suggestive lesions was required for a possible diagnosis, with a probable diagnosis requiring at minimum two diagnostic lesions. The threshold method, while conservative, allows for consistency in diagnosis and is useful for estimating prevalences in population based approaches in palaeopathology.

SPNB deposits on long bones have been considered by Snoddy et al. (2018) as diagnostic for scurvy when cranial SPNB is present. However, the presence of one case of probable and four cases of possible treponemal disease in subadults at Man Bac (11.4% of the subadult assemblage) suggests possible co-morbidity, therefore this diaphyseal SPNB was excluded from the diagnostic criteria for scurvy as these bone changes are a common occurrence in treponemal disease (Vlok et al. in press). Additionally, as scorbutic lesions are most commonly symmetrical, if a lesion was unilateral, it was not considered diagnostic for scurvy. Abnormal endochondral porosity exceeding 10mm from the proximal or distal metaphyseal plates were also here considered here as a diagnostic lesion for scurvy (Ortner et al. 2001; Snoddy et al. 2017).

The diagnostic criterion of thickened cortex in long bones for rickets by Brickley and Ives (2010) was here considered as a *suggestive* lesion as bilateral cortical enlargement of long bones are characteristic of a number of childhood diseases, including treponemal disease (Hackett 1976; Lewis 2017), that has been identified in the Man Bac assemblage (Vlok et al. in press). Long bone thickening is also difficult to define in infants due to the physiological alteration of cortical thickness and development of the medullary canal over the first six months of life (Rauch and Schoenau 2001). The diagnostic strength of radiographic lesions in rickets followed Schattmann et al. (2016) due to the possibility of co-morbidities between rickets and scurvy influencing diagnosis, as the expression of lesions in these two diseases overlap.

Lastly, active scurvy and active rickets were recorded as follows. Active scurvy was identified through the presence of at least one diagnostic SPNB lesion exhibiting no signs of remodelling, indicative of the most recent skeletal activity. We note that there remain challenges to identifying clear boundaries between active, healing, healed and recurrent episodes of scurvy. Following Mays et al. (2006) and Brickley and Mays (2019) rachitic porosity and fraying of metaphyses and rib ends, and porosity of the crania were considered signs of active rickets. As mentioned above, difficulties in associating long bone thickening

with rickets in the Man Bac sample impeded confidence in identifying healed rickets. Additionally, co-occurrence with other nutritional diseases such as scurvy and anaemia can impact the presentation of long bone thickening in healed rickets as these diseases are known to cause resorption of cortical bone (Jaffe 1972; Singh et al. 2015). However, data for the age distribution of long bone thickening are presented and discussed below.

***Table 2**: Diagnostic lesions of scurvy and rickets. One diagnostic lesion is consistent with a possible case. Two or more diagnostic lesions are consistent with a probable case. Suggestive lesions that supplement diagnoses are provided in Appendices 1 and 2.*

Lesion	**Differential Diagnosis**
Scurvy *(Brickley and Ives 2010: 65; Ortner et al. 2001; Snoddy et al. 2018; Snoddy et al. 2017)*	
Abnormal cortical porosity/ subperiosteal new bone (SPNB) on Ectocranial Parietal/Squamous Temporal	Trauma, infection, anaemia
Abnormal cortical porosity and SPNB on External Greater Wing of Sphenoid	Trauma, infection
SPNB around Foramen Rotundum	Appositional growth (juveniles)
Abnormal cortical porosity and SPNB on Pterygoid Fossae and/or Plates	Appositional growth (juveniles)
Abnormal cortical porosity/ SPNB on Anterior Surface of Maxillae/ Infraorbital Foramina	Trauma, infection
Abnormal cortical porosity/ SPNB on Posterior Surface of Maxilla	Alveolar resorption
Abnormal cortical porosity/ SPNB on Palatal Surface of Maxillae	Infection, trauma
Abnormal cortical porosity/ SPNB on medial surfaces of Coronoid Processes of Mandible	Infection, trauma
Abnormal cortical porosity/ SPNB on the Supraspinous Fossae of the Scapula	Trauma, appositional growth
Abnormal cortical porosity/ SPNB on the Infraspinous Fossae of the Scapula	Trauma, appositional growth
Abnormal cortical porosity/ SPNB on orbital roof	Trauma, anaemia
Abnormal endochondral porosity extending >10mm from the distal metaphyseal plate of long bones	Rickets, longitudinal growth
Radiographic: White Line of Fraenkel	Normal variation, lead toxicity, rickets
Radiographic: Trummerfeld Line	Osteopenia, trauma, amaemia
Radiographic: Wimberger Ring Sign	Normal variation
Corner Fracture at position of dense zone of calcification (Pelkan's spur)	Trauma
Rickets *(Brickley and Ives 2010: 103-107; Brickley and Mays 2019)*	
Layers of spiculated, irregular, porous new bone on ectocranium or endocranium, when healing there are irregular trabecular spurs	Normal growth, scurvy, anaemia
Medial angulation of mandibular ramus	
Kyphosis or scoliosis of the T9 to L3 vertebrae	Congenital or developmental anomalies
Alteration in rib neck angle (>3 months of age)	
Lateral straightening of rib shaft (>3 months of age)	
Enlargement of costochondral rib junction	scurvy
Acetabulae pushed dorsally and angled anteriorly (*protrusio acetabulae*)	Developmental abnormalities
Flaring and swelling of distal metaphyses	Scurvy

Fraying and or porosity of metaphyseal plate (macroscopic or radiological)	Postmortem damage
Bending deformities of the limbs	Developmental deformities
Angulation (depression) of the femoral neck (*coxa vara*)**	Osteopenia,
Cupping of metaphyseal plates	Postmortem damage, trauma, scurvy

2.6 Statistical Analysis

The association between age and morbidity of rickets, and scurvy was assessed using relative risk ratios. Relative risk ratios are a common statistical technique employed in clinical and epidemiological studies to assess whether a disease has differential influence across two independent categories (dichotomous variable) (Altman 1990). Relative risk ratios were employed here to test the probability that the dichotomous variables being assessed (e.g. presence or absence of scurvy or rickets) were associated with a positive (harmful) vs. a negative outcome, and that an *exposed* group was associated with a higher probability of a positive outcome, than the *treatment* group (McKillup 2006). The presence of combined probable and possible cases and probable only cases of scurvy, combined probable and possible cases, and probable only cases of rickets were treated as the positive outcomes. A relative risk ratio (RR) of less than one is indicative of reduced risk whereas an RR of more than one indicates increased risk. Differences in morbidity were tested at age of death before (exposed group) or after (control group): 1 year of age, 5 years of age and 10 years of age. Additionally, the prevalence of scurvy and rickets in infants before 6 months of age were compared to infants between 6 months and 1 year of age to assess the potential implications of passive immunity and nutrient transfer from the placenta and breastmilk on the morbidity of specific nutritional deficiencies at Man Bac. Relative risk ratios were calculated using MedCalc Software Ltd 2020. Due to the small sample size, statistical significance was set at $P<0.10$. The p-value was also considered in the context of the size of the effect.

3. Results

3.1 Lesion Distribution

Over ninety-five percent (95.4%; 42/44) of the assemblage had lesions in two or more skeletal elements, suggesting a pattern of systemic disease as defined by Ortner (1992) and Buckley and Tayles (2003). The lesions were predominantly bilateral and symmetrical islands of SPNB, with association of abnormal cortical porosity, particularly in the cranium. Ninety-three (40/43) percent had lesions on the crania with 88.6% having lesions on the postcrania (39/44). Vascular impressions were also present in association with SPNB and abnormal cortical porosity particularly in children under the age of five years on the anterior

and posterior zygomatic bones and maxillae. Bending of the shafts (8/44; 18.2%), flaring (10/44; 22.7%), fraying (5/44; 11.4%) and cupping (18/44; 40.9%) of the metaphyseal plates of long bones were also observed. Fifty-two-point-three percent (23/44) of the assemblage exhibited abnormal deep endochondral porosity extending more than 10mm from the metaphyseal plates. Skeletal deformities (cupping, fraying, flaring and bending) were moderate, and no severe cases of long bone deformities were present. Long bones were affected in 84.1% (37/44) of individuals, with long bone thickening (observed radiographically) present in 20.5% (9/44) of individuals.

3.2 Scurvy

Following Snoddy et al. (2018)'s criteria for diagnosis of scurvy, 79.5% (35/44) of the assemblage met the threshold criteria for probable scurvy and 95.5% (42/44) met the threshold criteria for, at minimum, possible scurvy (see Figure 3; Table 3). The relative risk of combined possible and probable, and probable only cases of scurvy were relatively equal across age cohorts (RR ~1) (Table 2). Therefore, overall, age does not appear to play a role in the morbidity of scurvy at Man Bac (Figure 4). However, in regards to probable only cases, there was a statistically significant increase in the prevalence of scurvy from the 0 to 6 months to the 6 months to 1 year old cohort when only considering the infants (<1 year of age) in the statistical analysis (n= 14, RR= 0.6250, p=0.0861; Table 5)). Infants over 6 months of age were 1.6 times more likely to have had scurvy than infants under 6 months of age. Detailed lesion descriptions and justification for scurvy diagnosis of each individual can be found in supplementary material (Table A.1).

Table 3: *Man Bac subadult scurvy prevalence. Table A.1 provides a detailed scurvy diagnosis outcome for all subadults at Man Bac. **= statistically significant, ***= statistical significance with size of the effect considered.*

Scurvy	**Possible**			**Probable**			**Possible and Probable**		
	Affected	*Observed*	*(%)*	*Affected*	*Observed*	*(%)*	*Affected*	*Observed*	*(%)*
0 to 6 months	3	8	37.5	5	8	62.5	8	8	100
6 months to 1 year	0	6	0	6	6	100	6	6	100
1 to 5 years	3	20	15	16	20	80	19	20	95
5 to 10 years	0	3	0	3	3	100	3	3	100
10 to 15 years	1	3	33.3	2	3	66.7	3	3	100
15 to 20 years	0	4	0	3	4	75	3	4	75
Total	7	44	16	35	44	79.5	42	44	95.5
Relative Risk				**RR**	**p-value**		**RR**	**p-value**	
Group 1: Infants only (<1 year)									
<0.5 months				**0.6250**	**0.0861****		1.0000	1.0000	
Group 2: All subadults									
<1 year				0.9821	0.9140		1.0714	0.1574	
<5 years				1.1030	0.7012		1.0067	0.5195	
<10 years				1.1351	0.6148		1.1351	0.4816	


a)
b)
c)
d)
e)
f)
g)
h)
i)
j)
k)

Figure 3: *Lesions in Man Bac subadults diagnostic for scurvy. a) Active subperiosteal new bone (SPNB) and abnormal cortical porosity on the palate (MB05M36, ~3 years) b) Active SPNB and abnormal cortical porosity on the anterior maxilla extending from the infraorbital foramen (MB05M36, ~3 years), c) Remodelled SPNB and abnormal cortical porosity on the anterior maxilla, note the vascular impressions (white arrows) (MB05M25, ~5 years), d) Active SPNB and abnormal cortical porosity on the medial coronoid process of the mandible (MB05M25, ~5 years), e) Active SPNB and abnormal cortical porosity in the supraspinous fossa of the scapula (MB05M5, ~1.5 years), f) Active SPNB and cortical porosity on the external sphenoid (MB05M12, ~2 years), g) Active SPNB and abnormal cortical porosity in the pterygoid fossae of the sphenoid (white arrows) (MB05M25, ~5 years), h) Abnormal endochondral porosity extending more than 10mm from the distal metaphyseal plate of the femur (MB07H2M16, ~1.5 years), i) White lines of Fraenkel and Trummerfeld zones of the distal long bones (MB07H2M6, ~2 years). j) Active SPNB and abnormal cortical porosity on the posterior zygoma (white arrow) (MB05M2, neonate). k) Mixed active and remodelled SPNB and abnormal cortical porosity on the anterior maxilla (white arrow) (MB05M2, neonate).*

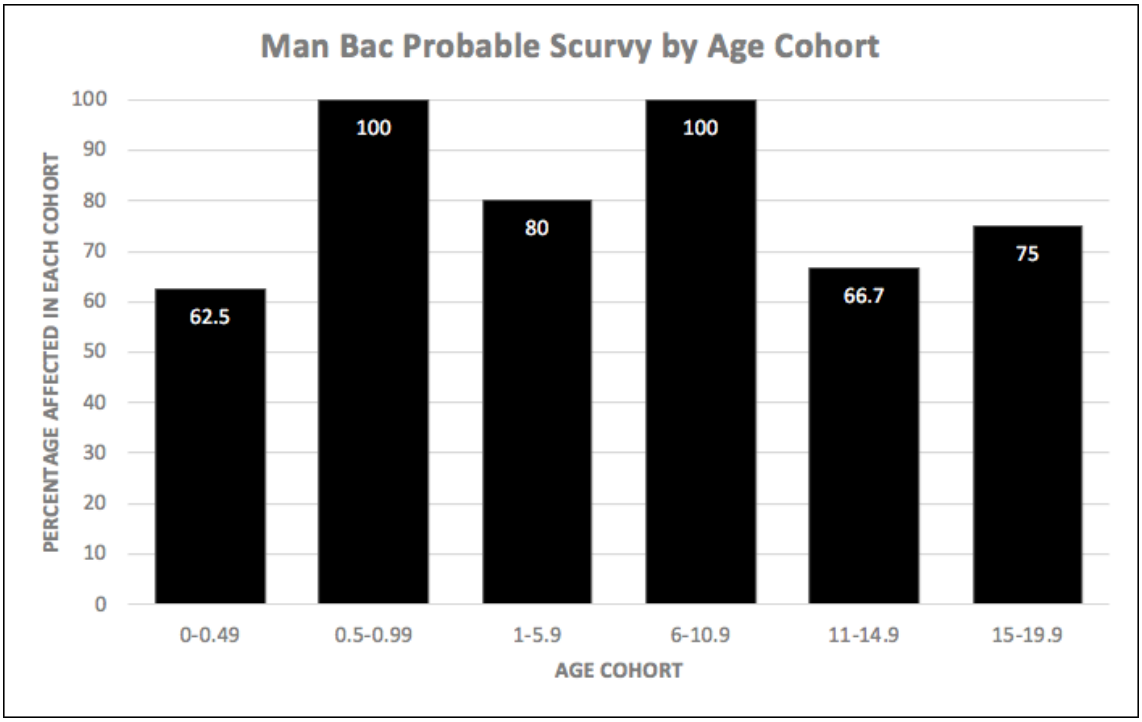

Figure 4: *Percentage prevalence of subadults meeting the threshold criteria for probable scurvy at Man Bac across age cohorts.*

3.3 Rickets

Following diagnosis with the Brickley and Ives (2010) criteria, 50% (22/44) of the assemblage met the criteria for, at minimum, a possible diagnosis, and 31.8% (14/44) met the criteria for probable diagnosis of rickets (Figure 5; Table 4). Age influenced the morbidity of rickets amongst the assemblage where individuals were over nine times more likely to have developed rickets before the age of 10 years old (n==44, RR= 9.4737, p= 0.1022). No evidence of rickets was found in individuals over 10 years of age. The most affected age cohort were infants between 6 months and 1 year of age (Figure 6). As was the case with probable scurvy, infants over 6 months old had significantly higher probable rickets morbidity risk than infants younger than 6 months of age (n=44, RR= 0.3000, p= 0.0595). While adults were not the focus of this study, bone mineralisation disorders were limited to subadults only. Detailed lesion

descriptions and justification for rickets diagnosis of each individual can be found in supplementary material (Table A.2).

Table 4: *Man Bac subadult rickets prevalence. Table A.2 provides a detailed rickets diagnosis outcome for all subadults at Man Bac. **= statistically significant, ***= statistical significance with size of the effect considered.*

Rickets	**Possible**			**Probable**			**Possible and Probable**		
	Affected	*Observed*	*(%)*	*Affected*	*Observed*	*(%)*	*Affected*	*Observed*	*(%)*
0 to 6 months	0	8	0	2	8	25	2	8	25
6 months to 1 year	0	6	0	5	6	83.3	5	6	83.3
1 to 5 years	7	20	35	6	20	30	13	20	65
5 to 10 years	1	3	33.3	1	3	33.3	2	3	66.7
10 to 15 years	0	3	0	0	3	0	0	3	0
15 to 20 years	0	4	0	0	4	0	0	4	0
Total	8	44	18.2	14	44	31.8	22	44	50
Relative Risk				**RR**	**p-value**		**RR**	**p-value**	
Group 1: Infants only (<1 year)									
<0.5 months				**0.3000**	**0.0595****		**0.3000**	**0.0595****	
Group 2: All subadults									
<1 year				**2.1429**	**0.0732****		1.0000	1.0000	
<5 years				4.3333	0.1336		2.1111	0.1464	
<10 years				6.1053	0.1914		**9.4737**	**0.1022*****	

Figure 5: *Lesions in Man Bac subadults consistent with a diagnosis for rickets. a) Thin layers of poorly mineralised new bone of the ectocranium and overall thinning of the cranial bone (MB07H2M21, ~9 months), b) Thick SPNB deposits on the femora and slight cupping of the distal metaphysis (MB05M30, ~6 months), c) Slight cupping of proximal tibia (MB05M25, ~5 years), d) Fraying, cupping and flaring of the proximal tibia (MB05M18, ~1.5 years), e) Fraying, flaring and cupping of the distal femur (MB05M18, ~1.5 years), f) Bending of the humeral shafts with fraying of the proximal metaphyses (MB05M3, ~6 months), g) Thickened cortex with coarsened trabeculae. Metaphyseal ends are also thickened. (MB05M30, ~6 months).*

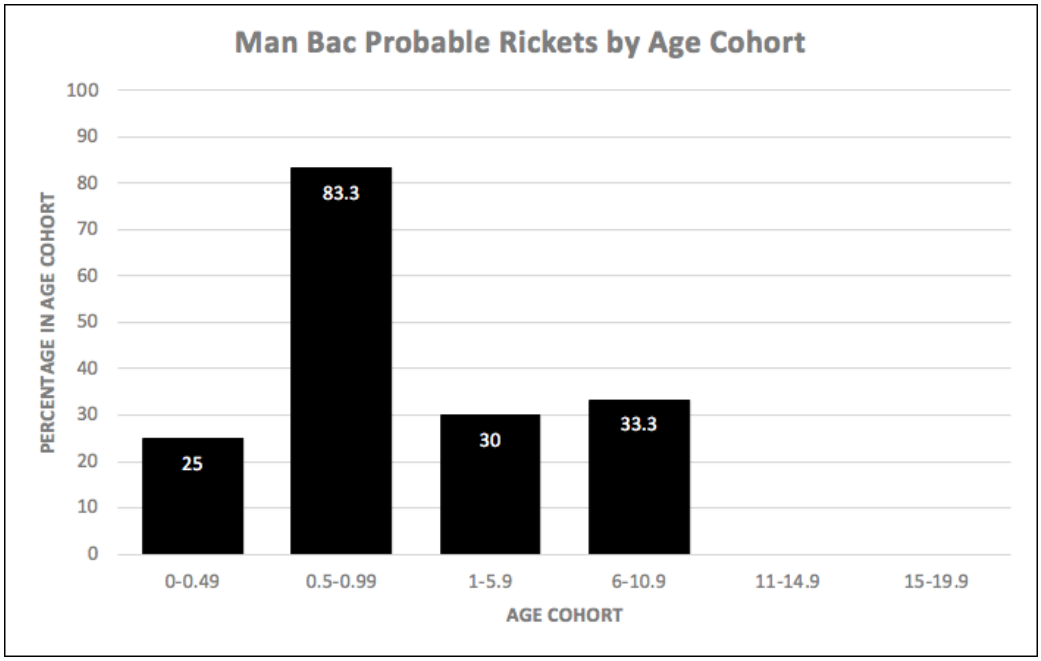

Figure 6: *Percentage prevalence of subadults meeting the threshold criteria for probable rickets at Man Bac across age cohorts.*

3.4 Co-morbidities and Activity of Rickets and Scurvy

Clear co-morbidities between rickets and scurvy are apparent at Man Bac with almost 32% of individuals having both probable rickets and probable scurvy (Table 5). All cases diagnosed as possible or probable rickets were also diagnosed with probable scurvy. Most subadults under the age of 5 years exhibited active scurvy, whereas evidence of remodelling was observed in most individuals over the age of 5 years (Table 6). No scorbutic subadult had completely remodelled lesions. Active rickets (fraying or porosity of the cranium and postcranium) was only observed in individuals under the age of 2 years of age. No clear trend is observable in possible signs of healed rickets, and long bone thickening was present in 50% (11/22) of individuals diagnosed with rickets. Individuals with fraying and porosity also exhibited long bone thickening, possibly consistent with re-occurrence of rickets.

Table 5: *Prevalence of co-morbidities at Man Bac.*

Rickets and Scurvy	**Probable**			**Possible and Probable**		
	Affected	*Observed*	*(%)*	*Affected*	*Observed*	*(%)*
0 to 6 months	2	8	25	2	8	25
6 months to 1 year	5	6	83.3	5	6	83.3
1 to 5 years	6	20	30	13	20	65
5 to 10 years	1	3	33.3	2	3	66.7
10 to 15 years	0	3	0	0	3	0
15 to 20 years	0	4	0	0	4	0
Total	14	44	31.8	22	44	50

Table 6: *Status of Scurvy and Rickets.*

	Active Scurvy			**Active Rickets**			**Possible Healed Rickets (Long Bone Thickening)**		
	Active	*Observed*	*(%)*	*Active*	*Observed*	*(%)*	*Healed*	*Observed*	*(%)*
0 to 6 months	7	8	87.5	2	2	100	2	2	100
6 months to 1 year	5	6	83.3	4	5	80	5	5	100
1 to 5 years	11	19	57.9	2	13	15.4	2	13	15.4
5 to 10 years	0	3	0	0	2	0	2	2	100
10 to 15 years	1	3	33	0	0	0	0	0	0
15 to 20 years	1	3	33	0	0	0	0	0	0
Total	25	42	59.5	8	22	36.4	11	22	50

4. Discussion

4.1 Causes of scurvy at Man Bac

Even in the absence of any other systematic study of nutritional diseases in the region, the levels of scurvy in Man Bac subadults is exceptionally high, but not entirely unexpected in a tropical context. Halcrow et al. (2014) report a case of scurvy in a subadult from historical period Cambodia and a high prevalence of the disease was reported from a population in subsistence transition from the Pacific islands (Buckley et al. 2014). The excellent preservation of bone surfaces at Man Bac may also have contributed to this high rate, as active SPNB can be lost through a range of taphonomic factors (Roberts and Connell 2004), and the excellent preservation of crania at Man Bac may also have contributed to this high observable prevalence (Brickley and Ives 2010; Snoddy et al. 2018). It is, also conceivable that the frequencies of possible cases of scurvy is an overrepresentation of individuals with clinical scurvy. As previously mentioned, treponemal disease has been identified in the Man Bac assemblage, possibly contributing to the SPNB recorded in the subadult assemblage (Vlok et al. in press). However, in regards to probable cases, 84.1% (37/44) of Man Bac subadults had more than three diagnostic lesions for scurvy, and 56.8% (25/44) also presented with radiographic signs of scurvy further strengthening the argument for high levels of subadult scurvy at Man Bac.

Man Bac inhabitants had a broad-based diet. It is currently not known to what degree rice was relied on or to what degree indigenous plants supplemented the diet at Man Bac. Evidence for fruits and nuts of a wide variety have been found in Pre-Neolithic sites in Northern Vietnam (Mai Huong 2013; Oxenham et al. 2018) and the diverse ecologies exploited by the Man Bac community may have provided a range of available fruits and nuts.

However, following climate cooling after the terminus of the Holocene Thermal Maximum approximately 5000 years ago, the ecology of the region would have changed significantly. Globally, dietary diversity decreased with the transition to agriculture, and this pattern is also present at Man Bac with a decrease in faunal taxa exploitation around the introduction of agriculture (Jones et al. 2019). It is possible a similar reduction in floral diversity also occurred with the introduction of rice and concurrent climate change, that may partly explain the high levels of scurvy identified at Man Bac. Both wild and cultivated food sources may have been occasionally disrupted by frequent tropical storms, potentially increasing the nutritional stress already experienced with the decrease in dietary diversity (Oxenham 2006), an interpretive point also used in the Pacific (Buckley et al. 2014).

Although at Man Bac there was a high reliance on various marine species from freshwater and brackish environments, all fish types provided inadequate levels of Vitamin C. Similarly, the terrestrial faunal assemblage would not have yielded sufficient levels of Vitamin C (Sawada et al. 2011). The cooking and processing of these foods would have further depleted the bioavailable Vitamin C (Mays 2013; Rumm-Kreuter and Demmel 1990). The interaction between local foragers and migrant farmers was also likely to have had an impact on nutritional stress as migrants adapted to establishing domesticated crops in new environments.

It is also worth noting the potential negative role age (and gender) based food taboos (see Oxenham 2016: 185-186) may have had on the nutritional health of children at Man Bac. While predominantly egalitarian, the inhabitants of Man Bac appear to have had an aged based hierarchy that may have favoured the allocation of resources to older individuals in the community (Oxenham et al. 2008), and will be explored in future publications.

Finally, adequate intake of Vitamin C is essential for immune function. A high pathogen load, where phagocytes are activated in the immune response, consequently increases oxidative stress and increases the demand for Vitamin C, an antioxidant, in the body (Hemilä 2017; Khaw and Woodhouse 1995; Rokkas et al. 1995). Indeed, in a subtropical climate a high pathogen load from many infectious diseases is expected. Hookworm, roundworm, *Shigella* sp., *Salmonella* sp., schistosomiasis, and *Escherichia coli* are all possible causes for infectious diarrhoea which decreases absorption of vitamin C (King et al. 2017; Oxenham 2016). Weanling diarrhoea, associated with the introduction of foods to supplement breast

feeding may have also increased the dietary requirement for Vitamin C in infants. This synergy is likely driving the frequencies of scurvy identified in the Man Bac infants and has been argued to be a contributing factor in other tropical environments (Buckley 2000). To date, no isotopic research has identified terminal age of weaning at Man Bac, but passive immunity from the maternal intrauterine environment is known to be reduced by 3 months of age (Lewis 2017). Furthermore, the high levels of fertility at Man Bac indicates shorter birth intervals which may have been facilitated by the early introduction of weaning foods (Buikstra et al. 1986; McFadden and Oxenham 2018). It is possible the increased frequency of probable scurvy after 6 months of age is related to the decreased efficacy of passive immunity from the intrauterine environment combined with introduction of weaning foods, thus increasing susceptibility of pathogens and the requirements for Vitamin C deficiency in these infants. In sum, a combination of restricted dietary diversity possibly due to environmental factors, combined with agricultural subsistence, and high pathogen loads are likely underlying the outcome of high levels of subadult scurvy at Man Bac.

4.2 Perinatal scurvy revisited

Recent research (see Buckley et al. 2014; Kinaston et al. 2009; Snoddy et al. 2017) has highlighted the possibility of the diagnosis of neonatal scurvy, facilitating discussion of maternal Vitamin C deficiency. At Man Bac all of the neonates (100%; 8/8) presented with possible or probable scurvy with 62.5% (5/8) having probable scurvy. Previously palaeopathologists have cautioned that normal SPNB growth may be incorrectly attributed to pathology in children under the age of 4 years and interpretations of these results should be treated with caution (e.g. Lewis 2017). While it is likely that growth is playing some role in the bone changes observed in the young infants at Man Bac, the frequency of neonates with probable scurvy was not higher than other age cohorts, which would be expected if the SPNB observed in the neonates was strictly due to growth. That active rickets was identified in 25% of Man Bac neonates supports the argument for the presence of neonatal scurvy. Furthermore, White lines of Fraenkel associated with Trummerfeld lines were present in 37.5% (3/8) of neonates (see Table A.1). These radiographic signs indicate disruptions to osteoid formation and do not share the same confounding factor of growth associated with macroscopic observations of SPNB. We argue here that the infant cohort of a skeletal assemblage should not be excluded from palaeopathological analyses. Furthermore, as demonstrated here with the diagnosis of rickets and scurvy, co-morbidities of nutritional disease can be used to further strengthen the argument for nutritional stress in young infants.

4.3 Causes of rickets at Man Bac

Rickets has been identified in a subadult assemblage from Southeast Asia at the Neolithic to Metal Age site of Niah Cave in Borneo (Schrenk 2017). However, the author attributes rickets simply to Vitamin D deficiency. Instead the causes for the skeletal manifestations of rickets are complex and result from an imbalance of calcium and phosphate regulation by Vitamin D and parathyroid hormones (Brickley and Ives 2010; Pettifor et al. 1981). Therefore, disturbances to any part of the mineralisation process can cause rickets. Hypophosphatemic rickets is most commonly caused by a genetic disorder, and hypophosphatemia from malnourishment is extremely rare (Lentz et al. 1978; Yamazaki et al. 2002). In the case of a high protein diet at Man Bac, phosphate deficiency is unlikely. Vitamin D deficiency is strongly associated with high latitudes, and reduced sun exposure which is unusual in subtropical regions unless social factors (such as clothing and containment inside) inhibit sun exposure (Mays et al. 2018) therefore, Vitamin D deficiency as a primary cause is unlikely in this context.

Rice is high in phytates and restricts calcium absorption in the gut while also having overall low calcium levels (Pettifor 2004). Rice is presumed to have approximately 32 mg/100g (*Oryza sativa japonica*) with levels less than 125mg/day resulting in skeletal deformities (Pettifor et al. 1981; US Department of Agriculture 2019). Therefore, calcium deficiency is a more likely cause for rickets in the infants and children of Man Bac than Vitamin D deficiency. This may also be supported by the presence of high levels of localised primary canine hypoplasia (LHPC) defects at Man Bac that have been partially attributed to calcium deficiency (McDonell and Oxenham 2014).

Calcium deficiency rickets has been documented in agriculturally dependent temperate and tropical regions globally (Fischer et al. 1999; Legius et al. 1989; Thacher 2003). Furthermore, calcium deficiency does not cause osteomalacia in adults (which is absent in the adults of Man Bac (unpublished data)), unlike in Vitamin D and phosphate deficiency (Pettifor 2004). The presence of high levels of rickets at 6 months to 1 year old and not younger, where breastfeeding likely provided a buffer against deficiency, also supports an argument for calcium deficiency as a more likely cause of rickets at Man Bac (Butte et al. 2002). Lower calcium levels are required in the tropics due to increased absorption of Vitamin D from UV rays (Pettifor 2004) so for this reason skeletal representation of calcium deficiency suggests

severe restriction of dietary calcium at Man Bac. Additionally, dietary requirements for calcium increase in the first 6 months after birth, compared to foetal requirements (Almaghamsi et al. 2018). A pregnant female's bones tend to be leached for calcium in periods of nutritional stress to compensate for the growing foetus, and research suggests dietary intake is independent of calcium secretion in breast milk, except in states of severe deficiency (Olausson et al. 2012). Given that 25% of neonates presented with probable active rickets suggests that in some Man Bac mothers, calcium deficiency was extreme. A continued decline of calcium deficiency with increasing age at Man Bac is not surprising due to the decline in calcium requirements of a growing child (Prentice 1995). As was the case with scurvy, a relationship with infectious diarrhoea and calcium deficiency has been observed (Foldenauer et al. 1998). The combination of high levels of scurvy and rickets at Man Bac suggests a restricted diet likely related to subsistence transition contributing to scarce micronutrients in the diet. Therefore, life stage was a significant factor in rickets, with dietary requirements increasing in infancy at a time where breastfeeding was insufficient to provide the required quantity of calcium for normal skeletal development.

4.4 Co-morbidities of nutritional stress

Co-morbidity of scurvy and rickets were particularly high for subadults between the ages of 6 months and 10 years. As all individuals with possible or probable rickets were also diagnosed with probable scurvy, it is possible that those with rickets indicate extreme severity of nutritional disease compared to other individuals affected by scurvy. This outcome further supports a shared aetiology of scurvy and rickets signalling a strong dietary cause. When considering probable only cases, it is clear that co-morbidity was highest around 6 months of age. An argument can be made for a dietary shift, whether due to depletion of vitamins in breastmilk or the introduction of vitamin-poor weaning foods.

Active lesions of both scurvy and rickets were highest under 1 year of age. While selective mortality is likely at play in the high prevalences of both scurvy and rickets in infants and young children, the increase in prevalence following the 6-month mark indicates factors influencing age of onset of rickets and scurvy. Concurrent evidence of active rickets with possible signs of healing in infants also suggests a particular age of onset where recurrent episodes of rickets may have occurred. The lack of a clear trend of healed rickets in older subadults does suggest that long bone thickening may not be a clear indicator of healed rickets in the Man Bac subadult assemblage.

4.5 Subadult health and the Neolithic transition in Southeast Asia

The adoption of agriculture in MSEA, and the degree of interactions between farmers and foragers were complex and non-linear, therefore variations in the impact to health is expected (Oxenham and Buckley 2016). Indeed, subsistence, population interaction, population density and sedentism vary throughout Neolithic sites in MSEA. Therefore, Man Bac does not reflect the overall impact of the Neolithic transition on health in the region. To date no other MSEA Neolithic site presents with subadult and adult SPNB levels as high as Man Bac (Halcrow et al. 2016; Pietrusewsky and Douglas 2002; Tayles 1999), further indicating Man Bac may be a unique case in the overall transition to agriculture in the region. Additionally, scurvy and rickets have to date not been identified in other prehistoric sites in MSEA. Interestingly, the skeletal evidence of non-specific stress at Man Bac, particularly in children is comparative to that of Khok Phanom Di (Halcrow et al. 2016; Oxenham and Domett 2011), possibly indicating that the initial adoption of agriculture may have had an impact on health. However, in order to fully appreciate shifts in health with the adoption of agriculture, further palaeopathological work on Pre-Neolithic sites is required. Oxenham et al. (2018) observed similarly high prevalences of cribra orbitalia at Con Co Ngua, a Pre-Neolithic site in Northern Vietnam, compared to Man Bac (Oxenham and Domett 2011), suggesting disease burdens were high prior to the Neolithic transition in this region. Con Co Ngua did not exhibit sizeable evidence for scurvy (Vlok et.al forthcoming).

Moreover, this trend in high burdens of disease identified at Man Bac is not observed in subsequent Bronze and Iron Age sites marking the intensification of agriculture (Halcrow et al. 2016). It is possible factors not directly related to the dietary effects of rice, rather secondary impacts of initial agricultural adoption, such as a significant increase in fertility, are the drivers for decline in health in the Neolithic of MSEA. It is worth noting that a correlation between fluctuating oral health and fertility has been demonstrated for MSEA (Willis and Oxenham 2013). A reappraisal of prehistoric MSEA sites, employing recent approaches to identifying specific nutritional diseases may be particularly useful in further investigating this trend.

The argument for no decline in health with the transition of agriculture across the entire prehistory of MSEA is not supported by this research. We argue that the impact of agricultural transition on health should be considered at a site level, and various lines of

palaeopathological study involving assessment of non-specific markers of stress *and* the diagnosis of specific diseases be incorporated in the analysis of changes of health with the agricultural transition in this region.

5. Conclusions

High levels of micronutrient deficiencies were identified in the Man Bac subadults. While a broad base diet exists for Man Bac, the exploitation of domesticated and wild fauna with domesticated rice likely contributed sufficient levels of macronutrients such as proteins, fatty acids and carbohydrates but excluded some micronutrients including calcium and Vitamin C. Additionally, gathered flora resources did not sufficiently supplement micronutrients to prevent nutritional disease in subadults. A high fertility rate at Man Bac likely contributed to population stress influencing the high levels of observed multi-nutrient deficiency. Similar analysis is required in other subadult assemblages throughout MSEA to explore intraregional variation in nutritional stress with the transition to and intensification of farming.

Acknowledgements

We would like to thank Dr. Ngo Anh Son, Mr. Bui Van Khanh and Ms. Nellissa Ling for their assistance with the radiographs, and Dr. Anne Marie Snoddy for discussions on the diagnosis of scurvy and comments on the manuscript.

Funding: This work was supported by a National Geographic Early Career Grant (EC-54332R-18); Royal Society of New Zealand Skinner Fund Grant; and a University of Otago Doctoral Scholarship.

References

Almaghamsi A, Almalki MH, and Buhary BM. 2018. Hypocalcemia in pregnancy: a clinical review update. Oman medical journal 33(6):453.

Altman DG. 1990. Practical Statistics for Medical Research. New York, USA: CRC press.

Bellwood P, and Oxenham M. 2008. The expansions of farming societies and the role of the Neolithic demographic transition. In: Bocquet-Appel J, and Bar-Yosef O, editors. The Neolithic Demographic Transition and its Consequences: Springer Science. p 13-34.

Bellwood P, Oxenham M, Hoang BC, Dzung NK, Willis A, Sarjeant C, Piper P, Matsumura H, Tanaka K, and Beavan-Athfield N. 2011. An Son and the Neolithic of Southern Vietnam. Asian Perspectives:144-175.

Bocquet-Appel J-P, Naji S, and Bandy M. 2008. Demographic and health changes during the transition to agriculture in North America. Recent Advances in Palaeodemography: Springer. p 277-292.

Bouis HE, and Welch RM. 2010. Biofortification—A Sustainable Agricultural Strategy for Reducing Micronutrient Malnutrition in the Global South. Crop Science 50(Supplement_1):S-20-S-32.

Brickley M, and Ives R. 2010. The Bioarchaeology of Metabolic Bone Disease. Oxford, UK: Academic Press.

Brickley MB, and Mays S. 2019. Metabolic Disease. In: Buikstra JE, editor. Ortner's Identification of Pathological Conditions in Human Skeletal Remains. 3rd ed. Cambridge, USA: Elsevier. p 531-566.

Buckley HR. 2000. Subadult Health and Disease in Prehistoric Tonga, Polynesia. American Journal of Physical Anthropology 113(4):481-505.

Buckley HR, Kinaston R, Halcrow SE, Foster A, Spriggs M, and Bedford S. 2014. Scurvy in a Tropical Paradise? Evaluating the Possibility of Infant and Adult Vitamin C Deficiency in the Lapita Skeletal Sample of Teouma, Vanuatu, Pacific islands. International Journal of Paleopathology 5:72-85.

Buckley HR, and Tayles N. 2003. Skeletal Pathology in a Prehistoric Pacific Island Sample: Issues in Lesion Recording, Quantification, and Interpretation. American Journal of Physical Anthropology 122(4):303-324.

Buikstra JE, Konigsberg LW, and Bullington J. 1986. Fertility and the development of agriculture in the prehistoric Midwest. American Antiquity 51(3):528-546.

Buikstra JE, and Ubelaker DH. 1994. Standards for Data Collection from Human Skeletal Remains: Proceedings of a Seminar at the Field Museum of Natural History, Arkansas Archaeological Survey Research Series No. 44. Fayetteville, USA: Arkansas Archaeological Survey.

Butte NF, Lopez-Alarcon MG, and Garza C. 2002. Nutrient adequacy of exclusive breastfeeding for the term infant during the first six months of life.

Carr AC, and Maggini S. 2017. Vitamin C and immune function. Nutrients 9(11):1211.

Castillo C. 2011. Rice in Thailand: the archaeobotanical contribution. Rice 4(3):114.

Castillo C, Fuller DQ, Piper PJ, Bellwood P, and Oxenham M. 2018. Hunter-Gatherer Specialization in the Late Neolithic of Southern Vietnam–The Case of Rach Nui. Quaternary international 489:63-79.

Domett KM, and Oxenham MF. 2011. The Demographic Profile of the Man Bac Cemetery Sample. In: Oxenham MF, Matsumura H, and Kim Dung N, editors. Man Bac: The Excavation of a Neolithic Site in Northern Vietnam, The Biology Terra Australis 33: ANU ePress. p 9-20.

Ekiz C, Agaoglu L, Karakas Z, Gurel N, and Yalcin I. 2005. The effect of iron deficiency anemia on the function of the immune system. The Hematology Journal 5(7):579-583.

Eshed V, Gopher A, Pinhasi R, and Hershkovitz I. 2010. Paleopathology and the origin of agriculture in the Levant. American Journal of Physical Anthropology 143(1):121-133.

Fain O. 2005. Musculoskeletal manifestations of scurvy. Joint Bone Spine 72(2):124-128.

Fischer P, Rahman A, Cimma J, Kyaw-Myint T, Kabir A, Talukder K, Hassan N, Manaster B, Staab D, and Duxbury J. 1999. Nutritional Rickets without Vitamin D Deficiency in Bangladesh. Journal of Tropical Pediatrics 45(5):291-293.

Foldenauer A, Vossbeck S, and Pohlandt F. 1998. Neonatal hypocalcaemia associated with rotavirus diarrhoea. European journal of pediatrics 157(10):838-842.

Hackett CJ. 1976. Diagnostic Criteria of Syphilis, Yaws and Treponarid (Treponematoses) and of Some Other Diseases in Dry Bones. Berlin, Germany: Springer.

Halcrow S, Harris N, Beavan N, and Buckley H. 2014. First Bioarchaeological Evidence of Probable Scurvy in Southeast Asia: Multifactorial Etiologies of Vitamin C Deficiency in a Tropical Environment. International Journal of Paleopathology 5:63-71.

Halcrow S, Harris N, Tayles N, Ikehara-Quebral R, and Pietrusewsky M. 2013. From the mouths of babes: dental caries in infants and children and the intensification of agriculture in mainland Southeast Asia. American Journal of Physical Anthropology 150(3):409-420.

Halcrow S, Tayles N, and King CL. 2016. Infant and Child Health and Disease with Agricultural Intensification in Mainland Southeast Asia. In: Oxenham M, and Buckley H, editors. The Routledge Handbook of Bioarchaeology in Southeast Asia and the Pacific Islands: Routledge. p 186-214.

Hemilä H. 2017. Vitamin C and infections. Nutrients 9(4):339.

Hiep T, and Phung H. 2004. Man Bac location and its relationship through ceramic data (in Vietnamese). Khao Co Hoc (Vietnamese Archaeology) 6:13-48.

Higham C. 2007. The Origins of the Civilization of Angkor Volume 2: The Excavation of Noen U-Loke and Non Muang Kao: Fine Arts Department of Thailand.

Higham C, Cameron J, Chang N, Castillo C, O'Reilly D, Petchey F, and Shewan L. 2014. The excavation of Non Ban Jak, Northeast Thailand-A report on the first three seasons.

Higham C, Higham T, and Kijngam A. 2011. Cutting a Gordian Knot: the Bronze Age of Southeast Asia: Origins, Timing and Impact. Antiquity 85(328):583-598.

Higham C, Manly B, Thosarat R, Buckley HR, Chang N, Halcrow S, Ward S, O'Reilly D, Shewan L, and Domett K. 2019a. Environmental and Social Change in Northeast Thailand during the Iron Age. Cambridge Archaeological Journal 29(4):549-569.

Higham C, and Thosarat R. 2005. Excavation of Khok Phanom Di, 7: summary and conclusions: Fine Arts Department of Thailand.

Higham CF, Higham TF, and Douka K. 2019b. Dating the Bronze Age of Southeast Asia. Why Does it Matter? Journal of Indo-Pacific Archaeology 43:43-67.

Higham T, Weiss A, Pigott V, Higham C, Ramsey C, D'Alpoim-Guedes J, Hanson S, Weber S, Rispolli F, and Ciarla R. in press. A New Chronology for a Prehistoric Copper Production Centre in Central Thailand using Kernel Density Estimates. Antiquity.

Jaffe HL. 1972. Metabolic, Degenerative, and Inflammatory Diseases of Bones and Joints. London: Lea and Febiger.

Jones RK. 2017. Transitions to animal domestication in Southeast Asia: Zooarchaeological analysis of Cồn Cổ Ngựa and Mán Bạc, Vietnam: Australian National University.

Jones RK, Piper PJ, Groves CP, Anh TN, Thi MHN, Thị HN, Hoang TH, and Oxenham MF. 2019. Shifting Subsistence Patterns from the Terminal Pleistocene to Late Holocene: A Regional Southeast Asian Analysis. Quaternary International 529:47-56.

Khaw K-T, and Woodhouse P. 1995. Interrelation of vitamin C, infection, haemostatic factors, and cardiovascular disease. Bmj 310(6994):1559-1563.

Kinaston RL, Buckley HR, Halcrow SE, Spriggs MJ, Bedford S, Neal K, and Gray A. 2009. Investigating foetal and perinatal mortality in prehistoric skeletal samples: a case study from a 3000-year-old Pacific Island cemetery site. Journal of Archaeological Science 36(12):2780-2787.

King CL, Bentley RA, Higham C, Tayles N, Viðarsdóttir US, Layton R, Macpherson CG, and Nowell G. 2014. Economic Change after the Agricultural Revolution in Southeast Asia? Antiquity 88(339):112-125.

King CL, Halcrow SE, Tayles N, and Shkrum S. 2017. Considering the Palaeoepidemiological Implications of Socioeconomic and Environmental Change in Southeast Asia. Archaeological Research in Asia 11:27-37.

Larsen CS. 1995. Biological Changes in Human Populations with Agriculture. Annual Review of Anthropology 24(1):185-213. DOI: 10.1146/annurev.an.24.100195.001153

Larsen CS. 2006. The Agricultural Revolution as Environmental Catastrophe: Implications for Health and Lifestyle in the Holocene. Quarternary International 150(1):12-20. DOI: 10.1016/j.quaint.2006.01.004

Legius E, Proesmans W, Eggermont E, Vandamme-Lombaerts R, Bouillon R, and Smet M. 1989. Rickets due to Dietary Calcium Deficiency. European Journal of Pediatrics 148(8):784-785.

Lentz RD, Brown DM, and Kjellstrand CM. 1978. Treatment of severe hypophosphatemia. Annals of internal medicine 89(6):941-944.

Lewis ME. 2017. Paleopathology of Children: Identification of Pathological Conditions in the Human Skeletal Remains of Non-Adults. London: Academic Press.

Lipson M, Cheronet O, Mallick S, Rohland N, Oxenham M, Pietrusewsky M, Pryce TO, Willis A, Matsumura H, and Buckley H. 2018. Ancient Genomes Document Multiple Waves of Migration in Southeast Asian Prehistory. Science 361(6397):92-95. DOI: 10.1126/science.aat3188

Mai Huong NT. 2013. Neolithic Vegetation in Northern Vietnam: An Indication of Early Agricultural Activities. Journal of Austronesian Studies 4:1.

Mai Huong NT. 2016. Burnt Rice from Four Archaeological Sites in Northern Vietnam. Vietnam Social Sciences(3):64-77.

Matsumura H, and Oxenham M. 2013. Population Dispersal from East Asia into Southeast Asia: Evidence from Cranial and Dental Morphology. In: Pechenkina EA, and Oxenham M, editors. Bioarchaeology of East Asia: Movement, Contact, Health. Gainesville, USA: University Press of Florida. p 179-212.

Matsumura H, and Oxenham M. 2014. Demographic Transitions and Migration in Prehistoric East/Southeast Asia Through the Lens of Nonmetric Dental Traits. American Journal of Physical Anthropology 155(1):45-65. DOI: 10.1002/ajpa.22537

Mays S. 2013. A Discussion of Some Recent Methodological Developments in the Osteoarchaeology of Childhood. Childhood in the Past 6(1):4-21.

Mays S, Brickley M, and Ives R. 2006. Skeletal Manifestations of Rickets in Infants and Young Children in a Historic Population from England. American Journal of Physical Anthropology 129(3):362-374.

Mays S, Prowse T, George M, and Brickley M. 2018. Latitude, Urbanization, Age, and Sex as Risk Factors for vitamin D Deficiency Disease in the Roman Empire. American Journal of Physical Anthropology 167(3):484-496.

McColl H, Racimo F, Vinner L, Demeter F, Gakuhari T, Moreno-Mayar JV, Van Driem G, Wilken UG, Seguin-Orlando A, and De la Fuente Castro C. 2018. The Prehistoric Peopling of Southeast Asia. Science 361(6397):88-92. DOI: 10.1126/science.aat3628

McDonell A, and Oxenham MF. 2014. Localised Primary Canine Hypoplasia: Implications for Maternal and Infant Health at Man Bac, Vietnam, 4000–3500 years BP. International Journal of Osteoarchaeology 24(4):531-539. DOI: 10.1002/oa.2239

McFadden C, Buckley H, Halcrow SE, and Oxenham MF. 2018. Detection of Temporospatially Localized Growth in Ancient Southeast Asia Using Human Skeletal Remains. Journal of Archaeological Science 98:93-101. DOI: 10.1016/j.jas.2018.08.010

McFadden C, and Oxenham MF. 2018. The D0-14/D ratio: A New Paleodemographic Index and Equation for Estimating Total fertility Rates. American Journal of Physical Anthropology 165(3):471-479. DOI: 10.1002/ajpa.23365

McGrath R, and Boyd WE. 2001. The chronology of the Iron Age 'moats' of northeast Thailand. Antiquity 75(288):349-360.

McKillup S. 2006. Statistics Explained: An Introductory Guide for Life Scientists. Cambridge UK: Cambridge University Press. 2006 p.

McKinley J. 2004. Compiling a Skeletal Inventory: Disarticulated and Co-Mingled Remains. In: Brickley M, and McKinley J, editors. Guidelines to the Standards for Recording Human Remains. Reading: BABAO/ Institute of Field Archaeologists.

Moorrees CF, Fanning EA, and Hunt EE. 1963. Formation and Resorption of Three Deciduous Teeth in Children. American Journal of Physical Anthropology 21(2):205-213.

Newton J, Domett KM, O'Reilly DJ, and Shewan L. 2013. Dental Health in Iron Age Cambodia: Temporal Variations with Rice Agriculture. International Journal of Paleopathology 3(1):1-10.

Olausson H, Goldberg GR, Laskey MA, Schoenmakers I, Jarjou LM, and Prentice A. 2012. Calcium economy in human pregnancy and lactation. Nutrition research reviews 25(1):40-67.

Ortner DJ. 1992. Skeletal Paleopathology; Probabilities, Possibilities and Impossibilities. In: Verano J, and Ubelaker D, editors. Demography in the Americas. Washington DC: Smithsonian Institution Press. p 5-13.

Ortner DJ. 2003. Identification of pathological conditions in human skeletal remains: Academic Press.

Ortner DJ, Butler W, Cafarella J, and Milligan L. 2001. Evidence of Probable Scurvy in Subadults from Archeological Sites in North America. American Journal of Physical Anthropology 114(4):343-351.

Ortner DJ, and Ericksen MF. 1997. Bone Changes in the Human Skull Probably resulting from Scurvy in Infancy and Childhood. International Journal of Osteoarchaeology 7(3):212-220.

Oxenham M. 2006. Biological Responses to Change in Prehistoric Viet Nam. Asian Perspectives 45(2):212-239.

Oxenham M. 2015. Mainland Southeast Asia: Towards a New Theoretical Approach. Antiquity 89(347):1221-1223.

Oxenham M. 2016. Bioarchaeology of Ancient Northern Vietnam: Archaeopress.

Oxenham M, and Buckley H. 2016. The population history of mainland and island Southeast Asia. In: Oxenham MF, and Buckley H, editors. The Routledge Handbook of Bioarchaeology in Southeast Asia and the Pacific. London: Routledge. p 9-23.

Oxenham M, Matsumura H, Domett K, Thuy NK, Dung NK, Cuong NL, Huffer D, and Muller S. 2008. Health and the Experience of Childhood in Late Neolithic Viet Nam. Asian Perspectives:190-209.

Oxenham M, and Tayles N. 2006. Synthesising Southeast Asian population history and palaeohealth. In: Oxenham M, and Tayles N, editors. Bioarchaeology of Southeast Asia. Cambridge, UK: Cmabridge University Press. p 335-349.

Oxenham MF, and Domett KM. 2011. Palaeohealth at Man Bac. In: Oxenham MF, Matsumura H, and Kim Dung N, editors. Man Bac: The Excavation of a Neolithic Site in Northern Vietnam The Biology. Canberra, Australia: ANU ePress. p 77-93.

Oxenham MF, Matsumura H, and Kim Dung N. 2011. Man Bac: The Excavation of a Neolithic Site in Northern Vietnam The Biology, Terra Australis 33. Canberra, Australia: ANU ePress.

Oxenham MF, Trinh HH, Willis A, Jones RK, Domett K, Castillo C, Wood R, Bellwood P, Tromp M, and Kells A. 2018. Between Foraging and Farming: Strategic Responses to

the Holocene Thermal Maximum in Southeast Asia. Antiquity 92(364):940-957. DOI: 10.15184/aqy.2018.69

Pettifor J, Ross F, Travers R, Glorieux F, and DeLuca H. 1981. Dietary calcium deficiency: A syndrome associated with bone deformities and elevated serum 1, 25-Dihyroxyvitamin D concentrations. Metabolic Bone Disease and Related Research 2(5):301-305.

Pettifor JM. 2004. Nutritional rickets: deficiency of vitamin D, calcium, or both? The American journal of clinical nutrition 80(6):1725S-1729S.

Pietrusewsky M, and Douglas MT. 2002. *Ban Chiang, a prehistoric village site in Northeast Thailand, Volume 1: The human skeletal remains* . Pennsylvania: University of Pennsylvania Museum of Archaeology.

Piper P, Campos F, Ngoc Kinh D, Amano N, Oxenham M, Chi Hoang B, Bellwood P, and Willis A. 2014. Early evidence for pig and dog husbandry from the Neolithic site of An Son, Southern Vietnam. International Journal of Osteoarchaeology 24(1):68-78.

Prentice A. 1995. Calcium requirements of children. Nutrition Reviews 53(2):37-40.

Rauch F, and Schoenau E. 2001. Changes in Bone Density during Childhood and Adolescence: An Approach based on Bone's Biological Organization. Journal of Bone and Mineral Research 16(4):597-604.

Resnick D. 1995. Diagnosis of Bone and Joint Disorders. Philadelphia, USA: Saunders.

Roberts CA, and Connell B. 2004. Guidance on recording palaeopathology. British Association for Biological Anthropology and Osteoarchaeology and ….

Rokkas T, Papatheodorou G, Karameris A, Mavrogeorgis A, Kalogeropoulos N, and Giannikos N. 1995. Helicobacter pylori infection and gastric juice vitamin C levels. Digestive diseases and sciences 40(3):615-621.

Rumm-Kreuter D, and Demmel I. 1990. Comparison of Vitamin Losses in Vegetables Due to Various Cooking Methods. Journal of Nutritional Science and Vitaminology 36(4):S7-S15.

Sawada J, Thuy NK, and Tuan NA. 2011. Faunal Remains at Man Bac. In: Oxenham MF, Matsumura H, and Kim Dung N, editors. Man Bac: The Excavation of a Neolithic Site in Northern Vietnam, The Biology Terra Australis 33. Canberra, Australia: ANU ePress. p 105-116.

Schattmann A, Bertrand B, Vatteoni S, and Brickley M. 2016. Approaches to Co-occurrence: Scurvy and Rickets in Infants and Young Children of 16–18th Century Douai, France. International journal of paleopathology 12:63-75.

Scheuer L, and Black S. 2000. Developmental Juvenile Osteology. Oxford, UK: Academic Press.

Schrenk A. 2017. Subadult Age at Death and Health Status at Niah Cave, Borneo (1500–200 bc). International Journal of Osteoarchaeology 27(5):801-812.

Singh J, Jain D, Verma RK, and Singh H. 2015. Scurvy: A Common Co-morbid Condition in Severe Acute Malnutrition. The Indian Journal of Pediatrics 82(8):761-762.

Snoddy AME, Buckley HR, Elliott GE, Standen VG, Arriaza BT, and Halcrow SE. 2018. Macroscopic Features of Scurvy in Human Skeletal Remains: A Literature Synthesis and Diagnostic Guide. American Journal of Physical Anthropology 167(4):876-895. DOI: 10.1002/ajpa.23699

Snoddy AME, Halcrow SE, Buckley HR, Standen VG, and Arriaza BT. 2017. Scurvy at the Agricultural Transition in the Atacama Desert (ca 3600–3200 BP): Nutritional Stress at the Maternal-Foetal Interface? International Journal of Paleopathology 18:108-120. DOI: 10.1016/j.ijpp.2017.05.011

Tanabe S, Saito Y, Vu QL, Hanebuth TJ, Ngo QL, and Kitamura A. 2006. Holocene Evolution of the Song Hong (Red River) Delta System, Northern Vietnam. Sedimentary Geology 187(1-2):29-61.

Tayles N. 1999. The Excavation of Khok Phanom Di a Prehistoric Site in Central Thailand Volume V: The People. London: Reports- Research Committee Society of Antiquaries London.

Tayles N, Domett K, and Nelsen K. 2000. Agriculture and dental caries? The case of rice in prehistoric Southeast Asia. World Archaeology 32(1):68-83.

Temple DH, and Larsen CS. 2013. Bioarchaeological Perspectives on Systemic Stress during the Agricultural Transition in Prehistoric Japan. In: Pechenkina K, and Oxenham M, editors. Bioarchaeology of East Asia: movement, contact, health: University Press of Florida. p 344-367.

Thacher TD. 2003. Calcium-Deficiency Rickets. In: Hochberg Z, editor. Vitamin D and Rickets. Basel, Switzerland: Karger. p 105-125.

Toizumi T, Thuy NK, and Sawada J. 2011. Fish Remains at Man Bac. In: Oxenham MF, Matsumura H, and Kim Dung N, editors. Man Bac: The Excavation of a Neolithic Site in Northern Vietnam The Biology, Terra Australis 33. Cannerra, Australia: ANU ePress. p 117-126.

Ubelaker DH. 1989. Human Skeletal Remains: Excavation, Analysis, Interpretation. Washington D.C, USA: Taraxacum Press.

US Department of Agriculture. 2019. FoodData Central. https://fdc.nal.usda.gov.

Vlok M, Oxenham M, Domett K, Tran MT, Mai Huong NT, Matsumura H, Trinh HH, Higham T, Higham CF, Huu NT et al. . in press. Two Probable Cases of Infection with *Treponema pallidum* during the Neolithic Period in Northern Vietnam (ca. 2000-1500B.C.). Bioarchaeology International.

Weber S, Lehman H, Barela T, Hawks S, and Harriman D. 2010. Rice or millets: early farming strategies in prehistoric central Thailand. Archaeological and Anthropological Sciences 2(2):79-88.

White TD, Black MT, and Folkens PA. 2000. Human Osteology. Oxford, UK: Academic press.

Willis A, and Oxenham MF. 2013. The Neolithic Demographic Transition and Oral Health: The Southeast Asian Experience. American Journal of Physical Anthropology 152(2):197-208.

Yamazaki Y, Okazaki R, Shibata M, Hasegawa Y, Satoh K, Tajima T, Takeuchi Y, Fujita T, Nakahara K, and Yamashita T. 2002. Increased circulatory level of biologically active full-length FGF-23 in patients with hypophosphatemic rickets/osteomalacia. The Journal of Clinical Endocrinology & Metabolism 87(11):4957-4960.

Yoneda M. 2008. Dietary reconstruction of ancient Vietnamese based on carbon and nitrogen isotopes. Man Bac Symposium. Institute of Archaeology, Hanoi, Vietnam.